APOPTOSIS INDUCTION/SUPPRESSION: A FEASIBLE APPROACH FOR NATURAL PRODUCTS TO TREATMENT OF DISEASES, VOLUME II

EDITED BY: Hong Zhang, Wei Peng and Xin Luan

PUBLISHED IN: Frontiers in Pharmacology and Frontiers in Oncology



frontiers Research Topics

Frontiers eBook Copyright Statement

The copyright in the text of individual articles in this eBook is the property of their respective authors or their respective institutions or funders. The copyright in graphics and images within each article may be subject to copyright of other parties. In both cases this is subject to a license granted to Frontiers.

The compilation of articles constituting this eBook is the property of Frontiers.

Each article within this eBook, and the eBook itself, are published under the most recent version of the Creative Commons CC-BY licence. The version current at the date of publication of this eBook is CC-BY 4.0. If the CC-BY licence is updated, the licence granted by Frontiers is automatically updated to the new version.

When exercising any right under the CC-BY licence, Frontiers must be attributed as the original publisher of the article or eBook, as applicable.

Authors have the responsibility of ensuring that any graphics or other materials which are the property of others may be included in the CC-BY licence, but this should be checked before relying on the CC-BY licence to reproduce those materials. Any copyright notices relating to those materials must be complied with.

Copyright and source acknowledgement notices may not be removed and must be displayed in any copy, derivative work or partial copy which includes the elements in question.

All copyright, and all rights therein, are protected by national and international copyright laws. The above represents a summary only. For further information please read Frontiers' Conditions for Website Use and Copyright Statement, and the applicable CC-BY licence.

ISSN 1664-8714
ISBN 978-2-88976-271-2
DOI 10.3389/978-2-88976-271-2

About Frontiers

Frontiers is more than just an open-access publisher of scholarly articles: it is a pioneering approach to the world of academia, radically improving the way scholarly research is managed. The grand vision of Frontiers is a world where all people have an equal opportunity to seek, share and generate knowledge. Frontiers provides immediate and permanent online open access to all its publications, but this alone is not enough to realize our grand goals.

Frontiers Journal Series

The Frontiers Journal Series is a multi-tier and interdisciplinary set of open-access, online journals, promising a paradigm shift from the current review, selection and dissemination processes in academic publishing. All Frontiers journals are driven by researchers for researchers; therefore, they constitute a service to the scholarly community. At the same time, the Frontiers Journal Series operates on a revolutionary invention, the tiered publishing system, initially addressing specific communities of scholars, and gradually climbing up to broader public understanding, thus serving the interests of the lay society, too.

Dedication to Quality

Each Frontiers article is a landmark of the highest quality, thanks to genuinely collaborative interactions between authors and review editors, who include some of the world's best academicians. Research must be certified by peers before entering a stream of knowledge that may eventually reach the public - and shape society; therefore, Frontiers only applies the most rigorous and unbiased reviews.
Frontiers revolutionizes research publishing by freely delivering the most outstanding research, evaluated with no bias from both the academic and social point of view. By applying the most advanced information technologies, Frontiers is catapulting scholarly publishing into a new generation.

What are Frontiers Research Topics?

Frontiers Research Topics are very popular trademarks of the Frontiers Journals Series: they are collections of at least ten articles, all centered on a particular subject. With their unique mix of varied contributions from Original Research to Review Articles, Frontiers Research Topics unify the most influential researchers, the latest key findings and historical advances in a hot research area! Find out more on how to host your own Frontiers Research Topic or contribute to one as an author by contacting the Frontiers Editorial Office: frontiersin.org/about/contact

APOPTOSIS INDUCTION/SUPPRESSION: A FEASIBLE APPROACH FOR NATURAL PRODUCTS TO TREATMENT OF DISEASES, VOLUME II

Topic Editors:
Hong Zhang, Shanghai University of Traditional Chinese Medicine, China
Wei Peng, Chengdu University of Traditional Chinese Medicine, China
Xin Luan, Shanghai University of Traditional Chinese Medicine, China

Citation: Zhang, H., Peng, W., Luan, X., eds. (2022). Apoptosis Induction/Suppression: A Feasible Approach for Natural Products to Treatment of Diseases, Volume II. Lausanne: Frontiers Media SA.
doi: 10.3389/978-2-88976-271-2

Table of Contents

06 ***Editorial: Apoptosis Induction/Suppression: A Feasible Approach for Natural Products to Treatment of Diseases, Volume II***
Wei Peng, Xin Luan and Hong Zhang

09 ***Ascorbic Acid Inhibits Liver Cancer Growth and Metastasis* in vitro *and* in vivo*, Independent of Stemness Gene Regulation***
Jingjing Wan, Juan Zhou, Lu Fu, Yubin Li, Huawu Zeng, Xike Xu, Chao Lv and Huizi Jin

20 ***Protective Effect of Pyxinol, One Active Ingredient of* Lichenes *on Cisplatin-Induced Nephrotoxicity via Ameliorating DNA Damage Response***
Yanting Yang, Xiuhong Zhu, Guohua Yu and Jinbo Ma

28 ***Total Flavonoids of Litchi Seed Attenuate Prostate Cancer Progression* Via *Inhibiting AKT/mTOR and NF-kB Signaling Pathways***
Ming Chang, Dan Zhu, Yanjiang Chen, Weiquan Zhang, Xi Liu, Xiao-Lan Li, Zhiping Cheng, Zhiheng Su, Jian Zhang, Yi Lu and Hongwei Guo

44 ***Molecular Basis of Prostate Cancer and Natural Products as Potential Chemotherapeutic and Chemopreventive Agents***
Bingke Bai, Qianbo Chen, Rui Jing, Xuhui He, Hongrui Wang, Yanfei Ban, Qi Ye, Weiheng Xu and Chengjian Zheng

84 ***Natural Products: A Promising Therapeutics for Targeting Tumor Angiogenesis***
Ruyi Li, Xin Song, Yanan Guo, Peng Song, Dongzhu Duan and Zhe-Sheng Chen

102 ***Safflower Polysaccharide Inhibits AOM/DSS-Induced Mice Colorectal Cancer Through the Regulation of Macrophage Polarization***
Qun Wang, Yun Huang, Min Jia, Dong Lu, Hong-Wei Zhang, Dan Huang, San-Hong Liu and Chao Lv

115 ***ROS/JNK/C-Jun Pathway is Involved in Chaetocin Induced Colorectal Cancer Cells Apoptosis and Macrophage Phagocytosis Enhancement***
Huihui Wang, Chuangyu Wen, Siyu Chen, Weiqian Li, Qiyuan Qin, Lu He, Fang Wang, Junxiong Chen, Weibiao Ye, Wende Li, Junsheng Peng, Xiangling Yang and Huanliang Liu

131 ***An Ethanolic Extract of* Cucurbita pepo *L. Seeds Modifies Neuroendocrine Disruption in Chronic Stressed Rats and Adrenal Expression of Inflammatory Markers and HSP70***
Hailah M. Almohaimeed, Shereen Hamed, Hanan S. Seleem, Ashwaq H. Batawi, Zuhair M. Mohammedsaleh, Maha Jameal Balgoon, Soad S. Ali, Soad Al Jaouni and Nasra Ayuob

145 ***Induction of PI3K/Akt-Mediated Apoptosis in Osteoclasts Is a Key Approach for* Buxue Tongluo *Pills to Treat Osteonecrosis of the Femoral Head***
Dan Wang, Yicheng Liu, Dandan Tang, Shujun Wei, Jiayi Sun, Lvqiang Ruan, Lin He, Ruolan Li, Qiang Ren, Xiaoping Tian and Yunhui Chen

164 ***Role of Borneol Induced Autophagy in Enhancing Radiosensitivity of Malignant Glioma***

Qinglin Li, Liang Xia, Caixing Sun, Huangjie Zhang, Mengying Zheng, Hongyan Zhang, Hongyang Lu and Zeng Wang

173 ***Sempervirine Inhibits Proliferation and Promotes Apoptosis by Regulating Wnt/β-Catenin Pathway in Human Hepatocellular Carcinoma***

Rongcai Yue, Haiping Liu, Yaxin Huang, Jing Wang, Dongmei Shi, Yanping Su, Yufei Luo, Ping Cai, Guilin Jin and Changxi Yu

184 ***Gastroprotective Effects of* Periplaneta americana *L. Extract Against Ethanol-Induced Gastric Ulcer in Mice by Suppressing Apoptosis-Related Pathways***

Shu Fu, Jiamei Chen, Chen Zhang, Jinfeng Shi, Xin Nie, Yichen Hu, Chaomei Fu, Xiaofang Li and Jinming Zhang

195 ***Network Pharmacology-Based Investigation and Experimental Exploration of the Antiapoptotic Mechanism of Colchicine on Myocardial Ischemia Reperfusion Injury***

Yuanjun Tang, Chenyang Shi, Yingyi Qin, Shuowen Wang, Hui Pan, Ming Chen, Xuemei Yu, Yuefen Lou and Guorong Fan

206 ***Ginsenoside Rb1 Attenuates Triptolide-Induced Cytotoxicity in HL-7702 Cells* via *the Activation of Keap1/Nrf2/ARE Pathway***

Hulinyue Peng, Longtai You, Chunjing Yang, Kaixin Wang, Manting Liu, Dongge Yin, Yuchen Xu, Xiaoxv Dong, Xingbin Yin and Jian Ni

221 ***Natural Products in Modulating Methamphetamine-Induced Neuronal Apoptosis***

Yiwei Zeng, Yunhui Chen, Su Zhang, Huan Ren, Jialin Xia, Mengnan Liu, Baozhi Shan and Yulan Ren

235 ***Apoptosis Induction, a Sharp Edge of Berberine to Exert Anti-Cancer Effects, Focus on Breast, Lung, and Liver Cancer***

Yi Zhu, Na Xie, Yilu Chai, Yisen Nie, Ke Liu, Yufei Liu, Yang Yang, Jinsong Su and Chuantao Zhang

254 ***Promoting Apoptosis, a Promising Way to Treat Breast Cancer With Natural Products: A Comprehensive Review***

Lie Yuan, Yongqing Cai, Liang Zhang, Sijia Liu, Pan Li and Xiaoli Li

299 ***Natural Products Modulate Cell Apoptosis: A Promising Way for the Treatment of Ulcerative Colitis***

Chenhao Liu, Yiwei Zeng, Yulong Wen, Xinggui Huang and Yi Liu

315 ***Apoptosis Triggering, an Important Way for Natural Products From Herbal Medicines to Treat Pancreatic Cancers***

Meiyan Li, Dandan Tang, Ting Yang, Die Qian and Runchun Xu

331 ***An Integrated Approach Based on Network Analysis Combined With Experimental Verification Reveals PI3K/Akt/Nrf2 Signaling Is an Important Way for the Anti-Myocardial Ischemia Activity of* Yi-Qi-Tong-Luo *Capsule***

Huxinyue Duan, Meiyan Li, Jia Liu, Jiayi Sun, Chunjie Wu, Yu Chen, Xiaohui Guo and Xinglong Liu

348 ***Sesquiterpene Lactones Attenuate Paclitaxel Resistance Via Inhibiting MALAT1/STAT3/ FUT4 Axis and P-Glycoprotein Transporters in Lung Cancer Cells***
Yaming Ding, Zhang Zhen, Muhammad Azhar Nisar, Farman Ali, Riaz Ud Din, Muhammad Khan, Tafail Akbar Mughal, Gulzar Alam, Linlin Liu and Muhammad Zubair Saleem

365 ***Curcumin-Loaded mPEG-PLGA Nanoparticles Attenuates the Apoptosis and Corticosteroid Resistance Induced by Cigarette Smoke Extract***
Xi Chen, Di Wang, Xuejun Guo, Xiaoming Li, Wenjing Ye, Yang Qi and Wen Gu

375 ***Inhibition of Myocardial Cell Apoptosis Is Important Mechanism for Ginsenoside in the Limitation of Myocardial Ischemia/Reperfusion Injury***
Zhihan Chen, Jingping Wu, Sijing Li, Caijiao Liu and Yulan Ren

389 ***Induction of Apoptosis by Metabolites of Rhei Radix et Rhizoma (Da Huang): A Review of the Potential Mechanism in Hepatocellular Carcinoma***
Huanyu Jiang, Wuyinuo Tang, Yang Song, Wei Jin and Quanyu Du

402 ***Maackiain Modulates miR-374a/GADD45A Axis to Inhibit Triple-Negative Breast Cancer Initiation and Progression***
Fu Peng, Li Wang, Liang Xiong, Hailin Tang, Junrong Du and Cheng Peng

416 ***Fengreqing Oral Liquid Exerts Anti-Inflammatory Effects by Promoting Apoptosis and Inhibiting PI3K/AKT and NF-κB Signaling Pathways***
Zhili Rao, Xiangyu Li, Xia Zhang, Jiuseng Zeng, Baojun Wang, Ruocong Yang and Nan Zeng

431 ***Extraction Optimization, Structural Characterization, and Anti-Hepatoma Activity of Acidic Polysaccharides From* Scutellaria barbata *D. Don***
Wenwen Su, Leilei Wu, Qichao Liang, Xiaoyue Lin, Xiaoyi Xu, Shikai Yu, Yitong Lin, Jiadong Zhou, Yang Fu, Xiaoyan Gao, Bo Zhang, Li Li, Dan Li, Yongkui Yin and Gaochen Song

frontiers | Frontiers in Pharmacology

EDITORIAL
published: 16 May 2022
doi: 10.3389/fphar.2022.923562

Editorial: Apoptosis Induction/Suppression: A Feasible Approach for Natural Products to Treatment of Diseases, Volume II

Wei Peng[1], *Xin Luan*[2] *and Hong Zhang*[2]*

[1]School of Pharmacy, Chengdu University of Traditional Chinese Medicine, Chengdu, China, [2]Institute of Interdisciplinary Integrative Medicine Research, Shanghai University of Traditional Chinese Medicine, Shanghai, China

Keywords: natural product, apoptosis, cancers, tumors, volume II

Editorial on the Research Topic

Apoptosis Induction/Suppression: A Feasible Approach for Natural Products to Treatment of Diseases, Volume II

INTRODUCTION

Apoptosis is the predominant form of programmed cell death, which is crucial for the normal cell development, organ growth and tissue homeostasis in organisms. In physiological conditions, the cell death and proliferate keep in a dynamic balance. In contrary, the unbalance of cell death and proliferation would result in lots of serious diseases, such as cancers, Alzheimer's disease, Parkinson's disease, and stroke, etc. Similar to the previous Volume I, the research topic "***Apoptosis Induction/Suppression: A Feasible Approach for Natural Products to Treatment of Diseases, Volume II***" provide an academic platform to discuss the novel signal molecules for the apoptosis-related signal pathway, and how natural products can be used to treat various diseases mentioned above via induction or suppression of apoptosis.

NATURAL PRODUCTS INDUCE APOPTOSIS IN TUMORS

Similar to Volume I of our topic for "***Apoptosis Induction/Suppression: A Feasible Approach for Natural Products to Treatment of Diseases***", most of the papers in Volume II suggested that inducing apoptosis is one of the predominant molecular mechanisms for natural products to treat cancers, such as lung, liver, colorectum, prostate, and breast cancers, *etc*.

It is known that lung cancer is the leading cause of cancer caused death worldwide. Ding et al. reported two natural sesquiterpene lactones named alantolactone and brevilin A attenuate the paclitaxel resistance induced pro-apoptotic effect in the paclitaxel-resistant A549 lung cancer cells. In addition, it is reported that natural products could be also used to treat another type of malignant tumor with promising prospect. Jiang et al. reviewed the antitumor effect of secondary metabolites from Rhei Radix et Rhzoma against liver cancer, which, including emodin, rhein, physcion, aloe-emodin, gallic acid, and resveratrol, could suppress liver cancer via induction of apoptosis owing to their multi-targets and multi-pathway characteristics. Su et al. reported the anti-cancer activity of acidic polysaccharides isolated from the *Scutellaria barbata* D. Don, which could induce apoptosis in

OPEN ACCESS

Edited by:
Michael Heinrich,
University College London,
United Kingdom

***Correspondence:**
Hong Zhang
zhanghong@shutcm.edu.cn

Specialty section:
This article was submitted to Ethnopharmacology, a section of the journal Frontiers in Pharmacology

Received: *19 April 2022*
Accepted: *29 April 2022*
Published: *16 May 2022*

Citation:
Peng W, Luan X and Zhang H (2022) Editorial: Apoptosis Induction/Suppression: A Feasible Approach for Natural Products to Treatment of Diseases, Volume II. Front. Pharmacol. 13:923562. doi: 10.3389/fphar.2022.923562

liver cancer cells via regulation of the apoptosis related proteins such as P53, Bax, Bcl-2 ratio, and cell cycle related proteins of cyclin D1 and CDK4. Sempervirine is an alkoloid isolated from *Gelsemium elegans* (G. elegans) Benth. considered as a toxic plant. Yue et al. reported the anticancer effects of sempervirnine on liver cancer *in vivo* and *in vitro*, and the potential molecular mechanisms are related to promote apoptosis via regulating the Wnt/β-catenin pathway. Besides, Wan et al. reported that ascorbic acid could suppress the growth and metastasis of liver cancer via promoting apoptosis of the cells by regulation of stemness genes.

Breast cancer is the most common malignancy in women with high morbidity and mortality, which is serious harm to the health of women, especially the subtype of triple negative breast cancer (TNBC). Yuan et al. present a review on the anticancer effects of natural compounds against breast cancer. The authors indicated that natural product could induce the apoptosis in breast cancer cells via multiple pathways, including mitochondria, FasL/Fas, PI3K/Akt, ROS, and MAPK. Maackiain is a natural compound isolated from the *Spatholobus suberectus* Dunn., which possesses significant anticancer effect against TNBC via induction of apoptosis and suppression of foci formation, migration and invasion of the cells by modulating miR-374a/GADD45A axis (Peng et al.). Besides, Zhu et al. present a review regarding berberine, a known natural compound isolated from the *Coptis chinensis* Franch., which possesses wide spectrum anticancer activities against lung cancer, liver cancer, and breast cancer, *etc*.

Similar to liver cancer, colorectal cancer is another type of cancer with high incidence, especially in China. Safflower polysaccharide is an active fraction isolated from the known traditional Chinese medicine of *Carthamus tinctorius* L. Wang et al. found that the safflower polysaccharide could induce apoptosis in colorectal cancer cells through macrophage polarization. Chaetocin is a natural product produced by a species of fungi of Chaetomium, which has anticancer effects against various type of cancers. Wang et al. investigated the anticancer effect of chaetocin on colorectal cancer, and found that this natural compound can induce apoptosis in colorectal cancer cells via regulation of ROS/JNK/C-Jun pathway. Prostate cancer is a commonly diagnosed malignant cancer in men, which does serious harm to the health of men. Bai et al. present a review regarding the anticancer effects and molecular mechanisms of natural products against prostate cancer. The authors suggested that natural products including extracts and monomers possess promising anticancer effects against prostate cancer, and the molecular mechanisms are related to induction of apoptosis. Chang et al. extracted the total flavonoids of Litchi seeds (TFLS), and studied their anticancer effect on prostate cancer *in vivo* and *in vitro*. The related results showed that TFLS induced the apoptosis and phenotypic reversal of EMT via inhibiting Akt/mTOR and NF-κB signaling pathways. Furthermore, Li et al. summarized the anticancer effects of natural products on pancreatic cancers via induction of apoptosis. Li et al. reported the anticancer effect of borneol against glioma related to induction of apoptosis and autophagy. Besides, another review by Li et al. suggested that natural products are promising therapeutics for treating cancers via induction of apoptosis and inhibition of angiogenesis.

NATURAL PRODUCTS INHIBIT APOPTOSIS TO TREAT OTHER DISEASES

Excessive apoptosis is the main reason for some diseases, such as ischemic heart disease (IHD), bone loss related diseases, and organs injury, *etc*. IHD is commonly caused by insufficient blood flow to the cardiac tissues, which has high morbidity and mortality. Chen et al. summarized the protective effects of ginsenoside on the myocardial ischemia/reperfusion injury (MIRI), and suggested that the potential molecular mechanisms are correlated to inhibition of myocardial cell apoptosis. Furthermore, Tang et al. reported that the colchicine, which is an alkaloid from *Colchicum autumnale*, can protect H_9C_2 cells from hypoxia/reoxygenation injury via anti-apoptosis by activating the PI3K/Akt/eNOS pathway. Besides, using network analysis, Duan et al. found the *Yi-Qi-Tong-Luo*-Capsule alleviates the myocardial ischemia by suppression of the oxidative stress induced apoptosis through the PI3K/Akt/Nrf2 pathway. Peng et al. reported the ginsenoside Rb1 attenuates the triptolide induced cell apoptosis in human normal liver cell line of HL-7702 cells by regulation of the Keap1/Nrf2/ARE signaling pathway. Chen et al. reported the curcumin could protect the rat tracheal epithelial cells from cigarette smoke extract induced apoptosis. Pyxinol is one of the active compounds from *Lichenes*. Yang et al. found that this compound could reduce the cisplatin induced nephrotoxicity via ameliorating DNA damage response. In addition, Fu et al. reported the *Periplaneta americana* L. extract has gastroprotective effects on ethanol-induced gastric ulcer in mice via inhibition of apoptosis related pathways. The apoptosis of intestinal epithelial cells (IECs) plays a crucial role in disease development of Ulcerative colitis (UC). Liu et al. present a review to summary the anti-apoptotic effects of natural products on IECs. Long-term abuse of methamphetamine could cause neurodegenerative changes in central dopaminergic neurons. Zeng et al. reviewed the protective effects of natural products against methamphetamine induced neuronal apoptosis and their potential molecular mechanisms. Besides, Almohaimeed et al. reported the extracts from *Cucurbita pepo* L. effectively ameliorate the chronic stress-induced behavioral, biochemical, and adrenal structural changes mostly through anti-apoptosis, antioxidant and anti-inflammatory effects.

Besides these mentioned above, the investigation by Wang et al. indicated that induction of PI3K/Akt related osteoclasts apoptosis plays an important role for *Buxue Tongluo* Pills to treat osteonecrosis of the femoral head. In addition, Rao et al. suggested the *Fengreqing Oral Liquid* exerts anti-inflammatory effects via promoting apoptosis through inhibiting PI3K/Akt and NF-κB signaling pathways.

We believe that this topic shows the latest studies regarding treatment of various diseases by natural products via regulating

apoptosis from fundamental theory and experiments *in vitro* and *in vivo*. Based on these works, it is suggested that apoptosis induction/suppression is helpful for treating various diseases, including cancers, ischemia-reperfusion (I/R) injury related diseases, bone loss related diseases, and organs injury, *etc*. However, similar to the previous Volume I, some other important apoptosis related diseases have not been mentioned in Volume II, such as Alzheimer's disease, Parkinson's disease, and rheumatoid arthritis, etc. Therefore, more works could be devoted to finding novel natural agents with pharmacological activities against these diseases via apoptosis induction/suppression.

AUTHOR CONTRIBUTIONS

WP and HZ concieved the paper, WP and XL wrote the original manuscript, HZ revised the final manuscript. All authors listed have made a substantial, direct, and intellectual contribution to the work, and approved it for publication.

Conflict of Interest: The authors declare that the research was conducted in the absence of any commercial or financial relationships that could be construed as a potential conflict of interest.

Publisher's Note: All claims expressed in this article are solely those of the authors and do not necessarily represent those of their affiliated organizations, or those of the publisher, the editors and the reviewers. Any product that may be evaluated in this article, or claim that may be made by its manufacturer, is not guaranteed or endorsed by the publisher.

Copyright © 2022 Peng, Luan and Zhang. This is an open-access article distributed under the terms of the Creative Commons Attribution License (CC BY). The use, distribution or reproduction in other forums is permitted, provided the original author(s) and the copyright owner(s) are credited and that the original publication in this journal is cited, in accordance with accepted academic practice. No use, distribution or reproduction is permitted which does not comply with these terms.

frontiers in Pharmacology

ORIGINAL RESEARCH
published: 24 August 2021
doi: 10.3389/fphar.2021.726015

Ascorbic Acid Inhibits Liver Cancer Growth and Metastasis *in vitro* and *in vivo*, Independent of Stemness Gene Regulation

Jingjing Wan[1†], Juan Zhou[2†], Lu Fu[2†], Yubin Li[2], Huawu Zeng[2], Xike Xu[2], Chao Lv[3] and Huizi Jin[1]**

[1]School of Pharmacy, Shanghai Jiao Tong University, Shanghai, China, [2]School of Pharmacy, Naval Medical University, Shanghai, China, [3]Institute of Interdisciplinary Integrative Medicine Research, Shanghai University of Traditional Chinese Medicine, Shanghai, China

OPEN ACCESS

Edited by:
Wei Peng,
Chengdu University of Traditional Chinese Medicine, China

Reviewed by:
Xin Xu,
Chinese Academy of Medical Sciences, China
Dongwei Zhang,
Beijing University of Chinese Medicine, China

***Correspondence:**
Huizi Jin
kimhz@sjtu.edu.cn
Chao Lv
lvchaoanhui@163.com

†These authors have contributed equally to this work

Specialty section:
This article was submitted to Pharmacology of Anti-Cancer Drugs, a section of the journal Frontiers in Pharmacology

Received: 16 June 2021
Accepted: 12 August 2021
Published: 24 August 2021

Citation:
Wan J, Zhou J, Fu L, Li Y, Zeng H, Xu X, Lv C and Jin H (2021) Ascorbic Acid Inhibits Liver Cancer Growth and Metastasis in vitro and in vivo, Independent of Stemness Gene Regulation. Front. Pharmacol. 12:726015. doi: 10.3389/fphar.2021.726015

Experimental and clinical evidence has indicated that the natural product ascorbic acid (AA) is effective in preventing and treating various types of cancers. However, the effect of AA on liver cancer metastasis has not yet been reported. Cancer stem cells (CSCs) play pivotal roles in cancer metastasis. Here, we demonstrated that AA selectively inhibited the viability of both liver cancer cells and CSCs, reduced the formation of cancer cell colonies and CSC spheres, and inhibited tumor growth *in vivo*. Additionally, AA prevented liver cancer metastasis in a xenotransplantation model without suppressing stemness gene expression in liver CSCs. Further study indicated that AA increased the concentration of H_2O_2 and induced apoptosis in liver CSCs. Catalase attenuated the inhibitory effects of AA on liver CSC viability. In conclusion, AA inhibited the viability of liver CSCs and the growth and metastasis of liver cancer cells *in vitro* and *in vivo* by increasing the production of H_2O_2 and inducing apoptosis. Our findings provide evidence that AA exerts its anti-liver cancer efficacy *in vitro* and *in vivo*, in a manner that is independent of stemness gene regulation.

Keywords: ascorbic acid, cancer stem cells, metastasis, stemness genes, H_2O_2, apoptosis

INTRODUCTION

One of the main causes of cancer-related death is distant metastasis that occurs in cancer patients, and cancer stem cells (CSCs) are an important driving force for cancer metastasis. CSCs, also referred to as tumor-initiating cells, have a stronger tumor-forming ability than somatic or non-tumorigenic cancer cells (Ponti et al., 2005; Ma et al., 2007). CSCs play key roles in the development of metastasis in multiple cancers. In colorectal cancer, $CD26^+$ CSCs caused distant metastasis when injected into the mouse cecal wall, while the presence of $CD26^+$ CSCs in primary tumors can predict distant metastasis in cancer patients (Pang et al., 2010). Also, $Lgr5^+$ or $CD44v6^+$ CSCs are required for the generation of metastatic tumors (Todaro et al., 2014; De Sousa e Melo et al., 2017). In squamous cell carcinoma of the head and neck, it was observed that $BMI1^+$ CSCs regulated the invasive growth and cervical lymph node metastasis in a mouse model (Chen D. et al., 2017). A recent study at the single-cell level in breast cancer has shown that early-stage metastatic cells possess a distinct stem-like gene expression signature (Wylie et al., 2015).

Liver cancer is a heterogeneous disease, and liver CSCs play important roles in the development of this disease. Inhibition of ICAM-1, a marker of hepatocellular CSCs, suppresses tumor formation

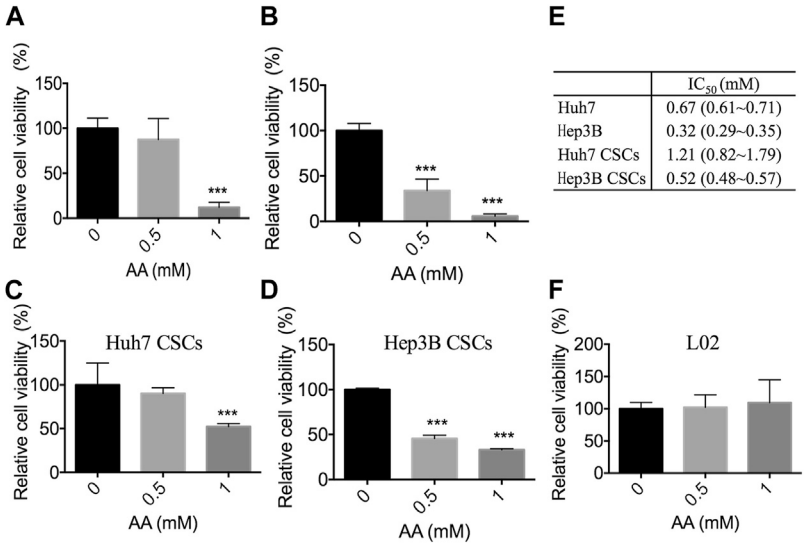


FIGURE 1 | Inhibitory effects of AA on the viability of liver cancer cells *in vitro*. Cells were treated with AA at the concentration as shown and cell viability was measured by CCK-8 assay. **(A)** Cell viability of Huh7 cells. **(B)** Cell viability of Hep3B cells. **(C)** Cell viability of Huh7 CSCs. **(D)** Cell viability of Hep3B CSCs. **(E)** IC50 values of AA, values are mean and 95% confidence. **(F)** Cell viability of L02 hepatocytes. ***$p < 0.001$.

and metastasis in mice (Liu et al., 2013). All-trans retinoic acid can effectively induce the differentiation of CSCs, and it also enhances the cytotoxicity of cisplatin and increases the inhibition of hepatocellular carcinoma (HCC) cell migration *in vitro* and metastasis *in vivo* in combination with cisplatin (Zhang et al., 2013). All of these studies have demonstrated a key role for CSCs in cancer metastasis and suggested that CSCs are a promising target for developing effective therapeutic agents that can be used to treat metastatic cancer.

The natural product ascorbic acid (AA) is an important water-soluble vitamin and is one of the early unorthodox therapies that has long been used in the field of alternative and complementary medicine for cancer treatment, with profound safety and anecdotal efficacy (Du et al., 2010; Chen et al., 2015). Many clinical and laboratory studies have revealed its effects on cancer prevention and treatment. AA inhibits the growth of prostate, ovarian, and pancreatic cancer cells and neuroblastoma cells. (Maramag et al., 1997; Carosio et al., 2007; Chen et al., 2008; Du et al., 2010; Yun et al., 2015; Schoenfeld et al., 2017). Cameron et al. demonstrated in the 1970s that there was a potential survival benefit for patients who received oral and intravenous administration of AA (Cameron and Pauling, 1976; Cameron and Pauling, 1978). However, two clinical studies performed at the Mayo Clinic have shown no significant difference between oral ascorbate-treated and placebo-treated patients (Moertel and Fleming, 1985; Creagan et al., 1979).

Additional research has shown that oral ingestion of high doses of AA rarely induce a plasma concentration greater than 200 μM, due to the limited absorption and renal excretion. By contrast, both intravenous (i.v.) and intraperitoneal (i.p.) administration of ascorbate result in pharmacologic serum ascorbate concentrations up to 20 mmol/L (Reczek and Chandel, 2015; Verrax and Calderon, 2009). Subsequent studies have shown that high-dose intravenous administration of AA alleviates symptoms and prolongs survival in patients with advanced cancer (Cameron and Pauling, 1976; Cameron and Pauling, 1978; Cameron and Campbell, 1974; Padayatty et al., 2006; Raymond et al., 2016). AA also significantly reduces the metastasis of B16FO melanoma cells injected into mice who were deficient in AA and unable to synthesize it (Cha et al., 2013). However, there have been no reports describing the effects of AA on liver cancer metastasis.

With the participation of transition metals (such as copper and iron), a high dose of AA as an electron donor produces extracellular ascorbate anion and H_2O_2, which play important roles in AA-induced anticancer activity (Chen et al., 2015). H_2O_2, an important reactive oxygen species (ROS), plays numerous roles in cancer cells, where a low concentration of H_2O_2 is involved in various signal transduction and cell functions, and a high concentration of H_2O_2 causes DNA damage and promotes cell apoptosis. Du et al. demonstrated that AA decreases the clonogenic survival of pancreatic cancer cell lines, while treatment of cells with H_2O_2 scavengers can reverse AA's anticancer activity (Du et al., 2010). Chen et al. reported that AA causes significant cytotoxicity in cancer cells, while glutathione reduces the cytotoxicity by attenuating AA-induced H_2O_2 production (Chen et al., 2005; Chen et al., 2011).

In this study, we investigated the inhibitory effects of AA on liver cancer cells and liver CSCs *in vitro* and *in vivo*. We found that AA inhibited the growth and metastasis of liver cancer cells and liver CSCs, although AA also increased the expression levels of stemness genes. Further molecular mechanism studies indicated that the increased concentration of H_2O_2 and the enhanced apoptosis by AA play vital roles in its efficacy against liver cancer.

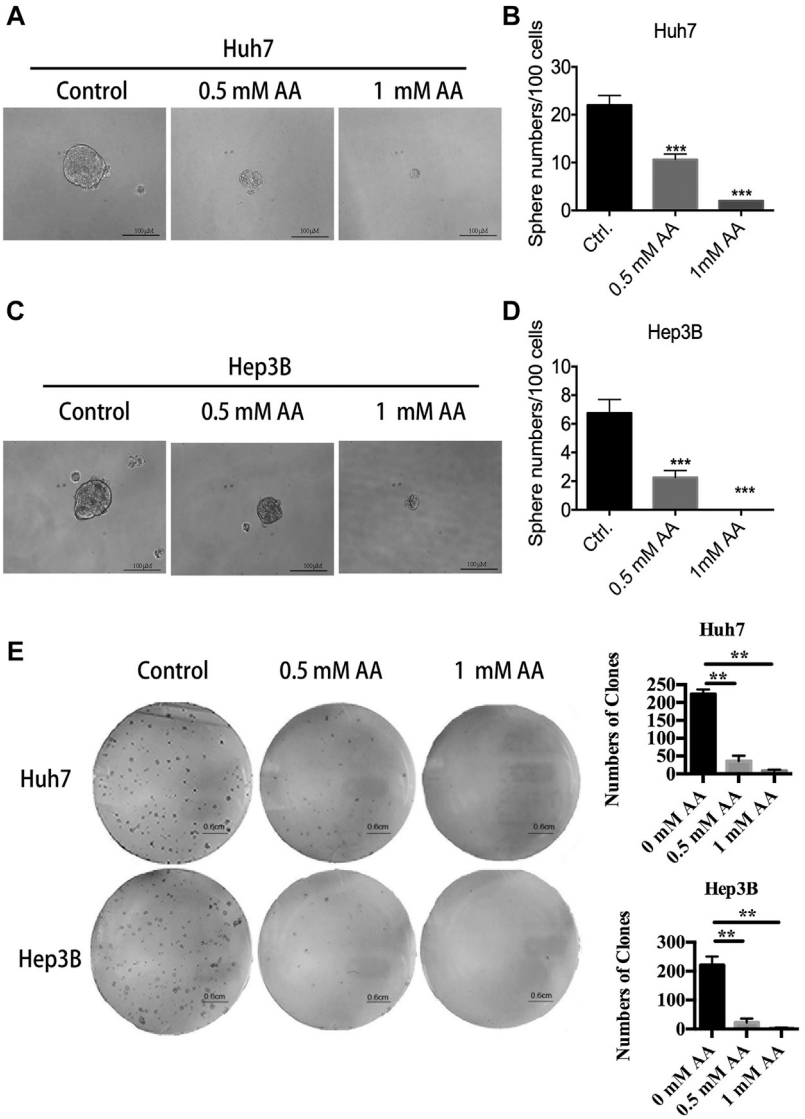


FIGURE 2 | AA reduces sphere formation and colony formation by liver cancer cells. **(A)** Image of spheres formed by Huh7 cells after treatment with AA at indicated concentrations for 14 days. **(B)** Sphere numbers of Huh7 cells after treatment with AA at indicated concentrations for 14 days. **(C)** Image of spheres formed by Hep3B cells after treatment with AA at indicated concentrations for 14 days. **(D)** Sphere numbers formed by Hep3B cells after treatment with AA at indicated concentrations for 14 days. **(E)** Colonies formed by Huh7 or Hep3B cells after treatment with AA at indicated concentrations for 14 days. ***$p < 0.001$.

MATERIALS AND METHODS

Cell Culture

Human liver cancer cell lines Huh7 and Hep3B and normal human liver cell line L02 cells were cultured in Dulbecco's modified Eagle's medium (DMEM) containing 10% fetal bovine serum (FBS) and 1% penicillin/streptomycin. Huh7 and Hep3B CSCs were enriched and maintained on poly-HEMA coated plates in serum-free DMEM/Nutrient Mixture F-12 (F-12) medium containing 20 ng/ml epidermal growth factor (EGF) (236-EG-200, R&D Systems), 10 ng/ml fibroblast growth factor (FGF) (233-FB-025, R&D Systems), and 1% penicillin/streptomycin (Pang et al., 2010; Li et al., 2015). For preparing poly-HEMA coated plates, 6-well plates were pre-coated with 1.2% (w/v) poly-HEMA (Re et al., 1994).

Detection of Cell Viability

Cell viability was measured by Cell Counting Kit-8 (CCK-8) (Dojindo Laboratories) according to the user's manual. The cell viability in each group is expressed as the percentage of untreated control cell viability (Wu et al., 2017).

Flow Cytometric Analysis

To examine the expression of CD133 and CD44, Huh7 and Hep3B stem cells were digested with 0.05% trypsin. Next, 10^6 cells/100 µl of single cells were resuspended and incubated with PE-labeled CD133

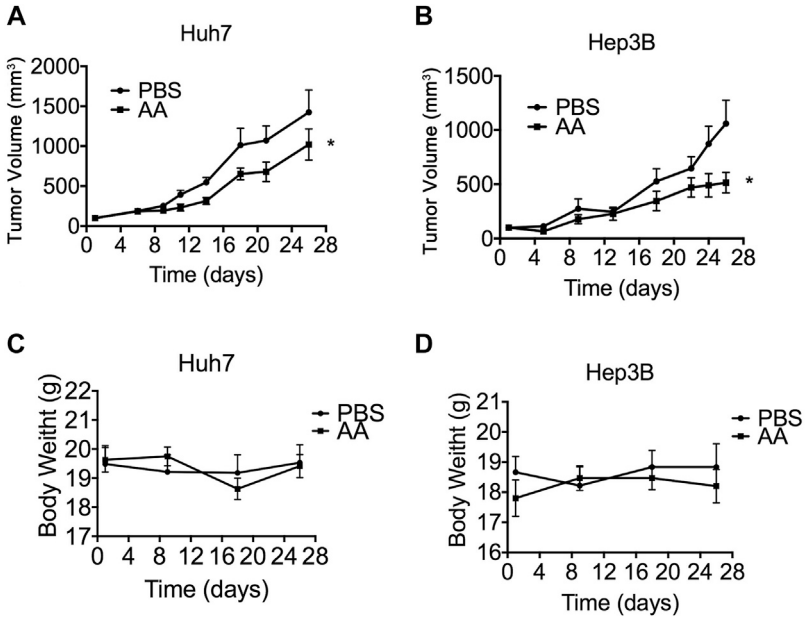


FIGURE 3 | AA suppresses tumor growth *in vivo*. 2×10^6 Huh7 or Hep3B cells were inoculated subcutaneously into nude mice. 3 weeks later, PBS (control group) or 4 g/kg AA was injected intraperitoneally twice daily for 26 days. Tumor volume was measured every 2–3 days and animal body weight was measured every 9 days. **(A)** Volumes of tumors formed by Huh7 cells. **(B)** Volumes of tumors formed by Hep3B cells. **(D)** Body weight of animals engrafted with Huh7 cells. **(D)** Body weight of animals engrafted with Hep3B cells $^*p < 0.05$.

(1:50, Miltenyi Biotec) or CD44 (1:50, Miltenyi Biotec) in the dark for 15 min, washed twice with cold phosphate-buffered saline (PBS), resuspended in 400 µl PBS, and analyzed using flow cytometry (Becton Dickinson FACS Vantage SE, San Jose, CA, United States).

To analyze cell apoptosis, Huh7 stem cells were digested with 0.05% trypsin. Then, 1×10^6 single cells were resuspended and mixed with 10 µl Annexin V-fluorescein isothiocyanate (FITC, 130-097-928, Miltenyi Biotec), incubated in darkness for 15 min, washed with 1 ml 1× Annexin V Binding Buffer and resuspended in 500 µl 1× Annexin V Binding Buffer, mixed with propidium iodide (PI) solution, and then analyzed by flow cytometry (Cheng et al., 2017).

RNA Isolation and Quantitative Real-Time PCR

Total RNA was isolated using a Tissue RNA Kit (R6311-01, Biomiga). RNA (1 µg) was reverse-transcribed into cDNA using GoScript Reverse Transcriptase (A5001, Promega). Quantitative real-time PCR was completed using the Power Up SYBR Green Master Mixture (Thermo Fisher) with the StepOne Plus Real-Time PCR System (Thermo Fisher), according to a protocol from a previous study (Wu et al., 2017). Specific primers for *CD90* and *EPCAM* were created according to Luo et al. (2015). Specific primers for *CD133, OCT4 (POU5F1), NANOG, SOX2*, and beta-actin were created according to Ma et al. (2010).

Animal Experiments

All of the mice were maintained in a pathogen-free facility, and all of the animal experiments were approved by the Committee on the Ethics of Animal Experiments of the Naval Medical University, China. For the animal experiments, 6-week-old female nude BABL/c mice were used, and 2×10^6 Huh7 or Hep3B cells were subcutaneously inoculated into the nude mice (Ma et al., 2018; Yuan et al., 2015). Three weeks later, PBS (control group) or 4 g/kg AA was injected intraperitoneally twice daily for 26 days. The tumor volume was calculated as: total volume = (length × width^2)/2 (Naito et al., 1986). Lung and liver tissues were fixed with 4% polyformaldehyde, and serial sections (four sections per tissue with a 30-µm step) were created and stained with hematoxylin and eosin (HE) (Cheng et al., 2017).

Western Blot

Western blot was completed according to a protocol from a previous study (Wu et al., 2017). Briefly, cells or tissues were lysed with Radioimmunoprecipitation Assay (RIPA) Lysis Buffer (P0013C, Beyotime Biotechnology, China) and centrifuged at 13,000 rpm for 15 min. The supernatant was separated by sodium dodecyl sulfate (SDS)-polyacrylamide gel and transferred to a polyvinylidene difluoride (PVDF) membrane. The membrane was incubated overnight with anti-NANOG (1:500, ab109250, Abcam), anti-SOX2 (1:500, ab92494, Abcam, UK), anti-ALDH1A1 (1:1,000, ab52492, Abcam), or anti-β-actin (1:1,000, 3700S, Cell Signaling Technology) primary antibodies, washed with Tris-buffered saline (TBS) containing 0.1% Tween-20 (TBST) three times, incubated with secondary antibody (926-32210, 1:20,000 for β-actin and 926-32211, 1:5,000 for others, LI-COR, Biosciences), and analyzed with the Odyssey Infrared Imaging System (LI-COR, Biosciences).

Detection of H_2O_2

The H_2O_2 concentration was measured using a H_2O_2 Assay Kit (S0038, Beyotime Biotechnology, China) according to the user's manual. Simply, 1×10^6 cells were lysed in 200 µl lysis buffer and

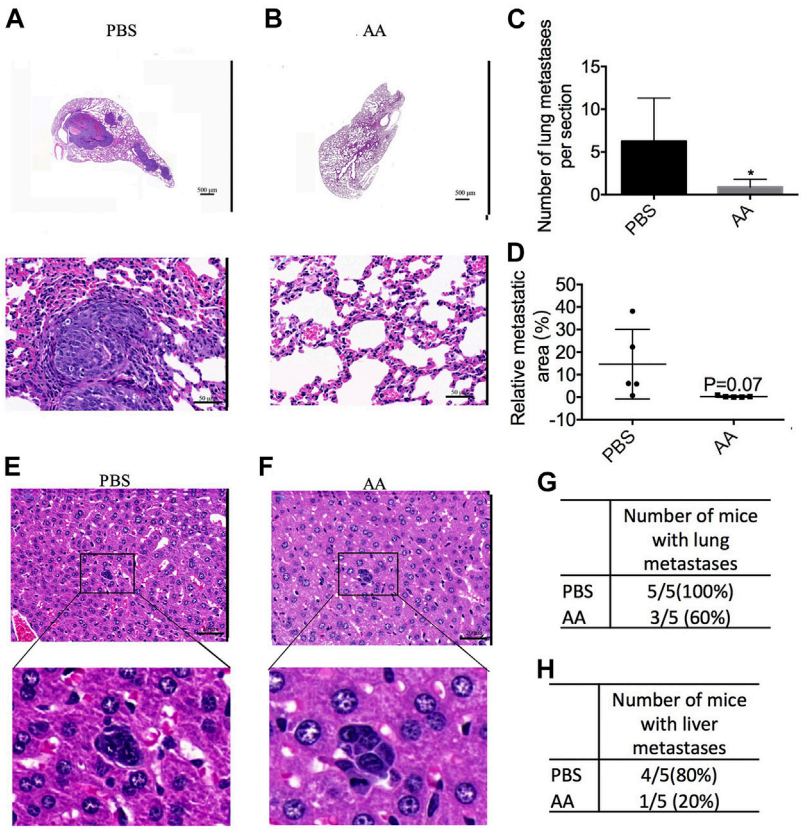


FIGURE 4 | AA prevents tumor metastasis *in vivo*. 2×10^6 Huh7 cells were inoculated subcutaneously into female BALB/c nude mice. After 3 weeks, PBS (control group) or 4 g/kg AA was injected intraperitoneally twice daily. At the end of the experiment, the animals were sacrificed to examine liver and lung metastasis. **(A,B)** HE staining of lung section (A: control group, B: AA group; A, B upper: 2× magnification; A, B lower: 40× magnification). **(C,D)** the number and area ratio of metastatic tumors in each lung section. **(E,F)** HE staining of liver section. (E: control group, F: AA group; 40 × magnification). **(G)** Number of mice with lung metastases in each group. **(H)** Number of mice with liver metastases in each group. $^*p < 0.05$.

centrifuged for 5 min at 12,000 rpm. Every 50 µl of the supernatant was mixed with 100 µl of H_2O_2 detection reagent and incubated for 30 min at room temperature. Absorbance was determined at 560 nm using an Epoch Microplate Spectrophotometer (BioTek). For catalase experiments, catalase was added prior to AA treatment.

Sphere Formation Assay and Colony Formation Assay

For the sphere formation experiment, cells were digested into single cells with trypsin. Then, 100 cells/well were plated into a 96-well ultra-low attachment plate and cultured for 2 weeks in serum-free DMEM/F-12 medium containing 20 ng/ml EGF, 10 ng/ml FGF, and AA (0, 0.5, or 1 mM). The number of spheres was counted and photographed.

For the colony formation experiment, 1,000 cells/well were plated into 6-well plates. The colonies were cultured in DMEM containing 10% fetal bovine serum, 1% penicillin/streptomycin, and AA (0, 0.5, or 1 mM). The colonies were then stained with 1% crystal violet.

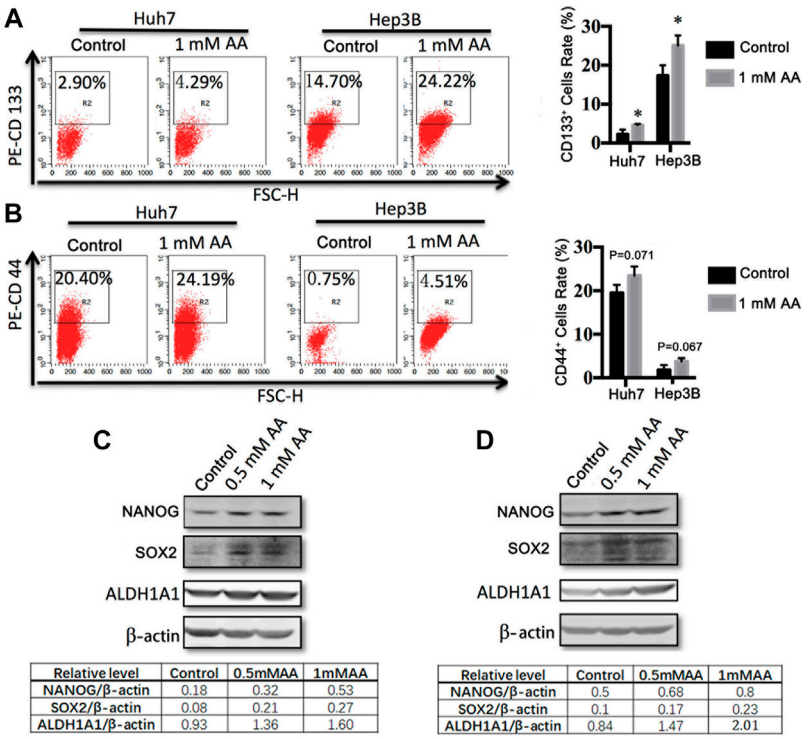
Statistical Analysis

Statistical analysis was performed using unpaired *t* tests when comparing two different groups or one-way ANOVA with Tukey's multiple comparison tests. IC50 values were calculated using Prism software (GraphPad, San Diego, CA, USA) by nonlinear regression to dose-response curves, and expressed as mean and 95% confidence intervals (CI). The data are expressed as the mean ± SEM. $p < 0.05$ was considered statistically significant.

RESULTS

AA Selectively Inhibited the Viability of Liver Cancer Cells and Liver CSCs *in vitro*

Two human liver cancer cell lines (Huh7 and Hep3B), the respective CSCs, and a normal human liver cell line L02 were treated with AA at the concentrations of 0, 0.5, or 1 mM, which are easily achievable clinically by intravenous infusion (Chen et al., 2008) (Hoffer et al., 2008). The results showed that AA inhibited the viabilities of liver cancer cells and liver CSCs in a concentration-dependent manner (**Figures 1A–D**). AA at the concentration of 1 mM decreased the viabilities of Huh7 and Hep3B cells to 12.15 and 5.77%, respectively (**Figures 1A,B**). For Huh7 and Hep3B CSCs, the viabilities were decreased to 52.37 and 33.04%, respectively, at 1 mM concentration of AA (**Figures 1C,D**). The IC50 values of AA for Huh7, Hep3B, and Huh7 CSCs and Hep3B CSCs were 0.67, 0.32,



Relative level	Control	0.5mMAA	1mMAA
NANOG/β-actin	0.18	0.32	0.53
SOX2/β-actin	0.08	0.21	0.27
ALDH1A1/β-actin	0.93	1.36	1.60

Relative level	Control	0.5mMAA	1mMAA
NANOG/β-actin	0.5	0.68	0.8
SOX2/β-actin	0.1	0.17	0.23
ALDH1A1/β-actin	0.84	1.47	2.01

FIGURE 5 | AA regulates the expression of stemness genes in liver cancer cells. **(A,B)** Flow cytometric analysis of the expressions of CD133 and CD44 in Huh7 **(A)** and Hep3B **(B)** stem cells treated with different concentrations of AA. **(C,D)** The protein levels of stemness genes in Huh7 **(C)** and Hep3B **(D)** stem cells treated with different concentrations of AA.

1.21, and 0.52 mM, respectively (**Figure 1E**). However, AA did not display significant inhibitory effects on the viability of L02 cells at 0.5 mM or 1 mM concentrations (**Figure 1F**). Together, these data indicated that AA was responsible for selective inhibitory effects on the viabilities of liver cancer cells and liver CSCs.

AA Inhibits Sphere Formation and Colony Formation in Liver Cancer Cells

We further examined the effects of AA on sphere formation and colony formation. As shown in **Figure 2A**, AA treatment reduced the volume of spheres formed by Huh7 cells. The number of spheres larger than 50 μm in diameter was markedly decreased in a concentration-dependent manner in AA-treated Huh7 cells (**Figure 2B**). Twenty-two spheres were formed for every 100 cells in the control group, whereas only two spheres were formed for every 100 cells in the group treated with 1 mM AA. Similar results were obtained for Hep3B cells (**Figures 2C,D**). As shown in **Figure 2E**, AA treatment also markedly decreased colony formation in a concentration-dependent manner in Huh7 and Hep3B cell lines. Collectively, our data showed that AA reduced sphere formation and colony formation by liver cancer cells, indicating the inhibitory effects of AA on self-renewal and tumorigenicity of liver cancer cells.

AA Inhibited Liver Tumor Growth *in vivo*

We determined the effects of AA on tumor growth in mice bearing Huh7 and Hep3B xenografts. As mentioned above, AA concentrations in human plasma and cells were tightly controlled. With the oral ingestion of high doses of vitamin C, even at 100 times the recommended dietary allowance, the plasma concentration rarely exceeds 200 μM. Both i.v. and i.p. administration of ascorbate induced pharmacologic serum ascorbate concentrations up to 20 mmol/L. To obtain a pharmacologic serum ascorbate concentration, the i.p. administration method was selected. Compared with the PBS control group, AA treatment significantly suppressed the growth of Huh7 and Hep3B xenograft tumors *in vivo* (**Figures 3A,B**) without significantly changing the animal's body weight (**Figures 3C,D**).

AA Prevents Tumor Metastasis *in vivo*

As shown in **Figures 4A,B**, AA-treated mice developed fewer metastatic lung tumors as compared to the control group. The number of metastatic lung tumors in AA-treated mice was 0.90 ± 0.40 (n = 5), and that in the control mice was 6.25 ± 2.27 (n = 5) (**Figure 4C**). The area ratio of metastatic lung tumors in AA-treated mice was 0.29 ± 0.17 (n = 5), and that in control mice was 14.61 ± 6.91 (n = 5) (**Figure 4D**). The metastatic tumors in the livers of either the control or AA groups were small (**Figures 4E,F**). In the control group, 5 of 5 mice developed metastatic lung tumors, whereas 3 of 5 mice exhibited metastatic lung tumors in the AA-treated group (**Figure 4G**). Additionally, in the control group, 4 of 5 mice developed metastatic liver tumors, while in the AA-treated group, 1 of 5 mice developed metastatic liver tumors (**Figure 4H**). In summary, our data demonstrated that AA

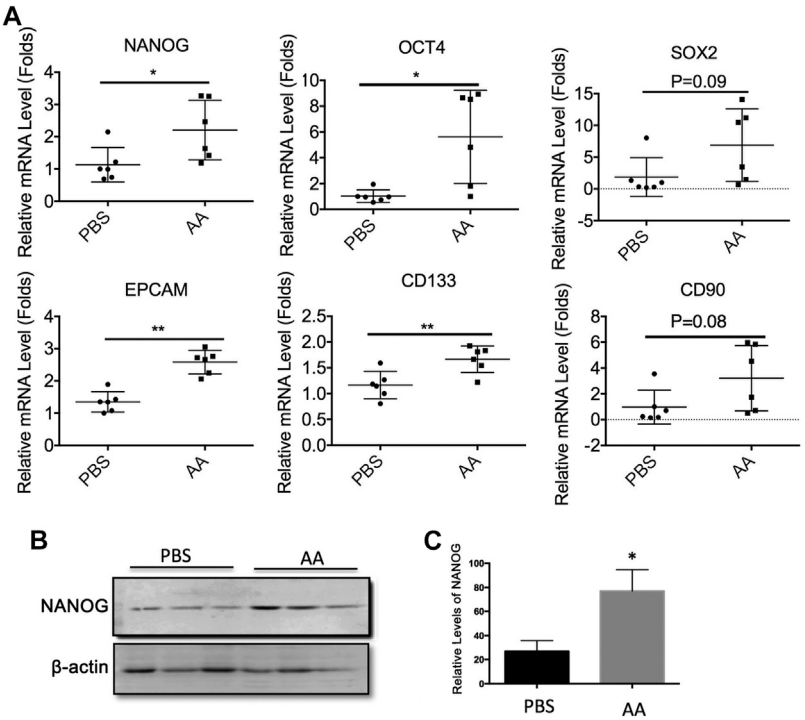


FIGURE 6 | AA regulates the expressions of stemness genes in liver tumors *in vivo*. 2×10^6 Huh7 cells were inoculated subcutaneously into female BALB/c nude mice. Three weeks later, PBS (control group) or 4 g/kg AA were injected intraperitoneally twice a day. At the end of treatment, the animals were sacrificed and tumors were collected for analysis. **(A)** mRNA levels of stemness genes in tumor tissue. **(B,C)** Protein levels of NANOG in tumor tissue. $^*p < 0.05$. $^{**}p < 0.01$.

treatment reduced liver and lung metastasis of liver cancer cells inoculated subcutaneously into nude mice.

AA Upregulated the Expression of Stemness Genes in Liver Cancer Cells and Tumors

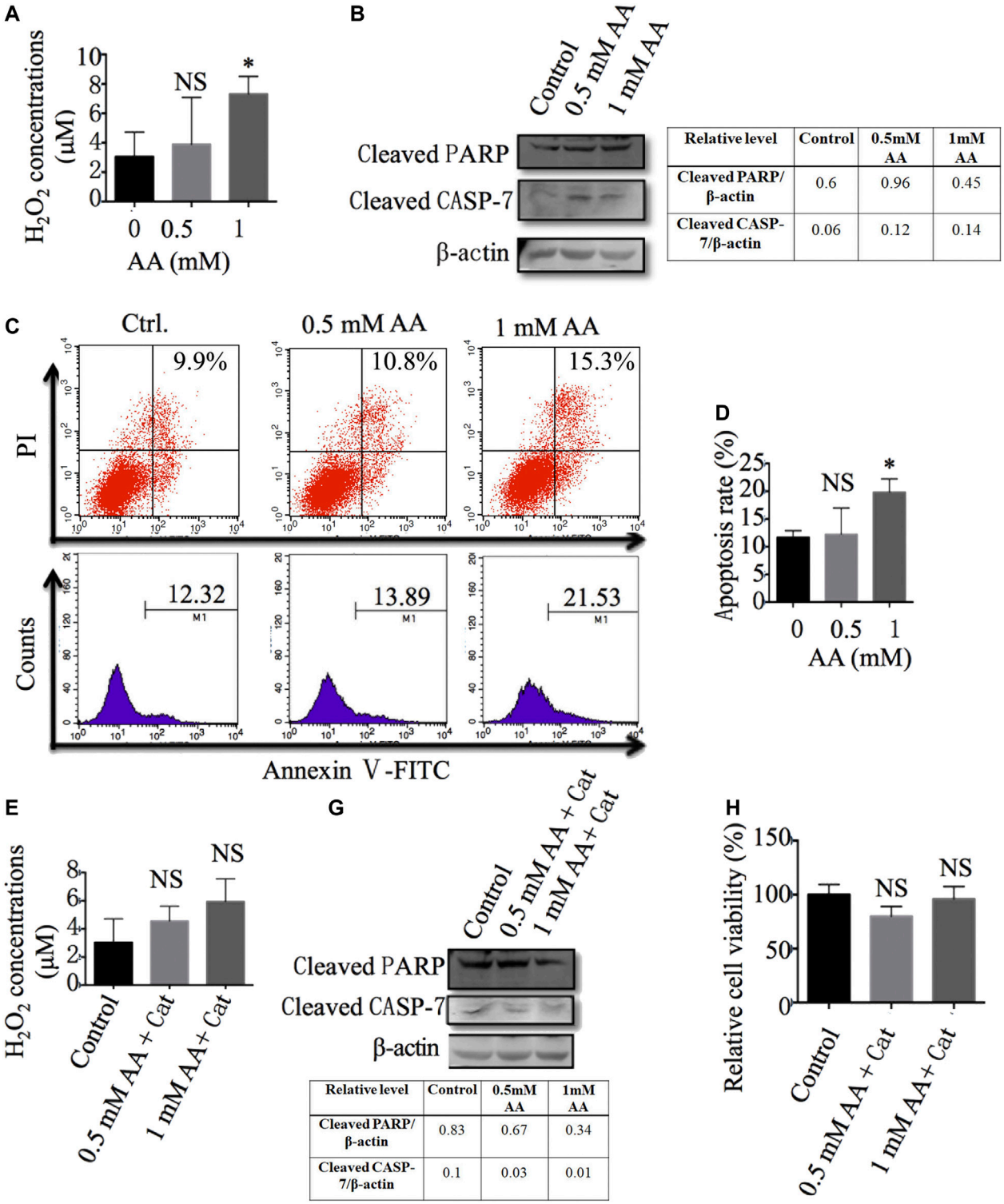
We investigated the effects of AA on the expression of stemness genes. Flow cytometric analysis showed that AA treatment increased $CD133^+$ cells and $CD44^+$ cells in both Huh7-and Hep3B-derived stem cells (**Figures 5A,B**). CD133 antigen was identified as a CSC marker in various cancer types, including liver cancer. CD44, a transmembrane glycoprotein, is also considered as an important liver CSC marker (Zhu et al., 2010; Yang et al., 2008). For Huh7 CSCs, AA at 1 mM increased $CD133^+$ cells and $CD44^+$ cells from 2.90 to 14.70%–4.29 and 24.19%, respectively (**Figures 5A,B**). For Hep3B CSCs, $CD133^+$ cells and $CD44^+$ cells were increased by AA from 20.40 to 0.75%–24.22 and 4.51%, respectively (**Figures 5A,B**). Western blot analysis showed that the protein levels of embryonic stem cell markers NANOG and SOX2 as well as liver CSC marker ALDH1A1 were increased after treatment with AA in Huh7-and Hep3B-derived stem cells (**Figures 5C,D**).

We also examined the effects of AA on the expression of stemness genes in liver tumors *in vivo*. Consistent with the *in vitro* results, the mRNA expression levels of *NANOG*, *OCT4*, *SOX2*, *EPCAM*, *CD133*, and *CD90* were upregulated in the AA-treated tumors (**Figure 6A**). Also, the protein level of NANOG was increased in the AA-treated group as compared with that of the control group (**Figures 6B,C**). Collectively, our data showed that AA upregulated the expression of stemness genes in liver cancer cells *in vitro* and *in vivo*.

AA Enhanced the Production of H_2O_2 and Promoted the Apoptosis of Liver CSCs

It was reported that H_2O_2 plays an important role in AA's anticancer activity (Lennicke et al., 2015; Chaiswing et al., 2018). To determine the role of H_2O_2 in the inhibitory effect of AA on liver CSCs, we first evaluated the concentrations of H_2O_2 in Huh7-derived CSCs with or without AA treatment. As shown in **Figure 7A**, AA treatment increased the concentration of H_2O_2 in Huh7-derived CSCs. Furthermore, AA increased the protein levels of cleaved poly (ADP-ribose) polymerase (PARP) and cleaved caspase-7 (**Figure 7B**) and promoted cell apoptosis (**Figures 7C,D**).

Catalase, as a specific H_2O_2 scavenger, converts the ROS H_2O_2 to water and oxygen and thereby mitigates the cytotoxic effects of H_2O_2. We also found that the addition of catalase reversed the effects of AA on the production of H_2O_2 and the cleavage of PARP and caspase-7 (**Figures 7E,F**). More importantly, the addition of catalase reduced the inhibitory effects of AA on



Relative level	Control	0.5mM AA	1mM AA
Cleaved PARP/β-actin	0.6	0.96	0.45
Cleaved CASP-7/β-actin	0.06	0.12	0.14

Relative level	Control	0.5mM AA	1mM AA
Cleaved PARP/β-actin	0.83	0.67	0.34
Cleaved CASP-7/β-actin	0.1	0.03	0.01

FIGURE 7 | AA reduces liver CSC viability *via* increasing the production of H2O2 and induction of cell apoptosis. **(A)** The content of H_2O_2 in Huh7 stem cells treated with different concentrations of AA. **(B)** The protein levels of cleaved PARP and caspase 7 in Huh7 stem cells treated with different concentrations of AA. **(C, D)** Apoptosis of Huh7 stem cells treated with different concentrations AA. **(E)** The content of H_2O_2 in Huh7 stem cells treated with different concentrations of AA in the presence of 100 μg/ml catalase (Cat: catalase, Sigma -Aldrich). **(F)** The protein levels of cleaved PARP and caspase 7 in Huh7 stem cells treated with different concentrations of AA in the presence of 100 μg/ml catalase. **(G)** Viabilities of Huh7 stem cells treated with different concentrations of AA in the presence of 100 μg/ml catalase. *$p < 0.05$.

liver CSC viability (**Figure 7G**), which was consistent with previous reports describing the dependence of AA's cytotoxicity on the generation of H_2O_2 (Du et al., 2010; Chen et al., 2015; Chen et al., 2005). In conclusion, our data indicate that AA exerts its inhibitory effects on liver CSCs through the production of H_2O_2 and the promotion of cell apoptosis.

DISCUSSION

Various factors lead to an increased risk of liver cancer. Among these factors, it has been reported that alcoholic liver disease is the most common cause of HCC, accounting for approximately 30% of all HCC cases (Morgan et al., 2004). Liver cancer is one of the common causes of cancer-related death. Metastasis and recurrence are the main causes of primary liver cancer-associated mortality. Liver CSCs, possessing a higher migration ability and tumorigenicity, are closely related to metastasis and recurrence of liver cancer. Liver CSCs are considered an important target for liver cancer therapy. For example, WYC-209, a synthetic retinoid, inhibited the proliferation of malignant murine melanoma tumor-repopulating cells and abrogated 87.5% of lung metastases of melanoma tumor-repopulating cells (Chen et al., 2018).

It was reported that AA inhibited the growth of various types of cancer, including colorectal cancer cells, neuroblastoma cells, and ovarian cancer cells. However, its effect on liver cancer metastasis has not yet been reported. Consistent with a previous study (Lv et al., 2018), we found that AA inhibited the viability of liver cancer cells without significantly inhibiting the viability of L02 cells, which are normal human hepatocytes. Furthermore, AA significantly attenuated the viability of liver CSCs and reduced the colony formation ability and sphere formation ability of liver cancer cells *in vitro*, indicating the inhibition by AA on self-renewal and tumorigenicity of liver cancer cells. Because CSCs are involved in important functions in cancer metastasis and AA shows inhibitory effects on liver CSCs, we further examined the effects of AA on liver cancer metastasis. As expected, AA inhibited the metastasis of liver cancer cells to the lung and liver in a subcutaneous xenotransplantation model.

Stemness genes play vital roles in regulating cancer metastasis. In most cases, stemness genes promote cancer metastasis (Lv et al., 2017; Baccelli et al., 2013; Tang et al., 2012; Celià-Terrassa and Kang, 2016). Sox2, a transcription factor involved in the regulation of embryonic development, functions as a novel regulator of cell invasion, migration, and metastasis in several cancer types (Feng and Lu, 2017; Weina and Utikal, 2014). However, it was recently reported that REX1, an embryonic stem cell marker, inhibits liver cancer metastasis, indicating the complex functions of stemness genes in the process of cancer metastasis (Luk et al., 2019). AA regulates the expression of stemness genes, and in human embryonic stem cells, AA caused specific DNA demethylation of 1,847 genes (including the important stem cell genes) (Chung et al., 2010) and also inhibited retinoic acid-induced differentiation of embryonic stem cells (Wu et al., 2014). Furthermore, AA alleviated cell aging and increased the production of induced pluripotent stem cells in mice and human cells (Esteban et al., 2010; Wang et al., 2011).

In adult stem cells, AA enhanced the stemness of mouse corneal epithelial stem cells/progenitor cells and promoted the healing of corneal epithelial injury (Chen J. et al., 2017). AA also reduced stemness gene expression in liver cancer (Lv et al., 2018). Unexpectedly, our data suggested that AA promoted the expression of genes related to cancer stemness. AA increased the production of $CD133^+$ and $CD44^+$ cells and the protein levels of NANOG, SOX2, and ALDH1A1 *in vitro* and upregulated the mRNA expression levels of *NANOG* and *SOX2* and the protein level of NANOG in Huh7 transplanted tumors. Our data suggest that AA inhibits liver cancer metastasis *via* a pathway independent of stemness gene regulation. However, the detailed mechanisms of AA-induced expression changes of stemness genes require further study.

Our results indicated that AA did not downregulate the expression of stem genes in liver cancer cells, which implies that other mechanisms are involved in the inhibition of liver cancer metastasis by AA. H_2O_2 plays an important role in AA's anticancer activity (Du et al., 2010; Chen et al., 2005; Chen et al., 2011). H_2O_2, a key ROS, is involved in cell differentiation, growth, and survival. High levels of H_2O_2 can induce cell cycle arrest and apoptosis in cells (Lennicke et al., 2015; Chaiswing et al., 2018). With the participation of transition metals (such as copper and iron), a high dose of AA as an electron donor produces extracellular ascorbate anion and H_2O_2. H_2O_2 is a cell permeant, and its accumulation induces DNA and mitochondrial damage, and apoptosis of tumor cells. The addition of H_2O_2 to tumor cells produced the same cell death effect as that caused by AA, while simultaneous use of the antioxidants N-acetylcysteine or catalase with AA inhibited AA-induced tumor cell death. These results further demonstrate the key role of H_2O_2 in AA's action upon tumor cells. (Chen et al., 2008; Verrax and Calderon, 2009; Chen et al., 2005; Chen et al., 2007). Normal cells exhibit both catalase and glutathione peroxidase activities, which efficiently detoxify H_2O_2. This might be the reason why AA selectively inhibited tumor cells, while it had no toxic effects on normal cells (Chen et al., 2005). We examined the changes in the H_2O_2 concentration in liver CSCs treated with AA and found that the H_2O_2 concentration was increased after AA treatment. AA treatment also increased the protein levels of apoptotic mediators including cleaved PARP and caspase-7 and enhanced the cell apoptosis of CSCs, while the addition of catalase reduced these effects. These results suggest that AA might induce CSC apoptosis by increasing the intracellular concentration of H_2O_2.

In conclusion, AA inhibited the viability of CSCs and prevented liver cancer metastasis without reducing the expression of stemness genes in liver cancer cells. The inhibitory effects of AA on liver CSCs can result from the production of H_2O_2 and promotion of cell apoptosis. Our findings provide evidence that supports AA as an effective therapeutic agent for liver cancer metastasis and suggest that additional effects other than inhibition of stemness genes may be considered during later evaluation of the effects of AA on CSCs and cancer metastasis.

DATA AVAILABILITY STATEMENT

The original contributions presented in the study are included in the article/Supplementary Material, further inquiries can be directed to the corresponding authors.

ETHICS STATEMENT

The animal study was reviewed and approved by the Committee on the Ethics of Animal Experiments of the Naval Medical University.

AUTHOR CONTRIBUTIONS

JW, JZ, LF, YL, and HWZ designed and conducted experiments, and wrote the manuscript. XK helped study design and interpretation of data. CL, HJ organized, conceived, and supervised the study. All authors read and approved the manuscript.

FUNDING

The work was supported by National Natural Science Foundation of China (81903510), National Major Project of China (2019ZX09201004-003-010).

REFERENCES

Baccelli, I., Schneeweiss, A., Riethdorf, S., Stenzinger, A., Schillert, A., Vogel, V., et al. (2013). Identification of a Population of Blood Circulating Tumor Cells from Breast Cancer Patients that Initiates Metastasis in a Xenograft Assay. *Nat. Biotechnol.* 31, 539–544. doi:10.1038/nbt.2576

Cameron, E., and Campbell, A. (1974). The Orthomolecular Treatment of Cancer II. Clinical Trial of High-Dose Ascorbic Acid Supplements in Advanced Human Cancer. *Chem. Biol. Interact.* 9, 285–315. doi:10.1016/0009-2797(74)90019-2

Cameron, E., and Pauling, L. (1976). Supplemental Ascorbate in the Supportive Treatment of Cancer: Prolongation of Survival Times in Terminal Human Cancer. *Proc. Natl. Acad. Sci.* 73, 3685–3689. doi:10.1073/pnas.73.10.3685

Cameron, E., and Pauling, L. (1978). Supplemental Ascorbate in the Supportive Treatment of Cancer: Reevaluation of Prolongation of Survival Times in Terminal Human Cancer*. *Proc. Natl. Acad. Sci.* 75, 4538–4542. doi:10.1073/pnas.73.10.3685

Carosio, R., Zuccari, G., Orienti, I., Mangraviti, S., and Montaldo, P. G. (2007). Sodium Ascorbate Induces Apoptosis in Neuroblastoma Cell Lines by Interfering with Iron Uptake. *Mol. Cancer* 6, 55. doi:10.1186/1476-4598-6-55

Celià-Terrassa, T., and Kang, Y. (2016). Distinctive Properties of Metastasis-Initiating Cells. *Genes Dev.* 30, 892–908. doi:10.1101/gad.277681.116

Cha, J., Roomi, M. W., Ivanov, V., Kalinovsky, T., Niedzwiecki, A., and Rath, M. (2013). Ascorbate Supplementation Inhibits Growth and Metastasisof B16FO Melanoma and 4T1 Breast Cancer Cellsin Vitamin C-Deficient Mice. *Int. J. Oncol.* 42, 55–64. doi:10.3892/ijo.2012.1712

Chaiswing, L., Clair, W. H. S., and Clair, D. K. S. (2018). Redox Paradox: A Novel Approach to Therapeutics-Resistant Cancer. *Antioxid. Redox Signal* 29, 1237–1272. doi:10.1089/ars.2017.7485

Chen, D., Wu, M., Li, Y., Chang, I., Yuan, Q., Ekimyan-Salvo, M., et al. (2017a). Targeting BMI1+Cancer Stem Cells Overcomes Chemoresistance and Inhibits Metastases in Squamous Cell Carcinoma. *Cell Stem Cell* 20, 621–634. e6. doi:10.1016/j.stem.2017.02.003

Chen, J., Cao, X., An, Q., Zhang, Y., Li, K., Yao, W., et al. (2018). Inhibition of Cancer Stem Cell like Cells by a Synthetic Retinoid. *Nat. Commun.* 9, 1–10. doi:10.1038/s41467-018-03877-7

Chen, J., Lan, J., Liu, D., Backman, L. J., Zhang, W., and Zhou, Q. (2017b). Ascorbic Acid Promotes the Stemness of Corneal Epithelial Stem/Progenitor Cells and Accelerates Epithelial Wound Healing in the Cornea. *Stem Cell Transl. Med.* 6, 1356–1365. doi:10.5966/sctm.2013-0122

Chen, P., Stone, J., Sullivan, G., Drisko, J. A., and Chen, Q. (2011). Anti-cancer Effect of Pharmacologic Ascorbate and its Interaction with Supplementary Parenteral Glutathione in Preclinical Cancer Models. *Free Radic. Biol. Med.* 51, 681–687. doi:10.1016/j.freeradbiomed.2011.05.031

Chen, Q., Espey, M. G., Krishna, M. C., Mitchell, J. B., Corpe, C. P., Buettner, G. R., et al. (2005). Pharmacologic Ascorbic Acid Concentrations Selectively Kill Cancer Cells: Action as a Pro-drug to Deliver Hydrogen Peroxide to Tissues. *Proc. Natl. Acad. Sci. U. S. A.* 102, 13604–13609. doi:10.1073/pnas.0506390102

Chen, Q., Espey, M. G., Sun, A. Y., Lee, J. H., Krishna, M. C., Shacter, E., et al. (2007). Ascorbate in Pharmacologic Concentrations Selectively Generates Ascorbate Radical and Hydrogen Peroxide in Extracellular Fluid *In Vivo*. *Proc. Natl. Acad. Sci. U. S. A.* 104, 8749–8754. doi:10.1073/pnas.0702854104

Chen, Q., Espey, M. G., Sun, A. Y., Pooput, C., Kirk, K. L., Krishna, M. C., et al. (2008). Pharmacologic Doses of Ascorbate Act as a Prooxidant and Decrease Growth of Aggressive Tumor Xenografts in Mice. *Proc. Natl. Acad. Sci.* 105, 11105–11109. doi:10.1073/pnas.0804226105

Chen, Q., Polireddy, K., Chen, P., and Dong, R. (2015). The Unpaved Journey of Vitamin C in Cancer Treatment. *Can. J. Physiol. Pharmacol.* 93, 1055–1063. doi:10.1139/cjpp-2014-0509

Cheng, Z., Yuan, X., Qu, Y., Li, X., Wu, G., Li, C., et al. (2017). Bruceine D Inhibits Hepatocellular Carcinoma Growth by Targeting β-catenin/jagged1 Pathways. *Cancer Lett.* 403, 195–205. doi:10.1016/j.canlet.2017.06.014

Chung, T. L., Brena, R. M., Kolle, G., Grimmond, S. M., Berman, B. P., Laird, P. W., et al. (2010). Vitamin C Promotes Widespread yet Specific DNA Demethylation of the Epigenome in Human Embryonic Stem Cells. *Stem Cells* 28, 1848–1855. doi:10.1002/stem.493

Creagan, E. T., Moertel, C. G., O'Fallon, J. R., Schutt, A. J., O'Connell, M. J., Rubin, J., et al. (1979). Failure of High-Dose Vitamin C (Ascorbic Acid) Therapy to Benefit Patients with Advanced Cancer. A Controlled Trial. *N. Engl. J. Med.* 301, 687–690. doi:10.1056/NEJM198603063141003

De Sousa e Melo, F., Kurtova, A. V., Harnoss, J. M., Kljavin, N., Hoeck, J. D., Hung, J., et al. (2017). A Distinct Role for Lgr5 + Stem Cells in Primary and Metastatic colon Cancer. *Nature* 543, 676–680. doi:10.1038/nature21713

Du, J., Martin, S. M., Levine, M., Wagner, B. A., Buettner, G. R., Wang, S. H., et al. (2010). Mechanisms of Ascorbate-Induced Cytotoxicity in Pancreatic Cancer. *Clin. Cancer Res.* 16, 509–520. doi:10.1158/1078-0432.CCR-09-1713

Esteban, M. A., Wang, T., Qin, B., Yang, J., Qin, D., Cai, J., et al. (2010). Vitamin C Enhances the Generation of Mouse and Human Induced Pluripotent Stem Cells. *Cell Stem Cell* 6, 71–79. doi:10.1016/j.stem.2009.12.001

Feng, X., and Lu, M. (2017). Expression of Sex-Determining Region Y-Box Protein 2 in Breast Cancer and its Clinical Significance. *Saudi Med. J.* 38, 685–690. doi:10.15537/smj.2017.7.19372

Hoffer, L. J., Levine, M., Assouline, S., Melnychuk, D., Padayatty, S. J., Rosadiuk, K., et al. (2008). Phase I Clinical Trial of i.V. Ascorbic Acid in Advanced Malignancy. *Ann. Oncol.* 19, 1969–1974. doi:10.1093/annonc/mdn377

Lennicke, C., Rahn, J., Lichtenfels, R., Wessjohann, L. A., and Seliger, B. (2015). Hydrogen Peroxide - Production, Fate and Role in Redox Signaling of Tumor Cells. *Cell Commun. Signal.* 13, 1–19. doi:10.1186/s12964-015-0118-6

Li, Y., Rogoff, H. a., Keates, S., Gao, Y., Murikipudi, S., Mikule, K., et al. (2015). Suppression of Cancer Relapse and Metastasis by Inhibiting Cancer Stemness. *Proc. Natl. Acad. Sci. U. S. A.* 112, 1839–1844. doi:10.1073/pnas.1424171112

Liu, S., Li, N., Yu, X., Xiao, X., Cheng, K., Hu, J., et al. (2013). Expression of Intercellular Adhesion Molecule 1 by Hepatocellular Carcinoma Stem Cells and Circulating Tumor Cells. *Gastroenterology* 144, 1031–1041. doi:10.1053/j.gastro.2013.01.046

Luk, S. T., Ng, K., Zhou, L., Tong, M., Wong, T., Yu, H., et al. (2019). Deficiency in Embryonic Stem Cell Marker REX1 Activates MKK6-dependent P38 MAPK Signaling to Drive Hepatocarcinogenesis. *Hepatology* 72, 183–197. doi:10.1002/hep.31020

Luo, Z. L., Cheng, S. Q., Shi, J., Zhang, H. L., Zhang, C. Z., Chen, H. Y., et al. (2015). A Splicing Variant of Merlin Promotes Metastasis in Hepatocellular Carcinoma. *Nat. Commun.* 6, 8457. doi:10.1038/ncomms9457

Lv, C., Li, F., Li, X., Tian, Y., Zhang, Y., Sheng, X., et al. (2017). MiR-31 Promotes Mammary Stem Cell Expansion and Breast Tumorigenesis by Suppressing Wnt Signaling Antagonists. *Nat. Commun.* 8, 1036–1053. doi:10.1038/s41467-017-01059-5

Lv, H., Wang, C., Fang, T., Li, T., Lv, G., Han, Q., et al. (2018). Vitamin C Preferentially Kills Cancer Stem Cells in Hepatocellular Carcinoma via SVCT-2. *Npj Precis. Oncol* 2, 1. doi:10.1038/s41698-017-0044-8

Ma, C., Han, M., Heinrich, B., Fu, Q., Zhang, Q., Sandhu, M., et al. (2018). Gut Microbiome–Mediated Bile Acid Metabolism Regulates Liver Cancer via NKT Cells. *Science* 360, eaan5931. doi:10.1126/science.aan5931

Ma, S., Chan, K. W., Hu, L., Lee, T. K. W., Wo, J. Y. H., Ng, I. O. L., et al. (2007). Identification and Characterization of Tumorigenic Liver Cancer Stem/Progenitor Cells. *Gastroenterology* 132, 2542–2556. doi:10.1053/j.gastro.2007.04.025

Ma, S., Tang, K. H., Chan, Y. P., Lee, T. K., Kwan, P. S., Castilho, A., et al. (2010). MiR-130b Promotes CD133+ Liver Tumor-Initiating Cell Growth and Self-Renewal via Tumor Protein 53-Induced Nuclear Protein 1. *Cell Stem Cell* 7, 694–707. doi:10.1016/j.stem.2010.11.010

Maramag, C., Menon, M., Balaji, K. C., Reddy, P. G., and Laxmanan, S. (1997). Effect of Vitamin C on Prostate Cancer Cells *In Vitro*: Effect on Cell Number, Viability, and DNA Synthesis. *Prostate* 32, 188–195. doi:10.1002/(SICI)1097-0045(19970801)32:3<188:AID-PROS5>3.0.CO;2-H

Moertel, C., and Fleming, T. (1985). High-dose Vitamin C versus Placebo in the Treatment of Patients with Advanced Cancer Who Have Had No Prior Chemotherapy: a Randomized Double-Blind Comparison. *New Engl. J.* 312, 137–141. doi:10.1056/NEJM198501173120301

Morgan, T. R., Mandayam, S., and Jamal, M. M. (2004). Alcohol and Hepatocellular Carcinoma. *Gastroenterology* 127, 87–96. doi:10.1053/j.gastro.2004.09.020

Naito, S., von Eschenbach, A. C., and Fidler, I. J. (1986). Growth and Metastasis of Tumor Cells Isolated from a Human Renal Cell Carcinoma Implanted into Different Organs of Nude Mice. *Cancer Res.* 46, 4109–4115.

Padayatty, S. J., Riordan, H. D., Hewitt, S. M., Katz, A., Hoffer, L. J., and Levine, M. (2006). Intravenously Administered Vitamin C as Cancer Therapy: Three Cases. *Cmaj* 174, 937–942. doi:10.1503/cmaj.050346

Pang, R., Law, W. L., Chu, A. C. Y., Poon, J. T., Lam, C. S. C., Chow, A. K. M., et al. (2010). A Subpopulation of CD26 + Cancer Stem Cells with Metastatic Capacity in Human Colorectal Cancer. *Cell Stem Cell* 6, 603–615. doi:10.1016/j.stem.2010.04.001

Ponti, D., Costa, A., Zaffaroni, N., Pratesi, G., Petrangolini, G., Coradini, D., et al. (2005). Isolation and *In Vitro* Propagation of Tumorigenic Breast Cancer Cells with Stem/Progenitor Cell Properties. *Cancer Res.* 65, 5506–5511. doi:10.1158/0008-5472.CAN-05-0626

Raymond, Y. C. F., Glenda, C. S. L., and Meng, L. K. (2016). Effects of High Doses of Vitamin C on Cancer Patients in Singapore: Nine Cases. *Integr. Cancer Ther.* 15, 197–204. doi:10.1177/1534735415622010

Re, F., Zanetti, A., Sironi, M., Polentarutti, N., Lanfrancone, L., Dejana, E., et al. (1994). Inhibition of anchorage-dependent Cell Spreading Triggers Apoptosis in Cultured Human Endothelial Cells. *J. Cel Biol.* 127, 537–546. doi:10.1083/jcb.127.2.537

Reczek, C. R., and Chandel, N. S. (2015). Revisiting Vitamin C and Cancer. *Science* 350, 1317–1318. doi:10.1126/science.aad8671

Schoenfeld, J. D., Sibenaller, Z. A., Mapuskar, K. A., Wagner, B. A., Cramer-Morales, K. L., Furqan, M., et al. (2017). O2− and H2O2-Mediated Disruption of Fe Metabolism Causes the Differential Susceptibility of NSCLC and GBM Cancer Cells to Pharmacological Ascorbate. *Cancer Cell* 31, 487–500. doi:10.1016/j.ccell.2017.02.018

Tang, K. H., Ma, S., Lee, T. K., Chan, Y. P., Kwan, P. S., Tong, C. M., et al. (2012). CD133 + Liver Tumor-Initiating Cells Promote Tumor Angiogenesis, Growth, and Self-Renewal through neurotensin/interleukin-8/CXCL1 Signaling. *Hepatology* 55, 807–820. doi:10.1002/hep.24739

Todaro, M., Gaggianesi, M., Catalano, V., Benfante, A., Iovino, F., Biffoni, M., et al. (2014). CD44v6 Is a Marker of Constitutive and Reprogrammed Cancer Stem Cells Driving colon Cancer Metastasis. *Cell Stem Cell* 14, 342–356. doi:10.1016/j.stem.2014.01.009

Verrax, J., and Calderon, P. B. (2009). Pharmacologic Concentrations of Ascorbate Are Achieved by Parenteral Administration and Exhibit Antitumoral Effects. *Free Radic. Biol. Med.* 47, 32–40. doi:10.1016/j.freeradbiomed.2009.02.016

Wang, T., Chen, K., Zeng, X., Yang, J., Wu, Y., Shi, X., et al. (2011). The Histone Demethylases Jhdm1a/1b Enhance Somatic Cell Reprogramming in a Vitamin-C-dependent Manner. *Cell Stem Cell* 9, 575–587. doi:10.1016/j.stem.2011.10.005

Weina, K., and Utikal, J. (2014). SOX2 and Cancer: Current Research and its Implications in the Clinic. *Clin. Transl. Med.* 3, 19. doi:10.1186/2001-1326-3-19

Wu, G., Zhu, L., Yuan, X., Chen, H., Xiong, R., Zhang, S., et al. (2017). Britanin Ameliorates Cerebral Ischemia-Reperfusion Injury by Inducing the Nrf2 Protective Pathway. *Antioxid. Redox Signal* 27, 754–768. doi:10.1089/ars.2016.6885

Wu, H., Wu, Y., Ai, Z., Yang, L., Gao, Y., Du, J., et al. (2014). Vitamin C Enhances Nanog Expression via Activation of the JAK/STAT Signaling Pathway. *Stem Cells* 32, 166–176. doi:10.1002/stem.1523

Wylie, B. J., Singh, M. P., Coull, B. A., Quinn, A., Yeboah-, K., Sabin, L., et al. (2015). Single-cell Analysis Reveals a Stem-Cell Program in Human Metastatic Breast Cancer Cells. *Nature* 526, 131–135. doi:10.1038/nature15260

Yang, Z. F., Ho, D. W., Ng, M. N., Lau, C. K., Yu, W. C., Ngai, P., et al. (2008). Significance of CD90+ Cancer Stem Cells in Human Liver Cancer. *Cancer Cell* 13, 153–166. doi:10.1016/j.ccr.2008.01.013

Yuan, D., Chen, L., Li, M., Xia, H., Zhang, Y., Chen, T., et al. (2015). Isolation and Characterization of Circulating Tumor Cells from Human Gastric Cancer Patients. *J. Cancer Res. Clin. Oncol.* 141, 647–660. doi:10.1007/s00432-014-1814-0

Yun, J., Mullarky, E., Lu, C., Kaitlyn, N., Kavalier, A., Rivera, K., et al. (2015). Vitamin C Selectively Kills KRAS and BRAF Mutant Colorectal Cancer Cells by Targeting GAPDH. *Science* 350, 1391–1396. doi:10.1126/science.aaa5004

Zhang, Y., Guan, D., Shi, J., Gao, H., Li, J., Zhao, J., et al. (2013). All-trans Retinoic Acid Potentiates the Chemotherapeutic Effect of Cisplatin by Inducing Differentiation of Tumor Initiating Cells in Liver Cancer. *J. Hepatol.* 59, 1255–1263. doi:10.1016/j.jhep.2013.07.009

Zhu, Z., Hao, X., Yan, M., Yao, M., Ge, C., Gu, J., et al. (2010). Cancer Stem/progenitor Cells Are Highly Enriched in CD133+CD44+ Population in Hepatocellular Carcinoma. *Int. J. Cancer* 126, 2067–2078. doi:10.1002/ijc.24868

Conflict of Interest: The authors declare that the research was conducted in the absence of any commercial or financial relationships that could be construed as a potential conflict of interest.

Publisher's Note: All claims expressed in this article are solely those of the authors and do not necessarily represent those of their affiliated organizations, or those of the publisher, the editors and the reviewers. Any product that may be evaluated in this article, or claim that may be made by its manufacturer, is not guaranteed or endorsed by the publisher.

Copyright © 2021 Wan, Zhou, Fu, Li, Zeng, Xu, Lv and Jin. This is an open-access article distributed under the terms of the Creative Commons Attribution License (CC BY). The use, distribution or reproduction in other forums is permitted, provided the original author(s) and the copyright owner(s) are credited and that the original publication in this journal is cited, in accordance with accepted academic practice. No use, distribution or reproduction is permitted which does not comply with these terms.

frontiers in Pharmacology

ORIGINAL RESEARCH
published: 06 September 2021
doi: 10.3389/fphar.2021.735731

Protective Effect of Pyxinol, One Active Ingredient of *Lichenes* on Cisplatin-Induced Nephrotoxicity via Ameliorating DNA Damage Response

Yanting Yang[1], *Xiuhong Zhu*[2], *Guohua Yu*[1,3]* *and Jinbo Ma*[1]*

[1]Department of Clinical Medicine, Binzhou Medical University, Yantai, China, [2]People's Hospital of Jimo District, Qingdao, China, [3]Department of Pathology, Affiliated Yantai Yuhuangding Hospital, Medical College of Qingdao University, Yantai, China

OPEN ACCESS

Edited by:
Xin Luan,
Shanghai University of Traditional Chinese Medicine, China

Reviewed by:
Yaswanth Kuthati,
Cathay General Hospital, Taiwan
Ye Yang,
Nanjing University of Chinese Medicine, China
Jing Jin,
Chinese Academy of Medical Sciences and Peking Union Medical College, China

***Correspondence:**
Guohua Yu
ygh0536@163.com
Jinbo Ma
jinbomayt@163.com

Specialty section:
This article was submitted to Pharmacology of Anti-Cancer Drugs, a section of the journal Frontiers in Pharmacology

Received: 03 July 2021
Accepted: 23 August 2021
Published: 06 September 2021

Citation:
Yang Y, Zhu X, Yu G and Ma J (2021) Protective Effect of Pyxinol, One Active Ingredient of Lichenes on Cisplatin-Induced Nephrotoxicity via Ameliorating DNA Damage Response. Front. Pharmacol. 12:735731. doi: 10.3389/fphar.2021.735731

Background: Cisplatin is a valuable chemotherapeutic agent against malignant tumors. However, the clinical use of cisplatin is limited by its side effects such as renal injury. Pyxinol is an active constituent of *Lichenes* and its effects on cisplatin-induced nephrotoxicity is currently unknown. This study aims to examine the potential protective effects of pyxinol on cisplatin-induced renal injury and explore the underlying mechanisms.

Methods: *In vivo* rat model of cisplatin-induced nephrotoxicity was induced by intraperitoneal (i.p) administration of cisplatin. The blood urea nitrogen and creatinine levels were measured and renal histological analysis was conducted to evaluate the renal function; The TUNEL staining, western blotting and real-time PCR assays were conducted to examine related molecular changes. Finally, the *in vivo* anti-tumor efficacy was examined in the xenograft tumor model using nude mice.

Results: Pretreatment with pyxinol attenuated cisplatin-induced increase in blood urea nitrogen, creatinine and urinary protein excretion and the magnitude of injury in the renal tubules. Pyxinol ameliorated the activation of p53 *via* attenuating the DNA damage response, which then attenuated the tubular cell apoptosis. Finally, pyxinol could potentiate the *in vivo* anti-tumor efficacy of cisplatin against the xenograft tumor of cervical cancer cells in nude mice.

Conclusions: Combining pyxinol with cisplatin could alleviate cisplatin-induced renal injury without decreasing its therapeutic efficacy, which might represent a beneficial adjunct therapy for cisplatin-based chemotherapeutic regimens in the clinic.

Keywords: cisplatin, nephrotoxicity, pyxino, DNA damage response, p53, apoptosis

Abbreviations: BUN, blood urea nitrogen; CMCS, carboxymethycellulose sodium; Cre, creatinine; HE, hematoxylin and eosin; i.p, intraperitoneal; m-CPBA, meta-chloroperbenzoic acid; PPD, 20 (S)-protopanaxadiol; RT-PCR, real-time polymerase chain reaction; TUNEL, terminal deoxynucleotidyl transferase-mediated dUTP nick end-labeling.

BACKGROUND

Cisplatin (cis-diamminedichloroplatinum II) is one of the most efficacious chemotherapeutic agents to treat solid tumors, such as non-small cell lung cancer, cervical cancer, testicular cancer (Pabla and Dong, 2008; Wang and Lippard, 2005) However, its use comes with several significant side effects. One of the major side effects of cisplatin use is nephrotoxicity, which is dose-dependent and as such limits its clinical use in certain patients (Arany and Safirstein, 2003; Pabla and Dong, 2008) Although current standard preventive protocols such as the hydration or diuretic therapies could decrease cisplatin-induced renal injury in many patients, a certain percentage of patients still suffer from cisplatin-induced nephrotoxicity (Perazella and Moeckel, 2010). Development of an effective adjunct therapy to curb or reduce cisplatin-induced nephrotoxicity could be a clinically beneficial approach to maximize its anti-tumor utility while reducing its side effects.

Despite decades of research attempting to uncover the molecular mechanisms attributable to cisplatin-induced nephrotoxicity, the exact mechanisms remain elusive. One of the increasingly recognized mechanisms underlying cisplatin-induced acute renal injury is DNA damage response (Yan et al., 2016; Zhu et al., 2015). Cisplatin is converted into a highly reactive molecule following aquation, which could bind to DNA and form intra-strand and inter-strand cross-linking. The cross-linking impedes DNA replication and/or transcription, causing DNA damage and ultimate cell apoptosis (Karasawa and Steyger, 2015; Zhu et al., 2015). As the guardian of genome, P53 would be immediately activated when the DNA damage occurred, to initiate the repair and/or the suicide program *via* regulating its downstream targets, such as *puma, bax*, *p21* (Jiang et al., 2004; Jiang et al., 2006; Man; Wei et al., 2007). Therefore, compounds that can attenuate the apoptosis *via* reducing DNA damage response could be potentially useful for the prevention and treatment of cisplatin-induced nephrotoxicity. Indeed, compounds such as lovastatin (Kruger et al., 2016) have been reported to demonstrate protective effect against cisplatin-induced nephrotoxicity *via* decreasing DNA damage response and attenuating tubular apoptosis.

Natural products provide rich resources for discovery of drug candidates or leading compounds (Pan and Pan, 2010). Indeed, natural products-derived bioactive ingredients have been tested against common side effects of chemotherapeutic agents, such as the cardiomyopathy of doxorubicin and the nephrotoxicity of cisplatin, and several compounds with novel structures have been identified using well-validated models. For example, F11 (Wang et al., 2014) and Rh2 (Wang et al., 2012), two novel pseudoginsenosides, are reportedly able to attenuate cisplatin-induced nephrotoxicity and doxorubicin-induced cardiotoxicity, respectively. Mahadev Rao reported that cystone, a constituent from Himalaya herbals, showed protective effects against cisplatin-induced renal toxicity *via* inhibiting the lipid peroxidation (Mahadev Rao, 1998). Recently, we find that pyxinol, an active constituent of *Lichenes*, demonstrates strong protective activity against myocardial ischemia-reperfusion injury *in vitro* and *in vivo* (Sahu et al., 2011). As part of our continuing effort to discover novel protective agents against cisplatin-induced renal injury, here we report that pyxinol (**Figure 1**) was able to attenuate cisplatin-induced nephrotoxicity without affecting its anti-tumor efficacy.

MATERIALS AND METHODS

Drugs and Chemicals

Pyxinol was prepared from 20 (S)-protopanaxadiol (PPD) as previously described (Bi et al., 2011). Briefly, after deriving 3, 12-diacetyl PPD with DMAP and Ac2O in pyridine, it was epoxidized with meta-chloroperbenzoic acid (m-CPBA) in dichloromethane to give 3, 12-diacetyl pyxinols. Then, 3, 12-diacetyl pyxinols was degraded with KOH in methanol to afford pyxinol (35% in three steps).

For *in vivo* study, pyxinol was dissolved in 0.5% carboxymethycellulose sodium (CMCS), and cisplatin (Qilu Pharm, Jinan, China) was dissolved in 0.9% sodium chloride solutions at proposed doses.

Animals

Male Sprague-Dawley rats and female nude mice were provided by the Institute of Laboratory Animal Science, Chinese Academy of Medical Sciences (Beijing, China). All the animals were raised in a the room with room temperature of 21–22°C and the relative humidity of 60–65% under 12/12 h light cycle. Animals had free access to standard rodent chow and water. All of the experimental protocols were approved by

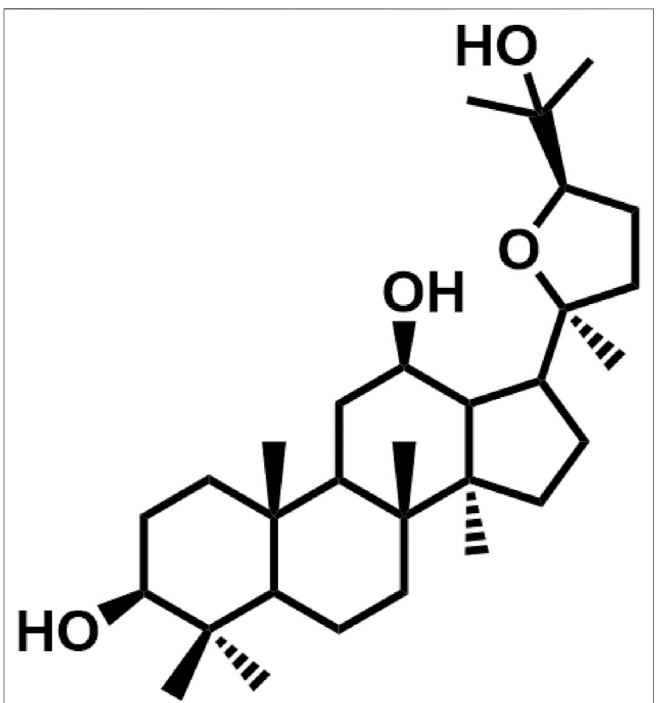


FIGURE 1 | Chemical structure of pyxinol.

TABLE 1 | Effects of pyxinol on the antitumor activity of cisplatin in nude mice.

Group	Dosage (mg/kg)	Number	Body Weight (g)		Tumor Weight (g)	Inhibitor Rate (100%)
		Initial/End	Initial	End		
Control	0	5/5	21.8 ± 1.0	22.4 ± 1.4	0.81 ± 0.26	
Cisplatin	3	5/5	23.1 ± 1.1	22.0 ± 1.1	0.36 ± 0.17[a]	56.2
Pyxinol	10	5/5	23.5 ± 1.2	24.2 ± 1.2	0.47 ± 0.56	41.7
Cisplatin plus Pyxinol	3 plus 10	5/5	21.8 ± 1.2	21.6 ± 1.2	0.20 ± 0.13[a]	75.2

Data are expressed as means ± SD (n = 5).
[a]$p < 0.05$: *compared with the control group.*

the Experimental Animal Research Committee of Yantai University and conducted strictly following the Animal [Scientific Procedures] Act 1986).

In vivo Rat Model of Cisplatin-induced Nephrotoxicity

Animals were randomly assigned into four groups. Nephrotoxicity was induced by intraperitoneal (i.p) administration of cisplatin dissolved in normal saline at the dose of 6.0 mg/kg body weight according to published literature (Wang et al., 2014). Animals in control group were given daily oral gavage of vehicle (0.5% carboxymethycellulose sodium (CMCS)) for 5 days. Animals in the pyxinol-treated group was given daily oral gavage of pyxinol dissolved in 0.5% (CMCS) at a dose of 10 mg/kg for 5 days. Right before the first pyxinol dosing, animals were treated with cisplatin dissolved in saline at a dose of 6 mg/kg only once. Five days after cisplatin treatment, rats were put into metabolic cages, and the 24-h urine samples were collected. Animals were euthanized thereafter. The kidney was harvested, weighed and calculated as percentage of the body weight. Blood and kidney samples were collected for the following analyses.

Biochemical Analysis

Plasma creatinine and blood urea nitrogen levels as well as 24-h urinary protein excretion were measured as indicators of renal function. Briefly, the blood was firstly collected in heparinized tubes, and the plasma was separated by centrifugation. Plasma creatinine and blood urea nitrogen levels were detected using commercial test kits following published protocol (Yang et al., 2018; Humanes et al., 2012). The protein concentration of the urine samples were analyzed using Pierce™ BCA protein assay kit (Thermo Fisher Scientific, United States).

Histological Analysis

Kidneys were isolated and fixed in 4% paraformaldehyde solution in PBS and then embedded in paraffin. Thereafter, tissue sections were performed for hematoxylin and eosin (HE) staining, in which the histopathological examination was conducted by a pathologist who was blind to the treatments following our published 4- point scale (Wang et al., 2014; Domitrovic et al., 2013): 0 = no damage, 1 = 0–20%, 2 = 20%–50%, 3 = 50–70%, and 4 = more than 70%. The mean score was calculated by counting at least 10 different fields for each sample.

Western Blot Assay

Kidney tissue was lysed using RAPI buffer, and the supernatants were used for western blot assay according to published literature (Yang et al., 2018). Briefly, total proteins (30–60 μg) were separated in a 10–12% SDS-polyacrylamide gel for different target proteins, and then transferred onto a PVDF membrane. After blocking with 5% BSA, the membranes were incubated with p53, p-p53 (Ser-15), p-γH2ax, p21 puma, and bax antibodies, followed by incubation with peroxidase-conjugated goat anti-mouse IgG antibody (1:2000) for 2 h. Bands were visualized using the ECL-plus western blotting detection system.

Terminal Deoxynucleotidyl Transferase dUTP Nick End Labeling (TUNEL)

The tubular cell apoptosis was detected with TUNEL staining using an apoptosis detection kit (*in situ* apoptosis detection kit) according to published protocol (Wang et al., 2010; Wang et al., 2011). Briefly, tissue sections (4 μm) were dewaxed and hydrated, and then permeabilized. Thereafter, the samples were incubated with 100 μl of reaction mixture containing the labeling enzyme and the TMR green labeled-dUTP at 37°C for 1 h in the moisture box. After extensive washing, the tissues were counterstained with DAPI and observed under a confocal fluorescence microscope, and the ratio of positive cells (the number of green cells divided by the number of the blue cells) was calculated for 10 different fields for each sample.

Real-time Polymerase Chain Reaction (RT-PCR)

Total RNA of the tissues was prepared using TRIzol (Invitrogen, United States) as previously described (Wang et al., 2011). After reverse transcription using a first-strand cDNA synthesis kit (Fermentas, United States), the cDNA was subjected to RT-PCR assays using the ABI 7500 RT-PCR System. Primer sequences were as follows:

P21, F: 5′-CTGGTGATGTCCGACCTGTTC-3′, R: 5′-CTG CTCAGTGGCGAAGTCAAA-3′; *Bax,* F: 5′-GATCAGCTCGGG

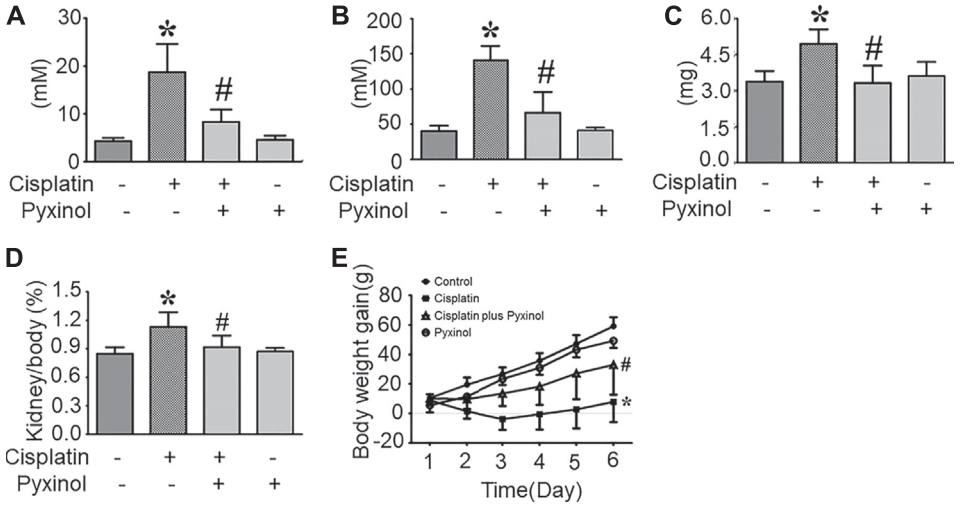


FIGURE 2 | Effects of pyxinol on the levels of BUN and Cre in cisplatin-treated rats. **(A)** plasma BUN level; **(B)** plasma Cre level; **(C)** Total 24-h urinary protein; **(D)** Kidney body ratio; **(E)** Body weight gain. All data were expressed as means ± SD (n = 6). *p < 0.05, compared with the control group; #p < 0.05, compared with the cisplatin group.

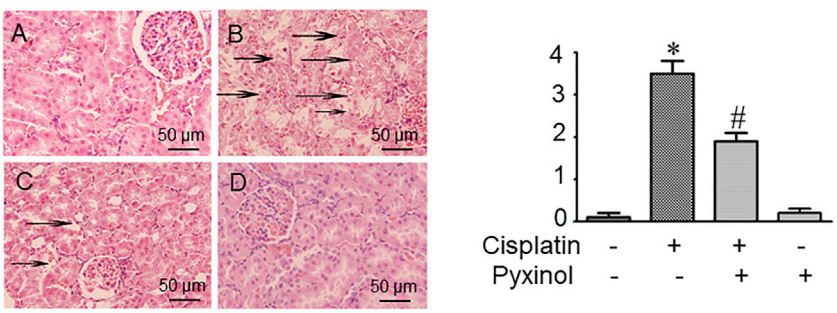


FIGURE 3 | Effects of pyxinol on the kidney histopathological damage induced by cisplatin in rats. Left: **(A)** Control group; **(B)** Cisplatin group; **(C)** Cisplatin plus pyxinol group; **(D)** Pyxinol group. The damage levels of the renal tubules were blindly assessed based on a 4- point scale, and the scores were expressed as means ± SD (n = 6). Representative histopathological changes were indicated using the black arrows: cell necrosis, cell swelling and vacuolization (×400 magnifications). Right: quantification of the histological damage. *p < 0.05, compared with the control group; #p < 0.05, compared with the cisplatin group.

CACTTTAG-3′, R: 5′-TGTTTGCTGATGGCAACTTC-3′; *Puma*, F: 5′-AGTGCGCCTTCACTTTGG-3′, R: 5′-CAGGAGGCTAGT GGTCAGGT-3′; ***β-actin***, F: 5′-CCCAGCACAATGAAGATCAA GATCAT-3′, R: 5′-ATCTGCTGGAAGGTGGACA GCGA-3′.

Xenograft Tumor Model

Female babc/nu mice were used to establish the xenograft tumor model of human cervical cancer (Hela) as previously reported (Lv et al., 2017, Carvalho Rodrigues et al., 2013). Briefly, the tumors were implanted at the dorsum after isolated from donor animals, which were established by injecting the HeLa cells. When the xenograft tumors reached an average volume of 100–300 mm^3, the animals were randomly assigned into four groups (n = 5): *1*) CMC group; *2*) 10 mg/kg pyxinol group; *3*) 3 mg/kg cisplatin group; *4*) 10 mg/kg pyxinol plus 3 mg/kg cisplatin group. The tumors were measured twice a week, and the relative tumor volume was calculated by the following formula: relative volume= $(width)^2$ plus length/2. At the end of the experiment, the animals were sacrificed, and xenograft tumors were weighed and used to calculate the percentage of inhibition.

Data Analyses and Statistics

The results were presented as mean ± SD. Comparisons between more than two groups were performed by analysis of variance (one way ANOVA) followed by Student t test. P < 0.05 was considered statistically significant unless indicated otherwise.

RESULTS

Pyxinol Attenuated Cisplatin-induced Renal Injury

Five days after cisplatin administration, the plasma BUN (blood urea nitrogen) and Cre levels, as well as 24-h urinary protein

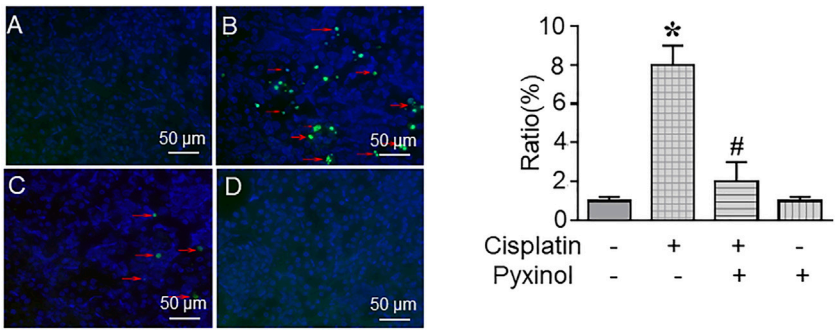


FIGURE 4 | Effects of pyxinol on cisplatin-induced renal tubular cell apoptosis. The paraffin kidney section was stained with TUNEL staining, and the slides were observed using a confocal fluorescence microscope, in which at least 2,000 tubule cells (blue cells) were randomly examined to quantify the ratio of apoptotic cells (green cells). **(A)** Control group; **(B)** Cisplatin group; **(C)** Cisplatin plus pyxinol group; **(D)** Pyxinol group. The apoptotic cells were indicated with red arrows. *$p < 0.05$, compared with the control group; #$p < 0.05$, compared with the cisplatin group.

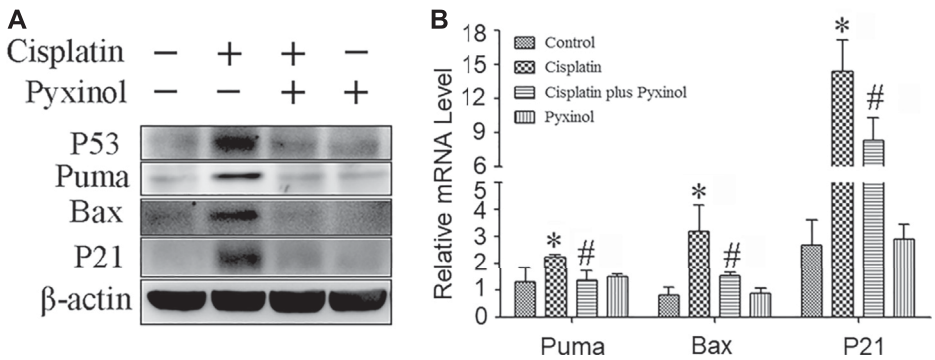


FIGURE 5 | Effects of pyxinol on the expression of P53 and its transcription activity induced by cisplatin in rats. **(A)** Representative western blotting band; **(B)** quantification of mRNA levels as measured by real-time PCR. *$p < 0.05$, compared with the control group; #$p < 0.05$, compared with the cisplatin group.

excretion, were significantly increased (**Figure 2**, $p < 0.05$, compared with the control group). 5 mg/kg pyxinol treatment significantly attenuated the increase of all the above biomarkers ($p < 0.05$, compared with the cisplatin group). Similar findings were observed on the body weight gain and the kidney/body ratio. Pyxinol alone showed no significant effect on any of the parameters.

Pyxinol Ameliorated Cisplatin-induced Histopathological Changes

In histopathological examination, typical acute structural damages in the renal tubules, such as cell necrosis, cell swelling and vacuolization, and desquamation of epithelial cells, were observed in cisplatin-treated rats (**Figure 3B**). The histological injury score was significantly higher as compared to control animals ($p < 0.05$). Five days of pyxinol treatment significantly alleviated the histopathological injury (**Figure 3C** compared to **Figure 3B**), along with reduced injury score ($p < 0.05$, compared with cisplatin group).

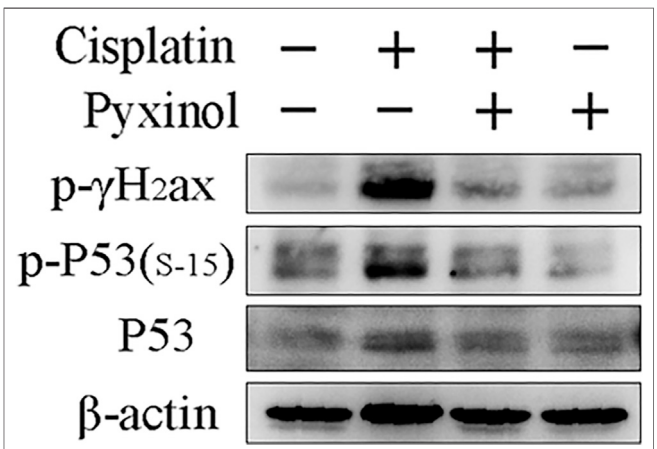


FIGURE 6 | Effects of pyxinol on the phosphorylation of P53 and γH2ax induced by cisplatin in rats. Total protein expressions were detected using western blotting assay.

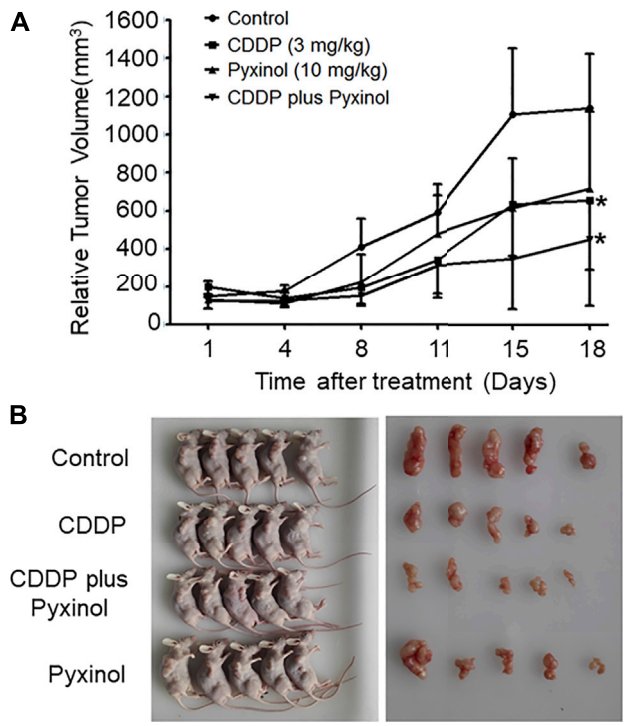


FIGURE 7 | Effects of pyxinol on the *in vivo* anti-tumor activity of cisplatin in nude mice. The balb/c nu mice were transplanted with human cervical cancer xenograft tumors (Hela), and treated as indicated. After treatment, the relative tumor volume was measured. **(A)**: Tumor volume. All data are expressed as means ± SD ($n = 5$).*$p < 0.05$, compared with the control group. **(B)**: Photos of the mice and tumors.

Pyxinol Reduced Cisplatin-induced Cell Apoptosis

The ratio of TUNEL-positive cells in kidney tissue was significantly increased in cisplatin-treated rats as compared to control rats (**Figure 4B**, $p < 0.05$). Five days of pyxinol treatment significantly attenuated the ratio and the number of apoptotic tubule cells (**Figure 4C**, $p < 0.05$, compared with the cisplatin group).

Pyxinol Attenuated Cisplatin-induced Increase of P53 Protein and its Downstream Molecules

To examine the potential molecular mechanisms, the protein and mRNA levels of p53 and its downstream molecules including p21, puma and bax were measured. Cisplatin treatment significantly increased the expression levels of both the proteins and mRNAs of the above signaling molecules (**Figure 5**), which were attenuated by pyxinol treatment. No significant changes were observed with these molecules in rats treated with pyxinol alone.

Pyxinol Ameliorated Cisplatin-induced DNA Damage Response

Cisplatin treatment increased the phosphorylation of p53 at serine 15, as well as the phosphorylation of γ-H2ax, two biomarkers of DNA damage (**Figure 6**). Pyxinol treatment attenuated the phosphorylation of p53 and γ-H2ax.

Pyxinol did Not Attenuate the *in vivo* Anti-tumor Efficacy of Cisplatin

To test the effect of pyxinol on the anti-tumor efficacy of cisplatin *in vivo*, the xenograft model in nude mice was established using human cervical cancer (Hela). At a dosage of 3 mg/kg, cisplatin significantly inhibited the growth of xenograft tumors (**Figure 7**, $p < 0.05$, compared with the control group; **Table 1**, $p < 0.05$, compared with the control group). Pyxinol (10 mg/kg) did not attenuate, but appeared to enhance, the anti-tumor activity of cisplatin ($p = 0.38$, compared with the cisplatin group). Pyxinol alone had no anti-tumor activity against cervical cancer *in vivo* ($p = 0.66$, compared with the control group).

DISCUSSION

Despite the well-established therapeutic efficacy against multiple solid tumors, side effects such as nephrotoxicity greatly limit the more extensive use of cisplatin in the clinic and available preventive strategies are only partially useful to reduce cisplatin-related toxicity. This reality inspires increasing research to develop adjunct therapies in the hope of finding combination therapy candidates with cisplatin to increase anti-tumor efficacy and/or reduce side effects (Arany and Safirstein, 2003; Perazella and Moeckel, 2010). In this study, we described the protective effects of a novel active constituent from *Lichenes*, pyixnol, on cisplatin-induced renal injury and examined the potential mechanisms underlying the apparent protective efficacy of pyixnol. We found that pyixnol demonstrated robust protective efficacy against cisplatin-induced renal injury as evidenced by drastically reduced BUN, creatinine and urinary protein excretion increase and the magnitude of renal tubule damage in cisplatin-treated animals. We also found that the protective effects of pyxinol were possibly achieved by attenuating the DNA damage response. Most importantly, these beneficial effects were achieved at the dose of pyxinol that did not affect the *in vivo* anti-tumor efficacy of cisplatin. Together, these results report for the first time the beneficial effects of pyxinol against cisplatin-induced nephrotoxicity and support the potential clinical utility of pyxinol as an adjunct to add to cisplatin chemotherapy.

It is well-established that the renal damage caused by cisplatin is at least partially due to the accumulation of cisplatin in the S3 segment of the renal tubules (Cristofori et al., 2007). As a result, the activity of the glomerular filtration is decreased and the concentration of plasma BUN and Cre is increased. Indeed, the animals in this study demonstrated significantly increased plasma BUN and CRE levels and content of albumen in the urine 5 days after a single injection of 6 mg/kg cisplatin, suggesting glomerulus damage. Pyxinol treatment significantly ameliorated all the above biomarkers. Similar findings were observed in the histopathological examinations, in which the representative changes such as cell necrosis, the desquamation of epithelial

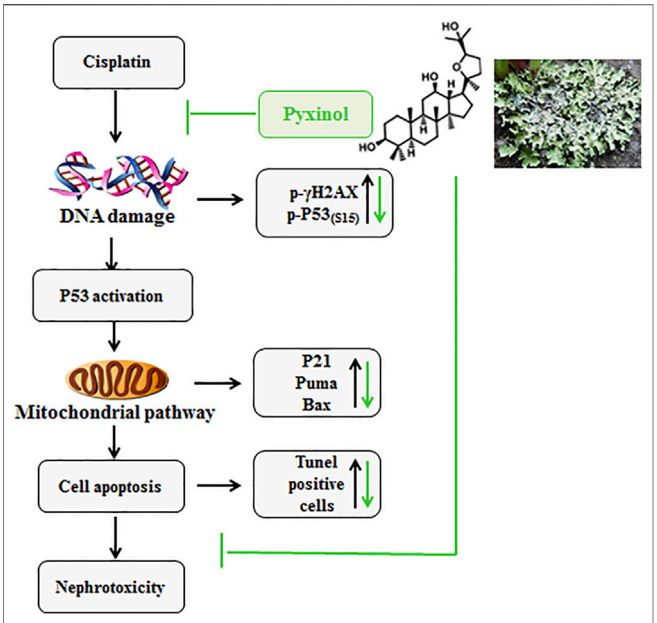


FIGURE 8 | The working model.

cells around proximal tubule, were all greatly improved after pyxinol treatment. These results provide strong evidence for the protective efficacy of pyxinol in cisplatin-induce renal injury.

One underlying mechanism of cisplatin-induced nephrotoxicity is cisplatin-provoked cell apoptosis, in which the oxidative stress and DNA damage-induced p53 activation acts as an initiator (Jiang et al., 2006; Yang et al., 2014). Consistent with the literature (Galgamuwa et al., 2016; Wang et al., 2014), we found that the renal tubule cells showed higher apoptosis ratio after treatment with cisplatin. The ratio of apoptotic cells was significantly decreased by pyxinol treatment, suggesting the protective effect of pyxinol against cisplatin-induced cell apoptosis in renal tubule. Interestingly, unlike our previous findings (Wang et al., 2014), pyxinol had no significant effect on cisplatin-induced oxidative stress in the kidney (data not shown). Similarly, pyxinol treatment also significantly attenuated cisplatin-evoked increase in the expression of p53 and its target genes such as p21, puma, bax as well as their protein levels, which are well-known players in the regulation of cisplatin-induced renal apoptosis (Yang et al., 2014). These data clearly showed that pyxinol could ameliorate the expression of p53 and suppressed its transcription after cisplatin exposure in the kidney.

There is clear evidence that DNA damage response is a crucial mechanism contributing to cisplatin-induced acute kidney injury. Following aquation, cisplatin could bind to DNA and form cross-linking in the kidney tubular cells, which causes replication stress and DNA damage (Wang and Lippard, 2005; Karasawa Steyger, 2015; Zhu et al., 2015). As the "sensors" of DNA lesions, ATM and ATR kinases phosphorylate p53 and γ-H2AX protein, two important biomarkers for the DNA damage, and initiate DNA repair, or induce cell cycle arrest and cell apoptosis. As expected, we found that cisplatin induced the phosphorylation of P53 (Ser-15) and γ-H2AX in the kidney tissue and pyxinol treatment attenuated such increases. These results suggest that pyxinol suppressed p53 activation was at least partially mediated *via* the decrease of cisplatin-induced DNA damage response.

As a potential adjunct therapy candidate, one crucial prerequisite is that pyixnol should not affect the anti-tumor efficacy of cisplatin. This possibility was tested using the xenograft tumor model in nude mice, and the results clearly showed that pyxinol did not affect the anti-tumor activity of cisplatin *in vivo*. A schematic model was proposed (**Figure 8**) to show the process and mechanism how pyixnol protects against cisplatin-induced renal injury.

CONCLUSION

Our study showed for the first time that pyxinol, one active constituents of *Lichenes*, was protective against cisplatin-induced nephrotoxicity through inhibiting tubular cell apoptosis *via* deceasing the DNA damage response. Importantly, pyxinol did not attenuate the anti-tumor efficacy of cisplatin, and therefore might be a novel potential adjunct therapy for cisplatin-based chemotherapeutic regimen in the clinic.

DATA AVAILABILITY STATEMENT

The data for the current study are available from the corresponding author on reasonable request.

ETHICS STATEMENT

The animal study was reviewed and approved by The Experimental Animal Research Committee of Binzhou Medical College.

AUTHOR CONTRIBUTIONS

Conception and design the experiments: JM and GY. Conducted the experiments: YY, JM, and GY, Data analysis and interpretation: XZ, YY, GY, and JM. Manuscript drafting: JM and YY. Final approval and critical revision: JM and GY. All authors read and approved the final manuscript.

FUNDING

This study was supported by National Natural Science Foundation of China (81903664) and the Technology Development Program Projects in Medicine and Health of Shandong Province (2017WS691).

SUPPLEMENTARY MATERIAL

The Supplementary Material for this article can be found online at: https://www.frontiersin.org/articles/10.3389/fphar.2021.735731/full#supplementary-material

REFERENCES

Arany, I., and Safirstein, R. L. (2003). Cisplatin Nephrotoxicity. *Semin. Nephrol.* 23, 460–464. doi:10.1016/s0270-9295(03)00089-5

Bi, Y., Tian, J., Wang, L., Zhao, F., Zhang, J., Wang, N., et al. (2011). Synthesis, Structural Determination and Protective Effects on Cultured Anoxia/reoxygen Injury Myocardiocytes of Ocotillol-type Derivatives. *J. Med. Plant Res.* 5, 2424–2429. doi:10.5897/jmpr11.713

Carvalho Rodrigues, M. A., Silva Faria, M. C., Santos, N. A., Gobe, G. C., and dos Santos, A. C. (2013). Carvedilol Efficiently Protects Kidneys Without Affecting the Antitumor Efficacy of Cisplatin in Mice. *Chem. Biol. Interact.* 206, 90–99. doi:10.1016/j.cbi.2013.08.015

Cristofori, P., Zanetti, E., Fregona, D., Piaia, A., and Trevisan, A. (2007). Renal Proximal Tubule Segment-specific Nephrotoxicity: An Overview on Biomarkers and Histopathology. *Toxicol. Pathol.* 35, 270–275. doi:10.1080/01926230601187430

Domitrovic, R., Cvijanovic, O., Pugel, E. P., Zagorac, G. B., Mahmutefendić, H., and Škoda, M. (2013). Luteolin Ameliorates Cisplatin-Induced Nephrotoxicity in Mice Through Inhibition of Platinum Accumulation, Inflammation and Apoptosis in the Kidney. *Toxicology* 310, 115–123. doi:10.1016/j.tox.2013.05.015

Galgamuwa, R., Hardy, K., Dahlstrom, J. E., Blackburn, A. C., Wium, E., Rooke, M., et al. (2016). Dichloroacetate Prevents Cisplatin-Induced Nephrotoxicity Without Compromising Cisplatin Anticancer Properties. *J. Am. Soc. Nephrol.* 27, 3331–3344. doi:10.1681/ASN.2015070827

Humanes, B., Lazaro, A., Camano, S., Moreno-Gordaliza, E., Lazaro, J. A., Blanco-Codesido, M., et al. (2012). Cilastatin Protects Against Cisplatin-Induced Nephrotoxicity Without Compromising its Anticancer Efficiency in Rats. *Kidney Int.* 82, 652–663. doi:10.1038/ki.2012.199

Jiang, M., Wei, Q., Wang, J., Du, Q., Yu, J., Zhang, L., et al. (2006). Regulation of PUMA-Alpha by P53 in Cisplatin-Induced Renal Cell Apoptosis. *Oncogene* 25, 4056–4066. doi:10.1038/sj.onc.1209440

Jiang, M., Yi, X., Hsu, S., Wang, C. Y., and Dong, Z. (2004). Role of P53 in Cisplatin-Induced Tubular Cell Apoptosis: Dependence on P53 Transcriptional Activity. *Am. J. Physiol. Ren. Physiol.* 287, F1140–F1147. doi:10.1152/ajprenal.00262.2004

Karasawa, T., and Steyger, P. S. (2015). An Integrated View of Cisplatin-Induced Nephrotoxicity and Ototoxicity. *Toxicol. Lett.* 237, 219–227. doi:10.1016/j.toxlet.2015.06.012

Krüger, K., Ziegler, V., Hartmann, C., Henninger, C., Thomale, J., Schupp, N., et al. (2016). Lovastatin Prevents Cisplatin-Induced Activation of Pro-apoptotic DNA Damage Response (DDR) of Renal Tubular Epithelial Cells. *Toxicol. Appl. Pharmacol.* 292, 103–114. doi:10.1016/j.taap.2015.12.023

Lv, G., Sun, D., Zhang, J., Xie, X., Wu, X., Fang, W., et al. (2017). Lx2-32c, A Novel Semi-synthetic Taxane, Exerts Antitumor Activity Against Prostate Cancer Cells In Vitro and In Vivo. *Acta Pharm. Sin B.* 7, 52–58. doi:10.1016/j.apsb.2016.06.005

Pabla, N., and Dong, Z. (2008). Cisplatin Nephrotoxicity: Mechanisms and Renoprotective Strategies. *Kidney Int.* 73, 994–1007. doi:10.1038/sj.ki.5002786

Pan, S. Y., Pan, S., Yu, Z.-L., Ma, D.-L., Chen, S.-B., Fong, W.-F., et al. (2010). New Perspectives on Innovative Drug Discovery: An Overview. *J. Pharm. Pharm. Sci.* 13, 450–471. doi:10.18433/j39w2g

Perazella, M. A., and Moeckel, G. W. (2010). Nephrotoxicity from Chemotherapeutic Agents: Clinical Manifestations, Pathobiology, and Prevention/therapy. *Semin. Nephrol.* 30, 570–581. doi:10.1016/j.semnephrol.2010.09.005

Rao, M., and Rao, M. N. (1998). Protective Effects of Cystone, A Polyherbal Ayurvedic Preparation, on Cisplatin-Induced Renal Toxicity in Rats. *J. Ethnopharmacol.* 62, 1–6. doi:10.1016/s0378-8741(98)00003-8

Sahu, B. D., Rentam, K. K., Putcha, U. K., Kuncha, M., Vegi, G. M., and Sistla, R. (2011). Carnosic Acid Attenuates Renal Injury in an Experimental Model of Rat Cisplatin-Induced Nephrotoxicity. *Food Chem. Toxicol.* 49, 3090–3097. doi:10.1016/j.fct.2011.08.018

Wang, D., and Lippard, S. J. (2005). Cellular Processing of Platinum Anticancer Drugs. *Nat. Rev. Drug Discov.* 4, 307–320. doi:10.1038/nrd1691

Wang, H., Kong, L., Zhang, J., Yu, G., Lv, G., Zhang, F., et al. (2014). The Pseudoginsenoside F11 Ameliorates Cisplatin-Induced Nephrotoxicity Without Compromising its Anti-tumor Activity In Vivo. *Sci. Rep.* 4, 4986. doi:10.1038/srep04986

Wang, H., Ma, X., Ren, S., Buolamwini, J. K., and Yan, C. (2011). A Small-Molecule Inhibitor of MDMX Activates P53 and Induces Apoptosis. *Mol. Cancer Ther.* 10, 69–79. doi:10.1158/1535-7163.MCT-10-0581

Wang, H., Mo, P., Ren, S., and Yan, C. (2010). Activating Transcription Factor 3 Activates P53 by Preventing E6-Associated Protein from Binding to E6. *J. Biol. Chem.* 285, 13201–13210. doi:10.1074/jbc.M109.058669

Wang, H., Yu, P., Gou, H., Zhang, J., Zhu, M., Wang, Z. H., et al. (2012). Cardioprotective Effects of 20(S)-Ginsenoside Rh2 Against Doxorubicin-Induced Cardiotoxicity In Vitro and In Vivo. *Evid Based. Complement. Altern. Med.* 2012, 506214. doi:10.1155/2012/506214

Wei, Q., Dong, G., Yang, T., Megyesi, J., Price, P. M., and Dong, Z. (2007). Activation and Involvement of P53 in Cisplatin-Induced Nephrotoxicity. *Am. J. Physiol. Ren. Physiol.* 293, F1282–F1291. doi:10.1152/ajprenal.00230.2007

Yan, M., Tang, C., Ma, Z., Huang, S., and Dong, Z. (2016). DNA Damage Response in Nephrotoxic and Ischemic Kidney Injury. *Toxicol. Appl. Pharmacol.* 313, 104–108. doi:10.1016/j.taap.2016.10.022

Yang, Y., Guan, D., Lei, L., Lu, J., Liu, J. Q., Yang, G., et al. (2018). H6, a Novel Hederagenin Derivative, Reverses Multidrug Resistance In Vitro and In Vivo. *Toxicol. Appl. Pharmacol.* 341, 98–105. doi:10.1016/j.taap.2018.01.015

Yang, Y., Liu, H., Liu, F., and Dong, Z. (2014). Mitochondrial Dysregulation and protection in Cisplatin Nephrotoxicity. *Arch. Toxicol.* 88, 1249–1256. doi:10.1007/s00204-014-1239-1

Zhu, S., Pabla, N., Tang, C., He, L., and Dong, Z. (2015). DNA Damage Response in Cisplatin-Induced Nephrotoxicity. *Arch. Toxicol.* 89, 2197–2205. doi:10.1007/s00204-015-1633-3

Conflict of Interest: The authors declare that the research was conducted in the absence of any commercial or financial relationships that could be construed as a potential conflict of interest.

Publisher's Note: All claims expressed in this article are solely those of the authors and do not necessarily represent those of their affiliated organizations, or those of the publisher, the editors and the reviewers. Any product that may be evaluated in this article, or claim that may be made by its manufacturer, is not guaranteed or endorsed by the publisher.

Copyright © 2021 Yang, Zhu, Yu and Ma. This is an open-access article distributed under the terms of the Creative Commons Attribution License (CC BY). The use, distribution or reproduction in other forums is permitted, provided the original author(s) and the copyright owner(s) are credited and that the original publication in this journal is cited, in accordance with accepted academic practice. No use, distribution or reproduction is permitted which does not comply with these terms.

frontiers in Pharmacology

ORIGINAL RESEARCH
published: 23 September 2021
doi: 10.3389/fphar.2021.758219

Total Flavonoids of Litchi Seed Attenuate Prostate Cancer Progression *Via* Inhibiting AKT/mTOR and NF-kB Signaling Pathways

Ming Chang[1,2,3†], Dan Zhu[4†], Yanjiang Chen[5†], Weiquan Zhang[1,4], Xi Liu[4], Xiao-Lan Li[1,4], Zhiping Cheng[4], Zhiheng Su[4], Jian Zhang[1,2,3], Yi Lu[1,2,3*] and Hongwei Guo[1,4*]*

[1]Key Laboratory of Longevity and Aging-Related Diseases of Chinese Ministry of Education, Center for Translational Medicine, Guangxi Medical University, Nanning, China, [2]School of Medicine, Southern University of Science and Technology, Shenzhen, China, [3]Guangdong Provincial Key Laboratory of Cell Microenvironment and Disease Research, Shenzhen, China, [4]Guangxi Key Laboratory of Bioactive Molecules Research and Evaluation, College of Pharmacy, Guangxi Medical University, Nanning, China, [5]Department of Surgery, University of Melbourne, Parkville, VIC, Australia

OPEN ACCESS

Edited by:
Hong Zhang,
Shanghai University of Traditional Chinese Medicine, China

Reviewed by:
Zhe-Sheng Chen,
St. John's University, United States
Xiuping Chen,
University of Macau, China

***Correspondence:**
Jian Zhang
zhangjian@sustech.edu.cn
Yi Lu
luy3@sustech.edu.cn
Hongwei Guo
hongweiguo@gxmu.edu.cn

[†]These authors have contributed equally to this work

Specialty section:
This article was submitted to Ethnopharmacology, a section of the journal Frontiers in Pharmacology

Received: 13 August 2021
Accepted: 13 September 2021
Published: 23 September 2021

Citation:
Chang M, Zhu D, Chen Y, Zhang W, Liu X, Li X-L, Cheng Z, Su Z, Zhang J, Lu Y and Guo H (2021) Total Flavonoids of Litchi Seed Attenuate Prostate Cancer Progression Via Inhibiting AKT/mTOR and NF-kB Signaling Pathways. Front. Pharmacol. 12:758219. doi: 10.3389/fphar.2021.758219

Litchi seeds have been traditionally used in Chinese herbal formula for urologic neoplasms including prostate cancer (PCa). However, the effective components of Litchi seeds and the mechanisms of their actions on PCa cell growth and metastasis remain unclear. In this study, we investigated the effects and molecular mechanisms of the Total Flavonoid of Litchi Seed (TFLS) in PCa PC3 and DU145 cell lines. We found that TFLS significantly inhibited the PCa cell proliferation, induced apoptosis, and prevented cell migration and invasion. Furthermore, we observed that TFLS upregulated the expression of epithelial biomarker E-cadherin and downregulated mesenchymal biomarker Vimentin. TFLS also increased the expression of cleaved-PRAP and Bax, and decreased the expression of Bcl-2 in both PC3 and DU145 cells. Besides, TFLS inhibited AKT signaling pathway by reducing the phosphorylation of AKT and activities of downstream signal transducers including mTOR, IκBα and NF-kB. Finally, TFLS treated mice exhibited a significant decrease in tumor size without toxicity in major organs *in vivo*. These results indicated that TFLS could suppress PCa cell growth *in vivo* and inhibit PCa cell proliferation and metastasis *in vitro* through induction of apoptosis and phenotypic reversal of EMT, which may be achieved by inhibiting the AKT/mTOR and NF-κB signaling pathways. Taken together, our data provide new insights into the role of TFLS as a novel potent anti-cancer agent for the treatment of PCa.

Keywords: total flavonoids of litchi seed, prostate cancer, apoptosis, proliferation, metastasis, Akt

INTRODUCTION

Prostate cancer is one of the most commonly diagnosed malignant tumors in men with high mortality, which causes a severe global health burden (Oliver et al., 1998; Karimi Roshan et al., 2019; Siegel et al., 2019). In China, the incidence of PCa has increased rapidly due to population aging, and PCa has the tendency to become the most common malignant tumor in the near future (Chen W. et al., 2016). Although patients with local PCa have a relatively high 5-year survival rate, most of the patients are diagnosed with bone metastasis, which almost inevitably causes deaths (Nieder et al., 2010). Currently, standard treatments for PCa include androgen antagonists, chemotherapy,

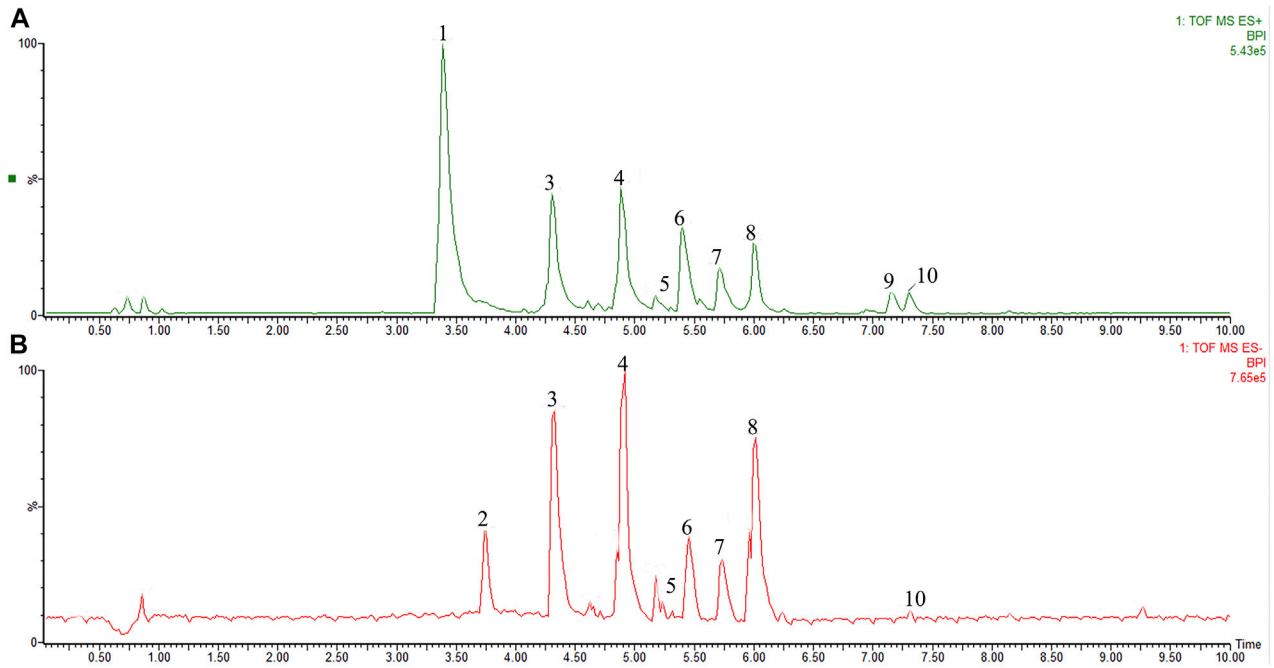


FIGURE 1 | The characterization of TFLS chemical profile. **(A)** positive ion mode; **(B)** negative ion mode; 1) Unknown ($C_{11}H_{18}N_3O$); 2) 2,5-Dihydroxybenzoic acid; 3) 3-O-p-Coumaroylquinic acid; 4) Epicatechin; 5) Rutin; 6) Proanthocyanidin A1; 7) Proanthocyanidin A2; 8) Litchioside. **(C)** 9) Berberine; 10) (-)-Pinocembrin7-O-Neohesperidoside).

radiotherapy and immunotherapy. These treatments are often accompanied with side effects that affect the general health and quality of life of patients (Farolfi et al., 2019). Hence, there is an urgent need to develop novel therapeutics that could effectively targeting PCa with low toxicity and few side effects.

In the past few years, natural herbal extracts have been of great research interests due to their drug specificity and limited side effects (Sharifi-Rad et al., 2019). As a supplement to conventional anticancer treatments, herbal extracts can alleviate clinical symptoms, prolong patient's survival and improve the quality of life of patients (Koga et al., 2017). Herbal extracts can also attenuate chemotherapy-related side effects, including nausea and vomiting. Therefore, herbal extracts could be promising therapeutic agents (Inoue et al., 2017).

Litchi chinensis Sonn (Litchi) belongs to the *Sapindaceae* family. Its seeds have been traditionally used in China for treating male urogenital diseases, including prostate cancer, prostatitis, benign prostatic hyperplasia and orchitis etc. (Cao et al., 2020). Accumulating pharmacological evidence suggested that the extracts of Litchi seeds have anticancer effects and can inhibit metastatic tumor growth (Hsu et al., 2012; Emanuele et al., 2018). We previously showed that the n-butyl alcohol extract of Litchi seeds demonstrated anti-prostate cancer properties both *in vitro* and *in vivo*, and flavonoid compounds were the most abundant chemical components (Guo et al., 2017). In this study, we examined the effects and mechanisms of Total Flavonoids of Litchi Seed (TFLS) on PCa. This study will provide the rationale for the clinical application of Litchi seeds for the treatment of PCa.

METHODS

Material and Chemical Reagents

The fetal bovine serum (FBS) was purchased from Gibco (Grand Island, NY, United States). BCA protein assay kit (No. P0011) and One Step TUNEL Apoptosis Assay Kit (No. C1089) were purchased from Beyotime (Shanghai, China). Transwell assay inserts (No. 354483) were purchased from Corning (Corning New York, NY, United States). Enhanced Chemiluminescence (ECL) was purchased from Thermofisher (Waltham, Massachusetts, United States). 1% crystal violet solution (No. V5265) was purchased from Sigma (St. Louis, MO, United States). Anti-rabbit IgG, HRP-linked Antibody, primary antibodies against E-cadherin, Vimentin, p-AMPKα, p-p44/42 MAPK, p-MEK1/2, p-AKT, AKT, p-mTOR, mTOR, p-IκBα, IκBα, p-NF-κB p65, NF-κB p65 and GAPDH were purchased from Cell Signaling Technology (Danvers, MA, United States). Primary antibody against Wnt 3a was purchased from Abcam (Cambridge, United Kingdom). The catalogue numbers of antibodies were shown in **Supplementary Table S1**. FITC Annexin V Apoptosis Detection Kit (No. 556547) and DNA Reagent Kit (No. 340242) were purchased from BD Biosciences (San Diego, CA, United States). Cell Titer 96® AQueous One Solution Cell Proliferation Assay (MTS, No. G3581) was purchased from Promega (Madison, WI, United States). The macroporous resin (No. M0032) was purchased from Solarbio Life Science (Beijing, China).

TABLE 1 | Characterization and identification of compounds in TFLS.

No.	Name	Molecular formula	Adduction		t_R/min		m/z	
					Positive	Negative	Positive	Negative
1	Unknown	$C_{11}H_{18}N_3O$		–	3.39	–	208.1438→149.0697, 131.0596, 103.0641	–
2	2,5-Dihydroxybenzoic acid	$C_7H_6O_4$	–	$[2M–H]^-$	–	3.733	–	307.0475→153.0208, 109.0298
3	3-O-*p*-Coumaroylquinic acid	$C_{16}H_{18}O_8$	$[M+H]^+$	$[2M–H]^-$	4.307	4.32	339.1146→321.0978, 293.0988, 147.0546	675.1933→337.0941, 191.0568, 173.0466, 163.0411
4	Epicatechin	$C_{15}H_{14}O_6$	$[M+H]^+$	$[M–H]^-$	4.88	4.92	291.0964→273.0862, 139.0494, 123.0542	289.0717→245.0764,179.0349,137.0243,125.0253,109.0304
5	Rutin	$C_{27}H_{30}O_{16}$	$[M+H]^+$	$[M–H]^-$	5.317	5.300	611.1637→465.1053, 303.0589	609.1454→301.0344
6	Proanthocyanidin A1	$C_{30}H_{24}O_{12}$	$[M+H]^+$	$[M–H]^-$	5.440	5.439	577.1346→559.1263, 425.0929, 287.0648	575.1179→557.1047, 423.0716, 271.0624, 137.0239, 125.0239
7	Proanthocyanidin A2	$C_{30}H_{24}O_{12}$	$[M+H]^+$	$[M–H]^-$	5.716	5.725	577.1343→425.0920, 287.0649	575.1193→423.0721, 285.0404, 271.0617, 137.0248, 125.0248
8	Litchioside C	$C_{19}H_{34}O_9$	$[M+Na]^+$	$[M–H]^-$	5.996	6.013	429.2141→407.2322, 245.1842, 241.1525, 227.1741	405.2130→243.1562, 239.1295, 225.1505
9	Berberine	$C_{20}H_{18}NO_4$	$[M]^+$	–	7.189	–	336.1302→321.1073, 320.0993, 292.1054	–
10	(-)-Pinocembrin7-O-Neohesperidoside	$C_{27}H_{32}O_{13}$	$[M+H]^+$	$[M–H]^-$	7.300	7.317	565.2033→257.0913, 239.0899, 153.0294, 105.0805, 103.0621, 101.0676	563.1774→255.0670

Cell Lines and Culture Conditions

PC3, DU145 and $PC3^{-luc}$ cells were obtained from the Center for Translational Medicine, Guangxi Medical University (Nanning, China) and cultured in RPMI 1640 containing 10% fetal bovine serum, 100 U/ml penicillin and 100 μg/ml streptomycin at 37°C and 5% CO_2.

Animal

Specific pathogen-free Kunming mice (20 ± 2 g, 4–5 weeks old) and nude male mice (18 ± 2 g, 5–6 weeks old) were purchased from Hunan SJA Laboratory Animal Co., Ltd. (Changsha, China). The mice were maintained in a ventilated room at an ambient temperature of 22 ± 2°C with a 12 h diurnal light cycle. The mice were given ad libitum access to food and water and allowed to acclimatize for 1 week before the experiments. All procedures were approved by the Institutional Animal Ethics Committee of Guangxi Medical University (IAEC, Nos. 201810146, 201903029).

Extraction and Composition Analysis of Total Flavonoid of Litchi Seed

The Litchi seeds (No. 181001) were purchased from Nanning Shengyuantang Chinese herbal medicine Co., Ltd. (Nanning, China). The voucher specimens (No. 20170713) were identified by Prof. Lilan Qin (Guangxi University of Chinese Medicine) and deposited at the College of Pharmacy of Guangxi Medical University. The seeds were cleaned with distilled water, dried and smashed into powder. Then the TFLS was isolated and purified as described previously (Zhang et al., 2021), and also shown in **Supplementary Figure S1**. The yield and purity of total flavonoids extract were 3.33 and 42.61% respectively. Then the chemical composition of TFLS was analyzed by ultra-performance liquid chromatography/quadrupole time-of-flight mass spectrometry (UPLC-Q-TOF/MS). The TFLS powder (1 g) was taken in a 10 ml volumetric flask, filled up to the final volume with acetonitrile: water (60:40). The sample concentration was 0.1 g/ml as filtered by a syringe filter (0.22 μm) and stored at 4°C until UPLC-Q-TOF/MS analysis.

Chromatographic analysis was performed on an Acquity UPLC HSS T3 column (100 mm × 2.1 mm, 1.8 μm) by Waters ACQUITY UPLC system (Waters Corp. Milford, MA, United States). The columns were maintained at 30°C and eluted at a flow rate of 0.30 ml/min. The mobile phase was composed of water containing 0.1% formic acid (A) and acetonitrile (B). The gradient program was optimized as follows: 0–1.5 min, 5% B; 1.5–5 min, 5% B to 30% B; 5–13 min, 30% B to 50% B; 13–14 min, 50% B to 5% B, 14–15 min, washing with 5% B. The injection volume was 5 μl.

The mass spectrometry with an electrospray ionization source operating in both positive and negative ion mode was performed on Waters definition accurate mass quadrupole time-of-flight Xevo G2-XS mass spectrometer (Waters Corp., Manchester, United Kingdom). The parameters were set as below: capillary voltage, 3 kV; sample and extraction cone voltage, 40 and 4.0 V; desolvation gas rate and temperature, 600 L/h and 300°C; source temperature, 100 C. Leucine-enkephalin was used as the lock

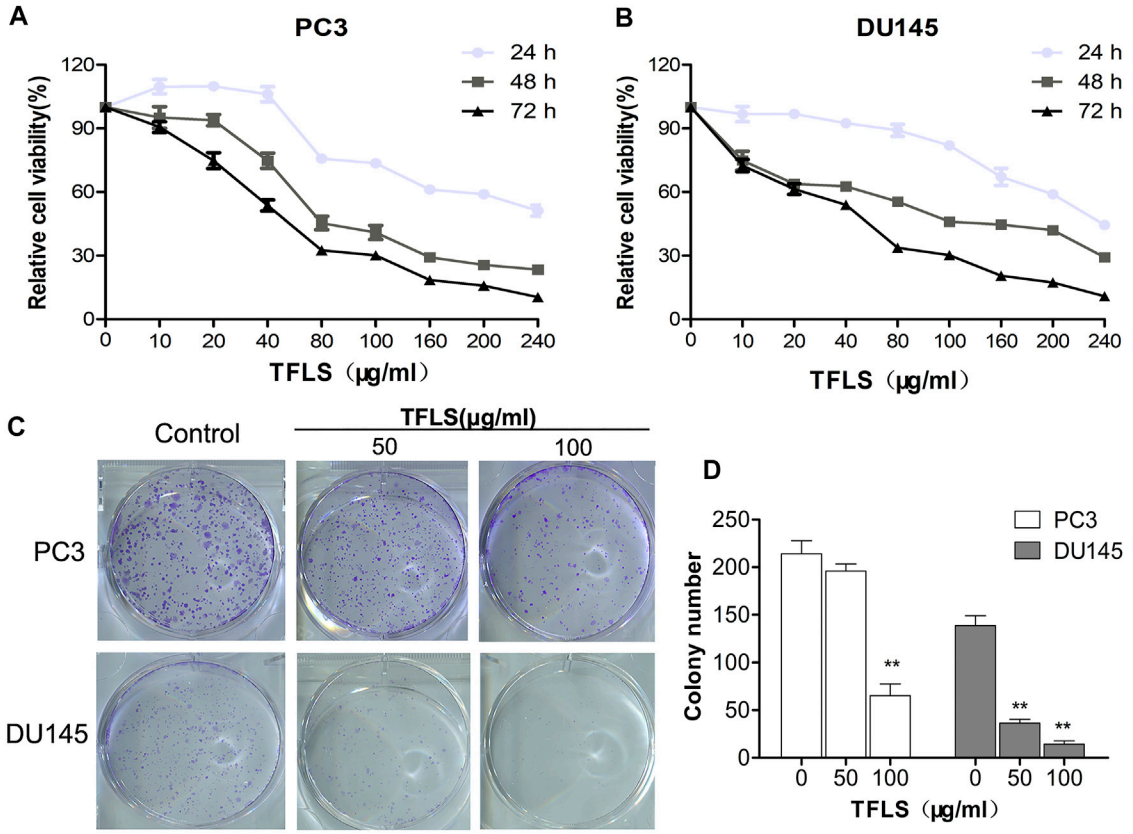


FIGURE 2 | TFLS inhibited the proliferation of PCa cells. **(A,B)** PC3 and DU145 cells were treated with different concentrations of TFLS (0–240 μg/ml) for 24, 48 and 72 h, and cell viability was detected by the MTS assay. **(C)** The colony formation of PC3 and DU145 cells treated with TFLS for 8 days. **(D)** Quantification of the number of colonies of PCa cells. The number of colonies was expressed by mean ± SEM, compared with the control group: $^{*}p < 0.05$; $^{**}p < 0.01$.

TABLE 2 | The IC_{50} value of TFLS on PCa cells.

PCa cells	IC_{50} (μg/ml)		
	24 h	48 h	72 h
PC3	245.2 ± 20.0	95.7 ± 10.6	61.5 ± 7.1
DU145	214.7 ± 15.7	84.6 ± 9.8	55.8 ± 5.1

mass in all analyses at a concentration of 400 ng/ml. Data was collected in MSE centroid mode from 50 m/z to 1,500 m/z.

Cell Proliferation Assay

Cell proliferation was assessed by MTS assay. PC3 and DU145 cells were separately seeded at 3,000 cells/well in 96-well plates and allowed to adhere overnight. Then 100 μl of RPMI-1640 complete medium containing various concentrations (0–240 μg/ml) of TFLS was added to each well and six replicates were used for each treatment concentration. After 24, 48 or 72 h, supernatant was removed and added with100 μl of RPMI-1640 medium. Then, cells were treated with 20 μl of MTS solution and incubated at 37°C for 2 h. Absorbance at 490 nm was determined by a microplate reader and relative cell viability was calculated by comparing treatment group cell viability to the control group. The half-maximal inhibitory concentration (IC_{50}) was calculated using SPSS version 20.0.

Colony Formation Assay

PCa cells (PC3, DU145) were seeded into 6-well plates at a concentration of 400 cells/well and incubated overnight, allowing cell attachment. Then cells were washed twice with phosphate-buffered saline (PBS), RPMI-1640 complete medium containing 50 or 100 μg/ml of TFLS was added to each well. Triplicates were used in each treatment group. Cell status was monitored until multiple macroscopic clones in the culture dish can be observed. Then the cells were fixed with 4% paraformaldehyde and stained with 0.025% crystal violet. After drying, the results of the experiment were imaged with a scanner, then the number of cell clones was calculated by Image J.

Cell Migration Assay

PC3 and DU145 cells were seeded into 6-well plates and allowed to grow until the cell confluence reaches >95%. Mitomycin at a concentration of 20 μg/ml was then added to the 6-well plate and incubated at 37°C for 2 h. Then a vertical wound was created using a sterile 10 μl pipette tip. Cells were treated with serum-free RPMI-1640 medium containing 50 or 100 μg/ml of TFLS. The same field at each well was imaged with a microscope (ECLIPSE Ti2, Nikon Corporation, Japan) at four time points (0, 8, 16 and 24 h) after treatments. Images were processed and analyzed using Image-Pro Plus software and the scratch areas of each

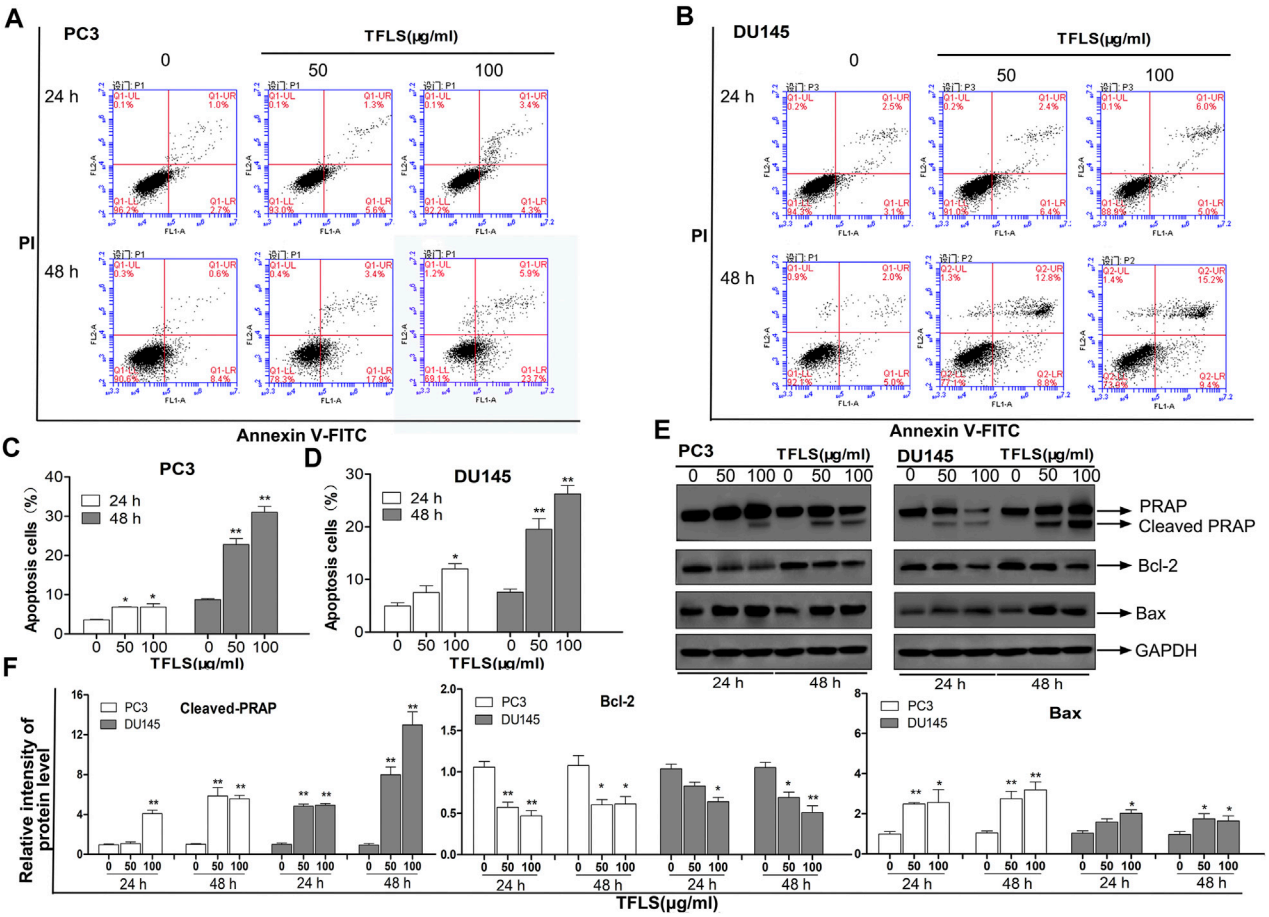


FIGURE 3 | TFLS induced apoptosis in PCa cells. PC3. **(A)** and DU145. **(B)** cells were treated with TFLS, the apoptotic cells were analyzed by Annexin V and PI double staining followed by flow cytometry analysis. The percentage of early apoptotic cells, late apoptotic cells and overall apoptotic cells were determined. Bar plot of overall apoptotic cells in PC3. **(C)** and DU145. **(D)** cells (Annexin V positive cells). **(E)** The expressions of apoptosis-related proteins in PC3 and DU145 cells were evaluated by Western blot. **(F)** Bar plots of the relative expressions of apoptosis-related proteins in PC3 and DU145 cells. Data are expressed as mean ± SEM. Compared with control group: $^{*}p < 0.05$; $^{**}p < 0.01$.

observation point at different times were measured to calculate the cell migration rate.

Cell Invasion Assay

PC3 and DU145 cells were cultured in the medium containing TFLS for 24 and 48 h before resuspension in a serum-free medium and seeding in the upper transwell chamber. The medium containing 20% FBS was added to the bottom of the lower chamber and allowed for invasion for 24 h. Later, the bottom of the chamber was rinsed with PBS, fixed with 4% paraformaldehyde and stained with 0.025% crystal violet. Then the cells were counted in five random microscopic fields (ECLIPSE Ti2, Nikon Corporation, Japan).

Flow Cytometry Analysis

Cell sample preparation and staining for Cell cycle and apoptosis analysis by flow cytometry were performed according to the manufacturer's manual. In brief, PC3 and DU145 cells were cultured in the medium containing 50 or 100 μg/ml TFLS for 24 and 48 h before the cells were harvested. For apoptosis analysis, the PCa cells were washed twice with PBS and resuspended in the Binding Buffer, then Annexin V-FITC and propidium iodide (PI) were added and incubated for 15 min in the dark. Cells were filtered after adding 400 μl 1× Binding Buffer while green fluorescence (Annexin V-FITC) and red fluorescence (PI) were detected by flow cytometry (Accuri C6, BD Biosciences, United States). In each group, 10,000 cells were analyzed. For cell cycle analysis, the harvested cells were incubated in sequence with solutions A, B, and C. After filtering the cells, the stained cells were analyzed by flow cytometry using FL-2A to score the DNA content of the cells. 10,000 cells were tested for each group.

TUNEL Assay

PC3 and DU145 cells were harvested after treating with TFLS for 24 and 48 h. Then, the harvested cells were grown on coverslips in a 12-well plate overnight. After washing with PBS, the cells were fixed and permeabilized, followed by TUNEL labeling using a One Step TUNEL Apoptosis Assay Kit. Finally, The DNA-binding dye 4′,6-diamidino-2-phenylindole (DAPI) dihydrochloride was

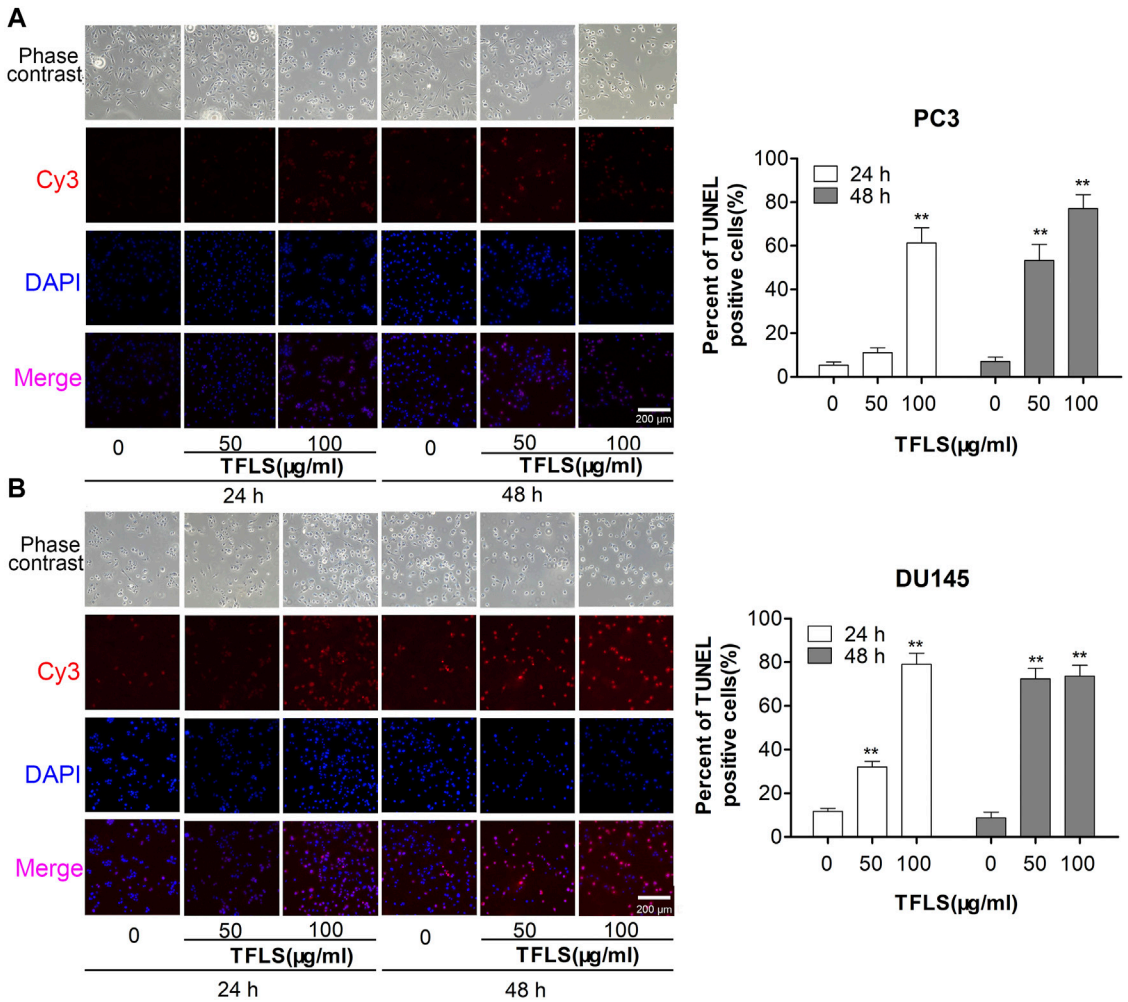


FIGURE 4 | PC3 and DU145 cells were treated with TFLS, and the apoptotic cells were detected by TUNEL assay. Representative images of apoptosis of PC3 and DU145 cells with 0, 50, 100 μg/ml of TFLS treatment for 24 or 48 h. TUNEL positive cells (red) were shown. Cell nuclei were detected by DAPI (blue). The images were obtained by a fluorescence microscope. Bar plots of the percentages of TUNEL positive cells [**(A)** PC3 cells; **(B)** DU145 cells]. Data are expressed as mean ± SEM. Compared with control group: $^{*}p < 0.05$; $^{**}p < 0.01$.

added for nuclear staining. Slides were observed under an inverted fluorescence microscope (ECLIPSE Ti2, Nikon Corporation, Japan). The cells with red fluorescence were defined as apoptotic cells.

Cell Morphology Assay

PCa cells (PC3, DU145) were inoculated into the cell culture dish and were washed twice with PBS after 24 h. RPMI-1640 complete medium containing 100 μg/ml of TFLS was then added and incubated for 48 h. After TFLS treatment, the morphology of PC3 and DU145 cells was observed using a microscope (ECLIPSE Ti2, Nikon Corporation, Japan). Representative fields were selected for taking pictures.

Western Blot Analysis

Total cell proteins were extracted and quantified by bicinchoninic acid (BCA) method. Sample proteins were denatured and analyzed by protein electrophoresis using 12% SDS polyacrylamide gel. Then sample proteins were transferred onto polyvinylidene difluoride (PVDF) membranes. After blocking, PVDF membranes were incubated with the corresponding primary antibodies (the dilution ratios of antibodies are showed in **Supplementary Table S1**) at 4°C overnight before the secondary antibody incubation. With the ECL chemiluminescence kit, the bands were visualized by chemiluminescence/fluorescence/condensation gel imaging analysis system (Champ Chemi 610 Plus, Beijing Saizhi Entrepreneur Technology Co., Ltd., China).

Immunofluorescence Analysis

After treatment with different concentrations of TFLS, PCa cells (PC3, DU145) were washed twice with PBS and seeded on coverslips in a 12-well plate overnight. After washing with PBS, the cells were fixed in 4% paraformaldehyde for 30 min. Following fixation, the

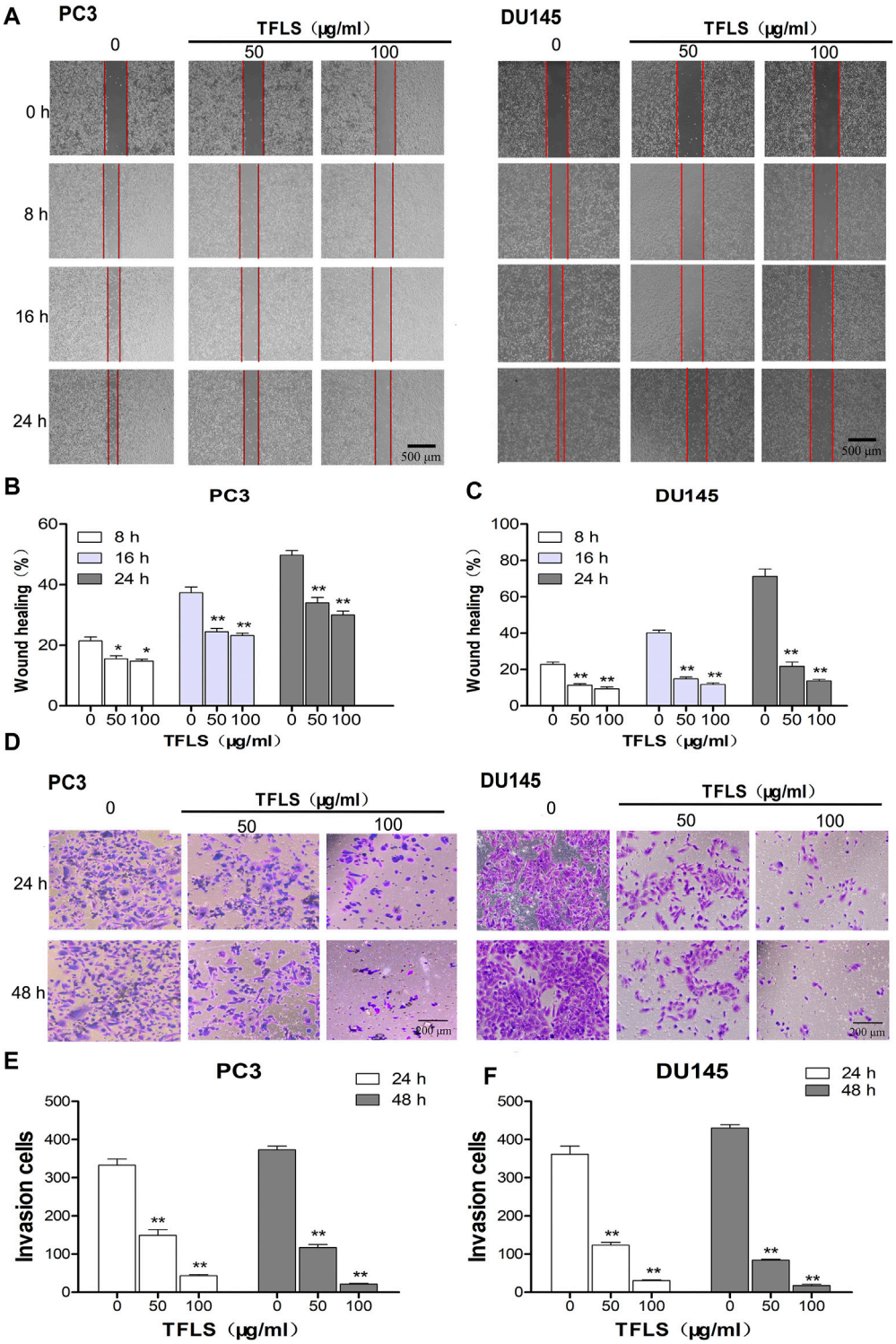


FIGURE 5 | TFLS inhibited the metastasis of PCa cells. **(A)** The effects of TFLS on the migration of PC3 and DU145 cells were analyzed using wound-healing assay. **(B,C)** Quantitative analysis of average wound healing degrees of PC3 and DU145 cells. **(D)** Invasiveness of PC3 and DU145 cells that underwent TFLS treatment determined by transwell invasion assay. **(E,F)** Invaded PC3 and DU145 cells were quantified; Data are expressed as mean ± SEM, compared with the control group: $^{*}p < 0.05$; $^{**}p < 0.01$.

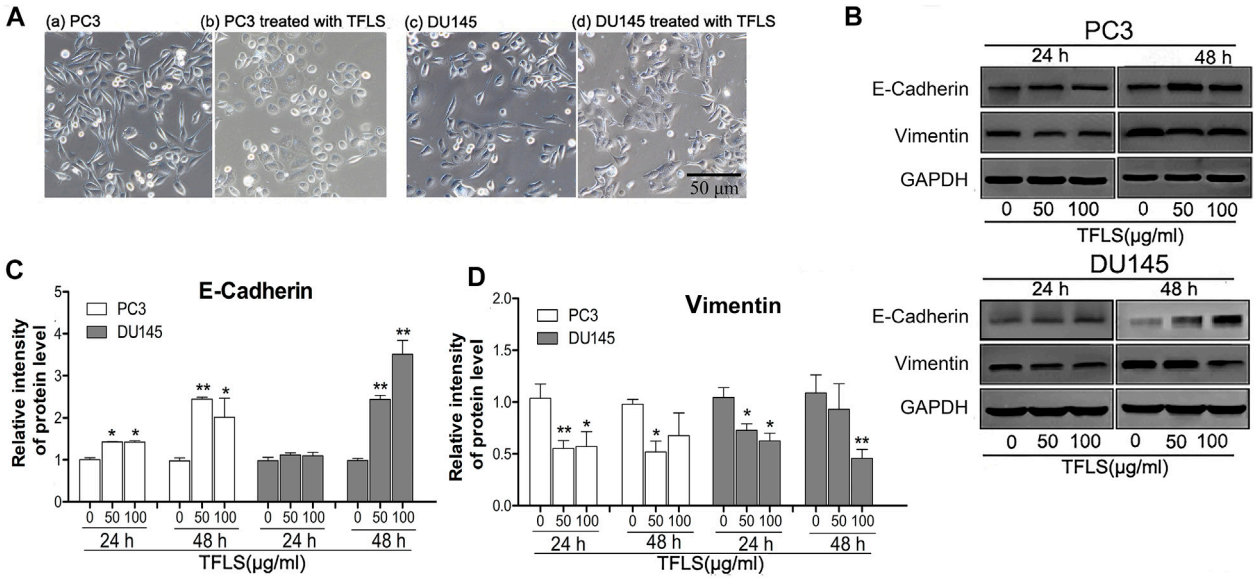


FIGURE 6 | TFLS inhibited EMT in PCa cells. **(A)** The morphology of PC3 and DU145 cells treated with or without TFLS (100 μg/ml) for 48 h (magnification 400×). **(B)** The expression of EMT-related proteins in PC3 and DU145 cells with 0, 50, 100 μg/ml of TFLS treatment for 24 or 48 h; Relative expression of E-cadherin **(C)** and Vimentin **(D)** was evaluated by ImageJ and shown as bar plots. Data are expressed as mean ± SEM, compared with the control group: $^{*}p < 0.05$; $^{**}p < 0.01$.

coverslips with PCa cells were washed with PBS three times and then permeabilized with 0.5% Triton X-100 for 15 min at room temperature. Cells were then washed with PBS three more times before incubating with primary antibodies against NF-κB p65 at 4°C overnight. The next day, the slides were stained with corresponding Alexa Fluor® 555-conjugated secondary antibodies for 2 h at room temperature. The cell nuclei were then stained with DAPI for 10 min and examined by fluorescence microscopy (Nikon Intensilight C-HGFI, Nikon Corporation, Japan).

Animal Model and Treatment

Thirty-two male nude mice were weighed, marked, and allowed for overnight fasting with free access to water. To establish a mouse PCa xenografts model, two million luciferase-expressing PC3 ($PC3^{-luc}$) cells were injected subcutaneously into each mouse's right flank (day 0). When the primary tumors had reached a mean volume of about 50 mm^3, the mice were randomly assigned to four groups based on tumor volumes and then treated. According to the clinical application of Lichi seeds in the Chinese Pharmacopoeia and the result of pilot experiment, the dosages of 40 and 80 mg/kg were selected in this experiment. The mice were orally treated with TFLS once daily. Paclitaxel (20 mg/kg), used as a reference drug for positive control, was administered intraperitoneally once per week. The body weight and tumor size of the mice were monitored every 3 days, and *in vivo* bioluminescence imaging was performed once a week by the IVIS imaging systems (Caliper Life Sciences, Hopkinton, MA, United States). At the end of experiment, mice were sacrificed with CO_2 inhalation. Then tumor volumes and tumor inhibitory rate of each group were respectively calculated using the following formula:

$$\text{Tumor inhibitory rate} = \frac{(\text{volume in control group} - \text{volume in experimental group})}{\text{volume in control group}} \times 100\%$$

$$\text{Tumor volumes (V)} = 1/2 \times (\text{length} \times \text{width}^2)$$

Acute Toxicity Test

The acute toxicity test for TFLS was conducted using the maximum-tolerated dose (MTD) method according to Technical Guidelines for Acute Toxicity Test for Traditional Chinese Medicine and Natural Medicine ([Z]GPT2-1, China Food and Drug Administration, 2005). Prior to treatment, animals were weighed, marked, and allowed for overnight fasting with free access to water. Then the mice were randomly assigned to two groups based on their individual body weight. Each group was comprised of five female and five male Kunming mice. 18 g/kg body weight TFLS was orally administered three times on the first day, with an interval of 6 h between doses. The general behavior and body weight of the mice were recorded every 24 h for 14 days. On day 14, all animals were sacrificed with CO_2 inhalation. Then the vital organs, including the heart, liver, lungs, spleen and kidney, were quickly removed and washed with ice-cold saline. The organs were then weighed, and organ weight index (OWI) was calculated using the following formula:

$$\text{Organ Weight Index (OWI)} = \frac{\text{Organ weight (g)}}{\text{Body weight of Mice on day of sacrifice (g)}} \times 100$$

Statistical Analysis

Data was presented as mean ± standard error of mean (SEM) of the biological replicates and analyzed by one-way ANOVA followed by LSD or Dunnett's T3 using SPSS

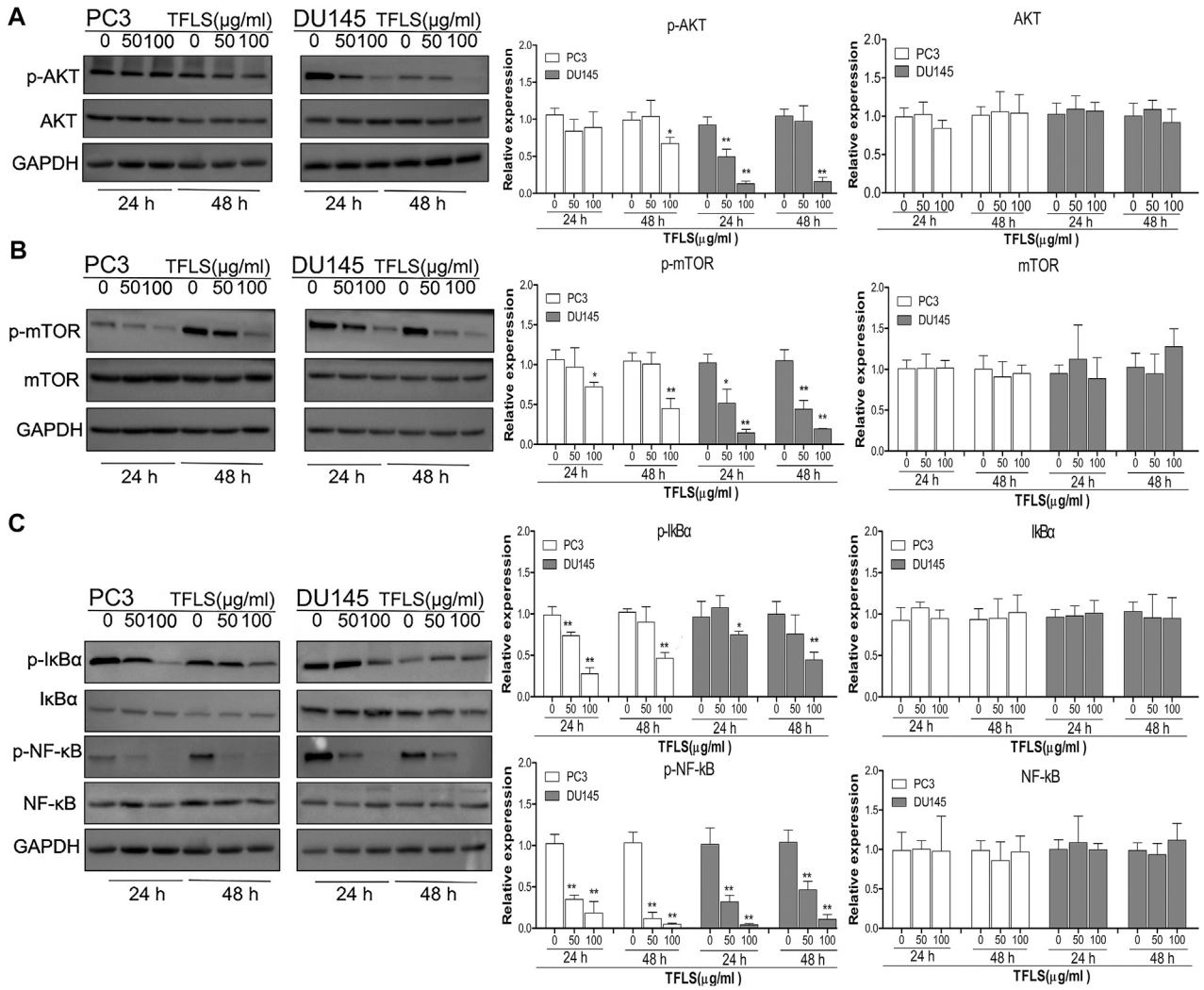


FIGURE 7 | TFLS inhibited the AKT/mTOR and NF-κB signaling pathways in PCa cells. PC3 and DU145 cells were treated with TFLS, the expression of key proteins in AKT pathway **(A)**, mTOR **(B)**, NF-κB **(C)** signaling pathways was analyzed by Western blot. GAPDH was used as a control. Data are expressed as mean ± SEM, compared with the control group: $^{*}p < 0.05$; $^{**}p < 0.01$.

version 20.0. A value of $p < 0.05$ was considered as statistically significant.

RESULTS

Analyzing the Components of Total Flavonoid of Litchi Seed

The chemical profile of the TFLS was shown in **Figure 1**. By comparing the m/z values in the databases such as METLIN, Pubchem, Massbank and published literature data, nine components in the TFLS were identified, including 2,5-Dihydroxybenzoic acid, 3-O-p-Coumaroylquinic acid, Epicatechin, Rutin, Proanthocyanidin A1, Proanthocyanidin A2, Litchioside C, Berberine, (-)-Pinocembrin7-O-Neohesperidoside. The detailed information of these components was listed in **Table 1** and **Supplementary Figure S2**.

Total Flavonoid of Litchi Seed Inhibited Proliferation and Viability of Prostate Cancer Cells

To investigate the effect of TFLS on cell proliferation, PCa cells were treated with different concentrations of TFLS (0–240 μg/ml) for 24, 48, or 72 h, and the cell viability was evaluated by MTS assay. We found that TFLS significantly inhibited the cell viability of both PC3 and DU145 cells in both dose- and time-dependent manners (**Figures 2A,B**). The IC_{50} values of TFLS on PC3 and DU145 cells at 72 h were 61.5 ± 7.1 and 55.8 ± 5.1 μg/ml respectively (**Table 2**).

In addition, we also assessed the effect of various concentrations of TFLS on the proliferative ability of PC3 and DU145 cells by colony formation assay. After 8 days of treatment, the colony-forming ability of DU145 cell was significantly reduced ($p < 0.01$). Compared with the control group, the number of colony formed by PC3 cells

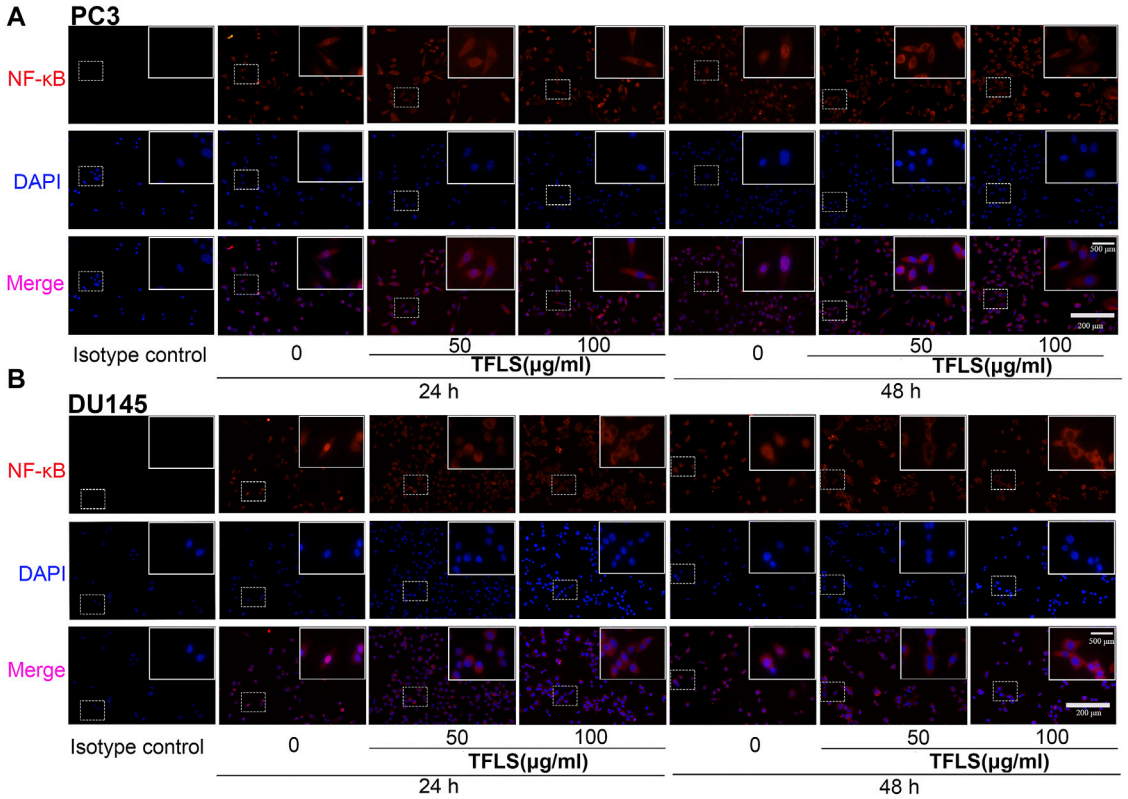


FIGURE 8 | TFLS inhibited the nucleus expression of NF-κB in PCa cells. **(A–B)** Representative images of immunofluorescence staining showing NF-κB p65 (red) in PC3 and DU145 cells treated without or with TFLS (50, 100 μg/ml). Cell nuclei were detected by DAPI (blue). The images were obtained by fluorescence microscope.

was reduced by approximately three quarters after treatment with high concentrations of TFLS (100 μg/ml) (**Figures 2C,D**).

Total Flavonoid of Litchi Seed Induced Apoptosis of Prostate Cancer Cells

To investigate the mechanism by which TFLS inhibited the PCa cell proliferation, we first assessed the effect of TFLS on cell cycle and apoptosis using flow cytometry analysis. The results (**Figures 3A–D**) showed that the percentage of apoptotic PC3 and DU145 cells was significantly higher in the TFLS treatment groups than that of the control groups. After 48 h treatment, the apopttic rates of PC3 and DU145 cells treated with 100 μg/ml TFLS were 31.10 ± 1.17% and 26.23 ± 1.34%, respectively. These results illustrated that TFLS might promote apoptosis of PCa cells. We further confirmed the effect of TFLS on cell apoptosis by TUNEL assay. We found that the number of TUNEL-positive cells was significantly increased in both the PC3 and DU145 cells treated with TFLS compared to the un-treated cells (**Figure 4**). These results suggested that TFLS could induce apoptosis of PCa cells.

To explore the mechanisms underlying TFLS-induced apoptosis of PCa cells, we screened the expression profiles of a panel of proteins involved in cellular apoptosis using Western blot. The data showed that TFLS increased the expression of cleaved- Poly ADP-ribose polymerase (PARP) and Bcl-2-associated X protein (Bax), while decreased the expression of B-cell lymphoma-2 (Bcl-2) in both PC3 and DU145 cells (**Figures 3E,F**). We also detected the effect of TFLS on cell cycle, and found that the cell cycle was not affected by TFLS treatment in these 2 cell lines (**Supplementary Figure S3**).

Total Flavonoid of Litchi Seed Inhibited Prostate Cancer Cell Migration and Invasion

In order to examine the effect of TFLS on metastasis in PCa cells, we firstly tested the cell migratory ability of PC3 and DU145 cells by wound-healing assay. As shown in **Figures 5A–C**, TFLS significantly reduced the gap closure rate. The percentage of PC3 cell migration reached 50% in the control group, the migratory rate was 29.4 ± 1.3% in cells treated with 100 μg/ml TFLS. Interestingly, TFLS showed a more potent inhibitory effect on DU145 cells after 24 h treatment. The migratory rate was reduced to 21.6 ± 2.3% in DU145 cells treated with 50 μg/ml of TFLS, which was further decreased to 13.6 ± 0.8% at 100 μg/ml. Similarly, it was found that TFLS reduced cell invasion in a dose-dependent manner in the transwell assay (**Figures 5D–F**).

Total Flavonoid of Litchi Seed Inhibited Epithelial-to-Mesenchymal Transition in Prostate Cancer Cells

EMT is one of the hallmarks of cancer metastasis. We investigated the inhibitory effects of TFLS on the EMT. We first observed the

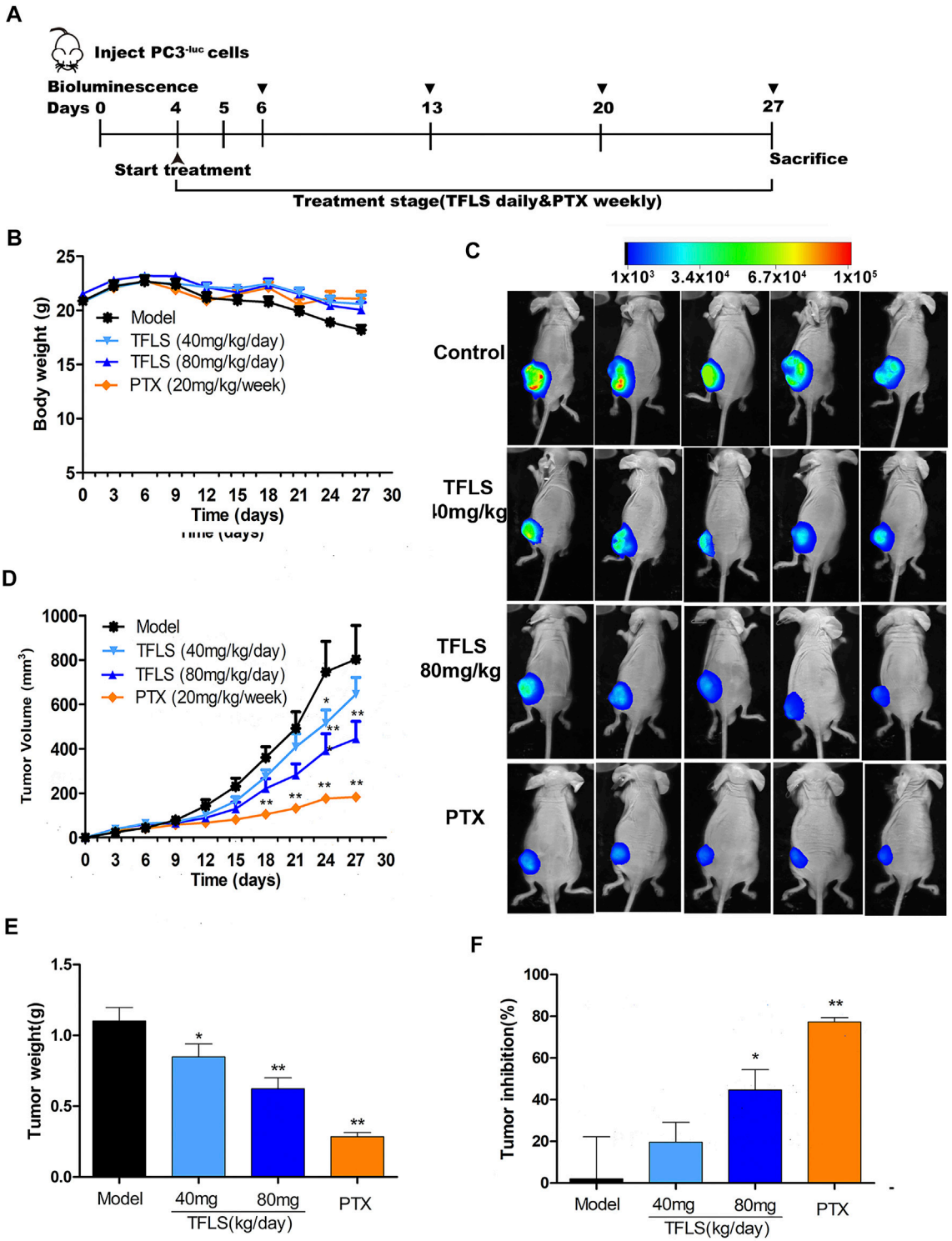


FIGURE 9 | TFLS suppressed tumor growth of PC3^{-luc} xenografts *in vivo*. **(A)** Outline of the animal experiment. **(B)** Body weight curves of mice in different groups during the whole treatment course. **(C)** Representative bioluminescence imaging of PC3^{-luc} xenograft tumors in different groups at the end of experiments. **(D)** Tumor growth curves of mice in different groups during the whole treatment course. **(E)** Tumor weight in different groups at the end of experiments. **(F)** Tumor inhibition rates in different groups at the end of experiments. Data are presented as mean ± SEM. Compared to control group: $^{*}p < 0.05$. $^{**}p < 0.01$. PTX: Paclitaxel.

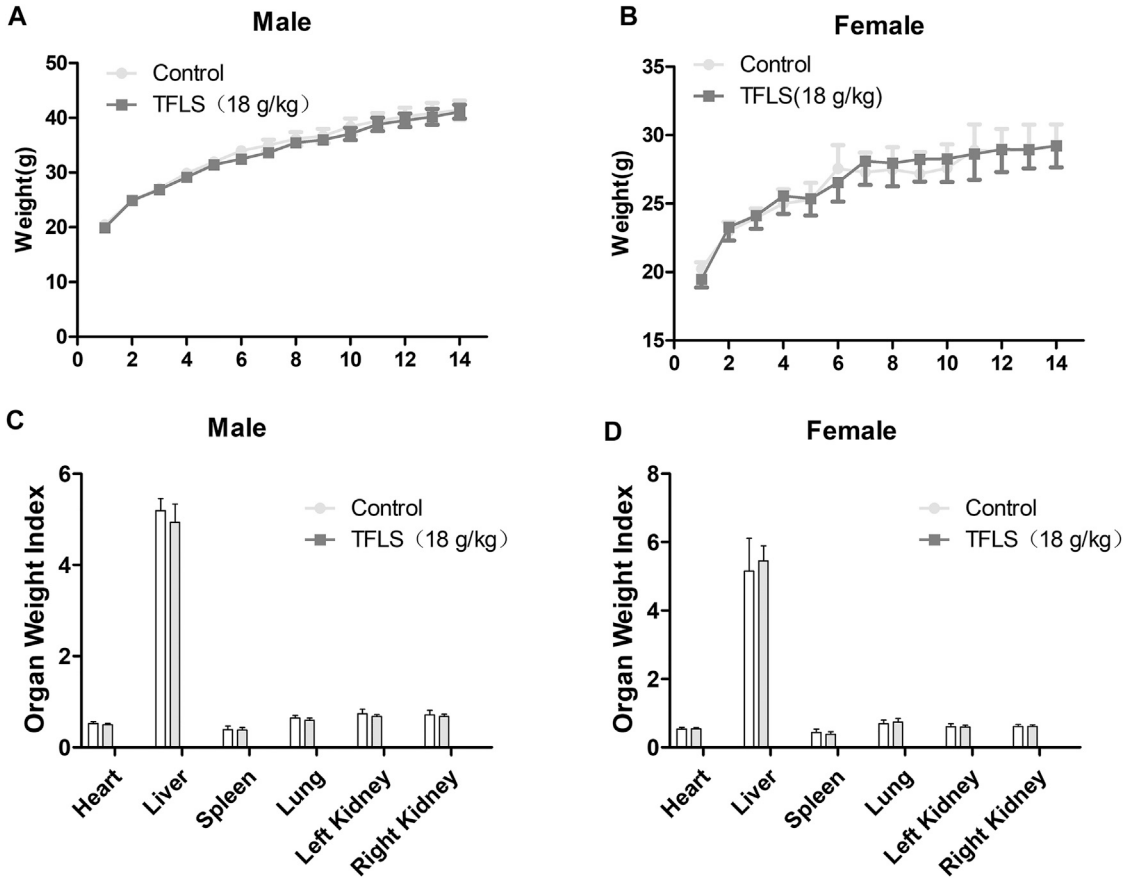


FIGURE 10 | The effects of TFLS on body weight and OWI. TFLS (18 g/kg body weight) was orally administered three times on the first day, with intervals of 6 h. The body weight was measured every day for 14 days in the male **(A)** and female **(B)** mice. On day 14, all animals were sacrificed. The vital organs were weighed and OWI was calculated **(C,D)**. Data are expressed as mean ± SEM.

effect of TFLS on cell morphology. It was found that the untreated PC3 and DU145 cells displayed a mesenchymal-like elongated spindle shape with sparse distribution, with observation of pseudopodium on some cells. However, after treating with TFLS, cells adapted to a more rounded shape accompanied by disappearance of pseudopodium (**Figure 6A**). These results suggested that TFLS might inhibit EMT in PCa.

To confirm the effect of TFLS on EMT, we evaluated the expression of EMT biomarkers, including E-cadherin and Vimentin. It was found that the expression of epithelial biomarker E-cadherin increased, while mesenchymal biomarker Vimentin's expression reduced after TFLS treatment compared with the control group, (**Figures 6B–D**). These results indicated that TFLS reduced migratory and invasive capabilities in PC3 and DU145 cells via phenotypic inversion of EMT.

Total Flavonoid of Litchi Seed Regulated AKT/mTOR and NF-κB Signaling Pathways

To further explore the underlying mechanisms of TFLS, we examined the expression of key proteins in signaling pathways implicated in cancer cell viability, proliferation and metastasis. For example, AKT, AMPK, MAPK and Wnt signaling pathways. We found that TFLS has little impact on p-AMPK, Wnt3a, p-MEK1/2 and p-P44/42 MAPK (**Supplementary Figure S4**). Interestingly, it was evidenced that the phosphorylation of AKT was effectively inhibited by TFLS in both PC3 and DU145 cells (**Figure 7A**), which may lead to changes in expression of several downstream proteins in the AKT signaling pathway. Hence, the total levels and activities of proteins involved in the AKT pathway were explored by Western blot. As shown in **Figures 7B,C**, after TFLS treatment, the levels of p-IκB α, p-NF-κB and p-mTOR in both PC3 and DU145 cells were significantly reduced compared to the control group. Notably, TFLS had no effect on the total expressions of AKT, IκB α, NF-κB and mTOR. The inhibitory effect of TFLS on the activation of NF-κB was further confirmed by immunofluorescence study. As shown in **Figure 8**, NF-κB p65 was mostly localized in the nucleus in the control group, as compared to a dispersed expression pattern in the treatment group.

Total Flavonoid of Litchi Seed Suppressed Tumor Growth of PC3 Xenografts *In Vivo*

To determine whether TFLS inhibits tumor progression *in vivo*, we established a nude mouse $PC3^{-luc}$ xenografts model. After treatment with TFLS, there was no significant difference in body

weight between the control group and TFLS treatment group (**Figure 9B**). However, the tumor weight and volume of TFLS-treated mice (at the dose of 40 and 80 mg/kg) was significantly lower than untreated mice (**Figures 9D,E**). Administration of either 40 or 80 mg/kg body weight TFLS showed a significant antitumor activity with tumor inhibition rates of 20.87 and 44.63%, respectively (**Figure 9F**). The bioluminescence imaging of $PC3^{-luc}$ xenograft tumors in different groups at the end of experiments showed consistent results (**Figure 9C**).

Acute Toxicity Test

Fourteen days after oral TFLS, no toxicity-related clinical symptom or mortality were observed. As shown in **Figures 10A,B**, there was no significant change in body weight by TFLS treatment in both male and female mice. In addition, no significant pathological change was observed in the textures, colors and organ weight index of vital organs, including the heart, liver, spleen, lung and kidney (**Figures 10C,D**). These results demonstrated that the median lethal dose (LD_{50}) of TFLS in mice is well-above 18 g/kg.

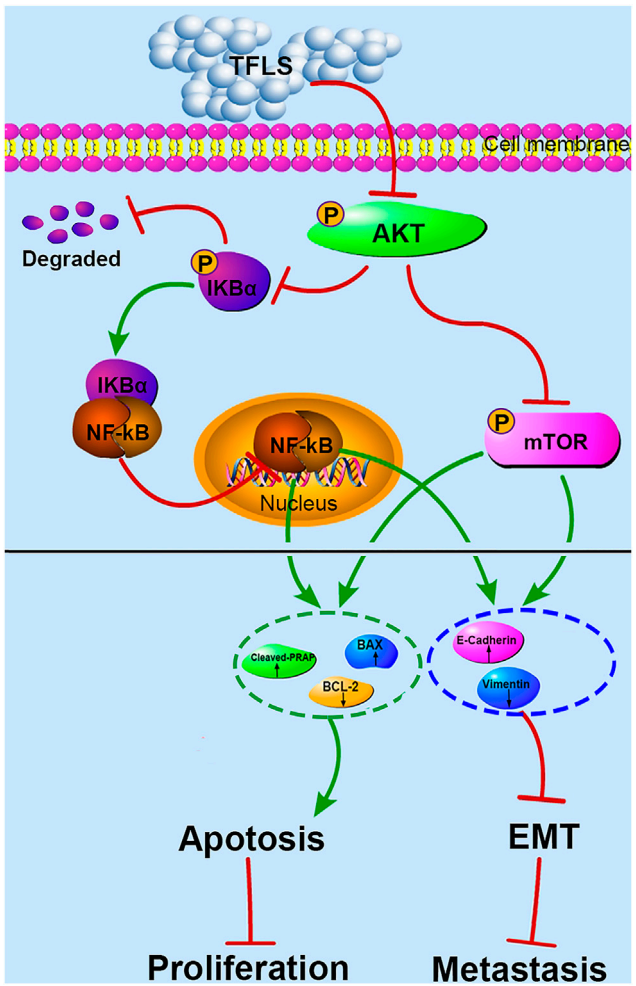


FIGURE 11 | Proposed mechanism of TFLS anti-PCa cells. In brief, TFLS inhibited the phosphorylation of AKT after entering cells, which resulted in decreased phosphorylation of mTOR and IκBα. Then, IκBα and NF-κB combined to form complex of NF-κB-IκBα, which suppressed NF-κB to translocate into the nucleus. The reduction of mTOR phosphorylation and inhibition of NF-κB's nuclear translocation thus regulated the expression of apoptosis- and EMT-related proteins. As a result, cancer progression was suppressed.

DISCUSSION

PCa is the second leading cause of cancer-related male mortality in Western countries. PCa is difficult to be treated with current clinical treatment modalities (Siegel et al., 2019). Hence, there is an urgent demand for novel anti-PCa therapies. Litchi seeds have been traditionally used in Chinese herbal formulas for urologic neoplasms including prostate cancer, renal carcinoma and bladder cancer (Hsu et al., 2012; Emanuele et al., 2018). In a previous study, we found that flavonoids were the most abundant chemical component among the extracts of Litchi seeds which exerted anti-PCa activity (Guo et al., 2017; Cao et al., 2020). Other studies also found that flavonoids extracted from Litchi pericarp such as epicatechin and proanthocyanidin B2 had anticancer activities (Koga et al., 2017). Therefore, in this study, we investigated the anticancer effects of TFLS on PCa cells. The results showed that TFLS significantly inhibited the proliferation and colony formation capability of PCa cells *in vitro*. More importantly, we also confirmed that TFLS could suppress tumor growth using a nude mouse $PC3^{-luc}$ xenograft model *in vivo*. Meanwhile, in the acute toxicity test, neither mortality nor abnormalities were detected in mice that were orally administered with 18 g/kg TFLS. The LD_{50} of TFLS in mice is well-above 18 g/kg. These findings demonstrated that TFLS might be a potent anti-tumor therapeutics with low toxicity and limited side effects. We investigated the molecular mechanisms of anti-PCa activity of TFLS *in vitro*. It was found that TFLS displays a dose- and time-dependent inhibitory effect on human breast cancer, which could be attributed, in part, to its regulation of apoptosis in cancer cells through upregulation and downregulation of multiple genes (Li and Jiang, 2007). So, we examined the effect of TFLS on cell cycle and apoptosis by flow cytometry and found that TFLS could induce apoptosis of PCa cells, which was further verified by TUNEL assay. In addition, our results showed that TFLS had little regulatory effect on the cell cycle. These findings indicated that the anti-proliferative function of TFLS on PCa cells was likely to be majorly exerted by apoptosis induction. So, we focused on the effect of TFLS on apoptosis-related proteins. The Bcl-2 family proteins are major regulators of the intrinsic apoptosis pathway. Among them, Bax was identified as a homologous binding partner of Bcl-2 that activates apoptosis (Boise et al., 1995). In contrast, PARP maintains cell viability (Satoh and Lindahl, 1992); Cleaved-PARP promotes cell disintegration and is considered as a biomarker of apoptosis (Oliver et al., 1998). Interestingly, in our study, we confirmed that TFLS treatment increased the expression of Bax and Cleaved-PRAP, while decreased the expression of Bcl-2, indicating that TFLS may induce intrinsic apoptosis by regulating the expression of Bcl-2 and Bax.

Tumor metastasis is one of the major characteristics of malignant tumors and remained an obstacle in cancer treatment. EMT is an essential process underlying metastasis, during which epithelial cells gradually gain mesenchymal properties with enhanced migratory and invasive capabilities (Huber et al., 2005). Because previous studies have shown EMT was an essential process underlying PCa metastasis, we examined if TFLS could prevent metastasis by inhibiting EMT. The changes in cellular properties and a group of molecular biomarkers are the main criteria for defining EMT status (Ievgenia and Cédric, 2019). In this study, we found that PC3 and DU145 cells gained epithelial property when treated with TFLS, suggesting that TFLS could prevent changes of cell morphology during EMT. We tested the expression of EMT protein biomarkers, including E-cadherin and Vimentin. E-cadherin is majorly expressed in epithelial cells to maintain cell-cell contact (Hay and Zuk, 1995), the downregulation of which was observed in embryogenesis, tissue fibrosis and cancer-related EMT. While the upregulation of Vimentin is strongly associated with tumor cell invasion and metastasis (Raymond and Leong, 1989). We found that TFLS significantly upregulated the expression of epithelial biomarker E-cadherin and inhibited the mesenchymal biomarker Vimentin. We confirmed that TFLS has an inhibitory effect on metastasis of PCa cells by preventing EMT based on the changes in cellular properties and expression of molecular biomarkers.

Furthermore, we tested the activation of signaling pathways that are highly associated with cell proliferation and metastasis upon TFLS treatment, including AKT, AMPK, MAPK and Wnt signaling pathways. AKT signaling pathway is critically implicated in both pathogenesis and development of PCa, the inhibition of which could induce cell apoptosis and inhibit metastasis (Tang et al., 2013). Upon stimulation and subsequent phosphorylation, AKT translocates into the nucleus and regulates target gene expression which is related to cancer cell viability, proliferation, apoptosis, cell cycle progression, metastasis and vasculogenesis (Chen H. et al., 2016). We found that TFLS could significantly decrease the phosphorylation of AKT in PC3 and DU145 cells. On the contrary, other signal pathways like AMPK, MEK1/2, P44/42 MAPK and Wnt 3a were not found to be affected by TFLS, suggesting that the anti-PCa property of TFLS was majorly exerted by inhibiting AKT signaling pathway. Hence, we hypothesized that TFLS induced apoptosis and inhibited metastasis of PCa cells by inhibiting the AKT signaling pathway.

To investigate the direct effect of TFLS on AKT, we tested the expression of the downstream proteins in this signaling pathway to further confirm the mechanism. IKK proteins, including IKK-α and IKK-β, could be activated by phosphorylated AKT. Their activation induces the phosphorylation and subsequent degradation of IκBα, leading to the dissociation of IκBα/NF-κB complex, nuclear translocation and activation of NF-κB signaling pathway (Chandrasekar et al., 2004). In our study, we found that TFLS inhibited NF-κB signaling pathway by decreasing the phosphorylation of IκBα and nucleus expression of NF-κB. This is supported by similar results showing that TFLS could attenuate the nuclear translocation of NF-κB in activated HSC-T6 (Qin et al., 2018). Meanwhile, our study confirmed that TFLS reduced the expression of phosphorylated NF-κB, which may also be resulted from the downregulation of NF-κB signaling pathway. NF-κB signaling pathway is highly associated with EMT and can promote a mesenchymal cell phenotype (Min et al., 2008). The activation of NF-κB promotes its binding to the VIM promoter, which upregulates Vimentin expression thus adaptation to a more mesenchymal phenotype (Lilienbaum and Paulin, 1993). Meanwhile, activated NF-κB inhibited the expression of E-cadherin by elevating transcriptional repressors of E-cadherin in multiple cancer types (Chua et al., 2007). Our study illustrated that NF-κB influenced EMT by regulating EMT-related proteins. In addition, it is well-established that the suppression of NF-κB could also promote cell apoptosis by upregulating pro-apoptosis proteins while downregulating anti-apoptosis proteins. Bcl-2 is transcriptionally regulated by NF-κB and this activity is mediated through a functional NF-κB site identified in the Bcl-2 p2 promoter in PCa cell lines (Catz and Johnson, 2001). NF-κB also regulates Bax gene expression through an indirect pathway by inducing PRAP caspase-3-mediated cleavage (Bentires-Alj et al., 2001). In accordance with the above findings, our study showed that TFLS increased the level of cleaved-PRAP and Bax, and reduced the level of Bcl-2. Hence, our results demonstrated that TFLS exerted pro-apoptosis and anti-metastatic effects in PCa cells by inhibiting the activation of AKT/NF-κB signaling pathway (**Figure 11**).

The mTOR is another important target protein downstream of the AKT signaling pathway and phosphorylated ATK could directly activate mTOR (Spirina et al., 2018). Interestingly, in this study, we also found that TFLS decreased phosphorylation level of mTOR. This finding implied that TFLS could inhibit AKT/mTOR signaling pathway. It has been reported that the mTOR signaling pathway plays a key role in the migration, invasion and EMT of PCa. Vo et al. (2013) confirmed that overactivation of AKT/mTOR signaling pathway enhanced the migration capability of PCa cells. We found that TFLS negatively regulates EMT, which could be mediated by inhibition of AKT/mTOR signalling pathway. It is reported that inhibition of Akt/mTOR reversed EMT by regulating the EMT-related proteins (Karimi Roshan et al., 2019). Our study also implied that the expression of E-Cadherin and Vimentin were regulated by AKT/mTOR pathway after TFLS treatment. Notably, activation of mTOR signaling pathway is also highly associated with tumor cell apoptosis, as evidenced by (Su et al., 2019). AKT/mTOR signaling pathway regulates the expression of apoptosis-related proteins, including Bcl-2, Bax and PRAP, etc (Xia et al., 2020). Therefore, we speculated that TFLS induced the apoptosis of PCa cells by inhibiting AKT/mTOR signaling pathway (**Figure 11**).

CONCLUSION

In summary, this study provides new insights into the role of TFLS as an anti-cancer agent in PCa. We show that TFLS could suppress the PCa growth *in vivo* and inhibit PCa cells proliferation, migration and invasion *in vitro* through induction of apoptosis and phenotypic

inversion of EMT, which may be realized by inhibiting AKT/mTOR and NF-κB signaling pathways.

DATA AVAILABILITY STATEMENT

The original contributions presented in the study are included in the article/**Supplementary Material**, further inquiries can be directed to the corresponding authors.

ETHICS STATEMENT

The animal study was reviewed and approved by the Institutional Animal Ethics Committee (IAEC, Nos. 201810146, 201903029), Guangxi Medical University.

AUTHOR CONTRIBUTIONS

HG, MC, and YL designed the study. MC, DZ, XL, WZ, ZC, and X-LL performed the experiments, HG, MC, and XL analyzed the data, YC and MC drafted the manuscript, HG, ZS, JZ, and YL contributed reagents/materials/analysis tools. All authors have read and agreed to the published version of the manuscript.

FUNDING

This work was supported by the National Natural Science Foundation of China (81660681, 82074347, 81773146, 81972766, 81972420), College Student's Innovative Entrepreneurial Training Plan Program (202110598024, 202110598028, 202110598242, 202110598112), Shenzhen Science and Technology Innovation Commission, Key project (JCYJ20170412152943794, JCYJ20170412154619484).

SUPPLEMENTARY MATERIAL

The Supplementary Material for this article can be found online at: https://www.frontiersin.org/articles/10.3389/fphar.2021.758219/full#supplementary-material

REFERENCES

Bentires-Alj, M., Dejardin, E., Viatour, P., Van Lint, C., Froesch, B., Reed, J. C., et al. (2001). Inhibition of the Nf-Kappa B Transcription Factor Increases Bax Expression in Cancer Cell Lines. *Oncogene* 20 (22), 2805–2813. doi:10.1038/sj.onc.1204343

Boise, L. H., Gottschalk, A. R., Quintáns, J., and Thompson, C. B. (1995). Bcl-2 and Bcl-2-Related Proteins in Apoptosis Regulation. *Curr. Top. Microbiol. Immunol.* 200, 107–121. doi:10.1007/978-3-642-79437-7_8

Cao, S., Han, Y., Li, Q., Chen, Y., Zhu, D., Su, Z., et al. (2020). Mapping Pharmacological Network of Multi-Targeting Litchi Ingredients in Cancer Therapeutics. *Front. Pharmacol.* 11, 451. doi:10.3389/fphar.2020.00451

Catz, S. D., and Johnson, J. L. (2001). Transcriptional Regulation of Bcl-2 by Nuclear Factor Kappa B and its Significance in Prostate Cancer. *Oncogene* 20 (50), 7342–7351. doi:10.1038/sj.onc.1204926

Chandrasekar, B., Marelli-Berg, F. M., Tone, M., Bysani, S., Prabhu, S. D., and Murray, D. R. (2004). Beta-Adrenergic Stimulation Induces Interleukin-18 Expression via Beta2-Ar, Pi3k, Akt, Ikk, and Nf-Kappab. *Biochem. Biophys. Res. Commun.* 319 (2), 304–311. doi:10.1016/j.bbrc.2004.04.185

Chen, H., Zhou, L., Wu, X., Li, R., Wen, J., Sha, J., et al. (2016a). The Pi3k/Akt Pathway in the Pathogenesis of Prostate Cancer. *Front. Biosci. Landmark Ed.* 21, 1084–1091. doi:10.2741/4443

Chen, W., Zheng, R., Baade, P. D., Zhang, S., Zeng, H., Bray, F., et al. (2016b). Cancer Statistics in China, 2015. *CA Cancer J. Clin.* 66 (2), 115–132. doi:10.3322/caac.21338

Chua, H. L., Bhat-Nakshatri, P., Clare, S. E., Morimiya, A., Badve, S., and Nakshatri, H. (2007). Nf-Kappab Represses E-Cadherin Expression and Enhances Epithelial to Mesenchymal Transition of Mammary Epithelial Cells: Potential Involvement of Zeb-1 and Zeb-2. *Oncogene* 26 (5), 711–724. doi:10.1038/sj.onc.1209808

Emanuele, S., Notaro, A., Palumbo Piccionello, A., Maggio, A., Lauricella, M., D'Anneo, A., et al. (2018). Sicilian Litchi Fruit Extracts Induce Autophagy versus Apoptosis Switch in Human Colon Cancer Cells. *Nutrients* 10 (10), 1490. doi:10.3390/nu10101490

Farolfi, A., Fendler, W., Iravani, A., Haberkorn, U., Hicks, R., Herrmann, K., et al. (2019). Theranostics for Advanced Prostate Cancer: Current Indications and Future Developments. *Eur. Urol. Oncol.* 2 (2), 152–162. doi:10.1016/j.euo.2019.01.001

Guo, H., Luo, H., Yuan, H., Xia, Y., Shu, P., Huang, X., et al. (2017). Litchi Seed Extracts Diminish Prostate Cancer Progression via Induction of Apoptosis and Attenuation of EMT through Akt/GSK-3β Signaling. *Sci. Rep.* 7, 41656. doi:10.1038/srep41656

Hay, E. D., and Zuk, A. (1995). Transformations between Epithelium and Mesenchyme: Normal, Pathological, and Experimentally Induced. *Am. J. Kidney Dis.* 26 (4), 678–690. doi:10.1016/0272-6386(95)90610-x

Hsu, C. P., Lin, C. C., Huang, C. C., Lin, Y. H., Chou, J. C., Tsia, Y. T., et al. (2012). Induction of Apoptosis and Cell Cycle Arrest in Human Colorectal Carcinoma by Litchi Seed Extract. *J. Biomed. Biotechnol.* 2012, 341479. doi:10.1155/2012/341479

Huber, M. A., Kraut, N., and Beug, H. (2005). Molecular Requirements for Epithelial-Mesenchymal Transition During Tumor Progression. *Curr. Opin. Cel Biol* 17 (5), 548–558. doi:10.1016/j.ceb.2005.08.001

Inoue, T., Takagi, H., Owada, Y., Watanabe, Y., Yamaura, T., Fukuhara, M., et al. (2017). The Efficacy of the Kampo Medicine Rikkunshito for Chemotherapy-Induced Anorexia (Rich Trial): Study Protocol for a Randomized Controlled Trial. *Trials* 18 (1), 485. doi:10.1186/s13063-017-2227-6

Karimi Roshan, M., Soltani, A., Soleimani, A., Rezaie Kahkhaie, K., Afshari, A. R., and Soukhtanloo, M. (2019). Role of Akt and Mtor Signaling Pathways in the Induction of Epithelial-Mesenchymal Transition (Emt) Process. *Biochimie* 165, 229–234. doi:10.1016/j.biochi.2019.08.003

Koga, N., Moriya, F., Waki, K., Yamada, A., Itoh, K., and Noguchi, M. (2017). Immunological Efficacy of Herbal Medicines in Prostate Cancer Patients Treated by Personalized Peptide Vaccine. *Cancer Sci.* 108 (12), 2326–2332. doi:10.1111/cas.13397

Li, J., and Jiang, Y. (2007). Litchi Flavonoids: Isolation, Identification and Biological Activity. *Molecules* 12 (4), 745–758. doi:10.3390/12040745

Lilienbaum, A., and Paulin, D. (1993). Activation of the Human Vimentin Gene by the Tax Human T-Cell Leukemia Virus. I. Mechanisms of Regulation by the Nf-Kappa B Transcription Factor. *J. Biol. Chem.* 268 (3), 2180–2188. doi:10.1016/s0021-9258(18)53979-x

Min, C., Eddy, S. F., Sherr, D. H., and Sonenshein, G. E. (2008). Nf-Kappab and Epithelial to Mesenchymal Transition of Cancer. *J. Cel Biochem* 104 (3), 733–744. doi:10.1002/jcb.21695

Nieder, C., Haukland, E., Pawinski, A., and Dalhaug, A. (2010). Anaemia and Thrombocytopenia in Patients with Prostate Cancer and Bone Metastases. *BMC Cancer* 10, 284. doi:10.1186/1471-2407-10-284

Oliver, F. J., de la Rubia, G., Rolli, V., Ruiz-Ruiz, M. C., de Murcia, G., and Murcia, J. M. (1998). Importance of Poly(Adp-Ribose) Polymerase and its Cleavage in Apoptosis. Lesson from an Uncleavable Mutant. *J. Biol. Chem.* 273 (50), 33533–33539. doi:10.1074/jbc.273.50.33533

Pastushenko, I., and Blanpain, C. (2019). EMT Transition States during Tumor Progression and Metastasis. *Trends Cel Biol.* 29 (3), 212–226. doi:10.1016/j.tcb.2018.12.001

Qin, G. J., Zhao, Y. Z., Liu, Y. X., Li, C., Cao, J., Cheng, Q. C., et al. (2018). Study on the Effects of Total Flavonoids from Litchi Nucleus on Nuclear Translocation of Nuclear Factor-Kappa B and Related Protein Expression in Rat Hepatic Stellate Cell. *Zhonghua Gan Zang Bing Za Zhi* 26 (7), 535–539. doi:10.3760/cma.j.issn.1007-3418.2018.07.011

Raymond, W. A., and Leong, A. S. (1989). Vimentin-A New Prognostic Parameter in Breast Carcinoma. *J. Pathol.* 158 (2), 107–114. doi:10.1002/path.1711580205

Satoh, M. S., and Lindahl, T. (1992). Role of Poly(Adp-Ribose) Formation in DNA Repair. *Nature* 356 (6367), 356–358. doi:10.1038/356356a0

Sharifi-Rad, J., Ozleyen, A., Boyunegmez Tumer, T., Oluwaseun Adetunji, C., El Omari, N., Balahbib, A., et al. (2019). Natural Products and Synthetic Analogs as a Source of Antitumor Drugs. *Biomolecules* 9 (11), 679. doi:10.3390/biom9110679

Siegel, R. L., Miller, K. D., and Jemal, A. (2019). Cancer Statistics, 2019. *CA Cancer J. Clin.* 69 (1), 7–34. doi:10.3322/caac.21551

Spirina, L. V., Kondakova, I. V., Tarasenko, N. V., Slonimskaya, E. M., Usynin, E. A., Gorbunov, A. K., et al. (2018). Targeting of the AKT/m-TOR Pathway: Biomarkers of Resistance to Cancer Therapy-AKT/m-TOR Pathway and Resistance to Cancer Therapy. *Zhongguo Fei Ai Za Zhi* 21 (1), 63–66. doi:10.3779/j.issn.1009-3419.2018.01.09

Su, C. C., Hsieh, K. L., Liu, P. L., Yeh, H. C., Huang, S. P., Fang, S. H., et al. (2019). Aicar Induces Apoptosis and Inhibits Migration and Invasion in Prostate Cancer Cells through an Ampk/Mtor-Dependent Pathway. *Int. J. Mol. Sci.* 20 (7), 1647. doi:10.3390/ijms20071647

Tang, Y. Q., Jaganath, I., Manikam, R., and Sekaran, S. D. (2013). Phyllanthus Suppresses Prostate Cancer Cell, PC-3, Proliferation and Induces Apoptosis through Multiple Signalling Pathways (MAPKs, PI3K/Akt, NFκB, and Hypoxia). *Evid. Based Complement. Alternat Med.* 2013, 609581. doi:10.1155/2013/609581

Vo, B. T., Morton, D., Jr., Komaragiri, S., Millena, A. C., Leath, C., and Khan, S. A. (2013). TGF-β Effects on Prostate Cancer Cell Migration and Invasion Are Mediated by PGE2 through Activation of PI3K/AKT/mTOR Pathway. *Endocrinology* 154 (5), 1768–1779. doi:10.1210/en.2012-2074

Xia, J., Dai, L., Wang, L., and Zhu, J. (2020). Ganoderic Acid Dm Induces Autophagic Apoptosis in Non-small Cell Lung Cancer Cells by Inhibiting the Pi3k/Akt/Mtor Activity. *Chem. Biol. Interact* 316, 108932. doi:10.1016/j.cbi.2019.108932

Zhang, W. Q., Li, X. L., Xue, W., Chang, M., and Guo, H. W. (2021). The Anti-proliferation Effect of Total Flavonoids of Litchi Seed Combined with Paclitaxel on Prostate Cancer Paclitaxel Resistant Cells. *Chin. Pharmacol. Bull.* 37 (4), 528–534. doi:10.3969/j.issn.1001-1978.2021.04.016

Conflict of Interest: The authors declare that the research was conducted in the absence of any commercial or financial relationships that could be construed as a potential conflict of interest.

Publisher's Note: All claims expressed in this article are solely those of the authors and do not necessarily represent those of their affiliated organizations, or those of the publisher, the editors and the reviewers. Any product that may be evaluated in this article, or claim that may be made by its manufacturer, is not guaranteed or endorsed by the publisher.

Copyright © 2021 Chang, Zhu, Chen, Zhang, Liu, Li, Cheng, Su, Zhang, Lu and Guo. This is an open-access article distributed under the terms of the Creative Commons Attribution License (CC BY). The use, distribution or reproduction in other forums is permitted, provided the original author(s) and the copyright owner(s) are credited and that the original publication in this journal is cited, in accordance with accepted academic practice. No use, distribution or reproduction is permitted which does not comply with these terms.

frontiers in Pharmacology

REVIEW
published: 23 September 2021
doi: 10.3389/fphar.2021.738235

Molecular Basis of Prostate Cancer and Natural Products as Potential Chemotherapeutic and Chemopreventive Agents

Bingke Bai[1†], Qianbo Chen[2†], Rui Jing[1†], Xuhui He[1], Hongrui Wang[1], Yanfei Ban[1], Qi Ye[3], Weiheng Xu[4]* and Chengjian Zheng[1]**

[1]Department of Chinese Medicine Authentication, School of Pharmacy, Second Military Medical University, Shanghai, China, [2]Department of Anesthesiology, Shanghai Eastern Hepatobiliary Surgery Hospital, Shanghai, China, [3]Department of Biological Science, College of Life Science, Fujian Agriculture and Forestry University, Fuzhou, China, [4]Department of Biochemical Pharmacy, School of Pharmacy, Second Military Medical University, Shanghai, China

OPEN ACCESS

Edited by:
Wei Peng,
Chengdu University of Traditional Chinese Medicine, China

Reviewed by:
Tao Guo,
Henan University of Traditional Chinese Medicine, China
Loh Teng Hern Tan,
Monash University Malaysia, Malaysia

***Correspondence:**
Qi Ye
qipharm@126.com
Weiheng Xu
xuweiheng7114@163.com
Chengjian Zheng
cjzheng1984@126.com

[†]These authors have contributed equally to this work

Specialty section:
This article was submitted to Ethnopharmacology, a section of the journal Frontiers in Pharmacology

Received: 08 July 2021
Accepted: 06 September 2021
Published: 23 September 2021

Citation:
Bai B, Chen Q, Jing R, He X, Wang H, Ban Y, Ye Q, Xu W and Zheng C (2021) Molecular Basis of Prostate Cancer and Natural Products as Potential Chemotherapeutic and Chemopreventive Agents. Front. Pharmacol. 12:738235. doi: 10.3389/fphar.2021.738235

Prostate cancer is the second most common malignant cancer in males. It involves a complex process driven by diverse molecular pathways that closely related to the survival, apoptosis, metabolic and metastatic characteristics of aggressive cancer. Prostate cancer can be categorized into androgen dependent prostate cancer and castration-resistant prostate cancer and cure remains elusive due to the developed resistance of the disease. Natural compounds represent an extraordinary resource of structural scaffolds with high diversity that can offer promising chemical agents for making prostate cancer less devastating and curable. Herein, those natural compounds of different origins and structures with potential cytotoxicity and/or *in vivo* anti-tumor activities against prostate cancer are critically reviewed and summarized according to the cellular signaling pathways they interfere. Moreover, the anti-prostate cancer efficacy of many nutrients, medicinal plant extracts and Chinese medical formulations were presented, and the future prospects for the application of these compounds and extracts were discussed. Although the failure of conventional chemotherapy as well as involved serious side effects makes natural products ideal candidates for the treatment of prostate cancer, more investigations of preclinical and even clinical studies are necessary to make use of these medical substances reasonably. Therefore, the elucidation of structure-activity relationship and precise mechanism of action, identification of novel potential molecular targets, and optimization of drug combination are essential in natural medicine research and development.

Keywords: prostate cancer, natural compounds, apoptosis, androgen receptor, mechanism

INTRODUCTION

It is nowadays evident that prostate cancer (PCa) is recognized as the second most common cancer and the fifth cause of cancer death in males (Torre et al., 2015)Initially, the usual therapy for prostate cancer is prostatectomy or radiation, which aims to remove or kill the malignant cells that have not spread or metastasized (Feldman and Feldman, 2001). However, numerous patients cannot be cured thoroughly by this treatment, and then followed by cancer recurrence and/or metastasis. The

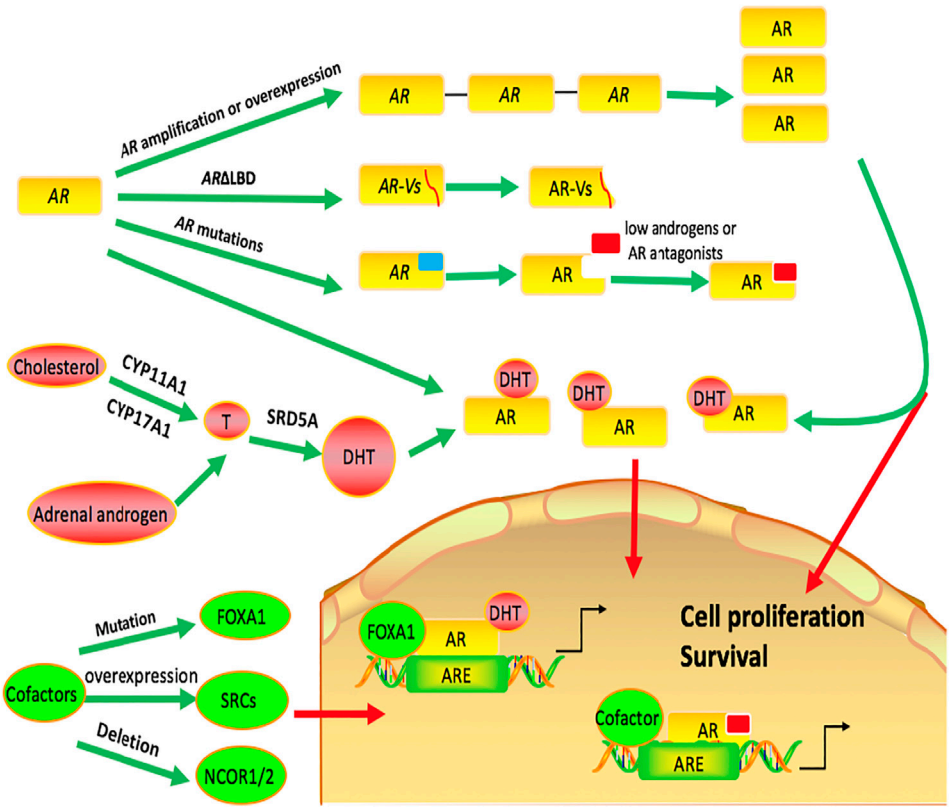


FIGURE 1 | Canonical AR in castration-resistant prostate cancer. Common alterations in *AR*, including *AR* amplification or overexpression, *AR* mutations and truncated *AR* lacking ligand-binding domains (*AR*ΔLBD), can increase its sensitivity to very low levels of androgens or lead to constitutive activation of AR signaling. There are two possible ways for the initial substrates to convert to intratumoral DHT in CRPC. The first way is that androgens are synthesized intratumorally via the *de novo* route and the second is that androgens are converted from adrenal androgens. Genomic and transcriptomic alterations in AR pathway coregulators are also associated with resistance to AR-targeted therapies in CRPC.

majority of prostate cancer growth is androgen dependent. Androgen deprivation therapy (ADT) such as surgery or gonadotropin-releasing hormone (GnRH) analog treatment, is the main therapeutic and dramatically effective intervention for the treatment of androgen dependent prostate cancer (ADPC) in putting patients with tumors in remission, as documented by the work on castration of Huggins, who was awarded the Nobel prize in 1966 (Huggins, 1978). Nevertheless, after this therapy, most of these prostate cancer patients gradually become androgen independent, go on to progress, metastasize and resist to ADT within 13–24 months accompanied by increased levels of prostate-specific antigen (PSA). Siegel et al. reported that failure of ADT is responsible for the ~27,000 metastatic prostate cancer deaths in the United States annually (Siegel et al., 2017). This stage of prostate cancer is called castration-resistant prostate cancer (CRPC), which has poor prognosis (Small et al., 2004). At present, there is no effective therapy for CRPC besides docetaxel, which has been demonstrated to prolong overall survival in this patient population. However, the efficacy of docetaxel is not satisfactory and there are many severe adverse effects such as anemia, neutropenia, diarrhea, and sensory neuropathy. Although, therapeutic options have expanded rapidly since 2011, including AR inhibitors (enzalutamide, abiraterone), immunotherapy (sipuleucel-T), bone seeking radionuclides (radium-223), and second-line chemotherapy (cabazitaxel), all of these agents or interventions only have shown a median survival benefit of 2–5 months (Ritch and Cookson, 2016). So searching for more effective anti-prostate cancer drugs, especially with high efficacy and low toxicity, remains an urgent problem that needs to be resolved. Natural compounds represent an irreplaceable resource of structural scaffolds that can offer chemical agents for making prostate cancer less devastating and curable. In recent years, many natural products and extracts have been scientifically investigated *in vitro* and/or *in vivo* and proved as potential anti-prostate cancer agents, which are currently scattered across various publications. So a systematic summary and knowledge of future prospects are necessary to facilitate further chemical and pharmacological studies for anti-prostate cancer agents.

Herein, we reviewed the detailed molecular causes of prostate cancer and critically summarized the natural

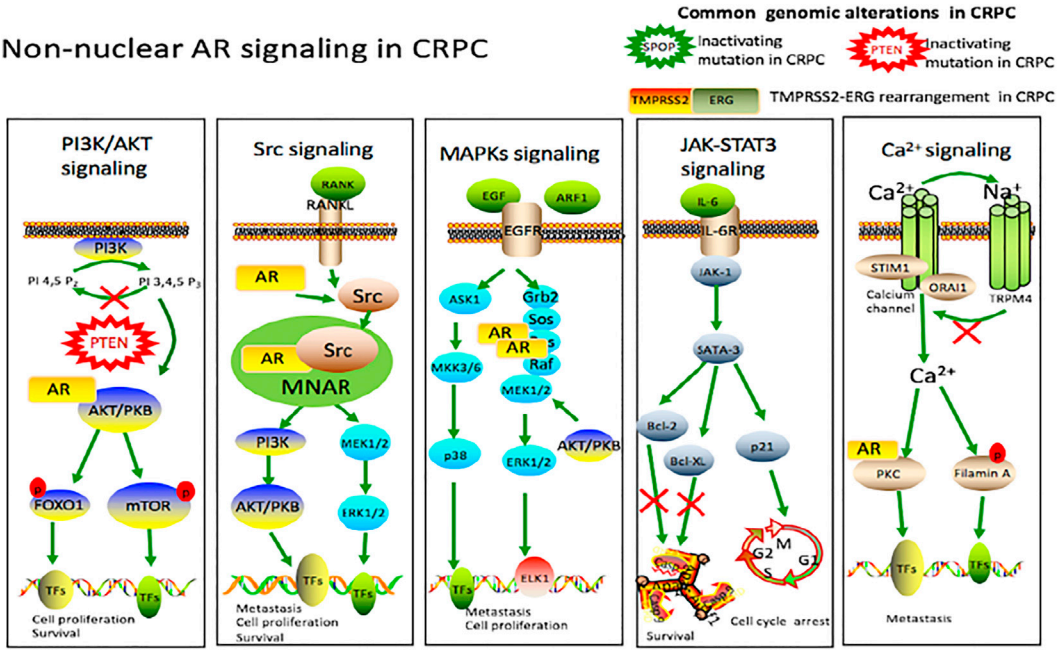


FIGURE 2 | Non-nuclear AR signaling in castration-resistant prostate cancer. Cytokines, interleukins and the growth factors secreted by the prostate cancer cells activate various signaling cascades like PI3K/AKT, Src, MAPKs and JAK/STAT3 pathways involved in castration-resistant prostate cancer, leading to cell proliferation, survival and tumor metastasis. Intracellular Ca^{2+} centration can be modulated through Calcium channel. This increase in intracellular Ca^{2+} can lead to activation of PKC and filamin A, ultimately influencing gene transcription through phosphorylation. TRPM4 is also activated by a rise in intracellular Ca^{2+} in prostate cancer cells. Upon activation, a Na^{+} influx via TRPM4 depolarizes the membrane potential, which decreases the driving force for Ca^{2+}, and thus contributes to migration of androgen-insensitive prostate cancer cells. There are other genomic alterations in castration-resistant prostate cancer, including *PTEN* mutation, *SPOP* mutation and *TMPRSS2-ERG* rearrangement.

compounds (or extracts and Chinese herb preparations) that have been reported to inhibit prostate cancer cells proliferation/tumor growth, induce prostate cancer cells apoptosis or exhibit effects on specific signaling pathways involved in prostate cancer *in vivo* and *in vitro*. In addition, we also provided possible novel targets for screening natural compounds (or extracts or Chinese herb preparations) with anti-prostate cancer activity and discuss the future prospects for the application of these compounds and extracts and the novel available approaches and technological improvements that should be explored to treat prostate cancer.

OVERVIEW OF THE MOLECULAR BASIS OF PROSTATE CANCER

Molecular Basis of Androgen Dependent Prostate Cancer

Androgens, principally testosterone (T) and dihydrotestosterone (DHT), are synthesized from cholesterol as the initial 27-carbon substrate via multiple enzymatic steps (Wadosky and Koochekpour, 2016). As a member of the ligand-activated nuclear hormone receptors superfamily, androgen receptor (AR) is a modular protein with four functional domains: an N-terminal regulatory domain (NTD), a DNA-binding domain (DBD), a small hinge region (H) and a ligand-binding domain (LBD) (Ho and Dehm, 2017). Upon binding to androgens, AR undergoes a conformational change, leading to nuclear translocation, phosphorylation, homodimer, and interaction with DNA (Li and Al-Azzawi, 2009). Subsequently, AR dimer binds to androgen-response elements (AREs), recruits essential co-factors and regulates the expression of androgen-regulated genes (Ho and Dehm, 2017).

The development and maintenance of the prostate is inseparable from androgen acting through the AR. Since Huggins and Hodges first demonstrated the responsiveness of prostate cancer to androgen deprivation, it has been clear that prostate cancer is dependent on androgen and AR activation for growth and survival (Huggins and Hodges, 1941). From then, hundreds of studies have demonstrated that androgen withdrawal results in initial regression of essentially all prostate cancers, albeit for a finite period, with the ultimate development of castration-resistant disease. Androgen deprivation therapy, via either orchidectomy or use of a gonadotropin-releasing hormone (GnRH) agonist has become the cornerstone of therapy in the treatment of prostate cancers. Newer agents, such as abiraterone, which block androgen synthetic pathways, have added clinical benefit in disseminated disease, demonstrating that even in "castration resistant disease" androgens may still be supporting prostate cancer growth

TABLE 1 | Natural compounds obtained from marine organisms or microorganisms with anti-prostate cancer activities.

Natural compound	Sort	Name of microorganisms	Cell type	Observation	Activity	Mechanism of action	Refs
C-phycocyanin	Proteins	*Limnothirix* sp.	LNCaP	*In vitro*	Induction of apoptosis	Increase of radical oxygen species (ROS) generation; increase of caspase-9 and caspase-3 activities.	Gantar et al. (2012)
Eusynstyelamide B(1)	Alkaloids	*Didemnum candidum*	LNCaP	*In vitro*	Antiproliferation	Induction of G2 cell cycle arrest; increase of CHK2 phosphorylation; upregulation of p21CIP1/WAF1; decrease of CDC2 expression.	Liberio et al. (2015)
Frondoside A(2)	Triterpene glycosides	*Cucumaria okhotensis*	DU145 LNCaP PC3 22Rv1 VCaP	*In vivo* *In vitro*	Antiproliferation Induction of apoptosis Inhibition of metastasis Inhibition of tumor growth	Induction of G2/M cell cycle arrest; upregulation of Bax, Bad, PTEN, cleavage of PARP and caspase-3; downregulation of anti-apoptotic proteins (survivin and Bcl-2); inhibition of pro-survival autophagy by upregulation of phospho-mTOR.	Dyshlovoy et al. (2016)
Galiellalactone(3)	Ketones	*Galiella ruffle*	DU145 LNCaP PC3	*In vivo* *In vitro*	Induction of apoptosis Inhibition of tumor growth	Inhibition of Stat3 activity; downregulation of the expressions of Bcl-2, Bcl-xL, c-myc and cyclin D1.	Hellsten et al. (2008)
Chaetocin(4)	Ketones	*Trichoderma virens*	PC3	*In vivo* *In vitro*	Antiangiogenesis Inhibition of tumor growth	Disruption of the HIF-1α/p300 complex.	Cook et al. (2009)
Chetomin(5)	Ketones	*Trichoderma virens*	PC3	*In vivo* *In vitro*	Antiangiogenesis Inhibition of tumor growth	Disruption of the HIF-1α/p300 complex.	Cook et al. (2009)
Gliotoxin(6)	Ketones	*Trichoderma virens*	PC3	*In vivo* *In vitro*	Antiangiogenesis Inhibition of tumor growth	Disruption of the HIF-1α/p300 complex.	Cook et al. (2009)
Halichondramide(7)	Trisoxazol-e macrolides	*Chondrosia corticata*	PC3	*In vivo*	Antiproliferation Inhibition of metastasis	The suppression of PRL-3 via downregulation phosphoinositide 3-kinase (PI3K) subunits p85 and p110 the expression; downregulation of matrix metalloproteases (MMPs).	Shin et al. (2013)
Lejimalide B(8)	Macrolide-s	*Eudistoma cf. rigida*	LNCaP PC3	*In vivo*	Antiproliferate Induction of apoptosis	Induction of G0/G1 cell cycle arrest and expression of p21waf1/cip1; downregulation of the expression of cyclin A, E, D survivin, p21B and BNIP3.	Wang et al. (2008b)
Jasplakinolide(9)	Cyclopent-apeptides	*Jaspis johnstoni*	LNCaP PC3 TSUPrl	*In vitro*	Antiproliferation	Not investigated.	Senderowicz et al. (1995)
Malformin A1(10)	Cyclopent-apeptides	*Aspergillus niger*	LNCaP PC3	*In vitro*	Antiproliferation Induction of apoptosis and necrosis	Induction of mitochondrial damage and autophagy.	Liu et al. (2016)
Stellettin A(11)	Triterpene-s	*Geodia japonica*	LNCaP	*In vivo*	Induction of oxidative stress and apoptosis	Upregulation of FasL and caspase-3 expression.	Liu et al. (2006)
Niphatenone B(12)	Glycerol ethers	*Niphates digitalis*	LNCaP PC3	*In vitro*	Antiproliferation	Binding with the activation function-1 (AF1) region of the AR N-terminus domain (NTD).	Meimetis et al. (2012)
4H-1,3-dioxin-4-one-2,3,6-trimethyl	Dioxin	*Trichoderma atroviride*	PC3	*In vitro* *In vivo*	Induction of apoptosis	Increase of expression of caspase -3	Ks et al. (2019)

(Continued on following page)

TABLE 1 | (*Continued*) Natural compounds obtained from marine organisms or microorganisms with anti-prostate cancer activities.

Natural compound	Sort	Name of microorganisms	Cell type	Observation	Activity	Mechanism of action	Refs
Alternol	unknown	*mutant fungus*	PC-3; 22RV1; BPH1	*in vitro*	Antiproliferation; Induction of apoptosis;	Interaction with multiple Krebs cycle enzymes	Li et al. (2019)
Hapalindole H (13)	indole-alkaloid	*Fischerella muscicola*	PC-3	*in vitro*	Antiproliferation;	Through the intrinsic mitochondrial pathway	Acua et al. (2018)
Heteronemin (14)	sesterterpenoid	*Hyrtios* sp.	LNcap; PC3	*In vitro* *In vivo*	Induction of apoptosis	Oxidative and ER Stress Combined with the Inhibition of Topoisomerase II and Hsp90	Lee et al. (2018)
xanthoquinodin JBIR-99 (15)	Quinolines	*Parengyodontium album* MEXU 30054	PC-3	*in vitro*	Induction of apoptosis	Though intrinsic and extrinsic apoptotic pathways	Anaya-Eugenio et al. (2019b)
Giluterrin (16)	alkaloid	*Aspergillus terreus* P63	PC-3	*in vitro*	Antiproliferation	Not investigated	Gubiani et al. (2019)
Elaiophylin (17)	antibiotic	*Actinomycete streptomyces*	22Rv1 ; VCaP	*in vitro* *in vivo*	blocking RORg transcriptional regulation activities	Inhibition of the expression of RORg target genes AR and AR variant	Zheng et al. (2020)
Urupocidin C (18)	bicyclic guanidine alkaloid	*Monanchora pulchra*	22Rv1; LNCaP	*in vitro*	Induction of apoptosis	Though mitochondria targeting	Dyshlovoy et al. (2020)
Pseudopterosin H	diterpene glycosides	*Pseudopterogorgia elisabethae*	PC-3	*in vitro*	reducing PC-3 cell viability	Inducing apoptosis and downregulating the production of intracellular reactive oxygen species	Bowers et al. (2021)
Nalidixic acid (19)	quinolone antibiotic	*Streptomyces* sp. (C-7)	PC3	*in vitro*	cytotoxic effect	Not investigated	Arora et al. (2018)
Discorhabdin L (20)	alkaloid	*Latrunculia* sp.		*in vivo*	Inhibition of cell growth	Not investigated	Harris et al. (2018)

(Morgentaler, 2009). These data support the notion that prostate cancer, in most cases, is a hormone (androgen) sensitive disease.

Overview of the Mechanisms of Castration-Resistant Prostate Cancer

Historically, there are much debate about the mechanisms of castration resistance, which are mainly summarized as the following by recent studies: canonical AR signaling, relying on AR nuclear translocation and AR-DNA binding, and non-nuclear AR signaling which requires neither AR nuclear translocation nor AR-DNA binding(Qin and Bin, 2019; Pisano et al., 2021).

Canonical AR Signaling

The potential mechanisms of canonical AR signaling that lead to CRPC can be categorized into three parts. 1) common alterations in AR, which can lead to AR increase its sensitivity to very low levels of androgens or constitutive activation of AR signaling; 2) AR activation by androgens converted from adrenalandrogens or synthesized intratumorally via the *de novo* route; 3) alterations in cofactors of the AR pathway (**Figure 1**).

Common Alterations in AR

One possible mechanism by which the prostate cancer becomes resistant to androgen deprivation therapy is alterations in *AR*, including *AR* amplification or overexpression, *AR* mutations and truncated *AR* lacking ligand-binding domains (*AR*ΔLBD). Thus, these changes in AR increase its sensitivity to very low levels of androgens or lead to constitutive activation of AR signaling. Strictly speaking, this mechanism of prostate cancers is not androgen-independent and the responses still depend on AR and androgen.

AR *Amplification or Overexpression.* Despite low circulating androgens in the CRPC patients, one potential mechanism that would allow tumor cell proliferation is by promoting the expression of the AR itself, which increases ligand-occupied receptor content (Feldman and Feldman, 2001). Plenty of studies have shown that approximately 50% of tumors that become castration resistant after ADT have amplified the AR gene, the most frequent genetic alteration reported for CRPC tumors, whereas none of the untreated primary tumors before androgen ablation had an AR gene amplification (Robinson et al., 2015; Djusberg et al., 2017).

Numerous studies provide the simplest explanation of how increased androgen receptor expression leads to resistance to anti-androgen therapy. According to one study, a three-to-five-fold increase in receptor levels could compensate for low ligand levels and restore androgen receptor signaling in xenotransplantation models. (Chen et al., 2004). Although tumors with AR amplification have

TABLE 2 | Alkaloids obtained from plants with anti-prostate cancer activities.

Natural compound	Botanical name	Cell type	Observation	Activity	Mechanism of action	Refs
Anibamine(21)	*Aniba panurensis*	DU145 M12 PC3	*In vitro*	Antiproliferation Inhibition of metastasis and invasion	Binding to the chemokine receptor CCR5.	Zhang et al. (2010b)
Berberine(22)	*Coptis chinensis* Franch.	DU145 LNCaP PC3 PC82 PWR1E	*In vitro* *In vivo*	Antiproliferation Induction of apoptosis and programmed necrosis	Inhibition of p53-Cyp-D association via decreasing the ROS production; downregulation of HIF-1α and VEGF expression; induction of G1 and G2/M cell cycle arrest by activating ATM-Chk1; induction of caspase-3 and -9 activation; upregulation of bax/bcl-2 expression.	Wang et al. (2012), Zhang et al. (2014)
Pipernonaline(23)	*Piper longum* L.	DU145 LNCap PC3	*In vitro*	Induction of apoptosis	Induction of sub-G1 and G0/G1 cell cycle arrest through downregulation of CDK2, CDK4, cyclin D1 and cyclin E; upregulation of procaspase-3/PARP cleavage; induction of ROS production and intracellular Ca2+, and mitochondrial membrane depolarization.	Lee et al. (2013b)
Piperlongumine(24)	*Piper longum* L.	LNCaP PC3	*In vitro*	Antiproliferation	Induction of G2/M phase cell cycle arrest; upregulation of bax/bcl-2 expression; activation of caspase-3; downregulation of PARP expression.	Kong et al. (2008)
Sanguinarine(25)	*Argemone mexicana* L.	PC3E RWPE1 TEM4-18	*In vitro*	Cytotoxicity	Inhibition of RGS17 activity.	Bodle et al. (2017)
Piperine (26)	*Piper nigrum* L. *and Piper longum* L.	DU145	*in vitro*	Inhibition of migration progression	downregulating the Akt/mTOR/MMP-9 signaling pathway	Yuan and Ying (2018)
Neferine (27)	*Nelumbo nucifera* Gaertn.	PC3, $CD44^+$ CSCs ; LNCaP	*in vitro*	Inhibition of proliferation and migration	through p38 MAPK/JNK activation	Erdogan and Turkekul (2020)

increased levels of AR, the signal for cell proliferation presumably continues to require androgen (Visakorpi et al., 1995). Maybe this can explain why tumors with castration resistance have increased sensitivity to androgens in a low androgen environment.

AR *Mutations.* In CRPC, the frequency of *AR* mutations in pre-treated tumors is 5–30% (Grasso et al., 2012; Robinson et al., 2015; Kumar et al., 2016). Most mutations identified in CRPC were located in the AR-LBD. These alterations could facilitate AR signaling in CRPC by offering: 1) ligand facilitation, thereby inducing AR activation even in the presence of low or absent levels of androgens and 2) agonist properties to AR antagonists (Coutinho et al., 2016). In addition, mutations can also occur in the AR-NTD that account for about a third of all mutations described in AR. And mutations can usually cause alterations that contribute to AR transactivation, such as facilitated recruitment of co-factors and other components of the transcriptional machinery, promoted N/C interaction, increased response to DHT activation and enhanced protein stability and nuclear retention (Network C. G. A., 2015; Coutinho et al., 2016).

Truncated* AR *Lacking Ligand-Binding Domains (ARΔLBD). Latest RNA sequencing data from big data sets, strongly suggests that constitutively active ARΔLBD may play a role in 40–50% of patients with CRPC (Robinson et al., 2015). Compared with hormone naïve PCa, ARΔLBDs are frequently upregulated in CRPC, and may serve as an adaptive response to therapies targeting the androgen/AR-signaling axis (Guo et al., 2009; Li et al., 2013). The recent genomic data on unique exon junctions reveals that at least 12 distinct *AR-V* mRNA species are detectable in primary PCa and 23 in CRPC (Abeshouse et al., 2015). However, among these variants, AR-V3/AR-V7 appears to be one of the most abundantly and ubiquitously expressed isoforms in our screening of a panel of human prostate cancer cell lines and tissues (Guo et al., 2009; Schweizer and Plymate, 2016). In addition, nonsense mutations leading to premature chain termination (Q641X, formerly Q640X) as well as enzymatic cleavage (tr-AR) were also shown to induce ARΔLBDs (Haile and Sadar, 2011). F. Zengerling et al. reported that inhibition of IGF-1R resulted in a down-regulation of AR, Q641X and AR-V7 signaling in PCa cells (Zengerling et al., 2016), which suggests that IGF-1/IGF-1R axis is a modulator of the ARΔLBD signaling, providing a rationale by targeting growth factor receptor for CRPC treatment.

AR Activation by DHT Synthesized Intratumorally via the de novo *Route or Converted From Adrenal Androgens*

There are two possible ways for the initial substrates to convert to intratumoral DHT in CRPC. The first way is that androgens are synthesized intratumorally via the *de novo* route and the second is that androgens are converted from adrenal androgens.

TABLE 3 | Flavanoids obtained from plants with anti-prostate cancer activities.

Natural compound	Botanical name	Cell type	Observation	Activity	Mechanism of action	Refs
Apigenin(28)	Distributed in various plants	C4-2B DU145 PC3 22Rv1	*In vitro* *In vivo*	Antiproliferation Anti-invasion Suppression of prostate cancer growth	Binding with IKKα; inhibition of NF-κB/p65 activity; inhibition of apoptosis proteins and Ku70-Bax interaction; inhibition of tumor suppressor ER-β degradation; inhibition of class I HDACs expression; inhibition of ABCB1 expression and sensitivity improvement of docetaxel-resistant prostate cancer cells to docetaxel treatment.	Zhu et al. (2013), Salmani et al. (2017)
Baicalein(29)	*Scutellaria baicalensis* Georgi	LNCaP PC3	*In vitro* *In vivo*	Antiproliferation Inhibition of tumor growth	Induction of G1 cell cycle arrest; inhibition of androgen receptor (AR) expression.	Haimson et al. (2005)
Cajanol(30)	*Cajanus cajan* (L.) Huth	PC3	*In vitro*	Induction of apoptosis	Induction of G1 and G2/M cell cycle arrest; modulation of the ERa-dependent PI3K pathway and induction of GSK3 and CyclinD1 activation.	Haimson et al. (2005)
Cryptocaryone(**31**)	*Cryptocarya wightiana* Thwaites	PC3	*In vitro*	Antiproliferation Induction of apoptosis	Induction of caspase-8 and 3 activation; upregulation of DR5 surface expression; induction of Fas clustering and the association of downstream signaling molecules, including FADD and procaspase-8; induction of DR4 and DR5 aggregation.	Chen et al. (2010)
CG901(32)	*Artocarpus altilis* (Parkinson) Fosberg	C4-2B DU145 PC3	*In vitro* *In vivo*	Antiproliferation	Selective inhibition of prostate cancer cell lines proliferation and mouse xenograft growth by inhibiting the expression of STAT3 target genes.	Jeon et al. (2015a)
Daidzein(33)	*Glycine max* (L.) Merr.	DU145 LNCaP PC3	*In vitro* *In vivo*	Antiproliferation Induction of apoptosis	Decrease the expression of VEGF and AR genes; induction of G2/M phase in the PC3 cells by downregulating Cyclin B1 and CDK1, and upregulating CDK inhibitors (p21 and p27); upregulation of Fas ligand (FasL) and the expression of proapoptotic Bim; downregulation of the expression of p-FOXO3a and increase of the nuclear stability of FOXO3a.	Labow and Layne, (1972)
Fisetin(34)	Distributed in various plants	DU145 LNCaP PC3 22Rv1	*In vitro* *In vivo*	Antiproliferation Inhibition of tumor growth	Downregulation of the expression of NudC protein; downregulation of MMP-2 and MMP-9 expressions.	(Shimoi, 1998; Afaq et al., 2008; Khan et al., 2008; Chien et al., 2010; Suh et al., 2010; Mukhtar et al., 2015)
Formononetin(35)	*Trifolium pratense* L.	PC3 RWPE1	*In vitro* *In vivo*	Antiproliferation Induction of apoptosis	Induction of G0/G1 phase cell cycle arrest; inhibition of the IGF-1/IGF-1R pathway and alteration of the Bax/Bcl-2 ratio; downregulation of expression levels of cyclin D1 and CDK4.	(Huang et al., 2013; Bi, 2014; Li et al., 2014)
Flavokawain B(36)	*Piper methysticum* G.Forst.	DU145 PC3 LNCaP LAPC4	*In vitro* *In vivo*	Antiproliferation Induction of apoptosis	Selective inhibition on androgen receptor (AR)-negative prostate cancer cell growth; induction of apoptosis with associated increased expressions of proapoptotic proteins: death receptor-5, Bim, Puma and downregulation of XIAP and survivin expressions.	Tang et al. (2010)

(Continued on following page)

TABLE 3 | (*Continued*) Flavanoids obtained from plants with anti-prostate cancer activities.

Natural compound	Botanical name	Cell type	Observation	Activity	Mechanism of action	Refs
Genistein(37)	*Glycine max* (L.) Merr.	DU145 PC3 PC-3M	*In vitro* *In vivo*	Inhibition of migration	Prevention of metastasis by directly binding to MEK4 and downregulation of p38 expression; downregulation of expression and activity of MMP-2.	(Li and Sarkar, 2002; Hsu et al., 2010)
Ginkgetin(38)	*Ginkgo biloba* L.	DU145 LNCaP PC3	*In vitro* *In vivo*	Antiproliferation Induction of apoptosis Inhibition of tumor growth	Induction of G0/G1 cell cycle arrest; selective suppression of STAT3 Tyr705 phosphorylation but not through inhibiting upstream tyrosine kinases and tyrosine phosphatase.	Jeon et al. (2015b)
Isoliquiritigenin(39)	Distributed in various plants	D4-2B LNCaP	*In vitro* *In vivo*	Antiproliferation Inhibition of tumor growth	Downregulation of the expression of NudC protein; downregulation of MMP-2 and MMP-9 expressions.	Zhang et al. (2010a)
Isoangustone A(40)	*Ginkgo biloba* L.	DU145 PC3	*In vitro* *In vivo*	Antiproliferation Induction of apoptosis Inhibition of tumor growth	Induction of p27kip1 tumor suppressor gene accumulation by attenuating p27kip1 at Thr 187 phosphorylation; inhibition of CDK2 activation through binding with the CDK2 complex; inhibition of mTOR kinase activity by binding with the mTOR complex.	Lee et al. (2013a)
Luteolin(41)	Distributed in various plants	LNCaP PC3	*In vitro* *In vivo*	Antiproliferation Prevention of metastasis	Inhibition of ANO1 expression; inhibition of the expression and/or function of ARs via regulation of prostate derived Ets transcription factor(PDEF); inhibition of IGF-1/IGF-1R system; decrease of the expression of E-cadherin through MDM.	Seo et al. (2017)
Licochalcone A(42)	*Glycyrrhiza glabra* L.	LNCaP	*In vitro*	Antiproliferation Induction of apoptosis	Induction of G2/M cell cycle arrest; downregulation of cyclin B1 and cdc2 expression; inhibition of phosphorylation of retinoblastoma (Rb); decrease of expression of transcription factor E2F, cyclin D1, CDKs 4 and 6; increase of expression of cyclin E.	Su et al. (2017)
Quercetin-6-C-b-D-glucopyranoside(43)	*Ulmus wallichiana* Planch.	DU145 LNCaP PC3 RWPE1	*In vitro*	Antiproliferation Induction of apoptosis	Induction of apoptosis via induction of cleaved PARP and Cas-3; induction of G0/G1 cell cycle arrest; inhibition of reactive oxygen generation and AKT/mTOR survival pathway via directly binding with aryl hydrocarbon receptor.	Hamidullah et al. (2015)
Quercetin(44)	Distributed in various plants	DU145 LNCaP PC3	*In vitro* *In vivo*	Induction of apoptosis	Increase of expression of c-Jun and its phosphorylation; decrease of expression of HSP72; intervention of BaP toxicity.	Asea et al. (2001), Yuan et al. (2004), Chaudhary et al., (2007), Aalinkeel et al. (2008)
Xanthohumol(45)	*Humulus lupulus* L.	BPH-1 PC3	*In vitro*	Antiproliferation Induction of apoptosis	Induction of S and Sub G1 cell cycle arrest; inhibition of NFkB activity and expression. Upregulation of pro- apoptotic proteins Bax and p53 expression.	Colgate et al. (2007)

(Continued on following page)

TABLE 3 | (*Continued*) Flavanoids obtained from plants with anti-prostate cancer activities.

Natural compound	Botanical name	Cell type	Observation	Activity	Mechanism of action	Refs
Vitexicarpin(46)	*Vitex rotundifolia* L.f.	PC3	*In vitro*	Induction of apoptosis	Induction of G2/M cell cycle arrest.	Meng et al. (2012)
2′,4′-dihydroxychalcone (47)	*Herba oxytropis*	PC3	*In vitro*	Induction of apoptosis	Induction of G1/S cell cycle arrest.	Sheng et al. (2015)
Auriculasin (48)	*Flemingia macrophylla* var. *philippinensis* (Merr. & Rolfe) H.Ohashi	LNCaP-FGC ; RWPE-1	*In vitro* *In vivo*	Induction of apoptosis; antiproliferation	Regulation of the PI3K/AKT/mTOR pathway in LNCaP prostate cancer cells;ROS accumulation	Cho et al. (2018)
Naringenin (49)	*citrus fruits and tomatoes*	MAT-LyLu cells	*In vitro*	Inhibition of metastasis	Blocking voltage-gated sodium channels	Gumushan Aktas and Akgun (2018)
Casticin (50)	*Vitex rotundifolia* L.f.,	DU 145	*In vitro*	Inhibition of prostate cancer cell metastasis	Inhibition of the protein levels of AKT, GSK3αβ, Snail, and MMPs (MMP-2, -9, -13, and -7); diminision of the expressions of NF-κB p65, GRB2, SOS-1, MEK,p-ERK1/2, and p-JNK1/2	Lin et al. (2019)

DHT Intratumorally via the* de novo *Route. The use of cholesterol for *de novo* steroidogenesis requires the components of the steroidogenic machinery present in the adrenals and gonads, including steroidogenic acute regulatory proteins, CYP11A1 and CYP17A1 (Miller and Auchus, 2011), which may play important roles in prostate cancer (Locke et al., 2008). Comparisons between primary prostate cancer and CRPC demonstrate that the transcription levels of these proteins are upregulated in CRPC (Montgomery et al., 2008) and CYP17A1 protein is detectable in a subset of metastatic CRPC cases (Efstathiou et al., 2012). In contrast to steroidogenesis in the adrenals and gonads, CRPC expresses steroid-5α-reductase (SRD5A1) with obvious 5α-reductase activity (Chang et al., 2011). One of the functions of robust SRD5A enzyme activity is that any *de novo* steroidogenesis would likely occur through the back door pathway that bypasses the requirement for T and involves 5-reduction of a 21-carbon steroid (progesterone or 17α-hydroxyprogesterone) instead of a 19-carbon androgen (Shaw et al., 2000; Auchus, 2004). Although this biochemical pathway may be engaged in CRPC, the relatively lengthy eight enzymatic steps required for conversion from cholesterol to DHT, the abundance of adrenal precursors present in serum, and the much closer pathway proximity of adrenal precursors to DHT, together suggest that adrenal precursors serve as the major substrate pool.

DHT Converted From Adrenal Androgens. There are two possible pathways from adrenal precursor steroids to DHT (Luu-The et al., 2008; Chang and Sharifi, 2012). The canonical adrenal pathway is the route that results in T synthesis as the penultimate metabolite, which undergoes 5-reduction to DHT (Scher and Sawyers, 2005; Ryan and Tindall, 2011; Hofland et al., 2012; Stein et al., 2012). This pathway is probably favored in the field because of the general notion that T must be the precursor to DHT and T is frequently detectable at concentrations greater than DHT in CRPC, as occurs with gonadal androgen physiology (Titus et al., 2005; Montgomery et al., 2008). In this pathway, DHEA is converted by 3β-hydroxysteroid dehydrogenase (3βHSD) to androstenedione (AD), which is then 17-keto reduced by aldo-keto reductase 1C3 (AKR1C3) or 17βHSD3 to T, the immediate precursor to DHT. The second possible pathway is that AD, like T, a 3-keto, △4-steroid, is also a potential substrate for SRD5A (Tomkins, 1957). AD is reduced to 5α-androstanedione (5α-dione), which then becomes the immediate precursor to DHT. The 5α-dione pathway is the major pathway for the synthesis of DHT in CRPC (Chang et al., 2011).

Alterations in Cofactors of the AR Pathway

Resistance to AR-targeted therapies in CRPC was also associated with genomic and transcriptomic alterations in coregulators of the AR pathway. Expression of 50 of the ~200 AR-associated coregulators is aberrant in clinical CRPC specimens (Liu et al., 2017). For example, a higher frequency of mutations in *FOXA1*, the gene encoding a pioneer factor that facilitates AR chromatin binding and transcriptional activation, was found in CRPC (12%) than in primary prostate cancer (4%) (Watson et al., 2013; Abeshouse et al., 2015). In addition, as one class of coregulators, steroid receptor coactivators (SRC-1, SRC-2 and SRC-3) play a key role in facilitating aberrant AR signaling in CRPC e. There have been studies reported that all 3 SRCs is elevated in CRPC (Taylor et al., 2010; Grasso et al., 2012; Abeshouse et al., 2015; Beltran et al., 2016; Bernemann et al., 2016). GATA2, another AR pioneer factor in the AR signaling axis, is aberrant expressed in CRPC and associated with poor outcome (He et al., 2014; Yan et al., 2014). Gupta et al. detected genomic copy number changes of circulating tumor cells from 16 patients with CRPC resistant to abiraterone or enzalutamide and revealed that multiple genes encoding AR coregulators had copy number alterations, including copy number gains BRD4 (43.75%) (Gupta et al., 2017). Moreover, changes of AR corepressors also play a key role in CRPC. For example, loss of activity of the key nuclear receptor corepressors NCOR1 and NCOR2, is prevalent

TABLE 4 | Terpenoids obtained from plants with anti-prostate cancer activities.

Natural compound	Botanical name	Cell type	Observation	Activity	Mechanism of action	Refs
Artemisinin(51)	*Artemisia annua* L.	DU145 PC3	*In vitro*	Induction of apoptosis	Increase of synthesis, and cleavage of procaspase-9, cleavage of caspase-3, and PARP-1 degradation.	Nakase et al. (2009)
Betulinic Acid(52)	*Bacopa monnieri* (L.) Wettst.	LNCaP	*In vitro* *In vivo*	Induction of apoptosis Inhibition of tumor growth	Activation of selective proteasome-dependent degradation of the transcription factors specificity protein 1(Sp1), Sp3, and Sp4; regulation of survivin and VEGF expression; downregulation of NF-kappaB expression.	Chintharlapalli et al. (2007)
Celastrol(53)	*Tripterygium wilfordii* Hook.f.	LNCaP PC3	*In vitro* *In vivo*	Induction of apoptosis	Accumulation of ubiquitinated proteins and three natural proteasome substrates IKB-A, Bax, and p27.	Wolfram et al. (2014)
Caseamembrin C(54)	*Casearia membranacea*	PC3	*In vitro*	Antiproliferation Induction of apoptosis	Downregulation of Bcl-2 and Bcl-xL expression; upregulation of Mcl-1S protein and activation of caspase-9 and caspase-3.	Huang et al. (2004)
Glycyrrhizin(55)	*Glycyrrhiza glabra* L.	DU145 LNCaP	*In vitro*	Antiproliferation Induction of apoptosis	Downregulation of the expression of caspase-3 and caspase-8.	Thirugnanam et al. (2008)
Lycopene(56)	Distributed in various plants	PC3	*In vitro* *In vivo*	Antiproliferation Antimetasis Induction of apoptosis	Inhibition of the androgen receptor element, resulting in decreased PSA velocity; inhibition signaling of insulin-like growth factor-I (IGF-I); decrease of the expression of αvβ3 and αvβ5 integrin.	(Bureyko et al., 2009; Wertz, 2009; Tang et al., 2011; Holzapfel et al., 2013)
Oridonin(57)	*Isodon rubescens* (Hemsl.) H.Hara	PC3	*In vivo* *In vitro*	Induction of apoptosis Inhibition of tumor growth Antiproliferation	Increase of expression of P21 and the mRNA level of beclin; increase of caspase-3 activity.	(Deepak and Handa, 2000; Xiang et al., 2012; Ming et al., 2016)
Pachymic acid(58)	*Poria cocos*	DU145 LNCaP	*In vitro*	Antiproliferation Induction of apoptosis	Decrease of prostaglandin synthesis and AKT activity.	Gapter et al. (2005)
Pseudolaric acid B(59)	*Larix kaempferi* (Lamb.) Carrière	DU145	*In vitro*	Antiproliferation Induction of apoptosis	Increase of ROS generation and Bcl-2 degradation.	Zhao et al. (2012)
Sugiol(60)	Salvia prionitis Hance	DU145 LNCaP PC3	*In vitro*	Antiproliferation	Induction of G0/G1 cell cycle arrest; downregulation the expression of STAT3; interaction with TKT.	Jung et al. (2015)
Triptolide(61)	*Tripterygium wilfordii* Hook.f.	DU145 LNCaP PC3 22Rv1	*In vitro* *In vivo*	Antiproliferation Induction of apoptosis	Decrease of CDK7-mediated phosphorylation; disruption of the phosphorylation of AR through XPB/CDK7.	Fei et al. (2016)
Ursolic Acid(62)	*Distributed in various plants*	DU145 LNCaP	*In vitro* *In vivo*	Antiproliferation Induction of apoptosis	Upregulation of DR5 activation of JNK; inhibition of NF-κB and STAT3 pathways.	(Deepak and Handa, 2000; Shanmugam et al., 2011; Meng et al., 2015)
Zerumbone(63)	*Zingiber zerumbet* (L.) Roscoe ex Sm.	DU145 HRPC PC3	*In vitro*	Antiproliferation Induction of apoptosis	Increase of MPM-2 expression; increase of Bcl-2 and Bcl-xL phosphorylation; induction of Cdk1 activity; induction of Cdc25C downregulation.	Chan et al. (2015)
β-elemene(64)	Distributed in various of plants	DU145 PC3	*In vitro*	Antiproliferation Induction of apoptosis	Downregulation of Bcl-2 expression; increase of cytochrome c; activation of PARP and caspase-3, -7, -9, and -10.	Li et al. (2010)

(Continued on following page)

TABLE 4 | (*Continued*) Terpenoids obtained from plants with anti-prostate cancer activities.

Natural compound	Botanical name	Cell type	Observation	Activity	Mechanism of action	Refs
7-xylosyl-10-deacetyl paclitaxel(65)	*Taxus wallichiana* Zucc.	PC3	*In vitro*	Antiproliferation Induction of apoptosis	Induction of G2/M cycle arrest; upregulation of pro-apoptotic Bax and Bad protein expressions and downregulation of anti-apoptotic Bcl-2 and Bcl-XL expressions.	Jiang et al. (2008)
25-OCH3-PPD (GS25)(66)	*Panax notoginseng* (Burkill) F.H.Chen	DU145 LNCAP PC3	*In vitro* *In vivo*	Induction of apoptosis	Decrease of MDM2 protein level; increase of the protein levels of the wild-type p53, Bax, cleaved-PARP.	Wang et al. (2008a)
Bakuchiol (67)	*Cullen corylifolium* (L.) Medik.	PC3	*In vitro*	Inhibition of cell proliferation and migration;	Inactivating NF-κB signaling via AR and ERβ	Miao et al. (2017)
Afrocyclamin A (68)	*Androsace umbellata* (Lour.) Merr.	DU145	*In vitro*; *In vivo*	Induction of apoptosis; inhibition of migration and invasion; inhibition of cell growth	Via the PI3k/Akt/mTOR pathway	Sachan et al. (2018)
Corosolic acid (69)	*Eriobotrya japonica* (Thunb.) Lindl.; *Crataegus pinnatifida* Bunge; *Actinidia chinensis* Planch.	PC-3; DU145; 22RV1; WPMY-1	*In vitro*	Inhibition of cell growth; Induction of apoptosis	The activation of endoplasmic reticulum (ER) stress-associated two pro-apoptoticsignaling pathways	Ma et al. (2018)
3-oxo-4-oxa-A-homo-25,26,27-trinordammarano-24,20-lactone triterpene (70)	*Cleome khorassanica* Bunge & Bien	DU-145 ; LNCaP	*In vitro*	Cell growth inhibition	Not investigated	Sajjadi et al. (2018)
20,25-dihydroxy-3-oxodammarane triterpene (71)	*Cleome khorassanica* Bunge & Bien	DU-145 ; LNCaP	*In vitro*	Cell growth inhibition	Not investigated	Sajjadi et al. (2018)
Britanin (72)	*Inula linariifolia* Turcz.	PC-3 ; PC-3-LU ; DU-145	*In vitro*; *In vivo*	Inhibition of cell proliferation, migration, and motility	Through PI3K/Akt/NF-κB Signaling Pathways	Zeng et al. (2020)
Linalool (73)	*herbs, spices and fruits*	22Rv1	*In vitro*; *In vivo*	Antiproliferation; Induction of apoptosis; Inhibition of migration invasion	Mitochondria-mediated intrinsic and death-receptor-mediated extrinsic pathways; inhibition of expression of Ki-67 and PCNA in the 22Rv1 xenograft model.	Zhao et al. (2020)
β-elemonic acid (74)	*Boswellia carterii* Birdw	DU145, PC-3 and 22RV1	*In vitro*	Induction of apoptosis	Through the suppression of JAK2/STAT3/MCL-1 and NF-κB signal pathways	Bao et al. (2021)
Heliantriol B2 (75)	*Chuquiraga erinacea* subsp. erinacea (Asteraceae)	PC-3; LNCaP	*In vitro*	Antiproliferation; Induction of apoptosis; Inhibition of migration invasion	Not investigated	Castro et al. (2019)

in CRPC due to mutation and/or deletion (Grasso et al., 2012; Abeshouse et al., 2015; Kumar et al., 2016).

Non-nuclear AR Signaling

Trafficking from the nucleus into the cytoplasm, AR may have unexpected consequences because AR has known functions in the cytoplasm, which is called non-genomic signaling (Foradori et al., 2008). One of the main characteristics of non-nuclear signaling is its rapidity with which it occurs. When steroid receptors stay in the cytosol, they can undergo several protein–protein interactions within seconds to minutes after steroid stimulation, which activates a variety of signaling pathways to promote the development of CRPC (**Figure 2**).

PI3K/AKT Signaling Pathway

The PI3K/AKT pathway is one of the most frequently activated signal transduction pathways in human cancer, including prostate cancer(Hoxhaj and Manning, 2020; Park et al., 2018; Braglia et al., 2020). Alterations of the PI3K/AKT pathway, including altered expression, mutation, and copy number alterations, have been reported in 42% of primary prostate tumors and 100% of metastatic tumors (Taylor et al., 2010). Androgens induce the accumulation of TORC2 complex, rapamycin insensitive chaperone of mTOR and stress activated protein kinase interacting protein 1 in the nucleus, thus stimulating TORC2 to activate Akt (Fang et al., 2012). Activated AKT can stimulate many downstream functions via

TABLE 5 | Polyphenols obtained from plants with anti-prostate cancer activities.

Natural compound	Botanical name	Cell type	Observation	Activity	Mechanism of action	Refs
Atraric acid (76)	*Prunus africana* (Hook.f.) Kalkman	LNCaP	*In vitro*	Inhibition of prostate cancer cell growth	Inhibition of AR nuclear translocation.	Schleich et al. (2006)
Curcumin(77)	*Curcuma longa* L.	DU145 PC3	*In vitro*	Antiproliferation	Inhibition of the expression of MT1-MMP and MMP2 proteins; inhibition of the DNA-binding ability of NICD.	Yang et al. (2017)
Ellagic Acid(78)	Distributed in various plants	LNCaP	*In vitro*	Antiproliferation Induction of apoptosis	Increase of Bax/Bcl2 ratio and increase caspases 3, caspases 6, caspases 8, and caspases 9 and PARP cleavage; inhibition of mTOR activation and reduction of intracellular levels of β-catenin; downregulation of the expressions of anti-apoptotic proteins, silent information regulator 1 (SIRT1), human antigen R (HuR) and heme oxygenase-1 (HO-1).	Vanella et al. (2013)
Gallic Acid(79)	*Toona sinensis* (Juss.) M.Roem.	DU145 PC3 22Rv1	*In vitro* *In vivo*	Inhibition of migration Induction of apoptosis	Activation of Chk1 and Chk2 and inhibition of Cdc25C and Cdc2 activities; blocking of the p38, JNK, PKC and PI3K/AKT signaling pathways and downregulation of NF-κB protein level; inhibition of MMP2 and MMP 9 gene expression.	(Hastak et al., 2003; Kaur et al., 2009)
Gossypol(80)	*Gossypium hirsutum* L.	DU145 PC3	*In vitro* *In vivo*	Antiproliferation Induction of apoptosis	Downregulation of Bcl-2 and Bcl-xl and the upregulation of Bax; activation of caspase3, caspase8 and caspase9 through the ROS-independent mitochondrial dysfunction pathway and the increase of PARP cleavage; suppression of the expression of AP-1and NF-κB blocked the activation of VEGF receptor 2 kinase.	Huang et al. (2006)
Honokiol(81)	Magnolia officinalis	PC3 LNCaP Myc-CaP	*In vitro* *In vivo*	Induction of apoptosis Inhibition of prostate tumor growth	Activation of Bax and/or Bak; decrease of expression of c-Myc.	Shigemura et al. (2007)
Nordihydroguaiaretic acid(82)	*Larrea tridentata* (DC.) Coville	PC3	*In vitro* *In vivo*	Inhibition of migration Antiproliferation	Suppression of NRP1 function.	Li et al. (2016)
Obovatol(83)	*Magnolia obovata* Thunb.	PC3 LNCaP	*In vitro*	Induction of apoptosis	Inhibition of TNF-α and TPA-induced DNA binding activity of NF-κB; translocation inhibition of p65 and p50 into nucleus via decreasing IκB phosphorylation; increase of the apoptotic genes expression: Bax, caspase-3, caspase-9; inhibition of the anti-apoptotic genes expression: Bcl-2, inhibitor of apoptosis protein (IAP-1) and X chromosome IAP (XIAP).	Soyong et al. (2009)
Resveratrol(84)	*Reynoutria japonica* Houtt.	DU145	*In vitro* *In vivo*	Induction of apoptosis	Downregulation of Bcl-2 and Bcl-xL and upregulation of Bax; activation of caspases-3, -8 and -9 and increased PARP cleavage.	Chang et al. (2013)
Procyanidin	*Arachis hypogaea* L.	DU145	*In vitro*	Antiproliferation	Induction of apoptotic cell death and cell cycle arrest at S phase;increase of intracellular ROS level and the decrease of Bcl-2/Bax ratio, and the activation of p53 and caspases-3	Chen et al. (2018)
Sinapic acid (85)	*various vegetables and fruit species*	PC3; LNCaP	*In vitro*	Antiproliferation;Induction of apoptosis;Inhibition of migration invasion	Increase of the expression of BAX, CASP3, CASP8, CYCS, FAS, TIMP-1 and CDH1,decrease of expression of MMP-9 in PC-3 cells;decrease of in the expressions of CDH2, MMP-2 and MMP-9 in LNCaP cells;increase of caspase-3 activity	Eroğlu et al. (2018)

(Continued on following page)

TABLE 5 | (*Continued*) Polyphenols obtained from plants with anti-prostate cancer activities.

Natural compound	Botanical name	Cell type	Observation	Activity	Mechanism of action	Refs
Carvacrol (86)	*Origanum and Thymus*	Human OSCC Tca-8113; SCC-25	*In vitro*	Antiproliferation, inhibition of metastasis and invasion; Induction of apoptosis	Regulating the cell cycle-associated proteins (P21, CCND1 and CDK4) and apoptosis-associated proteins (Cox2, Bcl-2, and Bax); inhibiting P-FAK, and reducing β-catenin, ZEB1, and MMP-2/9 expression	Dai et al. (2016)
Hispolon (87)	*Phellinus linteus*	DU145	*In vitro*	Induction of apoptosis	Via modulation of mitochondrial and STAT3 pathways	Masood et al. (2019)

TABLE 6 | Lignans obtained from plants with anti-prostate cancer activities.

Natural compound	Botanical name	Cell type	Observation	Activity	Mechanism of action	Refs
Deoxypodophyllotoxin(88)	*Anthriscus sylvestris* (L.) Hoffm.	LNCaP PC3	*In vitro*	Antiproliferation Induction of apoptosis	Accumulation of the reactive oxygen species, intracellular Ca^{2+}; increase of mitochondrial membrane potential.	Kim et al. (2013)
Magnolol (89)	*Magnolia officinalis* Rehder & E.H.Wilson	PC3 PrEC	*in vivo*	Cytotoxicity	Decrease of MMP-2 and MMP-9 expression; decrease of the level of phosphorylated AKT.	Lee et al. (2009)
Silibinin(90)	*Silybum marianum* (L.) Gaertn.	LNCaP 22Rv1	*In vitro* *In vivo*	Antiproliferation	Activation of acetyl-CoA carboxylase; reduction in hypoxia-induced NADPH oxidase (NOX) activity; increase of the lipid accumulation and NOX activity; downregulation of HIF-1α expression, lipid levels, clonogenicity and NOX activity.	Ting et al. (2016)
VB1(91)	*Vitex negundo* L.	PC3	*In vitro* *In vivo*	Induction of apoptosis	Activation of PARP cleavage.	Zhou et al. (2009)
Magnoline (92)	*Phellodendri amurensis cortex*	22RV1	*In vitro*	Antiproliferation	Disturbance of nutrition metabolism and energy metabolism	Sun et al. (2018)
Arctigenin (93)	*Arctium lappa* L.	PC-3M	*In vitro*	Induction of apoptosis and autophagy	Via PI3K/Akt/mTOR inhibition	Sun et al. (2021)
2-(5′-allyl-4‴,9‴-dihydroxyphenyl-furan)-3-hydroxy-7-methoxy-8-(6″,7″-dimethyl-furan-2″-one)-chromen-4-one. (94)	*Hosta plantaginea* (Lam.) Aschers	LNCaP	*In vitro*	Inhibition of cell growth	Not investigated	Wei et al. (2020)
2-(5′-allyl-3‴,5‴,9‴-trihydroxy-4‴-methoxyphenyl-furan)-3-hydroxy-7,8-furan-ring-chromen-4-one. (95)	*Hosta plantaginea* (Lam.) Aschers	LNCaP	*In vitro*	Inhibition of cell growth	Not investigated	Wei et al. (2020)
2,3-dehydrosilychristin (96)	*Hosta plantaginea* (Lam.) Aschers	LNCaP	*In vitro*	Inhibition of cell growth	Not investigated	Wei et al. (2020)
silychristin A (97)	*Hosta plantaginea* (Lam.) Aschers	LNCaP	*In vitro*	Inhibition of cell growth	Not investigated	Wei et al. (2020)

its kinase activity, including glycogen synthase kinase 3 (GSK3), tuberous sclerosis complex (TSC), FOXO transcription factors, NF-kappa-B and Bcl-2 family members BAD, which regulate a range of cellular processes (Liu et al., 2009; Courtney et al., 2010). It is estimated that genomic phosphatase and tensin homolog gene (PTEN) alterations, which is a negative inhibitor of PI3K/AKT pathway, occur in 9–45% of high-grade prostate intra-epithelial neoplasia (HG-PIN), 20–60% of localized prostate cancer, and up to 100% of cases of metastatic prostate cancer (Taylor et al., 2010; Jia et al., 2013).

Src Signaling Pathway

Preclinical studies have confirmed that non receptor tyrosine kinase c-Src and Src family kinase (SFK) regulate a complex signal network, driving the development of castration-resistance prostate cancer and bone metastasis. (Cai et al., 2011). After the establishment of bone metastasis, prostate cancer cells destroy the balance of osteoclasts and osteoblasts by secreting a variety of molecules, such as growth factors and cytokines that disrupt the normal process of bone maintenance and reconstruction (Yang et al., 2001; Mundy, 2002). The balance is in favor of

TABLE 7 | Other compounds obtained from plants with anti-prostate cancer activities.

Natural compound	Sort	Botanical name	Cell type	Observation	Activity	Mechanism of action	Refs
Aloe-emodin(98)	Anthraquin-ones	*Rheum palmatum* L.	PC3	*In vitro* *In vivo*	Antiproliferation Suppression of prostate cancer growth	Binding with mTOR complex2 ; Inhibition of mTORC2 kinase activity and downstream substrates of mTORC2, AKT and PKCa activity.	Liu et al. (2012a)
Calcitriol(99)	Secosteroids	Distributed in various plants	C4-2B LNCaP	*In vitro*	Antiproliferation Induction of apoptosis	Upregulation of Vitamin D receptor (VDR) expression; induction of BAX expression; increase of cleaved caspase-3 and downregulation of cdk2 expression.	Ben-Eltriki et al. (2016)
Diindolylmethane(100)	Indoles	Distributed in various plants	LNCaP PC3	*In vitro*	Antiproliferation Induction of apoptosis	Induction a [Ca^{2+}] rise by evoking phospholipase C-dependent Ca^{2+} release from the endoplasmic reticulum and Ca^{2+} entry via phospholipase A2-sensitive store-operated Ca^{2+} channels; regulation of FOXO3a/ β-catenin/GSK-3β signaling; regulation of estrogen metabolism and acting as an antiandrogen, finally leading downregulation of the AR and PSA.	Wang et al. (2016a)
Diallyl Trisulfide(101)	Trisulfides	*Allium sativum* L.	DU145 LNCap PC3	*In vitro* *In vivo*	Induction of apoptosis	Downregulation of XIAP protein expression.	Kim et al. (2011)
Embelin(102)	Quinones	*Embelia ribes* Burm.f.	C4-2B DU145 PC3	*In vitro*	Antiproliferation Induction of apoptosis	Induction of G1 cell cycle arrest; induction of apoptosis by triggering caspase 3 activation and PARP cleavage; inhibition of survivin expression by inhibiting AKT/NF-κB pathway.	Xu et al. (2017)
ESK246(103)	Glycosides	*Pittosporum venulosum*	LNCaP	*In vitro*	Antiproliferation	Inhibition of leucine uptake, leading to reduced mTORC1 signaling, cell cycle protein expression and cell proliferation.	Wang et al. (2014)
Ginsenoside Rg3(104)	Steroids	*Panax ginseng* C.A.Mey.	PC-3M	*In vitro*	Antiproliferation Antimetastasis	Suppression of aquaporin 1 (AQP1) water channel protein expression by activating p38 MAPK.	Pan et al. (2012)

(Continued on following page)

TABLE 7 | (*Continued*) Other compounds obtained from plants with anti-prostate cancer activities.

Natural compound	Sort	Botanical name	Cell type	Observation	Activity	Mechanism of action	Refs
Guggulsterone(105)	Steroids	*Commiphora mukul* (Hook. ex Stocks) Engl.	DU145 LNCaP PC3 PrEC	*In vitro*	Antiproliferation Induction of apoptosis	Increase of Bax expression, downregulation of Bcl-xl and Bcl-2 expression; increase of caspase-9 and caspase-8 cleavage; increase of ROI generation by activating JNK; selective inhibition of androgen receptor promoter activity in LNCaP cell.	Singh et al. (2005)
Guttiferone F(106)	Prenylated benzophenones	*Allanblackia stuhlmannii* (Engl.) Engl.	LNCaP PC3	*In vitro* *In vivo*	Induction of apoptosis	Increase of sub-G1 fraction and DNA fragmentation; down-regulation of androgen receptor expression and phosphorylation of ERK1/2.	Li et al. (2015c)
Indole-3-carbinol (I3C)(107)	Indoles	Distributed in various plants	LNCaP	*In vitro*	Antiproliferation	Induction of G1 cell-cycle arrest and downregulation of AR expression and inhibition of AR promoter activity.	Hsu et al. (2005)
Juglone(108)	Quinones	*Juglans mandshurica* Maxim.	LNCaP	*In vitro*	Antiproliferation Induction of apoptosis	Downregulation of AR expression; increase of caspase-3 and -9 activity.	Jiang et al. (2013)
Marchantin M(109)	Diphenyls	*Asterella angusta*	DU145 LNCaP PC3	*In vitro*	Induction of apoptosis	Inhibition of the 20S proteasome activity; induction of microtubule-associated protein-1 light chain-3 beta (LC3B) expression and conversion; induction of RNA-dependent protein kinase-like ER kinase activity; suppression of the PI3K/AKT/ mammalian target of rapamycin axis through preventing the activation and expression of AKT.	Jiang et al. (2013)
Moniliformediquinone (110)	Phenanthradiquinones	*Dendrobium moniliforme* (L.) Sw.	DU145 PC3	*In vitro* *In vivo*	Antiproliferation Induction of apoptosis Inhibition of tumor growth	Induction of S cell cycle arrest; induction of DNA damage response associated with Chk1, Chk2, c-Jun and JNK activation; induction of caspase-2,-3,7,8 and -9 cleavage through mitochondrial membrane loss and cytochrome c release.	Hsu et al. (2014)

(Continued on following page)

TABLE 7 | (*Continued*) Other compounds obtained from plants with anti-prostate cancer activities.

Natural compound	Sort	Botanical name	Cell type	Observation	Activity	Mechanism of action	Refs
Oleuropein (111)	Glycosides	*Olea europaea* L.	LNCaP DU145 BPH-1	*In vitro* *In vivo*	Anti-oxidation Cytotoxicity Inhibition of tumor cell growth and invasiveness	Not investigated.	Acquaviva et al. (2012)
Physapubescin B (112)	Steroids	*Physalis pubescens* L.	PC3	*In vitro In vivo*	Antiproliferation	Downregulation of Cdc25C protein expression; induction of G2/M cell cycle arrest; decrease of Cdc25C level and increase of levels of CyclinB1, P21 and p-Cdk1 (Tyr15).	Ding et al. (2015)
Pristimerin (113)	Esters	Distributed in various plants	PC3 LNCaP C4-2B	*In vitro*	Induction of apoptosis	Inhibition of proteasomal chymotrypsin-like activity assay and polyubiquitinated protein accumulation ; Interaction with the proteasomal β5 subunit in a conformation suitable for proteasome inhibition; increase of caspase-3 activation.	Yang et al. (2008)
Phenethyl-Isothiocyanat(PEITC) (114)	Isothiocyan-ates	Distributed in various plants	C4-2B DU145 LNCaP PC3	*In vitro* *In vivo*	Antiproliferation Induction of apoptosis	Increase in the G2-M phase; downregulate AR expression through inhibition of the transcription factor Sp1 and p300/CBP-associated factor (PCAF); upregulation of miR-194 via directly targeting BMP1, and downregulation of BMP1 led to decrease expression of key oncogenic matrix metalloproteinase, MMP2 and MMP9.	Wang et al. (2006), Yin et al. (2009), Jiang et al. (2013), Zhang et al. (2016)
Putrescine-1,4-dicinnamide (115)	Phenylprop-anoids	Distributed in various plants	DU145	*In vitro*	Induction of apoptosis	Increase the caspase-3 activity; increase of ROS generation.	Russo et al. (2007)
Physalins A(116)	Secosteriods	*Physalisalkekengi* var. *franchetii*	C4-2B 22Rv1	*In vitro*	Antiproliferation Induction of apoptosis	Inhibition of JNK and ERK activation; downregulation of AR expression and PAS expression.	Han et al. (2011)

(Continued on following page)

TABLE 7 | (*Continued*) Other compounds obtained from plants with anti-prostate cancer activities.

Natural compound	Sort	Botanical name	Cell type	Observation	Activity	Mechanism of action	Refs
Physalins B (117)	Secosteriods	*Physalisalkekengi* var. *franchetii*	C4-2B 22Rv1	*In vitro*	Antiproliferation Induction of apoptosis	Inhibition of JNK and ERK activation; downregulation of AR expression and PAS expression.	Han et al. (2011)
Physachenolide C (118)	Steroids	Disbributed in various plants	LNCaP PC3	*In vitro* *In vivo*	Cytotoxicity Inhibition of tumor cell growth	Not investigated.	Xu et al. (2015)
Reevesioside A (119)	Glycosides	*Reevesia formosana*	DU145 PC3	*In vitro*	Antiproliferation Induction of apoptosis	Induction of G1 cell cycle arrest by the downregulation of several related cell cycle regulators, including cyclin D1, cyclin E and CDC25A; increase of association between RB and E2F1 and the subsequent suppression of E2F1 activity via decreasing RB phosphorylation.	Leu et al. (2014)
Scopoletin(120)	Coumarins	*Erycibe obtusifolia*	LNCaP	*In vitro*	Antiproliferation Induction of apoptosis	Induction of G2/M cell cycle arrest by the downregulation of cyclin D1 expression.	Li et al. (2015a)
Sulforaphane(SNF) (121)	Sulfides	Disbributed in various plants	TRAMP C1	*In vitro* *In vivo*	Anti-oxidation	Regulation of Nrf2's CpGs demethylation and reactivation.	Zhang et al. (2013)
Thymoquinone (122)	Quinones	*Nigella sativa*	C2-2B DU145 LNCaP PC3	*In vitro*	Induction of apoptosis	Not investigated.	Trang et al. (1993)
Wedelolactone(123)	Esters	*Wedelia sinensis*	DU145 PrEC PC3 LNCaP	*In vitro*	Induction of apoptosis	Increase of c-JNK and caspase-3 activity by downregulation of PKCε without AKT inhibition.	Koka et al. (2010), Sarveswaran et al. (2012)
Z-Ligustilide(124)	Esters	*Angelica sinensis* (Oliv.) Diels	TRAMP C1	*In vitro*	Cytotoxicity	Increase of Nrf2 expression via the Nrf2 promoter CpGs demethylation.	Su et al. (2013)
2,5-dimethylphenol(125)	Phenols	*Chlaenius cordicolli*	PC3	*In vitro*	Cytotoxicity	Induction of $[Ca^{2+}]i$ rise through PKC-regulated store-operated Ca^{2+} channels and PLC-dependent Ca^{2+} release from the endoplasmic reticulum.	Wang et al. (2016a)
3-oxo-tirucallic acid(126)	Lupanic acids	*Boswellia carteri* Birdw.	LNCaP PC3	*In vitro* *In vivo*	Induction of apoptosis Inhibition of tumor cell growth	Inhibition of Akt activity and Akt signaling pathways, including glycogen synthase kinase-3β and BAD phosphorylation, and nuclear accumulation of p65, androgen receptor, β-catenin, and c-Myc.	Estrada et al. (2010)

(Continued on following page)

TABLE 7 | (*Continued*) Other compounds obtained from plants with anti-prostate cancer activities.

Natural compound	Sort	Botanical name	Cell type	Observation	Activity	Mechanism of action	Refs
3-α-acetoxy-tirucallic acid(127)	Lupanic acids	*Boswellia carteri* Birdw.	LNCaP PC3	*In vitro* *In vivo*	Induction of apoptosis Inhibition of tumor cell growth	Inhibition of Akt activity and Akt signaling pathways, including glycogen synthase kinase-3β and BAD phosphorylation, and nuclear accumulation of p65, androgen receptor, β-catenin, and c-Myc.	Estrada et al. (2010)
3-β-acetoxy-tirucallic acid(128)	Lupanic acids	*Boswellia carteri* Birdw.	LNCaP PC3	*In vitro* *In vivo*	Induction of apoptosis Inhibition of tumor cell growth	Inhibition of Akt activity and Akt signaling pathways, including glycogen synthase kinase-3β and BAD phosphorylation, and nuclear accumulation of p65, androgen receptor, β-catenin, and c-Myc.	Estrada et al. (2010)
6α-acetoxyanopterine(129)	Esters	*Anopterus macleayanus*	LNCaP PC3	*In vitro*	Antiproliferation Induction of apoptosis	Interaction with tubulin.	Levrier et al. (2016)
24-epibrassinolide(130)	Brassinoste-roids	Distributed in various plants	DU145 LNCaP	*In vitro* *In vivo*	Antiproliferation; Induction of apoptosis	Induction of G1 cell cycle arrest accompanied by reductions in cyclin D1, CDK4/6 and pRb expression in LNCaP cells; induction of G2/M cell cycle arrest by reductions in cyclin A, cyclin expression in DU145 cells.	Steigerova et al. (2012)
25-OH-PPD (131)	Saponins	*Panax ginseng* C.A.Mey.	LNCaP PC3	*In vitro* *In vivo*	Antiproliferation Induction of apoptosis Inhibition of tumor growth	Induction of G1 cell cycle arrest by downregulation of MDM2, E2F1, Bcl2, cdk2/4/6, and cyclin D1 expressions; increase of p21, p27, and Bax expressions; induction of PARP cleavage and caspases activation.	Wang et al. (2008a)
28-homocastasterone(132)	Brassinosteroids	Distributed in various plants	DU145 LNCaP	*In vitro* *In vivo*	Antiproliferation; Induction of apoptosis	Induction of G1 cell cycle arrest accompanied by reductions in cyclin D1, CDK4/6 and pRb expression in LNCaP cells; induction of G2/M cell cycle arrest via reductions in cyclin A expression.	Steigerova et al. (2012)

(Continued on following page)

TABLE 7 | (*Continued*) Other compounds obtained from plants with anti-prostate cancer activities.

Natural compound	Sort	Botanical name	Cell type	Observation	Activity	Mechanism of action	Refs
2′-Hydroxycinnamaldehyde (133)	Aldehydes	Cinnamomum verum J.Presl	DU145; LNCaP	*In vitro* *In vivo*	Antiproliferation; Induction of apoptosis	Signal transducer and activator of transcription 3 inactivation and reactive oxygen species generation	Yoon et al. (2019)
Methyllucidone (134)	cyclopentenedione	*Lindera erythrocarpa* Makino (Lauraceae)	DU145	*In vitro*	Inhibition of cell growth; Induction of apoptosis	Arrest of the cell cycle at G1 phase; regulation of the expression of the protein tyrosine phosphatase MEG2	Jin et al. (2018)
Ophiopogonin D ' (135)	triterpenoid saponins	Radix Ophiopogonis	PC3 ; DU145	*In vitro* *In vivo*	Induction of apoptosis	Via a RIPK1-related pathway	Lu et al. (2018)
Corchorusoside C(136)	steroid	*Streptocaulon juventas* (Lour.) Merr. (Apocynaceae)	DU-145	*In vitro* *In vivo*	Induction of apoptosis	Inhibition of activity and protein expression of NF-κB (p50 and p65), IKK(α and β), and ICAM-1; decrease of protein expression of Bcl-2 and increase of expression of PARP-1;increase of caspases 3 and 7	Anaya-Eugenio et al. (2019a)
Daucosterol (137)	steroid saponin	*Crateva adansonii* DC (Capparaceae)	LNCaP; DU145;PC3	*In vitro*	Antiproliferation; inhibition of cell growth;Induction of apoptosis	Downregulation of cell cycle proteins (cdk1, pcdk1, cyclin A and B) in DU145 and PC3 cells; downregulation of cdk2 in PC3 cells; downregulation of Akt, pAKT 18 and Bcl-2 proteins;up-regulation of Bax	Zingue et al. (2019)
Cyanidin 3-glucoside (138)	Glycosides	The dark purple glutinous rice (Oryza sativa L.) cultivar Luem Pua (LP)	PC3	*In vitro*	Inhibition of progressive cancer cell behaviors	Inhibit EMT through Smad signaling pathway(s) mediating Snail/E-cadherin expression	Jongsomchai et al. (2020)
Germacrone (139)	Ketones	Rhizoma Curcuma	PC-3;22RV1	*In vitro*	Antiproliferation; Induction of apoptosis	Inhibiting the Akt/mTOR signaling pathway	Yu et al. (2020)
Ineupatolide (140)	Esters	*Carpesium cernuum* L.	PC-3	*In vitro*	Antiproliferation	Promoting apoptosis and arresting the cell cycle in the G2and S phases;	Huang et al. (2021)
Jegosaponin A and B (141 and 142)	Saponins	*Styrax japonica* Siebold et al. Zuccarini.	PC-3	*In vitro* *In vivo*	Exhibiting cell membrane disruptive properties	Not investigated	Nishimura et al. (2021)
Isolobetyol (143)	polyacetylene	*Platycodon grandiflorus* (Jacq.) A.DC.	PC-3	*In vitro*	Antiproliferation	Not investigated	Li, (2020)
Lobetyol (144)	Alkynes	*Platycodon grandiflorus* (Jacq.) A.DC.	PC-3	*In vitro*	Antiproliferation	Not investigated	Li, (2020)
Lobetyolin (145)	Alkynosides	*Platycodon grandiflorus* (Jacq.) A.DC.	PC-3	*In vitro*	Antiproliferation	Not investigated	Li, (2020)

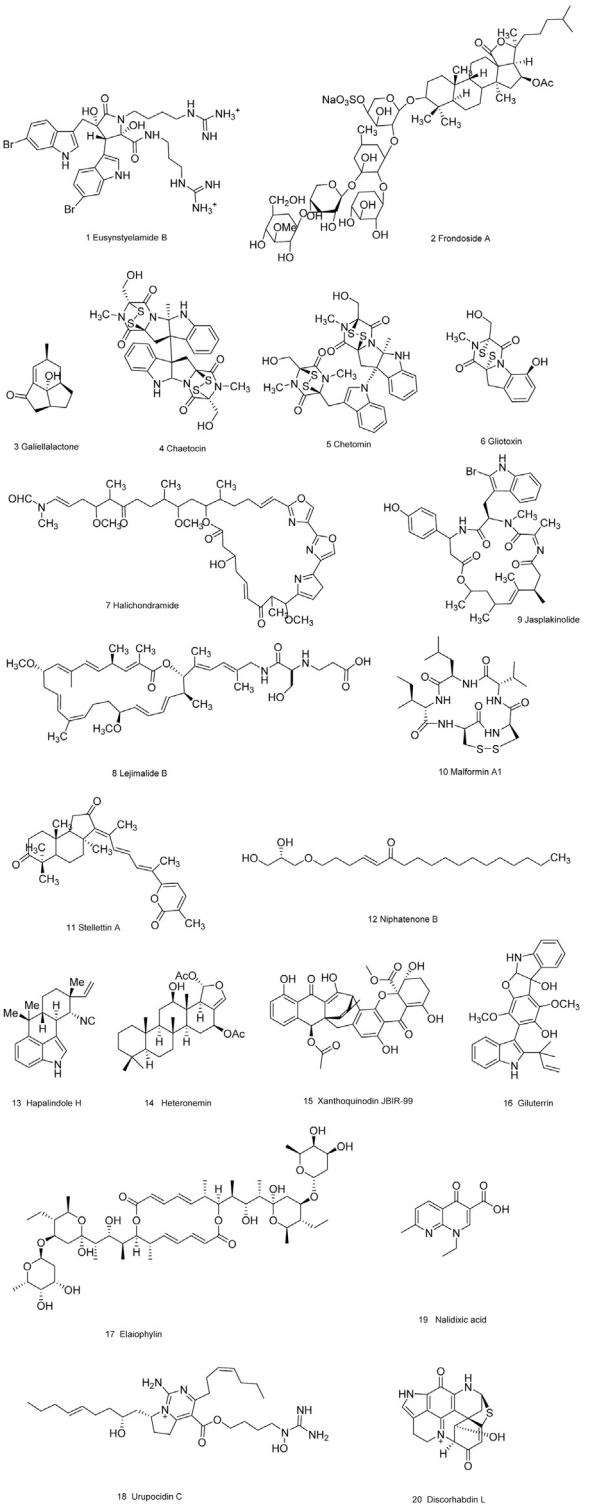


FIGURE 3 | Natural compounds obtained from marine organisms or microorganisms with anti-prostate cancer activities.

osteoblastogenesis, which explains the usual condensing aspect of PCa-derived bone metastases. Src activity specifically affects ruffled borders of osteoclasts (essential for bone resorption), through dynamic regulating the interactions of actin cytoskeleton and formation of podosomes (Horne et al., 2005; Destaing et al., 2011). Src and other SFKs also play important roles in the antiapoptotic signal transduction of RANKL and other tumor necrosis factor family members in osteoclasts (Xing et al., 2001). One essential role for Src in osteoblasts has also been demonstrated that reduction of Src expression decreases osteoblast(responsible for bone formation) proliferation and increases differentiation (Marilena et al., 2000).

Recently, a large number of studies have shown that the activation of SRC is an important mediator of AR signaling. (Asim et al., 2008). AR can form a tertiary complex with the scaffold protein modulator of non-genomic actions of the estrogen receptor (MNAR/PELP1) and Src (Unni et al., 2004). Initially, Src is inactive within this complex. However, when AR binds to Src, this results in the activation of Src in this complex (AR/MNAR/Src) and the subsequent activation of a downstream effector, MEK (Unni et al., 2004). Subsequent studies have shown that AR-induced Src activation can promote cell proliferation through cell cycle progression from G1 phase to S phase (Migliaccio et al., 2002).

MAPKs Signaling Pathway

The MAPKs signaling cascade play important roles in regulating diverse biological functions including cell proliferation, motility and survival, which are essential to prostate carcinogenesis (Rossomando et al., 1989; Armenia et al., 2018; Abida et al., 2019). Studies of DHT-responsiveness in prostate cancer cells show that DHT treatment induces phosphorylation of ERK-1/2 within 1–2 min and peak levels of phosphorylation within 5–10 min (Liao et al., 2013). Activated ERK-1/2 then translocate to the nucleus and directly interact with and phosphorylate transcription factors (TFs), such as nuclear ETS domain-containing Elk1 (Marais et al., 1993; Gille et al., 1995; Yang et al., 1998). Elk1 transcriptionally regulates immediate early genes (IEGs) such as c-fos (Gille et al., 1995; Unni et al., 2004), and regulates the expression of several genes related to cell proliferation (Marais et al., 1993; Unni et al., 2004). In addition, recent studies showed that other molecules induce prostate cancer via MAPK signaling. Jason et al. reported that ADP-ribosylation factor 1 (ARF1), a crucial regulator in vesicle-mediated membrane trafficking and involved in the activation of signaling molecules, promotes the occurrence of prostate cancer via targeting oncogenic MAPK signaling (Davis et al., 2016). Gonzalo et al. reported that epidermal growth factor (EGF) could stimulate G0/G1-S transition via p38 MAPK to overcome the growth restriction of androgen deprivation in prostate cancer cells (Rodriguez-Berriguete et al., 2016).

JAK-STAT3 Signaling Pathway

Janus kinases (JAK) signal transducers and activator of transcription (STAT) pathway play an important role in differentiation, hematopoiesis, immune function and cell growth (Bolli et al., 2003). Recently, accumulating evidence indicated that IL-6 is indispensable for activation of JAK/

TABLE 8 | Extracts obtained from plants with anti-prostate cancer activities.

Extract	Botanical name	Medicinal part	Cell type	Observation	Activity	Mechanism of action	Refs
Ethanol extract	*Vitex negundo* L.	Seed	PC3	*In vitro* *In vivo*	Antiproliferation	Induction of cleavage in poly ADP ribose polymerase protein; upregulation of Bax and downregulation of Bcl-2; increase of caspase-3 and -9.	Zhou et al. (2009)
Methanolic extract	*Aloe perryi* Baker	Fruit	HTB-81	*In vitro*	Induction of apoptosis	Not investigated.	Al-Oqail et al. (2016)
Ethanolic extract	*Annona muricata* L.	Leaf	PC3	*In vitro* *In vivo*	Antiproliferation Inhibition of tumor growth	Not investigated.	Yang et al. (2015)
Aqueous extract	*Camellia sinensis* (L.) Kuntze	Leaf	PC3	*In vitro* *In vivo*	Antiproliferation Induction of apoptosis Inhibition of tumor growth	Increase of Bax/Bcl-2 ratio and decrease of Ki67 protein expression; decrease of blood concentrations of tumor growth factors and tumor concentrations of VEGF and EGF expressions.	Wang et al. (2016b)
Methanolic extract	*Artocarpus altilis* (Parkinson) Fosberg	Leaf and stem	DU145 LNCap PC3	*In vitro* *In vivo*	Antiproliferation Induction of apoptosis Inhibition of tumor growth	Inhibition of STAT3 Ty705 phosphorylation and STAT3 activation.	Jeon et al. (2015a)
Hexane extract	*Juglans regia* L.	Leaf	PC3	*In vitro*	Antiproliferation Induction of apoptosis	Not investigated.	Li et al. (2015b)
Ammonia dichloromethane extract	*Berberis libanotica*	Root	DU145 PC3 22Rv1	*In vitro*	Antiproliferation Inhibition of metastasis	Induction of G0/G1 cell cycle arrest; eradication of self-renewal ability of highly resistant prostate cancer stem cells.	
Supercritical extract	*Azadirachta indica* A.Juss.	Leaf	LNCaP PC3	*In vitro* *In vivo*	Antiproliferation Induction of apoptosis Inhibition of tumor growth	Inhibition of calreticulin, integrin b1, and focal adhesion kinase activation; increase of the AKR1C2 level.	Wu et al. (2014)
Acetone extract	*Chaenomeles japonica* (Thunb.) Lindl. ex Spach	Fruit	PNT1A PC3	*In vitro*	Induction of apoptosis	Increase of Bax/Bcl-2 ration.	Lewandowska et al. (2013)
Hexanic lipidosterolic extract	*Serenoa repens* (W.Bartram) Small	Whole plant	LNCaP PC3	*In vitro*	Induction of apoptosis	Increase of caspase 9 activation and poly (ADP-ribose) polymerase 1 cleavage, and mitochondrial PTP activation.	Baron et al. (2009)
Aqueous extract	*Taraxacum officinale* F.H.Wigg.	Root	C4-2B LNCaP	*In vitro*	Inhibition of metastasis	Decrease of phosphorylation levels of FAK and SRC, and activities of matrix metalloproteinases (MMP-2 and MMP-9).	Sigstedt et al. (2008)
Ethyl acetate extract	*Commiphora mukul* (Hook. ex Stocks) Engl.	Bark	LNCaP PrEC	*In vitro*	Induction of apoptosis	Decrease of Bax expression; suppression of JNK activation.	Xiao et al. (2011)
Aqueous extract	*Cistus creticus* L. ; *Cistus monspeliensis* L.	Whole plant	PZ-HPV-7 PNT1A	*In vitro*	Antiproliferation	Not investigated.	Vitali et al. (2011)
Acidified dimethyl sulfoxide extract	*Morus nigra* L.	Fruit	PC3 CRL1435	*In vitro*	Antiproliferation Induction of apoptosis	Induction of G1 cell cycle arrest; decrease mitochondrial membrane potential.	Turan et al. (2017)

(Continued on following page)

TABLE 8 | (*Continued*) Extracts obtained from plants with anti-prostate cancer activities.

Extract	Botanical name	Medicinal part	Cell type	Observation	Activity	Mechanism of action	Refs
Dichloromethane extract	*Strobilanthes crispa* (L.) Blume	Leaf	DU145 PC3	*In vitro*	Induction of apoptosis	Increase of caspase 3 and/or 7 activity.	Visweswaran et al. (2010)
Punica granatum exeract	*Punica granatum* L.	Seed	LNCaP PC3	*In vitro*	Induction of apoptosis Inbition of metastasis	Upregulation of p21 and p27; increase of JNK phosphorylation; suppression of AKT/ mTOR signaling; modulation of the IGF-IGFBP axis.	Deng et al. (2017)
Hydroalcoholic extract	*Justicia spicigera* Schltdl.	stems; leaves	LNCaP	*In vitro*	Antiproliferation	cytostatic mechanism	Fernández-Pomares et al. (2017)
Ethyl acetate fraction	*Phoenix dactylifera* L. (Ajwa dates)	Fruit	PC3	*In vitro*	Induction of apoptosis	Arrest of the cell cycle in S phase	Mirza et al. (2018)
Ethyl acetate extract	*Kalanchoe flammea* Stapf (Crassulaceae)	Leaves	PC-3; LNCaP; PrEC	*In vitro*; *In vivo*	Induction of apoptosis	Phosphatidylserine translocation; overproduction of reactive oxygen species;release of Cytochrome C at mitochondrial level; activation of caspase-3 and -9;downregulation of apoptosis-related proteins Bcl-2, XIAP, and PKCε and DNA fragmentation and cell cycle arrest	Arias-González et al. (2018)
Hydroalcoholic extracts	*Euphorbia szovitsii* Fisch. & C.A.Mey., U. dioica and *Medicago sativa* L.	aerial parts	PC-3, DU145 ; HDF	*In vitro*	Antiproliferation	Not investigated	Asadi-Samani et al. (2018)
Ethanol extract	*Moringa oleifera flower*	flower	PC-3	*In vitro*	Induction of Apoptosis	Downregulation of AKT Pathway	Ju et al. (2018)
methanolic extract	*Paederia foetida* L.	leaves	PC-3, DU-145,HaCaT	*In vitro*	Inhibition of cell growth, migration; induction of apoptosis	Modulating chromatin modification enzymes and altering pro-inflammatory cytokine gene expression	Pradhan et al. (2019)
Ethanolic extract	*Moringa peregrina* (Forssk.) Fiori	seed	PC-3	*In vitro*	Induction of apoptosis	Cell cycle arrest at sub-G0 phase and DNA fragmentation.	Abou-Hashem et al. (2019)
Ethanolic extract	*dandelion* (Taraxacum officinale) *root* and *lemongrass* (Cymbopogon citratus)	Root		*In vivo*	Induction of apoptosis	Not investigated	Nguyen et al. (2019)
Ethanolic extract	*Glycyrrhiza glabra* (Fabaceae family)	roots	PC-3	*In vitro*	Antiproliferation	Both apoptosis and autophagy mechanisms	Gioti et al. (2020)
Dimethyl sulfoxide extract	*Ganoderma lucidum*	whole plant	PC3	*In vitro*	Induction of apoptosis	Inhibition of Jak-1/ STAT-3 activity	Wang et al. (2020)
Methanolic extract	*Moringa oleifera* Lam.	leaf	DU145; PC-3	*In vitro*	Antiproliferation; induction of apoptosis;G0/G1 cell cycle arrest	Downregulation of Notch signaling ; downregulation of Hedgehog Signaling Pathway	(Khan et al., 2020a; Khan et al., 2020b)
Dichloromethane and methanol extract	*Cecropia pachystachya* Trécul	leaves	PC3	*In vitro*	Senescence induction	β-galactosidase overexpression	Rosa et al. (2020)
Methanolic extract	*Dracocephalum palmatum* Stephan	leaves	PC-3	*In vitro*	Induction of apoptosis	Via the caspase-8-mediated extrinsic pathway	Lee et al. (2020)

(Continued on following page)

TABLE 8 | (*Continued*) Extracts obtained from plants with anti-prostate cancer activities.

Extract	Botanical name	Medicinal part	Cell type	Observation	Activity	Mechanism of action	Refs
Extract of multi-solvent systems(Cyclohexane, Hexane, Diethyl Ether, Ethyl Acetate, Methanol, Water)	*Hippophae rhamnoides* L. and *Hippophae tibetana* Schltdl.	leaves	LNCaP; C4-2	*In vitro*	Antiproliferation	Downregulation of androgen responsive genes, PSA, ELL2, EAF2 and CALR	Masoodi et al. (2020)
Ethanolic extract	*Salvia miltiorrhiza* Bunge.	roots	DU-145	*In vitro*; *In vivo*	Antiproliferation; induction of apoptosis;	Increase of the expression of p53 and reducion of the expression of Bcl-2 proteins	Bae et al. (2020)
Ethanolic extract	*Spirogyra neglecta* (Hassall) Kutzing	whole plant	PC3	*In vitro*	Antimetastasis activity	Inhibiting the Akt signaling pathway	Arjsri et al. (2021)
Methanolic extract	*Artemisia kruhsiana* subsp. alaskana (Rydb.) D.F.Murray & Elven	stems and leaves	PC-3	*In vitro*	Induction of autophagy;	Inhibitions of phosphor (p)-AKT, p-mTOR, Bcl-2, and Bax, activating beclin 1 and LC3 ratio in PC-3 cells	Lee et al. (2021)
Ethanolic extracts	*Treculia africana* Decne. (Moraceae) and *Entandrophragma angolense* Welw (Meliaceae)	whole plants	LNCaP, DU145 and PC3	*In vitro*	Antiproliferation; induction of apoptosis; anti-metastatic effects	Overexpression of caspase-3; low expression of Akt, pAkt and Bcl-2 proteins;a decrease of chemotaxis and cell migration	Zingue et al. (2021)
Ethanolic extracts	*Moringa oleifera* Lam.	Flower	PC-3	*In vitro*	Induction of apoptosis	Downregulation of AKT Pathway	Ju et al. (2018)

STAT pathway, which is involved in the oncogenesis of prostate cancer (Liu X. et al., 2012). Compared with men with normal prostates, benign prostatic hyperplasia, prostatitis and localized disease, approximately 50% of patients with advanced prostate cancer have increased levels of serum IL-6 (Twillie et al., 1995). Upon the binding of IL-6 to the IL-6 receptor, JAK-1 and STAT-3 become activated in sequence (C Schindler and Jr, 1995). L Tam et al. reported that cytoplasmic expression of IL-6 receptor and pSTAT3 Tyr705 are associated with the shortened biochemical recurrence time and death time from hormone relapse, respectively. Therefore, it is reasonable to target this pathway in hormone-refractory prostate cancer treatments (Tam et al., 2007).

Ca^{2+} Signaling Pathway

Ca^{2+}signaling is also involved in prostate cancer progression (Figiel et al., 2019; Chalmers and Monteith et al., 2018). Increased calcium intake from dairy products has been considered as a risk factor for prostate cancer (Foradori et al., 2007; Flourakis and Prevarskaya, 2009). As a primary signaling molecule, extracellular Ca^{2+} works through the Ca^{2+}-sensing receptor (CaR, a G protein coupled receptor) which directly regulates cell signal transduction and the Ca^{2+} channels (Vaz et al., 2015). Depletion of intracellular Ca^{2+} stores serves as a signal for the activation of Ca^{2+} influx across the plasma membrane. The proteins STIM1 and ORAI1 were identified as the key components of store-operated Ca^{2+} entry (SOCE). When Ca^{2+} is released from intracellular Ca^{2+} pool, Ca^{2+} dissociates from a luminal EF hand motif of STIM1. As a consequence, STIM1 proteins aggregate and recruit Orai1 Ca^{2+}channels, which then mediate SOCE (Kilch et al., 2016).

Recently, Huang et al. found that Ca^{2+} via CaR-mediated signaling induces filamin A cleavage, which is an actin-binding protein, and promotes the migration of AR-deficient and highly metastatic prostate cancer cells (Huang et al., 2016). In one additional study, Christian demonstrated that transient receptor potential melastatin 4 channel (TRPM4) is activated by a rise in intracellular Ca^{2+} in prostate cancer cells. Upon activation, a Na^{+} influx via TRPM4 depolarizes the membrane potential, which reduces the driving force for Ca^{2+} and limits SOCE, and thus promotes migration of androgen-insensitive prostate cancer cells (Christian et al., 2015).

Other Genomic Alterations in Castration-Resistant Prostate Cancer

Prostate cancer is characterized by a high genetic heterogeneity due to genomic alterations and instabilities associated with diverse PCa risk factors (Squire et al., 2011; Yap et al., 2016; Ciccarese et al., 2017; Rodrigues et al., 2017), which was evidenced by extensive genomic profiling analysis conducted on primary tumors (Network T. C. G. A., 2015) and on metastatic samples (Dan et al., 2015).

Speckle-type POZ protein (SPOP) is the substrate-binding subunit of a cullin-3 (CUL3)-based E3 ubiquitin ligase complex, which mediates the ubiquitylation and degradation of many target proteins. SPOP binds to the substrates through its N-terminal meprin and traf homology (MATH) domain, whereas it interacts with cullin-3 via BTB domain on its C terminal (Pintard et al., 2003; Xu et al., 2003; Zhuang et al.,

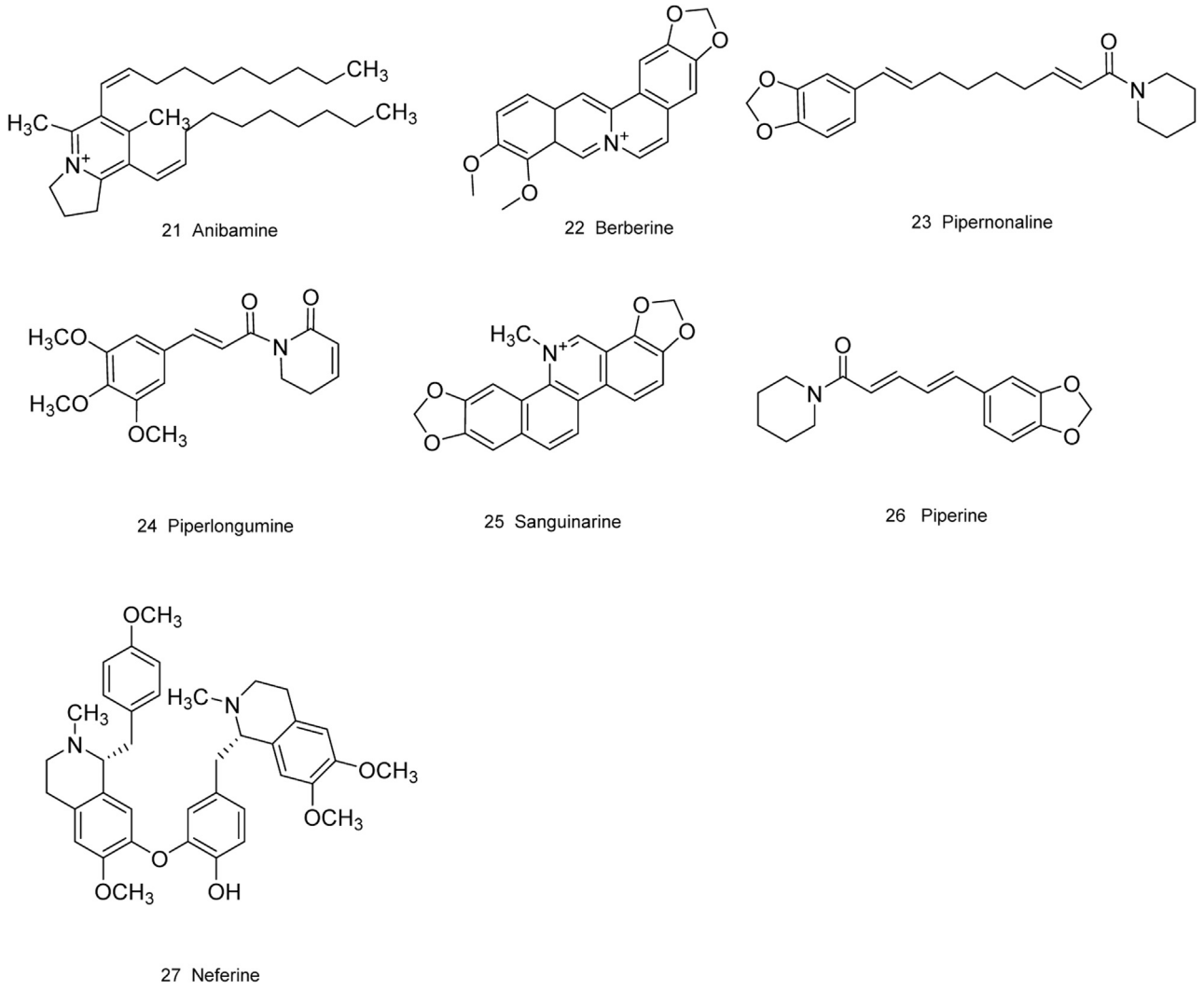


FIGURE 4 | Alkaloids obtained from plants with anti-prostate cancer activities.

2009). Recent cancer whole-genome and exome sequencing studies have shown that *SPOP* is the most frequently mutated gene (in up to 15% of cases) in primary prostate cancer (Barbieri et al., 2012; Network T. C. G. A., 2015). Interestingly, all *SPOP* somatic mutations identified in prostate cancer are clustered in its substrate binding MATH domain, thus having a dominant-negative effect on substrate binding and degradation (Theurillat et al., 2014). Recent studies have unanimously reported that SPOP interacts with bromodomain and extraterminal (BET) proteins that largely act as transcriptional coactivators and play vital roles in cell cycle, apoptosis, migration and invasion in physiological conditions. In addition, SPOP also promotes the ubiquitylation and proteasomal degradation of bromodomain-containing protein 2 (BRD2), BRD3 and BRD4, (Dai et al., 2017; Janouskova et al., 2017; Zhang et al., 2017). Pathologically, BET proteins are frequently overexpressed and are clinically linked to various types of human cancer (French et al., 2003; Crawford et al., 2008; Belkina and Denis, 2012). Recently, Janouskova *et al.* reported prostate cancer–associated *SPOP* mutants impaired its binding to BET proteins, leading to the reduced proteasomal degradation and accumulation of these proteins in prostate cancer cell lines and patient specimens, which subsequently causes resistance to BET inhibitors (Janouskova et al., 2017). Similar study has also demonstrated that *SPOP*-mutated prostate cancer cell lines and patient-derived organoids were intrinsically resistant to BET inhibitor-induced growth arrest and apoptosis (Dai et al., 2017). Furthermore, Dai et al. provided that stabilization of BRD4 may be a molecular mechanism for resistance to BET inhibitors in patients with prostate cancer bearing *SPOP* mutations (Dai et al., 2017). Taken together, these findings offer mechanistic insights into how *SPOP* mutations influence prostate cancer.

The *TMPRSS2-ERG* fusion gene arising from genetic rearrangement (fusion of encoding transmembrane protease

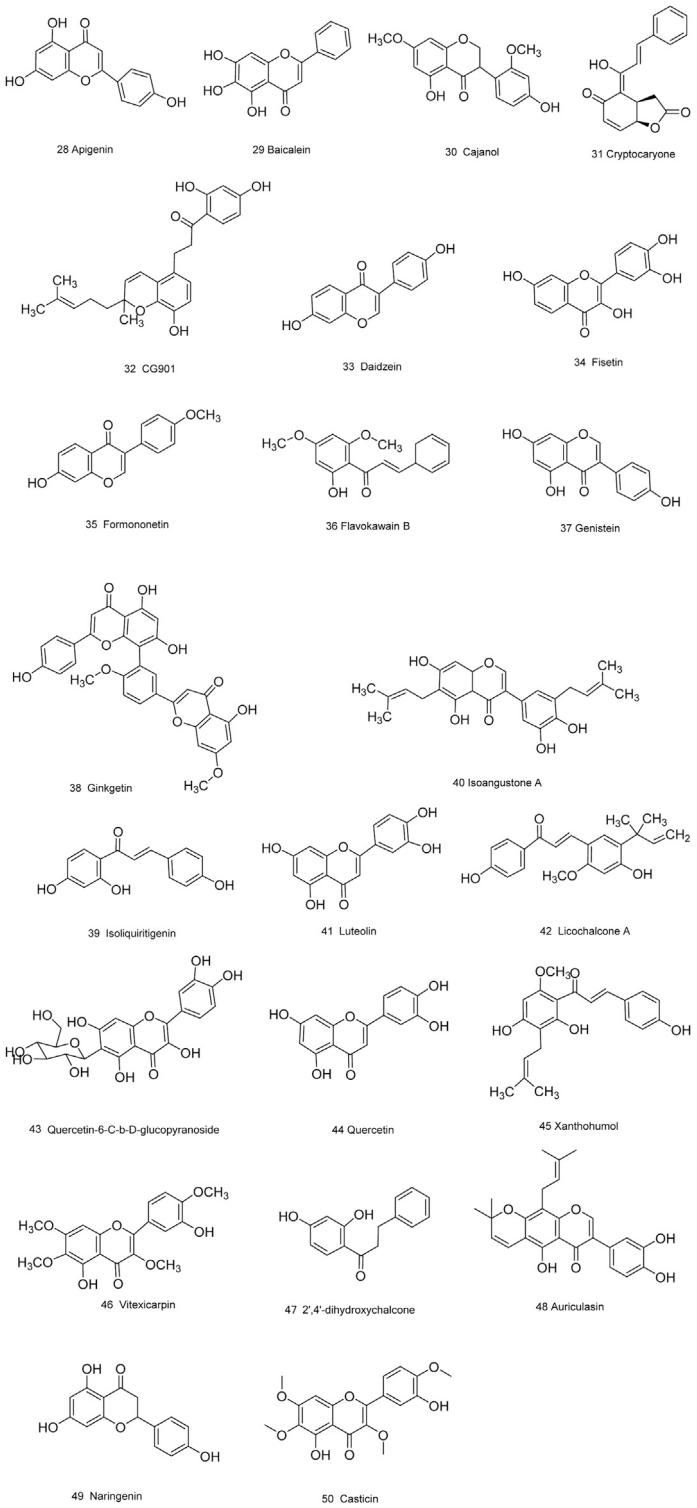


FIGURE 5 | Flavanoids obtained from plants with anti-prostate cancer activities.

serine 2, *TMPRSS2* gene, and *EST*-related gene, *ERG*) has also been a central focus in prostate cancer, which leads to aberrant expression of the *ETS* transcription factor *ERG* (Tomlins et al., 2005; Kandoth, 2013). *TMPRSS2-ERG* is the most common gene rearrangement in prostate cancer and is present in approximately 50% of prostate cancer tissues in Western countries (Cary and

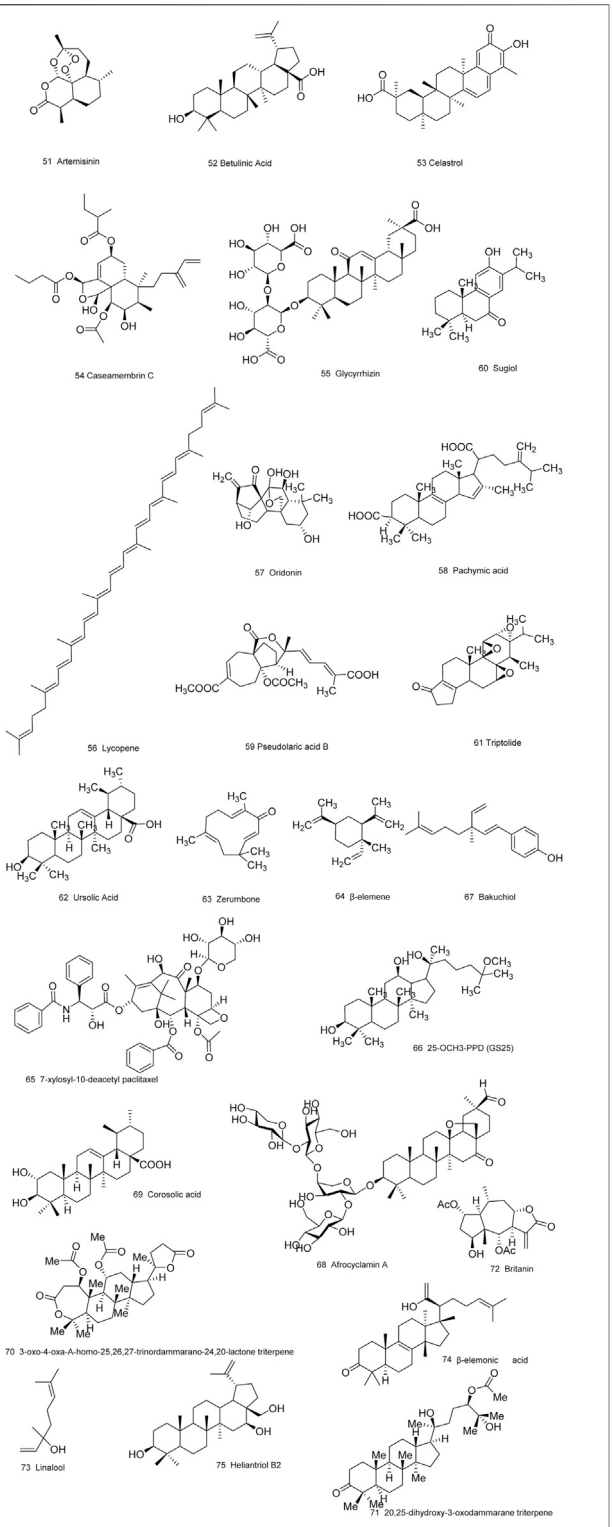


FIGURE 6 | Terpenoids obtained from plants with anti-prostate cancer activities.

Cooperberg, 2013). Previous studies indicated that *ERG* overexpression was driven by hijacking of androgen-responsive elements within the *TMPRSS2* promoter (Tomlins et al., 2005; Wang et al., 2007; Thangapazham et al., 2014). However, Kron et al. found that the molecular process is more complex. Their study indicated that the frequent deletion allows a cluster of regulatory elements (CORE) in the *TMPRSS2* promoter to expand into the rearranged ERG allele. This expanded CORE contains some CREs within the *ERG* locus that can promote *ERG* overexpression. Studies also revealed that overexpressed *ERG* co-opts prostate-specific master regulatory transcription factors, including AR, HOXB13 and FOXA1, in a process facilitated by their physical interaction with ERG and actives NOTCH signaling in primary prostate cancer (Kron et al., 2017). *ERG* overexpression is now an instrumental indicator in the diagnosis of prostate cancer. In addition, Graff et al. recently found that obesity and height might be correlated with the development of *TMPRSS2-ERG*-positive prostate cancer (Graff et al., 2018). Collectively, the functions and mechanisms of *TMPRSS2-ERG* increase the opportunities for finding new therapeutic targets for prostate cancer(Wang et al., 2017; Kong et al., 2020).

NATURAL COMPOUNDS THAT EXERT ANTI-PROSTATE EFFECTS

Natural compounds that have been found to inhibit prostate cancer cells proliferation/tumor growth, promote prostate cancer cells apoptosis, or modulate specific signaling pathways involved in prostate cancer *in vivo* and *in vitro* are categorized and presented according to their source of isolation (marine organisms, microorganisms and plants) and the structural scaffolds. Besides the effects on prostate cancer cells growth or apoptosis, special emphasis was given to the mechanism of action of a compound interfering specific signaling pathways involved in prostate cancer.

Natural Compounds Obtained From Marine Organisms or Microorganisms

As is well known, marine organisms or microorganisms possess the capacity to produce a large amount of diverse secondary metabolites with unique structural features and biological properties. Thus, marine and microbial organisms represent interesting and important sources of single molecules with promising skeletons and significant anti-prostate cancer activity. Up to now, a total of 24 natural compounds (**Figures 3**) isolated from marine organisms have been found to exhibit significant anti-prostate cancer activity either *in vivo* or *in vitro*. Detailed information about the compounds origin, activity and mechanism of action is listed in **Table 1**. Most of them exhibit antiproliferative, apoptosis inducing or metastasis inhibitory activities, with various acting mechanisms such as induction of autophagy, inhibition of AR activation, PI-3K/AKT/mTOR or JAK/STAT signaling pathways (Senderowicz et al., 1995; Liu et al., 2006; Wang WL. et al., 2008; Hellsten et al., 2008; Gantar et al., 2012; Meimetis et al., 2012; Shin et al., 2013; Liberio et al., 2015; Liu et al., 2016). Especially, frondoside A not only caused cell type

TABLE 9 | Chinese herbal compound preparations obtained from plants with anti-prostate cancer activities.

Medical formulation	Composition	Cell type	Observation	Activity	Mechanism of action	Refs
Zyflamend	Rosemary; Ginger; Turmeric; Green tea; Holy basil; Hu zhang; Chinese goldthread; Oregano; Barberry; *Scutellaria baicalensis.*	LNCaP	*In vitro*	Antiproliferation Induction of apoptosis	Inhibition of COX-1 and COX-2 enzyme activities; upregulation of p21 expression; downregulation of AR expression; induction of phosphorylation of Stat3 and PKCα/β.	Bemis et al. (2005)
PC-SPES	*Ganoderma lucidium; Dendranthema morifolium; Isatis indigotica; Glycyrrhiza glabra; Rabdosia rubescens; Panax pseudoginseng; Serenoa repens; Scutellaria baicalensis;.*	DU145 LNCaP PC3	*In vitro* *In vivo*	Induction of apoptosis Inhibition of tumor growth	Induction of G0/G1 and G2/M cell cycle arrest; upregulation of p21waf1 expression and downregulation of Bcl-2 expression.	Hsieh et al. (1997)
LCS101	*Atractylodes macrocephala; Astragalus membranaceus; Glehnia littoralis; Citrus reticulate; Lycium chinense; Ligustrum lucidum; Oldenlandia diffusa; Milletia reticulata; Ophiopogon japonicus; Paeonia obovata; Paeonia lactiflora; Prunella vulgaris; Poriae cocos; Scutellaria barbata.*	DU145 PC3	*In vitro*	Induction of apoptosis	Not investigated	Cohen et al. (2015)

specific cell cycle arrest and induction of caspase-dependent or -independent apoptosis *in vivo* but also significantly inhibited the cell growth of PC-3 and DU145 with a notable reduction of lung metastasis and decrease of circulating tumor cells in the peripheral blood (Dyshlovoy et al., 2016). In addition, gliotoxin, chaetocin and chetomin exhibited antiangiogenic effects *in vitro* and attenuated tumor growth mainly by disrupting the HIF-1α/p300 complex, which makes them attractive molecules for the design of future chemotherapeutic agents (Cook et al., 2009).

Natural Compounds Isolated From Plants

Medicinal plants have always been a very good source of drugs, which could produce plenty of secondary metabolites with high structural diversity and versatile bioactivities. Many candidates with promising anti-prostate activity have been reported, including 7 alkaloids, 23 flavanoids, 25 terpenoids, 13 polyphenols, 10 lignans and 48 other compounds (**Figures 4–9**). Almost all these candidates show anti-prostate cancer activities via anti-proliferation, apoptosis induction or metastasis and invasion inhibition, involved in canonical AR signaling and non-AR signaling like caspase cascades, AKT/mTOR pathway, MAPKs pathway, NF-κB pathway, Ca2+ pathway and JAK/STATs pathway. Additionally, there exist other acting mechanisms, for example, anibamine exhibited anti-prostate cancer activity by binding to the chemokine receptor CCR5; fisetin inhibited tumor growth by downregulating the expression of NudC protein, MMP-2 and MMP-9; lycopene showed anti-prostate cancer effects by inhibiting androgen receptor element and signaling of insulin-like growth factor-1 (Afaq et al., 2008; Khan et al., 2008; Bureyko et al., 2009; Wertz, 2009; Zhang et al., 2010b; Chien et al., 2010; Suh et al., 2010; Tang et al., 2011; Holzapfel et al., 2013; Mukhtar et al., 2015). Detailed information is provided in **Tables 2–7**.

EXTRACTS WITH ANTI-PROSTATE CANCER ACTIVITY

Extracts consist of a group of bioactive natural compounds, which may exert and possess the advantages of synergistic effects against diseases. Recently, nutraceuticals have also received increasing attention as the agents or dietary supplements for cancer prevention and treatment, as well as some extracts derived from edible sources. Thus in this section we will respectively review those extracts and nutraceuticals that have the potential effects against prostate cancer either *in vitro* or in prostate cancer mice models. Chinese herbal compound preparations of more than one medicinal plants that have been reported to inhibit prostate cancer are also presented in this review.

Herbal Extracts

Traditional and folk herbal medicines from medicinal plants offer great potential for the discovery of novel anti-prostate cancer drugs. The plant extracts listed in **Table 8** are complex mixtures, which need further investigations to reveal their bioative constituents through bioguided isolation and to clarify the roles of these different compounds in agaisnt prostate cancer when used alone or in combination. Also, the synergistic effect of the individual active components of these extracts and molecular mechanisms involved need further elucidation in order to evaluate the potential of these compounds as antineoplastic agents.

Chinese Herbal Compound Preparations

There are four traditional Chinese medical formulations reported to display significant anti-prostate cancer properties, that is, Zyflamend, PC-SPES and LCS101, which are composed of different medicinal plants (**Table 9**; Bemis et al., 2005; Hsieh et al., 1997; Cohen et al., 2015). Especially, PC-SPES significantly inhibited prostate tumor growth in tumor-bearing mouse model,

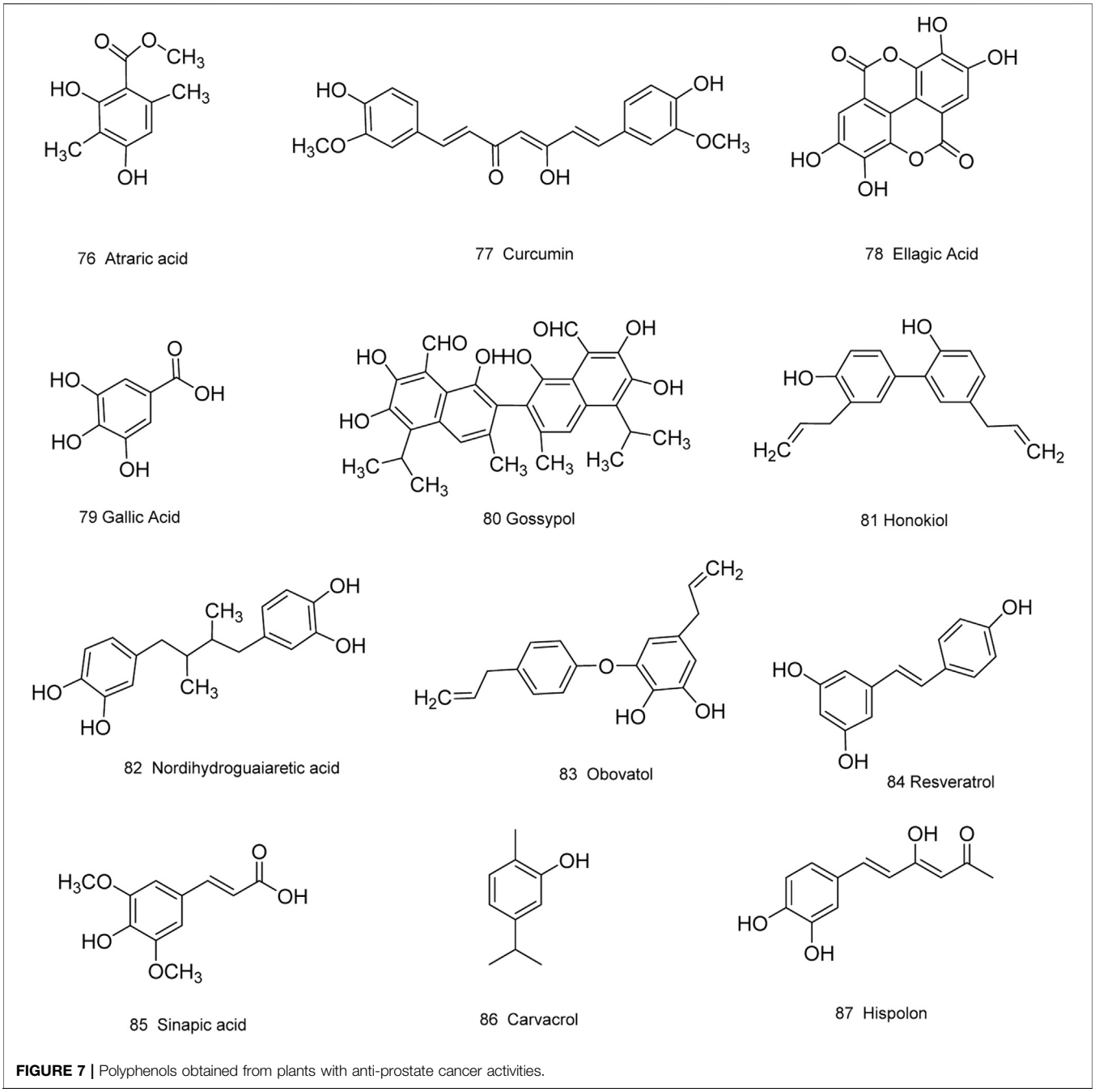


FIGURE 7 | Polyphenols obtained from plants with anti-prostate cancer activities.

mainly through cell cycle arrest and apoptosis induction, which is already clinically utilized for the treatment of clincal patients with prostate cancer (Hsieh et al., 1997).

Nutraceuticals and Extracts Derived From Edible Sources

Nowadays, dietary factors play an increasingly important role in the chemopreventive and/or therapeutic management of cancer (**Table 10**). The study of dietary agents (nutraceuticals or extracts derived from edible sources) in prostate cancer prevention is an important area of research since about 43–80% patients with prostate cancer are on alternative therapy based on dietary modification (Lippert et al., 1999; Nam et al., 1999). There are strong evidences that nutraceuticals and extracts derived from edible spices, vegetables or fruits such as vitamin D, pomegranate and tea polyphenols have demonstrated significant anti-prostate cancer activity when tested either *in vitro* and/or *in vivo* (Kasimsetty et al., 2009; Gregory et al., 2010; Koyama et al., 2010; Mordanmccombs et al., 2010; Hsu et al., 2011; Xiao et al., 2011; Turan et al., 2017). Especially, dietary phytochemicals that can selectively interfere cellular pathways involved in prostate

TABLE 10 | Nutraceuticals and extracts obtained from plants with anti-prostate cancer activities.

Dietary agents	Cell type	Observation	Activity	Mechanism of action	Refs
Epigallocatechin-3-Gallate (Green Tea)	Du145 LNCaP	*In vivo* *In vitro*	Antiproliferation Induction of apoptosis	Downregulation of ID2; increase of Bax/Bcl-2; inducing cell death via an ID2-related mechanism; Antiproliferation by increasing the activity of ERK 1/2 through a MEK-independent and PI3K-dependent mechanism.	Xiao et al. (2011), Turan et al. (2017)
Grape skin	C4-2B LNCaP ARCaP-E	*In vitro* *In vivo*	Induction of apoptosis Inhibition of metastasis	Decrease of nail and pSTAT3 expression; inhibition of Snail-mediated CatL activity.	Burton et al. (2015)
Modified Citrus Pectin	LNCaP PC3	*In vivo* *In vitro*	Induction of apoptosis	Cell growth inhibition and apoptosis induction via inhibiting MAPK/ERK signaling pathway and activating caspase 3.	Azémar et al. (2007), Yan and Katz (2010)
ProstaCaid	PC3	*In vitro*	Antiproliferation Inhibition of and migration invasion	Downregulation of expression CCND1, CDK4, E2F1and MAPK6; upregulation of CDKN1A expression; downregulation of CAV1, IGF2, NR2F1, and PLAU genes expression; suppression of the urokinase plasminogen activator (uPA) secretion.	Jiang et al. (2011)
Pomegranate	C4-2B DU145 LNCaP LNCaP-AR PC3 22Rv1	*In vitro* In vivo	Antiproliferation Induction of apoptosis Inhibition of metastasis	Inhibition of enzyme (cytochrome P450) expression and activity; inhibition of mTOR phosphorylation at Ser2448 and Ser2481 and IGF1 expression.	Malik et al. (2005), Hong et al. (2008), Kasimsetty et al., (2009), Koyama et al. (2010)
Selenium	C4-2B LNCaP PC3	*In vitro* *In vivo*	Antiproliferation Induction of apoptosis	Increase of p53 expression; apoptosis induction by superoxide generation through the mitochondrial-dependent pathway	Pinto et al. (2007), Xiang et al. (2009), Sarveswaran et al. (2010)
Soy	LNCaP PC3	*In vitro* *In vivo*	Antiproliferation Inhibition of tumor growth	Decreased of COX-2 RNA and protein expression; inhibition of the synthesis of prostaglandins; downregulation growth factors involved in angiogenesis (EGF and IGF-1) and the IL-8 gene; inhibition of ERK-1 and ERK-2 expression.	Wang et al. (2004), Swami et al. (2009), Rabiau et al. (2010)
Vitamin D	DU145 LNCaP PC3	*In vitro* *In vivo*	Antiproliferation Inhibition of migration	Increase of E-cadherin expression; decrease of urokinase plasminogen activator receptor levels.	Gregory et al. (2010), Mordanmccombs et al. (2010), Hsu et al. (2011)
Vitamin K2	VCaP	*in vitro*	Antiproliferation; Induction of apoptosis	Downregulation of the expression of androgen receptor, BiP, survivin, while activating caspase-3 and -7, PARP-1 cleavage, p21 and DNA damage response marker, phospho-H2AX	Dasari et al. (2018)
Algerian propolis	LNCaP	*in vitro*	Induction of apoptosis	Blocking the cell cycle at G0/G1 phase.	Zabaiou et al. (2019)

cancer cells have attracted research interest of scientists in prostate cancer therapies in recent years.

CONCLUSION AND PERSPECTIVES

Prostate cancer is the second most frequently diagnosed tumor and the fifth leading cause of cancer-related deaths in men in the worldwide (McEleny et al., 2002). And the mortality of prostate cancer mainly occurs as a result of the castrate resistant ones. Up to date, different kinds of drugs have been employed to improve the treatment condition, mainly including LHRH antagonists, antiandrogen (androgen receptor antagonists and androgen synthesis inhibitors), tyrosine kinase inhibitors, angiogenesis inhibitors, endothelin antagonists, matrix metalloproteinase inhibitors, antioxidants, and cell cycle inhibitors. However, as mentioned above, there is no effective therapy for CRPC at present, except for docetaxel, which is the only chemotherapeutic agent that has been proven to prolong the overall survival in CRPC patient population though with many adverse effects reported (Eyben et al., 2015). Hence, it is urgent for us to explore an effective treatment for prostate cancer, especially for CRPC. In recent years, many natural products and extracts have been scientifically investigated *in vitro* and/or *in vivo* and proved as potential anti-prostate cancer agents, which are currently scattered across various publications. So a systematic summary and knowledge of future prospects are necessary to facilitate further chemical and pharmacological studies for anti-prostate cancer agents.

In our review, we provided a comprehensive overview of the molecular basis of the incidence and development of prostate cancer, especially for castration-resistant prostate cancer (CRPC), which mainly including canonical AR signaling (AR

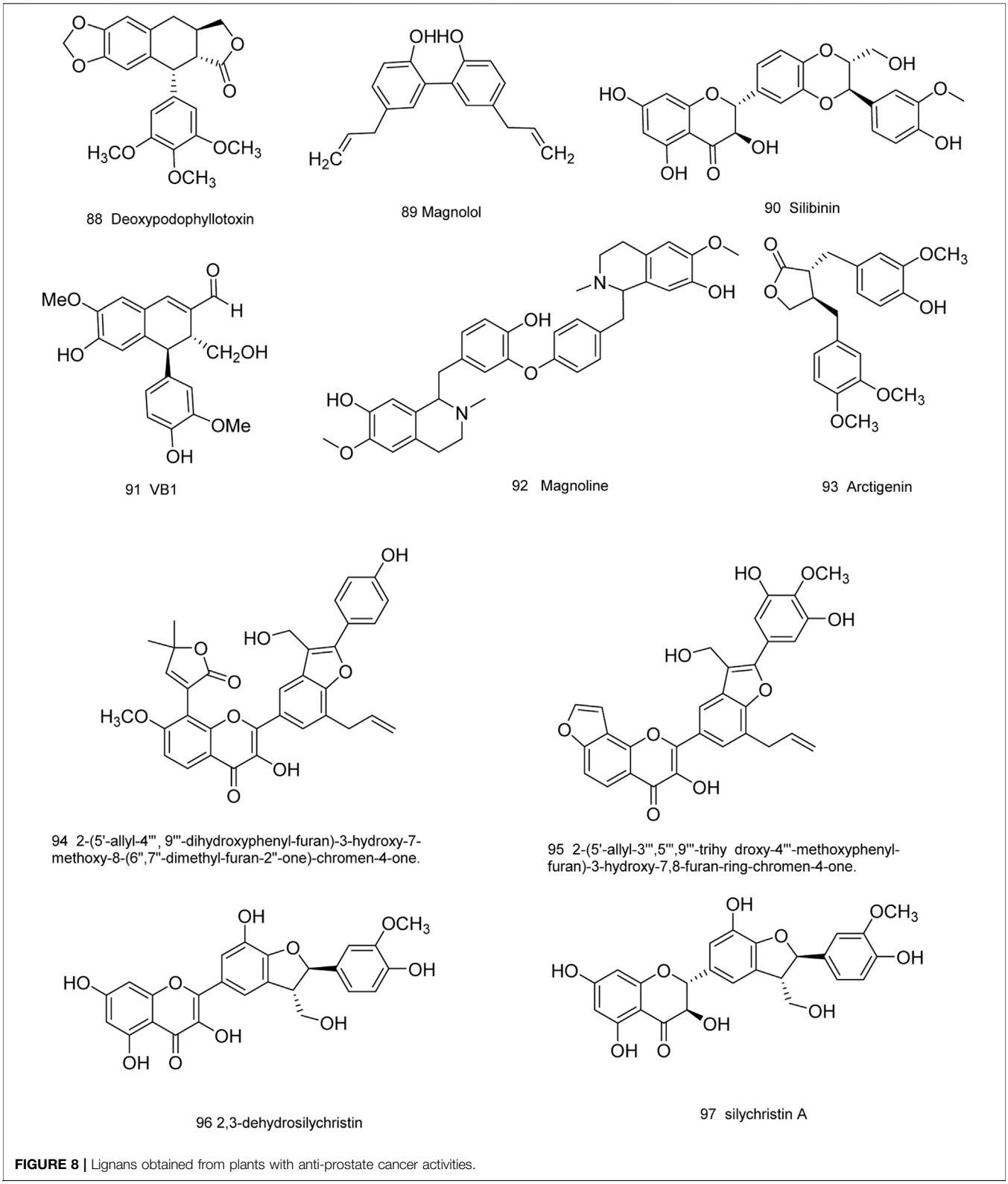


FIGURE 8 | Lignans obtained from plants with anti-prostate cancer activities.

amplification, over-expression, mutation, and unconventional activation), and non-nuclear AR signaling (PI3K/AKT, Src, MAPKs, JAK-STAT3, and Ca^{2+} signaling pathways). So most components involved in above-mentioned pathways represent potential targets for screening natural compounds and/or extracts with anti-prostate cancer activity. And natural compounds or

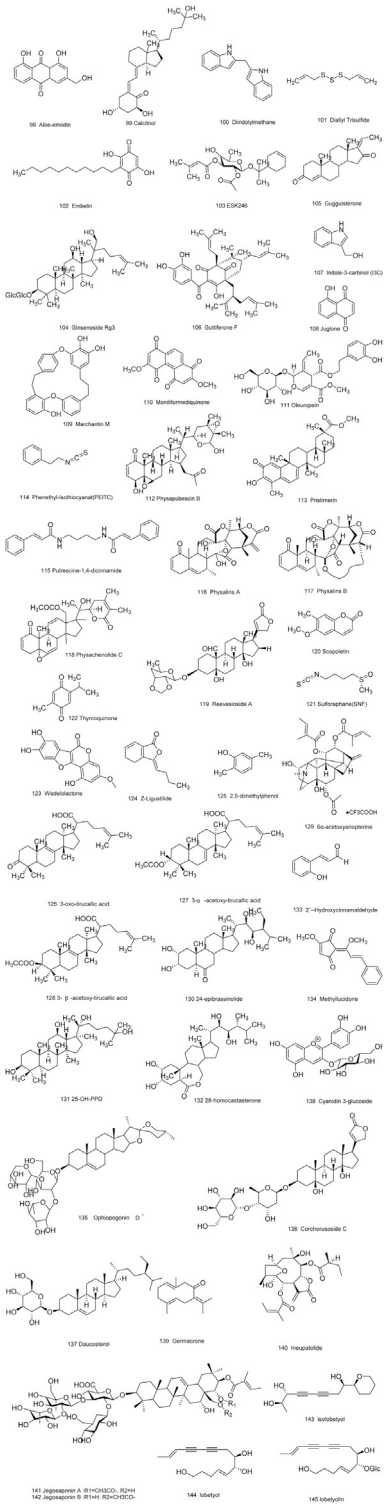


FIGURE 9 | Other compounds obtained from plants with anti-prostate cancer activities.

extracts that could function as modulators of canonical AR or non-nuclear AR signalling pathways thus can be regarded as promising candidates for anti-prostate interventions.

So far, a great amount of natural products isolated from diverse sources have been found to significantly inhibit prostate cancer cell proliferation/tumor growth or affected cellular signaling pathways in prostate cancer. As shown in our paper, the majority of natural compounds with direct relevance to prostate cancer are primarily derived from plants, with comparatively few molecules from marine and microbial sources. For these reported bioactive constituents, there is still plenty of room for improvement regarding the studies focused on efficacy enhancement and side effects amelioration by semi-synthetic modifications based on quantitative structural activity relationship elucidation. Since marine and microbial organisms represent important sources for single molecules exploit, more available and improved approaches should be included in finding novel natural products with significant anti-prostate cancer activity from these resource. Especially, engineering bacteria or fungus with novel gene clusters, currently used mainly for the identification of antibiotics or anti-tumor drugs, would be another promising approach for discovering natural compounds with anti-prostate activity. Extracts are another applicable option for anti-prostate purposes, in which case the chemical profile should be further elucidated, possibly affording a pure bioactive compound with precise mechanism of action. Also clinically used Chinese herb preparations should be profiled using techniques such as HPLC–MS to standardize the complex system to make it more controllable, stable, and reproducible in prostate cancer treatment. Furthermore, drug combination of these reported natural compounds with conventional chemotherapeutic agents may also be a promising way in finding solution for prostate cancer treatment. Finally, safty large-scale studies are needed to evaluate promising compounds or extracts and determing non-toxic doses for treating prostate cancer in mammals.

In conclusion, tackling prostate cancer (especially CRPC) is a much needed task that requires not only the great progress in understanding the genetic basis of prostate cancer, but also the significant technological improvements in tracking of bioactive natural compounds and structural characterization, which will facilitate the identification of novel natural compounds with significant anti-prostate cancer properties for drug development and therefore can be translated into significant health benefits for humans.

AUTHOR CONTRIBUTIONS

CZ, WX, and QY conceived and designed the outline of the manuscript; BB, QC, and RJ collated and summarized the literatures; XQ, HW and YB analyzed the data; RJ, BB, and CZ wrote the manuscript, QC, WX, and QY revised the manuscript and provided technical assistance to RJ and BB.

FUNDING

The work was supported by the National Nature Science Foundation of China (No. 82174081, 81770604), the Program of Shanghai Health System Subject Chief Scientist (2017BR004), and Shanghai Natural Science Fund (21ZR1478000).

REFERENCES

Aalinkeel, R., Bindukumar, B., Reynolds, J. L., Sykes, D. E., Mahajan, S. D., Chadha, K. C., et al. (2008). The Dietary Bioflavonoid, Quercetin, Selectively Induces Apoptosis of Prostate Cancer Cells by Down-Regulating the Expression of Heat Shock Protein 90. *Prostate* 68 (16), 1773–1789. doi:10.1002/pros.20845

Abeshouse, A., Ahn, J., Akbani, R., Ally, A., Amin, S., Andry, C. D., et al. (2015). The Molecular Taxonomy of Primary Prostate Cancer. *Cell* 163 (4), 1011–1025. doi:10.1016/j.cell.2015.10.025

Abou-Hashem, M. M. M., Abo-Elmatty, D. M., Mesbah, N. M., and Abd El-Mawgoud, A. M. (2019). Induction of Sub-G0 Arrest and Apoptosis by Seed Extract of Moringa Peregrina (Forssk.) Fiori in Cervical and Prostate Cancer Cell Lines. *J. Integr. Med.* 17 (6), 410–422. doi:10.1016/j.joim.2019.09.004

Acquaviva, R., Di Giacomo, C., Sorrenti, V., Galvano, F., Santangelo, R., Cardile, V., et al. (2012). Antiproliferative Effect of Oleuropein in Prostate Cell Lines. *Int. J. Oncol.* 41 (1), 31–38. doi:10.3892/ijo.2012.1428

Acuña, U. M., Mo, S., Zi, J., Orjala, J., and DE Blanco, E. J. C. (2018). Hapalindole H Induces Apoptosis as an Inhibitor of NF-κb and Affects the Intrinsic Mitochondrial Pathway in PC-3 Androgen-Insensitive Prostate Cancer Cells. *Anticancer Res.* 38 (6), 3299–3307. doi:10.21873/anticanres.12595

Afaq, F., Zaman, N., Khan, N., Syed, D. N., Sarfaraz, S., Zaid, M. A., et al. (2008). Inhibition of Epidermal Growth Factor Receptor Signaling Pathway by Delphinidin, an Anthocyanidin in Pigmented Fruits and Vegetables. *Int. J. Cancer* 123 (7), 1508–1515. doi:10.1002/ijc.23675

Al-Oqail, M. M., El-Shaibany, A., Al-Jassas, E., Al-Sheddi, E. S., Al-Massarani, S. M., and Farshori, N. N. (2016). *In Vitro* anti-proliferative Activities of Aloe Perryi Flowers Extract on Human Liver, colon, Breast, Lung, Prostate and Epithelial Cancer Cell Lines. *Pak J. Pharm. Sci.* 29 (2 Suppl. l), 723–729.

Anaya-Eugenio, G. D., Addo, E. M., Ezzone, N., Henkin, J. M., Ninh, T. N., Ren, Y., et al. (2019a). Caspase-Dependent Apoptosis in Prostate Cancer Cells and Zebrafish by Corchorusoside C from Streptocaulon Juventas. *J. Nat. Prod.* 82 (6), 1645–1655. doi:10.1021/acs.jnatprod.9b00140

Anaya-Eugenio, G. D., Rebollar-Ramos, D., González, M. D. C., Raja, H., Mata, R., and Carcache de Blanco, E. J. (2019b). Apoptotic Activity of Xanthoquinodin JBIR-99, from Parengyodontium Album MEXU 30054, in PC-3 Human Prostate Cancer Cells. *Chem. Biol. Interact* 311, 108798. doi:10.1016/j.cbi.2019.108798

Arias-González, I., García-Carrancá, A. M., Cornejo-Garrido, J., and Ordaz-Pichardo, C. (2018). Cytotoxic Effect of Kalanchoe Flammea and Induction of Intrinsic Mitochondrial Apoptotic Signaling in Prostate Cancer Cells. *J. Ethnopharmacol* 222, 133–147. doi:10.1016/j.jep.2018.04.038

Arjsri, P., Phetcharaburanin, J., Suksawat, M., Mapoung, S., Subkamkaew, C., Semmarath, W., et al. (2021). Spirogyra Neglecta (Hassall) Kützing Attenuates Metastasis of Castration-Resistant Human Prostate Cancer via the Blockage of AKT Signaling Pathway. *South Afr. J. Bot.* 139 (Suppl. 10), 26–37. doi:10.1016/j.sajb.2021.02.005

Arora, N., Kumar, S., Satti, N. K., Ali, A., Gupta, P., and Katoch, M. (2018). A Strain of Streptomyces Sp. Isolated from Rhizospheric Soil of Crataegus Oxycantha Producing Nalidixic Acid, a Synthetic Antibiotic. *J. Appl. Microbiol.* 124 (6), 1393–1400. doi:10.1111/jam.13736

Arulselvan, P., Ju, J., Gothai, S., Hasanpourghadi, M., Nasser, A., Aziz Ibrahim, I., et al. (2018). Anticancer Potential of Moringa Oleifera Flower Extract in Human Prostate Cancer PC-3 Cells via Induction of Apoptosis and Downregulation of AKT Pathway. *Phcog Mag.* 14 (58), 477. doi:10.4103/pm.pm_516_17

Asadi-Samani, M., Rafieian-Kopaei, M., Lorigooini, Z., and Shirzad, H. (2018). A Screening of Growth Inhibitory Activity of Iranian Medicinal Plants on Prostate Cancer Cell Lines. *Biomedicine (Taipei)* 8 (2), 8. doi:10.1051/bmdcn/2018080208

Asea, A., Ara, G., Teicher, B. A., Stevenson, M. A., and Calderwood, S. K. (2001). Effects of the Flavonoid Drug Quercetin on the Response of Human Prostate Tumours to Hyperthermia *In Vitro* and *In Vivo*. *Int. J. Hyperthermia* 17 (4), 347–356. doi:10.1080/02656730110053146

Asim, M., Siddiqui, I. A., Hafeez, B. B., Baniahmad, A., and Mukhtar, H. (2008). Src Kinase Potentiates Androgen Receptor Transactivation Function and Invasion of Androgen-independent Prostate Cancer C4-2 Cells. *Oncogene* 27 (25), 3596–3604. doi:10.1038/sj.onc.1211016

Auchus, R. J. (2004). The Backdoor Pathway to Dihydrotestosterone. *Trends Endocrinol. Metab.* 15 (9), 432–438. doi:10.1016/j.tem.2004.09.004

Azémar, M., Hildenbrand, B., Haering, B., Heim, M. E., and Unger, C. (2007). Clinical Benefit in Patients with Advanced Solid Tumors Treated with Modified Citrus Pectin: A Prospective Pilot Study. *Clin. Med. Oncol.* 1 (1), CMO.S285–80. doi:10.4137/CMO.S285

Bae, W. J., Choi, J. B., Kim, K. S., Ha, U. S., Hong, S. H., Lee, J. Y., et al. (2020). Inhibition of Proliferation of Prostate Cancer Cell Line DU-145 *In Vitro* and *In Vivo* Using Salvia Miltiorrhiza Bunge. *Chin. J. Integr. Med.* 26 (7), 533–538. doi:10.1007/s11655-017-2801-5

Bao, X., Zhu, J., Ren, C., Zhao, A., Zhang, M., Zhu, Z., et al. (2021). β-Elemonic Acid Inhibits Growth and Triggers Apoptosis in Human Castration-Resistant Prostate Cancer Cells through the Suppression of JAK2/STAT3/MCL-1 and NF-κb Signal Pathways. *Chem. Biol. Interact* 342, 109477. doi:10.1016/j.cbi.2021.109477

Barbieri, C. E., Baca, S. C., Lawrence, M. S., Demichelis, F., Blattner, M., Theurillat, J. P., et al. (2012). Exome Sequencing Identifies Recurrent SPOP, FOXA1 and MED12 Mutations in Prostate Cancer. *Nat. Genet.* 44 (6), 685–689. doi:10.1038/ng.2279

Baron, A., Mancini, M., Caldwell, E., Cabrelle, A., Bernardi, P., and Pagano, F. (2009). Serenoa Repens Extract Targets Mitochondria and Activates the Intrinsic Apoptotic Pathway in Human Prostate Cancer Cells. *BJU Int.* 103 (9), 1275–1283. doi:10.1111/j.1464-410X.2008.08266.x

Belkina, A. C., and Denis, G. V. (2012). BET Domain Co-regulators in Obesity, Inflammation and Cancer. *Nat. Rev. Cancer* 12 (7), 465–477. doi:10.1038/nrc3256

Beltran, H., Prandi, D., Mosquera, J. M., Benelli, M., Puca, L., Cyrta, J., et al. (2016). Divergent Clonal Evolution of Castration-Resistant Neuroendocrine Prostate Cancer. *Nat. Med.* 22 (3), 298–305. doi:10.1038/nm.4045

Bemis, D. L., Capodice, J. L., Anastasiadis, A. G., Katz, A. E., and Buttyan, R. (2005). Zyflamend, a Unique Herbal Preparation with Nonselective COX Inhibitory Activity, Induces Apoptosis of Prostate Cancer Cells that Lack COX-2 Expression. *Nutr. Cancer* 52 (2), 202–212. doi:10.1207/s15327914nc5202_10

Ben-Eltriki, M., Deb, S., Adomat, H., and Tomlinson Guns, E. S. (2016). Calcitriol and 20(S)-protopanaxadiol Synergistically Inhibit Growth and Induce Apoptosis in Human Prostate Cancer Cells. *J. Steroid Biochem. Mol. Biol.* 158, 207–219. doi:10.1016/j.jsbmb.2015.12.002

Bernemann, C., Schnoeller, T. J., Luedeke, M., Steinestel, K., Boegemann, M., Schrader, A. J., et al. (2017). Expression of AR-V7 in Circulating Tumour Cells Does Not Preclude Response to Next Generation Androgen Deprivation Therapy in Patients with Castration Resistant Prostate Cancer. *Eur. Urol.* 71, 1–3. doi:10.1016/j.eururo.2016.07.021

Bodle, C. R., Mackie, D. I., Hayes, M. P., Schamp, J. H., Miller, M. R., Henry, M. D., et al. (2017). Natural Products Discovered in a High-Throughput Screen Identified as Inhibitors of RGS17 and as Cytostatic and Cytotoxic Agents for Lung and Prostate Cancer Cell Lines. *J. Nat. Prod.* 80 (7), 1992–2000. doi:10.1021/acs.jnatprod.7b00112

Bolli, R., Dawn, B., and Xuan, Y. T. (2003). Role of the JAK-STAT Pathway in protection against Myocardial Ischemia/reperfusion Injury. *Trends Cardiovasc. Med.* 13 (2), 72–79. doi:10.1016/s1050-1738(02)00230-x

Bonham, M., Posakony, J., Coleman, I., Montgomery, B., Simon, J., and Nelson, P. S. (2005). Characterization of Chemical Constituents in Scutellaria Baicalensis with Antiandrogenic and Growth-Inhibitory Activities toward Prostate Carcinoma. *Clin. Cancer Res.* 11 (10), 3905–3914. doi:10.1158/1078-0432.CCR-04-1974

Bowers, Z., Caraballo, D., Jebelli, J., Famuyiwa, T., and Kumi-Diaka, J. (2021). Therapeutic Potential of Pseudopterosin H on a Prostate Cancer Cell Line. *FASEB* 35. doi:10.1096/fasebj.2021.35.S1.04601

Bureyko, T., Hurdle, H., Metcalfe, J. B., Clandinin, M. T., and Mazurak, V. C. (2009). Reduced Growth and Integrin Expression of Prostate Cells Cultured with Lycopene, Vitamin E and Fish Oil *In Vitro*. *Br. J. Nutr.* 101 (7), 990–997. doi:10.1017/S0007114508051684

Burton, L. J., Smith, B. A., Smith, B. N., Loyd, Q., Nagappan, P., McKeithen, D., et al. (2015). Muscadine Grape Skin Extract Can Antagonize Snail-Cathepsin L-Mediated Invasion, Migration and Osteoclastogenesis in Prostate and Breast Cancer Cells. *Carcinogenesis* 36 (9), 1019–1027. doi:10.1093/carcin/bgv084

Cai, H., Smith, D. A., Memarzadeh, S., Lowell, C. A., Cooper, J. A., and Witte, O. N. (2011). Differential Transformation Capacity of Src Family Kinases during the

Initiation of Prostate Cancer. *Proc. Natl. Acad. Sci. U S A.* 108 (16), 6579–6584. doi:10.1073/pnas.1103904108

Cary, K. C., and Cooperberg, M. R. (2013). Biomarkers in Prostate Cancer Surveillance and Screening: Past, Present, and Future. *Ther. Adv. Urol.* 5 (6), 318–329. doi:10.1177/1756287213495915

Castro, M. J., Careaga, V. P., Sacca, P. A., Faraoni, M. B., Murray, A. P., and Calvo, J. C. (2019). Lupane Triterpenoids and New Derivatives as Antiproliferative Agents against Prostate Cancer Cells. *Anticancer Res.* 39 (7), 3835–3845. doi:10.21873/anticanres.13533

Chan, M. L., Liang, J. W., Hsu, L. C., Chang, W. L., Lee, S. S., and Guh, J. H. (2015). Zerumbone, a Ginger Sesquiterpene, Induces Apoptosis and Autophagy in Human Hormone-Refractory Prostate Cancers through Tubulin Binding and Crosstalk between Endoplasmic Reticulum Stress and Mitochondrial Insult. *Naunyn Schmiedebergs Arch. Pharmacol.* 388 (11), 1223–1236. doi:10.1007/s00210-015-1152-z

Chang, H. T., Chou, C. T., Chen, I. L., Liang, W. Z., Kuo, D. H., Huang, J. K., et al. (2013). Mechanisms of Resveratrol-Induced Changes in [Ca(2+)]i and Cell Viability in PC3 Human Prostate Cancer Cells. *J. Recept Signal. Transduct Res.* 33 (5), 298–303. doi:10.3109/10799893.2013.822886

Chang, K. H., Li, R., Papari-Zareei, M., Watumull, L., Zhao, Y. D., Auchus, R. J., et al. (2011). Dihydrotestosterone Synthesis Bypasses Testosterone to Drive Castration-Resistant Prostate Cancer. *Proc. Natl. Acad. Sci. U S A.* 108 (33), 13728–13733. doi:10.1073/pnas.1107898108

Chang, K. H., and Sharifi, N. (2012). Prostate Cancer-From Steroid Transformations to Clinical Translation. *Nat. Rev. Urol.* 9 (12), 721–724. doi:10.1038/nrurol.2012.175

Chaudhary, A., Pechan, T., and Willett, K. L. (2007). Differential Protein Expression of Peroxiredoxin I and II by Benzo(a)pyrene and Quercetin Treatment in 22Rv1 and PrEC Prostate Cell Lines. *Toxicol. Appl. Pharmacol.* 220 (2), 197–210. doi:10.1016/j.taap.2006.12.030

Chen, C. D., Welsbie, D. S., Tran, C., Baek, S. H., Chen, R., Vessella, R., et al. (2004). Molecular Determinants of Resistance to Antiandrogen Therapy. *Nat. Med.* 10 (1), 33–39. doi:10.1038/nm972

Chen, L., Yan, F., Chen, W., Zhao, L., Zhang, J., Lu, Q., et al. (2018). Procyanidin from Peanut Skin Induces Antiproliferative Effect in Human Prostate Carcinoma Cells DU145. *Chem. Biol. Interact* 288, 12–23. doi:10.1016/j.cbi.2018.04.008

Chen, Y. C., Kung, F. L., Tsai, I. L., Chou, T. H., Chen, I. S., and Guh, J. H. (2010). Cryptocaryone, a Natural Dihydrochalcone, Induces Apoptosis in Human Androgen Independent Prostate Cancer Cells by Death Receptor Clustering in Lipid Raft and Nonraft Compartments. *J. Urol.* 183 (6), 2409–2418. doi:10.1016/j.juro.2010.01.065

Chiang, Y. T., Wang, K., Fazli, L., Qi, R. Z., Gleave, M. E., Collins, C. C., et al. (2014). GATA2 as a Potential Metastasis-Driving Gene in Prostate Cancer. *Oncotarget* 5 (2), 451–461. doi:10.18632/oncotarget.1296

Chien, C. S., Shen, K. H., Huang, J. S., Ko, S. C., and Shih, Y. W. (2010). Antimetastatic Potential of Fisetin Involves Inactivation of the PI3K/Akt and JNK Signaling Pathways with Downregulation of MMP-2/9 Expressions in Prostate Cancer PC-3 Cells. *Mol. Cel Biochem* 333 (1-2), 169–180. doi:10.1007/s11010-009-0217-z

Chintharlapalli, S., Papineni, S., Ramaiah, S. K., and Safe, S. (2007). Betulinic Acid Inhibits Prostate Cancer Growth through Inhibition of Specificity Protein Transcription Factors. *Cancer Res.* 67 (6), 2816–2823. doi:10.1158/0008-5472.Can-06-3735

Cho, H. D., Lee, J. H., Moon, K. D., Park, K. H., Lee, M. K., and Seo, K. I. (2018). Auriculasin-induced ROS Causes Prostate Cancer Cell Death via Induction of Apoptosis. *Food Chem. Toxicol.* 111, 660–669. doi:10.1016/j.fct.2017.12.007

Ciccarese, C., Massari, F., Iacovelli, R., Fiorentino, M., Montironi, R., Di Nunno, V., et al. (2017). Prostate Cancer Heterogeneity: Discovering Novel Molecular Targets for Therapy. *Cancer Treat. Rev.* 54, 68–73. doi:10.1016/j.ctrv.2017.02.001

Cohen, Z., Maimon, Y., Yoeli-Lerner, M., Yang, P., Samuels, N., and Berger, R. (2015). Selective Anticancer Effects and protection from Chemotherapy by the Botanical Compound LCS101: Implications for Cancer Treatment. *Int. J. Oncol.* 46 (1), 308–316. doi:10.3892/ijo.2014.2711

Colgate, E. C., Miranda, C. L., Stevens, J. F., Bray, T. M., and Ho, E. (2007). Xanthohumol, a Prenylflavonoid Derived from Hops Induces Apoptosis and Inhibits NF-kappaB Activation in Prostate Epithelial Cells. *Cancer Lett.* 246 (1-2), 201–209. doi:10.1016/j.canlet.2006.02.015

Cook, K. M., Hilton, S. T., Mecinovic, J., Motherwell, W. B., Figg, W. D., and Schofield, C. J. (2009). Epidithiodiketopiperazines Block the Interaction between Hypoxia-Inducible Factor-1alpha (HIF-1alpha) and P300 by a Zinc Ejection Mechanism. *J. Biol. Chem.* 284 (39), 26831–26838. doi:10.1074/jbc.M109.009498

Courtney, K. D., Corcoran, R. B., and Engelman, J. A. (2010). The PI3K Pathway as Drug Target in Human Cancer. *J. Clin. Oncol.* 28 (6), 1075–1083. doi:10.1200/Jco.2009.25.3641

Coutinho, I., Day, T. K., Tilley, W. D., and Selth, L. A. (2016). Androgen Receptor Signaling in Castration-Resistant Prostate Cancer: a Lesson in Persistence. *Endocr. Relat. Cancer* 23 (12), T179–T197. doi:10.1530/ERC-16-0422

Crawford, N. P., Alsarraj, J., Lukes, L., Walker, R. C., Officewala, J. S., Yang, H. H., et al. (2008). Bromodomain 4 Activation Predicts Breast Cancer Survival. *Proc. Natl. Acad. Sci. U S A.* 105 (17), 6380–6385. doi:10.1073/pnas.0710331105

Dai, W., Sun, C., Huang, S., and Zhou, Q. (2016). Carvacrol Suppresses Proliferation and Invasion in Human Oral Squamous Cell Carcinoma. *Onco Targets Ther.* 9, 2297–2304. doi:10.2147/ott.S98875

Dai, X., Gan, W., Li, X., Wang, S., Zhang, W., Huang, L., et al. (2017). Prostate Cancer-Associated SPOP Mutations Confer Resistance to BET Inhibitors through Stabilization of BRD4. *Nat. Med.* 23 (9), 1063–1071. doi:10.1038/nm.4378

Dan, R., Vanallen, E., Wu, Y. M., Schultz, N., Lonigro, R., Mosquera, J. M., et al. (2015). Integrative Clinical Genomics of Advanced Prostate Cancer. *Cell* 161 (5), 1215. doi:10.1016/j.cell.2015.05.001

Dasari, S., Samy, A. L. P. A., Kajdacsy-Balla, A., Bosland, M. C., and Munirathinam, G. (2018). Vitamin K2, a Menaquinone Present in Dairy Products Targets Castration-Resistant Prostate Cancer Cell-Line by Activating Apoptosis Signaling. *Food Chem. Toxicol.* 115, 218–227. doi:10.1016/j.fct.2018.02.018

Davis, J. E., Xie, X., Guo, J., Huang, W., Chu, W. M., Huang, S., et al. (2016). ARF1 Promotes Prostate Tumorigenesis via Targeting Oncogenic MAPK Signaling. *Oncotarget* 7 (26), 39834–39845. doi:10.18632/oncotarget.9405

Deepak, M., and Handa, S. S. (2000). Antiinflammatory Activity and Chemical Composition of Extracts of Verbena Officinalis. *Phytother Res.* 14 (6), 463–465. doi:10.1002/1099-1573(200009)14:6<463::aid-ptr611>3.0.co;2-g

Deng, Y., Li, Y., Yang, F., Zeng, A., Yang, S., Luo, Y., et al. (2017). The Extract from Punica Granatum (Pomegranate) Peel Induces Apoptosis and Impairs Metastasis in Prostate Cancer Cells. *Biomed. Pharmacother.* 93, 976–984. doi:10.1016/j.biopha.2017.07.008

Destaing, O., Block, M. R., Planus, E., and Albiges-Rizo, C. (2011). Invadosome Regulation by Adhesion Signaling. *Curr. Opin. Cel Biol* 23 (5), 597–606. doi:10.1016/j.ceb.2011.04.002

Ding, W., Hu, Z., Zhang, Z., Ma, Q., Tang, H., and Ma, Z. (2015). Physapubescin B Exhibits Potent Activity against Human Prostate Cancer *In Vitro* and *In Vivo*. *J. Agric. Food Chem.* 63 (43), 9504–9512. doi:10.1021/acs.jafc.5b03045

Djusberg, E., Jernberg, E., Thysell, E., Golovleva, I., Lundberg, P., Crnalic, S., et al. (2017). High Levels of the AR-V7 Splice Variant and Co-amplification of the Golgi Protein Coding YIPF6 in AR Amplified Prostate Cancer Bone Metastases. *Prostate* 77 (6), 625–638. doi:10.1002/pros.23307

Dyshlovoy, S. A., Kudryashova, E. K., Kaune, M., Makarieva, T. N., Shubina, L. K., Busenbender, T., et al. (2020). Urupocidin C: a New marine Guanidine Alkaloid Which Selectively Kills Prostate Cancer Cells via Mitochondria Targeting. *Sci. Rep.* 10 (1), 9764. doi:10.1038/s41598-020-66428-5

Dyshlovoy, S. A., Menchinskaya, E. S., Venz, S., Rast, S., Amann, K., Hauschild, J., et al. (2016). The marine Triterpene Glycoside Frondoside A Exhibits Activity *In Vitro* and *In Vivo* in Prostate Cancer. *Int. J. Cancer* 138 (10), 2450–2465. doi:10.1002/ijc.29977

Efstathiou, E., Titus, M., Tsavachidou, D., Tzelepi, V., Wen, S., Hoang, A., et al. (2012). Effects of Abiraterone Acetate on Androgen Signaling in Castrate-Resistant Prostate Cancer in Bone. *J. Clin. Oncol.* 30 (6), 637–643. doi:10.1200/JCO.2010.33.7675

Erdogan, S., and Turkekul, K. (2020). Neferine Inhibits Proliferation and Migration of Human Prostate Cancer Stem Cells through P38 MAPK/JNK Activation. *J. Food Biochem.* 44 (6). doi:10.1111/jfbc.13253

Eroğlu, C., Avcı, E., Vural, H., and Kurar, E. (2018). Anticancer Mechanism of Sinapic Acid in PC-3 and LNCaP Human Prostate Cancer Cell Lines. *Gene* 671, 127–134. doi:10.1016/j.gene.2018.05.049

Estrada, A. C., Syrovets, T., Pitterle, K., Lunov, O., Büchele, B., Schimana-Pfeifer, J., et al. (2010). Tirucallic Acids Are Novel Pleckstrin Homology

Domain-dependent Akt Inhibitors Inducing Apoptosis in Prostate Cancer Cells. *Mol. Pharmacol.* 77 (3), 378–387. doi:10.1124/mol.109.060475

Fang, Z., Zhang, T., Dizeyi, N., Chen, S., Wang, H., Swanson, K. D., et al. (2012). Androgen Receptor Enhances P27 Degradation in Prostate Cancer Cells through Rapid and Selective TORC2 Activation. *J. Biol. Chem.* 287 (3), 2090–2098. doi:10.1074/jbc.M111.323303

Feldman, B. J., and Feldman, D. (2001). The Development of Androgen-independent Prostate Cancer. *Nat. Rev. Cancer* 1 (1), 34–45. doi:10.1038/35094009

Fernández-Pomares, C., Juárez-Aguilar, E., Domínguez-Ortiz, M. Á., Gallegos-Estudillo, J., Herrera-Covarrubias, D., Sánchez-Medina, A., et al. (2018). Hydroalcoholic Extract of the Widely Used Mexican Plant Justicia Spicigera Schltdl. Exerts a Cytostatic Effect on LNCaP Prostate Cancer Cells. *J. Herbal Med.* 12, 66–72. doi:10.1016/j.hermed.2017.09.003

Flourakis, M., and Prevarskaya, N. (2009). Insights into Ca2+ Homeostasis of Advanced Prostate Cancer Cells. *Biochim. Biophys. Acta* 1793 (6), 1105–1109. doi:10.1016/j.bbamcr.2009.01.009

Foradori, C. D., Weiser, M. J., and Handa, R. J. (2008). Non-genomic Actions of Androgens. *Front. Neuroendocrinol* 29 (2), 169–181. doi:10.1016/j.yfrne.2007.10.005

Foradori, C. D., Werner, S. B., Sandau, U. S., Clapp, T. R., and Handa, R. J. (2007). Activation of the Androgen Receptor Alters the Intracellular Calcium Response to Glutamate in Primary Hippocampal Neurons and Modulates Sarco/endoplasmic Reticulum Calcium ATPase 2 Transcription. *Neuroscience* 149 (1), 155–164. doi:10.1016/j.neuroscience.2007.06.054

French, C. A., Miyoshi, I., Kubonishi, I., Grier, H. E., Perez-Atayde, A. R., and Fletcher, J. A. (2003). BRD4-NUT Fusion Oncogene: a Novel Mechanism in Aggressive Carcinoma. *Cancer Res.* 63 (2), 304–307. doi:10.1016/S0165-4608(02)00679-9

Gantar, M., Dhandayuthapani, S., and Rathinavelu, A. (2012). Phycocyanin Induces Apoptosis and Enhances the Effect of Topotecan on Prostate Cell Line LNCaP. *J. Med. Food* 15 (12), 1091–1095. doi:10.1089/jmf.2012.0123

Gapter, L., Wang, Z., Glinski, J., and Ng, K. Y. (2005). Induction of Apoptosis in Prostate Cancer Cells by Pachymic Acid from Poria Cocos. *Biochem. Biophys. Res. Commun.* 332 (4), 1153–1161. doi:10.1016/j.bbrc.2005.05.044

Gille, H., Kortenjann, M., Thomae, O., Moomaw, C., Slaughter, C., Cobb, M. H., et al. (1995). ERK Phosphorylation Potentiates Elk-1-mediated Ternary Complex Formation and Transactivation. *EMBO J.* 14 (5), 951–962. doi:10.1002/j.1460-2075.1995.tb07076.x

Gioti, K., Papachristodoulou, A., Benaki, D., Beloukas, A., Vontzalidou, A., Aligiannis, N., et al. (2020). Glycyrrhiza Glabra-Enhanced Extract and Adriamycin Antiproliferative Effect on PC-3 Prostate Cancer Cells. *Nutr. Cancer* 72 (2), 320–332. doi:10.1080/01635581.2019.1632357

Graff, R. E., Ahearn, T. U., Pettersson, A., Ebot, E. M., Gerke, T., Penney, K. L., et al. (2018). Height, Obesity, and the Risk of TMPRSS2:ERG-Defined Prostate Cancer. *Cancer Epidemiol. Biomarkers Prev.* 27 (2), 193–200. doi:10.1158/1055-9965.EPI-17-0547

Grasso, C. S., Wu, Y. M., Robinson, D. R., Cao, X., Dhanasekaran, S. M., Khan, A. P., et al. (2012). The Mutational Landscape of Lethal Castration-Resistant Prostate Cancer. *Nature* 487 (7406), 239–243. doi:10.1038/nature11125

Gregory, K. J., Zhao, B., Bielenberg, D. R., Dridi, S., Wu, J., Jiang, W., et al. (2010). Vitamin D Binding Protein-Macrophage Activating Factor Directly Inhibits Proliferation, Migration, and uPAR Expression of Prostate Cancer Cells. *PLoS One* 5 (10), e13428. doi:10.1371/journal.pone.0013428

Gubiani, J. R., Oliveira, M. C. S., Neponuceno, R. A. R., Camargo, M. J., Garcez, W. S., Biz, A. R., et al. (2019). Cytotoxic Prenylated Indole Alkaloid Produced by the Endophytic Fungus Aspergillus terreus P63. *Phytochemistry Lett.* 32, 162–167. doi:10.1016/j.phytol.2019.06.003

Gumushan Aktas, H., and Akgun, T. (2018). Naringenin Inhibits Prostate Cancer Metastasis by Blocking Voltage-Gated Sodium Channels. *Biomed. Pharmacother.* 106, 770–775. doi:10.1016/j.biopha.2018.07.008

Guo, Z., Yang, X., Sun, F., Jiang, R., Linn, D. E., Chen, H., et al. (2009). A Novel Androgen Receptor Splice Variant Is Up-Regulated during Prostate Cancer Progression and Promotes Androgen Depletion-Resistant Growth. *Cancer Res.* 69 (6), 2305–2313. doi:10.1158/0008-5472.Can-08-3795

Gupta, S., Li, J., Kemeny, G., Bitting, R. L., Beaver, J., Somarelli, J. A., et al. (2017). Whole Genomic Copy Number Alterations in Circulating Tumor Cells from Men with Abiraterone or Enzalutamide-Resistant Metastatic Castration-Resistant Prostate Cancer. *Clin. Cancer Res.* 23 (5), 1346–1357. doi:10.1158/1078-0432.CCR-16-1211

Haile, S., and Sadar, M. D. (2011). Androgen Receptor and its Splice Variants in Prostate Cancer. *Cell Mol Life Sci* 68 (24), 3971–3981. doi:10.1007/s00018-011-0766-7

Hamidullah Kumar, R., Singh Saini, K., Kumar, A., Kumar, S., Ramakrishna, E., et al. (2015). Quercetin-6-C-β-D-glucopyranoside, Natural Analog of Quercetin Exhibits Anti-prostate Cancer Activity by Inhibiting Akt-mTOR Pathway via Aryl Hydrocarbon Receptor. *Biochimie* 119, 68–79. doi:10.1016/j.biochi.2015.10.012

Han, H., Qiu, L., Wang, X., Qiu, F., Wong, Y., and Yao, X. (2011). Physalins A and B Inhibit Androgen-independent Prostate Cancer Cell Growth through Activation of Cell Apoptosis and Downregulation of Androgen Receptor Expression. *Biol. Pharm. Bull.* 34(10), 1584–1588. doi:10.1248/bpb.34.1584

Harris, E. M., Strope, J. D., Beedie, S. L., Huang, P. A., Goey, A. K. L., Cook, K. M., et al. (2018). Preclinical Evaluation of Discorhabdins in Antiangiogenic and Antitumor Models. *Mar. Drugs* 16 (7). doi:10.3390/md16070241

Hastak, K., Gupta, S., Ahmad, N., Agarwal, M. K., Agarwal, M. L., and Mukhtar, H. (2003). Role of P53 and NF-kappaB in Epigallocatechin-3-Gallate-Induced Apoptosis of LNCaP Cells. *Oncogene* 22 (31), 4851–4859. doi:10.1038/sj.onc.1206708

He, B., Lanz, R. B., Fiskus, W., Geng, C., Yi, P., Hartig, S. M., et al. (2014). GATA2 Facilitates Steroid Receptor Coactivator Recruitment to the Androgen Receptor Complex. *Proc. Natl. Acad. Sci. U S A.* 111 (51), 18261–18266. doi:10.1073/pnas.1421415111

Hellsten, R., Johansson, M., Dahlman, A., Dizeyi, N., Sterner, O., and Bjartell, A. (2008). Galiellalactone Is a Novel Therapeutic Candidate against Hormone-Refractory Prostate Cancer Expressing Activated Stat3. *Prostate* 68 (3), 269–280. doi:10.1002/pros.20699

Ho, Y., and Dehm, S. M. (2017). Androgen Receptor Rearrangement and Splicing Variants in Resistance to Endocrine Therapies in Prostate Cancer. *Endocrinology* 158 (6), 1533–1542. doi:10.1210/en.2017-00109

Hofland, J., van Weerden, W. M., Steenbergen, J., Dits, N. F., Jenster, G., and de Jong, F. H. (2012). Activin A Stimulates AKR1C3 Expression and Growth in Human Prostate Cancer. *Endocrinology* 153 (12), 5726–5734. doi:10.1210/en.2011-2065

Holzapfel, N. P., Holzapfel, B. M., Champ, S., Feldthusen, J., Clements, J., and Hutmacher, D. W. (2013). The Potential Role of Lycopene for the Prevention and Therapy of Prostate Cancer: from Molecular Mechanisms to Clinical Evidence. *Int. J. Mol. Sci.* 14 (7), 14620–14646. doi:10.3390/ijms140714620

Holzmann, C., Kappel, S., Kilch, T., Jochum, M. M., Urban, S. K., Jung, V., et al. (2015). Transient Receptor Potential Melastatin 4 Channel Contributes to Migration of Androgen-Insensitive Prostate Cancer Cells. *Oncotarget* 6 (39), 41783–41793. doi:10.18632/oncotarget.6157

Hong, M. Y., Seeram, N. P., and Heber, D. (2008). Pomegranate Polyphenols Down-Regulate Expression of Androgen-Synthesizing Genes in Human Prostate Cancer Cells Overexpressing the Androgen Receptor. *J. Nutr. Biochem.* 19 (12), 848–855. doi:10.1016/j.jnutbio.2007.11.006

Horne, W. C., Sanjay, A., Bruzzaniti, A., and Baron, R. (2005). The Role(s) of Src Kinase and Cbl Proteins in the Regulation of Osteoclast Differentiation and Function. *Immunol. Rev.* 208 (1), 106–125. doi:10.1111/j.0105-2896.2005.00335.x

Hsieh, T., Chen, S. S., Wang, X., and Wu, J. M. (1997). Regulation of Androgen Receptor (AR) and Prostate Specific Antigen (PSA) Expression in the Androgen-Responsive Human Prostate LNCaP Cells by Ethanolic Extracts of the Chinese Herbal Preparation, PC-SPES. *Biochem. Mol. Biol. Int.* 42 (3), 535–544. doi:10.1080/15216549700202941

Hsu, A., Bray, T. M., Helferich, W. G., Doerge, D. R., and Ho, E. (2010). Differential Effects of Whole Soy Extract and Soy Isoflavones on Apoptosis in Prostate Cancer Cells. *Exp. Biol. Med. (Maywood)* 235 (1), 90–97. doi:10.1258/ebm.2009.009128

Hsu, J. C., Zhang, J., Dev, A., Wing, A., Bjeldanes, L. F., and Firestone, G. L. (2005). Indole-3-carbinol Inhibition of Androgen Receptor Expression and Downregulation of Androgen Responsiveness in Human Prostate Cancer Cells. *Carcinogenesis* 26 (11), 1896–1904. doi:10.1093/carcin/bgi155

Hsu, J. L., Lee, Y. J., Leu, W. J., Dong, Y. S., Pan, S. L., Uang, B. J., et al. (2014). Moniliformediquinone Induces *In Vitro* and *In Vivo* Antitumor Activity through Glutathione Involved DNA Damage Response and Mitochondrial

Stress in Human Hormone Refractory Prostate Cancer. *J. Urol.* 191 (5), 1429–1438. doi:10.1016/j.juro.2013.11.102

Hsu, J. W., Yasmin-Karim, S., King, M. R., Wojciechowski, J. C., Mickelsen, D., Blair, M. L., et al. (2011). Suppression of Prostate Cancer Cell Rolling and Adhesion to Endothelium by 1α,25-Dihydroxyvitamin D3. *Am. J. Pathol.* 178 (2), 872–880. doi:10.1016/j.ajpath.2010.10.036

Huang, C., Miller, R. T., and Freter, C. E. (2016). Signaling Regulation and Role of Filamin A Cleavage in Ca2+-Stimulated Migration of Androgen Receptor-Deficient Prostate Cancer Cells. *Oncotarget* 8 (3), 3840–3853. doi:10.18632/oncotarget.9472

Huang, D. M., Shen, Y. C., Wu, C., Huang, Y. T., Kung, F. L., Teng, C. M., et al. (2004). Investigation of Extrinsic and Intrinsic Apoptosis Pathways of New Clerodane Diterpenoids in Human Prostate Cancer PC-3 Cells. *Eur. J. Pharmacol.* 503 (1-3), 17–24. doi:10.1016/j.ejphar.2004.09.040

Huang, W. J., Bi, L. Y., Li, Z. Z., Zhang, X., and Ye, Y. (2013). Formononetin Induces the Mitochondrial Apoptosis Pathway in Prostate Cancer Cells via Downregulation of the IGF-1/IGF-1R Signaling Pathway. *Pharm. Biol.* 52 (4), 466–470. doi:10.3109/13880209.2013.842600

Huang, Y. S., Mao, J. X., Zhang, L., Guo, H. W., Yan, C., and Chen, M. (2021). Antiprostate Cancer Activity of Ineupatolide Isolated from Carpesium Cernuum L. *Biomed. Res. Int.* 2021, 5515961. doi:10.1155/2021/5515961

Huang, Y. W., Wang, L. S., Chang, H. L., Ye, W., Dowd, M. K., Wan, P. J., et al. (2006). Molecular Mechanisms of (-)-Gossypol-Induced Apoptosis in Human Prostate Cancer Cells. *Anticancer Res.* 26 (3A), 1925–1933.

Huggins, C. (1978). Endocrine-induced Regression of Cancers. *Am. J. Surg.* 136 (2), 233–238. doi:10.1016/0002-9610(78)90235-0

Huggins, C., and Hodges, C. (1941). Studies in Prostate Cancer: the Effect of Castration, of Estrogen and of Androgen Injection on Serum Phosphatases in Metastatic Carcinoma of Prostate.

Janouskova, H., El Tekle, G., Bellini, E., Udeshi, N. D., Rinaldi, A., Ulbricht, A., et al. (2017). Opposing Effects of Cancer-type-specific SPOP Mutants on BET Protein Degradation and Sensitivity to BET Inhibitors. *Nat. Med.* 23 (9), 1046–1054. doi:10.1038/nm.4372

Jeon, Y. J., Jung, S. N., Chang, H., Yun, J., Lee, C. W., Lee, J., et al. (2015a). Artocarpus Altilis (Parkinson) Fosberg Extracts and Geranyl Dihydrochalcone Inhibit STAT3 Activity in Prostate Cancer DU145 Cells. *Phytother Res.* 29 (5), 749–756. doi:10.1002/ptr.5311

Jeon, Y. J., Jung, S. N., Yun, J., Lee, C. W., Choi, J., Lee, Y. J., et al. (2015b). Ginkgetin Inhibits the Growth of DU-145 Prostate Cancer Cells through Inhibition of Signal Transducer and Activator of Transcription 3 Activity. *Cancer Sci.* 106 (4), 413–420. doi:10.1111/cas.12608

Jia, S., Gao, X., Lee, S. H., Maira, S. M., Wu, X., Stack, E. C., et al. (2013). Opposing Effects of Androgen Deprivation and Targeted Therapy on Prostate Cancer Prevention. *Cancer Discov.* 3 (1), 44–51. doi:10.1158/2159-8290.CD-12-0262

Jiang, H., Sun, J., Xu, Q., Liu, Y., Wei, J., Young, C. Y., et al. (2013). Marchantin M: a Novel Inhibitor of Proteasome Induces Autophagic Cell Death in Prostate Cancer Cells. *Cell Death Dis* 4 (8), e761. doi:10.1038/cddis.2013.285

Jiang, J., Eliaz, I., and Sliva, D. (2011). Suppression of Growth and Invasive Behavior of Human Prostate Cancer Cells by ProstaCaidâ"¢: Mechanism of Activity. *Int. J. Oncol.* 38 (6), 1675–1682. doi:10.3892/ijo.2011.996

Jiang, S., Zu, Y., Fu, Y., Zhang, Y., and Efferth, T. (2008). Activation of the Mitochondria-Driven Pathway of Apoptosis in Human PC-3 Prostate Cancer Cells by a Novel Hydrophilic Paclitaxel Derivative, 7-Xylosyl-10-Deacetylpaclitaxel. *Int. J. Oncol.* 33 (1), 103–111. doi:10.3892/ijo.33.1.103

Jin, Y., Kim, Y. H., Park, J. Y., Lee, Y. J., Oh, H. M., Choi, S. K., et al. (2018). Methyllucidone Inhibits STAT3 Activity by Regulating the Expression of the Protein Tyrosine Phosphatase MEG2 in DU145 Prostate Carcinoma Cells. *Bioorg. Med. Chem. Lett.* 28 (5), 853–857. doi:10.1016/j.bmcl.2018.02.012

Jongsomchai, K., Leardkamolkarn, V., and Mahatheeranont, S. (2020). A rice Bran Phytochemical, Cyanidin 3-glucoside, Inhibits the Progression of PC3 Prostate Cancer Cell. *Anat. Cel Biol* 53 (4), 481–492. doi:10.5115/acb.20.085

Jung, S. N., Shin, D. S., Kim, H. N., Jeon, Y. J., Yun, J., Lee, Y. J., et al. (2015). Sugiol Inhibits STAT3 Activity via Regulation of Transketolase and ROS-Mediated ERK Activation in DU145 Prostate Carcinoma Cells. *Biochem. Pharmacol.* 97 (1), 38–50. doi:10.1016/j.bcp.2015.06.033

Kandoth, C. (2013). Cancer Genome Atlas Research Network. *Nature* 497 (7447), 67–73.

Kasimsetty, S. G., Bialonska, D., Reddy, M. K., Thornton, C., Willett, K. L., and Ferreira, D. (2009). Effects of Pomegranate Chemical Constituents/intestinal Microbial Metabolites on CYP1B1 in 22Rv1 Prostate Cancer Cells. *J. Agric. Food Chem.* 57 (22), 10636–10644. doi:10.1021/jf902716r

Kaur, M., Velmurugan, B., Rajamanickam, S., Agarwal, R., and Agarwal, C. (2009). Gallic Acid, an Active Constituent of Grape Seed Extract, Exhibits Anti-proliferative, Pro-apoptotic and Anti-tumorigenic Effects against Prostate Carcinoma Xenograft Growth in Nude Mice. *Pharm. Res.* 26 (9), 2133–2140. doi:10.1007/s11095-009-9926-y

Khan, F., Pandey, P., Ahmad, V., and Upadhyay, T. K. (2020a). Moringa Oleifera Methanolic Leaves Extract Induces Apoptosis and G0/G1 Cell Cycle Arrest via Downregulation of Hedgehog Signaling Pathway in Human Prostate PC-3 Cancer Cells. *J. Food Biochem.* 44 (8), e13338. doi:10.1111/jfbc.13338

Khan, F., Pandey, P., Jha, N. K., Jafri, A., and Khan, I. (2020b). Antiproliferative Effect of Moringa Oleifera Methanolic Leaf Extract by Down-Regulation of Notch Signaling in DU145 Prostate Cancer Cells. *Gene Rep.* 19, 100619. doi:10.1016/j.genrep.2020.100619

Khan, N., Asim, M., Afaq, F., Abu Zaid, M., and Mukhtar, H. (2008). A Novel Dietary Flavonoid Fisetin Inhibits Androgen Receptor Signaling and Tumor Growth in Athymic Nude Mice. *Cancer Res.* 68 (20), 8555–8563. doi:10.1158/0008-5472.CAN-08-0240

Kilch, T., Kappel, S., and Peinelt, C. (2016). Regulation of Ca(2+) Signaling in Prostate Cancer Cells. *Channels (Austin)* 10 (4), 170–171. doi:10.1080/19336950.2015.1137176

Kim, K. Y., Cho, H. J., Yu, S. N., Kim, S. H., Yu, H. S., Park, Y. M., et al. (2013). Interplay of Reactive Oxygen Species, Intracellular Ca2+ and Mitochondrial Homeostasis in the Apoptosis of Prostate Cancer Cells by Deoxypodophyllotoxin. *J. Cel Biochem* 114 (5), 1124–1134. doi:10.1002/jcb.24455

Kim, S. H., Bommareddy, A., and Singh, S. V. (2011). Garlic Constituent Diallyl Trisulfide Suppresses X-Linked Inhibitor of Apoptosis Protein in Prostate Cancer Cells in Culture and *In Vivo*. *Cancer Prev. Res. (Phila)* 4 (6), 897–906. doi:10.1158/1940-6207.CAPR-10-0323

Kimira, M., Arai, Y., Shimoi, K., and Watanabe, S. (1998). Japanese Intake of Flavonoids and Isoflavonoids from Foods. *J. Epidemiol.* 8 (3), 168–175. doi:10.2188/jea.8.168

Koka, P. S., Mondal, D., Schultz, M., Abdel-Mageed, A. B., and Agrawal, K. C. (2010). Studies on Molecular Mechanisms of Growth Inhibitory Effects of Thymoquinone against Prostate Cancer Cells: Role of Reactive Oxygen Species. *Exp. Biol. Med. (Maywood)* 235 (6), 751–760. doi:10.1258/ebm.2010.009369

Kong, E. H., Kim, Y. J., Kim, Y. J., Cho, H. J., Yu, S. N., Kim, K. Y., et al. (2008). Piplartine Induces Caspase-Mediated Apoptosis in PC-3 Human Prostate Cancer Cells. *Oncol. Rep.* 20 (4), 785–792. doi:10.3892/or_00000075

Koyama, S., Cobb, L. J., Mehta, H. H., Seeram, N. P., Heber, D., Pantuck, A. J., et al. (2010). Pomegranate Extract Induces Apoptosis in Human Prostate Cancer Cells by Modulation of the IGF-IGFBP axis. *Growth Horm. IGF Res.* 20 (1), 55–62. doi:10.1016/j.ghir.2009.09.003

Kron, K. J., Murison, A., Zhou, S., Huang, V., Yamaguchi, T. N., Shiah, Y. J., et al. (2017). TMPRSS2-ERG Fusion Co-opts Master Transcription Factors and Activates NOTCH Signaling in Primary Prostate Cancer. *Nat. Genet.* 49 (9), 1336–1345. doi:10.1038/ng.3930

Kumar, A., Coleman, I., Morrissey, C., Zhang, X., True, L. D., Gulati, R., et al. (2016). Substantial Interindividual and Limited Intraindividual Genomic Diversity Among Tumors from Men with Metastatic Prostate Cancer. *Nat. Med.* 22 (4), 369–378. doi:10.1038/nm.4053

Labow, R. S., and Layne, D. S. (1972). The Formation of Glucosides of Isoflavones and of Some Other Phenols by Rabbit Liver Microsomal Fractions. *Biochem. J.* 128 (3), 491–497. doi:10.1042/bj1280491

Lee, D. H., Szczepanski, M. J., and Lee, Y. J. (2009). Magnolol Induces Apoptosis via Inhibiting the EGFR/PI3K/Akt Signaling Pathway in Human Prostate Cancer Cells. *J. Cel Biochem* 106 (6), 1113–1122. doi:10.1002/jcb.22098

Lee, E., Son, J. E., Byun, S., Lee, S. J., Kim, Y. A., Liu, K., et al. (2013a). CDK2 and mTOR Are Direct Molecular Targets of Isoangustone A in the Suppression of Human Prostate Cancer Cell Growth. *Toxicol. Appl. Pharmacol.* 272 (1), 12–20. doi:10.1016/j.taap.2013.04.030

Lee, M. G., Liu, Y. C., Lee, Y. L., El-Shazly, M., Lai, K. H., Shih, S. P., et al. (2018). Heteronemin, a Marine Sesterterpenoid-type Metabolite, Induces Apoptosis in

Prostate LNcap Cells via Oxidative and ER Stress Combined with the Inhibition of Topoisomerase II and Hsp90. *Mar. Drugs* 16 (6). doi:10.3390/md16060204

Lee, S.-E., Sivtseva, S., Lim, C., Okhlopkova, Z., and Cho, S. (2021). Artemisia Kruhsiana Leaf Extract Induces Autophagic Cell Death in Human Prostate Cancer Cells. *Chin. J. Nat. Medicines* 19 (2), 134–142. doi:10.1016/s1875-5364(21)60014-6

Lee, S. E., Okhlopkova, Z., Lim, C., and Cho, S. (2020). Dracocephalum Palmatum Stephan Extract Induces Apoptosis in Human Prostate Cancer Cells via the Caspase-8-Mediated Extrinsic Pathway. *Chin. J. Nat. Med.* 18 (10), 793–800. doi:10.1016/s1875-5364(20)60019-x

Lee, S. Y., Cho, J. S., Yuk, D. Y., Moon, D. C., Jung, J. K., Yoo, H. S., et al. (2009). Obovatol Enhances Docetaxel-Induced Prostate and Colon Cancer Cell Death through Inactivation of Nuclear Transcription Factor-Kb. *J. Pharmacol. Sci.* 111 (2), 124–136. doi:10.1254/jphs.09048fp

Lee, W., Kim, K. Y., Yu, S. N., Kim, S. H., Chun, S. S., Ji, J. H., et al. (2013b). Pipernonaline from Piper Longum Linn. Induces ROS-Mediated Apoptosis in Human Prostate Cancer PC-3 Cells. *Biochem. Biophys. Res. Commun.* 430 (1), 406–412. doi:10.1016/j.bbrc.2012.11.030

Leu, W. J., Chang, H. S., Chan, S. H., Hsu, J. L., Yu, C. C., Hsu, L. C., et al. (2014). Reevesioside A, a Cardenolide Glycoside, Induces Anticancer Activity against Human Hormone-Refractory Prostate Cancers through Suppression of C-Myc Expression and Induction of G1 Arrest of the Cell Cycle. *Plos One* 9 (1), e87323. doi:10.1371/journal.pone.0087323

Levrier, C., Sadowski, M. C., Rockstroh, A., Gabrielli, B., Kavallaris, M., Lehman, M., et al. (2016). 6α-Acetoxyanopterine: A Novel Structure Class of Mitotic Inhibitor Disrupting Microtubule Dynamics in Prostate Cancer Cells. *Mol. Cancer Ther.* 16 (1), 3–15. doi:10.1158/1535-7163.mct-16-0325

Lewandowska, U., Szewczyk, K., Owczarek, K., Hrabec, Z., Podsędek, A., Koziołkiewicz, M., et al. (2013). Flavanols from Japanese Quince (Chaenomeles Japonica) Fruit Inhibit Human Prostate and Breast Cancer Cell Line Invasiveness and Cause Favorable Changes in Bax/Bcl-2 mRNA Ratio. *Nutr. Cancer* 65 (2), 273–285. doi:10.1080/01635581.2013.749292

Li, C., Han, X., Zhang, H., Wu, J., and Li, B. (2015a). Effect of Scopoletin on Apoptosis and Cell Cycle Arrest in Human Prostate Cancer Cells *In Vitro*. *Trop. J. Pharm. Res.* 14 (4), 611–617. doi:10.4314/tjpr.v14i4.8

Li, C., He, C., Xu, Y., Xu, H., Tang, Y., Chavan, H., et al. (2019). Alternol Eliminates Excessive ATP Production by Disturbing Krebs Cycle in Prostate Cancer. *Prostate* 79, 628–639. doi:10.1002/pros.23767

Li, J., and Al-Azzawi, F. (2009). Mechanism of Androgen Receptor Action. *Maturitas* 63 (2), 142–148. doi:10.1016/j.maturitas.2009.03.008

Li, Q. Q., Wang, G., Huang, F., Banda, M., and Reed, E. (2010). Antineoplastic Effect of Beta-Elemene on Prostate Cancer Cells and Other Types of Solid Tumour Cells. *J. Pharm. Pharmacol.* 62 (8), 1018–1027. doi:10.1111/j.2042-7158.2010.01135.x

Li, T., Zhao, X., Mo, Z., Huang, W., Yan, H., Ling, Z., et al. (2014). Formononetin Promotes Cell Cycle Arrest via Downregulation of Akt/Cyclin D1/CDK4 in Human Prostate Cancer Cells. *Cell Physiol Biochem* 34 (4), 1351–1358. doi:10.1159/000366342

Li, W. (2020). Isolobetyol, a New Polyacetylene Derivative from Platycodon Grandiflorum Root. *Nat. Prod. Res.*, 1–4. doi:10.1080/14786419.2020.1779269

Li, W., Li, D.-Y., Wang, H.-D., Zheng, Z.-J., Hu, J., and Li, Z.-Z. (2015b). Juglans Regia Hexane Extract Exerts Antitumor Effect, Apoptosis Induction and Cell Circle Arrest in Prostate Cancer Cells *In Vitro*. *Trop. J. Pharm. Res.* 14 (3), 399. doi:10.4314/tjpr.v14i3.7

Li, X., Fan, S., Pan, X., Xiaokaiti, Y., Duan, J., Shi, Y., et al. (2016). Nordihydroguaiaretic Acid Impairs Prostate Cancer Cell Migration and Tumor Metastasis by Suppressing Neuropilin 1. *Oncotarget* 7 (52), 86225–86238. doi:10.18632/oncotarget.13368

Li, X., Lao, Y., Zhang, H., Wang, X., Tan, H., Lin, Z., et al. (2015c). The Natural Compound Guttiferone F Sensitizes Prostate Cancer to Starvation Induced Apoptosis via Calcium and JNK Elevation. *BMC Cancer* 15 (1), 254. doi:10.1186/s12885-015-1292-z

Li, X., Li, X., Wang, J., Ye, Z., and Li, J. C. (2012). Oridonin Up-Regulates Expression of P21 and Induces Autophagy and Apoptosis in Human Prostate Cancer Cells. *Int. J. Biol. Sci.* 8 (6), 901–912. doi:10.7150/ijbs.4554

Li, Y., Chan, S. C., Brand, L. J., Hwang, T. H., Silverstein, K. A., and Dehm, S. M. (2013). Androgen Receptor Splice Variants Mediate Enzalutamide Resistance in Castration-Resistant Prostate Cancer Cell Lines. *Cancer Res.* 73 (2), 483–489. doi:10.1158/0008-5472.CAN-12-3630

Li, Y., and Sarkar, F. H. (2002). Inhibition of Nuclear Factor kappaB Activation in PC3 Cells by Genistein Is Mediated via Akt Signaling Pathway. *Clin. Cancer Res.* 8 (7), 2369–2377. doi:10.1159/000064924

Liao, R. S., Ma, S., Miao, L., Li, R., Yin, Y., and Raj, G. V. (2013). Androgen Receptor-Mediated Non-genomic Regulation of Prostate Cancer Cell Proliferation. *Transl Androl. Urol.* 2 (3), 187–196. doi:10.3978/j.issn.2223-4683.2013.09.07

Liberio, M. S., Sadowski, M. C., Davis, R. A., Rockstroh, A., Vasireddy, R., Lehman, M. L., et al. (2015). The Ascidian Natural Product Eusynstyelamide B Is a Novel Topoisomerase II Poison that Induces DNA Damage and Growth Arrest in Prostate and Breast Cancer Cells. *Oncotarget* 6 (41), 43944–43963. doi:10.18632/oncotarget.6267

Lin, C. C., Chen, K. B., Tsai, C. H., Tsai, F. J., Huang, C. Y., Tang, C. H., et al. (2019). Casticin Inhibits Human Prostate Cancer DU 145 Cell Migration and Invasion via Ras/Akt/NF-κB Signaling Pathways. *J. Food Biochem.* 43. doi:10.1111/jfbc.12902

Lippert, M. C., Mcclain, R., Boyd, J. C., and Theodorescu, D. (1999). Alternative Medicine Use in Patients with Localized Prostate Carcinoma Treated with Curative Intent. *Cancer* 86 (12), 2642–2648. doi:10.1002/(SICI)1097-0142(19991215)86:123.0.CO;2-4

Liu, K., Park, C., Li, S., Lee, K. W., Liu, H., He, L., et al. (2012a). Aloe-emodin Suppresses Prostate Cancer by Targeting the mTOR Complex 2. *Carcinogenesis* 33 (7), 1406–1411. doi:10.1093/carcin/bgs156

Liu, P., Cheng, H., Roberts, T. M., and Zhao, J. J. (2009). Targeting the Phosphoinositide 3-kinase Pathway in Cancer. *Nat. Rev. Drug Discov.* 8 (8), 627–644. doi:10.1038/nrd2926

Liu, S., Kumari, S., Hu, Q., Senapati, D., Venkadakrishnan, V. B., Wang, D., et al. (2017). A Comprehensive Analysis of Coregulator Recruitment, Androgen Receptor Function and Gene Expression in Prostate Cancer. *Elife* 6, e28482. doi:10.7554/eLife.28482

Liu, W. K., Cheung, F. W., and Che, C. T. (2006). Stellettin A Induces Oxidative Stress and Apoptosis in HL-60 Human Leukemia and LNCaP Prostate Cancer Cell Lines. *J. Nat. Prod.* 69 (6), 934–937. doi:10.1021/np058122y

Liu, X., He, Z., Li, C. H., Huang, G., Ding, C., and Liu, H. (2012b). Correlation Analysis of JAK-STAT Pathway Components on Prognosis of Patients with Prostate Cancer. *Pathol. Oncol. Res.* 18 (1), 17–23. doi:10.1007/s12253-011-9410-y

Liu, Y., Wang, M., Wang, D., Li, X., Wang, W., Lou, H., et al. (2016). Malformin A1 Promotes Cell Death through Induction of Apoptosis, Necrosis and Autophagy in Prostate Cancer Cells. *Cancer Chemother. Pharmacol.* 77 (1), 63–75. doi:10.1007/s00280-015-2915-4

Locke, J. A., Guns, E. S., Lubik, A. A., Adomat, H. H., Hendy, S. C., Wood, C. A., et al. (2008). Androgen Levels Increase by Intratumoral De Novo Steroidogenesis during Progression of Castration-Resistant Prostate Cancer. *Cancer Res.* 68 (15), 6407–6415. doi:10.1158/0008-5472.CAN-07-5997

Lu, Z., Wang, H., Zhu, M., Song, W., Wang, J., Wu, C., et al. (2018). Ophiopogonin D', a Natural Product from Radix Ophiopogonis, Induces *In Vitro* and *In Vivo* RIPK1-dependent and Caspase-independent Apoptotic Death in Androgen-independent Human Prostate Cancer Cells. *Front. Pharmacol.* 9, 432. doi:10.3389/fphar.2018.00432

Luu-The, V., Bélanger, A., and Labrie, F. (2008). Androgen Biosynthetic Pathways in the Human Prostate. *Best Pract. Res. Clin. Endocrinol. Metab.* 22 (2), 207–221. doi:10.1016/j.beem.2008.01.008

Ma, B., Zhang, H., Wang, Y., Zhao, A., Zhu, Z., Bao, X., et al. (2018). Corosolic Acid, a Natural Triterpenoid, Induces ER Stress-dependent Apoptosis in Human Castration Resistant Prostate Cancer Cells via Activation of IRE-1/JNK, PERK/CHOP and TRIB3. *J. Exp. Clin. Cancer Res.* 37 (1), 210. doi:10.1186/s13046-018-0889-x

Malik, A., Afaq, F., Sarfaraz, S., Adhami, V. M., Syed, D. N., and Mukhtar, H. (2005). Pomegranate Fruit Juice for Chemoprevention and Chemotherapy of Prostate Cancer. *Proc. Natl. Acad. Sci. U S A.* 102 (41), 14813–14818. doi:10.1073/pnas.0505870102

Marais, R., Wynne, J., and Treisman, R. (1993). The SRF Accessory Protein Elk-1 Contains a Growth Factor-Regulated Transcriptional Activation Domain. *Cell* 73 (2), 381–393. doi:10.1016/0092-8674(93)90237-k

Marilena, M., Sims, N. A., Susanne, V., Silvia, M., Anna, T., Silvia, B., et al. (2000). Decreased C-Src Expression Enhances Osteoblast Differentiation and Bone Formation. *J. Cel Biol.* 151 (2), 311–320.

Masood, M., Rasul, A., Sarfraz, I., Jabeen, F., Liu, S., Liu, X., et al. (2019).Hispolon Induces Apoptosis against Prostate DU145 Cancer Cells via Modulation of Mitochondrial and STAT3 Pathways*Pak J. Pharm. Sci.*, 32, 2237–2243.

Masoodi, K. Z., Wani, W., Dar, Z. A., Mansoor, S., Anam-ul-Haq, S., Farooq, I., et al. (2020). Sea Buckthorn (Hippophae Rhamnoides L.) Inhibits Cellular Proliferation, Wound Healing and Decreases Expression of Prostate Specific Antigen in Prostate Cancer Cells *In Vitro*. *J. Funct. Foods* 73, 104102. doi:10.1016/j.jff.2020.104102

McEleny, K. R., Watson, R. W., Coffey, R. N., O'Neill, A. J., and Fitzpatrick, J. M. (2002). Inhibitors of Apoptosis Proteins in Prostate Cancer Cell Lines. *Prostate* 51 (2), 133–140. doi:10.1002/pros.10061

Meimetis, L. G., Williams, D. E., Mawji, N. R., Banuelos, C. A., Lal, A. A., Park, J. J., et al. (2012). Niphatenones, Glycerol Ethers from the Sponge Niphates Digitalis Block Androgen Receptor Transcriptional Activity in Prostate Cancer Cells: Structure Elucidation, Synthesis, and Biological Activity. *J. Med. Chem.* 55 (1), 503–514. doi:10.1021/jm2014056

Meng, F. M., Yang, J. B., Yang, C. H., Jiang, Y., Zhou, Y. F., Yu, B., et al. (2012). Vitexicarpin Induces Apoptosis in Human Prostate Carcinoma PC-3 Cells through G2/M Phase Arrest. *Asian Pac. J. Cancer Prev.* 13 (12), 6369–6374. doi:10.7314/Apjcp.2012.13.12.6369

Meng, Y., Lin, Z. M., Ge, N., Zhang, D. L., Huang, J., and Kong, F. (2015). Ursolic Acid Induces Apoptosis of Prostate Cancer Cells via the PI3K/Akt/mTOR Pathway. *Am. J. Chin. Med.* 43 (7), 1471–1486. doi:10.1142/S0192415X15500834

Miao, L., Yun, X., Tao, R., Wang, Y., Fan, G., Zhu, Y., et al. (2018). Bakuchiol Exhibits Anti-metastasis Activity through NF-Kb Cross-Talk Signaling with AR and ERβ in Androgen-independent Prostate Cancer Cells PC-3. *J. Pharmacol. Sci.* 138, 1–8. doi:10.1016/j.jphs.2017.04.004

Migliaccio, A., Castoria, G., Di Domenico, M., de Falco, A., Bilancio, A., Lombardi, M., et al. (2002). Sex Steroid Hormones Act as Growth Factors. *J. Steroid Biochem. Mol. Biol.* 83 (1), 31–35. doi:10.1016/s0960-0760(02)00264-9

Miller, W. L., and Auchus, R. J. (2011). The Molecular Biology, Biochemistry, and Physiology of Human Steroidogenesis and its Disorders. *Endocr. Rev.* 32 (1), 81–151. doi:10.1210/er.2010-0013

Ming, M., Sun, F. Y., Zhang, W. T., and Liu, J. K. (2016). Therapeutic Effect of Oridonin on Mice with Prostate Cancer. *Asian Pac. J. Trop. Med.* 9 (2), 184–187. doi:10.1016/j.apjtm.2016.01.007

Mirza, M. B., Elkady, A. I., Al-Attar, A. M., Syed, F. Q., Mohammed, F. A., and Hakeem, K. R. (2018). Induction of Apoptosis and Cell Cycle Arrest by Ethyl Acetate Fraction of Phoenix Dactylifera L. (Ajwa Dates) in Prostate Cancer Cells. *J. Ethnopharmacol* 218, 35–44. doi:10.1016/j.jep.2018.02.030

Montgomery, R. B., Mostaghel, E. A., Vessella, R., Hess, D. L., Kalhorn, T. F., Higano, C. S., et al. (2008). Maintenance of Intratumoral Androgens in Metastatic Prostate Cancer: a Mechanism for Castration-Resistant Tumor Growth. *Cancer Res.* 68 (11), 4447–4454. doi:10.1158/0008-5472.CAN-08-0249

Mordan-McCombs, S., Brown, T., Wang, W. L., Gaupel, A. C., Welsh, J., Tenniswood, M., et al. (2010). Tumor Progression in the LPB-Tag Transgenic Model of Prostate Cancer Is Altered by Vitamin D Receptor and Serum Testosterone Status. *J. Steroid Biochem. Mol. Biol.* 121 (2), 368–371. doi:10.1016/j.jsbmb.2010.03.062

Morgentaler, A. (2009). Testosterone Therapy in Men with Prostate Cancer: Scientific and Ethical Considerations. *J. Urol.* 181 (3), 972–979. doi:10.1016/j.juro.2008.11.031

Mukhtar, E., Adhami, V. M., Sechi, M., and Mukhtar, H. (2015). Dietary Flavonoid Fisetin Binds to β-tubulin and Disrupts Microtubule Dynamics in Prostate Cancer Cells. *Cancer Lett.* 367 (2), 173–183. doi:10.1016/j.canlet.2015.07.030

Mundy, G. R. (2002). Metastasis to Bone: Causes, Consequences and Therapeutic Opportunities. *Nat. Rev. Cancer* 2 (8), 584–593. doi:10.1038/nrc867

Nakase, I., Gallis, B., Takatani-Nakase, T., Oh, S., Lacoste, E., Singh, N. P., et al. (2009). Transferrin Receptor-dependent Cytotoxicity of Artemisinin-Transferrin Conjugates on Prostate Cancer Cells and Induction of Apoptosis. *Cancer Lett.* 274 (2), 290–298. doi:10.1016/j.canlet.2008.09.023

Nam, R. K., Fleshner, N., Rakovitch, E., Klotz, L., Trachtenberg, J., Choo, R., et al. (1999). Prevalence and Patterns of the Use of Complementary Therapies Among Prostate Cancer Patients: an Epidemiological Analysis. *J. Urol.* 161 (5), 1521–1524. doi:10.1108/13598540910970072 10.1097/00005392-199905000-00028

Network, C. G. A. (2015a). The Molecular Taxonomy of Primary Prostate Cancer. *Cell* 163 (4), 1011–1025. doi:10.1016/j.cell.2015.10.025

Network, T. C. G. A. (2015b). The Molecular Taxonomy of Primary Prostate Cancer. *Cell* 163 (4), 1011–1025. doi:10.1016/j.cell.2015.10.025

Nguyen, C., Mehaidli, A., Baskaran, K., Grewal, S., Pupulin, A., Ruvinov, I., et al. (2019). Dandelion Root and Lemongrass Extracts Induce Apoptosis, Enhance Chemotherapeutic Efficacy, and Reduce Tumour Xenograft Growth *In Vivo* in Prostate Cancer. *Evid. Based Complement. Alternat Med.* 2019, 2951428. doi:10.1155/2019/2951428

Nishimura, M., Fuchino, H., Takayanagi, K., Kawakami, H., Nakayama, H., Kawahara, N., et al. (2021). Toxicity of Jegosaponins A and B from Styrax japonica Siebold Zuccarini in Prostate Cancer Cells and Zebrafish Embryos Resulting from Increased Membrane Permeability. *Ijms* 22 (12), 6354. doi:10.3390/ijms22126354

Pan, X. Y., Guo, H., Han, J., Hao, F., An, Y., Xu, Y., et al. (2012). Ginsenoside Rg3 Attenuates Cell Migration via Inhibition of Aquaporin 1 Expression in PC-3M Prostate Cancer Cells. *Eur. J. Pharmacol.* 683 (1–3), 27–34. doi:10.1016/j.ejphar.2012.02.040

Pintard, L., Willis, J. H., Willems, A., Johnson, J. L., Srayko, M., Kurz, T., et al. (2003). The BTB Protein MEL-26 Is a Substrate-specific Adaptor of the CUL-3 Ubiquitin-Ligase. *Nature* 425 (6955), 311–316. doi:10.1038/nature01959

Pinto, J. T., Sinha, R., Papp, K., Facompre, N. D., Desai, D., and El-Bayoumy, K. (2007). Differential Effects of Naturally Occurring and Synthetic Organoselenium Compounds on Biomarkers in Androgen Responsive and Androgen Independent Human Prostate Carcinoma Cells. *Int. J. Cancer* 120 (7), 1410–1417. doi:10.1002/ijc.22500

Pradhan, N., Parbin, S., Kausar, C., Kar, S., Mawatwal, S., Das, L., et al. (2019). Paederia Foetida Induces Anticancer Activity by Modulating Chromatin Modification Enzymes and Altering Pro-inflammatory Cytokine Gene Expression in Human Prostate Cancer Cells. *Food Chem. Toxicol.* 130, 161–173. doi:10.1016/j.fct.2019.05.016

Rabiau, N., Kossaï, M., Braud, M., Chalabi, N., Satih, S., Bignon, Y. J., et al. (2010). Genistein and Daidzein Act on a Panel of Genes Implicated in Cell Cycle and Angiogenesis by Polymerase Chain Reaction Arrays in Human Prostate Cancer Cell Lines. *Cancer Epidemiol.* 34 (2), 200–206. doi:10.1016/j.canep.2009.12.018

Ritch, C. R., and Cookson, M. S. (2016). Advances in the Management of Castration Resistant Prostate Cancer. *BMJ* 355, i4405. doi:10.1136/bmj.i4405

Robinson, D., Van Allen, E. M., Wu, Y. M., Schultz, N., Lonigro, R. J., Mosquera, J. M., et al. (2015). Integrative Clinical Genomics of Advanced Prostate Cancer. *Cell* 161 (5), 1215–1228. doi:10.1016/j.cell.2015.05.001

Rodrigues, D. N., Boysen, G., Sumanasuriya, S., Seed, G., Marzo, A. M., and de Bono, J. (2017). The Molecular Underpinnings of Prostate Cancer: Impacts on Management and Pathology Practice. *J. Pathol.* 241 (2), 173–182. doi:10.1002/path.4826

Rodríguez-Berriguete, G., Torrealba, N., Fraile, B., Paniagua, R., and Royuela, M. (2016). Epidermal Growth Factor Induces P38 MAPK-dependent G0/G1-To-S Transition in Prostate Cancer Cells upon Androgen Deprivation Conditions. *Growth Factors* 34 (1-2), 5–10. doi:10.3109/08977194.2015.1132712

Rosa, H. H., Carvalho, P., Ortmann, C. F., Schneider, N. F. Z., Reginatto, F. H., Simões, C. M. O., et al. (2020). Cytotoxic Effects of a Triterpene-Enriched Fraction of Cecropia Pachystachya on the Human Hormone-Refractory Prostate Cancer PC3 Cell Line. *Biomed. Pharmacother.* 130, 110551. doi:10.1016/j.biopha.2020.110551

Russo, A., Piovano, M., Clericuzio, M., Lombardo, L., Tabasso, S., Chamy, M. C., et al. (2007). Putrescine-1,4-dicinnamide from Pholiota Spumosa (Basidiomycetes) Inhibits Cell Growth of Human Prostate Cancer Cells. *Phytomedicine* 14 (2-3), 185–191. doi:10.1016/j.phymed.2006.09.010

Ryan, C. J., and Tindall, D. J. (2011). Androgen Receptor Rediscovered: the New Biology and Targeting the Androgen Receptor Therapeutically. *J. Clin. Oncol.* 29 (27), 3651–3658. doi:10.1200/JCO.2011.35.2005

Sachan, R., Kundu, A., Jeon, Y., Choi, W. S., Yoon, K., Kim, I. S., et al. (2018). Afrocyclamin A, a Triterpene Saponin, Induces Apoptosis and Autophagic Cell Death via the PI3K/Akt/mTOR Pathway in Human Prostate Cancer Cells. *Phytomedicine* 51, 139–150. doi:10.1016/j.phymed.2018.10.012

Sajjadi, S.-E., Ghanadian, M., Aghaei, M., and Salehi, A. (2018). Two New Dammarane Triterpenes Isolated from Cleome Khorassanica Bunge & Bien

with Cytotoxicity against DU-145 and LNCaP Prostate Cancer Cell Lines. *J. Asian Nat. Prod. Res.* 22, 38–46. doi:10.1080/10286020.2018.1538211

Salmani, J. M. M., Zhang, X. P., Jacob, J. A., and Chen, B. A. (2017). Apigenin's Anticancer Properties and Molecular Mechanisms of Action: Recent Advances and Future Prospectives. *Chin. J. Nat. Med.* 15 (5), 321–329. doi:10.1016/S1875-5364(17)30052-3

Saravanakumar, K., Mandava, S., Chellia, R., Jeevithan, E., Babu Yelamanchi, R. S., Mandava, D., et al. (2019). Novel Metabolites from Trichoderma Atroviride against Human Prostate Cancer Cells and Their Inhibitory Effect on *Helicobacter pylori* and Shigella Toxin Producing *Escherichia coli*. *Microb. Pathogenesis* 126, 19–26. doi:10.1016/j.micpath.2018.10.011

Sarveswaran, S., Gautam, S. C., and Ghosh, J. (2012). Wedelolactone, a Medicinal Plant-Derived Coumestan, Induces Caspase-dependent Apoptosis in Prostate Cancer Cells via Downregulation of PKCε without Inhibiting Akt. *Int. J. Oncol.* 41 (6), 2191–2199. doi:10.3892/ijo.2012.1664

Sarveswaran, S., Liroff, J., Zhou, Z., Nikitin, A. Y., and Ghosh, J. (2010). Selenite Triggers Rapid Transcriptional Activation of P53, and P53-Mediated Apoptosis in Prostate Cancer Cells: Implication for the Treatment of Early-Stage Prostate Cancer. *Int. J. Oncol.* 36 (6), 1419–1428. doi:10.3892/ijo_00000627

Scher, H. I., and Sawyers, C. L. (2005). Biology of Progressive, Castration-Resistant Prostate Cancer: Directed Therapies Targeting the Androgen-Receptor Signaling axis. *J. Clin. Oncol.* 23 (32), 8253–8261. doi:10.1200/JCO.2005.03.4777

Schindler, C., and Darnell, J. E. (1995). Transcriptional Responses to Polypeptide Ligands: the JAK-STAT Pathway. *Annu. Rev. Biochem.* 64 (64), 621–651. doi:10.1146/annurev.bi.64.070195.003201

Schleich, S., Papaioannou, M., Baniahmad, A., and Matusch, R. (2006). Activity-guided Isolation of an Antiandrogenic Compound of Pygeum Africanum. *Planta Med.* 72 (6), 547–551. doi:10.1055/s-2006-941472

Schweizer, M. T., and Plymate, S. R. (2016). Targeting Constitutively Active Androgen Receptor Splice Variants in Castration Resistant Prostate Cancer. *Expert Opin. Ther. Targets* 20 (8), 903–906. doi:10.1517/14728222.2016.1159676

Senderowicz, A. M., Kaur, G., Sainz, E., Laing, C., Inman, W. D., Rodríguez, J., et al. (1995). Jasplakinolide's Inhibition of the Growth of Prostate Carcinoma Cells *In Vitro* with Disruption of the Actin Cytoskeleton. *J. Natl. Cancer Inst.* 87 (1), 46–51. doi:10.1093/jnci/87.1.46

Seo, Y., Ryu, K., Park, J., Jeon, D. K., Jo, S., Lee, H. K., et al. (2017). Inhibition of ANO1 by Luteolin and its Cytotoxicity in Human Prostate Cancer PC-3 Cells. *PLoS One* 12 (3), e0174935. doi:10.1371/journal.pone.0174935

Shanmugam, M. K., Rajendran, P., Li, F., Nema, T., Vali, S., Abbasi, T., et al. (2011). Ursolic Acid Inhibits Multiple Cell Survival Pathways Leading to Suppression of Growth of Prostate Cancer Xenograft in Nude Mice. *J. Mol. Med. (Berl)* 89 (7), 713–727. doi:10.1007/s00109-011-0746-2

Shaw, G., Renfree, M. B., Leihy, M. W., Shackleton, C. H. L., Roitman, E., and Wilson, J. D. (2000). Prostate Formation in a Marsupial Is Mediated by the Testicular Androgen 5alpha -androstane-3alpha ,17beta -diol. *Proc. Natl. Acad. Sci.* 97 (22), 12256–12259. doi:10.1073/pnas.220412297

Sheng, Y., Zou, M., Wang, Y., and Li, Q. (2015). 2',4'-dihydroxychalcone, a Flavonoid Isolated from Herba Oxytropis, Suppresses PC-3 Human Prostate Cancer Cell Growth by Induction of Apoptosis. *Oncol. Lett.* 10 (6), 3737–3741. doi:10.3892/ol.2015.3795

Shigemura, K., Arbiser, J. L., Sun, S. Y., Zayzafoon, M., Johnstone, P. A., Fujisawa, M., et al. (2007). Honokiol, a Natural Plant Product, Inhibits the Bone Metastatic Growth of Human Prostate Cancer Cells. *Cancer* 109 (7), 1279–1289. doi:10.1002/cncr.22551

Shin, Y., Kim, G. D., Jeon, J. E., Shin, J., and Lee, S. K. (2013). Antimetastatic Effect of Halichondramide, a Trisoxazole Macrolide from the marine Sponge Chondrosia Corticata, on Human Prostate Cancer Cells via Modulation of Epithelial-To-Mesenchymal Transition. *Mar. Drugs* 11 (7), 2472–2485. doi:10.3390/md11072472

Siegel, R. L., Miller, K. D., Fedewa, S. A., Ahnen, D. J., Meester, R. G. S., Barzi, A., et al. (2017). Colorectal Cancer Statistics, 2017. *CA Cancer J. Clin.* 67 (3), 177–193. doi:10.3322/caac.21395

Sigstedt, S. C., Hooten, C. J., Callewaert, M. C., Jenkins, A. R., Romero, A. E., Pullin, M. J., et al. (2008). Evaluation of Aqueous Extracts of *Taraxacum officinale* on Growth and Invasion of Breast and Prostate Cancer Cells. *Int. J. Oncol.* 32 (5), 1085–1090. doi:10.3892/ijo.32.5.1085

Singh, S. V., Zeng, Y., Xiao, D., Vogel, V. G., Nelson, J. B., Dhir, R., et al. (2005). Caspase-dependent Apoptosis Induction by Guggulsterone, a Constituent of Ayurvedic Medicinal Plant Commiphora Mukul, in PC-3 Human Prostate Cancer Cells Is Mediated by Bax and Bak. *Mol. Cancer Ther.* 4 (11), 1747–1754. doi:10.1158/1535-7163.MCT-05-0223

Small, E. J., Halabi, S., Dawson, N. A., Stadler, W. M., Rini, B. I., Picus, J., et al. (2004). Antiandrogen Withdrawal Alone or in Combination with Ketoconazole in Androgen-independent Prostate Cancer Patients: a Phase III Trial (CALGB 9583). *J. Clin. Oncol.* 22 (6), 1025–1033. doi:10.1200/JCO.2004.06.037

Squire, J. A., Park, P. C., Yoshimoto, M., Alami, J., Williams, J. L., Evans, A., et al. (2011). Prostate Cancer as a Model System for Genetic Diversity in Tumors. *Adv. Cancer Res.* 112, 183–216. doi:10.1016/B978-0-12-387688-1.00007-7

Steigerová, J., Rárová, L., Oklešťková, J., Křížová, K., Levková, M., Sváchová, M., et al. (2012). Mechanisms of Natural Brassinosteroid-Induced Apoptosis of Prostate Cancer Cells. *Food Chem. Toxicol.* 50 (11), 4068–4076. doi:10.1016/j.fct.2012.08.031

Stein, M. N., Goodin, S., and Dipaola, R. S. (2012). Abiraterone in Prostate Cancer: a New Angle to an Old Problem. *Clin. Cancer Res.* 18 (7), 1848–1854. doi:10.1158/1078-0432.CCR-11-1805

Su, X., Li, T., Liu, Z., Huang, Q., Liao, K., Ren, R., et al. (2018). Licochalcone A Activates Keap1-Nrf2 Signaling to Suppress Arthritis via Phosphorylation of P62 at Serine 349. *Free Radic. Biol. Med.* 115, 471–483. doi:10.1016/j.freeradbiomed.2017.12.004

Su, Z. Y., Khor, T. O., Shu, L., Lee, J. H., Saw, C. L., Wu, T. Y., et al. (2013). Epigenetic Reactivation of Nrf2 in Murine Prostate Cancer TRAMP C1 Cells by Natural Phytochemicals Z-Ligustilide and Radix Angelica Sinensis via Promoter CpG Demethylation. *Chem. Res. Toxicol.* 26 (3), 477–485. doi:10.1021/tx300524p

Suh, Y., Afaq, F., Khan, N., Johnson, J. J., Khusro, F. H., and Mukhtar, H. (2010). Fisetin Induces Autophagic Cell Death through Suppression of mTOR Signaling Pathway in Prostate Cancer Cells. *Carcinogenesis* 31 (8), 1424–1433. doi:10.1093/carcin/bgq115

Sun, B. L., Cai, E. B., Zhao, Y., Wang, Y., Yang, L. M., and Wang, J. Y. (2021). Arctigenin Triggers Apoptosis and Autophagy via PI3K/Akt/mTOR Inhibition in PC-3M Cells. *Chem. Pharm. Bull. (Tokyo)* 69 (5), 472–480. doi:10.1248/cpb.c21-00021

Sun, H., Zhang, A. H., Liu, S. B., Qiu, S., Li, X. N., Zhang, T. L., et al. (2018). Cell Metabolomics Identify Regulatory Pathways and Targets of Magnoline against Prostate Cancer. *J. Chromatogr. B Analyt Technol. Biomed. Life Sci.* 1102–1103, 143–151. doi:10.1016/j.jchromb.2018.10.017

Swami, S., Krishnan, A. V., Moreno, J., Bhattacharyya, R. S., Gardner, C., Brooks, J. D., et al. (2009). Inhibition of Prostaglandin Synthesis and Actions by Genistein in Human Prostate Cancer Cells and by Soy Isoflavones in Prostate Cancer Patients. *Int. J. Cancer* 124 (9), 2050–2059. doi:10.1002/ijc.24161

Tam, L., Mcglynn, L. M., Traynor, P., Mukherjee, R., Bartlett, J. M., and Edwards, J. (2007). Expression Levels of the JAK/STAT Pathway in the Transition from Hormone-Sensitive to Hormone-Refractory Prostate Cancer. *Br. J. Cancer* 97 (3), 378–383. doi:10.1038/sj.bjc.6603871

Tang, Y., Li, X., Liu, Z., Simoneau, A. R., Xie, J., and Zi, X. (2010). Flavokawain B, a Kava Chalcone, Induces Apoptosis via Up-Regulation of Death-Receptor 5 and Bim Expression in Androgen Receptor Negative, Hormonal Refractory Prostate Cancer Cell Lines and Reduces Tumor Growth. *Int. J. Cancer* 127 (8), 1758–1768. doi:10.1002/ijc.25210

Tang, Y., Parmakhtiar, B., Simoneau, A. R., Xie, J., Fruehauf, J., Lilly, M., et al. (2011). Lycopene Enhances Docetaxel's Effect in Castration-Resistant Prostate Cancer Associated with Insulin-like Growth Factor I Receptor Levels. *Neoplasia* 13 (2), 108–119. doi:10.1593/neo.101092

Taylor, B. S., Schultz, N., Hieronymus, H., Gopalan, A., Xiao, Y., Carver, B. S., et al. (2010). Integrative Genomic Profiling of Human Prostate Cancer. *Cancer Cell* 18 (1), 11–22. doi:10.1016/j.ccr.2010.05.026

Thangapazham, R., Saenz, F., Katta, S., Mohamed, A. A., Tan, S. H., Petrovics, G., et al. (2014). Loss of the NKX3.1 Tumorsuppressor Promotes the TMPRSS2-ERG Fusion Gene Expression in Prostate Cancer. *BMC Cancer* 14 (1), 16. doi:10.1186/1471-2407-14-16

Theurillat, J. P., Udeshi, N. D., Errington, W. J., Svinkina, T., Baca, S. C., Pop, M., et al. (2014). Prostate Cancer. Ubiquitylome Analysis Identifies Dysregulation of Effector Substrates in SPOP-Mutant Prostate Cancer. *Science* 346 (6205), 85–89. doi:10.1126/science.1250255

Thirugnanam, S., Xu, L., Ramaswamy, K., and Gnanasekar, M. (2008). Glycyrrhizin Induces Apoptosis in Prostate Cancer Cell Lines DU-145 and LNCaP. *Oncol. Rep.* 20 (6), 1387–1392. doi:10.3892/or_00000157

Ting, H., Deep, G., Kumar, S., Jain, A. K., Agarwal, C., and Agarwal, R. (2016). Beneficial Effects of the Naturally Occurring Flavonoid Silibinin on the Prostate Cancer Microenvironment: Role of Monocyte Chemotactic Protein-1 and Immune Cell Recruitment. *Carcinogenesis* 37 (6), 589–599. doi:10.1093/carcin/bgw039

Titus, M. A., Schell, M. J., Lih, F. B., Tomer, K. B., and Mohler, J. L. (2005). Testosterone and Dihydrotestosterone Tissue Levels in Recurrent Prostate Cancer. *Clin. Cancer Res.* 11 (13), 4653–4657. doi:10.1158/1078-0432.CCR-05-0525

Tomkins, G. M. (1957). The Enzymatic Reduction of delta 4-3-ketosteroids. *J. Biol. Chem.* 225 (1), 13–24. doi:10.1016/S0002-9610(34)90209-910.1016/s0021-9258(18)64906-3

Tomlins, S. A., Rhodes, D. R., Perner, S., Dhanasekaran, S. M., Mehra, R., Sun, X. W., et al. (2005). Recurrent Fusion of TMPRSS2 and ETS Transcription Factor Genes in Prostate Cancer. *Science* 310 (5748), 644–648. doi:10.1126/science.1117679

Torre, L. A., Bray, F., Siegel, R. L., Ferlay, J., Lortet-Tieulent, J., and Jemal, A. (2015). Global Cancer Statistics, 2012. *CA Cancer J. Clin.* 65 (2), 87–108. doi:10.3322/caac.21262

Trang, N. T., Wanner, M. J., Phuong, le. V. N., Koomen, G. J., and Dung, N. X. (1993). Thymoquinone from Eupatorium Ayapana. *Planta Med.* 59 (1), 99. doi:10.1055/s-2006-959619

Turan, I., Demir, S., Kilinc, K., Burnaz, N. A., Yaman, S. O., Akbulut, K., et al. (2017). Antiproliferative and Apoptotic Effect of Morus Nigra Extract on Human Prostate Cancer Cells. *Saudi Pharm. J.* 25 (2), 241–248. doi:10.1016/j.jsps.2016.06.002

Twillie, D. A., Eisenberger, M. A., Carducci, M. A., Hseih, W. S., Kim, W. Y., and Simons, J. W. (1995). Interleukin-6: a Candidate Mediator of Human Prostate Cancer Morbidity. *Urology* 45 (3), 542–549. doi:10.1016/S0090-4295(99)80034-X

Unni, E., Sun, S., Nan, B., McPhaul, M. J., Cheskis, B., Mancini, M. A., et al. (2004). Changes in Androgen Receptor Nongenotropic Signaling Correlate with Transition of LNCaP Cells to Androgen independence. *Cancer Res.* 64 (19), 7156–7168. doi:10.1158/0008-5472.CAN-04-1121

Vanella, L., Di Giacomo, C., Acquaviva, R., Barbagallo, I., Cardile, V., Kim, D. H., et al. (2013). Apoptotic Markers in a Prostate Cancer Cell Line: Effect of Ellagic Acid. *Oncol. Rep.* 30 (6), 2804–2810. doi:10.3892/or.2013.2757

Vaz, C. V., Rodrigues, D. B., Socorro, S., and Maia, C. J. (2015). Effect of Extracellular Calcium on Regucalcin Expression and Cell Viability in Neoplastic and Non-neoplastic Human Prostate Cells. *Biochim. Biophys. Acta* 1853 (10 Pt A), 2621–2628. doi:10.1016/j.bbamcr.2015.07.006

Visakorpi, T., Hyytinen, E., Koivisto, P., Tanner, M., Keinänen, R., Palmberg, C., et al. (1995). *In Vivo* amplification of the Androgen Receptor Gene and Progression of Human Prostate Cancer. *Nat. Genet.* 9 (4), 401–406. doi:10.1038/ng0495-401

Vitali, F., Pennisi, G., Attaguile, G., Savoca, F., and Tita, B. (2011). Antiproliferative and Cytotoxic Activity of Extracts from Cistus Incanus L. And Cistus Monspeliensis L. on Human Prostate Cell Lines. *Nat. Prod. Res.* 25 (3), 188–202. doi:10.1080/14786410802583148

von Eyben, F., Kiljunen, T., Kangasmaki, A., Kairemo, K., von Eyben, R., and Joensuu, T. (2015). Management of Advanced Prostate Cancer. *Ann. Oncol.* 26 (11), 178–182. doi:10.1093/annonc/mdv327

Wadosky, K. M., and Koochekpour, a. S. (2016). Molecular Mechanisms Underlying Resistance to Androgen Deprivation Therapy in Prostate Cancer. *Oncotarget* 27, 64447–64470. doi:10.18632/oncotarget.10901

Wang, J., Eltoum, I. E., and Lamartiniere, C. A. (2004). Genistein Alters Growth Factor Signaling in Transgenic Prostate Model (TRAMP). *Mol. Cel Endocrinol* 219 (1–2), 171–180. doi:10.1016/j.mce.2003.12.018

Wang, J. L., Chou, C. T., Liang, W. Z., Yeh, J. H., Kuo, C. C., Lee, C. Y., et al. (2016a). Effect of 2,5-dimethylphenol on Ca(2+) Movement and Viability in PC3 Human Prostate Cancer Cells. *Toxicol. Mech. Methods* 26 (5), 327–333. doi:10.3109/15376516.2016.1158893

Wang, L. G., Liu, X. M., and Chiao, J. W. (2006). Repression of Androgen Receptor in Prostate Cancer Cells by Phenethyl Isothiocyanate. *Carcinogenesis* 27 (10), 2124–2132. doi:10.1093/carcin/bgl075

Wang, P., Henning, S. M., Magyar, C. E., Elshimali, Y., Heber, D., and Vadgama, J. V. (2016b). Green tea and Quercetin Sensitize PC-3 Xenograft Prostate Tumors to Docetaxel Chemotherapy. *J. Exp. Clin. Cancer Res.* 35 (1), 73. doi:10.1186/s13046-016-0351-x

Wang, Q., Grkovic, T., Font, J., Bonham, S., Pouwer, R. H., Bailey, C. G., et al. (2014). Monoterpene Glycoside ESK246 from Pittosporum Targets LAT3 Amino Acid Transport and Prostate Cancer Cell Growth. *ACS Chem. Biol.* 9 (6), 1369–1376. doi:10.1021/cb500120x

Wang, Q., Li, W., Liu, X. S., Carroll, J. S., Jänne, O. A., Keeton, E. K., et al. (2007). A Hierarchical Network of Transcription Factors Governs Androgen Receptor-dependent Prostate Cancer Growth. *Mol. Cel* 27 (3), 380–392. doi:10.1016/j.molcel.2007.05.041

Wang, W., Rayburn, E. R., Hao, M., Zhao, Y., Hill, D. L., Zhang, R., et al. (2008a). Experimental Therapy of Prostate Cancer with Novel Natural Product Anti-cancer Ginsenosides. *Prostate* 68 (8), 809–819. doi:10.1002/pros.20742

Wang, W. L., McHenry, P., Jeffrey, R., Schweitzer, D., Helquist, P., and Tenniswood, M. (2008b). Effects of Iejimalide B, a marine Macrolide, on Growth and Apoptosis in Prostate Cancer Cell Lines. *J. Cel Biochem* 105 (4), 998–1007. doi:10.1002/jcb.21898

Wang, X., Wang, B., Zhou, L., Wang, X., Veeraraghavan, V. P., Mohan, S. K., et al. (2020). Ganoderma Lucidum Put Forth Anti-tumor Activity against PC-3 Prostate Cancer Cells via Inhibition of Jak-1/STAT-3 Activity. *Saudi J. Biol. Sci.* 27 (10), 2632–2637. doi:10.1016/j.sjbs.2020.05.044

Wang, Y., Liu, Q., Liu, Z., Li, B., Sun, Z., Zhou, H., et al. (2012). Berberine, a Genotoxic Alkaloid, Induces ATM-Chk1 Mediated G2 Arrest in Prostate Cancer Cells. *Mutat. Res.* 734 (1-2), 20–29. doi:10.1016/j.mrfmmm.2012.04.005

Watson, I. R., Takahashi, K., Futreal, P. A., and Chin, L. (2013). Emerging Patterns of Somatic Mutations in Cancer. *Nat. Rev. Genet.* 14 (10), 703–718. doi:10.1038/nrg3539

Wei, R., Ma, Q., Zhong, G., He, J., and Sang, Z. (2020). Isolation and Characterization of Flavonoid Derivatives with Anti-prostate Cancer and Hepatoprotective Activities from the Flowers of Hosta Plantaginea (Lam.) Aschers. *J. Ethnopharmacol* 253, 112685. doi:10.1016/j.jep.2020.112685

Wertz, K. (2009). Lycopene Effects Contributing to Prostate Health. *Nutr. Cancer* 61 (6), 775–783. doi:10.1080/01635580903285023

Wolfram, J., Suri, K., Huang, Y., Molinaro, R., Borsoi, C., Scott, B., et al. (2014). Evaluation of Anticancer Activity of Celastrol Liposomes in Prostate Cancer Cells. *J. Microencapsul* 31 (5), 501–507. doi:10.3109/02652048.2013.879932

Wu, Q., Kohli, M., Bergen, H. R., 3rd, Cheville, J. C., Karnes, R. J., Cao, H., et al. (2014). Preclinical Evaluation of the Supercritical Extract of Azadirachta Indica (Neem) Leaves *In Vitro* and *In Vivo* on Inhibition of Prostate Cancer Tumor Growth. *Mol. Cancer Ther.* 13 (5), 1067–1077. doi:10.1158/1535-7163.MCT-13-0699

Xiang, N., Zhao, R., and Zhong, W. (2009). Sodium Selenite Induces Apoptosis by Generation of Superoxide via the Mitochondrial-dependent Pathway in Human Prostate Cancer Cells. *Cancer Chemother. Pharmacol.* 63 (2), 351–362. doi:10.1007/s00280-008-0745-3

Xiao, D., Zeng, Y., Prakash, L., Badmaev, V., Majeed, M., and Singh, S. V. (2011). Reactive Oxygen Species-dependent Apoptosis by Gugulipid Extract of Ayurvedic Medicine Plant Commiphora Mukul in Human Prostate Cancer Cells Is Regulated by C-Jun N-Terminal Kinase. *Mol. Pharmacol.* 79 (3), 499–507. doi:10.1124/mol.110.068551

Xing, L., Venegas, A. M., Chen, A., Garrett-Beal, L., Boyce, B. F., Varmus, H. E., et al. (2001). Genetic Evidence for a Role for Src Family Kinases in TNF Family Receptor Signaling and Cell Survival. *Genes Dev.* 15 (2), 241–253. doi:10.1101/gad.840301

Xu, L., Wei, Y., Reboul, J., Vaglio, P., Shin, T. H., Vidal, M., et al. (2003). BTB Proteins Are Substrate-specific Adaptors in an SCF-like Modular Ubiquitin Ligase Containing CUL-3. *Nature* 425 (6955), 316–321. doi:10.1038/nature01985

Xu, T., Li, T., Zhang, Y., Huan, S., Cui, T., and Sun, L. (2017). Inhibition of Akt/NF-κB/survivin Pathway by Embelin on Castration-Resistant Prostate Cancer Cells. *Oncotarget* 34, 3700–3710. doi:10.1038/onc.2014.302

Xu, Y. M., Liu, M. X., Grunow, N., Wijeratne, E. M., Paine-Murrieta, G., Felder, S., et al. (2015). Discovery of Potent 17β-Hydroxywithanolides for Castration-Resistant Prostate Cancer by High-Throughput Screening of a Natural Products Library for Androgen-Induced Gene Expression Inhibitors. *J. Med. Chem.* 58 (17), 6984–6993. doi:10.1021/acs.jmedchem.5b00867

Yaacob, N. S., Hamzah, N., Nik Mohamed Kamal, N. N., Zainal Abidin, S. A., Lai, C. S., Navaratnam, V., et al. (2010). Anticancer Activity of a Sub-fraction of Dichloromethane Extract of Strobilanthes Crispus on Human Breast and Prostate Cancer Cells *In Vitro*. *BMC Complement. Altern. Med.* 10 (1), 1–14. doi:10.1186/1472-6882-10-42

Yan, J., and Katz, A. (2010). PectaSol-C Modified Citrus Pectin Induces Apoptosis and Inhibition of Proliferation in Human and Mouse Androgen-dependent and- Independent Prostate Cancer Cells. *Integr. Cancer Ther.* 9 (2), 197–203. doi:10.1177/1534735410369672

Yang, C., Gundala, S. R., Mukkavilli, R., Vangala, S., Reid, M. D., and Aneja, R. (2015). Synergistic Interactions Among Flavonoids and Acetogenins in Graviola (Annona Muricata) Leaves Confer protection against Prostate Cancer. *Carcinogenesis* 36 (6), 656–665. doi:10.1093/carcin/bgv046

Yang, H., Landis-Piwowar, K. R., Lu, D., Yuan, P., Li, L., Reddy, G. P., et al. (2008). Pristimerin Induces Apoptosis by Targeting the Proteasome in Prostate Cancer Cells. *J. Cel Biochem* 103 (1), 234–244. doi:10.1002/jcb.21399

Yang, J., Fizazi, K., Peleg, S., Sikes, C. R., Raymond, A. K., Jamal, N., et al. (2001). Prostate Cancer Cells Induce Osteoblast Differentiation through a Cbfa1-dependent Pathway. *Cancer Res.* 61 (14), 5652–5659. doi:10.1016/S0165-4608(01)00481-2

Yang, J., Wang, C., Zhang, Z., Chen, X., Jia, Y., Wang, B., et al. (2017). Curcumin Inhibits the Survival and Metastasis of Prostate Cancer Cells via the Notch-1 Signaling Pathway. *Apmis* 125 (2), 134–140. doi:10.1111/apm.12650

Yang, S. H., Yates, P. R., Whitmarsh, A. J., Davis, R. J., and Sharrocks, A. D. (1998). The Elk-1 ETS-Domain Transcription Factor Contains a Mitogen-Activated Protein Kinase Targeting Motif. *Mol. Cel Biol* 18 (2), 710–720. doi:10.1128/MCB.18.2.710

Yap, T. A., Smith, A. D., Ferraldeschi, R., Al-Lazikani, B., Workman, P., and de Bono, J. S. (2016). Drug Discovery in Advanced Prostate Cancer: Translating Biology into Therapy. *Nat. Rev. Drug Discov.* 15 (10), 699–718. doi:10.1038/nrd.2016.120

Yin, P., Kawamura, T., He, M., Vanaja, D. K., and Young, C. Y. (2009). Phenethyl Isothiocyanate Induces Cell Cycle Arrest and Reduction of Alpha- and Beta-Tubulin Isotypes in Human Prostate Cancer Cells. *Cell Biol Int* 33 (1), 57–64. doi:10.1016/j.cellbi.2008.09.013

Yoon, Y. J., Kim, Y. H., Lee, Y. J., Choi, J., Kim, C. H., Han, D. C., et al. (2019). 2'-Hydroxycinnamaldehyde Inhibits Proliferation and Induces Apoptosis via Signal Transducer and Activator of Transcription 3 Inactivation and Reactive Oxygen Species Generation. *Cancer Sci.* 110 (1), 366–378. doi:10.1111/cas.13852

Yu, Z., Xu, J., Shao, M., and Zou, J. (2020). Germacrone Induces Apoptosis as Well as Protective Autophagy in Human Prostate Cancer Cells. *Cancer Manag. Res.* 12, 4009–4016. doi:10.2147/cmar.S250522

Yuan, H., Pan, Y., and Young, C. Y. (2004). Overexpression of C-Jun Induced by Quercetin and Resverol Inhibits the Expression and Function of the Androgen Receptor in Human Prostate Cancer Cells. *Cancer Lett.* 213 (2), 155–163. doi:10.1016/j.canlet.2004.04.003

Zabaiou, N., Fouache, A., Trousson, A., Buñay-Noboa, J., Marceau, G., Sapin, V., et al. (2019). Ethanolic Extract of Algerian Propolis Decreases Androgen Receptor Transcriptional Activity in Cultured LNCaP Cells. *J. Steroid Biochem. Mol. Biol.* 189, 108–115. doi:10.1016/j.jsbmb.2019.02.016

Zeng, Q., Zeng, Y., Nie, X., Guo, Y., and Zhan, Y. (2020). Britanin Exhibits Potential Inhibitory Activity on Human Prostate Cancer Cell Lines through PI3K/Akt/NF-Kb Signaling Pathways. *Planta Med.* 86 (18), 1401–1410. doi:10.1055/a-1211-4656

Zeng, Y., and Yang, Y. (2018). Piperine Depresses the Migration Progression via Downregulating the Akt/mTOR/MMP-9 S-ignaling P-athway in DU145 C-ells. *Mol. Med. Rep.* 17 (5). doi:10.3892/mmr.2018.8653

Zengerling, F., Azoitei, A., Herweg, A., Jentzmik, F., and Cronauer, M. V. (2016). Inhibition of IGF-1R Diminishes Transcriptional Activity of the Androgen Receptor and its Constitutively Active, C-Terminally Truncated Counterparts Q640X and AR-V7. *World J. Urol.* 34 (5), 633–639. doi:10.1007/s00345-015-1674-5

Zhang, C., Shu, L., Kim, H., Khor, T. O., Wu, R., Li, W., et al. (2016). Phenethyl Isothiocyanate (PEITC) Suppresses Prostate Cancer Cell Invasion Epigenetically through Regulating microRNA-194. *Mol. Nutr. Food Res.* 60 (6), 1427–1436. doi:10.1002/mnfr.201500918

Zhang, C., Su, Z. Y., Khor, T. O., Shu, L., and Kong, A. N. (2013). Sulforaphane Enhances Nrf2 Expression in Prostate Cancer TRAMP C1 Cells through Epigenetic Regulation. *Biochem. Pharmacol.* 85 (9), 1398–1404. doi:10.1016/j.bcp.2013.02.010

Zhang, L. Y., Wu, Y. L., Gao, X. H., and Guo, F. (2014). Mitochondrial Protein Cyclophilin-D-Mediated Programmed Necrosis Attributes to Berberine-Induced Cytotoxicity in Cultured Prostate Cancer Cells. *Biochem. Biophys. Res. Commun.* 450 (1), 697–703. doi:10.1016/j.bbrc.2014.06.039

Zhang, P., Wang, D., Zhao, Y., Ren, S., Gao, K., Ye, Z., et al. (2017). Intrinsic BET Inhibitor Resistance in SPOP-Mutated Prostate Cancer Is Mediated by BET Protein Stabilization and AKT-mTORC1 Activation. *Nat. Med.* 23(9), 1055–1062. doi:10.1038/nm.4379

Zhang, X., Haney, K. M., Richardson, A. C., Wilson, E., Gewirtz, D. A., Ware, J. L., et al. (2010b). Anibamine, a Natural Product CCR5 Antagonist, as a Novel lead for the Development of Anti-prostate Cancer Agents. *Bioorg. Med. Chem. Lett.* 20 (15), 4627–4630. doi:10.1016/j.bmcl.2010.06.003

Zhang, X., Yeung, E. D., Wang, J., Panzhinskiy, E. E., Tong, C., Li, W., et al. (2010a). Isoliquiritigenin, a Natural Anti-oxidant, Selectively Inhibits the Proliferation of Prostate Cancer Cells. *Clin. Exp. Pharmacol. Physiol.* 37 (8), 841–847. doi:10.1111/j.1440-1681.2010.05395.x

Zhang, X., Bi, L., Ye, Y., and Chen, J. (2014). Formononetin Induces Apoptosis in PC-3 Prostate Cancer Cells through Enhancing the Bax/Bcl-2 Ratios and Regulating the p38/Akt Pathway. *Nutr. Cancer* 66 (4), 656–661. doi:10.1080/01635581.2014.894098

Zhao, D., Lin, F., Wu, X., Zhao, Q., Zhao, B., Lin, P., et al. (2012). Pseudolaric Acid B Induces Apoptosis via Proteasome-Mediated Bcl-2 Degradation in Hormone-Refractory Prostate Cancer DU145 Cells. *Toxicol. Vitro* 26 (4), 595–602. doi:10.1016/j.tiv.2012.02.004

Zhao, F., Huang, W., Zhang, Z., Mao, L., Han, Y., Yan, J., et al. (2016). Triptolide Induces Protective Autophagy through Activation of the CaMKKβ-AMPK Signaling Pathway in Prostate Cancer Cells. *Oncotarget* 7 (5), 5366–5382. doi:10.18632/oncotarget.6783

Zhao, Y., Cheng, X., Wang, G., Liao, Y., and Qing, C. (2020). Linalool Inhibits 22Rv1 Prostate Cancer Cell Proliferation and Induces Apoptosis. *Oncol. Lett.* 20 (6), 289. doi:10.3892/ol.2020.12152

Zheng, J., Wang, J., Wang, Q., Zou, H., Wang, H., Zhang, Z., et al. (2020). Targeting Castration-Resistant Prostate Cancer with a Novel RORγ Antagonist Elaiophylin. *Acta Pharmaceutica Sinica B* 10, 2313–2322. doi:10.1016/j.apsb.2020.07.001

Zhou, Y., Liu, Y. E., Cao, J., Zeng, G., Shen, C., Li, Y., et al. (2009). Vitexins, Nature-Derived Lignan Compounds, Induce Apoptosis and Suppress Tumor Growth. *Clin. Cancer Res.* 15 (16), 5161–5169. doi:10.1158/1078-0432.CCR-09-0661

Zhu, Y., Liu, C., Nadiminty, N., Lou, W., Tummala, R., Evans, C. P., et al. (2013). Inhibition of ABCB1 Expression Overcomes Acquired Docetaxel Resistance in Prostate Cancer. *Mol. Cancer Ther.* 12 (9), 1829–1836. doi:10.1158/1535-7163.MCT-13-0208

Zhuang, M., Calabrese, M. F., Liu, J., Waddell, M. B., Nourse, A., Hammel, M., et al. (2009). Structures of SPOP-Substrate Complexes: Insights into Molecular Architectures of BTB-Cul3 Ubiquitin Ligases. *Mol. Cel* 36 (1), 39–50. doi:10.1016/j.molcel.2009.09.022

Zingue, S., Gbaweng Yaya, A. J., Michel, T., Ndinteh, D. T., Rutz, J., Auberon, F., et al. (2019). Bioguided Identification of Daucosterol, a Compound that Contributes to the Cytotoxicity Effects of Crateva Adansonii DC (Capparaceae) to Prostate Cancer Cells. *J. Ethnopharmacol* 247, 112251. doi:10.1016/j.jep.2019.112251

Zingue, S., Rutz, J., Maxeiner, S., Ndinteh, D. T., Chun, F. K.-H., Jüngel, E., et al. (2021). *In Vitro* pro-apoptotic and Anti-migratory Effects of Treculia Africana Decne. (Moraceae) and Entandrophragma Angolense Welw (Meliaceae) Extracts on Prostate Cancer Cells. *J. Herbal Med.* 28, 100443. doi:10.1016/j.hermed.2021.100443

Conflict of Interest: The authors declare that the research was conducted in the absence of any commercial or financial relationships that could be construed as a potential conflict of interest.

Publisher's Note: All claims expressed in this article are solely those of the authors and do not necessarily represent those of their affiliated organizations, or those of the publisher, the editors and the reviewers. Any product that may be evaluated in this article, or claim that may be made by its manufacturer, is not guaranteed or endorsed by the publisher.

Copyright © 2021 Bai, Chen, Jing, He, Wang, Ban, Ye, Xu and Zheng. This is an open-access article distributed under the terms of the Creative Commons Attribution License (CC BY). The use, distribution or reproduction in other forums is permitted, provided the original author(s) and the copyright owner(s) are credited and that the original publication in this journal is cited, in accordance with accepted academic practice. No use, distribution or reproduction is permitted which does not comply with these terms.

frontiers in Oncology

REVIEW
published: 22 October 2021
doi: 10.3389/fonc.2021.772915

Natural Products: A Promising Therapeutics for Targeting Tumor Angiogenesis

Ruyi Li[1†], *Xin Song*[2†], *Yanan Guo*[3,4], *Peng Song*[3,4*], *Dongzhu Duan*[5*] *and Zhe-Sheng Chen*[6*]

[1] Department of Respiratory and Critical Care Medicine, The First Affiliated Hospital of Zhengzhou University, Zhengzhou, China, [2] School of Life Science and Engineering, Lanzhou University of Technology, Lanzhou, China, [3] Research Center of Traditional Chinese Medicine in Gansu Province, Gansu University of Chinese Medicine, Lanzhou, China, [4] Key Laboratory of Prevention and Treatment for Chronic Diseases by Traditional Chinese Medicine in Gansu Province, Affiliated Hospital of Gansu University of Chinese Medicine, Lanzhou, China, [5] Shaanxi Key Laboratory of Phytochemistry and College of Chemistry & Chemical Engineering, Baoji University of Arts and Sciences, Baoji, China, [6] College of Pharmacy and Health Sciences, St. John's University, Queens, NY, United States

Tumor-associated angiogenesis is a key target for anti-cancer therapy. The imbalance between pro-angiogenic and anti-angiogenic signals elicited by tumor cells or tumor microenvironment always results in activating "angiogenic switch". Tumor angiogenesis functions in multi-aspects of tumor biology, including endothelial cell apoptosis, tumor metastasis, and cancer stem cell proliferation. Numerous studies have indicated the important roles of inexpensive and less toxic natural products in targeting tumor angiogenesis-associated cytokines and apoptotic signaling pathways. Our current knowledge of tumor angiogenesis is based mainly on experiments performed on cells and animals, so we summarized the well-established models for angiogenesis both *in vitro* and *in vivo*. In this review, we classified and summarized the anti-angiogenic natural agents (Polyphenols, Polysaccharides, Alkaloids, Terpenoids, Saponins) in targeting various tumor types according to their chemical structures at present, and discussed the mechanistic principles of these natural products on regulating angiogenesis-associated cytokines and apoptotic signaling pathways. This review is to help understanding the recent progress of natural product research for drug development on anti-tumor angiogenesis.

Keywords: tumor angiogenesis, natural products, angiogenic factors, endothelial cell apoptosis, anti-angiogenic mechanism, chemical structures

OPEN ACCESS

Edited by:
Xin Luan,
Shanghai University of Traditional Chinese Medicine, China

Reviewed by:
Jianbo Wan,
University of Macau, China
Haoyu Tang,
North Carolina State University, United States

****Correspondence:***
Peng Song
songp06@163.com
Dongzhu Duan
duandongzhu@126.com
Zhe-Sheng Chen
chenz@stjohns.edu

[†]These authors have contributed equally to this work

Specialty section:
This article was submitted to Pharmacology of Anti-Cancer Drugs, a section of the journal Frontiers in Oncology

Received: *08 September 2021*
Accepted: *04 October 2021*
Published: *22 October 2021*

Citation:
Li R, Song X, Guo Y, Song P, Duan D and Chen Z-S (2021) Natural Products: A Promising Therapeutics for Targeting Tumor Angiogenesis. Front. Oncol. 11:772915. doi: 10.3389/fonc.2021.772915

HIGHLIGHTS

1. The primary mechanism of tumor angiogenesis was depicted.
2. The current *in vivo* and *in vitro* models toward targeting angiogenesis were recapitulated.
3. Natural agents as therapeutics against tumor angiogenesis were summarized.

INTRODUCTION

Angiogenesis refers to the process of new blood vessel formation from pre-existing endothelial cells in established vessels. The main cellular element of newly formed capillaries is endothelial cells (ECs), that are primarily modulated by vascular endothelial growth factor (VEGF) (1). After stimulating by VEGF, ECs can migrate to the lead of growing capillaries, that are referred to as tip cells. Upon the transformation of ECs to tip cells, the following ECs (stalk cells) will proliferate and maintain the structural and functional integrity of nascent vessels (2). Unlike physiological condition, tumor cells exposed to hypoxic condition secrete high levels of pro-angiogenic factors, such as VEGF. VEGF is the key regulator of the proper development of tumor blood vessels. Members of the angiopoietins, platelet-derived growth factor (PDGF-B), transforming growth factor (TGF-β) families and basic fibroblast growth factor (bFGF) are also significant factors in the formation of an immature vascular network in tumors (3). Moreover, recent literature has demonstrated that a variety of pro-angiogenic factors (VEGF, angiopoietin-1, bFGF) have the ability of inhibiting EC apoptosis (4) in tumor angiogenesis.

Natural products isolated from plants have been used as medicine from ancient times. The discovery of natural products for treatment dated back to 2600 BC in Mesopotamia (5). Traditional Chinese medicine (TCM) and Indian Ayurveda system are well documented over thousands of years. Early experiments have verified their properties of anti-inflammatory, anti-allergic and anti-infectious diseases (6, 7). Natural phytochemicals have been applied to the therapy of various diseases, including tumors (8). These phytochemicals can effectively inhibit the initiation, development and progression of neoplasm by regulating cellular proliferation, apoptosis and metastasis (9). Recent studies have indicated the important roles of natural compounds in modulating tumor angiogenesis by promoting the apoptosis of endothelial cell and inhibiting the angiogenesis-associated cytokines (10). In this review, we recapitulate the process of tumor angiogenesis and present some natural products that have the effect of anti-tumor angiogenesis.

A systematic literature search was conducted in PubMed database from 2010 to 2020. The following search terms were used: "natural products (or) natural product (or) polyphenols (or) polysaccharides (or) alkaloids (or) terpenoids (or) saponins" and "tumor angiogenesis (or) anti-angiogenic (or) angiogenic factors (or) vascular endothelial cells". There were no language restrictions, and the abstracts of the papers identified by the initial search were evaluated by the lead reviewer Peng Song for appropriateness to this review. The inclusion criteria of references was that the abstracts of the references introduced the molecular mechanism investigation of natural products against tumor angiogenesis through *in vitro* or *in vivo* experiments.

PHYSIOLOGICAL VASCULATURE

The function of an extensive vascular network is to supply nutrients and oxygen and remove metabolic waste. During early embryogenesis, vascular growth is the results of combination of vasculogenesis and angiogenesis (11). Vasculogenesis refers to that new blood vessels are formed from primitive ECs precursors, as opposed to angiogenesis, in which the blood vessels developed from pre-existing ECs in established vessels (12). In adulthood, new blood vessels are rarely formed except in several physiological or pathological processes such as female reproductive cycling and wound healing. The sprouting, migration and proliferation of ECs are regulated by various cytokines, among them VEGF is a pivotal one (13).

NEOPLASM ANGIOGENESIS

Angiogenic Switch

At the early stage of neoplasm events, tumors present a balance between cell apoptosis and cell proliferation (14). Tumor cells produce pro-angiogenic factors, such as VEGF, PDGF and anti-angiogenic factors, such as angiostatin and thrombospondin. The secretion of these factors is in balance and tumors maintain at the "dormancy state". However, once the average volume of a tumor exceeds 1-2 mm^3, insufficient supply of oxygen and nutrients to tumor tissues will occur. Under hypoxic and/or acidic conditions, this balance is disturbed, and the tumors switch from a non-vascular to a vascular state, which turns on "angiogenic switch". At this state, hypoxia inducible factor 1 alpha (HIF1-α) is able to bind to hypoxia-regulators and induce the production of VEGF and other pro-angiogenic factors (15). Oncogene Ras and the mutated tumor suppressor gene TP53 also mediate this pro-angiogenic effect. The synthesis of anti-angiogenic factors are found decreased in these tumors (16). Even if only 1% of tumor cells turns on the "angiogenic switch", tumor growth occurs. In turn, the growth of neoplasm tissues promotes the initiation of angiogenesis (17).

Activated Factors and ECs Apoptosis in Tumor Angiogenesis

The most well-known receptors for tumor angiogenesis on the membrane of endothelial cells are tyrosine kinase receptors with their co-receptor, neuropilin. These receptors bind to VEGF or bFGF. The transcription of several pro-angiogenic factors can be initiated by the second messenger cascade of these receptors. High levels of VEGF can be found in most tumor types (1, 18). VEGF exerts the key role in the formation of new blood vessels and the proliferation of ECs. There are three tyrosine kinase receptors of VEGF, VEGFR-1 to -3. VEGFR-2 is the most prominent receptor in angiogenesis, which binds to VEGFA with strong tyrosine kinase activity (19). Moreover, latent forms of VEGF ligands are separated in the extracellular matrix, that are regulated by the release and activation of extracellular matrix-degrading proteases (e.g., MMP-9) (20). The up-regulation of other pro-angiogenic signals, such as FGF family, is involved in sustaining tumor angiogenesis (3, 21). Besides the VEGF signaling pathway, other signaling pathways and associated factors are involved in tumor angiogenesis. Angiopoietin 1 (ANGPT1) and ANGPT2 are important ligands from the ANGPT family, that bind to the receptor tyrosine kinase TIE2 on the membrane of ECs. Since ANGPT1 acts as an agonist of TIE2, its function is to promote vessel maturation. The activation of TIE2 mediated by ANGPT2 can induce vascular disruption and increase

angiogenesis (22). Another important system that regulates tumor angiogenesis is the Notch-Notch-ligand system. Endothelial-specific ligand Delta-like 4 (DLL4) mediates the formation of the tip and stalk cells following VEGF stimulation (23).

Apparently, neovasculature is strongly governed by ECs apoptosis. Both proangiogenic growth factors and extracellular matrix (ECM) act as the key roles in EC survival and angiogenesis (4). Induction of angiogenic growth factors and associated pathways are capable of inhibiting ECs apoptosis. For instance, ECs sustainment has been demonstrated to be linked with the modulation of cell apoptosis by VEGF (24). By increasing the expression of anti-apoptotic proteins, such as Bcl-2 and survivin, bFGF is able to decrease ECs apoptosis, which guarantees the cells survival (25). Of note, ANGPT1 involves in ECs apoptosis by modulating PI3K/Akt signaling and upregulating the anti-apoptotic protein surviving (26). Regarding the role of cell matrix and cell-cell interactions in angiogenesis, the anti-apoptotic effect of VEGF is dependent on the regulation of αvβ3-integrin and VE-cadherin protein (27, 28). Since the pivotal role of ECs in angiogenesis, many natural products are developed to target EC apoptosis. For example, resveratrol is able to increase Gly-LDL-induced vascular endothelial cell apoptosis (29). Similarly, *Physalis alkekengi L.* extract can reduce the apoptosis of ECs after exposing to hyperglycemia (30). Overall, angiogenic factors secreted by tumor cells (**Figure 1**) and EC apoptosis (**Figure 2**) are of significance in triggering and processing vessel formation in tumor microenvironment.

ANALYSIS OF VASCULATURE IN *IN VIVO* AND *IN VITRO* MODELS

Vasculature has been explored for many decades and the application of *in vitro* and *in vivo* assays to evaluate the induction and inhibition of vascularization has exerted a significant role for researchers to study and understand angiogenesis (31). The well-established *in vitro* models, such as the model of ECs, are easily analyzed and reproducible, yet the cells become senescent in the culture after a few passages (32). Unlike the *in vitro* models, *in vivo* models, for example, the model of chick chorioallantoic membrane (CAM), owns the advantages of short experimental period and low cost, which is available for drug screening (33). As an ideal anti-tumor angiogenesis model, zebrafish has been widely used in drug screening due to its small size, transparent embryos, easy large-scale rearing, strong reproductive capacity and short experimental period (34). The aortic ring test is a model of angiogenesis based on organ culture. In this model, the molecular mechanism in regulating angiogenesis can be clarified, but it cannot truly reflect the microvascular environment of tumor growth (35). Another widely used *in vivo* model is xenograft tumor in mice. Of note, tumor angiogenic environment in animals is different from human, so assays in animals could not replace that in human (31). We have summarized the advantages and disadvantages of the current common angiogenesis models both *in vitro* and *in vivo*, which will provide clues for human cancer study (**Table 1**).

NATURAL ANTI-TUMOR ANGIOGENIC COMPOUNDS DERIVED FROM PLANTS

Polyphenols

Polyphenols are members of a large family of chemical compounds with several phenolic groups, that can be found in foods and beverages of plant origin, including the spices, dried herbs, tea, red wine, coffee, cocoa products, seeds and nuts, vegetables, and fruits. Polyphenols are usually classified as phenolic acids, flavonoids, stilbenes, lignans, secoiridoids, among others. Polyphenols are of significance in the sustainment of human health. Recent studies have illustrated the pharmacologic functions of polyphenols that include antioxidation, vascular wall protection, improving enterogastric digestion, promoting immune response, and prevention of chronic disorders, such as tumor, atherosclerosis, hypertension, diabetes and

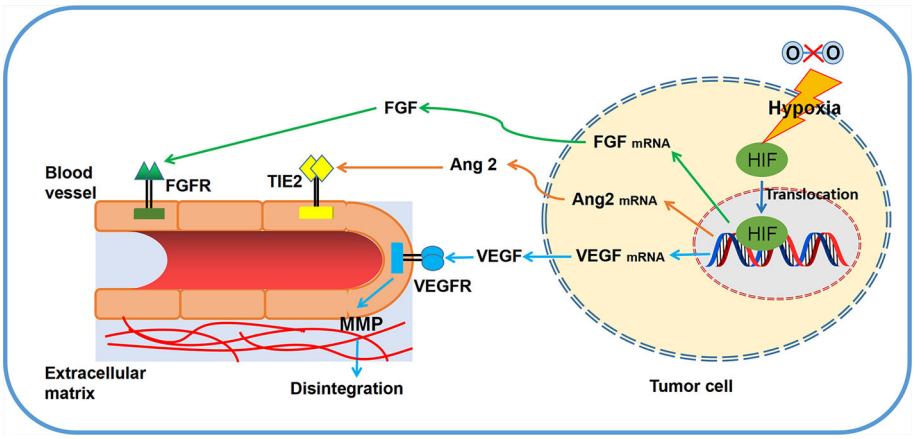


FIGURE 1 | Primary principles of angiogenesis in tumor microenvironment. Several significant regulators (VEGF, FGF, MMPs, TIE2) and related pathways are involved in tumor angiogenesis.

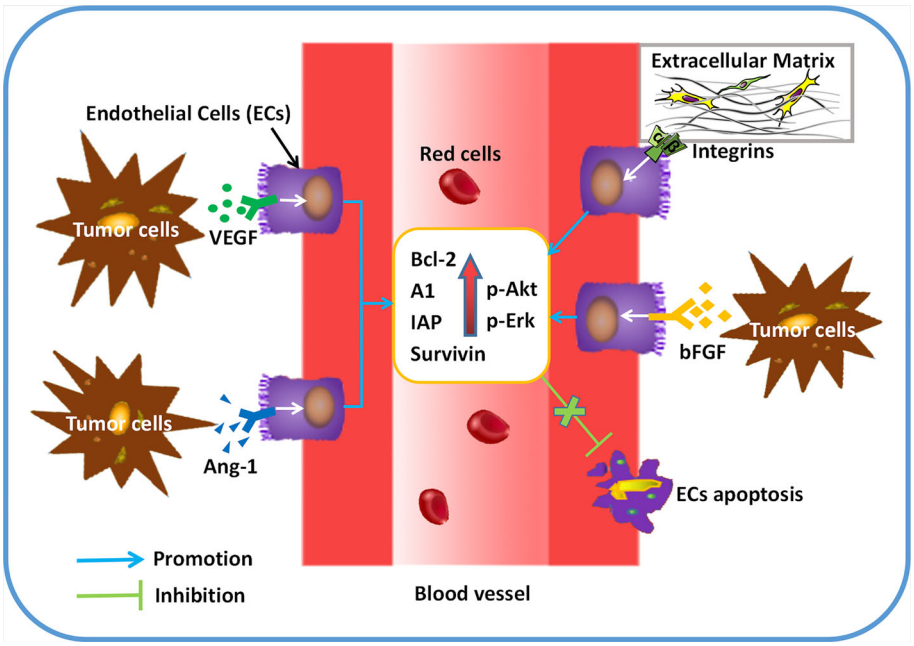


FIGURE 2 | ECs apoptosis can be regulated by pro-angiogenic factors in tumor angiogenesis. After secreting a variety of cytokines (VEGF, bFGF, Angiopoietin-1), tumor cells exerts the role of anti-apoptosis in ECs by binding to its receptors. Up-regulated expression of anti-apoptotic proteins (BCL-2, A1, IAP, etc) and protein kinases (Akt, Erk, etc) can be found in ECs, which results in more survival and less apoptosis in ECs.

so on. In addition to the summary of the chemical structures of polyphenols (**Figure 3**), the effect of several polyphenols (Ellagic acid, Chlorogenic acid, Quercetin, Catechin, Baicalin, Delphinidin, 6-methoxyequol, et al.) on tumor angiogenesis have also been studied in recent years (**Table 2**). Ellagic acid can inhibit angiogenesis by inhibiting the expression of VEGFR2 in ECV304 cell line. Moreover, researchers found that ellagic acid was able to regulate angiogenesis by inhibiting VEGF/VEGFR2, PI3K/Akt and MAPK signaling cascades in hamster cheek touch carcinogenesis model (39, 40). Chlorogenic acid is one of the hydroxygenic acid derivatives, which derives from *Eucommia ulmoides Oliv*. Chlorogenic acid suppressed tumor angiogenesis by blocking HIF-1α/Akt signaling pathway in lung cancer A549 cells (41). Quercetin, a flavanol-like compound, is derived from *Quercus iberica*. Quercetin reduces angiogenesis by inhibiting ERK phosphorylation and VEGFR-2 mRNA expression, and the calcineurin/NFAT signaling pathway (45, 46). Catechin is a flavanol-like compound and derived from black tea, which can affect angiogenesis by inhibiting VEGF (47). Baicalin, originated from *Scutellaria baicalensis Georgi*, can also inhibit tumor angiogenesis by regulating VEGFR (51). As for Delphinidin, it regulates angiogenesis by affecting the expression of HIF-1α and VEGF in A549 cells (56). 6-Methoxyquol is an isoflavone-like compound derived from soybean and can affect tumor angiogenesis through MAPK signaling pathway (59).

Polysaccharides

Polysaccharides are polymeric carbohydrate macromolecules, that are composed of long-chain monosaccharide units connected by glycosidic bonds. As pivotal bioactive macromolecules, polysaccharides are mainly extracted from plants, animals and microorganisms. Polysaccharides are currently applied to various biomedical products and functional foods because of their significant biological functions, such as inhibiting tumor growth, triggering immunity, antioxidation, anti-virus and neuroprotection. Recent studies indicated that polysaccharides extracted from higher plants showed anti-tumor activity by enhancing immunity. In addition to anti-tumor effect through immunomodulation, polysaccharides can directly inhibit tumor angiogenesis. Various polysaccharides, such as dandelion polysaccharide, sulfated polysaccharide, Fucoidan, LEP-2a, and Galactomannan, exert important roles in tumor angiogenesis (**Table 3**). Dandelion polysaccharide has been proved to inhibit angiogenesis both *in vivo* and *in vitro*. The PI3K/Akt signaling pathway is involved in this process, which inhibits the expression of VEGF and HIF-1α (66). Sulfurized polysaccharide is derived from *Phellinus ribis*. In the Lewis lung carcinoma (LLC) mouse model, sulfurized polysaccharide can inhibit vessel formation by modulating VEGF/VEGFR signaling pathway (67). Fucoidan, extracted from *Laminaria japonica*, regulates tumor angiogenesis by modulating MAPK and PI3K/Akt signaling pathways (68). Fucoidan is proved to reduce the expression of VEGF and PDGF in two chicken embryo chorioallantoic membrane (CAM) models (69). Moreover, in mice xenografted with DU-145 human prostate cancer cells, fucoidan can decrease tumor growth and angiogenesis by inhibiting JAK/STAT3/VEGF signaling pathway (70). Another important polysaccharide, Lep-2a, can restrain the expression of VEGF, CD105, bFGF, MMP-2 and MMP-9 in hepatocellular carcinoma (72). PSP001 is a galactomannan derived from the

TABLE 1 | Properties of common experimental models of angiogenesis *in vivo* and *in vitro*.

Assay type	Description	Advantages	Disadvantages	Refs
Endothelial cells	The proliferation of EC initializes the formation of blood vessel. Angiogenic-associated factors trigger the activation of EC, thereby degrading local basement membrane, promoting EC migration and invading the proximal ECM, which leads to EC sprout and capillary network formation. Therefore, vitro models of ECs were established to simulate angiogenesis in human body. 1. Evaluates EC proliferation by MTT and cell cycle. 2. Evaluates EC migration and invasion on a porous membrane with matrigel. 3. Evaluates EC capillary network formation on the matrigel.	Simple, reproducible, and quantitatively analyzed.	1. Limited use for the senescent property of ECs after a few passages. 2. Unrepresentative of the physiological reaction *in vivo*.	(32)
Tumor cells	Tumor cells are able to secrete a variety of cytokines in tumor growth, which affect tumor angiogenesis. Therefore, we can indirectly evaluate the role of tumor angiogenesis by detecting the expression of related cytokines. 1. Evaluates the expression of angiogenic factors secreted by tumor cells, such as VEGF, bFGF, etc. 2. Evaluates the expression of matrix metalloproteinases secreted by tumor cells, such as MMP-2, MMP-9, etc.	Specifically use for anti-angiogenic drugs development and drug detection of anti-angiogenic effects.	Unequal to human experiments because of the different local environment between tumor cell models and human models.	(36–38)
Chick chorioallantoic membrane (CAM)	CAMs is one of the most commonly used models to study the anti-angiogenic effect of drugs *in vivo*, which has been approved by FDA. At 6-8 days after hatching, the development of embryo membrane and vascular network is stable, but the immune system has not been completely established. Therefore, the embryo has no rejection to various foreign materials during this period, which makes it convenient to observe the effects of various drugs on angiogenesis. Methods: The 8-day-old fertile eggs were opened from the end of the air chamber. After the opening, we can observe the growth of blood vessels on CAM and determine the best position of drug intervention, thereby avoiding the damage of chicken embryo caused by mechanical stimulation and eggshell detachment.	1. Convenient to obtain materials and observe results. 2. Short experimental period and low cost. 3. Suitable for the screening of a large number of angiogenesis drugs.	The possibility of false positive results due to cellular damage, inflammatory reaction and fibrin degradation products	(33)
Rat aortic rings	Aortic ring assay is a model of vascular regeneration based on organ culture. In this assay, the angiogenic vessels developed from a small segment of the aorta. Methods: the rat aorta was removed, cut into 1 mm vascular rings, embedded with fibrin glue or collagen glue, and then cultured in serum-free MCDB131 medium. During the cultural process, the number of new microvessels produced by aortic rings was calculated and analyzed quantitatively.	1. A wide range of materials and simple observation method 2. Clear elucidation of angiogenic-associated molecular mechanism	Hardly reflection of the true microvascular environment of tumor growth	(35)
Zebrafish	As an ideal anti-tumor angiogenesis model, zebrafish has been widely used in drug screening: 1. Zebrafish tumor is highly similar to human cancer at the levels of histology, gene expression and genome. This model can be used for imaging and high-throughput genetic screening, which provides a unique opportunity for cancer genome research *in vivo*. 2. Using the techniques of forward genetics, reverse genetics, gene knockout, cancer cell transplantation and chemical inducers, we can conduct the replication of various zebrafish tumor models, the study of pathogenesis and the screening of antitumor drugs.	1. Small size, transparent embryos, easy large-scale rearing, strong reproductive capacity and short experimental period. 2. Highly similar to the human genome sequence (87%)	____	(34)
Xenograft mice with tumor cells	The model of mice bearing with tumor cells is used to study the potential antitumor activity of drugs and their effects on tumor size (diameter, area or volume) and survival time of animals. This model can also be used to study the potential anti-angiogenic activity, uptake and distribution of drugs. If a drug has the anti-angiogenic effect, it will prevent or reduce the number of tumor neovascularization.	____	1. Irreplacement of the local environment of spontaneous tumor growth 2. The differences about tumor growth environment between animal and human	(31)

fruit rind of *Punica granatum L.* A recent study found that galactomannan was able to suppress the expression of VEGF, MMP-2 and MMP-9 and up-regulate the expression of TIMP-1 and TIMP-2 in cancer cells (74).

Alkaloids

Alkaloids are a group of natural compounds with nitrogen structure and physiological function. Many alkaloids have complex nitrogen heterocyclic structures, and several compounds are organic amines with non-nitrogen heterocycles. Alkaloids have the properties of alkali, that are important active ingredients in Chinese herbal medicine. Although certain vitamins, amino acids and peptides from natural sources are also nitrogenous compounds, they are not included in the category of alkaloids. Alkaloids are ubiquitous in nature, especially in the plant kingdom. Alkaloids have been reported in at least 140 species of plants,

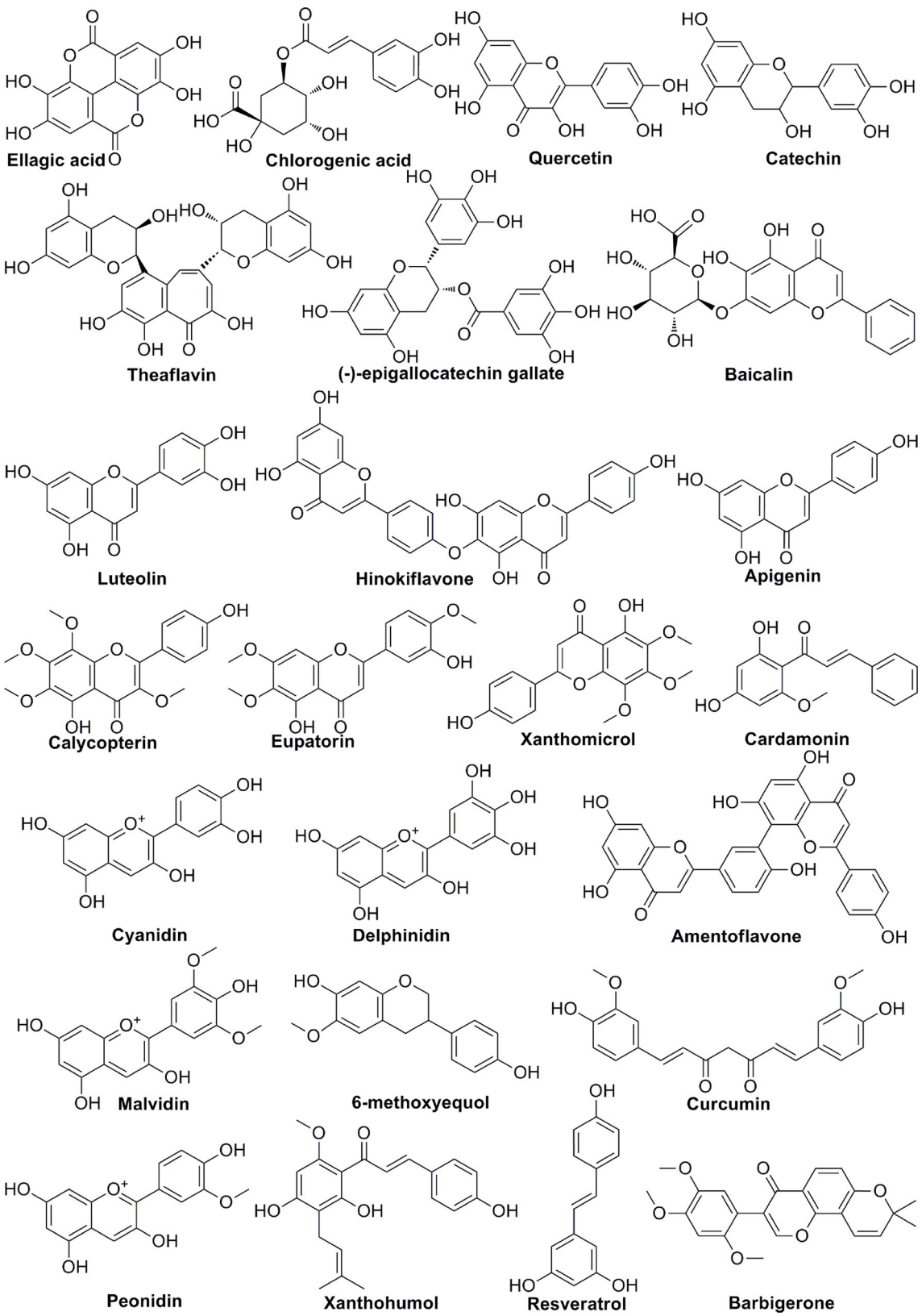


FIGURE 3 | The chemical structures of polyphenols involved in tumor angiogenesis.

TABLE 2 | Natural anti-tumor angiogenesis polyphenols and their sources, experimental models and anti-angiogenic mechanisms.

Category	Name	Source	Experimental model	Anti-angiogenic mechanism	Refs
Hydroxybenzoic acid derivative	Ellagic acid	blackberry	ECV304 cell line, Hamster cheek pouch carcinogenesis model, HUVEC cells	Inhibits VEGFR2 expression Inhibits VEGF/VEGFR2, PI3K/Akt and MAPK signaling cascades	(39, 40)
Hydroxycinamic acid derivatives	Chlorogenic acid	*Eucommia ulmoides Oliv*	A549 cells	Suppresses HIF-1α/Akt pathway	(41)
	Curcumin	*Curcuma aromatica Salisb*	A549 and PC-9 cells, Nude mice xenograft tumor model, T24 and UMUC2 cells, HUVEC cells	Blocks c-Met expression and PI3K/Akt/mTOR pathway Blocks IGF2 and IGF2 mediated PI3K/AKT/mTOR Signaling Pathway Cyclic nucleotide phosphodiesterases inhibition	(42–44)
Flavonols	Quercetin	Quercus iberica	MCF-7 cells, BALB/c nude mice xenograft model, HUVEC cells, Transgenic zebrafish embryos TG	Inhibits calcineurin/NFAT pathway, Inhibits ERK phosphorylation and VEGFR-2 expression	(45, 46)
Flavanols	Catechin	black tea	HUVEC and HASMC cells	Inhibits VEGF expression	(47)
	Theaflavin	black tea	OVCAR-3 and A2780/CP70, HUVEC	TF1 reduces VEGF secretion in a HIF1α-independent manner, while the others in a HIF1α-dependent way	(48)
	(-)-epigallocatechin gallate	green tea	SW620, HT-29, HCT116, Endothelial cells and xenografts	Suppresses JAK/STAT3/IL-8 pathway and VEGFR2 expression	(49, 50)
Flavones	Baicalin	*Scutellaria baicalensis Georgi*	A549 cell, Xenograft tumors in nude mice	VEGFR expression inhibition	(51)
	Apigenin	*Apium graveolens L.var.dulce DC.*	PC3-M and LNCaP C4-2B cells	Blocks TGF-β1-Smad-VEGF pathway	(52)
	Luteolin	*Reseda odorata L.*	Sprague-Dawley rat	VEGF expression inhibition	(53)
	Eupatorin	Isatis tinctoria	HUVEC cells	VEGF expression inhibition	(54)
	xanthomicrol	*Citrus reticulata* Blanco	HUVEC cells and rat aortic rings	VEGF expression inhibition	(55)
	calycopterin	Dracocephalum kotschyi	HUVEC cells and rat aortic rings	VEGF expression inhibition	(55)
Anthocyanins	Delphinidin	*Pharbitis nil(L.) Choisy*	A549 cell	Inhibits HIF-1α and VEGF expression	(56)
	Cyanidin	purple sweet potato	HUVEC and HRMEC	Blocks ERK pathways	(57)
	Peonidin	lycium ruthenicum	HUVEC and HRMEC cells	Blocks ERK pathways	(57)
	Malvidin	*Malva sinensis Cavan.*	SCC131 cells	Suppresses JAK/STAT-3 pathway	(58)
Isoflavone	6-methoxyequol	soybean	HUVECs A431 cells, Mouse xenograft tumors model	Suppresses MAPK pathway	(59)
Pyranoisoflavone	Barbigerone	soybean	B16F10 melanoma cells, Zebrafish and mouse xenograft tumors models	Suppresses MEK 3/6/p38 MAPK signaling pathway	(60)
Chalcone	Cardamonin	Alpinia katsumadaiHayata	SKOV3 cells	Inhibis VEGF and HIF-α expression	(61)
	Xanthohumol	*Humulus lupulus L.*	BxPC-3 cells	Blocks NF-κB expression	(62)
Biflavonoid	Amentoflavone	Selaginella tamariscina	TSGH8301 cell	Suppresses VEGF expression	(63)
	Hinokiflavone	*Platycladus orientalis* (Linn.) Franco	CT26 cell	–	(64)
Stilbens	Resveratrol	Peanut	Rats	MMP-9 expression inhibition	(65)

especially in Papaveraceae, tetrandridae, Solanaceae, Leguminosae, Apocynaceae, Ranunculaceae, and tillering family, et al. The common alkaloids include pyrrole, pyridine, quinoline, isoquinoline, indole, imidazole, purine, anisodamine, terpenoids, steroids, organic amines, and so on and the chemical structures of these alkaloids are shown in **Figure 4**. Current studies proved the biological activities of alkaloids, including anti-tumor, anti-bacterial, anti-inflammatory, antiviral, antiarrhythmic, analgesic, and antispasmodic effects. Voacangine is an indole-like compound, which is rich in *Ervatamia Stapf*. Treatment with voacangine decreases the VEGFR2 kinase activity in athymic nude mice bearing glioblastoma tumors and HUVECs, suggesting that its anti-angiogenic role is closely associated with VEGFR2 (81). Evodiamine is an indoloquinazoline-like compound, which is derived from *Euodia rutaecarpa (Juss.)*. Evodiamine is able to modulate angiogenesis by inhibiting the expression of VEGF through the c-Mer/Src/STAT3 signaling pathway (82). By inhibiting β-catenin, which reduces VEGF-A expression, Le Shi et al. found the anti-angiogenic role of evodiamine (83). As an isocarbostyril compound, narciclasine regulates HUVECs

TABLE 3 | Natural anti-tumor angiogenesis polysaccharides and their sources, experimental models and anti-angiogenic mechanisms.

Category	Name	Source	Experimental model	Anti-angiogenic mechanism	Refs
α-type polysaccharide	Dandelion Polysaccharide	the root of dandelion	HUVECs, CAM, Mice xenografted with Hepa1-6 and H22 cancer cells	Inhibits PI3K/AKT/HIF-1α/VEGF pathway	(66)
Sulfated polysaccharide	PRP-S16	*Phellinus ribis*	LLC (Lewis lung carcinoma) allografts tumor-bearing mice	Inhibits HIF-1α/VEGF/VEGFR-2/AKT pathway	(67)
A fucose-rich polysaccharide	Fucoidan	*Laminaria japonica, Fucus vesiculosus*	TNBC, HUVECs, CAM, Mice xenografted with DU-145 human prostate cancer	Suppresses MAPK and PI3K/AKT signaling pathway Inhibits VEGF and PDGF expression, Inhibits JAK/STAT3/VEGF pathway	(68–70)
Homogeneous polysaccharide	HH1-1	safflower	CAM, BxPC-3 xenograft model and PDX model	Impedes the combination of EGFR and Galectin-3 Inhibits Galectin-3/GFR/KT/OXO3 signaling pathway	(71)
Exopolysaccharide	LEP-2a	*Lachnum* sp.	H22 (hepatocellular carcinoma) allografts tumor-bearing mice	Suppresses VEGF, CD105, bFGF, MMP-2 and MMP-9 expression	(72)
Water-soluble polysaccharide	PTP	the roots of *Polygala tenuifolia*	SKOV3 xenograft, Tumor growth in BALB/c mice	Decreases EGFR, VEGF, and CD34 expression	(73)
Galactomannan	PSP001	the fruit rind of *Punica granatum L.*	CAM, A375 and A549 cells, B16F10	suppresses the expression of VEGF, MMP-2 and MMP-9 Upregulates the expression of TIMP-1 and TIMP-2	(74)
Water-soluble polysaccharide	STPC2	*Sargassum thunbergii*	HUVECs, A549 cells	Downregulates MMP-2, VEGF and HIF-1α expression	(75)
Apigalacturonan-Rich Polysaccharide	ZCMP	The sea grass *Zostera caespitosa* Miki	HUVECs	–	(76)
Pectic polysaccharide	Corn pectic polysaccharide (COPP)	corn (*Zea mays* L.)	Mice were given B16F10 and injected through the lateral tail vein	Suppresses the expression of VEGF, MMP-2 and MMP-9	(77)
Arabinogalactan	Arabinogalactan	flowers of *Panax notoginseng*	BxPC-3, Pancreatic cancer cell xenograft tumor in nude mice, HMEC-1	Inhibits BMP2/Smad/Id1 signaling pathway	(78)
Huaier polysaccharide	TP-1	Huaier fungus	To establish an *in vivo* pulmonary metastasis model, SMMC-7721 cells were injected into BALB/c nude mice *via* the tail vein	Inhibits HIF-1α/VEGF pathway	(79)
	SP-1	*Trametes robiniophila* murr (Huaier)	Mice xenografted with SMMC-7721 human hepatocellular carcinoma cells	Suppresses the expression of VEGF, MMP-2, HIF-1α, STAT3 and MMP-9	(80)

proliferation by a RhoA-independent activation of the Rho kinase Rock (84). Tetromethylpyrazine is an amide alkaloid, which is extracted from *Ligusticum chuanxiong hort*. Tetromethylpyrazine combined with paclitaxel inhibited angiogenesis both *in vivo* and *in vitro* through blocking ERK1/2 and AKT signaling pathways (85). Previous studies found that harmine, a β-carboline alkaloid, suppressed bladder cancer growth by its anti-angiogenic effect, which was linked to VEGFR2 signaling pathway (86). Oxysophocarpine is a quinolizidine alkaloid and it reduces the levels of HO-1, VEGF, MMP-9 and HIF-1 in OSCC cells (87). 3-acetyl-norerthrophlamide is a cassaditerpene alkaloid, which comes from *Erythrophleum fordii*. 3-acetyl-norerthrophlamide and exerts the anti-angiogenic function by inhibiting the eNOS activation and NO production (88). Many alkaloids, such as chuanbeinone, halofuginone, tetrandrine, also play significant roles in tumor angiogenesis (**Table 4**).

Terpenoids

Terpenoids are natural products that derive from mevalonic acid. Terpenoids are composed of multiple isoprene (C5) units with the general formula of $(C_5H_8)_n$. More than 20,000 terpenoids exist in nature and are widely distributed in the plant kingdom, such as Compositae, Ranunculaceae, Araliaceae, Oleaceae, Magnoliaceae, Lauraceae, Aristolochiaceae, and more. Based on the different molecular structures (**Figure 5**), terpenoids are divided into five groups: monoterpenes, sesquiterpenes, diterpenoids, triterpenoids and terpenes compound. Most of the bioactive terpenoids have been isolated from medicinal plants. For example, monoterpenes and sesquiterpenes are extracted from essential oils of medicinal plants and triterpenes are primarily available in balsams and resins. Recent studies have found that terpenoids have a variety of biological functions, including the regulation of enzyme system, cell surface signaling transduction, immune function, cell differentiation, tumor proliferation and angiogenesis. Important terpenoids (Perillyl Alcohol, β-elemene, Alantolactone, Tanshinone IIA, Triptolide, Ursolic acid, Koetjapic acid, et al) and their molecular signaling pathways participate in modulating tumor angiogenesis (**Table 5**). Perillyl Alcohol, hugely available in the essential oils of several plants (Lavendin, Mints, Cherries, etc.), possesses the anti-angiogenic property, the mechanism of which is probably to decrease the release of VEGF in cancer cells and stimulate the expression of Ang2 in endothelial cells (98). β-elemene is a

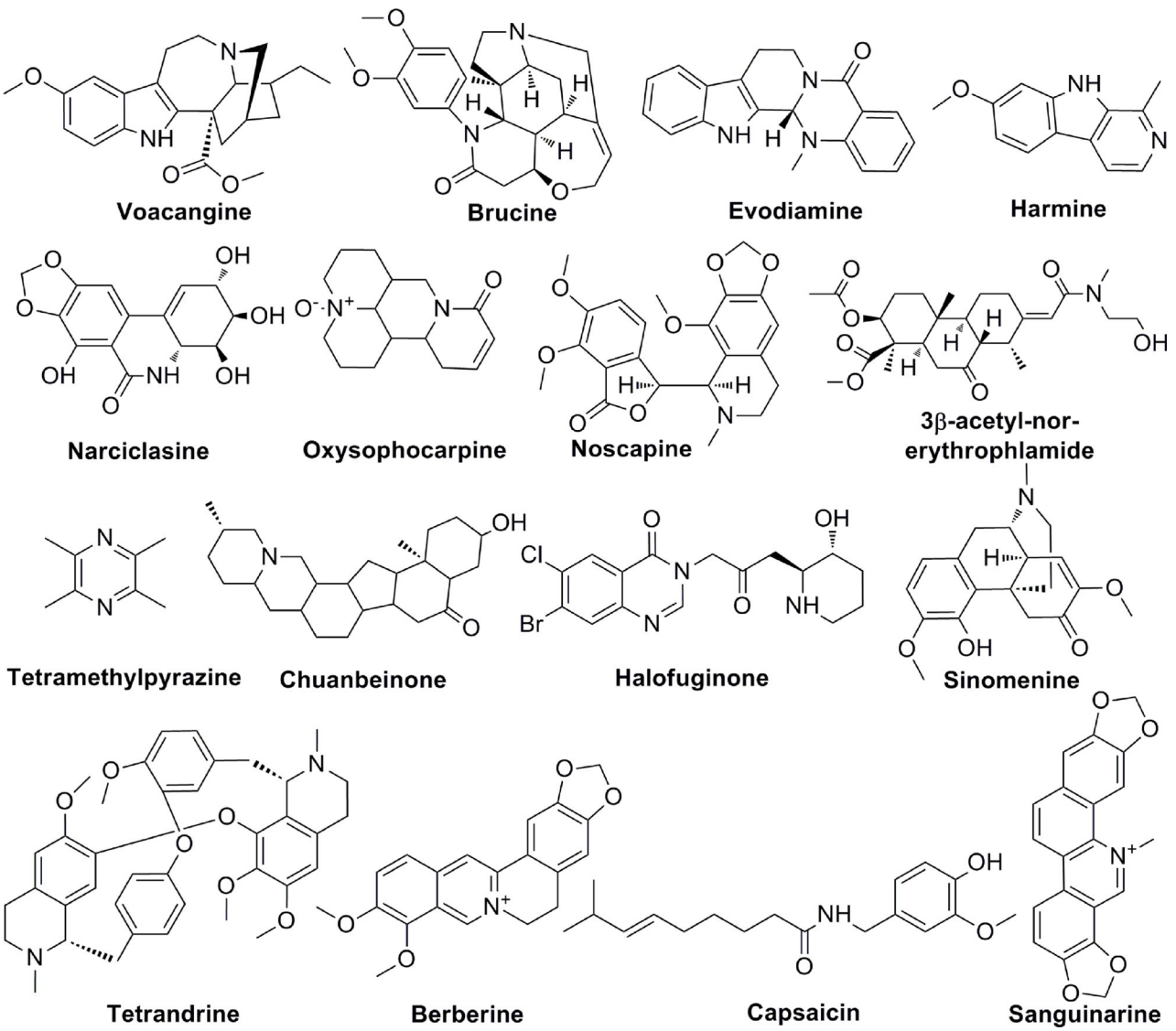


FIGURE 4 | The chemical structures of alkaloids involved in tumor angiogenesis.

sesquiterpene compound isolated from *Curcuma Zedoaria*. It inhibits the proliferation and metastasis of melanoma by suppressing VEGF-mediated angiogenesis (102). Alantolactone is also a sesquiterpene compound extracted from *Inula Helenium*. Alantolactone inhibits angiogenesis by reducing the phosphorylation of VEGFR2 and its downstream protein kinases, including PLCγ1, FAK, Src, and Akt in breast cancer (106). Tanshinone IIA is the key compound of Diterpene, isolated from *Salvia Miltiorrhiza Bunge*. Tanshinone IIA has anti-angiogenic activity in human EPCs, which is associated with the regulation of VEGF, PLC, Akt and JNK signaling pathways (109). Triptolide is also a Diterpene compound, derived from *Tripterygium Wilfordii*. Triptolide exerts the anti-angiogenic role in breast cancer by inhibiting ERK1/2-HIF1-α-VEGFA signaling pathway both *in vitro* and *in vivo* (113). As an important Triterpene compound, ursolic acid is able to decrease the expression of VEGF and iNOS in ehrlich ascites carcinoma (114). Koetjapic acid is also a significant Triterpene compound. Koetjapic acid is found to reduce the expression of VEGF in various angiogenic models, such as rat aortic ring, CAM and HUVECs (116).

Saponins

Saponins are composed of sapogenins and sugars. The sapogenins are triterpenes or spirostanes and the make-up sugars are commonly glucose, galactose, rhamnose, arabinose, xylose, glucuronic acid and galacturonic acid. Lipophilic sapogenins and hydrophilic sugar chains make the saponin an excellent surfactant. Saponins are mainly distributed in terrestrial higher plants and marine organisms, such as starfish and sea cucumber. Many

TABLE 4 | Natural anti-tumor angiogenesis alkaloids and their sources, experimental models and anti-angiogenic mechanisms.

Category	Name	Source	Experimental model	Anti-angiogenic mechanism	Refs
Indole	Voacangine	*Ervatamia Stapf*	Athymic nude mice bearing glioblastoma tumors consisting of U87MG glioblastoma, HUVECs	Inhibits VEGFR2 kinase activity and its downstream signaling by binding to the kinase domain of VEGFR2	(81)
	Brucine	*Strychnos nux-vomica Linn*	Human breast cancer cell line MDA-MB-231	Inhibits VEGF/VE-cadherin/EphA2/MMP-9/MMP-2 pathway	(89)
Indoloquinazoline alkaloid	Evodiamine	*Euodia rutaecarpa* (Juss.) Benth. (Rutaceae)	Human prostate cancer (PC-3 and DU145), Mouse xenograft model with HCC cell lines (HepG2, SMMC-7721, H22), HUVECs, The number of capillary sprouts from Matrigel embedded rat thoracic aortic rings	Inhibits c-Mer/Src/STAT3 pathway Inhibits VEGF and MMP-9 expression inhibits β-catenin expression	(82, 83)
Isocarbostyril alkaloid	Narciclasine	*Narcissus* and *Haemanthus* species	HUVECs	By the RhoA-independent activation of the Rho kinase ROCK downregulation of VEGFR2 expression	(84)
Amide alkeloid	Tetramethylpyrazine	*Ligusticum chuanxiong* hort	Ovarian cancer A2780 xenograft mouse models, HUVECs, SKOV3 cell	Inhibits ERK1/2 and Akt pathways	(85)
β-carboline alkaloid	Harmine	Pergamum harmala seeds	The xenograft mouse model assay of human bladder cancer used RT4 cell line, HUVECs, Rat aortic ring assay	Inhibits VEGFR2, ERK1/2 and Akt signaling pathways	(86)
Quinolizidine alkaloid	Oxysophocarpine	*Sophora flavescens* Ait. (Kushen), *S. alopecuroides L*. (Kudouzi or Kugancao), and other leguminous plants of the genus Robinia	HUVECs, BALB/c nude mice were injected with SCC-9 cells	Reduces the levels of HO-1, VEGF, MMP-9 and HIF-1α expression	(87)
Opium alkaloid	Noscapine	*Papaver somniferum L*	HUVECs	Inhibits growth of human endothelial cells, cord formation of human endothelial cells and chemotaxis factors responsible for the angiogenesis	(90)
Cassaine diterpene alkaloid	3β-acetyl-nor erythrophlamide	*Erythrophleum fordii*	HUVECs, A549 xenograft mouse model	Inhibits the VEGF-mediated eNOS activation and NO production	(88)
Isosteroidal Alkaloid	Chuanbeinone	Bulbus of *Fritillaria pallidiflora*	LLC and S180-bearing mice	Inhibits the expression of VEGF	(91)
quinazolinone alkaloid	Halofuginone	*Dichroa febrifuga* Lour.	NB4 and HUVEC cells, NOD/SCID mice were transplanted with leukemic cells	Reduces VEGF secretion and phosphorylation of SMAD-2 Blocks TGF-β signaling pathway	(92)
Bisbenzylisoquinoline alkaloid	Tetrandrine	the roots of the medicinal plant *Stephaniae tetrandrae S. Moore* (Han-Fang-Ji in Chinese)	Mouse endothelial cells (EOMA cell), Huh7 tumor xenografts	Inhibits EOMA cells proliferation *via* ROS/Akt pathway	(93)
Isoquinoline alkaloids	Berberine	*Coptis Rhizome*	MHCC-97L cells xenograft mouse model	Inhibits the expression of Id-1, VEGF	(94)
	Sinomenine	*Sinomenium actum Rehd.et wils.*	HUVEC, HOS-Luc cells xenograft mouse model	Inhibits the expression of VEGF, MMP-2, MMP-9, RANKL Inhibited invasion and metastasis *via* suppressing the CXCR4-STAT3 pathway	(95)
Benzophenanthridine alkaloid	Sanguinarine	the root of *Sanguinaria canadensis* and other poppy-fumaria species	Human microvascular endothelial cells (HMVECs), A549 cells	Inhibits the activation of serum starvation and hypoxia-induced VEGF promoter activity	(96)
Amide alkaloids	Capsaicin	*Capsicum annuum L.*	HUVEC, A549	Re-activation of p53-SMAR1, inhibits the expression of HIF-1α and Cox-2, down regulate VEGF	(97)

Chinese herbal medicines, such as *Ginseng, Polygala Tenuifolia, Platycodon grandiflorum, licorice, Anemarrhena and Bupleurum*, contain saponins as the main active ingredients. According to the different structures of sapogenins, saponins have the biological functions of anti-tumor, hypoglycemic, cholesterol lowering, liver protection, immune regulation, anti-inflammatory and anti-microbial effects. The chemical structures (**Figure 6**) and anti-angiogenic property of several saponins (Timosaponin AIII,

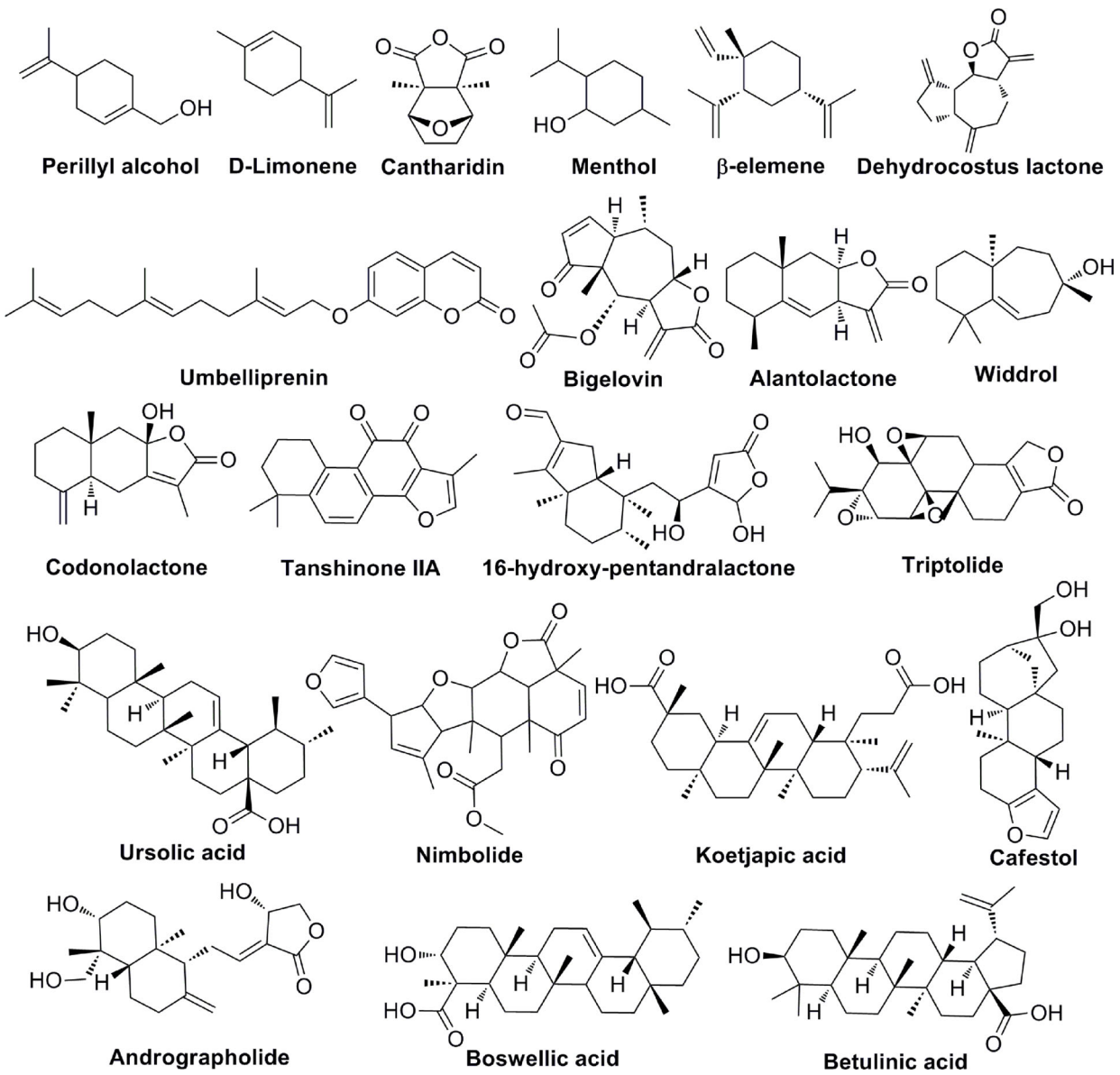


FIGURE 5 | The chemical structures of terpenoids involved in tumor angiogenesis.

Ginsenoside Rg3, β-Escin, sea cucumber saponins, et al) has been identified in recent years (**Table 6**). Timosaponin AIII is a steroidal saponin, derived from *Anemarrhena asphodeloides Bge*. It exerts anti-angiogenic effect through VEGF/PI3K/Akt/MAPK signaling pathway in the zebrafish embryos model (119). Ginsenoside Rg3 is a triterpene saponin, isolated from *Panax ginseng*. Ginsenoside Rg3 can decrease the expression of MMP-2, MMP-9 and VEGF in B16 cell tumor mouse model and *in vitro* B16 cell model (122). β-escin is also a kind of triterpene saponin, extracted from *Aesculus hippocastanum* seeds. β-escin can inhibit melanoma angiogenesis by increasing the expression of TIMP-1 and TIMP-2 (123). Sea cucumber saponins are crude saponins, that are prevalent in Holothuria leucospilota. The saponins extracted from sea cucumber can inhibit the expression of VEGF-D and TGF-β in MCF7 cells (126).

CONCLUSIONS

This review article shed a light on the role of natural compounds in cancer therapy by modulating angiogenic factors and ECs apoptosis. In addition, the chemical structures of natural compounds involved in tumor angiogenesis were summarized and shown in supplementary material with the format of CS

TABLE 5 | Natural anti-tumor angiogenesis terpenoids and their sources, experimental models and anti-angiogenic mechanisms.

Category	Name	Source	Experimental model	Anti-angiogenic mechanism	Refs
Monoterpene	Perillyl alcohol	the essential oils of several plants (lavendin, mints, cherries, etc.)	CAM, HUVECs, BLMVECs, K562	Inhibits VEGF and Akt pathways	(98)
	D-limonene rich volatile oil	blood orange (*Citrus sinensis* (L) Osbeck)	SW480 and HT-29 cells, HUVECs	Reduces the levels of VEGF, MMP-9 expression, inhibits the activation of VEGFR1	(99)
	Cantharidin	Mylabris	Subcutaneous and orthotopic pancreatic xenograft models with PANC-1 cells	Inhibits ERK, JNK, PKC, and NF-κB pathways	(100)
	Menthol	*Mentha haplocalyx Briq*	HepG2 cells	Inhibits the expression of VEGF	(101)
Sesquiterpene	β-elemene	the essential oil of *Curcuma zedoaria*	Rat aortic ring, Chick embryo chorioallantoic membrane, Melanoma growth and metastasis assay in C57BL/6 mice	Suppresses VEGF pathway	(102)
	Dehydrocostus lactone	Saussurea lappa and Laurus nobilis	lung cancer cells (A549 and H460 cells), Matrigel plugs were implanted in C57BL/6 mice	Suppresses of HIF-1a, Akt and pAkt, GSK-3β and pGSK-3β, as well as ERK, pERK, mTOR, and p-mTOR	(103)
	Umbelliprenin	Different spices of *Ferula* of umbeliferace	CT26 tumor cells, L929 cells	Inhibits MMP-2 and MMP-9 Inhibits the expression of VEGF, MMP2, MMP-9 and CD31 Potentiates immune response by IFN-γ increment and IL-4 decrease	(104)
	Bigelovin	*Inula helianthus-aquatica*	HCT 116 cells, Orthotopic tumor allografts and experimental metastatic models with colon 26-M01 cells	Interferes IL6/STAT3 and cofilin pathways	(105)
	Alantolactone	*Inula helenium*	HUVECs, human MDA-MB-231 breast cancer xenograft in mice	Suppresses the phosphorylation of VEGFR2 and its downstream protein kinase including PLCγ1, FAK, Src, and Akt	(106)
	Codonolactone	*Atractylodes lancea*	HUVECs, EA.hy 926 cells	Inhibits MMPs expression and VEGF secretion by down-regulating BMP/Runx2 activation	(107)
	Widdrol	*Juniperus chinensis*	HUVECs, Human colon adenocarcinoma HT29 cells	Suppresses phosphorylation of VEGFR2, AKT, FAK and eNOS	(108)
Diterpene	Tanshinone IIA	The dried root of *Salvia miltiorrhiza* Bunge	Human EPCs, CAM, Matrigel plug model	Inhibits EPC angiogenesis through the VEGF, PLC, Akt and JNK signaling pathways	(109)
	16-hydroxy-pentandralactone	*Vitex cofassus*	HUVECs	Inhibits VEGF-stimulated HUVEC proliferation	(110)
	Cafestol	Unfiltered coffee	HUVECs	Inhibits the phosphorylation of FAK and Akt and decreases nitric oxide production	(111)
	Andrographolide	*Andrographis paniculate*	HUVECs, A549 Cells	Inhibits MMP-9 expression	(112)
	Triptolide	*Tripterygium wilfordii*	HUVECs, Breast cancer cells (Hs578T and MDAMB231)	Inhibits the ERK1/2-HIF1-α-VEGFA signaling pathway	(113)
Triterpene	Ursolic acid	Many plant foods	Ehrlich ascites carcinoma (EAC) cells, Swiss albino mice with EAC cells	Inhibits VEGF and iNOS expression	(114)
	Nimbolide	*Azadirachta indica* leaves	HCT-116, HT-29, Caco-2, CRC cells	Inhibits VEGF and MMP-9 expression	(115)
	Koetjapic acid	*Sandoricum koetjaoe* Merr	rat aortic ring, CAM, HUVECs	Inhibits VEGF expression	(116)
	Boswellic acid	*Boswellia serrata*	Ehrlich ascites carcinoma (EAC) cells, Swiss albino mice with EAC cells	Inhibits VEGF and TNF-α expression	(117)
	Betulinic acid	The stembark of *Betula* ssp. and from many other plants	Human endometrial adenocarcinoma (EA) cells	Inhibits prolidase, HIF-1α and VEGF expressions	(118)

ChemDraw Drawing, which could be conveniently used for the related researchers. Natural products have presented as new stars in the field of anti-tumor neovascularization research for their easy availability and cost-effectiveness (128). A large number of epidemiological studies proved the reduction of cancer incidence upon the high nutritional ingestion of vegetables and fruits (129). Moreover, natural products emerged as SIRT6 modulators can be successfully applied to treat cancer, inflammation, Alzheimer's Disease, etc (130).

Currently, anti-angiogenic drugs are widely used and recognized in cancer treatments because they enriched the arsenal of chemotherapeutic drugs. The majority of modern targeted drugs fail to achieve the expected therapeutic effects. Consequently, the anti-cancer regimens have shifted to multi-targeted therapies using

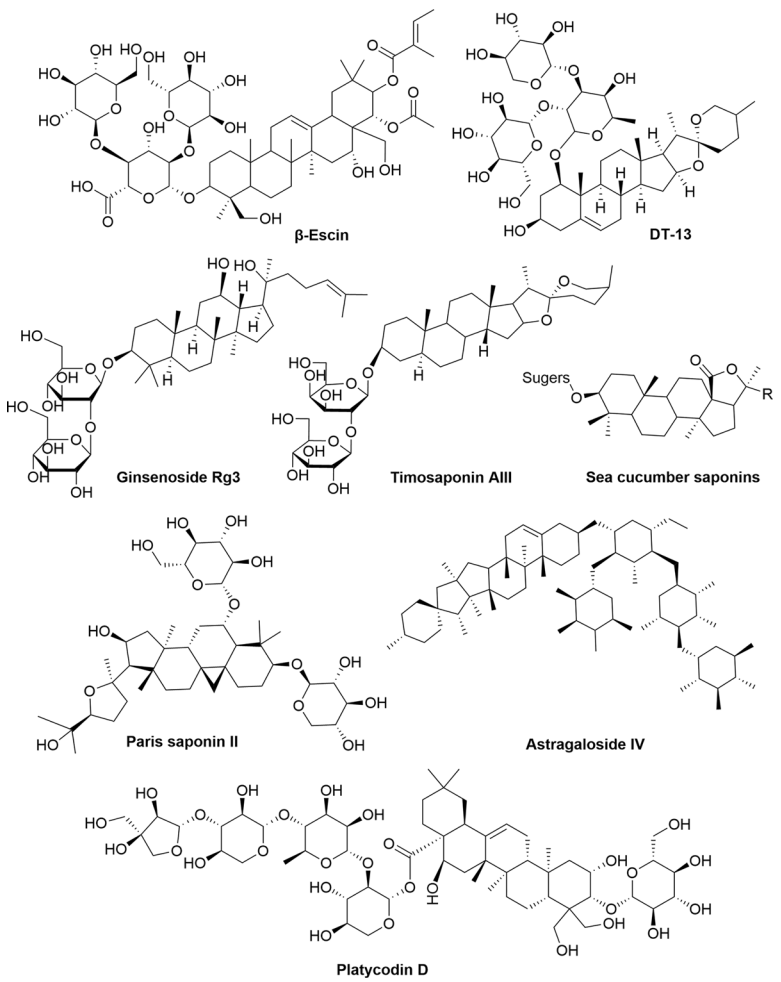


FIGURE 6 | The chemical structures of saponins involved in tumor angiogenesis.

TABLE 6 | Natural anti-tumor angiogenesis saponins and their sources, experimental models and anti-angiogenic mechanisms.

Category	Name	Source	Experimental model	Anti-angiogenic mechanism	Refs
Steroidal saponin	Timosaponin AIII	*Anemarrhena asphodeloides* Bge	Zebrafish embryos, HUVECs	Inhibits VEGF/PI3K/Akt/MAPK signaling cascade	(119)
	DT-13	Dwarf lilyturf tuber	HUVECs, CAM	Inhibits the levels of p-VEGFR-2, p-ERK1/2 and p-Akt, Inhibits the expression of VEGF	(120)
	Paris saponin II	*Rhizoma paridis*	HUVECs, SKOV3 cells	Suppresses NF-κB signaling	(121)
Triterpene saponin	Ginsenoside Rg3	*Panax ginseng*	B16 melanoma cells, C57BL/6 mice with B16 cells	Inhibits the expression of MMP-2, MMP-9 and VEGF	(122)
	β-Escin	*Aesculus hippocastanum* seeds	B16F10 and SK-MEL5 cells	Increases the expression of TIMP-1 and TIMP-2	(123)
	Astragaloside IV	*Astragali radix*	C57BL/6 mice with LLC cells	Blocks the M2 polarization of macrophages partially through the AMPK signaling pathway	(124)
	Platycodin D (PD)	the roots of Platycodon grandiflorum	C57BL/6 mice with H22 cells	Inhibits the expression of VEGF	(125)
Crude saponins	Sea cucumber saponins (SCS)	*Holothuria leucospilota* (sea cucumber)	MCF7 cells	Inhibits the expression of VEGF-D and TGF-β	(126)
	Rh.Sp saponins	*Rumex hastatus* D. Don.	CAM	–	(127)

traditional and integrative natural products. There is a huge number of natural products for anti-angiogenic substances and the study on the complex mechanisms of these compounds is just started. Studies on the role of different structures of natural compounds in inhibiting tumor angiogenesis would assist in anti-cancer drug discovery and development. The anti-angiogenic therapy of human cancer patients is based on pre-clinical models that simulate the pathogenesis of human cancers, and most of them are elucidated in this review. It is certain that future patients will be benefited from the novel discoveries of natural products, thus a lot of research works are warranted.

PERSPECTIVES AND LIMITATIONS

As for clinical application of natural products in tumor, issues have emerged during the past few decades. The bioavailability of natural products is the major restriction, since these compounds have the properties of poor aqueous solubility and low absorption rate. Prior to the use of natural products in anti-tumor therapy, the concentration problem needs to be resolved. At present, several carriers (nanoparticles, micelles, lipids, etc) with natural products are being developed to apply to the delivery of these compounds to human body systems. Therefore, as hopeful therapeutic targets towards tumor angiogenesis, more efforts should be made to the development of natural compounds and their modifiers according to their molecular mechanisms and involved signaling pathways in tumors.

AUTHOR CONTRIBUTIONS

PS, Z-SC, and DD conceived and designed the review. RL and XS created the tables and figures, and wrote the draft manuscript. RL, XS, and YG revised the manuscript and performed the table design. PS, Z-SC, and DD reviewed and edited the manuscript. All authors read and approved the final manuscript.

FUNDING

This work was supported by the National Natural Science Foundation of China (81803779); the Gansu Province Science Foundation for Distinguished Young Scholars (20JR10RA348) and the Gansu Province Science Foundation for B Program (1508RJZA018) from Gansu Provincial Sci. & Tech. Department; the Open Project of Research Center of Traditional Chinese Medicine, Gansu Province (zyzx-2020-zx1); the Open Project of Key Laboratory of Prevention and Treatment for Chronic Diseases by TCM in Gansu Province (GSMBKY2015-01); the Gansu Province Health Industry Scientific Research Program Management Project (GWGL2014-53); and the National Natural Science Foundation of Shaanxi Province (2018JQ2051).

ACKNOWLEDGMENTS

Thanks for the hard work of each author.

SUPPLEMENTARY MATERIAL

The Supplementary Material for this article can be found online at: https://www.frontiersin.org/articles/10.3389/fonc.2021.772915/full#supplementary-material

REFERENCES

1. Simon T, Gagliano T, Giamas G. Direct Effects of Anti-Angiogenic Therapies on Tumor Cells: VEGF Signaling. *Trends Mol Med* (2017) 23 (3):282–92. doi: 10.1016/j.molmed.2017.01.002
2. Haralambiev L, Neuffer O, Nitsch A, Kross NC, Bekeschus S, Hinz P, et al. Inhibition of Angiogenesis by Treatment With Cold Atmospheric Plasma as a Promising Therapeutic Approach in Oncology. *Int J Mol Sci* (2020) 21 (19):7098–113. doi: 10.3390/ijms21197098
3. Wang H, Yang J, Zhang K, Liu J, Li Y, Su W, et al. Advances of Fibroblast Growth Factor/Receptor Signaling Pathway in Hepatocellular Carcinoma and Its Pharmacotherapeutic Targets. *Front Pharmacol* (2021) 12:650388. doi: 10.3389/fphar.2021.650388
4. Chavakis E, Dimmeler S. Regulation of Endothelial Cell Survival and Apoptosis During Angiogenesis. *Arterioscler Thromb Vasc Biol* (2002) 22 (6):887–93. doi: 10.1161/01.atv.0000017728.55907.a9
5. Christensen SB. Natural Products That Changed Society. *Biomedicines* (2021) 9(5):472–502. doi: 10.3390/biomedicines9050472
6. Deng J, Wang C, Jiang Y. Warming Yang Method in Traditional Chinese Medicine for Depression: A Protocol for Systematic Review and Meta-Analysis. *Med (Baltimore)* (2020) 99(52):e23919. doi: 10.1097/MD.0000000000023919
7. Sharma B, Dutt V, Kaur N, Mittal A, Dabur R. Tinospora Cordifolia Protects From Skeletal Muscle Atrophy by Alleviating Oxidative Stress and Inflammation Induced by Sciatic Denervation. *J Ethnopharmacol* (2020) 254:112720. doi: 10.1016/j.jep.2020.112720
8. Parveen A, Sultana R, Lee SM, Kim TH, Kim SY. Phytochemicals Against Anti-Diabetic Complications: Targeting the Advanced Glycation End Product Signaling Pathway. *Arch Pharm Res* (2021) 44(4):378–401. doi: 10.1007/s12272-021-01323-9
9. Gaikwad S, Srivastava SK. Role of Phytochemicals in Perturbation of Redox Homeostasis in Cancer. *Antioxid (Basel)* (2021) 10(1):83–108. doi: 10.3390/antiox10010083
10. Fakhri S, Abbaszadeh F, Jorjani M, Pourgholami MH. The Effects of Anticancer Medicinal Herbs on Vascular Endothelial Growth Factor Based on Pharmacological Aspects: A Review Study. *Nutr Cancer* (2021) 73(1):1–15. doi: 10.1080/01635581.2019.1673451
11. Campos-Contreras ADR, Diaz-Munoz M, Vazquez-Cuevas FG. Purinergic Signaling in the Hallmarks of Cancer. *Cells* (2020) 9(7):1612–35. doi: 10.3390/cells9071612
12. Parmar D, Apte M. Angiopoietin Inhibitors: A Review on Targeting Tumor Angiogenesis. *Eur J Pharmacol* (2021) 899:174021. doi: 10.1016/j.ejphar.2021.174021
13. Jiang X, Wang J, Deng X, Xiong F, Zhang S, Gong Z, et al. The Role of Microenvironment in Tumor Angiogenesis. *J Exp Clin Cancer Res* (2020) 39 (1):204. doi: 10.1186/s13046-020-01709-5
14. Cho WC, Jour G, Aung PP. Role of Angiogenesis in Melanoma Progression: Update on Key Angiogenic Mechanisms and Other Associated Components. *Semin Cancer Biol* (2019) 59:175–86. doi: 10.1016/j.semcancer.2019.06.015
15. Teleanu RI, Chircov C, Grumezescu AM, Teleanu DM. Tumor Angiogenesis and Anti-Angiogenic Strategies for Cancer Treatment. *J Clin Med* (2019) 9 (1):84–104. doi: 10.3390/jcm9010084

16. Wheler JJ, Janku F, Naing A, Li Y, Stephen B, Zinner R, et al. TP53 Alterations Correlate With Response to VEGF/VEGFR Inhibitors: Implications for Targeted Therapeutics. *Mol Cancer Ther* (2016) 15 (10):2475–85. doi: 10.1158/1535-7163.MCT-16-0196
17. Ribatti D, Vacca A. Role of Endothelial Cells and Fibroblasts in Multiple Myeloma Angiogenic Switch. *Cancer Treat Res* (2016) 169:51–61. doi: 10.1007/978-3-319-40320-5_5
18. Yoshida GJ, Azuma A, Miura Y, Orimo A. Activated Fibroblast Program Orchestrates Tumor Initiation and Progression; Molecular Mechanisms and the Associated Therapeutic Strategies. *Int J Mol Sci* (2019) 20(9):2256–85. doi: 10.3390/ijms20092256
19. Zhang Y, Liu NM, Wang Y, Youn JY, Cai H. Endothelial Cell Calpain as a Critical Modulator of Angiogenesis. *Biochim Biophys Acta Mol Basis Dis* (2017) 1863(6):1326–35. doi: 10.1016/j.bbadis.2017.03.021
20. De Ieso ML, Yool AJ. Mechanisms of Aquaporin-Facilitated Cancer Invasion and Metastasis. *Front Chem* (2018) 6:135. doi: 10.3389/fchem.2018.00135
21. Liu G, Chen T, Ding Z, Wang Y, Wei Y, Wei X. Inhibition of FGF-FGFR and VEGF-VEGFR Signalling in Cancer Treatment. *Cell Prolif* (2021) 54(4): e13009. doi: 10.1111/cpr.13009
22. Monk BJ, Poveda A, Vergote I, Raspagliesi F, Fujiwara K, Bae DS, et al. Anti-Angiopoietin Therapy With Trebananib for Recurrent Ovarian Cancer (TRINOVA-1): A Randomised, Multicentre, Double-Blind, Placebo-Controlled Phase 3 Trial. *Lancet Oncol* (2014) 15(8):799–808. doi: 10.1016/S1470-2045(14)70244-X
23. Yang LI, Wang X, Sun J, Liu C, Li G, Zhu J, et al. Neuritin Promotes Angiogenesis Through Inhibition of DLL4/Notch Signaling Pathway. *Acta Biochim Biophys Sin (Shanghai)* (2021) 53(6):663–72. doi: 10.1093/abbs/gmab039
24. Gerber HP, Dixit V, Ferrara N. Vascular Endothelial Growth Factor Induces Expression of the Antiapoptotic Proteins Bcl-2 and A1 in Vascular Endothelial Cells. *J Biol Chem* (1998) 273(21):13313–6. doi: 10.1074/jbc.273.21.13313
25. O'Connor DS, Schechner JS, Adida C, Mesri M, Rothermel AL, Li F, et al. Control of Apoptosis During Angiogenesis by Survivin Expression in Endothelial Cells. *Am J Pathol* (2000) 156(2):393–8. doi: 10.1016/s0002-9440(10)64742-6
26. Kwak HJ, So JN, Lee SJ, Kim I, Koh GY. Angiopoietin-1 Is an Apoptosis Survival Factor for Endothelial Cells. *FEBS Lett* (1999) 448(2-3):249–53. doi: 10.1016/s0014-5793(99)00378-6
27. Carmeliet P, Lampugnani MG, Moons L, Breviario F, Compernolle V, Bono F, et al. Targeted Deficiency or Cytosolic Truncation of the VE-Cadherin Gene in Mice Impairs VEGF-Mediated Endothelial Survival and Angiogenesis. *Cell* (1999) 98(2):147–57. doi: 10.1016/s0092-8674(00)81010-7
28. Soldi R, Mitola S, Strasly M, Defilippi P, Tarone G, Bussolino F. Role of Alphavbeta3 Integrin in the Activation of Vascular Endothelial Growth Factor Receptor-2. *EMBO J* (1999) 18(4):882–92. doi: 10.1093/emboj/18.4.882
29. Sha W, Liu M, Sun D, Qiu J, Xu B, Chen L, et al. Resveratrol Improves Gly-LDL-Induced Vascular Endothelial Cell Apoptosis, Inflammatory Factor Secretion and Oxidative Stress by Regulating miR-142-3p and Regulating SPRED2-Mediated Autophagy. *Aging (Albany NY)* (2021) 13(5):6878–89. doi: 10.18632/aging.202546
30. Vicas LG, Jurca T, Baldea I, Filip GA, Olteanu D, Clichici SV, et al. Physalis Alkekengi L. Extract Reduces the Oxidative Stress, Inflammation and Apoptosis in Endothelial Vascular Cells Exposed to Hyperglycemia. *Molecules* (2020) 25(16):3747–65. doi: 10.3390/molecules25163747
31. Song P, Hai Y, Wang X, Zhao L, Chen B, Cui P, et al. Realgar Transforming Solution Suppresses Angiogenesis and Tumor Growth by Inhibiting VEGF Receptor 2 Signaling in Vein Endothelial Cells. *Arch Pharm Res* (2018) 41 (4):467–80. doi: 10.1007/s12272-018-1014-6
32. Gordon E, Schimmel L, Frye M. The Importance of Mechanical Forces for *In Vitro* Endothelial Cell Biology. *Front Physiol* (2020) 11:684. doi: 10.3389/fphys.2020.00684
33. Victorelli FD, Cardoso VMO, Ferreira NN, Calixto GMF, Fontana CR, Baltazar F, et al. Chick Embryo Chorioallantoic Membrane as a Suitable *In Vivo* Model to Evaluate Drug Delivery Systems for Cancer Treatment: A Review. *Eur J Pharm Biopharm* (2020) 153:273–84. doi: 10.1016/j.ejpb.2020.06.010
34. Brown HK, Schiavone K, Tazzyman S, Heymann D, Chico TJ. Zebrafish Xenograft Models of Cancer and Metastasis for Drug Discovery. *Expert Opin Drug Discovery* (2017) 12(4):379–89. doi: 10.1080/17460441.2017.1297416
35. Auerbach R, Akhtar N, Lewis RL, Shinners BL. Angiogenesis Assays: Problems and Pitfalls. *Cancer Metastasis Rev* (2000) 19(1-2):167–72. doi: 10.1023/a:1026574416001
36. Croci DO, Cerliani JP, Dalotto-Moreno T, Méndez-Huergo SP, Mascanfroni ID, Dergan-Dylon S, et al. Glycosylation-Dependent Lectin-Receptor Interactions Preserve Angiogenesis in Anti-VEGF Refractory Tumors. *Cell* (2014) 156(4):744–58. doi: 10.1016/j.cell.2014.01.043
37. Yu L, Wu X, Cheng Z, Lee CV, LeCouter J, Campa C, et al. Interaction Between Bevacizumab and Murine VEGF-A: A Reassessment. *Invest Ophthalmol Vis Sci* (2008) 49(2):522–7. doi: 10.1167/iovs.07-1175
38. Bonapace L, Coissieux MM, Wyckoff J, Mertz KD, Varga Z, Junt T, et al. Cessation of CCL2 Inhibition Accelerates Breast Cancer Metastasis by Promoting Angiogenesis. *Nature* (2014) 515(7525):130–3. doi: 10.1038/nature13862
39. Kowshik J, Giri H, Kishore TK, Kesavan R, Vankudavath RN, Reddy GB, et al. Ellagic Acid Inhibits VEGF/VEGFR2, PI3K/Akt and MAPK Signaling Cascades in the Hamster Cheek Pouch Carcinogenesis Model. *Anticancer Agents Med Chem* (2014) 14(9):1249–60. doi: 10.2174/1871520614666140723114217
40. Wang N, Wang ZY, Mo SL, Loo TY, Wang DM, Luo HB, et al. Ellagic Acid, a Phenolic Compound, Exerts Anti-Angiogenesis Effects *via* VEGFR-2 Signaling Pathway in Breast Cancer. *Breast Cancer Res Treat* (2012) 134 (3):943–55. doi: 10.1007/s10549-012-1977-9
41. Park JJ, Hwang SJ, Park JH, Lee HJ. Chlorogenic Acid Inhibits Hypoxia-Induced Angiogenesis *via* Down-Regulation of the HIF-1alpha/AKT Pathway. *Cell Oncol (Dordr)* (2015) 38(2):111–8. doi: 10.1007/s13402-014-0216-2
42. Abusnina A, Keravis T, Zhou Q, Justiniano H, Lobstein A, Lugnier C. Tumour Growth Inhibition and Anti-Angiogenic Effects Using Curcumin Correspond to Combined PDE2 and PDE4 Inhibition. *Thromb Haemost* (2015) 113(2):319–28. doi: 10.1160/TH14-05-0454
43. Jiao D, Wang J, Lu W, Tang X, Chen J, Mou H, et al. Curcumin Inhibited HGF-Induced EMT and Angiogenesis Through Regulating C-Met Dependent PI3K/Akt/mTOR Signaling Pathways in Lung Cancer. *Mol Ther Oncolytics* (2016) 3:16018. doi: 10.1038/mto.2016.18
44. Tian B, Zhao Y, Liang T, Ye X, Li Z, Yan D, et al. Curcumin Inhibits Urothelial Tumor Development by Suppressing IGF2 and IGF2-Mediated PI3K/AKT/mTOR Signaling Pathway. *J Drug Target* (2017) 25(7):626–36. doi: 10.1080/1061186X.2017.1306535
45. Zhao D, Qin C, Fan X, Li Y, Gu B. Inhibitory Effects of Quercetin on Angiogenesis in Larval Zebrafish and Human Umbilical Vein Endothelial Cells. *Eur J Pharmacol* (2014) 723:360–7. doi: 10.1016/j.ejphar.2013.10.069
46. Zhao X, Wang Q, Yang S, Chen C, Li X, Liu J, et al. Quercetin Inhibits Angiogenesis by Targeting Calcineurin in the Xenograft Model of Human Breast Cancer. *Eur J Pharmacol* (2016) 781:60–8. doi: 10.1016/j.ejphar.2016.03.063
47. Negrao R, Costa R, Duarte D, Gomes TT, Azevedo I, Soares R. Different Effects of Catechin on Angiogenesis and Inflammation Depending on VEGF Levels. *J Nutr Biochem* (2013) 24(2):435–44. doi: 10.1016/j.jnutbio.2011.12.011
48. Gao Y, Rankin GO, Tu Y, Chen YC. Inhibitory Effects of the Four Main Theaflavin Derivatives Found in Black Tea on Ovarian Cancer Cells. *Anticancer Res* (2016) 36(2):643–51.
49. Jin G, Yang Y, Liu K, Zhao J, Chen X, Liu H, et al. Combination Curcumin and (-)-Epigallocatechin-3-Gallate Inhibits Colorectal Carcinoma Microenvironment-Induced Angiogenesis by JAK/STAT3/IL-8 Pathway. *Oncogenesis* (2017) 6(10):e384. doi: 10.1038/oncsis.2017.84
50. Xu H, Becker CM, Lui WT, Chu CY, Davis TN, Kung AL, et al. Green Tea Epigallocatechin-3-Gallate Inhibits Angiogenesis and Suppresses Vascular Endothelial Growth Factor C/vascular Endothelial Growth Factor Receptor 2 Expression and Signaling in Experimental Endometriosis *In Vivo*. *Fertil Steril* (2011) 96(4):1021–8. doi: 10.1016/j.fertnstert.2011.07.008
51. Yan Y, Yao L, Sun H, Pang S, Kong X, Zhao S, et al. Effects of Wogonoside on Invasion and Migration of Lung Cancer A549 Cells and Angiogenesis in Xenograft Tumors of Nude Mice. *J Thorac Dis* (2020) 12(4):1552–60. doi: 10.21037/jtd-20-1555
52. Mirzoeva S, Franzen CA, Pelling JC. Apigenin Inhibits TGF-Beta-Induced VEGF Expression in Human Prostate Carcinoma Cells *via* a Smad2/3- and

Src-Dependent Mechanism. *Mol Carcinog* (2014) 53(8):598–609. doi: 10.1002/mc.22005
53. Cook MT, Mafuvadze B, Besch-Williford C, Ellersieck MR, Goyette S, Hyder SM. Luteolin Suppresses Development of Medroxyprogesterone Acetate-Accelerated 7,12-Dimethylbenz(a)Anthracene-Induced Mammary Tumors in Sprague-Dawley Rats. *Oncol Rep* (2016) 35(2):825–32. doi: 10.3892/or.2015.4431
54. Doleckova I, Rarova L, Gruz J, Vondrusova M, Strnad M, Krystof V. Antiproliferative and Antiangiogenic Effects of Flavone Eupatorin, an Active Constituent of Chloroform Extract of Orthosiphon Stamineus Leaves. *Fitoterapia* (2012) 83(6):1000–7. doi: 10.1016/j.fitote.2012.06.002
55. Abbaszadeh H, Ebrahimi SA, Akhavan MM. Antiangiogenic Activity of Xanthomicrol and Calycopterin, Two Polymethoxylated Hydroxyflavones in Both *In Vitro* and Ex Vivo Models. *Phytother Res* (2014) 28(11):1661–70. doi: 10.1002/ptr.5179
56. Kim MH, Jeong YJ, Cho HJ, Hoe HS, Park KK, Park YY, et al. Delphinidin Inhibits Angiogenesis Through the Suppression of HIF-1alpha and VEGF Expression in A549 Lung Cancer Cells. *Oncol Rep* (2017) 37(2):777–84. doi: 10.3892/or.2016.5296
57. Tanaka J, Nakamura S, Tsuruma K, Shimazawa M, Shimoda H, Hara H. Purple Rice (Oryza Sativa L.) Extract and Its Constituents Inhibit VEGF-Induced Angiogenesis. *Phytother Res* (2012) 26(2):214–22. doi: 10.1002/ptr.3533
58. Baba AB, Nivetha R, Chattopadhyay I, Nagini S. Blueberry and Malvidin Inhibit Cell Cycle Progression and Induce Mitochondrial-Mediated Apoptosis by Abrogating the JAK/STAT-3 Signalling Pathway. *Food Chem Toxicol* (2017) 109(Pt 1):534–43. doi: 10.1016/j.fct.2017.09.054
59. Bellou S, Karali E, Bagli E, Al-Maharik N, Morbidelli L, Ziche M, et al. The Isoflavone Metabolite 6-Methoxyequol Inhibits Angiogenesis and Suppresses Tumor Growth. *Mol Cancer* (2012) 11:35. doi: 10.1186/1476-4598-11-35
60. Yang JH, Hu J, Wan L, Chen LJ. Barbigerone Inhibits Tumor Angiogenesis, Growth and Metastasis in Melanoma. *Asian Pac J Cancer Prev* (2014) 15 (1):167–74. doi: 10.7314/apjcp.2014.15.1.167
61. Xue ZG, Niu PG, Shi DH, Liu Y, Deng J, Chen YY. Cardamonin Inhibits Angiogenesis by mTOR Downregulation in SKOV3 Cells. *Planta Med* (2016) 82(1-2):70–5. doi: 10.1055/s-0035-1557901
62. Saito K, Matsuo Y, Imafuji H, Okubo T, Maeda Y, Sato T, et al. Xanthohumol Inhibits Angiogenesis by Suppressing Nuclear factor-kappaB Activation in Pancreatic Cancer. *Cancer Sci* (2018) 109(1):132–40. doi: 10.1111/cas.13441
63. Chiang CH, Yeh CY, Chung JG, Chiang IT, Hsu FT. Amentoflavone Induces Apoptosis and Reduces Expression of Anti-Apoptotic and Metastasis-Associated Proteins in Bladder Cancer. *Anticancer Res* (2019) 39(7):3641–9. doi: 10.21873/anticanres.13512
64. Zhou J, Zhao R, Ye T, Yang S, Li Y, Yang F, et al. Antitumor Activity in Colorectal Cancer Induced by Hinokiflavone. *J Gastroenterol Hepatol* (2019) 34(9):1571–80. doi: 10.1111/jgh.14581
65. Pandey AK, Bhattacharya P, Shukla SC, Paul S, Patnaik R. Resveratrol Inhibits Matrix Metalloproteinases to Attenuate Neuronal Damage in Cerebral Ischemia: A Molecular Docking Study Exploring Possible Neuroprotection. *Neural Regener Res* (2015) 10(4):568–75. doi: 10.4103/1673-5374.155429
66. Ren F, Wu K, Yang Y, Yang Y, Wang Y, Li J. Dandelion Polysaccharide Exerts Anti-Angiogenesis Effect on Hepatocellular Carcinoma by Regulating VEGF/HIF-1alpha Expression. *Front Pharmacol* (2020) 11:460. doi: 10.3389/fphar.2020.00460
67. Ding J, Jia W, Cui Y, Jin J, Zhang Y, Xu L, et al. Anti-Angiogenic Effect of a Chemically Sulfated Polysaccharide From Phellinus Ribis by Inhibiting VEGF/VEGFR Pathway. *Int J Biol Macromol* (2020) 154:72–81. doi: 10.1016/j.ijbiomac.2020.03.068
68. Hsu WJ, Lin MH, Kuo TC, Chou CM, Mi FL, Cheng CH, et al. Fucoidan From Laminaria Japonica Exerts Antitumor Effects on Angiogenesis and Micrometastasis in Triple-Negative Breast Cancer Cells. *Int J Biol Macromol* (2020) 149:600–8. doi: 10.1016/j.ijbiomac.2020.01.256
69. Oliveira C, Granja S, Neves NM, Reis RL, Baltazar F, Silva TH, et al. Fucoidan From Fucus Vesiculosus Inhibits New Blood Vessel Formation and Breast Tumor Growth *In Vivo*. *Carbohydr Polym* (2019) 223:115034. doi: 10.1016/j.carbpol.2019.115034
70. Rui X, Pan HF, Shao SL, Xu XM. Anti-Tumor and Anti-Angiogenic Effects of Fucoidan on Prostate Cancer: Possible JAK-STAT3 Pathway. *BMC Complement Altern Med* (2017) 17(1):378. doi: 10.1186/s12906-017-1885-y
71. Yao Y, Zhou L, Liao W, Chen H, Du Z, Shao C, et al. HH1-1, a Novel Galectin-3 Inhibitor, Exerts Anti-Pancreatic Cancer Activity by Blocking Galectin-3/EGFR/AKT/FOXO3 Signaling Pathway. *Carbohydr Polym* (2019) 204:111–23. doi: 10.1016/j.carbpol.2018.10.008
72. Zong S, Li J, Yang L, Huang Q, Ye Z, Hou G, et al. Synergistic Antitumor Effect of Polysaccharide From Lachnum Sp. In Combination With Cyclophosphamide in Hepatocellular Carcinoma. *Carbohydr Polym* (2018) 196:33–46. doi: 10.1016/j.carbpol.2018.05.006
73. Yao H, Cui P, Xu D, Liu Y, Tian Q, Zhang F. A Water-Soluble Polysaccharide From the Roots of Polygala Tenuifolia Suppresses Ovarian Tumor Growth and Angiogenesis In Vivo. *Int J Biol Macromol* (2018) 107 (Pt A):713–8. doi: 10.1016/j.ijbiomac.2017.09.043
74. Varghese S, Joseph MM, S RA, B SU, Sreelekha TT. The Inhibitory Effect of Anti- Tumor Polysaccharide From Punica Granatum on Metastasis. *Int J Biol Macromol* (2017) 103:1000–10. doi: 10.1016/j.ijbiomac.2017.05.137
75. Ou M, Sun X, Liang J, Liu F, Wang L, Wu X, et al. A Polysaccharide From Sargassum Thunbergii Inhibits Angiogenesis via Downregulating MMP-2 Activity and VEGF/HIF-1alpha Signaling. *Int J Biol Macromol* (2017) 94(Pt A):451–8. doi: 10.1016/j.ijbiomac.2016.10.046
76. Lv Y, Shan X, Zhao X, Cai C, Zhao X, Lang Y, et al. Extraction, Isolation, Structural Characterization and Anti-Tumor Properties of an Apigalacturonan-Rich Polysaccharide From the Sea Grass Zostera Caespitosa Miki. *Mar Drugs* (2015) 13(6):3710–31. doi: 10.3390/md13063710
77. Jayaram S, Kapoor S, Dharmesh SM. Pectic Polysaccharide From Corn (Zea Mays L.) Effectively Inhibited Multi-Step Mediated Cancer Cell Growth and Metastasis. *Chem Biol Interact* (2015) 235:63–75. doi: 10.1016/j.cbi.2015.04.008
78. Wang P, Zhang L, Yao J, Shi Y, Li P, Ding K. An Arabinogalactan From Flowers of Panax Notoginseng Inhibits Angiogenesis by BMP2/Smad/Id1 Signaling. *Carbohydr Polym* (2015) 121:328–35. doi: 10.1016/j.carbpol.2014.11.073
79. Li C, Wu X, Zhang H, Yang G, Hao M, Sheng S, et al. A Huaier Polysaccharide Restrains Hepatocellular Carcinoma Growth and Metastasis by Suppression Angiogenesis. *Int J Biol Macromol* (2015) 75:115–20. doi: 10.1016/j.ijbiomac.2015.01.016
80. Zou Y, Xiong H, Xiong H, Lu T, Zhu F, Luo Z, et al. A Polysaccharide From Mushroom Huaier Retards Human Hepatocellular Carcinoma Growth, Angiogenesis, and Metastasis in Nude Mice. *Tumour Biol* (2015) 36 (4):2929–36. doi: 10.1007/s13277-014-2923-8
81. Kim Y, Sugihara Y, Kim TY, Cho SM, Kim JY, Lee JY, et al. Identification and Validation of VEGFR2 Kinase as a Target of Voacangine by a Systematic Combination of DARTS and MSI. *Biomolecules* (2020) 10(4):508–25. doi: 10.3390/biom10040508
82. Hwang ST, Um JY, Chinnathambi A, Alharbi SA, Narula AS, Namjoshi OA, et al. Evodiamine Mitigates Cellular Growth and Promotes Apoptosis by Targeting the C-Met Pathway in Prostate Cancer Cells. *Molecules* (2020) 25 (6):1320–33. doi: 10.3390/molecules25061320
83. Shi L, Yang F, Luo F, Liu Y, Zhang F, Zou M, et al. Evodiamine Exerts Anti-Tumor Effects Against Hepatocellular Carcinoma Through Inhibiting Beta-Catenin-Mediated Angiogenesis. *Tumour Biol* (2016) 37(9):12791–803. doi: 10.1007/s13277-016-5251-3
84. Brautigam J, Bischoff I, Schurmann C, Buchmann G, Epah J, Fuchs S, et al. Narciclasine Inhibits Angiogenic Processes by Activation of Rho Kinase and by Downregulation of the VEGF Receptor 2. *J Mol Cell Cardiol* (2019) 135:97–108. doi: 10.1016/j.yjmcc.2019.08.001
85. Zou L, Liu X, Li J, Li W, Zhang L, Li J, et al. Tetramethylpyrazine Enhances the Antitumor Effect of Paclitaxel by Inhibiting Angiogenesis and Inducing Apoptosis. *Front Pharmacol* (2019) 10:707. doi: 10.3389/fphar.2019.00707
86. Hai-Rong C, Xiang H, Xiao-Rong Z. Harmine Suppresses Bladder Tumor Growth by Suppressing Vascular Endothelial Growth Factor Receptor 2-Mediated Angiogenesis. *Biosci Rep* (2019) 39(5):1–10. doi: 10.1042/BSR20190155
87. Liu R, Peng J, Wang H, Li L, Wen X, Tan Y, et al. Oxysophocarpine Retards the Growth and Metastasis of Oral Squamous Cell Carcinoma by Targeting

the Nrf2/HO-1 Axis. *Cell Physiol Biochem* (2018) 49(5):1717–33. doi: 10.1159/000493615
88. Tae N, Hung TM, Kim O, Kim N, Lee S, Na S, et al. A Cassaine Diterpene Alkaloid, 3beta-Acetyl-Nor-Erythrophlamide, Suppresses VEGF-Induced Angiogenesis and Tumor Growth *via* Inhibiting eNOS Activation. *Oncotarget* (2017) 8(54):92346–58. doi: 10.18632/oncotarget.21307
89. Mingzhu LP SUO, Mei ZHANG, Yaodong ZHU, Mengran XU, LI W. Brucine Inhibits Vasculogenic Mimicry of Breast Cancer Cell Lines *In Vitro* and the Related Mechanism. *China Oncol* (2018) 28(4):241–7. doi: 10.19401/j.cnki.1007-3639.2018.04.001
90. Meher RK, Naik MR, Bastia B, Naik PK. Comparative Evaluation of Anti-Angiogenic Effects of Noscapine Derivatives. *Bioinformation* (2018) 14 (5):236–40. doi: 10.6026/97320630014236
91. Wang D, Li Z, Zhang L, Atanasov AG, Wang S. Characterization of the Isosteroidal Alkaloid Chuanbeinone From Bulbus of Fritillaria Pallidiflora as Novel Antitumor Agent *In Vitro* and *In Vivo*. *Planta Med* (2016) 82(3):195–204. doi: 10.1055/s-0035-1558156
92. Assis PA, De Figueiredo-Pontes LL, Lima AS, Leao V, Candido LA, Pintao CT, et al. Halofuginone Inhibits Phosphorylation of SMAD-2 Reducing Angiogenesis and Leukemia Burden in an Acute Promyelocytic Leukemia Mouse Model. *J Exp Clin Cancer Res* (2015) 34:65. doi: 10.1186/s13046-015-0181-2
93. Xiao W, Jiang Y, Men Q, Yuan L, Huang Z, Liu T, et al. Tetrandrine Induces G1/S Cell Cycle Arrest Through the ROS/Akt Pathway in EOMA Cells and Inhibits Angiogenesis *In Vivo*. *Int J Oncol* (2015) 46(1):360–8. doi: 10.3892/ijo.2014.2735
94. Tsang CM, Cheung KC, Cheung YC, Man K, Lui VW, Tsao SW, et al. Berberine Suppresses Id-1 Expression and Inhibits the Growth and Development of Lung Metastases in Hepatocellular Carcinoma. *Biochim Biophys Acta* (2015) 1852(3):541–51. doi: 10.1016/j.bbadis.2014.12.004
95. Xie T, Ren HY, Lin HQ, Mao JP, Zhu T, Wang SD, et al. Sinomenine Prevents Metastasis of Human Osteosarcoma Cells *via* S Phase Arrest and Suppression of Tumor-Related Neovascularization and Osteolysis Through the CXCR4-STAT3 Pathway. *Int J Oncol* (2016) 48(5):2098–112. doi: 10.3892/ijo.2016.3416
96. Xu JY, Meng QH, Chong Y, Jiao Y, Zhao L, Rosen EM, et al. Sanguinarine is a Novel VEGF Inhibitor Involved in the Suppression of Angiogenesis and Cell Migration. *Mol Clin Oncol* (2013) 1(2):331–6. doi: 10.3892/mco.2012.41
97. Chakraborty S, Adhikary A, Mazumdar M, Mukherjee S, Bhattacharjee P, Guha D, et al. Capsaicin-Induced Activation of P53-SMAR1 Auto-Regulatory Loop Down-Regulates VEGF in Non-Small Cell Lung Cancer to Restrain Angiogenesis. *PloS One* (2014) 9(6):e99743. doi: 10.1371/journal.pone.0099743
98. Loutrari H, Hatziapostolou M, Skouridou V, Papadimitriou E, Roussos C, Kolisis FN, et al. Perillyl Alcohol Is an Angiogenesis Inhibitor. *J Pharmacol Exp Ther* (2004) 311(2):568–75. doi: 10.1124/jpet.104.070516
99. Chidambara Murthy KN, Jayaprakasha GK. Patil BS. D-Limonene Rich Volatile Oil From Blood Oranges Inhibits Angiogenesis, Metastasis and Cell Death in Human Colon Cancer Cells. *Life Sci* (2012) 91(11-12):429–39. doi: 10.1016/j.lfs.2012.08.016
100. Xu MD, Liu L, Wu MY, Jiang M, Shou LM, Wang WJ, et al. The Combination of Cantharidin and Antiangiogenic Therapeutics Presents Additive Antitumor Effects Against Pancreatic Cancer. *Oncogenesis* (2018) 7(11):94. doi: 10.1038/s41389-018-0102-2
101. Jin TX-kZX-tWH-cDHC. Effect of Menthol on Proliferation, Migration and Expressions of IL-8, CXCL-12 and VEGF in Hepatoma HepG2 Cells. *Chin J Exp Tradit Med Formulae* (2019) 25(21):60–5. doi: 10.13422/j.cnki.syfjx.20192124
102. Chen W, Lu Y, Wu J, Gao M, Wang A, Xu B. Beta-Elemene Inhibits Melanoma Growth and Metastasis *via* Suppressing Vascular Endothelial Growth Factor-Mediated Angiogenesis. *Cancer Chemother Pharmacol* (2011) 67(4):799–808. doi: 10.1007/s00280-010-1378-x
103. Sheng W, Mao H, Wang C, Yang N, Zhang Z, Han J. Dehydrocostus Lactone Enhances Chemotherapeutic Potential of Doxorubicin in Lung Cancer by Inducing Cell Death and Limiting Metastasis. *Med Sci Monit* (2018) 24:7850–61. doi: 10.12659/MSM.911410
104. Naderi Alizadeh M, Rashidi M, Muhammadnejad A, Moeini Zanjani T, Ziai SA. Antitumor Effects of Umbelliprenin in a Mouse Model of Colorectal Cancer. *Iran J Pharm Res* (2018) 17(3):976–85.
105. Li M, Yue GG, Song LH, Huang MB, Lee JK, Tsui SK, et al. Natural Small Molecule Bigelovin Suppresses Orthotopic Colorectal Tumor Growth and Inhibits Colorectal Cancer Metastasis *via* IL6/STAT3 Pathway. *Biochem Pharmacol* (2018) 150:191–201. doi: 10.1016/j.bcp.2018.02.017
106. Liu YR, Cai QY, Gao YG, Luan X, Guan YY, Lu Q, et al. Alantolactone, a Sesquiterpene Lactone, Inhibits Breast Cancer Growth by Antiangiogenic Activity *via* Blocking VEGFR2 Signaling. *Phytother Res* (2018) 32(4):643–50. doi: 10.1002/ptr.6004
107. Wang S, Cai R, Ma J, Liu T, Ke X, Lu H, et al. The Natural Compound Codonolactone Impairs Tumor Induced Angiogenesis by Downregulating BMP Signaling in Endothelial Cells. *Phytomedicine* (2015) 22(11):1017–26. doi: 10.1016/j.phymed.2015.07.009
108. Jin S, Yun HJ, Jeong HY, Oh YN, Park HJ, Yun SG, et al. Widdrol, a Sesquiterpene Isolated From Juniperus Chinensis, Inhibits Angiogenesis by Targeting Vascular Endothelial Growth Factor Receptor 2 Signaling. *Oncol Rep* (2015) 34(3):1178–84. doi: 10.3892/or.2015.4075
109. Lee HP, Liu YC, Chen PC, Tai HC, Li TM, Fong YC, et al. Tanshinone IIA Inhibits Angiogenesis in Human Endothelial Progenitor Cells *In Vitro* and *In Vivo*. *Oncotarget* (2017) 8(65):109217–27. doi: 10.18632/oncotarget.22649
110. Rasyid FA, Fukuyoshi S, Ando H, Miyake K, Atsumi T, Fujie T, et al. A Novel Clerodane Diterpene From Vitex Cofassus. *Chem Pharm Bull (Tokyo)* (2017) 65(1):116–20. doi: 10.1248/cpb.c16-00775
111. Wang S, Yoon YC, Sung MJ, Hur HJ, Park JH. Antiangiogenic Properties of Cafestol, a Coffee Diterpene, in Human Umbilical Vein Endothelial Cells. *Biochem Biophys Res Commun* (2012) 421(3):567–71. doi: 10.1016/j.bbrc.2012.04.046
112. Guo X, Zhao M, Lin Y, Chen W, Wang S, Dai J. [Inhibitory Effect of Andrographolide on Angiogenesis Induced by the Supernatant From Cultured Tumor Cells]. *Zhong Nan Da Xue Xue Bao Yi Xue Ban* (2018) 43(8):821–5. doi: 10.11817/j.issn.1672-7347.2018.08.001
113. Liu H, Tang L, Li X, Li H. Triptolide Inhibits Vascular Endothelial Growth Factor-Mediated Angiogenesis in Human Breast Cancer Cells. *Exp Ther Med* (2018) 16(2):830–6. doi: 10.3892/etm.2018.6200
114. Saraswati S, Agrawal SS, Alhaider AA. Ursolic Acid Inhibits Tumor Angiogenesis and Induces Apoptosis Through Mitochondrial-Dependent Pathway in Ehrlich Ascites Carcinoma Tumor. *Chem Biol Interact* (2013) 206(2):153–65. doi: 10.1016/j.cbi.2013.09.004
115. Gupta SC, Prasad S, Sethumadhavan DR, Nair MS, Mo YY, Aggarwal BB. Nimbolide, a Limonoid Triterpene, Inhibits Growth of Human Colorectal Cancer Xenografts by Suppressing the Proinflammatory Microenvironment. *Clin Cancer Res* (2013) 19(16):4465–76. doi: 10.1158/1078-0432.CCR-13-0080
116. Nassar ZD, Aisha AF, Ahamed MB, Ismail Z, Abu-Salah KM, Alrokayan SA, et al. Antiangiogenic Properties of Koetjapic Acid, a Natural Triterpene Isolated From Sandoricum Koetjaoe Merr. *Cancer Cell Int* (2011) 11(1):12. doi: 10.1186/1475-2867-11-12
117. Agrawal SS, Saraswati S, Mathur R, Pandey M. Antitumor Properties of Boswellic Acid Against Ehrlich Ascites Cells Bearing Mouse. *Food Chem Toxicol* (2011) 49(9):1924–34. doi: 10.1016/j.fct.2011.04.007
118. Karna E, Szoka L, Palka JA. Betulinic Acid Inhibits the Expression of Hypoxia-Inducible Factor 1alpha and Vascular Endothelial Growth Factor in Human Endometrial Adenocarcinoma Cells. *Mol Cell Biochem* (2010) 340 (1-2):15–20. doi: 10.1007/s11010-010-0395-8
119. Zhou ZY, Zhao WR, Xiao Y, Zhou XM, Huang C, Shi WT, et al. Antiangiogenesis Effect of Timosaponin AIII on HUVECs *In Vitro* and Zebrafish Embryos *In Vivo*. *Acta Pharmacol Sin* (2020) 41(2):260–9. doi: 10.1038/s41401-019-0291-z
120. Zhao R, Sun L, Lin S, Bai X, Yu B, Yuan S, et al. The Saponin Monomer of Dwarf Lilyturf Tuber, DT-13, Inhibits Angiogenesis Under Hypoxia and Normoxia *via* Multi-Targeting Activity. *Oncol Rep* (2013) 29(4):1379–86. doi: 10.3892/or.2013.2272
121. Yang M, Zou J, Zhu H, Liu S, Wang H, Bai P, et al. Paris Saponin II Inhibits Human Ovarian Cancer Cell-Induced Angiogenesis by Modulating NF-kappaB Signaling. *Oncol Rep* (2015) 33(5):2190–8. doi: 10.3892/or.2015.3836

122. Meng L, Ji R, Dong X, Xu X, Xin Y, Jiang X. Antitumor Activity of Ginsenoside Rg3 in Melanoma Through Downregulation of the ERK and Akt Pathways. *Int J Oncol* (2019) 54(6):2069–79. doi: 10.3892/ijo.2019.4787
123. Kwak H, An H, Alam MB, Choi WS, Lee SY, Lee SH. Inhibition of Migration and Invasion in Melanoma Cells by Beta-Escin *via* the ERK/NF-kappaB Signaling Pathway. *Biol Pharm Bull* (2018) 41(10):1606–10. doi: 10.1248/bpb.b18-00251
124. Xu F, Cui WQ, Wei Y, Cui J, Qiu J, Hu LL, et al. Astragaloside IV Inhibits Lung Cancer Progression and Metastasis by Modulating Macrophage Polarization Through AMPK Signaling. *J Exp Clin Cancer Res* (2018) 37 (1):207. doi: 10.1186/s13046-018-0878-0
125. Li W, Tian YH, Liu Y, Wang Z, Tang S, Zhang J, et al. Platycodin D Exerts Anti-Tumor Efficacy in H22 Tumor-Bearing Mice *via* Improving Immune Function and Inducing Apoptosis. *J Toxicol Sci* (2016) 41(3):417–28. doi: 10.2131/jts.41.417
126. Soltani M, Parivar K, Baharara J, Kerachian MA, Asili J. Transcriptional Analysis of VEGF-D and TGFbeta Genes in MCF7 Cells Exposed to Saponin Isolated From Holothuria Leucospilota (Sea Cucumber). *Rep Biochem Mol Biol* (2015) 4(1):25–31.
127. Ahmad S, Ullah F, Ayaz M, Zeb A, Ullah F, Sadiq A. Antitumor and Anti-Angiogenic Potentials of Isolated Crude Saponins and Various Fractions of Rumex Hastatus D. Don. *Biol Res* (2016) 49:18. doi: 10.1186/s40659-016-0079-2
128. Dutta S, Mahalanobish S, Saha S, Ghosh S, Sil PC. Natural Products: An Upcoming Therapeutic Approach to Cancer. *Food Chem Toxicol* (2019) 128:240–55. doi: 10.1016/j.fct.2019.04.012
129. Zamora-Ros R, Béraud V, Franceschi S, Cayssials V, Tsilidis KK, Boutron-Ruault MC, et al. Consumption of Fruits, Vegetables and Fruit Juices and Differentiated Thyroid Carcinoma Risk in the European Prospective Investigation Into Cancer and Nutrition (EPIC) Study. *Int J Cancer* (2018) 142(3):449–59. doi: 10.1002/ijc.30880
130. Akter R, Afrose A, Rahman MR, Chowdhury R, Nirzhor SSR, Khan RI, et al. A Comprehensive Analysis Into the Therapeutic Application of Natural Products as SIRT6 Modulators in Alzheimer's Disease, Aging, Cancer, Inflammation, and Diabetes. *Int J Mol Sci* (2021) 22(8):4180–202. doi: 10.3390/ijms22084180

Conflict of Interest: The authors declare that the research was conducted in the absence of any commercial or financial relationships that could be construed as a potential conflict of interest.

Publisher's Note: All claims expressed in this article are solely those of the authors and do not necessarily represent those of their affiliated organizations, or those of the publisher, the editors and the reviewers. Any product that may be evaluated in this article, or claim that may be made by its manufacturer, is not guaranteed or endorsed by the publisher.

Copyright © 2021 Li, Song, Guo, Song, Duan and Chen. This is an open-access article distributed under the terms of the Creative Commons Attribution License (CC BY). The use, distribution or reproduction in other forums is permitted, provided the original author(s) and the copyright owner(s) are credited and that the original publication in this journal is cited, in accordance with accepted academic practice. No use, distribution or reproduction is permitted which does not comply with these terms.

frontiers in Pharmacology

ORIGINAL RESEARCH
published: 22 October 2021
doi: 10.3389/fphar.2021.761641

Safflower Polysaccharide Inhibits AOM/DSS-Induced Mice Colorectal Cancer Through the Regulation of Macrophage Polarization

Qun Wang[1†], Yun Huang[1†], Min Jia[2], Dong Lu[1], Hong-Wei Zhang[1], Dan Huang[3*], San-Hong Liu[1*] and Chao Lv[1*]*

[1]Institute of Interdisciplinary Integrative Medicine Research, Shanghai University of Traditional Chinese Medicine, Shanghai, China, [2]College of Pharmaceutical Sciences, Zhejiang Chinese Medical University, Hangzhou, China, [3]Department of Pathology, Fudan University Shanghai Cancer Center, Shanghai, China

OPEN ACCESS

Edited by:
Wei Peng,
Chengdu University of Traditional Chinese Medicine, China

Reviewed by:
Yan Binbin,
China Academy of Chinese Medical Sciences, China
Min Chen,
Southwest University, China

***Correspondence:**
Qun Wang
qunwang0523@163.com
Chao Lv
lvchaoanhui@163.com
San-Hong Liu
liush@shutcm.edu.cn
Dan Huang
Danhuang@shca.org.cn

[†]These authors have contributed equally to this work

Specialty section:
This article was submitted to Pharmacology of Anti-Cancer Drugs, a section of the journal Frontiers in Pharmacology

Received: 20 August 2021
Accepted: 16 September 2021
Published: 22 October 2021

Citation:
Wang Q, Huang Y, Jia M, Lu D, Zhang H-W, Huang D, Liu S-H and Lv C (2021) Safflower Polysaccharide Inhibits AOM/DSS-Induced Mice Colorectal Cancer Through the Regulation of Macrophage Polarization. Front. Pharmacol. 12:761641. doi: 10.3389/fphar.2021.761641

Safflower polysaccharide (SPS) is one of the active fractions extracted from safflower petals (*Carthamus tinctorius L.*) which has been reported to possess antitumor and immune control roles. However, its antitumor mechanisms by regulating the immune pathway remain barely understood. In this study, a mouse model was established by azoxymethane (AOM)/dextran sodium sulfate (DSS) to evaluate the antitumor effect of SPS on colorectal cancer (CRC). The results showed that 50 mg/kg SPS-1, an active fraction isolated from SPS, could significantly inhibit CRC induced by AOM/DSS and changed the polarization of macrophages to the M1 phenotype. Meanwhile, SPS-1 treatment significantly alleviated the characteristic AOM/DSS-induced pathological symptoms, in terms of decreasing the nucleoplasmic ratio, nuclear polarity extinction, and gland hyperplasia. However, the results *in vitro* showed that SPS-1 did not directly inhibit the growth of CRC cells but could upregulate the NF-κB signal and trigger M1 macrophage transformation. Thus, the condition medium (CM) of Mφ pretreated with SPS-1 was used against CRC cells. As expected, SPS-1–activated Raw 264.7 markedly exhibited antitumor effects by inhibiting cell proliferation and suppressing cell colony formation. In addition, SPS-1–activated Raw 264.7 could also induce CRC cell apoptosis by upregulating the levels of tumor necrosis factor-α (TNF-α) and nitric oxide (NO). Further results suggested that SPS-1–induced transition of the macrophage phenotype could be suppressed by an NF-κB inhibitor, PDTC. Moreover, SPS-1–activated Raw 264.7 inhibiting CRC cell proliferation and inducing apoptosis were also rescued by PDTC. Taken together, all results suggested that SPS-1 could be a therapeutic option for the prevention and treatment of CRC.

Keywords: safflower polysaccharide, colorectal cancer, apoptosis, macrophages, NF-κB

INTRODUCTION

Colorectal cancer (CRC) is the third most common malignant tumor in the world, with morbidity and mortality second to gastric and liver cancer, respectively (Li et al., 2013; Mármol et al., 2017). In 2020, there were 1.93 million new cases of colon cancer, and 935,173 people died of colorectal cancer–related diseases (Siegel.et al., 2020). According to previous reports, most CRC cases are closely associated with environmental factors including chemicals and dietary causing genetic

TABLE 1 | Primer sequences for qPCR analysis.

Gene name	Primer sequences
GAPDH	F: 5′-AACTTTGGCATTGTGGAAGG-3′ R: 5′-GGATGCAGGGATGTTCT-3′
IL-4	F: 5′-GAATGTACCAGGAGCCATATC-3′ R: 5′-CTCAGTACTACGAGTAATCCA-3′
IL-23	F: 5′-CAGCAGCTCTCTCGGAATCT-3′ R: 5′-TGGATACGGGGCACATTATT-3′
TNF-α	F: 5′-CGGTGCCTATGTCTCAGCCT-3′ R: 5′-GAGGGTCTGGGCCATAGAAC-3′
IL-6	F: 5′-TCGTGGAAATGAGAAAAGAGTTG-3′ R: 5′-AGTGCATCATCGTTGTTCATACA-3′

instabilities in intestinal cells, specific intestinal symbiont, and pathogen, and only about 20% of CRC cases exhibit familial hereditary properties (Jasperson et al., 2010; Valle, 2017; Jackson and Theiss, 2020). Epidemiological data also show that chronic intestinal inflammation is the most important underlying etiologies of carcinogenesis. The mechanism may be to cause defects in the host's antitumor immune system and promote the cancerous process (Jackson and Theiss, 2020).

The early signs of CRC are not obvious until abdominal pain and blood in the stool can be detected. Patients with advanced conditions like anemia and weight loss can only be treated with surgery (Ladabaum et al., 2020). In addition, the tolerance and toxicity of chemotherapeutics limit their clinical application (Kaufmann et al., 2019). Therefore, to prevent colitis-related CRC, the discovery and development of drugs with small side effects and low tolerability are the current priorities. When evaluating the effects of drug candidates on CRC, it is crucial to select a suitable tumor model of CRC. According to short formation time, tumor stability, and similar characteristics to human CRC, the AOM/DSS model is the most suitable for studying the occurrence and development of CRC (Tanaka et al., 2003; Venkatachalam et al., 2020).

Natural polysaccharides possess multiple therapeutic characteristics, including antitumor, anti-inflammation, and immunomodulation (Zhao et al., 2020). Currently, polysaccharide drugs including chondroitin sulfate, ginseng polysaccharide, and lentinan polysaccharide have been widely applied in cancer therapy (Wang et al., 2016; Zheng et al., 2020). Safflower polysaccharide (SPS), one of the active components of safflower, has antitumor and immune regulation effects (Ando et al., 2002). According to previous studies, SPS could significantly inhibit the invasion and migration of various tumor cells, such as gastric cancer and ovarian cancer (Cui et al., 2018). In this study, a polysaccharide fraction (SPS-1) was isolated from SPS; it exhibited no cytotoxicity to colon cancer cells within a dose range of 1–1,000 μg/ml but could induce macrophages to produce TNF-α and NO associated with M1-type macrophages. M1-type tumor-associated macrophages (TAM) can inhibit tumor growth in the microenvironment, while M2-type TAM can facilitate tumor cell survival, proliferation, invasion, angiogenesis, and immunosuppression (Li et al., 2021). Therefore, we explored the antitumor effect and potential mechanisms of SPS-1 on colorectal cancer cells by regulating the polarization of tumor-associated macrophages.

MATERIALS AND METHODS

Materials

Dextran sulfate sodium (DSS) and azoxymethane (AOM) were obtained from Yeasen Biotechnology Co., Ltd. (Shanghai, China). Antibodies of p-IκBα, p-p65, IκBα, p65, and GAPDH were purchased from Cell Signaling Technology (Danvers, MA, United States). Human TNF-α and the IL-6 ELISA kit were obtained from eBioscience (Vienna, Austria). Anti–CD16-PE, CD11c-FITC, CD11b-FITC, F4/80-PE, CD-3-APC, CD80-PE, and CD206-PE were obtained from eBioscience (Minneapolis, MN, United States). The Annexin V-FITC/PI apoptosis detection kit was obtained from BD Biosciences (San Jose, CA, United States). Calcein-AM/PI was acquired from Beyotime (Haimen, China). PDTC was purchased from MedchemExpress (Monmouth Junction, NJ, United States). Safflower polysaccharide (SPS) was obtained from Shanghai Yuanye Bio-Technology Co., Ltd. (Shanghai, China).

Cell Culture

The cell lines of HCT116, RKO, SW480, LoVo, MC38, and RAW 264.7 were obtained from Cell Bank of Shanghai Institute of Cell Biology, Chinese Academy of Sciences (SIBS, CAS). The RAW 264.7, LoVo, and MC38 cell lines were cultured in DMEM (Hyclone, Logan, UT, United States) with 10% FBS (Biological Industries, Cromwell, CT, United States). The HCT116 cell line was cultured in McCoy's 5A medium (Gibco, Carlsbad, CA, United States) supplemented with 10% FBS. The SW480 cell line was maintained in the L-15 medium (Gibco, Carlsbad, CA, United States) supplemented with 10% FBS. The RKO cell line was cultured in the MEM medium (Hyclone, Logan, UT, United States) with 10% FBS.

Detection of Cell Viability

The cell lines of HCT116, RKO, SW480, LoVo, MC38, and RAW 264.7 were planted into 96-well plates (1×10^4 cells/ml) containing different concentrations of SPS-1 or CM. After treatment for 48 h, the effect of SPS-1 on cell viability was measured by Cell Counting Kit-8 (CCK-8, Dojindo), according to the instructions.

Conditioned Medium Collection

The RAW 264.7 cells were treated with different concentrations of SPS-1 (100, 500, and 1,000 μg/ml, respectively) for 24 h, and then the supernatant was collected and filtered through a 0.22-μm filter. In addition, cells treated by LPS (50 ng/ml) and untreated RAW 264.7 cells were used as a positive control and a negative control, respectively.

Colony Formation Assay

For colony formation experiment, 1,000 cells (RKO and HCT116) were planted into a 12-well plate and cultured for 7 days in CM. Then cells were stained with Giemsa for colony counting.

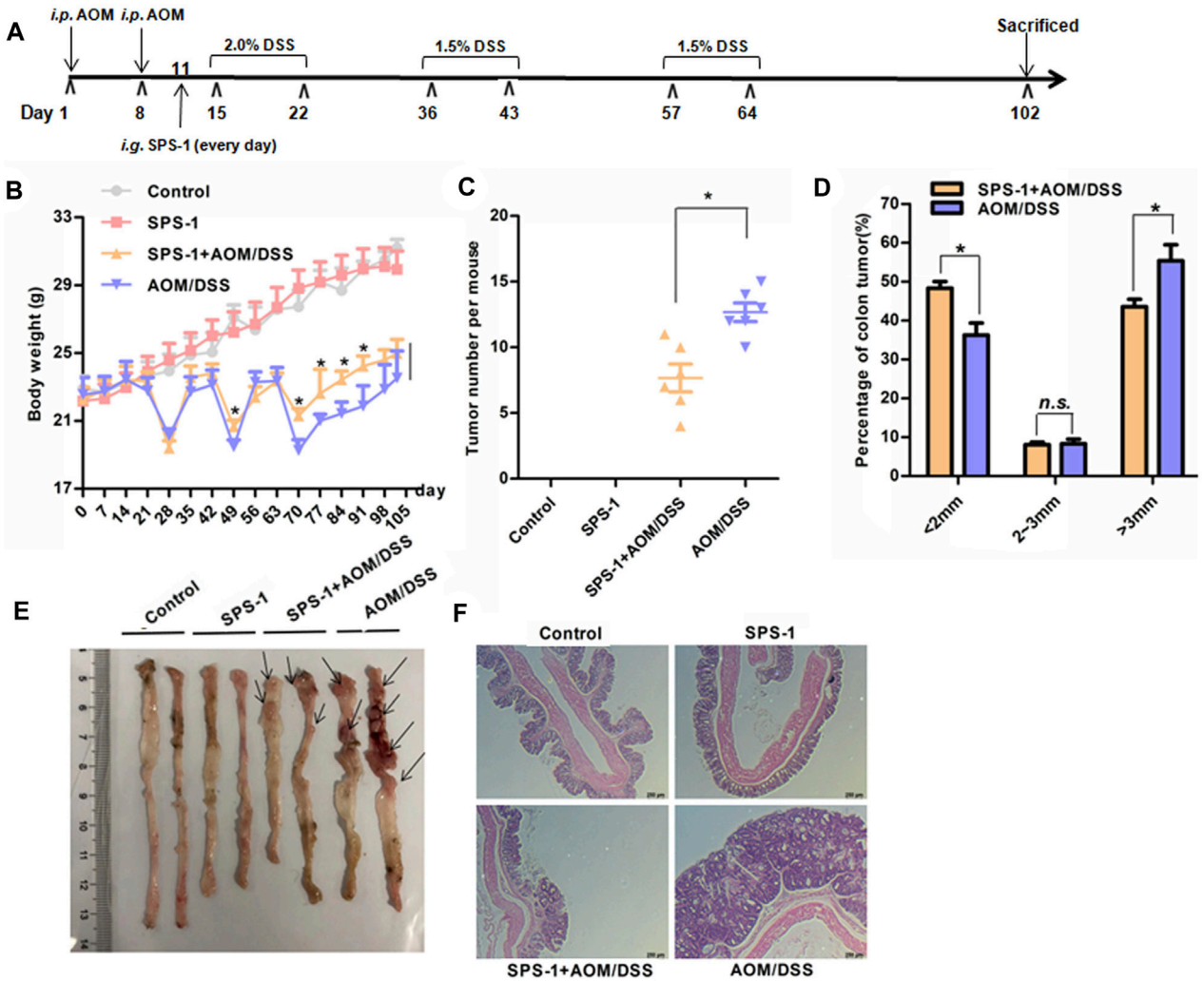


FIGURE 1 | Effects of SPS-1 on AOM/DSS-induced CRC in mice. **(A)** Schematic explanation of the experimental procedure for the AOM/DSS model. The mice body weight **(B)**, the total number **(C)**, and the size distributions of tumors **(D,E)** after 102 days induction. **(F)** Representative gross morphology of mice colon by H&E staining of colon tissues. Data are shown as mean ± SEM. * indicates $p < 0.05$ compared with the AOM/DSS group.

Nitrite Determination, IL-6, and TNF-α Assays

The production of nitric oxide (NO) was detected by using the Griess reaction. The RAW 264.7 cells were planted into 12-well plates (5×10^3 cells/ml) and treated with different concentrations of SPS-1 (100, 500, and 1,000 μg/ml, respectively) for 24 h. Then 50 μl of the culture supernatant was mixed with an equal volume of Griess reagent for 30 min at room temperature. The absorbance was measured by a microplate reader at 450 nm. The levels of IL-6 and TNF-α in RAW 264.7 cells in cell-free supernatant were detected by an ELISA assay kit, according to the instructions (Ebioscience).

Flow Cytometric Analysis

RAW 264.7 cells were treated with SPS-1 (100, 500, and 1,000 μg/ml, respectively) for 24 h, incubated with PE-labeled CD80, CD16, and CD206 in the dark for 15 min, washed twice with cold PBS, and resuspended with 300 μl PBS. In addition, RKO and HCT116 cells were planted into six-well plates (5×10^5 cells/ml) containing different concentrations of CM. The ratio of the conditioned medium to the normal medium is 3:1, and the medium is changed every 24 h. After 72 h of CM treatment, cells were collected and washed twice with PBS, and then cells were resuspended with 300 μl PBS in tubes. Propidium iodide (PI) or Annexin V was added to the tubes for 20 min according to the corresponding experiment. The result was detected by flow cytometry (BD Biosciences); each analysis was performed using 10,000 cells.

RNA Isolation and Quantitative Real-Time PCR Analysis

RAW 264.7 cells (2×10^6 cells/six-well plate) were treated with SPS-1 (100, 500, and 1,000 μg/ml, respectively) for 12 h. Total

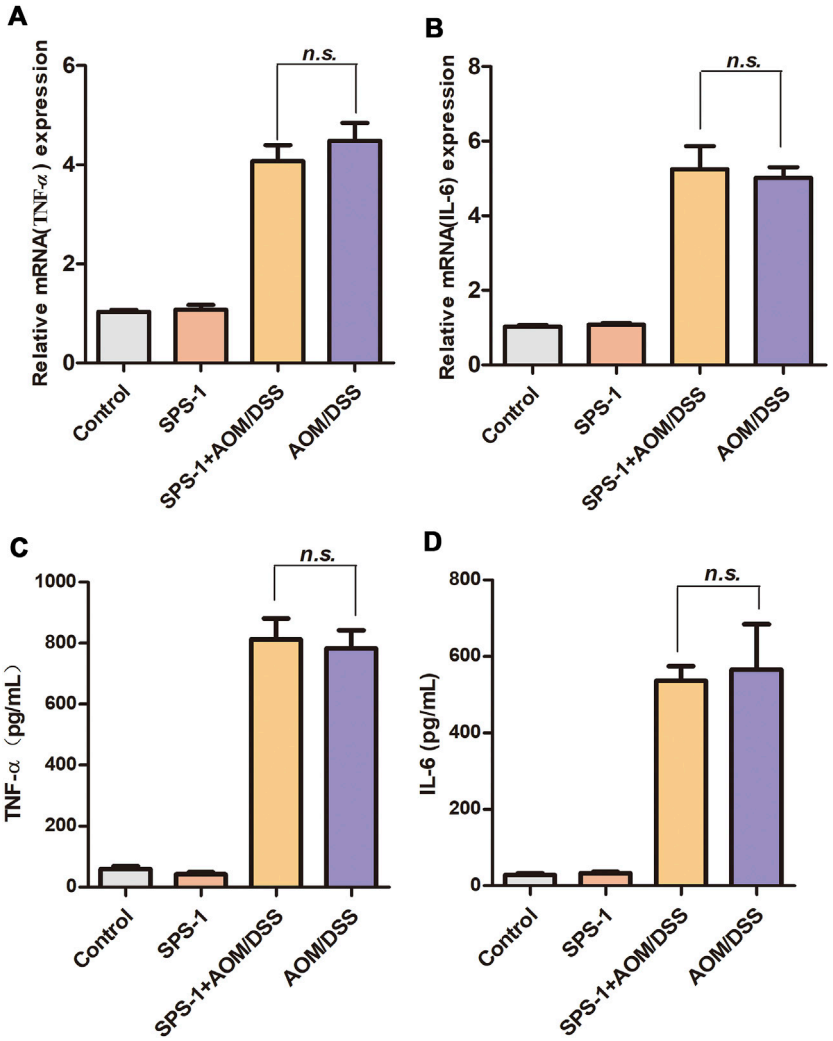


FIGURE 2 | Effect of SPS-1 on AOM/DSS-induced expression of cytokines in colon tissue and serum. **(A,B)** The colon tissue was collected after the experiment, and the mRNA levels of TNF-α and IL-6 were assessed by qRT-PCR. **(C,D)** Blood samples were taken on day 102, and serum levels of TNF-α and IL-6 were assayed by ELISA. Data are shown as mean ± SEM. *n.s.* indicates no significant difference compared with the AOM/DSS group.

TABLE 2 | Effects of SPS-1 on cell viability of colorectal cancer cells after 48 h treatment.

SPS-1 (μg/ml)	HCT116 (%)	SW480 (%)	LoVo (%)	RKO (%)	MC38 (%)
0	99.34 ± 1.54	109.12 ± 0.23	101.11 ± 0.34	88.29 ± 1.98	109.07 ± 1.09
100	100.23 ± 0.53	99.21 ± 1.19	99.34 ± 0.49	100.21 ± 2.01	100.12 ± 1.11
200	101.32 ± 2.20	89.99 ± 4.12	98.18 ± 0.02	99.13 ± 0.97	100.39 ± 0.44
400	109.12 ± 0.67	98.39 ± 0.91	99.89 ± 1.20	99.12 ± 2.99	99.54 ± 1.08
800	98.90 ± 1.98	98.86 ± 0.26	99.29 ± 1.22	98.14 ± 0.98	99.10 ± 0.98
1,000	99.87 ± 1.11	101.01 ± 0.30	100.80 ± 0.65	109.99 ± 1.11	100.32 ± 2.11

Each data point represents the mean ± SEM of independent three experiments.

RNA was isolated by RNAiso Plus (Takara, Dalian, China). RNA (1 μg) was reverse-transcribed using the PrimeScript RT Reagent Kit (Takara, Dalian, China). Quantitative RT-PCR was performed using a Roche LightCycler480, and the sequences of the primers are indicated in **Table 1**. Results were finally normalized to the level of GAPDH gene expression.

Animal Experiments

All mice were maintained in a pathogen-free facility, and all animal experiments were approved by the Committee on the Ethics of Animal Experiments of the Shanghai University of Traditional Chinese Medicine (SHUTCM). 6-week-old C57 mice were used in animal experiments. The mice were randomly and equally divided into four groups (n = 6):

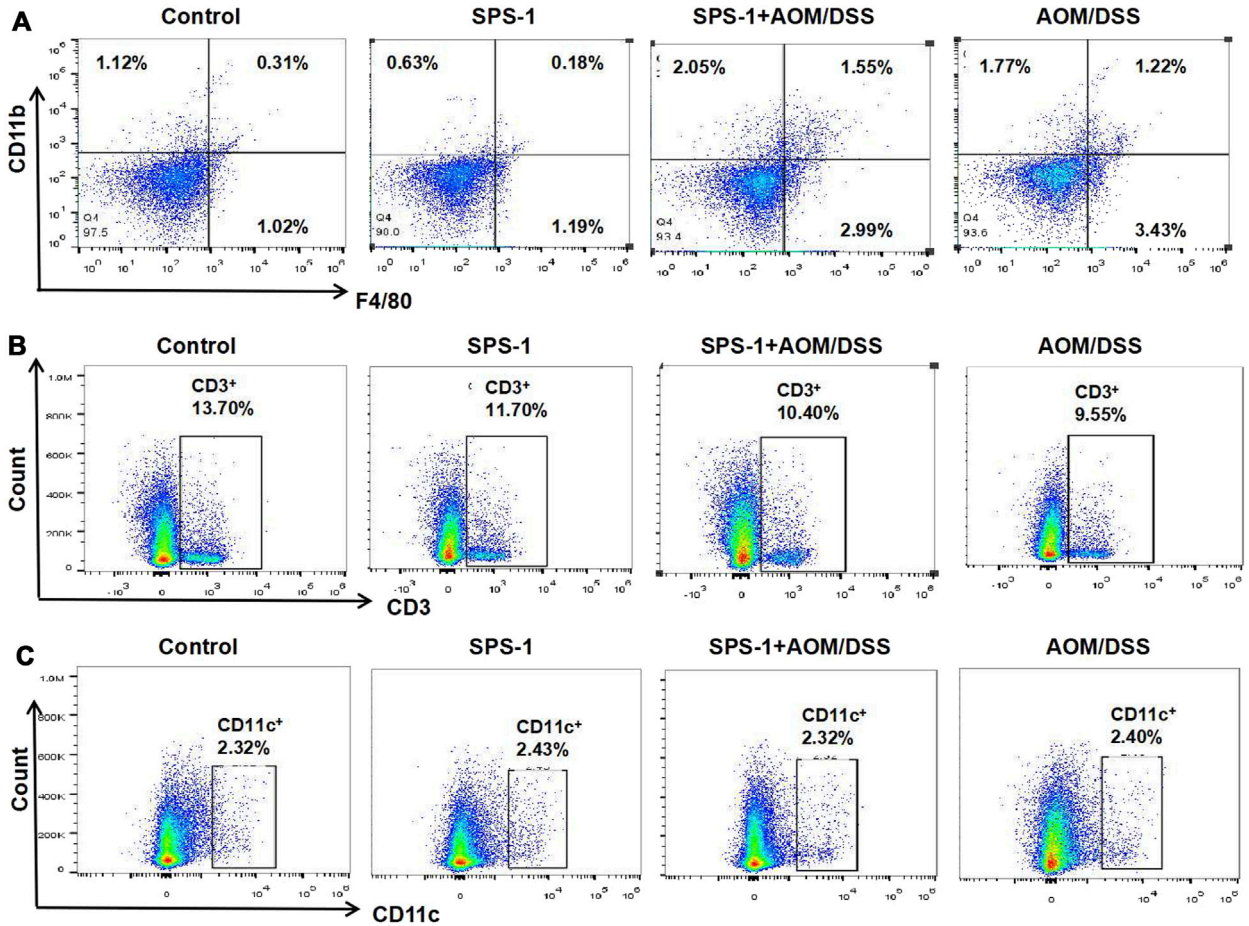


FIGURE 3 | Effect of SPS-1 on the number of **(A)** macrophage, **(B)** T Cells, and **(C)** dendritic cells (DC) in colon tissue of CRC mice. The cells obtained from colon tissue were incubated with different flow cytometric antibodies (CD11b, F4/80, CD3, and CD11c) and detected by flow cytometry.

control, SPS-1, AOM/DSS, and AOM/DSS+SPS-1. The AOM/DSS and AOM/DSS+SPS-1 groups were injected with 10 mg/kg of AOM intraperitoneally. Seven days after the AOM injection, the mice were given DSS in their drinking water for the third (2% DSS), sixth (1.5% DSS), and ninth (1.5% DSS) week. The same procedure was performed with intraperitoneal normal saline and drinking distilled water instead of the AOM/DSS treatment in the control and SPS-1 groups. The SPS-1 and AOM/DSS+SPS-1 groups were administered by a dosage of 50 mg/kg SPS-1 every day. Mice in AOM/DSS and control groups were treated by gavage equal volume of saline. All mice were sacrificed by cervical dislocation 102 days after the administration of SPS-1.

Western Blot

RAW 264.7 cells (2×10^6 cells/six-well plate) were treated with SPS (100, 500, and 1,000 μg/ml, respectively) for 30 min to activate the NF-κB signaling pathway. Cells were washed with PBS, and total cells were collected in 100 μl of a lysis buffer. The lysates were centrifuged for 15 min at 4°C, and the supernatant was collected. Proteins were subjected to 10% sodium dodecyl sulfate–polyacrylamide gel electrophoresis (SDS-PAGE) and then transferred to PVDF membranes. The membranes were incubated with primary antibodies at manufacturer's recommended dilutions at 4°C overnight, and secondary antibodies were added at the recommended dilutions and the incubation continued for another 1 h at room temperature. The protein bands were analyzed with an imaging system (Bio-Rad, United States).

Statistical Analysis

Statistical analysis was performed with an unpaired t-test when comparing two different groups or one-way ANOVA with Tukey's multiple comparison tests. The data are expressed as mean ± SEM. $p < 0.05$ was considered significant.

RESULTS

Safflower Polysaccharide-1 Suppressed Colorectal Cancer Formation and Growth in Azoxymethane/Dextran Sodium Sulfate-Induced Mice

SPS-1 is the major component of SPS, and its chemical properties such as the separation spectrum,

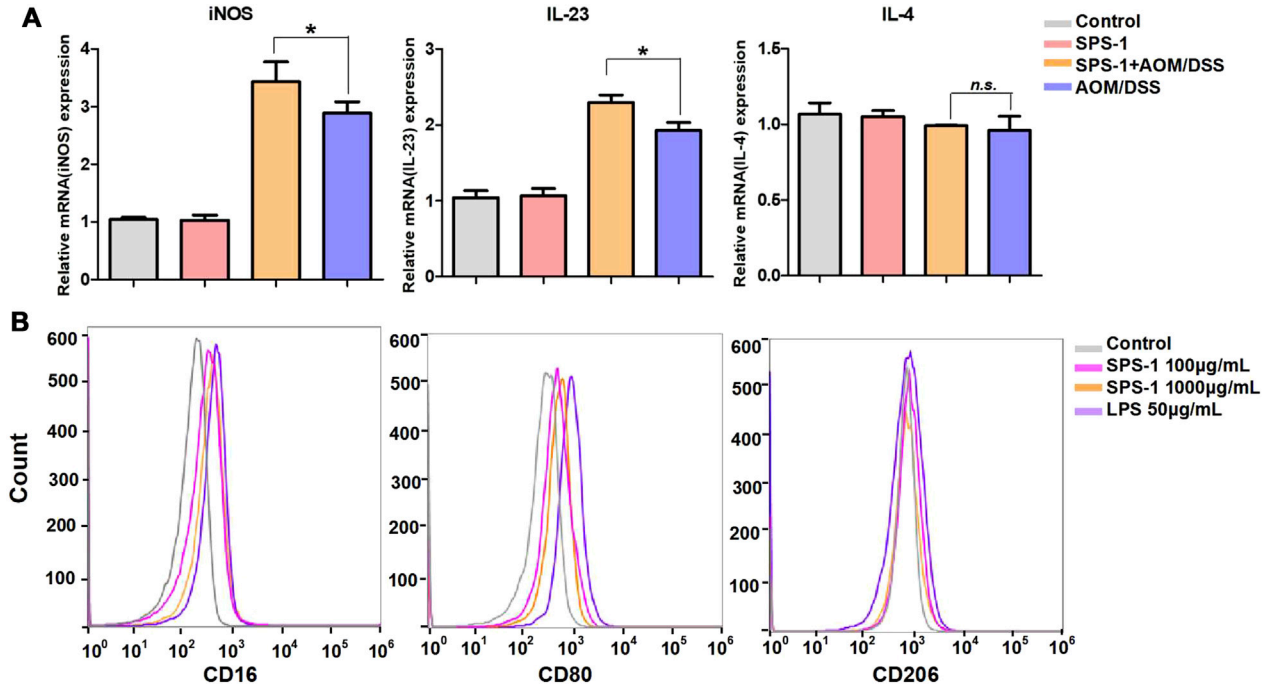


FIGURE 4 | Effect of SPS-1 on macrophage polarization *in vivo* and *in vitro*. **(A)** mRNA levels analysis of M1 markers iNOS, interleukin (IL)-23, and M2 markers IL-4 in colons tissue of the mice. **(B)** CD16, CD80, and CD206 expression on Raw 264.7 stimulated with SPS-1 was analyzed by flow cytometry. Data are shown as mean ± SEM. * indicate $p < 0.05$ compared with the AOM/DSS group.

monosaccharide composition, average molecular weight, and the infrared spectrum are provided in the supplementary materials (**Supplementary Figure S1–S4**). To study the antitumor activity of SPS-1, a mouse model was established by AOM/DSS as described previously (Angelou et al., 2018). As shown in **Figure 1A**, the mice were treated with SPS-1 at a dosage of 50 mg/kg/day *via* gavage. In the model group, we found that mice that freely drank DSS solution for seven consecutive days in the first, second and third cycles showed obvious body weight loss as compared to the control group. In contrast, a significant improvement in weight loss was observed in the SPS-1–treated AOM/DSS group, especially during the third cycle (**Figure 1B**). Next, we determined the occurrence of CRC in these mice by calculating the number and size distribution of tumors. As shown in **Figures 1C,E**, the number of tumors in the model group was more than those in the SPS-1–treated AOM/DSS group. Furthermore, the tumor diameters in the model group were mainly distributed > 3 mm (55.39 ± 3.29%), while the diameters in the SPS-1–treated AOM/DSS group were predominantly < 2 mm (55.31 ± 6.39%) (**Figures 1D,E**). There was no difference between the SPS-1–treated AOM/DSS group and the model group with a diameter of 2–3 mm (**Figures 1D,E**). Moreover, histologic examination showed that SPS-1 treatment significantly alleviated the characteristic AOM/DSS-induced pathological symptoms, in terms of an increased nucleoplasmic ratio, nuclear polarity extinction, and gland hyperplasia (**Figure 1F**). These results showed that SPS-1 could significantly reduce the AOM/DSS-induced tumor formation and growth in mice.

Safflower Polysaccharide-1 Inhibited the Occurrence of Colorectal Cancer Neither by Reducing Intestinal Inflammation nor by Killing Tumor Cells Directly

To investigate the underlying mechanisms of SPS-1 antitumor effects, qRT-PCR was used to detect the mRNA level of inflammatory cytokines in colon tissue. Compared with the control group, AOM/DSS treatment resulted in a significant increase in the mRNA levels of IL-6 and TNF-α. However, these inflammatory cytokines of the SPS-1–treated AOM/DSS group were not reduced as compared to the model group (**Figures 2A,B**). Consistent with the qRT-PCR results, there was also no difference in serum levels of IL-6 and TNF-α between the SPS-1–treated AOM/DSS and model groups (**Figures 2C,D**).

To further explore the underlying antitumor mechanisms of SPS-1, five types of CRC cells were selected to evaluate SPS-1 effects on proliferation. As shown in **Table 2**, there was no obvious cytotoxicity of SPS-1 (0–1,000 μg/ml) on HCT116, SW480, LoVo, RKO, and MC38 cells. These results showed that SPS-1 neither reduced intestinal inflammation nor directly killed tumor cells to inhibit the occurrence of CRC.

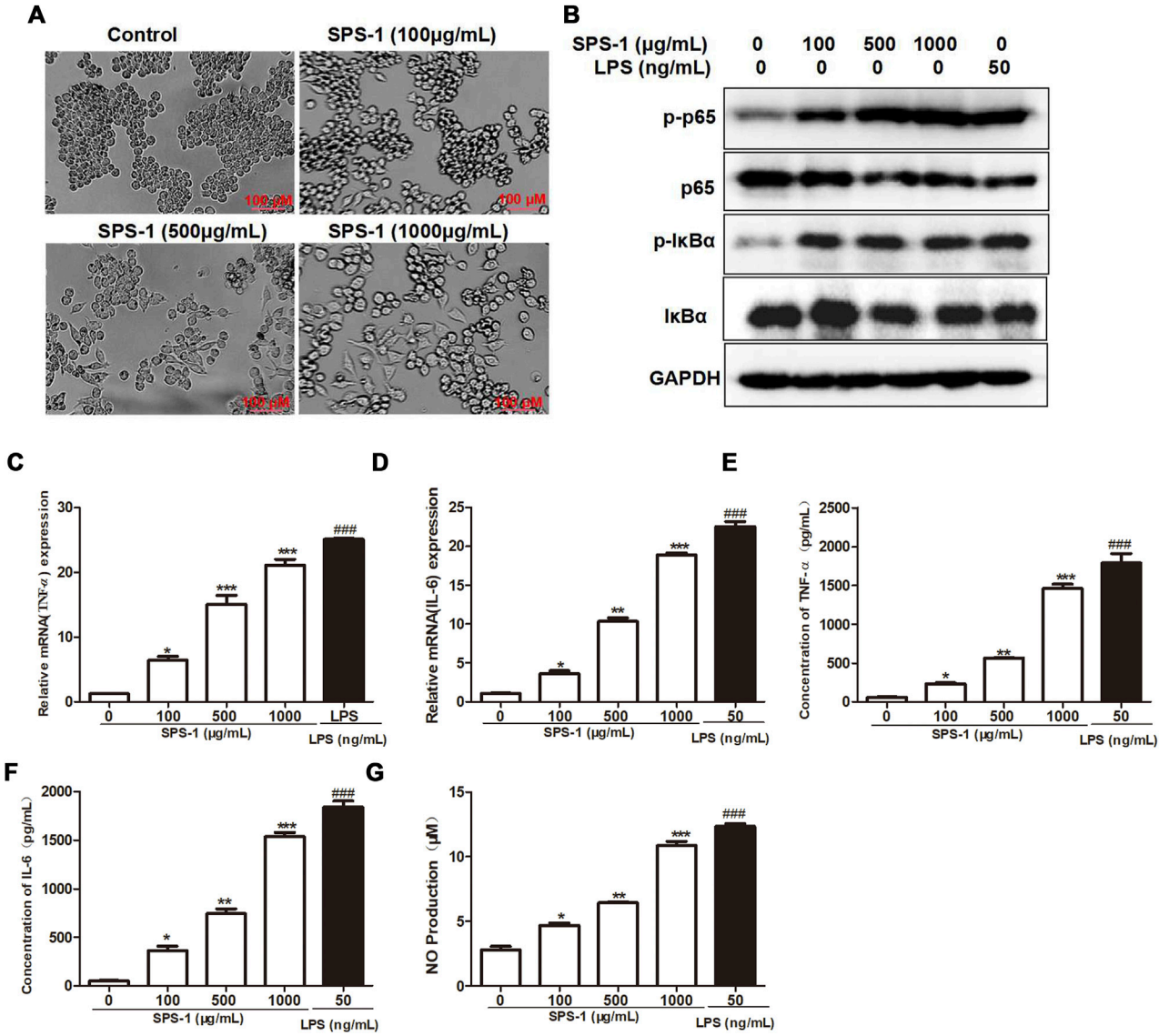


FIGURE 5 | SPS-1 activated macrophages to release TNF-α, IL-6, and NO through the NF-κB signaling pathway. **(A)** Morphology of RAW 264.7 after treatment with SPS-1. **(B)** The expression of IκBα, p-IκBα, p65, and p-p65 after being treated with SPS-1. The mRNA levels of TNF-α **(C)** and IL-6 **(D)** in RAW 264.7 after being treated with SPS-1. The levels of TNF-α **(E)**, IL-6 **(F)**, and NO **(G)** in RAW 264.7 after being treated with SPS-1. Data are shown as mean ± SEM. * indicate $p < 0.05$, ** and $^{\#\#}$ indicate $p < 0.01$, *** and $^{\#\#\#}$ indicate $p < 0.001$ compared with the control group.

Safflower Polysaccharide-1 Shifted Macrophage Polarization Toward the M1 Phenotype *In Vivo* and *In Vitro*

Based on the above results, we speculated that SPS-1 inhibited CRC by activating the immune system *in vivo*. In this study, the proportion of T cells, dendritic cells (DC), and macrophages in the CRC tissue was determined by flow cytometry. As shown in **Figure 3A**, macrophages (F480/CD11b) in the colon tissue of the model group were significantly higher than those in the control group. After SPS-1 treatment, the number of macrophages was further increased in the proportion from 1.22% to 1.55%. However, the T-cell levels in colon tissues of the model group and the SPS-1–treated AOM/DSS group were lower than those of the control group (**Figure 3B**). Also, the proportion of DC cells was not changed in the control group, the SPS-1 group, the AOM/DSS group, and the SPS-1–treated AOM/DSS group (**Figure 3C**). These results suggested that SPS-1 could selectively activate macrophages *in vivo*.

To describe the differential phenotype of macrophages, CRC tissues were isolated from mice and the expression of M1 and M2 markers was analyzed by real-time PCR. The results showed that the mRNA levels of M1 markers (iNOS and IL-23) were significantly upregulated after SPS-1 treatment, while the M2 marker (IL-4) was not changed (**Figure 4A**). To further study the relationship between SPS-1 treatment and macrophage

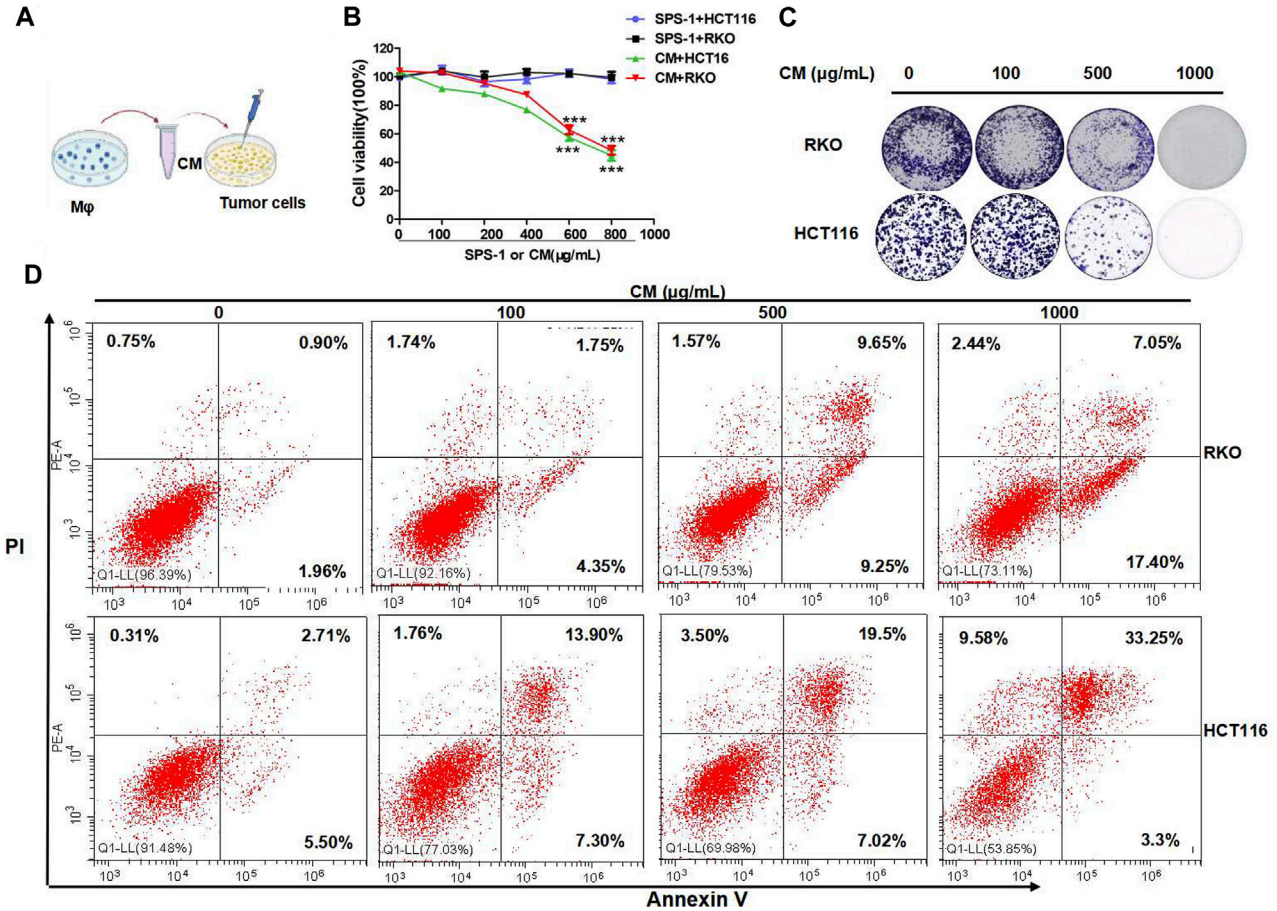


FIGURE 6 | SPS-1–activated Mφ inhibited colon cancer cells proliferation and induced apoptosis. **(A)** The condition medium (CM) of Mφ was pretreated with SPS-1. **(B)** CM of SPS-1–activated Mφ inhibited the growth of RKO and HCT116 cells in different concentrations. **(C)** The effect of SPS-1 or the condition medium (CM) on the proliferation of RKO and HCT116 cells. **(D)** The apoptosis induced by CM in RKO and HCT116 cells was analyzed by flow cytometry. *** and ###indicate $p < 0.001$ compared with the control group.

polarization, LPS was used to polarize Raw 264.7 cells into M1 type *in vitro*. As shown in **Figure 4B**, M1 marker genes (CD16 and CD80) were increased and M2 marker genes (CD206) remained unchanged after being treated by SPS-1. These results suggested that SPS-1 treatment could increase the propensity of Mφ polarizing to the M1 phenotype *in vivo* and *in vitro*.

Safflower Polysaccharide-1 Activated Macrophages to Release TNF-α, IL-6, and Nitric Oxide Through the NF-κB Signaling Pathway

The change in cell morphology is an important marker for macrophage activation (Sica and Mantovani, 2021). Bright field imaging results showed that the RAW 264.7 cells morphology was significantly changed after SPS-1 treatment, together with long protrusions and pseudopodia (**Figure 5A**). The activation of protein kinases such as IκBα and p65 has been proven to activate macrophages (Yang et al., 2019). To examine whether NF-κB signaling was involved in SPS-1–regulated cell activation, RAW 264.7 cells were treated with increasing concentrations of SPS-1, and then the phosphorylation levels of IκBα and p65 were analyzed. As shown in **Figure 5B**, SPS-1 could increase IκBα phosphorylation, as well as the phosphorylation of the p65 NF-κB subunit in RAW 264.7 in a concentration-dependent manner. Subsequently, we also tested the cytokines released by macrophages after the activation of SPS-1. As shown in **Figures 5C,D**, the mRNA levels of TNF-α and IL-6 were significantly increased after SPS-1 treatment. Meanwhile, ELISA results showed that the secretion of TNF-α and IL-6 was also significantly increased when RAW 264.7 was treated with SPS-1 (**Figures 5E,F**). In addition, the production NO by macrophages was also increased significantly in a concentration-dependent manner after SPS-1 treatment (**Figure 5G**). These results showed that SPS-1 activated macrophages to release TNF-α, IL-6, and NO through the NF-κB signaling pathway.

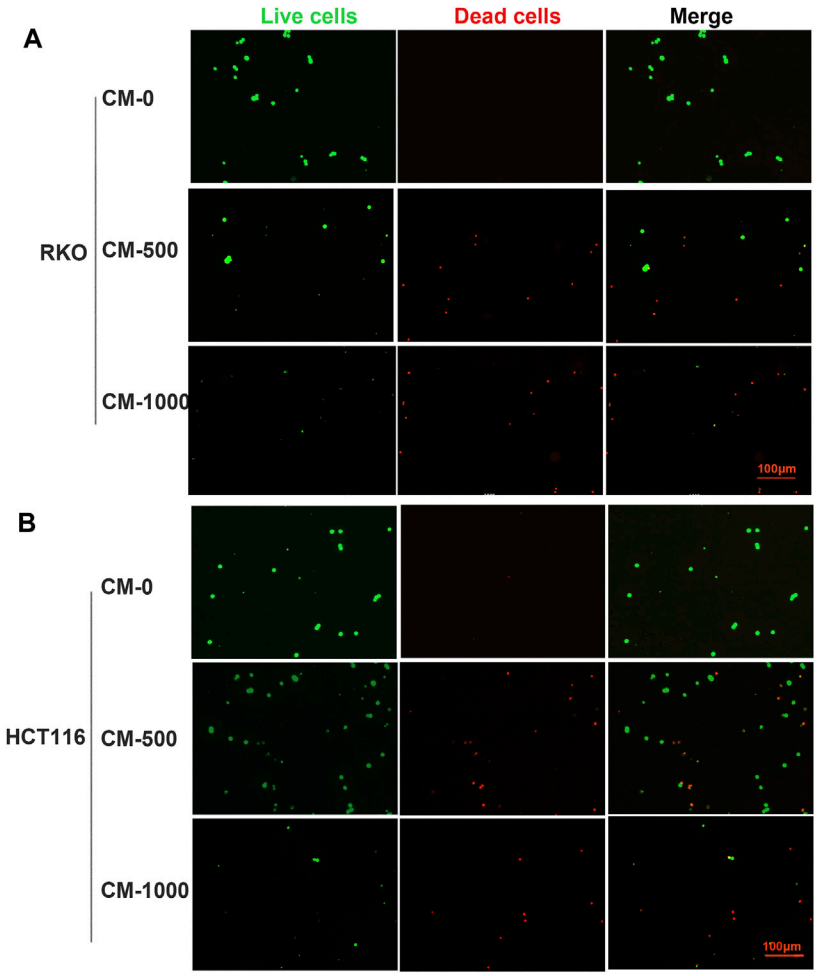


FIGURE 7 | Live/dead staining evaluated the effect of CM on CRC cells apoptosis. **(A)** RKO and **(B)** HCT116 were inoculated into six-well plates (5×10^5 cells/ml) containing different concentrations of CM for 72 h. Then, cells were stained with calcein-AM and PI after exposure to CM (100–1,000 μg/ml). Imaging was performed using a fluorescence tracing microscope.

Safflower Polysaccharide-1–Activated Mφ Inhibited Colorectal Cancer Cells Proliferation and Induced Apoptosis

To further study the antitumor activity of SPS-1–activated Mφ, the condition medium (CM) of Mφ pretreated with SPS-1 was established (**Figure 6A**). As shown in **Figure 6B**, the CM of Mφ pretreated with SPS-1 exhibited a significant inhibitory effect on the proliferation of RKO and HCT116 cells. Meanwhile, clonogenic survival of RKO and HCT116 cells after being treated with CM was measured by a colony-forming unit assay. The results showed that the colony-forming efficiency of RKO and HCT116 cells treated with CM of Mφ pretreated with SPS-1 was significantly inhibited (**Figure 6C**). Furthermore, the flow cytometry analysis to evaluate the role of CM of Mφ pretreated with SPS-1 in RKO and HCT116 cell apoptosis was performed. As shown in **Figure 6D**, the apoptotic rates of RKO and HCT116 cells were significantly increased in a concentration-dependent manner of SPS-1. Moreover, the effect of CM of Mφ pretreated with SPS-1 on CRC cells apoptosis was also determined with live/dead staining. The results showed that the numbers of live cells stained with calcein-AM were markedly decreased and dead cells with red fluorescence were significantly increased in RKO and HCT116 cells after treatment with CM (**Figures 7A,B**).

Safflower Polysaccharide-1–Activated Mφ Induced Colorectal Cancer Cells Apoptosis Through the NF-κB Signaling Pathway

To further evaluate whether SPS-1 activated macrophages through the NF-κB signaling pathway, the NF-κB inhibitor (PDTC) was used to block the NF-κB pathway in macrophages. As shown in **Figures 8A,B**, PDTC treatment reversed the effects of SPS-1 on the release of TNF-α and NO, and reduced the expression of CD16 and CD80 (**Figures 8C,D**). Furthermore, CCK-8 experiments demonstrated that PDTC

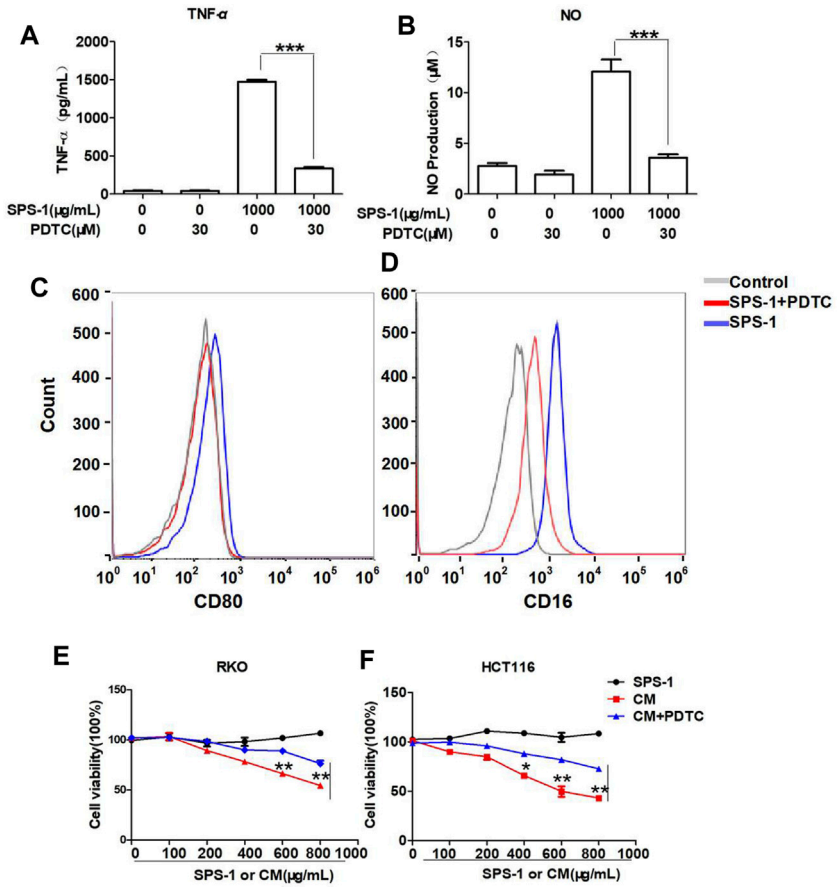


FIGURE 8 | SPS-1 activated Mφ through the NF-κB signaling pathway inhibited CRC cells proliferation. RAW 264.7 cells were preincubated with or without PDTC (30 μM) for 1 h and then treated with 1,000 μg/ml of SPS-1. RNA expression of TNF-α **(A)** was tested by qRT-PCR, and the production of NO by RAW 264.7 cells was detected by the NO kit. The expression of CD80 **(C)** and CD16 **(D)** was analyzed by flow cytometry. Next, the effect of SPS-1, CM, and CM+PDTC on the proliferation of RKO **(E)** and HCT116 **(F)** cells was measured by the Cell Counting Kit-8. Data are shown as mean ± SEM. **indicate $p < 0.01$, ***indicate $p < 0.001$ compared with the SPS-1+PDTC group.

could significantly reduce the inhibitory effect of CM on RKO and HCT116 cells in a concentration-dependent manner (**Figures 8E,F**). In addition, live/dead staining results showed that the antitumor effect of CM could be significantly reversed after pretreatment of macrophages with PDTC (**Figures 9A,B**). These results suggested that SPS-1–activated Mφ inhibited CRC cells proliferation and induced apoptosis mainly through the NF-κB signaling pathway.

DISCUSSION

In this study, we found that SPS-1, an active fraction extracted from SPS, could significantly inhibit AOM/DSS-induced CRC *in vivo*. The repeated AOM challenges resulted in increasing levels of IL-6 and TNF-α in serum and intestinal tissue, which contributes to AOM/DSS-induced CRC (Wang et al., 2019). However, the expression of these pro-inflammatory factors was not significantly reduced by SPS-1 treatment, indicating that SPS-1 did not prevent the occurrence of CRC through relieving inflammation. The tumor microenvironment is essential for tumorigenesis and development. When detecting the number of immune cells in CRC tissue induced by AOM/DSS, it was found that only the proportion of macrophages increased significantly. Therefore, we speculated that SPS-1 activation of macrophages is the main way against AOM/DSS-induced CRC.

Macrophages play important roles in the tumor immune microenvironment due to their heterogeneity and plasticity and can be polarized when affected by external microenvironmental factors (Pan et al., 2020). The blood vessel nutrition and oxygen supply in tumor tissue are insufficient during tumor growth, which leads to increased secretion of lactic acid and TGF-β and induces macrophages to differentiate into M2-type (Zhou et al., 2017). Therefore, macrophages in tumor tissues are generally M2-type and contribute to tumor proliferation, invasion, and metastasis (Katoh, 2016). However, in CRC model mice, modulating the differentiation of macrophages to M1 type could effectively inhibit tumor growth and metastasis (Chen et al., 2019). Thus, the regulation of the macrophage differentiation phenotype is one

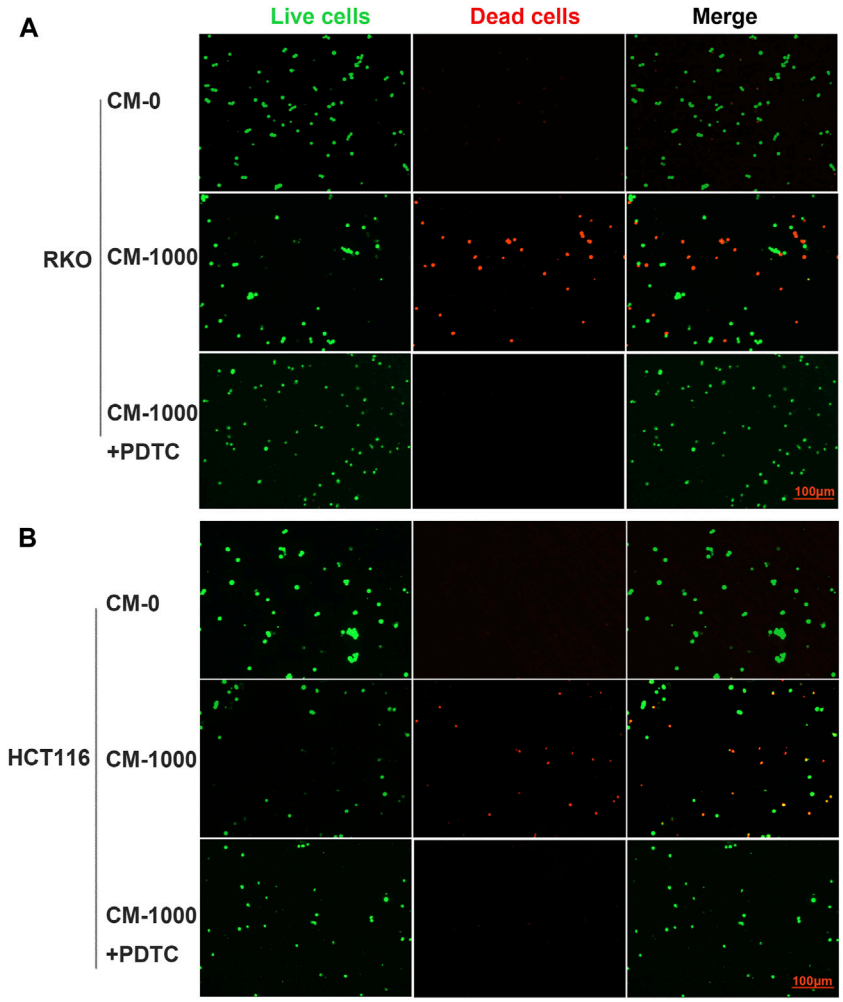


FIGURE 9 | Live/dead staining evaluated the effect of CM or CM+PDTC on CRC cells apoptosis. PDTC was used to block the NF-κB pathway in macrophages and collected the condition medium (CM) of Mφ pretreated with SPS-1 or SPS-1+PDTC. **(A)** RKO and **(B)** HCT116 were inoculated into six-well plates (5×10^5 cells/ml) containing different concentrations of CM. Then cells were stained with calcein-AM and PI after exposure to CM (100–1,000 μg/ml). Imaging was performed using a fluorescence tracing microscope.

of the important research directions of CRC immunotherapy. In this research, we found that the morphology of the macrophage could be changed and induced to be of M1-type after 24 h of treatment with SPS-1, and the expression of M1-related genes was also significantly upregulated. Consistent with the *in vivo* results, *in vitro* results also demonstrated that SPS-1 could induce the polarization of macrophages to M1-type. In general, cytokines and chemokines are primary regulators of immune defense and some cytokines produced by macrophages are mediators of tumor cytotoxicity (Najafi et al., 2019). TNF-α, which is produced mainly by activated macrophages/monocytes, has the broadest activity (Cruceriu et al., 2020). Besides, NO is a kind of free radical gas, as one of the smallest and simplest biologically active molecules in nature, which can effectively inhibit the growth of tumor cells and induce apoptosis (Balkwill., 2019). The current research results showed that SPS-1 could activate macrophages with the increase of NO and TNF-α but it cannot directly induce tumor cell apoptosis. Encouragingly, SPS-1–mediated CM significantly inhibited the proliferation of cancer cells and induced apoptosis in a dose-dependent manner. These results indicated that SPS-1–activated Mφ possessed markedly antitumor activity on CRC cells.

Activation of the NF-κB signaling pathway is closely related to the polarization of macrophages (Sica and Mantovani, 2012). As previous studies, some Chinese medicines and their extracts regulate the phenotype polarization of macrophages *via* this pathway (Wang.et al., 2015). In this study, the SPS-1 could activate macrophages through the NF-κB signaling pathway. Subsequently, when macrophages were treated with the NF-κB inhibitor, PDTC, M1 polarization induced by SPS-1 was significantly inhibited. In addition, the effect of CM on tumor proliferation and apoptosis was also reversed. These results suggested that SPS-1 induced the M1-type polarization of

macrophages by activating the NF-κB signaling pathway, thus exhibiting antitumor activity.

In summary, SPS-1 exhibited tumor suppressive effect by activating macrophages and inducing them to M1-type polarization through the NF-κB signaling pathway. This finding provided a new insight for the development of clinical strategies for CRC immunotherapy, which could be used alone or in combination with chemotherapy drugs to prevent the development of CRC and improve the survival of patients.

DATA AVAILABILITY STATEMENT

The datasets presented in this study can be found in online repositories. The names of the repository/repositories and accession number(s) can be found in the article/ **Supplementary Material**.

ETHICS STATEMENT

The animal study was reviewed and approved by the Committee on the Ethics of Animal Experiments of the Shanghai University of Traditional Chinese Medicine (SHUTCM).

AUTHOR CONTRIBUTIONS

CL, SL, and DH contributed to the conception and design of the experiment. QW and YH performed experiments. HZ and DL performed the statistical analysis. QW and MJ wrote the manuscript.

FUNDING

This study w supported by grants from the China Postdoctoral Science Foundation (2021M692154); Shanghai Natural Science Foundation (19ZR1410200); National Natural Science Foundation of China (81903510); National Major Project of China (2019ZX09201004-003-010); and Opening Project of Zhejiang Provincial Preponderant and Characteristic Subject of Key University (Traditional Chinese Pharmacology), Zhejiang Chinese Medical University (No. ZYAOX2018018).

SUPPLEMENTARY MATERIAL

The Supplementary Material for this article can be found online at: https://www.frontiersin.org/articles/10.3389/fphar.2021.761641/full#supplementary-material

REFERENCES

Ando, I., Tsukumo, Y., Wakabayashi, T., Akashi, S., Miyake, K., Kataoka, T., et al. (2002). Safflower Polysaccharides Activate the Transcription Factor NF-Kappa B via Toll-like Receptor 4 and Induce Cytokine Production by Macrophages. *Int. Immunopharmacol* 2 (8), 1155–1162. doi:10.1016/s1567-5769(02)00076-0

Angelou, A., Andreatos, N., Antoniou, E., Zacharioudaki, A., Theodoropoulos, G., Damaskos, C., et al. (2018). A Novel Modification of the AOM/DSS Model for Inducing Intestinal Adenomas in Mice. *Anticancer Res.* 38 (6), 3467–3470. doi:10.21873/anticanres.12616

Balkwill, F. (2019). Tumour Necrosis Factor and Cancer. *Nat. Rev. Cancer* 9 (5), 361–371. doi:10.1038/nrc2628

Chen, L., Zhou, L., Wang, C., Han, Y., Lu, Y., Liu, J., et al. (2019). Tumor-Targeted Drug and CpG Delivery System for Phototherapy and Docetaxel-Enhanced Immunotherapy with Polarization toward M1-type Macrophages on Triple Negative Breast Cancers. *Adv. Mater.* 31 (52). doi:10.1002/adma.201904997e1904997

Cruceriu, D., Baldasici, O., Balacescu, O., and Berindan-Neagoe, I. (2020). The Dual Role of Tumor Necrosis Factor-Alpha (TNF-α) in Breast Cancer: Molecular Insights and Therapeutic Approaches. *Cel Oncol (Dordr)* 43 (1), 1–18. doi:10.1007/s13402-019-00489-1

Cui, D., Zhao, D., Wang, B., Liu, B., Yang, L., Xie, H., et al. (2018). Safflower (Carthamus tinctorius L.) Polysaccharide Attenuates Cellular Apoptosis in Steroid-Induced Avascular Necrosis of Femoral Head by Targeting Caspase-3-dependent Signaling Pathway. *Int. J. Biol. Macromol* 116, 106–112. doi:10.1016/j.ijbiomac.2018.04.181

Jackson, D. N., and Theiss, A. L. (2020). Gut Bacteria Signaling to Mitochondria in Intestinal Inflammation and Cancer. *Gut Microbes* 11 (3), 285–304. doi:10.1080/19490976.2019.1592421

Jasperson, K. W., Tuohy, T. M., Neklason, D. W., and Burt, R. W. (2010). Hereditary and Familial colon Cancer. *Gastroenterology* 138 (6), 2044–2058. doi:10.1053/j.gastro.2010.01.054

Katoh, M. (2016). FGFR Inhibitors: Effects on Cancer Cells, Tumor Microenvironment and Whole-Body Homeostasis (Review). *Int. J. Mol. Med.* 38 (1), 3–15. doi:10.3892/ijmm.2016.2620

Kaufmann-Molnàr, I., Hofmann Checchini, H., and Fringer, A. (2019). Chemotherapeutic Side Effects in colon Cancer. A Qualitative Study from the point of View of Those Affected. *Pflege* 32 (3), 129–136. doi:10.1024/1012-5302/a000676

Ladabaum, U., Dominitz, J. A., Kahi, C., and Schoen, R. E. (2020). Strategies for Colorectal Cancer Screening. *Gastroenterology* 158 (2), 418–432. doi:10.1053/j.gastro.2019.06.043

Li, H., Somiya, M., and Kuroda, S. (2021). Enhancing Antibody-dependent Cellular Phagocytosis by Re-education of Tumor-Associated Macrophages with Resiquimod-Encapsulated Liposomes. *Biomaterials* 268, 120601. doi:10.1016/j.biomaterials.2020.120601

Li, J., Yuan, Y., Yang, F., Wang, Y., Zhu, X., Wang, Z., et al. (2013). Expert Consensus on Multidisciplinary Therapy of Colorectal Cancer with Lung Metastases (2019 Edition). *J. Hematol. Oncol.* 12 (1), 16. doi:10.1186/s13045-019-0702-0

Mármol, I., Sánchez-de-Diego, C., Pradilla Dieste, A., Cerrada, E., and Rodriguez Yoldi, M. J. (2017). Colorectal Carcinoma: A General Overview and Future Perspectives in Colorectal Cancer. *Int. J. Mol. Sci.* 18 (1), 197. doi:10.3390/ijms18010197

Miller, K. D., Fidler-Benaoudia, M., Keegan, T. H., Hipp, H. S., Jemal, A., and Siegel, R. L. (2020). Cancer Statistics for Adolescents and Young Adults, 2020. *CA Cancer J. Clin.* 70 (1), 443–459. doi:10.3322/caac.21637

Najafi, M., Hashemi Goradel, N., Farhood, B., Salehi, E., Nashtaei, M. S., Khanlarkhani, N., et al. (2019). Macrophage Polarity in Cancer: A Review. *J. Cel Biochem* 120 (3), 2756–2765. doi:10.1002/jcb.27646

Pan, Y., Yu, Y., Wang, X., and Zhang, T. (2020). Tumor-Associated Macrophages in Tumor Immunity. *Front. Immunol.* 11 (11), 583084. doi:10.3389/fimmu.2020.583084

Sica, A., and Mantovani, A. (2012). Macrophage Plasticity and Polarization: *In Vivo* Veritas. *J. Clin. Invest.* 122 (3), 787–795. doi:10.1172/JCI59643

Song, M., Chan, A. T., and Sun, J. (2020). Influence of the Gut Microbiome, Diet, and Environment on Risk of Colorectal Cancer. *Gastroenterology* 158 (2), 322–340. doi:10.1053/j.gastro.2019.06.048

Tanaka, T., Kohno, H., Suzuki, R., Yamada, Y., Sugie, S., and Mori, H. (2003). A Novel Inflammation-Related Mouse colon Carcinogenesis Model Induced by Azoxymethane and Dextran Sodium Sulfate. *Cancer Sci.* 94 (11), 965–973. doi:10.1111/j.1349-7006

Valle, L. (2017). Recent Discoveries in the Genetics of Familial Colorectal Cancer and Polyposis. *Clin. Gastroenterol. Hepatol.* 15 (6), 809–819. doi:10.1016/j.cgh.2016.09.148

Venkatachalam, K., Vinayagam, R., Arokia Vijaya Anand, M., Isa, N. M., and Ponnaiyan, R. (2020). Biochemical and Molecular Aspects of 1,2-dimethylhydrazine (DMH)-induced colon Carcinogenesis: a Review. *Toxicol. Res. (Camb)* 9 (1), 2–18. doi:10.1093/toxres/tfaa004

Wang, C. C., Cui, L., Zhang, Z. H., Feng, L., Liu, D., Jia, X. B., et al. (2016). [Research Thoughts on Tumor Immune Responses by Polysaccharide of Chinese Medicine via Oral Administration]. *Zhongguo Zhong Yao Za Zhi* 41 (10), 1965–1971. doi:10.4268/cjcmm20161034

Wang, S. Q., Cui, S. X., and Qu, X. J. (2019). Metformin Inhibited Colitis and Colitis-Associated Cancer (CAC) through Protecting Mitochondrial Structures of Colorectal Epithelial Cells in Mice. *Cancer Biol. Ther.* 20 (3), 338–348. doi:10.1080/15384047.2018.1529108

Wang, Y. L., Bian, K., and Zhang, D. D. (2015). [Advance in Studies on Regulatory Mechanism of Phenotype Polarization of Macrophages and Intervention with Traditional Chinese Medicines]. *Zhongguo Zhong Yao Za Zhi* 40 (2), 180–184. doi:10.4268/cjcmm20150204

Yang, Y., Chen, J., Lei, L., Li, F., Tang, Y., Yuan, Y., et al. (2019). Acetylation of Polysaccharide from Morchella Angusticeps peck Enhances its Immune Activation and Anti-inflammatory Activities in Macrophage RAW264.7 cells. *Food Chem. Toxicol.* 125, 38–45. doi:10.1016/j.fct10.1016/j.fct.2018.12.036

Zhao, Y., Yan, B., Wang, Z., Li, M., and Zhao, W. (2020). Natural Polysaccharides with Immunomodulatory Activities. *Mini Rev. Med. Chem.* 20 (2), 96–106. doi:10.2174/1389557519666190913151632

Zheng, Y., Ren, W., Zhang, L., Zhang, Y., Liu, D., and Liu, Y. (2020). A Review of the Pharmacological Action of Astragalus Polysaccharide. *Front. Pharmacol.* 11 (11), 349. doi:10.3389/fphar.2020.00349

Zhou, Q., Xian, M., Xiang, S., Xiang, D., Shao, X., Wang, J., et al. (2017). All-Trans Retinoic Acid Prevents Osteosarcoma Metastasis by Inhibiting M2 Polarization of Tumor-Associated Macrophages. *Cancer Immunol. Res.* 5 (7), 547–559. doi:10.1158/2326-6066.CIR-16-0259

Conflict of Interest: The authors declare that the research was conducted in the absence of any commercial or financial relationships that could be construed as a potential conflict of interest.

Publisher's Note: All claims expressed in this article are solely those of the authors and do not necessarily represent those of their affiliated organizations, or those of the publisher, the editors, and the reviewers. Any product that may be evaluated in this article, or claim that may be made by its manufacturer, is not guaranteed or endorsed by the publisher.

Copyright © 2021 Wang, Huang, Jia, Lu, Zhang, Huang, Liu and Lv. This is an open-access article distributed under the terms of the Creative Commons Attribution License (CC BY). The use, distribution or reproduction in other forums is permitted, provided the original author(s) and the copyright owner(s) are credited and that the original publication in this journal is cited, in accordance with accepted academic practice. No use, distribution or reproduction is permitted which does not comply with these terms.

frontiers in Pharmacology

ORIGINAL RESEARCH
published: 27 October 2021
doi: 10.3389/fphar.2021.729367

ROS/JNK/C-Jun Pathway is Involved in Chaetocin Induced Colorectal Cancer Cells Apoptosis and Macrophage Phagocytosis Enhancement

Huihui Wang[1,2†], Chuangyu Wen[2,3†], Siyu Chen[4†], Weiqian Li[2], Qiyuan Qin[2], Lu He[2], Fang Wang[2], Junxiong Chen[1,2], Weibiao Ye[5], Wende Li[4], Junsheng Peng[2,6], Xiangling Yang[1,2] and Huanliang Liu[1,2]**

[1]Department of Clinical Laboratory, The Sixth Affiliated Hospital, Sun Yat-sen University, Guangzhou, China, [2]Guangdong Provincial Key Laboratory of Colorectal and Pelvic Floor Diseases, Guangdong Institute of Gastroenterology, The Sixth Affiliated Hospital, Sun Yat-sen University, Guangzhou, China, [3]Department of Obstetrics and Gynecology, Affiliated Dongguan Hospital, Southern Medical University, Dongguan, China, [4]Guangdong Laboratory Animals Monitoring Institute, Guangdong Key Laboratory Animal Lab, Guangzhou, China, [5]Department of Pathology, Affiliated Dongguan Hospital, Southern Medical University, Dongguan, China, [6]Department of Gastrointestinal Surgery, The Sixth Affiliated Hospital, Sun Yat-sen University, Guangzhou, China

OPEN ACCESS

Edited by:
Wei Peng,
Chengdu University of Traditional Chinese Medicine, China

Reviewed by:
Feng Wang,
Affiliated Hospital of Nantong University, China
Qing Zhang,
Chengdu University of Traditional Chinese Medicine, China

***Correspondence:**
Huanliang Liu
liuhuanl@mail.sysu.edu.cn
Xiangling Yang
yangxl28@mail.sysu.edu.cn

†These authors have contributed equally to this work.

Specialty section:
This article was submitted to Pharmacology of Anti-Cancer Drugs, a section of the journal Frontiers in Pharmacology

Received: 23 June 2021
Accepted: 11 October 2021
Published: 27 October 2021

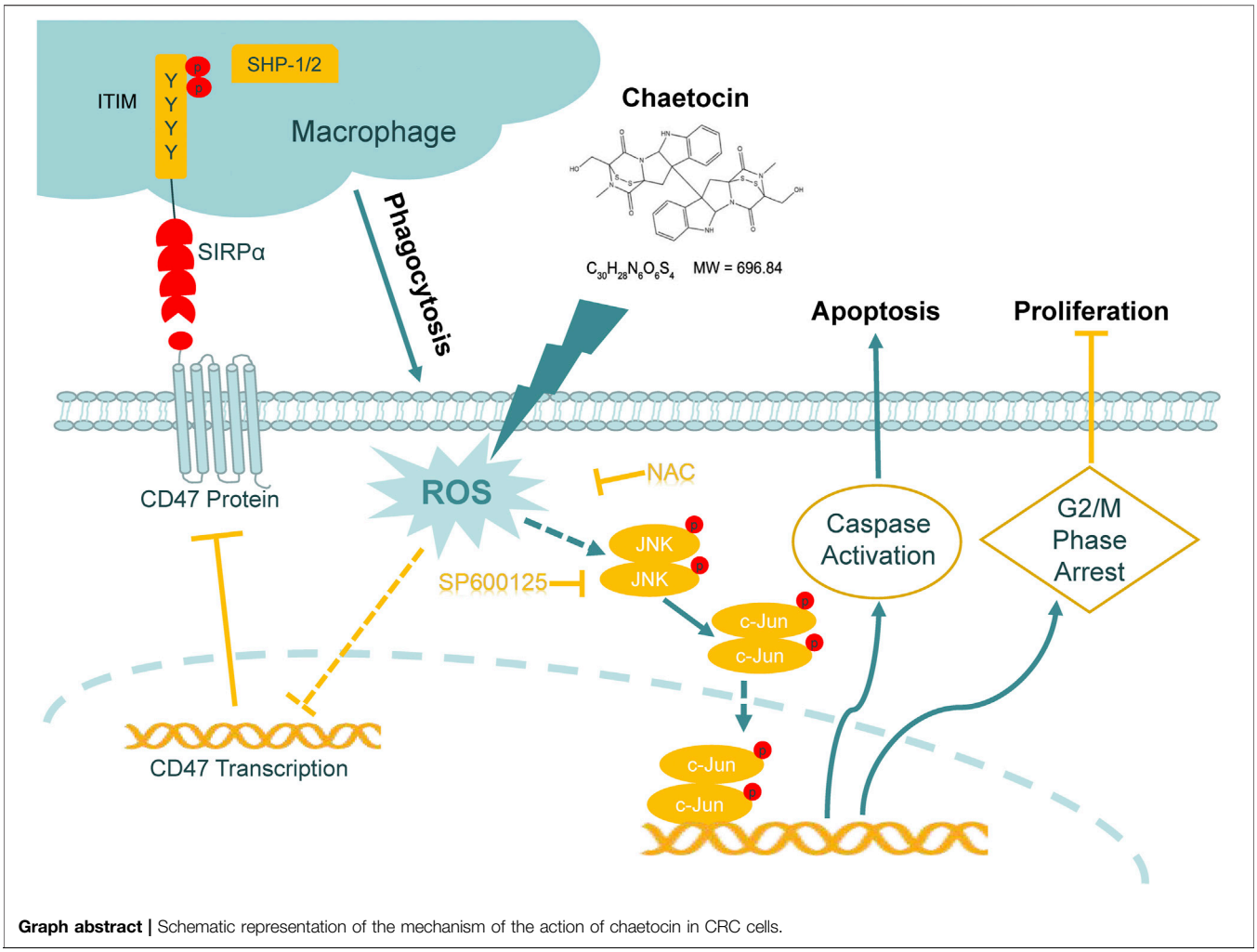
Citation:
Wang H, Wen C, Chen S, Li W, Qin Q, He L, Wang F, Chen J, Ye W, Li W, Peng J, Yang X and Liu H (2021) ROS/JNK/C-Jun Pathway is Involved in Chaetocin Induced Colorectal Cancer Cells Apoptosis and Macrophage Phagocytosis Enhancement. Front. Pharmacol. 12:729367. doi: 10.3389/fphar.2021.729367

There is an urgent need for novel agents for colorectal cancer (CRC) due to the increasing number of cases and drug-resistance related to current treatments. In this study, we aim to uncover the potential of chaetocin, a natural product, as a chemotherapeutic for CRC treatment. We showed that, regardless of 5-FU-resistance, chaetocin induced proliferation inhibition by causing G2/M phase arrest and caspase-dependent apoptosis in CRC cells. Mechanically, our results indicated that chaetocin could induce reactive oxygen species (ROS) accumulation and activate c-Jun N-terminal kinase (JNK)/c-Jun pathway in CRC cells. This was confirmed by which the JNK inhibitor SP600125 partially rescued CRC cells from chaetocin induced apoptosis and the ROS scavenger N-acetyl-L-cysteine (NAC) reversed both the chaetocin induced apoptosis and the JNK/c-Jun pathway activation. Additionally, this study indicated that chaetocin could down-regulate the expression of CD47 at both mRNA and protein levels, and enhance macrophages phagocytosis of CRC cells. Chaetocin also inhibited tumor growth in CRC xenograft models. In all, our study reveals that chaetocin induces CRC cell apoptosis, irrelevant to 5-FU sensitivity, by causing ROS accumulation and activating JNK/c-Jun, and enhances macrophages phagocytosis, which suggests chaetocin as a candidate for CRC chemotherapy.

Keywords: chaetocin, colorectal cancer, ROS, JNK/c-Jun pathway, apoptosis, CD47

INTRODUCTION

Colorectal cancer (CRC) is one of the most frequently diagnosed cancer in the world (Sung et al., 2021). The clinical options available for CRC include surgery, radiotherapy, chemotherapy, targeted therapy and immunotherapy (Dekker et al., 2019). 5-FU remains the first-line chemo drug for CRC, but resistance and adverse side effects significantly limit its efficacy (Biagi et al., 2011). Although



Graph abstract | Schematic representation of the mechanism of the action of chaetocin in CRC cells.

molecular targeted agents like cetuximab, a epidermal growth factor receptor inhibitor, have been approved for CRC patients, high mutation rates of KRAS and BRAF result in unsatisfactory effects of these drugs (Gunjur, 2019). Due to the particular feature of CRC, the effectiveness of immunotherapy includes PD-1/PD-L1 inhibitors is really limited on CRC patients (Ganesh et al., 2019). Therefore, novel agents with better efficacy are urgently needed for CRC treatment.

Reactive oxygen species (ROS) has been proven to participate in many biological events, including cell growth, differentiation and death through interacting with multiple signaling pathways (Holmström and Finkel, 2014). Considerable evidence has showed that various diseases like diabetes mellitus, atherosclerosis and cancer are closely related to the accumulation of ROS (Reuter et al., 2010). *Cancer* initiation, metastasis and drug resistance may benefit from the moderate increase in ROS levels, but excessive ROS accumulation causes cancer cell death, and cancer cells preserves a higher concentration of ROS comparing to that in their normal counterparts (Tafani et al., 2016; Galadari et al., 2017). Therefore, cancer cells are more vulnerable to ROS accumulation, and redox-targeted agents may be highly efficacious in inducing cancer cell death and can be developed for cancer treatment.

With the deeper understanding of tumor microenvironment, immune checkpoint inhibitors (ICIs) have achieved rapid development (Liu, 2019). Although ICIs including ipilimumab (targets CTLA-4), nivolumab (targets PD-1), and atezolizumab (targets PD-L1) are also approved for CRC by the Food and Drug Administration, due to their limitations such as poor efficiency and drug resistance in CRC treatment, it is also of great importance to study on new immune checkpoint and inhibitors (Franke et al., 2019; Sclafani, 2019). Cluster of differentiation 47 (CD47), also called integrin related proteins (IAP), is a member of the immunoglobulin superfamily. CD47, by binding to signal-regulatory protein α (SIRPα), transmits the signal "Don't Eat Me" to avoid phagocytosis by immune system (Matlung et al., 2017; Russ et al., 2018). In addition, it is verified that tumor cells overexpress CD47 to escape from immune surveillance in various malignant tumors such as leukemia,

lymphoma, breast and colon cancer, and antagonism CD47 has significant anti-tumor effects (Horrigan, 2017; Lian et al., 2019; Hu et al., 2020). As a result, CD47 is considered as an emerging immune checkpoint molecule to be studied. Although some CD47 antibodies are in clinical development currently (Jalil et al., 2020), due to the liabilities exhibited in clinical trials and the limitation of antibodies in modification, searching for small organic molecules that inhibit CD47 should be another effective strategy for the development of immunotherapy (Miller et al., 2019; Burgess et al., 2020).

Natural products are valuable sources for new cancer drug discovery and development. More than 50% of the approved drugs for cancer treatment are of natural origin (Newman and Cragg, 2020). Therefore, exploring efficient anticancer drugs from natural products seems to be an attractive strategy. The natural product chaetocin, which is produced by a species of fungi called Chaetomium (Sekita et al., 1981) has a potent inhibitory effect on various type of cancers, from the result of number of studies (Isham et al., 2007; Lee et al., 2011; Chaib et al., 2012; Dixit et al., 2014; Liu et al., 2015; Wen et al., 2019). Several studies showed that the anticancer effects of chaetocin depended on the accumulation of ROS (Isham et al., 2007; Tibodeau et al., 2009; Dixit et al., 2014; Li et al., 2019; Ozyerli-Goknar et al., 2019; Wen et al., 2019). The growth inhibition of chaetocin in several CRC cell lines has been reported (Isham et al., 2012), indicating the potential of chaetocin as a chemotherapeutic agent. However, the mechanism behind such effects is unclear, and it has not been investigated whether chaetocin could overcome the resistance to 5-FU and whether chaetocin has immunomodulatory effects.

In the present study, we investigated whether the chaetocin's proliferation inhibition and apoptosis inducing effects extended to CRC cells. In addition, whether this effect would be influenced by 5-FU sensitivity and translated well to animal studies. Mechanism wise, we showed that chaetocin induced apoptosis is channeled by JNK/c-Jun in CRC cells and also chaetocin's effect in immune surveillance modulation through CD47. Together, the results from this study highlight the potential of chaetocin as a novel chemo agent for CRC patients.

MATERIALS AND METHODS

Reagents

Chaetocin (#C9492, Sigma-Aldrich, St Louis, MO, United States), z-VAD-fmk (#ALX-260–020, Enzo, New York, NY, United States), N-acetyl-L-cysteine (NAC) (#A7250, Sigma-Aldrich) and SP600125 (#S5567, Sigma-Aldrich) were dissolved in DMSO to form the 10mM, 50mM, 0.5M and 20 mM solution respectively. These reagents were stored at −20°C. Primary antibodies against PARP (#9542), caspase-3 (#9662), cleaved-caspase-3 (#9661), caspase-8 (#9746), caspase-9 (#9508), BCL-2 (#15071), BCL-XL (#2764), MCL-1 (#4572), XIAP (#14334), JNK (#9252) and phospho-JNK (Thr183/Tyr185) (#4668) were purchased from Cell Signaling Technology (Beverly, MA, United States). Anti-c-Jun (#ab131497), anti-Ser63 phosphor-c-Jun (#ab28807), anti-CD47 (#ab9089) anti-α-tubulin (#ab233661) and β-actin (#ab8226) were purchased from Abcam (Cambridge, MA, United States), FITC anti-human CD47 (#323106) was purchased from Biolegend (San Diego, CA, United States). Anti-mouse immunoglobulin G (#B900620) and anti-rabbit immunoglobulin G (#B900610) horseradish peroxidase-conjugated secondary antibodies were purchased from Proteintech Group (Chicago, IL, United States).

Cell Culture

LIM1215 cell line was obtained from the European Collection of Authenticated Cell Cultures (Salisbury, Wiltshire, United Kingdom). The other CRC cell lines were purchased from Culture Collection of Chinese Academy of Science (Shanghai, China). The 5-FU-resistant HCT-15/5FU-R cell line was established from HCT-15 as previously described (Wen et al., 2015; Wen et al., 2016; Wang et al., 2020). DLD-1, LS174T, Caco-2, LIM1215, HCT-8, SW620, HCT116 and SW480 cells were cultured in RPMI 1640 (Gibco Life Technologies, Carlsbad, CA, United States). HT-29, LoVo, RKO, HCT-15 and HCT-15/5FU-R cells were cultured in DMEM (Gibco Life Technologies) supplemented with 10% fetal bovine serum (Gibco Life Technologies), 100 units/mL penicillin and 10 μg/ml streptomycin (Gibco Life Technologies). Incubations were controlled in a humidified atmospheric environment of 5% CO2 at 37°C.

Cell Viability Assay

To test CRC cell viability after chaetocin treatment, CCK-8 assay (Nanjing KeyGen Biotech Co., Ltd., Nanjing, Jiangsu, China) was performed. Cells seeded in 96-well plates were left to grow overnight. The next day, chaetocin at various concentrations were added, and incubated for 24 h. Cells were assessed after 4 h of incubation with 10 μL of CCK-8 solution. The results were carried out using Varioskan Flash multimode reader (Thermo Fisher Scientific, Waltham, MA, United States) at 450 nm.

Colony Formation Assay

500 cells/well of HCT116 and LS174T cells and 1,000 cells/well of LIM1215 and HCT–15/5-FU-R cells were seeded in 6-well plates. Chaetocin at various concentration were then added. Plates were left for incubation for different duration. Before imaging, we fixed cells using ice-cold methanol for 5 min and then cells were stained using 0.1% crystal violet. Colonies were counted from images obtained by Epson scanner (Suwa, Nagano, Japan).

Real-Time Cell Impedance Analysis

To dynamically monitor cell proliferation, xCELLigence system from Roche Applied Science (Mannheim, Baden-Wuerttemberg, Germany) was utilized. Briefly, cells in 100 μL of media were seeded into E-plate and incubated overnight. Chaetocin treatment took place the next day. The impedance measurement was performed according to the manufacturer's manual. The measurable impedance should increase when cells proliferate.

Cell Cycle Analysis

FACSCanto II flow cytometry (BD Biosciences) with Propidium Iodide (PI, BD Biosciences, Franklin Lakes, NJ, United States) staining was performed. After chaetocin treatment, cells were

collected, washed before fixed overnight with 66% cold ethanol at 4°C. After discarding the ethanol, cells were washed with PBS, followed by staining with PI.

Cell Apoptosis Analysis

Flow cytometry with Annexin V-FITC/PI staining (Nanjing KeyGen Biotech Co., Ltd.) was used to identify the apoptotic population of CRC cells. After chaetocin treated, both suspended and attached cells were collected, washed with PBS and stained in a working solution (500 μL of binding buffer with 5 μL of Annexin V-FITC and 5 μL of PI) for 15 min at room temperature in the dark. FACSCanto II flow cytometry (BD Biosciences) were then carried out, while cells with positive Annexin V-FITC staining were considered as apoptotic cells.

Analysis of Cell Surface CD47

HCT116 cells and LS174T were treated with 0.5 and 1 μM chaetocin for 24 and 12 h respectively. After PBS washed, cells were then incubated with anti-CD47-FITC antibody for 15 min on ice in the dark. The expression of cell surface CD47 was analyzed using FACSCanto II flow cytometry (BD Biosciences).

Real-Time Quantitative Polymerase Chain Reaction (PCR)

Total RNA was extracted from chaetocin-treated CRC cells using Trizol reagent (Ambion, Carlsbad, CA, United States). cDNA was then synthesized from 500 ng RNA of each sample using the PrimeScript RT reagent Kit (TaKaRa, Dalian, Liaoning, China). Real-time PCR using SYBR Premix Ex Taq II Kit (TaKaRa) was performed according to manufacturer's instruction. The specific primers for real-time PCR are as follows: CD47 forward, 5′-TGG TGG GAA ACT ACA CTT GCG-3′; CD47 reverse, 5′- CGT GCG GTT TTT CAG CTC TAT-3′; actin forward, 5′-GTG ACG TTG ACA TCC GTA AAG A-3′; actin reverse, 5′- GCC GGA CTC ATC GTA CTC C-3′; actin was chosen as endogenous control and the CD47 gene expression was analyzed using $2^{-\Delta\Delta Ct}$ method. The CD47 gene expression is shown as fold change of control.

Mitochondrial Membrane Potential Measurement

The mitochondrial membrane potential of CRC cells was measured using the JC-1 mitochondrial membrane potential assay kit (Nanjing KeyGen Biotech Co., Ltd.), following the manufacturer's protocol. In brief, chaetocin treated cells were stained at 37°C for 20 min, then rinsed, using solutions provided in the kit. The fluorescence intensity results were obtained using FACSCanto II flow cytometry (BD Biosciences), whilst mitochondrial JC-1 aggregates which stained red were considered as mitochondria from health cells.

ROS Measurement

The cells were incubated with 10 μM of 2′,7′-dichlorofluorescin diacetate (DCFH-DA) (Beyotime Institute of Biotechnology, Shanghai, China), a fluorescent probe, at 37°C for 30 min. Following chaetocin treatments, cells were washed with serum-free media and resuspended in 500 μL of PBS before fluorescence measurements using flow cytometry (BD Biosciences).

Western Blot Analysis

RIPA lysis buffer (Cell Signaling Technology) containing protease and phosphatase inhibitors (Nanjing KeyGen Biotech Co., Ltd.) was used to extract proteins from chaetocin treated cells. BCA assay (Pierce, Thermo Fisher Scientific) was implemented to ensure a normalised protein concentration. Equal amounts of protein were resolved by SDS-PAGE and were then transferred to nitrocellulose membranes (Merck Millipore, Burlington, MA, United States). Next, the membranes were first blocked by 5% nonfat dry milk, followed by primary antibody incubation overnight at 4°C. After washing the membranes with TBST the next day, HRP-conjugated secondary antibody was applied and left for incubation for 1 h at room temperature before ECL detection. α-tubulin was used as loading control.

In vitro Phagocytosis Assay

Preparation of human macrophages: monocyte-differentiated macrophages were prepared as described previously (Lou et al., 2019). Monocytes extraction from blood of healthy adult donor was done using MACS using anti-CD14 microbeads (Miltenyi Biotec, Auburn, CA, United States). Monocytes were then cultured in RPMI 1640 (Gibco Life Technologies) supplemented with 10% fetal bovine serum (Gibco Life Technologies), 100 units/mL penicillin and 10 μg/ml streptomycin (Gibco Life Technologies), 200 mM glutamine (Gibco Life Technologies) and 25 mM HEPES (Gibco Life Technologies) and treated with 25 ng/ml human recombinant macrophage colony-stimulating factor (M-CSF) for 7 days to differentiate to macrophages.

Preparation of tumor cells: Live HCT116 cells were stained with 5 μM carboxyfluorescein diacetate succinimidyl ester (CFSE) at 37°C for 15 min after 0.5 μM chaetocin treatment for 24 h. After washed with ice-cold D-PBS, stained cells were resuspended in serum-free RPMI 1640.

For *in vitro* phagocytosis assay, 1×10^5 macrophages were added to 2×10^5 CFSE-stained tumor cells per well in the 24-well plate for 24 h incubation. Cells were then stained with CD14-APC (Ebiosciences, San Diego, CA, United States) and phagocytosis was analyzed by flow cytometry. CD14-APC plus CFSE positive cells were determined as macrophages which had successfully phagocytized tumor cells.

Tumor Xenografts in Nude Mice

5×10^6 HCT116 cells were injected subcutaneously into the flank of five-week-old female BALB/c nude mice from Guangdong Laboratory Animals Monitoring Institute. After waited 1 week for measurable tumors to form (approximately 50 mm^3), the animals were divided randomly into two groups ($n = 6$ each group) which was either treated with vehicle (10% DMSO, 20% cremophor EL

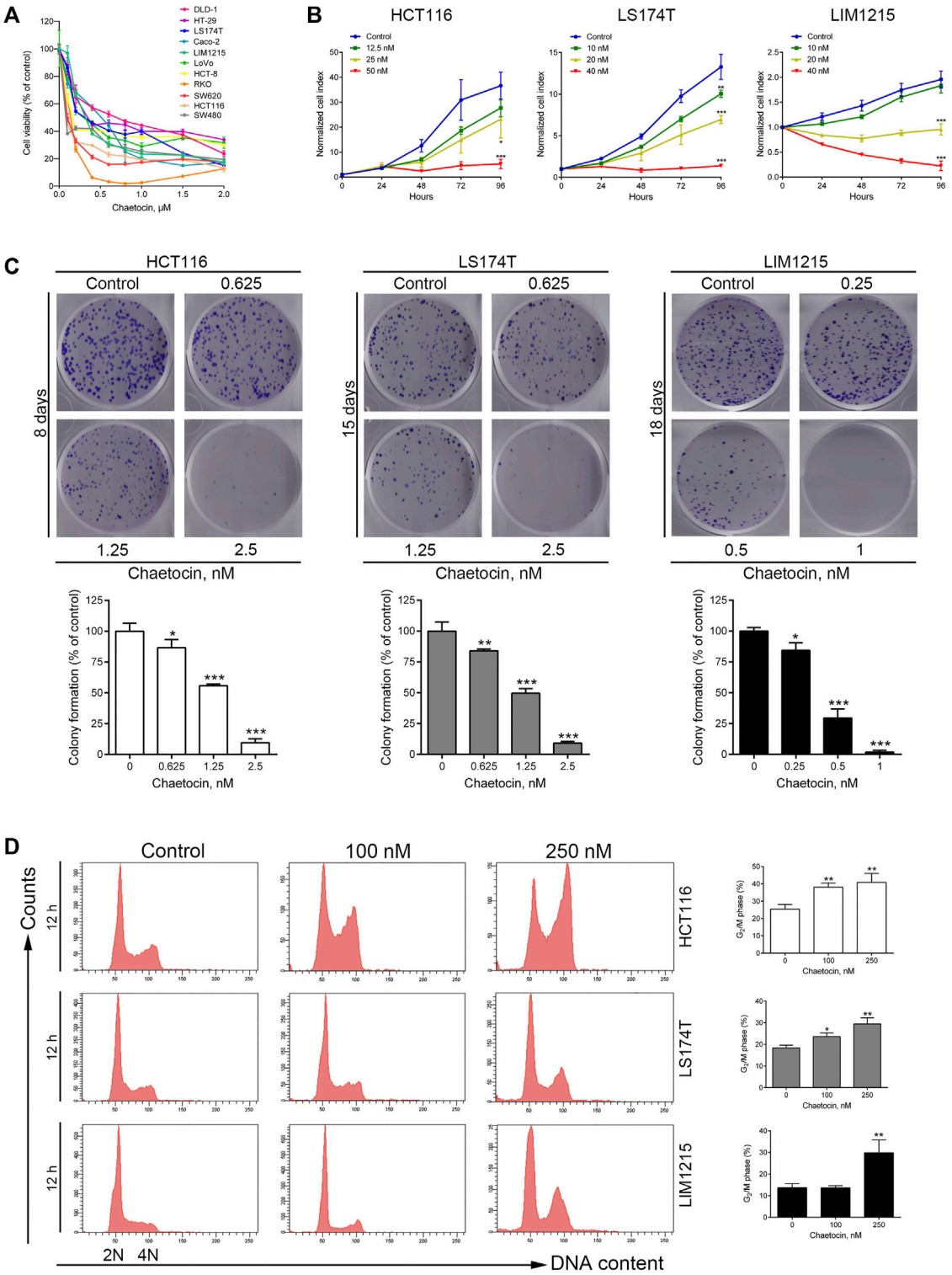


FIGURE 1 | Chaetocin Inhibits cell proliferation and causes G2/M phase arrest. **(A)** Followed by treated with chaetocin at increasing concentrations for 24 h, CCK8 assay was used to measure the viability of CRC cells.**(B)** Real-time cell analysis results on the proliferation of HCT116, LS174T and LIM1215 cells. **(C)** After treated with chaetocin for indicated days, number of new colonies formed were counted. **(D)** Cell cycle distribution analysis on CRC cell lines after 12 h chaetocin treatment at various concentrations detected by PI-stained flow cytometry. For **(C)** and **(D)**, results were shown as mean ± SD of three independent experiments. $^{*}p < 0.05$, $^{**}p < 0.01$, $^{***}p < 0.001$, versus control group.

TABLE 1 | Effects on viability of chaetocin on various CRC cells.

Cell line	IC_{50} (μM)
DLD-1	0.64
HT-29	0.57
LS174T	0.40
Caco-2	0.39
LIM1215	0.37
LoVo	0.35
HCT-8	0.19
RKO	0.13
SW620	0.071
HCT116	0.059
SW480	0.052

estimated as the following formula: $a^2 \times b \times 0.5$, where a is the smallest diameter and b is the diameter perpendicular to a. At the end of the study, the tumors from sacrificed mice were removed, weighed and stored for further experiments. All animal studies conducted were approved by the Institutional Animal Care and Use Committee of Guangdong Laboratory Animals Monitoring Institute.

Statistical Analysis

All experiments were performed at least in triplicate, and the results were shown as mean ± SD where applicable. One-way analysis of variance followed by Tukey's test by GraphPad Prism 7.00 (GraphPad Software Inc., La Jolla, CA, United States) was used to analyze significant differences among the results. $^*p < 0.05$ was considered statistically significant.

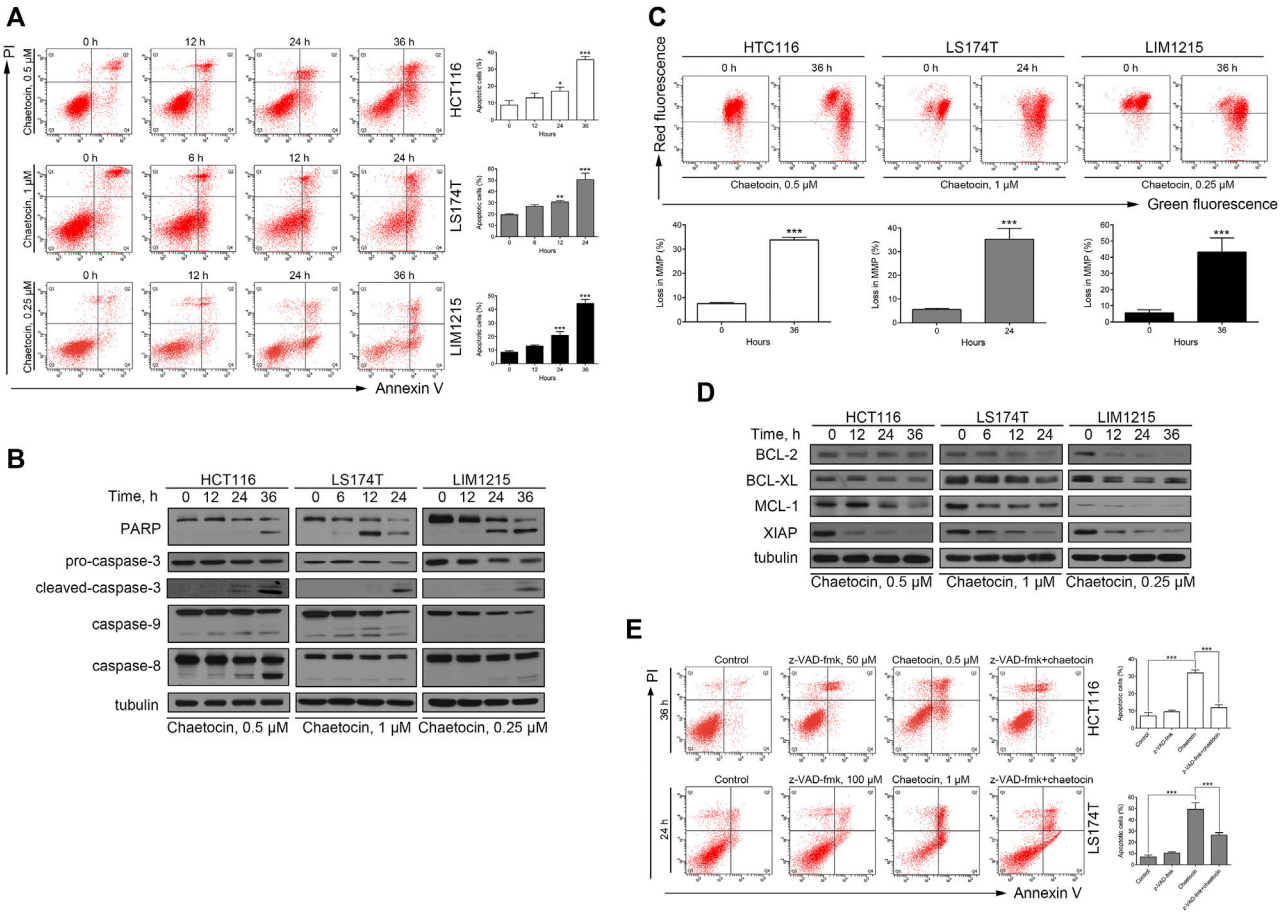


FIGURE 2 | Chaetocin induces caspase-dependent apoptosis in CRC cells. **(A)** Flow cytometry results with Annexin V-FITC/PI staining on apoptotic population of HCT116, LS174T and LIM1215 after chaetocin treatment. **(B)** Western blot analysis of PARP, caspase-3, capase-9 and caspase-8 expression levels in HCT116, LS174T and LIM1215 cells. **(C)** Flow cytometry results with JC-1 staining on three CRC cell lines. **(D)** Western blot results to evaluate the protein level of BCL-2, BCL-XL, MCL-1 and XIAP in CRC cell lines. **(E)** A 2 h z-VAD-fmk pretreatment could rescue some HCT116 and LS174T cells from apoptosis induced by chaetocin. For **(A)**, **(C)** and **(E)**, results were shown as mean ± SD of three independent experiments. $^*p < 0.05$, $^{**}p < 0.01$, $^{***}p < 0.001$. For **(A)** and **(C)**, comparison was against 0 h group.

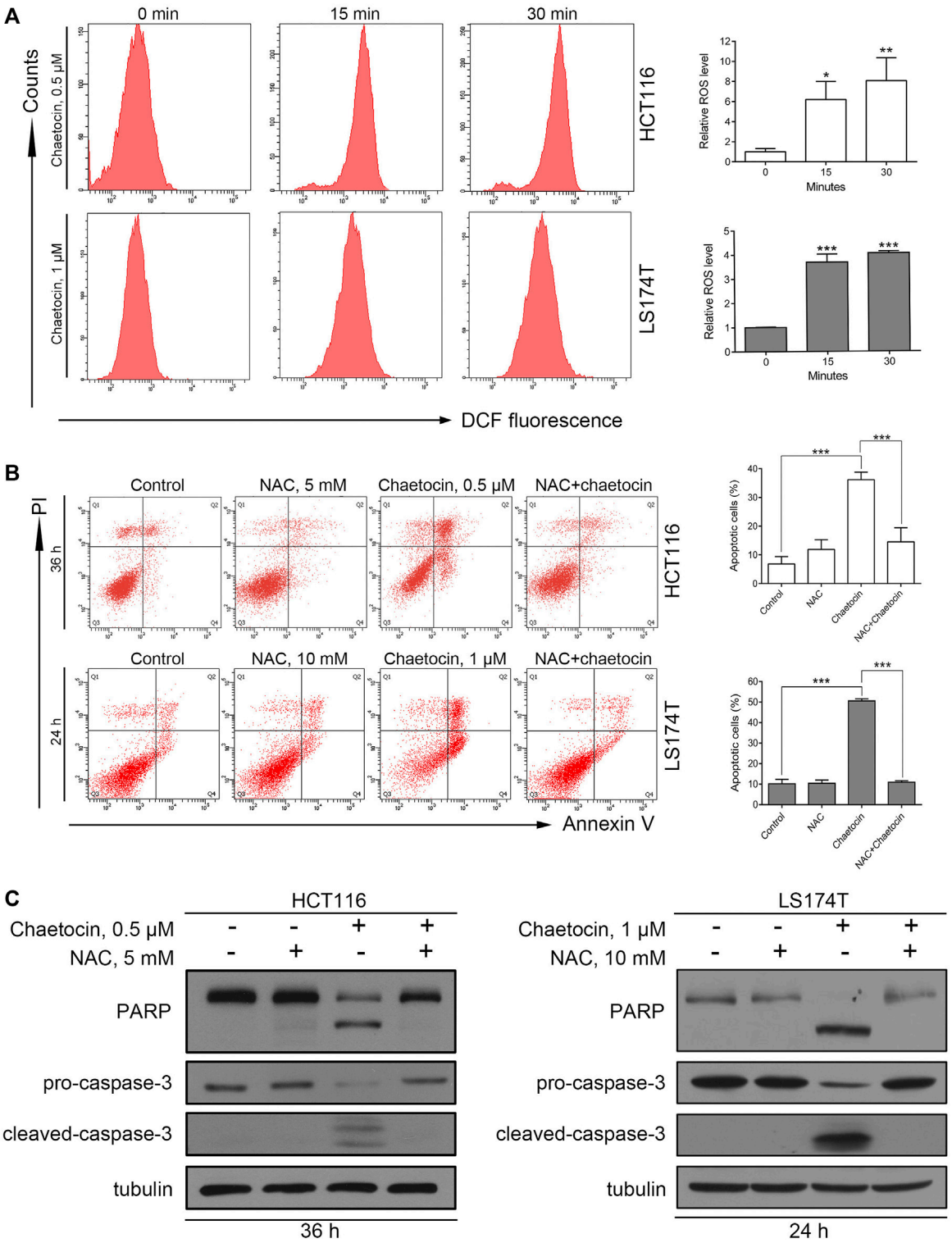


FIGURE 3 | Chaetocin-induced ROS accumulation is required for cell apoptosis. **(A)** ROS levels of HCT116 and LS174T cells were verified using flow cytometry, after DCFH-DA labeling and chaetocin treatments. HCT116 and LS174T cells were pretreated with NAC for 2 h and then cotreated with chaetocin for another indicated times. **(B)** Flow cytometry analysis on apoptotic CRC cells. **(C)** Western blot of PARP and caspase-3 protein level. For **(A)** and **(B)**, results were shown as mean ± SD of three independent experiments. $^{*}p < 0.05$, $^{**}p < 0.01$, $^{***}p < 0.001$, versus control group.

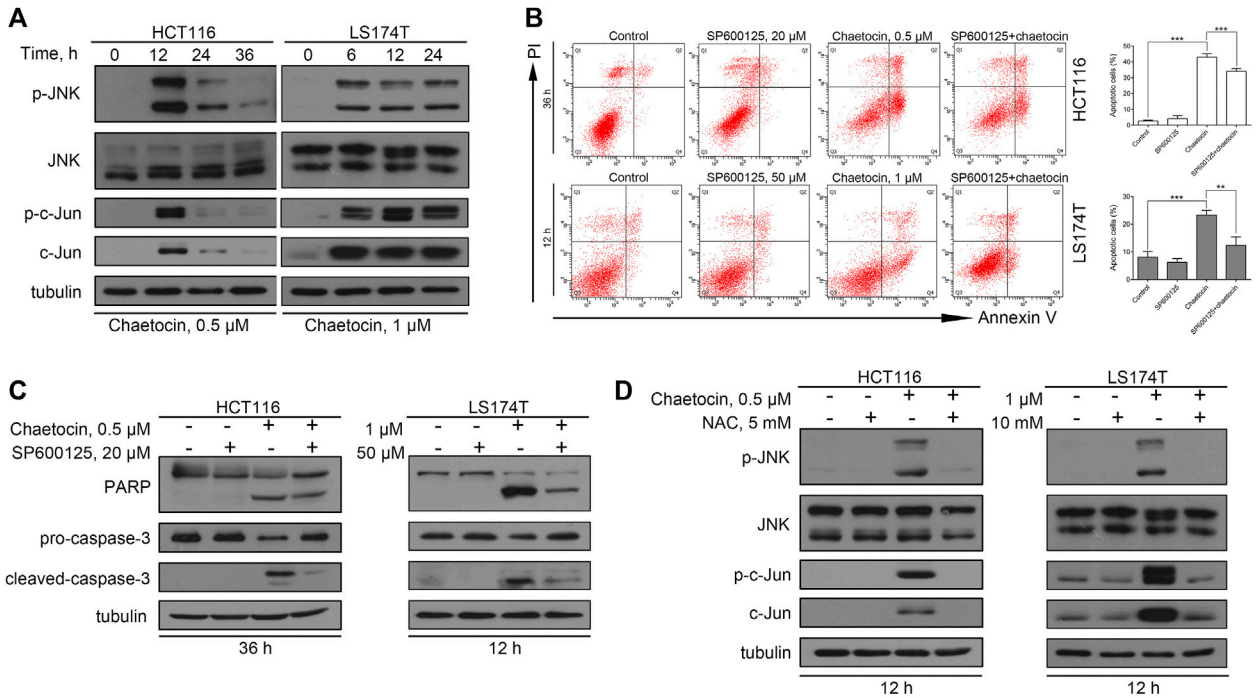


FIGURE 4 | The involvement of ROS/JNK/c-Jun in ROS-mediated cell apoptosis. **(A)** The protein level of JNK and c-Jun in HCT116 and LS174T cells after chaetocin treatment by western blot. CRC cells were pretreated with SP600125 for 2 h before chaetocin treatment for indicated hours. **(B)** Cell apoptosis was measured by flow cytometry. Results were shown as mean ± SD of three independent experiments. $^{**}p < 0.01$, $^{***}p < 0.001$. **(C)** Expression of PARP and caspase-3 was analyzed by western blot. **(D)** The expression levels of JNK and c-Jun after NAC pretreatment for 2 h and then cotreatment of chaetocin for 12 h in HCT116 and LS174T cells were analyzed by western blot.

RESULTS

Chaetocin Suppresses Cell Growth and Triggers G_2/M Cell Cycle Arrest in CRC Cells

Chaetocin has a thiodioxopiperazine structure as shown in **Supplementary Figure 1** (Wen et al., 2019). Firstly, the cytotoxic effects of chaetocin were tested on various CRC cells. After treated with chaetocin for 24 h at increasing concentrations, from 0 to 2 μM, CCK8 results showed a progressive inhibition in cell viability across a dozen of various CRC cell lines, with IC50 values between 0.052 and 0.64 μM (**Figure 1A** and **Table 1**). Real-time cell analysis showed that the normalized cell index was inhibited by chaetocin in a dose-dependent manner in HCT116, LS174T and LIM1215 cells (**Figure 1B**), indicating that the cell proliferation of CRC cells was markedly restrained by chaetocin. Moreover, colony formation assay also revealed a decrease in both size and numbers in CRC colonies (**Figure 1C**). Collectively, our results demonstrated that chaetocin suppressed CRC cell growth *in vitro*. To determine whether chaetocin achieved this by inducing cell cycle arrest, cell cycle distribution analysis was carried out using flow cytometry. As shown in **Figure 1D**, after HCT116, LS174T and LIM1215 cells were treated with chaetocin for 12 h, the population of HCT116, LS174T and LIM1215 cells at the G_2/M phase increased substantially, indicating that chaetocin Inhibits CRC cell proliferation by prompting G2/M phase arrest.

Chaetocin Induces CRC Cells Apoptosis in a Caspase-dependent Manner

Our previous studies have shown that chaetocin induces apoptosis in gastric cancer cell lines HGC-27 and AGS (Wen et al., 2019), whether the same would occur in CRC cells was investigated. After chaetocin treated, as shown in **Figure 2A**, flow cytometry exhibited that chaetocin increased the apoptotic cell populations in HCT116, LS174T and LIM1215 cells, and the apoptotic population increases as the duration of treatment lengthened. Because caspase pathway activation is crucial to apoptosis (Mandal et al., 2020), caspase family proteins were then assessed by western blot analysis. Chaetocin decreased the levels of the precursor forms of caspase-3, -8, and -9 but increased cleavage of those proteins in HCT116, LS174T and LIM1215 cells (**Figure 2B**). Consistently, chaetocin induced PARP cleavage which is the known downstream protein of caspase pathway (**Figure 2B**), illustrating that chaetocin induces CRC cell apoptosis which may depend on caspase activation. When apoptosis occurs, the integrity of the mitochondrial membrane will decrease, a phenomenon recognized as an indicator of apoptosis (Lindsay et al., 2011). As shown in **Figure 2C**, the integrity of the mitochondrial membrane was disrupted in HCT116, LS174T and LIM1215 cells after chaetocin treatment. To further confirm this, western blot was performed to

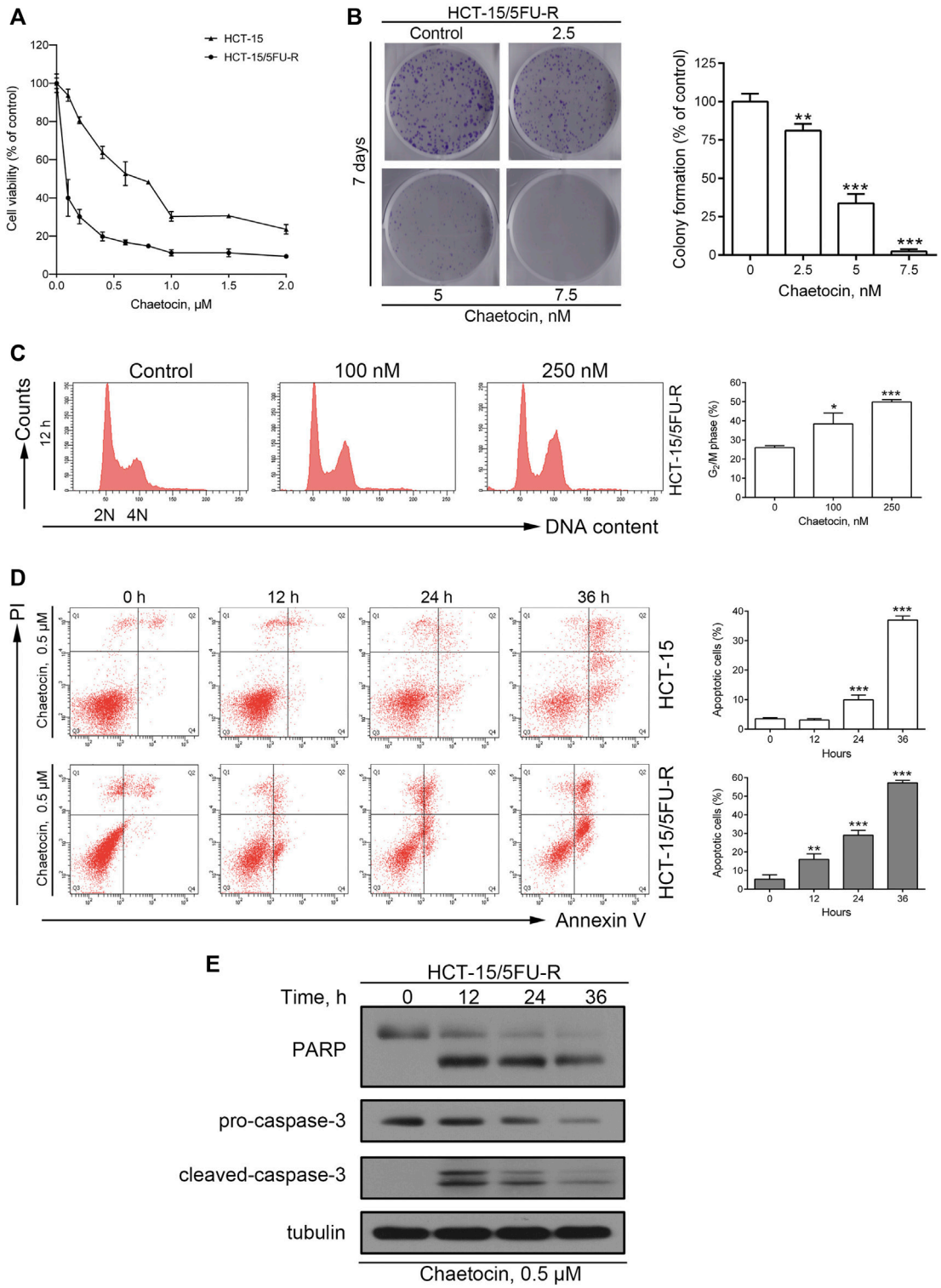


FIGURE 5 | Chaetocin overcomes 5-FU resistance in CRC cells. **(A)** The CCK8 cell viability assay on 5-FU resistant and sensitive HCT-15 cell lines. **(B)** After 7 days chaetocin treatment, colony formation result of HCT-15/5FU-R cells. **(C)** Cell cycle distribution results of HCT-15/5FU-R cells after 12 h chaetocin treatment at indicated concentration were analyzed by flow cytometry with PI staining. **(D)** Apoptotic population analysis by flow cytometry with Annexin V-FITC/PI staining of HCT-15 and HCT-15/5FU-R cells, after 0.5 μM chaetocin. **(E)** Western blot results on PARP and caspase-3 expression level in HCT-15/5FU-R cells. For **a**, **(B)**, **(C)** and **(D)**, results were shown as mean ± SD of three independent experiments. $^{*}p < 0.05$, $^{**}p < 0.01$, $^{***}p < 0.001$, versus control group.

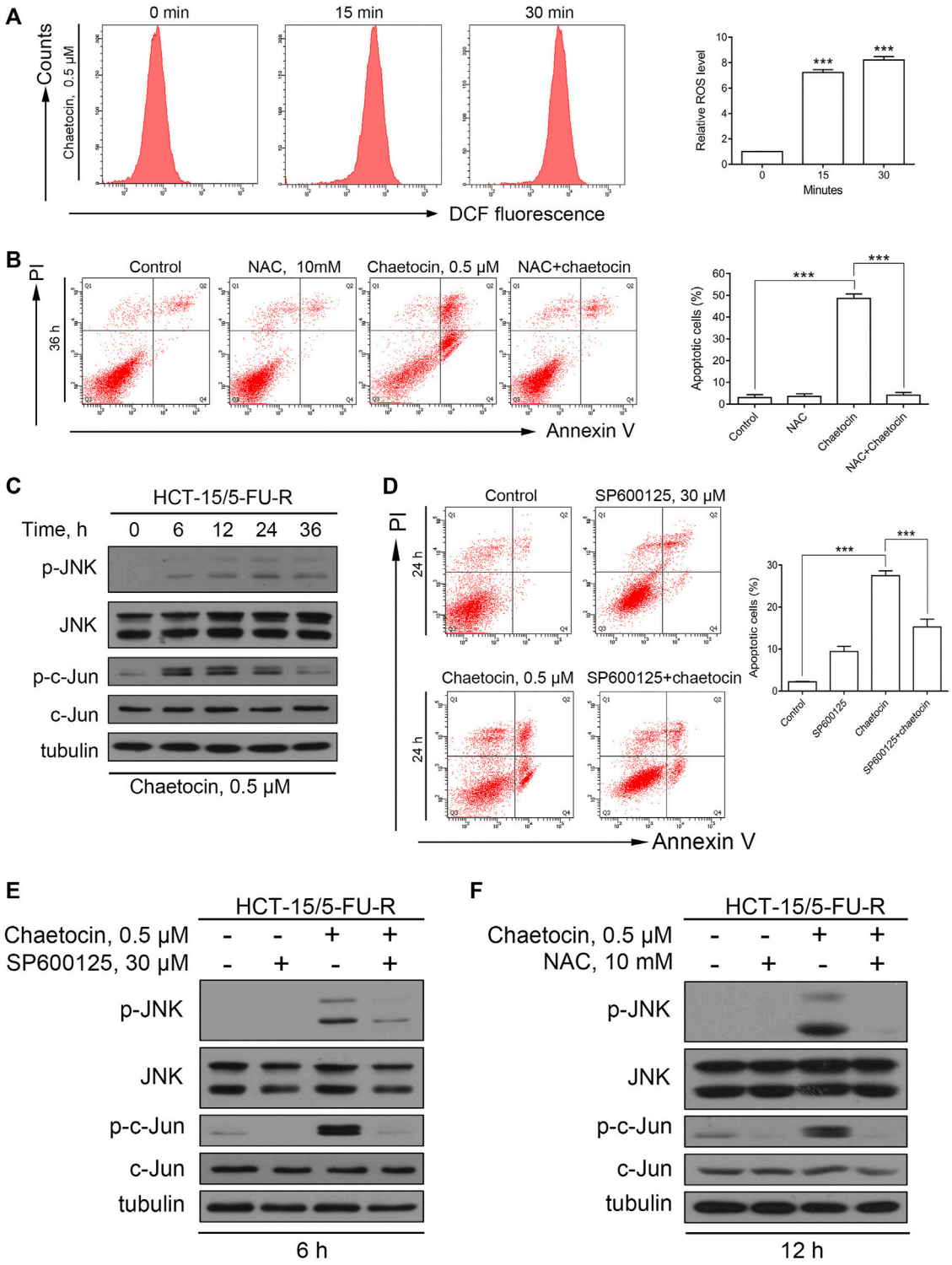


FIGURE 6 | Chaetocin-induced apoptosis in HCT-15/5FU-R cells is associated with the ROS/JNK/c-Jun pathway. **(A)** The ROS levels of HCT-15/5FU-R cells. Results were shown as mean ± SD of three independent experiments. ***$p < 0.001$, versus control group. **(B)** HCT-15/5FU-R cells apoptosis induced by chaetocin were rescued by 2 h of NAC pretreatment (***$p < 0.001$). **(C)** The expression level JNK and c-Jun protein in 5-FU-resistant CRC cells by western blot after chaetocin treatment. **(D)** HCT-15/5FU-R cells were cotreated with chaetocin for 24 h after 2 h SP600125 preincubation. Flow cytometry were used analyze the rescued population (***$p < 0.001$). **(E)** After pretreated with SP600125 for 2 h and then cotreated with chaetocin for another 6 h, the expression of JNK and c-Jun in HCT-15/5FU-R cells were analyzed by western blot. **(F)** The expression levels of JNK and c-Jun in HCT-15/5FU-R cells were evaluated by western blot after 2 h of NAC pretreatment followed by chaetocin cotreatment for 12 h.

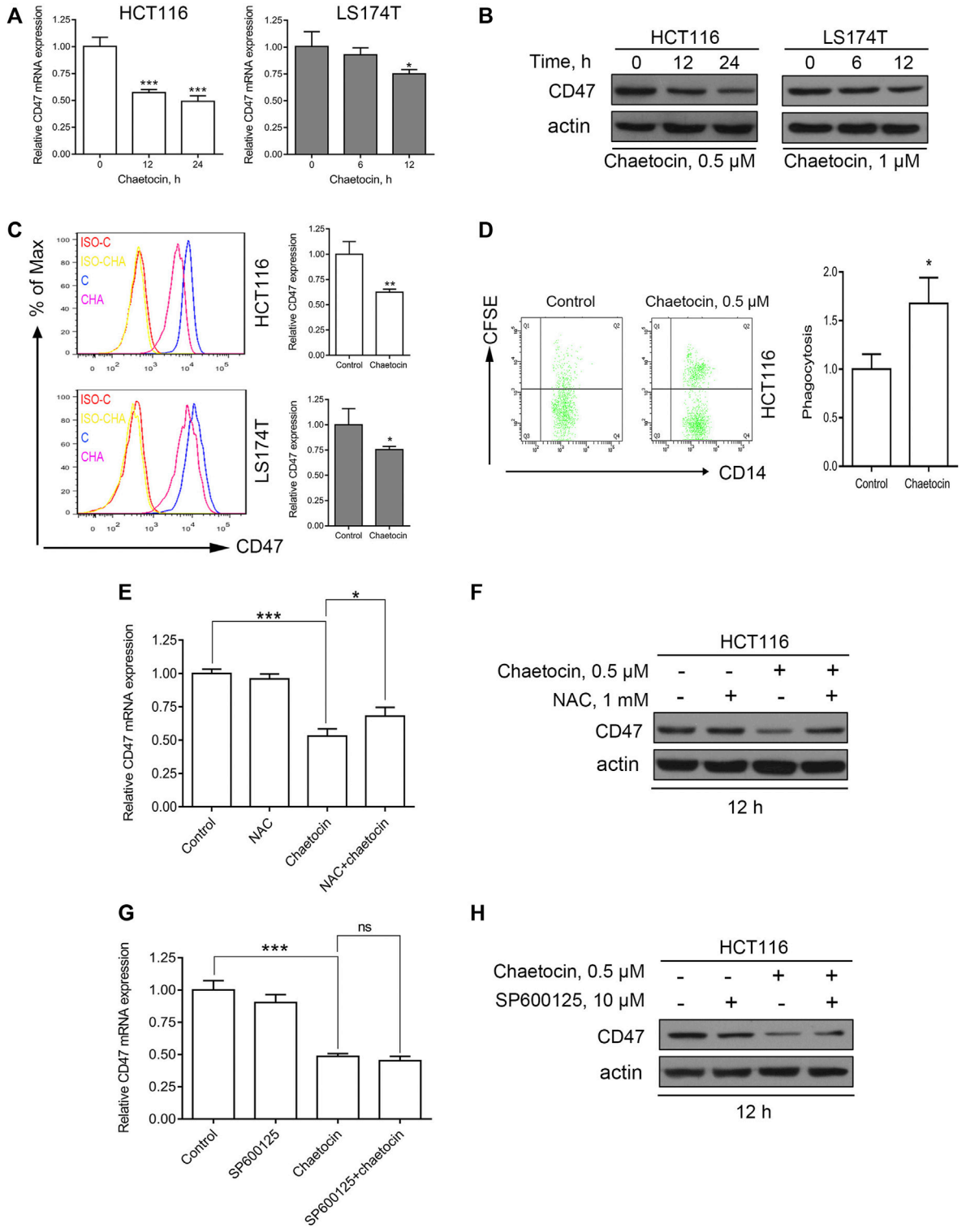


FIGURE 7 | Chaetocin decreases the expression of CD47 in CRC cells and enhances the phagocytosis of macrophages. **(A)** The expression of CD47 at mRNA levels was detected by qPCR after HCT116 and LS174T cells treated with chaetocin (0.5 μM chaetocin for HCT116 cells and 1 μM chaetocin for LS174T cells) for the indicated times. *$p < 0.05$, ***$p < 0.001$. **(B)** The expression of total CD47 protein was analyzed by western blot after chaetocin treatment. **(C)** The expression of membrane CD47 protein was detected by flow cytometry after HCT116 and LS174T were treated as described (*$p < 0.05$, **$p < 0.01$). **(D)** HCT116 cells were pretreated with 0.5 μM chaetocin for 24 h and then co-cultured with macrophages for another 24 h, the phagocytosis of HCT116 cells by macrophages was detected by flow cytometry. *$p < 0.05$. HCT116 cells were pretreated with 1 mM NAC for 2 h and then co-treated with 0.5 μM chaetocin for another 12 h **(E)** The mRNA level of CD47 was detected by qPCR. *$p < 0.05$, ***$p < 0.001$. **(F)** The expression of total CD47 protein was detected by western blot. SP600125 rescue analysis was done as previously mentioned. **(G)** mRNA expression of CD47 detection by qPCR (***$p < 0.001$). **(H)** The amount of CD47 protein expressed was evaluated by western blot.

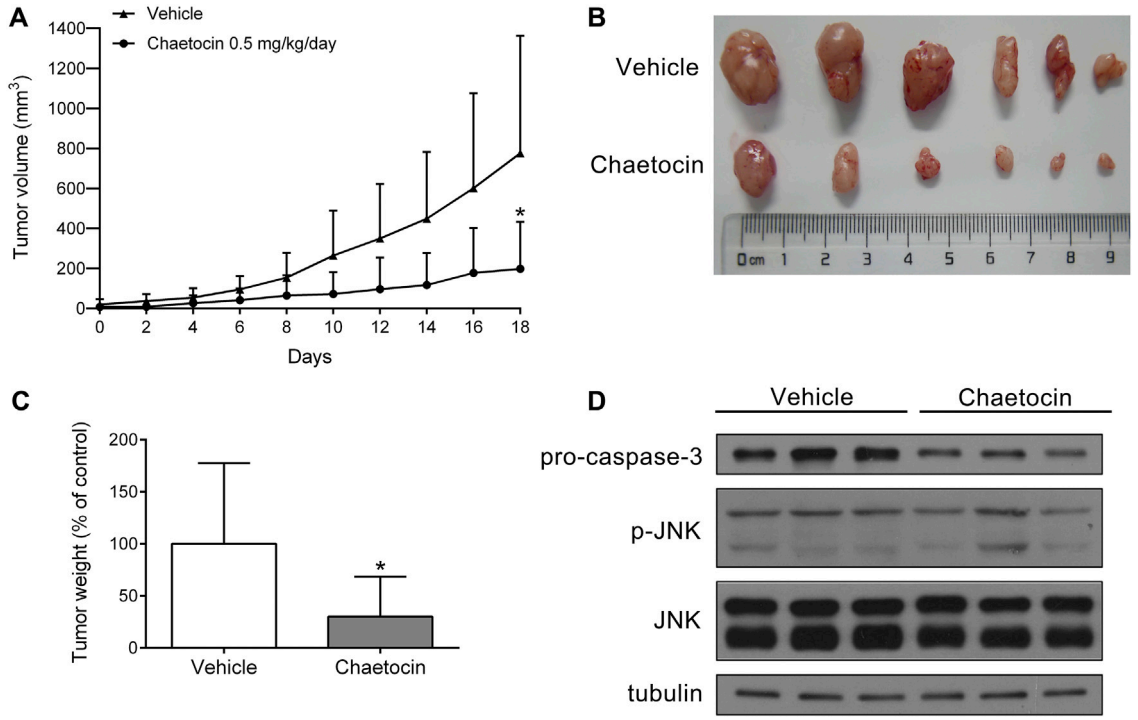


FIGURE 8 | Chaetocin inhibits the growth of CRC cell xenografts. Nude mice subcutaneously inoculated with HCT116 cells were subjected to chaetocin (0.5 mg/kg/day) treatment for 18 days, control group was treated with vehicle. **(A)** Tumor growth curves were recorded every other day.**(B)** and **(C)** The image of tumor tissue at the end of the experiment. **(D)** The protein levels of pro-caspase-3 and JNK in tumor tissues were detected by western blot. For **(A)** and **(C)**, results were shown as mean ± SD of six mice in each group. *$p < 0.05$, versus vehicle group.

evaluate the expression of several antiapoptotic proteins (BCL-2, BCL-XL, MCL-1 and XIAP) in CRC cells lines (**Figure 2D**). The decrease in antiapoptotic proteins expression further established that chaetocin induces apoptosis in CRC cells. Lastly, z-VAD-fmk, a pan-caspase inhibitor, was implemented as a pretreatment. After the caspase pathway was restrained by z-VAD-fmk (**Supplementary Figure 2**), the apoptotic cell population following treatment with chaetocin was significantly restored in CRC cells (**Figure 2E**), indicating that chaetocin-elicited apoptosis of CRC cells depends on caspase activation.

The Accumulation of ROS is Crucial in Chaetocin-Induced CRC Cell Apoptosis

It was previously reported that chaetocin induces apoptosis through the accumulation of ROS in gastric cancer, glioma, and myeloma cells (Isham et al., 2007; Dixit et al., 2014; Wen et al., 2019). The fluorescent probe DCFH/DA was first used to validate that the ROS level rises after chaetocin treatment in HCT116 and LS174T cells (**Figure 3A**). Next, a ROS scavenger, NAC was used. Flow cytometry analysis showed that NAC almost abolished chaetocin-induced apoptosis in HCT116 and LS174T cells (**Figure 3B**). Moreover, PARP and caspase-3 cleavage induced by chaetocin were reversed when cells were cotreated with NAC (**Figure 3C**). These results suggest that Chaetocin-induced apoptosis in CRC cells relies on ROS accumulation.

The ROS/JNK/C-Jun Pathway Is Involved in Chaetocin-Induced CRC Cell Apoptosis

It is well known that ROS induce cancer cell apoptosis by activating the JNK/c-Jun pathway (Aggarwal et al., 2019). To explore whether chaetocin-induced apoptosis take on the same ROS/JNK/c-Jun route, several experiments were carried out. First, western blot results showed a markedly increase in JNK and c-Jun phosphorylation after chaetocin treatment (**Figure 4A**), suggesting JNK/c-Jun pathway activation. SP600125, owing to its ability to suppress JNK/c-Jun pathway, was then used to prove that chaetocin-induced cell death depends on JNK/c-Jun activation. As shown by the results of flow cytometry and western blot, SP600125 partially restored chaetocin-induced apoptosis in HCT116 and LS174T cells (**Figures 4B,C**). We finally investigated if ROS accumulation induced by chaetocin relates to JNK/c-Jun activation. As shown in **Figure 4D**, NAC restored the abnormal increase in phosphorylation of JNK and c-Jun after chaetocin treatment. The above results suggest that Chaetocin induces cell death through the ROS/JNK/c-Jun axis.

Chaetocin Induces Proliferation Inhibition and Apoptosis in 5-FU-resistant CRC Cells

We then explored whether chaetocin's effect could stretch into 5-FU-resistant CRC cells, using cell lines that has already been

established by our group (Wen et al., 2015; Wen et al., 2016). A similar and decent IC50 value of 0.054 μM was exhibited in the CCK8 cell viability assay (**Figure 5A**). Moreover, the same dose-dependent colony formation inhibition pattern could be observed in **Figure 5B** as well as the Increase in G2/M population as shown in **Figure 5C**. Flow cytometry and western blot results also certified that chaetocin induced apoptosis in HCT-15/5FU-R cells by caspase activation like that in normal CRC cells **Figures 5D,E**. These results illustrated that chaetocin could by pass 5-FU resistance in CRC cells.

Chaetocin-Induced Apoptosis in HCT-15/5FU-R Cells is Associated With the ROS/JNK/C-Jun Pathway

To check that chaetocin induces cell death through the same pathway in 5-FU resistant strains of CRC, similar experiments were performed in HCT-15/5FU-R cells. Similar increase in ROS was detected in HCT-15/5FU-R cells (**Figure 6A**). NAC overturned the apoptotic effect induced by chaetocin (**Figure 6B**). The above results established that chaetocin induces accumulation of ROS and ultimately leads to apoptosis. Moreover, the increase in phosphorylation of JNK and c-Jun confirms that chaetocin leads to JNK/c-Jun pathway activation in HCT-15/5FU-R cells (**Figure 6C**). Also SP600125 was able to partially reverse the effect of chaetocin-induced apoptosis (**Figures 6D,E**). In addition, chaetocin was no longer able to induce JNK/c-Jun activation after the ROS in cells were scavenged by NAC (**Figure 6F**). The above results illustrated that chaetocin Induces apoptosis in HCT-15/5FU-R cells through the same ROS/JNK/c-Jun axis as in 5-FU-sensitive CRC cell lines.

Chaetocin Decreases the Expression of CD47 in CRC Cells and Enhances Macrophage Phagocytosis

In recent years, more and more studies have shown that CD47 could be one of the key immune checkpoint molecules in tumor therapy (Lian et al., 2019; Hayat et al., 2019). The present study showed that chaetocin not only reduced the expression of CD47 at mRNA levels (**Figure 7A**), but also inhibited the expression of total CD47 protein and membrane CD47 protein in CRC cells (**Figures 7B,C**). The highly expressed CD47 on the surface enables tumor cells to evade from immune surveillance of macrophages (Russ et al., 2018). Our results showed that macrophages had an enhanced phagocytosis of HCT116 cells which were pretreated with chaetocin (**Figure 7D**), indicating that chaetocin could reduce the expression of CD47 in CRC cells and enhance macrophages phagocytosis of CRC cells. As ROS/JNK/c-Jun involvement in chaetocin treatment was established in our study, whether the expression of CD47 was down-regulated through ROS/JNK/c-Jun signaling pathway was then investigated. When NAC was used to scavenge ROS in chaetocin-treated HCT116 cells, the inhibitory effects of CD47 at mRNA and protein levels were both partially reversed (**Figures 7E,F**), indicating that ROS accumulation down-regulated the expression of CD47 in CRC cells at transcriptional levels. Although SP600125 did not reverse the reduction of CD47 at mRNA level, it reversed the reduction of CD47 at protein level in HCT116 cells (**Figures 7G,H**), indicating a post-transcriptional regulation of JNK/c-Jun on CD47. All these results illustrated that chaetocin decreased the expression of CD47 at both mRNA and protein levels in CRC cells and enhanced macrophages phagocytosis.

Chaetocin Suppresses the Growth of CRC Cell Xenografts

The role of chaetocin in tumor growth was assessed *in vivo* using a nude mouse xenograft model by subcutaneously inoculating them with HCT116 cells. Mice were treated with vehicle and chaetocin (0.5 mg/kg) by intraperitoneal injection every day for 18 days. As shown in **Figures 8A–C**, the volume and weight of tumor in HCT116 xenografts were effectively suppressed in the chaetocin-treated group compared with control group, suggesting that chaetocin effects tumor proliferation both *in vitro* and *in vivo*. The protein levels of pro-caspase-3 were decreased in chaetocin-treated tumors, while p-JNK levels were increased (**Figure 8D**), indicating that chaetocin induces cell apoptosis like *in vitro*, undertaking the JNK/c-Jun pathway in CRC cell xenografts.

DISCUSSION

Novel agents for CRC treatment are urgently needed to be developed, and natural products are important sources for new cancer drug discovery and development. In the present study, by investigating the natural product chaetocin, we found that chaetocin not only caused cell cycle arrest and induced cell death both *in vitro* and *in vivo* with decent efficacy, it also downregulated CD47 and the consequent phagocytosis by macrophages in CRC cells. This study highlights the promising role of chaetocin for CRC treatment.

It has been reported that basal ROS levels are higher in CRC than that in the normal counterparts (Haklar et al., 2001; Rainis et al., 2007), and CRC cells are more vulnerable to the accumulation of ROS, inducing intracellular ROS accumulation should be an efficient strategy for CRC treatment. Chaetocin has been found to cause ROS accumulation and hence leads to significant growth inhibition in various cancer cells such as gastric cancer cells, glioma and leukemia cells (Isham et al., 2007; Truitt et al., 2014; Wen et al., 2019). Consistent with these reports, we found that chaetocin also significantly increased ROS levels in CRC cells (**Figure 3A**) and chaetocin-induced CRC cells apoptosis was almost abrogated by the ROS scavenger NAC (**Figures 3B,C**).

Tibodeau *et al.* has reported that chaetocin is a competitive inhibitor of thioredoxin reductase (TRXR), an enzyme that decrease intracellular ROS levels in an extracellular model (Tibodeau et al., 2009), which is consistent with the results of our previous study that chaetocin lead to ROS accumulation by inactivating TRXR in GC cells (Wen et al., 2019). But in our CRC cells, chaetocin was unable to inactivate with TRXR (data not shown), even though the ROS levels in CRC cells with chaetocin treatment rose up distinctly. These results indicated that chaetocin elevated ROS in different ways owning to the model, and the direct target of chaetocin to elevate ROS in CRC cells remains to be verified. Hypoxia-inducible factor-1α (HIF-1α) have also been reported to be the target of chaetocin in hepatoma (Lee et al., 2011), however, this HIF-1α-targeting mechanism does not hold in other cancer cells

(Isham et al., 2012). Similarly, Chaetocin has also been reported to directly inhibit the methyl-transferase for lysine nine tri-methylation on histone H3 (SUV39H1) in acute myeloid leukemia (Lai et al., 2015), but some other studies reported that the inhibition of chaetocin in SU(VAR)three to nine was regulated by the accumulation of ROS induced by chaetocin (Chaib et al., 2012; Dixit et al., 2014; Zhang et al., 2017). Thus, we speculated that chaetocin exerts its multiple functions by inducing ROS accumulation.

It is widely known that JNK is an important downstream effector of ROS and induces apoptosis mainly by affecting cell mitochondria (Castro-Caldas et al., 2012; Sinha et al., 2013). Consistent with the report that chaetocin induces apoptosis via JNK activation in glioma cells (Dixit et al., 2014), chaetocin-activated JNK and c-Jun in CRC cells were also detected in our study (**Figure 4A**). Moreover, ROS inhibitor NAC reversed both the JNK/c-Jun activation and apoptosis (**Figure 4D**) further strengthened our speculation that chaetocin-induced CRC cell apoptosis through the ROS/JNK/c-Jun pathway. However, since SP600125, a JNK inhibitor, could not fully rescue CRC cells from apoptosis, this calls for future studies to fully reveal the whole picture of chaetocin-induced apoptosis in CRC cells.

Although 5-FU is able to induce cancer cell death by upregulating ROS levels, by genetic and epigenetic alterations, 5-FU-resistant CRC cells avoid the death threshold induced by the accumulation of ROS (Hwang et al., 2001; Kang et al., 2014). In this case, 5-FU-resistant CRC cells were able to withstand higher level of ROS, and hence may render them more sensitive to redox-targeted agents (Kang et al., 2014; Yao et al., 2017), which is consistent with our results (**Supplementary Figure 4** and **Figures 5A,D**). Therefore, chaetocin may be a promising agent in overcoming 5-FU resistance.

Different from what Lu et al. reported that chaetocin downregulated PD-L1 by inhibiting a histone-lysine N-methyltransferase 2A (Lu et al., 2017), our study indicated that chaetocin downregulated the expression of CD47 at both mRNA and protein levels via the accumulation of ROS. However, SP600125 was only able to reverse the inhibitory effect of chaetocin on CD47 at protein level, not mRNA level, in CRC cells (**Figures 7G,H**), which indicated that JNK/c-Jun could not regulate the expression of CD47 in CRC cells transcriptionally. It has been reported that the mRNA expression of CD47 could be regulated by NF-κB pathway in liver cancer cells (Lo et al., 2015) and Wnt/β-catenin in glioma cell (Gowda et al., 2018), which could both be regulated by ROS (Vallée and Lecarpentier, 2018; Capece et al., 2019). Combining the results of this study with those reported by others, here is a speculation that chaetocin regulates the expression of CD47 by regulating NF-κB and Wnt/β-catenin pathways via the accumulation of ROS. However, the regulation of CD47 by chaetocin in CRC cells remains further exploration. Although the enhancement of macrophage phagocytosis of CRC cells induced by chaetocin is shown in our study, this effect of chaetocin still needs further verification in animals.

CONCLUSION

This study not only showed the cytotoxic effects of chaetocin on killing CRC cells ignoring 5-FU resistance, but also showed the reduction of CD47 and enhancement of macrophages phagocytosis of CRC cells induced by chaetocin (As shown in the graph abstract). Our research confirmed the excellent anti-tumor effect of chaetocin in CRC with "double dimensions", highlighting the potential of chaetocin as a promising agent for CRC treatment.

DATA AVAILABILITY STATEMENT

The original contributions presented in the study are included in the article/**Supplementary Material**, further inquiries can be directed to the corresponding authors.

ETHICS STATEMENT

The studies involving human participants were reviewed and approved by The Medical Ethics Committee of the Sixth Affiliated Hospital of Sun Yat-sen University, Guangzhou, China. Written informed consent for participation was not required for this study in accordance with the national legislation and the institutional requirements. The animal study was reviewed and approved by The Public Health Service Policy on Humane Care of Laboratory Animals and approved by the Institution Animal Care and Use Committee (IACUC) at Guangdong Laboratory Animals Monitoring Institute.

AUTHOR CONTRIBUTIONS

HW: Conceptualization, Investigation, Writing—original draft. CW: Conceptualization, Validation, Writing—review and editing. SC: Investigation, Methodology. WL: Investigation, Writing - review and editing. QQ: Methodology, Writing - review and editing. LH: Investigation. FW: Investigation, Validation. JC: Validation. WY: Writing - review and editing. WL: Project administration. JP: Resources. XY: Conceptualization, Supervision. HL: Conceptualization, Supervision.

FUNDING

This work was supported by China Postdoctoral Science Foundation (grant number 2020M683114); National Natural Science Foundation of China (grant number 81672413); Project to Attract High Level Foreign Experts (grant number G20190019023) and National Key Clinical Discipline.

SUPPLEMENTARY MATERIAL

The Supplementary Material for this article can be found online at: https://www.frontiersin.org/articles/10.3389/fphar.2021.729367/full#supplementary-material

REFERENCES

Aggarwal, V., Tuli, H. S., Varol, A., Thakral, F., Yerer, M. B., Sak, K., et al. (2019). Role of Reactive Oxygen Species in Cancer Progression: Molecular Mechanisms and Recent Advancements. *Biomolecules* 9. doi:10.3390/biom9110735

Biagi, J. J., Raphael, M. J., Mackillop, W. J., Kong, W., King, W. D., and Booth, C. M. (2011). Association between Time to Initiation of Adjuvant Chemotherapy and Survival in Colorectal Cancer: a Systematic Review and Meta-Analysis. *JAMA* 305, 2335–2342. doi:10.1001/jama.2011.749

Burgess, T. L., Amason, J. D., Rubin, J. S., Duveau, D. Y., Lamy, L., Roberts, D. D., et al. (2020). A Homogeneous SIRPα-CD47 Cell-Based, Ligand-Binding Assay: Utility for Small Molecule Drug Development in Immuno-Oncology. *PLoS One* 15, e0226661. doi:10.1371/journal.pone.0226661

Capece, D., Verzella, D., Di Francesco, B., Alesse, E., Franzoso, G., and Zazzeroni, F. (2019). NF-kappaB and Mitochondria Cross Paths in Cancer: Mitochondrial Metabolism and beyond. *Semin. Cel Dev Biol* 98, 118–128. doi:10.1016/j.semcdb.2019.05.021

Castro-Caldas, M., Carvalho, A. N., Rodrigues, E., Henderson, C., Wolf, C. R., and Gama, M. J. (2012). Glutathione S-Transferase Pi Mediates MPTP-Induced C-Jun N-Terminal Kinase Activation in the Nigrostriatal Pathway. *Mol. Neurobiol.* 45, 466–477. doi:10.1007/s12035-012-8266-9

Chaib, H., Nebbioso, A., Prebet, T., Castellano, R., Garbit, S., Restouin, A., et al. (2012). Anti-leukemia Activity of Chaetocin via Death Receptor-dependent Apoptosis and Dual Modulation of the Histone Methyl-Transferase SUV39H1. *Leukemia* 26, 662–674. doi:10.1038/leu.2011.271

Dekker, E., Tanis, P. J., Vleugels, J. L. A., Kasi, P. M., and Wallace, M. B. (2019). Colorectal Cancer. *Lancet* 394, 1467–1480. doi:10.1016/S0140-6736(19)32319-0

Dixit, D., Ghildiyal, R., Anto, N. P., and Sen, E. (2014). Chaetocin-induced ROS-Mediated Apoptosis Involves ATM-YAP1 axis and JNK-dependent Inhibition of Glucose Metabolism. *Cell Death Dis* 5, e1212. doi:10.1038/cddis.2014.179

Franke, A. J., Skelton, W. P., Starr, J. S., Parekh, H., Lee, J. J., Overman, M. J., et al. (2019). Immunotherapy for Colorectal Cancer: A Review of Current and Novel Therapeutic Approaches. *J. Natl. Cancer Inst.* 111, 1131–1141. doi:10.1093/jnci/djz093

Galadari, S., Rahman, A., Pallichankandy, S., and Thayyullathil, F. (2017). Reactive Oxygen Species and Cancer Paradox: To Promote or to Suppress. *Free Radic. Biol. Med.* 104, 144–164. doi:10.1016/j.freeradbiomed.2017.01.004

Ganesh, K., Stadler, Z. K., Cercek, A., Mendelsohn, R. B., Shia, J., Segal, N. H., et al. (2019). Immunotherapy in Colorectal Cancer: Rationale, Challenges and Potential. *Nat. Rev. Gastroenterol. Hepatol.* 16, 361–375. doi:10.1038/s41575-019-0126-x

Gowda, P., Patrick, S., Singh, A., Sheikh, T., and Sen, E. (2018). Mutant Isocitrate Dehydrogenase 1 Disrupts PKM2-β-Catenin-BRG1 Transcriptional Network-Driven CD47 Expression. *Mol. Cel Biol* 38, e00001. doi:10.1128/MCB.00001-18

Gunjur, A. (2019). Targeted Therapy for BRAF-Mutant Colorectal Cancer. *Lancet Oncol.* 20, e618. doi:10.1016/S1470-2045(19)30644-8

Haklar, G., Sayin-Ozveri, E., Yüksel, M., Aktan, A. O., and Yalçin, A. S. (2001). Different Kinds of Reactive Oxygen and Nitrogen Species Were Detected in colon and Breast Tumors. *Cancer Lett.* 165, 219–224. doi:10.1016/s0304-3835(01)00421-9

Hayat, S. M. G., Bianconi, V., Pirro, M., Jaafari, M. R., Hatamipour, M., and Sahebkar, A. (2019). CD47: Role in the Immune System and Application to Cancer Therapy. *Cel Oncol (Dordr)* 43 (1), 19–30. doi:10.1007/s13402-019-00469-5

Holmström, K. M., and Finkel, T. (2014). Cellular Mechanisms and Physiological Consequences of Redox-dependent Signalling. *Nat. Rev. Mol. Cel Biol* 15, 411–421. doi:10.1038/nrm3801

Horrigan, S. K. (2017). Replication Study: The CD47-Signal Regulatory Protein Alpha (SIRPa) Interaction Is a Therapeutic Target for Human Solid Tumors. *Elife* 6, e18173. doi:10.7554/eLife.18173

Hu, T., Liu, H., Liang, Z., Wang, F., Zhou, C., Zheng, X., et al. (2020). Tumor-intrinsic CD47 Signal Regulates Glycolysis and Promotes Colorectal Cancer Cell Growth and Metastasis. *Theranostics* 10, 4056–4072. doi:10.7150/thno.40860

Hwang, P. M., Bunz, F., Yu, J., Rago, C., Chan, T. A., Murphy, M. P., et al. (2001). Ferredoxin Reductase Affects P53-dependent, 5-Fluorouracil-Induced Apoptosis in Colorectal Cancer Cells. *Nat. Med.* 7, 1111–1117. doi:10.1038/nm1001-1111

Isham, C. R., Tibodeau, J. D., Bossou, A. R., Merchan, J. R., and Bible, K. C. (2012). The Anticancer Effects of Chaetocin Are Independent of Programmed Cell Death and Hypoxia, and Are Associated with Inhibition of Endothelial Cell Proliferation. *Br. J. Cancer* 106, 314–323. doi:10.1038/bjc.2011.522

Isham, C. R., Tibodeau, J. D., Jin, W., Xu, R., Timm, M. M., and Bible, K. C. (2007). Chaetocin: a Promising New Antimyeloma Agent with *In Vitro* and *In Vivo* Activity Mediated via Imposition of Oxidative Stress. *Blood* 109, 2579–2588. doi:10.1182/blood-2006-07-027326

Jalil, A. R., Andrechak, J. C., and Discher, D. E. (2020). Macrophage Checkpoint Blockade: Results from Initial Clinical Trials, Binding Analyses, and CD47-Sirpα Structure-Function. *Antib Ther.* 3, 80–94. doi:10.1093/abt/tbaa006

Kang, K. A., Piao, M. J., Kim, K. C., Kang, H. K., Chang, W. Y., Park, I. C., et al. (2014). Epigenetic Modification of Nrf2 in 5-Fluorouracil-Resistant colon Cancer Cells: Involvement of TET-dependent DNA Demethylation. *Cel Death Dis* 5, e1183. doi:10.1038/cddis.2014.149

Lai, Y. S., Chen, J. Y., Tsai, H. J., Chen, T. Y., and Hung, W. C. (2015). The SUV39H1 Inhibitor Chaetocin Induces Differentiation and Shows Synergistic Cytotoxicity with Other Epigenetic Drugs in Acute Myeloid Leukemia Cells. *Blood Cancer J.* 5, e313. doi:10.1038/bcj.2015.37

Lee, Y. M., Lim, J. H., Yoon, H., Chun, Y. S., and Park, J. W. (2011). Antihepatoma Activity of Chaetocin Due to Deregulated Splicing of Hypoxia-Inducible Factor 1α Pre-mRNA in Mice and *In Vitro*. *Hepatology* 53, 171–180. doi:10.1002/hep.24010

Li, Z., Huang, L., Wei, L., Hou, Z., Ye, W., and Huang, S. (2019). Chaetocin Induces Caspase-dependent Apoptosis in Ovarian Cancer Cells via the Generation of Reactive Oxygen Species. *Oncol. Lett.* 18, 1915–1921. doi:10.3892/ol.2019.10507

Lian, S., Xie, X., Lu, Y., and Jia, L. (2019). Checkpoint CD47 Function on Tumor Metastasis and Immune Therapy. *Onco Targets Ther.* 12, 9105–9114. doi:10.2147/OTT.S220196

Lindsay, J., Esposti, M. D., and Gilmore, A. P. (2011). Bcl-2 Proteins and Mitochondria-Sspecificity in Membrane Targeting for Death. *Biochim. Biophys. Acta* 1813, 532–539. doi:10.1016/j.bbamcr.2010.10.017

Liu, D. (2019). Cancer Biomarkers for Targeted Therapy. *Biomark Res.* 7, 25. doi:10.1186/s40364-019-0178-7

Liu, X., Guo, S., Liu, X., and Su, L. (2015). Chaetocin Induces Endoplasmic Reticulum Stress Response and Leads to Death Receptor 5-dependent Apoptosis in Human Non-small Cell Lung Cancer Cells. *Apoptosis* 20, 1499–1507. doi:10.1007/s10495-015-1167-4

Lo, J., Lau, E. Y., Ching, R. H., Cheng, B. Y., Ma, M. K., Ng, I. O., et al. (2015). Nuclear Factor Kappa B-Mediated CD47 Up-Regulation Promotes Sorafenib Resistance and its Blockade Synergizes the Effect of Sorafenib in Hepatocellular Carcinoma in Mice. *Hepatology* 62, 534–545. doi:10.1002/hep.27859

Lou, Q., Liu, R., Yang, X., Li, W., Huang, L., Wei, L., et al. (2019). miR-448 Targets Ido1 and Regulates CD8+ T Cell Response in Human colon Cancer. *J. Immunother. Cancer* 7, 210. doi:10.1186/s40425-019-0691-0

Lu, C., Paschall, A. V., Shi, H., Savage, N., Waller, J. L., Sabbatini, M. E., et al. (2017). The MLL1-H3K4me3 Axis-Mediated PD-L1 Expression and Pancreatic Cancer Immune Evasion. *J. Natl. Cancer Inst.* 109, djw283. doi:10.1093/jnci/djw283

Mandal, R., Barrón, J. C., Kostova, I., Becker, S., and Strebhardt, K. (2020). Caspase-8: The Double-Edged Sword. *Biochim. Biophys. Acta Rev. Cancer* 1873, 188357. doi:10.1016/j.bbcan.2020.188357

Matlung, H. L., Szilagyi, K., Barclay, N. A., and van den Berg, T. K. (2017). The CD47-Sirpα Signaling axis as an Innate Immune Checkpoint in Cancer. *Immunol. Rev.* 276, 145–164. doi:10.1111/imr.12527

Miller, T. W., Amason, J. D., Garcin, E. D., Lamy, L., Dranchak, P. K., Macarthur, R., et al. (2019). Quantitative High-Throughput Screening Assays for the Discovery and Development of SIRPα-CD47 Interaction Inhibitors. *PLoS One* 14, e0218897. doi:10.1371/journal.pone.0218897

Newman, D. J., and Cragg, G. M. (2020). Natural Products as Sources of New Drugs over the Nearly Four Decades from 01/1981 to 09/2019. *J. Nat. Prod.* 83, 770–803. doi:10.1021/acs.jnatprod.9b01285

Ozyerli-Goknar, E., Sur-Erdem, I., Seker, F., Cingöz, A., Kayabolen, A., Kahya-Yesil, Z., et al. (2019). The Fungal Metabolite Chaetocin Is a Sensitizer for Pro-apoptotic Therapies in Glioblastoma. *Cel Death Dis* 10, 894. doi:10.1038/s41419-019-2107-y

Rainis, T., Maor, I., Lanir, A., Shnizer, S., and Lavy, A. (2007). Enhanced Oxidative Stress and Leucocyte Activation in Neoplastic Tissues of the colon. *Dig. Dis. Sci.* 52, 526–530. doi:10.1007/s10620-006-9177-2

Reuter, S., Gupta, S. C., Chaturvedi, M. M., and Aggarwal, B. B. (2010). Oxidative Stress, Inflammation, and Cancer: How Are They Linked. *Free Radic. Biol. Med.* 49, 1603–1616. doi:10.1016/j.freeradbiomed.2010.09.006

Russ, A., Hua, A. B., Montfort, W. R., Rahman, B., Riaz, I. B., Khalid, M. U., et al. (2018). Blocking "don't Eat Me" Signal of CD47-Sirpα in Hematological Malignancies, an In-Depth Review. *Blood Rev.* 32, 480–489. doi:10.1016/j.blre.2018.04.005

Sclafani, F. (2019). MEK and PD-L1 Inhibition in Colorectal Cancer: a Burning Blaze Turning into a Flash in the pan. *Lancet Oncol.* 20, 752–753. doi:10.1016/S1470-2045(19)30076-2

Sekita, S., Yoshihira, K., Natori, S., Udagawa, S., Muroi, T., Sugiyama, Y., et al. (1981). Mycotoxin Production by Chaetomium Spp. And Related Fungi. *Can. J. Microbiol.* 27, 766–772. doi:10.1139/m81-119

Sinha, K., Das, J., Pal, P. B., and Sil, P. C. (2013). Oxidative Stress: the Mitochondria-dependent and Mitochondria-independent Pathways of Apoptosis. *Arch. Toxicol.* 87, 1157–1180. doi:10.1007/s00204-013-1034-4

Sung, H., Ferlay, J., Siegel, R. L., Laversanne, M., Soerjomataram, I., Jemal, A., et al. (2021). *Global Cancer Statistics 2020: GLOBOCAN Estimates of Incidence and Mortality Worldwide for 36 Cancers in 185 Countries*. CA: A Cancer Journal for Clinicians.

Tafani, M., Sansone, L., Limana, F., Arcangeli, T., De Santis, E., Polese, M., et al. (2016). The Interplay of Reactive Oxygen Species, Hypoxia, Inflammation, and Sirtuins in Cancer Initiation and Progression. *Oxid Med. Cel Longev* 2016, 1–18. doi:10.1155/2016/3907147

Tibodeau, J. D., Benson, L. M., Isham, C. R., Owen, W. G., and Bible, K. C. (2009). The Anticancer Agent Chaetocin Is a Competitive Substrate and Inhibitor of Thioredoxin Reductase. *Antioxid. Redox Signal.* 11, 1097–1106. doi:10.1089/ars.2008.2318

Truitt, L., Hutchinson, C., DeCoteau, J. F., and Geyer, C. R. (2014). Chaetocin Antileukemia Activity against Chronic Myelogenous Leukemia Cells Is Potentiated by Bone Marrow Stromal Factors and Overcomes Innate Imatinib Resistance. *Oncogenesis* 3, e122. doi:10.1038/oncsis.2014.37

Vallée, A., and Lecarpentier, Y. (2018). Crosstalk between Peroxisome Proliferator-Activated Receptor Gamma and the Canonical WNT/β-Catenin Pathway in Chronic Inflammation and Oxidative Stress during Carcinogenesis. *Front. Immunol.* 9, 745. doi:10.3389/fimmu.2018.00745

Wang, H., Wen, C., Chen, S., Wang, F., He, L., Li, W., et al. (2020). Toosendanin-induced Apoptosis in Colorectal Cancer Cells Is Associated with the κ-opioid Receptor/β-Catenin Signaling axis. *Biochem. Pharmacol.* 177, 114014. doi:10.1016/j.bcp.2020.114014

Wen, C., Chen, J., Zhang, D., Wang, H., Che, J., Qin, Q., et al. (2016). Pseudolaric Acid B Induces Mitotic Arrest and Apoptosis in Both 5-Fluorouracil-Sensitive and -resistant Colorectal Cancer Cells. *Cancer Lett.* 383, 295–308. doi:10.1016/j.canlet.2016.09.007

Wen, C., Huang, L., Chen, J., Lin, M., Li, W., Lu, B., et al. (2015). Gambogic Acid Inhibits Growth, Induces Apoptosis, and Overcomes Drug Resistance in Human Colorectal Cancer Cells. *Int. J. Oncol.* 47, 1663–1671. doi:10.3892/ijo.2015.3166

Wen, C., Wang, H., Wu, X., He, L., Zhou, Q., Wang, F., et al. (2019). ROS-mediated Inactivation of the PI3K/AKT Pathway Is Involved in the Antigastric Cancer Effects of Thioredoxin Reductase-1 Inhibitor Chaetocin. *Cel Death Dis* 10, 809. doi:10.1038/s41419-019-2035-x

Yao, C. W., Kang, K. A., Piao, M. J., Ryu, Y. S., Fernando, P. M. D. J., Oh, M. C., et al. (2017). Reduced Autophagy in 5-Fluorouracil Resistant Colon Cancer Cells. *Biomol. Ther. (Seoul)* 25, 315–320. doi:10.4062/biomolther.2016.069

Zhang, S., Yin, J., and Zhong, J. (2017). Chaetocin Reactivates the Lytic Replication of Epstein-Barr Virus from Latency via Reactive Oxygen Species. *Sci. China Life Sci.* 60, 66–71. doi:10.1007/s11427-016-0286-7

Conflict of Interest: The authors declare that the research was conducted in the absence of any commercial or financial relationships that could be construed as a potential conflict of interest.

Publisher's Note: All claims expressed in this article are solely those of the authors and do not necessarily represent those of their affiliated organizations, or those of the publisher, the editors and the reviewers. Any product that may be evaluated in this article, or claim that may be made by its manufacturer, is not guaranteed or endorsed by the publisher.

Copyright © 2021 Wang, Wen, Chen, Li, Qin, He, Wang, Chen, Ye, Li, Peng, Yang and Liu. This is an open-access article distributed under the terms of the Creative Commons Attribution License (CC BY). The use, distribution or reproduction in other forums is permitted, provided the original author(s) and the copyright owner(s) are credited and that the original publication in this journal is cited, in accordance with accepted academic practice. No use, distribution or reproduction is permitted which does not comply with these terms.

frontiers in Pharmacology

ORIGINAL RESEARCH
published: 10 November 2021
doi: 10.3389/fphar.2021.749766

An Ethanolic Extract of *Cucurbita pepo* L. Seeds Modifies Neuroendocrine Disruption in Chronic Stressed Rats and Adrenal Expression of Inflammatory Markers and HSP70

*Hailah M. Almohaimeed[1], Shereen Hamed[2], Hanan S. Seleem[3,4], Ashwaq H. Batawi[5], Zuhair M. Mohammedsaleh[6], Maha Jameal Balgoon[7], Soad S. Ali[8,9], Soad Al Jaouni[9,10] and Nasra Ayuob[11]**

[1]Department of Basic Science, College of Medicine, Princess Nourah Bint Abdulrahman University (PNU), Riyadh, Saudi Arabia, [2]Department of Medical Histology and Cell Biology, Faculty of Medicine, Mansoura University, Mansoura, Egypt, [3]Histology Department, Faculty of Medicine, Menoufia University, Shebin ElKoum, Egypt, [4]Department of Basic Medical Sciences, Unaizah College of Medicine and Medical Sciences, Qassim University, Buraydah, Saudi Arabia, [5]Department of Biological Science, Faculty of Science, King Abdulaziz University, Jeddah, Saudi Arabia, [6]Department of Medical Laboratory Technology, Faculty of Applied Medical Sciences, University of Tabuk, Tabuk, Saudi Arabia, [7]Department of Biochemistry, Faculty of Science, King Abdulaziz University, Jeddah, Saudi Arabia, [8]Department of Histology and Cell Biology, Faculty of Medicine, Assuit University, Asyut, Egypt, [9]Yousef Abdullatif Jameel Chair of Prophetic Medical Applications (YAJCPMA), Faculty of Medicine, King Abdulaziz University, Jeddah, Saudi Arabia, [10]Department of Hematology/Pediatric Oncology, King Abdulaziz University Hospital (KAUH), Faculty of Medicine, King Abdulaziz University, Jeddah, Saudi Arabia, [11]Department of Medical Histology, Faculty of Medicine, Damietta University, Damietta, Egypt

OPEN ACCESS

Edited by:
Hong Zhang,
Shanghai University of Traditional Chinese Medicine, China

Reviewed by:
Stefania Schiavone,
University of Foggia, Italy
Sladjana Dronjak,
University of Belgrade, Serbia

***Correspondence:**
Nasra Ayuob
nasraayuob@gmail.com

Specialty section:
This article was submitted to Ethnopharmacology, a section of the journal Frontiers in Pharmacology

Received: *29 July 2021*
Accepted: *30 September 2021*
Published: *10 November 2021*

Citation:
Almohaimeed HM, Hamed S, Seleem HS, Batawi AH, Mohammedsaleh ZM, Balgoon MJ, Ali SS, Al Jaouni S and Ayuob N (2021) An Ethanolic Extract of Cucurbita pepo *L. Seeds Modifies Neuroendocrine Disruption in Chronic Stressed Rats and Adrenal Expression of Inflammatory Markers and HSP70. Front. Pharmacol. 12:749766. doi: 10.3389/fphar.2021.749766*

Background: Pumpkins (*Cucurbita pepo* L.) were described to have antioxidant, anti-inflammatory, anti-fatigue, and antidepressant-like effect. The adrenal gland is an important stress-responsive organ that maintains homeostasis during stress.

Objectives: This study aimed to assess the efficacy of the administration of *Cucurbita pepo* L. (CP) extract in relieving behavioral, biochemical, and structural changes in the adrenal gland induced by exposure to chronic unpredictable mild stress (CUMS) and to explore the mechanism behind this impact.

Materials and Methods: Forty male albino rats were divided into 4 groups (n = 10): control, CUMS, fluoxetine-treated, and CP-treated groups. Behavioral changes, corticosterone level, pro-inflammatory cytokines TNF-α and IL-6, and oxidant/antioxidant profile were assessed in the serum at the end of the experiment. Adrenal glands were processed for histopathological and immunohistochemical assessment. Gene expression of caspase-3 and Ki67 and heat shock protein 70 (HSP70) were assessed in adrenal glands using RT-PCR.

Results: The CP extract significantly reduced the corticosterone level ($p < 0.001$), immobility time ($p < 0.001$), and inflammatory and oxidative changes associated with CUMS-induced depression compared to the untreated group. The CP extract alleviated CUMS-induced adrenal histopathological changes and significantly reduced apoptosis ($p < 0.001$) and significantly upregulated antioxidant levels in the serum.

Conclusion: *Cucurbita pepo* L. effectively ameliorated the chronic stress-induced behavioral, biochemical, and adrenal structural changes mostly through its antioxidant and anti-inflammatory effects.

Keywords: pumpkin, stress, depression, caspase-3, ki67, Hsp70, apoptosis

INTRODUCTION

More than 264 million people of all ages suffer depression all over the world (WHO, 2020). The performance of the depressed person is generally poor at school, at work, and in the family. Depression may lead to suicide; so, it is considered the second leading cause of death in 15- to 29-year-olds (WHO, 2020). Mammals can survive stressful events by activation of appropriate physiological responses to these events. The adrenal gland is part of the hypothalamic–pituitary–adrenocortical (HPA) axis and the sympatho–adrenomedullary axis that maintain homeostasis during stress (Ulrich-Lai et al., 2006). It was reported that exposure to thermal stress results in rapid expression of HSP70 in the adrenal cortex (Huang et al., 2001). These proteins share intracellular trafficking, antigen presentation, apoptosis, and many other actions (Khar et al., 2001). It has been described that exogenous hormones or interference with endogenous hormones, during the critical periods of development, can have permanent effects on the physiological and behavioral pathways regulated by hypothalamic neuroendocrine circuits (Gore and Patisaul, 2010). Neuroendocrine disruption was also described to extend the concept of endocrine disruption to include the full breadth of integrative physiology; therefore, it is more than hormonal upset (Waye and Trudeau, 2011).

Changes in neuroendocrine regulation, metabolism, and diet/microbiota are considered triggers for inflammation and predispose to developing depression (Huang et al., 2019). It was postulated that depression—one of the neuropsychiatric disorders—and inflammation have a two-way relationship. While depression promotes inflammatory reactions, inflammation promotes neuropsychiatric disorders including depression (Bauer and Teixeira, 2019).

Fluoxetine, a classical antidepressant, is among the drugs available in the market for treatment of depression. It is now considered as an emerging neuroendocrine disruptor. This effect of fluoxetine is a side effect, rather than main therapeutic targets in mammals (León-Olea et al., 2014). Therefore, there is a need for safer antidepressant with no side effects on the neuroendocrine status.

Pumpkins (*Cucurbita pepo* L.) are economically important species cultivated worldwide. They have nutritional and health benefits as they are rich in phenolics, flavonoids, amino acids, carbohydrates, and vitamins (Wang et al., 2002). Several research studies revealed that pumpkins have extensive bioactivities, such as antidiabetic, anticancer, antioxidant, anti-inflammatory, anti-fatigue, and antidepressant-like effect (Wang et al., 2012; Zhang et al., 2012; Nawirska-Olszańska et al., 2013; Kim Nr et al., 2016). Traditional medicine mainly Ayurvedic systems and Chinese medicine have used different parts of the pumpkin, including flesh of the fruits and seeds (Perez Gutierrez, 2016). The antidepressant efficacy of Sweetme Sweet Pumpkin (SSP) and *Cucurbita moschata Duch* was previously tested in an *in vivo* study using a forced swimming test (FST)–induced animal model of depression and was compared with fluoxetine (Kim Nr et al., 2016). In one of the relatively recent reviews that summarized that the antidepressant foods, such as pumpkin seeds, were described to have an antidepressant food score of 47%, providing its antidepressant-like effect (Lachance and Ramsey, 2018). Recently, Dotto and Chacha endorsed conducting more animal- and clinical trial-based research studies in order to confirm the ameliorative effect of pumpkin seeds on depression (Dotto and Chacha, 2020).

These reports were encouraging to test the efficacy of pumpkins in alleviating the impact of chronic stress on the adrenal glands. Therefore, this study was performed to assess the effect of oral administration of the *Cucurbita pepo L.* (CP) extract on relieving the chronic unpredictable mild stress (CUMS)–induced behavioral, biochemical, and adrenal structure and to explore the mechanism behind this impact.

MATERIALS AND METHODS

Extraction and Dosage of Pumpkin

Cucurbita pepo L. (voucher specimen: AQJ_95) were purchased from the local market at Jeddah, Saudi Arabia. They were identified in the King Abdulaziz University herbarium using specimens of herbarium and the flora of KSA (Chaudhary, 2001). Voucher specimens were deposited in the herbarium. CP was identified by the authors and was verified by a botanist from the Faculty of Science, King Abdulaziz University.

Extraction of CP was done according to the previous studies (Wang et al., 2012). The raw fruits with the peel were cut using a slicer and dried using a lyophilizer (FD5508; ilShinBioBase Co., Ltd., Korea) and then crushed by using an electrical grinding machine. The powder was passed through a 40-mesh sieve to get a fine powder and stored in an airtight container. The dried powder (50 g) was mixed with 450 ml of 80% ethanol and left for 1 day at 37°C in a shaker (JSSI-100T; JS Research Inc., Compact Shaking Incubator., Korea) and then was filtered with cotton and filter paper on the second day. This extraction process was repeated twice at 37°C to get an ethanol extract.

Identification of the Constituents of CP

The chemical composition of PE was analyzed using a trace gas chromatography GC-TSQ evo 8000 mass spectrometer (Thermo Scientific, Austin, TX, United States) with a direct capillary column TG–5MS (30 m × 0.25 mm × 0.25 μm film thickness).

TABLE 1 | List of the stressors used in the CUMS protocol used in this study during the 1st week. These stressors were repeated during the 2nd, 3rd, and 4th weeks at different time points (Doron et al., 2014).

	Week
Day 1	Restraint stress (4 h)
Day 2	Placement in an empty cage with water at the bottom and lights on (4 h)
Day 3	Title cages at 30° (4 h)
Day 4	Placing mice in cages with wet sawdust (4 h)
Day 5	Placing mice in soiled cages of other mice (4 h)
Day 6	Restraint stress (4 h)
Day 7	Reversal of the light/dark cycle (4 h)

The column oven temperature was initially set to 50°C and then increased by 5°C/min to 250°C and held for 2 min and then increased to a final temperature of 300°C by 25°C/min and held for 2 min. The injector and MS transfer line temperatures were kept at 270 and 260°C, respectively; helium was used as a carrier gas at a constant flow rate of 1 ml/min. The solvent delay was 4 min, and diluted samples of 3 µl were injected automatically using an Autosampler AS1300 coupled with GC in the splitless mode in a PTV injector. EI mass spectra were collected at 70 eV ionization voltages over the range of m/z 50–650 in the full scan mode. The ion source temperature was set at 250°C. The components were identified by comparison of their mass spectra with those of WILEY 09 and NIST 14 mass spectral database that are used to identify and study the chemical composition of unknown components in any extract (Wiley, 2006; Mikaia et al., 2014). Analysis had been done in qualitative type using Thermo Scientific™ Xcalibur™ 2.2 software, and all values were reported in relative percentage (Abd El-Kareem et al., 2016).

Experimental Design

This study was approved by the Biomedical Research Ethics Committee at the Faculty of Medicine, King Abdulaziz University, Jeddah, KSA (reference number 45-20). In this study, forty male albino rats weighing 150–200 g and aged 2–3 months were obtained from the King Fahd Medical Research Center (KFMRC). Before starting the experiment, the rats were left to acclimatize to the laboratory conditions for 1 week. Ten rats were assigned as the control group which was left unexposed to CUMS. The other thirty rats were subjected to the procedure of CUMS for 4 weeks that included different types of stressors at different times during the day in order to prevent habituation to stress. The CUMS procedure was fully described in previous works (Ayuob et al., 2016; Ali et al., 2017) and was shown in **Table 1**. The rats exposed to CUMS were divided into 3 groups (n = 10). The untreated group (CUMS) received the vehicle 0.03% carboxymethyl cellulose (CMC-Na) by gavage for 2 weeks. The FLU-treated group received FLU (Dar Al Dawa Pharmaceuticals Co., Ltd., Amman, Jordan), an antidepressant used for pharmacological validation, dissolved in CMC-Na 0.03% at a dose of 20 mg/kg by gastric gavage (Li et al., 2014). The CP-treated group received the CP extract dissolved in distilled water at a dose of 100 mg/kg by gavage for 2 weeks according to Wang et al. (2012).

Behavioral Changes Assessment

The FST was performed after 4 weeks to confirm the effect of CUMS on the rats (Ali et al., 2017). During this test, each rat was placed in a glassy cylindrical container (height 20 cm, diameter 14 cm) with 15 cm of water at 25 ± 2°C. The rat was videotaped for 6 min using behavior software (Noldus Information Technology, EthoVision XT®), and the total time spent immobile during the 6 min was measured by a technician blind to the experiment groups. The total time, in seconds, spent by the rats without limb movement, except for the minor movement necessary to keep the mouse afloat, "immobility time" during the 6 min was determined.

Biochemical Techniques

Twenty four hours after finishing the behavior test, blood samples were taken from the intra-orbital sinus of rats after being anesthetized with 4% isoflurane (SEDICO Pharmaceuticals Company, Cairo, Egypt) in 100% oxygen. After that, the rats were euthanized by cervical dislocation. Blood samples were centrifuged at 3,000 rpm for 15 min at 4°C to obtain the serum and were kept at −18°C for biochemical assessment.

The level of corticosterone (ALPCO Diagnostics, Orangeburg, NY, United States) was assessed using enzyme-linked immunosorbent assay kits according to the manufacturer's instructions. According to the manufacturer's instructions, TNF-α and IL-6 (Quantakin R&D system, USA Kit) were assessed by using enzyme-linked immunosorbent assay. The optical density of each sample was determined in duplicate with a microplate ELISA reader set to 450 nm.

The thiobarbituric acid reactive substances (TBARS) assay kit (Biodiagnostic; Egypt) was utilized to measure the level of malondialdehyde (MDA) spectrophotometrically at 535 nm (Gamal et al., 2018). The level of superoxide dismutase (SOD) was measured by using the SOD assay kit (Biodiagnostic; Egypt) (Packer, 2002). The assessment of the glutathione peroxidase (GPX) level was performed by using the GPX kit (Randox Labs, Crumlin, United Kingdom). To quantify the activity of catalase (CAT), a calibration curve was generated for the assay and all samples, using assay kits (Biodiagnostic; Egypt). The method is previously described (Gamal et al., 2018).

Quantitative Real-Time PCR

RNA extraction from the tissue samples was done using the TriFast™ reagent (PeqLab, Germany, Cat No.: 30-2010), as described in the manufacturer's protocol. The concentration of

the purified RNA was estimated by using a NanoDrop 2000c spectrophotometer (Thermo Scientific, United States). The extracted RNA from each sample was reverse transcribed using the SensiFAST™ cDNA synthesis kit for RT-qPCR (Bioline USA Inc., United States, Cat No.: BIO-65053), following the manufacturer's instruction. The synthesized cDNA was stored at -80°C until utilization for qRT-PCR.

The qRT-PCR reactions were performed using the SensiFAST™ SYBR Lo-ROX kit (Bioline USA Inc., United States, Cat No.: BIO-94002) on the Applied Biosystems 7500 real-time PCR detection system (Life technology, United States). Gene-specific primers for rats, used in this study, were designed by Primer3 software (v.0.4.0),and their specificity was checked using NCBI/Primer-BLAST program. The primers were then purchased from Willowfort™ (United Kingdom). The primers were GAPDH (5′-TGCACCACCAACTGCTTAGC-3′, 5′-GGC ATGGACTGTGGTCATGAG-3′), caspase-3 (forward 5- TGT ATGCTTACTCTACCGCACCCG-3, reverse 5-GCGCAAAGT GACTGGATGAACC-3), HSP70 (5′-ACGAGGGTCTCAAGG GCAAG-3′, 5′-CTCTTTCTCAGCCAGCGTGTTAG-3′).

Ki67 (forward 5-AGAAGAGCCCACAGCACAGAGAA-3, reverse 5-AGAAGAGCCCACAGCACAGAGAA 3). The PCR mixture was prepared as follows: 10 µl SensiFAST™ SYBR Lo-ROX mix, 0.8 µl forward primer, 0.8 µl reverse primer, 2 µl template cDNA, and 6.4 µl nuclease-free water. The reaction mix was transferred to a thermal cycler that was previously programmed to hold at 95°C for 2 min, followed by 40 cycles of 95°C for 15 s, and then 60°C for 30 s. A negative control reaction containing no template was run in each experiment.

Melting curve analysis was carried out to prove specificity of PCR products, and the Ct value for each reaction was obtained from amplification plots. The relative quantification for each gene expression in the tissue samples was calculated using the comparative threshold (ΔΔCt) method with GAPDH as the internal control gene. For the overall fold change, it was calculated and linearized by the $2^{-\Delta\Delta Ct}$ arithmetic formula.

Histological Techniques

At the end of the experiment and after the rats were anesthetized, the abdomen was opened and the right adrenal gland was dissected out. To obtain paraffin blocks, fixation of the adrenal gland in 10% neutral buffered formalin and further processes were performed. The paraffin sections of 4-µm thickness were prepared and stained with hematoxylin and eosin (H&E). Moreover, other paraffin sections were immunohistochemically stained using the streptavidin–biotin–peroxidase technique. Slides were incubated overnight at 4°C, and then they were incubated with monoclonal anti-Ki67 (Dako Cytomation, United States, at dilution 1:1,000) for demonstration of cell proliferation. In addition, polyclonal anti-caspase-3 antibody (Santa Cruz Biotechnology, United States, at dilution 1:1,000) was utilized for the detection of apoptosis. A polyclonal antibody against heat shock protein-70 (HSP70) (Dako, Carpinteria, CA, United States, at dilution 1:1,000) was also utilized. Corresponding biotinylated conjugated secondary antibody from the Dako staining system was used. The slides stained with the secondary antibody only were used as negative controls.

The nuclei were counterstained with hematoxylin. Brown cytoplasmic staining was considered a positive reaction. The stained sections were examined and photographed using an Olympus Microscope BX-51 (Olympus) connected to a digital camera and a computer. Semiquantitative analysis of antibody immunoreactivity was done by Pro Plus image analysis software. The percentage area of the immunopositive reaction was assessed in 30 fields at ×400 magnification. The positive cells were counted per 1.0 mm^2 of area, as described by Zhou et al. (2016). At least five fields from each slide were examined, and the mean was calculated for each animal.

For morphometric analysis, four sections were examined in each animal (magnification ×100). The thickness of different zones of the adrenal gland was measured in micrometers. The adrenal cortex thickness was obtained by measuring the distance between the medulla and the adrenal capsule in a straight line, one measurement being taken in each quadrant of the adrenal cortex.

Statistical Analysis

The behavioral, biochemical, and immunohistochemical data were analyzed by the Statistical Package for the Social Sciences (SPSS) version 16. The study variables were affected by two independent factors: stress exposure and treatment. Therefore, analysis using a mixed-model two-way ANOVA based on Bonferroni post hoc was performed. Statistical significance was considered at $p < 0.05$.

RESULTS

Behavioral Results

The immobility time during the FST was significantly higher ($p = 0.03$) in the CUMS group than the control, whereas it was significantly lower ($p = 0.01$, $p = 0.001$) in FLU- and CP-treated groups than in the CUMS group (**Figure 1A**).

Results of CP Extract Analysis Using GC-MS

The main compounds detected in CP mainly include oleic acid (about 56%), palmitic acid (about 8.9%), linolenic acid 3.5%, and linoleic acid 2.8% besides many other compounds (**Table 2**; **Figure 2**). Among the compounds of CP that were reported to have anti-inflammatory effect, there are oleic acid, palmitic acid, linolenic acid, betulin, and linoleic acid, while those with an antioxidant effect are palmitic acid and 10-octadecenoic acid and methyl ester.

Biochemical Assessment

Corticosterone Level in the Serum

The corticosterone level significantly increased ($p < 0.001$) in untreated rats exposed to CUMS compared to that in the control rats, while those treated with FLU and CP showed a significant reduction ($p < 0.001$) in serum corticosterone level

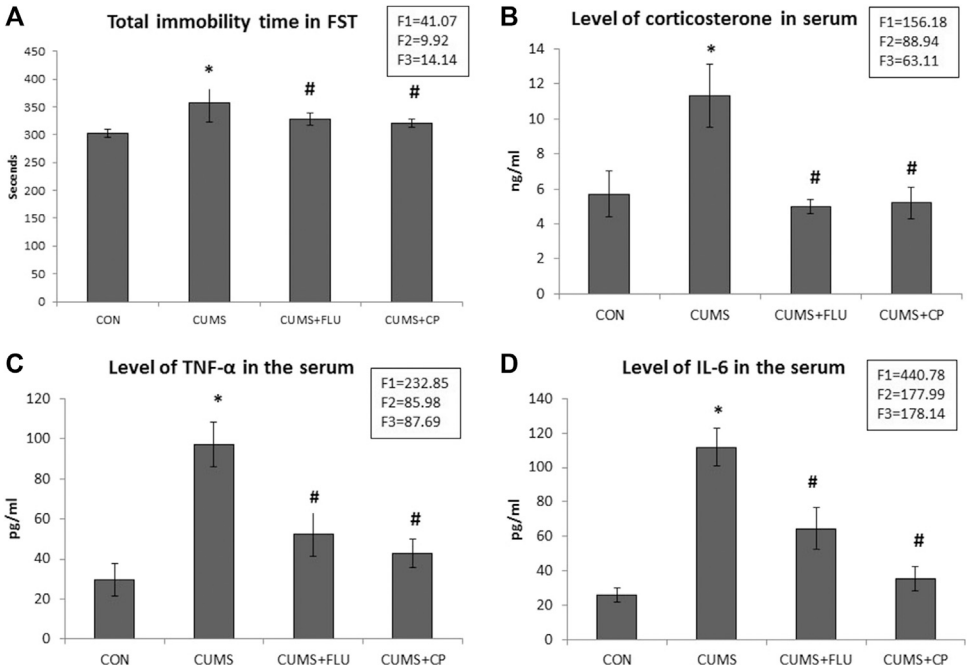


FIGURE 1 | Immobility time during the forced swimming test (FST) **(A)**, serum corticosterone level **(B)**, TNF-α serum level **(C)**, and IL-6 serum level **(D)** in the studied groups. Data are analyzed using mixed-model two-way ANOVA based on the Bonferroni post hoc test. Results are expressed as mean ± SD (n = 10), dF = 36, F1 = effect of stress, F2 = effect of treatment, F3 = interaction between stress and treatment. A p value <0.05 was considered significant. * significance versus the control group (CON), # significance versus the chronic unpredictable mild stress (CUMS) group. CON: control, CUMS: chronic unpredictable mild stress, Flu: fluoxetine, CP: *Cucurbita pepo*.

compared to that in the untreated rats exposed to CUMS (**Figure 1B**).

TNF-α and IL-6 Levels in the Serum

At the end of the experiment, assessment of serum TNF-α and IL-6 showed that they were significantly elevated ($p < 0.001$) in the CUMS group, whereas they showed a significant reduction ($p < 0.001$) in FLU- and CP-treated groups compared with those in the untreated rats exposed to CUMS (**Figures 1C,D**).

MDA, SOD, GPX, and CAT Levels in the Serum

It was noticed that the level of serum MDA was significantly higher ($p < 0.001$) in the CUMS group than in the control rats, while that in CP-treated groups was significantly lower ($p = 0.003$) than that in untreated rats exposed to CUMS. FLU administration could not significantly reduce the MDA level in rats exposed to CUMS (**Figure 3A**).

In contrast, levels of SOD, GPX, and CAT in the serum of the CUMS group were significantly lower ($p < 0.001$, $p < 0.001$, $p = 0.002$) than those in the serum of the control group, while their levels showed a significant increase ($p = 0.01$, $p = 0.003$, $p = 0.03$) in the CP-treated group compared to those in the CUMS-exposed group. FLU administration could not significantly increase SOD, GPX, and CAT in rats exposed to CUMS (**Figures 3B–D**).

Gene Expression of Ki67, Caspase-3, and HSP70

RT-PCR revealed insignificantly high Ki67 gene expression ($p = 0.14$) in the adrenal glands of the CUMS group compared to the control group, while that of FLU- and CP-treated groups showed significant high expression ($p = 0.02$, $p = 0.01$) compared to that of the CUMS-exposed group (**Figure 3E**).

Regarding caspase-3, its gene expression was significantly increased ($p < 0.001$) in the adrenal glands of the CUMS group compared to the control group, while that of FLU- and CP-treated groups showed a significant decrease ($p = 0.03$, $p = 0.04$) compared to that of the CUMS-exposed group (**Figure 3F**).

When it came to HSP70 gene expression, it recorded a significant higher ($p < 0.001$) levels in the adrenal glands of the CUMS group than in the control group, while that of FLU- and CP-treated groups showed an insignificant decrease ($p = 0.07$, $p = 0.08$) compared to that of the CUMS-exposed group (**Figure 3G**).

Histopathological Assessment

Adrenal glands of control rats have an intact structure with a preserved architecture of the cortex included zona glomerulosa, zona fasciculata, and zona reticularis as well as the medulla (**Figure 4**). Adrenal glands of CUMS-exposed rats showed many cells in the ZG, ZF, and ZR with obvious vacuolation and degenerated nuclei and sometimes deeply stained nuclei with

TABLE 2 | Components of *Cucurbita pepo* L. extract identified using gas chromatography and mass spectrometer (GC–MS) analysis.

SN	Name of the compound	Molecular formula	Molecular weight	Retention time (minutes)	Relative percentage	NIST match factor (Mikaia et al., 2014)	Activity
1.	Hexadecanoic acid, methyl ester (palmitic acid methyl ester)	$C_{17}H_{34}O_2$	270	21.50	3.02	839	Anti-inflammatory action through inhibition of the cyclooxygenase II enzyme (Hema et al., 2011)Antioxidant, hypocholesterolemic, lubricant, antiandrogenic (Duke, 1992)
2.	Hexadecanoic acid (palmitic acid)	$C_{16}H_{32}O_2$	256	22.61	8.90	821	Anti-inflammatory through inhibition of phospholipase A2 (Aparna et al., 2012) Antioxidant, hypocholesterolemic, lubricant, antiandrogenic (Duke, 1992)
3.	9-octadecenoic acid (Z)-	$C_{18}H_{34}O_2$	256	22.82	4.40	894	-
4.	10-octadecenoic acid, methyl ester	$C_{19}H_{36}O_2$	296	24.13	4.82	804	Antibacterial, antifungal, antioxidant (Asghar and Choudahry, 2011)
5.	Butyl 9,12,15-octadecatrienoate	$C_{22}H_{38}O_2$	334	24.73	1.60	743	No activity reported
6.	9-octadecenoic acid (oleic acid)	$C_{18}H_{34}O_2$	282	25.14	56.59	901	Anti-inflammatory actions through peroxisome proliferator-activated receptor gamma (PPAR-γ) activation (Song et al., 2019)
7.	9,12-octadecadienoic acid (Z,Z)- (linolenic acid)	$C_{18}H_{32}O_2$	280	25.42	3.52	855	Anti-inflammatory, hypocholesterolemic, antiandrogenic, antihistaminic, antieczemic (Duke 1992)
8.	*cis*-13-octadecenoic acid (linoleic acid)	$C_{18}H_{34}O_2$	282	26.01	1.75	796	Anti-inflammatory, antiandrogenic, antileukotriene-D4, hypocholesterolemic, flavor (Duke 1992)
9.	9-octadecenoic acid (Z)-, anhydride (oleic anhydride)	$C_{36}H_{66}O_3$	546	28.98	3.60	800	Anti-inflammatory (Song et al., 2019)
10.	Linoleic acid ethyl ester (ethyl linoleate)	$C_{20}H_{36}O_2$	308	29.21	1.08	782	No activity reported
11.	Stigmast-5-en-3-Ol	$C_{29}H_{50}O$	414	35.65	3.08	725	Decrease endothelial leukocyte and platelet adhesion (Duke, 1992; Kikuchi et al., 2015)
12.	Betulin	$C_{30}H_{50}O_2$	442	40.49	2.35	644	Anti-inflammatory and antitumor effect (Kikuchi et al., 2015; Jonnalagadda et al., 2017)

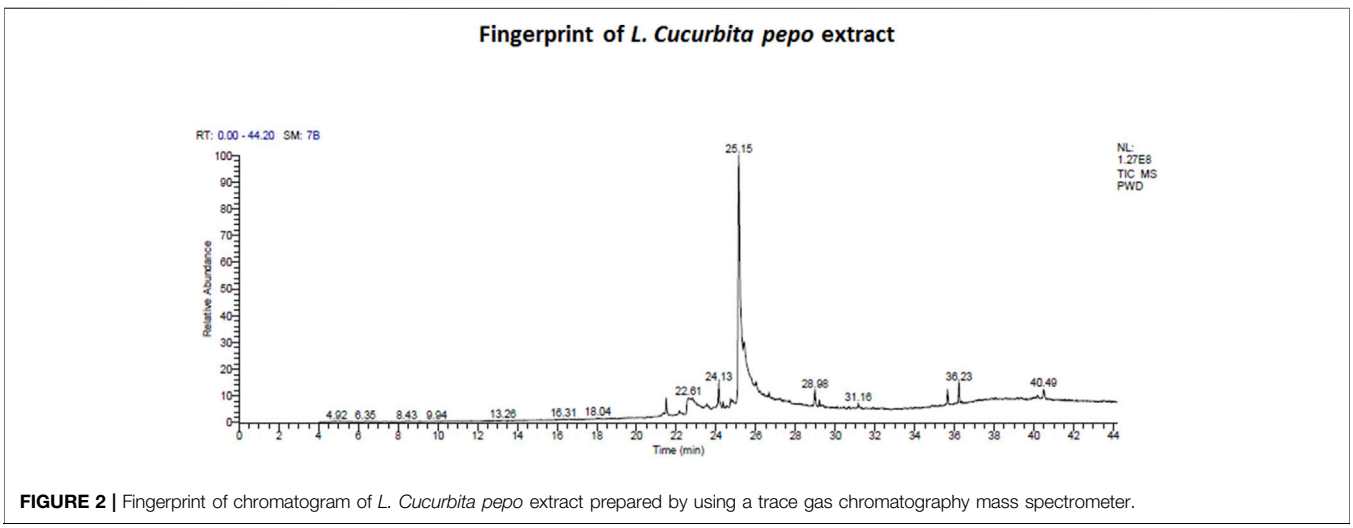


FIGURE 2 | Fingerprint of chromatogram of *L. Cucurbita pepo* extract prepared by using a trace gas chromatography mass spectrometer.

moderate thickening in the capsule and connective tissue trabeculae. Many cells of the ZR appeared dark with brown lipofuscin pigments. On the other hand, adrenal glands of CP-treated rats showed fewer obviously vacuolated cells and deeply stained nuclei in the ZG, and ZF and ZR revealed few dark cells (**Figure 4**).

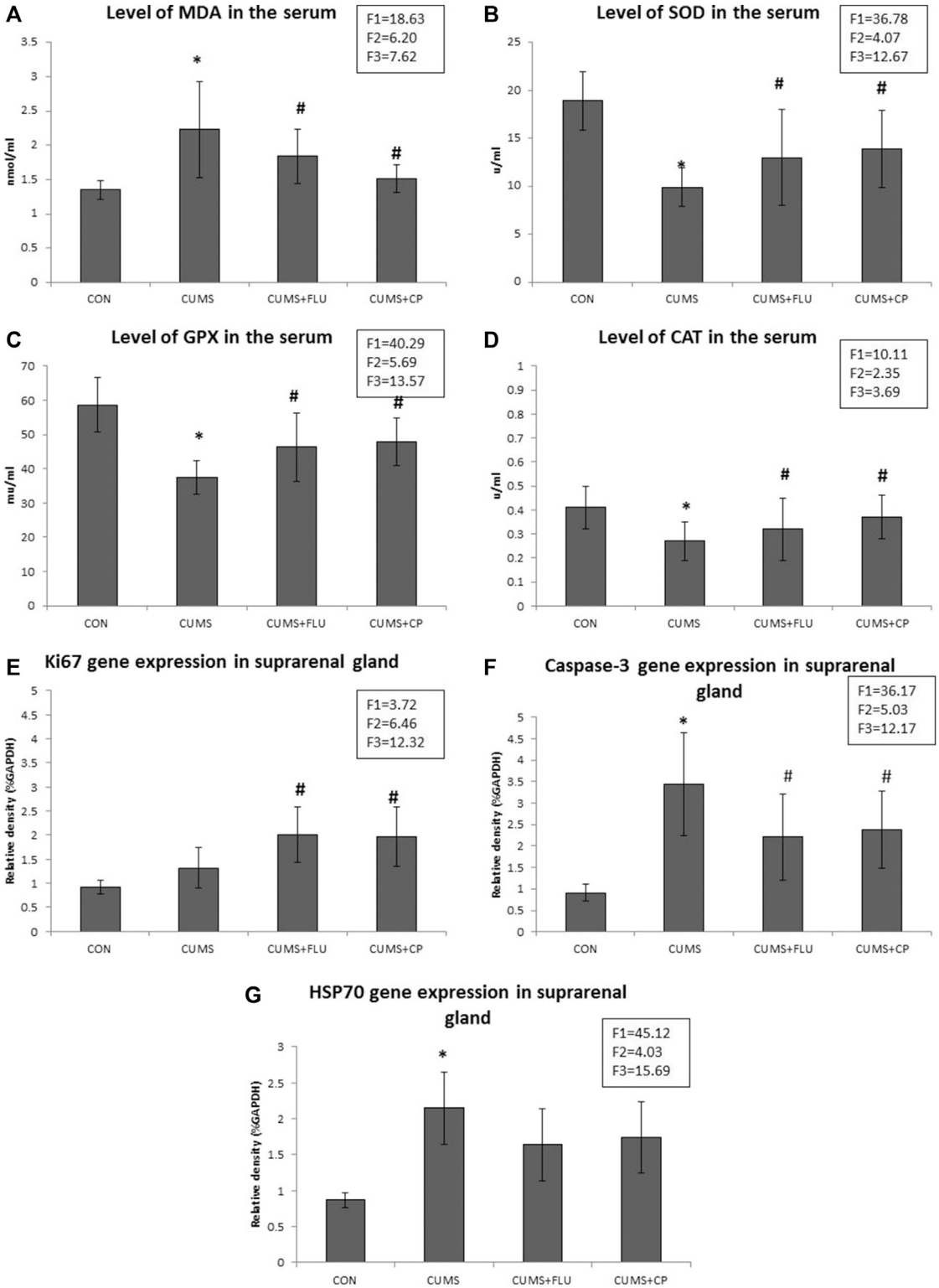


FIGURE 3 | Levels of MDA **(A)**, SOD **(B)**, GPX **(C),** and CAT **(D)** assessed in the serum of the studied groups using ELIZA. Levels of gene expression of Ki67 **(E)**, caspase-3 **(F),** and HSP70 **(G)** assessed in the suprarenal glands of the studied groups using qRT-PCR. Data are analyzed using mixed-model two-way ANOVA based on the Bonferroni post hoc test. Results are expressed as mean ± SD (n = 10), dF = 36, F1 = effect of stress, F2 = effect of treatment, F3 = interaction between stress and treatment. A p value <0.05 was considered significant. * significance versus the control group (CON), # significance versus the chronic unpredictable mild stress (CUMS) group. CON: control, CUMS: chronic unpredictable mild stress, Flu: fluoxetine, CP: *Cucurbita pepo*.

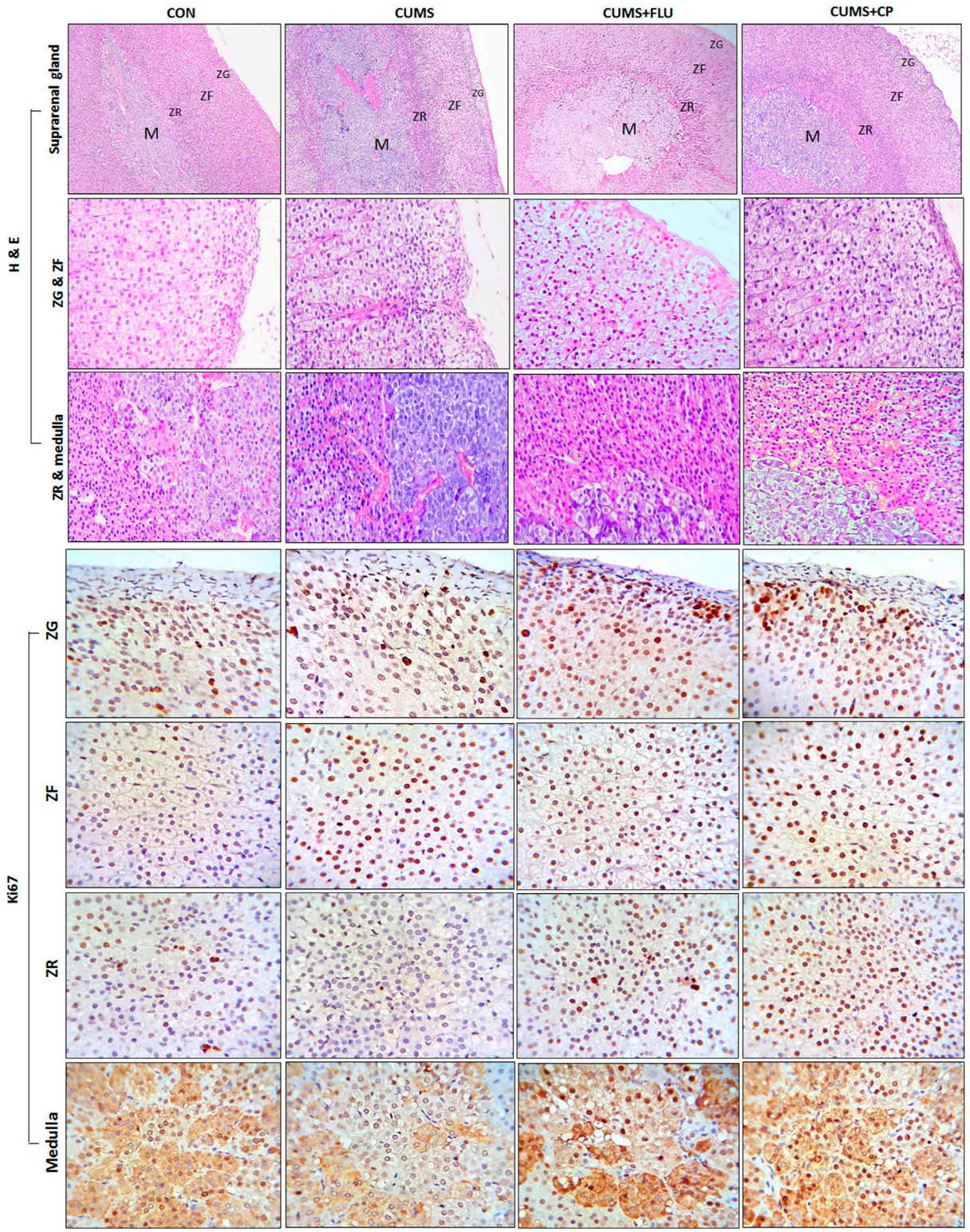


FIGURE 4 | Sections of the adrenal gland of studied groups stained with H&E staining and Ki67 antibody (H&E x100 and 40, immunohistochemical staining X100). ZG, Zona glomerulosa, ZF: Zona fasciculata, ZR: Zona reticularis. CON: control, CUMS: chronic unpredictable mild stress, Flu: fluoxetine, CP: *Cucurbita pepo*.

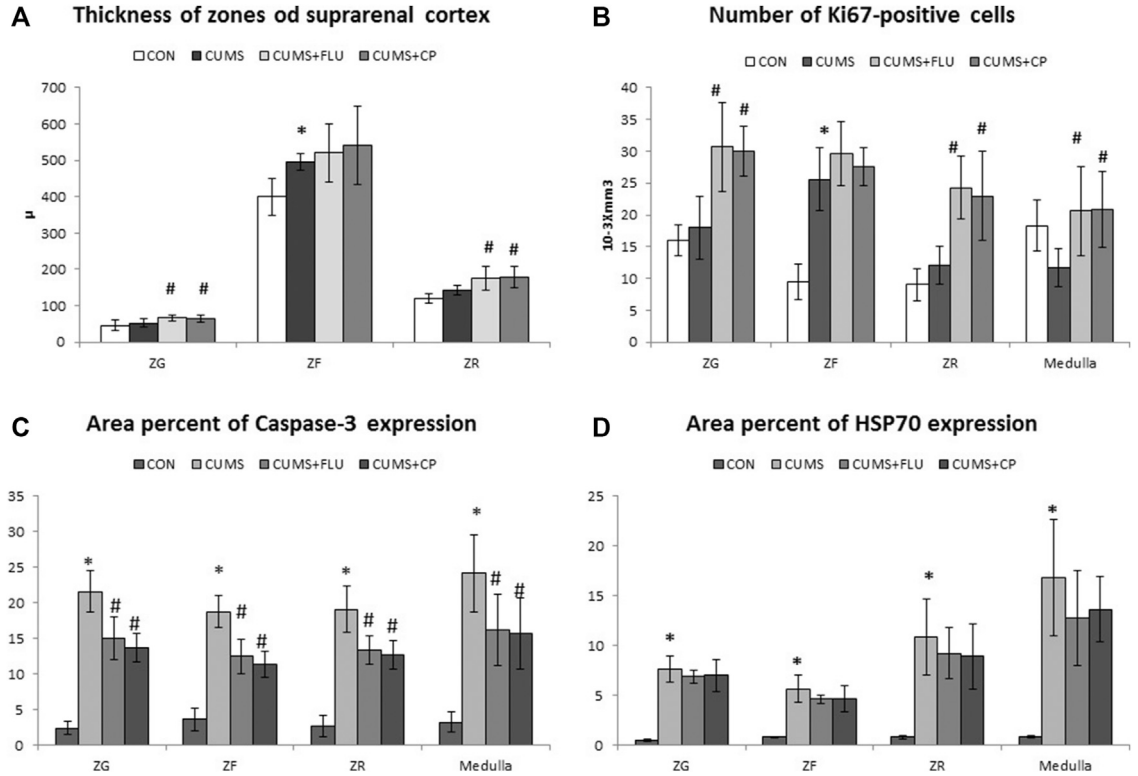


FIGURE 5 | Thickness of the suprarenal cortical zones **(A)**, Immuno-expression of Ki67 **(B)**, caspase-3 **(C)**, and HSP70 **(D)** in the studied groups. Data are analyzed using mixed-model two-way ANOVA based on the Bonferroni post hoc test. Results are expressed as mean ± SD (n = 10), dF = 36. Results are expressed as mean ± SD (n = 10). A p value <0.05 was considered significant. * significance versus the control group (CON), # significance versus the chronic unpredictable mild stress (CUMS) group. ZG: zona glomerulosa, ZF: zona fasciculata, ZR: zona reticularis. CON: control, CUMS: chronic unpredictable mild stress, Flu: fluoxetine, CP: *Cucurbita pepo*.

Morphometric measurements showed that the thickness of the ZG and ZR showed an insignificant increase after exposure to CUMS, while they were significantly increased in FLU- ($p = 0.01$, $p = 0.02$) and CP- treated groups ($p = 0.02$, $p = 0.001$), respectively. Regarding the thickness of the ZF, it was significantly increased ($p = 0.02$) in the CUMS-exposed group, and it was further increased, but insignificantly, in FLU- and CP-treated groups compared to that in the untreated CUMS group.

In order to determine whether cellular hyperplasia was restricted to a specific subregion of the adrenal gland, immunohistochemical labeling for Ki67 (the marker of the dividing cell) was used. The number of Ki67-positive proliferating cells was significantly increased ($p < 0.001$) in the ZF after exposure to CUMS, while treatment with FLU and CP insignificantly increased it compared to the untreated CUMS group. Although the number of proliferating cells was insignificantly increased in the ZG and ZR and insignificantly decreased in the medulla of the CUMS group compared to the control group, treatment with FLU and CP significantly increased the number of proliferating cells in the ZG ($p = 0.001$, $p = 0.003$), ZR ($p < 0.001$) and medulla ($p = 0.004$, $p = 0.003$) compared to the untreated CUMS group (**Figures 4**, **5**).

Immunohistochemical staining using caspase-3 was performed to assess apoptosis (**Figure 6**). It was noticed that the percent area of caspase-3 expression significantly increased ($p < 0.001$) in all zones of the gland following exposure to CUMS for 4 weeks in comparison to that of the control group. The CP-treated group showed a significant reduction in caspase-3 expression in the ZG ($p < 0.001$), ZF ($p < 0.001$), ZR ($p < 0.001$, $p = 0.005$), and medulla ($p = 0.004$, $p = 0.001$), in comparison to that of the CUMS group (**Figures 5**, **6**).

The area percent of HSP70 expression significantly increased ($p < 0.001$) in all zones of the cortex as well as in the medulla of the adrenal gland of the CUMS group compared to that of the control group, whereas it was insignificantly reduced in all zones and medulla of FLU- and CP-treated groups compared to that of the CUMS group (**Figures 5**, **6**).

DISCUSSION

Modern society is obviously full of stress that may arise from daily problems, health care, and job-related issues. These stressors may cause the so-called stress-related disorders (Clayton and Mccance, 2014). In this study, the ethanolic extract of the flesh and peel of *Cucurbita pepo* L. was used to investigate its potential in alleviating the CUMS-induced depressive behavior and its impact on the adrenal gland. This was proved by a

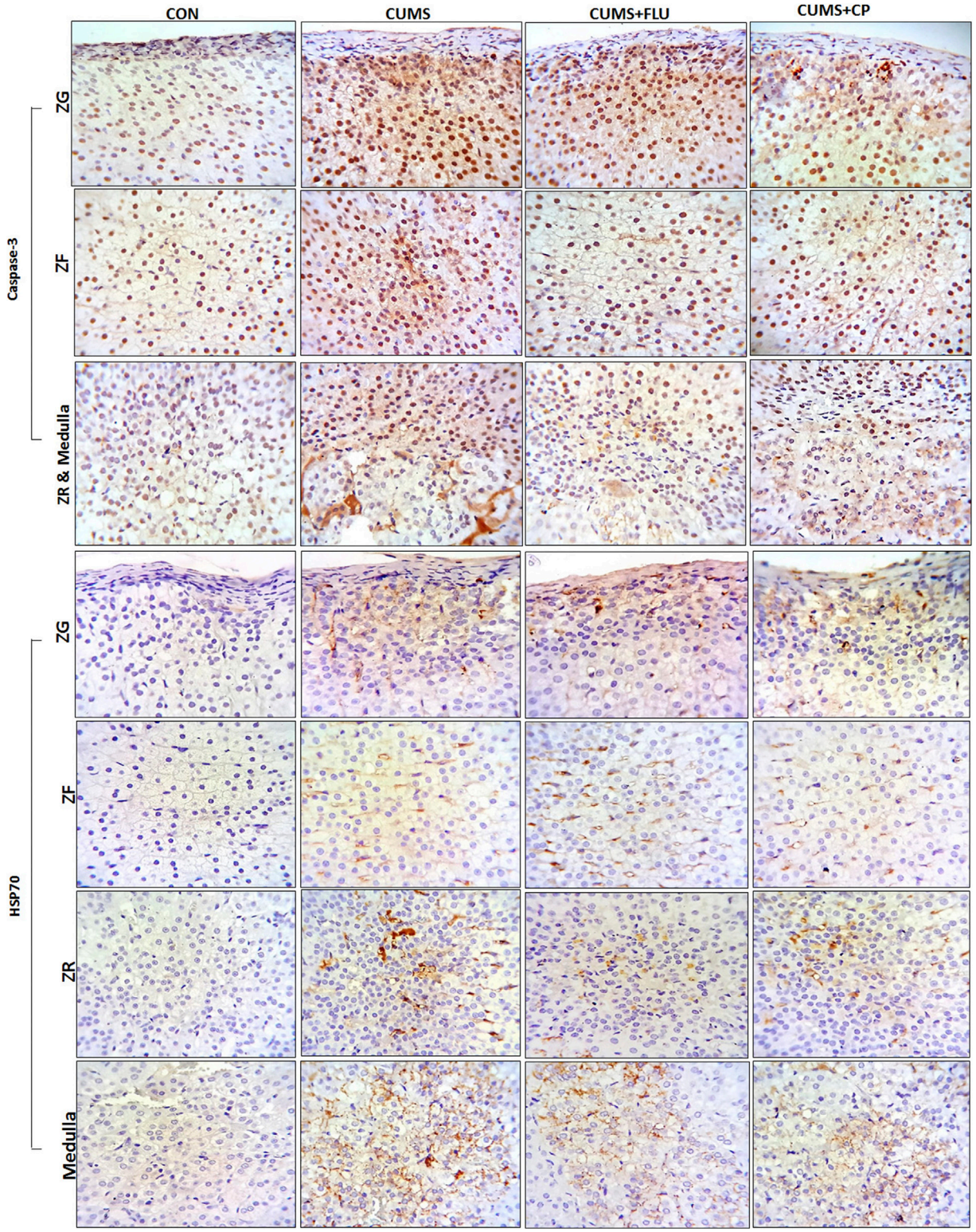


FIGURE 6 | Sections of the adrenal gland of studied groups stained immunohistochemically with caspase-3 and HSP70 antibodies. ZG: zona glomerulosa, ZF: zona fasciculata, ZR: zona reticularis. CON: control, CUMS: chronic unpredictable mild stress, Flu: fluoxetine, CP: *Cucurbita pepo*.

significant increase in the serum corticosterone level and verified by a prolonged immobility time during the FST. These findings were consistent with those previously reported (Tang et al., 2015).

Both TNF-α and IL-6 were reported to be involved in pathogenesis of depression (Taraz et al., 2015; Pedraz-Petrozzi et al., 2020). It was reported that mice deficient in IL-6 or TNF-α receptors are resistant to depressive behaviors (Viana et al., 2010). Therefore, they were assessed in this study, and it was observed that both TNF-α and IL-6 were significantly increased in the serum of rats exposed to CUMS for 4 weeks, indicating that they were depressed. This finding was supported by Numakawa et al. (2014) in mice with behavioral despair and by Taraz et al. (2015) in patients with depression.

In this study, administration of pumpkin extract was associated with amelioration of the depressive behavior, evident by the significant reduction of the immobility time of the FST and confirmed by the significant reduction in corticosterone and inflammatory cytokines TNF-α and IL-6 in the serum. These findings were supported by Kim Nr et al. (2016) who reported that SSP for 28 days decreased the level of inflammatory cytokines in the depressed rats. The anti-inflammatory activity of pumpkin might be attributed to the active compounds of the pumpkin such as oleic and palmitic acids and estradiol.

Downregulation of oleic acid, palmitic acid, and linoleic acid was described in depression (Conklin et al., 2010; Martín et al., 2010). It was reported that oleic acid–mediated neuroprotection is linked to its anti-inflammatory effect mediated by peroxisome proliferator–activated receptor gamma (PPAR-γ) activation (Song et al., 2019). Adding to that, palmitic acid was reported to inhibit phospholipase A(2), and therefore considered as an anti-inflammatory compound (Aparna et al., 2012). Estradiol was one of the compounds of the pumpkin detected in this study. Estradiol was reported to induce an anti-inflammatory effect and subsequently alleviate the depressive behavior (Xu et al., 2015). Another mechanism by which estradiol can induce an antidepressant effect is upregulation of expression of brain-derived neurotropic factor (BDNF) and ERK phosphorylation by the activation of ER-β in the brain (Yang et al., 2010).

In this study, the serum level of MDA was increased, while SOD, GPX, and CAT levels were decreased in the CUMS-exposed rats. Similar changes were documented following the exposure to CUMS in previous studies, and they added that these biochemical changes resulted in oxidative stress and impairment of HPA (Nabavi et al., 2015). Liu T. et al. (2015) also reported that development of depression may be attributed to the low content of antioxidants in the body. The antioxidant properties of the pumpkin fruit extract were frequently reported (Bahramsoltani et al., 2017). In addition, the flesh and peel of the *Cucurbita pepo* L. was reported to process higher antioxidant activity than the other parts, for example, seeds (Oyeleke et al., 2019). Pumpkin extract administration, in many previous studies, significantly increased the levels of SOD and GPX and reduced MDA in the serum of mice (Guo-Hua et al., 2000; Dang, 2004), and this effect was also documented in this study. Therefore, the antioxidant activity of pumpkins could be behind its antidepressant effect evident in this study. This is in a line with the observations of Kim Nr et al. (2016). It was reported that natural products with anti-inflammatory, antioxidant, and anti-fatigue effects also have an antidepressant-like effect (Jeong et al., 2015). All these previous activities were proved in pumpkins.

Increased cytoplasmic vacuolation of adrenal cortical cells, observed in the CUMS group in this study, might be attributed to increase demand for lipids, which forms the cornerstone for cortisol synthesis. Cigankova et al. (2005) observed that long-lasting experimental hypodynamia resulted in coalescence of multiple cytoplasmic lipid droplets of cortical cells. These lipid droplets contain cholesterol, which is the principal precursor in the synthesis of steroid hormones. However, Koldysheva and Lushnikova (2008) reported that stress resulted in a significant decrease in lipid droplets in cells of the adrenal cortex, especially ZF (Koldysheva and Lushnikova, 2008). It was described that upon exposure to physical stress, pain stimuli are transmitted to the hypothalamus, resulting in CRH secretion into the hypophyseal portal system, which increases ACTH secretion and stimulates its receptors in the ZF and ZR to increase cortisol secretion (Patti et al., 2018). The thickened adrenal capsule and trabeculae observed in CUMS-exposed rats were previously reported (El-Desouki et al., 2011; Altayeb and Salem, 2017) as a result of increased collagen synthesis by fibroblasts on exposure to immobilization stress.

Many cells in the adrenal glands of CUMS-exposed rats showed deeply stained nuclei, indicating that they underwent apoptosis that was confirmed by caspase-3 immunohistochemical staining. Similar observation was reported by Altayeb and Salem, (2017), while they were studying the effect of immobilization stress on adrenal glands of rats. Liu Q. et al. (2015) reported that excessive oxidative stress, evident following exposure to CUMS in this study, modifies the expression levels of "apoptosis-related genes" and induces cell apoptosis and degeneration through signaling pathways of Bcl-2, Bax, and caspase-3. This mechanism was confirmed in this study by RT-PCR that revealed significant upregulation of caspase-3 gene expression. On reviewing the literature, there was no direct effect of *Cucurbita pepo* on caspase-3–mediated apoptosis in different tissues. It seems that reduction in caspase-3–positive apoptotic cells detected in the adrenal glands was attributed to the antioxidant effect of *Cucurbita pepo* documented in this study. This is supported by many previous studies conducted on other plants and herbs with significant antioxidant activities (Banagozar Mohammadi et al., 2019; Ghazizadeh et al., 2020).

This study showed that exposure to CUMS increased Ki67-positive cells in the adrenal cortex that was significantly evident in the ZF, indicating an increased number of proliferating cells, and as a result, the thickness of this layer was significantly increased. On the other hand, the number of Ki67-positive proliferating cells insignificantly decreased in the medulla in response to CUMS. These observations were in a line with those of Ulrich-Lai et al. (2006) who reported an increase in Ki67-positive cell nuclei only in the outer ZF after exposure to chronic variable stress, while the medulla showed cellular hypertrophy and not hyperplasia. Moreover, Laborie et al., (2003) reported a generalized increase in medullary function after exposure to chronic stress,

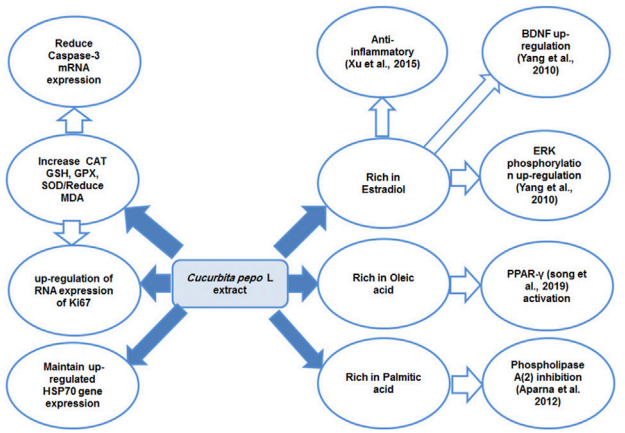


FIGURE 7 | Diagram summarizing the proposed mechanism of antidepressant effect of the *Cucurbita pepo* L extract. Peroxisome proliferator–activated receptor gamma (PPAR-γ), extracellular signal–regulated kinase (ERK), brain-derived neurotropic factor (BDNF), catalase (CAT), glutathione peroxidase (GPX), reduced glutathione (GSH), and superoxide dismutase heat shock protein (HSP70).

suggesting that chronic stress may lead to medullary hypertrophy. In this study, administration of the pumpkin extract significantly increased cell proliferation, evident by the upregulation of the Ki67 gene and immuno-expression in almost all zones and the medulla of the adrenal gland compared to CUMS. This explained increased thickness of the gland zones recorded in this study. It also may compensate the apoptotic effect induced by exposure to CUMS. This finding is supported by Kim Hy et al. (2016) who reported a significant upregulation of the mRNA expression of Ki67 and proliferation of splenocytes isolated from the spleen of BALB/c mice treated with SSP, streamed and *Cucurbita moschata Duch* and its major component, β-carotene.

In the present study, exposure to CUMS significantly increased gene expression and immuno-expression of HSP70 in all zones of the adrenal gland. In concordance with that, Zheng et al. (2008) also proved that augmented HSP70 expression after exposure to stressful conditions modulates inflammatory responses by inhibiting activation of the inflammatory transcription factor, the nuclear factor-kappa B (NF-kappaB). In addition, HSP70 may directly interfere with apoptosis and necrosis (Yenari et al., 2005). More recently, Li et al. (2019) reported an upregulation of HSP70 expression in the porcine adrenal gland tissue following exposure to heat stress, which indicates the role of HSP70 in adrenal gland injury and emphasizes its relevance to inflammatory responses. The rapid induction of HSP70 in response to stress is considered essential to the cellular protection process.

In our study, treating CUMS-exposed rats with pumpkins was associated with an insignificant reduction in HSP70 expression which was associated with reduced apoptosis and inflammatory responses. This might point to the beneficial effect of the relatively high level of HSP70 induced by both FLU and CP as it resulted in the reduction of caspase-3–mediated apoptosis and release of inflammatory cytokines. Although the effect of pumpkins on heat shock protein family was not previously described, oleic acid, which represents the main constituents of pumpkins used in this study, was described to downregulate the expression of the HSP60 in the human T lymphocyte cell line (Martins De Lima et al., 2004), which is supportive to our study finding. The proposed mechanism of action of *Cucurbita pepo* as an antidepressant-like substance is summarized in **Figure 7**. Among the limitations of this study was the inability to further investigate the in-depth mechanism of the antidepressant effect of CP, and therefore, further study is encouraged to do that.

In conclusion, this study provides science-based evidence of the efficacy of *Cucurbita pepo* L. extract to alleviate CUMS-induced behavioral and biochemical changes as well as the histopathological impact on the adrenal glands. These effects were evident through the downregulation of apoptosis and HSP70 expression and seemed to be mediated through the antioxidant and anti-inflammatory effect of the *Cucurbita pepo* L. extract. Although this study and some other recent studies have documented the antidepressant-like effect of *Cucurbita pepo* and explored its mechanism, further studies including clinical studies are needed to affirm this effect in humans.

DATA AVAILABILITY STATEMENT

The original contributions presented in the study are included in the article/**Supplementary Material**, further inquiries can be directed to the corresponding authors.

ETHICS STATEMENT

The animal study was reviewed and approved by the Biomedical Research Ethics Committee at the Faculty of Medicine, King Abdulaziz University, Jeddah, KSA (reference numbers 45-20).

AUTHOR CONTRIBUTIONS

All the authors listed have made a substantial, direct, and intellectual contribution to the work and approved it for publication.

ACKNOWLEDGMENTS

This research was funded by the Deanship of Scientific Research at Princess Nourah bint Abdulrahman University through the Fast-track Research Funding Program.

SUPPLEMENTARY MATERIAL

The Supplementary Material for this article can be found online at: https://www.frontiersin.org/articles/10.3389/fphar.2021.749766/full#supplementary-material

REFERENCES

Abd-El-Kareem, M. S. M. A., Rabbih, M. A. E. F., Selim, E. T. M., Elsherbiny, E. A. E.-M., and El-Khateeb, A. Y. (2016). Application of GC/EIMS in Combination with Semi-empirical Calculations for Identification and Investigation of Some Volatile Components in Basil Essential Oil. *Ijamsc* 04, 14–25. doi:10.4236/ijamsc.2016.41002

Ali, S. S., Abd El Wahab, M. G., Ayuob, N. N., and Suliaman, M. (2017). The Antidepressant-like Effect of Ocimum Basilicum in an Animal Model of Depression. *Biotech. Histochem.* 92, 390–401. doi:10.1080/10520295.2017.1323276

Altayeb, Z., and Salem, M. (2017). Light and Electron Microscopic Study on the Effect of Immobilization Stress on Adrenal Cortex of Adult Rats and Possible Ameliorative Role of Vitamin E. *J. Med. Histology* 1, 44–56. doi:10.21608/jmh.2017.961.1012

Aparna, V., Dileep, K. V., Mandal, P. K., Karthe, P., Sadasivan, C., and Haridas, M. (2012). Anti-inflammatory Property of N-Hexadecanoic Acid: Structural Evidence and Kinetic Assessment. *Chem. Biol. Drug Des.* 80, 434–439. doi:10.1111/j.1747-0285.2012.01418.x

Asghar, S. F., and Choudahry, M. (2011). Gas Chromatography-Mass Spectrometry (GC-MS) Analysis of Petroleum Ether Extract (Oil) and Bio-Assays of Crude Extract of Iris Germanica. *Int. J. Genet. Mol. Biol.* 3, 95–100. doi:10.5897/IJGMB.9000024

Ayuob, N. N., Ali, S. S., Suliaman, M., El Wahab, M. G. A., and Ahmed, S. M. (2016). The Antidepressant Effect of Musk in an Animal Model of Depression: a Histopathological Study. *Cell Tissue Res.* 366, 271–284. doi:10.1007/s00441-016-2468-9

Bahramsoltani, R., Farzaei, M. H., Abdolghaffari, A. H., Rahimi, R., Samadi, N., Heidari, M., et al. (2017). Evaluation of Phytochemicals, Antioxidant and Burn Wound Healing Activities of Cucurbita Moschata Duchesne Fruit Peel. *Iran J. Basic Med. Sci.* 20, 798–805. doi:10.22038/IJBMS.2017.9015

Banagozar Mohammadi, A., Torbati, M., Farajdokht, F., Sadigh-Eteghad, S., Fazljou, S. M. B., Vatandoust, S. M., et al. (2019). Sericin Alleviates Restraint Stress Induced Depressive- and Anxiety-like Behaviors via Modulation of Oxidative Stress, Neuroinflammation and Apoptosis in the Prefrontal Cortex and hippocampus. *Brain Res.* 1715, 47–56. doi:10.1016/j.brainres.2019.03.020

Bauer, M. E., and Teixeira, A. L. (2019). Inflammation in Psychiatric Disorders: what Comes First? *Ann. N. Y Acad. Sci.* 1437, 57–67. doi:10.1111/nyas.13712

Chaudhary, S. (2001). *Flora of the Kingdom of Saudi Arabia: Illustrated Riyadh: Ministry of Agriculture and Water, National Herbarium, National Agriculture and Water Research Center*, 2. Riyadah: Anatomy and morphology.

Cigankova, V., Zibrin, M., Bod A, K., and Holovska, K. (2005). Effect of Long-Term Experimental Hypodynamy on the Adrenal Glands of Japanese Quails: and Ultrastructural Study. *BULLETIN-VETERINARY INSTITUTE PULAWY* 49, 449.

Clayton, M., and Mccance, K. (2014). "Stress and Disease," in *Pathophysiology the Biologic Basis for Disease in Adults and Children*. Editors K. Mccance, S. Huether, V. Brashers, and N. Rote. 7th ed. (USA: Canada Elsevier).

Conklin, S. M., Runyan, C. A., Leonard, S., Reddy, R. D., Muldoon, M.F., and Yao, J. K. (2010). Age-related Changes of N-3 and N-6 Polyunsaturated Fatty Acids in the Anterior Cingulate Cortex of Individuals with Major Depressive Disorder. *Prostaglandins Leukot. Essent. Fatty Acids* 82, 111–119. doi:10.1016/j.plefa.2009.12.002

Dang, C. (2004). Effect of Pumpkin Distillable Subject on Lipid Peroxidation and the Activity of Antioxidative Enzyme Induced by Plumbum in Mouse. *Chin. J. Clin. Rehabil.* 8, 4378–4379.

Doron, R., Lotan, D., Versano, Z., Benatav, L., Franko, M., Armoza, S., et al. (2014). Escitalopram or Novel Herbal Mixture Treatments during or Following Exposure to Stress Reduce Anxiety-like Behavior through Corticosterone and BDNF Modifications. *PloS One* 9, e91455. doi:10.1371/journal.pone.0091455

Dotto, J. M., and Chacha, J. S. (2020). The Potential of Pumpkin Seeds as a Functional Food Ingredient: A Review. *Scientific Afr.* 10, e00575. doi:10.1016/j.sciaf.2020.e00575

Duke, J. A. (1992). *Handbook of Phytochemical Constituents of GRAS Herbs and Other Economic Plants*. [Online]. Boca Raton: FL: CRC Press. Available at: https://phytochem.nal.usda.gov/phytochem/search.

El-Desouki, N., El-Refaiy, A., Abdel-Azeem, H., and El-Baely, M. (2011). Histological and Ultrasructural Studies of the Effect of Immobilization Stress on the Adrenal Cortex of Albino Rat and the Ameliorative Role of Diazepam. *J. Egypt. Ger. Soc. Zool* 62, 25–45.

Gamal, M., Moawad, J., Rashed, L., Morcos, M. A., and Sharawy, N. (2018). Possible Involvement of Tetrahydrobiopterin in the Disturbance of Redox Homeostasis in Sepsis - Induced Brain Dysfunction. *Brain Res.* 1685, 19–28. doi:10.1016/j.brainres.2018.02.008

Ghazizadeh, J., Hamedeyazdan, S., Torbati, M., Farajdokht, F., Fakhari, A., Mahmoudi, J., et al. (2020). Melissa Officinalis L. Hydro-Alcoholic Extract Inhibits Anxiety and Depression through Prevention of central Oxidative Stress and Apoptosis. *Exp. Physiol.* 105, 707–720. doi:10.1113/EP088254

Gore, A. C., and Patisaul, H. B. (2010). Neuroendocrine Disruption: Historical Roots, Current Progress, Questions for the Future. *Front. Neuroendocrinol.* 31, 395–399. doi:10.1016/j.yfrne.2010.07.003

Guo-Hua, X., Zhi-Hong, H., and Yong-Fangl, W. (2000). A Study of the Possible Anti-tumour Effect and Immunompetence of Pumpkin Polysaccharide. *J. Wuhan Prof. Med. Coll.* 28, 1–4.

Hema, R., Kumaravel, S., and Alagusundaram, K. (2011). GC/MS Determination of Bioactive Components of Murraya Koenigii. *J. Am. Sci.* 7, 80–83.

Huang, L., Mivechi, N. F., and Moskophidis, D. (2001). Insights into Regulation and Function of the Major Stress-Induced Hsp70 Molecular Chaperone *In Vivo*: Analysis of Mice with Targeted Gene Disruption of the hsp70.1 or hsp70.3 Gene. *Mol. Cel, Biol.* 21, 8575–8591. doi:10.1128/MCB.21.24.8575-8591.2001

Huang, Q., Liu, H., Suzuki, K., Ma, S., and Liu, C. (2019). Linking what We Eat to Our Mood: a Review of Diet, Dietary Antioxidants, and Depression. *Antioxidants* 8, 376. doi:10.3390/antiox8090376

Jeong, H. J., Kim, J. H., Kim, N. R., Yoou, M. S., Nam, S. Y., Kim, K. Y., et al. (2015). Antidepressant Effect of Stillen. *Arch. Pharm. Res.* 38, 1223–1231. doi:10.1007/s12272-014-0472-8

Jonnalagadda, S. C., Suman, P., Morgan, D. C., and Seay, J. N. (2017). "Chapter 2 - Recent Developments on the Synthesis and Applications of Betulin and Betulinic Acid Derivatives as Therapeutic Agents," in *Studies in Natural Products Chemistry*. Editor R. Atta Ur (Elsevier).

Khar, A., Ali, A. M., Pardhasaradhi, B. Y., Varalakshmi, C. H., Anjum, R., and Kumari, A. L. (2001). Induction of Stress Response Renders Human Tumor Cell Lines Resistant to Curcumin-Mediated Apoptosis: Role of Reactive Oxygen Intermediates. *Cell Stress Chaperones* 6, 368–376. doi:10.1379/1466-1268(2001)006<0368:iosrrh>2.0.co;2

Kikuchi, T., Ando, H., Maekawa, K. I., Arie, H., Yamada, T., and Tanaka, R. (2015). Two New Ent-kaurane-type Diterpene Glycosides from Zucchini (Cucurbita Pepo L.) Seeds. *Fitoterapia* 107, 69–76. doi:10.1016/j.fitote.2015.09.019

Kim, H. Y., Nam, S. Y., Yang, S. Y., Kim, H. M., and Jeong, H. J. (2016a). Cucurbita Moschata Duch. And its Active Component, β-carotene Effectively Promote the Immune Responses through the Activation of Splenocytes and Macrophages. *Immunopharmacol. Immunotoxicol.* 38, 319–326. doi:10.1080/08923973.2016.1202960

Kim, N. R., Kim, H. Y., Kim, M. H., Kim, H. M., and Jeong, H. J. (2016b). Improvement of Depressive Behavior by Sweetme Sweet Pumpkin™ and its Active Compound, β-carotene. *Life Sci.* 147, 39–45. doi:10.1016/j.lfs.2016.01.036

Koldysheva, E. V., and Lushnikova, E. L. (2008). Ultrastructural Reorganization of Rat Adrenal Cortex after Whole Body Hyperthermia. *Bull. Exp. Biol. Med.* 145, 650–655. doi:10.1007/s10517-008-0160-0

Laborie, C., Van Camp, G., Bernet, F., Montel, V., and Dupouy, J. P. (2003). Metyrapone-induced Glucocorticoid Depletion Modulates Tyrosine Hydroxylase and Phenylethanolamine N-Methyltransferase Gene Expression in the Rat Adrenal Gland by a Noncholinergic Transsynaptic Activation. *J. Neuroendocrinol.* 15, 15–23. doi:10.1046/j.1365-2826.2003.00859.x

Lachance, L. R., and Ramsey, D. (2018). Antidepressant Foods: An Evidence-Based Nutrient Profiling System for Depression. *World J. Psychiatry* 8, 97–104. doi:10.5498/wjp.v8.i3.97

León-Olea, M., Martyniuk, C. J., Orlando, E. F., Ottinger, M. A., Rosenfeld, C., Wolstenholme, J., et al. (2014). Current Concepts in Neuroendocrine Disruption. *Gen. Comp. Endocrinol.* 203, 158–173. doi:10.1016/j.ygcen.2014.02.005

Li, J. Y., Yong, Y. H., Gong, D. L., Shi, L., Wang, X. M., Gooneratne, R., et al. (2019). Proteomic Analysis of the Response of Porcine Adrenal Gland to Heat Stress. *Res. Vet. Sci.* 122, 102–110. doi:10.1016/j.rvsc.2018.11.004

Li, M., Fu, Q., Li, Y., Li, S., Xue, J., and Ma, S. (2014). Emodin Opposes Chronic Unpredictable Mild Stress Induced Depressive-like Behavior in Mice by Upregulating the Levels of Hippocampal Glucocorticoid Receptor and Brain-Derived Neurotrophic Factor. *Fitoterapia* 98, 1–10. doi:10.1016/j.fitote.2014.06.007

Liu, Q., Si, T., Xu, X., Liang, F., Wang, L., and Pan, S. (2015a). Electromagnetic Radiation at 900 MHz Induces Sperm Apoptosis through Bcl-2, Bax and Caspase-3 Signaling Pathways in Rats. *Reprod. Health* 12, 65–69. doi:10.1186/s12978-015-0062-3

Liu, T., Zhong, S., Liao, X., Chen, J., He, T., Lai, S., et al. (2015b). A Meta-Analysis of Oxidative Stress Markers in Depression. *PloS One* 10, e0138904. doi:10.1371/journal.pone.0138904

Martín, V., Fabelo, N., Santpere, G., Puig, B., marín, R., Ferrer, I., et al. (2010). Lipid Alterations in Lipid Rafts from Alzheimer's Disease Human Brain Cortex. *J. Alzheimers Dis.* 19, 489–502. doi:10.3233/JAD-2010-1242

Martins De Lima, T., De Oliveira Rodrigues, L., Bengtson, M. H., Sogayar, M. C., Bezerra, C. N., Rebouças, N. A., et al. (2004). Identification of Genes Regulated by Oleic Acid in Jurkat Cells by Suppressive Subtractive Hybridization Analysis. *FEBS Lett.* 576, 320–324. doi:10.1016/j.febslet.2004.09.025

Mikaia, A., Ei, P. E. W. V., Ei, V. Z., Ei, D. Z., Ei, O. D. S., Neta, P., et al. (2014). *NIST Standard Reference Database 1A. Standard Reference Data*. Gaithersburg, MD, USA: NIST.

Nabavi, Sf., Braidy, N., Habtemariam, S., Orhan, Ie., Daglia, M., Manayi, A., et al. (2015). Neuroprotective Effects of Chrysin: From Chemistry to Medicine. *Neurochem. Int.* 90, 224–231. doi:10.1016/j.neuint.2015.09.006

Nawirska-Olszańska, A., Kita, A., Biesiada, A., Sokół-Łętowska, A., and Kucharska, A. Z. (2013). Characteristics of Antioxidant Activity and Composition of Pumpkin Seed Oils in 12 Cultivars. *Food Chem.* 139, 155–161. doi:10.1016/j.foodchem.2013.02.009

Numakawa, T., Richards, M., Nakajima, S., Adachi, N., Furuta, M., Odaka, H., et al. (2014). The Role of Brain-Derived Neurotrophic Factor in Comorbid Depression: Possible Linkage with Steroid Hormones, Cytokines, and Nutrition. *Front. Psychiatry* 5, 136. doi:10.3389/fpsyt.2014.00136

Oyeleke, A. W., Oluwajuyitan, D. T., Oluwamukomi, O. M., and Enujiugha, N. V. (2019). Amino Acid Profile, Functional Properties and *In-Vitro* Antioxidant Capacity of Cucurbita Maxima and Cucurbita Mixta Fruit Pulps and Seeds. *Ejnfs*, 224–241. doi:10.9734/ejnfs/2019/v10i430117

Packer, L. (2002). *Superoxide Dismutase*. Elsevier.

Patti, G., Guzzeti, C., Di Iorgi, N., maria Allegri, A. E., Napoli, F., Loche, S., et al. (2018). Central Adrenal Insufficiency in Children and Adolescents. *Best Pract. Res. Clin. Endocrinol. Metab.* 32, 425–444. doi:10.1016/j.beem.2018.03.012

Pedraz-Petrozzi, B., Neumann, E., and Sammer, G. (2020). Pro-inflammatory Markers and Fatigue in Patients with Depression: A Case-Control Study. *Sci. Rep.* 10, 66532–66536. doi:10.1038/s41598-020-66532-6

Perez Gutierrez, R. M. (2016). Review of Cucurbita Pepo (Pumpkin) its Phytochemistry and Pharmacology. *Med. Chem.* 6, 012–021. doi:10.4172/2161-0444.1000316

Song, J., Kim, Y. S., Lee, D. H., Lee, S. H., Park, H. J., Lee, D., et al. (2019). Neuroprotective Effects of Oleic Acid in Rodent Models of Cerebral Ischaemia. *Sci. Rep.* 9, 10732–10813. doi:10.1038/s41598-019-47057-z

Tang, M., Jiang, P., Li, H., Cai, H., Liu, Y., Gong, H., et al. (2015). Antidepressant-like Effect of N-3 PUFAs in CUMS Rats: Role of tPA/PAI-1 System. *Physiol. Behav.* 139, 210–215. doi:10.1016/j.physbeh.2014.11.054

Taraz, M., Taraz, S., and dashti-Khavidaki, S. (2015). Association between Depression and Inflammatory/anti-Inflammatory Cytokines in Chronic Kidney Disease and End-Stage Renal Disease Patients: a Review of Literature. *Hemodial. Int.* 19, 11–22. doi:10.1111/hdi.12200

Ulrich-Lai, Y. M., Figueiredo, H. F., Ostrander, M. M., Choi, D. C., Engeland, W. C., and Herman, J. P. (2006). Chronic Stress Induces Adrenal Hyperplasia and Hypertrophy in a Subregion-specific Manner. *Am. J. Physiol. Endocrinol. Metab.* 291, E965–E973. doi:10.1152/ajpendo.00070.2006

Viana, A. F., Maciel, I. S., Dornelles, F. N., Figueiredo, C. P., Siqueira, J. M., Campos, M. M., et al. (2010). Kinin B1 Receptors Mediate Depression-like Behavior Response in Stressed Mice Treated with Systemic *E. coli* Lipopolysaccharide. *J. Neuroinflammation* 7, 98. doi:10.1186/1742-2094-7-98

Wang, P., Liu, J., Zhao, Q., and Hao, L. (2002). Studies on Nutrient Composition and Utilization of Pumpkin Fruit. *J. Inner Mongolia Agric. Univ. (Natural Sci. Edition)* 23, 52–54. doi:10.5772/intechopen.89274

Wang, S. Y., Huang, W. C., Liu, C. C., Wang, M. F., Ho, C. S., Huang, W. P., et al. (2012). Pumpkin (Cucurbita Moschata) Fruit Extract Improves Physical Fatigue and Exercise Performance in Mice. *Molecules* 17, 11864–11876. doi:10.3390/molecules171011864

Waye, A., and Trudeau, V. L. (2011). Neuroendocrine Disruption: More Than Hormones Are Upset. *J. Toxicol. Environ. Health B Crit. Rev.* 14, 270–291. doi:10.1080/10937404.2011.578273

Who (2020). Who Health Organization [Online]. Available at: https://www.who.int/news-room/fact-sheets/detail/depression.

Wiley, J. (2006). *Wiley Registry of Mass Spectral Data*. John Wiley.

Xu, Y., Sheng, H., Tang, Z., Lu, J., and Ni, X. (2015). Inflammation and Increased Ido in hippocampus Contribute to Depression-like Behavior Induced by Estrogen Deficiency. *Behav. Brain Res.* 288, 71–78. doi:10.1016/j.bbr.2015.04.017

Yang, L. C., Zhang, Q. G., Zhou, C. F., Yang, F., Zhang, Y. D., Wang, R. M., et al. (2010). Extranuclear Estrogen Receptors Mediate the Neuroprotective Effects of Estrogen in the Rat hippocampus. *PloS One* 5, e9851. doi:10.1371/journal.pone.0009851

Yenari, M. A., Liu, J., Zheng, Z., Vexler, Z. S., Lee, J. E., and Giffard, R. G. (2005). Antiapoptotic and Anti-inflammatory Mechanisms of Heat-Shock Protein protection. *Ann. N. Y Acad. Sci.* 1053, 74–83. doi:10.1196/annals.1344.007

Zhang, B., Huang, H., Xie, J., Xu, C., Chen, M., Wang, C., et al. (2012). Cucurmosin Induces Apoptosis of BxPC-3 Human Pancreatic Cancer Cells via Inactivation of the EGFR Signaling Pathway. *Oncol. Rep.* 27, 891–897. doi:10.3892/or.2011.1573

Zheng, Z., Kim, J. Y, Ma, H., Lee, J. E., and Yenari, M. A. (2008). Anti-inflammatory Effects of the 70 kDa Heat Shock Protein in Experimental Stroke. *J. Cereb. Blood Flow Metab.* 28, 53–63. doi:10.1038/sj.jcbfm.9600502

Zhou, P., Yang, X., Jia, X., Yu, J., Asenso, J., Xiao, F., et al. (2016). Effect of 6'-acetylpaeoniflorin on Dinitrochlorobenzene-Induced Allergic Contact Dermatitis in BALB/c Mice. *Immunol. Res.* 64, 857–868. doi:10.1007/s12026-016-8788-8

Conflicts of Interest: The authors declare that the research was conducted in the absence of any commercial or financial relationships that could be construed as a potential conflict of interest.

Publisher's Note: All claims expressed in this article are solely those of the authors and do not necessarily represent those of their affiliated organizations, or those of the publisher, the editors, and the reviewers. Any product that may be evaluated in this article, or claim that may be made by its manufacturer, is not guaranteed or endorsed by the publisher.

Copyright © 2021 Almohaimeed, Hamed, Seleem, Batawi, Mohammedsaleh, Balgoon, Ali, Al Jaouni and Ayuob. This is an open-access article distributed under the terms of the Creative Commons Attribution License (CC BY). The use, distribution or reproduction in other forums is permitted, provided the original author(s) and the copyright owner(s) are credited and that the original publication in this journal is cited, in accordance with accepted academic practice. No use, distribution or reproduction is permitted which does not comply with these terms.

frontiers in Pharmacology

ORIGINAL RESEARCH
published: 29 November 2021
doi: 10.3389/fphar.2021.729909

Induction of PI3K/Akt-Mediated Apoptosis in Osteoclasts Is a Key Approach for *Buxue Tongluo* Pills to Treat Osteonecrosis of the Femoral Head

Dan Wang[1†], Yicheng Liu[2†], Dandan Tang[1], Shujun Wei[1], Jiayi Sun[1], Lvqiang Ruan[2], Lin He[1], Ruolan Li[1], Qiang Ren[3], Xiaoping Tian[1]* and Yunhui Chen[1]**

[1]School of Pharmacy, School of Basic Medicine, Innovative Institute of Chinese Medicine and Pharmacy, School of Acupuncture and Tuina, Chengdu University of Traditional Chinese Medicine, Chengdu, China, [2]Neijiang Hospital of Traditional Chinese Medicine Affiliated to Chengdu University of Traditional Chinese Medicine, Neijiang, China, [3]Hospital of Chengdu University of Traditional Chinese Medicine, Chengdu, China

OPEN ACCESS

Edited by:
Hong Zhang,
Shanghai University of Traditional Chinese Medicine, China

Reviewed by:
Xiaofei Zhang,
Shaanxi University of Chinese Medicine, China
Lei Chen,
Guangdong Pharmaceutical University, China

***Correspondence:**
Qiang Ren
401627406@qq.com
Xiaoping Tian
tianxiaoping@cdutcm.edu.cn
Yunhui Chen
chenyunhui@cdutcm.edu.cn

[†]These authors have contributed equally to this work and share first authorship

Specialty section:
This article was submitted to Ethnopharmacology, a section of the journal Frontiers in Pharmacology

Received: 24 June 2021
Accepted: 04 October 2021
Published: 29 November 2021

Citation:
Wang D, Liu Y, Tang D, Wei S, Sun J, Ruan L, He L, Li R, Ren Q, Tian X and Chen Y (2021) Induction of PI3K/Akt-Mediated Apoptosis in Osteoclasts Is a Key Approach for Buxue Tongluo Pills to Treat Osteonecrosis of the Femoral Head. Front. Pharmacol. 12:729909. doi: 10.3389/fphar.2021.729909

The *Buxue Tongluo* pill (BTP) is a self-made pill with the functions of nourishing blood, promoting blood circulation, dredging collaterals, and relieving pain. It consists of *Angelica sinensis* (Oliv.) Diels, *Pheretima aspergillum* (E.Perrier), *Panax notoginseng* (Burk.) F. H. Chen, *Astragalus membranaceus* (Fisch.) Bge, and *Glycyrrhiza uralensis* Fisch. Various clinical practices have confirmed the therapeutic effect of BTP on osteonecrosis of the femoral head (ONFH), but little attention has been paid to the study of its bioactive ingredients and related mechanisms of action. In this study, UPLC/MS-MS combined with GEO data mining was used to construct a bioactive ingredient library of BTP and a differentially expressed gene (DEG) library for ONFH. Subsequently, Cytoscape (3.7.2) software was used to analyze the protein–protein interaction between BTP and DEGs of ONFH to screen the key targets, and functional annotation analysis and pathway enrichment analysis were carried out. Finally, 34 bioactive compounds were screened, which acted on 1,232 targets. A total of 178 DEGs were collected, and 17 key genes were obtained after two screenings. By bioinformatics annotation on these key genes, a total of 354 gene ontology (GO) functional annotation analyses and 42 Kyoto Encyclopedia of Genes and Genomes (KEGG) pathways were obtained. The present study found that GO and KEGG enrichment were mainly related to apoptosis, suggesting that BTP may exert an anti-ONFH effect by promoting osteoclast apoptosis. Experiments *in vitro* demonstrated that BTP could increase the mitochondrial membrane potential (MMP) and induce remarkable apoptosis in osteoclasts. Furthermore, we determined the apoptosis marker of cleaved(C)-caspase-3, bcl-2, and bax and found that BTP could upregulate the C-caspase-3 and bax expression in osteoclasts and decrease the expression of bcl-2, p-Akt, and p-PI3K in a dose-dependent manner, indicating that BTP could induce PI3K/Akt-mediated apoptosis in osteoclasts to treat ONFH. This study explored the pharmacodynamic basis and mechanism of BTP against ONFH from the perspective of systemic pharmacology, laying a foundation for further elucidating the therapeutic effects of BTP against ONFH.

Keywords: buxue tongluo pill, osteonecrosis of the femoral head, GEO database, apoptosis, PI3K/AKT

INTRODUCTION

Osteonecrosis of the femoral head (ONFH) refers to a disease in which the blood supply of the femoral head is damaged or interrupted, leading to the death of bone marrow components and bone cells and the structural change and collapse of the femoral head (Pouya and Kerachian, 2015). It has also been considered a debilitating disease of multifactorial genesis, predominately affecting young people aged 20–40 years with the destruction of hip joints in their third, fourth, or fifth decade of life (Sun and Li, 2013). Currently, approximately 20,000–30,000 patients in the United States are diagnosed with ONFH annually, bringing pain and a substantial economic burden to the patients. Treatment options available for ONFH include pharmaceutical intervention and surgical treatment. Unfortunately, the former often fails to achieve satisfactory results due to the rapid progress of ONFH, and concerns regarding the longevity of the hip replacement have always existed. Thus, ONFH has been widely regarded as a global problem (Ping, 2021). Recently, traditional Chinese medicine (TCM) has been gradually accepted as a complementary and alternative medicine for the treatment of multiple diseases due to low toxicity and good curative effects (Xu et al., 2021; Zhang et al., 2021). A growing amount of TCM compounds and monomers, such as *Bushen Huoxue* decoction (Sun and Li, 2013), *Huangqi Shenggu* decoction (Ping, 2021), *Taohong Siwu* decoction (Zhao, 2020), Gastrodin (Zheng et al., 2014), and luteolin (Yan et al., 2020), have been reported to exert a significant therapeutic effect on ONFH.

BTP is a TCM formula that has been proven effective in treating ONFH with the functions of "promoting blood supply". It is composed of *Angelica sinensis* (Oliv.) Diels, *Pheretima aspergillum* (E.Perrier), *Panax notoginseng* (Burk.) F. H. Chen, *Astragalus membranaceus* (Fisch.) Bge, and *Glycyrrhiza uralensis* Fisch. Although it is frequently used to treat ONFH in clinical practice, there is no research for the specific mechanism regarding the anti-ONFH effect of BTP. Moreover, the TCM formula is characteristic of multicomponents, multitargets, and multipathways, making it difficult to reveal their mechanisms of action (Xu et al., 2021). Network pharmacology is a technology that can systematically analyze the interaction network of drug components, targets, diseases, and genes, which is consistent with the overall concept of the TCM theoretical system (Hopkins, 2008). At present, increasing studies have confirmed the great potential of network pharmacology in investigating the possible molecular mechanisms of TCM (Shan et al., 2018; Cui et al., 2018; Daina et al., 2019; Wang et al., 2020; Xia et al., 2021). Thus, it is an inevitable trend to apply network pharmacology to investigate the material basis and molecular mechanism of the TCM formula (Qing and Jia, 2021; Qing and Hu, 2021; Qing and Jia, 2019). In the current study, UPLC-MS/MS was used to identify the active ingredients of BTP, and network pharmacology was used to study the molecular mechanisms of BTP against ONFH. Besides, experiments *in vitro* were performed to provide scientific evidence for the predicted results with the network pharmacology. The general experimental procedures are shown in **Figure 1**.

METHODS

Preparation of the Extracts of BTP

BTP samples were prepared and provided by Neijiang traditional Chinese medicine hospital (Neijiang, China). The powder of BTP (10 g) was ultrasonically dissolved with 300 ml, 75% ethanol, followed by concentrating to 100 ml using a rotary evaporator. Then, the supernatant was filtered by microporous membranes with a pore size of 0.22 μm. Then, the obtained 10 μl filtrates of BTP were analyzed by UPLC-MS/MS.

UPLC-MS/MS Analysis

For qualitative analysis, a Thermo Scientific Q Exactive Orbitrap HRMS (Thermo Fisher Scientific, Massachusetts, United States) was connected to a Thermo Scientific Vanquish UPLC (Thermo Fisher Scientific, Massachusetts, United States). Chromatographic separation was achieved on a Thermo Scientific Accucore C_{18} (3 × 100 mm, 2.6 μm) in a thermostatically controlled column compartment (30 °C). The aqueous and organic mobile phases used were acetonitrile (A) and 0.1% phosphoric acid aqueous solution (B), respectively. The gradient elution program was set up as follows: 0–20 min, 12–25% A; 20.1–30 min, 25–28% A; 30.1–32 min, 28–40% A; 32.1–40 min, 40–50% A; 40.1–60 min, 50% A; 60.1–65 min, 12% A. The flow rate was set as 0.3 ml/min, and 2 μl of the extraction was injected into the UPLC system. The instrument was operated in the positive ion mode to perform full-scan analysis over an m/z range of 100–1,500. The optimized parameters were set as follows: a sheath gas flow rate of 35 L/min; a spray voltage of 3000 V; a capillary temperature of 320 V; an aux gas flow rate of 10.00 L/min; a max spray current of 100 A; a probe heater temperature of 350 C; and an S-lens RF level of 50.00%.

Establishment of Effective Compounds and the Target Library of BTP

Compounds of BTP were analyzed by UPLC-MS/MS. Subsequently, targets regarding these identified compounds via UPLC-MS/MS were obtained from the online database of SwissTargetPrediction (http://www.swisstargetprediction.ch/) (Daina et al., 2019).

Establishment of the ONFH Target Library

As a common worldwide resource for gene expression studies, the Gene Expression Omnibus (GEO) database (https://www.ncbi.nlm.nih.gov/geo) allows open access to high-throughput gene expression and other functional genomics datasets (Clough and

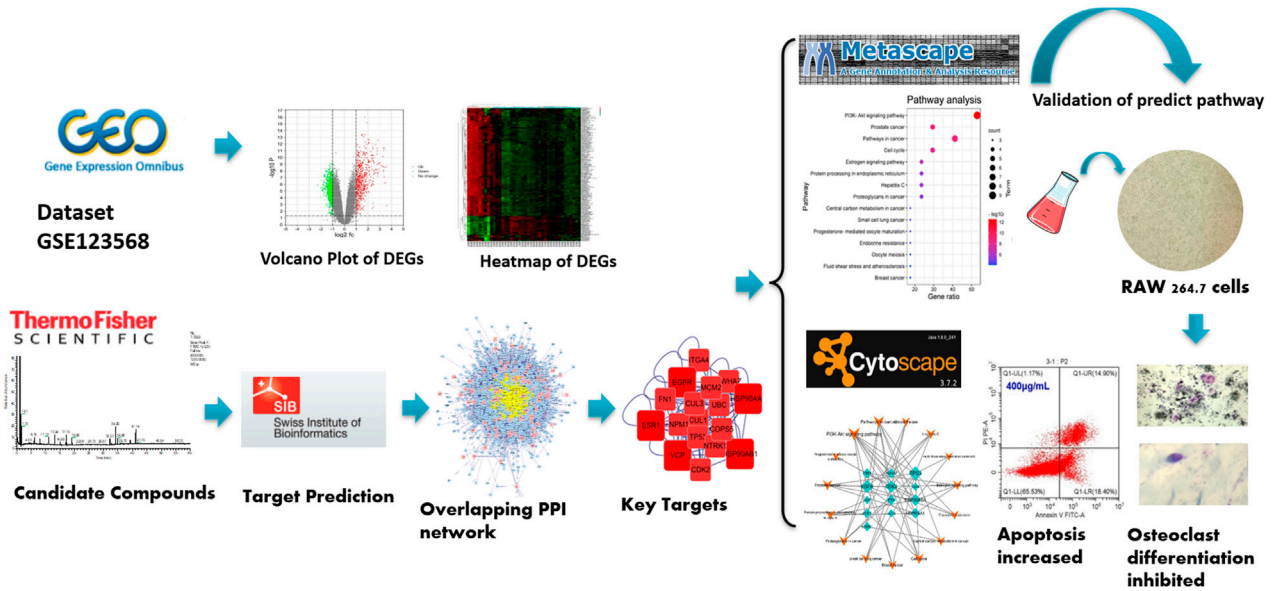


FIGURE 1 | Whole experiment process in our study.

Barrett, 2016). The GEO database was searched using "osteonecrosis of femoral head" as the keyword. We aimed to find a comparison of gene expression data sets between femoral head samples from patients with ONFH and normal femoral head samples. In order to ensure the stability and credibility of the analysis results, only data sets with a sample size larger than 10 were selected. Finally, only one suitable data set of ONFH was downloaded from the GEO database, namely, dataset GSE123568. In this dataset, 10 normal femoral head samples and 30 ONFH samples were included.

Acquisition of Differentially Expressed Genes

In order to obtain DEGs, dataset GSE123568 was analyzed with GEO2R, which was the official differential expression analysis tool of the GEO database. In this study, the difference with logFC (fold change) ≥1.3 and *p*-values <0.01 was statistically significant, and the corresponding genes were identified as DEGs.

Construction of the Protein–Protein Interaction Based on Bisogenet

In this study, the protein–protein interaction (PPI) of BTP and DEGs from ONFH were constructed by Cytoscape software (3.7.2). Then, the overlapping PPI network was obtained by using BisoGenet in Cytoscape. The median of three important attribute values, namely, degree, betweenness, and closeness, was employed for screening to obtain the core gene. After two screenings, a PPI network containing 17 nodes and 114 edges was obtained and used for enrichment analysis. The detailed attribute values and screening process of these targets are presented in **Table 3** and **Figure 3**, respectively.

Functional Enrichment and Constructing the Network of BTP-DEGs-Pathway

The Metascape platform (http://metascape.org/gp/index.html) has a comprehensive annotation function and data of gene annotation monthly updated (Zhou et al., 2019). In this study, functional annotation of gene ontology (GO) and KEGG pathways was performed with the Metascape platform. The main biological processes and involved metabolic pathways were analyzed by submitting the core targets of BTP-DEGs from ONFH to Metascape with $p < 0.01$. Then, the results were saved and visualized by Bioinformatics (http://www.bioinformatics.com.cn/) (Huang, 2009). Afterward, as shown in **Figure 4**, the network of the BTP-DEGs-Pathway was constructed with Cytoscape (3.7.2).

EXPERIMENTAL VALIDATION

Chemicals and Reagents

Fetal bovine serum (FBS), phosphate-buffered saline (PBS), penicillin–streptomycin, 0.25% trypsin–EDTA (1x), and Dulbecco's modified eagle's medium (DMEM) were purchased from GIBCO (Grand Island, NY, United States). A cell counting kit-8 (CCK8) detection kit was purchased from the Beijing 4A Biotech Co., Ltd. (Beijing, China). The assay kits for DCFH-DA, horseradish peroxidase (HPR)-conjugated secondary antibodies, β-actin, BCA protein assay reagents, and primary antibodies for cleaved (C) caspase-3 were purchased from Boster Biol. Tech. (Wuhan, China). Primary antibodies for phosphorylation- (p-) Akt, Akt, PI3K, and P-PI3K were obtained from ImmunoWay Biotechnology Co. (Suzhou, China). Annexin V-FITC/PI apoptosis kits were obtained from US Everbright® Inc

TABLE 1 | Precursor and product ions of constituents in the *Buxue Tongluo* Pill.

No.	Compound	RT	Formula	MS^1	MS^2	Herbal medicine	Ref.
1	DL-Arginine	1.19	$C_6H_{14}N_4O_2$	175 $[M + H]^+$	116, 71, 70, 60	*P. aspergillum*	(Zhang et al., 2017)
2	Asparagine	1.23	$C_4H_8N_2O_3$	131 $[M-H]^-$	114, 113, 95, 72	*A. membranaceus*	(Liu et al., 2013)
3	Choline	1.24	$C_5H_{13}NO$	104 $[M + H]^+$	60	*A. membranaceus*	(Wu et al., 2020)
4	Sucrose	1.25	$C_{12}H_{22}O_{11}$	729 $[2M + FA-H]^-$	683.625, 387.11475, 179.89	*A. membranaceus*	(Wu et al., 2020)
5	Adenine	1.26	$C_5H_5N_5$	136 $[M + H]^+$	119, 109	*P. aspergillum*	(Wu et al., 2020)
6	Guanine	1.33	$C_5H_5N_5O$	152 $[M + H]^+$	135, 110, 81, 55	*P. aspergillum*	(Zhang et al., 2017)
7	Guanosine	1.33	$C_{10}H_{13}N_5O_5$	284 $[M + H]^+$	152, 135,110	*P. aspergillum*	(Zhang et al., 2017)
8	Hypoxanthine	1.34	$C_5H_4N_4O$	137 $[M + H]^+$	119, 110	*P. aspergillum*	(Zhang et al., 2017)
9	Nicotinic acid	1.37	$C_6H_5NO_2$	124 $[M-H]^-$	96, 80, 78, 52	*P. aspergillum*	(Zhang et al., 2017)
10	Phenylalanine	1.41	$C_9H_{11}NO_2$	166 $[M + H]^+$	120, 103	*P. aspergillum*	(Zhang et al., 2017)
11	Succinic acid	1.46	$C_4H_6O_4$	117 $[M-H]^-$	99, 73	*P. aspergillum*	(Zhang et al., 2017)
12	Tryptophan	2.44	$C_{11}H_{12}N_2O_2$	205 $[M + H]^+$	188, 170, 159, 142, 132, 130, 118	*P. aspergillum*	(Zhang et al., 2017)
13	Caffeic acid	3.01	$C_9H_8O_4$	179 $[M-H]^-$	135	*A. sinensis*/*P. notoginseng*	(Liu et al., 2017)
14	Benzoic acid	5.19	$C_7H_6O_2$	121 $[M-H]^-$	93	*A. sinensis*	(Liu et al., 2017)
15	3-Coumaric acid	6.47	$C_9H_8O_3$	163 $[M-H]^-$	119, 93	*P. notoginseng*	(Liu et al., 2019)
16	Calycosin-7-O-β-D-glucoside	7.37	$C_{22}H_{22}O_{10}$	447 $[M + Na]^+$	285, 270	*A. membranaceus*	(Zhang et al., 2008)
17	Chlorogenic acid	8.08	$C_{16}H_{18}O_9$	355.10 $[M + H]^+$	191, 179, 173	*A. sinensis*	(Liu et al., 2017)
18	Liquiritin	8.12	$C_{21}H_{22}O_9$	417 $[M-H]^-$	255, 135, 119	*G. uralensis*	[Meng et al., 2010]
19	Ferulic acid	13.24	$C_{10}H_{10}O_4$	195 $[M + H]^+$	177, 145	*A. sinensis*	(Chen et al., 2009)
20	Isoliquiritin	14.99	$C_{21}H_{22}O_9$	419 $[M + H]^+$	257, 147, 137	*G. uralensis*	(Zhang et al., 2011)
21	Daidzein	15.31	$C_{15}H_{10}O_4$	255 $[M + H]^+$	137.91	*A. membranaceus*	[Meng et al., 2010]
22	Ononin	17.11	$C_{22}H_{22}O_9$	431 $[M + H]^+$	268	*A. membranaceus*	(Luo et al., 2020)
23	Formononetin	17.34	$C_{16}H_{12}O_4$	269 $[M + H]^+$	254, 237,137	*A. membranaceus*	(Luo et al., 2020)
24	Ginsenoside Re	17.41	$C_{48}H_{82}O_{18}$	991 $[M-H]^-$	789, 441	*P. notoginseng*	(Liu et al., 2004)
25	Biochanin A	19.06	$C_{16}H_{12}O_5$	285 $[M + H]^+$	270, 253	*A. membranaceus*	(Luo et al., 2020)
26	Licoricesaponin G2	31.46	$C_{42}H_{62}O_{17}$	837 $[M-H]^-$	351,113	*G. uralensis*	(Meng et al., 2009)
27	Psoralen	32.23	$C_{11}H_6O_3$	186 $[M + H]^+$	187.03, 131.04	*P. notoginseng*	(Yang et al., 2010)
28	Ginsenoside Rb_1	33.90	$C_{54}H_{92}O_{23}$	1,107.59 $[M-2H]^{2-}$	945.54, 783.48, 621.43	*P. notoginseng*	(Liu et al., 2004)
29	Pimpinellin	34.20	$C_{13}H_{10}O_5$	247 $[M + H]^+$	231,217,203,186,176	*A. membranaceus*	(Liu et al., 2012)
30	Gypenoside XVII	34.27	$C_{48}H_{82}O_{18}$	991 $[M-H]^-$	945.54, 783.48, 621.43	*P. notoginseng*	(Jia et al., 2019)
31	Isoliquiritigenin	34.96	$C_{15}H_{12}O_4$	257 $[M + H]^+$	147, 137	*G. uralensis*	(Zhao et al., 2016)
32	Glycyrrhizic acid	34.97	$C_{42}H_{62}O_{16}$	821 $[M-H]^-$	645, 351	*G. uralensis*	(Liu et al., 2004)
33	Licochalcone A	39.42	$C_{21}H_{22}O_4$	339 $[M + H]^+$	297, 121	*G. uralensis*	(Zhang et al., 2011)
34	Z-Ligustilide	41.13	$C_{12}H_{14}O_2$	232.13 $[M + ACN + H]^+$	191, 173	*A. sinensis*	(Sheng et al., 2020)

MW, molecular weight, C7DG, calycosin-7-O-β-D-glucoside.

(Suzhou, China). Polyvinylidene fluoride (PVDF) membranes were purchased from Sigma-Aldrich (Shanghai, China). 5,5′,6,6′-Tetrachloro-1.1′,3.3′-tetraethyl-imidacarbocyanine iodide (JC-1) was obtained from Jiangsu KeyGen Biotech (Nanjing, China).

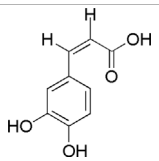
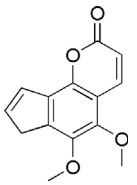
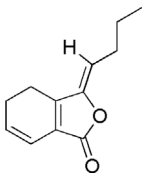
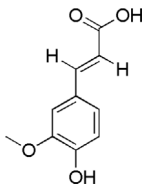
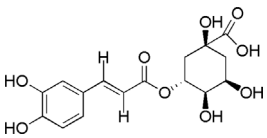
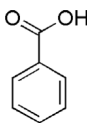
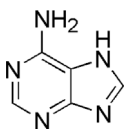
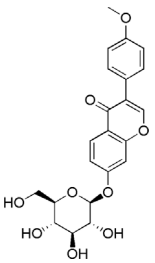
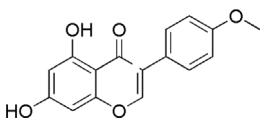
Cell Culture

The RAW 264.7 cells were purchased from Wuhan Pu-nuo-sai Life Technology Co., Ltd. (Wuhan, China) and used throughout the study. The RAW264.7 cells were cultured in DMEM containing 10% FBS (v/v) and 1% penicillin–streptomycin (v/v) at 37°C in a humidified atmosphere of 5% CO_2.

Cell Activity Detection

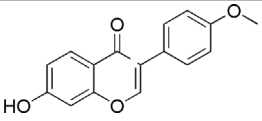
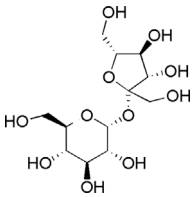
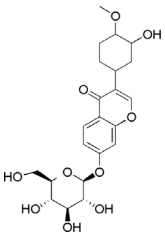
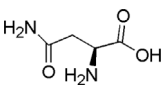
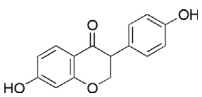
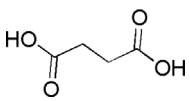
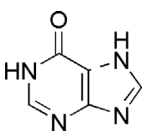
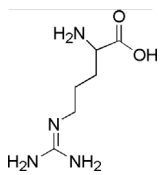
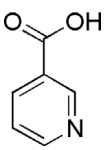
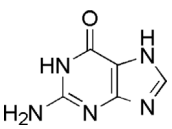
The RAW 264.7 cells were incubated in 96-well plates (1×10^4 cells/well) with different concentrations (0, 5, 10, 20, 40, 60, 80, 100, 150, and 200 μg/ml) of BTP, followed by induction with RANKL (100 ng/ml). After incubation for 24 and 48 h, the supernatant was discarded, and the cells were washed three

TABLE 2 | Active compounds of the *Buxue Tongluo* Pill.

Id	Molid	Name	Structure
DG1	MOL000414	Caffeic acid	
DG2	MOL004781	Pimpinellin	
DG3	MOL002122	Z-Ligustilide	
DG4	MOL000360	Ferulic acid	
DG5	MOL001955	Chlorogenic acid	
DG6	MOL000219	Benzoic acid	
HQ1	MOL001788	Adenine	
HQ2	MOL000391	Ononin	
HQ3	MOL000510	Biochanin A	

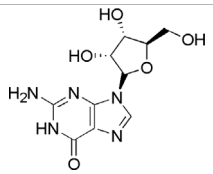
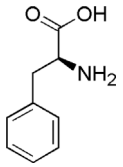
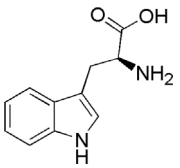
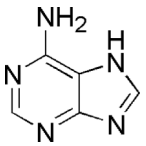
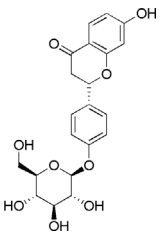
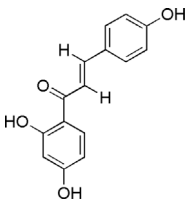
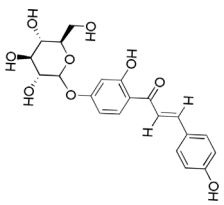
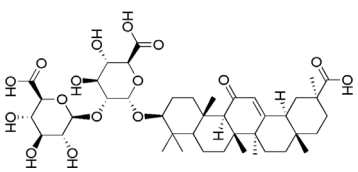
(Continued on following page)

TABLE 2 | (*Continued*) Active compounds of the *Buxue Tongluo* Pill.

Id	Molid	Name	Structure
HQ4	MOL000392	Formononetin	
HQ5	MOL000842	Sucrose	
HQ6	MOL009290	Calycosin-7-O-β-D-glucoside	
HQ7	MOL000429	Asparagine	
HQ8	MOL000390	Daidzein	
DL1	MOL000346	Succinic acid	
DL2	MOL001831	Hypoxanthine	
DL3	MOL000054	DL-Arginine	
DL4	MOL000421	Nicotinic acid	
DL5	MOL001757	Guanine	

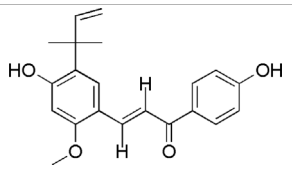
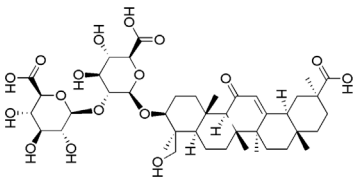
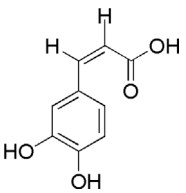
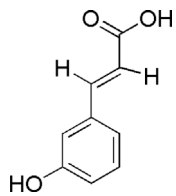
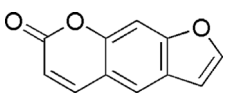
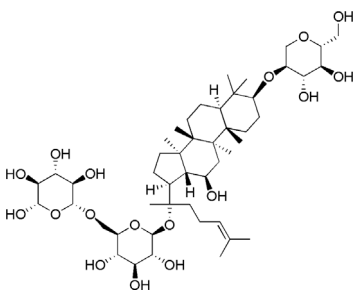
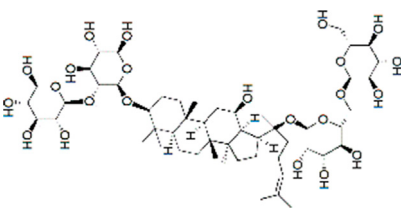
(Continued on following page)

TABLE 2 | (*Continued*) Active compounds of the *Buxue Tongluo* Pill.

Id	Molid	Name	Structure
DL6	MOL002687	Guanosine	
DL7	MOL000041	Phenylalanine	
DL8	MOL001780	Tryptophan	
DL9	MOL001788	Adenine	
GC1	MOL004903	Liquiritin	
GC2	MOL001789	Isoliquiritigenin	
GC3	MOL004951	Isoliquiritin	
GC4	MOL004876	Glycyrrhizic acid	

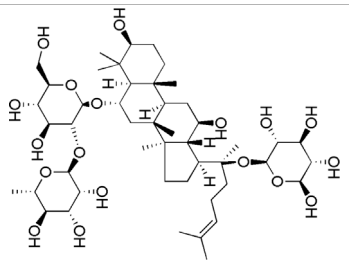
(Continued on following page)

TABLE 2 | (*Continued*) Active compounds of the *Buxue Tongluo* Pill.

Id	Molid	Name	Structure
GC5	MOL000497	Licochalcone A	
GC6	MOL004892	Licoricesaponin G2	
SQ1	MOL000414	Caffeic acid	
SQ2	MOL004549	3-Coumaric acid	
SQ3	MOL001950	Psoralen	
SQ4	MOL007495	Gypenoside XVII	
SQ5	MOL007476	Ginsenoside Rb1	

(Continued on following page)

TABLE 2 | (*Continued*) Active compounds of the *Buxue Tongluo* Pill.

Id	Molid	Name	Structure
SQ6	MOL005338	Ginsenoside Re	

times with PBS. Then, 10 μl CCK-8 was added to each well and incubated for 0.5 h. The optical density (OD) values were measured at 450 nm by the microtablet reader (Bio-RAD, United States). Each experiment was repeated three times. The concentration- and time-dependent effects of BTP on raw 264.7 cells are presented in **Figure 5**.

Osteoclastogenesis and TRAP Staining

The RAW 264.7 cells were seeded in 24-well plates (1×10^5 cells/well) and then pretreated with BTP (0, 50, 75, and 100 μg/ml) for 24 h, followed by induction with RANKL (100 ng/ml) for 7 days. Untreated cells were used as a negative control, while only RANKL-induced cells were used as a positive control group. During the induction period, the medium was changed every other day. After 7 days, the cells were washed with PBS, followed by fixing with 4% paraformaldehyde for 30 min, and then stained to detect TRAP activity. Finally, trap-positive cells were enumerated via a microscope. Mature osteoclasts with more than three nuclei were counted in a random area in each replicate sample.

Bone Resorption Assay

The RAW 264.7 cells were seeded in 96-well plates (1×10^4 cells/well) containing bovine bone slices and then pretreated with

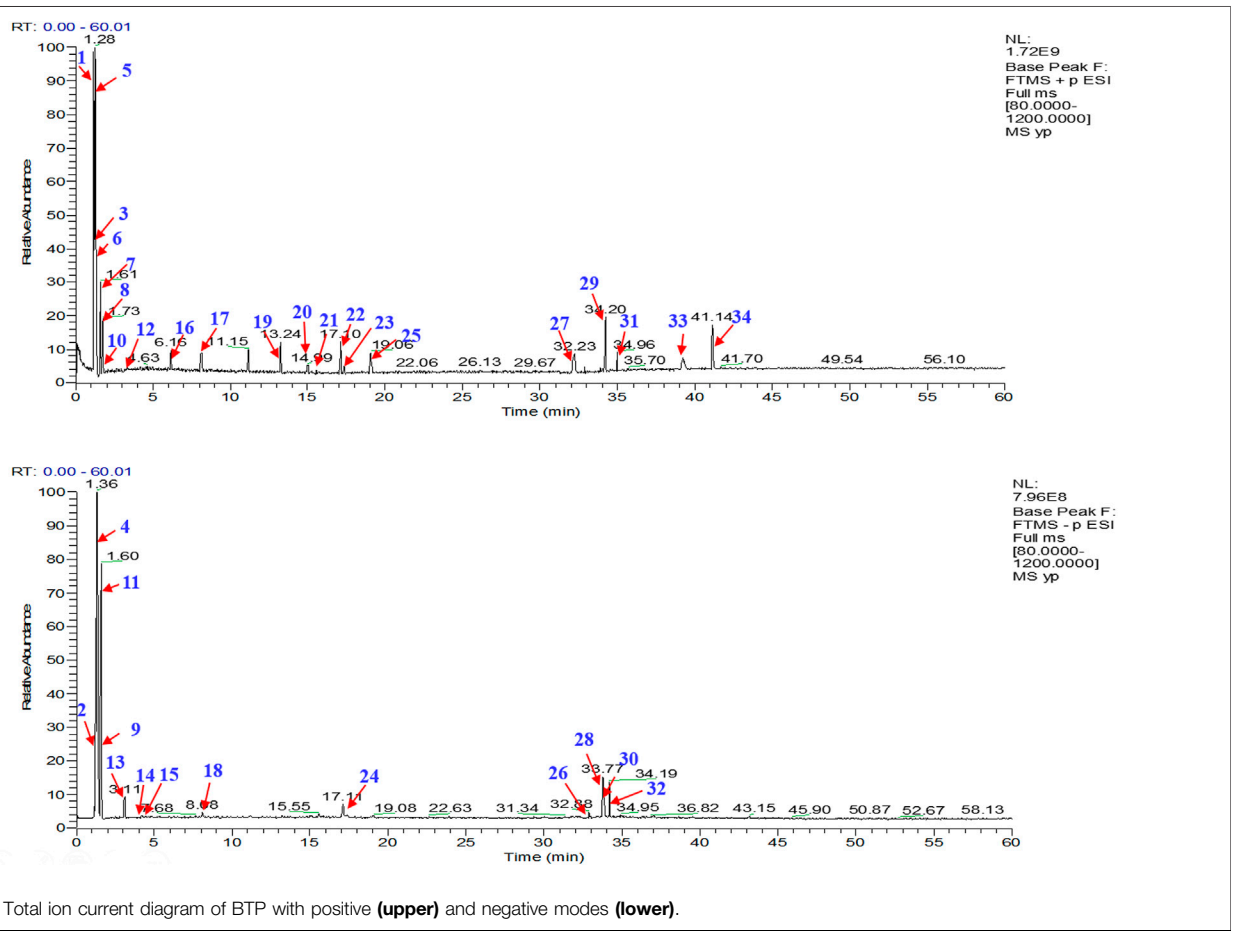


FIGURE 2 | Total ion current diagram of BTP with positive **(upper)** and negative modes **(lower)**.

different concentrations of BTP (0, 50, 75, and 100 μg/ml) for 24 h, followed by induction with RANKL (100 ng/ml) for 9 days. Then, bovine bone slices seeded with cells were washed with PBS, fixed in 2.5% glutaraldehyde over 10 min, ultrasonically cleaned with 0.25 mol/l ammonia hydroxide, and stained with 1% toluidine blue over 10 min. After washing with ddH2O, the osteolysis pits were photographed with a light microscope. Bone resorption capacity was defined as the bone resorption relative area (resorption area/total bone area).

Apoptosis Assay Using a Flow Cytometer

Cell apoptosis was detected by flow cytometry (CytoFLEX FCM, Beckman Coulter Inc., Atlanta, Georgia, United States). The RAW 264.7 cells were incubated in 6-well plates with RANKL (100 ng/ml) for 5 days and then treated with BTP (0, 50, 75, and 100 μg/ml) for 24 h. Subsequently, cell apoptosis was detected with the manufacturer's instructions of the Annexin V/PI apoptosis kit and cell cycle kit; the cells were stained with Annexin V-FITC and PI, respectively, and then detected by flow cytometer analysis. Each experiment was repeated three times.

Mitochondrial Membrane Potential (MMP) Determination

The change of intracellular mitochondrial membrane potential (MMP, ΔΨm) is generally recognized as an important indicator of mitochondrial dysfunction, and JC-1 is commonly considered as an ideal probe to evaluate ΔΨm. In this study, the cells were inoculated in laser confocal dishes (1×10^4/well), treated with different concentrations of BTP for 24 h, and subsequently induced with RANKL (100 ng/ml) for 5 days. After the induction, the cells were incubated with the JC-1 probe (10 μg/ml) in the dark for 30 min. Confocal laser microscopy was used to observe the green and the red fluorescence (Leica, SP8 SR, Wetzlar, Germany) of cells at 488 and 647 nm, respectively, and the images were recorded.

Immunofluorescence Assay of AKT/P-AKT

The RAW 264.7 cells were seeded in the confocal dish (1×10^5) and processed as described above. Then, they were washed three times with PBS, fixed with 4% paraformaldehyde for 30 min, and then washed three times with PBS. Afterward, the cells were treated with 0.5% Triton-X-100 for 30 min, followed by blocking with goat serum for 1 h at room temperature, and then, PI3K and P-PI3K antibodies (1:500) were added separately and incubated overnight at 4°C. Soon afterward, antirabbit IgG (H&L) Alexa Fluor® 488 and antimouse IgG (H + L) Alexa Fluor® 647 were added and incubated at room temperature for 1 h in the dark. Then, PBS was used to wash out the unbound secondary antibody, and the nuclei were stained with DAPI. Then, AKT/P-AKT and their fluorescence intensity were observed using a confocal laser microscope (Leica, SP8 SR, Wetzlar, Germany).

Western Blotting Assay

The RAW 264.7 cells were inoculated in 6-well plates (2×10^6/well) at 37°C in a humidified atmosphere of 5% CO_2 and incubated for 24 h. Then, the RAW 264.7 cells were treated with RANKL (100 ng/ml) for 5 days and then treated with BTP (50, 75, and 100 μg/ml) for 24 h. At the end of the treatment, 100 μl of RIPA cell lysates was used to extract the total cell protein. The protein concentrations were determined using BCA protein assay reagents. Then, the total protein was separated by 12% SDS-PAGE and then transferred to the PVDF membrane. After blocking by 5% skimmed milk, the PVDF membrane was incubated overnight with diluted primary antibodies of PI3K, P-PI3K, C-caspase-3, Akt, and p-Akt (dilution 1:1,000) at 4°C. Subsequently, the PVDF membrane was incubated for 1 h with the diluted secondary antibody. Finally, the protein bands were stained with ECL detection kits, and β-actin was used as the internal reference. Image analysis software ImageJ (version 1.51, National Institutes of Health, MD, United States) was utilized for gray analysis.

Statistical Analysis

All the data were presented as the mean ± standard deviations (SDs), statistical comparisons were evaluated using one-way analysis of variance (ANOVA), and significant differences between the mean values were measured using Duncan's multiple range test. $p < 0.01$ was deemed statistically significant.

RESULTS

Effective Compounds of BTP

A total of 34 components were identified from BTP, of which six compounds belonged to *Angelica sinensis* (Oliv.) Diels, seven to *Astragalus membranaceus* (Fisch.) Bge, six to *Glycyrrhiza uralensis* Fisch., six to *Panax notoginseng* (Burk.) F. H. Chen, and nine to *Pheretima aspergillum* (E.Perrier). Their specific information and total ion current diagram are shown in **Table 1**, **Table 2**, and **Figure 2**, respectively. Moreover, a total of 1,232 related targets were obtained from the online databases.

Establishment of the ONFH Target Library

A total of 178 DEGs were screened out, including 143 upregulated genes and 35 downregulated genes, and were visualized with a volcano plot, as shown in **Figure 2**. In the volcano plot, the vertical axis represents $\log_2$ FC (fold change), and the horizontal axis represents $\log_{10}$ (p-value). The DEGs with $\log_2$ FC > 0 were defined as upregulated genes, and the others were downregulated genes. Additionally, the expression situation regarding all the DEGs was visualized with a heatmap, as shown in **Figure 3A**. In the heatmap, the vertical axis represents DEGs, while the horizontal axis represents the sample. DEGs were effectively divided into normal and ONFH groups. Red indicates the upregulated gene, and green represents the downregulated genes.

Acquisition of Core Genes Regarding BTP Against ONFH

Centrality expresses the degree of a node in a certain network in the center of the whole network. The degree is defined as the sum of direct connections between nodes and represents the cohesion of a given node in a certain network. Furthermore, betweenness indicates the number of shortest paths passing through a node. These three factors are the indispensable basis for assessing the importance of a specific target. Through screening, 17 core targets with 114 vital interactions were obtained, and the detailed information and identification process of core targets are shown in **Table 3** and **Figure 3C**, respectively.

Functional Enrichment of Core Targets

The signal pathway of core targets was analyzed using the Metascape platform, and the results were visualized by bioinformatics. The results showed that the functions of core targets were closely related to the occurrence of ONFH. KEGG and GO enrichment are presented in **Table 4** and **Figure 4**, respectively.

Based on the results of KEGG enrichment, as shown in **Table 4**, multiple pathways jointly contributed to the antiONFH effect of BTP, including the PI3k-Akt signaling pathway, prostate cancer, pathways in cancer, the cell cycle, the estrogen signaling pathway, protein processing in the endoplasmic reticulum, hepatitis c, proteoglycans in cancer, the central carbon metabolism in cancer, small-cell lung cancer, progesterone-mediated oocyte maturation, endocrine resistance, oocyte meiosis, fluid shear stress and atherosclerosis, and breast cancer. Thus, it suggested that the antiONFH effect of BTP might associate with a synergistic effect of multiple pathways.

In conformity with the results of GO enrichment, the biological processes (BPs) in which BTP chiefly participated involved DNA repair, cell cycle phase transition, regulation of cell cycle phase transition, regulation of the cell cycle process, mitotic cell cycle G1/S transition, cell cycle G1/S phase transition, mitotic cell cycle phase transition, positive regulation of the cell cycle, the DNA biosynthetic process, response to topologically incorrect protein, protein insertion into the membrane, the proteasome-mediated ubiquitin-dependent protein catabolic process, regulation of mitotic cell cycle phase transition, regulation of cell cycle G2/M phase transition, and developmental growth involved in morphogenesis.

Such effects were primarily reflected in several aspects, including ubiquitin-protein ligase binding, ubiquitin-like protein ligase binding, nitric-oxide synthase regulator activity, disordered domain specific binding, kinase binding, protein kinase binding, protein domain specific binding, protease binding, cell adhesion molecule binding, histone deacetylase binding, unfolded protein binding, integrin binding, protein phosphatase binding, phosphatase binding, and chromatin binding. The targets of this action were chiefly concentrated in multiple cell sites, including vesicle lumen, melanosomes, pigment granules, secretory granule lumen, cytoplasmic vesicle lumen, the perinuclear region of the cytoplasm, ficolin-1-rich granule lumen, the intracellular protein-containing complex, focal adhesion, the cell–substrate junction, growth cones, neuronal cell bodies, sites of polarized growth, ficolin-1-rich granules, and the protein-DNA complex.

Based on the above bioinformatics analysis, previous reports, and our preliminary experiments, we deduced that the molecular mechanisms of this TCM formula might attribute to PI3K/Akt-related cell apoptosis.

Construction of Key Targets-Pathway Network

The network of key targets-pathway was constructed with Cytoscape (3.7.2), as presented in **Figure 3B**. V represents the pathway, and the diamond represents the DEGs. The greater the significance, the larger the volume of the graph was. The results showed that the targets of TP53, EGFR, and CDK2 and the pathways of the PI3K-AKT signaling pathway and cell cycle were more critical in the entire network. Therefore, subsequent experiments chose these two pathways for verification.

Cytotoxic Effect of BTP on RAW264.7 Cells

The cytotoxicity of BTP on normal RAW 264.7 cells was assessed by CCK-8 assays. As shown in **Figure 5**, BTP at concentrations up to 200 mg/ml did not exhibit obvious cytotoxicity on RAW264.7 cells within 24 and 48 h of incubation.

BTP Inhibits Osteoclastogenesis and Bone Resorption in Osteoclasts

At 7 days after inducting RAW 264.7 cells with RANKL (100 ng/ml), TRAP-positive multinucleated cells were observed under a light microscope, as shown in **Figure 6**. Interestingly, BTP at 20, 40, and 80 μg/ml markedly decreased the number of osteoclasts in a dose-dependent manner ($p < 0.05$ at 100 μg/ml, $p < 0.005$ at 200 μg/ml, $p < 0.0001$ at 400 μg/ml). In addition, the significant inhibitory effect of BTP on bone resorption *in vitro* has also been confirmed. As shown in **Figure 8**, compared with the control group, BTP dose-dependently reduced the area of bone resorption.

BTP Induces Cell Apoptosis in Osteoclasts

In this study, two comprehensively recognized cell apoptosis detection methods, including AO-EB double staining and FITC-conjugated Annexin V/PI staining, were carried out using a laser confocal microscope and flow cytometry analysis. Therefore, we further explored the apoptosis induced by BTP treatments. As shown in **Figure 7A**, our present results confirmed our hypothesis. After 5 days of RANKL treatment, the RAW 264.7 cells were induced to osteoclasts. As shown in **Figure 7A**, BTP at the concentrations of 50, 75, and 100 μg/ml could induce apoptosis in osteoclasts, compared to the control osteoclasts. Moreover, the results of immunofluorescence also presented the same trend. As far as we know, JC-1 aggregates in the mitochondrial matrix to form polymers that emit red fluorescence under normal physiological conditions and green fluorescence when MMP is reduced. Thus, the changes of $\Delta\Psi m$

TABLE 3 | Detailed attribute values of core targets.

Name	Degree	Betweenness	Closeness
TP53	417	8838.351	0.625
EGFR	413	4978.824	0.584532
ESR1	362	4732.667	0.595238
YWHAZ	354	5282.821	0.602968
FN1	401	5764.932	0.616114
UBC	421	7284.354	0.608614
NTRK1	715	15501.89	0.680628
CUL3	519	8497.666	0.643564
CUL1	331	4143.496	0.604651
CDK2	352	5856.056	0.605778
COPS5	364	4224.348	0.605214
HSP90AB1	304	3368.986	0.577265
ITGA4	298	3802.689	0.592525
HSP90AA1	368	3823.474	0.587703
VCP	301	3662.213	0.579839
NPM1	291	3407.6	0.590909
MCM2	403	6534.106	0.617871

could be directly reflected by the fluorescence transformation. In **Figure 7B**, compared with the control group, the green fluorescence of the experimental group was getting stronger, while the red fluorescence was getting weaker, indicating that MMP breakdown happened.

The results suggested that BTP (50, 75, and 100 μg/ml) could induce remarkable apoptosis in osteoclasts (RANKL induced RAW 264.7 cells). Furthermore, the apoptosis markers of C-caspase-3, bcl-2, and bax were determined. As shown in **Figure 8**, BTP could upregulate the expression of C-caspase three and bax, downregulating bcl-2 expression in osteoclasts in a dose-dependent manner.

BTP Regulates the PI3K/AKT Signal Pathway in Osteoclasts

The PI3K/Akt pathway is a classical signaling pathway responsible for regulating cell proliferation, differentiation, apoptosis, and a

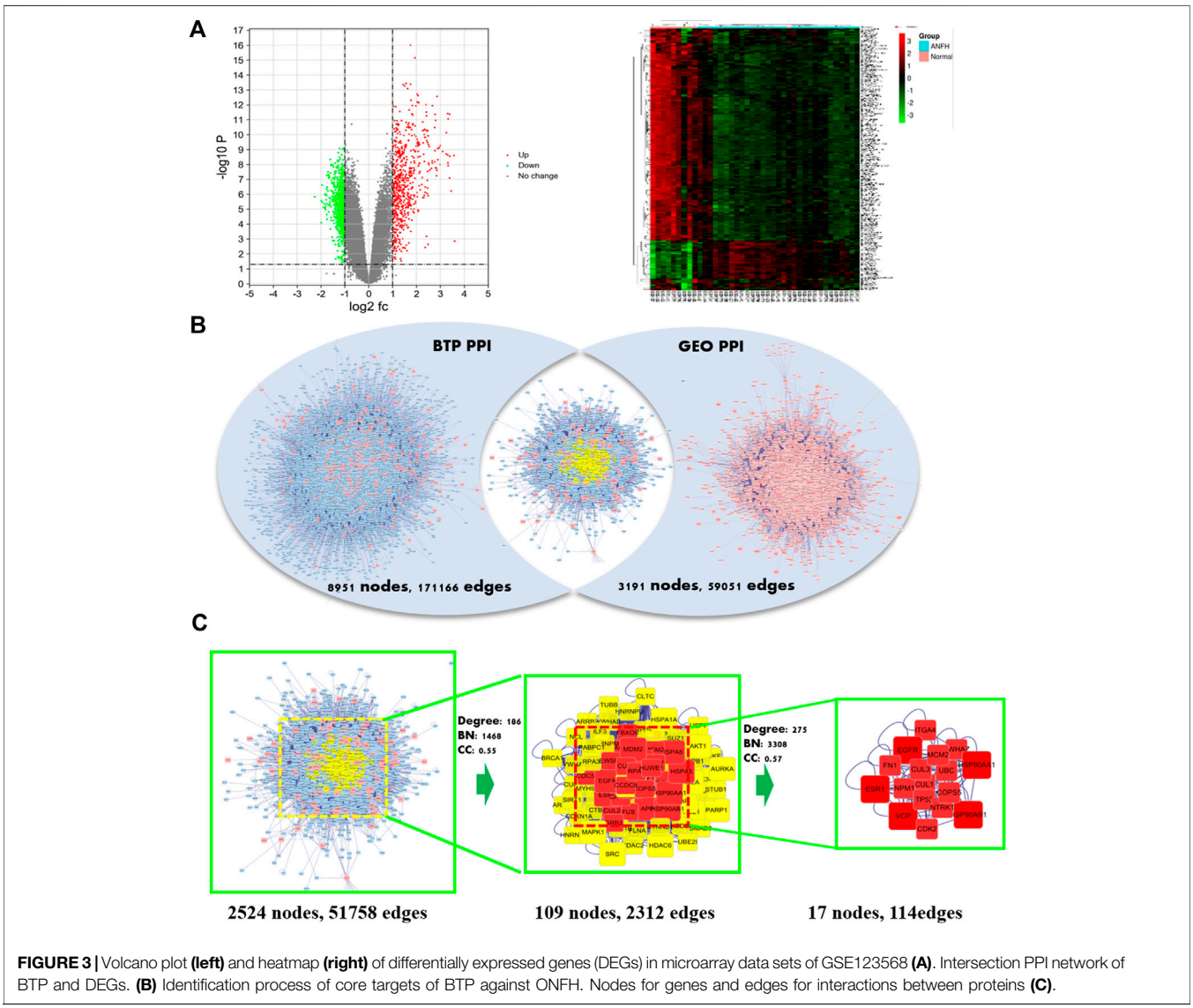


FIGURE 3 | Volcano plot **(left)** and heatmap **(right)** of differentially expressed genes (DEGs) in microarray data sets of GSE123568 **(A)**. Intersection PPI network of BTP and DEGs. **(B)** Identification process of core targets of BTP against ONFH. Nodes for genes and edges for interactions between proteins **(C)**.

TABLE 4 | Functional enrichment of the core targets of BTP-DEGs.

Term	Category	Count	*p* Value	Gene ratio
KEGG	PI3K-Akt signaling pathway	9	2.982E-13	52.94117647
	Prostate cancer	5	1.505E-09	29.41176471
	Pathways in cancer	7	1.745E-09	41.17647059
	Cell cycle	5	9.05E-09	29.41176471
	Estrogen signaling pathway	4	3.169E-07	23.52941176
	Protein processing in endoplasmic reticulum	4	2.61E-06	23.52941176
	Hepatitis C	4	2.802E-06	23.52941176
	Proteoglycans in cancer	4	5.796E-06	23.52941176
	Central carbon metabolism in cancer	3	7.797E-06	17.64705882
	Small cell lung cancer	3	1.689E-05	17.64705882
	Progesterone-mediated oocyte maturation	3	2.521E-05	17.64705882
	Endocrine resistance	3	2.521E-05	17.64705882
	Oocyte meiosis	3	5.416E-05	17.64705882
	Fluid shear stress and atherosclerosis	3	8.104E-05	17.64705882
	Breast cancer	3	8.447E-05	17.64705882
GO BP	DNA repair	8	5.631E-10	
	cell cycle phase transition	8	1.399E-09	
	regulation of cell cycle phase transition	7	6.522E-09	
	regulation of the cell cycle process	8	7.122E-09	
	G1/S transition of the mitotic cell cycle	6	9.284E-09	
	cell cycle G1/S phase transition	6	1.498E-08	
	mitotic cell cycle phase transition	7	2.936E-08	
	positive regulation of the cell cycle	6	7.962E-08	
	DNA biosynthetic process	5	9.436E-08	
	response to the topologically incorrect protein	5	1.149E-07	
	protein insertion into the membrane	4	1.196E-07	
	proteasome-mediated ubiquitin-dependent protein catabolic process	6	1.243E-07	
	regulation of mitotic cell cycle phase transition	6	1.484E-07	
	regulation of cell cycle G2/M phase transition	5	1.558E-07	
	developmental growth involved in morphogenesis	5	1.782E-07	
GO MF	ubiquitin protein ligase binding	9	2.855E-14	
	ubiquitin-like protein ligase binding	9	5.039E-14	
	nitric-oxide synthase regulator activity	4	1.142E-11	
	disordered domain specific binding	4	4.166E-09	
	Kinase binding	8	4.315E-09	
	protein kinase binding	7	5.903E-08	
	protein domain specific binding	7	8.076E-08	
	Protease binding	4	1.015E-06	
	cell adhesion molecule binding	5	1.313E-05	
	histone deacetylase binding	3	4.105E-05	
	unfolded protein binding	3	4.912E-05	
	integrin binding	3	8.104E-05	
	protein phosphatase binding	3	9.162E-05	
	Phosphatase binding	3	0.0002008	
	chromatin binding	4	0.0002956	
GO CC	vesicle lumen	5	1.147E-06	
	melanosome	3	3.392E-05	
	pigment granule	3	3.392E-05	
	secretory granule lumen	4	3.55E-05	
	cytoplasmic vesicle lumen	4	3.725E-05	
	perinuclear region of the cytoplasm	5	5.163E-05	
	ficolin-1-rich granule lumen	3	5.416E-05	
	intracellular protein-containing complex	5	5.621E-05	
	focal adhesion	4	9.86E-05	
	cell-substrate junction	4	0.0001051	
	growth cone	3	0.0001582	
	neuronal cell body	4	0.0001585	
	site of polarized growth	3	0.0001744	
	ficolin-1-rich granule	3	0.0001772	
	protein-DNA complex	3	0.0002502	

series of critical physiological activities. Nevertheless, only the phosphorylation of PI3K and Akt mainly participate in these physiological activities. Besides, growing numbers of studies have found that cell apoptosis is closely related to the PI3K/Akt pathway (Xue and Feng, 2018; Zhan and Yan, 2020). Therefore, we evaluated the effect of BTP on the PI3K/Akt pathway in osteoclasts.

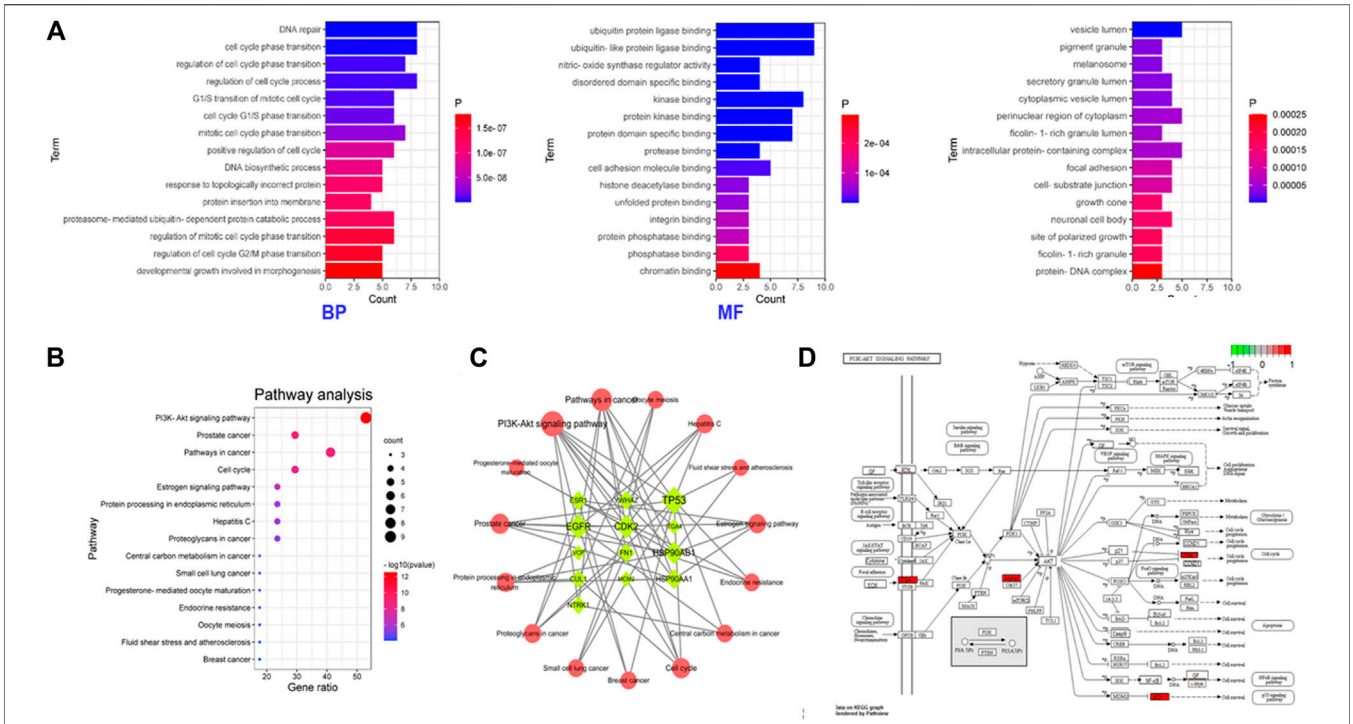


FIGURE 4 | Functional enrichment of the core targets of BTP-DEGs. **(A)** GO enrichment. **(B)** KEGG enrichment. **(C)** Network of Key Targets-Pathway. **(D)** Pathway map of key targets.

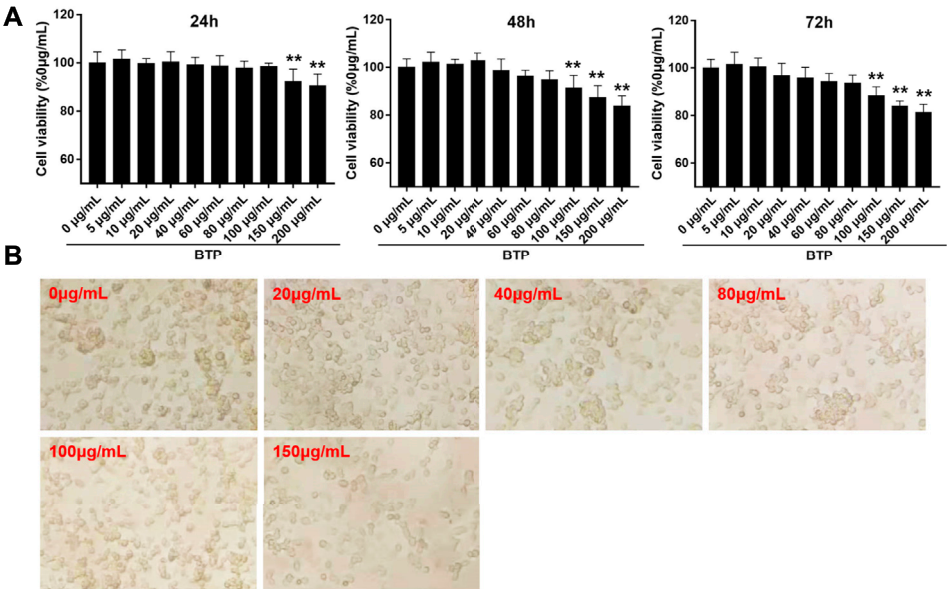


FIGURE 5 | Cytotoxic effect of BTP on RAW264.7 cells. **(A)** Cell viability assays of RAW 264.7 cells treated with series doses of BTP at 24, 48, and 72 h, respectively. **(B)** Representative figures of RAW264.7 cells treated with series doses of BTP for 24 h.

In the present study, both immunofluorescence and western blot assays were performed to determine the effect of BTP on the PI3K/Akt signaling pathway in osteoclasts. The results revealed that after pretreatment with BTP, the expression of p-Akt and p-PI3K was reduced, while no noticeable change was evident in the expression of AKT and PI3K compared to the control group (**Figure 8B**). Likewise, as presented in **Figure 8C**, the result of the immunofluorescence revealed that green fluorescence becomes

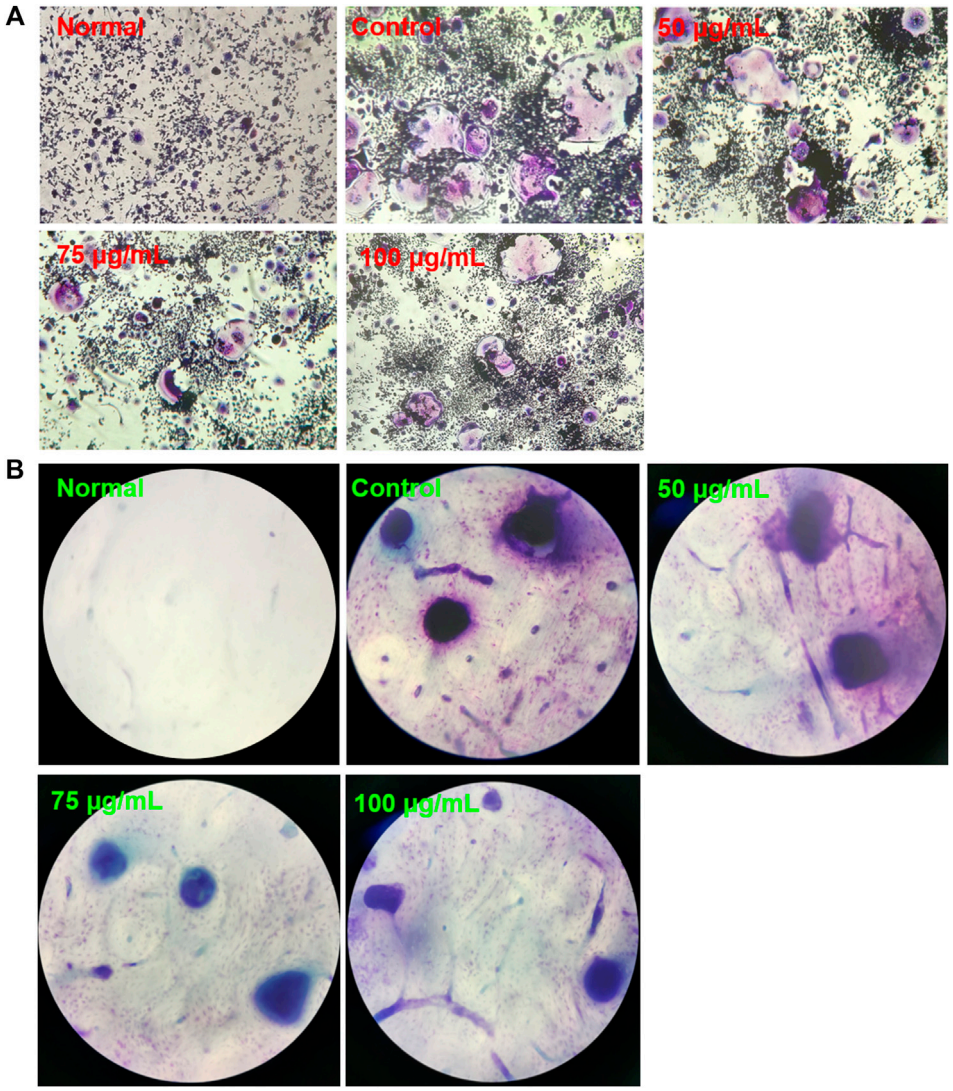


FIGURE 6 | Osteoclastogenesis with TRAP staining **(A)** and bone resorption assay **(B)**.

weaker, indicating that the expression of p-Akt was reduced, and the red fluorescence (the expression of Akt) had no apparent change.

DISCUSSION

It is widely known that TCM has shown broad application prospects in treating various intractable diseases and has become increasingly recognized globally (Zhang et al., 2021; Long et al., 2020). TCM also provides abundant resources for the development of new drugs. However, it remains a challenge to study the mechanisms of action of the TCM formula due to their characteristic of multicomponents, multitargets, and multipathways (Yu and Qi, 2020). Network pharmacology, first put forward by Hopkins in 2007, can analyze the connection of components, targets, and diseases in the network systematically and study the multilayer and multipathway mechanism of action of medications comprehensively, which coincides with the fundamental concept of holism in TCM (Hopkins, 2007; Sheng et al., 2020). Thus, it has become increasingly indispensable for performing qualified basic research of TCM formulas (Zhang et al., 2021). In addition, network pharmacology may realize "drug relocation" and explore new biological activities of drugs, thus expanding the application scope. As a result, it has been widely used in pharmacological research regarding TCM.

BTP has a long history of clinical applications for ONFH treatment and is composed of *Angelica sinensis* (Oliv.) Diels, *Pheretima aspergillum* (E.Perrier), *Panax notoginseng* (Burk.) F. H. Chen, *Astragalus membranaceus* (Fisch.) Bge, and *Glycyrrhiza uralensis* Fisch. This TCM formula has the effects of nourishing

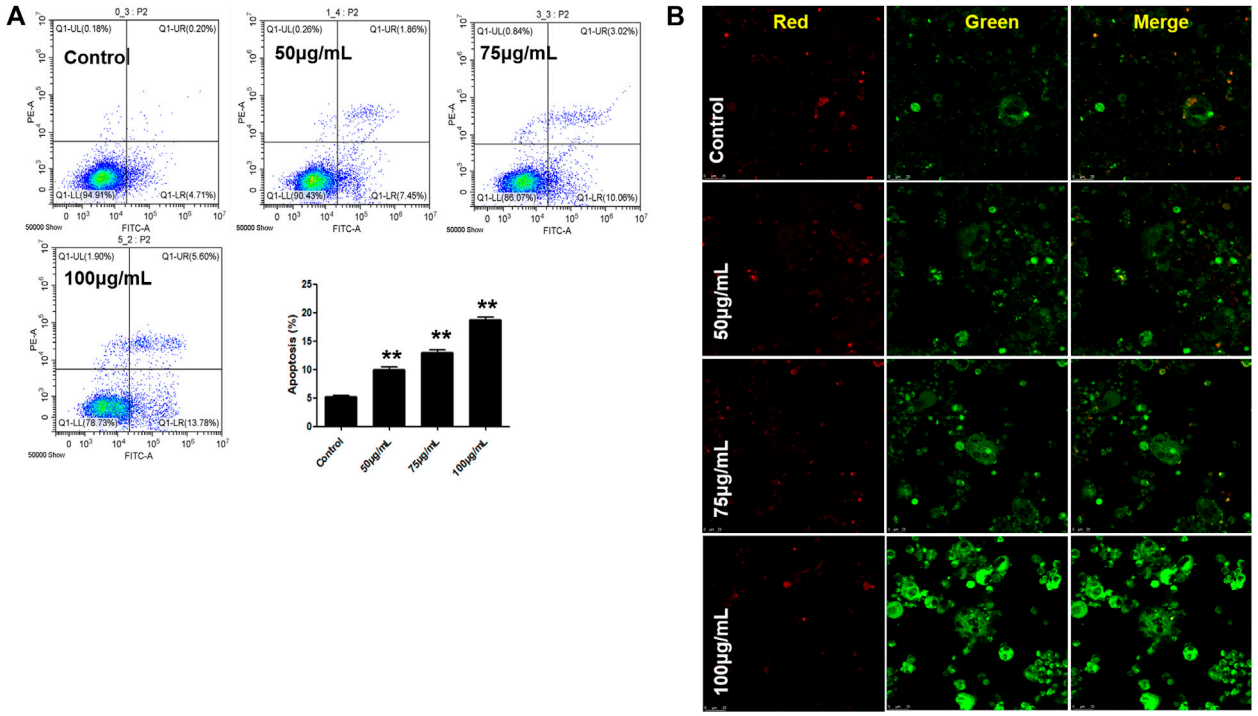


FIGURE 7 | BTP induces cell apoptosis **(A)** and decreases MMP **(B)** in osteoclasts (× 400).

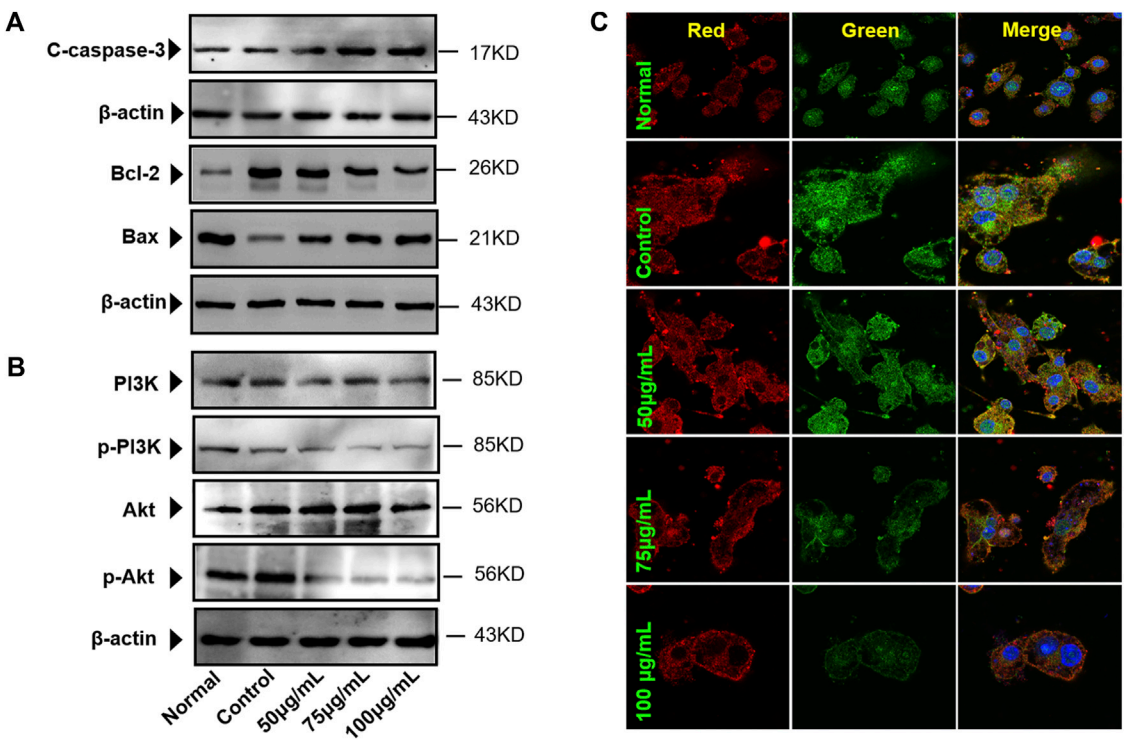


FIGURE 8 | BTP regulates apoptotic proteins in osteoclasts. **(A)** Caspase-3, Bcl-2, and Bax **(B)** Akt and PI3K in osteoclasts. **(C)** Akt/p-Akt expressions in cells (× 400), p-Akt (green) and Akt (red).

blood, promoting blood circulation, dredging collaterals, and relieving pain. Although the anti-ONFH effect of BTP has been well documented, its active components and mechanisms of action remain obscure and need further research. In this study, a total of 34 compounds were identified. Among these, six compounds (caffeic acid, pimpinellin, Z-ligustilide, ferulic acid, chlorogenic acid, and benzoic acid) belonged to *Angelica sinensis* (Oliv.) Diels, seven (ononin, biochanin a, formononetin, sucrose, calycosin-7-O-β-D-glucoside, asparagine, and daidzein) to *Astragalus membranaceus* (Fisch.)Bge, six (liquiritin, isoliquiritigenin, isoliquiritin, glycyrrhizic acid, licochalcone A, and licoricesaponin g2) to *Glycyrrhiza uralensis* Fisch., eight (caffeic acid, 3-coumaric acid, psoralen, gypenoside xvii, ginsenoside Rb1, and ginsenoside re) to *Panax notoginseng* (Burk.), and nine (succinic acid, hypoxanthine, DL-arginine, nicotinic acid, guanine, guanosine, phenylalanine, tryptophan, and inosine) to *Pheretima aspergillum* (E. Perrier). Formononetin and daidzein have been reported to inhibit RANKL-induced osteoclast differentiation and regulate osteogenic differentiation, indicating that they may become potential drugs for preventing and treating bone destruction in ONFH. In addition, another study has shown that the extract of *Panax notoginseng* (Burk.) could significantly promote the repair of the femoral head in rabbits with ONFH and improve the bone density and bone microstructure (Gui et al., 2019), which was also supported by clinical research (Jia et al., 2011).

KEGG is one of the most used tools to predict the possible molecular mechanisms of drugs, particularly herbal medicines. In our present study, the KEGG enrichment of the core target genes revealed that these genes were significantly enriched in the PI3K-AKT signaling pathway and cell cycle. Numerous studies have confirmed that cell apoptosis is often accompanied by growth arrest, suggesting that cell cycle arrest correlates with apoptosis closely (Duan et al., 2021; Zhang et al., 2021). When CAF and theobromine, which can shorten the G2/M block time, were added before the exposure, the ratio of the G2/M phase decreased with more noticeable increases in apoptosis. In contrast, when TPA, IBMX, and 3-aminoben extending the G2/M block time were added, the G2/M ratio increased, while the apoptosis ratio decreased (Zhao et al., 1999). Shinomiya *et al.* used CAF to reduce the G2 blockade of mouse lymphoma cells EL-4 caused by *cis*-diamminedichloroplatinum and promote the occurrence of apoptosis (Shinomiya et al., 1997). As a result, we designed a series of *in vitro* experiments to verify our hypothesis. In the present study, CCK-8 results showed that BTP had no toxicity to RAW 264.7 cells under 150 μg/ml for 24 h treatment.

Therefore, we applied the concentration of 50, 75, and 100 μg/ml to the follow-up experiments. TRAP staining results showed that BTP at 75 and 100 μg/ml inhibited the formation of TRAP-positive multinucleated cells. In addition, the area of bone resorption *in vitro* was also significantly suppressed, illustrating that BTP could inhibit the formation of osteoclasts. In addition, the results of flow cytometry revealed that BTP could induce remarkable apoptosis in osteoclasts (RANKL-induced RAW 264.7 cells) and decrease the mitochondrial membrane potential (MMOP, $\Delta\Psi$). Consequently, we determined the apoptosis-related proteins of C-caspase-3, Bax, and Bcl-2, and found that BTP could upregulate the proapoptosis proteins of C-caspase-3 and Bax but downregulate the antiapoptosis protein of Bcl-2, which is consistent with the flow cytometry and MMOP analysis. The PI3K-Akt signaling pathway is closely related to cell apoptosis and has been recognized as a potential target for regulating cell survival and apoptosis (Zhang et al., 2019). Therefore, we speculated that the treatment effects of BTP on ONFH might associate with PI3K/Akt-mediated apoptosis. In our bioinformatics analysis, the results indicated that the effects of BTP might be closely related to the PI3K/Akt signaling pathway, which is also an important upstream signaling for apoptosis. Therefore, we determined the expressions of PI3K/Akt signal-related proteins, including PI3K, phosphorylation (p)-PI3K, Akt, and p-Akt. Our results demonstrated that BTP treatment could downregulate the expressions of p-PI3K and p-Akt, subsequently resulting in cell apoptosis of osteoclasts (RANKL induced RAW 264.7 cells).

CONCLUSION

In conclusion, our present results suggested that BTP treatment could be beneficial for the osteonecrosis of the femoral head (ONFH), and the possible mechanisms are related to suppressing the formation of osteoclasts and induction of apoptosis in osteoclasts via regulation of the PI3K/Akt signaling pathway (Calder et al., 2004, Dhomen et al., 2012, Huang et al., 2004, Hua, 2017, Kimura et al., 2006, Lanaya et al., 2014, Linder et al., 2018, Lv et al., 2021, Mettey et al., 2003, Okuma et al., 2008, Poeta et al., 2007, Roovers et al., 2007, Ren et al., 2013, Savio et al., 2014, Schneider et al., 2009, Soussi, 2000, Xu et al., 2020, Yu et al., 2020, Zhang et al., 2014).

DATA AVAILABILITY STATEMENT

The datasets presented in this study can be found in online repositories. The names of the repository/repositories and accession number(s) can be found below: PRIDE (Proteomics Identification Database, https://www.ebi.ac.uk/pride/archive). The Project Name: Analysis of components of Buxuetongluo Pills by LC-MS/MS, Project accession: PXD027269.

AUTHOR CONTRIBUTIONS

All authors contributed to the article and approved the submitted version. YHC, QR, and XPT conceived and designed this paper. DW, YCL, DT completed the main experiment content. HL, RL processed all the pictures in the article. DW and YCL analyzed the data and wrote the original draft of the paper. YHC reviewed and edited the paper. Additionally, WS helped complete the test of osteogenic differentiation and bone resorption, and SJ helped complete all the confocal imaging.

FUNDING

This research was supported by the Sichuan Science and Technology Program (Grant No. 2020YFS0525), the

International Cooperation and Exchange Project of Sichuan Provincial Science and Technology Department (Grant No. 2017HH0004), the National Natural Science Foundation of China (Grant No. 81603537), the Sichuan Provincial Administration of Traditional Chinese Medicine (Grant No. 2021MS464), and the Youth Scholarship of Chengdu University of Traditional Chinese Medicine (Grant No. QNXZ2019043).

REFERENCES

Calder, J. D., Buttery, L., Revell, P. A., Pearse, M., and Polak, J. M. (2004). Apoptosis--a Significant Cause of Bone Cell Death in Osteonecrosis of the Femoral Head. *J. Bone Jt. Surg Br* 86 (8), 1209–1213. doi:10.1302/0301-620x.86b8.14834

Chen, L., Qi, J., Chang, Y. X., Zhu, D., and Yu, B. (2009). Identification and Determination of the Major Constituents in Traditional Chinese Medicinal Formula *Danggui-Shaoyao-San* by HPLC-DAD-ESI-MS/MS. *J. Pharm. Biomed. Anal.* 50 (2), 127–137. doi:10.1016/j.jpba.2009.03.039

Clough, E., and Barrett, T. (2016). The Gene Expression Omnibus Database. *Methods Mol. Biol.* 1418, 93–110. doi:10.1007/978-1-4939-3578-9_5

Cui, Y., Li, C., Zeng, C., Li, J., Zhu, Z., Chen, W., et al. (2018). *Tongmai Yangxin* Pills Anti-oxidative Stress Alleviates Cisplatin-Induced Cardiotoxicity: Network Pharmacology Analysis and Experimental Evidence. *Biomed. Pharmacother.* 108, 1081–1089. doi:10.1016/j.biopha.2018.09.095

Daina, A., Michielin, O., and Zoete, V. (2019). SwissTargetPrediction: Updated Data and New Features for Efficient Prediction of Protein Targets of Small Molecules. *Nucleic Acids Res.* 47 (W1), W357–W364. doi:10.1093/nar/gkz382

Dhomen, N. S., Mariadason, J., Tebbutt, N., and Scott, A. M. (2012). Therapeutic Targeting of the Epidermal Growth Factor Receptor in Human Cancer. *Crit. Rev. Oncog* 17 (1), 31–50. doi:10.1615/critrevoncog.v17.i1.40

Duan, H., Zhang, Q., Liu, J., Li, R., Wang, D., Peng, W., et al. (2021). Suppression of Apoptosis in Vascular Endothelial Cell, the Promising Way for Natural Medicines to Treat Atherosclerosis. *Pharmacol. Res.* 168, 105599. doi:10.1016/j.phrs.2021.105599

Gui, X., Jiang, Z., Chen, B., Yu, J., and Yang, Y. (2019). Effect of Radix et *Rhizoma Notoginseng* on the microstructure of femoral head in rabbits with steroid-induced osteonecrosis of femoral head and Its Mechanism. *J. New Chin. Med.* 51 (12), 9–12.

Hopkins, A. L. (2007). Network Pharmacology. *Nat. Biotechnol.* 25(10), 1110–1111. doi: doi:10.1038/nbt1007-1110

Hopkins, A. L. (2008). Network Pharmacology: The Next Paradigm in Drug Discovery. *Nat. Chem. Biol.* 4 (11), 682–690. doi:10.1038/nchembio.118

Hua, Y. (2017). Expression of P53 Gene in the Blood of Patients with Alcohol-Induced Avascular Necrosis of the Femoral Head and its Mechanism on Osteoblast Apoptosis. *Anat. Res* 39 (02), 136–139.

Huang, da. W., Sherman, B. T., and Lempicki, R. A. (2009). Bioinformatics Enrichment Tools: Paths toward the Comprehensive Functional Analysis of Large Gene Lists. *Nucleic Acids Res.* 37 (1), 1–13. doi:10.1093/nar/gkn923

Huang, Y., Luo, X., Guo, K., An, H., and Jiang, D. (2004). Effect of Endogenous Glucocorticoid on Expression of P53 and Bcl-2 Proteins in Osteocyte Apoptosis in Avascular Necrosis of the Femoral Head Induced by Alcoholism. *Guizhou. Med. J.* 12, 1059–1062.

Jia, B., Fan, W., Chen, G., Li, Y., Zhang, G., Yang, Sh., et al. (2019). Development of UPLC-MS Combined with HPLC Technique to Explore the Effects of Exogenous Substances on the Saponin Contents and Growth of *Panax Notoginseng* Leaves. *J. Yunnan Agric. Univ.* 34 (01), 116–123. doi:10.12101/j.issn.1004-390X(n).201712011

Jia, F., Sun, R., Li, Y., Liu, B., Zhao, F., and Xiong, Y. (2011). Study on Prevention and Treatment of Femoral Head Necrosis after Femoral Neck Fracture with *Sanqi Danshen* Tablet. *Chin. J. Orthop. Traumatol.* 6, 12–14.

Kimura, H., Fujiwara, Y., Sone, T., Kunitoh, H., Tamura, T., Kasahara, K., et al. (2006). EGFR Mutation Status in Tumour-Derived DNA from Pleural Effusion Fluid Is a Practical Basis for Predicting the Response to Gefitinib. *Br. J. Cancer* 95 (10), 1390–1395. doi:10.1038/sj.bjc.6603428

Lanaya, H., Natarajan, A., Komposch, K., Li, L., Amberg, N., Chen, L., et al. (2014). EGFR Has a Tumour-Promoting Role in Liver Macrophages during Hepatocellular Carcinoma Formation. *Nat. Cel Biol.* 16 (10), 972–977. doi:10.1038/ncb3031

Linder, M., Hecking, M., Glitzner, E., Zwerina, K., Holcmann, M., Bakiri, L., et al. (2018). EGFR Controls Bone Development by Negatively Regulating mTOR-Signaling during Osteoblast Differentiation. *Cell Death Differ* 25 (6), 1094–1106. doi:10.1038/s41418-017-0054-7

Liu, J., Wang, X., Cai, S., Katsuko, K., and Tsuneo, N. (2004). Analysis of the Constituents in the Chinese Drug Notoginseng by Liquid Chromatography-Electrospray Mass Spectrometry. *Chin. Pharm. J.* 13 (4). doi:10.1021/ja961604z

Liu, L., Duan, J., and Tang, Y. (2017). Study on Chemical Component and Synergetic Effect of Concerted Application of Chinese Angelica and Safflower by Using UHPLC-Q-TOF-MS. *Chin. J. Tradit. Chin. Med. Pharm.* 3, 996–1000.

Liu, M. H., Tong, X., Wang, J. X., Zou, W., Cao, H., and Su, W. W. (2013). Rapid Separation and Identification of Multiple Constituents in Traditional Chinese Medicine Formula Shenqi Fuzheng Injection by Ultra-fast Liquid Chromatography Combined with Quadrupole-Time-Of-Flight Mass Spectrometry. *J. Pharm. Biomed. Anal.* 74, 141–155. doi:10.1016/j.jpba.2012.10.024

Liu, M., Hui, O., Jia, J., Huang, W., Guo, S., He, M., et al. (2019). Analysis of Anti-complement Activity and Active Ingredients of *Gynura Procumbens* by UPLC-Q-TOF-MS. *Chin. Tradit Pat Med.* 41 (11), 2681–2687.

Liu, Z., Jiang, M., Lu, X., Qin, F., Song, Y., Wen, J., et al. (2012). Simultaneous Determination of Pimpinellin, Isopimpinellin and Phellopterin in Rat Plasma by a Validated UPLC-MS/MS and its Application to a Pharmacokinetic Study after Administration of *Toddalia Asiatica* Extract. *J. Chromatogr. B Analyt Technol. Biomed. Life Sci.* 891-892, 102–108. doi:10.1016/j.jchromb.2012.02.022

Luo, L., Gao, W., Zhang, Y., Liu, C., Wang, G., Wu, H., et al. (2020). Integrated Phytochemical Analysis Based on UPLC-MS and Network Pharmacology Approaches to Explore the Quality Control Markers for the Quality Assessment of *Trifolium Pratense* L. *Molecules* 25 (17), 3787. doi:10.3390/molecules25173787

Lv, W., Yu, M., Yang, Q., Kong, P., and Yan, B. (2021). Total Flavonoids of Rhizoma Drynariae Ameliorate Steroid-induced A-vascular N-ecrosis of the F-emoral H-ead via the PI3K/AKT P-athway. *Mol. Med. Rep.* 23 (5). doi:10.3892/mmr.2021.11984

Meng, X., Li, H., Song, F., Liu, C., Liu, Z., and Liu, S. (2009). Studies on Triterpenoids and Flavones inGlycyrrhiza uralensisFisch. By HPLC-ESI-MSnand FT-ICR-MSn. *Chin. J. Chem.* 27 (2), 299–305. doi:10.1002/cjoc.200990048

Mettey, Y., Gompel, M., Thomas, V., Garnier, M., Leost, M., Ceballos-Picot, I., et al. (2003). Aloisines, a New Family of CDK/GSK-3 Inhibitors. SAR Study, crystal Structure in Complex with CDK2, Enzyme Selectivity, and Cellular Effects. *J. Med. Chem.* 46 (2), 222–236. doi:10.1021/jm020319p

Okuma, C., Kaketa, T., Hikita, A., Matsuda, K., Nakamura, M., Nagase, Y., et al. (2008). Potential Involvement of P53 in Ischemia/reperfusion-Induced Osteonecrosis. *J. Bone Miner Metab.* 26 (6), 576–585. doi:10.1007/s00774-007-0849-6

Ping, C. (2021). Clinical Observation on Non-traumatic Femoral Head Necrosis Treated by Operation Combined with Huangqi Shenggu Decoction. *J. Tradit Chin. Med.* 37 (03), 427–429.

Poeta, M. L., Manola, J., Goldwasser, M. A., Forastiere, A., Benoit, N., Califano, J. A., et al. (2007). TP53 Mutations and Survival in Squamous-Cell Carcinoma of the Head and Neck. *N. Engl. J. Med.* 357 (25), 2552–2561. doi:10.1056/NEJMoa073770

Pouya, F., and Kerachian, M. A. (2015). Avascular Necrosis of the Femoral Head: Are Any Genes Involved?. *Arch. Bone Jt. Surg.* 3 (3), 149–155. doi:10.22038/abjs.2015.4294

Qing, Z., Xinyue, D., Ruolan, L., Jiayi, S., Jia, L., Wei, P., et al. (2021). Inducing Apoptosis and Suppressing Inflammatory Reactions in Synovial Fibroblasts Are Two Important Ways for Guizhi-Shaoyao-Zhimu Decoction against Rheumatoid Arthritis. *J. Inflamm. Res.* 14, 217–236. doi:10.2147/jir.s287242

Ren, Y., Zhu, Z., Zhang, W., Zhang, Y., and Zhang, H. (2013). HPLC-MS/MS Determination of Puerarin and Daidzein in Puerarin Root. *Phys. Test. Chem Anal B* 49 (04), 464–467.

Roovers, R. C., Laeremans, T., Huang, L., De Taeye, S., Verkleij, A. J., Revets, H., et al. (2007). Efficient Inhibition of EGFR Signaling and of Tumour Growth by Antagonistic Anti-EFGR Nanobodies. *Cancer Immunol. Immunother.* 56 (3), 303–317. doi:10.1007/s00262-006-0180-4

Savio, A. L., da Silva, G. N., de Camargo, E. A., and Salvadori, D. M. (2014). Cell Cycle Kinetics, Apoptosis Rates, DNA Damage and TP53 Gene Expression in Bladder Cancer Cells Treated with Allyl Isothiocyanate (Mustard Essential Oil). *Mutat. Res.* 762, 40–46. doi:10.1016/j.mrfmmm.2014.02.006

Schneider, M. R., Sibilia, M., and Erben, R. G. (2009). The EGFR Network in Bone Biology and Pathology. *Trends Endocrinol. Metab.* 20 (10), 517–524. doi:10.1016/j.tem.2009.06.008

Shan, J., Yang, R., Zhang, X., Shen, C., Shen, C., Ji, J., et al. (2018). Network Pharmacological Study of Antitussive and Expectorant Effective of Jiegeng Decotion. *Chin. Tradit Herb Drugs* 49, 3501–3508.

Sheng, S., Huang, Y., Yang, Z., Li, J., and Xu, F. (2020). Conventional Drugs in New Use: Recognition on Pharmacological Effects of Tanshinone IIA Based on Gene Expression Profile and Connectivity Map. *Chin. J. Integr. Med. Cardio-/cerebrovascuiar Dis.* 18 (18), 2967–2973.

Shinomiya, N., Takemura, T., Iwamoto, K., and Rokutanda, M. (1997). Caffeine Induces S-phase Apoptosis in Cis-Diamminedichloroplatinum-Treated Cells, whereas Cis-Diamminedichloroplatinum Induces a Block in G2/M. *Cytometry* 27 (4), 365–373. doi:10.1002/(sici)1097-0320(19970401)27:4<365:aid-cyto8>3.0.co;2-b

Soussi, T. (2000). The P53 Tumor Suppressor Gene: from Molecular Biology to Clinical Investigation. *Ann. N. Y Acad. Sci.* 910, 121–129. doi:10.1111/j.1749-6632.2000.tb06705.x

Sun, B., and Li, G. (2013). Observation on 38 Cases of Femoral Head Necrosis Treated with Bushen Huoxue Decoction. *J. Tradit Chin. Med.* 29 (12), 987–988.

Wang, S., Tong, Y., Yang, Y., and Shi, Y. (2020). Mechanism of Wuling Powder in Treatment of Diabetic Kidney Disease Based on Network Pharmacology. *World Chin. Med.* 15 (22), 3383–3390. doi:10.3969/j.issn.1673-7202.2020.22.004

Wu, H., Zhong, S., Peng, L., Wu, W., Li, Z., and Li, W. (2020). HPLC-ESI-MS/MS Analysis of Active Component Differences in astragalus before and after Honey-Fried. *J. Chin. Mass. Spectr. Soc.* 41 (06), 117–127. doi:10.7538/zpxb.2019.0121

Xia, W., Hu, S., Wang, M., Xu, F., Han, L., and Peng, D. (2021). Exploration of the Potential Mechanism of the *Tao Hong Si Wu* Decoction for the Treatment of Postpartum Blood Stasis Based on Network Pharmacology and *In Vivo* Experimental Verification. *J. Ethnopharmacol.* 268, 113641. doi:10.1016/j.jep.2020.113641

Xu, H., Chen, S., Zhang, H., Zou, Y., Zhao, J., Yu, J., et al. (2020). Network-based Analysis Reveals Novel Gene Signatures in the Peripheral Blood of Patients with Sporadic Nonsyndromic Thoracic Aortic Aneurysm. *J. Cel Physiol* 235 (3), 2478–2491. doi:10.1002/jcp.29152

Xu, Q., Guo, Q., Wang, C. X., Zhang, S., Wen, C. B., Sun, T., et al. (2021). Network Differentiation: a Computational Method of Pathogenesis Diagnosis in Traditional Chinese Medicine Based on Systems Science. *Artif. Intell. Med.* 118():102134, doi:10.1016/j.artmed.2021.102134

Xu, Q., Wang, X., Zhong, N., Wang, Y., Li, Z., and Cai, Y. (2021). A Network Pharmacology and Molecular Docking Study on Treatment Mechanism of Bacterial Dysentery of *Huanglian-Huangqin-Huangbo* Herb Pair. doi: doi:10.21203/rs.3.rs-147874/v1

Xue, X. H., Feng, Z. H., Li, Z. X., and Pan, X. Y. (2018). Salidroside Inhibits Steroid-Induced Avascular Necrosis of the Femoral Head via the PI3K/Akt Signaling Pathway: *In Vitro* and *In Vivo* Studies. *Mol. Med. Rep.* 17 (3), 3751–3757. doi:10.3892/mmr.2017.8349

Yan, Z., Zhan, J., Qi, W., Lin, J., Huang, Y., Xue, X., et al. (2020). The Protective Effect of Luteolin in Glucocorticoid-Induced Osteonecrosis of the Femoral Head. *Front. Pharmacol.* 11, 1195. doi:10.3389/fphar.2020.01195

Yang, W., Feng, C., Kong, D., Shi, X., Cui, Y., Liu, M., et al. (2010). Simultaneous and Sensitive Determination of Xanthotoxin, Psoralen, Isoimpinellin and Bergapten in Rat Plasma by Liquid Chromatography-Electrospray Ionization Mass Spectrometry. *J. Chromatogr. B Analyt Technol. Biomed. Life Sci.* 878 (5-6), 575–582. doi:10.1016/j.jchromb.2009.12.035

Yu, L., Qiyue, Y., Yan, X., Yulu, Z., Jinyan, W., Songyu, L., et al. (2020). Nose to Brain Drug Delivery - a Promising Strategy for Active Components from Herbal Medicine for Treating Cerebral Ischemia Reperfusion. *Pharmacol. Res.* 159, 104795. doi:10.1016/j.phrs.2020.104795

Zhan, J., Yan, Z., Zhao, M., Qi, W., Lin, J., Lin, Z., et al. (2020). Allicin Inhibits Osteoblast Apoptosis and Steroid-Induced Necrosis of Femoral Head Progression by Activating the PI3K/AKT Pathway. *Food Funct.* 11, 7830–7841. doi:10.1039/D0FO00837K

Zhang, J.-Z., Gao, W.-Y., Gao, Y., Liu, D., Liu, D.-L., and Huang, L.-Q. (2011). Analysis of Influences of Spaceflight on Chemical Constituents in Licorice by HPLC-ESI-MS/MS. *Acta Physiol. Plant* 33, 2511–2520. doi:10.1007/s11738-011-0796-7

Zhang, Q., Duan, H. X., Li, R. L., Sun, J. Y., Liu, J., Peng, W., et al. (2021). Inducing Apoptosis and Suppressing Inflammatory Reactions in Synovial Fibroblasts Are Two Important Ways for Guizhi-Shaoyao-Zhimu Decoction against Rheumatoid Arthritis. *J. Inflamm. Res.* 14, 217–236. doi:10.2147/JIR.S287242

Zhang, Q., Liu, J., Duan, H., Li, R., Peng, W., and Wu, C. (2021). Activation of Nrf2/HO-1 Signaling: An Important Molecular Mechanism of Herbal Medicine in the Treatment of Atherosclerosis via the protection of Vascular Endothelial Cells from Oxidative Stress. *J. Adv. Res.* doi:10.1016/j.jare.2021.06.023

Zhang, Q., Liu, J., Zhang, M., Wei, S., Li, R., Gao, Y., et al. (2019). Apoptosis Induction of Fibroblast-like Synoviocytes Is an Important Molecular-Mechanism for Herbal Medicine along with its Active Components in Treating Rheumatoid Arthritis. *Biomolecules* 9, 795. doi:10.3390/biom9120795

Zhang, X., Qi, L. W., Yi, L., Li, P., Wen, X. D., and Yu, Q. T. (2008). Screening and Identification of Potential Bioactive Components in a Combined Prescription of Danggui Buxue Decoction Using Cell Extraction Coupled with High Performance Liquid Chromatography. *Biomed. Chromatogr.* 22 (2), 157–163. doi:10.1002/bmc.910

Zhang, X., Zhu, J., Liu, F., Li, Y., Chandra, A., Levin, L. S., et al. (2014). Reduced EGFR Signaling Enhances Cartilage Destruction in a Mouse Osteoarthritis Model. *Bone. Res.* 2, 14015. doi:10.1038/boneres.2014.15

Zhang, Y., Long, Y., Yu, S., Li, D., Yang, M., Guan, Y., et al. (2021). Natural Volatile Oils Derived from Herbal Medicines: A Promising Therapy Way for Treating Depressive Disorder. *Pharmacol. Res.* 164, 105376. doi:10.1016/j.phrs.2020.105376

Zhang, Y., Wei, W., Huo, J., and Wang, W. (2017). Serum Pharmacochemistry Study of *Pheretima Aspergillum* by UPLC-Q-TOF-MS. *J. Chin. Med. Mat.* 40 (004), 848–853.

Zhao, H. (2020). Clinical Observation on 47 Cases of Early Non-traumatic Femoral Head Necrosis Treated by Taohong Siwu Decoction Combined with Acupuncture. *Chin. J. Ethn. Ethn.* 29 (14), 99–101.

Zhao, W., Shou, H., and Chen, J. (1999). G2-M Phase Block and Tumor. *Foreign Med. Sci.* 2, 13–15.

Zhao, Y., Liu, S., Zhang, C., Liu, D., and Zhang, T. (2016). Analysis on chemical constituents from *Glycyrrhizae Radix* et Rhizoma by HPLC-Q-TOF-M. *Chin. Med. Mat* 47 (12), 2061–2068. doi:10.7501/j.issn.0253-2670.2016.12.007

Zheng, H., Yang, E., Peng, H., Li, J., Chen, S., Zhou, J., et al. (2014). Gastrodin Prevents Steroid-Induced Osteonecrosis of the Femoral Head in Rats by Anti-apoptosis. *Chin. Med. J. (Engl)* 127 (22), 3926–3931. doi:10.3760/cma.j.issn.0366-6999.20141371

Zhou, Y., Zhou, B., Pache, L., Chang, M., Chanda, S. K., Khodabakhshi, A. H., et al. (2019). Metascape Provides a Biologist-Oriented Resource for the Analysis of Systems-Level Datasets. *Nat. Commun.* 10 (1), 1523. doi:10.1038/s41467-019-09234-6

Conflict of Interest: The authors declare that the research was conducted in the absence of any commercial or financial relationships that could be construed as a potential conflict of interest.

Publisher's Note: All claims expressed in this article are solely those of the authors and do not necessarily represent those of their affiliated organizations or those of the publisher, the editors, and the reviewers. Any product that may be evaluated in this article or claim that may be made by its manufacturer is not guaranteed or endorsed by the publisher.

Copyright © 2021 Wang, Liu, Tang, Wei, Sun, Ruan, He, Li, Ren, Tian and Chen. This is an open-access article distributed under the terms of the Creative Commons Attribution License (CC BY). The use, distribution or reproduction in other forums is permitted, provided the original author(s) and the copyright owner(s) are credited and that the original publication in this journal is cited, in accordance with accepted academic practice. No use, distribution or reproduction is permitted which does not comply with these terms.

frontiers in Oncology

ORIGINAL RESEARCH
published: 30 November 2021
doi: 10.3389/fonc.2021.749987

Role of Borneol Induced Autophagy in Enhancing Radiosensitivity of Malignant Glioma

Qinglin Li[1], Liang Xia[2], Caixing Sun[2], Huangjie Zhang[3], Mengying Zheng[4], Hongyan Zhang[3], Hongyang Lu[5]* and Zeng Wang[3]**

[1] Department of Scientific Research, The Cancer Hospital of the University of Chinese Academy of Sciences (Zhejiang Cancer Hospital), Institute of Basic Medicine and Cancer (IBMC), Chinese Academy of Sciences, Hangzhou, China, [2] Department of Neurotumor Surgery, The Cancer Hospital of the University of Chinese Academy of Sciences (Zhejiang Cancer Hospital), Institute of Basic Medicine and Cancer (IBMC), Chinese Academy of Sciences, Hangzhou, China, [3] Department of Pharmacy, The Cancer Hospital of the University of Chinese Academy of Sciences (Zhejiang Cancer Hospital), Institute of Basic Medicine and Cancer (IBMC), Chinese Academy of Sciences, Hangzhou, China, [4] Department of Medical School, Zhejiang University City College, Hangzhou, China, [5] Department of Thoracic Oncology, The Cancer Hospital of the University of Chinese Academy of Sciences (Zhejiang Cancer Hospital), Institute of Basic Medicine and Cancer (IBMC), Chinese Academy of Sciences, Hangzhou, China

OPEN ACCESS

Edited by:
Xin Luan,
Shanghai University of Traditional Chinese Medicine, China

Reviewed by:
Yang Li,
Anhui Medical University, China
Ye Yang,
Nanjing University of Chinese Medicine, China

***Correspondence:**
Zeng Wang
wangzeng@zjcc.org.cn
Hongyang Lu
Luhy@zjcc.org.cn
Hongyan Zhang
Zhanghy@zjcc.org.cn

Specialty section:
This article was submitted to Pharmacology of Anti-Cancer Drugs, a section of the journal Frontiers in Oncology

Received: *30 July 2021*
Accepted: *01 November 2021*
Published: *30 November 2021*

Citation:
Li Q, Xia L, Sun C, Zhang H, Zheng M, Zhang H, Lu H and Wang Z (2021) Role of Borneol Induced Autophagy in Enhancing Radiosensitivity of Malignant Glioma. Front. Oncol. 11:749987. doi: 10.3389/fonc.2021.749987

Glioma is the common primary craniocerebral malignancy with unfavorable prognosis. It is currently treated by surgical resection supplemented by radiotherapy, although the resistance of glioma cells to radiation limits the therapeutic outcomes. The aim of the present study was to determine the potential radiosensitizing effects of borneol and the underlying mechanisms. We found that borneol administration along with radiotherapy significantly inhibited the growth of primary glioma cells *in vitro* and *in vivo*. Furthermore, borneol markedly increased the number of autophagosomes in the glioma cells, which coincided with increased expression of beclin-1 and LC3. And the combination of borneol and radiation exposure significantly decreased the expression levels of HIF-1α, mTORC1 and eIF4E. In addition, silencing mTORC1 and eIF4E upregulated Beclin-1 and LC3 and decreased the expression of HIF-1α, thereby inhibiting tumor cell proliferation. Our findings suggest that borneol sensitizes glioma cells to radiation by inducing autophagy *via* inhibition of the mTORC1/eIF4E/HIF-1α regulatory axis.

Keywords: natural product, borneol, malignant glioma, autophagy, HIF-1α

1 INTRODUCTION

Glioma accounts for about 60% of all brain tumors and is the most common primary craniocerebral malignancy originating from glial cells of the brain and spinal cord (1–3). Currently, gliomas are classified by the World Health Organization (WHO) into low and high-grade neurogliomas (4). Glioblastoma (GBM) is the most aggressive and common form of adult brain cancer, and is characterized by high recurrence and mortality, and low cure rates (5). In addition, most malignant gliomas infiltrate into the surrounding tissues resulting in lack of clearly demarcated boundaries. The average survival duration of GBM patients is only 14 months, and the five-year mortality rate

exceeds 95% (6–8). Currently, surgical resection, radiotherapy and adjuvant chemotherapy are the primary treatment strategies for GBM, although radiation tolerance often leads to tumor recurrence.

Hypoxia-inducible factor-1α (HIF-1α) is activated in the hypoxic tumor microenvironment and promotes the transcription of genes associated with tumor invasion, proliferation and radio-resistance (9–13). The tumor cells often develop resistance to hypoxia *via* autophagy, a lysosome-dependent mechanism of degrading damaged proteins and organelles that ensures nutrient recycling, protein synthesis, cellular homeostasis and survival during stress (14–16). Autophagy is initiated with the formation of a "bubble" of lipid bilayer around the proteins/organelles, which is then elongated to vesicles known as autophagosomes in the presence of LC3 (17, 18). Beclin-1 also plays a crucial role in the induction of autophagy, and is an established tumor suppressor that inhibits the genesis and progression of tumors by promoting autophagy and apoptosis. It is aberrantly expressed in various tumors, and is regulated by HIF-1α. Studies show that Beclin-1 downregulation and HIF-1α overexpression are conducive to tumor progression and metastasis, and therefore portend poor prognosis (19, 20).

The mammalian target of rapamycin (mTOR) pathway is the key regulator of autophagy, and is activated in response to growth factors, metabolic stress, low energy levels, hypoxia and nutrient deficiency (21–23). In a previous study, we found that the natural terpene derivative borneol inhibited HIF-1α in primary glioma cells by regulating the mTORC1/eIF4E pathway, and induced autophagy and apoptosis. The aim of the present study was to evaluate the potential radio-sensitizing effect of borneol on glioma cells and explore the role of autophagy.

2 EXPERIMENTAL METHODS

2.1 Establishment of Rodent C6 Intracranial Tumor Transplantation Model and Treatment Regimen

SPF male SD rats were provided by Shanghai Sipur Bikai Experimental Animal Co. Ltd. After 2 weeks of acclimatization, the animals were divided into the control, radiotherapy, borneol and combination therapy groups (n=6 each). Glioma cells were inoculated to establishment the tumor model as previously described (24). Two weeks later, the animals from the appropriate groups were anesthetized with pentobarbital and irradiated once with 15Gy dosage. Borneol (16 mg/kg) was administered for 7 days before and 3 days after radiotherapy. The general condition and survival of the animals were recorded, and the relative tumor volume was measured.

2.2 Immunohistochemistry (IHC)

The tumor tissues were fixed in formalin, dehydrated, embedded in paraffin and cut into ultra-thin sections. After rehydration and antigen retrieval, the sections were incubated overnight with the specific primary antibody at 4°C, followed by biotinylated secondary antibody. The sections were then washed with PBS, probed with avidin-horseradish peroxidase complex, developed with the DAB chromogenic agent, rinsed with water, and counterstained with hematoxylin. The stained sections were dehydrated, cleared with xylene, sealed with neutral gum, and observed under a light microscope. The positively stained cells were counted in 6 random non-overlapping fields at 10x-40x magnification.

2.3 Transmission Electron Microscopy

The glioma tissues were washed with 0.1mM phosphate buffer, fixed with 1% osmium acid for 2 hours, rinsed again with the same solution, and dehydrated through an alcohol gradient. After drying to critical point, the tissues were coated with platinum for 10 minutes, and observed by transmission electron microscopy (TEM).

2.4 Human Primary Glioma Cell Culture and CCK-8 Assay

Human primary glioma cells were isolated as previously described (24). The cells in the logarithmic growth phase were seeded into 96-well plates, and incubated for 24h. After irradiating with X-ray at the dose of 5Gy, the cells were cultured in the presence of varying concentrations of borneol (10, 20, 40 and 80μg/ml) for 48h. Untreated and non-irradiated controls were included. Ten microliters CCK-8 solution was added to each well and after a 2h incubation, the absorbance at 450nm was measured using a microplate analyzer. Each condition was tested in triplicates.

2.5 SiRNA/Gene Transfection

HIF-1α overexpression siRNA vectors were designed and synthesized as in our previous study (24), and the primary glioma cells were transfected with the respective constructs with Opti-MEM and Oligofectamine according to the manufacturer's instructions. The stably transfected cells were irradiated (5Gy) and cultured with 20μg/ml borneol for 48h. Cell viability was evaluated as described in section *Human primary glioma cell culture and CCK-8 assay*.

2.6 Immunofluorescence and Western Blotting

The expression levels of HIF-1α, mTORC1, eIF4E, LC3 and Beclin1 proteins in the suitably transfected/treated cells were evaluated by immunofluorescence and western blotting with specific antibodies as previously described (24).

2.7 Statistical Analysis

SPSS22.0 was used for statistical analysis. All data were expressed as mean ± standard deviation (x ± s). T-test (homogeneity of variance) or Kruskal-Wallish test (heterogeneity of variance) was used to compare the means of two experimental groups. $P<0.05$ was considered statistically significant.

3 RESULTS

3.1 The Combination of Borneol and Radiotherapy Inhibited Glioma Growth by Inducing Autophagy

Compared to the untreated controls and the borneol group, borneol combined with radiotherapy group significantly decreased the tumor volume (P<0.05, P<0.05), and the tumor inhibition rate of the combination therapy was higher than the radiotherapy alone (**Figure 1**). As shown in **Figure 2**, the expression levels of HIF-1α, mTORC1 and eIF4E in glioma tissues was markedly lower in the animals treated with borneol and/or radiation compared to the untreated tumor-bearing group (P<0.05 or P<0.01). Furthermore, the different therapies increased the expression of LC3 and Beclin-1 in the gliomas (P<0.01). Consistent with this, TEM examination of the glioma tissues (**Figure 3A**) showed numerous autophagosomes in the borneol, radiotherapy and combination therapy groups compared to the untreated controls (**Figure 3B**). Taken together, borneol induced autophagy in the glioma cells and augmented radiation-mediated tumor inhibition.

3.2 Borneol Sensitized Glioma Cells to Radiation by Targeting the mTORC1/eIF4E/HIF-1α Pathway

As shown in **Figure 4**, borneol significantly decreased the viability of the glioma cells *in vitro* in a dose-dependent manner when combined with 5Gy irradiation compared to cells subjected to either treatment (P < 0.05 for 20μg/ml and 40μg/ml borneol and p < 0.01 for 80μg/ml borneol).

HIF-1α knockdown decreased the percentage of viable glioma cells, whereas ectopic expression of HIF-1α had the opposite effect (P > 0.05). However, the survival rate of the HIF-1α-overexpressing cells decreased significantly when treated with borneol and/or 5Gy radiation (P<0.05 or P<0.01), and the inhibitory effect of the combination treatment was greater. In the HIF-1α-silenced cells, borneol and radiotherapy further inhibited the proliferation rates (**Figure 5**).

Furthermore, the combination of borneol and radiation exposure significantly decreased the expression levels of HIF-1α, mTORC1 and eIF4E proteins (**Figures 6**, **7**) in the glioma cells compared to the untreated controls (p < 0.05 or p < 0.01). Compared to radiotherapy alone, the combination treatment had a stronger inhibitory effect (p< 0.05 or p < 0.01).

As shown in **Figure 8A**, mTORC1 knockdown significantly decreased HIF-1α expression in glioma cells (P < 0.01), and increased that of LC3 and Beclin-1 (P <0.01). Furthermore, the expression levels of LC3 and Beclin-1 were also upregulated in the eIF4E-silenced glioma cells (P <0.01)(**Figure 8B**). Taken together, borneol sensitized glioma cells to radiation by targeting the mTORC1/eIF4E/HIF-1α pathway.

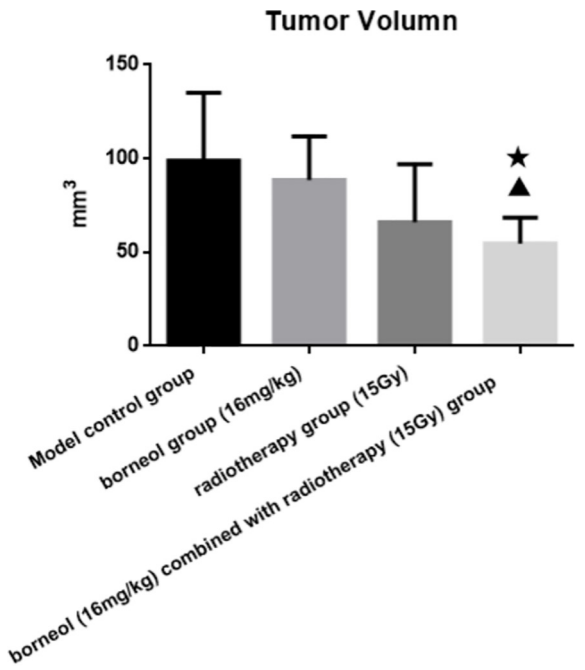


FIGURE 1 | Tumor volume of brain glioma in rats after borneol and radiotherapy treatment($\bar{x}$ ± S, n=6). Compared with the control group, ▲P<0.05; Compared with borneol group, ★P<0.05.

4 DISCUSSION

Glioblastoma accounts for 50% of all gliomas, and is the most aggressive tumor of the central nervous system in adults, with high recurrence and low cure rates. Despite advances in neurosurgery and the widespread use of chemotherapy and radiotherapy against newly diagnosed GBM, patient survival has improved only marginally. Radiotherapy is the primary treatment strategy for advanced glioma (25, 26), although its outcomes are limited due to hypoxia-induced resistance. HIF-1α is activated in the hypoxic microenvironment of solid tumors, and promotes tumor cell survival by increasing glucose uptake and utilization. In a previous study, we showed that borneol inhibited HIF-1α in primary human glioma cells and rat glioma tissues by targeting the mTORC1/eIF4E pathway, which is also involved in autophagy regulation. Although autophagy generally ensures cell survival and homeostasis by recycling damaged organelles and proteins, excessive autophagy may induce cell death. Therefore, we hypothesized that borneol induces autophagy in glioma cells by targeting the mTORC1/eIF4E signaling pathway, which in turn downregulates HIF-1α and sensitizes the cells to radiotherapy.

HIF-1α activation promotes glioma cell survival, proliferation and metastasis under hypoxic conditions, and is therefore a promising therapeutic target. We found that HIF-1α silencing significantly decreased the proliferation rate of the irradiated glioma cells whereas HIF-1α overexpression had the opposite effect, which confirmed the crucial role of HIF-1α in the response to radiotherapy. Borneol significantly augmented the tumor cell killing effect of radiation *in vitro* and *in vivo*, which

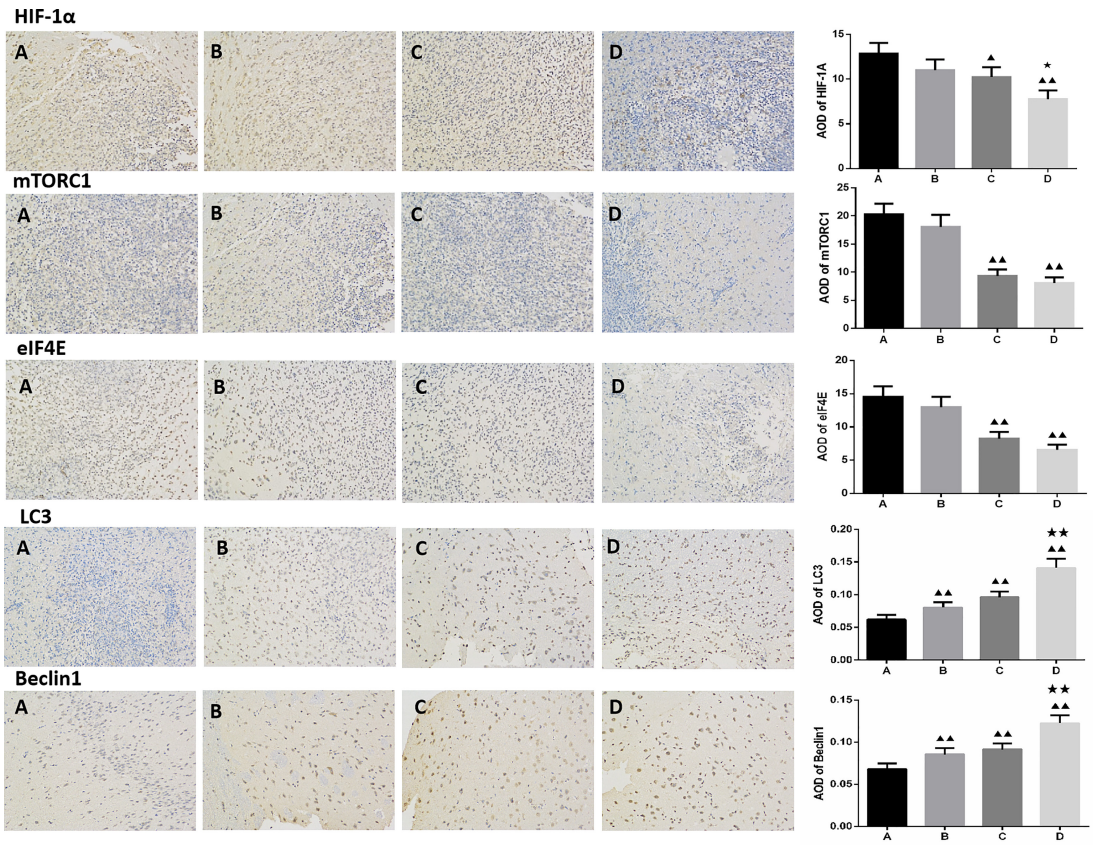


FIGURE 2 | Immunohistochemical detection of HIF-1α, mTOR, eIF4E, LC3 and Beclin1 expression levels in glioma tissues treated by borneol and radiotherapy (n=3, ×200 times). **(A)** Control group **(B)** Borneol 16mg/Kg **(C)** Radiotherapy 15Gy group **(D)** Borneol 16mg/Kg combined radiotherapy 15Gy group. Compared with control group, ▲P<0.05, ▲▲P< 0.01; Compared with the radiation 5Gy group, ★P<0.05, ★★P< 0.01.

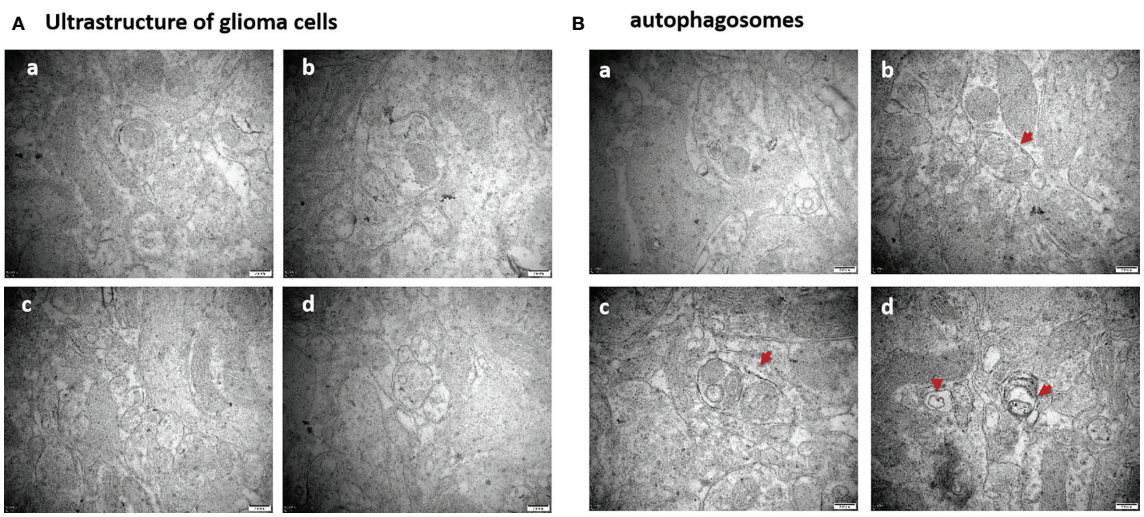


FIGURE 3 | **(A)** Ultrastructure of glioma tissues observed by transmission electron microscopy (×60000 times); **(B)** Observation of the formation of autophagosomes in glioma tissues by transmission electron microscopy (×60000 times). The red arrows are autophagosomes. **(a)** Control group **(b)** Borneol 16mg/Kg **(c)** Radiotherapy 15Gy group **(d)** Borneol 16mg/Kg combined radiotherapy 15Gy group.

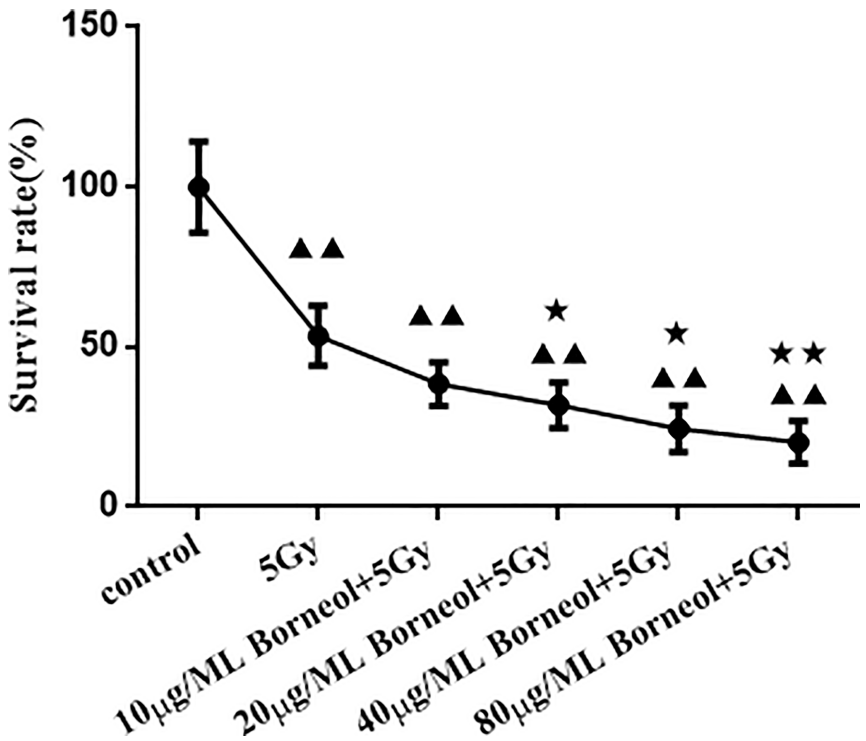


FIGURE 4 | Effects of different concentrations of borneol on the growth of human glioma primary cultured cells under the radiation dose of 5Gy ($\bar{x}$ ± S,*n*=3). Compared with control group, ▲▲P< 0.01; Compared with the radiation 5Gy group, ★P<0.05, ★★P< 0.01.

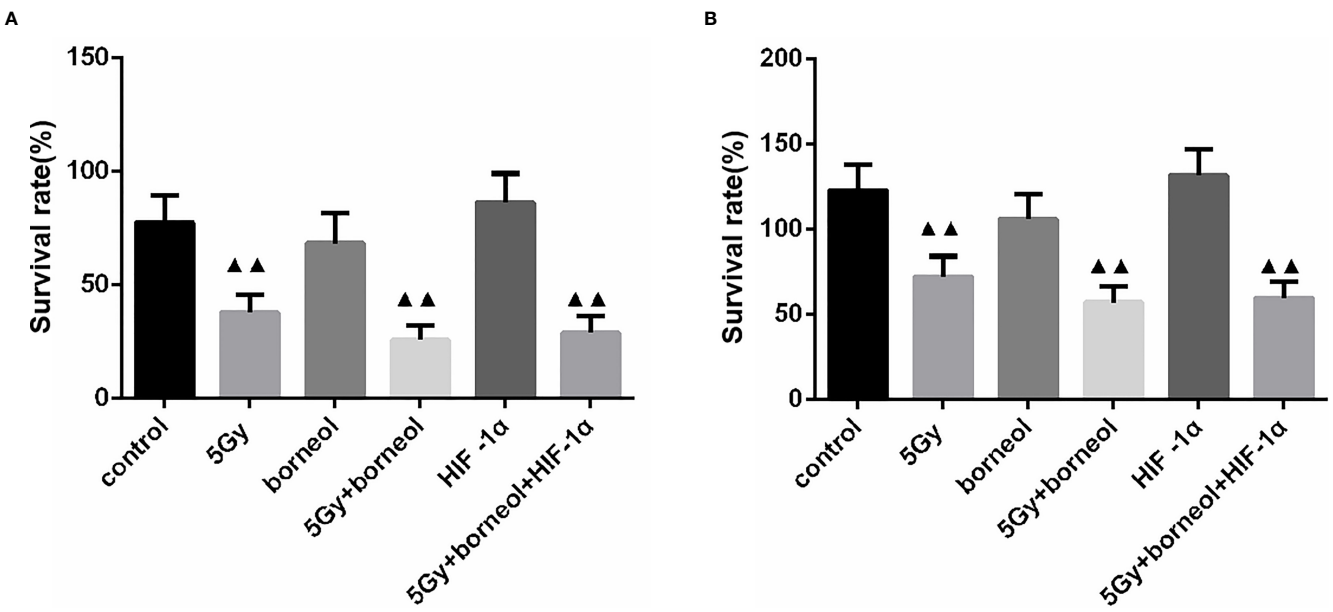


FIGURE 5 | Cell growth Of borneol and radiotherapy treatment on HIF-1α silence **(A)** or overexpressing **(B)** cell ($\bar{x}$ ± S,*n*=3). Compared with the control group, ▲▲P <0.01.

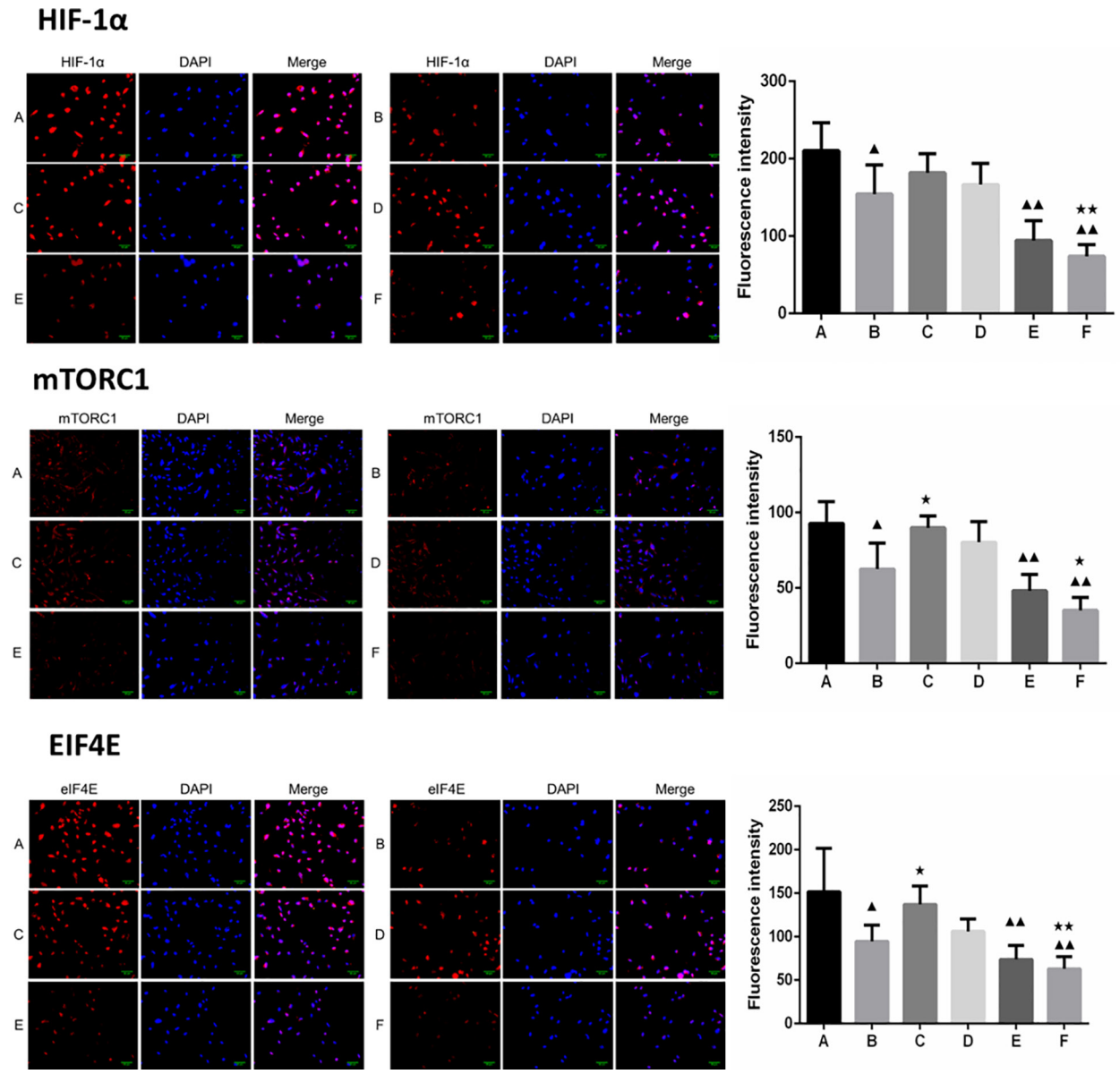


FIGURE 6 | Expression of HIF-1α, mTORC1 and eIF4E in each group after borneol and radiotherapy treatment (200×) ($\bar{x}$ ± S,*n*=5). **(A)** Control group **(B)** Radiotherapy 5Gy group **(C)** Borneol 20μg/ml 24h group **(D)** Borneol 20μg/ml 48h group **(E)** Borneol 20 μg/ml combined radiotherapy 5Gy group **(F)** Borneol 20μg/ml 48h combined radiotherapy 5Gy group. Compared with the control group, ▲P<0.05, ▲▲P< 0.01; Compared with radiotherapy group, ★P<0.05, ★★P< 0.01.

coincided with an increase in the number of autophagosomes in the glioma cells/tissues, along with upregulation in LC3 and Beclin1 levels. Beclin1 initiates the process of autophagy by regulating autophagosome formation and maturity. LC3 is a structural component of autophagosomes and a marker of autophagy flux. These results indicate that borneol accelerates autophagy in the irradiated glioma cells, resulting in increased cell death and tumor inhibition. Akt/mTOR inhibitors induce autophagic death in radiation-resistant and radiation-sensitive U87 glioma cell lines, but have no effect on the apoptosis rates and radiosensitivity of glioma cells (27). Consistent with this, borneol significantly downregulated HIF-1α, mTORC1 and eIF4E in the irradiated human glioma primary culture cells, and the inhibitory effect of the combination therapy was stronger compared to radiotherapy alone. Thus, borneol sensitizes glioma cells to radiation by inducing autophagy *via* the inhibition of the mTORC1/eIF4E/HIF-1A pathway. Other studies have shown that inhibition of PI3K/Akt/mTOR pathway and HIF-1α can inhibit the migration and invasion of human glioblastoma U87 cells (28). Consistent with this, silencing of either mTORC1 or eIF4E significantly decreased the levels of HIF-1α in glioma cells, and increased that of LC3 and Beclin-1. This suggests that

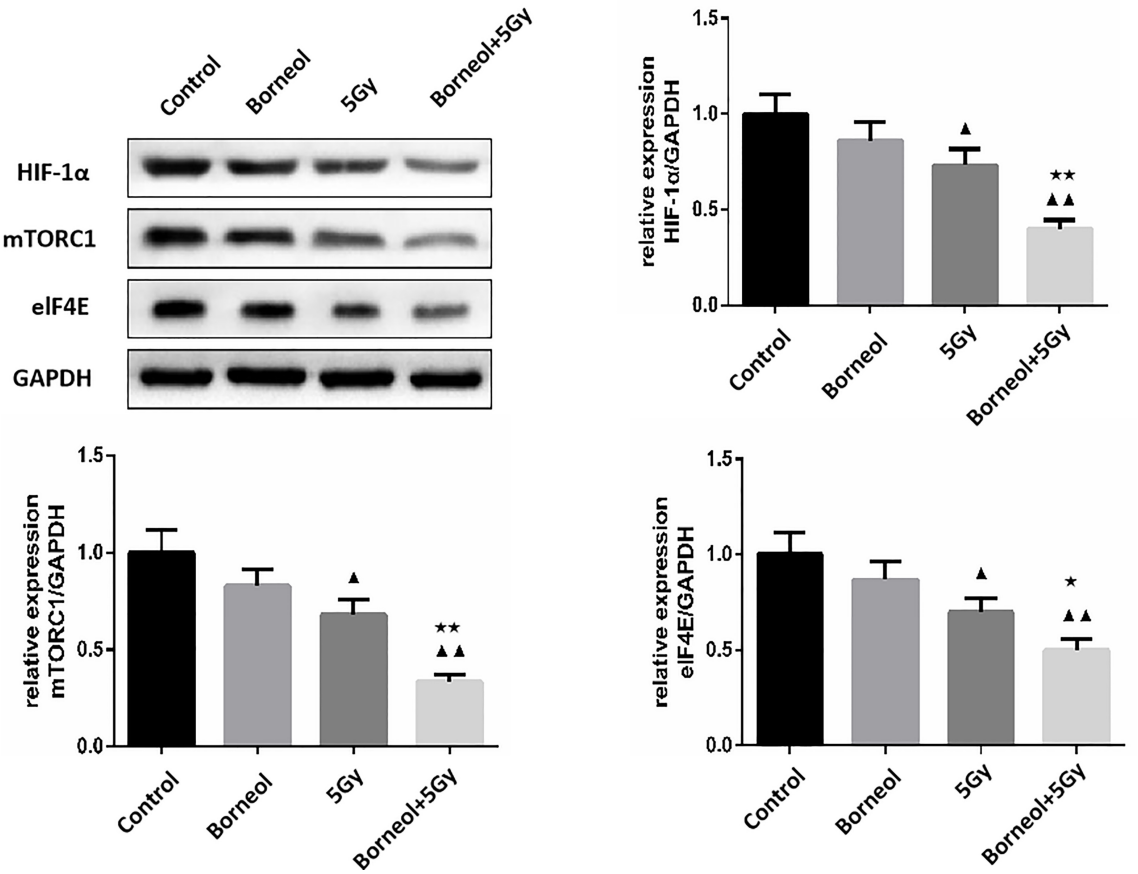


FIGURE 7 | Expression levels of HIF-1α, mTORC1 and eIF4E in human glioma cells after borneol and radiotherapy treatment($\bar{x}$ ± S,n=3). Compared with the control group, ▲P <0.05, ▲▲P <0.01;Compared with radiotherapy group, ★P<0.05, ★★P< 0.01.

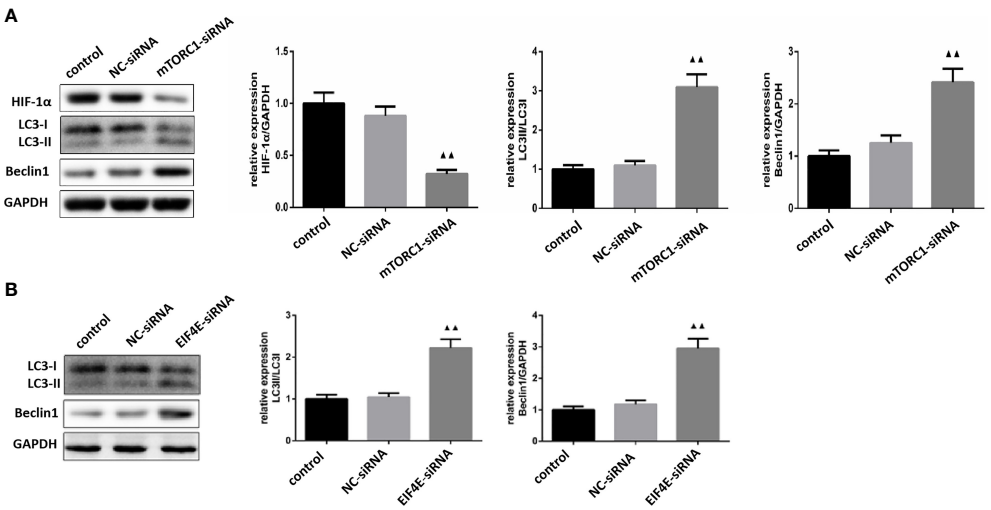


FIGURE 8 | **(A)** Expression levels of HIF-1α, LC3 and Beclin1 in glioma cells silenced by mTOR C1($\bar{x}$ ± S,n=3). **(B)** Expression levels of LC3 and Beclin1 proteins in glioma cells silenced by eIF4E ($\bar{x}$ ± S,n=3). Compared with the normal control group, ▲▲ P <0.01.

inhibition of the mTORC1/eIF4E pathway promotes radiosensitivity by inducing autophagy and inactivating HIF-1α.

In conclusion, borneol sensitized glioma cells to radiation by accelerating autophagic cell death through the mTORC1/eIF4E/HIF-1α axis, and should be considered for the treatment of advanced gliomas.

DATA AVAILABILITY STATEMENT

The raw data supporting the conclusions of this article will be made available by the authors, without undue reservation.

ETHICS STATEMENT

The animal study was reviewed and approved by Animal ethics committee of Zhejiang Cancer Hospital.

AUTHOR CONTRIBUTIONS

Conceptualization and methodology by HL and HYZ. Experiments design: QL, LX, CS. Experiments performance: HJZ and MZ. Data analysis: ZW. Writing – Original draft: ZW. Writing – Review & Editing: QL and HL. All authors contributed to the article and approved the submitted version.

FUNDING

This work was supported by the 1022 Talent Training Program of Zhejiang Cancer Hospital, National Science of Foundation of China (NO 81502147), Zhejiang Provincial National Science Foundation of China (NO LY20H290003, LGF18H280003, YY18H300008, LYQ20H280001), Zhejiang Medical and Health Science and Technology Project (NO 2020KY477, 2020364926, 2019RC127, 2018KY291,2016KYB038, 2019ZD024), Chinese medicine science and technology plan of Zhejiang Province (NO 2022ZB052, 2021ZB036, 2016ZQ009, 2020ZQ005).

SUPPLEMENTARY MATERIAL

The Supplementary Material for this article can be found online at: https://www.frontiersin.org/articles/10.3389/fonc.2021.749987/full#supplementary-material

REFERENCES

1. Ohgaki H, Kleihues P. Epidemiology and Etiology of Gliomas. *Acta Neuropathol* (2005) 109:93–108. doi: 10.1007/s00401-005-0991-y
2. Valor LM, Hervás-Corpión I. The Epigenetics of Glioma Stem Cells: A Brief Overview. *Front Oncol* (2020) 10:602378. doi: 10.3389/fonc.2020.602378
3. Chen R, Smith-Cohn M, Cohen AL, Colman H. Glioma Subclassifications and Their Clinical Significance. *Neurotherapeutics* (2017) 14:284–97. doi: 10.1007/s13311-017-0519-x
4. Sharma P, Debinski W. Receptor-Targeted Glial Brain Tumor Therapies. *Int J Mol Sci* (2018) 19:3326. doi: 10.3390/ijms19113326
5. Nayak L, Reardon DA. High-Grade Gliomas. *Continuum (Minneap Minn).* (2017) 23:1548–63. doi: 10.1212/CON.0000000000000554
6. Xiong L, Wang F, Qi Xie X. Advanced Treatment in High-Grade Gliomas. *J BUON* (2019) 24:424–30.
7. Xu S, Tang L, Li X, Fan F, Liu Z. Immunotherapy for Glioma: Current Management and Future Application. *Cancer Lett* (2020) 476:1–12. doi: 10.1016/j.canlet.2020.02.002
8. Gusyatiner O, Hegi ME. Glioma Epigenetics: From Subclassification to Novel Treatment Options. *Semin Cancer Biol* (2018) 51:50–8. doi: 10.1016/j.semcancer.2017.11.010
9. Vordermark D, Horsman MR. Hypoxia as a Biomarker and for Personalized Radiation Oncology. *Recent Results Cancer Res* (2016) 198:123–42. doi: 10.1007/978-3-662-49651-0_6
10. Huang W, Ding X, Ye H, Wang J, Shao J, Huang T. Hypoxia Enhances the Migration and Invasion of Human Glioblastoma U87 Cells Through PI3K/Akt/mTOR/HIF-1alpha Pathway. *Neuroreport* (2018) 29:1578–85. doi: 10.1097/WNR.0000000000001156
11. Meng FW, FS L, WH L, Li L, Jie LL. Formation of New Lymphatic Vessels in Glioma: An Immunohistochemical Analysis. *Neuropathology* (2020) 40:215–23. doi: 10.1111/neup.12625
12. Liu S, Liu X, Zhang C, Shan W, Qiu X. T-Cell Exhaustion Status Under High and Low Levels of Hypoxia-Inducible Factor 1alpha Expression in Glioma. *Front Pharmacol* (2021) 12:711772. doi: 10.3389/fphar.2021.711772
13. Jiao X, Yu Y, Meng J, He M, Zhang CJ, Geng W, et al. Dual-Targeting and Microenvironment-Responsive Micelles as a Gene Delivery System to Improve the Sensitivity of Glioma to Radiotherapy. *Acta Pharm Sin B* (2019) 9:381–96. doi: 10.1016/j.apsb.2018.12.001
14. Parzych KR, Klionsky DJ. An Overview of Autophagy: Morphology, Mechanism, and Regulation. *Antioxid Redox Signal* (2014) 20:460–73. doi: 10.1089/ars.2013.5371
15. Onorati AV, Dyczynski M, Ojha R, Amaravadi RK. Targeting Autophagy in Cancer. *Cancer* (2018) 124:3307–18. doi: 10.1002/cncr.31335
16. Escamilla-Ramírez A, Castillo-Rodríguez RA, Zavala-Vega S, Jimenez-Farfan D, Anaya-Rubio I, Briseño E, et al. Autophagy as a Potential Therapy for Malignant Glioma. *Pharmaceuticals (Basel)* (2020) 13:156. doi: 10.3390/ph13070156
17. Sanchez Gomez-, SM Y-D, Rodri guez-Arribas MR, Bravo-San Pedro JM, Martínez-Chacón G, Uribe-Carretero E, et al. mRNA and Protein Dataset of Autophagy Markers(LC3 and P62)in Several Cell Lines. *Data Brief* (2016) 7:641–7. doi: 10.1016/j.dib.2016.02.085
18. Cj P, Hv E, Vijayakurup V, R Menon G, Nair S, Gopala S. High LC3/Beclin Expression Correlates With Poor Survival in Glioma: A Definitive Role for Autophagy as Evidenced by. *In Vitro Autophagic Flux. Pathol Oncol Res* (2019) 25:137–48. doi: 10.1007/s12253-017-0310-7
19. Osman NA, Abd El-Rehim DM, Kamal IM. Defective Beclin-1 and Elevated Hypoxia-Inducible Factor (HIF)-1alpha Expression Are Closely Linked to Tumorigenesis, Differentiation, and Progression of Hepatocellular Carcinoma. *Tumour Biol* (2015) 36:4293–9. doi: 10.1007/s13277-015-3068-0
20. Radwan SM, Hamdy NM, Hegab HM, El-Mesallamy HO. Beclin-1 and Hypoxia-Inducible Factor-1alpha Genes Expression: Potential Biomarkers in Acute Leukemia Patients. *Cancer Biomark* (2016) 16:619–26. doi: 10.3233/CBM-160603
21. Wang Y, Zhang H. Regulation of Autophagy by mTOR Signaling Pathway. *Adv Exp Med Biol* (2019) 1206:67–83. doi: 10.1007/978-981-15-0602-4_3
22. Zhu Y, Liu X, Zhao P, Zhao H, Gao W, Wang L. Celastrol Suppresses Glioma Vasculogenic Mimicry Formation and Angiogenesis by Blocking the PI3K/Akt/mTOR Signaling Pathway. *Front Pharmacol* (2020) 11:25. doi: 10.3389/fphar.2020.00025
23. Nan Y, Guo H, Guo L, Wang L, Ren B, Yu K, et al. MiRNA-451 Inhibits Glioma Cell Proliferation and Invasion Through the mTOR/HIF-1alpha/VEGF Signaling Pathway by Targeting Cab39. *Hum Gene Ther Clin Dev* (2018) 29:156–66. doi: 10.1089/humc.2018.133

24. Wang Z, Li Q, Xia L, Li X, Sun C, Wang Q, et al. Borneol Promotes Apoptosis of Human Glioma Cells Through Regulating HIF-1a Expression *via* Mtorc1/Eif4e Pathway. *J Cancer* (2020) 11:4810–22. doi: 10.7150/jca.45304
25. Shen H, Cook K, Gee HE, Hau E. Hypoxia, Metabolism, and the Circadian Clock: New Links to Overcome Radiation Resistance in High-Grade Gliomas. *J Exp Clin Cancer Res* (2020) 39:129. doi: 10.1186/s13046-020-01639-2
26. Saeed H, Tseng YD, Lo SS. Narrative Review of Palliative Hypofractionated Radiotherapy for High Grade Glioma. *Ann Palliat Med* (2021) 10:846–62. doi: 10.21037/apm-20-1246
27. Fujiwara K, Iwado E, Mills GB, Sawaya R, Kondo S, Kondo Y. Akt Inhibitor Shows Anticancer and Radiosensitizing Effects in Malignant Glioma Cells by Inducing Autophagy. *Int J Oncol* (2007) 31:753–60. doi: 10.3892/ijo.31.4.753
28. Huang W, Ding X, Ye H, Wang J, Shao J, Huang T. Hypoxia Enhances the Migration and Invasion of Human Glioblastoma U87 Cells Through PI3K/Akt/mTOR/HIF-1α Pathway. *Neuroreport* (2018) 29:1578–85. doi: 10.1097/WNR.0000000000001156

Conflict of Interest: The authors declare that the research was conducted in the absence of any commercial or financial relationships that could be construed as a potential conflict of interest.

Publisher's Note: All claims expressed in this article are solely those of the authors and do not necessarily represent those of their affiliated organizations, or those of the publisher, the editors and the reviewers. Any product that may be evaluated in this article, or claim that may be made by its manufacturer, is not guaranteed or endorsed by the publisher.

Copyright © 2021 Li, Xia, Sun, Zhang, Zheng, Zhang, Lu and Wang. This is an open-access article distributed under the terms of the Creative Commons Attribution License (CC BY). The use, distribution or reproduction in other forums is permitted, provided the original author(s) and the copyright owner(s) are credited and that the original publication in this journal is cited, in accordance with accepted academic practice. No use, distribution or reproduction is permitted which does not comply with these terms.

frontiers in Pharmacology

ORIGINAL RESEARCH
published: 07 December 2021
doi: 10.3389/fphar.2021.806091

Sempervirine Inhibits Proliferation and Promotes Apoptosis by Regulating Wnt/β-Catenin Pathway in Human Hepatocellular Carcinoma

Rongcai Yue[1,2†], Haiping Liu[1†], Yaxin Huang[1†], Jing Wang[1], Dongmei Shi[1], Yanping Su[1], Yufei Luo[1], Ping Cai[3], Guilin Jin[1,2]* and Changxi Yu[1,2]**

[1]School of Pharmacy, Fujian Medical University, Fuzhou, China, [2]Fujian Key Laboratory of Drug Target Discovery and Structural and Functional Research, Fujian Medical University, Fuzhou, China, [3]Fujian Provincial Key Laboratory of Environment Factors and Cancer, School of Public Health, Fujian Medical University, Fuzhou, China

OPEN ACCESS

Edited by:
Hong Zhang,
Shanghai University of Traditional Chinese Medicine, China

Reviewed by:
Liu Ying,
Shanghai University, China
Feng Jiao,
Shanghai Jiao Tong University, China

***Correspondence:**
Changxi Yu
changxiyu@mail.fjmu.edu.cn
Guilin Jin
jinguilin0611@163.com
Ping Cai
caipingfjmu@163.com

†These authors have contributed equally to this work

Specialty section:
This article was submitted to Pharmacology of Anti-Cancer Drugs, a section of the journal Frontiers in Pharmacology

Received: 31 October 2021
Accepted: 19 November 2021
Published: 07 December 2021

Citation:
Yue R, Liu H, Huang Y, Wang J, Shi D, Su Y, Luo Y, Cai P, Jin G and Yu C (2021) Sempervirine Inhibits Proliferation and Promotes Apoptosis by Regulating Wnt/β-Catenin Pathway in Human Hepatocellular Carcinoma. Front. Pharmacol. 12:806091. doi: 10.3389/fphar.2021.806091

Gelsemium elegans (*G. elegans*) Benth., recognized as a toxic plant, has been used as traditional Chinese medicine for the treatment of neuropathic pain and cancer for many years. In the present study, we aim to obtain the anti-tumor effects of alkaloids of *G. elegans* and their active components in hepatocellular carcinoma (HCC) and the potential mechanism was also further investigated. We demonstrated that sempervirine induced HCC cells apoptosis and the apoptosis was associated with cell cycle arrest during the G_1 phase, up-regulation of p53 and down-regulation of cyclin D1, cyclin B1 and CDK2. Furthermore, sempervirine inhibited HCC tumor growth and enhances the anti-tumor effect of sorafenib *in vivo*. In addition, inactivation of Wnt/β-catenin pathway was found to be involved in sempervirine-induced HCC proliferation. The present study demonstrated that alkaloids of *G. elegans* were a valuable source of active compounds with anti-tumor activity. Our findings justified that the active compound sempervirine inhibited proliferation and induced apoptosis in HCC by regulating Wnt/β-catenin pathway.

Keywords: sempervirine, wnt/β-catenin, alkaloids, *Gelsemium elegans* benth., hepatocellular carcinoma

INTRODUCTION

Hepatocellular carcinoma (HCC), the most common form of primary liver cancer, is the fourth leading cause of cancer-related death worldwide (Villanueva, 2019). Despite improvements in detection and clinical treatment strategies, the 5-years survival rate for HCC is less than 20% (Yu et al., 2021). Conventional chemotherapeutic and radio therapeutic treatments have caused serious problems, and resistance to chemotherapy is frequently observed (Craig et al., 2020). Sorafenib is recommended as the first-line treatment options for HCC patients, with primary concerns of high dose toxicity and limited anti-cancer effects (Wang et al., 2021). Therefore, developing novel efficient drugs and searching more effective therapies or synergistic agents are necessary for improving HCC therapy.

For over decades, a goal of clinical oncology has been the development of therapies promoting the effective elimination of cancer cells by apoptosis (Ichim and Tait, 2016; Carneiro and El-Deiry, 2020). In addition, the cell cycle is a complex and strictly controlled process, which is controlled by several cyclin dependent kinase (CDK) complexes. p53 is the most widely studied tumor suppressor and mediates a variety of anti-proliferative processes through cell cycle and apoptosis (Hu et al., 2021).

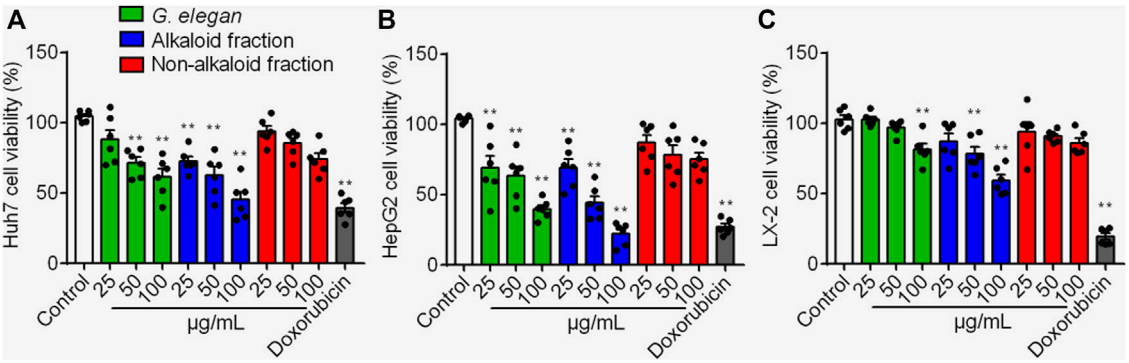


FIGURE 1 | The cytotoxic effects of the alkaloid fraction, non-alkaloid fraction, and whole extracts of *G. elegans* on Huh7 **(A)** HepG2 **(B)** and LX-2 **(C)** cells. Cell viability was assayed for 24 h $^{**}p < 0.01$ *vs*. Control.

Wnt signaling pathway, as one of the important conserved pathways in mammal, is involved in the differentiation, development and formation of all human organs, hematopoietic system and reproductive system (Perugorria et al., 2019). Therefore, the disorder of Wnt pathway is closely related to a variety of diseases, including tumors (Wang et al., 2019; Parsons et al., 2021). In normal cells, the Wnt pathway switch is not turned on. At this time, the Wnt pathway activity remains at a low level, which is mainly controlled by β-catenin complex, which is presented the excess in the ubiquitinated cytoplasm to the proteasome for degradation, thus silencing the downstream target genes. When Wnt pathway is activated, the binding of upstream Wnt ligands and receptors leads to the disintegration of β-catenin complex, the accumulation of β-catenin in the cytoplasm, entering the nucleus and binding with transcription factor TCF to start the expression of downstream oncogenes, including c-Myc, cyclin D1 and surviving (Li et al., 2021). At present, several drugs targeting Wnt pathway are undergoing clinical trials and are expected to be on the market (Martin-Orozco et al., 2019; Ashrafizadeh et al., 2020). Hence, Wnt pathway inhibitors can not only inhibit the growth of HCC cells, but also reduce the drug resistance of cells and sensitize chemotherapeutic drugs.

Natural products from plants are potentially important resources in the context of drug discovery for cancer therapy (Greco et al., 2021). Importantly, increasing evidence has reported that apoptosis induction or suppression might be one of the predominant molecular mechanisms whereby natural products could be used to treat cancer (Carneiro and El-Deiry, 2020). In addition, lots of active natural products based on apoptosis regulation, such as taxol, camptothecin and curcumin (Ashrafizadeh et al., 2020), have been used as clinical drugs to treat cancer (Mullard, 2016). *Gelsemium elegans* Benth. (*G. elegans*), also known as heartbreaking grass, has been used as a traditional Chinese medicine for the treatment of neuropathic pain and cancer for many years (Wang et al., 2015). Studies on the chemical constituents of the genus plants show that all species are rich in alkaloids, especially indole alkaloids, including gelsdine, gelsmeine, humantenine, koumine, sarpagine and yohimbane (Jin et al., 2014). Among them, structurally representative alkaloids sempervirine, gelsemine, humantene, and koumine have possessed anti-tumor, analgesic, anti-inflammatory and immunomodulatory pharmacological activities (Zhang and Wang, 2015; Pan et al., 2016; Yue et al., 2019; Jin et al., 2021). In the present study, we demonstrated that sempervirine inhibited proliferation and promoted apoptosis by regulating Wnt/β-catenin pathway in HCC.

MATERIALS AND METHODS

Reagents and Materials

DMEM culture medium and fetal bovine serum (FBS) were purchased from Gibco (Grand Island, NY). The doxorubicin (DOX, catalog #ST1285), CCK8 (catalog #C0043), apoptosis detection kit (catalog #C1062L), TOPFlash (catalog #D2501) and FOPFlash (catalog #D2503) was purchased from Beyotime (Shanghai, China). Anti-human β-catenin (catalog #8480), cyclin D1 (catalog #55506), cyclin B1 (catalog # 12,231), survivin (catalog # 2808), c-Myc (catalog #18583), CDK2 (catalog #18048), p53 (catalog #2527), β-actin (catalog #4970) and Histone H3 (catalog #4499) antibodies were bought from Cell Signaling Technology (Beverly, MA, United States). FH535 (catalog #HY-15721) and BML-284 (catalog #HY-19987) was purchased from Med Chem Express (MCE, United States). Humantenidine, gelsemine, koumine, gelsenicin, gelsevirine, and sempervirine (HPLC≥98%) were purchased from Shanghai Yuanye Bio-Technology Co., Ltd. The roots and stems of *G. elegans* were bought from a commercial source and authenticated by the Department of Pharmacognosy, School of Pharmacy, Fujian Medical University as previous reported (Liu Hao et al., 2008). Other chemicals were of analytical grade and commercially available.

Extraction the Total Alkaloid and Isolation of Alkaloid Compounds

The total alkaloid was extracted as previously described (Su et al., 2011). Briefly, *G. elegans* dry powder was refluxed in 95% ethanol for 3 h and the extraction was repeated for three times. The extracts were combined, dissoluted by 2% hydrochloric acid, and extracted again for another three times. The pH was adjusted to 11 with 5 M NaOH prior to extraction of total alkaloids. At the same time, the total extract and non alkaloid fraction were also

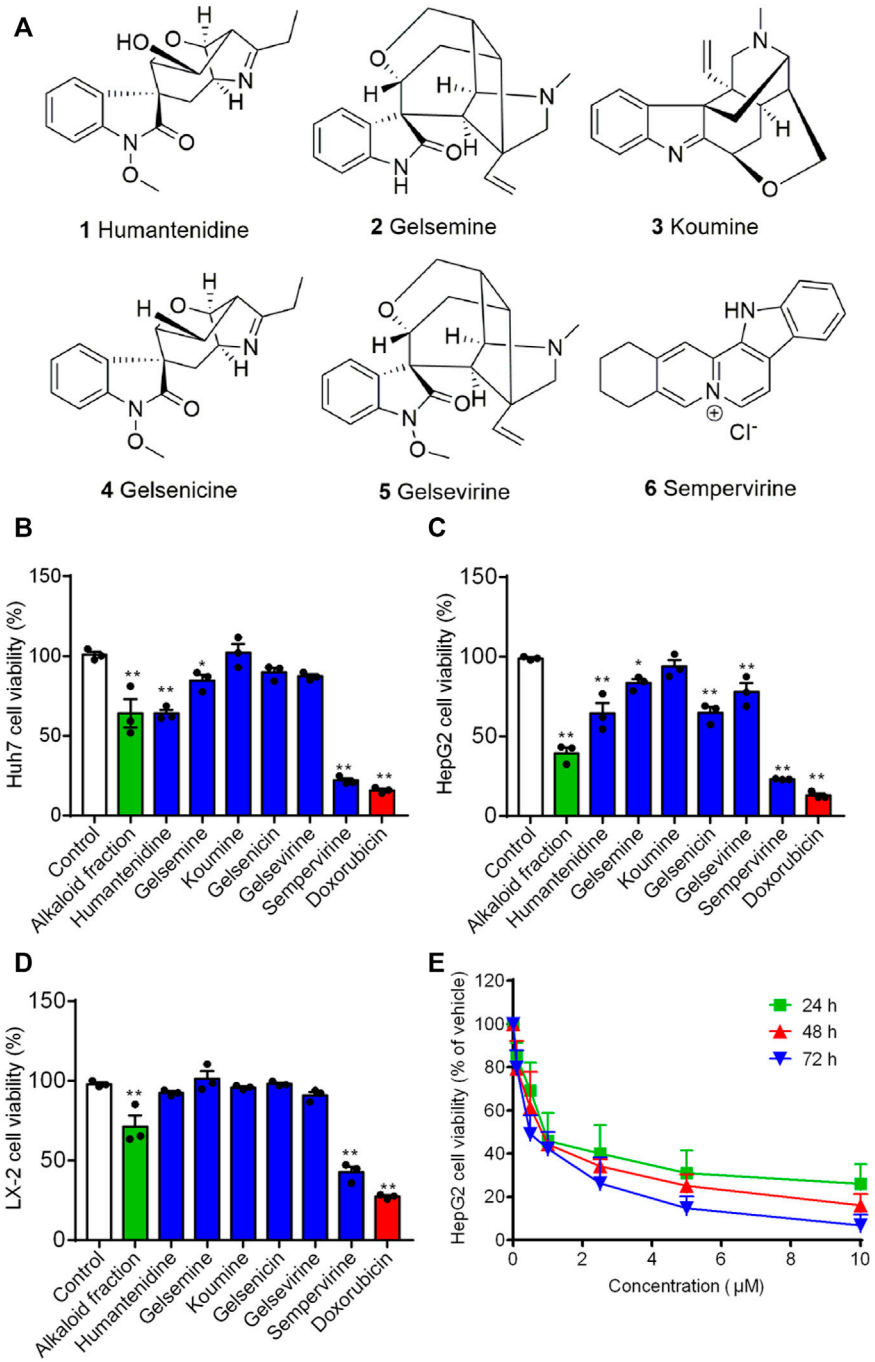


FIGURE 2 | The effect of alkaloids on growth-inhibiting activity in HepG2, Huh7 and LX-2 cells. **(A)** The chemical structure of alkaloids. Huh7 **(B)** HepG2 **(C)** and LX-2 **(D)** cells were treated for 24 h. Cell viability was assayed by CCK8. **(E)** Sempervirine (0, 0.1, 0.5, 1, 2.5, 5, 10 μM) inhibited HepG2 cells growth for 24, 48, and 72 h $^{*}p < 0.05$; $^{**}p < 0.01$ *vs*. Control.

reserved for subsequent experiment to detect activity. Alkaloidal compounds were then successfully separated using pH-zone-refining counter-current chromatography and compared with commercial standards purchased from Shanghai yuanye Bio-Technology Co., Ltd.

Cell Lines and Cell Culture

HepG2, Huh7 and the normal cell line LX-2 were obtained from GuangZhou Jennio Biotech Co.,Ltd. The cells were grown under standard conditions (37°C with 5% CO_2) using DMEM medium supplemented with 10% FBS.

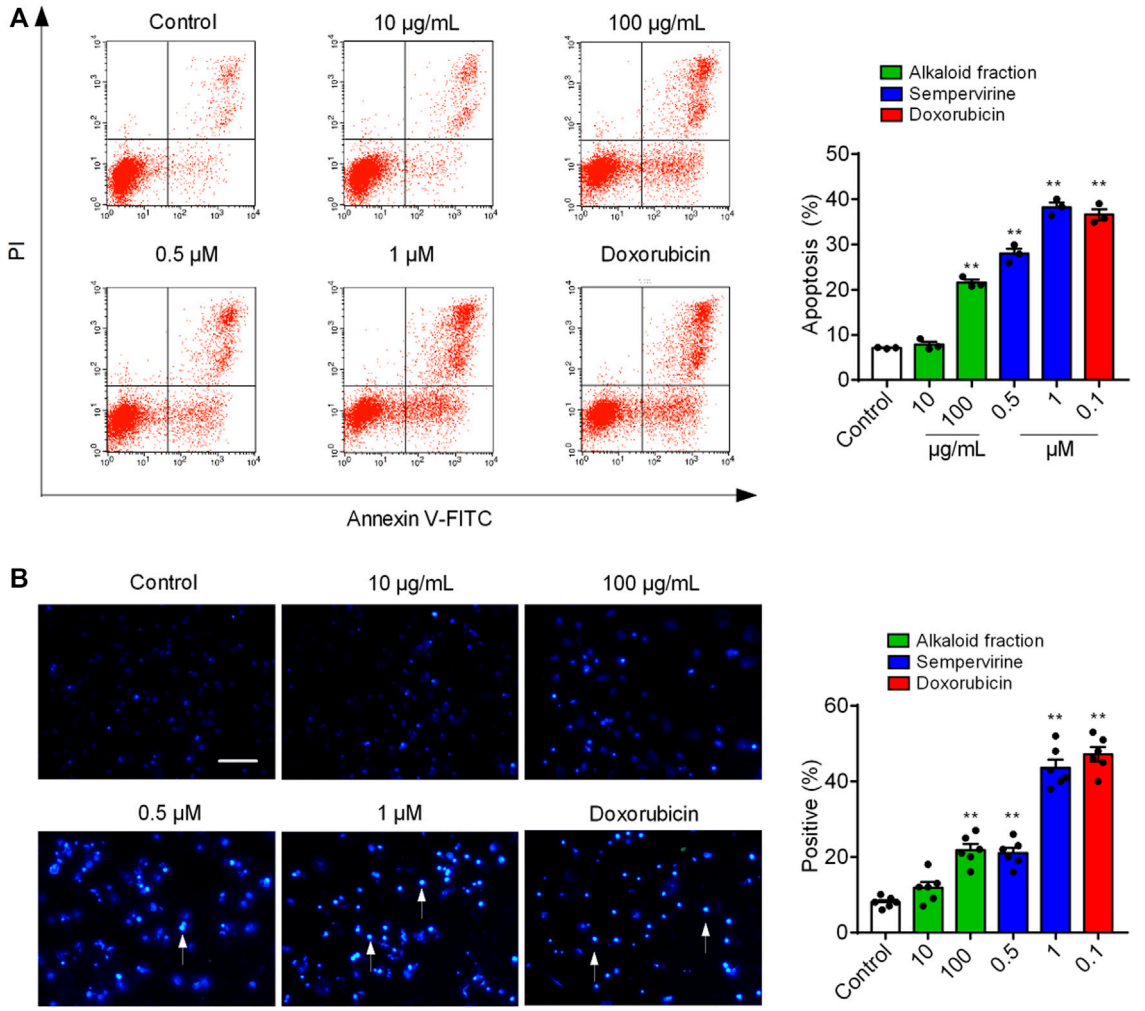


FIGURE 3 | Sempervirine induced apoptosis in HepG2 cells. **(A)** Apoptosis was evaluated by flow cytometry. The *X*- and *Y*-axes represent annexin V-FITC staining and PI, respectively. **(B)** The morphological nuclear changes in HepG2 cells treated with sempervirine at different concentrations. The cells were stained with Hoechst 33258 for 30 min in the dark to examine the cleaved nuclei. $^{**}p < 0.01$ *vs*. Control.

Cell Viability Assay

Cell viability was determined by the CCK8 assay. Cells were treated with sempervirine (0, 0.1, 0.5, 1, 2.5, 5, and 10 μM) for 24, 48, and 72 h, respectively. 0.1 μM Doxorubicin was used as a positive control. The absorbance at 450 nm was read using a BioTek Synergy two plate reader (BioTek Instruments, Inc.).

Cell Apoptosis Assay

After digestion with trypsin, the cells were collected, washed with PBS and resuspended by 1× Binding buffer. Annexin V-FITC and solution were added and react at room temperature for 15 min, then detected by flow cytometry (FACSCalibur, BD) within 1 h.

Cell Cycle Assay

Cells were incubated with sempervirine (0.5 and 1 μM) for 24 h. After treatment, the cells were fixed with cold 75% ethanol overnight at 4°C. Then the cells were incubated with PI staining solution (50 μg/mL) and RNase A solution (100 μg/mL) and incubated for 30 min. Cell cycle distribution were analyzed by flow cytometry (FACSCalibur, BD).

Luciferase Reporter Assay

Cells were co-transfected with TOPflash or FOPflash vector together with luciferase reporter vector pRL-TK as the control for transfection efficiency as previous reported (Cheng et al., 2017). After 12 h of transfection, cells were incubated with sempervirine for another 24 h. Luciferase activity was measured and normalized according to the recommended protocol (Promega).

Western Blot Analysis

30 μg amounts of protein and 5× loading buffer was fully mixed and boiled in a constant temperature water bath at 95°C for 5 min to denature the protein. The protein was separated by sodium dodecyl sulfate polyacrylamide gel electrophoresis and transferred to PVDF membranes. The

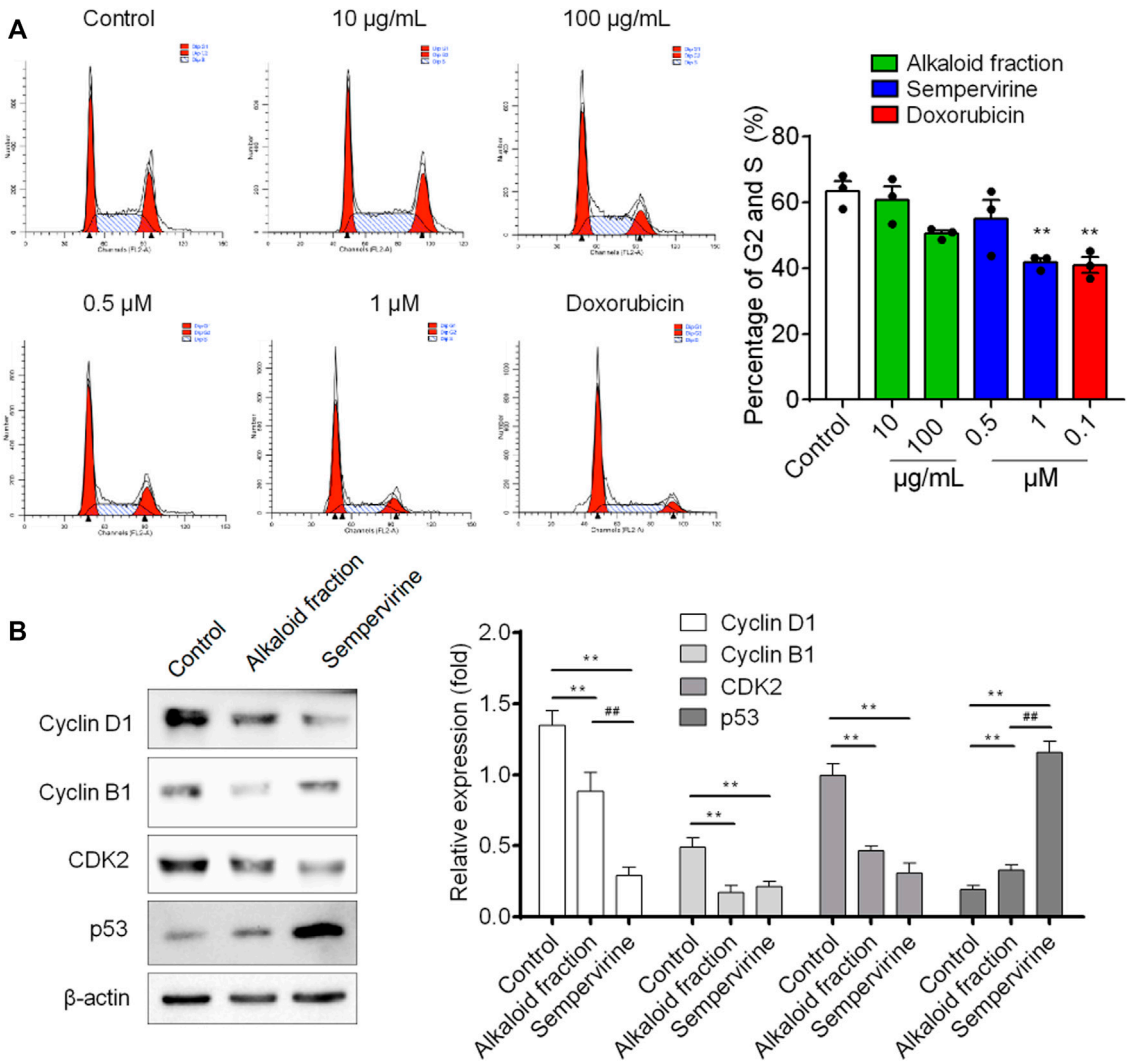


FIGURE 4 | The effect of sempervirine on the cell cycle and the expression of cell cycle regulators in HepG2 cells. **(A)** Sempervirine treatment induced a dose dependent increase in the proportion of cells in the G1 phase and a decrease in cells in the S and G2 phases compared to the control. **(B)** Representative pictures for p53, CDK2, cyclin B1 and cyclin D1 protein expression by western blot analysis. $^{**}p < 0.01$ *vs*. Control, $^{\#\#}p < 0.01$ *vs*. the alkaloid fraction.

membranes were incubated with primary antibodies overnight at 4°C, horseradish peroxidase-conjugated secondary antibodies for 2 h at room temperature and enhanced chemiluminescence kit (Sigma, United States) according to the manufacturer's instructions and visualized with a ChemiDoc XRS gel imaging system (Bio-Rad, United States).

Histopathological Examination

The tumor tissues of three nude mice in each group were randomly taken for histopathological examination. The tumor tissues were conducted fixation, dehydration, transparent, wax dipping, embedding and then cut into 4 μm slices for hematoxylin and eosin (HE) staining, the expression of Ki67, TUNEL and β-catenin according to the manufacturer's instructions and appropriate dilution ratio. The stained slides visualized under a TCS SP8 microscope (Leica, Germany).

HCC Xenograft Model

The HepG2 cells grown were digested and centrifuged, resuspended in PBS solution, and 5×10^6 cells were injected into the right back of each four-week-old male Balb/c nude mouse (Shanghai SLAC Lab. Animal Co., Ltd.). After 2 weeks, when the tumor grew to about 1 cm^3, mice were treated with 1 mg/kg sempervirine by intraperitoneal injection once daily for 2 weeks. Sorafenib is given orally at 10 and 30 mg/kg, respectively. The growth of tumor and the physical condition of nude mice were observed every day. Animal experiments were approved by the Committee on the Ethics of Animal Experiments of the Fujian Medical University.

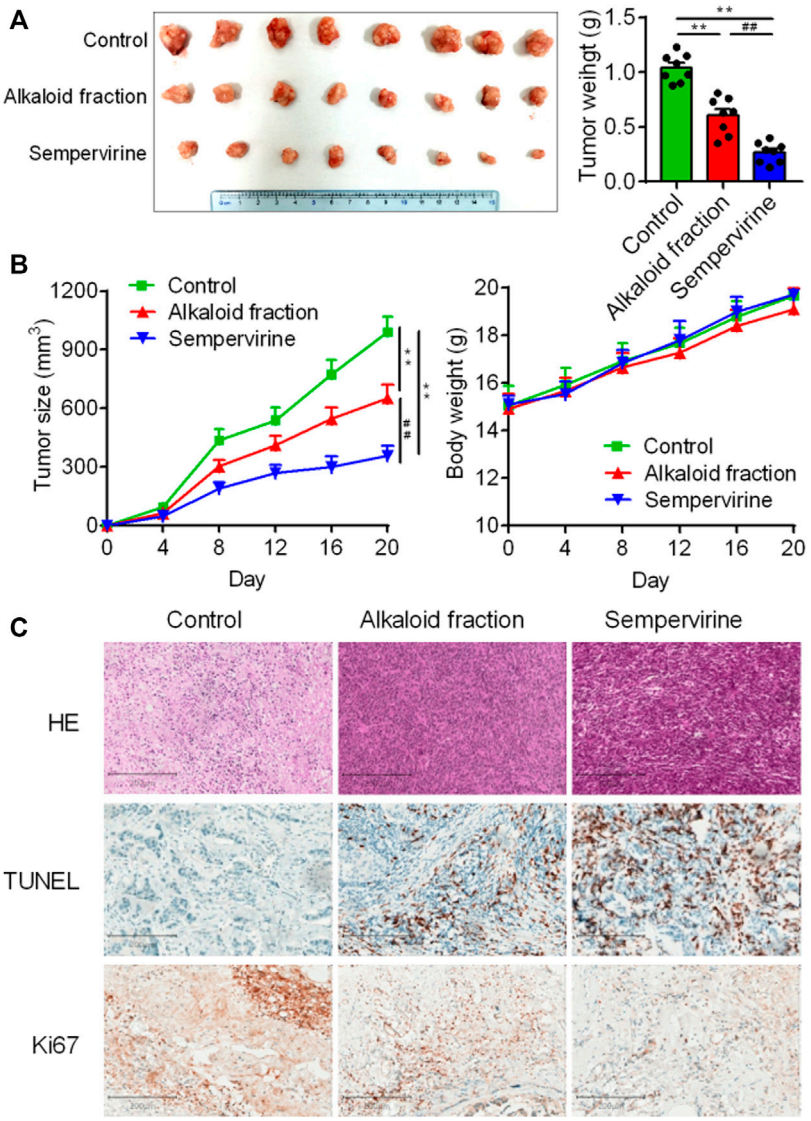


FIGURE 5 | Sempervirine inhibited HCC *in vivo*. **(A)** Images of HepG2 subcutaneous inoculation tumors in mice intravenously treated with the sempervirine for 2 weeks. Quantification of the volumes of tumors was shown. **(B)** Growth curves of the tumors and quantification of body weights of the mice during treatment. **(C)** Representative HE staining, the proliferation marker Ki67 and the apoptosis marker TUNEL of xenografts treated with the sempervirine and the alkaloid fraction. Scale bars = 200 μm. Data are presented as means ± SEM. $^{**}p < 0.01$ *vs*. Control, $^{\#\#}p < 0.01$ *vs*. the alkaloid fraction.

Statistical Analysis

Results were expressed as mean ± SEM from three independent experiments. The results were statistically evaluated using by one-way analysis of variance (ANOVA) followed by the Dunnett's test. A value of $p < 0.05$ indicates a significant difference.

RESULTS

Sempervirine Exhibited Selective Cytotoxicity Toward HCC

HepG2, Huh7 and LX-2 were used to assess the inhibition effects of the alkaloid fraction, non-alkaloid fraction, and whole extracts of *G. elegans* (**Figure 1**). Furthermore, six alkaloid compounds extracted from the alkaloid fraction of *G. elegans* were evaluated the cytotoxicity *in vitro* (chemical structure shown in **Figure 2A**). Among the alkaloids examined at 10 μM, sempervirine showed best effects to inhibit the proliferation of Huh7 and HepG2 cells (**Figures 2B,C**). Interestingly, cytotoxicity analysis showed that sempervirine was found to be relatively low cytotoxic to LX-2 cells (**Figure 2D**). In addition, the CCK8 results indicated that sempervirine inhibited HCC growth in a dose and time dependent manner (**Figure 2E**).

Sempervirine Induced Cell Apoptosis

We next determined whether sempervirine could induce cell apoptosis (**Figure 2A**). 24 h after the alkaloid fraction (10 and

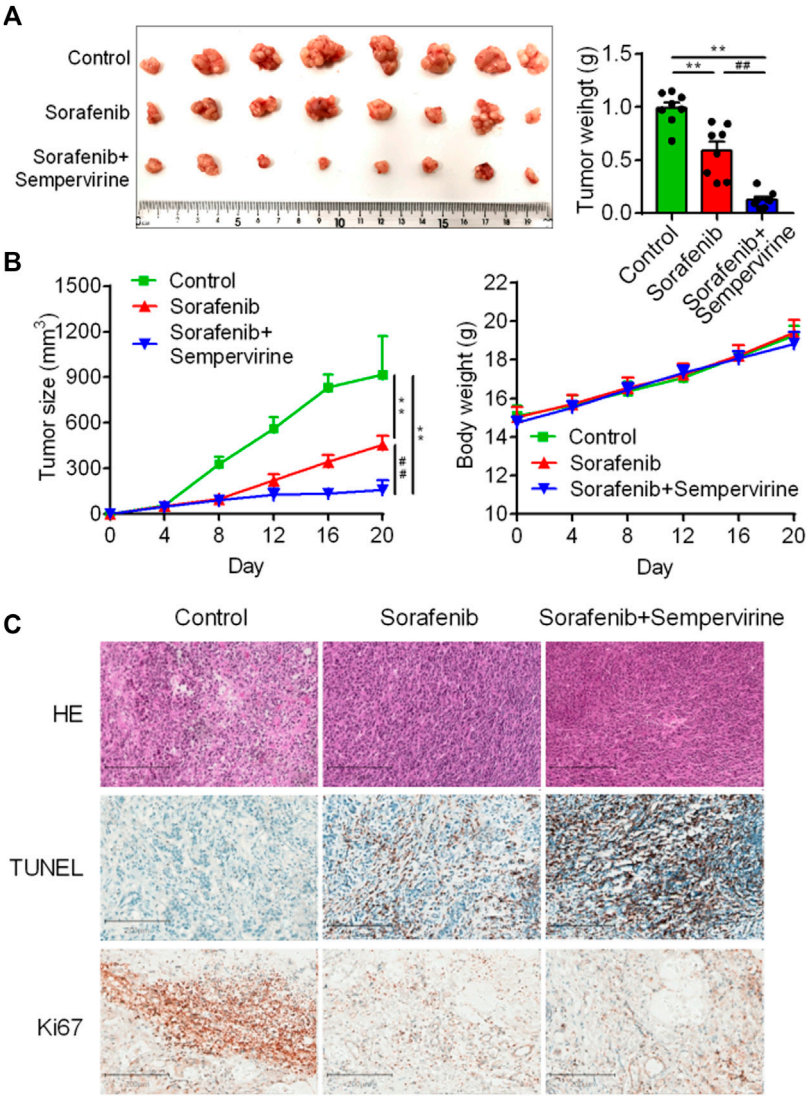


FIGURE 6 | Sempervirine enhanced anti-tumor activity of sorafenib. **(A)** Representative bioluminescence images of HepG2 hepatic tumors in mice treated with sempervirine and sorafenib for 2 weeks. **(B)** Quantification of tumor volumes and tumor growth curves in mice. **(C)** Representative HE staining, Ki67 and TUNE of xenografts treated with the sempervirine and the combination group. Scale bars = 200 μm. Data are presented as means ± SEM. $^{**}p < 0.01$ *vs*. Control, $^{\#\#}p < 0.01$ *vs*. the combination.

100 μg/mL) and sempervirine (1 and 10 μM) treatment, HepG2 cells were suffered significantly apoptosis. Next, we analyzed morphological nuclear changes and found that sempervirine significantly causes nuclear contraction and DNA breakage in HCC (**Figure 2B**). The data indicated that sempervirine induces HepG2 cells apoptosis.

Sempervirine Induced Cell Cycle Arrest in G1 Phase

Flow cytometry was used to analyze the DNA content. Sempervirine induced a dose-dependent increase in the proportion of G_1 phase and decrease in the S and G_2 phases (**Figure 3A**). Furthermore, the expression levels of p53 was markedly increased, whereas cyclin D1, cyclin B1 and CDK2 expression were significantly decreased after sempervirine treatment (**Figure 4B**). These results revealed that sempervirine induced p53 activation and arrested cell cycle in G_1 phase.

Sempervirine Inhibited HCC *In Vivo*

Further *in vivo* results shown that sempervirine treatment significantly inhibited HepG2 tumor growth rate and size (**Figure 5A**). No body weight loss was observed in sempervirine-treated mice (**Figure 5B**). In addition, Ki67 and TUNEL assay of xenograft tumor tissues were performed to measure proliferation and apoptosis of HepG2 cells in the xenograft model, the results suggested that sempervirine

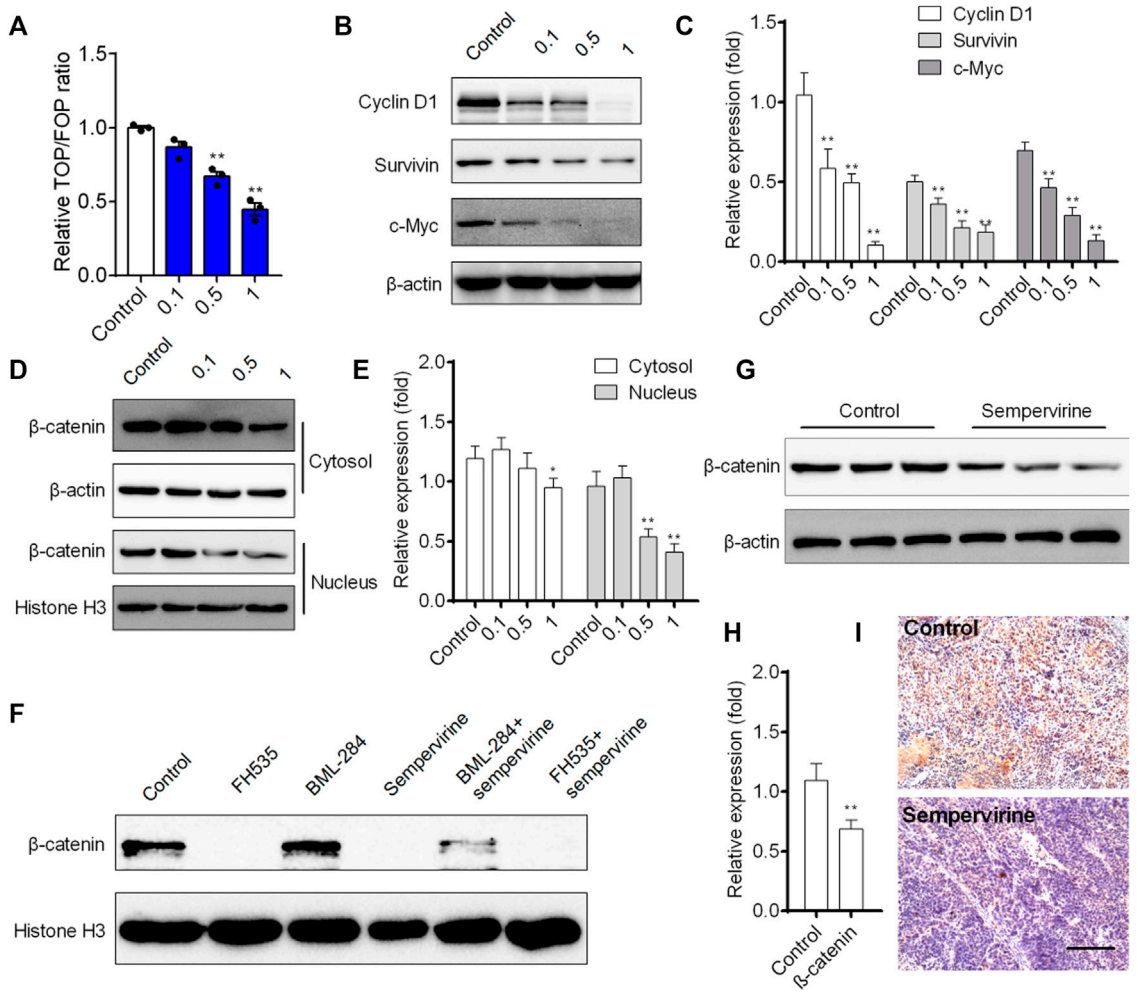


FIGURE 7 | Sempervirine inhibited Wnt/β-catenin pathway and induced apoptosis *in vivo*. **(A)** Cells were treated with different concentrations of sempervirine for 24 h to TOPflash assay. **(B, C)** Western blotting analysis of Wnt/β-catenin target genes survivin, cyclin D1, and c-Myc in HepG2 cells after treated with different concentrations of sempervirine. **(D, E)** HepG2 cells were pretreated with sempervirine for 24 h and the fractioned lysates were analyzed by Western blotting. **(F)** HepG2 cells treated with 10 μM Wnt activator BML-284 or 10 μM Wnt inhibitor FH535 for 24 h in the presence of sempervirine were analyzed by western blots. **(G–I)** The effect of sempervirine on the expression of β-catenin protein *in vivo*. Scale bars = 100 μm. Data are presented as means ± SEM. $^{*}p < 0.05$; $^{**}p < 0.01$ *vs*. Control.

significantly inhibit cell proliferation and induce apoptosis (**Figure 5C**). These results indicated that sempervirine is a potential therapeutic agent for HCC *in vivo*.

Sempervirine Enhanced the Anti-tumor Effects of Sorafenib

Sorafenib is a clinically first-line drug for advanced HCC, with limited curative effect and easy to develop drug resistance. Therefore, the synergist of sorafenib is also one of the hotspots in the development of HCC drugs. The results showed that the effect of the combination of sorafenib (10 mg/kg) and sempervirine was more excellent to that of sorafenib at high dose (30 mg/kg) (**Figures 6A,B**). HE staining showed that the combination of sorafenib and BD and sorafenib high dose treatment could significantly induce tumor tissue necrosis, TUNEL showed that the combination group and sorafenib high dose group could significantly induce the apoptosis of hepatoma tumor cells, and Ki67 showed that the combination group and sorafenib high dose group could significantly inhibit the proliferation of hepatoma tumor cells (**Figure 6C**). These findings proved that sempervirine possessed synergistic effect with sorafenib.

Sempervirine Inhibited Wnt/β-Catenin Pathway and Induced Apoptosis *In Vivo*

We further investigated the effects of sempervirine on the transcriptional activity of Wnt/β-catenin pathway in HepG2 cells. Our results showed that sempervirine inhibited transcription of TCF/LEF in HepG2 cells with a dose-dependent manner (**Figure 7A**). Furthermore, Wnt/β-catenin target genes survivin, cyclin D1, and c-Myc were significantly decreased after different concentrations of sempervirine treatment in HepG2 cells (**Figures 7B,C**). The results of separation and detection of nuclear protein and cytoplasmic protein showed that sempervirine could significantly inhibit the level of

β-catenin in the nucleus (**Figures 7D,E**). In addition, the effect of Wnt inhibitor FH535 and agonist BML-284 were used to evaluate the regulatory effect of sempervirine on the lever of β-catenin in nucleus. Sempervirine also decreased the lever of β-catenin in BML-284-treated cells, while the amount of β-catenin after combined treatment with sempervirine was the same as that treated with sempervirine alone (**Figure 7F**). Moreover, sempervirine suppressed the expression of β-catenin in a xenograft model (**Figures 7G,H**). These results suggest that sempervirine can significantly inhibit the nuclear aggregation level of β-catenin and inhibit the transcription level of Wnt pathway and thus may induce HepG2 cell apoptosis *via* the Wnt/β-catenin pathway.

DISCUSSION

Primary liver cancer is one of the common malignant tumors in the world. At present, the first-line drugs for advanced liver cancer are still mainly multiple tyrosine kinase receptor inhibitors. Sorafenib is a first-line anti HCC drug and demonstrates broad oral antitumor efficacy given orally at 7.5–60 mg/kg in panel of human tumor xenograft models. Daily oral administration of Sorafenib (30–60 mg/kg) produces complete tumor stasis during treatment in five of the six models (Wilhelm et al., 2004). However, Sorafenib is easy to develop drug resistance. Drug development strategy of advanced liver cancer is mainly to find molecules targeting new pathways or molecules sensitized by sorafenib. Previous reports indicated that *G. elegans* possessed ideal natural compounds for the treatment of cancer (Liang et al., 2013; Que et al., 2021). Sempervirine, an alkaloid isolated from *G. elegans*, have shown anti-cancer activity (Pan et al., 2016; Caggiano et al., 2020). Our data demonstrated that sempervirine inhibited HCC growth in a dose dependent manner. More interestingly, sempervirine could have synergistic effect with sorafenib *in vitro*.

HCC has the characteristics of rapid proliferation and high degree of malignancy and the treatment of HCC is still an enormous problem (Forner et al., 2012). Several apoptosis inducer have been proven to be clinically effective (Ashkenazi et al., 2017). The present CCK8 assays revealed that sempervirine inhibited induce apoptosis activity. In addition, the growth inhibition induced by sempervirine occurs through the G_1 phase arrest. Moreover, sempervirine could downregulate the expression of cyclin D1, cyclin B1 and CDK2 and increase p53. Consistently, sempervirine has been identified as a potent inhibitor of MDM2 on p53 (Sasiela et al., 2008).

Wnt pathway is closely related to the differentiation and development of liver and mediates the occurrence and development of a variety of liver diseases (Khalaf et al., 2018; Taciak et al., 2018; Wen et al., 2020). Its key transduction factor β-catenin is closely related to the activation of hepatic progenitor cells. In the mouse liver regeneration model, β-catenin could regulate the specific differentiation of hepatic progenitor cells and induce liver regeneration. In a variety of hepatoma cell lines, β-catenin is closely related to the ability of liver tumor regeneration and invasion (He and Tang, 2020). The over activation of Wnt pathway can induce the occurrence of primary liver cancer in mice. In patients with liver cancer, Wnt pathway is the signal pathway with the highest mutation rate except p53 (Trejo-Solis et al., 2021). Wnt pathway inhibitors can not only inhibit the growth of HCC cells, but also reduce the drug resistance of cells and sensitize chemotherapeutic drugs (Vilchez et al., 2016). β-catenin protein is the key transduction factor to start Wnt pathway transcription. In the inactive Wnt pathway, the level of β-catenin is strictly regulated by GSK3β complex, which keeps Wnt activity at a low level. In tumor cells, Wnt pathway mutation or upstream signal activation makes a large amount of β-catenin accumulate and transfer to the nucleus. Thus, excessive activation of Wnt pathway can promote tumor occurrence and development. The present study found that sempervirine could significantly inhibit the nuclear aggregation level of β-catenin, indicating that sempervirine may act on the transcriptional activity of β-catenin to regulate cell proliferation.

In conclusion, the present study maintained that sempervirine inhibited HCC by arresting G_1 cell cycle and inducing apoptosis. Furthermore, sempervirine inhibited HCC growth *in vivo* and increatingly, possessed a synergistic effect with sorafenib. In addition, sempervirine could significantly inhibit the nuclear aggregation level of β-catenin and inhibit the transcription level of Wnt pathway and thus might induce HCC apoptosis *via* the Wnt/β-catenin pathway.

DATA AVAILABILITY STATEMENT

The original contributions presented in the study are included in the article/**Supplementary Material**, further inquiries can be directed to the corresponding authors.

ETHICS STATEMENT

The animal study was reviewed and approved by Fujian Medical University.

AUTHOR CONTRIBUTIONS

PC, GJ, CY, and RY designed research; RY, HL, YH, DS, YL, YL, and YS performed the experiments; RY, HL, YH and GJ analyzed data; and RY and CY wrote the manuscript.

FUNDING

This work was supported by the National Natural Science Foundation of China (82000554, 81973309), the Natural Science Foundation of Fujian Province (2019J01303, 2020J01640, 2020J01618), the Science and Technology Project of Fujian Province (2018Y2001), the Research Initiation Fund for High-level Talents of Fujian Medical University (XRCZX2018015), the Startup Fund of Fujian Medical University (2018QH1015), the Joint Funds for the Innovation of Science and Technology, Fujian Province (2018Y9075, 2019Y9009) and the Open Project Fund of Fujian Provincial Key Laboratory of Environment Factors and Cancer (GWSZD-202003).

ACKNOWLEDGMENTS

We thank Junjin Lin from the Public Technology Service Center (Fujian Medical University, China) for the assistance in flow cytometry analysis.

SUPPLEMENTARY MATERIAL

The Supplementary Material for this article can be found online at: https://www.frontiersin.org/articles/10.3389/fphar.2021.806091/full#supplementary-material

REFERENCES

Ashkenazi, A., Fairbrother, W. J., Leverson, J. D., and Souers, A. J. (2017). From Basic Apoptosis Discoveries to Advanced Selective BCL-2 Family Inhibitors. *Nat. Rev. Drug Discov.* 16, 273–284. doi:10.1038/nrd.2016.253

Ashrafizadeh, M., Ahmadi, Z., Mohamamdinejad, R., Yaribeygi, H., Serban, M. C., Orafai, H. M., et al. (2020). Curcumin Therapeutic Modulation of the Wnt Signaling Pathway. *Curr. Pharm. Biotechnol.* 21, 1006–1015. doi:10.2174/1389201021666200305115101

Caggiano, C., Guida, E., Todaro, F., Bielli, P., Mori, M., Ghirga, F., et al. (2020). Sempervirine Inhibits RNA Polymerase I Transcription Independently from P53 in Tumor Cells. *Cell Death Discov* 6, 111. doi:10.1038/s41420-020-00345-4

Carneiro, B. A., and El-Deiry, W. S. (2020). Targeting Apoptosis in Cancer Therapy. *Nat. Rev. Clin. Oncol.* 17, 395–417. doi:10.1038/s41571-020-0341-y

Cheng, Z., Yuan, X., Qu, Y., Li, X., Wu, G., Li, C., et al. (2017). Bruceine D Inhibits Hepatocellular Carcinoma Growth by Targeting β-catenin/jagged1 Pathways. *Cancer Lett.* 403, 195–205. doi:10.1016/j.canlet.2017.06.014

Craig, A. J., Von Felden, J., Garcia-Lezana, T., Sarcognato, S., and Villanueva, A. (2020). Tumour Evolution in Hepatocellular Carcinoma. *Nat. Rev. Gastroenterol. Hepatol.* 17, 139–152. doi:10.1038/s41575-019-0229-4

Forner, A., Llovet, J. M., and Bruix, J. (2012). Hepatocellular Carcinoma. *Lancet* 379, 1245–1255. doi:10.1016/s0140-6736(11)61347-0

Greco, G., Catanzaro, E., and Fimognari, C. (2021). Natural Products as Inducers of Non-canonical Cell Death: A Weapon against Cancer. *Cancers (Basel)* 13, 304. doi:10.3390/cancers13020304

He, S., and Tang, S. (2020). WNT/β-catenin Signaling in the Development of Liver Cancers. *Biomed. Pharmacother.* 132, 110851. doi:10.1016/j.biopha.2020.110851

Hu, J., Cao, J., Topatana, W., Juengpanich, S., Li, S., Zhang, B., et al. (2021). Targeting Mutant P53 for Cancer Therapy: Direct and Indirect Strategies. *J. Hematol. Oncol.* 14, 157. doi:10.1186/s13045-021-01169-0

Ichim, G., and Tait, S. W. (2016). A Fate Worse Than Death: Apoptosis as an Oncogenic Process. *Nat. Rev. Cancer* 16, 539–548. doi:10.1038/nrc.2016.58

Jin, G. L., Hong, L. M., Liu, H. P., Yue, R. C., Shen, Z. C., Yang, J., et al. (2021). Koumine Modulates Spinal Microglial M1 Polarization and the Inflammatory Response through the Notch-RBP-Jκ Signaling Pathway, Ameliorating Diabetic Neuropathic Pain in Rats. *Phytomedicine* 90, 153640. doi:10.1016/j.phymed.2021.153640

Jin, G. L., Su, Y. P., Liu, M., Xu, Y., Yang, J., Liao, K. J., et al. (2014). Medicinal Plants of the Genus Gelsemium (Gelsemiaceae, Gentianales)-Aa Review of Their Phytochemistry, Pharmacology, Toxicology and Traditional Use. *J. Ethnopharmacol.* 152, 33–52. doi:10.1016/j.jep.2014.01.003

Khalaf, A. M., Fuentes, D., Morshid, A. I., Burke, M. R., Kaseb, A. O., Hassan, M., et al. (2018). Role of Wnt/β-Catenin Signaling in Hepatocellular Carcinoma, Pathogenesis, and Clinical Significance. *J. Hepatocell Carcinoma* 5, 61–73. doi:10.2147/jhc.s156701

Li, Q., Sun, M., Wang, M., Feng, M., Yang, F., Li, L., et al. (2021). Dysregulation of Wnt/β-Catenin Signaling by Protein Kinases in Hepatocellular Carcinoma and its Therapeutic Application. *Cancer Sci.* 112, 1695–1706. doi:10.1111/cas.14861

Liang, S., He, C.-Y., Szabó, L. F., Feng, Y., Lin, X., and Wang, Y. (2013). Gelsochalotine, a Novel Indole Ring-Degraded Monoterpenoid Indole Alkaloid from Gelsemium Elegans. *Tetrahedron Lett.* 54, 887–890. doi:10.1016/j.tetlet.2012.11.122

Liu Hao, X. Y., Shi, D., and Yu, C. (2008). Pharmacognostical Study on the Gelsem Ium Elegans Benth. From Fuzhou. *Hai Xia Yao Xue* 20, 62–64.

Martin-Orozco, E., Sanchez-Fernandez, A., Ortiz-Parra, I., and Ayala-San Nicolas, M. (2019). WNT Signaling in Tumors: The Way to Evade Drugs and Immunity. *Front. Immunol.* 10, 2854. doi:10.3389/fimmu.2019.02854

Mullard, A. (2016). Pioneering Apoptosis-Targeted Cancer Drug Poised for FDA Approval. *Nat. Rev. Drug Discov.* 15, 147–149. doi:10.1038/nrd.2016.23

Pan, X., Yang, C., Cleveland, J. L., and Bannister, T. D. (2016). Synthesis and Cytoxicity of Sempervirine and Analogues. *J. Org. Chem.* 81, 2194–2200. doi:10.1021/acs.joc.6b00022

Parsons, M. J., Tammela, T., and Dow, L. E. (2021). WNT as a Driver and Dependency in Cancer. *Cancer Discov.* 11, 2413–2429. doi:10.1158/2159-8290.cd-21-0190

Perugorria, M. J., Olaizola, P., Labiano, I., Esparza-Baquer, A., Marzioni, M., Marin, J. J. G., et al. (2019). Wnt-β-catenin Signalling in Liver Development, Health and Disease. *Nat. Rev. Gastroenterol. Hepatol.* 16, 121–136. doi:10.1038/s41575-018-0075-9

Que, W., Chen, M., Yang, L., Zhang, B., Zhao, Z., Liu, M., et al. (2021). A Network Pharmacology-Based Investigation on the Bioactive Ingredients and Molecular Mechanisms of Gelsemium Elegans Benth against Colorectal Cancer. *BMC Complement. Med. Ther.* 21, 99. doi:10.1186/s12906-021-03273-7

Sasiela, C. A., Stewart, D. H., Kitagaki, J., Safiran, Y. J., Yang, Y., Weissman, A. M., et al. (2008). Identification of Inhibitors for MDM2 Ubiquitin Ligase Activity from Natural Product Extracts by a Novel High-Throughput Electrochemiluminescent Screen. *J. Biomol. Screen.* 13, 229–237. doi:10.1177/1087057108315038

Su, Y. P., Shen, J., Xu, Y., Zheng, M., and Yu, C. X. (2011). Preparative Separation of Alkaloids from Gelsemium Elegans Benth. Using pH-Zone-Refining Counter-current Chromatography. *J. Chromatogr. A.* 1218, 3695–3698. doi:10.1016/j.chroma.2011.04.025

Taciak, B., Pruszynska, I., Kiraga, L., Bialasek, M., and Krol, M. (2018). Wnt Signaling Pathway in Development and Cancer. *J. Physiol. Pharmacol.* 69, 185–196. doi:10.26402/jpp.2018.2.07

Trejo-Solis, C., Escamilla-Ramirez, A., Jimenez-Farfan, D., Castillo-Rodriguez, R. A., Flores-Najera, A., and Cruz-Salgado, A. (2021). Crosstalk of the Wnt/β-Catenin Signaling Pathway in the Induction of Apoptosis on Cancer Cells. *Pharmaceuticals (Basel)* 14, 871. doi:10.3390/ph14090871

Vilchez, V., Turcios, L., Marti, F., and Gedaly, R. (2016). Targeting Wnt/β-Catenin Pathway in Hepatocellular Carcinoma Treatment. *World J. Gastroenterol.* 22, 823–832. doi:10.3748/wjg.v22.i2.823

Villanueva, A. (2019). Hepatocellular Carcinoma. *N. Engl. J. Med.* 380, 1450–1462. doi:10.1056/NEJMra1713263

Wang, J., Liu, R., Zhao, Y., Ma, Z., Sang, Z., Wen, Z., et al. (2021). Novel Microcrystal Formulations of Sorafenib Facilitate a Long-Acting Antitumor Effect and Relieve Treatment Side Effects as Observed with Fundus Microcirculation Imaging. *Front. Oncol.* 11, 743055. doi:10.3389/fonc.2021.743055

Wang, W., Smits, R., Hao, H., and He, C. (2019). Wnt/β-Catenin Signaling in Liver Cancers. *Cancers (Basel)* 11, 926. doi:10.3390/cancers11070926

Wang, Y., Wu, S., Chen, Z., Zhang, H., and Zhao, W. (2015). Inhibitory Effects of Cytochrome P450 Enzymes CYP1A2, CYP2A6, CYP2E1 and CYP3A4 by Extracts and Alkaloids of Gelsemium Elegans Roots. *J. Ethnopharmacol.* 166, 66–73. doi:10.1016/j.jep.2015.03.002

Wen, X., Wu, Y., Awadasseid, A., Tanaka, Y., and Zhang, W. (2020). New Advances in Canonical Wnt/β-Catenin Signaling in Cancer. *Cancer Manag. Res.* 12, 6987–6998. doi:10.2147/cmar.s258645

Wilhelm, S. M., Carter, C., Tang, L., Wilkie, D., McNabola, A., Rong, H., et al. (2004). BAY 43-9006 Exhibits Broad Spectrum Oral Antitumor Activity and Targets the RAF/MEK/ERK Pathway and Receptor Tyrosine Kinases Involved in Tumor Progression and Angiogenesis. *Cancer Res.* 64, 7099–7109. doi:10.1158/0008-547210.1158/0008-5472.CAN-04-1443

Yu, S., Cai, L., Liu, C., Gu, R., and Cai, L. (2021). Identification of Prognostic Alternative Splicing Events Related to the Immune Microenvironment of Hepatocellular Carcinoma. *Mol. Med.* 27, 36. doi:10.1186/s10020-021-00294-3

Yue, R., Jin, G., Wei, S., Huang, H., and Su, L. (2019). Immunoregulatory Effect of Koumine on Nonalcoholic Fatty Liver Disease Rats. *J. Immunol. Res.* 2019, 8325102. doi:10.1155/2019/8325102

Zhang, J. Y., and Wang, Y. X. (2015). Gelsemium Analgesia and the Spinal glycine Receptor/allopregnanolone Pathway. *Fitoterapia* 100, 35–43. doi:10.1016/j.fitote.2014.11.002

Conflict of Interest: The authors declare that the research was conducted in the absence of any commercial or financial relationships that could be construed as a potential conflict of interest.

Publisher's Note: All claims expressed in this article are solely those of the authors and do not necessarily represent those of their affiliated organizations, or those of the publisher, the editors and the reviewers. Any product that may be evaluated in this article, or those of the publisher, the editors and the reviewers. Any product that may be evaluated in this article, or claim that may be made by its manufacturer, is not guaranteed or endorsed by the publisher.

Copyright © 2021 Yue, Liu, Huang, Wang, Shi, Su, Luo, Cai, Jin and Yu. This is an open-access article distributed under the terms of the Creative Commons Attribution License (CC BY). The use, distribution or reproduction in other forums is permitted, provided the original author(s) and the copyright owner(s) are credited and that the original publication in this journal is cited, in accordance with accepted academic practice. No use, distribution or reproduction is permitted which does not comply with these terms.

frontiers in Pharmacology

ORIGINAL RESEARCH
published: 15 December 2021
doi: 10.3389/fphar.2021.798421

Gastroprotective Effects of *Periplaneta americana* L. Extract Against Ethanol-Induced Gastric Ulcer in Mice by Suppressing Apoptosis-Related Pathways

Shu Fu[1], Jiamei Chen[1], Chen Zhang[1], Jinfeng Shi[2], Xin Nie[1], Yichen Hu[3], Chaomei Fu[1], Xiaofang Li[1] and Jinming Zhang[1]**

[1]State Key Laboratory of Southwestern Chinese Medicine Resources, College of Pharmacy, Chengdu University of Traditional Chinese Medicine, Chengdu, China, [2]School of Pharmacy, Chengdu Medical College, Chengdu, China, [3]Key Laboratory of Coarse Cereal Processing, Ministry of Agriculture and Rural Affairs, Sichuan Engineering & Technology Research Center of Coarse Cereal Industralization, School of Food and Biological Engineering, Chengdu University, Chengdu, China

OPEN ACCESS

Edited by:
Hong Zhang,
Shanghai University of Traditional Chinese Medicine, China

Reviewed by:
Qiu Li,
Qingdao Agricultural University, China
Hongwei Gao,
Guangxi University of Chinese Medicine, China
Shengpeng Wang,
University of Macau, China

***Correspondence:**
Xiaofang Li
lixiaofang@cdutcm.edu.cn
Jinming Zhang
zhangjinming1987@126.com

Specialty section:
This article was submitted to Ethnopharmacology, a section of the journal Frontiers in Pharmacology

Received: *20 October 2021*
Accepted: *03 December 2021*
Published: *15 December 2021*

Citation:
Fu S, Chen J, Zhang C, Shi J, Nie X, Hu Y, Fu C, Li X and Zhang J (2021) Gastroprotective Effects of Periplaneta americana *L. Extract Against Ethanol-Induced Gastric Ulcer in Mice by Suppressing Apoptosis-Related Pathways. Front. Pharmacol. 12:798421. doi: 10.3389/fphar.2021.798421*

Although *Periplaneta americana* L. and its modern preparation, Kangfuxin liquid, have been extensively applied for ulcerative diseases in gastrointestinal tract (e.g., gastric ulcer (GU) and ulcerative colitis, the effective components and potential mechanisms) remain unclear. In accordance with the accumulating research evidences, the relieving/exacerbating of GU is noticeably correlated to focal tissue programmed cell death. Herein, gastro-protective effects of the effective *Periplaneta americana* L. extract (PAE) fraction were assessed *in vitro* and *in vivo*, involving in programmed cell death-related signaling channels. To screen the effective PAE fraction exerting gastroprotective effects, several PAE fractions were gained based on a wide range of ethanol solution concentration, and they were assessed on ethanol-induced ulcer mice. Based on HPLC investigation with the use of nucleosides, the chemical composition of screened effective PAE, extracted by 20% ethanol, was analyzed in terms of quality control. Based on CCK-8 assay, the protective effects on GES-1 cells, impaired by ethanol, of PAE were assessed. After 3 days pre-treatment with PAE (200, 400, 800 mg/kg), the gastric lesions were assessed by tissue morphology, and periodic acid-schiff (PAS) staining, as well as hematoxylin and eosin (H&E) based histopathology-related investigation. The levels for inflammation cytokines (IL1-β, TNF-α, IL-18, PGE2, and IL-6), antioxidant indices (SOD and MDA) were examined via ELISA. In the meantime, based on Western Blotting assay, the expression levels of some programmed cell death-related protein targets (NLRP3, caspase-1, NF-κB p65, MyD88, and TLR4) were analyzed. As revealed from the results, PAE is capable of alleviating gastric mucosa impairment, suppressing the inflammatory cytokines, and down-regulating the MyD88/NF-κB channels. Accordingly, 20% ethanol extract of *Periplaneta americana* L. would contribute its gastroprotective effects, thereby providing the evidence that its anti-GU mechanisms correlated with inhibiting programmed cell death channel.

Keywords: *Periplaneta americana* L., gastric ulcer, MyD88/NF-κB, PAS staining, HPLC

INTRODUCTION

Gastric ulcer (GU) refers to a prevailing disorder relating to the stomach and intestines with effects on more populations globally (Boligon et al., 2014). GU popularity reaches 2.4% within west people as well as 6.1% within Chinese population (Xie et al., 2020). Though GU has disputed etiology and the origination and development of the disease, the disbalance assumption of destruction and offense factor pertaining to mucosal barriers was extensively recognized (Chen et al., 2015; Chen et al., 2018). Different elements are likely to facilitate the process of forming GU [e.g., nonsteroidal anti-inflammation drug (NSAID), consumption of alcohol, tobacco-smoking, *Helicobacter pylori* infection, and psychology stress (Adhikary et al., 2011)]. More and more research reported that programmed cell death is critical channels under the catalysis from caspases downstream pertaining to impairment of gastrointestinal mucosa epithelium (Ahmed et al., 2021). It acts via molecule signaling channels exhibiting the characteristics of the cell regulatory cycle's initiating, mediating, executing and regulating processes. A recent research built correlations of apoptosis and autophagy to indomethacin-triggered mucosa erosion and ulceration (Gebril et al., 2020). Besides, mitochondrion channel mitigated programmed cell death had correlations to the act or process of causing or getting *H. pylori*. The act or process of causing or getting *H. pylori* up-regulated pro-apoptosis protein Bax, whereas it down-regulate anti-apoptosis protein Bcl-2 condition within gastric mucosa (Liu et al., 2005). It is noticeable that stimulation for caspase three and nine is reported within one gastric adenocarcinoma cell line for responding *H. pylori* culture (Zhang et al., 2007).

A number of drugs (e.g., H2 receptor antagonist drug, antacid drug, proton pump inhibiting drug (omeprazole) and antibiotic drug) can be used in terms of treating GU (Ren et al., 2020). Nevertheless, the mentioned medications encounter pivotal issues as impacted by their insufficient efficacy in resisting GU as well as noticeable side effect (e.g., cardiovascular disease risk, hypergastrinaemia, osteoporotic bone fracture, impotence, hypoacidity and gynecomastia) (Chakravarty and Gaur, 2019; Zhang et al., 2019a; Kulikova et al., 2020; Zhou et al., 2020). For this reason, novel drugs capable of being highly efficient and less toxic should be developed to prevent and treat GU.

Hence, the application of traditional Chinese medicine and their extracts turns out to be a hotspot of widespread concern. Clinically and experimentally related research reported their clinically related benefit and less side effect to treat GU (Bi et al., 2014). *Periplaneta americana* L. (PA) (Song et al., 2017), i.e., American cockroach, generally acts as crude drugs exhibiting the long clinically related use history. Given the relevant records within Shennong's Classic of Materia Medica, the classics of traditional Chinese medicine (TCM), PA was primarily adopted for promoting circulations of blood, removing blood stasis in accordance with TCM (Ma et al., 2018). Kangfuxin (KFX), an extract of PA, gained the approval from China Food and Drug Administration (CFDA) in 1998, involving primarily small molecular peptide, amino acid and nucleotide (Lu et al., 2019). KFX was extensively applied in terms of healing of tissue wounds, particularly within gastric and duodenal ulcer (Chen et al., 2016). In accordance with increasing literature, KFX can exert gastroprotective influence through the decrease in oxidation stresses and endoplasmic reticulum stress in resisting gastric ulcer triggered by ethanol in rats (Chen et al., 2016; Shen et al., 2017). Considerable clinically related tests proved KFX to help cure GU, under the support from animals experiments (Zou et al., 2019).

On the whole, in accordance with the mentioned research, KFX refers to a therapeutic drug with high prospect to treat GU. However, the active substance composition and protective system pertaining to KFX to improve GU remain not clear. In accordance with existing reports, the anti-GU active parts of PA were screened and the quality of the effective parts was controlled. The anti-GU mechanism of *Periplaneta americana* L. was assessed from the perspective of inhibition of programmed cell death channel.

MATERIALS AND METHODS

Materials

The reference standards uracil, hypoxanthine, inosine and gland pyrimidine were purchased from National Institute for Food and Drug Control (Beijing, China). Sucralfate was purchased from Abcam Co., Ltd. Gastric epithelial cell line (GES-1), Dulbecco's modified Eagle's Medium (DMEM), and fetal bovine serum (FBS) were purchased from Boster Biological Technology Co., Ltd., China) China. Mouse monoclonal anti-beta-actin and rabbit polyclonal anti-TLR4 were obtained from Multisciences BIOTECH, Co., Ltd. (Hangzhou, China). Rabbit polyclonal anti-NALP3/CIAS1 and rabbit polyclonal anti-Caspase1 p20 were obtained from Abcam (Cambridge, UK). Rabbit polyclonal anti-MyD88 was purchased from Boster Biological Technology Co. Ltd. (China). Rabbit polyclonal anti-NF-κB p65 was obtained from Servicebio, Technology Co., Ltd. (Wuhan, China).

Preparation of PAEs With Several Concentrations of Ethanol

Periplaneta americana L. (PA) was primarily identified by microscopic and thin layer chromatography identification, according to Chinese Pharmacopoeia 2020 edition. 1 kg of dry PA was crashed into crude powder and degreased twice with petroleum ether (1:10) for 3 h every time, and dried by a vaccum drying method. Each of 100 g the degreased PA powder was extracted with 1000 ml of 20, 40, 60, and 80% ethanol through reflux extraction for 2 h. All extracts were collected and concentrated with one rotary evaporating device at 40°C. Subsequently, the extracts received the lyophilization after filtration. The yield of PAEs was calculated.

Screening the Effective PAE Fraction on Ulcer Mice Triggered by Ethanol

Male Sprague-Dawley (200–250 g) mice were raised in the specific pathogen free (SPF) animal center at Chengdu

TABLE 1 | Gastric ulcer scoring system based on the severity of ulcer.

Ulcer score	Gastric lesions
0	No lesion
1	Mucosal edema and petechiae
2	One to five small lesions (1–2 mm)
3	More than five small lesions or one intermediate lesion (3–4 mm)
4	Two to more intermediate lesions or one gross lesion (>4 mm)
5	Perforated ulcers

University of TCM with one animal quarter under air conditioning with 12 h lightness/without light, temperature 22 ± 2°C and humidity 50 ± 10% cycle. The mice could freely have food and water. The animal experiments here were carried out based on the International Guideline recommendation in terms of using and caring experiment-related animal, as permitted by the Committee responsible for animal experiment ethics in Chengdu University of TCM.

We launched rat gastric mucosa impairment in accordance with our previous study. When the acclimatization was achieved for a week, the experiment mice were administrated with absolute ethanol 6 ml/kg animal and received the random classification to five groups (n = 6 per group). (1) Model group; (2) 20% ethanol extract (20 mg/kg) group; (3) 40% ethanol extract (20 mg/kg) group; (4) 60% ethanol extract (20 mg/kg) group; and (5) 80% ethanol extract (20 mg/kg) group. The mice were treated orally with PAE once a day for 14 consecutive days except for model cohorts which were administered saline. On the last day of the treatment, the experimental mice were deprived of food but allowed free access to water for 24 h after the final administration. Next, the animals were sacrificed, and the stomach tissues were removed, rinsed gently with cold saline and then photographed. The ulcer index in terms of square millimeters (mm^2) and ulcer inhibition percentage (%) were achieved in accordance with the previous method with a slight change. In this method, the surface of the injured area was ascertained with a ruler, and the degree of the ulcer's degree was determined based on the severity of the ulcer with the use of **Table 1**.

HPLC Investigation

HPLC investigation was performed for PAE, together with reference compounds uracil, hypoxanthine, inosine and gland pyrimidine based on high performance liquid chromatography (HPLC) System (LC-2030C, SHIMADZU, Japan) with an auto-injector sampler programmed at 10 μL, with the use of a C_{18} column (Agilent five HC-C_{18} 250 × 4.6 mm) at a column temperature of 25°C. All operations, acquisitions and data investigation were regulated with the use of the Chemstation software (SHIMADZU, Japan). The mobile phase was composed by A (methanol: water: acetic acid = 30:69.8:0.2, v/v) and B (methanol: water = 1:1, v/v). Samples were eluted in accordance with the following gradient: 0–10 min 100% A isocratic, 10–20 min 100–70% A, 20–21 min 70–50% A, 21–22 min 50–100% A, 22–25 min 100% A isocratic. The flow rate and the optimized detection wavelength reached 0.6 ml/min and 254 nm, respectively.

Cell Culture

We incubated human gastric epithelial cell line (GES-1) in cell culture medium (CCM) covering 89% Dulbecco's modified Eagle's Medium (DMEM), 10% fetal bovine serum (FBS), 1% antibiotic antimycotic solution. Then, the culture was performed at 5% CO_2, 37°C.

Gastroprotective Effects of PAE *In Vitro*

The effects of PAE on the proliferation of GES-1 cells after 24 and 48 h treatment were assessed. To specific, the GES-1 cells were seeded in a 96-well plate with the density of 6×10^3 cells per well to adhere for 24 h, and then treated with PAE at several concentrations (5, 10, 20, 40, and 80 μg/ml) for 24 and 48 h, respectively. CCK-8 assay was performed to assess the proliferation of GES-1 cells with PAE.

To assess the gastro-protective effects of PAE on cell impairment model under the cause of ethanol, the GES-1 cells treated with 100 μM ethanol was employed. Several concentrations of PAE were treated with the mentioned cells. Briefly, 6.0×10^3 cells/well were cultured in 96-well plates for 16 h. And then, the mentioned cells were divided into the control (medium), model (medium + ethanol) and PAE treatment cohorts with several concentrations of PAE (5, 10, 20, 40, and 80 μg/ml). After 24 h culture, the CCK-8 assay tool was employed to assess cell viability.

Gastroprotective Effect on Ulcer Mice Triggered by Ethanol *in vivo*

The ICR mice (6–8 weeks of age) were purchased from SPF (Beijing) Biotechnology Co. Ltd. (Chengdu, China). Mice were housed in collective cages at 25 ± 1°C with free access to laboratory chow and distilled water. The animal experiments were approved by the ethics committee of the Chengdu University of Traditional Chinese Medicine (CDUTCM, permit SYXK (Chuan) 2020-124), and all animal experiments were conducted in strict accordance with the Guidelines for the Care and Use of Laboratory Animals of the Ministry of Science and Technology of China.

After 3 days of adaptive feeding, the mice were randomly divided into six cohorts: normal control cohort (saline), gastric ulcer model cohort (saline + ethanol) and positive control cohort (200 mg/kg of sucralfate), PAE-L cohort (200 mg/kg of PAE), PAE-M cohort (400 mg/kg of PAE), and PAE-H cohort (800 mg/kg of PAE). All drugs were pre-administrated intragastrically once daily for 3 days before induction. On the third day, following a 24 h fast with free access to water, except normal control cohort, all mice were administrated intragastrically with absolute ethanol 6 ml/kg animal. After 2 weeks, the animals were sacrificed, and the stomach tissues were removed, then rinsed gently with cold saline and photographed. To measure the gastric lesions, the lesioned gastric area rate was determined with the use of the program Image J (Zhang et al., 2019b).

Histopathological Investigation

For histopathological investigation, gastric tissues fixed in 4% paraformaldehyde were embedded in paraffin and then cut into

5 mm thick sections. The mentioned tissue sections were stained with hematoxylin and eosin (H&E), periodic acid-schiff (PAS). Under a light microscope (Olympus, Tokyo, Japan), an assessment was blindly conducted on the sections by an experienced and board-certified pathologist in accordance with the criteria (Zhang et al., 2021).

Determination of Inflammatory Cytokines

The gastric tissue segments were homogenized with nine folds of cold PBS, centrifuged for 15 min at 6000 rpm/min, and the supernatant was collected. The amounts of MPO, SOD, IL1-β, IL-6, IL-18, PGE2, and TNF-α in gastric homogenate were achieved with the use of the commercial detection tools.

Western Blotting

Homogenized gastric tissue was lysed with radioimmunoprecipitation assay (RIPA) lysis buffer (Beyotime, Nanjing, China) covering protease and phosphatase inhibitors, and centrifuged at 12,000 rpm for 20 min at 4°C. The overall protein concentration was ascertained with the use of a BCA protein assay tool in the light of the manufacturers' instructions. Commensurable protein was resolved by 10% sodium dodecyl sulfate-polyacrylamide gels and subsequently transferred to polyvinylidene fluoride membrane (Xu et al., 2021). The blots were blocked for 2 h with 5% skim milk in TBST buffer, followed by incubation throughout the night under the temperature of 4°C based on primary antibody: mouse monoclonal anti-beta-actin (1:3,000), rabbit polyclonal anti-NALP3/CIAS1(1:1,000), rabbit polyclonal anti-Caspase1 p20 (1:1,000, rabbit polyclonal anti-TLR4 (1:1,000), rabbit polyclonal anti-MyD88 (1:1,000) and rabbit polyclonal anti-NF-κB p65 (1:1,000). Subsequently, the washing was achieved for immunoblots by employing TBST 3 times, and the probing process was achieved by adopting anti-rabbit horseradish peroxidase-conjugated secondary antibody (1: 15,000 dilution in TBST) under the ambient temperature for 2 h. Next, the detection was achieved for immunoreactive protein with the use of an optimized system for chemiluminescence western blotting detection (GE Health Care; Little Chalfont, Buckinghamshire, UK). The immunoblotting tests were performed 3 times.

Statistical Investigation

All data had the expression of mean ± standard deviation (SD). Statistical investigation was carried out with the use of SPSS 17.0 statistical software with One-way ANOVA or Kruskal-Wallis H-test and all charts were drawn by Graphpad Prism 5.0 (Graphpad Software, San Diego, USA). p-values of <0.05 had statistical significance.

RESULTS

Bioactive Fraction Screening

Acute gastric lesion was triggered through administrating ethanol in intra-gastric. According to **Figure 1**, we found a significantly broadening area of the formation of gastric ulcer within ethanol-stimulated mice. Treatment with PAE with several ethanol extraction processes achieved different therapeutic efficacies. In the gastric ulcer triggered by ethanol model cohort, mucosa tissues were extensively destroyed and necrotic, exhibiting severe hemorrhage, edema and leukocyte infiltration. The 20% EE, 40% EE, and 60% EE could effectively prevent the severe gastric mucosa impairment attributed to ethanol. In particular, mice pretreated with 20% EE before ethanol intoxication exhibited good protective effect against tissue impairment by ethanol, in which mucosa color was normally pink while not being thickened, also hemorrhages and congestion were not identified. The ulcer index score of ethanol treatment cohort rose to 3.59, whereas pretreatment of 20% EE, 40% EE, and 60% EE significantly ($p < 0.05$) decreased the UI scores in comparison with the ethanol treatment cohort. The ulcer index of 20% EE was lowest. Almost none of macroscopic ulcer or hemorrhagic spot could be found. Coupled with the high yield of 20% EE (36.7 ± 6.2%), therefore, we employed the 20% EE fraction for the subsequent experiments.

Chemical Composition of PAE (20% EE)

According to **Figure 2**, an analysis was conducted on four standard substances under the mixture, and a satisfied separation degree and methodology study was acquired. The normal curve and linear scope of the mentioned compounds included: hypoxanthine: y = 312163.70x + 103.22 (r^2 = 0.999992, 0.11–0.44 mg/ml), uracil: y = 1110949x + 371 (r^2 = 0.999991, 0.12 mg/ml~0.49 mg/ml), adenine: y = 909935x + 3705 (r^2 = 0.9998, 0.039–0.12 mg/ml) and inosine: y = 75123x − 24 (r^2 = 0.99995, 0.18–0.75 mg/ml). Accordingly, we found four compounds, i.e., hypoxanthine, uracil, adenine and inosine, in PAE through the contrast with the retention time (t_R) and UV spectrum of the relevant peaks within mixed standard solution. Their contents in PAE were achieved based on the external standard approach as 0.54, 1.21, 0.20, 0.87 mg/g, respectively.

PAE Promoted GES-1 Cells Proliferation

For the assessment of the effect exerted by PAE on the cytotoxicity and proliferating process of normal GES-1 and ethanol-impaired GES-1 cells, we carried out the treatment for cells by using PAE (5–80 μg/ml) under 100 μM ethanol or not. After 24 and 48 h of treatment with PAE in normal GES-1 cells, GES-1 cells' proliferation was promoted in a dose- & time-dependent manner (**Figure 3A**). This data indicated that PAE had no cytotoxicity and could facilitate the proliferation of epithelial cells. Additionally, the treatment with 100 μM ethanol would alter the appearance of GES-1 cells. The GES-1 cells treated by ethanol exhibited the poor cell adherence. Cytoplasm of the mentioned cells was shrunk, indicated the cytotoxicity and early programmed cell death. Some suspended cells could be found in culture medium. In accordance with CCK-8 assay, the cell viability of GES-1 cells treated by 100 μM ethanol was remarkably dropped (**Figure 3B**). However, the concentrations of 5, 10, 20, 40, and 80 μg/ml of PAE boosted GES-1 cell proliferation, in contrast with the reduced cell proliferation of GES-1 injured by ethanol. This implied that PAE was likely to facilitate GES-1 cell proliferation and protect the cell impairment by ethanol.

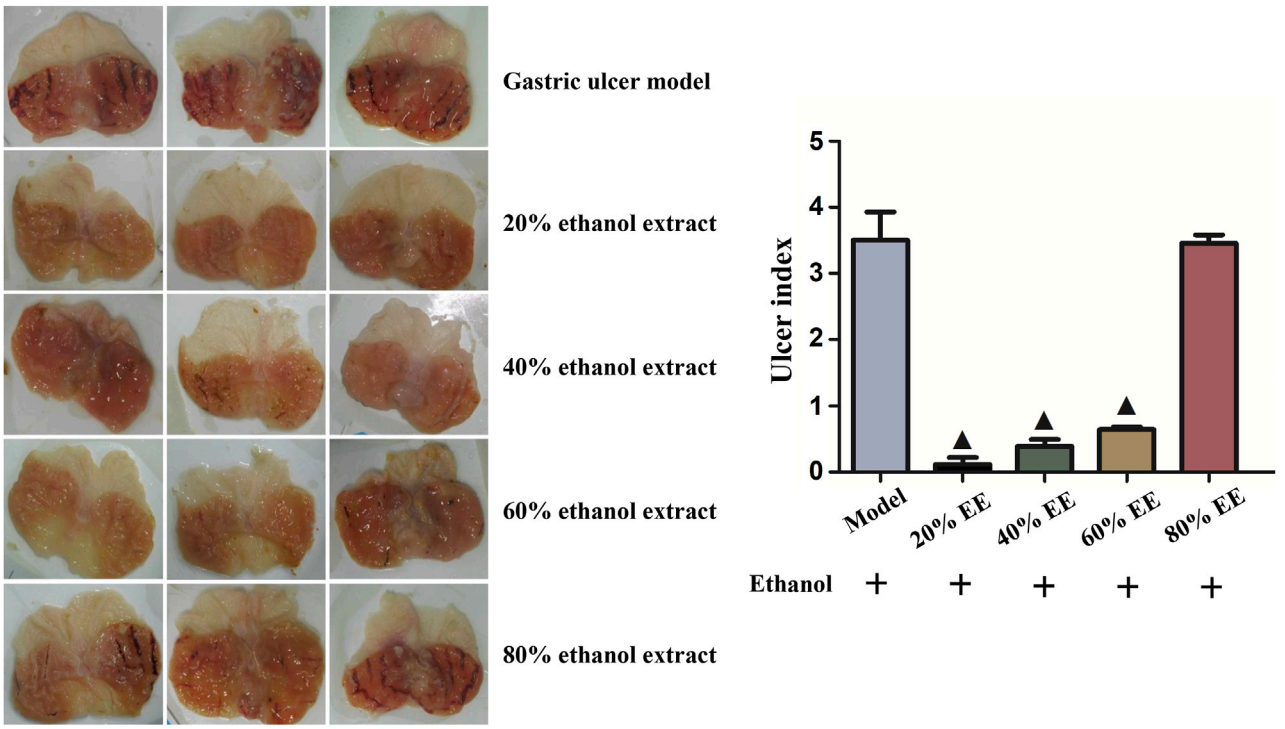


FIGURE 1 | Effects of PAE extracted by a series of concentration of ethanol on the gross appearance of the gastric mucosa and ulcer index in ethanol-induced gastric ulcer in rats. ▲$p < 0.05$, PAE treatment group vs. ethanol-induced group.

Protective Effect of PAE Against Gastric Ulcer Triggered by Ethanol *In Vivo*

Representative of images of the mentioned split stomachs were shown in **Figure 4A**. We reported significant tissue impairment and visible haemorrhagic mucosa lesions within the stomachs of the ethanol treatment mice, while the mice under the saline treatment indicated no lesion within gastric mucosa. As opposed to the mentioned, the administration of either SUC or PAE, particularly at the dosage of 400 mg/kg and 800 mg/kg PAE, would relieve the ulcer effectively. At the assistance of vernier caliper, the gastric ulcer area in stomach tissue was counted. According to **Figure 4B**, the ulcer area reached 27.6 ± 5.8 mm^2 in the ethanol induce model cohort; pretreatment with PAE (200, 400, and 800 mg/kg) and 200 mg/kg of sucralfate efficiently attenuated the mentioned abnormal varieties, which was dependent of concentrations.

Histological changes in the stomach mucosa of the ulcer mice were visualized by PAS and H&E staining (**Figure 4C**). To specific, the change of mucin depletion in the inner membrane of mucosa was scored by PAS staining assay. As shown, the degree of purplish red on the surface of gastric tissue of gastric ulcer model cohort was much reduced in contrast with normal control cohort, indicated that the lower mucin content in ulcer cohort. Nevertheless, the treatment of SUC and PAE could relieve the mucin depletion. In particular, after administration of SUC and high dose of PAE (800 mg/kg), the positive rates of PAS staining were significantly augmented, which exhibited the similar level as normal control cohort. Histological assessment by H&E staining suggested more severe erosion of the gastric mucosa with hemorrhagic lesions extending deeply into the mucosa and submucosa, as well as extensive edema and leukocyte infiltration of the submucosal layer in ulcer cohort. However, the ulcerated mice pretreated with SUC and PAE exhibited less mucosa impairment in comparison with the ulcerated model mice, also complying with the remission of the ulcer area, edema, and leukocyte infiltration (**Figure 4A**).

Levels of MPO and SOD in Gastric Tissue

MPO, as the indicator of neutrophils stimulation, is commonly used to assess the inflammation reaction. According to **Figure 5A**, in comparison with the control cohort, ulcer model cohort under the cause of ethanol significantly increased the levels of MPO ($p < 0.05$). After treatment of SUC and PAE at low, middle, and high dosage, the elevated level of MPO could be significantly dropped ($p < 0.05$), suggesting the alleviative inflammation in the mentioned treatment cohorts. Given oxygen free radicals involved in the occurrence and development of mucosa lesions, SOD is critical to preventing and treating gastric mucosa impairment and ulceration. According to **Figure 5B**, the level of SOD in ulcer mice triggered by ethanol were remarkably attenuated, in contrast with control cohort. Pretreatment with both SUC and PAE significantly increased the gastric SOD level ($p < 0.05$).

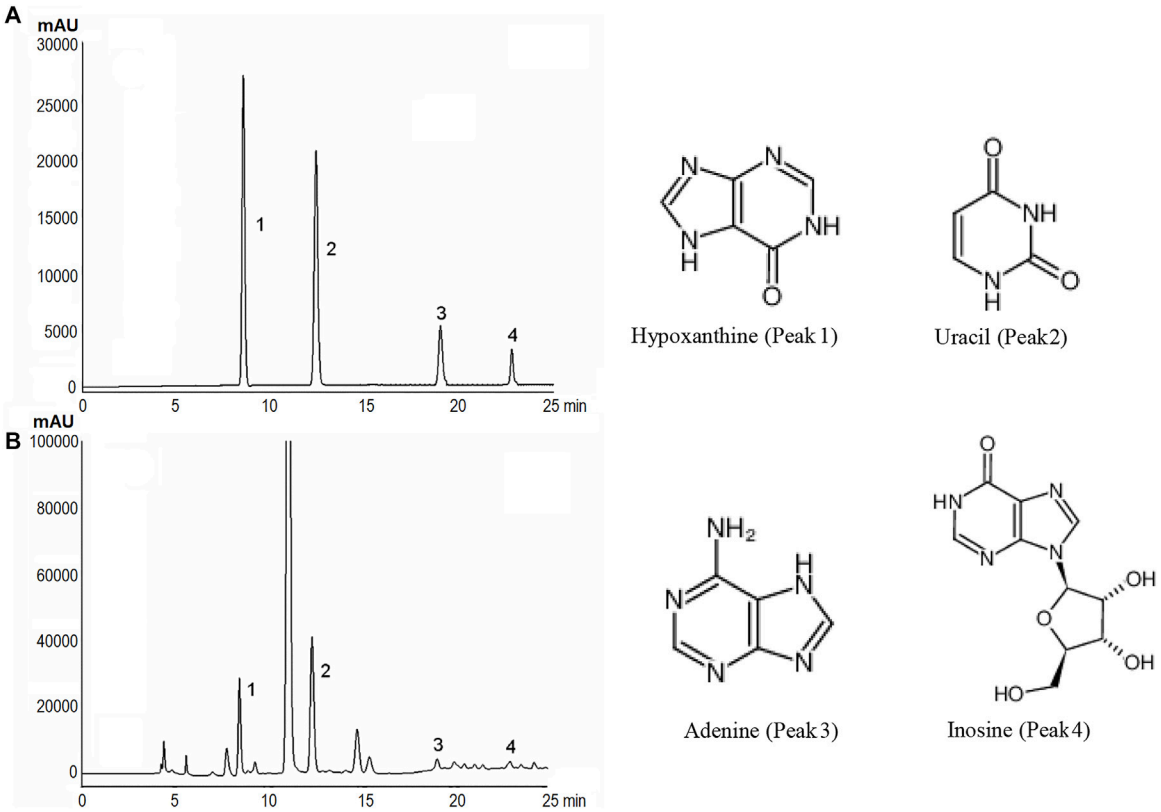


FIGURE 2 | HPLC spectra and chemical structures of these representative markers of PAE obtained with 20% ethanol extraction. **(A, B)** represented the chromatogarm of four representative markers and PAE.

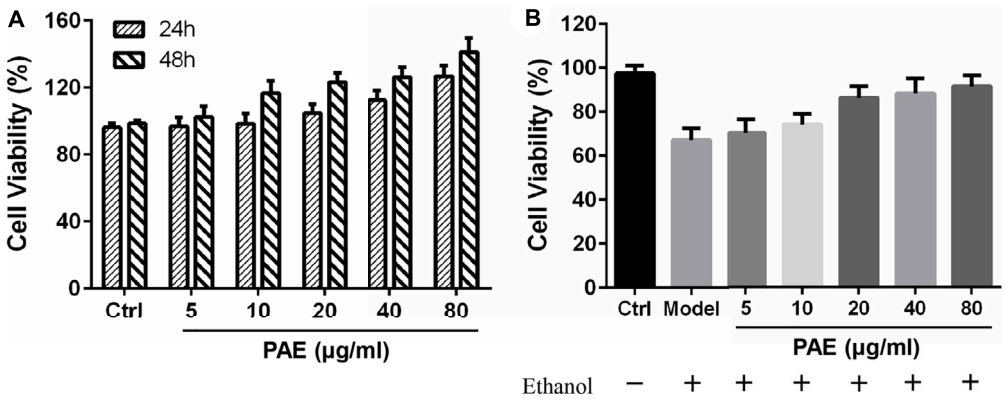


FIGURE 3 | Effects of PAE on the proliferation of GES-1 cells. **(A)** The pretreatment of PAE promoted cell viability with 24 and 48 h treatment **(B)** Cell viability in the presence or absence of 100 μM ethanol for 24 h treatment.

Levels of Inflammatory Cytokines in Gastric Tissue

Inflammatory response is an inevitable mitigated factor in gastric ulcer triggered by ethanol, as commonly evidenced by the increased expression of pro-inflammatory cytokines. According to **Figure 6**, ethanol inducement would significantly increase the gastric pro-inflammatory cytokines (IL-1β, IL-6, TNF-α, IL-18). In contrast with control cohort, the amounts of IL-1β, IL-6, TNF-α, IL-18 in ulcer model cohort increased to 8.52-, 5.24-, 7.86-, and 4.16-folds, respectively. However, SUC and PAE could noticeably reverse this overproduction ($p < 0.05$). The down-regulation efficacy of PAE on pro-inflammatory cytokines exhibited a dose-dependent manner. The administration of high dose of PAE shown the strongest anti-inflammatory effects.

In addition, prostaglandin E2 (PGE2) was proven as a crucial mediator for sustaining the integrity of gastric mucosa defense and for gastric ulcer healing. PGE2 would control gastric acid

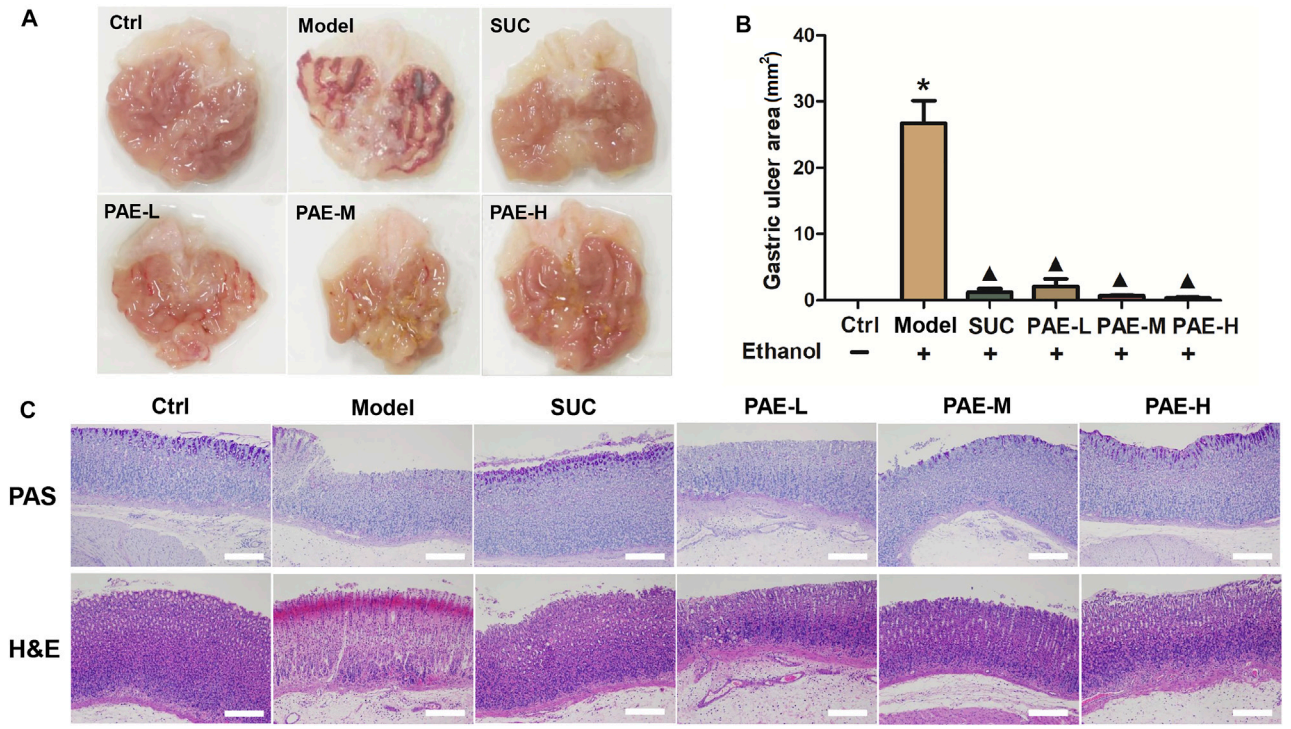


FIGURE 4 | (A) Macroscopic view of the gastric tissue in gastric ulcer triggered by ethanol mice after administration of PAE. **(B)** Gastric ulcer area in each cohort. *$p < 0.05$, Ctrl group vs. Gastric ulcer model group; ▲$p < 0.05$, PAE/SUC treatment group vs. Gastric ulcer model group; **(C)** Representative photomicrographs of sections from gastric wall samples by PAS and H&E staining.

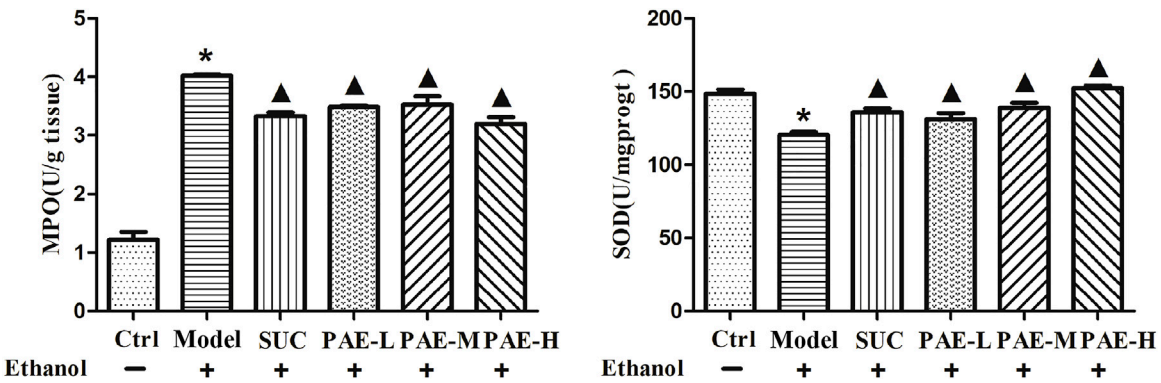


FIGURE 5 | Effect of PAE on the levels of MPO and SOD in ethanol-stimulated gastric tissues. *$p < 0.05$, Ctrl group vs. Gastric ulcer model group; ▲$p < 0.05$, PAE/SUC treatment group vs. Gastric ulcer model group.

secretion, stabilize mast cell membrane and stimulate tissue repair process, thereby critically impacting ulcer healing. The previous study revealed that the decreased level of PGE2 at the gastric mucosa would be involved in gastric ulceration and aggravate precancerosis. Thus, ethanol inducement could dramatically reduce PGE2, in contrast with normal control cohort, while either SUC or PAE significantly modulated the PGE2 level in the gastric homogenate in comparison with ulcer model cohort under the cause of ethanol ($p < 0.05$). The mentioned results suggested that PAE could prominently suppress the inflammatory response in stomach.

Effects on Programmed Cell Death-Related Signal Channel

The inflammasome, part of innate immunity and inflammation response, is critical to gastric impairment's pathogenesis and progression under the cause of ethanol. It was acknowledged that to suppress the activity of nucleotide-binding domain-like receptor family pyrin domain-covering 3 (NLRP3) is an effective mechanism in resisting gastric mucosa impairment under the cause of ethanol. Herein, the NLRP3/caspase-1 cascade was examined mitigated by detecting the

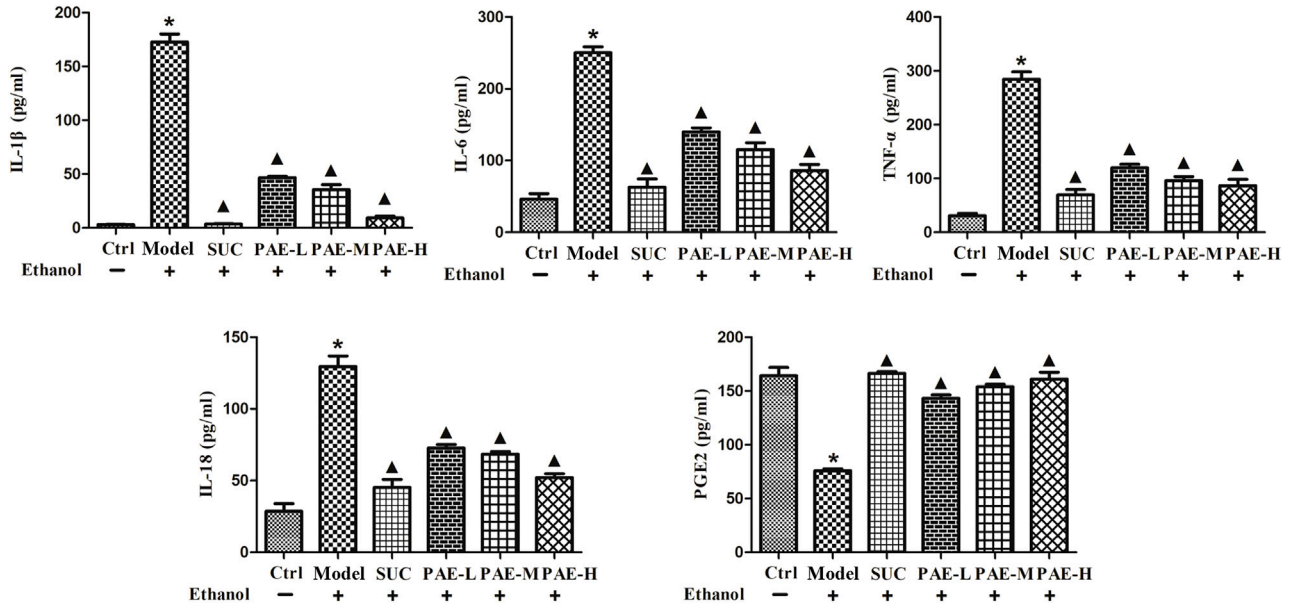


FIGURE 6 | Effect of PAE on the levels of inflammatory cytokines, i.e., IL-1β, IL-6, TNF-α, IL-18, and PGE2, in ethanol-stimulated gastric tissues. *$p < 0.05$, Ctrl group vs. Gastric ulcer model group; ▲$p < 0.05$, PAE/SUC treatment group vs. Gastric ulcer model group.

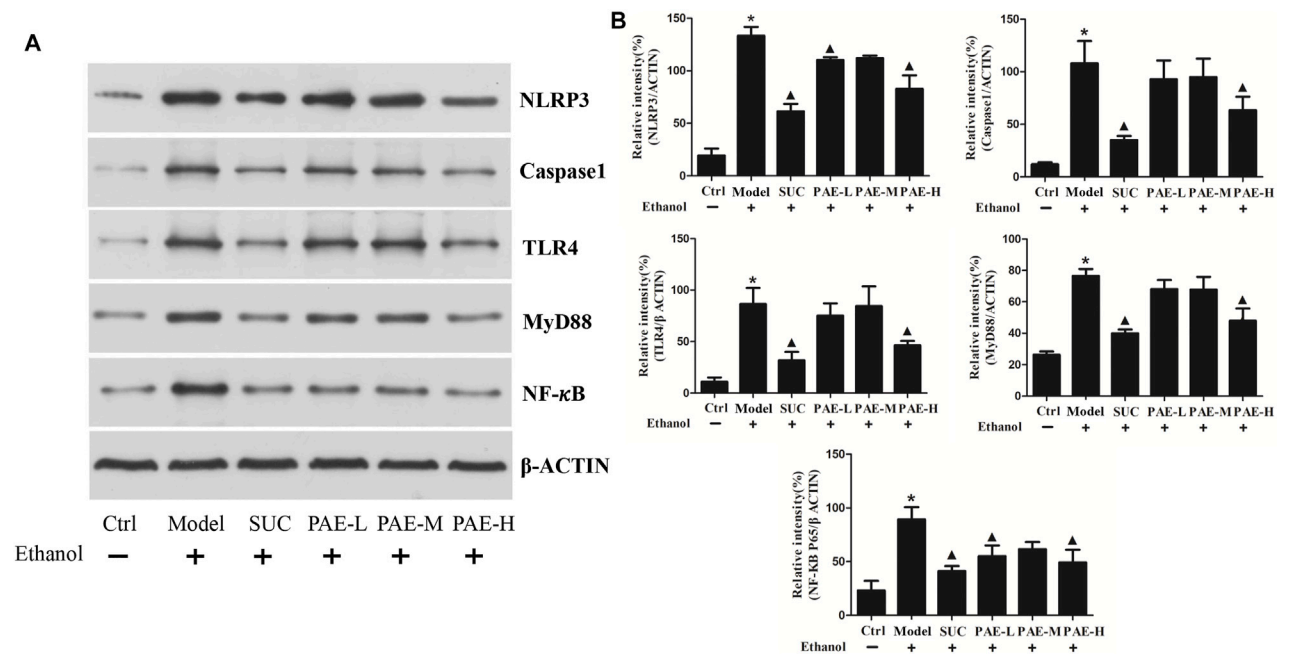


FIGURE 7 | Influence of PAE on the expressions of programmed cell death-related proteins in ethanol-stimulated gastric tissues by western blotting. *$p < 0.05$, Ctrl group vs. Gastric ulcer model group; ▲$p < 0.05$, PAE/SUC treatment group vs. Gastric ulcer model group.

protein expression of NLRP3 and caspase-1 by western blotting assay. According to **Figure 7**, ethanol administration triggered the stimulation of the NLRP3/caspase-1 channel as demonstrated by 4.6-fold increase of NLRP3, and 4.12-fold increase of caspase-1, respectively, versus the control cohort. The stimulation of the NLRP3/caspase-1 channel was lowered by PAE administration, according to down-regulated protein expressions of NLRP3 and Caspase-1 levels by 38.6 and 41.2%, respectively in high dose of PAE cohort.

Moreover, the effects on the expressions of TLR4, MyD88, NF-κB P65 were achieved by western blotting assay. As illustrated, ethanol significantly up-regulated the expressions of the mentioned programmed cell death-related proteins, i.e., TLR4, MyD88, NF-κB P65. Nevertheless, pretreatment with PAE (800 mg/kg) and SUC effectively down-regulated the mentioned protein expressions. The mentioned findings denote that inhibition of the NLRP3/caspase-1 and NF-κB channels, at least partially, facilitates he ameliorative effects of PAE against gastric ulcer triggered by ethanol.

DISCUSSION

Researchers have widely used gastric ulcer model triggered by ethanol to study various promising agents for antiulcer treatment (Liu et al., 2012). One reason is that high alcohol consumption was considered as one of the most prevalent causes of GU in humans. It was proven that ethanol at high concentrations is capable of directly eroding gastric mucosa in 30–60 min, leading to gastric mucosa lesion and upper gastrointestinal bleeding (UGIB) (Liang et al., 2018). Moreover, ethanol induced GU model has the advantage over other GU models, such as pylorus ligation and stress (Ren et al., 2021). Through excessive oral administration of absolute ethanol in animal models, mucous membrane can be solubilized and then exposed to the proteolytic and hydrolytic actions of hydrochloric acid and pepsin, thereby causing gastric lesions. The mentioned lesions exhibit infiltration of inflammatory cell, desquamation of epithelial cell, hemorrhage and extensive submucosal edema, thereby resembling considerable characteristics exhibited by acute human peptic ulcer disease (Mousa et al., 2019). However, the underlying mechanisms of gastric ulcer triggered by ethanol are complex and still controversial. Many research cohorts have reported that the pathology of gastric ulcer triggered by ethanol generally involves three dimensions: oxidative stress, programmed cell death and inflammatory response (Liang et al., 2018; Badr et al., 2019; Zhou et al., 2020).

Notably, increasing evidence has shown that programmed cell death plays a key role in the gastrointestinal mucosa epithelial impairment. Gastroprotective effect of chlorogenic acid (Ahmed et al., 2021), gallic acid, patchoulene epoxide (Liang et al., 2018), and silymarin (Arafa Keshk et al., 2017) against GU in mice involves the modulation of programmed cell death signaling channel. Besides, programmed cell death cascade is closely correlated to oxidative stress and inflammatory response. To specific, overexposure to ROS and TNF-α can trigger caspase-dependent programmed cell death (Abdelwahab, 2013). Therefore, products having a strong apoptosis-resisting activity, with additional anti-inflammatory, and/or antioxidative properties, may represent potential candidates for GU therapy. Recent studies have demonstrated the inextricable link between NLRP3 inflammasome stimulation and cell death, covering ferroptosis, necroptosis, programmed cell death, as well as pyroptosis (Zheng and Kanneganti, 2020). Considerable cell death effectors (e.g., caspase-8, c-FLIP, GPX4 and MLKL) were confirmed to regulate inflammasome NLRP3 directly or indirectly stimulation and IL-1β release in response to a wide range of impairment-associated molecular patterns (DAMPs) and pathogen-associated molecular pattern molecules (PAMPs) (He et al., 2016).

We reported the cytoprotective, antiulcer, anti-inflammatory, antioxidant and apoptosis-resisting action of PAE in resisting GU under the cause of ethanol within SD mice initially. Besides, PAE is capable of noticeably rising programmed cell death-related protein (P65, NF-KB, MyD88, and TLR4) within gastric tissue under the cause of ethanol. Besides, when cells undergo oxidative stress under the cause of ethanol, they can induce and activate the release of the inflammation-associated factor NLRP3 inflammasome, activate Caspase-1 and eventually mature the effector pro-inflammatory cytokines (Hou et al., 2021). Our study has showed that PAE administration is capable of lowering the stimulation of the NLRP3/caspase-1 channel triggered by ethanol administration, while impacting inflammation and oxidative stress by regulating pro-inflammatory cytokines (IL-18, TNF-α, IL-6, IL-1β) and oxidative stress factors (MPO and SOD). Our result is also consistent with previous study. On the whole, we show vital evidences in relation to the noticeable anti-ulcer efficacy of PAE in resisting GU under the cause of ethanol on the basis of significant apoptosis-resisting activity.

CONCLUSION

20% ethanol extract of *Periplaneta americana* L. exhibits significant gastroprotective effects against ethanol impairment *in vitro* and *in vivo*, indicating that this extract possessed a good potential as the anti-gastric ulcer agent. Pretreatment of *Periplaneta americana* L. extract could play a remarkable protective role on gastric tissue programmed cell death induced by ethanol, mitigated by MyD88/NF-κB signaling channels.

DATA AVAILABILITY STATEMENT

The raw data supporting the conclusion of this article will be made available by the authors, without undue reservation.

ETHICS STATEMENT

The animal study was reviewed and approved by Committee responsible for animal experiment ethics in Chengdu University of TCM.

AUTHOR CONTRIBUTIONS

SF and CZ: implemented the experiments. JC, JS, and XN: analyzed the data and wrote the manuscript. YH and CF: provided technical support. XL and JZ: conceived and designed the experiments. All authors contributed to the article and approved the submitted version.

FUNDING

The authors gratefully acknowledge the financial supports of Young Elite Scientists Sponsorship Program by CAST (2018QNRC1-01).

REFERENCES

Abdelwahab, S. I. (2013). Protective Mechanism of Gallic Acid and its Novel Derivative against Ethanol-Induced Gastric Ulcerogenesis: Involvement of Immunomodulation Markers, Hsp70 and Bcl-2-Associated X Protein. *Int. Immunopharmacol* 16, 296–305. doi:10.1016/j.intimp.2013.04.005

Adhikary, B., Yadav, S. K., Roy, K., Bandyopadhyay, S. K., and Chattopadhyay, S. (2011). Black tea and Theaflavins Assist Healing of Indomethacin-Induced Gastric Ulceration in Mice by Antioxidative Action. *Evid. Based Complement. Alternat Med.* 2011, 546560. doi:10.1155/2011/546560

Ahmed, M. A. E., Mohanad, M., Ahmed, A. A. E., Aboulhoda, B. E., and El-Awdan, S. A. (2021). Mechanistic Insights into the Protective Effects of Chlorogenic Acid against Indomethacin-Induced Gastric Ulcer in Rats: Modulation of the Cross Talk between Autophagy and Apoptosis Signaling. *Life Sci.* 275, 119370. doi:10.1016/j.lfs.2021.119370

Arafa Keshk, W., Zahran, S. M., Katary, M. A., and Abd-Elaziz Ali, D. (2017). Modulatory Effect of Silymarin on Nuclear Factor-Erythroid-2-Related Factor 2 Regulated Redox Status, Nuclear Factor-Kb Mediated Inflammation and Apoptosis in Experimental Gastric Ulcer. *Chem. Biol. Interact* 273, 266–272. doi:10.1016/j.cbi.2017.06.022

Badr, A. M., El-Orabi, N. F., and Ali, R. A. (2019). The Implication of the Crosstalk of Nrf2 with NOXs, and HMGB1 in Ethanol-Induced Gastric Ulcer: Potential Protective Effect Is Afforded by Raspberry Ketone. *PloS one* 14, e0220548. doi:10.1371/journal.pone.0220548

Bi, W. P., Man, H. B., and Man, M. Q. (2014). Efficacy and Safety of Herbal Medicines in Treating Gastric Ulcer: A Review. *World J. Gastroenterol.* 20, 17020–17028. doi:10.3748/wjg.v20.i45.17020

Boligon, A. A., de Freitas, R. B., de Brum, T. F., Waczuk, E. P., Klimaczewski, C. V., de Ávila, D. S., et al. (2014). Antiulcerogenic Activity of Scutia Buxifolia on Gastric Ulcers Induced by Ethanol in Rats. *Acta Pharm. Sin B* 4, 358–367. doi:10.1016/j.apsb.2014.05.001

Chakravarty, K., and Gaur, S. (2019). Role of Probiotics in Prophylaxis of *Helicobacter P* Infection. *Curr. Pharm. Biotechnol.* 20, 137–145. doi:10.2174/1389201020666190227203107

Chen, H., Liao, H., Liu, Y., Zheng, Y., Wu, X., Su, Z., et al. (2015). Protective Effects of Pogostone from Pogostemonis Herba against Ethanol-Induced Gastric Ulcer in Rats. *Fitoterapia* 100, 110–117. doi:10.1016/j.fitote.2014.11.017

Chen, P., Shen, Y., Shi, H., Ma, X., Lin, B., Xiao, T., et al. (2016). Gastroprotective Effects of Kangfuxin-Against Ethanol-Induced Gastric Ulcer via Attenuating Oxidative Stress and ER Stress in Mice. *Chem. Biol. Interact* S9, 30509. doi:10.1016/j.cbi.2016.10.021

Chen, X., Liu, R., Liu, X., Xu, C., and Wang, X. (2018). L-Ascorbic Acid-2-Glucoside Inhibits Helicobacter Pylori-Induced Apoptosis through Mitochondrial Pathway in Gastric Epithelial Cells. *Biomed. Pharmacother.* 97, 75–81. doi:10.1016/j.biopha.2017.10.030

Gebril, S. M., Ito, Y., Shibata, M. A., Maemura, K., Abu-Dief, E. E., Hussein, M. R. A., et al. (2020). Indomethacin Can Induce Cell Death in Rat Gastric Parietal Cells through Alteration of Some Apoptosis- and Autophagy-Associated Molecules. *Int. J. Exp. Pathol.* 101, 230–247. doi:10.1111/iep.12370

He, Y., Hara, H., and Núñez, G. (2016). Mechanism and Regulation of NLRP3 Inflammasome Activation. *Trends Biochem. Sci.* 41, 1012–1021. doi:10.1016/j.tibs.2016.09.002

Hou, J., Lei, Z., Cui, L., Hou, Y., Yang, L., An, R., et al. (2021). Polystyrene Microplastics lead to Pyroptosis and Apoptosis of Ovarian Granulosa Cells via NLRP3/Caspase-1 Signaling Pathway in Rats. *Ecotoxicol Environ. Saf.* 212, 112012. doi:10.1016/j.ecoenv.2021.112012

Kulikova, O. I., Stvolinsky, S. L., Migulin, V. A., Andreeva, L. A., Nagaev, I. Y., Lopacheva, O. M., et al. (2020). A New Derivative of Acetylsalicylic Acid and Carnosine: Synthesis, Physical and Chemical Properties, Biological Activity. *Daru* 28, 119–130. Tehran University of Medical Sciences. doi:10.1007/s40199-019-00323-x

Liang, J., Dou, Y., Wu, X., Li, H., Wu, J., Huang, Q., et al. (2018). Prophylactic Efficacy of Patchoulene Epoxide against Ethanol-Induced Gastric Ulcer in Rats: Influence on Oxidative Stress, Inflammation and Apoptosis. *Chem. Biol. Interact* 283, 30–37. doi:10.1016/j.cbi.2018.01.014

Liu, H. F., Liu, W. W., Wang, G. A., and Teng, X. C. (2005). Effect of *Helicobacter P* Infection on Bax Protein Expression in Patients with Gastric Precancerous Lesions. *World J. Gastroenterol.* 11, 5899–5901. doi:10.3748/wjg.v11.i37.5899

Liu, Y., Tian, X., Gou, L., Fu, X., Li, S., Lan, N., et al. (2012). Protective Effect of L-Citrulline against Ethanol-Induced Gastric Ulcer in Rats. *Environ. Toxicol. Pharmacol.* 34, 280–287. doi:10.1016/j.etap.2012.04.009

Lu, S., Wu, D., Sun, G., Geng, F., Shen, Y., Tan, J., et al. (2019). Gastroprotective Effects of Kangfuxin against Water-Immersion and Restraint Stress-Induced Gastric Ulcer in Rats: Roles of Antioxidation, Anti-Inflammation, and Pro-survival. *Pharm. Biol.* 57, 770–777. doi:10.1080/13880209.2019.1682620

Ma, X., Hu, Y., Li, X., Zheng, X., Wang, Y., Zhang, J., et al. (2018). *Periplaneta A* Ameliorates Dextran Sulfate Sodium-Induced Ulcerative Colitis in Rats by Keap1/Nrf-2 Activation, Intestinal Barrier Function, and Gut Microbiota Regulation. *Front. Pharmacol.* 9, 944. doi:10.3389/fphar.2018.00944

Mousa, A. M., El-Sammad, N. M., Hassan, S. K., Madboli, A. E. N. A., Hashim, A. N., Moustafa, E. S., et al. (2019). Antiulcerogenic Effect of Cuphea Ignea Extract against Ethanol-Induced Gastric Ulcer in Rats. *BMC Complement. Altern. Med.* 19, 345. doi:10.1186/s12906-019-2760-9

Ren, S., Wei, Y., Wang, R., Wei, S., Wen, J., Yang, T., et al. (2020). Rutaecarpine Ameliorates Ethanol-Induced Gastric Mucosal Injury in Mice by Modulating Genes Related to Inflammation, Oxidative Stress and Apoptosis. *Front. Pharmacol.* 11, 600295. doi:10.3389/fphar.2020.600295

Ren, S., Wei, Y., Niu, M., Li, R., Wang, R., Wei, S., et al. (2021). Mechanism of Rutaecarpine on Ethanol-Induced Acute Gastric Ulcer Using Integrated Metabolomics and Network Pharmacology. *Biomed. Pharmacother.* 138, 111490. doi:10.1016/j.biopha.2021.111490

Shen, Y., Sun, J., Niu, C., Yu, D., Chen, Z., Cong, W., et al. (2017). Mechanistic Evaluation of Gastroprotective Effects of Kangfuxin on Ethanol-Induced Gastric Ulcer in Mice. *Chem. Biol. Interact* 273, 115–124. doi:10.1016/j.cbi.2017.06.007

Song, Q., Xie, Y., Gou, Q., Guo, X., Yao, Q., and Gou, X. (2017). JAK/STAT3 and Smad3 Activities Are Required for the Wound Healing Properties of *Periplaneta A* Extracts. *Int. J. Mol. Med.* 40, 465–473. doi:10.3892/ijmm.2017.3040

Xie, L., Guo, Y. L., Chen, Y. R., Zhang, L. Y., Wang, Z. C., Zhang, T., et al. (2020). A Potential Drug Combination of Omeprazole and Patchouli Alcohol Significantly Normalizes Oxidative Stress and Inflammatory Responses against Gastric Ulcer in Ethanol-Induced Rat Model. *Int. Immunopharmacol* 85, 106660. doi:10.1016/j.intimp.2020.106660

Xu, H., Luo, R., Dong, L., Pu, X., Chen, Q., Ye, N., et al. (2021). pH/ROS Dual-Sensitive and Chondroitin Sulfate Wrapped Poly (β-Amino Ester)-SA-PAPE Copolymer Nanoparticles for Macrophage-Targeted Oral Therapy for Ulcerative Colitis. *Nanomedicine : nanotechnology, Biol. Med.* 39, 102461. doi:10.1016/j.nano.2021.102461

Zhang, C., Chen, Z., He, Y., Xian, J., Luo, R., Zheng, C., et al. (2021). Oral Colon-Targeting Core-Shell Microparticles Loading Curcumin for Enhanced Ulcerative Colitis Alleviating Efficacy. *Chin. Med.* 16, 92. doi:10.1186/s13020-021-00449-8

Zhang, C., Gao, F., Gan, S., He, Y., Chen, Z., Liu, X., et al. (2019). Chemical Characterization and Gastroprotective Effect of an Isolated Polysaccharide Fraction from Bletilla Striata against Ethanol-Induced Acute Gastric Ulcer. *Food Chem. Toxicol.* 131, 110539. doi:10.1016/j.fct.2019.05.047

Zhang, H., Fang, D. C., Lan, C. H., and Luo, Y. H. (2007). *Helicobacter P* Infection Induces Apoptosis in Gastric Cancer Cells through the Mitochondrial Pathway. *J. Gastroenterol. Hepatol.* 22, 1051–1056. doi:10.1111/j.1440-1746.2007.04959.x

Zhang, K., Liu, Y., Wang, C., Li, J., Xiong, L., Wang, Z., et al. (2019). Evaluation of the Gastroprotective Effects of 20 (S)-Ginsenoside Rg3 on Gastric Ulcer Models in Mice. *J. Ginseng Res.* 43, 550–561. doi:10.1016/j.jgr.2018.04.001

Zheng, M., and Kanneganti, T. D. (2020). The Regulation of the ZBP1-NLRP3 Inflammasome and its Implications in Pyroptosis, Apoptosis, and Necroptosis (PANoptosis). *Immunol. Rev.* 297, 26–38. doi:10.1111/imr.12909

Zhou, D., Yang, Q., Tian, T., Chang, Y., Li, Y., Duan, L. R., et al. (2020). Gastroprotective Effect of Gallic Acid against Ethanol-Induced Gastric Ulcer in Rats: Involvement of the Nrf2/HO-1 Signaling and Anti-Apoptosis Role. *Biomed. Pharmacother.* 126, 110075. doi:10.1016/j.biopha.2020.110075

Zou, J. B., Zhang, X. F., Shi, Y. J., Tai, J., Wang, Y., Liang, Y. L., et al. (2019). Therapeutic Efficacy of Kangfuxin Liquid Combined with PPIs in Gastric Ulcer. *Evid. Based Complement. Alternat Med.* 2019, 1324969. doi:10.1155/2019/1324969

Conflict of Interest: The authors declare that the research was conducted in the absence of any commercial or financial relationships that could be construed as a potential conflict of interest.

The reviewer SW declared a past collaboration with one of the authors CF to the handling editor.

Publisher's Note: All claims expressed in this article are solely those of the authors and do not necessarily represent those of their affiliated organizations, or those of the publisher, the editors and the reviewers. Any product that may be evaluated in this article, or claim that may be made by its manufacturer, is not guaranteed or endorsed by the publisher.

Copyright © 2021 Fu, Chen, Zhang, Shi, Nie, Hu, Fu, Li and Zhang. This is an open-access article distributed under the terms of the Creative Commons Attribution License (CC BY). The use, distribution or reproduction in other forums is permitted, provided the original author(s) and the copyright owner(s) are credited and that the original publication in this journal is cited, in accordance with accepted academic practice. No use, distribution or reproduction is permitted which does not comply with these terms.

frontiers in Pharmacology

ORIGINAL RESEARCH
published: 16 December 2021
doi: 10.3389/fphar.2021.804030

Network Pharmacology-Based Investigation and Experimental Exploration of the Antiapoptotic Mechanism of Colchicine on Myocardial Ischemia Reperfusion Injury

Yuanjun Tang[1†], Chenyang Shi[1†], Yingyi Qin[2†], Shuowen Wang[1], Hui Pan[1], Ming Chen[1], Xuemei Yu[1], Yuefen Lou[3] and Guorong Fan[1]**

[1]Department of Clinical Pharmacy, Shanghai General Hospital, Shanghai Jiaotong University School of Medicine, Shanghai, China, [2]Department of Health Statistics, Naval Medical University, Shanghai, China, [3]Department of Pharmacy, Shanghai Fourth People's Hospital Affiliated to Tongji University School of Medicine, Shanghai, China

OPEN ACCESS

Edited by:
Hong Zhang,
Shanghai University of Traditional Chinese Medicine, China

Reviewed by:
Zhang Yuefan,
Shanghai University, China
Jianguo Xing,
Xinjiang Institute of Materia Medica, China

***Correspondence:**
Yuefen Lou
louyuefen@sina.cn
Guorong Fan
guorfan@163.com

†These authors have contributed equally to this work and share first authorship

Specialty section:
This article was submitted to Ethnopharmacology, a section of the journal Frontiers in Pharmacology

Received: 28 October 2021
Accepted: 29 November 2021
Published: 16 December 2021

Citation:
Tang Y, Shi C, Qin Y, Wang S, Pan H, Chen M, Yu X, Lou Y and Fan G (2021) Network Pharmacology-Based Investigation and Experimental Exploration of the Antiapoptotic Mechanism of Colchicine on Myocardial Ischemia Reperfusion Injury. Front. Pharmacol. 12:804030. doi: 10.3389/fphar.2021.804030

Background: The beneficial effects of colchicine on cardiovascular disease have been widely reported in recent studies. Previous research demonstrated that colchicine has a certain protective effect on ischemic myocardium and has the potential to treat myocardial ischemia reperfusion injury (MIRI). However, the potential targets and pharmacological mechanism of colchicine to treat MIRI has not been reported.

Methods: In this study, we used network pharmacology and experimental verification to investigate the pharmacological mechanisms of colchicine for the treatment of MIRI. Potential targets of colchicine and MIRI related genes were screened from public databases. The mechanism of colchicine in the treatment of MIRI was determined by protein-protein interaction (PPI), gene ontology (GO) and Kyoto Encyclopedia of Genes and Genomes (KEGG) pathway enrichment analysis. Additionally, we evaluated the effect of colchicine on H9C2 cell activity using CCK-8 assays, observed the effect of colchicine on H9C2 cell apoptosis via flow cytometry, and further verified the expression of key targets after colchicine treated by Western blot.

Results: A total of 626 target genes for colchicine and 1549 MIRI disease targets were obtained. 138 overlapping genes were determined as potential targets of colchicine in treating MIRI. the PPI network analysis demonstrated that the targets linked to MIRI were ALB, TNF, ACTB, AKT1, IL6, TP53, IL1B, CASP3 and these targets showed nice affinity with colchicine in molecular docking experiments. The results of GO analysis and KEGG pathway enrichment demonstrated that the anti-MIRI effect of colchicine involves in apoptotic signaling pathway. Further tests suggested that colchicine can protect H9C2 cell from Hypoxia/Reoxygenation (H/R) injury through anti-apoptotic effects. Western blot results demonstrated that colchicine can inhibited MIRI induced apoptosis of H9C2 cell by enhancing the decreased levels of Caspase-3 in myocardial injure model induced by H/R and activating the PI3K/AKT/eNOS pathway.

Conclusions: we performed network pharmacology and experimental evaluation to reveal the pharmacological mechanism of colchicine against MIRI. The results from this study could provide a theoretical basis for the development and clinical application of colchicine.

Keywords: colchicine, myocardial ischemia reperfusion injury, network pharmacology, experimental verification, apoptosis

INTRODUCTION

Acute Myocardial Infarction is the necrosis of myocardial tissue caused by acute or persistent ischemia and hypoxia of coronary arteries, which seriously threatens the lives of patients (Castro-Dominguez et al., 2018; Gulati et al., 2020). The most effective treatment for reducing the area of myocardial infarction is reperfusion timely (Bajaj et al., 2015; Toldo and Abbate, 2018). However, after restoring blood supply to the damaged myocardial tissue, many patients suffered more severe damage to the heart structure, more disordered energy metabolism of myocardial cells and even some irreversible damage such as re-enlargement of myocardial infarction area, life-threatening arrhythmia and so forth, therefore, we called it myocardial ischemia reperfusion injury (MIRI) (Buja, 2005; Marchant et al., 2012). Studies have revealed that the physiological mechanisms of MIRI are apoptosis, calcium overload, oxidative stress, autophagy, inflammation, endoplasmic reticulum stress, mitochondrial disorders, etc (Walters et al., 2012; Munzel et al., 2017). Previous research found that cardiomyocyte apoptosis is the core factor of MIRI, and about 50% of MIRI is related with cardiomyocyte apoptosis (Buja, 2005). Myocardial ischemia triggers the process of cardiomyocyte apoptosis, and reperfusion further aggravates the degree of this process, which would result in malignant arrhythmia, heart failure and even sudden cardiac death (Nagai et al., 2010; Fujiwara et al., 2019). Myocardial ischemia and hypoxia can induce the expression of a variety of apoptosis-related factors and inflammatory factors, which could promote abnormal apoptosis of myocardial cells (Yao et al., 2020). As an important factor affecting the progression of disease, the imbalance of myocardial cell apoptosis is also an important regulatory pathway for drugs to play a therapeutic role. Unfortunately, at present, there are few effective medicines for the treatment of MIRI in clinical practice.

Colchicine, which is a zhuophenone alkaloid extracted from the bulb of *Colchicum autumnale*, has extensive anti-inflammatory, immunosuppressive and strong anti-fibrosis effects, it is the first-line drug for the treatment of acute gout attack (Downing, 2000; Terkeltaub, 2009; Roubille et al., 2013). A retrospective study suggested that the use of colchicine in gout patients can reduce the incidence of acute myocardial infarction (Crittenden et al., 2012). Studies have reported that STEMI patients with chest pain less than 12 h were randomly treated with colchicine or placebo for 5 days after percutaneous coronary intervention (PCI), the CK-MB level in the colchicine group was declined and the area of infarction decreased significantly (Deftereos et al., 2015). The COLCOT study have demonstrated that colchicine can reduce the risk of recurring myocardial ischemic in patients after acute myocardial infarction and it has good safety in low dose (Tardif et al., 2019). What's more, the earlier you start using colchicine after acute myocardial infarction, the greater the benefit (Bouabdallaoui et al., 2020). Above all, colchicine has a certain protective effect on ischemic myocardium and has the potential to treat MIRI, but its mechanism is still unclear.

Network pharmacology is developed based on the theories of systems biology, network biology, multidirectional pharmacology and omics. It reveals the interaction mechanism between the body and disease from the aspects of protein, molecule and gene, and provides a basis for the development and mechanism research of multi-target drugs (Hopkins, 2007; Huang et al., 2014; Zhang et al., 2017). This study screened the potential targets and functional characteristics of colchicine in the treatment of MIRI through network pharmacology. The colchicine multi-target network was constructed, and the key targets were enriched. In addition, the key targets were identified by experimental verification to further confirm the effect of colchicine on related signal pathways. The process of network pharmacology analysis is shown in **Figure 1**. The main purpose of this study is to explore the therapeutic targets and key signal pathways of colchicine in treatment of MIRI, and provide potential strategies for disease treatment.

MATERIAL AND METHODS

Prediction of Potential Targets of Colchicine

The 2D molecular structure and PubChem CID of Colchicine were obtained from PubChem (https://pubchem.ncbi.nlm.nih.gov/, update time:2021-02-04), which is the world's largest database of free access to chemical information. Swiss Target Prediction (http://www.swisstargetprediction.ch, update time: 2019) (Daina et al., 2019), Comparative Toxicogenomics database (CTD, http://ctdbase.org/about/, update time: 2021-09-02) (Davis et al., 2019), BATMAN-TCM database (http://bionet.ncpsb.org.cn/batman-tcm/, update time: 2020-07-29) (Liu et al., 2016) and PharmMapper (http://lilab-ecust.cn/pharmmapper/, update time: 2017) (Wang et al., 2017) were used to obtain the targets name, gene name, UniProt ID and FIT score of colchicine. Then the names of target genes were converted into the official symbols using UniProt database (http://www.uniprot.org/, update time: 2021-04) (UniProt, 2019) and types was selected to "Homo sapiens".

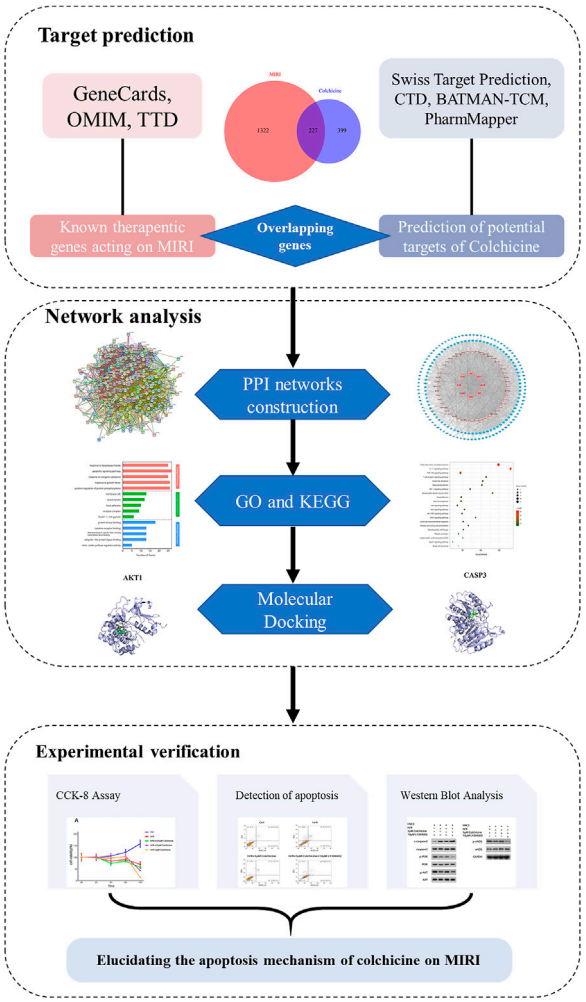


FIGURE 1 | The workflow of action mechanism of Colchicine on treating MIRI in this study.

Acquisition of MIRI Related Genes

The therapeutic targets for MIRI were collected from the Online Mendelian Inheritance in Man (OMIM, http://www.omim.org/, update time: 2021-09-02) (Amberger et al., 2015), Therapeutic Target database (TTD, https://db.idrblab. org/ttd/, update time: 2021-09-29) (Wang et al., 2020) and GeneCards (https://www.genecards.org/, update time: 2021-09-13) (Fishilevich et al., 2016). The MIRI was used as the searching keyword and the putative targets of colchicine and the known therapeutic targets on MIRI amalgamated.

Protein-Protein Interaction (PPI) Networks Construction

The STRING database is a database of known and predicted protein-protein interaction. The potential targets of colchicine in the treatment of MIRI were put into STRING V11.5 (https://string-db.org/cgi/input.pl, update time: 2021) (Szklarczyk et al., 2017) to build the PPI network interaction. Cytoscape V3.8.2 (http://www.cytoscape.org/, update time: 2020-10-29) (Shannon et al., 2003) were used to construct and visualize the PPI network. The topological properties of PPI network were examined by 'Network analyzer' a cytoscape plugin app. Nodes in the network are connected by edges if there are regulatory relations. The parameters of "Degree", "Average Shortest Path Length", "Betweenness Centrality", "Closeness Centrality", "Clustering Coefficient" were estimated, and the value of "Degree" was used as a reference for the importance of the target.

Gene Ontology (GO) and Kyoto Encyclopedia of Genes and Genomes (KEGG) Pathway Enrichment Analysis

Metascape (http://metascape.org/gp/index.html, update time: 2021-10-18) (Zhou et al., 2019) was used to conducted GO enrichment analysis and KEGG pathway enrichment analysis. The operation is simply to copy and paste the core genes in the Metascape's gene list and then select the species of Homo sapiens. In the Enrichment section of the analysis page, KEGG Pathways, GO Molecular Functions, GO Biological Processes and GO Cellular Components were selected for enrichment analysis of KEGG Pathways, GO Molecular Functions, GO Biological Processes and GO Cellular Components respectively. The visualization of the important enrichment results of GO and KEGG pathways was implemented by "ggplot2" package of R version 4.0.2 software (update time: 2020-06-22).

Molecular Docking

The 3D structure of the target protein was downloaded from the PDB database (https://www.rcsb.org/). The target protein is processed by removing ligand and water motifs and adding hydrogen using AutoDockTools-1.5.6 (update time: 2014-09-17) (Trott and Olson, 2010). The protein receptors and ligand were converted to PDBQT format. Finally, AutoDock vina software will be used for molecular docking, and the lowest free energy model is selected for visual analysis by using PyMOL. The docking score is carried out for each docking. The smaller the docking score, the better the docking result. Docking score < -6 indicates good binding affinity.

Experimental Chemicals and Reagents

Fetal bovine serum (FBS), phosphate buffered saline (PBS), Krebs-Ringer Bicarbonate buffer, penicillin-streptomycin, trypsin-EDTA and dulbecco modified eagle medium (DMEM) were purchased from GIBCO (Grand Island, NY, United States). Protease inhibitor, RIPA Lysis buffer and BCA protein assay kit were obtained from Beyotime Biotechnology (Shanghai, China). Cell Counting Kit-8 (CCK8) detection kit was obtained from the BBI Life Sciences company (Shanghai, China). Annexin V-FITC/PI apoptosis kits were purchased from YEASEN biological technology company (Shanghai, China). Polyvinylidene fluoride (PVDF) membrane was purchased from Millipore company, (United States). Enhanced chemiluminescence kit (ECL) reagent was obtained from ThermoFisher Scientific, Ltd, (United States). Colchicine and LY294002 were obtained from MedChemExpress company (Shanghai, China) with the purity over 98%. Primary antibodies

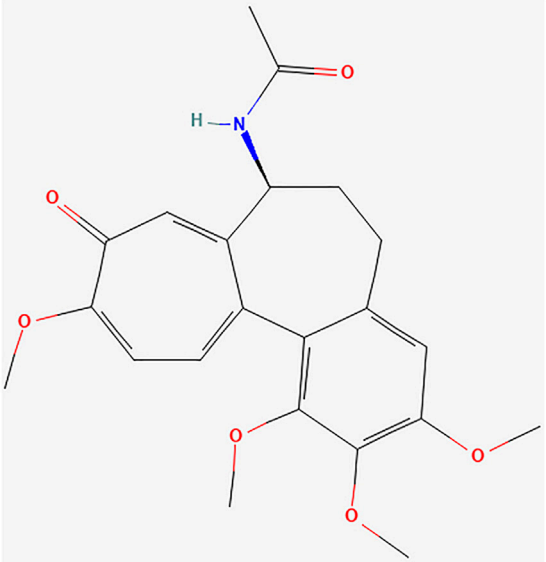


FIGURE 2 | Chemical structure of Colchicine (PubChem CID: 6167).

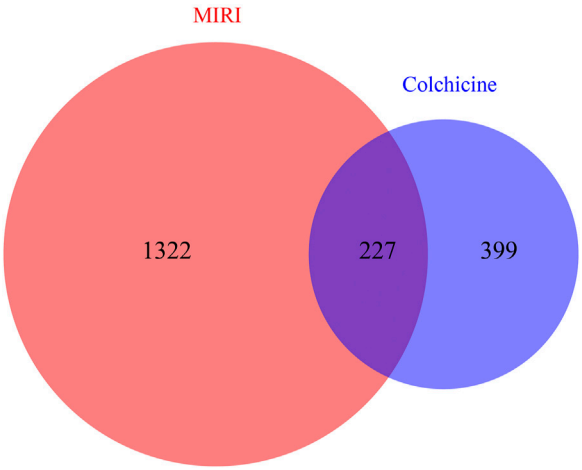


FIGURE 3 | Venn diagrams showing the number of shared and unique targets by Colchicine and MIRI were represented. A total of 227 targets of colchicine with therapeutic potential for MIRI were identified.

against Phospho-PI3K, Phospho-AKT, Phospho-eNOS, caspase3, GAPDH and antibodies against PI3K, AKT, eNOS, c-Caspase3 were purchased from ZEN-BIOSCIENCE company (Chendu, China).

H9C2 Myocardial Cell Culture and Treatments

H9C2 cells were purchased from the National Collection of Authenticated Cell Cultures (Shanghai, China) and cultured in DMEM containing 10% FBS and 1% penicillin/streptomycin in CO_2 incubator at 37°C and 95% relative humidity.

The H9C2 cells were pretreated with colchicine (0–5 μM) for 24 h, then the drug-containing medium was removed from the colchicine-treated cells and replaced by Krebs–Ringer Bicarbonate buffer, and cells were put into a modular incubator chamber saturated with 99.99% N_2 and cultured in a normal incubator for the indicated time (0–16 h). Then the cells were subjected to reoxygenation by changing the DMEM back, and cultured under normoxia (21% O_2) for 2 h. The H9C2 cells Hypoxia/Reoxygenation (H/R) model were established.

Detection of Cell Viability

CCK-8 assays were carried out to detect the effect of colchicine on H9C2 cell activity. Briefly, the H9C2 cells were seeded into 96-well plates at the density of 3×10^3 cells in culture medium. After processing the cells as previously described, 10 μL of CCK-8 was then added to each well and placed the 96-well plate in the incubator for 1 h. The absorbance values of each well were determined spectrophotometrically at 450 nm using a microplate reader (Bio-Tek, United States). Each experiment was repeated 5 times.

Detection of Apoptosis

H9C2 cell apoptosis was detected by flow cytometry (Beckman Coulter Inc, Atlanta, Georgia, United States). The cells were trypsinized using 0.25% trypsin. The H9C2 cells in suspension (1×10^6 cells) were extracted and washed using phosphate-buffered saline. The cells were resuscitated with 100 μL of binding buffer, mixed with 5 μL of Annexin V-FITC and 10 μL of PI, and incubated at room temperature in dark for 15 min. The samples were assessed using flow cytometer analysis. Each experiment was repeated 3 times.

Western Blot Analysis

To determine anti-MIRI effects of colchicine through caspase3 and PI3K/AKT/eNOS signaling, protein phosphorylation was measured by western blotting assay. Briefly, H9C2-cell lysates were prepared in RIPA Lysis buffer after drug administration. The protein concentrations were analyzed by the BCA protein assay kit. Protein extracts were separated by 8–15% SDS-PAGE according to different molecular weights, and then transferred onto PVDF membrane. The membranes were blocked with 5% nonfat dry milk in TBST for 1 h at room temperature, and were then incubated overnight at 4°C with the following primary antibodies: p-PI3K (1:1,000), *p*-Akt (1:1,000), *p*-eNOS (1:1,000), Caspase-3 (1:1,000) and GAPDH (1:1,000). The membranes were then incubated for 1 h with goat anti-rabbit IgG-HRP (1:5,000) as the secondary antibody. Antibody-bound protein was detected by ECL reagent. GAPDH served as the internal control. ImageJ Java 1.8.0 software (update time: 2021-09-28) (NIH, United States) was used to analyze the imaging map and calculate the ratios of PI3K, AKT, eNOS and Cascapse3 proteins in each group.

Statistical Analysis

All the data are expressed as the mean ± SD. The statistical analysis was performed with SPSS version 21.0 (update time: 2020) (IBM Corporation, Armonk, NY). For multiple comparisons, one-way analysis of variance (ANOVA) was performed, and comparisons between two groups were

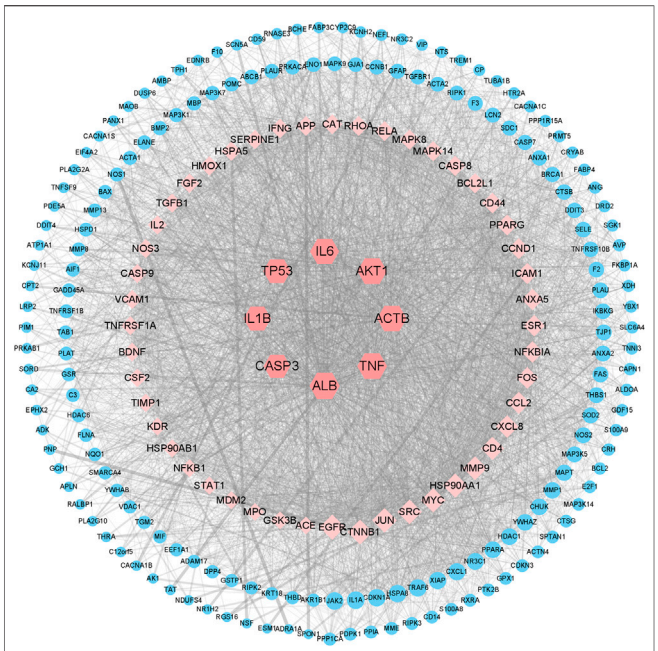


FIGURE 4 | Network pharmacology revealed the targets characteristics of colchicine with therapeutic potential for MIRI. A protein network of known targets of colchicine with therapeutic potential for MIRI was generated by Cytoscape.

analyzed using an LSD test. A value of $p < 0.05$ was regarded as statistically significant.

Ethics Statements

This study is not animal study, human study and have no identifiable human images/data.

RESULTS

Active Components and Potential Targets of Colchicine on MIRI

The molecular formula of colchicine is C22H25NO6, and its molecular structure is shown in **Figure 2**. We searched the PharmMapper, Swiss Target Prediction, CTD, and BATMAN-TCM database, and a total of 626 target genes for colchicine were obtained by UniProt gene annotation simultaneously (**Supplementary Table S1**). For MIRI, we collected 1,549 disease targets through OMIM, GeneCards, and TTD (**Supplementary Table S2**). By matching the targets of colchicine with MIRI related targets, 227 cross-genes were derived, which were potential targets of colchicine in treating MIRI **(Figure 3)**.

Conversion of Target Proteins Into Network and Analysis

We uploaded a total of 227 cross-genes into the STRING database for PPI analysis. Then we imported the results from STRING database into Cytoscape to estimate the topological properties of PPI network. From **Supplementary Figure S1**, a total of 227 nodes and 4,709 edges were acquired. We selected 56 core target genes based on the Q3 of node degree (61), included ALB, TNF, ACTB, AKT1, IL6, TP53, IL1B, CASP3, et al. **Figure 4** showed the topological properties results of these 56 core target genes with no isolated nodes. Nodes represented proteins, and each edge represented the interaction relationship between proteins. The more lines, the greater the correlation degree. The average clustering coefficient is 0.4931, average degree is 89.6250, average shortest path length is between 1.3097 ~ 1.7655, and betweenness centrality is between 0.0013 ~ 0.0747. According to our results, it is suggested that ALB, TNF, ACTB, AKT1, IL6, TP53, IL1B, CASP3, may be the key targets of colchicine in the treatment of MIRI.

Gene Ontology Enrichment Analysis

We imported the selected potential 56 core target genes into the Metascape for GO analysis. A total of 98 biological processes were enrichment, such as response to lipopolysaccharide, apoptotic signaling pathway, response to inorganic substance, and et al. A total of 14 cellular component were enrichment, such as membrane raft, vesicle lumen, focal adhesion, and et al. A total of 23 molecular function were enrichment, such as protein kinase binding, cytokine receptor binding, RNA polymerase II-specific DNA-binding transcription factor binding, and et al. (**Figure 5A**).

KEGG Pathway Enrichment Analysis

We conducted KEGG pathway enrichment analysis on potential 56 core target genes using Metascape and screened out 21 pathways. **Figure 5B** showed these 21 pathways, such as Fluid shear stress and atherosclerosis, IL-17 signaling pathway, PI3K-Akt signaling pathway, T cell receptor signaling pathway, and et al. As shown in **Figure 5B**, colchicine may play an anti-MIRI role by regulating cascade reactions of multiple signaling pathways. Interestingly, consistent with the results of the previous GO functional annotation, the KEGG pathway also enriched the apoptotic pathways. It is known that apoptosis plays an important role in MIRI injury of myocardial cells. Therefore, it is suggesting that colchicine may protect ischemic myocardium by inhibiting apoptosis in myocardial cells. Based on the enriched pathway of apoptosis, the PI3K/AKT signaling pathway (https://www.kegg.jp/kegg/) was obtained through further screening in the apoptotic mechanism (**Figure 6**).

Molecular Docking Analysis

Molecular docking analysis was conducted to evaluate the binding affinity of colchicine with key target proteins. In order to evaluate the biological activity of colchicine, the docking simulation of colchicine and the key target proteins were implemented by molecular docking analysis. As can be seen from **Figure 7** and **Table 1**, the results showed that docking scores of colchicine with ALB, TNF, ACTB, AKT1, IL6, TP53, IL1B and CASP3 ranged from -6.1 to -7.6, and all the hub proteins showed better binding affinity with colchicine. Most of these hub proteins are involved in cell apoptosis.

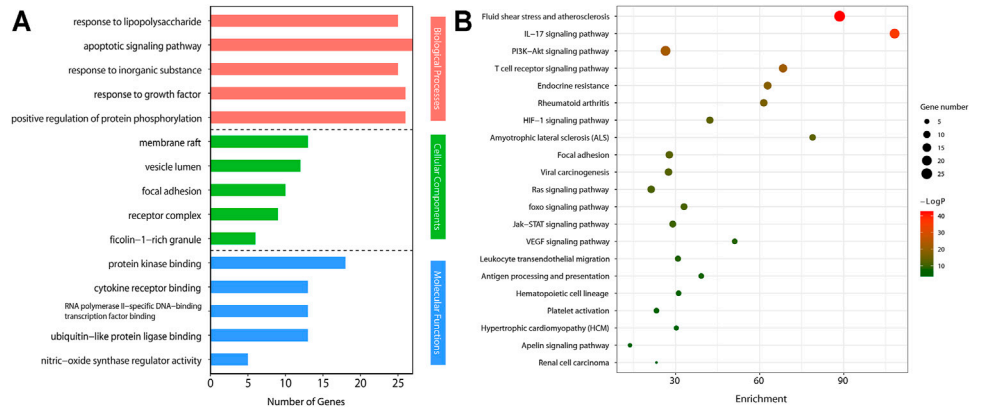


FIGURE 5 | Gene Ontology (GO) analyses and Kyoto Encyclopedia of Genes and Genomes (KEGG) pathways by Metascape.**(A)** GO enrichment analysis of target genes. The number of GO entries in the functional categories of biological process (BP), cell composition (CC), and molecular function (MF) ($p < 0.05$).**(B)** KEGG pathways of target genes ($p < 0.05$).

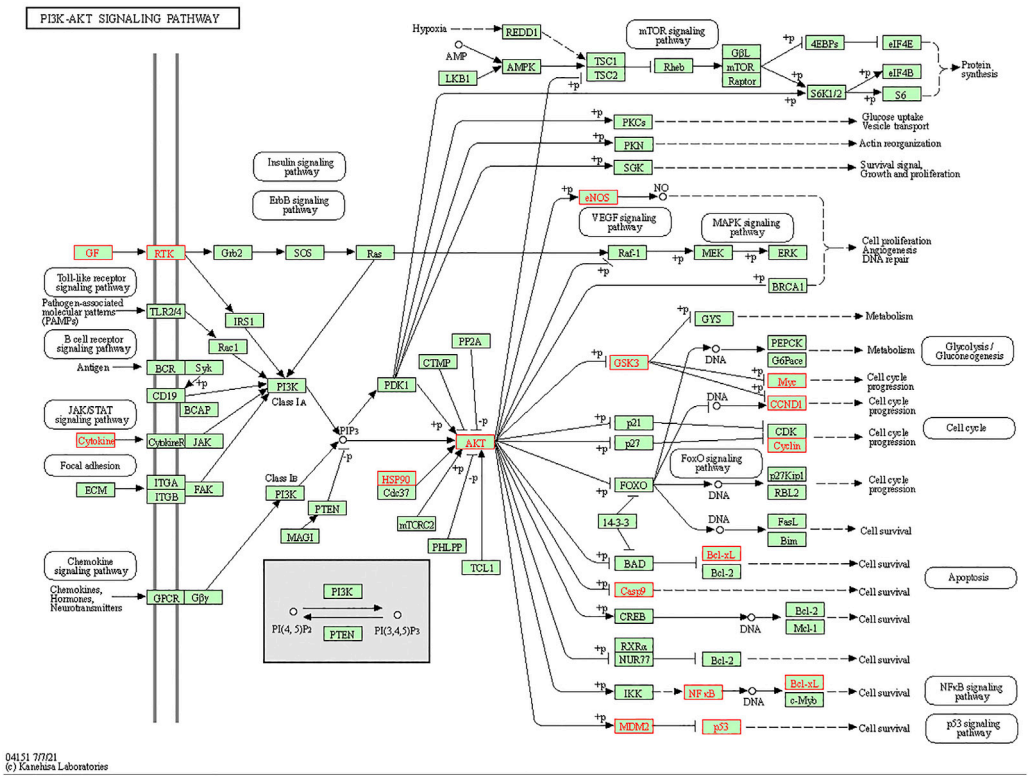


FIGURE 6 | Screening of PI3K/AKT signaling pathway in apoptosis. The red marked nodes represent overlapping targets of colchicine and MIRI.

Result of CCK-8 Cell Viability Assay

To determine the effect of colchicine on H9C2 cells, we used different concentrations of colchicine (0.05, 0.5, 5 μM) to stimulate H9C2 cells and detected the cell viability by CCK8 assay. The cell viability was also measured after incubation with various time of H/R (0, 2, 4, 8, 16 h). From **Figure 8**, we found that groups with 0.5 μM or 5 μM colchicine have significantly higher cell viability than others hypoxia groups before 8 h, and the results of 5 μM colchicine group were more stable (the SD was smaller). We also observed that there was a significant decrease in cell viability of 0.5 and 5 μM colchicine groups at 16 h. Maybe it's the toxic effects of colchicine. Therefore, we choose 5 μM as the optimum concentration of colchicine to anti-MIRI at 8 h.

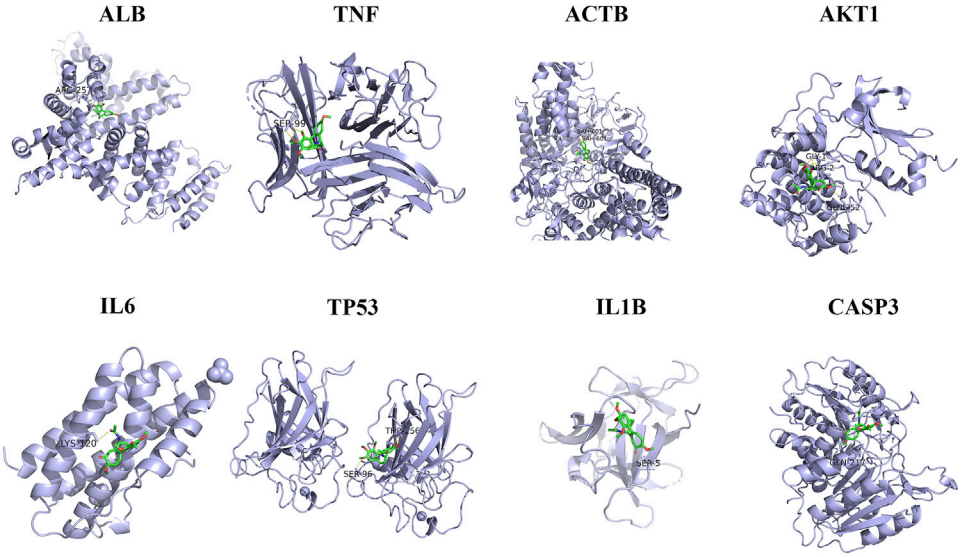


FIGURE 7 | Structural interactions of colchicine and key target receptors.

TABLE 1 | The docking scores of colchicine with key proteins.

Tagret	Drug	PDB ID	Docking score
ALB	Colchicine	1E7E	−7.6
TNF	—	6OOY	−6.6
ACTB	—	6ICV	−7.0
AKT1	—	3CQU	−6.5
IL6	—	1ALU	−6.1
TP53	—	6SHZ	−6.5
IL1B	—	1HIB	−6.2
CASP3	—	1CP3	−6.6

Result of Apoptosis Detection

CCK-8 assay results suggested that colchicine can protect H9C2 cell form H/R injury. To determine whether this anti-MIRI effect was related to apoptosis, flow cytometry was used to detect the apoptosis-inducing effect of colchicine on H9C2 cells and the percentage of apoptotic cells was also detected by Annexin V-FITC and PI double staining. As shown in **Figure 9**, the apoptosis rate was increased in 6.182%, which is significantly when cells were treated with H/R compared with the controls (1.214%). However, colchicine with 5 μM caused a significant reduction (4.490%) of early apoptotic cells as compared with the H/R only groups. Additionally, LY294002 (PI3K inhibitor) significantly attenuated the effects of colchicine, which can be observed from the apoptotic rate increased to 7.993%. These results suggested that colchicine plays an antiapoptotic role partly on H/R injury of H9C2 cell.

Result of Western Blot Analysis

PI3K/AKT is one of the main signal transduction pathways involved in cell proliferation and apoptosis, and eNOS is a downstream of PI3K/AKT which related to the anti-MIRI effect of colchicine base on the result of GO enrichment and KEGG enrichment (Zhang et al., 2019). To further study the mechanisms underlying the antiapoptotic effects of colchicine and the effects of colchicine on PI3K/AKT/eNOS signaling pathway, we detected the apoptosis-related protein caspase3 and the key proteins of PI3K, AKT, eNOS in the signaling pathway. From **Figure 10**, it could be seen that after H/R injury in H9C2 cell, phosphorylation levels of PI3K, AKT, and eNOS proteins were significantly decreased compared with those in the control group ($p < 0.001$). Compared with the H/R group, 5 μM colchicine observably increased the phosphorylation levels of PI3K, AKT, and eNOS ($p < 0.01$). Simultaneously, c-Caspase3 was significantly increased expression in H/R treated H9C2 cell ($p < 0.001$), however, markedly reduced by 5 μM colchicine treatment ($p < 0.01$). Moreover, the use of LY294002 (PI3K inhibitor) significantly prevented the effects of colchicine ($p < 0.001$), which can be shown from the protein expression of p-PI3K, *p*-AKT, *p*-eNOS and c-Caspase-3. Our results demonstrated that colchicine can inhibited MIRI induced apoptosis of H9C2 cell by activating the PI3K/AKT/eNOS pathway.

DISCUSSION

MIRI is a common pathophysiological injury in ischemic heart disease, shock, extracorporeal circulation, cardiovascular surgery and other diseases or treatments. It causes damage to tissues, organs, etc. through an excessive cascade reaction (Gao et al., 2012). Moreover, together with the injury caused by ischemia, it determines the final region of myocardial infarction and the process of ventricular remodeling, and eventually develops into heart failure (Herr et al., 2020). At present, endogenous protective methods are widely used to reduce reperfusion injury and improve the prognosis of patients with acute myocardial

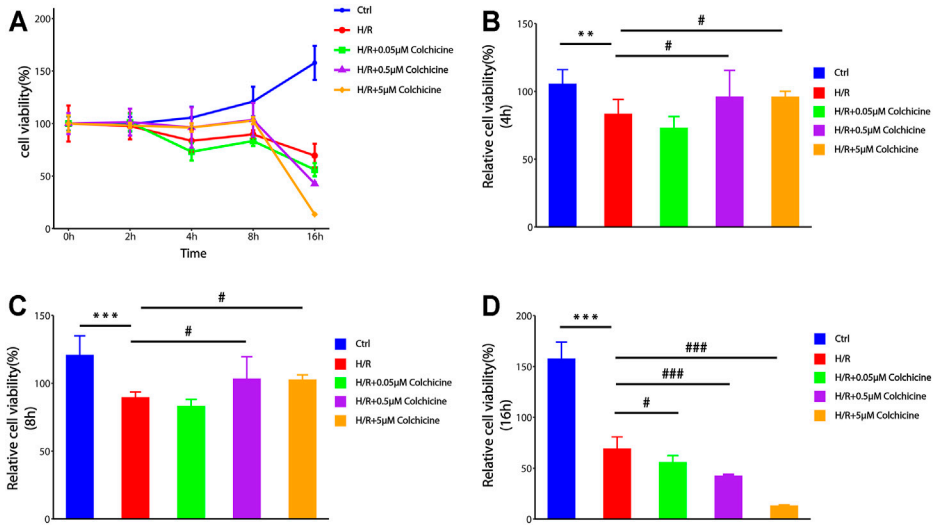


FIGURE 8 | The effect of different concentrations of colchicine and different time of H/R-damaged on the viability of H9C2 cell by CCK-8 assays.**(A)** Optimum concentration of colchicine in appropriate time H/R-damaged was determined by CCK8 assay.**(B–D)** The effect of different colchicine concentrations on H9C2 cell viability after 4 h/8 h/16 h H/R injury (***$p < 0.001$, **$p < 0.01$ compared with control; #$p < 0.05$, ###$p < 0.001$ compared with H/R group).

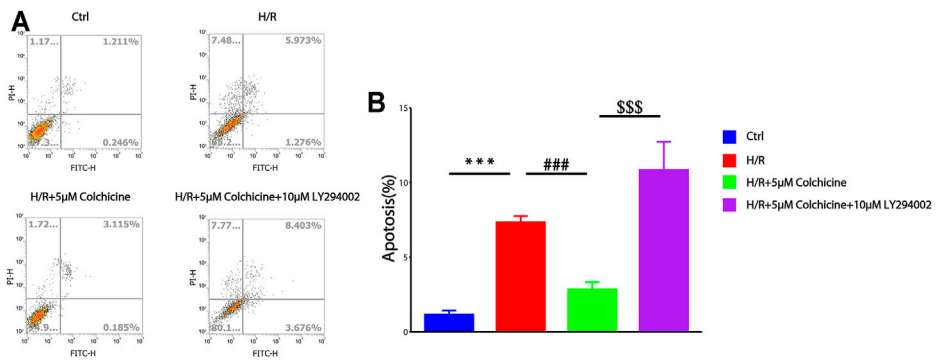


FIGURE 9 | Flow cytometry was used to detect the apoptosis-inducing effect of colchicine on H9C2 cells. **(A)** the apoptotic effects of colchicine was measured through flow cytometry.**(B)** The quantitative results were analyzed. The data were expressed as mean ± SD (***$p < 0.001$ compared with control; ###$p < 0.001$ compared with H/R group; $$$$p < 0.001$ compared with colchicine treated alone).

infarction, for example, ischemic preconditioning, ischemic post-conditioning and pharmacological post-conditioning (Wu et al., 2018). Nevertheless, there are few effective drugs for the treatment of MIRI clinically. Therefore, finding a resultful drug to treat MIRI makes sense (Bellis et al., 2020). Network pharmacology is an emerging discipline based on systems biology, which is used to analyze biological system networks to select specific signal nodes, so that the potential interaction between drugs and targets can be accurately determined (Barabasi et al., 2011; Zhao et al., 2016). For these reasons, there is no doubt that network pharmacology is one of the efficacious strategies for discovering new drugs (Hopkins, 2008). This study discovered the potential therapeutic targets and pathways of colchicine through network pharmacology, and explored the mechanism of colchicine on MIRI. Our works provide new ideas for understanding the pharmacological mechanisms of drugs from the perspective of the network.

Colchicine has various biological activities such as anti-inflammatory, anti-hepatic fibrosis, and enhance the effects of sympathomimetic drugs and so on (Leung et al., 2015). The beneficial effects of colchicine on cardiovascular disease have been widely reported in recent studies (Roubille et al., 2014; Martinez et al., 2018; Akodad et al., 2020). Previous reports had shown that colchicine has a certain protective effect on ischemic myocardium, which can reduce the coronary plaque and the area of myocardial infarction in patients with myocardial infarction by inhibiting inflammation response (Nidorf et al., 2019; Nidorf et al., 2020). However, the potential regulatory targets and pharmacological mechanisms of colchicine in MIRI injury

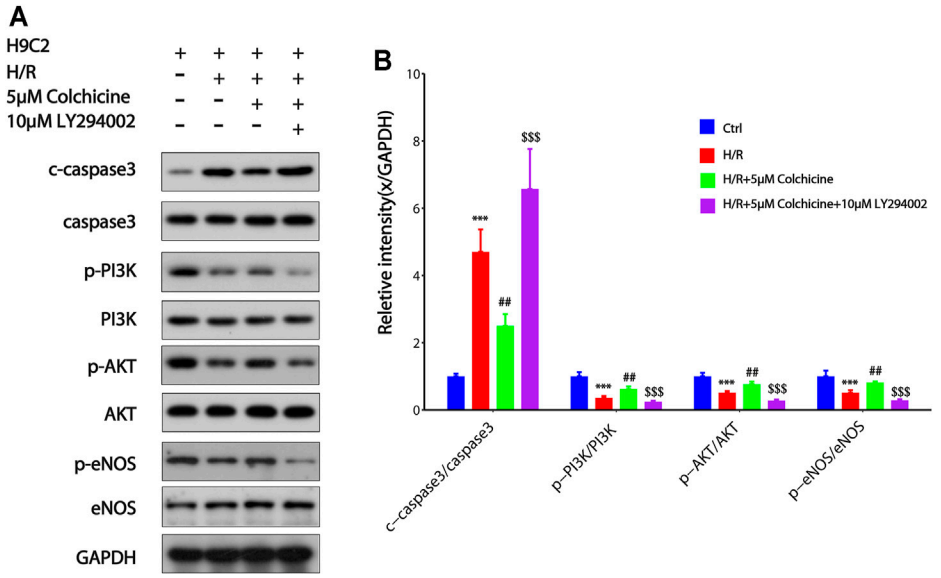


FIGURE 10 | Colchicine inhibited MIRI-induced apoptosis of H9C2 by regulating the PI3K/AKT/eNOS pathway.**(A)** Protein expression of p-PI3K, *p*-AKT, *p*-eNOS, and Caspase-3 were detected by western blot analysis;**(B)** Protein content was quantified using densitometric analysis with GAPDH as internal control. The values of control group were set as one. Data were expressed as mean ± SD (***$p < 0.001$ compared with control; ##$p < 0.01$ compared with H/R group; $$$$p < 0.001$ compared with colchicine treated alone).

remain unclear. In this study, 227 overlapping genes related to colchicine were identified by connecting targets of colchicine with targets of disease. the PPI network analysis demonstrated that the targets linked to MIRI were ALB, TNF, ACTB, AKT1, IL6, TP53, IL1B, CASP3 and these targets showed nice affinity with colchicine in molecular docking experiments, we found that most of the hub targets are involved in external or internal apoptotic pathways. The results of GO analysis and KEGG pathway enrichment demonstrated that the anti-MIRI effect of colchicine involves in apoptotic signaling pathway and the PI3K/AKT signaling pathway was obtained through further screening in the apoptotic mechanism. Previous studies have extensively reported the beneficial effects of inhibition of cardiomyocyte apoptosis on MIRI (Tao et al., 2011; Konstantinidis et al., 2012). However, the effect of colchicine on cardiomyocyte apoptosis induced by MIRI has not been reported. Therefore, network pharmacology can help us understand the mechanism of colchicine in the treatment of MIRI from a general view and lays a good foundation for further discussion of the anti-MIRI pharmacological target and molecular mechanism of colchicine.

Based on KEGG pathway enrichment and the result of molecular docking in the core targets, we chose the key proteins of PI3K/AKT/eNOS signaling pathway and the apoptosis-related protein Caspase-3 for validation the mechanisms underlying the anti-MIRI effects of colchicine. The PI3K/Akt signal pathway can regulate the migration, proliferation, differentiation, apoptosis and metabolism of various types of cells, which is connected to cardiomyocyte apoptosis (Brand et al., 2019; Cui et al., 2020). PI3K is activated and generates phosphatidylinositol 3,4,5-trisphosphate, which induces the phosphorylation of AKT (*p*-AKT), *p*-AKT then activates endothelial nitric oxide synthase (eNOS) and produces NO, NO produced by eNOS activation has been shown to play an important role in the process of MIRI (Cohen et al., 2006; Ying et al., 2015). CASP3, as one of the most concerned proteins in caspase family, can catalyze the specific cleavage of a variety of key cell proteins, which is one of the most critical apoptotic protease in the process of apoptosis (Miura, 2011). Activation of caspase-3 is a common ultimate signal in response to factors that induce apoptosis, such as plays an important role in the apoptosis of cardiomyocytes (Gundapaneni et al., 2017).

Our present data provide ample evidence to support the protective role of colchicine in MIRI injury through reducing apoptosis. In this study, we found that colchicine could systematically and significantly inhibit the apoptosis cells from H/R injure. Additionally, LY294002 (PI3K inhibitor) significantly attenuated the effects of colchicine. Our results demonstrated that colchicine markedly enhanced the decreased levels of Caspase-3 in myocardial injure model induced by H/R. Then, Western blot results further confirmed that colchicine inhibited H/R induced cardiomyocyte apoptosis by regulating the PI3K/AKT/eNOS pathway. After PI3K/AKT/eNOS signal pathway was specifically blocked (LY294002 group), cardiomyocyte apoptosis induced by ischemia-reperfusion was aggravated. This further suggested that colchicine plays a protective role against MIRI through the apoptosis pathway. R. Singhal et al. found that the activation of PI3K/AKT/eNOS pathway induced by colchicine could reduce apoptosis, inflammation and fibrosis in heart failure cardiomyocytes, which may in part contribute to the improvement of cardiac function (Singhal et al., 2014). This result is consistent with the PI3K/AKT/eNOS signaling pathway and key targets related to apoptosis obtained in our study.

CONCLUSION

In summary, we performed network pharmacology and experimental evaluation to reveal the pharmacological mechanism of colchicine against MIRI. Moreover, a further *in-vitro* validation experiment illustrated that colchicine substantially inhibited apoptosis of myocardial cell via regulating PI3K/Akt/eNOS signaling pathway and inhibiting the expression of pro-apoptotic protein Caspase-3. Our findings may guide further pharmacological investigations on the therapeutic effects of colchicine on MIRI and the discovery of new drugs for MIRI treatment. However, this study still has some limitations. Network pharmacology approaches await further improvements, and it is necessary to conduct *in vivo* experimental study to verify the efficacy and mechanism of colchicine in the treatment of MIRI in our future research.

DATA AVAILABILITY STATEMENT

The original contributions presented in the study are included in the article/**Supplementary Material**, further inquiries can be directed to the corresponding authors.

AUTHOR CONTRIBUTIONS

YT and GF designed the study. YT, CS, YQ was responsible for data analysis and interpretation and drafting of the manuscript. SW, HP, MC and XY were involved in data acquisition and experimentation. YL was responsible for the data curation and the revision of the manuscript. GF was responsible for funding acquisition and project administration.

FUNDING

This work is financially supported by grants from the National Natural Science Foundation of China (81973289), the National Natural Science Foundation of China (81902395).

SUPPLEMENTARY MATERIAL

The Supplementary Material for this article can be found online at: https://www.frontiersin.org/articles/10.3389/fphar.2021.804030/full#supplementary-material

REFERENCES

Akodad, M., Sicard, P., Fauconnier, J., and Roubille, F. (2020). Colchicine and Myocardial Infarction: A Review. *Arch. Cardiovasc. Dis.* 113 (10), 652–659. doi:10.1016/j.acvd.2020.04.007

Amberger, J. S., Bocchini, C. A., Schiettecatte, F., Scott, A. F., and Hamosh, A. (2015). OMIM.org: Online Mendelian Inheritance in Man (OMIM®), an Online Catalog of Human Genes and Genetic Disorders. *Nucleic Acids Res.* 43, D789–D798. doi:10.1093/nar/gku1205

Bajaj, A., Sethi, A., Rathor, P., Suppogu, N., and Sethi, A. (2015). Acute Complications of Myocardial Infarction in the Current Era: Diagnosis and Management. *J. Investig. Med.* 63 (7), 844–855. doi:10.1097/JIM.0000000000000232

Barabási, A. L., Gulbahce, N., and Loscalzo, J. (2011). Network Medicine: a Network-Based Approach to Human Disease. *Nat. Rev. Genet.* 12 (1), 56–68. doi:10.1038/nrg2918

Bellis, A., Mauro, C., Barbato, E., Di Gioia, G., Sorriento, D., Trimarco, B., et al. (2020). The Rationale of Neprilysin Inhibition in Prevention of Myocardial Ischemia-Reperfusion Injury during ST-Elevation Myocardial Infarction. *Cells* 9 (9), 2134. doi:10.3390/cells9092134

Bouabdallaoui, N., Tardif, J. C., Waters, D. D., Pinto, F. J., Maggioni, A. P., Diaz, R., et al. (2020). Time-to-treatment Initiation of Colchicine and Cardiovascular Outcomes after Myocardial Infarction in the Colchicine Cardiovascular Outcomes Trial (COLCOT). *Eur. Heart J.* 41 (42), 4092–4099. doi:10.1093/eurheartj/ehaa659

Brand, C. S., Lighthouse, J. K., and Trembley, M. A. (2019). Protective Transcriptional Mechanisms in Cardiomyocytes and Cardiac Fibroblasts. *J. Mol. Cel Cardiol* 132, 1–12. doi:10.1016/j.yjmcc.2019.04.023

Buja, L. M. (2005). Myocardial Ischemia and Reperfusion Injury. *Cardiovasc. Pathol.* 14 (4), 170–175. doi:10.1016/j.carpath.2005.03.006

Castro-Dominguez, Y., Dharmarajan, K., and McNamara, R. L. (2018). Predicting Death after Acute Myocardial Infarction. *Trends Cardiovasc. Med.* 28 (2), 102–109. doi:10.1016/j.tcm.2017.07.011

Cohen, M. V., Yang, X. M., and Downey, J. M. (2006). Nitric Oxide Is a Preconditioning Mimetic and Cardioprotectant and Is the Basis of many Available Infarct-Sparing Strategies. *Cardiovasc. Res.* 70 (2), 231–239. doi:10.1016/j.cardiores.2005.10.021

Crittenden, D. B., Lehmann, R. A., Schneck, L., Keenan, R. T., Shah, B., Greenberg, J. D., et al. (2012). Colchicine Use Is Associated with Decreased Prevalence of Myocardial Infarction in Patients with Gout. *J. Rheumatol.* 39 (7), 1458–1464. doi:10.3899/jrheum.111533

Cui, Z. H., Zhang, X. J., Shang, H. Q., Wang, X., and Rong, D. (2020). Glutamine Protects Myocardial Ischemia-Reperfusion Injury in Rats through the PI3K/Akt Signaling Pathway. *Eur. Rev. Med. Pharmacol. Sci.* 24 (1), 444–451. doi:10.26355/eurrev_202001_19944

Daina, A., Michielin, O., and Zoete, V. (2019). SwissTargetPrediction: Updated Data and New Features for Efficient Prediction of Protein Targets of Small Molecules. *Nucleic Acids Res.* 47 (W1), W357–W364. doi:10.1093/nar/gkz382

Davis, A. P., Grondin, C. J., Johnson, R. J., Sciaky, D., McMorran, R., Wiegers, J., et al. (2019). The Comparative Toxicogenomics Database: Update 2019. *Nucleic Acids Res.* 47 (D1), D948–D954. doi:10.1093/nar/gky868

Deftereos, S., Giannopoulos, G., Angelidis, C., Alexopoulos, N., Filippatos, G., Papoutsidakis, N., et al. (2015). Anti-Inflammatory Treatment with Colchicine in Acute Myocardial Infarction: A Pilot Study. *Circulation* 132 (15), 1395–1403. doi:10.1161/CIRCULATIONAHA.115.017611

Downing, K. H. (2000). Structural Basis for the Interaction of Tubulin with Proteins and Drugs that Affect Microtubule Dynamics. *Annu. Rev. Cel Dev Biol* 16, 89–111. doi:10.1146/annurev.cellbio.16.1.89

Fishilevich, S., Zimmerman, S., Kohn, A., Iny Stein, T., Olender, T., Kolker, E., et al. (2016). Genic Insights from Integrated Human Proteomics in GeneCards. *Database* 2016, baw030. doi:10.1093/database/baw030

Fujiwara, M., Matoba, T., Koga, J. I., Okahara, A., Funamoto, D., Nakano, K., et al. (2019). Nanoparticle Incorporating Toll-like Receptor 4 Inhibitor Attenuates Myocardial Ischaemia-Reperfusion Injury by Inhibiting Monocyte-Mediated Inflammation in Mice. *Cardiovasc. Res.* 115 (7), 1244–1255. doi:10.1093/cvr/cvz066

Gao, H., Kiesewetter, D. O., Zhang, X., Huang, X., Guo, N., Lang, L., et al. (2012). PET of Glucagonlike Peptide Receptor Upregulation after Myocardial Ischemia or Reperfusion Injury. *J. Nucl. Med.* 53 (12), 1960–1968. doi:10.2967/jnumed.112.109413

Gulati, R., Behfar, A., Narula, J., Kanwar, A., Lerman, A., Cooper, L., et al. (2020). Acute Myocardial Infarction in Young Individuals. *Mayo Clin. Proc.* 95 (1), 136–156. doi:10.1016/j.mayocp.2019.05.001

Gundapaneni, K. K., Shyamala, N., Galimudi, R. K., Kupsal, K., Gantala, S. R., Padala, C., et al. (2017). Polymorphic Variants of Caspase Genes (8 & 3) in the Risk Prediction of Coronary Artery Disease. *Gene* 627, 278–283. doi:10.1016/j.gene.2017.06.035

Herr, D. J., Singh, T., Dhammu, T., and Menick, D. R. (2020). Regulation of Metabolism by Mitochondrial Enzyme Acetylation in Cardiac Ischemia-Reperfusion Injury. *Biochim. Biophys. Acta Mol. Basis Dis.* 1866 (6), 165728. doi:10.1016/j.bbadis.2020.165728

Hopkins, A. L. (2007). Network Pharmacology. *Nat. Biotechnol.* 25 (10), 1110–1111. doi:10.1038/nbt1007-1110

Hopkins, A. L. (2008). Network Pharmacology: the Next Paradigm in Drug Discovery. *Nat. Chem. Biol.* 4 (11), 682–690. doi:10.1038/nchembio.118

Huang, C., Zheng, C., Li, Y., Wang, Y., Lu, A., and Yang, L. (2014). Systems Pharmacology in Drug Discovery and Therapeutic Insight for Herbal Medicines. *Brief Bioinform* 15 (5), 710–733. doi:10.1093/bib/bbt035

Konstantinidis, K., Whelan, R. S., and Kitsis, R. N. (2012). Mechanisms of Cell Death in Heart Disease. *Arterioscler Thromb. Vasc. Biol.* 32 (7), 1552–1562. doi:10.1161/ATVBAHA.111.224915

Leung, Y. Y., Yao Hui, L. L., and Kraus, V. B. (2015). Colchicine--Update on Mechanisms of Action and Therapeutic Uses. *Semin. Arthritis Rheum.* 45 (3), 341–350. doi:10.1016/j.semarthrit.2015.06.013

Liu, Z., Guo, F., Wang, Y., Li, C., Zhang, X., Li, H., et al. (2016). BATMAN-TCM: a Bioinformatics Analysis Tool for Molecular mechANism of Traditional Chinese Medicine. *Sci. Rep.* 6, 21146. doi:10.1038/srep21146

Marchant, D. J., Boyd, J. H., Lin, D. C., Granville, D. J., Garmaroudi, F. S., and McManus, B. M. (2012). Inflammation in Myocardial Diseases. *Circ. Res.* 110 (1), 126–144. doi:10.1161/CIRCRESAHA.111.243170

Martínez, G. J., Celermajer, D. S., and Patel, S. (2018). The NLRP3 Inflammasome and the Emerging Role of Colchicine to Inhibit Atherosclerosis-Associated Inflammation. *Atherosclerosis* 269, 262–271. doi:10.1016/j.atherosclerosis.2017.12.027

Miura, M. (2011). Apoptotic and Non-apoptotic Caspase Functions in Neural Development. *Neurochem. Res.* 36 (7), 1253–1260. doi:10.1007/s11064-010-0341-x

Münzel, T., Camici, G. G., Maack, C., Bonetti, N. R., Fuster, V., and Kovacic, J. C. (2017). Impact of Oxidative Stress on the Heart and Vasculature: Part 2 of a 3-Part Series. *J. Am. Coll. Cardiol.* 70 (2), 212–229. doi:10.1016/j.jacc.2017.05.035

Nagai, T., Anzai, T., Kaneko, H., Anzai, A., Mano, Y., Nagatomo, Y., et al. (2010). Impact of Systemic Acidosis on the Development of Malignant Ventricular Arrhythmias after Reperfusion Therapy for ST-Elevation Myocardial Infarction. *Circ. J.* 74 (9), 1808–1814. doi:10.1253/circj.cj-10-0229

Nidorf, S. M., Fiolet, A. T. L., Eikelboom, J. W., Schut, A., Opstal, T. S. J., Bax, W. A., et al. (2019). The Effect of Low-Dose Colchicine in Patients with Stable Coronary Artery Disease: The LoDoCo2 Trial Rationale, Design, and Baseline Characteristics. *Am. Heart J.* 218, 46–56. doi:10.1016/j.ahj.2019.09.011

Nidorf, S. M., Fiolet, A. T. L., Mosterd, A., Eikelboom, J. W., Schut, A., Opstal, T. S. J., et al. (2020). Colchicine in Patients with Chronic Coronary Disease. *N. Engl. J. Med.* 383 (19), 1838–1847. doi:10.1056/NEJMoa2021372

Roubille, F., Busseuil, D., Merlet, N., Kritikou, E. A., Rhéaume, E., and Tardif, J. C. (2014). Investigational Drugs Targeting Cardiac Fibrosis. *Expert Rev. Cardiovasc. Ther.* 12 (1), 111–125. doi:10.1586/14779072.2013.839942

Roubille, F., Kritikou, E., Busseuil, D., Barrere-Lemaire, S., and Tardif, J. C. (2013). Colchicine: an Old Wine in a New Bottle? *Antiinflamm Antiallergy Agents Med. Chem.* 12 (1), 14–23. doi:10.2174/1871523011312010004

Shannon, P., Markiel, A., Ozier, O., Baliga, N. S., Wang, J. T., Ramage, D., et al. (2003). Cytoscape: a Software Environment for Integrated Models of Biomolecular Interaction Networks. *Genome Res.* 13 (11), 2498–2504. doi:10.1101/gr.1239303

Singhal, R., Chang, S. L., Chong, E., Hsiao, Y. W., Liu, S. H., Tsai, Y. N., et al. (2014). Colchicine Suppresses Atrial Fibrillation in Failing Heart. *Int. J. Cardiol.* 176 (3), 651–660. doi:10.1016/j.ijcard.2014.07.069

Szklarczyk, D., Morris, J. H., Cook, H., Kuhn, M., Wyder, S., Simonovic, M., et al. (2017). The STRING Database in 2017: Quality-Controlled Protein-Protein Association Networks, Made Broadly Accessible. *Nucleic Acids Res.* 45 (D1), D362–D368. doi:10.1093/nar/gkw937

Tao, J., Zhu, W., Li, Y., Xin, P., Li, J., Liu, M., et al. (2011). Apelin-13 Protects the Heart against Ischemia-Reperfusion Injury through Inhibition of ER-dependent Apoptotic Pathways in a Time-dependent Fashion. *Am. J. Physiol. Heart Circ. Physiol.* 301 (4), H1471–H1486. doi:10.1152/ajpheart.00097.2011

Tardif, J. C., Kouz, S., Waters, D. D., Bertrand, O. F., Diaz, R., Maggioni, A. P., et al. (2019). Efficacy and Safety of Low-Dose Colchicine after Myocardial Infarction. *N. Engl. J. Med.* 381 (26), 2497–2505. doi:10.1056/NEJMoa1912388

Terkeltaub, R. A. (2009). Colchicine Update: 2008. *Semin. Arthritis Rheum.* 38 (6), 411–419. doi:10.1016/j.semarthrit.2008.08.006

Toldo, S., and Abbate, A. (2018). The NLRP3 Inflammasome in Acute Myocardial Infarction. *Nat. Rev. Cardiol.* 15 (4), 203–214. doi:10.1038/nrcardio.2017.161

Trott, O., and Olson, A. J. (2010). AutoDock Vina: Improving the Speed and Accuracy of Docking with a New Scoring Function, Efficient Optimization, and Multithreading. *J. Comput. Chem.* 31 (2), 455–461. doi:10.1002/jcc.21334

UniProt, C. (2019). UniProt: a Worldwide Hub of Protein Knowledge. *Nucleic Acids Res.* 47 (D1), D506–D515. doi:10.1093/nar/gky1049

Walters, A. M., Porter, G. A., Jr., and Brookes, P. S. (2012). Mitochondria as a Drug Target in Ischemic Heart Disease and Cardiomyopathy. *Circ. Res.* 111 (9), 1222–1236. doi:10.1161/CIRCRESAHA.112.265660

Wang, X., Shen, Y., Wang, S., Li, S., Zhang, W., Liu, X., et al. (2017). PharmMapper 2017 Update: a Web Server for Potential Drug Target Identification with a Comprehensive Target Pharmacophore Database. *Nucleic Acids Res.* 45 (W1), W356–W360. doi:10.1093/nar/gkx374

Wang, Y., Zhang, S., Li, F., Zhou, Y., Zhang, Y., Wang, Z., et al. (2020). Therapeutic Target Database 2020: Enriched Resource for Facilitating Research and Early Development of Targeted Therapeutics. *Nucleic Acids Res.* 48 (D1), D1031–D1041. doi:10.1093/nar/gkz981

Wu, M. Y., Yiang, G. T., Liao, W. T., Tsai, A. P., Cheng, Y. L., Cheng, P. W., et al. (2018). Current Mechanistic Concepts in Ischemia and Reperfusion Injury. *Cell Physiol Biochem* 46 (4), 1650–1667. doi:10.1159/000489241

Yao, B., Wan, X., Zheng, X., Zhong, T., Hu, J., Zhou, Y., et al. (2020). Critical Roles of microRNA-141-3p and CHD8 in Hypoxia/reoxygenation-Induced Cardiomyocyte Apoptosis. *Cell Biosci* 10, 20. doi:10.1186/s13578-020-00384-5

Ying, Z., Xie, X., Chen, M., Yi, K., and Rajagopalan, S. (2015). Alpha-lipoic Acid Activates eNOS through Activation of PI3-kinase/Akt Signaling Pathway. *Vascul Pharmacol.* 64, 28–35. doi:10.1016/j.vph.2014.11.004

Zhang, X., Huang, L. F., Hua, L., Feng, H. K., and Shen, B. (2019). Resveratrol Protects Myocardial Apoptosis Induced by Ischemia-Reperfusion in Rats with Acute Myocardial Infarction via Blocking P13K/Akt/e-NOS Pathway. *Eur. Rev. Med. Pharmacol. Sci.* 23 (4), 1789–1796. doi:10.26355/eurrev_201902_17142

Zhang, Y., Wang, Z., and Wang, Y. (2017). Multi-hierarchical Profiling: an Emerging and Quantitative Approach to Characterizing Diverse Biological Networks. *Brief Bioinform* 18 (1), 57–68. doi:10.1093/bib/bbv112

Zhao, Z., Zhang, Y., Gai, F., and Wang, Y. (2016). Confirming an Integrated Pathology of Diabetes and its Complications by Molecular Biomarker-Target Network Analysis. *Mol. Med. Rep.* 14 (3), 2213–2221. doi:10.3892/mmr.2016.5478

Zhou, Y., Zhou, B., Pache, L., Chang, M., Khodabakhshi, A. H., Tanaseichuk, O., et al. (2019). Metascape Provides a Biologist-Oriented Resource for the Analysis of Systems-Level Datasets. *Nat. Commun.* 10 (1), 1523. doi:10.1038/s41467-019-09234-6

Conflict of Interest: The authors declare that the research was conducted in the absence of any commercial or financial relationships that could be construed as a potential conflict of interest.

Publisher's Note: All claims expressed in this article are solely those of the authors and do not necessarily represent those of their affiliated organizations, or those of the publisher, the editors and the reviewers. Any product that may be evaluated in this article, or claim that may be made by its manufacturer, is not guaranteed or endorsed by the publisher.

Copyright © 2021 Tang, Shi, Qin, Wang, Pan, Chen, Yu, Lou and Fan. This is an open-access article distributed under the terms of the Creative Commons Attribution License (CC BY). The use, distribution or reproduction in other forums is permitted, provided the original author(s) and the copyright owner(s) are credited and that the original publication in this journal is cited, in accordance with accepted academic practice. No use, distribution or reproduction is permitted which does not comply with these terms.

frontiers in Pharmacology

ORIGINAL RESEARCH
published: 03 January 2022
doi: 10.3389/fphar.2021.723784

Ginsenoside Rb1 Attenuates Triptolide-Induced Cytotoxicity in HL-7702 Cells *via* the Activation of Keap1/Nrf2/ARE Pathway

Hulinyue Peng[1†], Longtai You[1†], Chunjing Yang[2], Kaixin Wang[1], Manting Liu[1], Dongge Yin[1], Yuchen Xu[1], Xiaoxv Dong[1], Xingbin Yin[1]* and Jian Ni[1]**

[1]School of Chinese Materia Medica, Beijing University of Chinese Medicine, Beijing, China, [2]Department of Pharmacy, Beijing Shijitan Hospital Affiliated to Capital University of Medical Sciences, Beijing, China

OPEN ACCESS

Edited by:
Hong Zhang,
Shanghai University of Traditional Chinese Medicine, China

Reviewed by:
Sun Young Park,
Pusan National University, South Korea
Zhenzhou Jiang,
China Pharmaceutical University, China

***Correspondence:**
Xiaoxv Dong
dxiaoxv@163.com
Xingbin Yin
yxbtcm@163.com
Jian Ni
njtcm@263.net

[†]These authors have contributed equally to this work

Specialty section:
This article was submitted to "Ethnopharmacology", a section of the journal Frontiers in Pharmacology

Received: 11 June 2021
Accepted: 06 December 2021
Published: 03 January 2022

Citation:
Peng H, You L, Yang C, Wang K, Liu M, Yin D, Xu Y, Dong X, Yin X and Ni J (2022) Ginsenoside Rb1 Attenuates Triptolide-Induced Cytotoxicity in HL-7702 Cells via the Activation of Keap1/Nrf2/ARE Pathway. Front. Pharmacol. 12:723784. doi: 10.3389/fphar.2021.723784

Triptolide (TP) is the major bioactive compound extracted from *Tripterygium wilfordii* Hook F. It exerts anti-inflammatory, antirheumatic, antineoplastic, and neuroprotective effects. However, the severe hepatotoxicity induced by TP limits its clinical application. Ginsenoside Rb1 has been reported to possess potential hepatoprotective effects, but its mechanism has not been fully investigated. This study was aimed at investigating the effect of ginsenoside Rb1 against TP-induced cytotoxicity in HL-7702 cells, as well as the underlying mechanism. The results revealed that ginsenoside Rb1 effectively reversed TP-induced cytotoxicity in HL-7702 cells. Apoptosis induced by TP was suppressed by ginsenoside Rb1 *via* inhibition of death receptor-mediated apoptotic pathway and mitochondrial-dependent apoptotic pathway. Pretreatment with ginsenoside Rb1 significantly reduced Bax/Bcl-2 ratio and down-regulated the expression of Fas, cleaved poly ADP-ribose polymerase (PARP), cleaved caspase-3, and -9. Furthermore, ginsenoside Rb1 reversed TP-induced cell cycle arrest in HL-7702 cells at S and G2/M phase, *via* upregulation of the expressions of cyclin-dependent kinase 2 (CDK2), cyclin E, cyclin A, and downregulation of the expressions of p53, p21, and p-p53. Ginsenoside Rb1 increased glutathione (GSH) and superoxide dismutase (SOD) levels, but decreased the reactive oxygen species (ROS) and malondialdehyde (MDA) levels. Pretreatment with ginsenoside Rb1 enhanced the expression levels of nuclear factor-erythroid 2-related factor 2 (Nrf2), total Nrf2, NAD(P)H: quinone oxidoreductases-1 (NQO-1), heme oxygenase-1 (HO-1), and Kelch-like ECH-associated protein 1 (Keap1)/Nrf2 complex. Therefore, ginsenoside Rb1 effectively alleviates TP-induced cytotoxicity in HL-7702 cells through activation of the Keap1/Nrf2/ARE antioxidant pathway.

Keywords: ginsenoside Rb1, triptolide, HL-7702 cells, Keap1/Nrf2/ARE pathway, apoptosis, cytotoxicity

1 INTRODUCTION

Triptolide (TP) (**Figure 1A**) is a major diterpenoid extracted from *Tripterygium wilfordii* Hook F (TWHF), a rhizome used as a traditional Chinese medicinal herb (Tan et al., 2018). Studies have revealed that TP exerts significant pharmacological effects such as antirheumatic, anti-inflammatory, antineoplastic, and neuroprotective properties. These properties account for its wide application in

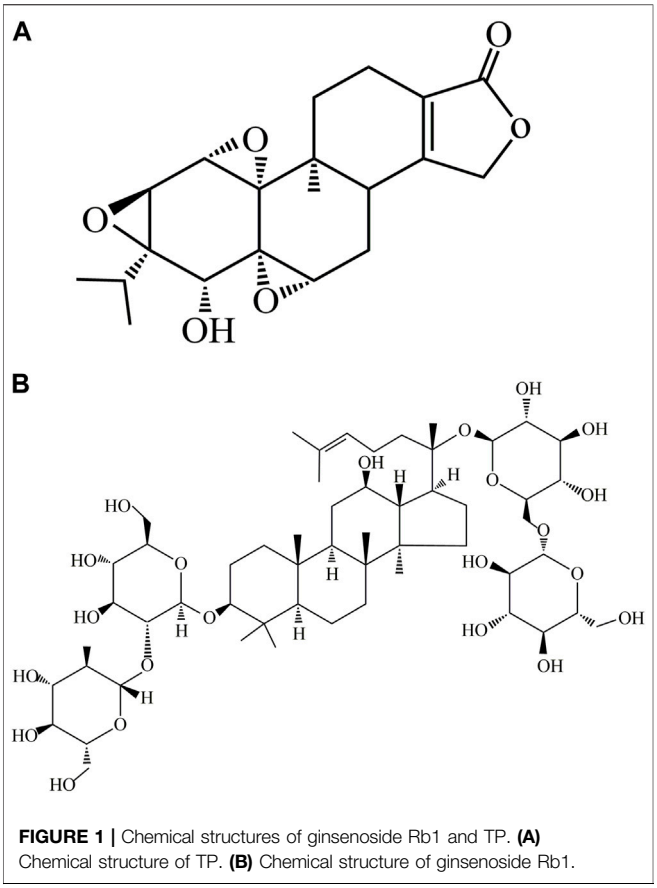


FIGURE 1 | Chemical structures of ginsenoside Rb1 and TP. **(A)** Chemical structure of TP. **(B)** Chemical structure of ginsenoside Rb1.

the treatment of systemic lupus erythematosus, rheumatoid arthritis, central nervous system diseases, and nephrotic syndrome (Li et al., 2014). However, the clinical application of TP is hampered by its toxic effects on multiple cells and organs: it has been associated with nephrotoxicity, hepatotoxicity, cardiotoxicity, and reproductive toxicity (Ruan et al., 2017; You et al., 2018; Wang et al., 2019a; Xu et al., 2019b). The hepatotoxicity of TP is of widely concern since it may cause liver damage in animals and humans (Zhou et al., 2017a).

Oxidative stress-induced apoptosis and hepatocyte dysfunction are thought to be involved in the potential mechanisms underlying TP-induced hepatotoxicity (You et al., 2018). It has been reported that TP stimulated increases in levels of intracellular reactive oxygen species (ROS) and oxidative stress (Lee et al., 2015). Overproduction of intracellular ROS impairs the structure of Kelch-like ECH-associated protein 1 (Keap1)/nuclear factor-erythroid 2-related factor 2 (Nrf2) complex, resulting in activation Nrf2 which then binds to antioxidant response elements (ARE) in the nucleus. The Nrf2/ARE complex stimulates the transcription and translation of oxidoreductases such as heme oxygenase-1 (HO-1), glutamate cysteine ligase catalytic (GCLC), and NAD(P)H: quinone oxidoreductases-1 (NQO-1), which play important roles in antioxidant defense (Ci et al., 2017; Tan et al., 2018; Cinegaglia et al., 2020). As a result, the activation of Nrf2 pathway effectively regulates the levels of ROS and attenuates cell damage caused by oxidative stress.

Apoptosis is a physiological phenomenon which is initiated under the regulation of a series of genes when cells are exposed to drug or external stimuli (Garcia-Caballero et al., 2017; Nori-Garavand et al., 2020). One of the main regulatory pathways of apoptosis is death receptor-mediated pathway, also known as extrinsic pathway. Fas is an important death receptor that mediates apoptosis. The interaction between Fas and its ligand FasL activates caspase-8, thereby triggering activation of downstream effector caspase-3, and ultimately initiating apoptosis (Zhou et al., 2017b; Xu et al., 2019b; You et al., 2019). Another major pathway for regulation of apoptosis is the mitochondrial-dependent intrinsic apoptosis pathway. A key step in the intrinsic apoptosis pathway involves increased mitochondrial membrane permeability which leads to increased release of cytochrome *c* into the cytoplasm. Under oxidative stress, the excessive ROS interact with Bax, thereby enhancing the release of cytochrome *c* from the mitochondria. In the cytoplasm, cytochrome *c* forms an apoptotic body through interaction with caspase-9, which further stimulates the expression of downstream effector caspase-3, and ultimately initiates apoptosis (Li et al., 2016; Pan et al., 2018; Cao et al., 2019; Li et al., 2019). Studies *in vivo* and *in vitro* have shown that TP induces apoptosis through these two pathways (You et al., 2018; Huo et al., 2019; Hasnat et al., 2020).

Ginsenoside Rb1 (**Figure 1B**) is a dammarane-type triterpene saponin compound isolated from the widely used Chinese herb *Panax notoginseng* (Burk.) F. H. Chen (*P. notoginseng*) (Yu et al., 2019). It exerts significant pharmacological effects such as antioxidant, anti-inflammatory, cardioprotective, and neuroprotective properties (Zhu et al., 2012; Zhang et al., 2018; Jiang et al., 2021; Wang et al., 2021; Wei et al., 2021). Although the mechanism involved in the use of ginsenoside Rb1 for the treatment of certain diseases has been gradually understood over the past few years, its hepatoprotective potential has not been elucidated (Na et al., 2012; Lai et al., 2021). Therefore, this study was aimed at investigating the protective effect of ginsenoside Rb1 against TP-induced cytotoxicity, and its underlying mechanism, so as to provide new strategies for the intervention and treatment of hepatotoxicity caused by TP.

2 MATERIALS AND METHODS

2.1 Reagents and Chemicals

The HL-7702 cells were purchased from China Infrastructure of Cell Line Resources. TP (batch no. 7675; purity: 99.7%), and ginsenoside Rb1 (batch no. 8786; purity: 100.0%) were purchased from Standard Technology Co., Ltd. (Shanghai, China). Fetal bovine serum (FBS), penicillin and streptomycin solution, and Dulbecco's Modified Eagle's Medium (DMEM) were purchasedfrom Corning (NY, United States). Phosphate buffered saline (PBS) and 0.05% trypsin were purchased from Gibco, Invitrogen (Carlsbad, CA, United States). 3-(4,5-Dimethylthiazol-2-yl-)-2,5-diphenyltetrazolium bromide

(MTT) (ST316), N-acetylcysteine (NAC) (ST1546), LDH assay kits (C0017), malondialdehyde (MDA) kits (S0131S), GSH kits (S0053), TdT-mediated dUTP Nick-End Labeling (TUNEL) analysis kits (S1098), ROS detection kits (S0033S), SOD kits (S0087), bicinchoninic acid (BCA) protein quantification kits (P0012), dimethyl sulfoxide (DMSO), and JC-1 kits (C2003S) were products of Beyotime Biotechnology (Shanghai, China). Antibodies against Nrf2 (ab62352), Bax (ab53154), COX IV (ab16056), p53 (ab241556), Keap1 (ab118285), CDK2 (ab32147), cyclin A (ab181591), Bcl-2 (ab185002), Fas (ab82419), cyclin E (ab33911), cleaved caspase-3 (ab2302), cytochrome *c* (ab90529), p21 (188224), NQO1 (ab80588), β-actin (ab8226), cleaved caspase-9 (ab2324), and Histone H3 (ab1791) were purchased from Abcam (Cambridge, United Kingdom). Antibodies against cleaved PARP (5625S), HO-1 (86806S), Keap1 (4678S), and p-p53 (9286S) were purchased from Cell Signaling Technology, Beverly (MA, United States). ML385 (SML 1833) was purchased from Sigma-Aldrich (St. Louis, MO, United States).

2.2 Cell Cultures and Treatment

The HL-7702 cells were cultured in DMEM containing 1% penicillin/streptomycin and 10% FBS in a humidified 5%-CO_2 incubator with at 37°C. Ginsenoside Rb1 and TP were dissolved in DMSO and preserved at 4°C. In all experiments, DMSO concentration was always kept below 0.1%. The HL-7702 cells were incubated, with or without pretreatment with ginsenoside Rb1 for 6 h, prior to treatment with 400 nM TP for 48 h. In this study, cells in logarithmic growth phase were used in all experiments.

2.3 Cell Viability Assay

The cells were seeded overnight in 96-well plates at a density of 5.0×10^3 cells/well. Then, cells in pretreatment groups were exposed to 5–20 μM ginsenoside Rb1 for 6 h. Subsequently, the cells were exposed to TP (400 nM) for 48 h. Thereafter, 100 μL of MTT (0.5 mg/ml) working solution was added to the cells, followed by incubation for 4 h. Thereafter, the MTT medium was removed, and 150 μL of DMSO was added to the wells in order to dissolve the resultant formazan crystals. Then, the absorbance of the formazan solution was read at 490 nm in a microplate reader (Thermo Fisher Scientific, NYC, United States).

2.4 LDH Cytotoxicity Assay

The cells were seeded in 96-well plates at a density of 1.0×10^4 cells/well, and they were cultured in DMEM overnight. Subsequent incubation was carried out as described in **Section 2.2**. The activity of LDH in the supernatant was assayed using LDH assay kit.

2.5 TUNEL Staining

The cells were seeded in 6-well plates at a density of 4.0×10^5 cells/well. After exposure to ginsenoside Rb1 and TP or TP alone, the cells in the different groups were treated with 4% paraformaldehyde solution. Then, TUNEL analysis kit was used to determine apoptosis according to the instructions in the kit. Apoptotic cells were identified and photographed under a florescence microscope (BX51-DSU; Olympus, Tokyo, Japan) at ×200 magnification.

2.6 Apoptosis Assay

The cell culture procedure used was as described in **Section 2.2**. After washing with PBS, the cells were re-suspended in 295 μL binding buffer, followed by incubation with. Annexin V-FITC and propidium iodide for 20 min at room temperature, in the dark. Thereafter, the cells were injected into a flow cytometer (BD Biosciences, New Jersey, United States) for fluorescence analysis.

2.7 Measurement of ROS Levels

The using DCFH-DA assay was used to measure the levels of ROS in HL-7702 cells. The cells were cultured as indicated in **Section 2.2**. Then, 10 μM DCFH-DA was added to the cells, followed by incubation at 37°C for 30 min in the dark. The cells were rinsed in PBS and re-suspended in the same PBS prior to injection into a flow cytometer for measurement of levels of ROS.

2.8 Determination of the Oxidative Stress Index

The cells were seeded in 6-well plates at a density of 4.0×10^5 cells/well, and cultured for 24 h. Then, the cells were incubated with 5, 10, and 20 μM of ginsenoside Rb1 for 6 h, followed by incubation with 400 nM TP for 48 h. Thereafter, the cells were centrifuged 10 min at 12,000 rpm and lysed with radio-immunoprecipitation assay (RIPA) buffer. The protein content of the lysate was determined with CA protein quantification kit. The levels of intracellular malondialdehyde (MDA), GSH, and SOD were measured using their respective assay kits.

2.9 Measurement of Mitochondrial Membrane Potential ($\Delta\psi$m)

The assay of mitochondrial membrane potential (MMP) assay was done using JC-1. In normal cells with high mitochondrial membrane potential, a large amount JC-1 in the mitochondrial matrix produces red fluorescence. In contrast, in apoptotic cells, the reduced MMP promotes the transfer of JC-1 to the cytoplasm, where it appears green fluorescence (Luo et al., 2018). Therefore, changes in MMP can be judged by changes in fluorescence of JC-1. In this assay, the cells incubation and drug treatment methods were the same as described in **Section 2.2**. Thereafter, the cells were rinsed in PBS and incubated with in culture medium mixed with JC-1 staining solution at 37°C for 30 min. After washing twice with PBS, the changes in MMP were analyzed in a flow cytometer.

2.10 Cell Cycle Assay

The cells were incubated and treated with drugs as described in **Section 2.2**. After discarding the medium, the cells were digested using trypsin and washed with PBS, followed by re-suspension in 75% ethanol overnight at 4°C. Then, the cells were incubated with propidium iodide (PI) and ribonuclease (RNase) for 30 min in the dark, followed by analysis of cell cycle using a flow cytometry.

2.11 Western Blot Analysis

The methods used for cell culture and drug treatment were as indicated in **Section 2.2**. Total protein was extracted by lysing the cells with ice-cold RIPA buffer (Sigma, St. Louis, MO, United States). The lysate was centrifuged for 10 min at 12,000 rpm, and the protein content of the supernatant was determined using BCA protein assay kit. In a parallel experiment, the mitochondrial and cytosolic fractions were separated using the ProteoExtract® Cytosol/Mitochondria Fractionation Kit (Millipore, Billerica, MA, United States) according to the manufacturer's instructions. Then, equal amounts of target protein were separated using sodium dodecyl sulfate-polyacrylamide gel electrophoresis (SDS-PAGE) and transferred to a polyvinylidene fluoride (PVDF) membrane. The protein-loaded membranes were blocked with 5% skim milk in TBST buffer (25 mM Tris, 150 mM NaCl, and 0.1% Tween 20) pH 7.4 for 1 h at room temperature. Thereafter, the membrane was incubated overnight at 4°C with specific primary antibodies against cytochrome *c* (1:1,000), Bcl-2 (1:1,000), Bax (1:1,000), Fas (1:1,000), p53 (1:1,000), p21 (1:1,000), p-p53 (1:1,000), CDK2 (1:1,000), cyclin A (1:1,000), cyclin E (1:1,000), cleaved-caspase-3 (1:1,000), cleaved-PARP (1:1,000), cleaved-caspase-9 (1:1,000), Nrf2 (1:1,000), Keap1 (1:1,000), HO-1 (1:1,000), NQO1 (1:1,000), COX IV (1:1,000), Histone H3 (1:1,000), and β-actin (1:1,000). Then, the immunoblots were incubated with and corresponding secondary antibodies were incubated together at room temperature for 1 h. Finally, the relative expression levels were determined using intensive ECL detection system (UVP, United States), with β-actin and COX IV as loading controls (cytosolic and mitochondrial, respectively).

2.12 Co-Immunoprecipitation Assay

Following treatment with ginsenoside Rb1, the HL-7702 cells were exposed to TP for 48 h. Then, the cells were lysed using protease inhibitor-containing RIPA buffer so that Nrf2 existed in the cells in the form of Keap1/Nrf2 complex. The lysed product was incubated with corresponding primary antibody overnight at 4°C. Before being mixed with the cell lysate, protein A/G magnetic beads were washed thrice with RIPA buffer, followed by centrifugation for 3 min at 3,000 rpm. The mixture was incubated at 4°C for 4 h to ensure that the antibody was bound to the protein A/G magnetic beads. Then, 2 μg anti-Keap1 antibody or anti-Nrf2 antibody was added to the cell lysate and incubated for 24 h, after which the complex was washed 3–5 times, and boiled for 5 min in SDS sample buffer. Then, the supernatant was subjected to SDS-PAGE electrophoresis to obtain Nrf2 or Keap1 antibody immunoblot.

2.13 siRNA Transient Transfection

Nrf2 was silenced in HL-7702 cells by using Nrf2 siRNA. The following siRNA-encoding DNA oligonucleotides containing inner palindromic sequences (sense: 5′-CGAGAAGUGUUU GACUUUATT-3′; antisense: 5′-UAAAGUCAAACACUUCUC GTT-3′, and negative control siRNA (NC siRNA) (sense: 5′-UUC UCCGAACGUGUCACGUTT-3′; antisense: 5′-ACGUGACAC GUUCGGAGAATT-3′) were synthesized (GenePharma, United States). HL-7702 cells were transiently transfected with Nrf2 siRNA or NC siRNA by using Lipofectamine 2000 (Invitrogen, Carlsbad, CA, United States) according to the associated protocol. Moreover, at 24 h post-transfection, the cells were treated by indicated drugs and collected for Western blot analysis.

2.14 Statistical Analysis

All experimental data were expressed as mean ± S.D (n = 3). GraphPad Prism 8.0 was used to analyze the experiment data. Statistical differences were determined with one-way ANOVA and LSD test. Values of $p < 0.05$ were considered indicative of statistically significant differences.

3 RESULTS

3.1 Ginsenoside Rb1 Inhibited Triptolide-Induced Cytotoxicity in HL-7702 Cells

The HL-7702 cells were exposed with 100, 200, 400, and 800 nM of TP for 24, 48, and 72 h, respectively, aim at determining the dose and treatment time of TP according to the result of cell viability using MTT assay. Compared with control group, TP dose-dependently reduced the viability of HL-7702 cells, suggesting that it exerted toxic effects on HL-7702 cells (**Figure 2A**). After repeated experiments, it was found that 400 nM TP treat for 48 h had stable and obvious cytotoxicity on HL-7702 cells. As a result, 400 nM TP was used as the condition in the subsequent experiments. In contrast, ginsenoside Rb1 (at concentrations of 5, 10, and 20 μM) dose-dependently enhanced the viability of HL-7702 cells (**Figure 2B**). Therefore, 5, 10, and 20 μM ginsenoside Rb1 were used in follow-up experiments. The HL-7702 cells were treated with ginsenoside Rb1 at doses of 5, 10, and 20 μM for 6 h, followed incubation with 400 nM TP for 48 h. Results from MTT assay showed that the viability of ginsenoside Rb1-treated cells at each of the three concentrations was markedly higher than that of the control group, indicating that ginsenoside Rb1 protected HL-7702 cells from TP-induced toxicity (**Figure 2C**). Results from LDH assay were consistent with those from cell viability assay: ginsenoside Rb1 reversed the TP-induced LDH release in a dose-dependent manner (**Figure 2D**). These results suggest that ginsenoside Rb1 dose-dependently inhibited TP-induced cytotoxicity in HL-7702 cell.

3.2 Ginsenoside Rb1 Inhibited Triptolide-Induced HL-7702 Cell Apoptosis

TUNEL nuclear staining and Annexin V-FITC/PI flow cytometry were used to determine the protective effect of ginsenoside Rb1 against TP-induced apoptosis in HL-7702 cells. The percentage of apoptosis i.e., TUNEL-positive cells due to TP treatment was significantly increased (**Figures 3A,B**). In contrast, ginsenoside Rb1 pretreatment at doses of 5, 10, and 20 μM inhibited TP-induced apoptosis. The purpose of Annexin V-FITC/PI flow cytometry assay was to quantify the degree of apoptosis in each group of treated cells. In 5, 10, and 20 μM ginsenoside

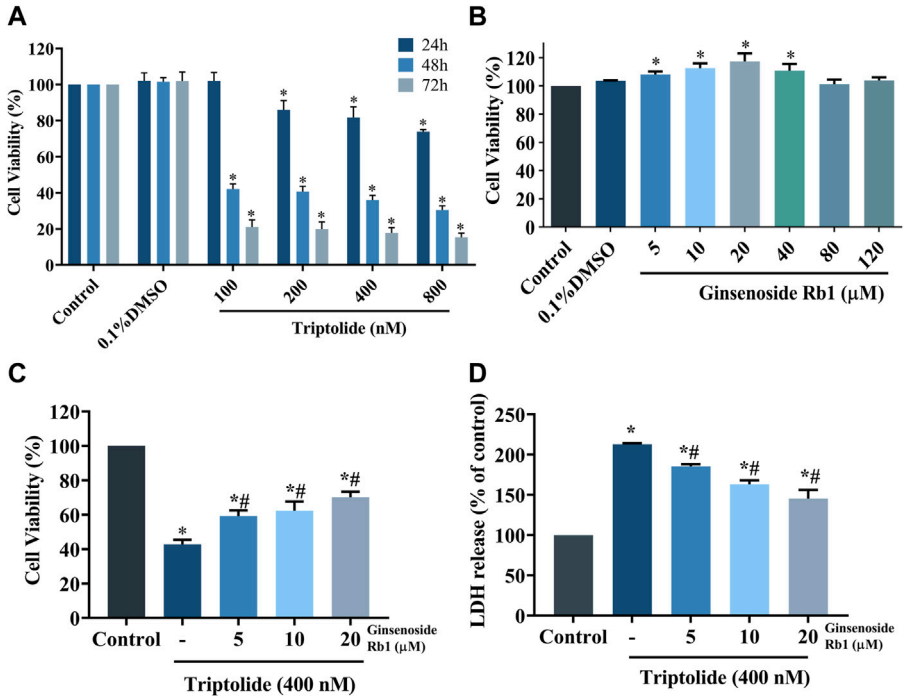


FIGURE 2 | Protective effect of ginsenoside Rb1 on TP-induced cytotoxicity in HL-7702 cells. **(A)** Viability of HL-7702 cells after treatment with different concentrations of TP for different time durations, as determined with MTT assay. **(B)** Viability of HL-7702 cells treated with various concentrations of ginsenoside Rb1 for 24 h. **(C)** HL-7702 cells were pretreated with ginsenoside Rb1 for 6 h, and then exposed to 400 nM TP for 48 h, after which cell viability was determined with MTT assay. **(D)** Protective effect of ginsenoside Rb1 on TP-induced LDH release from HL-7702 cells. LDH is mainly located in the cytoplasm, and its release indicates the damage of cell membrane integrity. Data are expressed as mean ± S.D, $n = 3$. ($^{*}p < 0.05$ *vs.* untreated cells in control group; $^{\#}p < 0.05$ *vs.* TP-only group).

Rb1-pretreatment groups, the percentage of viable HL-7702 cells was markedly higher than that in cells treated with TP only, indicating that ginsenoside Rb1 suppressed apoptosis induced by TP (**Figure 4A**). Moreover, the percentages of early and late apoptotic cells were markedly increased in the TP-treated group, but the pretreatment ginsenoside Rb1 effectively reversed this change (**Figure 4B**). It is known that NAC, a type of ROS inhibitor, partially blocks TP-induced apoptosis. Following treatment with NAC, the percentage of viable cells was significantly increased, while the percentage of early and late apoptotic cells were decreased, which were similar to the effect of ginsenoside Rb1. These results suggested that ginsenoside Rb1 may inhibit the production of ROS, thereby inhibiting the occurrence of apoptosis (**Figures 4A,B**). Overall, the results indicated that ginsenoside Rb1 suppressed TP-induced HL-7702 cell apoptosis.

3.3 Effect of Ginsenoside Rb1 on Triptolide-Induced Cell Cycle Arrest in HL-7702 Cells

The effect of ginsenoside Rb1 on the cell cycle distribution in TP-treated HL-7702 cells was determined with flow cytometry. Treatment of the cells with TP led to marked increases in the percentages of cell in G2/M and S phases of the cell cycle, but the percentage of cell in the G1 phase was significantly reduced (**Figure 5A**). In contrast, ginsenoside Rb1 pretreatment significantly mitigated G2/M and S phase cell cycle arrest induced by TP. These results are in agreement with the expression levels of proteins related in the G2/M and S phases. In TP-treated group, the protein expression levels of p53, p-p53, and p21 were markedly increased, but the protein expressions of cyclin A, cyclin E, and CDK2 significantly downregulated (**Figure 5B**). However, ginsenoside Rb1 pretreatment effectively reversed the pattern of expressions of these proteins. Thus, ginsenoside Rb1 pretreatment effectively inhibited TP-induced cell cycle arrest in HL-7702 cells.

3.4 Effect of Ginsenoside Rb1 on the Modulation of Apoptosis-Related Proteins in Triptolide-Treated HL-7702 Cells

The expressions of apoptosis-related proteins were assayed with Western blotting so as to further identify the potential regulatory mechanism involved in the effect of ginsenoside Rb1 on cell apoptosis. In the group treated with TP only, the protein expressions of Fas (one of the most typical death receptors) and Bax were significantly increased. However, these increases were reversed by ginsenoside Rb1 in a dose-dependent manner (**Figure 6**). Exposure of the HL-7702 cells to 400 nM TP for 48 h resulted in significant increases in the protein expressions of cleaved caspase-3, cleaved PARP, and cleaved caspase-9.

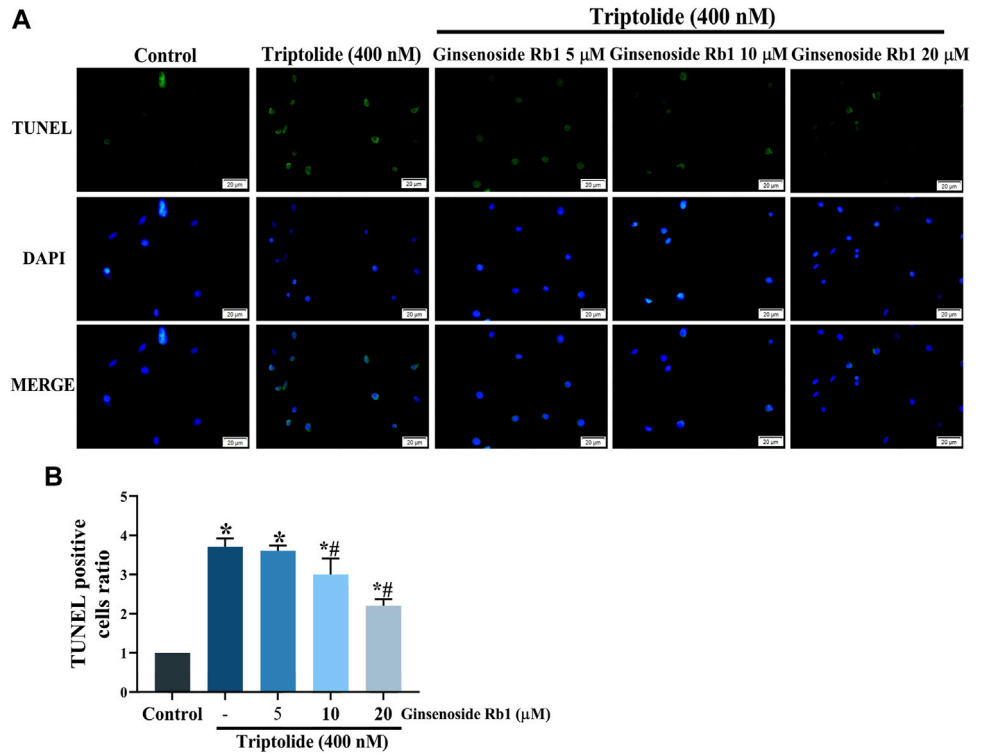


FIGURE 3 | Protective effect of ginsenoside Rb1 against apoptosis in HL-7702 cells. **(A)** TUNEL staining of apoptotic cells under fluorescence microscopy (scale bar = 20 μm). TUNEL reagents were used to label the apoptotic cells and all cell nuclei were stained with DAPI. **(B)** Histogram of proportion of TUNEL positive cells. Data are expressed as mean ± S. D, $n = 3$. (*$p < 0.05$ *vs.* untreated cells in control group; $^{\#}p < 0.05$ *vs.* TP-only group).

However, these increases were dose-dependently reversed by pretreatment with ginsenoside Rb1. These results indicated that ginsenoside Rb1 inhibited TP-induced cell apoptosis through suppression of the activation of extrinsic and intrinsic apoptotic pathways.

3.5 Ginsenoside Rb1 Suppressed Triptolide-Induced Oxidative Stress Activation and Mitochondrial Dysfunction in HL-7702 Cells

3.5.1 Ginsenoside Rb1 Inhibited Triptolide-Induced Oxidative Stress in HL-7702 Cells

High levels of ROS and MDA, and reduced levels of SOD and GSH, are indicators of oxidative stress, and apoptosis (Aleksandrova et al., 2021). As expected, TP markedly increased the levels of ROS and MDA, when compared with untreated cells, while it decreased the levels of SOD, and GSH (**Figures 7A,B**). In contrast, the levels of intracellular ROS and MDA were decreased in ginsenoside Rb1-pretreated groups, while GSH and SOD levels were increased. These results indicated that ginsenoside Rb1 blocked TP-induced oxidative stress. Moreover, the results indicated that NAC reduced HL-7702 cell apoptosis, and demonstrated that ROS overproduction was correlated with oxidative stress-induced apoptosis (**Figure 4A**). Overall, ginsenoside Rb1 protected HL-7702 cells from oxidative stress-mediated apoptosis.

3.5.2 Effect of Ginsenoside Rb1 on Triptolide-Induced Mitochondrial Dysfunction in HL-7702 Cells

Studies have revealed that loss of MMP increases the permeability of the mitochondrial outer membrane, resulting in severe mitochondrial dysfunction due to rapid leakage of cytochrome *c* from the mitochondria into the cytoplasm (Chen et al., 2016). Compared with untreated cells, the MMP of HL-7702 cells was markedly decreased after treatment with TP only (**Figures 8A,B**). However, in ginsenoside Rb1+TP groups, MMP was markedly elevated in a concentration-dependent manner. Bax (a proapoptotic protein) and Bcl-2 (an antiapoptotic protein) are the apoptosis regulatory proteins involved in the mitochondria-dependent apoptotic pathway (Jia et al., 2015). Compared with untreated cells, treatment with TP markedly enhanced Bax/Bcl-2 ratio in HL-7702 cells (**Figure 6**). However, pretreatment with 5–20 μM ginsenoside Rb1 effectively reversed the TP-mediated expression patterns of Bax and Bcl-2. Besides, there was marked reduction in amount of cytochrome *c* transferred to the cytoplasm in ginsenoside Rb1+TP groups, when compared to the corresponding level in cells treated with TP lone (**Figure 8C**). These results suggested that the mechanism underlying the effect of ginsenoside Rb1 on TP-induced apoptosis of HL-7702 cells may involve the repair of mitochondrial dysfunction.

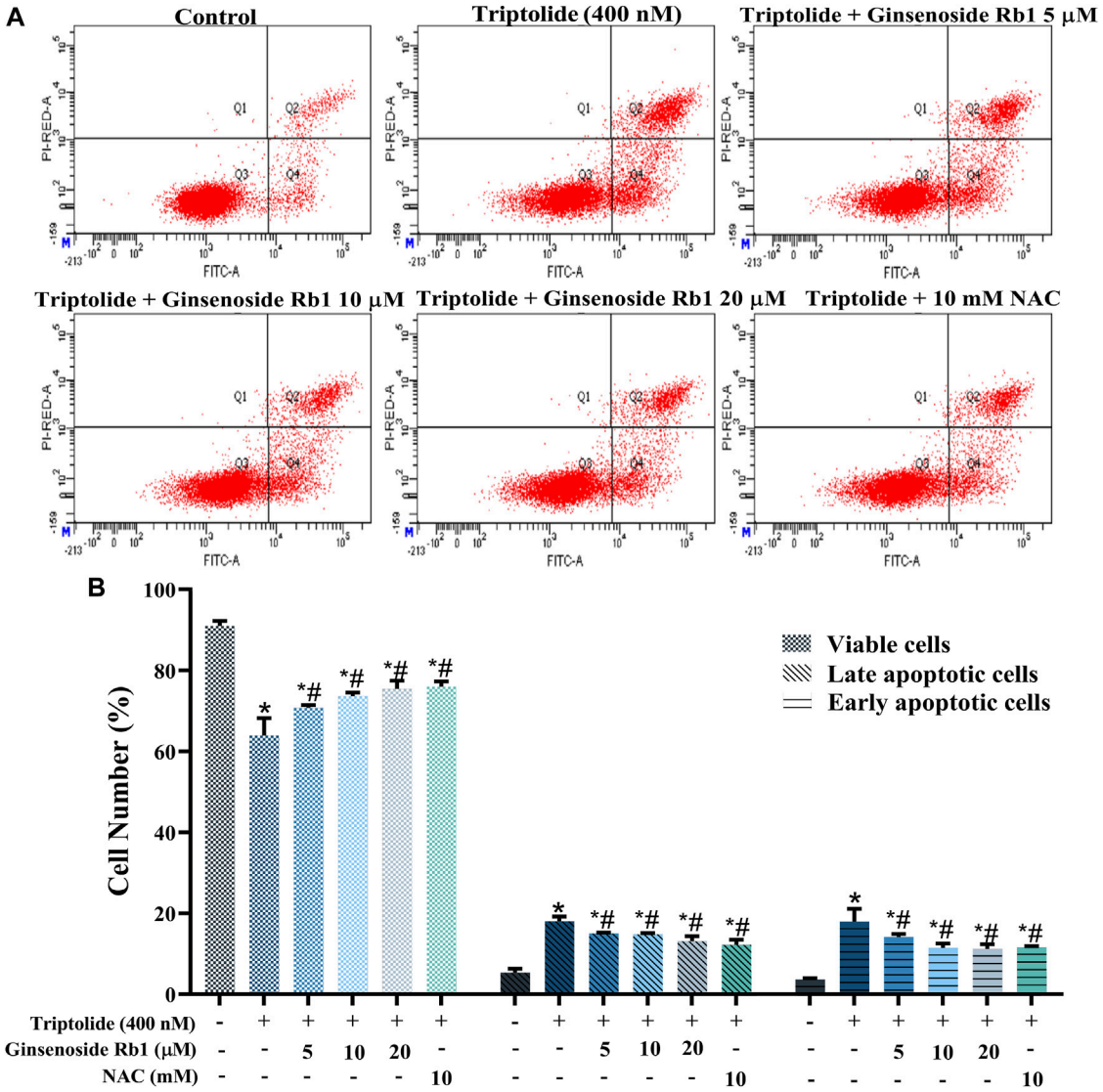


FIGURE 4 | Protective effect of ginsenoside Rb1 against apoptosis in HL-7702 cells. **(A)** Apoptosis of HL-7702 cells treated with 5, 10, 20 μM ginsenoside Rb1, as determined using Annexin V-FITC/PI double staining and flow cytometry. The Q3 region represents viable cells, while Q4 region represents early apoptotic cells. The Q2 region represents late apoptotic cells, while Q1 region represents necrotic cells or mechanical damaged cells. **(B)** Histogram showing the average percentages of viable, early apoptotic, and late apoptotic cells. Data are expressed as mean ± S.D, $n = 3$. (*$p < 0.05$ *vs.* untreated cells in control group; $^{\#}p < 0.05$ *vs.* TP-only group).

3.6 Ginsenoside Rb1 Activated Keap1/Nrf2/ARE Pathway in HL-7702 Cells Under Oxidative Stress

It has been demonstrated that Nrf2 plays a central role in the cellular defense system against oxidative stress: Nrf2 activation upregulates the expressions of downstream antioxidant enzymes, especially NQO1 and HO-1 (Zhang et al., 2008). In this study, TP treatment significantly downregulated the expressions of total Nrf2, nuclear Nrf2, NQO1, and HO-1 and simultaneously increased the protein expression level of Keap1 in the cytoplasm, relative to untreated cells (**Figures 9A,B**). However, these TP-induced changes were significantly reversed by treatment with ginsenoside Rb1. Under regular physiological conditions, Nrf2 is rapidly ubiquitinated and degraded upon binding to Keap1, thereby inhibiting its nuclear translocation (Nguyen et al., 2009). Results from immunoprecipitation assays showed that ginsenoside Rb1 pretreatment promoted the dissociation of Nrf2/Keap1 complex in the cytoplasm (**Figure 9C**). In addition, the result of Nrf2 inhibitor experiment showed that ML385 could block the ginsenoside Rb1-mediated increase in the expression of total-Nrf2 protein in TP-treated HL-7702 cells (**Figure 9D**). What's more, Nrf2 siRNA was used to knockdown the expression of Nrf2, and the results showed that the apoptosis of Nrf2 siRNA group was significantly higher than that of NC siRNA, while ginsenoside Rb1 effectively inhibited Nrf2 siRNA-induced apoptosis. Meanwhile, the results of WB assay showed that ginsenoside

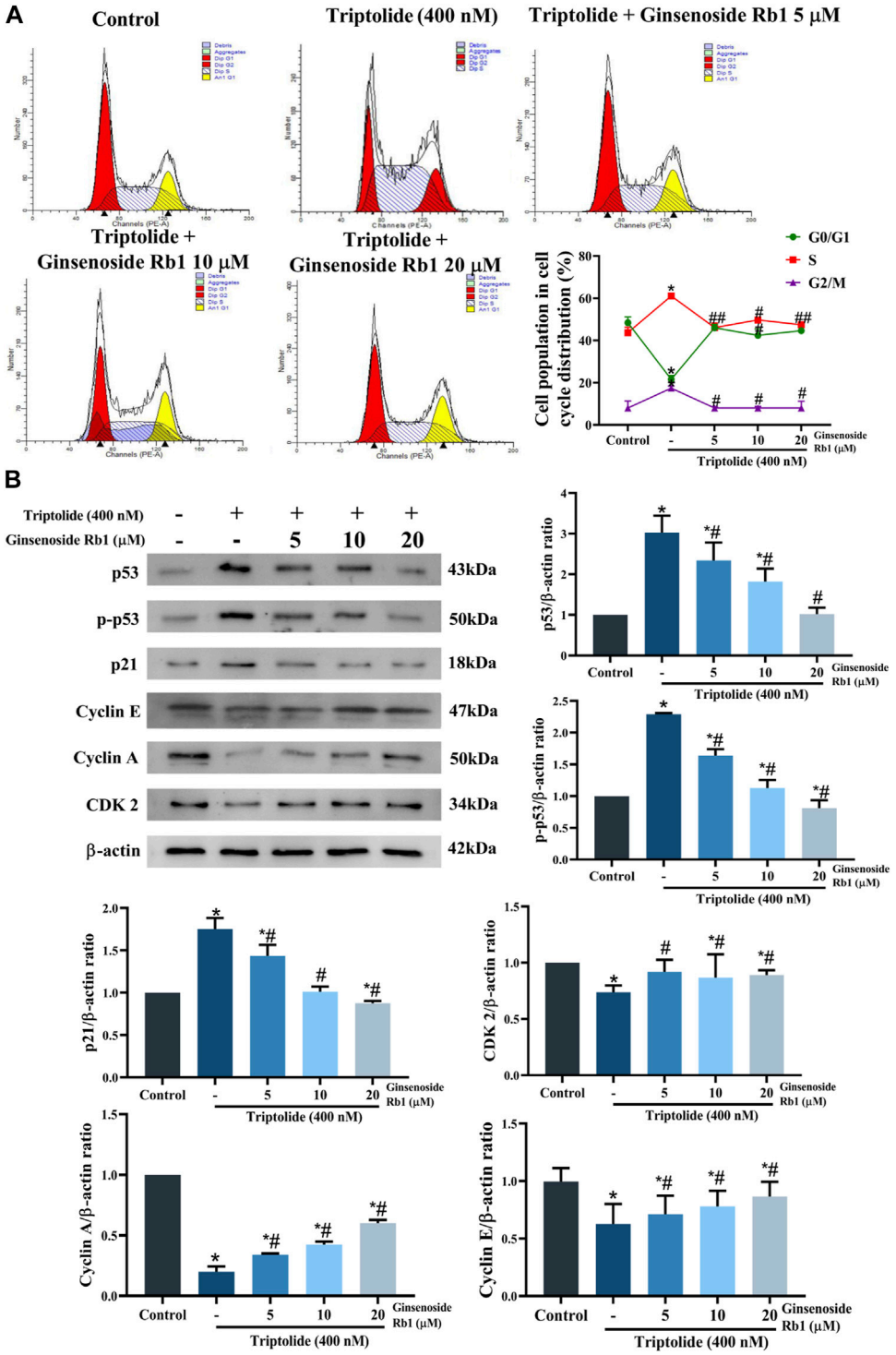


FIGURE 5 | Effect of ginsenoside Rb1 on TP-induced cell cycle arrests in HL-7702 cells. **(A)** Effect of 5, 10, and 20 μM ginsenoside Rb1 on the cell cycle. **(B)** Effect of 5, 10, and 20 μM ginsenoside Rb1 on the expressions of proteins related to the cell cycle, as determined with Western blotting. Data are expressed as mean ± S.D, $n = 3$. (*$p < 0.05$ *vs.* untreated cells in control group; $^{\#}p < 0.05$ *vs.* TP-only group).

Rb1 effectively reversed the decrease of Nrf2 expression induced by Nrf2 siRNA (**Figure 9E**). Above all, these results indicated that ginsenoside Rb1 effectively repaired TP-induced oxidative stress damage in HL-7702 cells through activation of the Keap1/Nrf2/ARE antioxidant pathway, thereby regulating cellular oxidation-antioxidation homeostasis.

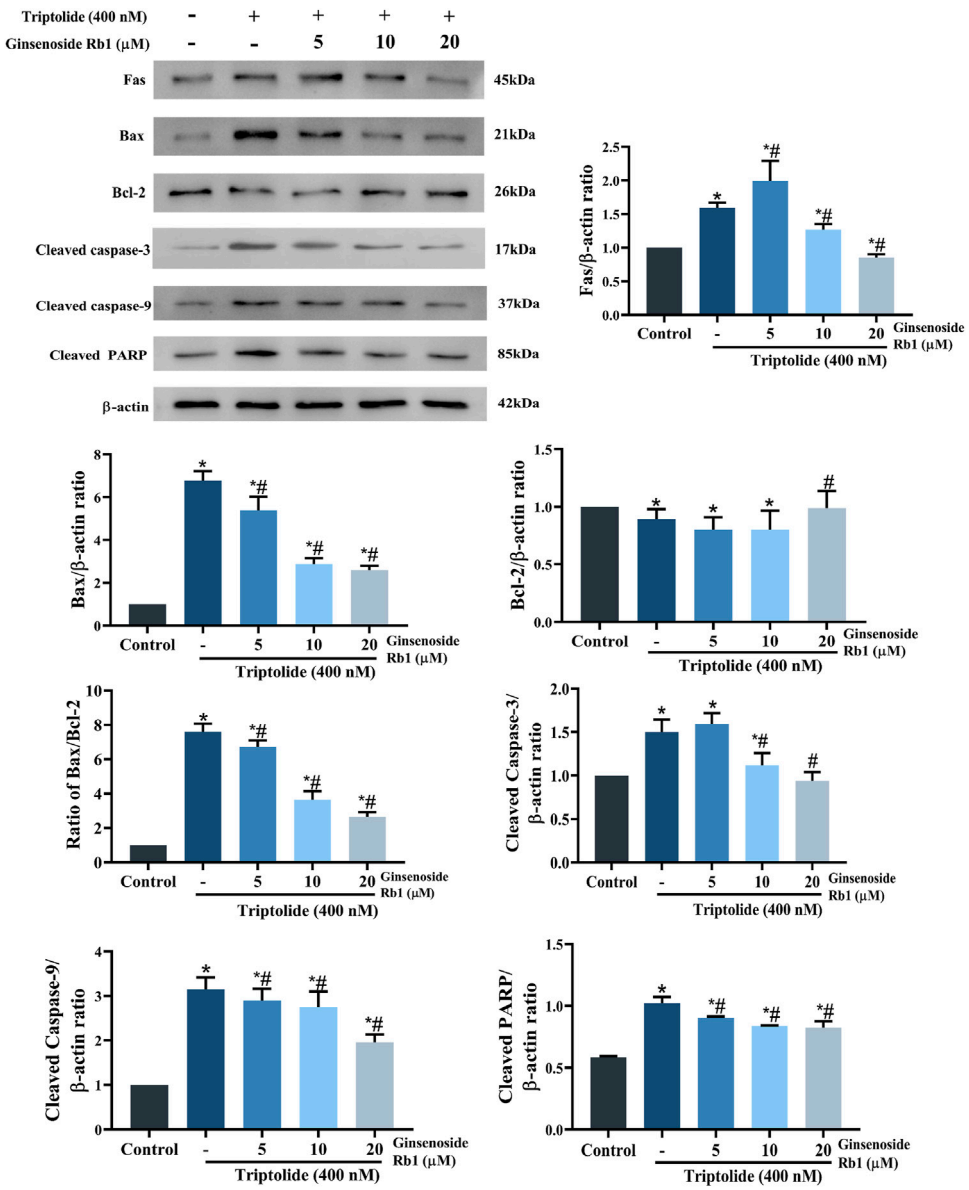


FIGURE 6 | Effect of ginsenoside Rb1 on the expressions of apoptosis-related proteins in TP-treated HL-7702 cells. Data are expressed as mean ± S.D, $n = 3$. (*$p <$ 0.05 *vs.* untreated cells in control group; $^{\#}p < 0.05$ *vs.* TP-only group).

4 DISCUSSION

Triptolide (TP), the main bioactive compound in TWHF, exerts significant antineoplastic, and anti-inflammatory properties. (Yang et al., 2017). However, TP is also the main component involved in the hepatotoxicity of TWHF, which greatly limits its clinical application (Zou et al., 2020; Zheng et al., 2021). Ginsenoside Rb1 is a panaxadiol saponin extracted from *ginseng*, *Panax notoginseng*, American ginseng, and other Araliaceae plants. It has been reported that ginsenoside Rb1 exerts multiple pharmacological actions such as cerebral protection, cardiovascular system protection, immunoregulation and anti-leukemia effects (Zymone et al., 2018; Fan et al., 2019; Cao et al., 2020). Although the pharmacological effects of ginsenoside Rb1 have been gradually understood over the years, its potential hepatotoxic effect (especially TP-induced hepatotoxicity), and the mechanism involved, remain unclear. Results from MTT and LDH assays indicated that TP exerted obvious cytotoxic effect on HL-7702 cells. However, HL-7702 cell viability was increased after treatment with ginsenoside Rb1, indicating, significant attenuation of TP-induced cytotoxic effect on the cells. Apoptosis is triggered by exogenous and endogenous pathways, and the caspase family plays a crucial role in both pathways (Shao et al., 2019; Wang et al., 2019b). Fas is one of the most typical death receptors in the exogenous death receptor-

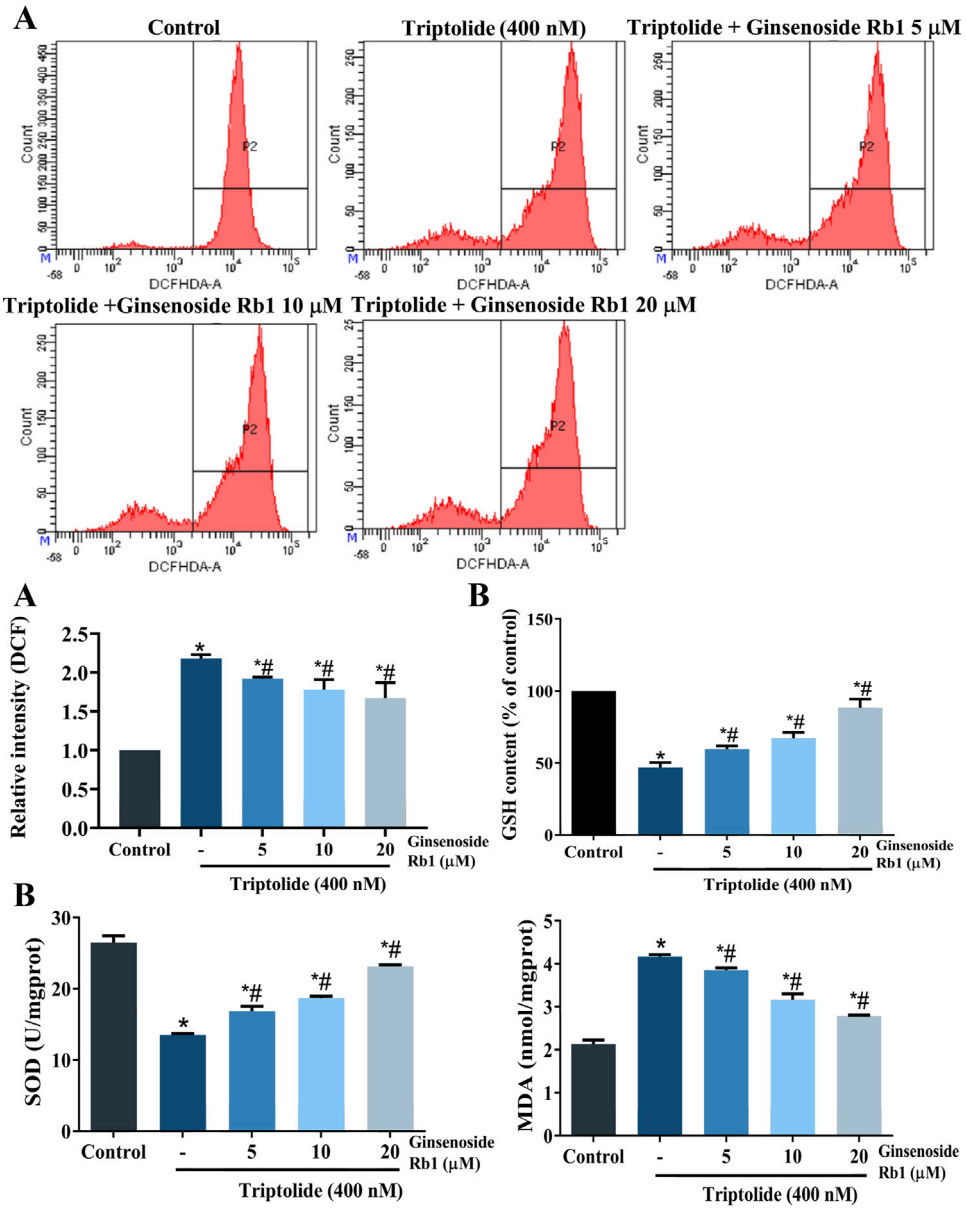


FIGURE 7 | Effect of ginsenoside Rb1 on ROS levels and antioxidant enzyme activity in TP-treated HL-7702 cells. **(A)** Effects of TP and ginsenoside Rb1 on ROS levels in HL-7702 cells, as determined with DCFH-DA staining and flow cytometry. Intracellular ROS could oxidize nonfluorescent and colorless DCFH-DA into DCF, which could emit fluorsecence. Thus, fluorescence intensity coule reflect the level of intracellular ROS. **(B)** Effect of TP and ginsenoside Rb1 on levels of MDA, SOD, and GSH. Data are expressed as mean ± S.D, $n = 3$. (*$p < 0.05$ *vs.* untreated cells in control group; $^{\#}p < 0.05$ *vs.* TP-only group).

mediated apoptosis pathway. It recruits Fas-associated death domain (FADD) after binding to FasL (the specific ligand of Fas), thereby activating caspase-8. Then the release of caspase-8 into the cytoplasm activates caspase-3, ultimately triggering apoptosis (Xu et al., 2020). The endogenous apoptotic pathway is also called mitochondria-dependent apoptotic pathway. The Bcl-2 protein family and cytochrome *c* are involved in the mitochondria-dependent apoptotic pathway (Berg et al., 2013). Bax is one of the important pro-apoptotic proteins in Bal-2 family. The transfer of activated Bax into the mitochondria impairs mitochondrial membrane permeability and causes increased of cytochrome *c* into the cytoplasm. In the presence of ATP, cytochrome *c* forms a polymer complex with apoptosis protease activating factor-1 (Apaf-1), and then activates pro caspase-9 to form apoptotic bodies composed of cytochrome *c*, caspase-9, and Apaf-1. Subsequently, the apoptotic bodies enhance the transcription and translation of downstream proteins, especially caspase-3, eventually leading to apoptosis (Jia et al., 2015; Li et al., 2017; Chen et al., 2018). However, Bcl-2 (one of the most typical anti-apoptotic proteins) suppresses

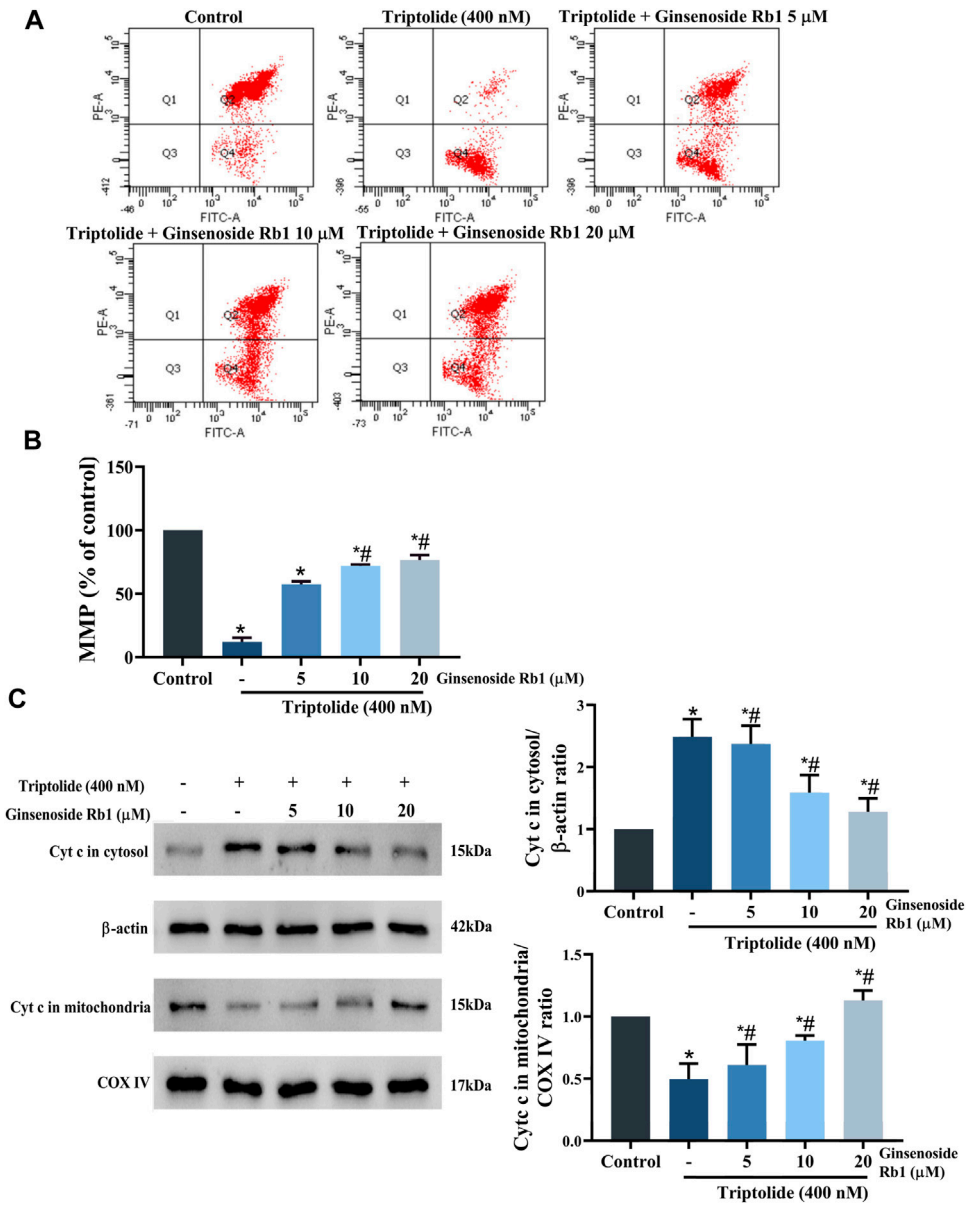


FIGURE 8 | Effect of ginsenoside Rb1 on MMP in HL-7702 cells treated with TP. **(A)** Changes in MMP in the cells after treatment with TP and ginsenoside Rb1, as measured using JC-1 staining. JC-1 is a mitochondria-specific lipophilic cationic fluorescence dye able to selectively enter the mitochondria. When the mitochondrial membrane potential decreased, JC-1 transferred from the mitochondria to the cytoplasm, and the fluorescence changed from red to green. **(B)** Histogram of average JC-1 fluorescence in cells. **(C)** Effect of TP and ginsenoside Rb1 on the quantity of cytochrome *c* in the cytosol and mitochondria, as determined using Western blotting, with β-actin and COX IV as loading controls (cytosolic and mitochondrial, respectively). Data are expressed as mean ± S.D, $n = 3$. (*$p < 0.05$ *vs.* untreated cells in control group; $^{\#}p < 0.05$ *vs.* TP-only group).

Bax activity and plays an anti-apoptotic part by inhibiting cytochrome *c* release and attenuating mitochondrial membrane damage (Xu et al., 2019c). This study has demonstrated that TP treatment markedly upregulated the expressions of cleaved caspase-3, cleaved PARP, cleaved caspase-9, and Fas, and increase the ratio of Bax/Bcl-2 in HL-7702 cells. In addition, TP induced increased release of cytochrome *c*. However, these TP-induced changes in HL-7702 cells were suppressed by pretreatment with ginsenoside Rb1. Overall, these results indicated that ginsenoside Rb1 effectively protected the HL-7702 cells from apoptosis induced by TP through inhibition of death receptor-mediated and mitochondrial-dependent apoptotic pathways.

Mitochondrial dysfunction caused by oxidative stress is an important event in apoptosis. Excessive ROS in cells is a sign of oxidative stress (Li et al., 2018; Chen et al., 2020). Slight increases in intracellular ROS levels are beneficial to cell proliferation, while excessive ROS cause structural changes in related proteins and

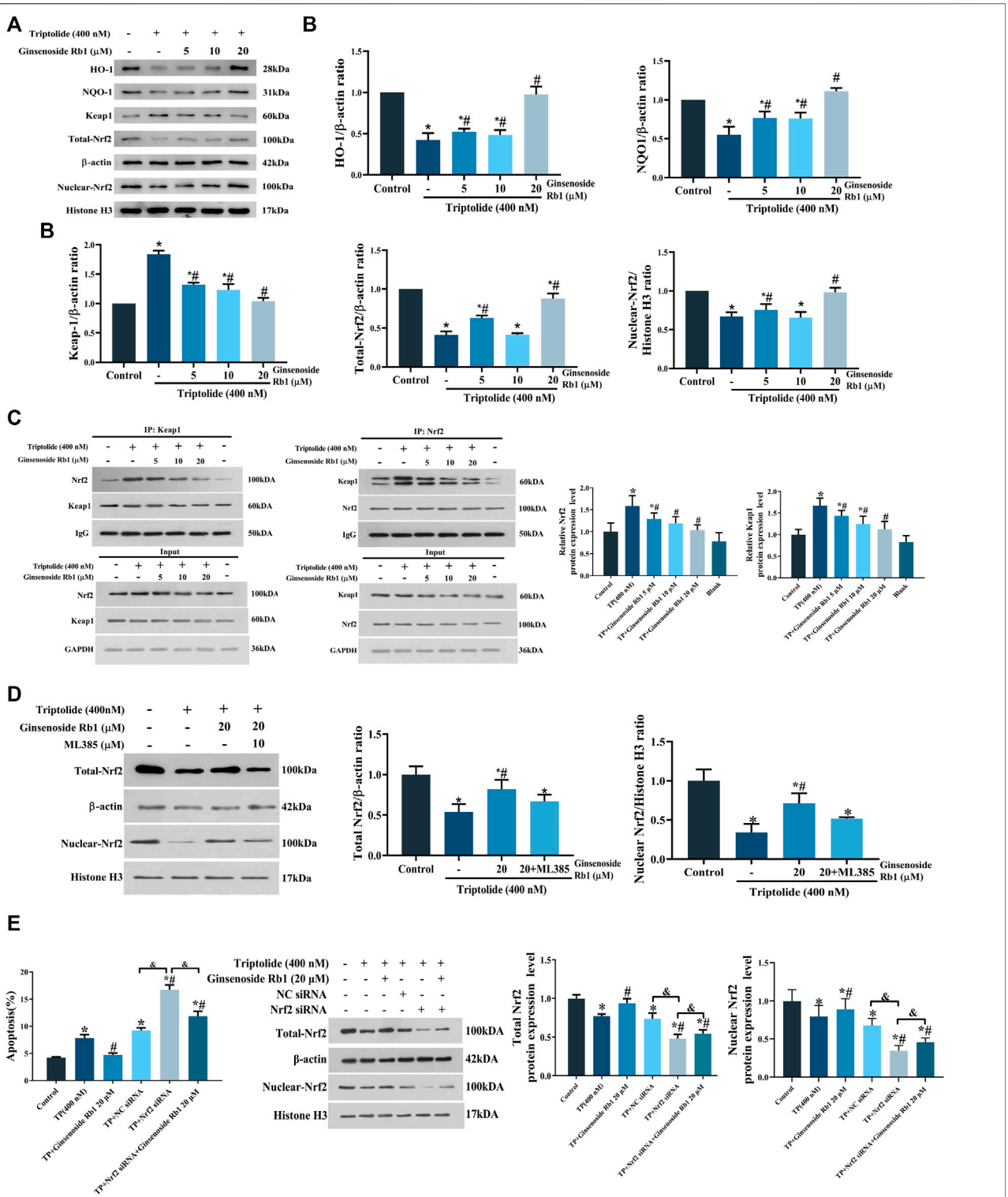


FIGURE 9 | Effect of ginsenoside Rb1 on the Keap1/Nrf2/ARE pathway in HL-7702 cells treated with TP. **(A)** Effect of different concentrations of ginsenoside Rb1 on protein expression levels of Keap1, nuclear Nrf2, total Nrf2, NQO1, and HO-1, as was determined using Western blotting. Histone H3 was used as an internal control for nucleoprotein, while β-actin was used as internal control for total protein. **(B)** Quantitative protein bands of Keap1, nuclear Nrf2, total Nrf2, NQO1, and HO-1, as determined using optical density analysis. **(C)** Effect of ginsenoside Rb1 on the production of Keap1/Nrf2 complex, as determined using co-immunoprecipitation assay. **(D)** Expression levels and quantitative protein bands of Nrf2 after adding ML385 to the high-dose ginsenoside Rb1+TP group, as determind with Western blotting and optical density analysis. **(E)** The effect of Nrf2 knockdown on apoptosis and Nrf2 expression measured by flow cytometry and Western blotting. Data are expressed as mean ± S.D, $n = 3$. ($^{*}p < 0.05$ *vs.* untreated cells in control group; $^{\#}p < 0.05$ *vs.* TP-only group; $^{\&}p < 0.05$ indicates significant differences between different groups).

lipid peroxidation, resulting in mitochondrial dysfunction which is manifested in increased mitochondrial membrane permeability, decreased mitochondrial membrane potential, and increased cytochrome *c* release (Chen et al., 2016; Kong et al., 2018). SOD and GSH are typical antioxidants, which inhibit oxygen free radical production and scavenge lipid peroxides produced by ROS (Song et al., 2018). In this study, TP markedly increased intracellular ROS levels and Bax/Bcl-2 ratio in HL-7702 cells, and reduced the MMP and levels of SOD and GSH, while the MDA level was increased. However, ginsenoside Rb1 pretreatment reversed the TP-induced increases in levels of ROS and MDA, and increased the levels of SOD and GSH. Moreover, it was observed that NAC pretreatment markedly reversed TP-induced apoptosis in HL-7702 cells. In general, these results have demonstrated that ginsenoside Rb1 effectively inhibited TP-induced oxidative stress and promoted the antioxidant capacity of HL-7702 cells.

The Nrf2 pathway is considered to be an important route for combating oxidative damage caused by excessive ROS (Liu et al., 2018). Normally, Nrf2 exists in the cytoplasm in the form of Keap1/Nrf2 complex. When the levels of intracellular ROS increase, Nrf2 binds to ARE in the nucleus, thereby upregulating the expressions of HO-1, and NQO-1 (Yang et al., 2020). In this study, TP markedly reduced the levels of total Nrf2 and nuclear Nrf2, while ginsenoside Rb1 effectively reversed these changes. Moreover, ginsenoside Rb1 suppressed the production of Nrf2/Keap1 complex. Addition of ML385 to the high-dose ginsenoside Rb1+TP group blocked the increase of the total Nrf2 expression. In addition, Nrf2 siRNA was used to knockdown the expression of Nrf2 in HL-7702 cells. The results indicated that ginsenoside Rb1 could significantly inhibit the apoptosis of HL-7702 cells and reverse the decrease of Nrf2 expression induced by Nrf2 siRNA. Thus, ginsenoside Rb1 effectively activated antioxidant defenses through stimulation of the Keap1/Nrf2/ARE pathway. Pretreatment with ginsenoside Rb1 triggered the transcription and translation of downstream antioxidant proteins such as NQO-1, and HO-1, indicating that it played an antioxidant role. The activation of Keap1/Nrf2/ARE signaling pathway appears to be one of the crucial mechanisms through which ginsenoside Rb1 protected HL-7702 cells from TP-induced oxidative damage.

Studies have shown that oxidative stress may cause DNA damage and cell cycle arrest (Samikkannu et al., 2015). It has been reported that p53 mediates oxidative stress in cells with irreparable DNA damage, and induces apoptosis in concert with other apoptotic proteins e.g., Bax (Hori et al., 2013). The combination of cyclin A and CDK2 or CDK1 regulates S phase and mitosis (Wang et al., 2019b). Cyclin E-CDK2 complex regulates the duplication of intracellular chromosomes which promote the entry of cells into the S phase, and on entering the G2 phase, there is a gradual decrease in cyclin E content (Shang et al., 2020). Moreover, p21 is one of the most typical cyclin-dependent kinase inhibitors. By binding to cyclin and CDK, p21 inactivates the cyclin-CDK complex, and blocks each stage of the cell cycle (Lee et al., 2017). In this study, the HL-7702 cells were arrested at G2/M and S phases after treatment with TP, and TP upregulated the expressions of p21, p-p53, and p53, while downregulated the expressions of cyclin A, cyclin E and CDK2. However, these expression patterns were effectively reversed by ginsenoside Rb1 pretreatment. These results indicated that excessive ROS production caused DNA damage, and further led to arrest of HL-7702 cells at G2/M and S phases of the cell cycle, and mitochondria-dependent apoptosis. Therefore, it can be hypothesized that ginsenoside Rb1 protected HL-7702 cellular DNA from oxidative damage by inhibiting ROS production, thereby indirectly reversing G2/M and S cell cycle arrest while inhibiting endogenous apoptosis pathway.

5 CONCLUSION

The results of this study have shown that ginsenoside Rb1 protects HL-7702 cells from TP-induced apoptosis and cell cycle arrest via activation the Keap1/Nrf2/ARE pathway. This study has reported, for the first time, that ginsenoside Rb1 can alleviate TP-induced cytotoxicity in HL-7702 cells, and its potential mechanism is elucidated from the perspective of combination medication, providing new strategies for clinical treatment of TP-induced hepatotoxicity.

DATA AVAILABILITY STATEMENT

The original contributions presented in the study are included in the article/Supplementary Material, further inquiries can be directed to the corresponding authors.

AUTHOR CONTRIBUTIONS

LY, XD, XY, and JN designed the study. CY, KW, ML, DY, YX, and HP conducted the experiments. HP and LY conducted the data analyses and wrote the paper. All authors have reviewed and approved the final version of the article.

FUNDING

This study was generously supported by the Fundamental Research Funds for the Central Universities (No. 2020-JYB-ZDGG-046).

REFERENCES

Aleksandrova, K., Koelman, L., and Rodrigues, C. E. (2021). Dietary Patterns and Biomarkers of Oxidative Stress and Inflammation: A Systematic Review of Observational and Intervention Studies. *Redox Biol.* 42, 101869. doi:10.1016/j.redox.2021.101869

Cao, L., Gao, Y., Zhu, J., Zhang, J., Dong, M., and Mao, Y. (2020). Protective Action of the Ginsenoside Rh3 in a Rat Myocardial Ischemia-Reperfusion Injury Model by Inhibition of Apoptosis Induced via P38 Mitogen-Activated Protein Kinase/caspase-3 Signaling. *J. Int. Med. Res.* 48 (12), 300060520969090. doi:10.1177/0300060520969090

Cao, Y., Dai, F., Li, Y., Jia, L., Luan, Y., and Zhao, Y. (2019). The Research on the Mechanism of Tsoong Inhibiting for colon Cancer. *Saudi J. Biol. Sci.* 26 (3), 605–613. doi:10.1016/j.sjbs.2018.11.007

Chen, G., Lin, Y., Chen, L., Zeng, F., Zhang, L., Huang, Y., et al. (2020). Role of DRAM1 in Mitophagy Contributes to Preeclampsia Regulation in Mice. *Mol. Med. Rep.* 22 (3), 1847–1858. doi:10.3892/mmr.2020.11269

Chen, H., Dong, Y., He, X., Li, J., and Wang, J. (2018). Paeoniflorin Improves Cardiac Function and Decreases Adverse Postinfarction Left Ventricular Remodeling in a Rat Model of Acute Myocardial Infarction. *Drug Des. Devel Ther.* 12, 823–836. doi:10.2147/DDDT.S163405

Chen, W., Zou, P., Zhao, Z., Chen, X., Fan, X., Vinothkumar, R., et al. (2016). Synergistic Antitumor Activity of Rapamycin and EF24 via Increasing ROS for the Treatment of Gastric Cancer. *Redox Biol.* 10, 78–89. doi:10.1016/j.redox.2016.09.006

Ci, X., Zhou, J., Lv, H., Yu, Q., Peng, L., and Hua, S. (2017). Betulin Exhibits Anti-inflammatory Activity in LPS-Stimulated Macrophages and Endotoxin-Shocked Mice through an AMPK/AKT/Nrf2-dependent Mechanism. *Cell Death Dis* 8, e2798. doi:10.1038/cddis.2017.39

Cinegaglia, N., Acosta-Navarro, J., Rainho, C., Antoniazzi, L., Mattioli, S., Pimentel, C., et al. (2020). Association of Omnivorous and Vegetarian Diets with Antioxidant Defense Mechanisms in Men. *J. Am. Heart Assoc.* 9 (12), e015576. doi:10.1161/JAHA.119.015576

Fan, C., Ma, Q., Xu, M., Qiao, Y., Zhang, Y., Li, P., et al. (2019). Ginsenoside Rb1 Attenuates High Glucose-Induced Oxidative Injury via the NAD-PARP-SIRT Axis in Rat Retinal Capillary Endothelial Cells. *Int. J. Mol. Sci.* 20 (19), 4936–4954. doi:10.3390/ijms20194936

García-Caballero, M., Martínez-Poveda, B., Medina, M. A., and Quesada, A. R. (2017). The Natural Antiangiogenic Compound AD0157 Induces Caspase-dependent Apoptosis in Human Myeloid Leukemia Cells. *Front. Pharmacol.* 8, 802. doi:10.3389/fphar.2017.00802

Hasnat, M., Yuan, Z., Ullah, A., Naveed, M., Raza, F., Baig, M. M. F. A., et al. (2020). Mitochondria-dependent Apoptosis in Triptolide-Induced Hepatotoxicity Is Associated with the Drp1 Activation. *Toxicol. Mech. Methods* 30 (2), 124–133. doi:10.1080/15376516.2019.1669247

Hori, Y. S., Kuno, A., Hosoda, R., and Horio, Y. (2013). Regulation of FOXOs and P53 by SIRT1 Modulators under Oxidative Stress. *PLoS One* 8 (9), e73875. doi:10.1371/journal.pone.0073875

Huo, J., Yu, Q., Zhang, Y., Liu, K., Hsiao, C. D., Jiang, Z., et al. (2019). Triptolide-induced Hepatotoxicity via Apoptosis and Autophagy in Zebrafish. *J. Appl. Toxicol.* 39 (11), 1532–1540. doi:10.1002/jat.3837

Jia, J., Dai, S., Sun, X., Sang, Y., Xu, Z., Zhang, J., et al. (2015). A Preliminary Study of the Effect of ECRG4 Overexpression on the Proliferation and Apoptosis of Human Laryngeal Cancer Cells and the Underlying Mechanisms. *Mol. Med. Rep.* 12 (4), 5058–5064. doi:10.3892/mmr.2015.4059

Jiang, L., Yin, X., Chen, Y. H., Chen, Y., Jiang, W., Zheng, H., et al. (2021). Proteomic Analysis Reveals Ginsenoside Rb1 Attenuates Myocardial Ischemia/reperfusion Injury through Inhibiting ROS Production from Mitochondrial Complex I. *Theranostics* 11 (4), 1703–1720. doi:10.7150/thno.43895

Kong, S. Z., Li, J. C., Li, S. D., Liao, M. N., Li, C. P., Zheng, P. J., et al. (2018). Anti-Aging Effect of Chitosan Oligosaccharide on D-Galactose-Induced Subacute Aging in Mice. *Mar. Drugs* 16 (6), 181. doi:10.3390/md16060181

Lai, Y., Tan, Q., Xv, S., Huang, S., Wang, Y., Li, Y., et al. (2021). Ginsenoside Rb1 Alleviates Alcohol-Induced Liver Injury by Inhibiting Steatosis, Oxidative Stress, and Inflammation. *Front. Pharmacol.* 12, 616409. doi:10.3389/fphar.2021.616409

Lee, C., Chun, W., Zhao, R., Kim, Y. D., Nam, M. M., Jung, D. H., et al. (2017). Anticancer Effects of an Extract from the Scallop Patinopecten Yessoensis on MCF-7 Human Breast Carcinoma Cells. *Oncol. Lett.* 14 (2), 2207–2217. doi:10.3892/ol.2017.6424

Lee, S. E., Yang, H., Son, G. W., Park, H. R., Park, C. S., Jin, Y. H., et al. (2015). Eriodictyol Protects Endothelial Cells against Oxidative Stress-Induced Cell Death through Modulating ERK/Nrf2/ARE-Dependent Heme Oxygenase-1 Expression. *Int. J. Mol. Sci.* 16 (7), 14526–14539. doi:10.3390/ijms160714526

Li, Q., Cui, S., Jing, G., Ding, H., Xia, Z., and He, X. (2019). The Role of PI3K/Akt Signal Pathway in the Protective Effects of Propofol on Intestinal and Lung Injury Induced by Intestinal Ischemia/reperfusion1. *Acta Cir Bras* 34 (1), e20190010000005. doi:10.1590/s0102-865020190010000005

Li, S., Bao, L., Si, L., Wang, X., and Bo, A. (2018). Research on Roles of Mongolian Medical Warm Acupuncture in Inhibiting P38 MAPK Activation and Apoptosis of Nucleus Pulposus Cells. *Evid. Based Complement. Alternat Med.* 2018, 6571320. doi:10.1155/2018/6571320

Li, X. J., Jiang, Z. Z., and Zhang, L. Y. (2014). Triptolide: Progress on Research in Pharmacodynamics and Toxicology. *J. Ethnopharmacol* 155 (1), 67–79. doi:10.1016/j.jep.2014.06.006

Li, Y., Li, A., Wu, J., He, Y., Yu, H., Chai, R., et al. (2016). MiR-182-5p Protects Inner Ear Hair Cells from Cisplatin-Induced Apoptosis by Inhibiting FOXO3a. *Cel Death Dis* 7, e2362. doi:10.1038/cddis.2016.246

Li, Z., Zheng, X., Li, P., Itoua, E. S., Moukassa, D., and Ndinga Andely, F. (2017). Effects of Acupuncture on mRNA Levels of Apoptotic Factors in Perihematomal Brain Tissue during the Acute Phase of Cerebral Hemorrhage. *Med. Sci. Monit.* 23, 1522–1532. doi:10.12659/msm.897689

Liu, Q., Ci, X., Wen, Z., and Peng, L. (2018). Diosmetin Alleviates Lipopolysaccharide-Induced Acute Lung Injury through Activating the Nrf2 Pathway and Inhibiting the NLRP3 Inflammasome. *Biomol. Ther. (Seoul)* 26 (2), 157–166. doi:10.4062/biomolther.2016.234

Luo, J., Qin, J., Fu, Y., Zhang, S., Zhang, X., and Yang, M. (2018). 6'-Hydroxy Justicidin B Triggers a Critical Imbalance in Ca2+ Homeostasis and Mitochondrion-dependent Cell Death in Human Leukemia K562 Cells. *Front. Pharmacol.* 9, 601. doi:10.3389/fphar.2018.00601

Na, J. Y., Kim, S., Song, K., Lim, K. H., Shin, G. W., Kim, J. H., et al. (2012). Anti-apoptotic Activity of Ginsenoside Rb1 in Hydrogen Peroxide-Treated Chondrocytes: Stabilization of Mitochondria and the Inhibition of Caspase-3. *J. Ginseng Res.* 36 (3), 242–247. doi:10.5142/jgr.2012.36.3.242

Nguyen, T., Nioi, P., and Pickett, C. B. (2009). The Nrf2-Antioxidant Response Element Signaling Pathway and its Activation by Oxidative Stress. *J. Biol. Chem.* 284 (20), 13291–13295. doi:10.1074/jbc.R900010200

Nori-Garavand, R., Hormozi, M., Narimani, L., Beigi Boroujeni, N., Rajabzadeh, A., Zarei, L., et al. (20202020). Effect of Selenium on Expression of Apoptosis-Related Genes in Cryomedia of Mice Ovary after Vitrification. *Biomed. Res. Int.* 2020, 1–8. doi:10.1155/2020/5389731

Pan, H., Li, J., Rankin, G. O., Rojanasakul, Y., Tu, Y., and Chen, Y. C. (2018). Synergistic Effect of Black tea Polyphenol, Theaflavin-3,3'-Digallate with Cisplatin against Cisplatin Resistant Human Ovarian Cancer Cells. *J. Funct. Foods* 46, 1–11. doi:10.1016/j.jff.2018.04.037

Ruan, Q., Xu, Y., Xu, R., Wang, J., Hua, Y., Wang, M., et al. (2017). The Adverse Effects of Triptolide on the Reproductive System of *Caenorhabditis elegans*: Oogenesis Impairment and Decreased Oocyte Quality. *Int. J. Mol. Sci.* 18 (2). doi:10.3390/ijms18020464

Samikkannu, T., Ranjith, D., Rao, K. V., Atluri, V. S., Pimentel, E., El-Hage, N., et al. (2015). HIV-1 Gp120 and Morphine Induced Oxidative Stress: Role in Cell Cycle Regulation. *Front. Microbiol.* 6, 614. doi:10.3389/fmicb.2015.00614

Shao, D., Wu, Z. Q., Bai, S. Y., Fu, G. W., and Zou, Z. Q. (2019). The Function of miRNA-153 Against Isoflurane-Induced Neurotoxicity via Nrf2/ARE Cytoprotection. *Mol. Med. Rep.* 19 (5), 4001–4010. doi:10.3892/mmr.2019.10056

Shang, L., Wang, K., Liu, D., Qin, S., Huang, J., Zhao, Y., et al. (2020). TMEM16A Regulates the Cell Cycle of Pulmonary Artery Smooth Muscle Cells in High-Flow-Induced Pulmonary Arterial Hypertension Rat Model. *Exp. Ther. Med.* 19 (5), 3275–3281. doi:10.3892/etm.2020.8589

Song, K., Im, S. H., Yoon, Y. J., Kim, H. M., Lee, H. J., and Park, G. S. (2018). A 60 Hz Uniform Electromagnetic Field Promotes Human Cell Proliferation by Decreasing Intracellular Reactive Oxygen Species Levels. *PLoS One* 13 (7), e0199753. doi:10.1371/journal.pone.0199753

Tan, Q. Y., Hu, Q., Zhu, S. N., Jia, L. L., Xiao, J., Su, H. Z., et al. (2018). Licorice Root Extract and Magnesium Isoglycyrrhizinate Protect against Triptolide-Induced Hepatotoxicity via Up-Regulation of the Nrf2 Pathway. *Drug Deliv.* 25 (1), 1213–1223. doi:10.1080/10717544.2018.1472676

van den Berg, E., van Woensel, J. B., and Bem, R. A. (2013). Apoptosis in Pneumovirus Infection. *Viruses* 5 (1), 406–422. doi:10.3390/v5010406

Wang, M., Wang, R., Sun, H., Sun, G., and Sun, X. (2021). Ginsenoside Rb1 Ameliorates Cardiotoxicity Triggered by Aconitine via Inhibiting Calcium Overload and Pyroptosis. *Phytomedicine* 83, 153468. doi:10.1016/j.phymed.2021.153468

Wang, S., Chen, M., Yin, Y., and Storey, K. B. (2019b). MiR-200-3p Is Potentially Involved in Cell Cycle Arrest by Regulating Cyclin A during Aestivation in Apostichopus Japonicus. *Cells* 8 (8). doi:10.3390/cells8080843

Wang, S. R., Chen, X., Ling, S., Ni, R. Z., Guo, H., and Xu, J. W. (2019a). MicroRNA Expression, Targeting, Release Dynamics and Early-Warning Biomarkers in Acute Cardiotoxicity Induced by Triptolide in Rats. *Biomed. Pharmacother.* 111, 1467–1477. doi:10.1016/j.biopha.2018.12.109

Wei, E., Fang, X., Jia, P., Li, M., Jin, P., Li, F., et al. (2021). Ginsenoside Rb1 Alleviates Lipopolysaccharide-Induced Inflammatory Injury by Downregulating miR-222 in WI-38 Cells. *Cel Transpl.* 30, 9636897211002787. doi:10.1177/09636897211002787

Xu, J. C., Zhou, X. P., Wang, X. A., Xu, M. D., Chen, T., Chen, T. Y., et al. (2019a). Cordycepin Induces Apoptosis and G2/M Phase Arrest through the ERK Pathways in Esophageal Cancer Cells. *J. Cancer* 10 (11), 2415–2424. doi:10.7150/jca.32071

Xu, L. Y., Wu, W., Cheng, R., Sun, L. X., Jiang, Z. Z., Zhang, L. Y., et al. (2019b). Toxic Effects of Triptolide on Adrenal Steroidogenesis in H295R Cells and Female Rats. *J. Biochem. Mol. Toxicol.* 33 (11), e22394. doi:10.1002/jbt.22394

Xu, Z., Zhang, K., Wang, Q., and Zheng, Y. (2019c). MicroRNA-124 I-mproves F-unctional R-ecovery and S-uppresses Bax-dependent A-poptosis in R-ats F-ollowing S-pinal C-ord I-njury. *Mol. Med. Rep.* 19 (4), 2551–2560. doi:10.3892/mmr.2019.9904

Xu, Z., Zhang, Y., and Cao, Y. (2020). The Roles of Apoptosis in Swine Response to Viral Infection and Pathogenesis of Swine Enteropathogenic Coronaviruses. *Front. Vet. Sci.* 7, 572425. doi:10.3389/fvets.2020.572425

Yang, C., Shi, Z., You, L., Du, Y., Ni, J., and Yan, D. (2020). Neuroprotective Effect of Catalpol via Anti-oxidative, Anti-inflammatory, and Anti-apoptotic Mechanisms. *Front. Pharmacol.* 11, 690. doi:10.3389/fphar.2020.00690

Yang, G., Wang, L., Yu, X., Huang, Y., Qu, C., Zhang, Z., et al. (20172017). Protective Effect of 18β-Glycyrrhetinic Acid against Triptolide-Induced Hepatotoxicity in Rats. *Evid. Based Complement. Alternat Med.* 2017, 3470320. doi:10.1155/2017/3470320

You, L., Dong, X., Ni, B., Fu, J., Yang, C., Yin, X., et al. (2018). Triptolide Induces Apoptosis through Fas Death and Mitochondrial Pathways in HepaRG Cell Line. *Front. Pharmacol.* 9, 813. doi:10.3389/fphar.2018.00813

You, L., Yang, C., Du, Y., Liu, Y., Chen, G., Sai, N., et al. (20192019). Matrine Exerts Hepatotoxic Effects via the ROS-dependent Mitochondrial Apoptosis Pathway and Inhibition of Nrf2-Mediated Antioxidant Response. *Oxidative Med. Cell Longevity* 2019, 1–15. doi:10.1155/2019/1045345

Yu, L., Chen, Y., Shi, J., Wang, R., Yang, Y., Yang, L., et al. (2019). Biosynthesis of Rare 20(R)-protopanaxadiol/protopanaxatriol Type Ginsenosides through *Escherichia coli* Engineered with Uridine Diphosphate Glycosyltransferase Genes. *J. Ginseng Res.* 43 (1), 116–124. doi:10.1016/j.jgr.2017.09.005

Zhang, Y., Guan, L., Wang, X., Wen, T., Xing, J., and Zhao, J. (2008). Protection of Chlorophyllin against Oxidative Damage by Inducing HO-1 and NQO1 Expression Mediated by PI3K/Akt and Nrf2. *Free Radic. Res.* 42 (4), 362–371. doi:10.1080/10715760801993076

Zhang, Y. L., Liu, Y., Kang, X. P., Dou, C. Y., Zhuo, R. G., Huang, S. Q., et al. (2018). Ginsenoside Rb1 Confers Neuroprotection via Promotion of Glutamate Transporters in a Mouse Model of Parkinson's Disease. *Neuropharmacology* 131, 223–237. doi:10.1016/j.neuropharm.2017.12.012

Zheng, N., Wei, A., Wu, T., Long, L., Yang, H., Li, H., et al. (2021). Triptolide and Atorvastatin Synergistically Promote Hepatotoxicity in Cultured Hepatocytes and Female Sprague-Dawley Rats by Inhibiting Pregnane X Receptor-Mediated Transcriptional Activation of CYP3A4. *Toxicol. Lett.* 342, 85–94. doi:10.1016/j.toxlet.2021.02.008

Zhou, L. L., Zhou, C., Liang, X. W., Feng, Z., Liu, Z. P., Wang, H. L., et al. (2017a). Self-protection against Triptolide-Induced Toxicity in Human Hepatic Cells via Nrf2-ARE-NQO1 Pathway. *Chin. J. Integr. Med.* 23 (12), 929–936. doi:10.1007/s11655-017-2546-6

Zhou, X., Hong, T., Yu, Q., Nie, S., Gong, D., Xiong, T., et al. (2017b). Exopolysaccharides from Lactobacillus Plantarum NCU116 Induce C-Jun Dependent Fas/Fasl-Mediated Apoptosis via TLR2 in Mouse Intestinal Epithelial Cancer Cells. *Sci. Rep.* 7, 14247. doi:10.1038/s41598-017-14178-2

Zhu, J., Jiang, Y., Wu, L., Lu, T., Xu, G., and Liu, X. (2012). Suppression of Local Inflammation Contributes to the Neuroprotective Effect of Ginsenoside Rb1 in Rats with Cerebral Ischemia. *Neuroscience* 202, 342–351. doi:10.1016/j.neuroscience.2011.11.070

Zou, M., Nong, C., Yu, Z., Cai, H., Jiang, Z., Xue, R., et al. (2020). The Role of Invariant Natural Killer T Cells and Associated Immunoregulatory Factors in Triptolide-Induced Cholestatic Liver Injury. *Food Chem. Toxicol.* 146, 111777. doi:10.1016/j.fct.2020.111777

Zymone, K., Raudone, L., Raudonis, R., Marksa, M., Ivanauskas, L., and Janulis, V. (2018). Phytochemical Profiling of Fruit Powders of Twenty Sorbus L. Cultivars. *Molecules* 23 (10). doi:10.3390/molecules23102593

Conflict of Interest: The authors declare that the research was conducted in the absence of any commercial or financial relationships that could be construed as a potential conflict of interest.

Publisher's Note: All claims expressed in this article are solely those of the authors and do not necessarily represent those of their affiliated organizations, or those of the publisher, the editors and the reviewers. Any product that may be evaluated in this article, or claim that may be made by its manufacturer, is not guaranteed or endorsed by the publisher.

Copyright © 2022 Peng, You, Yang, Wang, Liu, Yin, Xu, Dong, Yin and Ni. This is an open-access article distributed under the terms of the Creative Commons Attribution License (CC BY). The use, distribution or reproduction in other forums is permitted, provided the original author(s) and the copyright owner(s) are credited and that the original publication in this journal is cited, in accordance with accepted academic practice. No use, distribution or reproduction is permitted which does not comply with these terms.

frontiers in Pharmacology

REVIEW
published: 04 January 2022
doi: 10.3389/fphar.2021.805991

Natural Products in Modulating Methamphetamine-Induced Neuronal Apoptosis

Yiwei Zeng[1†‡], Yunhui Chen[1†‡], Su Zhang[1], Huan Ren[1], Jialin Xia[1], Mengnan Liu[2], Baozhi Shan[3*] and Yulan Ren[1*]*

[1]College of Acupuncture-moxibustion and Tuina, College of Basic Medicine, College of Nursing, College of Chinese Classics, Chengdu University of Traditional Chinese Medicine, Chengdu, China, [2]Traditional Chinese Medicine Hospital Affiliated to Southwest Medical University, Luzhou, China, [3]School of Humanities, Jiangxi University of Traditional Chinese Medicine, Nanchang, China

Methamphetamine (METH), an amphetamine-type psychostimulant, is highly abused worldwide. Chronic abuse of METH causes neurodegenerative changes in central dopaminergic neurons with numerous neuropsychiatric consequences. Neuronal apoptosis plays a critical role in METH-induced neurotoxicity and may provide promising pharmacological targets for preventing and treating METH addiction. In recent years, accumulating evidence has revealed that natural products may possess significant potentials to inhibit METH-evoked neuronal apoptosis. In this review, we summarized and analyzed the improvement effect of natural products on METH-induced neuronal apoptosis and their potential molecular mechanisms on modulating dopamine release, oxidative stress, mitochondrial-dependent apoptotic pathway, endoplasmic reticulum stress-mediated apoptotic pathway, and neuroinflammation. Hopefully, this review may highlight the potential value of natural products in modulating METH-caused neuronal apoptosis and provide useful information for future research and developments of novel and efficacious pharmacotherapies in this field.

Keywords: methamphetamine, dopaminergic neurons, apoptosis, natural products, neurodegenaration

OPEN ACCESS

Edited by:
Hong Zhang,
Shanghai University of Traditional Chinese Medicine, China

Reviewed by:
Jia Liu,
China Academy of Chinese Medical Sciences, China
Mailan Liu,
Hunan University of Chinese Medicine, China

***Correspondence:**
Yunhui Chen
chenyunhui@cdutcm.edu.cn
Baozhi Shan
shanbaozhi@jxutcm.edu.cn
Yulan Ren
renyulan@cdutcm.edu.cn

‡ORCID:
Yiwei Zeng,
https://orcid.org/0000-0002-7042-2503
Yunhui Chen,
https://orcid.org/0000-0002-3555-8018

†These authors have contributed equally to this work

Specialty section:
This article was submitted to Ethnopharmacology, a section of the journal Frontiers in Pharmacology

Received: *31 October 2021*
Accepted: *09 December 2021*
Published: *04 January 2022*

Citation:
Zeng Y, Chen Y, Zhang S, Ren H, Xia J, Liu M, Shan B and Ren Y (2022) Natural Products in Modulating Methamphetamine-Induced Neuronal Apoptosis. Front. Pharmacol. 12:805991. doi: 10.3389/fphar.2021.805991

INTRODUCTION

Methamphetamine (METH), also known as "ice" or "crystal," is one of the most widely used and abused illicit amphetamine-type stimulants (Courtney and Ray, 2014; Jones et al., 2020). Statistics reveal that in 2019, approximately 27 million people (0.5% of the global population) reported using METH (UNODC, 2020). The number of METH abusers in China and the United States reached an estimated 1.18 million (out of 2.14 million drug users) and 1.7 million (more than half of them suffering METH use disorder), respectively (CNNCC, 2019; Elinore, 2020). Studies also demonstrate that METH administration is highly prevalent in Australia, Canada, and South Africa (Australian Institute of Health and Welfare, 2020; Bach et al., 2020; Sorsdahl et al., 2021). This highly addictive stimulant drug causes serious societal and public health concerns globally, and considerable attention and effort need to be devoted to researching and developing effective intervention strategies against METH-evoked neurotoxic consequences.

Epidemiological and clinical studies have demonstrated that METH is a potent central nervous system stimulant and can significantly impact the human body physically, behaviorally, cognitively, and psychiatrically (Schep et al., 2010; Kevil et al., 2019). Acute METH intake may cause euphoria, delusions, agitations, hypersexuality, or even hyperthermia, cerebrovascular hemorrhages, arrhythmias, heart attacks, and renal failure in high doses (Courtney and Ray, 2014; Glasner-

Edwards and Mooney, 2014; Baradhi et al., 2019; Kevil et al., 2019). Long-term METH abuse elicits neuropsychiatric impairments, including cognitive decline, altered decision-making, psychosis, and psychomotor dysfunction (Krasnova and Cadet, 2009; Dean et al., 2013; Lappin et al., 2018; Mizoguchi and Yamada, 2019). Its withdrawal symptoms in abstinence include depression, agitation, fatigue, and intense craving (Krasnova and Cadet, 2009; Feng et al., 2020). These neuropsychiatric complications are mostly attributed to METH-induced neurotoxicity. Animal-based studies and human neuroimaging analysis have revealed that repeated use of METH can induce neurodegeneration of dopaminergic and serotoninergic terminals in the striatum, cortex, and hippocampus and primarily affects the nigrostriatal dopaminergic pathway (Ernst et al., 2000; Friend and Keefe, 2013; McFadden et al., 2018; Golsorkhdan et al., 2020). METH-evoked neurotoxicity may include direct damage to terminals, oxidative stress, mitochondria dysfunction, neuronal excitotoxicity, endoplasmic reticulum stress, and neuroinflammation, leading to dopaminergic neuron apoptosis (Jayanthi et al., 2004; Yang et al., 2018; Kim et al., 2020). Although substantial progress has been made in deciphering the mechanisms of METH-induced neuronal apoptosis, currently effective pharmacotherapies for METH addiction remain scarce (Yang et al., 2018). Hence, exploration of natural products as potential interventions against METH-elicited complications has become a research hotspot in recent years (Moszczynska and Callan, 2017; Chiang et al., 2019).

Natural products are bioactive components from natural organisms, including plants, animals, insects, marine organisms, microorganisms (Xie et al., 2021). These agents have been widely used by human societies for thousands of years (Baker et al., 2007), and their bioactivities are of great interest to enormous research fields (Ekiert and Szopa, 2020). In recent decades, a growing body of research has demonstrated that natural products exert anti-apoptotic effects on METH-induced neurotoxicity and may yield promising targets for further investigation of effective pharmacological interventions. Converging lines of evidence suggest that natural products can attenuate symptoms of addiction and drug use disorders and modulate the complex mechanisms underlying METH-evoked apoptosis in various ways (Lu et al., 2009). Moreover, METH users have been reported to have an increased risk of developing Parkinson's disease. Natural products may garner considerable neuroprotective properties and effectively mitigate neurodegeneration of Parkinson's disease that partially shares pathogenesis with METH-induced apoptosis, including dopamine release, oxidative stress, and mitochondria damage (Rios et al., 2016; Solayman et al., 2017). Their application may merit further research and development as a promising strategy for pharmacological intervention against METH-induced neuronal apoptosis. Hence, to provide useful insights for future research and development of novel and efficacious pharmacotherapies in this field, a systematic and comprehensive review is of necessity.

In this review, electronic databases, including PubMed, EMBASE, Web of Science, Cochrane Library, China National Knowledge Infrastructure, China Biomedical Literature Database, Wanfang Database, and Chinese Scientific Journals Database, were searched from the inception to August 2021 to identify eligible studies. All the included individual studies were assessed according to the Best practice in research—Overcoming common challenges in phytopharmacological research (Heinrich et al., 2020). The anti-apoptotic effects of natural products on METH-evoked neurotoxic consequences through mediating multiple pathways were summarized and analyzed, including dopamine release, oxidative stress, mitochondrial-dependent apoptotic pathway, endoplasmic reticulum stress-mediated apoptotic pathway, and neuroinflammation. The detailed information of natural products and their potential effects with mechanisms on modulating METH-evoked neuronal apoptosis are illustrated in **Tables 1**, **2**.

MAIN MECHANISMS UNDERLYING METH-INDUCE NEURONAL APOPTOSIS

METH-Induced Dopamine Release

Dopamine (DA) is a key neurotransmitter associated with the reinforcement effects of drug addiction. METH is a cationic molecule and chiral compound based around a phenylethylamine core (Homer et al., 2008) and can modulate the DA system with a myriad of influences on DA release. It has a high lipid solubility, penetrates the blood-brain barrier readily (Nordahl et al., 2003; Schep et al., 2010), and can be taken up by dopaminergic cells through binding to the dopamine transporter (DAT) due to its chemical similarity with DA (Iversen, 2006). Physiologically, DAT removes DA from the synapse to terminate its neurotransmitter effects (Wang et al., 2015). The binding of METH to DAT causes the blockage of the extracellular DA reuptake and the reverse transportation of DA outside the cell, leading to the increase of DA concentration in the synaptic cleft (Panenka et al., 2013). METH in high concentrations can cross the axons through lipophilic diffusion, exacerbating the accumulation of extracellular DA (Shin et al., 2018). Another primary substrate molecule involved in METH-induced DA release is the vesicular monoamine transporter-2 (VMAT-2), an integral membrane protein transporting DA from the cytosol to synaptic vesicles (Fleckenstein et al., 2009). This transportation is coupled to a vacuolar-type H^+ pump ATPase. Studies show that METH, as a "weak base," can disrupt the proton gradient of inner and outer sides of the vesicle required for DA sequestration, eliciting the DA leakage from the vesicle to the cytosol (Schwartz et al., 2006; Panenka et al., 2013). Moreover, METH may induce a decrease of VMAT-2 function and its density on the membrane (Eyerman and Yamamoto, 2005; McFadden et al., 2012). These interactions of METH with DAT and VMAT-2 result in excessive DA accumulation in the intracellular and extracellular surroundings.

METH-Induced Oxidative Stress and Mitochondria-Dependent Cell Apoptosis

Multiple pathways are involved in the complicated mechanism of METH-caused neurotoxicity, and oxidative stress has been considered an essential contributor to neuronal apoptosis.

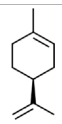
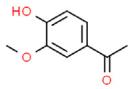
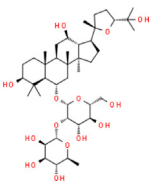
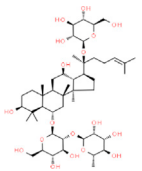
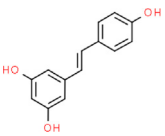
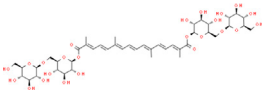
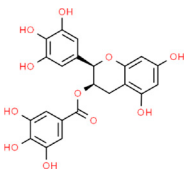
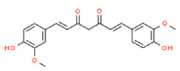
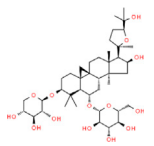
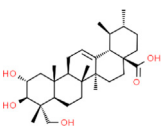
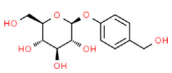
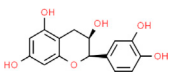
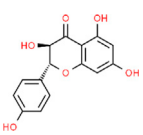
TABLE 1 | Anti-apoptotic activities of natural products in METH-induced neuronal apoptosis.

Extracts/Monomers	Cells/Animal	Dosage	Related mechanisms	Detailed pathways	Refs
Ginseng total saponin	Male Swiss-Webster mice	50, 100 mg/kg	DA release	Blocking DA uptake inhibiting degradation of DA by MAO	Oh et al. (1997a); Oh et al. (1997b)
Limonene	Male Sprague-Dawley rats and ICR mice	200, 400, 600 mg/kg	DA release	Increasing GABA levels through activating GABA B receptors	Yun (2014)
Apocynin	Male Sprague–Dawley rats	0.01–100 μM	DA release	Not conclusive	Miller et al. (2014)
	Male ICR mice	50 mg/kg daily for 7 days	DA release Oxidative stress Neuroinflammation	Inhibiting ERK-dependent p47phox activation	Dang et al. (2016)
Pseudoginsenoside-F11	Male ICR mice	8 mg/kg daily for 5 days	DA release	Regulating GABAergic neurons and μ-opioid receptors.	Li et al. (2000)
	Male Wistar rats	3, 6 mg/kg for 12 days	Oxidative stress	Increasing SOD and GSH Decreasing MDA	Chen et al. (2016)
Ginsenoside RE	C57BL/6 mice	10, 20 mg/kg, p.o., twice a day	Oxidative stress Neuroinflammation	Inactivating PKCδ Inducing GPx activity	Shin et al. (2014)
Resveratrol	Dopaminergic neurons of mice	20 μM	Oxidative stress ERS	Decreasing ROS production Decreasing intracellular Ca^{2+} concentration	Sun et al. (2015)
	C57BL/6 mice	10, 100 mg/kg	Oxidative stress	Activating the Keap1-Nrf2 pathway	Zeng et al. (2021)
	N27 dopaminergic cells	10 μM	Mitochondria-dependent pathway	Blocking caspase-3 activation	Kanthasamy et al. (2011)
Crocin	Male Wistar rats	30, 60, 90 mg/kg	Oxidative stress Neuroinflammation	Increasing SOD and GSH Decreasing MDA and TNF-α Regulating CREB-BDNF signaling pathway	Shafahi et al. (2018); Mozaffari et al. (2019)
Epigallocatechin gallate	CD-1 male mice	2 mg/kg	Oxidative stress	Increasing GPx-4 protein Decreasing SOD-1 protein	Pan et al. (2020)
TCPE	PC12 cells	6.25–400 μg/ml	Oxidative stress	Increasing SOD and GPx Decreasing ROS and MDA	Zeng et al. (2020)
Curcumin	Male Wistar rats	100, 200 mg/kg for 7 days	Oxidative stress Neuroinflammation	Increasing SOD and GPx Decreasing TNF-α and MDA	Hadizadeh-Bazaz et al. (2021)
Astragaloside IV	Male Wistar rats	10, 20 mg/kg	Mitochondria-dependent pathway	Increasing Bcl-2 Decreasing caspase-3	Lu et al. (2015)
Asiatic acid	SH-SY5Y cells	20 μM	Neuroinflammation Mitochondria-dependent pathway	Decreasing TNF-α and IL-6 Inhibiting translocation of NF-κB/STAT3 and ERK phosphorylation Inhibiting cleavage of procasepase-3	Park et al. (2017)
Antrodia camphorata enzymes	PC12 cells	62.5, 125, 250 μg/ml	Mitochondria-dependent pathway Oxidative stress	Inhibiting activity of caspase-3 Decreasing ROS production	Chi et al. (2017)
Gastrodin	Cortical neurons of SD rats	25 mg/L	Mitochondria-dependent pathway	Decreasing caspase-3 Regulating CREB-BNDF signaling pathway	Ma et al. (2020); Shin et al. (2011); Yang et al. (2020)
Epicatechin	HT22 hippocampal cells	10–20 μM	ERS	Down-regulating CHOP, ROS, caspase-3, -8, -9, PARP	Kang et al. (2019)
Aromadendrin	SH-SY5Y Cells	10–40 μM	ERS P13K/Akt/mTOR pathway	Decreasing CHOP, Bax; Increasing bcl-2; Inhibiting mTOR phosphorylation	Lee et al. (2021)

DA, dopamine; MAO, monoamine oxidase; GABA, gamma-aminobutyric acid; ERK, extracellular signal-regulated kinase; SOD, superoxide dismutase; GSH, glutathione; MDA, malondialdehyde; PKCδ, protein kinase C-δ; GPx, glutathione peroxidase; ROS, reactive oxygen species; ER, endoplasmic reticulum; CHOP, TNF-α, tumor necrosis factor-α; CREB, cyclic AMP response element binding protein; BNDF, brain-derived neurotrophic factor; Keap-1, Kelch-like ECH associated protein-1; Nrf2, nuclear factor erythroid 2-related factor 2; Bcl-2, B-cell lymphoma 2; IL-6, interleukin 6; TCPE, terminalia chebula polyphenol extract; NF-κB, nuclear factor kappa B; STAT3, signal transducer and activator of transcription proteins 3; PARP, poly ADP-ribose polymerase.

METH-induced cytosolic and synaptic DA accumulation results in the production of quinone and semi-quinone through autoxidation to generate large amounts of reactive oxygen species (ROS), such as hydrogen peroxide, hydroxyl radicals, and superoxide radicals. Furthermore, a small portion of DA produces H_2O_2 with the mediation of monoamine oxidase (MAO) (Hermida-Ameijeiras et al., 2004; McDonnell-Dowling and Kelly, 2017; Yang et al., 2018). METH also inhibits the production of antioxidants, including glutathione, superoxide dismutase (SOD), and catalase (Tata and Yamamoto, 2007; Huang et al., 2013). Thus, the imbalance between ROS and free radical scavengers contributes to the oxidative stress in

TABLE 2 | Detailed information and chemical structures of natural products.

Monomers	Systematic name	Origin	Chemical structures
Limonene	(4S)-4-Isopropenyl-1-methylcyclohexene	Fruits *of Citrus L.,* Rutaceae	
Apocynin	1-(4-Hydroxy-3-methoxyphenyl)-ethanone	*Picrorhiza kurroa* Royle ex Benth, Plantaginaceae	
Pseudoginsenoside-F11	(3beta,6alpha,12beta,24R)-3,12,25-Trihydroxy-20,24-epoxydammaran-6-yl 2-O-(6-deoxy-alpha-L-mannopyranosyl)-beta-D-mannopyranoside	*Panax quinquefolius L,* Araliaceae	
Ginsenoside RE	(3beta,6alpha,12beta)-20-(beta-D-Glucopyranosyloxy)-3,12-dihydroxydammar-24-en-6-yl 2-O-(6-deoxy-alpha-L-mannopyranosyl)-beta-D-glucopyranoside	*Panax ginseng* C. A. Mey., Araliaceae	
Resveratrol	5-[(E)-2-(4-Hydroxyphenyl)vinyl]-1,3-benzenediol	Red wine	
Crocin	Bis [(2S,3R,4S,5S,6R)-3,4,5-trihydroxy-6-({[(2R,3R,4S,5S,6R)-3,4,5-trihydroxy-6-(hydroxymethyl)tetrahydro-2H-pyran-2-yl]oxy}methyl)tetrahydro-2H-pyran-2-yl] (2E,4E,6E,8E,10E,12E,14E)-2,6,11,15-tetramet hyl-2,4,6,8,10,12,14-hexadecaheptaenedioate	*Crocus sativus L.,* Iridaceae	
Epigallocatechin gallate	(2R,3R)-5,7-Dihydroxy-2-(3,4,5-trihydroxyphenyl)-3,4-dihydro-2H-chromen-3-yl 3,4,5-trihydroxybenzoate	*Camellia sinensis L.*, Theaceae	
Curcumin	(1E,6E)-1,7-Bis(4-hydroxy-3-methoxyphenyl)-1,6-heptadiene-3,5-dione	*Curcuma longa L.,* Zingiberaceae	
Astragaloside IV	(3beta,6alpha,9beta,16beta,20R,24S)-16,25-Dihydroxy-3-(beta-D-xylopyranosyloxy)-20,24-epoxy-9,19-cyclolanostan-6-yl beta-D-glucopyranoside	*Astragalus mongholicus* bunge, Fabaceae	
Asiatic acid	(2alpha,3beta)-2,3,23-Trihydroxyurs-12-en-28-oic acid	*Centella asiatica (L.)* Urb, Apiaceae	
Gastrodin	4-(Hydroxymethyl)phenyl beta-D-glucopyranoside	*Gastrodia elata* Blume, Orchidacea	
Epicatechin	(2R,3R)-2-(3,4-Dihydroxyphenyl)-3,5,7-chromanetriol	*Camellia sinensis* (*L.*) kuntze, Theaceae	
Aromadendrin	(2R,3R)-3,5,7-Trihydroxy-2-(4-hydroxyphenyl)-2,3-dihydro-4H-chromen-4-one	*Abies sibirica* Ledeb. (Syn. *Pinus sibirica* Ledeb), Pinaceae	

dopaminergic terminals. Excessive ROS may result in lipids and protein metabolism disruption, mitochondrial dysfunction, and nuclear DNA damage, increasing susceptibility to neuronal damage and death (Potashkin and Meredith, 2006).

Mitochondria is an important site of METH-evoked ROS generation in neural cells. Several investigations have suggested that mitochondria dysfunction plays a crucial role in METH-induced dopaminergic apoptosis. ROS can inhibit key enzymes in the electron transport chain (ETC) of mitochondria, including complex II-III and IV (Wu et al., 2007; Halpin et al., 2014a; Dawson and Dawson, 2017; Moratalla et al., 2017). METH diffuses into mitochondria, and its accumulation disrupts oxidative phosphorylation and suppresses ATP synthesis (Krasnova and Cadet, 2009). In addition, METH inhibits the tricarboxylic acid cycle and ETC, which are essential to ATP production (Barbosa et al., 2015). In turn, the inhibition of ETC enhances ROS production, which may further restrain ETC components through positive feedback, aggravating the dysfunction of mitochondrial metabolism (Yang et al., 2018). Another critical mechanism underlying mitochondria dysfunction triggered by METH is the alteration of mitochondrial dynamics (biogenesis, fusion, fission, and mitophagy) (Michel et al., 2012; Anne Stetler et al., 2013). METH can decrease the expression of certain key molecules related to mitochondrial biogenesis (Valian et al., 2017; Beirami et al., 2018). Mitochondrial dysfunction causes the mitochondrial membrane permeabilization (Kroemer et al., 2007), and subsequently the release of cytochrome-c (Cyt-c), apoptosis-inducing factor (AIF), and Smac/Diablo into the cytosol (Cadet et al., 2003; Jayanthi et al., 2004). METH administration has been shown to up-regulate the expression of pro-apoptotic proteins (Bax, Bak, and Bid) and down-regulate the expression of anti-apoptotic proteins (Bcl-2, Bcl-XL, and BclW) (Jayanthi et al., 2001; Cadet et al., 2003). The increase in the Bax, Bak, and Bid can promote the release of Cyt-c from mitochondria to the cytosol (Roth and D'Sa, 2001). Subsequently, apoptosis protease activating factor 1 (Apaf-1) is activated, initiating the mitochondria-dependent cell apoptosis pathway (the intrinsic pathway) (Cain et al., 2002). Apaf-1 binding to Cyto-c constitutes the "apoptosome," which serves as a molecular platform for the caspase-9 activation (Jiang and Wang, 2000; Bratton and Salvesen, 2010) and induces sequential caspase-3, -6, and -7 activations (Roth and D'Sa, 2001; Shin et al., 2018). Additionally, several studies have reported that protein kinase C-δ (PKCδ), a member of the PKC family, plays a critical role in the mitochondrial-dependent apoptotic cascade. PKCδ can be proteolytically activated by caspase-3, then translocate to the nucleus mediating DNA fragmentation and apoptosis. In turn, the activated PKCδ enhances caspase-3 production through a positive-feedback loop (Kanthasamy et al., 2003; Kaul et al., 2003).

METH-Induced Excitotoxicity and Endoplasmic Reticulum Stress

Excitotoxicity refers to the overloaded intracellular calcium levels initiated by excessive glutamate (Glu) release, activating apoptotic pathways, eventually resulting in cellular damage (Halpin et al., 2014b). Glu is the major excitatory neurotransmitter in the brain, and METH has been shown to evoke the excessive release of Glu in the striatum (Stephans and Yamamoto, 1994; Mark et al., 2004). Accumulated Glu binds to amino-5hydroxy-3-methyl-4-isoxazole propionic acid receptors and N-methyl-D-aspartate receptors to initiate downstream signaling pathways, leading to a surge of Ca^{2+} influx (Riddle et al., 2006; Halpin et al., 2014b; Kim et al., 2020). Ca^{2+} is an important intracellular second manager responsible for multiple signal transductions, which can be regulated by the endoplasmic reticulum (ER) through the sequestration of Ca^{2+}. METH-induced excess intracellular Ca^{2+} causes the disturbance of intracellular Ca^{2+} concentrations, activates the protein kinases, phosphatase, and nitric oxide synthase (NOS) and eventually results in endoplasmic reticulum stress (ERS) (Bahar et al., 2016; Moratalla et al., 2017). In stress conditions, a decrease in the protein-folding capacity of ER may induce the accumulation of unfolded and misfolded proteins in ER, which causes unfold protein response (UPR) to remove those proteins and maintain ER homeostasis (Go et al., 2017). UPR is mediated by IRE1α, PERK, and ATF6 signaling proteins, triggering UPR-dependent apoptotic signaling by activating C/EBP homologous protein (CHOP) (Sano and Reed, 2013; Bahar et al., 2016). As a transcription factor, CHOP can up-regulate the expressions of Bax and Bak and down-regulate the expressions of Bcl-2 and Bcl-XL to promote apoptosis (Hu et al., 2018). The elevated Ca^{2+} activates the calpain, a cytosolic calcium-activated neutral cysteine endopeptidase. The activated calpain translocates from the cytosol to the membrane, where it cleaves procaspase-12 (Nakagawa and Yuan, 2000), then the active caspase-12 initiates positive feedback to activate caspase-9 and -3 to potentiate apoptosis (Martinez et al., 2010).

METH-Induced Neuroinflammation

The neuroinflammation induced by METH is closely related to the microglial activation and the production of pro-inflammatory cytokines (Goncalves et al., 2008). Microglial cells monitor neuronal homeostasis, serve as the immune defense against neuronal damage, and can be activated upon neuronal injury and neurotoxic agents (Lull and Block, 2010; Shaerzadeh et al., 2018). METH stimulation may elicit the morphological alteration of microglial cells (Xu et al., 2017). Neuroimaging has demonstrated that chronic METH administration induces microgliosis reaction in humans (Sekine et al., 2008). Activated microglial cells secrete enormous pro-inflammatory cytokines, including interleukin6 (IL-6) and tumor necrosis factor-α (TNF-α), which induce prolonged neuroinflammation (Goncalves et al., 2010). This inflammatory response may be associated with certain signaling pathways, such as nuclear factor kappa B (NF-κB) and signal transducer and transcription (STAT) pathway activator. Research has shown that METH can activate the NF-κB pathway, inducing its transfer from the cytoplasm to the nucleus and promoting the transcription of pro-inflammatory cytokines in microglia (Shah et al., 2012). METH also causes the increase of signal transducer and activator of transcription proteins 3 (STAT3) and its translocation to the nucleus (Zhao et al., 2019), which carries out

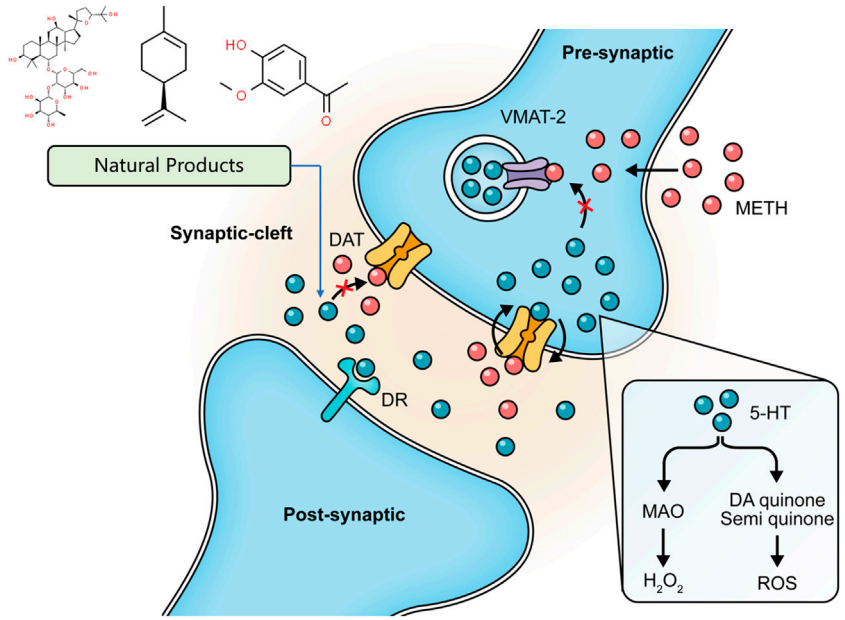


FIGURE 1 | Natural products targeting DA release to attenuate METH-induced apoptosis.

the IL-6 signaling (Coelho-Santos et al., 2012). Additionally, studies have demonstrated that mitogen-activated protein kinase (MAPK) may play a crucial role in the METH-induced release of inflammatory cytokines (Yan et al., 2014; Park et al., 2017). The chronic neuroinflammation leads to overexpression of PUMA (p53-up-regulated modulator of apoptosis), a pro-apoptotic protein of the Bcl-2 family that drives Cyt-c release from the mitochondria to initiate caspase cascades (Yang et al., 2018).

EFFECTS AND MECHANISMS OF NATURAL PRODUCTS ON METH-INDUCED APOPTOSIS

Natural Products Targeting DA Release to Modulate METH-Induced Apoptosis

As described above, METH interferes with DA reuptake and causes DA oxidation. Elevated levels of DA readily diffuse in cells and cause oxidative damage, which is closely related to METH-initiated neurotoxic effects. Ginseng total saponin (GTS), an active biological component derived from *Panax ginseng* C. A. Mey., has been reported to be an effective intervention for the central dopaminergic system more than 2 decades ago. Studies conducted in 1994 and 1996 by Kim et al. first identified that GTS could attenuate conditioned place preference in mice, and this effect might be associated with inhibition of METH-induced dopaminergic activation (Kim et al., 1995; Kim et al., 1996). Their follow-up studies demonstrated that GTS pretreatment could partially protect striatal dopaminergic neurons from METH-induced depletions and reduce DA release and its degradation by MAO (Oh et al., 1997a; Oh et al., 1997b). The property of reducing DA release in GTS may alleviate DA autoxidation and ensuing oxidative stress and apoptosis activation. Limonene is a major compound in the essential oils of citrus fruit peels. In 2014, Lin et al. demonstrated that Limonene reduced extracellular DA levels elevated by METH in the nucleus accumbens of rats, which might be resulted from the increase of gamma-aminobutyric acid (GABA) levels (Yun, 2014). In the same year, Miller et al. proposed that subchronic use of Apocynin, a phenolic compound isolated from *Picrorhiza kurroa* Royle ex Benth., could significantly reduce the METH-stimulated DA release in rat striatum (Miller et al., 2014). In 2016, Dang et al. further studied the neuroprotective effects of Apocynin and found that this compound could attenuate mitochondrial dysfunction, microglial activation, and causal apoptotic signaling process through inhibiting the extracellular signal-regulated kinase (ERK)-dependent activation of p47phox (Dang et al., 2016). The major mechanisms of how natural products target DA release to attenuate METH-induced apoptosis are summarized in **Figure 1**.

Natural Products Targeting Oxidative Stress and Mitochondria-Dependent Pathway to Modulate METH-Induced Apoptosis

Oxidative stress and mitochondria dysfunction have been considered major mechanisms underlying METH-induced apoptosis. Regulating the generation of ROS and antioxidants may be efficacious strategies to ameliorate mitochondria dysfunction and neural damage. Pseudoginsenoside-F11 (PF11), an ocotillol-type saponin derived from American Ginseng (*Panax quinquefolius L.*) (Li et al., 2000), has been demonstrated to mediate neuroinflammation through decreasing the activation of microglial and the subsequent expression of pro-inflammatory factors and oxidative stress

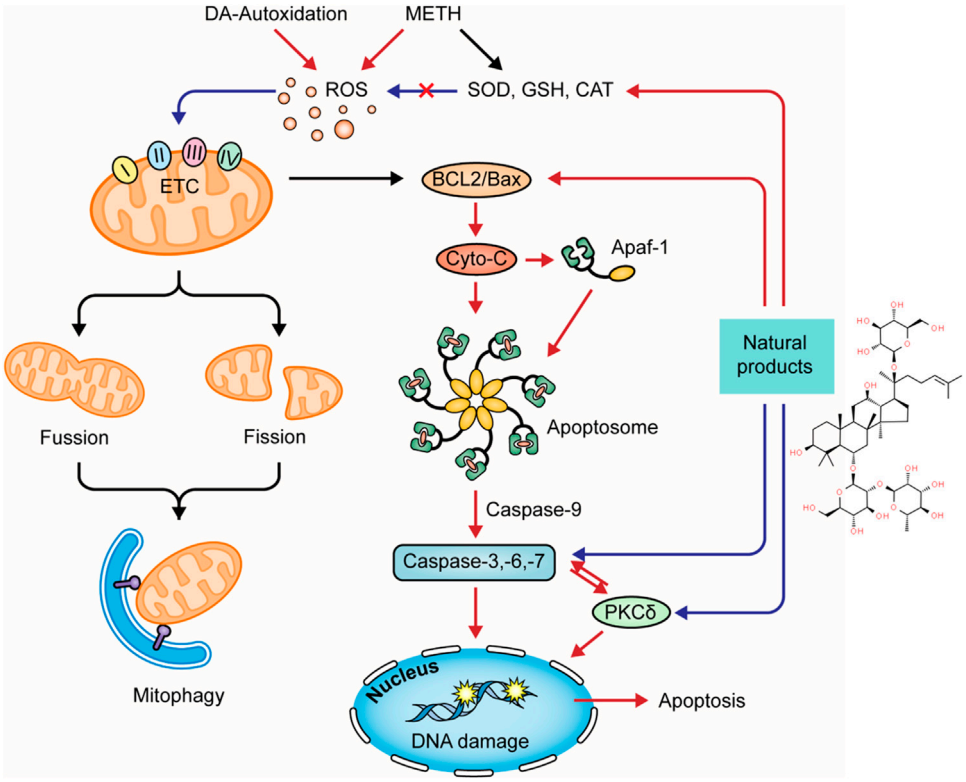


FIGURE 2 | Natural products targeting on oxidative stress and mitochondria-dependent apoptotic pathway to attenuate METH-induced apoptosis.

through increasing antioxidant activity (Wang et al., 2014; Zhang et al., 2019). In 2003, a study by Wu et al. showed that PF11 could antagonize the depletion of dopaminergic contents in mice induced by chronic METH administration (Wu et al., 2003). In 2016, Chen et al. further revealed that PF11 could attenuate the METH-evoked oxidative stress in the hippocampus of rats through increasing SOD and GSH-Px activities and decreasing malondialdehyde (MDA) level (Chen. et al., 2016). PF11 also regulated GABAergic neurons and μ-opioid receptors, which are considered to be involved in METH-induced DA release (Fu et al., 2016). *Gastrodia elata* Blume is a well-known herb in traditional Chinese medicine and has often been used to treat various neurological disorders. In early 2011, Shin et al. reported that its methanol extract could significantly attenuate METH-induced ROS in striatal dopaminergic neurons of mice (Shin et al., 2011). Ginsenoside RE, a validated constituent extracted from *Panax ginseng* C. A. Mey. (Liu et al., 2019), showed an antioxidative effect against METH-induced apoptosis. In 2014, Shin et al. proved the mediation effect of Ginsenoside RE for oxidative stress in mitochondria through inhibiting PKCδ (Shin et al., 2014). In 2015, *in vitro* studies by Nam et al. also suggested that Ginsenoside RE could induce the cytosolic and mitochondrial GPx activity and the mitochondrial translocation of cleaved PKCδ (Nam et al., 2015). Resveratrol, a polyphenol found in red wine, has considerable neuroprotective effects, including antioxidation, anti-inflammation, and anti-apoptosis (Howitz et al., 2003). In 2015, Sun et al. reported that it could significantly decrease METH-induced ROS production *in vitro* and the compensatory SOD generation. They also observed that resveratrol might reduce the intracellular Ca^{2+} concentration, suggesting it exerts neuroprotective effects on METH-caused apoptosis through targeting oxidative stress and ER stress (Sun et al., 2015). Another study by Zeng et al. also suggested that the antioxidative effect of resveratrol might attribute to the activation of the keap1-Nrf2 pathway (Zeng et al., 2021). In 2018, Shafahi et al. reported that intervention with crocin, a bioactive constituent of saffron (*Crocus sativus L.*), could regulate the increased SOD and GSH and the ensuing decreased caspase-3 activation in rats stimulated by METH (Shafahi et al., 2018). In 2019, an *in vivo* study by Mozaffari et al. demonstrated that the neuroprotective effects of crocin might be associated with the Cyclic AMP response element-binding protein (CREB) and the Brain-derived neurotrophic factor (BDNF) signaling pathway (Mozaffari et al., 2019). Epigallocatechin gallate (EGCG), a polyphenol compound derived from green tea, is a potent antioxidant. In 2020, Pan et al. observed that EGCG pretreatment could reverse the reduced GPx-4 protein level in the striatum of mice and the overexpression of compensatory SOD-1 protein induced by METH, indicating its effects in preventing METH-caused apoptosis (Pan et al., 2020). Terminalia chebula polyphenol extract (TCPE) is obtained

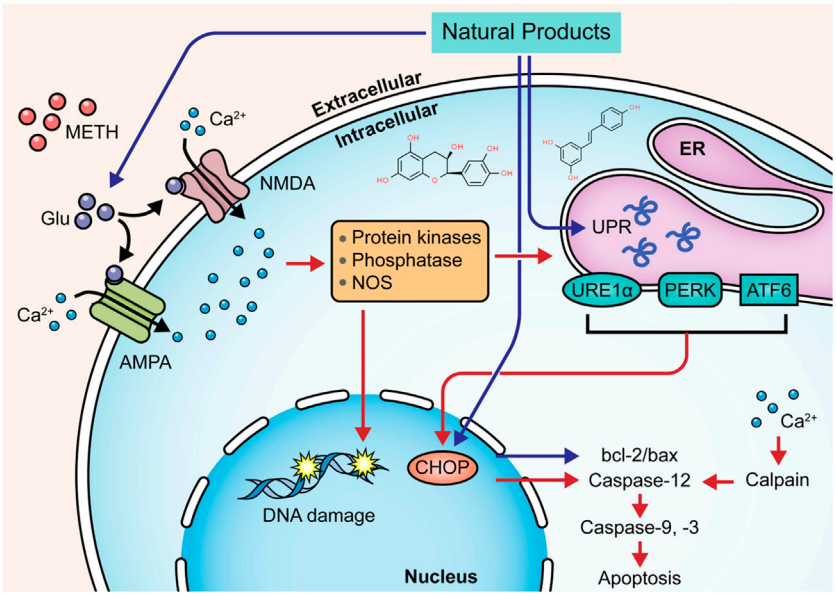


FIGURE 3 | Natural products targeting ERS-mediated pathway to attenuate METH-induced apoptosis.

from *Terminalia chebula* Retz. In 2020, Zeng et al. reported that TCPE could protect PC12 cells from METH-elicited DNA damage and apoptosis, which might be related to the inhibition of intracellular ROS and MDA production and the enhancement of SOD and GPx activities (Zeng et al., 2020). Curcumin (CUR) is the main component of turmeric (*Curcuma longa L.*). In 2021, a study by Hadizadeh-Bazaz et al. reported that CUR could increase SOD and GSH and decrease MDA in the hippocampal neurons of mice injected with METH. They also found that CUR could reduce the TNF-α levels to attenuate the neuroinflammation. These effects of CUR contributed to a significant reduction in METH-induced apoptosis (Hadizadeh-Bazaz et al., 2021).

Several natural products targeting mitochondria-related apoptotic proteins have been explored in recent years. In 2011, Kanthas et al. reported that resveratrol pretreatment could protect dopaminergic cells from MTTH-induced cell death through blocking caspase-3 activation and the subsequent DNA fragmentation (Kanthasamy et al., 2011). Astragaloside IV is the main bioactive component in *Astragalus mongholicus* bunge. In 2015, a study by Sui et al. revealed that the Bcl-2 and caspase-3 were overexpressed in METH-dependent mice, and the former might be a compensatory reaction against apoptosis. Astragaloside IV could enhance the Bcl-2 expression and inhibit the caspase-3 expression and activation (Lu et al., 2015). Asiatic acid is a pentacyclic triterpene extracted from *Centella asiatica* (*L.*) Urb. and possesses multiple bioactivities, including antioxidation, anti-inflammation, and anti-apoptosis. An *in vitro* study conducted in 2017 by Park et al. revealed that Asiatic acid inhibited the cleavage of caspase-3 to reduce the subsequent cleavage of PARP (Park et al., 2017). *Antrodia camphorata* (M. Zang et C. H. Su) Sheng. H. Wu, Ryvarden et T. T. Chang is a medicinal mushroom endemic to Southeast China. In 2017, a study by Chi et al. showed that its enzymes could suppress the METH-evoked mitochondrial apoptosis pathway in PC12 cells by reducing the intracellular ROS levels and inhibiting procaspase-3 cleavage (Chi et al., 2017). In 2020, Yan et al. investigated the anti-apoptotic effect of Gastrodin (GAS), the major bioactive component of *Gastrodia elata* Blume, and reported that GAS intervention could decline the METH-stimulated caspase-3 overexpression in cortical neurons of rats (Yan et al., 2020). An *in vitro* experiment by Ma et al. also observed that GAS could decrease TUNEL-positive cells in the cortical neurons stimulated by METH through modulating CREB/BNDF signaling pathway (Ma et al., 2020). The major mechanisms of how natural products target oxidative stress and mitochondria-dependent apoptotic pathway to attenuate METH-induced apoptosis are summarized in **Figure 2**.

Natural Products Targeting Endoplasmic Reticulum Stress-Mediated Pathway to Modulate METH-Induced Apoptosis

Targeting the ERS-mediated pathway is also a feasible way for natural products to modulate METH-induced neuronal apoptosis. In 2015, Sun et al. observed that resveratrol might reduce the intracellular Ca^{2+} overload and exert neuroprotective effects on METH-caused apoptosis of dopaminergic neurons through attenuating ERS (Sun et al., 2015). In 2019, Kang et al. reported that Epicatechin, a bioactive flavonoid in green tea, could protect hippocampal neurons from METH-induced cell apoptosis via reducing ERS, and its potential mechanisms might associate with the down-regulation of CHOP, ROS, caspase-3, -8, -9, and PARP (Kang et al., 2019). In 2021, Lee et al. revealed that pretreatment with aromadendrin, a flavonoid obtained from *Abies sibirica* Ledeb. (Syn. *Pinus sibirica* Ledeb),

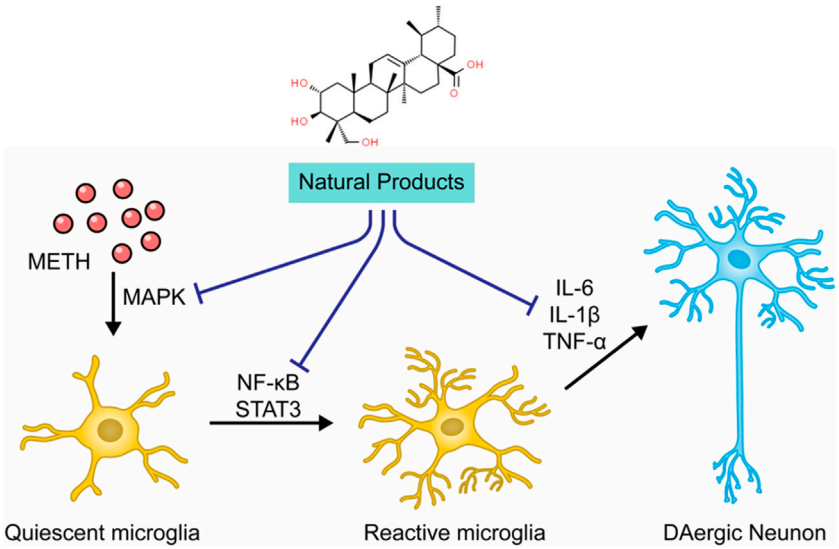


FIGURE 4 | Natural products targeting neuroinflammation to attenuate METH-induced apoptosis.

suppressed METH-induced cell death in SH-SY5Y cells by decreasing CHOP and Bax and increasing Bcl-2. It also exhibited a preventative effect on cell apoptosis via restoring the phosphorylation of mTOR to inhibit the PI3K/Akt/mTOR pathway (Lee et al., 2021). The major mechanisms of how natural products target ERS to attenuate METH-induced apoptosis are summarized in **Figure 3**.

Natural Products Targeting Neuroinflammation to Modulate METH-Induced Apoptosis

As stated before, the neuroinflammation induced by activated microglia is crucial in METH-caused neurotoxicity. Accordingly, ameliorating neuroinflammation may be a promising approach to control METH-induced neurotoxicity. In 2014, Shin et al. found that Ginsenoside RE could attenuate the METH-induced activation of microglial in PKCδ (+/+) mice, suggesting that Ginsenoside RE could mediate apoptosis via inactivation of PKCδ (Shin et al., 2014). In 2017, an investigation by Park et al. demonstrated that Asiatic acid could relieve METH-mediated dopaminergic neuroinflammation of SH-SY5Y cells by reducing pro-inflammatory cytokines secretion, such as TNFα and IL-6, and down-regulated the expression of TNF receptor via inhibiting NF-κB, STAT3, and MAPK-ERK signaling pathway. Moreover, Asiatic acid also exerted the inhibitory effects on caspase-3 cleavage and the subsequent PARP cleavage and the mediative effects on Bcl-2 and Bax (Park et al., 2017). In addition, in 2018, Shafahi et al. reported that crocin treatment could reduce the level of TNF-α in the hippocampus of rats stimulated by METH, suggesting that crocin could also exert an antiapoptotic effect by mediating METH-induced neuroinflammation (Shafahi et al., 2018). The major mechanisms of how natural products target neuroinflammation to attenuate METH-induced apoptosis are summarized in **Figure 4**.

CONCLUSION AND PERSPECTIVES

Most of the METH-elicited neuropsychiatric consequences are attributable to its neurotoxicity, including direct damage to central dopaminergic and serotonergic terminals and the subsequent neurodegenerative changes upon the activation of neuronal autophagy, apoptosis, and necrosis (Davidson et al., 2001; Yu et al., 2015; Sanchez et al., 2018). In recent years, important progress has been achieved in interpreting the complex mechanism underlying METH-produced neurotoxicity. Neuronal apoptosis has been considered the main pathogenic factor in METH-induced neurodegeneration. Animal studies have confirmed that pro-apoptotic changes in the brain are highly associated with METH-induced neuropsychiatric symptoms, such as locomotor sensitization, psychosis, memory impairments, and cognitive impairments (Shin et al., 2017). With the decrease of central monoaminergic terminals and the depletion of dopamine and serotonin, these psychiatric complications are sustained (Rusyniak, 2013), leading to failed anti-addiction treatments, relapse to drug use, and increased risk of various neurodegenerative diseases (Shukla and Vincent, 2020). In view of the devastating societal and public health burdens caused by METH abuse, further in-depth explorations in pharmacotherapies are highly anticipated. In this review, we summarized and analyzed these natural products that have been proven to possess significantly *in vitro* and *in vivo* protective effects against METH-induced neuronal apoptosis through mediating multiple pro-apoptotic factors, such as DA release, oxidative stress, mitochondria-dependent apoptotic pathway, ERS-mediated apoptotic pathway, and neuroinflammation.

Notwithstanding the numerous studies conducted to excavate the effects of natural agents in the prevention and treatment of METH-caused neuronal apoptosis, the discovery and development of novel and effective novel pharmacotherapies still require more sophisticated works in both preclinical and clinical investigations. First, METH abuse involves the activation of multiple apoptotic pathways. However, current research has primarily focused on using a single natural agent to block a single pathway. Given the complex nature of METH-initiated neurotoxicity, strategies that combine multiple natural compounds and target multiple pathways may yield more encouraging medications. Interestingly, the protective effect of certain natural products, such as Crocin, Resveratrol, Curcumin, and Apocynin, on METH-evoked apoptosis have been attributed to the regulation of multiple targets simultaneously. From the perspective of optimal "cocktail" drug design, they may yield a promising future in novel anti-METH strategies (Radhakrishnan and Tidor, 2008). Approaches combining systems biology with traditional computational-aided drug design are applicable for developing drug "cocktail" regimens to modulate the core target network of METH. Second, the available studies have focused on the effects of natural products on oxidative stress, and the interpretation of their actions on other pathogenic factors is still insufficient. Several natural agents have demonstrated promising potential to regulate neuronal apoptosis in other fields, including neurodegenerative diseases (Kim and Kim, 2018), which indicate that discovery and exploration of more potential natural candidates can be anticipated.

Third, the specific molecular and genetic mechanisms underlying the anti-apoptotic effects of natural products are still elusive. The safety of natural products and their interaction with conventional drugs have become major concerns. Therefore, further studies on their pharmacokinetics, pharmacodynamics, and toxicological profiles are of great necessity (Jha and Rathi, 2008; Nauffal and Gabardi, 2016; Gaston et al., 2020). Follow-up studies need to be performed to evaluate the potential toxicity of the natural agents. In addition, no clinical trial regarding the anti-apoptotic effects of natural products for METH-induced neuronal apoptosis has been documented, and future studies may devote more efforts to designing high-quality and well-designed clinical trials to verify their therapeutic effects and explore the relative mechanism. Lastly, new and emerging insightful scientific findings on METH-induced neuronal apoptosis have continually updated our understanding of its biomechanisms. For example, recent studies confirmed that CCAAT/enhancer-binding protein (C/EBP-β), Lipocalin2 (lcn2), and Sigma-1 receptor (σ-1R) might play an important role in METH-induced microglial apoptosis (Shen et al., 2016; Chen et al., 2019). These new findings may provide new directions for future studies of natural agents and yield more refined and robust evidence. In addition, it is also worth noting that except for the natural products stated above, other agents, such as Vitamin C (L-ascorbate) and Melatonin, also have the potentials to be developed as candidate anti-apoptotic drugs in clinical management (Huang et al., 2012; Nguyen et al., 2015).

In conclusion, this review summarized and analyzed these natural products with anti-apoptotic properties to prevent and treat METH-induced neurotoxicity by modulating DA release, oxidative stress, mitochondria dysfunction, caspase cascades, and neuroinflammation. Hopefully, this review may provide helpful information for their further exploration preclinically and clinically.

AUTHOR CONTRIBUTIONS

All authors contributed to the article. YR, YC, and BS conceived and designed this paper. YZ, YC, SZ, HR, JX, ML, and YR summarized and analyzed the data. YZ and YC drafted the paper. YC, BS, and YR revised and edited the paper.

FUNDING

This research was supported by the Major Research and Development Project and the International Cooperation and Exchange Project of Sichuan Provincial Science and Technology Department (No. 2018SZ071, No. 2017HH0004), the National Natural Science Foundation of China (No. 81873239, No. 81603537), the Sichuan Provincial Administration of Traditional Chinese Medicine (No. 2021MS464), and the Youth Scholarship of Chengdu University of Traditional Chinese Medicine (No. QNXZ2019043).

REFERENCES

Anne Stetler, R., Leak, R. K., Gao, Y., and Chen, J. (2013). The Dynamics of the Mitochondrial Organelle as a Potential Therapeutic Target. *J. Cereb. Blood Flow Metab.* 33 (1), 22–32. doi:10.1038/jcbfm.2012.158

Australian Institute of Health and Welfare (2020). National Drug Strategy Household Survey 2019. Available at: https://www.aihw.gov.au/reports/illicit-use-of-drugs/national-drug-strategy-household-survey-2019/contents/summary (Accessed July 10, 2021).

Bach, P., Hayashi, K., Milloy, M. J., Nosova, E., Kerr, T., Wood, E., et al. (2020). Characterising the Increasing Prevalence of crystal Methamphetamine Use in Vancouver, Canada, from 2006-2017: A Gender-Based Analysis. *Drug Alcohol. Rev.* 39 (7), 932–940. doi:10.1111/dar.13126

Bahar, E., Kim, H., and Yoon, H. (2016). ER Stress-Mediated Signaling: Action Potential and Ca(2+) as Key Players. *Int. J. Mol. Sci.* 17 (9), 1558. doi:10.3390/ijms17091558

Baker, D. D., Chu, M., Oza, U., and Rajgarhia, V. (2007). The Value of Natural Products to Future Pharmaceutical Discovery. *Nat. Prod. Rep.* 24 (6), 1225–1244. doi:10.1039/b602241n

Baradhi, K. M., Pathireddy, S., Bose, S., and Aeddula, N. R. (2019). Methamphetamine (N-Methylamphetamine)-Induced Renal Disease: Underevaluated Cause of End-Stage Renal Disease (ESRD). *BMJ Case Rep.* 12 (9), e230288. doi:10.1136/bcr-2019-230288

Barbosa, D. J., Capela, J. P., Feio-Azevedo, R., Teixeira-Gomes, A., Bastos, M. D. L., and Carvalho, F. (2015). Mitochondria: Key Players in the Neurotoxic Effects of Amphetamines. *Arch. Toxicol.* 89 (10), 1695–1725. doi:10.1007/s00204-015-1478-9

Beirami, E., Oryan, S., Seyedhosseini Tamijani, S. M., Ahmadiani, A., and Dargahi, L. (2018). Intranasal Insulin Treatment Restores Cognitive Deficits and Insulin Signaling Impairment Induced by Repeated Methamphetamine Exposure. *J. Cel Biochem.* 119 (2), 2345–2355. doi:10.1002/jcb.26398

Bratton, S. B., and Salvesen, G. S. (2010). Regulation of the Apaf-1-Caspase-9 Apoptosome. *J. Cel Sci.* 123 (Pt 19), 3209–3214. doi:10.1242/jcs.073643

Cadet, J. L., Jayanthi, S., and Deng, X. (2003). Speed Kills: Cellular and Molecular Bases of Methamphetamine-Induced Nerve Terminal Degeneration and Neuronal Apoptosis. *FASEB J.* 17 (13), 1775–1788. doi:10.1096/fj.03-0073rev

Cain, K., Bratton, S. B., and Cohen, G. M. (2002). The Apaf-1 Apoptosome: a Large Caspase-Activating Complex. *Biochimie* 84 (2-3), 203–214. doi:10.1016/s0300-9084(02)01376-7

Chen, X., Yang, X., Wang, J., and Li, X. (2016). Effects of Psuedoginsenoside F11 on the Oxidation Material Levels in the Serum and Brain Tissue of Methamphetamine - Dependent Rats (China). *West China J. Pharm. Sci.* 31 (02), 152–153. doi:10.13375/j.cnki.wcjps.2016.02.013

Chen, X., Lu, J., Zhao, X., Chen, C., Qiao, D., Wang, H., et al. (2019). Role of C/EBP-β in Methamphetamine-Mediated Microglial Apoptosis. *Front. Cel Neurosci.* 13, 366. doi:10.3389/fncel.2019.00366

Chi, D., Sun, Y., and Pan, S. (2017). The Protective Effect and its Mechanism of Antrodia Camphorata Enzyme on the Cytotoxicity Injury of PC12 Cells Induced by Amphetamine (China). *Chin. J. Clin. Anat.* 35 (4), 397408–398401. doi:10.13418/j.issn.1001-165x.2017.04.009

Chiang, M., Lombardi, D., Du, J., Makrum, U., Sitthichai, R., Harrington, A., et al. (2019). Methamphetamine-associated Psychosis: Clinical Presentation, Biological Basis, and Treatment Options. *Hum. Psychopharmacol.* 34 (5), e2710. doi:10.1002/hup.2710

CNNCC (2019). National Drug Report. China National Narcotics Control Committee. Available at: http://www.gov.cn/xinwen/2020-06/28/content_5522443.htm (Accessed July 10, 2021).

Coelho-Santos, V., Gonçalves, J., Fontes-Ribeiro, C., and Silva, A. P. (2012). Prevention of Methamphetamine-Induced Microglial Cell Death by TNF-α and IL-6 through Activation of the JAK-STAT Pathway. *J. Neuroinflammation* 9, 103. doi:10.1186/1742-2094-9-103

Courtney, K. E., and Ray, L. A. (2014). Methamphetamine: an Update on Epidemiology, Pharmacology, Clinical Phenomenology, and Treatment Literature. *Drug Alcohol Depend.* 143, 11–21. doi:10.1016/j.drugalcdep.2014.08.003

Dang, D. K., Shin, E. J., Nam, Y., Ryoo, S., Jeong, J. H., Jang, C. G., et al. (2016). Apocynin Prevents Mitochondrial Burdens, Microglial Activation, and Pro-apoptosis Induced by a Toxic Dose of Methamphetamine in the Striatum of Mice via Inhibition of P47phox Activation by ERK. *J. Neuroinflammation* 13, 12. doi:10.1186/s12974-016-0478-x

Davidson, C., Gow, A. J., Lee, T. H., and Ellinwood, E. H. (2001). Methamphetamine Neurotoxicity: Necrotic and Apoptotic Mechanisms and Relevance to Human Abuse and Treatment. *Brain Res. Brain Res. Rev.* 36 (1), 1–22. doi:10.1016/s0165-0173(01)00054-6

Dawson, T. M., and Dawson, V. L. (2017). Mitochondrial Mechanisms of Neuronal Cell Death: Potential Therapeutics. *Annu. Rev. Pharmacol. Toxicol.* 57, 437–454. doi:10.1146/annurev-pharmtox-010716-105001

Dean, A. C., Groman, S. M., Morales, A. M., and London, E. D. (2013). An Evaluation of the Evidence that Methamphetamine Abuse Causes Cognitive Decline in Humans. *Neuropsychopharmacology* 38 (2), 259–274. doi:10.1038/npp.2012.179

Ekiert, H. M., and Szopa, A. (2020). Biological Activities of Natural Products. *Molecules* 25 (23), 5769. doi:10.3390/molecules25235769

Elinore, F. M (2020). *National Survey on Drug Use and Health-2019*. Substance Abuse and Mental Health Services Administration. Available at: https://www.samhsa.gov/data/data-we-collect/nsduh-national-survey-drug-use-and-health (Accessed July 10, 2021).

Ernst, T., Chang, L., Leonido-Yee, M., and Speck, O. (2000). Evidence for Long-Term Neurotoxicity Associated with Methamphetamine Abuse: A 1H MRS Study. *Neurology* 54 (6), 1344–1349. doi:10.1212/wnl.54.6.1344

Eyerman, D. J., and Yamamoto, B. K. (2005). Lobeline Attenuates Methamphetamine-Induced Changes in Vesicular Monoamine Transporter 2 Immunoreactivity and Monoamine Depletions in the Striatum. *J. Pharmacol. Exp. Ther.* 312 (1), 160–169. doi:10.1124/jpet.104.072264

Feng, L., He, W., Lin, S., Ruan, Y., Yuan, C., Qiu, H., et al. (2020). The Association between Interleukin-8 Levels and the Development of Withdrawal Symptoms during Methamphetamine Abstinence. *Hum. Psychopharmacol.* 35 (4), e2736. doi:10.1002/hup.2736

Fleckenstein, A. E., Volz, T. J., and Hanson, G. R. (2009). Psychostimulant-induced Alterations in Vesicular Monoamine Transporter-2 Function: Neurotoxic and Therapeutic Implications. *Neuropharmacology* 56 (Suppl. 1), 133–138. doi:10.1016/j.neuropharm.2008.07.002

Friend, D. M., and Keefe, K. A. (2013). A Role for D1 Dopamine Receptors in Striatal Methamphetamine-Induced Neurotoxicity. *Neurosci. Lett.* 555, 243–247. doi:10.1016/j.neulet.2013.08.039

Fu, K., Lin, H., Miyamoto, Y., Wu, C., Yang, J., Uno, K., et al. (2016). Pseudoginsenoside-F11 Inhibits Methamphetamine-Induced Behaviors by Regulating Dopaminergic and GABAergic Neurons in the Nucleus Accumbens. *Psychopharmacology* 233 (5), 831–840. doi:10.1007/s00213-015-4159-8

Gaston, T. E., Mendrick, D. L., Paine, M. F., Roe, A. L., and Yeung, C. K. (2020). "Natural" Is Not Synonymous with "Safe": Toxicity of Natural Products Alone and in Combination with Pharmaceutical Agents. *Regul. Toxicol. Pharmacol.* 113, 104642. doi:10.1016/j.yrtph.2020.104642

Glasner-Edwards, S., and Mooney, L. J. (2014). Methamphetamine Psychosis: Epidemiology and Management. *CNS Drugs* 28 (12), 1115–1126. doi:10.1007/s40263-014-0209-8

Go, B. S., Kim, J., Yang, J. H., and Choe, E. S. (2017). Psychostimulant-Induced Endoplasmic Reticulum Stress and Neurodegeneration. *Mol. Neurobiol.* 54 (6), 4041–4048. doi:10.1007/s12035-016-9969-0

Golsorkhdan, S. A., Boroujeni, M. E., Aliaghaei, A., Abdollahifar, M. A., Ramezanpour, A., Nejatbakhsh, R., et al. (2020). Methamphetamine Administration Impairs Behavior, Memory and Underlying Signaling Pathways in the hippocampus. *Behav. Brain Res.* 379, 112300. doi:10.1016/j.bbr.2019.112300

Gonçalves, J., Martins, T., Ferreira, R., Milhazes, N., Borges, F., Ribeiro, C. F., et al. (2008). Methamphetamine-induced Early Increase of IL-6 and TNF-Alpha mRNA Expression in the Mouse Brain. *Ann. N. Y Acad. Sci.* 1139, 103–111. doi:10.1196/annals.1432.043

Gonçalves, J., Baptista, S., Martins, T., Milhazes, N., Borges, F., Ribeiro, C. F., et al. (2010). Methamphetamine-induced Neuroinflammation and Neuronal Dysfunction in the Mice hippocampus: Preventive Effect of Indomethacin. *Eur. J. Neurosci.* 31 (2), 315–326. doi:10.1111/j.1460-9568.2009.07059.x

Hadizadeh-Bazaz, M., Vaezi, G., Khaksari, M., and Hojati, V. (2021). Curcumin Attenuates Spatial Memory Impairment by Anti-oxidative, Anti-apoptosis, and Anti-inflammatory Mechanism against Methamphetamine Neurotoxicity in Male Wistar Rats: Histological and Biochemical Changes. *Neurotoxicology* 84, 208–217. doi:10.1016/j.neuro.2021.03.011

Halpin, L. E., Collins, S. A., and Yamamoto, B. K. (2014a). Neurotoxicity of Methamphetamine and 3,4-methylenedioxymethamphetamine. *Life Sci.* 97 (1), 37–44. doi:10.1016/j.lfs.2013.07.014

Halpin, L. E., Northrop, N. A., and Yamamoto, B. K. (2014b). Ammonia Mediates Methamphetamine-Induced Increases in Glutamate and Excitotoxicity. *Neuropsychopharmacology* 39 (4), 1031–1038. doi:10.1038/npp.2013.306

Heinrich, M., Appendino, G., Efferth, T., Fürst, R., Izzo, A. A., Kayser, O., et al. (2020). Best Practice in Research - Overcoming Common Challenges in Phytopharmacological Research. *J. Ethnopharmacol.* 246, 112230. doi:10.1016/j.jep.2019.112230

Hermida-Ameijeiras, A., Méndez-Alvarez, E., Sánchez-Iglesias, S., Sanmartín-Suárez, C., and Soto-Otero, R. (2004). Autoxidation and MAO-Mediated Metabolism of Dopamine as a Potential Cause of Oxidative Stress: Role of Ferrous and Ferric Ions. *Neurochem. Int.* 45 (1), 103–116. doi:10.1016/j.neuint.2003.11.018

Homer, B. D., Solomon, T. M., Moeller, R. W., Mascia, A., DeRaleau, L., and Halkitis, P. N. (2008). Methamphetamine Abuse and Impairment of Social Functioning: a Review of the Underlying Neurophysiological Causes and Behavioral Implications. *Psychol. Bull.* 134 (2), 301–310. doi:10.1037/0033-2909.134.2.301

Howitz, K. T., Bitterman, K. J., Cohen, H. Y., Lamming, D. W., Lavu, S., Wood, J. G., et al. (2003). Small Molecule Activators of Sirtuins Extend *Saccharomyces cerevisiae* Lifespan. *Nature* 425 (6954), 191–196. doi:10.1038/nature01960

Hu, H., Tian, M., Ding, C., and Yu, S. (2018). The C/EBP Homologous Protein (CHOP) Transcription Factor Functions in Endoplasmic Reticulum Stress-Induced Apoptosis and Microbial Infection. *Front. Immunol.* 9, 3083. doi:10.3389/fimmu.2018.03083

Huang, Y. N., Wang, J. Y., Lee, C. T., Lin, C. H., Lai, C. C., and Wang, J. Y. (2012). L-ascorbate Attenuates Methamphetamine Neurotoxicity through Enhancing the Induction of Endogenous Heme Oxygenase-1. *Toxicol. Appl. Pharmacol.* 265 (2), 241–252. doi:10.1016/j.taap.2012.08.036

Huang, M. C., Lin, S. K., Chen, C. H., Pan, C. H., Lee, C. H., and Liu, H. C. (2013). Oxidative Stress Status in Recently Abstinent Methamphetamine Abusers. *Psychiatry Clin. Neurosci.* 67 (2), 92–100. doi:10.1111/pcn.12025

Iversen, L. (2006). Neurotransmitter Transporters and Their Impact on the Development of Psychopharmacology. *Br. J. Pharmacol.* 147 (Suppl. 1), S82–S88. doi:10.1038/sj.bjp.0706428

Jayanthi, S., Deng, X., Bordelon, M., McCoy, M. T., and Cadet, J. L. (2001). Methamphetamine Causes Differential Regulation of Pro-death and Anti-death Bcl-2 Genes in the Mouse Neocortex. *FASEB J.* 15 (10), 1745–1752. doi:10.1096/fj.01-0025com

Jayanthi, S., Deng, X., Noailles, P. A., Ladenheim, B., and Cadet, J. L. (2004). Methamphetamine Induces Neuronal Apoptosis via Cross-Talks between Endoplasmic Reticulum and Mitochondria-dependent Death Cascades. *FASEB J.* 18 (2), 238–251. doi:10.1096/fj.03-0295com

Jha, V., and Rathi, M. (2008). Natural Medicines Causing Acute Kidney Injury. *Semin. Nephrol.* 28 (4), 416–428. doi:10.1016/j.semnephrol.2008.04.010

Jiang, X., and Wang, X. (2000). Cytochrome C Promotes Caspase-9 Activation by Inducing Nucleotide Binding to Apaf-1. *J. Biol. Chem.* 275 (40), 31199–31203. doi:10.1074/jbc.C000405200

Jones, C. M., Compton, W. M., and Mustaquim, D. (2020). Patterns and Characteristics of Methamphetamine Use Among Adults - United States, 2015-2018. *Morb. Mortal. Wkly. Rep.* 69 (12), 317–323. doi:10.15585/mmwr.mm6912a1

Kang, Y., Lee, J. H., Seo, Y. H., Jang, J. H., Jeong, C. H., Lee, S., et al. (2019). Epicatechin Prevents Methamphetamine-Induced Neuronal Cell Death via Inhibition of ER Stress. *Biomol. Ther. (Seoul)* 27 (2), 145–151. doi:10.4062/biomolther.2018.092

Kanthasamy, A. G., Kitazawa, M., Kanthasamy, A., and Anantharam, V. (2003). Role of Proteolytic Activation of Protein Kinase Cdelta in Oxidative Stress-Induced Apoptosis. *Antioxid. Redox Signal.* 5 (5), 609–620. doi:10.1089/152308603770310275

Kanthasamy, K., Gordon, R., Jin, H., Anantharam, V., Ali, S., Kanthasamy, A. G., et al. (2011). Neuroprotective Effect of Resveratrol against Methamphetamine-Induced Dopaminergic Apoptotic Cell Death in a Cell Culture Model of Neurotoxicity. *Curr. Neuropharmacol.* 9 (1), 49–53. doi:10.2174/157015911795017353

Kaul, S., Kanthasamy, A., Kitazawa, M., Anantharam, V., and Kanthasamy, A. G. (2003). Caspase-3 Dependent Proteolytic Activation of Protein Kinase C delta Mediates and Regulates 1-Methyl-4-Phenylpyridinium (MPP+)-induced Apoptotic Cell Death in Dopaminergic Cells: Relevance to Oxidative Stress in Dopaminergic Degeneration. *Eur. J. Neurosci.* 18 (6), 1387–1401. doi:10.1046/j.1460-9568.2003.02864.x

Kevil, C. G., Goeders, N. E., Woolard, M. D., Bhuiyan, M. S., Dominic, P., Kolluru, G. K., et al. (2019). Methamphetamine Use and Cardiovascular Disease. *Arterioscler Thromb. Vasc. Biol.* 39 (9), 1739–1746. doi:10.1161/ATVBAHA.119.312461

Kim, C., and Kim, B. (2018). Anti-Cancer Natural Products and Their Bioactive Compounds Inducing ER Stress-Mediated Apoptosis: A Review. *Nutrients* 10 (8), 1021. doi:10.3390/nu10081021

Kim, H. S., Kang, J. G., Rheu, H. M., Cho, D. H., and Oh, K. W. (1995). Blockade by Ginseng Total Saponin of the Development of Methamphetamine Reverse Tolerance and Dopamine Receptor Supersensitivity in Mice. *Planta Med.* 61 (1), 22–25. doi:10.1055/s-2006-957991

Kim, H. S., Jang, C. G., Park, W. K., Oh, K. W., Rheu, H. M., Cho, D. H., et al. (1996). Blockade by Ginseng Total Saponin of Methamphetamine-Induced Hyperactivity and Conditioned Place Preference in Mice. *Gen. Pharmacol.* 27 (2), 199–204. doi:10.1016/0306-3623(95)02023-3

Kim, B., Yun, J., and Park, B. (2020). Methamphetamine-Induced Neuronal Damage: Neurotoxicity and Neuroinflammation. *Biomol. Ther. (Seoul)* 28 (5), 381–388. doi:10.4062/biomolther.2020.044

Krasnova, I. N., and Cadet, J. L. (2009). Methamphetamine Toxicity and Messengers of Death. *Brain Res. Rev.* 60 (2), 379–407. doi:10.1016/j.brainresrev.2009.03.002

Kroemer, G., Galluzzi, L., and Brenner, C. (2007). Mitochondrial Membrane Permeabilization in Cell Death. *Physiol. Rev.* 87 (1), 99–163. doi:10.1152/physrev.00013.2006

Lappin, J. M., Darke, S., and Farrell, M. (2018). Methamphetamine Use and Future Risk for Parkinson's Disease: Evidence and Clinical Implications. *Drug Alcohol Depend.* 187, 134–140. doi:10.1016/j.drugalcdep.2018.02.032

Lee, H.-S., Kim, E.-N., and Jeong, G.-S. (2021). Aromadendrin Protects Neuronal Cells from Methamphetamine-Induced Neurotoxicity by Regulating Endoplasmic Reticulum Stress and PI3K/Akt/mTOR Signaling Pathway. *Int. J. Mol. Sci.* 22 (5), 2274. doi:10.3390/ijms22052274

Li, Z., Wu, C. F., Pei, G., Guo, Y. Y., and Li, X. (2000). Antagonistic Effect of Pseudoginsenoside-F11 on the Behavioral Actions of Morphine in Mice. *Pharmacol. Biochem. Behav.* 66 (3), 595–601. doi:10.1016/s0091-3057(00)00260-4

Liu, M., Bai, X., Yu, S., Zhao, W., Qiao, J., Liu, Y., et al. (2019). Ginsenoside Re Inhibits ROS/ASK-1 Dependent Mitochondrial Apoptosis Pathway and Activation of Nrf2-Antioxidant Response in Beta-Amyloid-Challenged SH-SY5Y Cells. *Molecules* 24 (15), 2687. doi:10.3390/molecules24152687

Lu, L., Liu, Y., Zhu, W., Shi, J., Liu, Y., Ling, W., et al. (2009). Traditional Medicine in the Treatment of Drug Addiction. *Am. J. Drug Alcohol. Abuse* 35 (1), 1–11. doi:10.1080/00952990802455469

Lu, S., Xinxin, L., and Kun, L. (2015). Caspase-3 and Bcl-2 Expression in Methamphetamine-dependent Rat Brain Interfered with Astragaloside IV (China). *J. Apoplexy Nervous Dis.* 32 (6), 505–507. doi:10.19845/j.cnki.zfysjjbzz.2015.06.007

Lull, M. E., and Block, M. L. (2010). Microglial Activation and Chronic Neurodegeneration. *Neurotherapeutics* 7 (4), 354–365. doi:10.1016/j.nurt.2010.05.014

Ma, C. L., Li, L., Yang, G. M., Zhang, Z. B., Zhao, Y. N., Zeng, X. F., et al. (2020). Neuroprotective Effect of Gastrodin in Methamphetamine-Induced Apoptosis through Regulating cAMP/PKA/CREB Pathway in Cortical Neuron. *Hum. Exp. Toxicol.* 39 (8), 1118–1129. doi:10.1177/0960327120911438

Mark, K. A., Soghomonian, J. J., and Yamamoto, B. K. (2004). High-dose Methamphetamine Acutely Activates the Striatonigral Pathway to Increase Striatal Glutamate and Mediate Long-Term Dopamine Toxicity. *J. Neurosci.* 24 (50), 11449–11456. doi:10.1523/JNEUROSCI.3597-04.2004

Martinez, J. A., Zhang, Z., Svetlov, S. I., Hayes, R. L., Wang, K. K., and Larner, S. F. (2010). Calpain and Caspase Processing of Caspase-12 Contribute to the ER Stress-Induced Cell Death Pathway in Differentiated PC12 Cells. *Apoptosis* 15 (12), 1480–1493. doi:10.1007/s10495-010-0526-4

McDonnell-Dowling, K., and Kelly, J. P. (2017). The Role of Oxidative Stress in Methamphetamine-Induced Toxicity and Sources of Variation in the Design of Animal Studies. *Curr. Neuropharmacol.* 15 (2), 300–314. doi:10.2174/1570159x14666160428110329

McFadden, L. M., Stout, K. A., Vieira-Brock, P. L., Allen, S. C., Nielsen, S. M., Wilkins, D. G., et al. (2012). Methamphetamine Self-Administration Acutely Decreases Monoaminergic Transporter Function. *Synapse* 66 (3), 240–245. doi:10.1002/syn.21506

McFadden, L. M., Cordie, R., Livermont, T., and Johansen, A. (2018). Behavioral and Serotonergic Changes in the Frontal Cortex Following Methamphetamine Self-Administration. *Int. J. Neuropsychopharmacol.* 21 (8), 758–763. doi:10.1093/ijnp/pyy044

Michel, S., Wanet, A., De Pauw, A., Rommelaere, G., Arnould, T., and Renard, P. (2012). Crosstalk between Mitochondrial (Dys)function and Mitochondrial Abundance. *J. Cel Physiol.* 227 (6), 2297–2310. doi:10.1002/jcp.23021

Miller, D. K., Oelrichs, C. E., Sun, G. Y., and Simonyi, A. (2014). Subchronic Apocynin Treatment Attenuates Methamphetamine-Induced Dopamine Release and Hyperactivity in Rats. *Life Sci.* 98 (1), 6–11. doi:10.1016/j.lfs.2013.12.031

Mizoguchi, H., and Yamada, K. (2019). Methamphetamine Use Causes Cognitive Impairment and Altered Decision-Making. *Neurochem. Int.* 124, 106–113. doi:10.1016/j.neuint.2018.12.019

Moratalla, R., Khairnar, A., Simola, N., Granado, N., García-Montes, J. R., Porceddu, P. F., et al. (2017). Amphetamine-related Drugs Neurotoxicity in Humans and in Experimental Animals: Main Mechanisms. *Prog. Neurobiol.* 155, 149–170. doi:10.1016/j.pneurobio.2015.09.011

Moszczynska, A., and Callan, S. P. (2017). Molecular, Behavioral, and Physiological Consequences of Methamphetamine Neurotoxicity: Implications for Treatment. *J. Pharmacol. Exp. Ther.* 362 (3), 474–488. doi:10.1124/jpet.116.238501

Mozaffari, S., Ramezany Yasuj, S., Motaghinejad, M., Motevalian, M., and Kheiri, R. (2019). Crocin Acting as a Neuroprotective Agent against Methamphetamine-Induced Neurodegeneration via CREB-BDNF Signaling Pathway. *Iran J. Pharm. Res.* 18 (2), 745–758. doi:10.22037/ijpr.2019.2393

Nakagawa, T., and Yuan, J. (2000). Cross-talk between Two Cysteine Protease Families. Activation of Caspase-12 by Calpain in Apoptosis. *J. Cel Biol.* 150 (4), 887–894. doi:10.1083/jcb.150.4.887

Nam, Y., Wie, M. B., Shin, E. J., Nguyen, T. T., Nah, S. Y., Ko, S. K., et al. (2015). Ginsenoside Re Protects Methamphetamine-Induced Mitochondrial Burdens

and Proapoptosis via Genetic Inhibition of Protein Kinase C δ in Human Neuroblastoma Dopaminergic SH-SY5Y Cell Lines. *J. Appl. Toxicol.* 35 (8), 927–944. doi:10.1002/jat.3093

Nauffal, M., and Gabardi, S. (2016). Nephrotoxicity of Natural Products. *Blood Purif.* 41 (1-3), 123–129. doi:10.1159/000441268

Nguyen, X. K., Lee, J., Shin, E. J., Dang, D. K., Jeong, J. H., Nguyen, T. T., et al. (2015). Liposomal Melatonin Rescues Methamphetamine-Elicited Mitochondrial Burdens, Pro-apoptosis, and Dopaminergic Degeneration through the Inhibition PKCδ Gene. *J. Pineal Res.* 58 (1), 86–106. doi:10.1111/jpi.12195

Nordahl, T. E., Salo, R., and Leamon, M. (2003). Neuropsychological Effects of Chronic Methamphetamine Use on Neurotransmitters and Cognition: a Review. *J. Neuropsychiatry Clin. Neurosci.* 15 (3), 317–325. doi:10.1176/jnp.15.3.317

Oh, K. W., Kim, H. S., and Wagner, G. C. (1997a). Inhibitory Effects of Ginseng Total Saponin on Methamphetamine-Induced Striatal Dopamine Increase in Mice. *Arch. Pharm. Res.* 20 (5), 516–518. doi:10.1007/BF02973952

Oh, K. W., Kim, H. S., and Wagner, G. C. (1997b). Ginseng Total Saponin Inhibits the Dopaminergic Depletions Induced by Methamphetamine. *Planta Med.* 63 (1), 80–81. doi:10.1055/s-2006-957610

Pan, A. L., Hasalliu, E., Hasalliu, M., and Angulo, J. A. (2020). Epigallocatechin Gallate Mitigates the Methamphetamine-Induced Striatal Dopamine Terminal Toxicity by Preventing Oxidative Stress in the Mouse Brain. *Neurotox Res.* 37 (4), 883–892. doi:10.1007/s12640-020-00177-1

Panenka, W. J., Procyshyn, R. M., Lecomte, T., MacEwan, G. W., Flynn, S. W., Honer, W. G., et al. (2013). Methamphetamine Use: a Comprehensive Review of Molecular, Preclinical and Clinical Findings. *Drug Alcohol Depend.* 129 (3), 167–179. doi:10.1016/j.drugalcdep.2012.11.016

Park, J. H., Seo, Y. H., Jang, J. H., Jeong, C. H., Lee, S., and Park, B. (2017). Asiatic Acid Attenuates Methamphetamine-Induced Neuroinflammation and Neurotoxicity through Blocking of NF-kB/STAT3/ERK and Mitochondria-Mediated Apoptosis Pathway. *J. Neuroinflammation* 14 (1), 240. doi:10.1186/s12974-017-1009-0

Potashkin, J. A., and Meredith, G. E. (2006). The Role of Oxidative Stress in the Dysregulation of Gene Expression and Protein Metabolism in Neurodegenerative Disease. *Antioxid. Redox Signal.* 8 (1-2), 144–151. doi:10.1089/ars.2006.8.144

Radhakrishnan, M. L., and Tidor, B. (2008). Optimal Drug Cocktail Design: Methods for Targeting Molecular Ensembles and Insights from Theoretical Model Systems. *J. Chem. Inf. Model.* 48 (5), 1055–1073. doi:10.1021/ci700452r

Riddle, E. L., Fleckenstein, A. E., and Hanson, G. R. (2006). Mechanisms of Methamphetamine-Induced Dopaminergic Neurotoxicity. *AAPS J.* 8 (2), E413–E418. doi:10.1007/BF02854914

Ríos, J. L., Onteniente, M., Picazo, D., and Montesinos, M. C. (2016). Medicinal Plants and Natural Products as Potential Sources for Antiparkinson Drugs. *Planta Med.* 82 (11-12), 942–951. doi:10.1055/s-0042-107081

Roth, K. A., and D'Sa, C. (2001). Apoptosis and Brain Development. *Ment. Retard. Dev. Disabil. Res. Rev.* 7 (4), 261–266. doi:10.1002/mrdd.1036

Rusyniak, D. E. (2013). Neurologic Manifestations of Chronic Methamphetamine Abuse. *Psychiatr. Clin. North. Am.* 36 (2), 261–275. doi:10.1016/j.psc.2013.02.005

Sanchez, A., Malaty, I. A., Khanna, A., Busl, K., Youn, T. S., Nagaraja, N., et al. (2018). Bilateral Basal Ganglia Necrosis Secondary to Methamphetamine. *Mov Disord. Clin. Pract.* 5 (5), 555–556. doi:10.1002/mdc3.12649

Sano, R., and Reed, J. C. (2013). ER Stress-Induced Cell Death Mechanisms. *Biochim. Biophys. Acta* 1833 (12), 3460–3470. doi:10.1016/j.bbamcr.2013.06.028

Schep, L. J., Slaughter, R. J., and Beasley, D. M. (2010). The Clinical Toxicology of Metamfetamine. *Clin. Toxicol. (Phila)* 48 (7), 675–694. doi:10.3109/15563650.2010.516752

Schwartz, K., Weizman, A., and Rehavi, M. (2006). The Effect of Psychostimulants on [3H]dopamine Uptake and Release in Rat Brain Synaptic Vesicles. *J. Neural Transm. (Vienna)* 113 (9), 1347–1352. doi:10.1007/s00702-005-0383-4

Sekine, Y., Ouchi, Y., Sugihara, G., Takei, N., Yoshikawa, E., Nakamura, K., et al. (2008). Methamphetamine Causes Microglial Activation in the Brains of Human Abusers. *J. Neurosci.* 28 (22), 5756–5761. doi:10.1523/JNEUROSCI.1179-08.2008

Shaerzadeh, F., Streit, W. J., Heysieattalab, S., and Khoshbouei, H. (2018). Methamphetamine Neurotoxicity, Microglia, and Neuroinflammation. *J. Neuroinflammation* 15 (1), 341. doi:10.1186/s12974-018-1385-0

Shafahi, M., Vaezi, G., Shajiee, H., Sharafi, S., and Khaksari, M. (2018). Crocin Inhibits Apoptosis and Astrogliosis of Hippocampus Neurons against Methamphetamine Neurotoxicity via Antioxidant and Anti-inflammatory Mechanisms. *Neurochem. Res.* 43 (12), 2252–2259. doi:10.1007/s11064-018-2644-2

Shah, A., Silverstein, P. S., Singh, D. P., and Kumar, A. (2012). Involvement of Metabotropic Glutamate Receptor 5, AKT/PI3K Signaling and NF-κB Pathway in Methamphetamine-Mediated Increase in IL-6 and IL-8 Expression in Astrocytes. *J. Neuroinflammation* 9, 52. doi:10.1186/1742-2094-9-52

Shen, K., Zhang, Y., Lv, X., Chen, X., Zhou, R., Nguyen, L. K., et al. (2016). Molecular Mechanisms Involving Sigma-1 Receptor in Cell Apoptosis of BV-2 Microglial Cells Induced by Methamphetamine. *CNS Neurol. Disord. Drug Targets* 15 (7), 857–865. doi:10.2174/1871527315666160518122816

Shin, E. J., Bach, J. H., Nguyen, T. T., Nguyen, X. K., Jung, B. D., Oh, K. W., et al. (2011). Gastrodia Elata Bl Attenuates Methamphetamine-Induced Dopaminergic Toxicity via Inhibiting Oxidative Burdens. *Curr. Neuropharmacol.* 9 (1), 118–121. doi:10.2174/157015911795016967

Shin, E. J., Shin, S. W., Nguyen, T. T., Park, D. H., Wie, M. B., Jang, C. G., et al. (2014). Ginsenoside Re Rescues Methamphetamine-Induced Oxidative Damage, Mitochondrial Dysfunction, Microglial Activation, and Dopaminergic Degeneration by Inhibiting the Protein Kinase Cδ Gene. *Mol. Neurobiol.* 49 (3), 1400–1421. doi:10.1007/s12035-013-8617-1

Shin, E. J., Dang, D. K., Tran, T. V., Tran, H. Q., Jeong, J. H., Nah, S. Y., et al. (2017). Current Understanding of Methamphetamine-Associated Dopaminergic Neurodegeneration and Psychotoxic Behaviors. *Arch. Pharm. Res.* 40 (4), 403–428. doi:10.1007/s12272-017-0897-y

Shin, E. J., Tran, H. Q., Nguyen, P. T., Jeong, J. H., Nah, S. Y., Jang, C. G., et al. (2018). Role of Mitochondria in Methamphetamine-Induced Dopaminergic Neurotoxicity: Involvement in Oxidative Stress, Neuroinflammation, and Pro-apoptosis-A Review. *Neurochem. Res.* 43 (1), 66–78. doi:10.1007/s11064-017-2318-5

Shukla, M., and Vincent, B. (2020). The Multi-Faceted Impact of Methamphetamine on Alzheimer's Disease: From a Triggering Role to a Possible Therapeutic Use. *Ageing Res. Rev.* 60, 101062. doi:10.1016/j.arr.2020.101062

Solayman, M., Islam, M. A., Alam, F., Khalil, M. I., Kamal, M. A., and Gan, S. H. (2017). Natural Products Combating Neurodegeneration: Parkinson's Disease. *Curr. Drug Metab.* 18 (1), 50–61. doi:10.2174/1389200217666160709204826

Sorsdahl, K., Stein, D. J., Pasche, S., Jacobs, Y., Kader, R., Odlaug, B., et al. (2021). A Novel Brief Treatment for Methamphetamine Use Disorders in South Africa: a Randomised Feasibility Trial. *Addict. Sci. Clin. Pract.* 16 (1), 3. doi:10.1186/s13722-020-00209-3

Stephans, S. E., and Yamamoto, B. K. (1994). Methamphetamine-induced Neurotoxicity: Roles for Glutamate and Dopamine Efflux. *Synapse* 17 (3), 203–209. doi:10.1002/syn.890170310

Sun, D., Yue, Q., Guo, W., Li, T., Zhang, J., Li, G., et al. (2015). Neuroprotection of Resveratrol against Neurotoxicity Induced by Methamphetamine in Mouse Mesencephalic Dopaminergic Neurons. *Biofactors* 41 (4), 252–260. doi:10.1002/biof.1221

Tata, D. A., and Yamamoto, B. K. (2007). Interactions between Methamphetamine and Environmental Stress: Role of Oxidative Stress, Glutamate and Mitochondrial Dysfunction. *Addiction* 102 (Suppl. 1), 49–60. doi:10.1111/j.1360-0443.2007.01770.x

UNODC (2020). World Drug Report 2021. Available at: https://wdr.unodc.org/wdr2020/index.html (Accessed July 10, 2021).

Valian, N., Ahmadiani, A., and Dargahi, L. (2017). Escalating Methamphetamine Regimen Induces Compensatory Mechanisms, Mitochondrial Biogenesis, and GDNF Expression, in Substantia Nigra. *J. Cel Biochem* 118 (6), 1369–1378. doi:10.1002/jcb.25795

Wang, X., Wang, C., Wang, J., Zhao, S., Zhang, K., Wang, J., et al. (2014). Pseudoginsenoside-F11 (PF11) Exerts Anti-neuroinflammatory Effects on LPS-Activated Microglial Cells by Inhibiting TLR4-Mediated TAK1/IKK/NF-κB, MAPKs and Akt Signaling Pathways. *Neuropharmacology* 79, 642–656. doi:10.1016/j.neuropharm.2014.01.022

Wang, K. H., Penmatsa, A., and Gouaux, E. (2015). Neurotransmitter and Psychostimulant Recognition by the Dopamine Transporter. *Nature* 521 (7552), 322–327. doi:10.1038/nature14431

Wu, C. F., Liu, Y. L., Song, M., Liu, W., Wang, J. H., Li, X., et al. (2003). Protective Effects of Pseudoginsenoside-F11 on Methamphetamine-Induced Neurotoxicity in Mice. *Pharmacol. Biochem. Behav.* 76 (1), 103–109. doi:10.1016/s0091-3057(03)00215-6

Wu, C. W., Ping, Y. H., Yen, J. C., Chang, C. Y., Wang, S. F., Yeh, C. L., et al. (2007). Enhanced Oxidative Stress and Aberrant Mitochondrial Biogenesis in Human Neuroblastoma SH-SY5Y Cells during Methamphetamine Induced Apoptosis. *Toxicol. Appl. Pharmacol.* 220 (3), 243–251. doi:10.1016/j.taap.2007.01.011

Xie, Q., Li, H., Lu, D., Yuan, J., Ma, R., Li, J., et al. (2021). Neuroprotective Effect for Cerebral Ischemia by Natural Products: A Review. *Front. Pharmacol.* 12, 607412. doi:10.3389/fphar.2021.607412

Xu, E., Liu, J., Liu, H., Wang, X., and Xiong, H. (2017). Role of Microglia in Methamphetamine-Induced Neurotoxicity. *Int. J. Physiol. Pathophysiol. Pharmacol.* 9 (3), 84–100.

Yan, T., Li, L., Sun, B., Liu, F., Yang, P., Chen, T., et al. (2014). Luteolin Inhibits Behavioral Sensitization by Blocking Methamphetamine-Induced MAPK Pathway Activation in the Caudate Putamen in Mice. *PLoS One* 9 (6), e98981. doi:10.1371/journal.pone.0098981

Yang, X., Wang, Y., Li, Q., Zhong, Y., Chen, L., Du, Y., et al. (2018). The Main Molecular Mechanisms Underlying Methamphetamine- Induced Neurotoxicity and Implications for Pharmacological Treatment. *Front. Mol. Neurosci.* 11, 186. doi:10.3389/fnmol.2018.00186

Yang, G., Zeng, X., Li, J., Leung, C. K., Zhang, D., Hong, S., et al. (2020). Protective Effect of Gastrodin for Methamphetamine-Induced Neurotoxicity (China). *Chinses Pharmacol. Bull.* 36 (2), 238–245. doi:10.3969/j.issn.1001-1978.2020.02.017

Yu, S., Zhu, L., Shen, Q., Bai, X., and Di, X. (2015). Recent Advances in Methamphetamine Neurotoxicity Mechanisms and its Molecular Pathophysiology. *Behav. Neurol.* 2015, 103969. doi:10.1155/2015/103969

Yun, J. (2014). Limonene Inhibits Methamphetamine-Induced Locomotor Activity via Regulation of 5-HT Neuronal Function and Dopamine Release. *Phytomedicine* 21 (6), 883–887. doi:10.1016/j.phymed.2013.12.004

Zeng, Q., Lin, K., Liang, Z., Xiong, Q., Duan, J., Li, C., et al. (2020). Protective Effect and Mechanism of Terminalia Chebula Polyphenol Extract on Methamphetamine-Induced Injury in PC12 Cells. *Sci. Techn. Food Industry* 41 (05), 299–304. doi:10.13386/j.issn1002-0306.2020.05.049

Zeng, Q., Xiong, Q., Zhou, M., Tian, X., Yue, K., Li, Y., et al. (2021). Resveratrol Attenuates Methamphetamine-Induced Memory Impairment via Inhibition of Oxidative Stress and Apoptosis in Mice. *J. Food Biochem.* 45 (2), e13622. doi:10.1111/jfbc.13622

Zhang, Z., Yang, H., Yang, J., Xie, J., Xu, J., Liu, C., et al. (2019). Pseudoginsenoside-F11 Attenuates Cognitive Impairment by Ameliorating Oxidative Stress and Neuroinflammation in D-galactose-T-reated M-ice. *Int. Immunopharmacol.* 67, 78–86. doi:10.1016/j.intimp.2018.11.026

Zhao, L., Du, L., Zhang, Y., Chao, J., Duan, M., Yao, H., et al. (2019). Role of PUMA in the Methamphetamine-Induced Migration of Microglia. *Metab. Brain Dis.* 34 (1), 61–69. doi:10.1007/s11011-018-0319-y

Conflict of Interest: The authors declare that the research was conducted in the absence of any commercial or financial relationships that could be construed as a potential conflict of interest.

Publisher's Note: All claims expressed in this article are solely those of the authors and do not necessarily represent those of their affiliated organizations, or those of the publisher, the editors and the reviewers. Any product that may be evaluated in this article, or claim that may be made by its manufacturer, is not guaranteed or endorsed by the publisher.

Copyright © 2022 Zeng, Chen, Zhang, Ren, Xia, Liu, Shan and Ren. This is an open-access article distributed under the terms of the Creative Commons Attribution License (CC BY). The use, distribution or reproduction in other forums is permitted, provided the original author(s) and the copyright owner(s) are credited and that the original publication in this journal is cited, in accordance with accepted academic practice. No use, distribution or reproduction is permitted which does not comply with these terms.

frontiers in Pharmacology

REVIEW
published: 27 January 2022
doi: 10.3389/fphar.2022.803717

Apoptosis Induction, a Sharp Edge of Berberine to Exert Anti-Cancer Effects, Focus on Breast, Lung, and Liver Cancer

Yi Zhu[1†], Na Xie[2†], Yilu Chai[1†], Yisen Nie[1†], Ke Liu[1], Yufei Liu[1], Yang Yang[1], Jinsong Su[3] and Chuantao Zhang[1]**

[1]Department of Respiratory Medicine, Hospital of Chengdu University of Traditional Chinese Medicine, Chengdu, China, [2]College of Pharmacy, Chengdu University of Traditional Chinese Medicine, Chengdu, China, [3]State Key Laboratory of Southwestern Chinese Medicine Resources, Innovative Institute of Chinese Medicine and Pharmacy, Chengdu University of Traditional Chinese Medicine, Chengdu, China

OPEN ACCESS

Edited by:
Hong Zhang,
Shanghai University of Traditional Chinese Medicine, China

Reviewed by:
Dhanasekhar Reddy,
Central University of Kerala, India
Lei Gao,
Southern Medical University, China
Xiaoping Pan,
Zhejiang Chinese Medical University, China

***Correspondence:**
Chuantao Zhang
zhangchuantao@cdutcm.edu.cn
Jinsong Su
1508113999@qq.com

†These authors have contributed equally to this work and share first authorship

Specialty section:
This article was submitted to Ethnopharmacology, a section of the journal Frontiers in Pharmacology

Received: *28 October 2021*
Accepted: *10 January 2022*
Published: *27 January 2022*

Citation:
Zhu Y, Xie N, Chai Y, Nie Y, Liu K, Liu Y, Yang Y, Su J and Zhang C (2022) Apoptosis Induction, a Sharp Edge of Berberine to Exert Anti-Cancer Effects, Focus on Breast, Lung, and Liver Cancer. Front. Pharmacol. 13:803717. doi: 10.3389/fphar.2022.803717

Cancer is the leading cause of death and one of the greatest barriers to increased life expectancy worldwide. Currently, chemotherapy with synthetic drugs remains one of the predominant ways for cancer treatment, which may lead to drug resistance and normal organ damage. Increasing researches have suggested that apoptosis, a type of programmed cell death, is a promising way for cancer therapy. Furthermore, natural products are important sources for finding new drugs with high availability, low cost and low toxicity. As a well-known isoquinoline alkaloid, accumulating evidence has revealed that berberine (BBR) exerts potential pro-apoptotic effects on multiple cancers, including breast, lung, liver, gastric, colorectal, pancreatic, and ovarian cancers. The related potential signal pathways are AMP-activated protein kinase, mitogen-activated protein kinase, and protein kinase B pathways. In this review, we provide a timely and comprehensive summary of the detailed molecular mechanisms of BBR in treating three types of cancer (breast, lung and liver cancer) by inducing apoptosis. Furthermore, we also discuss the existing challenges and strategies to improve BBR's bioavailability. Hopefully, this review provides valuable information for the comprehension of BBR in treating three types of cancer and highlight the pro-apoptotic effects of BBR, which would be beneficial for the further development of this natural compound as an effective clinical drug for treating cancers.

Keywords: berberine, bioavailability, ADMET, anticancer effects, apoptosis induction

INTRODUCTION

Cancer is one of the leading causes of death worldwide with estimated 19.3 million new cases and approximately 10 million deaths in 2020 (gco.iarc.fr; Sung et al., 2021). According to the Global Cancer Observatory, lung cancer is the second most diagnosed cancer and the leading cause of cancer mortality, and it is also the leading cause of death in men. In 2020, 2.2 million new lung cancer cases and 1.8 million deaths were predicted, accounting for 18% of all cancer-related deaths. Among women, lung cancer is the principal cause of cancer-related death in many countries, such as most cities in Eastern Europe, West Asia, East Asia (China), and Southeast Asia (gco.iarc.fr). The

incidence rate is generally higher in young women than in young men, which cannot be explained by smoking (Fidler-Benaoudia et al., 2020). Breast cancer is the most commonly diagnosed cancer and the most common cause of death in women. In 2020, approximately 2.3 million women were newly diagnosed with breast cancer and 684,996 women with breast cancer died (gco.iarc.fr). Although the incidence and mortality of breast cancer in high-income countries have been declining, those in low- and middle-income countries have been increasing (Lortet-Tieulent et al., 2020). Globally, the incidence of breast cancer is still on the rise, and there has been a 3.1% annual rate of increase in global breast cancer incidences beginning with 641,000 cases in 1980 to over 1.6 million in 2010 (Bray et al., 2015). Liver cancer was the sixth most commonly diagnosed cancer in the world in 2020 and the third leading cause of cancer-related deaths, with approximately 906,000 new cases and 830,000 deaths. The morbidity and mortality rate of liver cancer in men is two to three times that of women worldwide (gco.iarc.fr). Liver cancer progresses rapidly unless diagnosed early, and the patient's odds are very low (Gravitz, 2014). Currently, the common treatment methods for cancer include radiotherapy, chemotherapy, and surgery; as research progresses, targeted therapy (Mollaei et al., 2019; Thakkar et al., 2020; Song et al., 2021), immunotherapy (Anderson et al., 2021; Myers and Miller, 2021) and metabolic therapy (Park et al., 2020) have also been used to treat various types of cancer. However, despite the advances that have been made in therapeutic approaches, these treatments may lead to chemotherapy resistance (Zhang et al., 2019d), cancer development (Zhao et al., 2020) and normal organ damage (Zhang et al., 2020b). Owing to socio-economic development, population aging, and lifestyle changes, the incidence of cancer continues to rise worldwide, necessitating the search for safe and effective therapeutic drugs (Sung et al., 2021).

Various natural products have been proven to have anticancer effects and the potential to be effective in cancer treatment (Peng et al., 2015; Wu et al., 2015; Luo et al., 2019a). For example, curcumin can inhibit cancer development and proliferation (Giordano and Tommonaro, 2019), and baicalin promotes apoptosis in pancreatic cancer (Huang et al., 2019b). Natural products are believed to be safer than chemical products (Hou et al., 2021; Xu et al., 2021), as they kill cancer cells without affecting normal cells (El Khalki et al., 2020). Owing to their high availability, low cost, and low toxicity, the application of natural products in cancer therapy has been recommended (Anwanwan et al., 2020). Berberine (BBR) is a well-known isoquinoline alkaloid with multiple biological effects that has been used in medicine for many years (Habtemariam, 2020). It can be easily obtained from medicinal plants and can be synthesized (Kong et al., 2004; Huang et al., 2011). BBR has attracted attention because of its low cytotoxicity and wide variety of pharmacological effects, including antiviral, hypoglycemic, anti-inflammatory, hypotensive, hypolipidemic, and anticancer activities (Feng et al., 2019; Wang et al., 2019; Samadi et al., 2020; Song et al., 2020; Warowicka et al., 2020).

Recently, BBR, a well-known natural alkaloid from the *Coptis chinensis* Franch. has shown good potential anticancer effects via the inhibition of cell proliferation, metastasis and invasiveness through apoptosis. The involved mechanisms were related to the regulation of the AMP-activated protein kinase (AMPK), mitogen-activated protein kinase (MAPK), and protein kinase B (AKT) pathways (**Figure 1**). In this review, we offer a comprehensive summary of the mechanisms of BBR in treating breast, lung and liver cancer, providing a valuable reference for future research.

PHYSICOCHEMICAL PROPERTIES OF BBR

BBR ($C_{20}H_{18}NO_4$), with a molecular weight of 336.36 g/mol, is a quaternary amine isoquinoline alkaloid. It is yellow, odorless, and has a very bitter taste. BBR has a wide range of sources, such as *Coptis chinensis* Franch., *Phellodendron chinense* C. K. Schneid., *Berberis vulgaris* L., *Hydrastis canadensis* L., *Arcangelisia flava* (L.) Merr., *Berberis aquifolium* Pursh, and *Berberis aristata* DC. (Peng et al., 2004; Wang et al., 2004) (**Table 1**). *Berberis vulgaris* L. is the most widely distributed natural source of BBR, containing approximately 2.44% BBR (Ahmad et al., 2019) (**Figure 2**). BBR is slightly soluble in water, ethanol, or methanol, readily soluble in hot water and hot ethanol, and hardly soluble in organic solvents such as benzene, chloroform and acetone. The salt form is relatively soluble, especially in the sulfate and phosphate forms (Battu et al., 2010; Wang et al., 2017c; Guo and Kang, 2018). Methanol, ethanol, and aqueous or acidified methanol and ethanol are the most commonly used extraction solvents (Teng and Choi, 2014). BBR is sensitive to decomposition under high-temperature and light conditions, and it should be kept at a proper temperature and away from light (Neag et al., 2018).

THE ADMET PROPERTIES OF BBR

BBR has poor intestinal absorption and oral bioavailability in humans and rats. Its absolute oral bioavailability is only 0.37 ± 0.11% (Feng et al., 2020). In humans, after oral administrations of 400 mg BBR, the mean maximum plasma concentration is approximately 0.4 ng/ml (Hua et al., 2007). The most ionized form of BBR under physiological conditions (pKa = ~15) results in lower oral bioavailability (Spinozzi et al., 2014). P-glycoprotein (P-gp) expressed in the apical membrane of intestinal mucosal cells secretes xenobiotics into the lumen, thereby limiting the net intestinal absorption of BBR (Maeng et al., 2002). In addition, extensive intestinal first-pass elimination leads to BBR remaining in the gastrointestinal lumen, which is finally excreted in the stool (Liu et al., 2010; Wang et al., 2017c). Moreover, after absorption through the intestine, BBR is widely distributed in organs, predominantly in liver (Liu et al., 2010; Tan et al., 2013), thereby making the BBR content of the organs much higher than the plasma concentration (Wang et al., 2017b). *In vivo*, BBR undergoes extensive metabolism and simultaneously exists with its metabolites (Wang et al., 2017b) (**Figure 3**).

The acute toxicity of BBR depends on the method of administration, and basic acute toxicity studies have illustrated that the median lethal dose (LD_{50}) of BBR from intravenous and

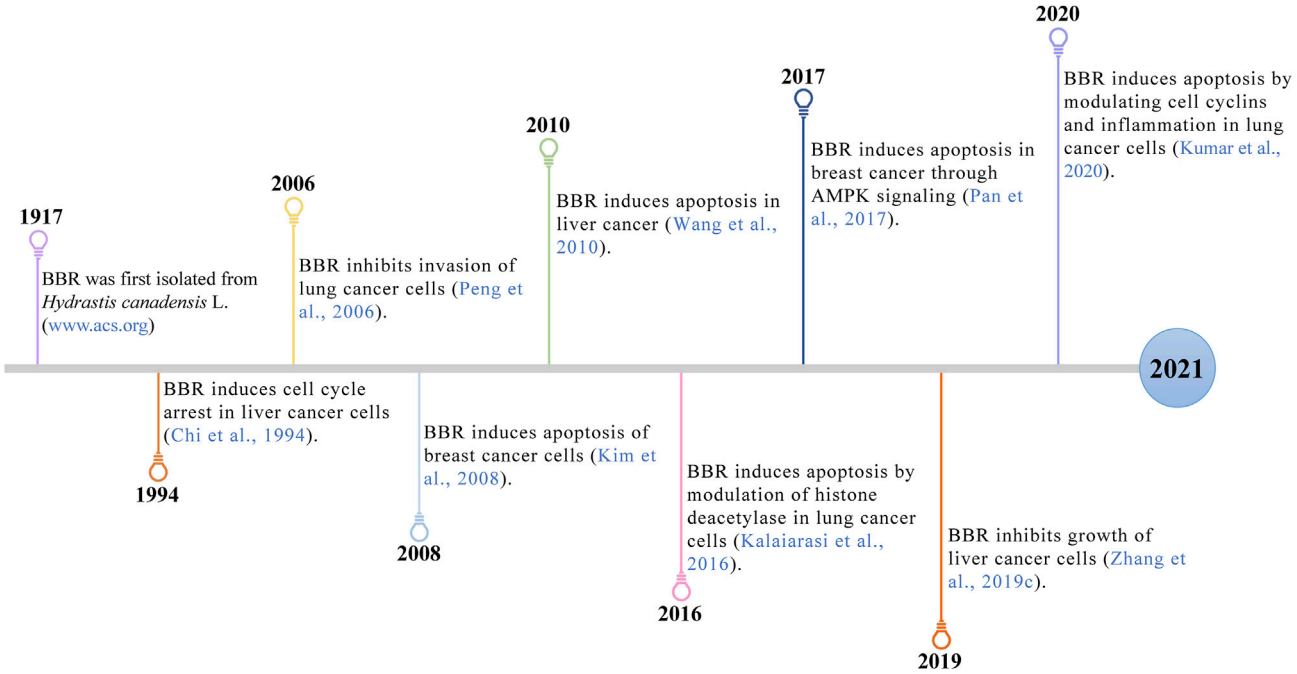


FIGURE 1 | Timeline: Continuous evidences of BBR anticancer effects on three cancers.

TABLE 1 | The plant sources of BBR.

Family	Plant source	Used part	Detection method	Ref.
Ranunculaceae	*Coptis chinensis* Franch.	Rhizome	UHPLC-ESI-MS/MS	Liu et al. (2016)
		Root	HPLC	Roh et al. (2020)
	Coptis deltoidea C. Y. Cheng and P. K. Hsiao	Rhizome	UHPLC-ESI-MS/MS	Liu et al. (2016)
	Coptis teeta Wall.	Root	HPLC	Liu et al. (2020a)
		Rhizome	HPTLC	Goswami et al. (2019)
	Hydrastis canadensis L.	Rhizome, root	LC-MS, HPLC	Ettefagh et al. (2011); Mandal et al. (2020)
	Coptis japonica (Thunb.) Makino	Rhizome	HPLC	Min et al. (2006)
Berberidaceae	*Berberis vulgaris* L.	Root	HPLC	Ahmad et al. (2019)
	Berberis koreana Palib.	Stem	HPLC	Lee et al. (2010)
	Berberis thunbergii DC.	Leaf	HPLC-MS	Fernández-Poyatos et al. (2019)
		—	UPLC-MS/MS	Och et al. (2017)
	Berberis aristata DC.	Stem bark	HPTLC	Khan et al. (2020)
	Berberis asiatica Roxb. ex DC.	Root, stem bark	HPLC	Andola et al. (2010)
	Berberis aquifolium Pursh	Stem bark	Spectrophotometry	Slobodníková et al. (2004)
	Mahonia bealei (Fort.) Carr.	Stem	HPLC, qNMR	Wang et al. (2015b)
		—	SFC	Huang et al. (2019c)
	Berberis aetnensis C. Presl	Root	HPLC	Campisi et al. (2014)
Rutaceae	*Phellodendron chinense* C. K. Schneid.	Bark	TLC	Zhou and Gu. (1995)
	Phellodendron amurense Rupr.	—	HPLC	Wang et al. (2015a)
Papaveraceae	*Chelidonium majus* L.	—	UPLC	Gu et al. (2010)

Note: UHPLC-ESI-MS/MS: ultra-high performance liquid chromatography-electrospray ionization tandem mass spectrometry. qNMR: quantitative nuclear magnetic resonance spectroscopy. HPLC: high-performance liquid chromatography. SFC: supercritical fluid chromatography. HPTLC: high-performance thin-layer chromatography. TLC: thin layer chromatography. UPLC: ultra-performance liquid chromatography. MS: tandem mass spectrometry. -: no relevant data.

intraperitoneal injection is 9.0386 and 57.6103 mg/kg, respectively, in mice. Interestingly, no LD_{50} was found after oral administration, possibly because of its poor oral bioavailability (Kheir et al., 2010). Previous studies have revealed that BBR is cardiotoxic, leading to total amplitude and beating rate inhibition at 10 μM in cardiomyocytes (Zhang et al., 2018). Animal experiments have suggested that BBR exerts toxic and teratogenic effects in developing zebrafish embryos at 400 mg/L for a-48 h administration, as evidenced by pericardial edema, damaged heart morphogenesis, vascular defects, and death (Martini et al., 2020). BBR treatment during vertebrate development leads to the impairment of cardiovascular

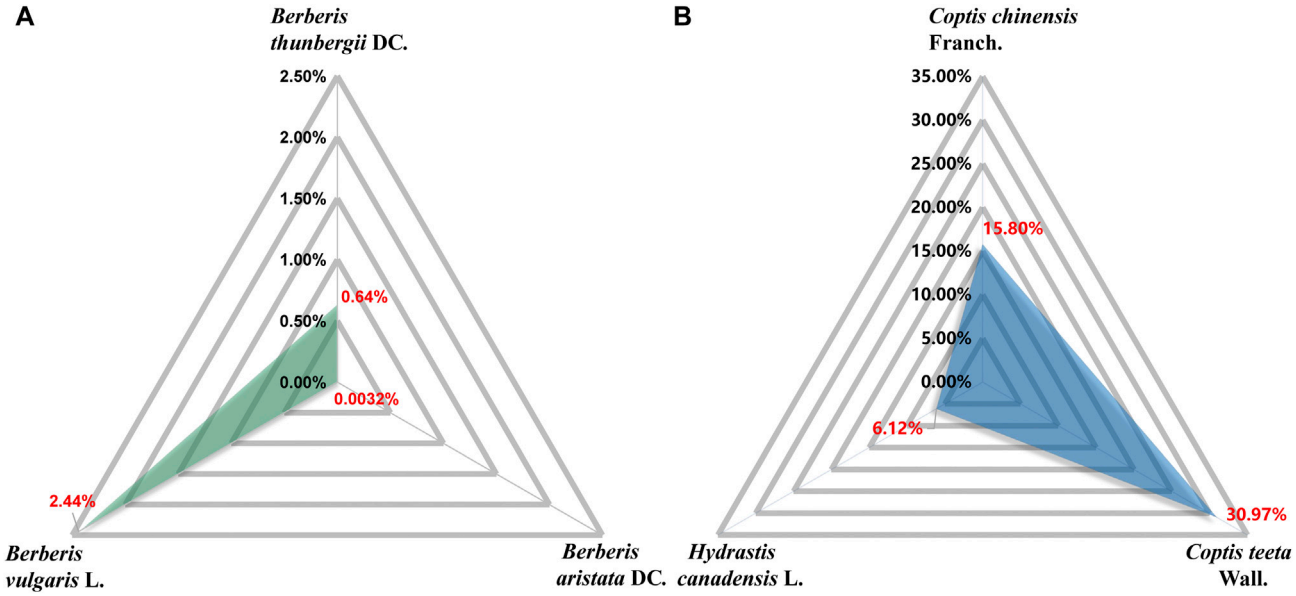


FIGURE 2 | Content of BBR in corresponding plant parts. *Berberis vulgaris* L. dry root: 2.44% (Ahmad et al., 2019). *Berberis thunbergii* DC.: 0.64% (Och et al., 2017). *Berberis aristata* DC. stem bark: 0.0032% (Khan et al., 2020). *Hydrastis canadensis* L. root: 6.12% (Ettefagh et al., 2011). *Coptis chinensis* Franch. water extracts: 15.80% (Roh et al., 2020). *Coptis teeta* Wall. rhizome: 30.97% (Goswami et al., 2019).

system morphogenesis and functionality, suggesting it should be used with caution during pregnancy and lactation. In addition, BBR shows a risk of potential neurotoxicity and immunotoxicity (Kysenius et al., 2014; Mahmoudi et al., 2016), and high doses of BBR (10 mg/kg) can suppress both cellular and humoral immune functions in treated hosts. BBR at 5 mg/kg appeared to affect only delayed-type hypersensitivity responses and lymphoproliferation (Mahmoudi et al., 2016). Moreover, several studies have shown that the concomitant use of BBR with macrolides or 5-aminosalicylic acid may induce cardiac or splenic toxicity, respectively (Zhi et al., 2015; Li et al., 2016). However, the above-mentioned data are derived from animal experiments, and recent clinical trials have shown that BBR is well tolerated in the human body with only some gastrointestinal side effects (Zhang et al., 2020c; Zhao et al., 2021b). Cardioprotective effects have also been confirmed (Qing et al., 2018; Mercurio et al., 2020; Zhao et al., 2021a). These differences may be related to administration time, concentration, and species. Overall, current research proves that BBR is safe for humans, but the rare embryo- and immune-related toxicity suggests its potential risk for pregnant women and children. In addition, the interaction between BBR and drugs requires further research (**Table 2**).

MECHANISMS OF BBR ANTICANCER EFFECTS

BBR is shown to exert pro-apoptotic effects in multiple cancers (**Table 3**). In the following section, we provide a comprehensive summary of the anticancer mechanisms.

Breast Cancer

Numerous experiments have shown that BBR is effective for treating breast cancer through diverse mechanisms, including the inhibition of cancer cell proliferation, metastasis; regulation of metabolism, the immune system, and cancer-related pathways; and the promotion of DNA damage (**Figure 4**).

BBR Inhibits Cell Proliferation to Induce Apoptosis

Proliferation and apoptosis are considered opposing cellular phenomena, and the occurrence of tumors is believed to be related to blocked apoptosis and abnormal proliferation. According to the literature, higher doses of BBR (100 μM) are predominantly distributed in the nucleolus, which causes a nucleolar stress response to upregulate p53 and induce cell proliferation inhibition and cell death (Sakaguchi et al., 2020). In addition, BBR downregulates metadherin (MTDH) to exert an antiproliferative effect (Sun et al., 2019). In triple-negative breast cancer (TNBC) cell lines, BBR inhibits the proliferation of TNBC cells with IC_{50} values ranging from 0.19 to 16.7 μM including different pathways, such as AKT/extracellular regulated protein kinases (ERK) pathways and p38. Moreover, the cell cycle kinase complex cyclin A/cyclin-dependent kinase (CDK) 1, and cyclin D/CDK4 are suppressed (Lin et al., 2019; El Khalki et al., 2020). Furthermore, recent studies have indicated that, with cell proliferation inhibition, BBR induces apoptotic cell death through the activation of caspase-9/cytochrome c; the cleavage of poly ADP-ribose polymerase (PARP), caspase-7, and caspase-8 proteins, and upregulation of pro-apoptotic B-cell lymphoma-2 (Bcl-2) proteins via p53 (Zhao et al., 2017; Carneiro and El-Deiry, 2020; El Khalki et al., 2020).

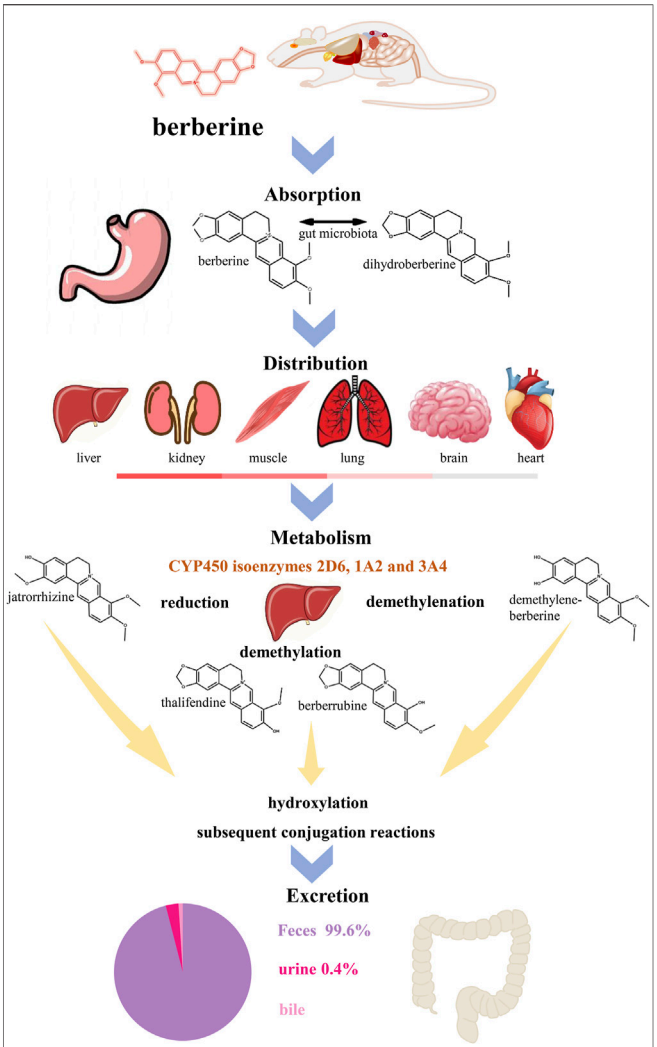


FIGURE 3 | The ADME process of BBR in rats. BBR has a poor oral bioavailability which is below 1% (Habtemariam, 2020). After oral administration in rats, BBR is absorptive by gastrointestinal system, involving the reciprocal transformation between BBR and dihydroberberine (Feng et al., 2015). BBR has wildly distribution in the liver, kidney, muscle, lung, brain and heart (decreasing order) (Tan et al., 2013). In liver, BBR metabolizes in five ways, reduction, demethylation, demethylenation, hydroxylation and subsequent conjugation reactions (Wang et al., 2017b). Cytochrome P450 (CYP450) isoenzymes 2D6, 1A2 and 3A4 (Li et al., 2011) play an important role in metabolism and jatrorrhizine, thalifendine, berberrubine and demethylene-berberine are the main products of phase I metabolism. Meanwhile, the four metabolites can be detected in feces, urine and bile (Ma et al., 2013). The main way of metabolism of BBR and its metabolites is through feces.

BBR Inhibits Cell Invasion and Metastasis to Potentially Induce Apoptosis

Metastasis is a characteristic of tumor invasiveness. Several studies have shown that BBR inhibits colony formation and migration by decreasing the phosphorylation of c-Jun and c-Fos (Zhao et al., 2017; Yao et al., 2019; Zhao and Zhang, 2020). Recent studies have indicated that BBR downregulates ephrin-B2 and transforming growth factor beta 1 (TGF-β1) to decrease the expression levels of matrix metalloproteinase (MMP)2 and MMP9, thereby inhibiting cell growth and migration (Ma et al., 2017; Kim et al., 2018a). MMPs are known to be involved in all steps of tumor progression. For example, MMP11 inhibits apoptosis and promotes cancer development. As an MMP inhibitor, BBR may be able to regulate MMPs and tissue inhibitors of MMPs to induce apoptosis (Cabral-Pacheco et al., 2020). In addition, BBR suppresses the toll-like receptor 9 (TLR9)-myeloid differentiation factor 88 (MyD88)–nuclear factor kappa-B (NF-κB) pathway and partly reverses doxorubicin (Dox)-exacerbated breast cancer metastasis (Zheng et al., 2021). NF-κB is a transcription factor that reduces apoptosis and has been shown to be involved in cell apoptosis in the phosphoinositide-3-kinase (PI3K)/AKT/NF-κB/MMP9 signaling pathway (Yang et al., 2019). The overexpression of vasodilator-stimulated phosphoprotein (VASP) and fibronectin (FN) is related to the poor prognosis of breast cancer, BBR not only binds to VASP to induce changes in its secondary structure but also decreases the expression of FN to inhibit cell proliferation and migration (Su et al., 2016; Jeong et al., 2018). In particular, serine phosphorylation of VASP regulates colon cancer cell survival and apoptosis, while FN protects lung cancer cells against docetaxel-induced apoptosis (Ali et al., 2015; Qin et al., 2016). Ultimately, the inhibition of cell invasion and metastasis may be a potential target for BBR to induce apoptosis.

BBR Regulates Metabolism to Synergistically Induce Apoptosis

Metabolic disorders are characterized by several pathological states such as chronic inflammation, dyslipidemia and insulin resistance, which are related to the incidence of breast cancer. Therefore, targeting the metabolism to treat cancer is a feasible approach. BBR has the ability to regulate metabolism or metabolic functions to affect the outcome of breast cancer (Cazzaniga and Bonanni, 2018). Previous studies have shown that BBR interferes with breast cancer cell metabolism and induces apoptosis via a mitochondrial-dependent pathway (Patil et al., 2010; Tan et al., 2015a; Tan et al., 2015b). As mentioned earlier, BBR targets p53, which regulates multiple metabolic pathways, including glucose, lipid, mitochondrial, serine, nucleotide metabolism and oxidative phosphorylation, thereby synergistically inducing apoptosis (Liu et al., 2019a). Although its specific mechanism remains unclear, the use of BBR in breast cancer patients has been recommended (Cazzaniga and Bonanni, 2018).

BBR Regulates the Immune System to Active Apoptosis Pathway

Cancer immunosurveillance usually challenges cells that have undergone tumor transformation. Only the most immune-evasive or highly mutagenic tumor cells can escape immune surveillance and produce clinically relevant tumors. Therefore, cancer cells in established tumors can resist antitumor immunity. Thus, overcoming the immune-evasive phenotype has become a new strategy for effective cancer therapies (Garg and Agostinis, 2017). Physiologically, the immune system can activate the mitochondrial apoptosis pathway and the Fas death receptor apoptosis pathway

TABLE 2 | Toxicity researches of BBR.

Animals/cell lines	Dose	Administration method	Duration	Detail	Ref.
Fourth instar larvae	10 mg/L BBR plus near UVA	—	24 h	Decreased larval survival	Philogène et al. (1984)
Wistar and Sprague-Dawley rats	2, 10, 20 μg/g	intraperitoneal injection	7 days	Higher mean serum bilirubin concentration	Chan (1993)
Balb/c mice	10 mg/kg	intraperitoneal injection	14 days	Cellular and humoral immune functions suppression	Mahmoudi et al. (2016)
	5 mg/kg			Delayed-type hypersensitivity responses, lymphoproliferation	
Zebrafish embryos	100 mg/L	—	24–96 h	Teratogenic effect, developmental toxicity, pericardial edema, cardiac looping defects, late heart morphogenesis impairment, early cardiac functionality impairment	Martini et al. (2020)
Cerebellar granule neurons, hippocampal neurons	0.01–10 μM		0.5–24 h	Severe disruption of neuritic and nuclear integrity, functional and morphological alterations of neuronal mitochondria	Kysenius et al. (2014)
Sprague-Dawley rat cardiomyocytes	10 μM	—	24 h	Cardiac arrest, total beating rate and amplitude inhibition	Zhang et al. (2018)

Note- :no relevant data.

without causing inflammation or tissue destruction (Nagata and Tanaka, 2017). Recently, BBR and exercise have been shown to slow the progression of breast cancer in 4T1 tumor-bearing rats. Synergistic therapy regulates intestinal microbial metabolites to improve the immune system by activating the mitochondrial apoptosis pathway and the Fas death receptor apoptosis pathway, thereby exerting anticancer effects (Ma et al., 2020). Collectively, these results provide evidence that BBR regulates immunity during cancer treatment.

BBR Promotes DNA Damage to Induce Apoptosis

DNA fragmentation is a hallmark of apoptosis, and BBR can induce DNA fragmentation in MDA-MB-231 cells. Further studies have shown that BBR markedly downregulates the levels of X-ray cross-complementing protein 1 and excision repair cross-complementing group 1, thereby inhibiting cell DNA repair and sensitizing MDA-MB-231 cells to chemotherapeutic drugs (Gao et al., 2019). Another study showed (El Khalki et al., 2020) that after 120 h of BBR treatment, both BT-20 and HCC70 showed significant H2A.X variant histone (H2AX) phosphorylation, which is a sign of DNA damage. Finally, DNA damage promotes p53 expression, leading to the activation of apoptosis (Hafner et al., 2019).

BBR Suppresses Inflammation to Induce Apoptosis

Infection and inflammation account for approximately a quarter of the causes of cancers, and tumors can be described as wounds that never heal and are infiltrated by numerous inflammatory and immune cells. Tumor-related chronic inflammation is generally believed to be a sign of cancer that promotes the progression to metastatic stage, and plays an important role in tumor development and treatment (Suarez-Carmona et al., 2017; Murata, 2018). After BBR treatment, P2X7-mediated NLR family pyrin domain containing 3 (NLRP3) inflammasome activation was inhibited, as evidenced by the suppressed expressing of NLRP3, caspase-1, and interleukin 1 beta (IL-1β) in MDA-MB-231 cells (Yao et al., 2019). BBR can also inhibit the secretion of tumor necrosis factor alpha (TNF-α) and interleukin-6 (IL-6) by increasing the expression of the nuclear factor of kappa light polypeptide gene enhancer in B-cells inhibitor, alpha (IκBα), thus inhibiting p65 protein and NF-κB (Zhao and Zhang, 2020). Similarly, in breast cancer-bearing rats treated with BBR (50 mg/kg), the increased levels of lipid peroxide (malonaldehyde), pro-inflammatory cytokines (IL-1β, IL-6 and TNF-α), enzymatic antioxidants (superoxide dismutase and catalase), non-enzymatic antioxidants (glutathione and vitamin C), and transcription factor NF-κB were significantly decreased by the administration of BBR. Furthermore, NF-κB and proliferating cell nuclear antigen (PCNA) in breast cancer were also downregulated (Karnam et al., 2017). Finally, with NF-κB downregulation, apoptosis was induced in breast cancer cells.

BBR Regulates Cancer-Related Pathways to Induce Apoptosis

AMPK Pathway

In breast cancer, AMPK phosphorylation induces multiple cellular responses, including cell growth inhibition, cell cycle arrest and apoptosis (Ponnusamy et al., 2020b). Salt-inducible kinase 3 (SIK3) belongs to the AMPK-related kinase family. The combination of emodin and BBR attenuates SIK3, leading to cell cycle arrest, decreased cell growth and increased apoptosis in breast cancer cells (Ponnusamy et al., 2020a). Interestingly, low-dose BBR enhances Dox sensitivity to drug-resistant breast cancer through the AMPK- hypoxia-inducible factor-1α (HIF-1α) -P-gp pathway. High-dose BBR directly induces apoptosis by activating the AMPK-p53 pathway. Therefore, BBR is both a chemotherapy sensitizer and chemotherapy drug (Pan et al., 2017).

MAPK Pathway

Overwhelming evidence indicates that the aberrant activation of the MAPK pathway contributes to breast cancer growth, invasion, metastasis, and reduced apoptosis. For example, MAPK promotes breast cancer cell invasion and metastasis

TABLE 3 | Pro-apoptotic effect of BBR on the three cancers *in vitro*.

Disease	Cell lines	Dose of BBR	Duration	Detail	Ref.
Breast cancer	MCF-7 cells	1, 10 μM 100 μM	24, 48, 72 h 72 h	Cell proliferation inhibition, cell cycle arrest Cell death	Sakaguchi et al. (2020)
	MCF-7 cells, MDA-MB-231 cells	50, 100 μM	24, 48 h	Apoptosis	Sun et al. (2019)
	MDA-MB-468 cells MDA-MB-231 cells MDA-MB-453 cells BT-549 cells	3, 6, 12 μM 6.25, 12.5, 25 μM 2.5, 5, 10 μM 5, 10, and 20 μM	1, 2, 3, 4 days	Cell proliferation inhibition	Lin et al. (2019)
	HCC70 cells BT-20 cells MDA-MB-468 cells	0.5, 1 μM	120, 144 h	Apoptosis	El Khalki et al. (2020)
	MDA-MB-231 cells	5 μg/ml	48 h	Apoptosis	Zhao et al. (2017)
	MDA-MB-231 cells	2.5–100 μg/ml	48 h	Cell proliferation, growth and metastasis inhibition	Yao et al. (2019)
	MDA-MB-231 cells	25 μmol/L	48 h	Cell migration inhibition	Zhao and Zhang. (2020)
	ZR-75-30 cells	0.78, 1.56, 3.12 μM	48 h	Cell proliferation, migration inhibition	Ma et al. (2017)
	MDA-MB-231 cells	20, 40, 80, 160 μmol/L	48, 72 h	DNA breaks	Gao et al. (2019)
	Multidrug-resistant MCF-7 cells	80, 160, 320 μM	24, 48, 72 h	Apoptosis	Pan et al. (2017)
	MCF-7 cells, MDA-MB-231 cells	100 μM	48,72 h	Apoptosis	Jabbarzadeh Kaboli et al. (2019)
	MCF-7 cells, MDA-MB-231 cells	20, 40, 80 μM	24, 48 h	Cell cycle arrest	Tak et al. (2019)
	Dox resistant MCF-7 cells	50, 100, 150, 200 μM	48 h	Cell growth inhibition	Wang et al. (2020)
Lung cancer	H1975 cells, A549 cells	6.25, 12.5, 25, 50 and 100 μM	24, 48, 72 h	Cell growth, migration and invasion inhibition, cell cycle arrest	Zheng et al. (2018a)
	H1299 cells, A549 cells	20, 100 μM	48 h	Apoptosis	Fu et al. (2013)
	A549 cells	3.15, 6.25, 12.5, 25 μM 40, 80,120 μM	48 h 48 h	Apoptosis Apoptosis	Kumar et al. (2020) Chen et al. (2019)
	H1975 cells, H1650 cells	0.78125–12.5 μM	24 h	Cell growth inhibition	Fan et al. (2018)
	A549 cells	20–200 μM	24, 36, and 48 h.	Apoptosis	Kalaiarasi et al. (2016)
	H1975 cells	25 μmol/L	24 h	Apoptosis	Zheng et al. (2020)
Liver cancer	HepG2 cells	5 μg/ml	4 days	Limits DOX-exacerbated HCC repopulation	Zhang et al. (2019b)
	Hep3B cells, BEL-7404 cells	50, 75, 100, 125 μM	12, 24, 48 h	Cell proliferation inhibition	Zhang et al. (2019c)
	HepG2 cells	10, 50, and 100 μg/ml	24, 48, 72 h	Cell proliferation inhibition, apoptosis	Li et al. (2017)
	HepG2 cells	50, 100 μM	18, 24 h	Apoptosis	Saxena et al. (2018)
	Huh-7.HCVrep cells	100 μM	24, 48 h	Apoptosis	Tai et al. (2020)
	MHCC97L Cells, PLC/PRF/5 cells	7.8125–1,000 μM	24 h	Apoptosis	Guo et al. (2020)
	HepG2 cells, Hep3B cells, SNU-182 cells	10, 20, 50, 100 μM	72 h	Cell proliferation inhibition	Chuang et al. (2017)
	HepG2 cells	100 μM	24 h	Cell growth inhibition	Chen et al. (2016)
	HepG2 cells	50, 100 μM	6 h	Cell invasion and metastasis inhibition	Wang et al. (2016)
	HepG2 cells	3.125 μM	7 days	Chemotherapy-induced apoptosis promoted migration inhibition	Zhao et al. (2020)
	Huh-7 cells, HepG2 cells	30 μM	14 days	Cell cycle arrest	Li et al. (2018a)
	Huh7 cells	50 μM	72 h	Apoptosis	Vishnoi et al. (2021)
	MHCC97-H cells, HepG2 cells	50, 100, 200 μM	24 h	Apoptosis	Song et al. (2019b)

Note: Huh-7.HCVrep cells: AB12-A2 Huh-7 replicon cells carrying the HCV genotype 1b subgenomic RNA.

via interleukin 32 (Wen et al., 2019). MAPK promotes breast cancer cell growth via linc-RoR (Peng et al., 2017). Downregulated MAPK has been shown to induce apoptosis and inhibit the proliferation of breast cancer cells (Zhu et al., 2020). The epidermal growth factor receptor (EGFR) is a surface marker of breast cancer. Dysregulation of EGFR/MAPK is common in this disease. BBR downregulates EGFR/MAPK to induce apoptosis (Jabbarzadeh Kaboli et al., 2019). BBR also reduces the expression of interleukin-8 (IL-8) by downregulating the EGFR/mitogen-activated protein kinase (MEK)/ERK pathway to induce cell growth and inhibit invasion (Kim et al., 2018c).

AKT Pathway

Aberrant AKT expression is associated with increased invasion, metastasis and drug resistance (Shariati and Meric-Bernstam, 2019). Several lines of evidence have suggested that BBR induces cell cycle arrest and death by suppressing AKT (Tak et al., 2019; Ponnusamy et al., 2020a). BBR modulates the phosphatase and tensin homolog (PTEN)/

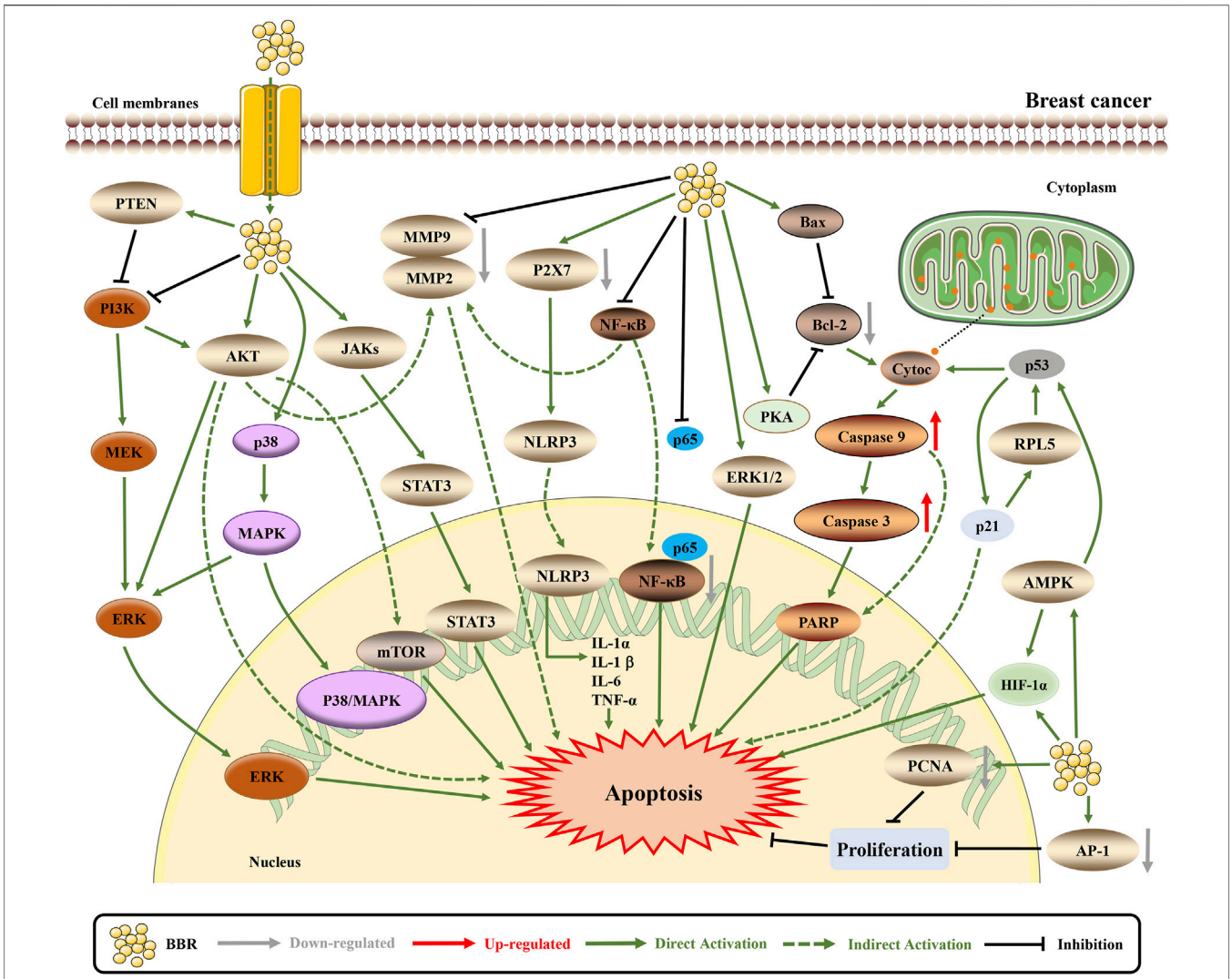


FIGURE 4 | The pro-apoptotic mechanisms of BBR in breast cancer. BBR exerts anti-cancer effects by influencing breast cancer related pathways. BBR induces apoptosis through downregulating MTDH (Sun et al., 2019). BBR actives the mitochondrial apoptotic pathway and upregulates AMPK to promote apoptosis (Pan et al., 2017; Zhao et al., 2017; Ma et al., 2020). Furthermore, BBR downregulates AKT/ERK pathway to induce cell cycle arrest and apoptosis (Lin et al., 2019). BBR inhibits NLRP3 and NF-κB inflammasome pathway to suppress inflammation and EMT, thus inducing apoptosis (Karnam et al., 2017; Yao et al., 2019; Zhao and Zhang, 2020). The mechanism of BBR inhibiting cell proliferation, invasion and growth may be induced by EGFR/ERK and EGFR/AKT signaling pathways (Kim et al., 2018c; Jabbarzadeh Kaboli et al., 2019). BBR affects certain protein expression and structure via VASP, and downregulates AP-1 and PCNA to inhibit cell proliferation and migration, which also decreases resistance to apoptosis (Su et al., 2016; Karnam et al., 2017; Jeong et al., 2018).

AKT/mammalian target of rapamycin (mTOR) signaling pathway to reverse Dox resistance and induce apoptosis (Wang et al., 2020).

BBR Reverses Drug Resistance to Induce Apoptosis

Lapatinib is a new type of human epidermal growth factor receptor 2 (HER2)/EGFR tyrosine kinase inhibitor used for the treatment of HER2-positive breast cancer. However, acquired drug resistance is inevitable. Studies have shown that BBR can increase the level of reactive oxygen species (ROS) to induce apoptosis in lapatinib-resistant cells and reverse the drug resistance of breast cancer cells (Zhang et al., 2016). In addition, BBR and Dox synergistically enhanced the inhibitory effect on cancer cells by reducing P-gp and multidrug resistance protein 1 expression with the best BBR/Dox ratio of = 2:1 (Qian et al., 2021).

Lung Cancer

As documented in the literature, BBR exhibits anti-lung cancer activity via multiple molecular mechanisms (**Figure 5**). BBR can significantly inhibit the growth of lung cancer cells by reducing the protein expression of transcription factors Sp1 and 3-phosphoinositide dependent protein kinase 1 (PDPK1), both of which are related to cancer growth and progression (Zheng

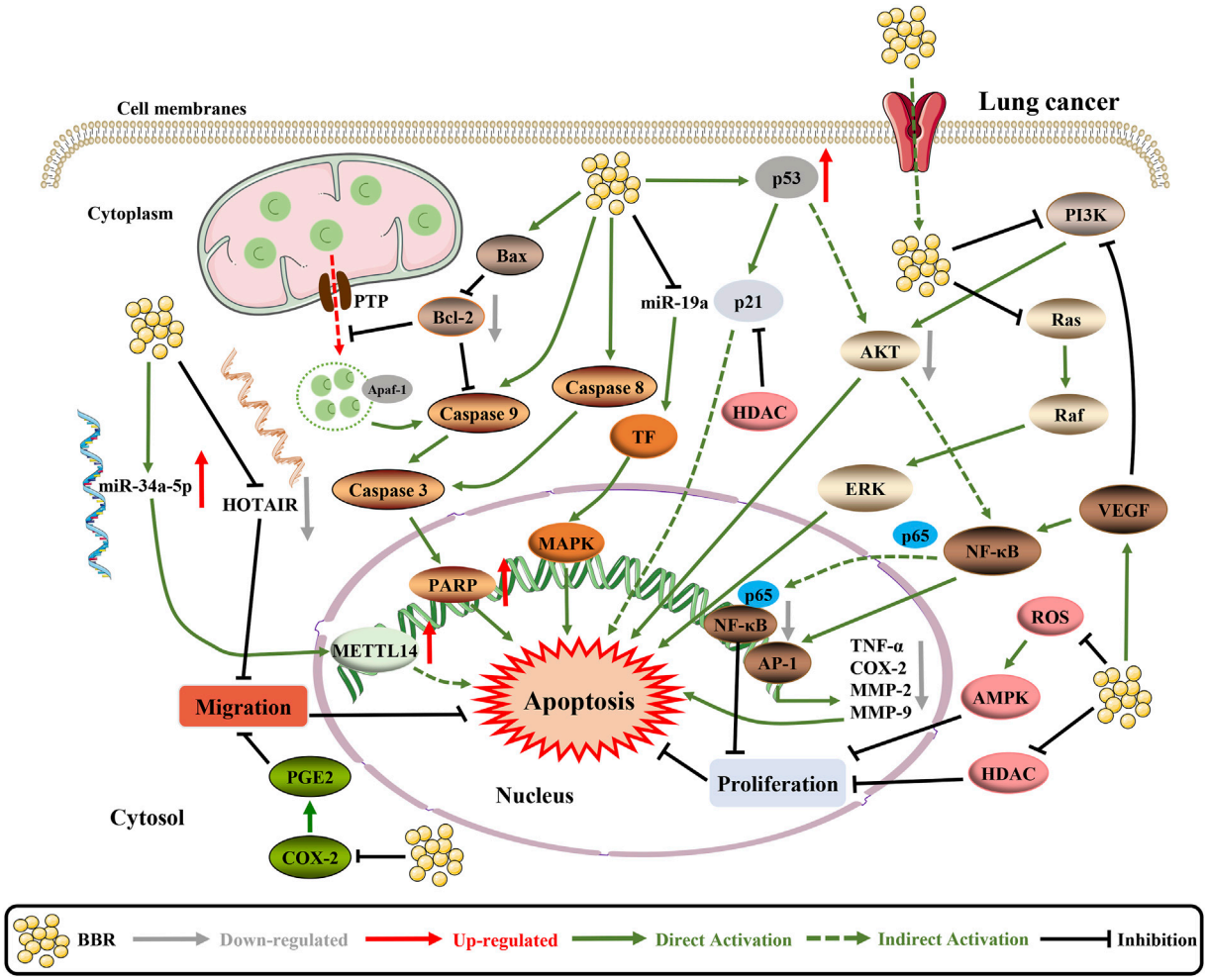


FIGURE 5 | The pro-apoptotic mechanisms of BBR in lung cancer. BBR increases the activity of the Bcl-2/Bax signaling pathway and inhibits the VEGF/NF-κB/AP-1 signaling pathway to enhance cell apoptosis (Li et al., 2018b). BBR upregulates tumor suppressor genes (p21 and p53) mRNA and protein by inhibiting HDAC (Kalaiarasi et al., 2016). On the top of this, BBR can regulate the expression and interaction of HOTAIR and miR-34a-5p in human lung cancer cells, which significantly inhibits EMT and induces apoptosis (Zheng et al., 2020). In addition, BBR inhibits the cell proliferation by targeting PI3K/AKT and ROS/AMPK signaling pathways to activate apoptosis (Fu et al., 2013; Bhattacharyya et al., 2017).

et al., 2018a). Furthermore, BBR induces apoptosis by modulating cell cyclins, inflammation, and the PI3K/AKT pathway. However, it was also observed that the proliferation inhibitory effect of BBR was transient, and no significant inhibitory effect was observed in the second-generation cells (Fu et al., 2013; Kumar et al., 2020). Another study showed that the tissue factor (TF) is a direct inhibitory target of miR-19a in non-small cell lung cancer (NSCLC) cells and BBR induces apoptosis through the miR-19a/TF/MAPK axis (Chen et al., 2019). In addition, BBR can cause mitochondrial dysfunction. By activating the ROS/AMPK pathway, BBR inhibits lipogenesis and cell proliferation (Fan et al., 2018). The combination of BBR and UVA can significantly increase cytotoxicity, and the phototoxicity of BBR is mediated by the production of ROS, mitochondrial membrane permeabilization and caspase-9/caspase-3 activation (Bhattacharyya et al., 2017). BBR also mediates epigenetic reprogramming by inhibiting histone deacetylase (HDAC) to downregulate oncogenes such as TNF-α, cyclooxygenase (COX)-2, MMP2, and MMP9 and cancer suppressor genes (p21 and p53) mRNA and protein upregulation. Besides, BBR regulates Bcl-2/Bcl-2 associated X protein (Bax) family proteins and triggers the caspase cascade apoptotic pathway (Kalaiarasi et al., 2016).

Epithelial-mesenchymal transition (EMT) is a process through which epithelial cells acquire mesenchymal features. EMT is associated with cancer initiation, invasion, metastasis, and resistance to therapy (Nieto et al., 2016). BBR and gefitinib can regulate the expression and interaction of HOX transcript antisense intergenic RNA (HOTAIR) and miR-34a-5p in human lung cancer cells to inhibit EMT. HOTAIR is an important oncogenic lncRNA, that is involved in tumorigenesis and invasion, and miR-34a-5p is a tumor suppressor. HOTAIR is significantly elevated in NSCLC cells and promotes migration and invasion, whereas depletion of HOTAIR reduces the

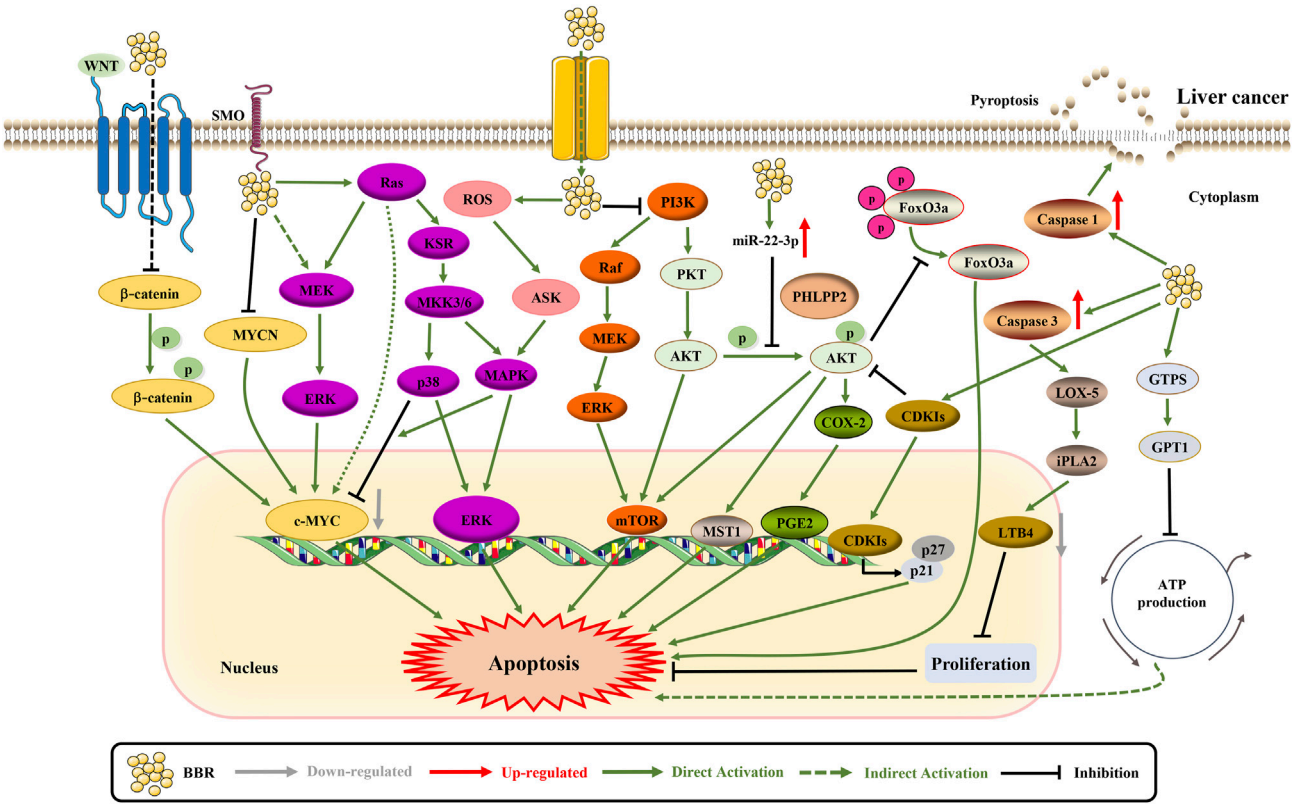


FIGURE 6 | The pro-apoptotic mechanisms of BBR in liver cancer. BBR promotes apoptosis by suppressing the expression of SLC1A5 and c-MYC (Zhang et al., 2019c; Tai et al., 2020). BBR increases the expression of CDKIs $p21^{Cip1}$ and $p27^{Kip1}$ via regulating the AKT/FoxO3a signaling pathway (Guo et al., 2020). Likewise, BBR induces apoptosis through iPLA2/LOX-5/LTB4 pathway and PHLPP2-AKT-MST1 axis (Saxena et al., 2018; Zhao et al., 2020). Besides, BBR inhibits cell proliferation through ERK1/2 and GPT1 axis (Chuang et al., 2017; Guo et al., 2020). BBR can regulate adenylate cyclase signaling in association with MKK3/6 stabilization to exert necroptosis (Sengupta et al., 2017). BBR upregulates miR-22-3p to inhibit cell proliferation (Chen et al., 2016). Furthermore, BBR simultaneously inhibits NF-κB p65 and β-catenin translation to promote apoptosis (Li et al., 2017). The apoptosis promotion of BBR may also be related to the inhibition of PI3K/AKT, p38 MAPK/ERK-COX2 and HIF-1α (Luo et al., 2019b; Song et al., 2019b; Qi and Liu, 2021).

migration and invasion ability of NSCLC cells (Zheng et al., 2020).

In vitro studies have shown that continuous Dox treatment causes transformation of HL-60 cells to N2 neutrophils, thereby inducing chemotherapy resistance. The combined treatment of Dox and 2 μM BBR caused HL-60 cells to differentiate into N1 neutrophils and stimulates immune clearance in HL-60 cells. In addition, BBR can also downregulate the expression of Dox-derived neutrophils CD133 and CD309 to prevent chemotherapy sensitivity and immune rejection (Zhang et al., 2019d).

Liver Cancer

Through continued research, numerous anti-liver cancer activities of BBR are being recognized (**Figure 6**).

BBR Inhibits Cell Proliferation and Growth to Induce Apoptosis

Cancer cells undergo specific metabolic reprogramming to sustain their proliferation. In Hep3B and BEL-7404 cells, BBR treatment decreases the rate of glutamine uptake by inhibiting solute carrier family 1 member 5 (SLC1A5) to in turn inhibit cell proliferation (Zhang et al., 2019c). In addition, BBR treatment inhibits chemotherapy-exacerbated hepatocellular carcinoma (HCC) cell population through the caspase-3-calcium-independent phospholipase A2 (iPLA2) -COX-2 pathway (Zhang et al., 2019b). BBR treatment can also inhibit cell proliferation by targeting Sp1 to upregulate miR-22-3p and suppress NF-κB p65 to induce apoptosis (Li et al., 2017). The pleckstrin homology domain leucine-rich repeat protein phosphatase 2 (PHLPP2), a tumor suppressor gene, can upregulate PHLPP2 from the PHLPP2-AKT-mammalian sterile 20-like kinase 1 (MST1) axis, exerting anti-proliferative effects (Saxena et al., 2018). A recent study revealed that BBR treatment enhanced ROS production and increased apoptosis (Tai et al., 2020). BBR treatment inhibits the growth of HCC cells by inhibiting glutamic-pyruvic transaminase 1 (GPT1) (Guo et al., 2020). Similarly, BBR treatment inhibits HCC cell proliferation by activating ERK1/2 phosphorylation (Chuang et al., 2017). The combination of S-allyl-cysteine and BBR can regulate adenylate cyclase signaling in association with stabilization of mitogen-activated protein kinase 3/6 (MKK3/6) to inhibit necroptosis and proliferation (Sengupta et al., 2017). BBR also regulates miR-22-3p to inhibit HCC

development and progression (Chen et al., 2016). Overall, these results suggest that BBR induces apoptosis by inhibiting cell proliferation and growth.

BBR Inhibits Cell Invasion and Metastasis to Potentially Induce Apoptosis

Cyclin D1 is overexpressed in HCC and is associated with invasiveness. Studies have shown that BBR can inhibit cyclin D1 expression in liver cancer cells (Wang et al., 2016). Apoptotic cancer cells induced by chemotherapeutics can also change the tumor microenvironment by activating the lipoxygenase (LOX) pathway, and release inflammatory factors such as leukotriene B4 (LTB4) to stimulate the adhesion and migration of a small number of surviving cells. BBR can reverse FN adhesion and migration in HepG2 cells by inhibiting the iPLA2/LOX-5/LTB4 pathway (Zhao et al., 2020).

BBR Regulates Cancer-Related Pathways to Induce Apoptosis

First, BBR promotes the expression of cyclin-dependent kinase inhibitors (CDKIs) $p21^{Cip1}$ and $p27^{Kip1}$ by regulating the AKT/Forkhead box O3a (FoxO3a)/S-phase kinase-associated protein 2 (Skp2) axis and further induces HCC cell cycle arrest (Li et al., 2018a). Second, BBR antagonizes the β-catenin pathway to induce apoptosis, thereby reducing the survival rate of HCC cells (Vishnoi et al., 2021). However, BBR combined with HMQ1611 has also been shown to inhibit the WNT/β-catenin pathway and inhibit the proliferation and metastasis of HCC (Dai et al., 2019). Third, BBR can inhibit the PI3K/AKT pathway to inhibit cell growth, migration and invasion, and induce apoptosis (Song et al., 2019b). In Western countries, liver cancer is increasingly caused by nonalcoholic fatty liver disease/nonalcoholic steatohepatitis (NAFLD/NASH). Interestingly, BBR might alleviate NASH-HCC via the p38MAPK and ERK/COX-2 pathways (Luo et al., 2019b).

BBR Induces Cell Pyroptosis

Pyroptosis is a caspase-1-dependent programmed cell death. However, the role of pyroptosis in HCC remains unclear. Pyrolysis in HCC tissues and cells is suppressed. Administration of BBR inhibited the viability, migration and invasion of HepG2 cells by inducing cell pyrolysis, which was attenuated by the caspase-1 inhibitor Ac-YVAD-CMK. In summary, pyroptosis is involved in the pathogenesis of HCC and may be a new target for HCC treatment (Chu et al., 2016).

BBR Promotes Chemosensitivity and Radiosensitivity to Induce Apoptosis

Regorafenib resistance is an important barrier to the treatment of advanced liver cancer. BBR enhances the cytotoxicity of regorafenib in liver cancer cells. The combination of these two factors significantly inhibits the proliferation of HCC cells and induces apoptosis (Wang et al., 2021). Similarly, BBR can induce cell apoptosis and inhibit proliferation by resisting sorafenib resistance (Huang et al., 2018). 10-hydroxycamptothecin (10-HCPT) is an effective topoisomerase I inhibitor used in the treatment of liver cancer. The high expression of HIF-1α in liver cancer tissues is related to 10-HCPT resistance, which is considered a potential cancer target for natural products (Li et al., 2020). The upregulation of HIF-1α has been confirmed to exert anti-apoptotic effects (Tang et al., 2021). Conversely, BBR can inhibit the expression of HIF-1α as a synergistic treatment for liver cancer (Qi and Liu, 2021). Radiotherapy, which can be enhanced by BBR, is a common treatment for liver cancer. For instance, BBR enhances radiation-induced oxidative stress and apoptosis in Huh7 and HepG2 cells by suppressing the nuclear factor erythroid 2–related factor 2 (Nrf2) signaling pathway (You et al., 2019).

ANTICANCER EFFECT OF BBR AGAINST OTHER CANCERS

There is growing evidence that BBR exhibits other anticancer activities. Nasopharyngeal carcinoma (NPC) is a malignancy derived from the epithelial cells of the nasopharynx cavity, and is closely associated with Epstein-Barr virus infection, BBR decreases the expression of EBNA1 to exhibit an antitumor effect against NPC (Wang et al., 2017a). BBR represses human gastric cancer cell growth by inducing cytostatic autophagy via the inhibition of MAPK/mTOR/p70 ribosomal S6 protein kinase and AKT (Zhang et al., 2020a). Moreover, BBR can regulate metabolism and exert anticancer effects. Lipid metabolism is a significant component of energy homeostasis, and BBR may partially inhibit colon cancer growth by targeting the SREBP cleavage-activating protein/sterol regulatory element-binding protein-1 pathway driving lipogenesis (Liu et al., 2020b). BBR also inhibits overactive glucose metabolism in colon cancer cells by suppressing mTOR-dependent HIF-1α protein synthesis (Mao et al., 2018). Furthermore, BBR promotes the degradation of sonic hedgehog mRNA in colorectal cancer cells, interrupting the paracrine hedgehog signaling pathway activity thus suppressing colorectal cancer growth (Shen et al., 2021). Additionally, BBR regulates the TGF-β pathway and reverses EMT in normal colonic epithelial cells (Huang et al., 2019a). In gynecology, BBR has been shown to suppress the growth and metastasis of endometrial cancer cells via miR-101/COX-2, and the combination therapy of BBR and cisplatin markedly enhances ovarian cancer cell death by inducing apoptosis and necroptosis, which may improve the anticancer effect of chemotherapy drugs (Liu et al., 2019b). Collectively, these results indicate that BBR has a wide range of anticancer effects.

ANTICANCER EFFECT OF BBR DERIVATIVES

BBR derivatives have better bioavailability, specific targeting, and stronger anticancer effects than those of BBR. The BBR derivative 8-cetylBBR (HBBR) is more effective for targeting lungs, and its anticancer properties are also significantly stronger than those of BBR. Animal experiments have proven that the oral administration of HBBR at a dose of 10 mg/kg significantly inhibited tumor growth and was more effective than the 120 mg/kg dose of BBR treatment (Xiao et al., 2018). Esters, amides, and sulfonates of BBR have also been

developed for small-molecule cancer immunotherapy, such as 2,3-methylenedioxy-9-((2,2,3,3-tetramethylcyclopropane-1-carbonyl) oxy)-10-methoxyprotoberberine chloride and 2,3-methylenedioxy-9-(2-(adamantan-1-yl) acetoxy)-10-methoxyberberine chloride (Wang et al., 2018). BBR derivatives with a long alkyl chain branched by hydroxyl and methoxycarbonyl groups at position 9 showed 3.6-fold higher intracellular concentrations and 60-fold increased anti-proliferation activity against A549 cells compared with BBR (Liu et al., 2020c). 9-O-gernylberberrubine bromide and 9-O-farnesylberberrubine bromide showed greater growth inhibition, cell cycle regulation, and migration reduction (Chang et al., 2021). Combined with nanotechnology, 9-O-octadecyl substituted BBR derivative induce mitochondrial apoptosis (Song et al., 2019a). 13-dichlorophenylalkyl BBR semisynthetic derivatives, especially 13-[3-(2,4-dichlorophenyl)propyl]-9,10-dimethoxy-5,6-dihy-drobenzo[*g*]-1,3benzodioxolo[5,6-a]quinolizinium chloride induced apoptosis in breast cancer cells, while, 13-[2-(4-chlorophenyl)ethyl]berberine iodide (NAX014) reduced HER2 overexpressing breast cancer cell migration, and intragastric administration of 20 mg/kg NAX014 in HER2/neu transgenic mice delayed the onset of mammary tumors with no negative effects on health and survival (Pierpaoli et al., 2018; Pierpaoli et al., 2021).13-Ethylberberine induces apoptosis through the mitochondria-related apoptotic pathway in radiotherapy-resistant breast cancer cells (Jin et al., 2019). 9-/13-lipophilic substituted BBR derivatives, such as 9-O-dodecyl-BBR, 13-dodecyl-BBR, and 13-O-dodecyl-BBR, show significant photocytotoxic effects on HepG2 cells and induce remarkable cancer cell apoptosis (Lin et al., 2020).

Collectively, although BBR derivatives have higher anticancer efficacy, their specific mechanisms need to be further studied, and preclinical evidence is scarce.

STRATEGIES TO IMPROVE THE BIOAVAILABILITY OF BBR

The poor bioavailability of BBR limits its clinical application in cancer treatment. At present, apart from BBR derivatives, several other effective methods have been adopted. Structural modification of BBR not only improves its bioavailability but also enhances its anticancer effects. As mentioned earlier, BBR is sensitive to temperature and is widely distributed in organs after absorption. Evidence indicates that cationic or lipophilic substituted BBR derivatives increase their potential to penetrate the phospholipid bilayer (Popiołek et al., 2019; Lin et al., 2020). Demonstrating good stability at 4°C and 25°C, BBR liposomes showed a sustained-release behavior and displayed significantly increased retention in rat blood circulation, as evidenced by the significantly increased half-life ($t_{1/2}$) and area under the curve (AUC) compared with BBR. In addition, BBR liposomes selectively increased the concentration in the liver, lungs and tumors, while reducing their distribution in the heart and kidney (Wang et al., 2017d). Similarly, the forms of esters, amides, and sulfonates of BBR have also been developed (Wang et al., 2018). In particular, BBR hydrochloride and BBR sulfate have higher solubilities than BBR (Feng et al., 2020). In addition, BBR hydrochloride induced cell proliferation and apoptosis of A549 cells by increasing the activity of the Bcl-2/Bax signaling pathway and inhibiting the Janus kinase 2 (Jak2)/vascular endothelial growth factor (VEGF)/NF-κB/transcription factor AP-1 (AP-1) signaling pathway (Li et al., 2018b). Second, co-administration can significantly improve the bioavailability and anticancer effects of BBR, such as theophylline (Hashemi-Niasari et al., 2018), cinnamaldehyde (Meng et al., 2017), icotinib (Chen et al., 2021), evodiamine (Du et al., 2017), HMQ1611 (Dai et al., 2019), s-allyl-cysteine (Sengupta et al., 2017), resveratrol (D'arcy et al., 2021), and Dox (Zhang et al., 2020b). All these factors may have a synergistic effect with BBR. Furthermore, the advent of nanotechnology has led to considerable improvements in enhancing the targeting and efficacy of BBR. For example, nanofabrication methods generate BBR-loaded liposomes with uniform size, high entrapment efficiency, and extended drug release time (Duong et al., 2021). Collagen gold nanoparticulate nanocarriers conjugated with BBR showed greater cell uptake capacity and pro-apoptotic effect on breast cancer cells (Chiu et al., 2021). Similarly, BBR-loaded Janus gold mesoporous silica nanocarriers were used in chemo/radio/photothermal therapy for the treatment of liver cancer and had a protective effect on normal tissues (Li et al., 2019b). The fluorescence of BBR-loaded polylactic acid nanoparticles (NPs) taken up by HCT116 colon carcinoma cells was approximately 2-fold higher than that of BBR (Ghaffarzadegan et al., 2020). Nano-co-delivery can further improve these effects. Nanoliposomes loaded with P-gp inhibitors and BBR chloride significantly increased BBR chloride content in cells (Vanti et al., 2021). Nano-co-delivery of BBR and Dox using poly lactic-co-glycolic acid NPs resulted in an almost 14-fold increase in half-life and an increased plasma concentration in rats (Khan et al., 2019), while BBR and zinc oxide-based NPs provided safe chemo-photothermal therapy for lung cancers (Kim et al., 2018b). Dual-functionalized spray-dried casein micelles combined with BBR and diosmin showed superior cytotoxicity and higher cellular uptake in HepG2 cells (Abdelmoneem et al., 2018). Targeting the lung delivery of layer-by-layer lipid NPs for the dual delivery of BBR and rapamycin (RAP) enhanced the sensitivity of lung cancer cells to RAP and the toxicity of drugs to cancer cells (Kabary et al., 2018). With BBR mitochondrial targeting, a paclitaxel-ss-BBR conjugate (PTX-ss-BBR NPs) and camptothecin-ss-BBR were prepared, which had stronger anti-A549 cell proliferation and pro-apoptotic effects (Cheng et al., 2020; Cheng and Ji, 2020). In addition, BBR derivatives and Dox nanomedicines target mitochondria-enhanced apoptosis (Lin et al., 2021). Dendrimer-encapsulated BBR improved pharmacokinetic parameters, such as AUC and half-life ($t_{1/2}$) of BBR (Gupta et al., 2017). The gram-scale production of carrier-free fluorescent BBR microrods exhibited good optical properties and, pH-responsive drug-release behavior (Zheng et al., 2018b).

Therefore, the enhancement of BBR bioavailability primarily includes derivatizations, modifications, co-administration, and nanotechnology.

CONCLUSION AND FUTURE PERSPECTIVES

Lung cancer, breast cancer, and liver cancer are common types of cancers globally with a rising incidence rate. Conventional cancer therapies may lead to drug resistance and serious toxicities. Thus,

novel therapeutic approaches are urgently needed. Natural products are a valuable source of new drugs, and BBR is a known isoquinoline alkaloid with outstanding activities. It can be extracted from various medicinal plants, such as *C. chinensis*, *P. chinense,* and *B. vulgaris*. In recent decades, accumulated studies have shown that BBR has considerable anticancer effects. As mentioned above, BBR can significantly inhibit the proliferation, metastasis, and invasiveness of cancer cells to induce apoptosis, the related signal pathways are AMPK, MAPK, and AKT pathways. This article reviews the chemical properties, ADMET, therapeutic effects and mechanisms of BBR in treating three types of cancers (breast, lung and liver cancer). Which are expected to serve as a reference for follow-up research.

However, there are some issues require further clarification in future research before clinical usage of this natural compound. Firstly, due to multi-target characteristics, the anticancer mechanisms of BBR have not yet been fully elucidated, and more verification is still needed, for example, study shows BBR regulates immunity during cancer treatment, but its targets are not fully clarified, more research is needed in the future. By means of network pharmacology, research has demonstrated that traditional medicines show a synergistic effect through multiple targets and pathways (Yuan et al., 2017). Therefore, we suggest to search for possible targets of BBR and to find drugs or natural products that have a synergistic effect with BBR through network pharmacology.

Secondly, most of the current existing researches focus on the cellular level, there is still a lack of corresponding clinical data to evaluate anticancer efficacy and corresponding dose in humans, which should be studied further.

Thirdly, the pharmacokinetics of BBR in humans have not been fully elucidated. The metabolites of BBR in the body also need to be further studied. A previous study identified 96 metabolites in rats, with most metabolites excreted in urine (Wang et al., 2017b). However, how metabolites interact with BBR requires further research to better understand their biological activities. Therefore, we recommend more *in vivo* studies to understand the metabolism of BBR.

Fourthly, low bioavailability of BBR seriously limits its clinical application, fortunately, structural modification of BBR has a significant effect on improving efficacy, selectivity, and safety. Some BBR derivatives, such as position 9 or 13 of the alkaloid skeleton, have better bioavailability and anticancer effects, which have been predicted to improve clinical efficacy and safety of BBR (Zhang et al., 2019a). Besides, nanotechnology have significantly enhanced the bioavailability of BBR, also, nanotechnology enables BBR to reach specific sites and exert pharmacological effects. Moreover, nanocarriers can enhance the anticancer effects of BBR through co-delivery. Therefore, a combination of structural modification, BBR derivatives, and nanotechnology is expected to be a comprising way to improve bioavailability of BBR.

Fifthly, regarding safety, as described herein, toxicity of BBR depends on the method of administration and mild gastrointestinal reactions may occur in some patients after oral administration (Imenshahidi and Hosseinzadeh, 2019). Paradoxically, BBR has shown adverse effects and even toxicity under specific circumstances, such as liver toxicity, cardiotoxicity and immunotoxicity. But BBR has been shown to possess cardioprotective, hepatoprotective effects and immunomodulatory capacities in human body. Such contradictory results may be related to mode of administration, dose of BBR and administration time. Hence, we suggest comprehensive strategies to investigate the balance between toxicity and therapeutic efficacy of BBR. Especially, long-term clinical trials are needed to better determine the human safety of BBR.

Sixthly, recently, clinical research on BBR has increased, primarily focusing on metabolic diseases, such as nonalcoholic liver disease, diabetes, and hyperlipidemia (Li et al., 2019a; Zhang et al., 2020c; Di Bisceglie et al., 2020; Zhao et al., 2021b; Harrison et al., 2021), and digestive system diseases, such as ulcerative colitis (Xu et al., 2020) and colorectal adenoma (Chen et al., 2020). BBR ursodeoxycholate and BBR chloride are involved in this process. They provide reliable evidence for the safety and effectiveness of the clinical use of BBR, but a lack of high-quality clinical research on cancers remains. Furthermore, most research is limited to Chinese studies, which may not be appliance for other groups of people. So large sample and multi-center studies are recommended.

Lastly, multidrug resistance has become a challenge in anticancer therapy and BBR has been valued as a chemosensitizer, chemoprotector and radiotherapy protector. Therefore, the sensitization effect of BBR on radiotherapy and chemotherapy warrants further study.

In conclusion, many studies have revealed anticancer effects of BBR through apoptosis, and more *in vivo* and *in vitro* studies are needed to further confirm anticancer effects of BBR. Hopefully, with further research, the therapeutic effect of BBR on cancers will likely be clinically accepted and applied.

AUTHOR CONTRIBUTIONS

YZ and KL searched the literature, wrote the first draft of the manuscript. NX and YL conducted ADMET analysis. YC and YY draught mechanism diagrams. YN processed the radar graph and the table in the manuscript. CZ and JS contributed to the manuscript revision. All authors read and approved the submitted version.

FUNDING

Financial support was provided by the Sichuan Science and technology program, Grant/Award Number: 2020JDRC0114, 2020YFH0164; Special subject of scientific research on traditional Chinese Medicine of Sichuan Administration of Traditional Chinese Medicine, Grant/Award Number: 2021MS093; "100 Talent Plan" Project of Hospital of Chengdu University of Traditional Chinese Medicine, Grant/Award Number: Hospital office (2021) 42.

REFERENCES

Abdelmoneem, M. A., Mahmoud, M., Zaky, A., Helmy, M. W., Sallam, M., Fang, J. Y., et al. (2018). Dual-Targeted Casein Micelles as Green Nanomedicine for Synergistic Phytotherapy of Hepatocellular Carcinoma. *J. Control. Release* 287, 78–93. doi:10.1016/j.jconrel.2018.08.026

Ahmad, S., Hussain, A., Hussain, A., Abdullah, I., Ali, M. S., Froeyen, M., et al. (2019). Quantification of Berberine in Berberis Vulgaris L. Root Extract and its Curative and Prophylactic Role in Cisplatin-Induced *In Vivo* Toxicity and *In Vitro* Cytotoxicity. *Antioxidants (Basel)* 8, 185. doi:10.3390/antiox8060185

Ali, M., Rogers, L. K., and Pitari, G. M. (2015). Serine Phosphorylation of Vasodilator-Stimulated Phosphoprotein (Vasp) Regulates Colon Cancer Cell Survival and Apoptosis. *Life Sci.* 123, 1–8. doi:10.1016/j.lfs.2014.12.018

American Chemical Society (2022). *American Chemical Society*. [Online]. Available: https://www.acs.org/content/acs/en/molecule-of-the-week/archive/b/berberine.html (Accessed November 21, 2021).

Anderson, N. R., Minutolo, N. G., Gill, S., and Klichinsky, M. (2021). Macrophage-Based Approaches for Cancer Immunotherapy. *Cancer Res.* 81, 1201–1208. doi:10.1158/0008-5472.Can-20-2990

Andola, H. C., Gaira, K. S., Rawal, R. S., Rawat, M. S., and Bhatt, I. D. (2010). Habitat-Dependent Variations in Berberine Content of Berberis Asiatica Roxb. Ex. Dc. In Kumaon, Western Himalaya. *Chem. Biodivers.* 7, 415–420. doi:10.1002/cbdv.200900041

Anwanwan, D., Singh, S. K., Singh, S., Saikam, V., and Singh, R. (2020). Challenges in Liver Cancer and Possible Treatment Approaches. *Biochim. Biophys. Acta Rev. Cancer* 1873 (1), 188314. doi:10.1016/j.bbcan.2019.188314

Battu, S. K., Repka, M. A., Maddineni, S., Chittiboyina, A. G., Avery, M. A., and Majumdar, S. (2010). Physicochemical Characterization of Berberine Chloride: A Perspective in the Development of a Solution Dosage Form for Oral Delivery. *AAPS PharmSciTech* 11, 1466–1475. doi:10.1208/s12249-010-9520-y

Bhattacharyya, R., Saha, B., Tyagi, M., Bandyopadhyay, S. K., Patro, B. S., and Chattopadhyay, S. (2017). Differential Modes of Photosensitisation in Cancer Cells by Berberine and Coralyne. *Free Radic. Res.* 51, 723–738. doi:10.1080/10715762.2017.1368506

Bray, F., Ferlay, J., Laversanne, M., Brewster, D. H., Gombe Mbalawa, C., Kohler, B., et al. (2015). Cancer Incidence in Five Continents: Inclusion Criteria, Highlights from Volume X and the Global Status of Cancer Registration. *Int. J. Cancer* 137, 2060–2071. doi:10.1002/ijc.29670

Cabral-Pacheco, G. A., Garza-Veloz, I., Castruita-De La Rosa, C., Ramirez-Acuña, J. M., Perez-Romero, B. A., Guerrero-Rodriguez, J. F., et al. (2020). The Roles of Matrix Metalloproteinases and Their Inhibitors in Human Diseases. *Ijms* 21 (24), 9739. doi:10.3390/ijms21249739

Campisi, A., Acquaviva, R., Bonfanti, R., Raciti, G., Amodeo, A., Mastrojeni, S., et al. (2014). Antioxidant Properties of Berberis Aetnensis C. Presl (Berberidaceae) Roots Extract and Protective Effects on Astroglial Cell Cultures. *ScientificWorldJournal* 2014, 315473. doi:10.1155/2014/315473

Carneiro, B. A., and El-Deiry, W. S. (2020). Targeting Apoptosis in Cancer Therapy. *Nat. Rev. Clin. Oncol.* 17, 395–417. doi:10.1038/s41571-020-0341-y

Cazzaniga, M., and Bonanni, B. (2018). Relationship between Metabolic Disorders and Breast Cancer Incidence and Outcomes. Is There a Preventive and Therapeutic Role for Berberine? *Anticancer Res.* 38, 4393–4402. doi:10.21873/anticanres.12741

Chan, E. (1993). Displacement of Bilirubin from Albumin by Berberine. *Biol. Neonate.* 63, 201–208. doi:10.1159/000243932

Chang, J. M., Wu, J. Y., Chen, S. H., Chao, W. Y., Chuang, H. H., Kam, K. H., et al. (2021). 9-O-Terpenyl-Substituted Berberrubine Derivatives Suppress Tumor Migration and Increase Anti-human Non-small-cell Lung Cancer Activity. *Int. J. Mol. Sci.* 22, 9864. doi:10.3390/ijms22189864

Chen, J., Wu, F. X., Luo, H. L., Liu, J. J., Luo, T., Bai, T., et al. (2016). Berberine Upregulates Mir-22-3p to Suppress Hepatocellular Carcinoma Cell Proliferation by Targeting Sp1. *Am. J. Transl. Res.* 8, 4932–4941.

Chen, P., Dai, C. H., Shi, Z. H., Wang, Y., Wu, J. N., Chen, K., et al. (2021). Synergistic Inhibitory Effect of Berberine and Icotinib on Non-small Cell Lung Cancer Cells via Inducing Autophagic Cell Death and Apoptosis. *Apoptosis* 26, 639–656. doi:10.1007/s10495-021-01694-w

Chen, Q. Q., Shi, J. M., Ding, Z., Xia, Q., Zheng, T. S., Ren, Y. B., et al. (2019). Berberine Induces Apoptosis in Non-small-cell Lung Cancer Cells by Upregulating Mir-19a Targeting Tissue Factor. *Cancer Manag. Res.* 11, 9005–9015. doi:10.2147/cmar.S207677

Chen, Y. X., Gao, Q. Y., Zou, T. H., Wang, B. M., Liu, S. D., Sheng, J. Q., et al. (2020). Berberine versus Placebo for the Prevention of Recurrence of Colorectal Adenoma: A Multicentre, Double-Blinded, Randomised Controlled Study. *Lancet Gastroenterol. Hepatol.* 5, 267–275. doi:10.1016/s2468-1253(19)30409-1

Cheng, Y., and Ji, Y. (2020). Mitochondria-Targeting Nanomedicine Self-Assembled from Gsh-Responsive Paclitaxel-Ss-Berberine Conjugate for Synergetic Cancer Treatment with Enhanced Cytotoxicity. *J. Control. Release* 318, 38–49. doi:10.1016/j.jconrel.2019.12.011

Cheng, Y., Ji, Y., and Tong, J. (2020). Triple Stimuli-Responsive Supramolecular Nanoassembly with Mitochondrial Targetability for Chemophotothermal Therapy. *J. Control. Release* 327, 35–49. doi:10.1016/j.jconrel.2020.08.006

Chi, C. W., Chang, Y. F., Chao, T. W., Chiang, S. H., P'eng, F. K., Lui, W. Y., et al. (1994). Flowcytometric Analysis of the Effect of Berberine on the Expression of Glucocorticoid Receptors in Human Hepatoma Hepg2 Cells. *Life Sci.* 54, 2099–2107. doi:10.1016/0024-3205(94)00719-5

Chiu, C. F., Fu, R. H., Hsu, S. H., Yu, Y. A., Yang, S. F., Tsao, T. C., et al. (2021). Delivery Capacity and Anticancer Ability of the Berberine-Loaded Gold Nanoparticles to Promote the Apoptosis Effect in Breast Cancer. *Cancers (Basel)* 13, 5317. doi:10.3390/cancers13215317

Chu, Q., Jiang, Y., Zhang, W., Xu, C., Du, W., Tuguzbaeva, G., et al. (2016). Pyroptosis Is Involved in the Pathogenesis of Human Hepatocellular Carcinoma. *Oncotarget* 7, 84658–84665. doi:10.18632/oncotarget.12384

Chuang, T. Y., Wu, H. L., Min, J., Diamond, M., Azziz, R., and Chen, Y. H. (2017). Berberine Regulates the Protein Expression of Multiple Tumorigenesis-Related Genes in Hepatocellular Carcinoma Cell Lines. *Cancer Cel Int* 17, 59. doi:10.1186/s12935-017-0429-3

D'arcy, M. S., Pike, C. V. S., and Coussons, P. J. (2021). A Novel Combined Resveratrol/Berberine Phytochemotheraputic Using the Hepg2 Cell Line as a Model for the Treatment of Hepatocarcinoma. *Cell Biol Int* 45, 2499–2509. doi:10.1002/cbin.11695

Dai, B., Ma, Y., Yang, T., Fan, M., Yu, R., Su, Q., et al. (2019). Synergistic Effect of Berberine and Hmq1611 Impairs Cell Proliferation and Migration by Regulating Wnt Signaling Pathway in Hepatocellular Carcinoma. *Phytother. Res.* 33, 745–755. doi:10.1002/ptr.6267

Di Bisceglie, A. M., Watts, G. F., Lavin, P., Yu, M., Bai, R., and Liu, L. (2020). Pharmacokinetics and Pharmacodynamics of Htd1801 (Berberine Ursodeoxycholate, Budca) in Patients with Hyperlipidemia. *Lipids Health Dis.* 19, 239. doi:10.1186/s12944-020-01406-4

Du, J., Sun, Y., Lu, Y. Y., Lau, E., Zhao, M., Zhou, Q. M., et al. (2017). Berberine and Evodiamine Act Synergistically against Human Breast Cancer Mcf-7 Cells by Inducing Cell Cycle Arrest and Apoptosis. *Anticancer Res.* 37, 6141–6151. doi:10.21873/anticanres.12063

Duong, T. T., Isomäki, A., Paaver, U., Laidmäe, I., Tõnisoo, A., Yen, T. T. H., et al. (2021). Nanoformulation and Evaluation of Oral Berberine-Loaded Liposomes. *Molecules* 26 (9), 2591. doi:10.3390/molecules26092591

El Khalki, L., Maire, V., Dubois, T., and Zyad, A. (2020). Berberine Impairs the Survival of Triple Negative Breast Cancer Cells: Cellular and Molecular Analyses. *Molecules* 25 (3), 506. doi:10.3390/molecules25030506

Ettefagh, K. A., Burns, J. T., Junio, H. A., Kaatz, G. W., and Cech, N. B. (2011). Goldenseal (Hydrastis Canadensis L.) Extracts Synergistically Enhance the Antibacterial Activity of Berberine via Efflux Pump Inhibition. *Planta Med.* 77, 835–840. doi:10.1055/s-0030-1250606

Fan, X. X., Leung, E. L., Xie, Y., Liu, Z. Q., Zheng, Y. F., Yao, X. J., et al. (2018). Suppression of Lipogenesis via Reactive Oxygen Species-Ampk Signaling for Treating Malignant and Proliferative Diseases. *Antioxid. Redox Signal.* 28, 339–357. doi:10.1089/ars.2017.7090

Feng, R., Shou, J. W., Zhao, Z. X., He, C. Y., Ma, C., Huang, M., et al. (2015). Transforming Berberine into its Intestine-Absorbable Form by the Gut Microbiota. *Sci. Rep.* 5, 12155. doi:10.1038/srep12155

Feng, X., Sureda, A., Jafari, S., Memariani, Z., Tewari, D., Annunziata, G., et al. (2019). Berberine in Cardiovascular and Metabolic Diseases: From Mechanisms to Therapeutics. *Theranostics* 9, 1923–1951. doi:10.7150/thno.30787

Feng, X., Wang, K., Cao, S., Ding, L., and Qiu, F. (2020). Pharmacokinetics and Excretion of Berberine and its Nine Metabolites in Rats. *Front. Pharmacol.* 11, 594852. doi:10.3389/fphar.2020.594852

Fernández-Poyatos, M. D. P., Ruiz-Medina, A., Zengin, G., and Llorent-Martínez, E. J. (2019). Phenolic Characterization, Antioxidant Activity, and Enzyme Inhibitory Properties of Berberis Thunbergii Dc. Leaves: A Valuable Source of Phenolic Acids. *Molecules* 24 (22), 4171. doi:10.3390/molecules24224171

Fidler-Benaoudia, M. M., Torre, L. A., Bray, F., Ferlay, J., and Jemal, A. (2020). Lung Cancer Incidence in Young Women vs. Young Men: A Systematic Analysis in 40 Countries. *Int. J. Cancer* 147, 811–819. doi:10.1002/ijc.32809

Fu, L., Chen, W., Guo, W., Wang, J., Tian, Y., Shi, D., et al. (2013). Berberine Targets AP-2/hTERT, NF-Kb/cox-2, HIF-1α/VEGF and Cytochrome-c/Caspase Signaling to Suppress Human Cancer Cell Growth. *PLoS One* 8, e69240. doi:10.1371/journal.pone.0069240

Gao, X., Wang, J., Li, M., Wang, J., Lv, J., Zhang, L., et al. (2019). Berberine Attenuates Xrcc1-Mediated Base Excision Repair and Sensitizes Breast Cancer Cells to the Chemotherapeutic Drugs. *J. Cel. Mol. Med.* 23, 6797–6804. doi:10.1111/jcmm.14560

Garg, A. D., and Agostinis, P. (2017). Cell Death and Immunity in Cancer: From Danger Signals to Mimicry of Pathogen Defense Responses. *Immunol. Rev.* 280, 126–148. doi:10.1111/imr.12574

Ghaffarzadegan, R., Khoee, S., and Rezazadeh, S. (2020). Fabrication, Characterization and Optimization of Berberine-Loaded Pla Nanoparticles Using Coaxial Electrospray for Sustained Drug Release. *DARU* 28, 237–252. doi:10.1007/s40199-020-00335-y

Giordano, A., and Tommonaro, G. (2019). Curcumin and Cancer. *Nutrients* 11, 2376. doi:10.3390/nu11102376

Global Cancer Observatory (2021). *Global Cancer Observatory*. [Online]. Available: https://gco.iarc.fr/(Accessed November 21, 2021).

Goswami, A. K., Gogoi, N., Shakya, A., and Sharma, H. K. (2019). Development and Validation of High-Performance Thin-Layer Chromatographic Method for Quantification of Berberine in Rhizomes of Coptis Teeta Wall, an Endangered Species Collected from Arunachal Pradesh, India. *J. Chromatogr. Sci.* 57, 411–417. doi:10.1093/chromsci/bmz009

Gravitz, L. (2014). Liver Cancer. *Nature* 516, S1. doi:10.1038/516S1a

Gu, Y., Qian, D., Duan, J. A., Wang, Z., Guo, J., Tang, Y., et al. (2010). Simultaneous Determination of Seven Main Alkaloids of Chelidonium Majus L. By Ultra-performance Lc with Photodiode-Array Detection. *J. Sep. Sci.* 33, 1004–1009. doi:10.1002/jssc.200900690

Guo, L., and Kang, W. Y. (2018). *Chemistry of Chinese Materia Medica*. Beijing: China Medical Science Press.

Guo, W., Tan, H. Y., Li, S., Wang, N., and Feng, Y. (2020). Glutamic-Pyruvic Transaminase 1 Facilitates Alternative Fuels for Hepatocellular Carcinoma Growth-A Small Molecule Inhibitor, Berberine. *Cancers (Basel)* 12, 1854. doi:10.3390/cancers12071854

Gupta, L., Sharma, A. K., Gothwal, A., Khan, M. S., Khinchi, M. P., Qayum, A., et al. (2017). Dendrimer Encapsulated and Conjugated Delivery of Berberine: A Novel Approach Mitigating Toxicity and Improving *In Vivo* Pharmacokinetics. *Int. J. Pharm.* 528, 88–99. doi:10.1016/j.ijpharm.2017.04.073

Habtemariam, S. (2020). Berberine Pharmacology and the Gut Microbiota: A Hidden Therapeutic Link. *Pharmacol. Res.* 155, 104722. doi:10.1016/j.phrs.2020.104722

Hafner, A., Bulyk, M. L., Jambhekar, A., and Lahav, G. (2019). The Multiple Mechanisms that Regulate P53 Activity and Cell Fate. *Nat. Rev. Mol. Cel Biol.* 20, 199–210. doi:10.1038/s41580-019-0110-x

Harrison, S. A., Gunn, N., Neff, G. W., Kohli, A., Liu, L., Flyer, A., et al. (2021). A Phase 2, Proof of Concept, Randomised Controlled Trial of Berberine Ursodeoxycholate in Patients with Presumed Non-alcoholic Steatohepatitis and Type 2 Diabetes. *Nat. Commun.* 12, 5503. doi:10.1038/s41467-021-25701-5

Hashemi-Niasari, F., Rabbani-Chadegani, A., Razmi, M., and Fallah, S. (2018). Synergy of Theophylline Reduces Necrotic Effect of Berberine, Induces Cell Cycle Arrest and Parp, Hmgb1, Bcl-2 Family Mediated Apoptosis in Mda-Mb-231 Breast Cancer Cells. *Biomed. Pharmacother.* 106, 858–867. doi:10.1016/j.biopha.2018.07.019

Hou, Y., Wang, X., Zhang, Y., Wang, S., and Meng, X. (2021). Highland Mate: Edible and Functional Foods in Traditional Medicine for the Prevention and Treatment of Hypoxia-Related Symptoms. *Curr. Opin. Pharmacol.* 60, 306–314. doi:10.1016/j.coph.2021.07.018

Hua, W., Ding, L., Chen, Y., Gong, B., He, J., and Xu, G. (2007). Determination of Berberine in Human Plasma by Liquid Chromatography-Electrospray Ionization-Mass Spectrometry. *J. Pharm. Biomed. Anal.* 44, 931–937. doi:10.1016/j.jpba.2007.03.022

Huang, C., Tao, L., Wang, X. L., and Pang, Z. (2019a). Berberine Reversed the Epithelial-Mesenchymal Transition of normal Colonic Epithelial Cells Induced by SW480 Cells through Regulating the Important Components in the TGF-β Pathway. *J. Cel. Physiol* 234, 11679–11691. doi:10.1002/jcp.27835

Huang, Q., Zhang, J., Peng, J., Zhang, Y., Wang, L., Wu, J., et al. (2019b). Effect of Baicalin on Proliferation and Apoptosis in Pancreatic Cancer Cells. *Am. J. Transl. Res.* 11, 5645–5654.

Huang, Y., Jiang, Z., Wang, J., Yin, G., Jiang, K., Tu, J., et al. (2019c). Quality Evaluation of Mahonia Bealei (Fort.) Carr. Using Supercritical Fluid Chromatography with Chemical Pattern Recognition. *Molecules* 24 (20), 3684. doi:10.3390/molecules24203684

Huang, Y., Wang, K., Gu, C., Yu, G., Zhao, D., Mai, W., et al. (2018). Berberine, a Natural Plant Alkaloid, Synergistically Sensitizes Human Liver Cancer Cells to Sorafenib. *Oncol. Rep.* 40, 1525–1532. doi:10.3892/or.2018.6552

Huang, Z. J., Zeng, Y., Lan, P., Sun, P. H., and Chen, W. M. (2011). Advances in Structural Modifications and Biological Activities of Berberine: An Active Compound in Traditional Chinese Medicine. *Mini Rev. Med. Chem.* 11, 1122–1129. doi:10.2174/138955711797655362

Imanshahidi, M., and Hosseinzadeh, H. (2008). Pharmacological and Therapeutic Effects of Berberis Vulgaris and its Active Constituent, Berberine. *Phytother Res.* 22, 999–1012. doi:10.1002/ptr.2399

Imenshahidi, M., and Hosseinzadeh, H. (2019). Berberine and Barberry (Berberis Vulgaris): A Clinical Review. *Phytother. Res.* 33, 504–523. doi:10.1002/ptr.6252

Inbaraj, J. J., Kukielczak, B. M., Bilski, P., Sandvik, S. L., and Chignell, C. F. (2001). Photochemistry and Photocytotoxicity of Alkaloids from Goldenseal (Hydrastis Canadensis L.) 1. Berberine. *Chem. Res. Toxicol.* 14, 1529–1534. doi:10.1021/tx0155247

Jabbarzadeh Kaboli, P., Leong, M. P., Ismail, P., and Ling, K. H. (2019). Antitumor Effects of Berberine against Egfr, Erk1/2, P38 and Akt in Mda-Mb231 and Mcf-7 Breast Cancer Cells Using Molecular Modelling and *In Vitro* Study. *Pharmacol. Rep.* 71, 13–23. doi:10.1016/j.pharep.2018.07.005

Jeong, Y., You, D., Kang, H. G., Yu, J., Kim, S. W., Nam, S. J., et al. (2018). Berberine Suppresses Fibronectin Expression through Inhibition of C-Jun Phosphorylation in Breast Cancer Cells. *J. Breast Cancer* 21, 21–27. doi:10.4048/jbc.2018.21.1.21

Jin, H., Ko, Y. S., Park, S. W., Chang, K. C., and Kim, H. J. (2019). 13-Ethylberberine Induces Apoptosis through the Mitochondria-Related Apoptotic Pathway in Radiotherapy-Resistant Breast Cancer Cells. *Molecules* 24 (13), 2448. doi:10.3390/molecules24132448

Kabary, D. M., Helmy, M. W., Elkhodairy, K. A., Fang, J. Y., and Elzoghby, A. O. (2018). Hyaluronate/Lactoferrin Layer-By-Layer-Coated Lipid Nanocarriers for Targeted Co-delivery of Rapamycin and Berberine to Lung Carcinoma. *Colloids Surf. B Biointerfaces* 169, 183–194. doi:10.1016/j.colsurfb.2018.05.008

Kalaiarasi, A., Anusha, C., Sankar, R., Rajasekaran, S., John Marshal, J., Muthusamy, K., et al. (2016). Plant Isoquinoline Alkaloid Berberine Exhibits Chromatin Remodeling by Modulation of Histone Deacetylase to Induce Growth Arrest and Apoptosis in the A549 Cell Line. *J. Agric. Food Chem.* 64, 9542–9550. doi:10.1021/acs.jafc.6b04453

Karnam, K. C., Ellutla, M., Bodduluru, L. N., Kasala, E. R., Uppulapu, S. K., Kalyankumarraju, M., et al. (2017). Preventive Effect of Berberine against Dmba-Induced Breast Cancer in Female Sprague Dawley Rats. *Biomed. Pharmacother.* 92, 207–214. doi:10.1016/j.biopha.2017.05.069

Khan, I., Joshi, G., Nakhate, K. T., AjazuddinKumar, R., Kumar, R., and Gupta, U. (2019). Nano-Co-Delivery of Berberine and Anticancer Drug Using Plga Nanoparticles: Exploration of Better Anticancer Activity and *In Vivo* Kinetics. *Pharm. Res.* 36, 149. doi:10.1007/s11095-019-2677-5

Khan, M. I., Rahman, M. A., Khalid, M., Khushtar, M., and Mujahid, M. (2020). Quality Control Standardization and Evaluation of Antimicrobial Potential of Daruhaldi (Berberis Aristata Dc) Stem Bark. *J. Diet. Suppl.* 17, 97–109. doi:10.1080/19390211.2018.1484405

Kheir, M. M., Wang, Y., Hua, L., Hu, J., Li, L., Lei, F., et al. (2010). Acute Toxicity of Berberine and its Correlation with the Blood Concentration in Mice. *Food Chem. Toxicol.* 48, 1105–1110. doi:10.1016/j.fct.2010.01.033

Kim, J. B., Lee, K. M., Ko, E., Han, W., Lee, J. E., Shin, I., et al. (2008). Berberine Inhibits Growth of the Breast Cancer Cell Lines Mcf-7 and Mda-Mb-231. *Planta Med.* 74, 39–42. doi:10.1055/s-2007-993779

Kim, S., Lee, J., You, D., Jeong, Y., Jeon, M., Yu, J., et al. (2018a). Berberine Suppresses Cell Motility through Downregulation of TGF-B1 in Triple Negative Breast Cancer Cells. *Cell Physiol. Biochem.* 45, 795–807. doi:10.1159/000487171

Kim, S., Lee, S. Y., and Cho, H. J. (2018b). Berberine and Zinc Oxide-Based Nanoparticles for the Chemo-Photothermal Therapy of Lung Adenocarcinoma. *Biochem. Biophys. Res. Commun.* 501, 765–770. doi:10.1016/j.bbrc.2018.05.063

Kim, S., You, D., Jeong, Y., Yu, J., Kim, S. W., Nam, S. J., et al. (2018c). Berberine Down-Regulates Il-8 Expression through Inhibition of the Egfr/Mek/Erk Pathway in Triple-Negative Breast Cancer Cells. *Phytomedicine* 50, 43–49. doi:10.1016/j.phymed.2018.08.004

Kong, W., Wei, J., Abidi, P., Lin, M., Inaba, S., Li, C., et al. (2004). Berberine Is a Novel Cholesterol-Lowering Drug Working through a Unique Mechanism Distinct from Statins. *Nat. Med.* 10, 1344–1351. doi:10.1038/nm1135

Kumar, R., Awasthi, M., Sharma, A., Padwad, Y., and Sharma, R. (2020). Berberine Induces Dose-dependent Quiescence and Apoptosis in A549 Cancer Cells by Modulating Cell Cyclins and Inflammation Independent of Mtor Pathway. *Life Sci.* 244, 117346. doi:10.1016/j.lfs.2020.117346

Kysenius, K., Brunello, C. A., and Huttunen, H. J. (2014). Mitochondria and Nmda Receptor-dependent Toxicity of Berberine Sensitizes Neurons to Glutamate and Rotenone Injury. *PLoS One* 9, e107129. doi:10.1371/journal.pone.0107129

Lee, H. Y., He, X., and Ahn, J. (2010). Enhancement of Antimicrobial and Antimutagenic Activities of Korean Barberry (Berberis Koreana Palib.) by the Combined Process of High-Pressure Extraction with Probiotic Fermentation. *J. Sci. Food Agric.* 90, 2399–2404. doi:10.1002/jsfa.4098

Li, F., Dong, X., Lin, P., and Jiang, J. (2018a). Regulation of Akt/Foxo3a/Skp2 Axis Is Critically Involved in Berberine-Induced Cell Cycle Arrest in Hepatocellular Carcinoma Cells. *Int. J. Mol. Sci.* 19, 327. doi:10.3390/ijms19020327

Li, G., Zhao, M., Qiu, F., Sun, Y., and Zhao, L. (2019a). Pharmacokinetic Interactions and Tolerability of Berberine Chloride with Simvastatin and Fenofibrate: An Open-Label, Randomized, Parallel Study in Healthy Chinese Subjects. *Drug Des. Devel Ther.* 13, 129–139. doi:10.2147/dddt.S185487

Li, J., Liu, F., Jiang, S., Liu, J., Chen, X., Zhang, S., et al. (2018b). Berberine Hydrochloride Inhibits Cell Proliferation and Promotes Apoptosis of Non-small Cell Lung Cancer via the Suppression of the Mmp2 and Bcl-2/Bax Signaling Pathways. *Oncol. Lett.* 15, 7409–7414. doi:10.3892/ol.2018.8249

Li, M., Zhang, M., Zhang, Z. L., Liu, N., Han, X. Y., Liu, Q. C., et al. (2017). Induction of Apoptosis by Berberine in Hepatocellular Carcinoma HepG2 Cells via Downregulation of NF-Kb. *Oncol. Res.* 25, 233–239. doi:10.3727/096504016x14742891049073

Li, R. L., He, L. Y., Zhang, Q., Liu, J., Lu, F., Duan, H. X., et al. (2020). HIF-1α Is a Potential Molecular Target for Herbal Medicine to Treat Diseases. *Drug Des. Devel. Ther.* 14, 4915–4949. doi:10.2147/dddt.S274980

Li, X.-D., Wang, Z., Wang, X.-R., Shao, D., Zhang, X., Li, L., et al. (2019b). Berberine-Loaded Janus Gold Mesoporous Silica Nanocarriers for Chemo/Radio/Photothermal Therapy of Liver Cancer and Radiation-Induced Injury Inhibition. *Ijn* 14, 3967–3982. doi:10.2147/ijn.S206044

Li, Y., Ren, G., Wang, Y. X., Kong, W. J., Yang, P., Wang, Y. M., et al. (2011). Bioactivities of Berberine Metabolites after Transformation through Cyp450 Isoenzymes. *J. Transl. Med.* 9, 62. doi:10.1186/1479-5876-9-62

Li, Y. H., Zhang, M., Fu, H. B., Xiao, H. T., and Bian, Z. X. (2016). Pre-Clinical Toxicity of a Combination of Berberine and 5-Aminosalicylic Acid in Mice. *Food Chem. Toxicol.* 97, 150–158. doi:10.1016/j.fct.2016.08.031

Lin, C., Yang, X., Li, H., Zou, Y., Mohammad, I. S., Rong, H., et al. (2021). Self-Assembled Nanomedicine Combining a Berberine Derivative and Doxorubicin for Enhanced Antitumor and Antimetastatic Efficacy via Mitochondrial Pathways. *Nanoscale* 13, 6605–6623. doi:10.1039/d1nr00032b

Lin, H. J., Ho, J. H., Tsai, L. C., Yang, F. Y., Yang, L. L., Kuo, C. D., et al. (2020). Synthesis and *In Vitro* Photocytotoxicity of 9-/13-Lipophilic Substituted Berberine Derivatives as Potential Anticancer Agents. *Molecules* 25, 677. doi:10.3390/molecules25030677

Lin, Y. S., Chiu, Y. C., Tsai, Y. H., Tsai, Y. F., Wang, J. Y., Tseng, L. M., et al. (2019). Different Mechanisms Involved in the Berberine-Induced Antiproliferation Effects in Triple-Negative Breast Cancer Cell Lines. *J. Cel Biochem.* 120, 13531–13544. doi:10.1002/jcb.28628

Liu, J., Zhang, C., Hu, W., and Feng, Z. (2019a). Tumor Suppressor P53 and Metabolism. *J. Mol. Cel Biol.* 11, 284–292. doi:10.1093/jmcb/mjy070

Liu, L., Fan, J., Ai, G., Liu, J., Luo, N., Li, C., et al. (2019b). Berberine in Combination with Cisplatin Induces Necroptosis and Apoptosis in Ovarian Cancer Cells. *Biol. Res.* 52, 37. doi:10.1186/s40659-019-0243-6

Liu, L., Wang, Z. B., Song, Y., Yang, J., Wu, L. J., Yang, B. Y., et al. (2016). Simultaneous Determination of Eight Alkaloids in Rat Plasma by Uhplc-Ms/Ms after Oral Administration of Coptis Deltoidea C. Y. Cheng Et Hsiao and Coptis Chinensis Franch. *Molecules* 21, 913. doi:10.3390/molecules21070913

Liu, T. H., Zhang, X. M., Tian, S. Z., Chen, L. G., and Yuan, J. L. (2020a). Bioinformatics Analysis of Endophytic Bacteria Related to Berberine in the Chinese Medicinal Plant Coptis Teeta Wall. *3 Biotech.* 10, 96. doi:10.1007/s13205-020-2084-y

Liu, Y., Hua, W., Li, Y., Xian, X., Zhao, Z., Liu, C., et al. (2020b). Berberine Suppresses Colon Cancer Cell Proliferation by Inhibiting the Scap/Srebp-1 Signaling Pathway-Mediated Lipogenesis. *Biochem. Pharmacol.* 174, 113776. doi:10.1016/j.bcp.2019.113776

Liu, Y., Zhu, K. X., Cao, L., Xie, Z. F., Gu, M., Lü, W., et al. (2020c). Berberine Derivatives with a Long Alkyl Chain Branched by Hydroxyl Group and Methoxycarbonyl Group at 9-Position Show Improved Anti-proliferation Activity and Membrane Permeability in A549 Cells. *Acta Pharmacol. Sin* 41, 813–824. doi:10.1038/s41401-019-0346-1

Liu, Y. T., Hao, H. P., Xie, H. G., Lai, L., Wang, Q., Liu, C. X., et al. (2010). Extensive Intestinal First-Pass Elimination and Predominant Hepatic Distribution of Berberine Explain its Low Plasma Levels in Rats. *Drug Metab. Dispos.* 38, 1779–1784. doi:10.1124/dmd.110.033936

Lortet-Tieulent, J., Georges, D., Bray, F., and Vaccarella, S. (2020). Profiling Global Cancer Incidence and Mortality by Socioeconomic Development. *Int. J. Cancer* 147, 3029–3036. doi:10.1002/ijc.33114

Luo, H., Vong, C. T., Chen, H., Gao, Y., Lyu, P., Qiu, L., et al. (2019a). Naturally Occurring Anti-cancer Compounds: Shining from Chinese Herbal Medicine. *Chin. Med.* 14, 48. doi:10.1186/s13020-019-0270-9

Luo, Y., Tian, G., Zhuang, Z., Chen, J., You, N., Zhuo, L., et al. (2019b). Berberine Prevents Non-alcoholic Steatohepatitis-Derived Hepatocellular Carcinoma by Inhibiting Inflammation and Angiogenesis in Mice. *Am. J. Transl. Res.* 11, 2668–2682.

Ma, J. Y., Feng, R., Tan, X. S., Ma, C., Shou, J. W., Fu, J., et al. (2013). Excretion of Berberine and its Metabolites in Oral Administration in Rats. *J. Pharm. Sci.* 102, 4181–4192. doi:10.1002/jps.23718

Ma, W., Zhu, M., Zhang, D., Yang, L., Yang, T., Li, X., et al. (2017). Berberine Inhibits the Proliferation and Migration of Breast Cancer Zr-75-30 Cells by Targeting Ephrin-B2. *Phytomedicine* 25, 45–51. doi:10.1016/j.phymed.2016.12.013

Ma, W., Zhang, Y., Yu, M., Wang, B., Xu, S., Zhang, J., et al. (2020). In-Vitro and In-Vivo Anti-breast Cancer Activity of Synergistic Effect of Berberine and Exercise through Promoting the Apoptosis and Immunomodulatory Effects. *Int.Immunopharmacology* 87, 106787. doi:10.1016/j.intimp.2020.106787

Maeng, H. J., Yoo, H. J., Kim, I. W., Song, I. S., Chung, S. J., and Shim, C. K. (2002). P-Glycoprotein-Mediated Transport of Berberine across Caco-2 Cell Monolayers. *J. Pharm. Sci.* 91, 2614–2621. doi:10.1002/jps.10268

Mahmoudi, M., Zamani Taghizadeh Rabe, S., Balali-Mood, M., Karimi, G., Memar, B., Rahnama, M., et al. (2016). Immunotoxicity Induced in Mice by Subacute Exposure to Berberine. *J. Immunotoxicol.* 13, 255–262. doi:10.3109/1547691x.2015.1058306

Mandal, S. K., Maji, A. K., Mishra, S. K., Ishfaq, P. M., Devkota, H. P., Silva, A. S., et al. (2020). Goldenseal (Hydrastis Canadensis L.) and its Active Constituents: A Critical Review of Their Efficacy and Toxicological Issues. *Pharmacol. Res.* 160, 105085. doi:10.1016/j.phrs.2020.105085

Mao, L., Chen, Q., Gong, K., Xu, X., Xie, Y., Zhang, W., et al. (2018). Berberine Decelerates Glucose Metabolism via Suppression of mTOR-dependent HIF-1α Protein Synthesis in colon Cancer Cells. *Oncol. Rep.* 39, 2436–2442. doi:10.3892/or.2018.6318

Martini, D., Pucci, C., Gabellini, C., Pellegrino, M., and Andreazzoli, M. (2020). Exposure to the Natural Alkaloid Berberine Affects

Cardiovascular System Morphogenesis and Functionality during Zebrafish Development. *Sci. Rep.* 10, 17358. doi:10.1038/s41598-020-73661-5

Meng, M., Geng, S., Du, Z., Yao, J., Zheng, Y., Li, Z., et al. (2017). Berberine and Cinnamaldehyde Together Prevent Lung Carcinogenesis. *Oncotarget* 8, 76385–76397. doi:10.18632/oncotarget.20059

Mercurio, V., Pucci, G., Bosso, G., Fazio, V., Battista, F., Iannuzzi, A., et al. (2020). A Nutraceutical Combination Reduces Left Ventricular Mass in Subjects with Metabolic Syndrome and Left Ventricular Hypertrophy: A Multicenter, Randomized, Double-Blind, Placebo-Controlled Trial. *Clin. Nutr.* 39, 1379–1384. doi:10.1016/j.clnu.2019.06.026

Min, Y. D., Yang, M. C., Lee, K. H., Kim, K. R., Choi, S. U., and Lee, K. R. (2006). Protoberberine Alkaloids and Their Reversal Activity of P-Gp Expressed Multidrug Resistance (Mdr) from the Rhizome of Coptis Japonica Makino. *Arch. Pharm. Res.* 29, 757–761. doi:10.1007/bf02974076

Mollaei, H., Safaralizadeh, R., and Rostami, Z. (2019). Microrna Replacement Therapy in Cancer. *J. Cel Physiol* 234, 12369–12384. doi:10.1002/jcp.28058

Murata, M. (2018). Inflammation and Cancer. *Environ. Health Prev. Med.* 23, 50. doi:10.1186/s12199-018-0740-1

Myers, J. A., and Miller, J. S. (2021). Exploring the Nk Cell Platform for Cancer Immunotherapy. *Nat. Rev. Clin. Oncol.* 18, 85–100. doi:10.1038/s41571-020-0426-7

Nagata, S., and Tanaka, M. (2017). Programmed Cell Death and the Immune System. *Nat. Rev. Immunol.* 17, 333–340. doi:10.1038/nri.2016.153

Neag, M. A., Mocan, A., Echeverría, J., Pop, R. M., Bocsan, C. I., Crişan, G., et al. (2018). Berberine: Botanical Occurrence, Traditional Uses, Extraction Methods, and Relevance in Cardiovascular, Metabolic, Hepatic, and Renal Disorders. *Front. Pharmacol.* 9, 557. doi:10.3389/fphar.2018.00557

Nieto, M. A., Huang, R. Y., Jackson, R. A., and Thiery, J. P. (2016). Emt: 2016. *Cell* 166, 21–45. doi:10.1016/j.cell.2016.06.028

Ning, N., Wang, Y. Z., Zou, Z. Y., Zhang, D. Z., Wang, D. Z., and Li, X. G. (2015). Pharmacological and Safety Evaluation of Fibrous Root of Rhizoma Coptidis. *Environ. Toxicol. Pharmacol.* 39, 53–69. doi:10.1016/j.etap.2014.11.006

Och, A., Szewczyk, K., Pecio, Ł., Stochmal, A., Załuski, D., and Bogucka-Kocka, A. (2017). Uplc-Ms/Ms Profile of Alkaloids with Cytotoxic Properties of Selected Medicinal Plants of the Berberidaceae and Papaveraceae Families. *Oxid Med. Cel Longev* 2017, 9369872. doi:10.1155/2017/9369872

Pan, Y., Zhang, F., Zhao, Y., Shao, D., Zheng, X., Chen, Y., et al. (2017). Berberine Enhances Chemosensitivity and Induces Apoptosis through Dose-Orchestrated Ampk Signaling in Breast Cancer. *J. Cancer* 8, 1679–1689. doi:10.7150/jca.19106

Park, J. H., Pyun, W. Y., and Park, H. W. (2020). Cancer Metabolism: Phenotype, Signaling and Therapeutic Targets. *Cells* 9, 2308. doi:10.3390/cells9102308

Patil, J. B., Kim, J., and Jayaprakasha, G. K. (2010). Berberine Induces Apoptosis in Breast Cancer Cells (Mcf-7) through Mitochondrial-dependent Pathway. *Eur. J. Pharmacol.* 645, 70–78. doi:10.1016/j.ejphar.2010.07.037

Peng, P. L., Hsieh, Y. S., Wang, C. J., Hsu, J. L., and Chou, F. P. (2006). Inhibitory Effect of Berberine on the Invasion of Human Lung Cancer Cells via Decreased Productions of Urokinase-Plasminogen Activator and Matrix Metalloproteinase-2. *Toxico.l Appl. Pharmacol.* 214, 8–15. doi:10.1016/j.taap.2005.11.010

Peng, W., Hu, C., Shu, Z., Han, T., Qin, L., and Zheng, C. (2015). Antitumor Activity of Tatariside F Isolated from Roots of Fagopyrum Tataricum (L.) Gaertn against H22 Hepatocellular Carcinoma via Up-Regulation of P53. *Phytomedicine* 22, 730–736. doi:10.1016/j.phymed.2015.05.003

Peng, W. H., Wu, C. R., Chen, C. S., Chen, C. F., Leu, Z. C., and Hsieh, M. T. (2004). Anxiolytic Effect of Berberine on Exploratory Activity of the Mouse in Two Experimental Anxiety Models: Interaction with Drugs Acting at 5-Ht Receptors. *Life Sci.* 75, 2451–2462. doi:10.1016/j.lfs.2004.04.032

Peng, W. X., Huang, J. G., Yang, L., Gong, A. H., and Mo, Y. Y. (2017). Linc-Ror Promotes Mapk/Erk Signaling and Confers Estrogen-independent Growth of Breast Cancer. *Mol. Cancer* 16, 161. doi:10.1186/s12943-017-0727-3

Philogène, B. J., Arnason, J. T., Towers, G. H., Abramowski, Z., Campos, F., Champagne, D., et al. (1984). Berberine: A Naturally Occurring Phototoxic Alkaloid. *J. Chem. Ecol.* 10, 115–123. doi:10.1007/bf00987648

Pierpaoli, E., Fiorillo, G., Lombardi, P., Salvatore, C., Geroni, C., Piacenza, F., et al. (2018). Antitumor Activity of Nax060: A Novel Semisynthetic Berberine Derivative in Breast Cancer Cells. *Biofactors* 44, 443–452. doi:10.1002/biof.1440

Pierpaoli, E., Piacenza, F., Fiorillo, G., Lombardi, P., Orlando, F., Salvatore, C., et al. (2021). Antimetastatic and Antitumor Activities of Orally Administered Nax014 Compound in a Murine Model of Her2-Positive Breast Cancer. *Int. J. Mol. Sci.* 22, 2653. doi:10.3390/ijms22052653

Ponnusamy, L., Kothandan, G., and Manoharan, R. (2020a). Berberine and Emodin Abrogates Breast Cancer Growth and Facilitates Apoptosis through Inactivation of Sik3-Induced Mtor and Akt Signaling Pathway. *Biochim. Biophys. Acta Mol. Basis Dis.* 1866, 165897. doi:10.1016/j.bbadis.2020.165897

Ponnusamy, L., Natarajan, S. R., Thangaraj, K., and Manoharan, R. (2020b). Therapeutic Aspects of Ampk in Breast Cancer: Progress, Challenges, and Future Directions. *Biochim. Biophys. Acta Rev. Cancer* 1874, 188379. doi:10.1016/j.bbcan.2020.188379

Popiołek, I., Niziołek, A., Kamiński, K., Kwolek, U., Nowakowska, M., and Szczubiałka, K. (2019). Cellular Delivery and Enhanced Anticancer Activity of Berberine Complexed with a Cationic Derivative of γ-cyclodextrin. *Bioorg. Med. Chem.* 27, 1414–1420. doi:10.1016/j.bmc.2019.02.042

Qi, Y., and Liu, G. (2021). Berberine-10-hydroxy Camptothecine-Loaded Lipid Microsphere for the Synergistic Treatment of Liver Cancer by Inhibiting Topoisomerase and HIF-1α. *Drug Deliv.* 28, 171–182. doi:10.1080/10717544.2020.1870020

Qian, K., Tang, C.-y., Chen, L.-y., Zheng, S., Zhao, Y., Ma, L.-s., et al. (2021). Berberine Reverses Breast Cancer Multidrug Resistance Based on Fluorescence Pharmacokinetics *In Vitro* and *In Vivo*. *ACS Omega* 6, 10645–10654. doi:10.1021/acsomega.0c06288

Qin, S., Zhang, B., Xiao, G., Sun, X., Li, G., Huang, G., et al. (2016). Fibronectin Protects Lung Cancer Cells against Docetaxel-Induced Apoptosis by Promoting Src and Caspase-8 Phosphorylation. *Tumour Biol.* 37, 13509–13520. doi:10.1007/s13277-016-5206-8

Qing, Y., Dong, X., Hongli, L., and Yanhui, L. (2018). Berberine Promoted Myocardial Protection of Postoperative Patients through Regulating Myocardial Autophagy. *Biomed. Pharmacother.* 105, 1050–1053. doi:10.1016/j.biopha.2018.06.088

Roh, K. B., Ryu, D. H., Cho, E., Weon, J. B., Park, D., Kweon, D. H., et al. (2020). Coptis Chinensis Franch Directly Inhibits Proteolytic Activation of Kallikrein 5 and Cathelicidin Associated with Rosacea in Epidermal Keratinocytes. *Molecules* 25, 5556. doi:10.3390/molecules25235556

Sakaguchi, M., Kitaguchi, D., Morinami, S., Kurashiki, Y., Hashida, H., Miyata, S., et al. (2020). Berberine-Induced Nucleolar Stress Response in a Human Breast Cancer Cell Line. *Biochem. Biophys. Res. Commun.* 528, 227–233. doi:10.1016/j.bbrc.2020.05.020

Samadi, P., Sarvarian, P., Gholipour, E., Asenjan, K. S., Aghebati-Maleki, L., Motavalli, R., et al. (2020). Berberine: A Novel Therapeutic Strategy for Cancer. *IUBMB life* 72, 2065–2079. doi:10.1002/iub.2350

Saxena, S., Shukla, S., and Kakkar, P. (2018). Berberine Induced Modulation of Phlpp2-Akt-Mst1 Kinase Signaling Is Coupled with Mitochondrial Impairment and Hepatoma Cell Death. *Toxicol. Appl. Pharmacol.* 347, 92–103. doi:10.1016/j.taap.2018.03.033

Sengupta, D., Chowdhury, K. D., Chatterjee, S., Sarkar, A., Paul, S., Sur, P. K., et al. (2017). Modulation of Adenylate Cyclase Signaling in Association with Mkk3/6 Stabilization under Combination of Sac and Berberine to Reduce Hepg2 Cell Survivability. *Apoptosis* 22, 1362–1379. doi:10.1007/s10495-017-1407-x

Shariati, M., and Meric-Bernstam, F. (2019). Targeting Akt for Cancer Therapy. *Expert Opin. Investig. Drugs* 28, 977–988. doi:10.1080/13543784.2019.1676726

Shen, Z. Q., Wang, J., Tan, W. F., and Huang, T. M. (2021). Berberine Inhibits Colorectal Tumor Growth by Suppressing Shh Secretion. *Acta Pharmacol. Sin.* 42, 1190–1194. doi:10.1038/s41401-020-00514-2

Slobodníková, L., Kost'álová, D., Labudová, D., Kotulová, D., and Kettmann, V. (2004). Antimicrobial Activity of Mahonia Aquifolium Crude Extract and its Major Isolated Alkaloids. *Phytother. Res.* 18, 674–676. doi:10.1002/ptr.1517

Song, D., Hao, J., and Fan, D. (2020). Biological Properties and Clinical Applications of Berberine. *Front. Med.* 14, 564–582. doi:10.1007/s11684-019-0724-6

Song, J., Lin, C., Yang, X., Xie, Y., Hu, P., Li, H., et al. (2019a). Mitochondrial Targeting Nanodrugs Self-Assembled from 9-O-Octadecyl Substituted Berberine Derivative for Cancer Treatment by Inducing Mitochondrial Apoptosis Pathways. *J. Control. Release* 294, 27–42. doi:10.1016/j.jconrel.2018.11.014

Song, L., Luo, Y., Wang, X., Almutairi, M. M., Pan, H., Li, W., et al. (2019b). Exploring the Active Mechanism of Berberine against Hcc by Systematic Pharmacology and Experimental Validation. *Mol. Med. Rep.* 20, 4654–4664. doi:10.3892/mmr.2019.10698

Song, X., Liu, C., Wang, N., Huang, H., He, S., Gong, C., et al. (2021). Delivery of Crispr/Cas Systems for Cancer Gene Therapy and Immunotherapy. *Adv. Drug Deliv. Rev.* 168, 158–180. doi:10.1016/j.addr.2020.04.010

Spinozzi, S., Colliva, C., Camborata, C., Roberti, M., Ianni, C., Neri, F., et al. (2014). Berberine and its Metabolites: Relationship between Physicochemical Properties and Plasma Levels after Administration to Human Subjects. *J. Nat. Prod.* 77, 766–772. doi:10.1021/np400607k

Su, K., Hu, P., Wang, X., Kuang, C., Xiang, Q., Yang, F., et al. (2016). Tumor Suppressor Berberine Binds Vasp to Inhibit Cell Migration in Basal-like Breast Cancer. *Oncotarget* 7, 45849–45862. doi:10.18632/oncotarget.9968

Suarez-Carmona, M., Lesage, J., Cataldo, D., and Gilles, C. (2017). Emt and Inflammation: Inseparable Actors of Cancer Progression. *Mol. Oncol.* 11, 805–823. doi:10.1002/1878-0261.12095

Sun, Y., Wang, W., and Tong, Y. (2019). Berberine Inhibits Proliferative Ability of Breast Cancer Cells by Reducing Metadherin. *Med. Sci. Monit.* 25, 9058–9066. doi:10.12659/msm.914486

Sung, H., Ferlay, J., Siegel, R. L., Laversanne, M., Soerjomataram, I., Jemal, A., et al. (2021). Global Cancer Statistics 2020: Globocan Estimates of Incidence and Mortality Worldwide for 36 Cancers in 185 Countries. *CA Cancer J. Clin.* 71, 209–249. doi:10.3322/caac.21660

Tai, C. J., Jassey, A., Liu, C. H., Tai, C. J., Richardson, C. D., Wong, S. H., et al. (2020). Targeting Autophagy Augments Bbr-Mediated Cell Death in Human Hepatoma Cells Harboring Hepatitis C Virus Rna. *Cells* 9, 908. doi:10.3390/cells9040908

Tak, J., Sabarwal, A., Shyanti, R. K., and Singh, R. P. (2019). Berberine Enhances Posttranslational Protein Stability of P21/Cip1 in Breast Cancer Cells via Down-Regulation of Akt. *Mol. Cel. Biochem.* 458, 49–59. doi:10.1007/s11010-019-03529-4

Tan, W., Li, N., Tan, R., Zhong, Z., Suo, Z., Yang, X., et al. (2015a). Berberine Interfered with Breast Cancer Cells Metabolism, Balancing Energy Homeostasis. *Anticancer Agents Med. Chem.* 15, 66–78. doi:10.2174/1871520614666140910120518

Tan, W., Zhong, Z., Wang, S., Suo, Z., Yang, X., Hu, X., et al. (2015b). Berberine Regulated Lipid Metabolism in the Presence of C75, Compound C, and Tofa in Breast Cancer Cell Line Mcf-7. *Evid. Based Complement. Alternat Med.* 2015, 396035. doi:10.1155/2015/396035

Tan, X. S., Ma, J. Y., Feng, R., Ma, C., Chen, W. J., Sun, Y. P., et al. (2013). Tissue Distribution of Berberine and its Metabolites after Oral Administration in Rats. *PLoS One* 8, e77969. doi:10.1371/journal.pone.0077969

Tang, Y., Hou, Y., Zeng, Y., Hu, Y., Zhang, Y., Wang, X., et al. (2021). Salidroside Attenuates CoCl2-Simulated Hypoxia Injury in PC12 Cells Partly by Mitochondrial protection. *Eur. J. Pharmacol.* 912, 174617. doi:10.1016/j.ejphar.2021.174617

Teng, H., and Choi, Y. H. (2014). Optimization of Ultrasonic-Assisted Extraction of Bioactive Alkaloid Compounds from Rhizoma Coptidis (Coptis Chinensis Franch.) Using Response Surface Methodology. *Food Chem.* 142, 299–305. doi:10.1016/j.foodchem.2013.06.136

Thakkar, S., Sharma, D., Kalia, K., and Tekade, R. K. (2020). Tumor Microenvironment Targeted Nanotherapeutics for Cancer Therapy and Diagnosis: A Review. *Acta Biomater.* 101, 43–68. doi:10.1016/j.actbio.2019.09.009

Vanti, G., Coronnello, M., Bani, D., Mannini, A., Bergonzi, M. C., and Bilia, A. R. (2021). Co-Delivery of Berberine Chloride and Tariquidar in Nanoliposomes Enhanced Intracellular Berberine Chloride in a Doxorubicin-Resistant K562 Cell Line Due to P-Gp Overexpression. *Pharmaceutics* 13, 306. doi:10.3390/pharmaceutics13030306

Vishnoi, K., Ke, R., Saini, K. S., Viswakarma, N., Nair, R. S., Das, S., et al. (2021). Berberine Represses β-Catenin Translation Involving 4E-BPs in Hepatocellular Carcinoma Cells. *Mol. Pharmacol.* 99, 1–16. doi:10.1124/molpharm.120.000029

Wang, C., Wang, H., Zhang, Y., Guo, W., Long, C., Wang, J., et al. (2017a). Berberine Inhibits the Proliferation of Human Nasopharyngeal Carcinoma Cells via an Epstein-Barr Virus Nuclear Antigen 1-Dependent Mechanism. *Oncol. Rep.* 37, 2109–2120. doi:10.3892/or.2017.5489

Wang, F., Zhao, G., Cheng, L., Zhou, H. Y., Fu, L. Y., and Yao, W. X. (2004). Effects of Berberine on Potassium Currents in Acutely Isolated Ca1 Pyramidal Neurons of Rat Hippocampus. *Brain Res.* 999, 91–97. doi:10.1016/j.brainres.2003.11.036

Wang, J., Wang, L., Lou, G. H., Zeng, H. R., Hu, J., Huang, Q. W., et al. (2019). Coptidis Rhizoma: A Comprehensive Review of its Traditional Uses, Botany, Phytochemistry, Pharmacology and Toxicology. *Pharm. Biol.* 57, 193–225. doi:10.1080/13880209.2019.1577466

Wang, K., Chai, L., Feng, X., Liu, Z., Liu, H., Ding, L., et al. (2017b). Metabolites Identification of Berberine in Rats Using Ultra-high Performance Liquid Chromatography/Quadrupole Time-Of-Flight Mass Spectrometry. *J. Pharm. Biomed. Anal.* 139, 73–86. doi:10.1016/j.jpba.2017.02.038

Wang, K., Feng, X., Chai, L., Cao, S., and Qiu, F. (2017c). The Metabolism of Berberine and its Contribution to the Pharmacological Effects. *Drug Metab. Rev.* 49, 139–157. doi:10.1080/03602532.2017.1306544

Wang, K., Yu, G., Lin, J., Wang, Z., Lu, Q., Gu, C., et al. (2021). Berberine Sensitizes Human Hepatoma Cells to Regorafenib via Modulating Expression of Circular Rnas. *Front. Pharmacol.* 12, 632201. doi:10.3389/fphar.2021.632201

Wang, N., Feng, Y., Zhu, M., Tsang, C. M., Man, K., Tong, Y., et al. (2010). Berberine Induces Autophagic Cell Death and Mitochondrial Apoptosis in Liver Cancer Cells: The Cellular Mechanism. *J. Cel. Biochem.* 111, 1426–1436. doi:10.1002/jcb.22869

Wang, N., Wang, X., Tan, H. Y., Li, S., Tsang, C. M., Tsao, S. W., et al. (2016). Berberine Suppresses Cyclin D1 Expression through Proteasomal Degradation in Human Hepatoma Cells. *Int. J. Mol. Sci.* 17, 1899. doi:10.3390/ijms17111899

Wang, W., Li, Q., Liu, Y., and Chen, B. (2015a). Ionic Liquid-Aqueous Solution Ultrasonic-Assisted Extraction of Three Kinds of Alkaloids from Phellodendron Amurense Rupr and Optimize Conditions Use Response Surface. *Ultrason. Sonochem.* 24, 13–18. doi:10.1016/j.ultsonch.2014.10.009

Wang, W., Ma, X., Guo, X., Zhao, M., Tu, P., and Jiang, Y. (2015b). A Series of Strategies for Solving the Shortage of Reference Standards for Multi-Components Determination of Traditional Chinese Medicine, Mahoniae Caulis as a Case. *J. Chromatogr. A.* 1412, 100–111. doi:10.1016/j.chroma.2015.08.015

Wang, X., Wang, Q., Liu, Z., and Zheng, X. (2017d). Preparation, Pharmacokinetics and Tumour-Suppressive Activity of Berberine Liposomes. *J. Pharm. Pharmacol.* 69, 625–632. doi:10.1111/jphp.12692

Wang, Y., Liu, Y., Du, X., Ma, H., and Yao, J. (2020). Berberine Reverses Doxorubicin Resistance by Inhibiting Autophagy through the Pten/Akt/Mtor Signaling Pathway in Breast Cancer. *Onco Targets Ther.* 13, 1909–1919. doi:10.2147/ott.S241632

Wang, Y. X., Pang, W. Q., Zeng, Q. X., Deng, Z. S., Fan, T. Y., Jiang, J. D., et al. (2018). Synthesis and Biological Evaluation of New Berberine Derivatives as Cancer Immunotherapy Agents through Targeting Ido1. *Eur. J. Med. Chem.* 143, 1858–1868. doi:10.1016/j.ejmech.2017.10.078

Warowicka, A., Nawrot, R., and Goździcka-Józefiak, A. (2020). Antiviral Activity of Berberine. *Arch. Virol.* 165, 1935–1945. doi:10.1007/s00705-020-04706-3

Wen, S., Hou, Y., Fu, L., Xi, L., Yang, D., Zhao, M., et al. (2019). Cancer-associated Fibroblast (CAF)-derived IL32 Promotes Breast Cancer Cell Invasion and Metastasis via Integrin β3-p38 MAPK Signalling. *Cancer Lett.* 442, 320–332. doi:10.1016/j.canlet.2018.10.015

Wu, L. S., Jia, M., Chen, L., Zhu, B., Dong, H. X., Si, J. P., et al. (2015). Cytotoxic and Antifungal Constituents Isolated from the Metabolites of Endophytic Fungus Do14 from Dendrobium Officinale. *Molecules* 21, E14. doi:10.3390/molecules21010014

Xiao, Y., Tian, C., Huang, T., Han, B., Wang, M., Ma, H., et al. (2018). 8-Cetylberberine Inhibits Growth of Lung Cancer *In Vitro* and *In Vivo*. *Life Sci.* 192, 259–269. doi:10.1016/j.lfs.2017.11.012

Xu, L., Zhang, Y., Xue, X., Liu, J., Li, Z. S., Yang, G. Y., et al. (2020). A Phase I Trial of Berberine in Chinese with Ulcerative Colitis. *Cancer Prev. Res. (Phila)* 13, 117–126. doi:10.1158/1940-6207.Capr-19-0258

Xu, T., Wu, X., Liu, J., Sun, J., Wang, X., Fan, G., et al. (2021). The Regulatory Roles of Dietary Fibers on Host Health via Gut Microbiota-Derived Short Chain Fatty Acids. *Curr. Opin. Pharmacol.* 62, 36–42. doi:10.1016/j.coph.2021.11.001

Yang, H. L., Thiyagarajan, V., Shen, P. C., Mathew, D. C., Lin, K. Y., Liao, J. W., et al. (2019). Anti-Emt Properties of Coq0 Attributed to Pi3k/Akt/Nfkb/Mmp-9 Signaling Pathway through Ros-Mediated Apoptosis. *J. Exp. Clin. Cancer Res.* 38, 186. doi:10.1186/s13046-019-1196-x

Yao, M., Fan, X., Yuan, B., Takagi, N., Liu, S., Han, X., et al. (2019). Berberine Inhibits Nlrp3 Inflammasome Pathway in Human Triple-Negative Breast Cancer Mda-Mb-231 Cell. *BMC Complement. Altern. Med.* 19, 216. doi:10.1186/s12906-019-2615-4

You, X., Cao, X., and Lin, Y. (2019). Berberine Enhances the Radiosensitivity of Hepatoma Cells by Nrf2 Pathway. *Front. Biosci. (Landmark Ed.* 24, 1190–1202. doi:10.2741/4775

Yuan, H., Ma, Q., Cui, H., Liu, G., Zhao, X., Li, W., et al. (2017). How Can Synergism of Traditional Medicines Benefit from Network Pharmacology? *Molecules* 22, 1135. doi:10.3390/molecules22071135

Zhang, C., Sheng, J., Li, G., Zhao, L., Wang, Y., Yang, W., et al. (2019a). Effects of Berberine and its Derivatives on Cancer: A Systems Pharmacology Review. *Front. Pharmacol.* 10, 1461. doi:10.3389/fphar.2019.01461

Zhang, F., Jia, Y., Zheng, X., Shao, D., Zhao, Y., Wang, Z., et al. (2019b). Janus Nanocarrier-Based Co-delivery of Doxorubicin and Berberine Weakens Chemotherapy-Exacerbated Hepatocellular Carcinoma Recurrence. *Acta Biomater.* 100, 352–364. doi:10.1016/j.actbio.2019.09.034

Zhang, M. Y., Yu, Y. Y., Wang, S. F., Zhang, Q., Wu, H. W., Wei, J. Y., et al. (2018). Cardiotoxicity Evaluation of Nine Alkaloids from Rhizoma Coptis. *Hum. Exp. Toxicol.* 37, 185–195. doi:10.1177/0960327117695633

Zhang, P., Wang, Q., Lin, Z., Yang, P., Dou, K., and Zhang, R. (2019c). Berberine Inhibits Growth of Liver Cancer Cells by Suppressing Glutamine Uptake. *Onco Targets Ther.* 12, 11751–11763. doi:10.2147/ott.S235667

Zhang, Q., Wang, X., Cao, S., Sun, Y., He, X., Jiang, B., et al. (2020a). Berberine Represses Human Gastric Cancer Cell Growth *In Vitro* and *In Vivo* by Inducing Cytostatic Autophagy via Inhibition of Mapk/Mtor/P70s6k and Akt Signaling Pathways. *Biomed. Pharmacother.* 128, 110245. doi:10.1016/j.biopha.2020.110245

Zhang, R., Qiao, H., Chen, S., Chen, X., Dou, K., Wei, L., et al. (2016). Berberine Reverses Lapatinib Resistance of Her2-Positive Breast Cancer Cells by Increasing the Level of Ros. *Cancer Biol. Ther.* 17, 925–934. doi:10.1080/15384047.2016.1210728

Zhang, R., Zhang, Y., Zhang, Y., Wang, X., Gao, X., Liu, Y., et al. (2020b). Ratiometric Delivery of Doxorubicin and Berberine by Liposome Enables superior Therapeutic index Than Doxil®. *Asian J. Pharm. Sci.* 15, 385–396. doi:10.1016/j.ajps.2019.04.007

Zhang, S., Zhou, L., Zhang, M., Wang, Y., Wang, M., Du, J., et al. (2019d). Berberine Maintains the Neutrophil N1 Phenotype to Reverse Cancer Cell Resistance to Doxorubicin. *Front. Pharmacol.* 10, 1658. doi:10.3389/fphar.2019.01658

Zhang, Y., Gu, Y., Ren, H., Wang, S., Zhong, H., Zhao, X., et al. (2020c). Gut Microbiome-Related Effects of Berberine and Probiotics on Type 2 Diabetes (The Premote Study). *Nat. Commun.* 11, 5015. doi:10.1038/s41467-020-18414-8

Zhao, J. V., Yeung, W. F., Chan, Y. H., Vackova, D., Leung, J. Y. Y., Ip, D. K. M., et al. (2021a). Effect of Berberine on Cardiovascular Disease Risk Factors: A Mechanistic Randomized Controlled Trial. *Nutrients* 13, 2550. doi:10.3390/nu13082550

Zhao, L., and Zhang, C. (2020). Berberine Inhibits Mda-Mb-231 Cells by Attenuating Their Inflammatory Responses. *Biomed. Res. Int.* 2020, 3617514. doi:10.1155/2020/3617514

Zhao, M. M., Lu, J., Li, S., Wang, H., Cao, X., Li, Q., et al. (2021b). Berberine Is an Insulin Secretagogue Targeting the Kcnh6 Potassium Channel. *Nat. Commun.* 12, 5616. doi:10.1038/s41467-021-25952-2

Zhao, Y., He, K., Zheng, H., Sun, M., Shi, T., Zheng, X., et al. (2020). Berberine Inhibits the Apoptosis-Induced Metastasis by Suppressing the Ipla2/Lox-5/Ltb4 Pathway in Hepatocellular Carcinoma. *Onco Targets Ther.* 13, 5223–5230. doi:10.2147/ott.S243357

Zhao, Y., Jing, Z., Lv, J., Zhang, Z., Lin, J., Cao, X., et al. (2017). Berberine Activates Caspase-9/Cytochrome C-Mediated Apoptosis to Suppress Triple-Negative Breast Cancer Cells *In Vitro* and *In Vivo*. *Biomed. Pharmacother.* 95, 18–24. doi:10.1016/j.biopha.2017.08.045

Zheng, F., Li, J., Ma, C., Tang, X., Tang, Q., Wu, J., et al. (2020). Novel Regulation of Mir-34a-5p and Hotair by the Combination of Berberine and Gefitinib Leading to Inhibition of Emt in Human Lung Cancer. *J. Cel. Mol. Med.* 24, 5578–5592. doi:10.1111/jcmm.15214

Zheng, F., Wu, J., Tang, Q., Xiao, Q., Wu, W., and Hann, S. S. (2018a). The Enhancement of Combination of Berberine and Metformin in Inhibition of Dnmt1 Gene Expression through Interplay of Sp1 and Pdpk1. *J. Cel. Mol. Med.* 22, 600–612. doi:10.1111/jcmm.13347

Zheng, X., Zhang, F., Shao, D., Zhang, Z., Cui, L., Zhang, J., et al. (2018b). Gram-Scale Production of Carrier-free Fluorescent Berberine Microrods for Selective Liver Cancer Therapy. *Biofactors* 44, 496–502. doi:10.1002/biof.1450

Zheng, X., Zhao, Y., Jia, Y., Shao, D., Zhang, F., Sun, M., et al. (2021). Biomimetic Co-assembled Nanodrug of Doxorubicin and Berberine Suppresses Chemotherapy-Exacerbated Breast Cancer Metastasis. *Biomaterials* 271, 120716. doi:10.1016/j.biomaterials.2021.120716

Zhi, D., Feng, P. F., Sun, J. L., Guo, F., Zhang, R., Zhao, X., et al. (2015). The Enhancement of Cardiac Toxicity by Concomitant Administration of Berberine and Macrolides. *Eur. J. Pharm. Sci.* 76, 149–155. doi:10.1016/j.ejps.2015.05.009

Zhou, H., and Gu, Y. (1995). Determination of Berberine in Phellodendron Chinense Schneid and its Processed Products by Tlc (Thin Layer Chromatography) Densitometry. *Zhongguo Zhong Yao Za Zhi* 20, 405447–447. doi:10.3321/j.issn:1001-5302.1995.07.019

Zhu, X., Qiu, J., Zhang, T., Yang, Y., Guo, S., Li, T., et al. (2020). Microrna-188-5p Promotes Apoptosis and Inhibits Cell Proliferation of Breast Cancer Cells via the Mapk Signaling Pathway by Targeting Rap2c. *J. Cel. Physiol.* 235, 2389–2402. doi:10.1002/jcp.29144

Zhu, Y., Ma, N., Li, H. X., Tian, L., Ba, Y. F., and Hao, B. (2014). Berberine Induces Apoptosis and DNA Damage in MG-63 Human Osteosarcoma Cells. *Mol. Med. Rep.* 10, 1734–1738. doi:10.3892/mmr.2014.2405

Conflict of Interest: The authors declare that the research was conducted in the absence of any commercial or financial relationships that could be construed as a potential conflict of interest.

Publisher's Note: All claims expressed in this article are solely those of the authors and do not necessarily represent those of their affiliated organizations, or those of the publisher, the editors and the reviewers. Any product that may be evaluated in this article, or claim that may be made by its manufacturer, is not guaranteed or endorsed by the publisher.

Copyright © 2022 Zhu, Xie, Chai, Nie, Liu, Liu, Yang, Su and Zhang. This is an open-access article distributed under the terms of the Creative Commons Attribution License (CC BY). The use, distribution or reproduction in other forums is permitted, provided the original author(s) and the copyright owner(s) are credited and that the original publication in this journal is cited, in accordance with accepted academic practice. No use, distribution or reproduction is permitted which does not comply with these terms.

frontiers in Pharmacology

REVIEW
published: 28 January 2022
doi: 10.3389/fphar.2021.801662

Promoting Apoptosis, a Promising Way to Treat Breast Cancer With Natural Products: A Comprehensive Review

Lie Yuan[1,2,3], Yongqing Cai[4], Liang Zhang[1,2,3], Sijia Liu[1,2,3], Pan Li[5] and Xiaoli Li[1,2,3]**

[1]Department of Pharmacology, College of Pharmacy, Chongqing Medical University, Chongqing, China, [2]Chongqing Key Laboratory of Drug Metabolism, Chongqing, China, [3]Key Laboratory for Biochemistry and Molecular Pharmacology of Chongqing, Chongqing, China, [4]Department of Pharmacy, Daping Hospital, Army Medical University, Chongqing, China, [5]Department of Pharmacy, Fengdu County Hospital of Traditional Chinese Medicine, Chongqing, China

Breast cancer is one of the top-ranked malignant carcinomas associated with morbidity and mortality in women worldwide. Chemotherapy is one of the main approaches to breast cancer treatment. Breast cancer initially responds to traditional first- and second-line drugs (aromatase inhibitor, tamoxifen, and carboplatin), but eventually acquires resistance, and certain patients relapse within 5 years. Chemotherapeutic drugs also have obvious toxic effects. In recent years, natural products have been widely used in breast cancer research because of their low side effects, low toxicity, and good efficacy based on their multitarget therapy. Apoptosis, a programmed cell death, occurs as a normal and controlled process that promotes cell growth and death. Inducing apoptosis is an important strategy to control excessive breast cancer cell proliferation. Accumulating evidence has revealed that natural products become increasingly important in breast cancer treatment by suppressing cell apoptosis. In this study, we reviewed current studies on natural product–induced breast cancer cell apoptosis and summarized the proapoptosis mechanisms including mitochondrial, FasL/Fas, PI3K/AKT, reactive oxygen species, and mitogen-activated protein kinase–mediated pathway. We hope that our review can provide direction in the search for candidate drugs derived from natural products to treat breast cancer by promoting cell apoptosis.

Keywords: breast cancer, apoptosis, natural products, monomer, mechanism

OPEN ACCESS

Edited by:
Wei Peng,
Chengdu University of Traditional Chinese Medicine, China

Reviewed by:
Guobing Li,
The Third Military Medical University, China
Yunhui Chen,
Chengdu University of Traditional Chinese Medicine, China

****Correspondence:***
Xiaoli Li
plum181181@126.com
Pan Li
756248601@qq.com

Specialty section:
This article was submitted to Ethnopharmacology, a section of the journal Frontiers in Pharmacology

Received: *25 October 2021*
Accepted: *13 December 2021*
Published: *28 January 2022*

Citation:
Yuan L, Cai Y, Zhang L, Liu S, Li P and Li X (2022) Promoting Apoptosis, a Promising Way to Treat Breast Cancer With Natural Products: A Comprehensive Review. Front. Pharmacol. 12:801662. doi: 10.3389/fphar.2021.801662

INTRODUCTION

Breast cancer (BC) is one of the most common malignancies occurring in women, with its morbidity increasing annually, thereby threatening human health (Georgalas et al., 2015). BC is characterized by high incidence, high mortality, high heterogeneity, high recurrence rate, and poor prognosis (Qian et al., 2019), which have collectively led to its morbidity and mortality surpassing that of lung cancer in women (Sung et al., 2021).

BC can mainly be divided into three subtypes according to histopathological features: estrogen receptor–positive (ER^+), HER2-positive ($HER2^+$), and triple-negative (TN). ER^+ BC can be treated with tamoxifen and aromatase inhibitors. $HER2^+$ BC can be treated with monoclonal antibodies against HER2, such as trastuzumab. TNBC does not express specific molecules; therefore, standard cytotoxic chemotherapy (doxorubicin, docetaxel, 5-fluorouracil, platinum drugs, and other agents in

different combinations) remains the standard of care for patients with TNBC (Nøhr-Nielsen et al., 2020; Su et al., 2020; Pal and Rakshit, 2021; Shimanuki et al., 2021). However, regardless of the treatment strategy, the potential side effects, including lymphedema, weight reduction, pain, and chemotherapy-induced peripheral neuropathy, are significant (Binkley et al., 2012). Furthermore, BC initially responds to traditional chemotherapy. However, it eventually acquires resistance and metastasis in the advanced stage. Moreover, certain patients relapse within 5 years. Therefore, the discovery of additional or substituted drugs to treat BC is urgently required.

In the last 2 decades, natural products, such as alkaloids, flavonoids, terpenoids, and phenylpropanoids, have been widely used in preclinical studies of BC because of their rich natural resources, low toxicity and good efficacy (Ateba et al., 2018; Hematpoor et al., 2018; Kushwaha et al., 2020; Sindhu et al., 2021). They can target various apoptosis-related signaling pathways (PI3K/AKT, mitogen-activated protein kinase [MAPK], and p53) to induce apoptosis in BC cells (Khojasteh Poor et al., 2021; Li et al., 2021). Therefore, natural products are an important resource in the search for candidate drugs to treat BC. However, there is no systematic analysis or review of natural products for treating BC by promoting apoptosis. Herein, the purpose of our review is to summarize the latest research on natural products, including monomers and extracts, on anti-BC treatment through different molecular mechanisms to induce cell apoptosis. We hope that this article will provide direction for follow-up studies of natural products for BC treatment.

APOPTOSIS AND BC

Cell death is indispensable in the growth, development, senescence, and death of an organism (Liu et al., 2018a). It can occur through numerous regulatory mechanisms, including apoptosis, necrosis, necroptosis, pyroptosis, and ferroptosis (Zhang et al., 2021b). Apoptosis and autophagy are known as type I and type II programmed cell death, respectively. Autophagy is a double-edged sword in tumor cells. It can degrade and recycle cellular components in an orderly manner to maintain homeostasis and promote the survival of tumor cells. However, excessive autophagy can lead to autophagic cell death (Yu et al., 2008). Unlike autophagy, apoptosis has been identified as a highly regulated and controlled process that promotes tumor cell death.

Apoptosis is a form of cellular suicide triggered by extracellular (extrinsic apoptosis) or intracellular (intrinsic apoptosis) signals (Suraweera et al., 2020). Its biochemical features include cell contraction, nuclear fragmentation, chromatin aggregation, DNA fragmentation, mRNA decay, and the formation of apoptotic bodies (Roos and Kaina, 2013). Excessive apoptosis leads to atrophy, whereas inadequate apoptosis is associated with uncontrolled cell proliferation, as observed in tumors. In normal breast cells, there is a balance between cell proliferation and apoptosis, antiapoptosis and proapoptosis to maintain the cell homeostasis (Parton et al., 2001). Once the balance is disrupted, activated antiapoptotic signal pathway or proapoptosis pathway deficiency can lead to uncontrolled cell proliferation, therapeutic resistance, and cancer cell recurrence (Mohammad et al., 2015). In BC cells, multiple factors, including growth factor, DNA damage, reactive oxygen species (ROS), and UV radiation, can promote uncontrolled cell growth through mitochondrial, FasL/Fas–, PI3K/AKT–, ROS-, nuclear factor κB (NF-κB)–, and MAPK–mediated pathways, to break the balance of proapoptotic and antiapoptotic effects. Therefore, targeting apoptotic pathways is an efficient strategy for identifying candidate drugs derived from natural products to treat BC (Rajabi et al., 2021).

PROAPOPTOTIC EFFECTS OF MONOMERS FROM NATURAL PRODUCTS ON BC

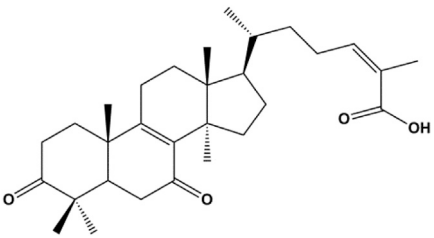
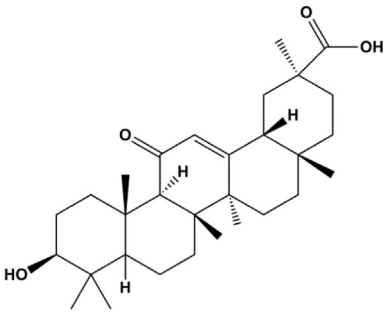
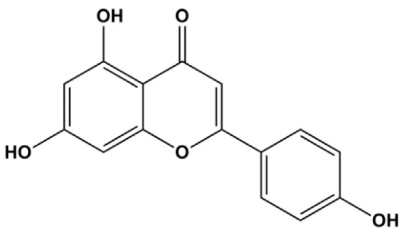
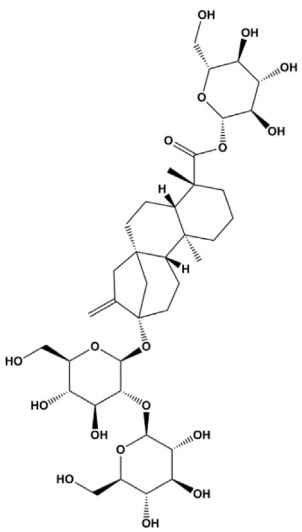
An increasing number of studies have comprehensively demonstrated the proapoptotic effects of natural products on BC. In this study, we reviewed the effect and mechanism of monomers derived from natural products on apoptosis in BC (**Table 1**).

Mitochondrial Pathway–Mediated Apoptosis

The mitochondrial pathway can be triggered by various cellular stresses, such as UV radiation, DNA damage, ROS, hypoxia, and endoplasmic reticulum stress (ERS). It is also known as an intrinsic pathway that induces apoptosis. The mechanism of mitochondrial pathway–mediated apoptosis is related to altered mitochondrial membrane potential (MMP) and promotes cytochrome c (CytoC) release to activate initiator caspase-9, which then activated caspase-9 cleaves caspase-3, resulting in cell apoptosis. CytoC is regulated by the evolutionarily conserved B-cell lymphoma-2 (Bcl-2) family, which includes proapoptotic and antiapoptotic members (Suraweera et al., 2020). Antiapoptotic members, Bcl-2, Bcl-2–like (Bcl2L), and Bcl-2–related protein long isoform (BclXL), are located in the outer membrane of mitochondria and can prevent the release of CytoC. Proapoptotic members, Bcl-2–associated X-protein (Bax), BH3-interacting death domain (Bid), and Bcl-2–interacting protein (Bim), must be transferred to mitochondria to induce apoptosis.

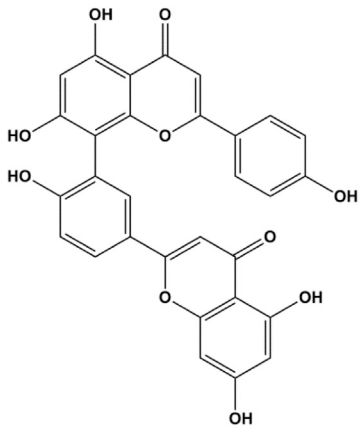
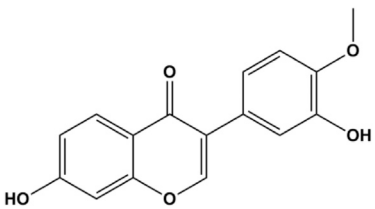
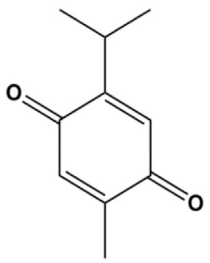
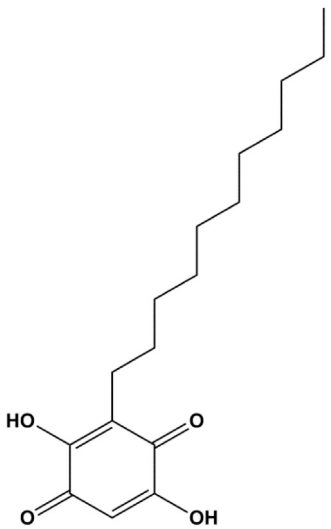
Numerous studies have suggested that certain natural products induce BC cell apoptosis through the mitochondrial pathway (**Figure 1**). Ganoderic acid DM is an active monomer of *Ganoderma lucidum*. In 2012, Wu et al. (2012) reported that ganoderic acid DM significantly induced DNA breakage and poly-ADP-ribose polymerase (PARP) cleavage, reduced MMP, and ultimately induced MCF-7 cell apoptosis. Sharma et al. (2012) also reported that 18β-glycyrrhetinic acid induced apoptosis through the mitochondrial death cascade, characterized by the absence of MMP, promoting the release of CytoC and activation of caspase-9. Stevioside is a diterpenoid glycoside found in *Stevia rebaudiana* (Bertoni) Bertoni leaves. A study by Paul et al. (2012) revealed that stevioside can reduce

TABLE 1 | Proapoptotic effects of monomers from natural products on breast cancer cells.

Monomers	Chemical structure	Detail mechanisms		Cell model	Refs
Mitochondrial pathway–mediated apoptosis					
Ganoderic acid DM (50 μM)		Cleaved PARP, γ-H2AX	CDK2, CDK6, p-Rb, CytoC	MCF-7	Wu et al. (2012)
18β-Glycyrrhetinic acid (100 μM)		CytoC, activated caspase-9, Bax	Bcl-2	MCF-7	Sharma et al. (2012)
Apigenin (10, 20, 40, 80 μM)		p53, p21, Bax, p-Cdc2, cleaved caspase-3, cleaved PARP	Bcl-2, cyclin B1, Cdc2	T47D	Liu et al. (2012)
Stevioside (10 μM)		Bax, Caspase-9	Bcl-2	MCF7	Paul et al. (2012)

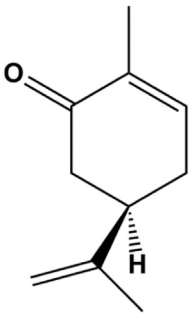
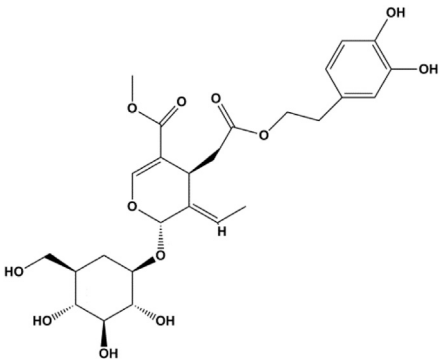
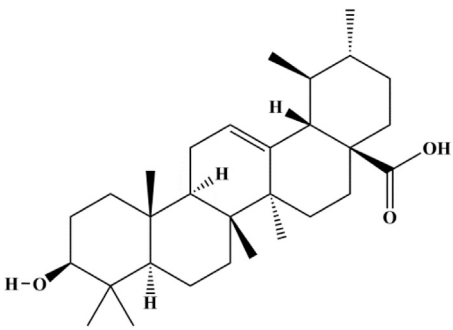
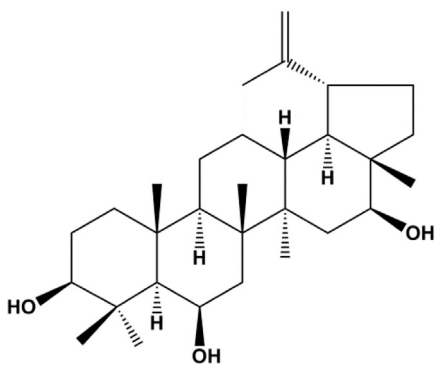
(Continued on following page)

TABLE 1 | (*Continued*) Proapoptotic effects of monomers from natural products on breast cancer cells.

Monomers	Chemical structure	Detail mechanisms		Cell model	Refs
Amentoflavone (250 μM)		Bax, p53	Bid	MCF-7	Pei et al. (2012)
Calycosin (25, 50, 100 μM)		Bax	Bcl-2	MCF-7	Tian et al. (2013)
Thymoquinon (with 12.30 ± 0.62 μM in MDA-MB-468 with 18.06 ± 0.71 μM in T-47D)		p27, Bax, CytoC, pro–caspase-3, cleaved PARP	Cyclin D1, cyclin E, Bcl-2, BclXL, survivin, p-PDK1, p-PTEN, p-Akt, p-GSK-3β, p-Bad, 4E-BP1, eIF4E, p-S6R, p-p70S6K	MDA-MB-468 T-47D	Rajput et al. (2013)
Embelin (40, 80 μg/mL)		Bax, CytoC, caspase-3, caspase-9	Bcl-2	MCF-7	Li et al. (2013)

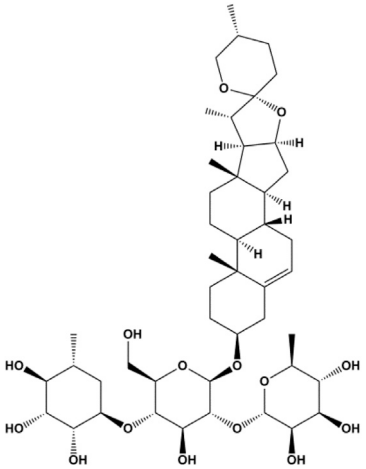
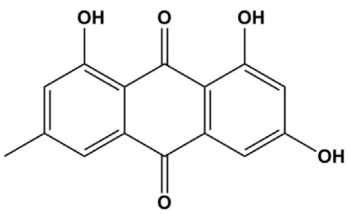
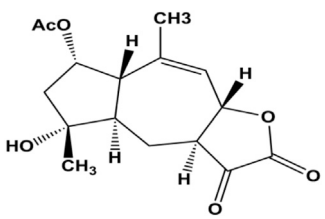
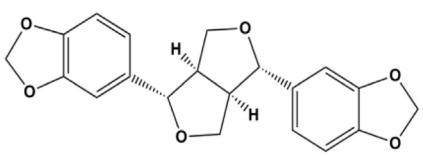
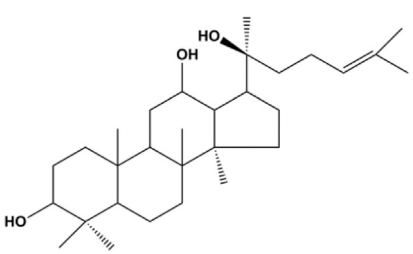
(Continued on following page)

TABLE 1 | (*Continued*) Proapoptotic effects of monomers from natural products on breast cancer cells.

Monomers	Chemical structure	Detail mechanisms		Cell model	Refs
L-Carvone (0.3–2.4 mM)		p53, Bad, cleaved caspase-3, cleaved PARP	MCF-7	MDA-MB-231	Patel and Thakkar, (2014)
Oleuropein (100, 200 μM)		p53, Bax	Bcl-2	MCF-7	Hassan et al. (2014)
Ursolic acid (20, 40, 80 μmol/L)		p16, p27, activated caspase-3, activated caspase-9		MDA-MB-231	Ma and Sun, (2014)
3β, 6β, 16β-trihydroxylup-20 (29)-ene (TTHL) (0.5, 1.36, 3.70 μg/mL)		Cleaved caspase-9, ROS		MCF-7	Viau et al. (2014)

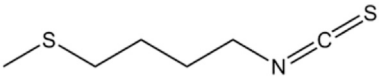
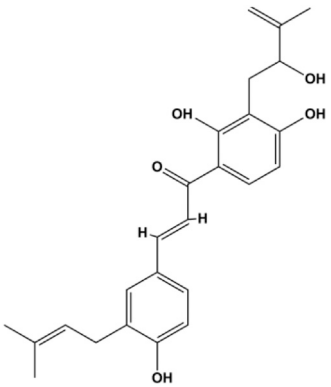
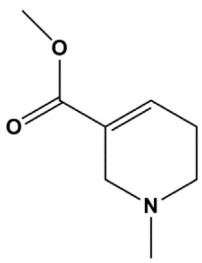
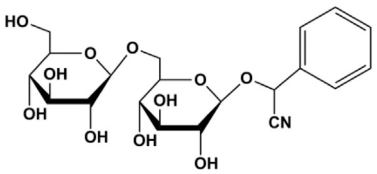
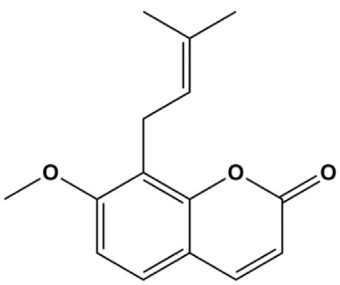
(Continued on following page)

TABLE 1 | (*Continued*) Proapoptotic effects of monomers from natural products on breast cancer cells.

Monomers	Chemical structure	Detail mechanisms		Cell model	Refs
Dioscin (1, 2, 4, 6,8 μM)		Cleaved caspase-3, cleaved PARP	Bcl-2, cIAP-1, Mcl-1	MDA-MB-231	Kim et al. (2014)
Emodin (10, 40 μM)		Cleaved caspase-3, PARP, p53, Bax	Bcl-2	Bcap-37 ZR-75-30	Zu et al. (2015)
Gaillardin (1, 10, 100 mM)		Bax, p53	Bcl-2	MCF-7 MDA-MB-468	Fallahian et al. (2015)
Sesamin (1, 10, 50 μM)		Bax, caspase-3, p53		MCF-7	Siao et al. (2015)
20(S)-protopanaxadiol (0–60 ml)		Bax, cleaved PARP, p53	Bcl-2, CytoC, cyclin D1, CDK4	MCF-7	Zhang et al. (2018a)

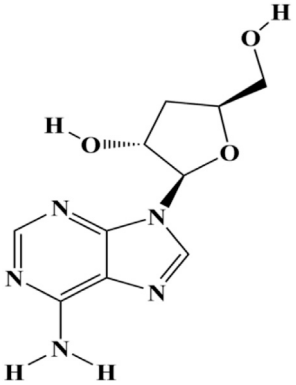
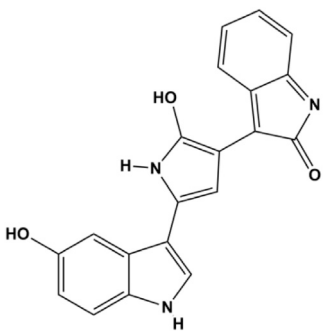
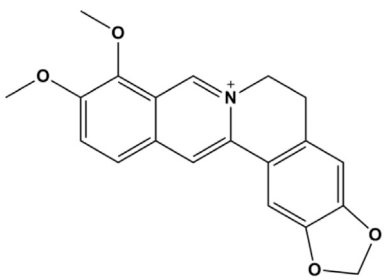
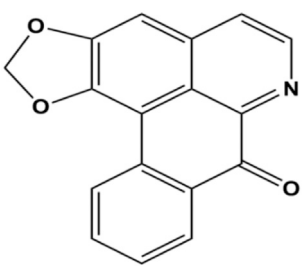
(Continued on following page)

TABLE 1 | (*Continued*) Proapoptotic effects of monomers from natural products on breast cancer cells.

Monomers	Chemical structure	Detail mechanisms		Cell model	Refs
4-Methylthiobutyl isothiocyanate (2.5, 5, 10, 20 μM)		Cleaved caspase-9, cleaved caspase-3	PARP	MDA-MB-231 MCF-7	Li et al. (2015)
Paratocarpin E (10, 20, 30, 40 μM)		Cleaved caspase-8, cleaved caspase-9, Bax, CytoC	Bcl-2	MCF-7	Gao et al. (2016)
Arecoline (10, 30, 50, 100, 300, 500 μmol/L)		p53, Bax	Bcl-2	MCF-7	Feng et al. (2016)
Amygdalin (10, 20, 40 mg/mL)		Bax, activated caspase-3, cleaved PARP, p-p38	Bcl-2	Hs578T	Lee and Moon, (2016)
Osthole (25, 50, 100 μmol/L)		Bax, p53, p21, CytoC	Bcl-2	MCF-7	Zhang and Zhu, (2016)

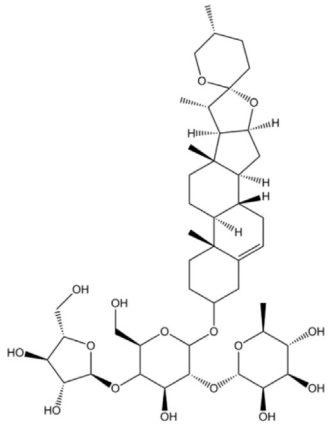
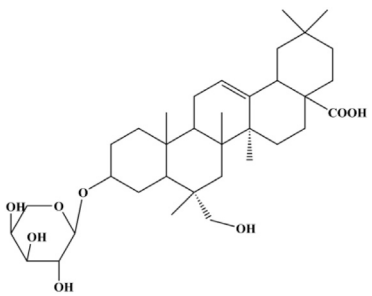
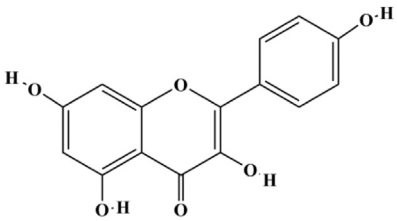
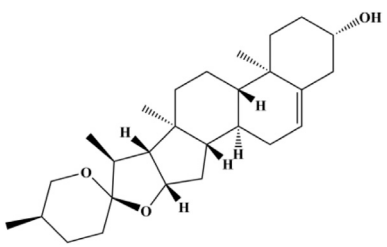
(Continued on following page)

TABLE 1 | (*Continued*) Proapoptotic effects of monomers from natural products on breast cancer cells.

Monomers	Chemical structure	Detail mechanisms		Cell model	Refs
Cordycepin (50, 100 μM)		Cleaved caspase-8, cleaved caspase-9, cleaved caspase-3, Bax	Bcl-2	MCF-7 MDA-MB-231	Wang et al. (2016)
Violacein (0.45, 4.5 μM)		Bax, p53, caspase-3, Fas, FADD	Bcl-2, MDM2	MCF-7	Alshatwi et al. (2016)
Berberine (5, 10, 20, 40 μg/mL)		Cleaved caspase-3, cleaved caspase-9, Bax, CytoC	Bcl-2	BT549 MDA-MB-231	Zhao et al. (2017)
Liriodenine (0.1, 1, 10 μM)		p53	Bcl-2, cyclin D1	MCF-7	Li et al. (2017b)
Polyphyllin I (8 μM)				MDA-MB-231	Li et al. (2017a)

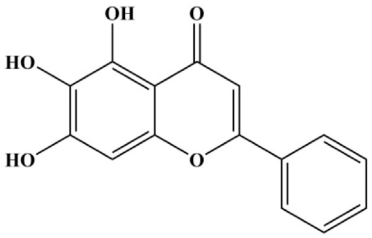
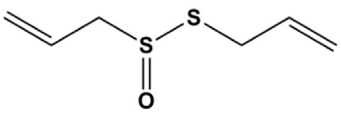
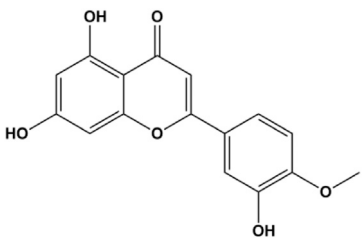
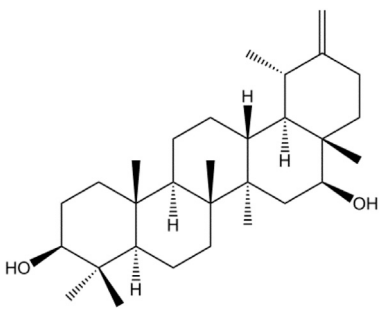
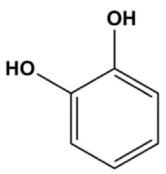
(Continued on following page)

TABLE 1 | (*Continued*) Proapoptotic effects of monomers from natural products on breast cancer cells.

Monomers	Chemical structure	Detail mechanisms		Cell model	Refs
		Cleaved caspase-9, cleaved caspase-3, cleaved PARP			
Clematis hederagenin saponin (0.08, 0.4, 2, 10 μg/mL)		Caspase-3, caspase-9	Apaf-1, CytoC	MCF-7 MDA-MB-231	Cheng et al. (2018)
Kaempferol (50 μmol/L)		Cleaved caspase-9, cleaved caspase-3, p-A TM		MDA-MB-231 cells	Zhu and Xue, (2019)
Diosgenin (5, 10, 20, 40 μM)		CytoC, cleaved caspase-9	Bcl-2	MCF-7 Hs578T	Liao et al. (2019)

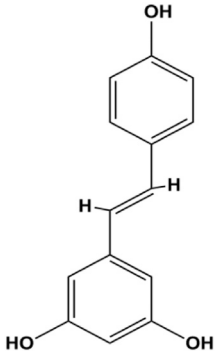
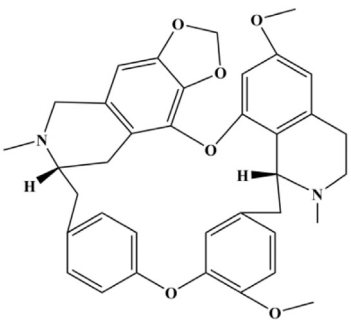
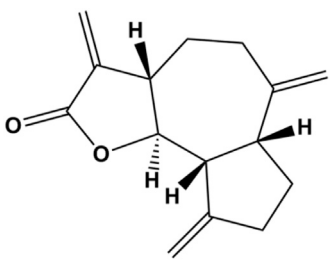
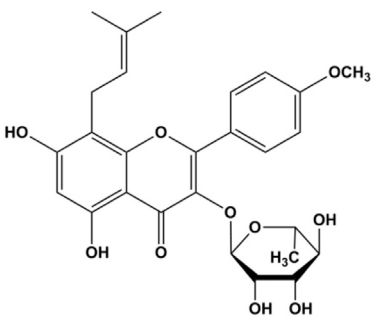
(Continued on following page)

TABLE 1 | (*Continued*) Proapoptotic effects of monomers from natural products on breast cancer cells.

Monomers	Chemical structure	Detail mechanisms		Cell model	Refs
Baicalein (50, 100 μM)		Bax, CytoC, cleaved caspase-9, cleaved caspase-3	Bcl-2	MCF-7	Liu et al. (2019)
Allicin (20, 45 μM)		Activated caspase-3, activated caspase-8, activated caspase-9 NOXA, p21, Bak	BclXL	MCF-7 HCC-70	Rosas-Gonzalez et al. (2020)
Diosmetin (5, 10, 20, 30, 40, 50, 60, 70 μm/L)		p53, Bax, caspase-3	Bcl-2	MCF-7	Wang et al. (2020)
Arnidiol (60 μM)		PARP, cleaved caspase-3		MDA-MB-231	Hu et al. (2020)
Catechol (10, 40, 80 μM)		p-H2AX, p-ATM, p-ATR, cleaved caspase -9, cleaved caspase-3, Bax	BclXL, Bcl-2	MDA-MB-231	Vazhappilly et al. (2021)

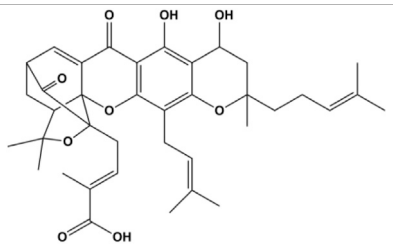
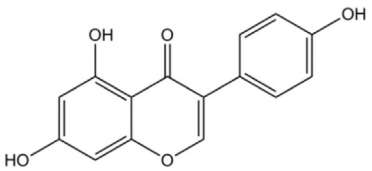
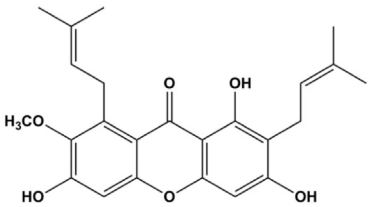
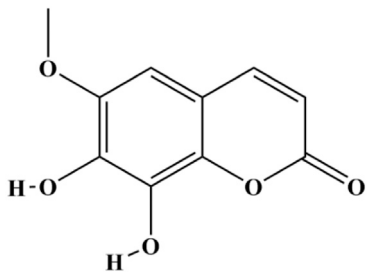
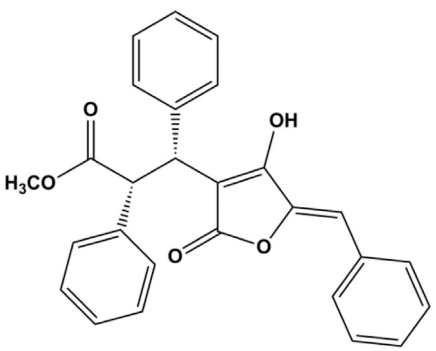
(Continued on following page)

TABLE 1 | (*Continued*) Proapoptotic effects of monomers from natural products on breast cancer cells.

Monomers	Chemical structure	Detail mechanisms	Cell model	Refs
Resveratrol (12.5, 25, 50, 100, 200 μM)		Cleaved PARP1, cleaved caspase-3 PCNA, Bcl-2	MDA-MB-231	Liang et al. (2021)
Cepharanthine (2 μM)		Cleaved caspase-3, cleaved PARP	MDA-MB-231	Shen et al. (2021)
Dehydrocostuslactone (5, 10, 20, 30, 40, 50, 60, 80, 100 μmol/L)		Bax, caspase-3, cleaved caspase-3 Bcl-2	SK-BR-3	Ma et al. (2021)
FasL-Fas–mediated apoptosis				
Icariside II (25, 50, 75 μM)		CytoC, cleaved caspase-3, cleaved PARP, cleaved caspase-7, cleaved caspase-8, Fas, FADD, BclXL, Bax, Bim	MCF7	Huang et al. (2012)

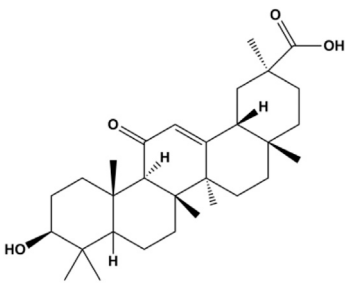
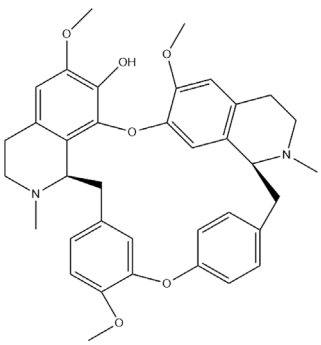
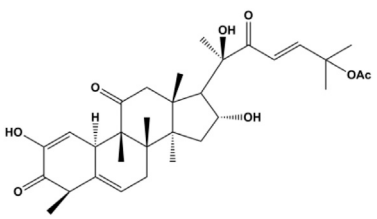
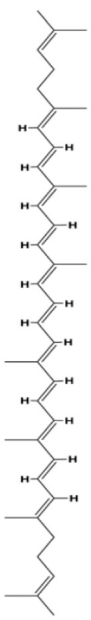
(Continued on following page)

TABLE 1 | (*Continued*) Proapoptotic effects of monomers from natural products on breast cancer cells.

Monomers	Chemical structure	Detail mechanisms		Cell model	Refs
Gambogenic acid (0.4, 0.6, 0.8, 1.0 μg/mL)		Fas, cleaved caspase-3, cleaved caspase-8, cleaved caspase-9, Bax	Bcl-2	MDA-MB-231	Zhou et al. (2013)
Genistein (0, 5, 10, 20 μmol/L)		FADD, cleaved caspase-8, FasL		MDA-MB-231	Wang et al. (2013a)
α-Mangostin (1, 2, 3, 4 μM)		Cleaved PARP, Bax	Fas, Bcl-2, p-Fak	MCF-7 MDA-MB-231	Li et al. (2014)
Fraxetin (20, 40, 60 μM)		Fas, FasL, Bax	Bcl-2	MCF-7	Liu et al. (2017a)
Pulveraven A (50,100 μM)		FADD, cleaved caspase-7, cleaved caspase-8, cleaved PARP, Bax	Bcl-2	MCF-7	Lee et al. (2021)

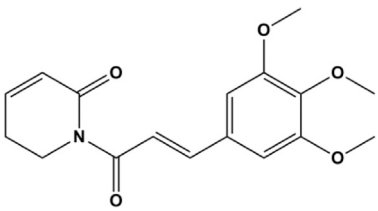
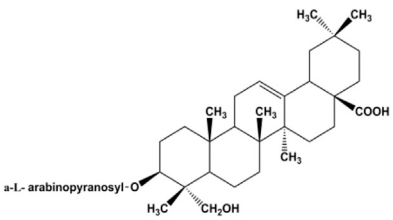
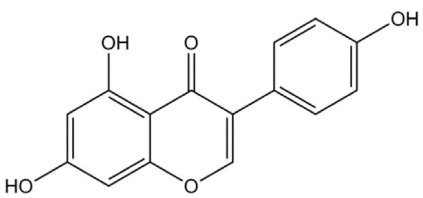
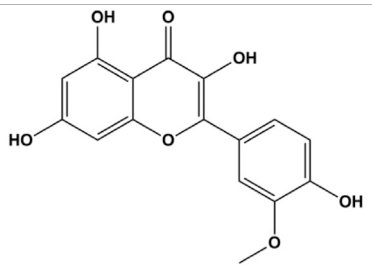
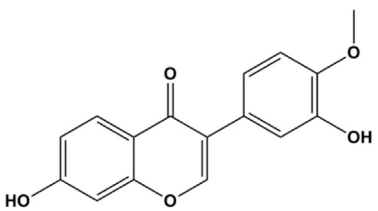
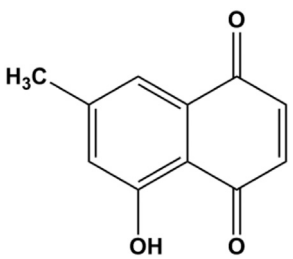
(Continued on following page)

TABLE 1 | (*Continued*) Proapoptotic effects of monomers from natural products on breast cancer cells.

Monomers	Chemical structure	Detail mechanisms		Cell model	Refs
PI3K/AKT pathway–mediated apoptosis					
18β-Glycyrrhetinic acid (100 μM)		CytoC, activated caspase-9, Bax	Bcl-2	MCF-7	Sharma et al. (2012)
Fangchinoline (5, 10, 20 μmol/L)			p-PI3K, p-Akt, p-mTOR	MDA-MB-231	Zhang et al. (2017)
Cucurbitacin E (100–200 nM)		Cleaved caspase-3, cleaved PARP	Cyclin D1, survivin, Mcl-1, XIAP, Bcl-2, p-STAT3, p-ERK, p-AKT	MDA-MB-468	Kong et al. (2014)
Lycopene (100 μM)		Cleaved PARP, p21, Bax	p-Akt, p-mTOR, cyclin D1	MDA-MB-468	Takeshima et al. (2014)

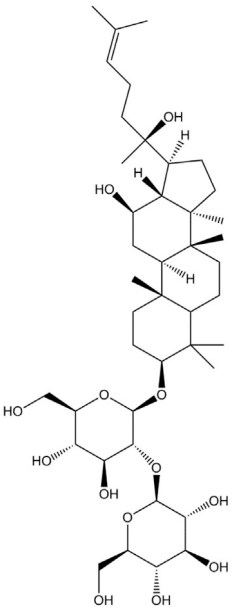
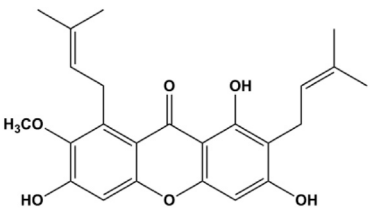
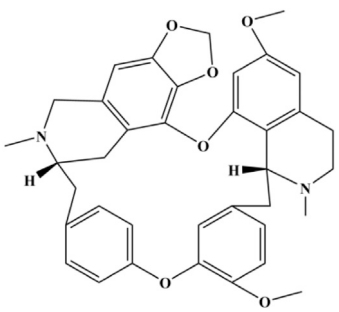
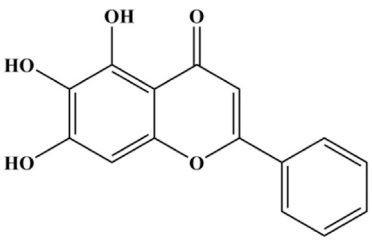
(Continued on following page)

TABLE 1 | (*Continued*) Proapoptotic effects of monomers from natural products on breast cancer cells.

Monomers	Chemical structure	Detail mechanisms		Cell model	Refs
Piperlongumine (5, 10, 15, 20, 25 μM)		Bax, CytoC	p-Akt, p70S6K1, 4EBP1, cyclin D1, Bcl-2, p53	MDA-MB-231	Shrivastava et al. (2014)
D-Rhamnose β hederin (20, 30, 40 μg/mL)			p-PI3K, p-Akt	MDA-MB-231 MCF-7	Cheng et al. (2014)
Genistein (0, 20, 40, 80 μM)		Bax	p-Akt, Bcl-2	MCF-7	Chen et al. (2015b)
Isorhamnetin (10 μM)		Bax, cleaved caspase-3	p-Akt, p-mTOR, p-MEK1/2, p-ERK1/2, Bcl-2, BclXL	MCF7 MDA-MB-468	Hu et al. (2015)
Calycosin (80 μM)			p-Akt, HOTAIR	MCF-7	Chen et al. (2015c)
Ramentaceone (5, 10, 15 μM)		Bax, Bak, cleaved caspase-3, cleaved PARP	PI3K p85, p-PI3K, p-Akt (Ser473), Bcl-2	BT47 SKBR3 MCF-7 MDA-MB-231	Kawiak and Lojkowska, (2016)

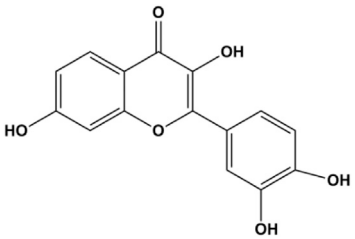
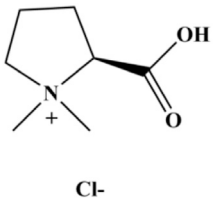
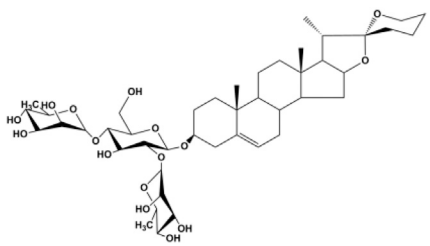
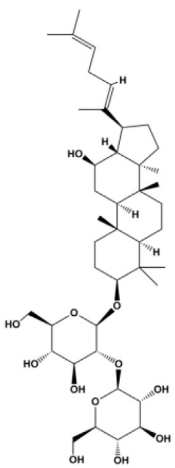
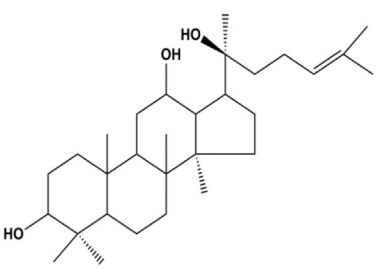
(Continued on following page)

TABLE 1 | (*Continued*) Proapoptotic effects of monomers from natural products on breast cancer cells.

Monomers	Chemical structure	Detail mechanisms		Cell model	Refs
Ginsenoside Rg3 (100 ng/mL)			p-Akt, MGBA	MDA-MB-231	Peng et al. (2016)
α-Mangostin (15, 30 μM)		Cleaved caspase-3, cleaved caspase-9	Bcl-2, Mcl-1	T47D	Kritsanawong et al. (2016)
Cepharanthine (with 10 μM in MCF-7 cells, with 6 μM in MDA-MB-231 cells)		Bax, Bad, cleaved caspase-3, cleaved caspase-9	Bcl-2	MCF-7 MDA-MB-231	Gao et al. (2017)
Baicalein (10, 20, 40 μM)		IκB	p-Akt, p-mTOR, NF-κB, p-IκB	MCF-7 MDA-MB-231	Yan et al. (2018)

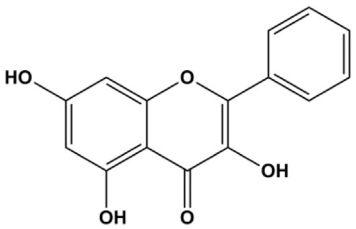
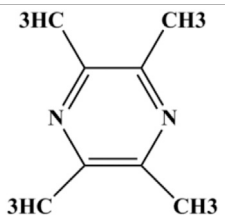
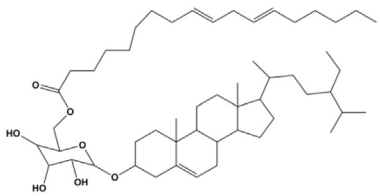
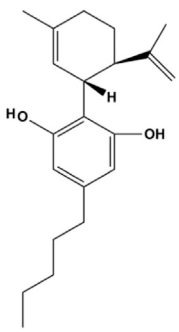
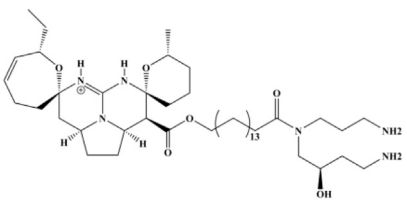
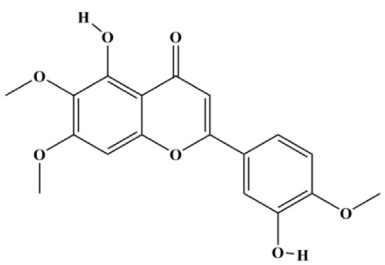
(Continued on following page)

TABLE 1 | (*Continued*) Proapoptotic effects of monomers from natural products on breast cancer cells.

Monomers	Chemical structure	Detail mechanisms		Cell model	Refs
Fisetin (20μM, 40μM, 80 μM)		Bax, caspase-3, caspase-8, caspase-9	p-PI3K, p-Akt, p-mTOR, p-P70	4T1	SUN et al. (2018)
Stachydrine hydrochloride (5, 20, 50, 100, 200 μM)		Cleaved caspase-3	Bcl-2, p-Akt, p-ERK	MCF-7 T47D	Wang et al. (2017)
Paris saponins (XA2) (1.25, 2.5, 5 μM)			p-Akt, p-mTOR, p-P70S6K	MCF-7 MDA-MB-231	Xie et al. (2017)
Ginsenoside Rg5 (10, 20 mg/kg)		Ras, cleaved caspase-8, cleaved caspase-9, Bax, CytoC	Bcl-2	MCF-7	Liu and Fan, (2018)
20(S)-protopanaxadiol (15, 30, 60 μM)		p-PTEN, p53	p-Akt (Thr308), p-Akt (Ser473), p-mTOR (Ser2448), p-FoxO1 (Ser256), p-MDM2 (Ser166), p-NF-κB, p65 (Ser536), p-GSK-3β (Ser9), p27kip1, CytoC	MCF-7	Zhang et al. (2018a)

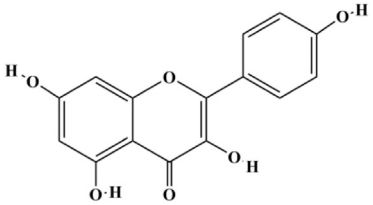
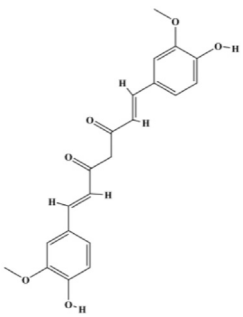
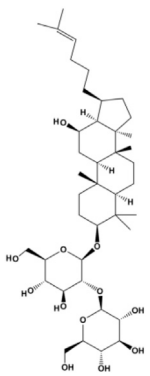
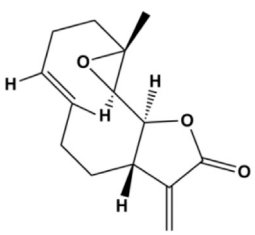
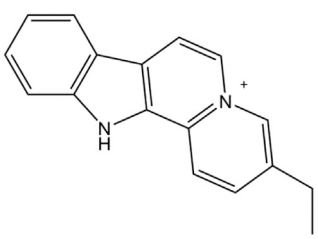
(Continued on following page)

TABLE 1 | (*Continued*) Proapoptotic effects of monomers from natural products on breast cancer cells.

Monomers	Chemical structure	Detail mechanisms		Cell model	Refs
Galangin (20, 40, 80, 160 μmol/L)		Bax, cleaved caspase-9, cleaved caspase-8, cleaved caspase-3, cleaved Bid, Bad, p21, p27, p53	Bcl-2, p-PI3K, p-Akt, cyclin D3, cyclin B1, CDK1, CDK2, CDK4	MCF-7	Liu et al. (2018b)
Tetramethylpyrazine (800, 1,600, 3,200 μM)		Cleaved caspase-3	p-Akt	MDA-MB-231	Shen et al. (2018)
Daucosterol linoleate (25, 50, 100 mg/mL)		Cleaved caspase-3, cleaved caspase-7, cleaved caspase-8, cleaved caspase-9, cleaved PARP-1, Bax, Bad	BclXL, Bcl-2, XIAP	MCF-7	Han et al. (2018)
Cannabidiol (1–7 μM)		PPARγ	mTOR, cyclin D1	MDA-MB-231 T-47D	Sultan et al. (2018)
Crambescidin 800 (0.01, 0.1, 0.5, 1, 5, 10,15, 20 μM)		p21	Cyclin D1, CDK4, CDK6	T11 SUM159PT	Shrestha et al. (2018)
Eupatorin (5 μg/mL)		Bak1, HIF1A, Bax, Bad, CytoC, SMAC/Diablo, activated caspase-9, activated caspase-8, Rb-Raf-1, GSK-3β	Akt (pan), p-PDK1	MDA-MB-231	Razak et al. (2019)

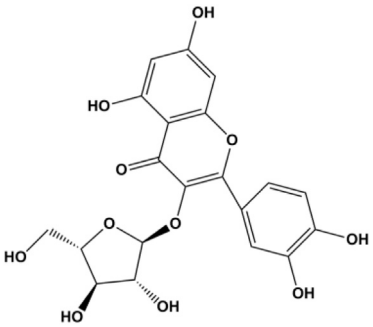
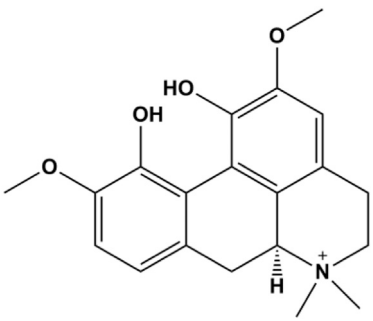
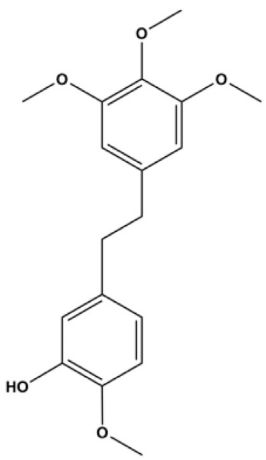
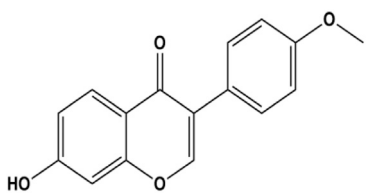
(Continued on following page)

TABLE 1 | (*Continued*) Proapoptotic effects of monomers from natural products on breast cancer cells.

Monomers	Chemical structure	Detail mechanisms		Cell model	Refs
Kaempferol (25, 50, 100 μmol/L)			p-PI3K, p-AKT, p-GSK-3β	SUM190	Zhao et al. (2019)
Curcumin (10, 30 μM)		p21, Bax, cleaved caspase-3	CDC25, CDC2, Bcl-2	T47D MCF-7	Hu et al. (2018)
Ginsenoside Rk1 (40, 80, 120 μM)		Bax, CytoC, cleaved caspase-3, cleaved caspase-8, cleaved caspase-9	Bcl-2	MDA-MB-231	Hong and Fan, (2019)
Parthenolide (5, 10 μmol/L)		Caspase-3	Bcl-2	MDA-MB-231 MCF-7	Han et al. (2019)
Flavopereirine (5, 10, 15 μM)		Cyclin D1, cyclin E1, p21, 27, activated caspase-3, activated caspase-9, cleaved PARP, p-ERK1/2, p38	Cyclin A2, CDK-2, BclxL, cleaved caspase-8	MDA-MB-231	Yeh et al. (2019)

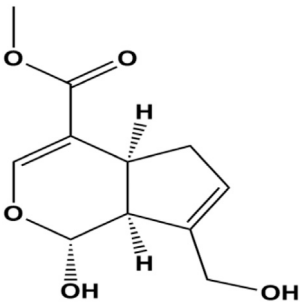
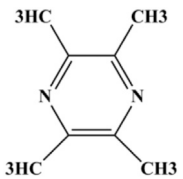
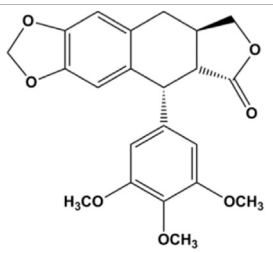
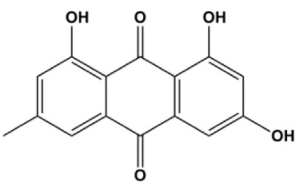
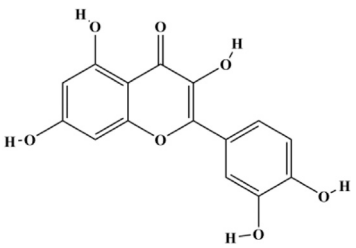
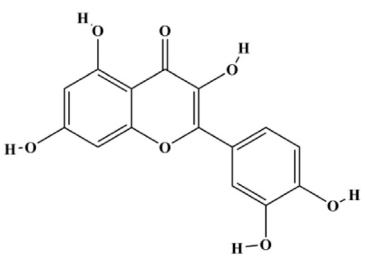
(Continued on following page)

TABLE 1 | (*Continued*) Proapoptotic effects of monomers from natural products on breast cancer cells.

Monomers	Chemical structure	Detail mechanisms		Cell model	Refs
Avicularin (6.25, 12.5, 25, 50, 100 μmol/L)			PI3K, p-PI3K, AKT, p-Akt, Bcl-2, BclXL, CDK2	MDA-MB-231	Yu et al. (2020)
Magnoflorine (1.25, 2.5, 5 μM) and Doxorubicin (0.1, 0.25, 0.5, 1 μM)		p21, p53, cleaved caspase-9, cleaved caspase-3, Beclin-1, LC3-I	CDK1, CDK2, cyclin B1, Bcl-2, p62	MCF-7 MDA-MB-231	Wei et al. (2020)
Erianin (40, 80, 160 nM)		p21, p27, PARP, Bax, caspase-3, caspase-9	CDK1, cyclin B1, p-PI3K, p-Akt	MDA-MB-231 EFM-192A cell	Xu et al. (2021)
MAPK pathway–mediated apoptosis					
Formononetin (25, 50, 100 μM)		Bax, Ras, Raf, p-p38	Bcl-2	MCF-7	Chen and Sun, (2012)

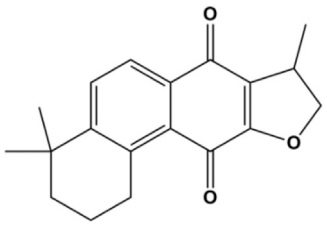
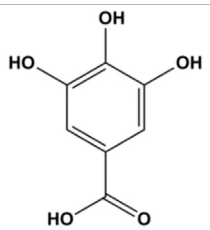
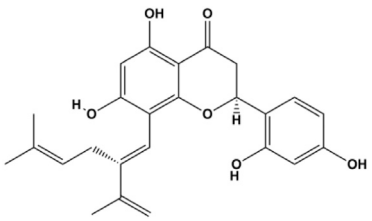
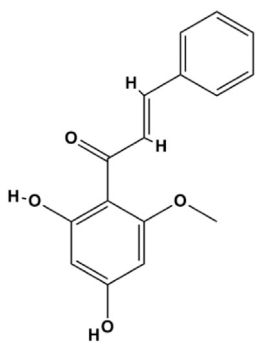
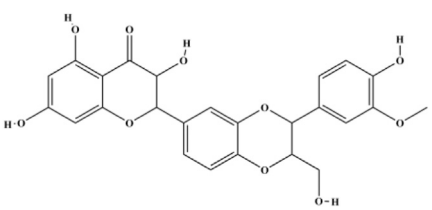
(Continued on following page)

TABLE 1 | (*Continued*) Proapoptotic effects of monomers from natural products on breast cancer cells.

Monomers	Chemical structure	Detail mechanisms		Cell model	Refs
Genipin (0.05, 0.1, 1 mM)		Bax, activated caspase-3, p38, p-JNK	Bcl-2	MDA-MB-231	Kim et al. (2012)
Tetramethylpyrazine (0.25, 0.50, 1.00, 1.50, 2.00 mg/mL)		p-p38, p-JNK	p-ERK	MCF7	Lai et al. (2016)
Deoxypodophyllotoxin (10^1–10^4 ng/mL)		Cleaved caspase-3, ERK1/2, IkB-α	p-ERK	MB231	Benzina et al. (2015)
Emodin (20, 40, 80 μmol/mL)		AP-1		MCF-7	Fan et al. (2015)
Quercetin (40 μM)		p21	Cyclin D1, Twist, p-p38	MCF-7	Ranganathan et al. (2015)
Quercetin (20 μM)		FasL, GADD45, p53, p21, p-JNK, translocation of Foxo3a		MDA-MB-231	Nguyen et al. (2017)

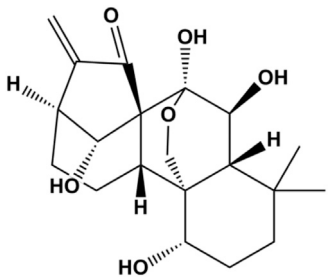
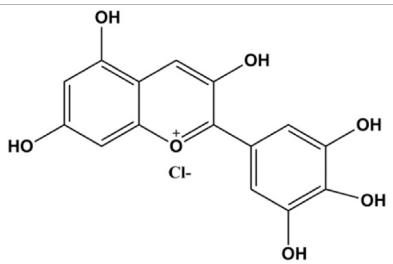
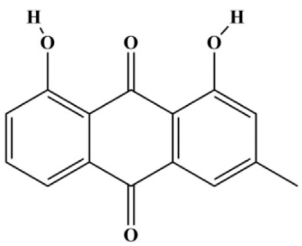
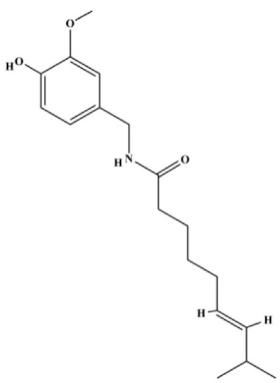
(Continued on following page)

TABLE 1 | (*Continued*) Proapoptotic effects of monomers from natural products on breast cancer cells.

Monomers	Chemical structure	Detail mechanisms		Cell model	Refs
Isocryptotanshinone (2.5, 5, 10 μM)		Bsx, Bak, cleaved PARP, cleaved caspase-3, cleaved caspase-9, p-JNK, p-ERK, p-p38	Bcl-2, BclXL	MCF-7	Zhang et al. (2015a)
Gallic acid (5, 25, 50 μM)		$p21^{Cip1}$, $p27^{Kip1}$, activated caspase-9, activated caspase-3	Cyclin D1/CDK4, cyclin E/CDK2	MDA-MB-231	Lee et al. (2017)
Sophoraflavanone G (5, 10, 15, 20, 30 μM)		Cleaved caspase-8, cleaved caspase-3, cleaved caspase-9	Bcl-2, BclXL	MDA-MB-231	Huand et al. (2019)
Cardamonin (CD) (20 μM)		Foxo3a, p27, p21, Bim, p-JNK, cleaved caspase-3	Cyclin D1	MDA-MB 231 MCF-7	Kong et al. (2019)
Silymarin (100, 200 μg/mL)		Bax, cleaved PARP, cleaved caspase-9, p-JNK	Bcl-2, p-p38, p-ERK1/2	MDA-MB-231 MCF-7	Kim et al. (2021)

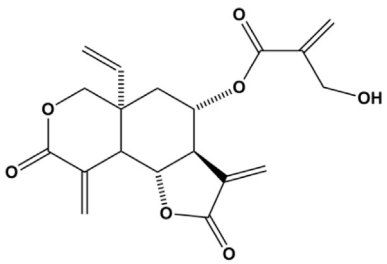
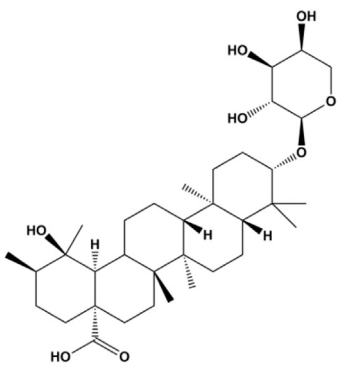
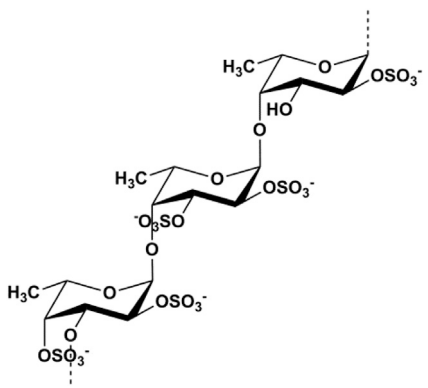
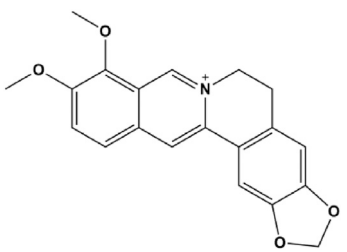
(Continued on following page)

TABLE 1 | (*Continued*) Proapoptotic effects of monomers from natural products on breast cancer cells.

Monomers	Chemical structure	Detail mechanisms		Cell model	Refs
NF-κB–mediated apoptosis					
Oridonin (20 μM)		Bax, cleaved PARP, Fas, PPARγ	Bcl-2, caspase-8, NF-κB (p65), IKKα, IKKβ, p-mTOR	MDA-MB-231 MCF-7	Wang et al. (2013b)
Delphintin (10, 20, 40, 80, 160 μmol/L)		IκBα, IKKα, IKKβ, PKCα	p-NF-κB/p65, p-IκBα, p-IKKα/β, p-PKCα	MDA-MB-453 BT-474	Wu et al. (2018a)
Chrysophanol (5, 10, 20 μM)		p27, cleaved caspase-3, cleaved PARP	Cyclin D1, cyclin E, Bcl-2, p65, IκB	MCF-7 MDA-MB-231	Ren et al. (2018)
Capsaicin (100, 150 μmol/L)		Bax, cleaved caspase-3	FBI-1, Ki-67, Bcl-2, survivin	MCF-7 MDA-MB-231	Chen et al. (2021)

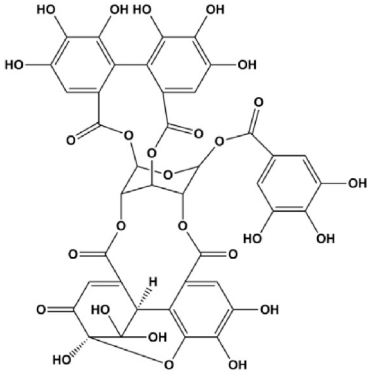
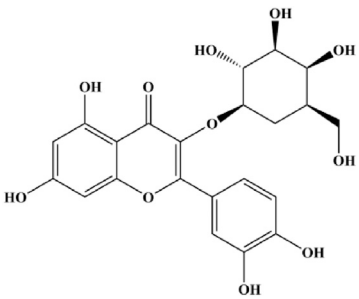
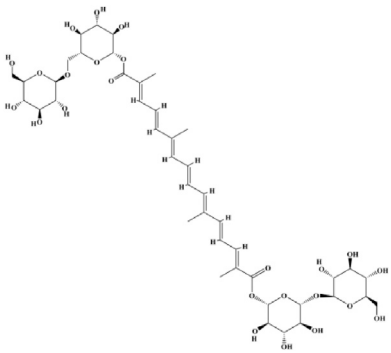
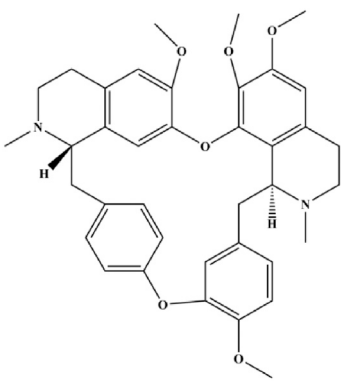
(Continued on following page)

TABLE 1 | (*Continued*) Proapoptotic effects of monomers from natural products on breast cancer cells.

Monomers	Chemical structure	Detail mechanisms		Cell model	Refs
ROS-mediated apoptosis					
Vernodalin (3.125, 6.25, 12.5 μg/mL)		CytoC, cleaved PARP, caspase-3, cleaved caspase-7, cleaved caspase-9	Bcl-2, BclxL, MMP	MCF-7 MDA-MB-231	Looi et al. (2013)
Ziyuglycoside II (2.5, 10, 40 μM)		p21/WAF1, p-Cdc25C, p-Cdc2	Cdc25C, Cdc2, cyclin A, cyclin B1	MDA-MB-231 MCF-7	Zhu et al. (2014)
Fucoidan (0.2–1 mg/mL)		Caspase-8, CytoC, Bax	Cyclin D1, CDK-4, Bcl-2	MCF-7	Banafa et al. (2013)
Berberine (50 μM)		Bax, ROS, p-JNK, CytoC, AIF, activated caspase-3	Bcl-2	MDA-MB-231 MCF-7	Xie et al. (2015)

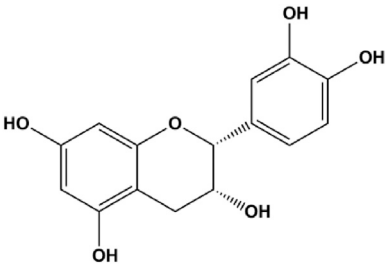
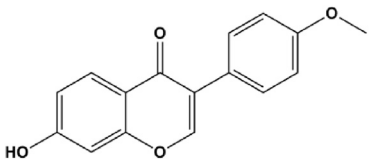
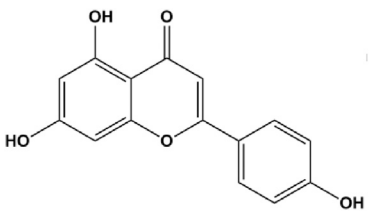
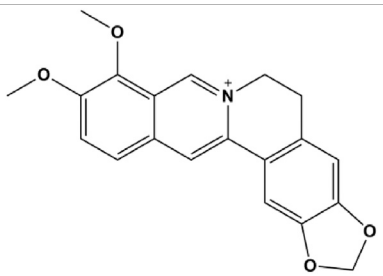
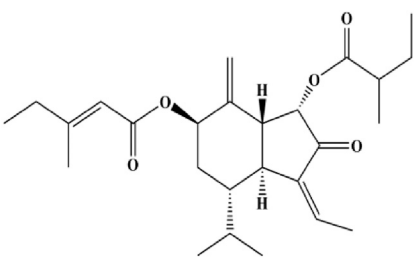
(Continued on following page)

TABLE 1 | (*Continued*) Proapoptotic effects of monomers from natural products on breast cancer cells.

Monomers	Chemical structure	Detail mechanisms		Cell model	Refs
Geraniin (5, 10, 25 μM)		Cleaved PARP, cleaved caspase-3	Bcl-2, p-ERK1/2, p-Akt, p-p38	MCF-7	Zhai et al. (2016)
Hyperoside (25, 50, 100 μM)		Bax, cleaved caspase-3	Bcl-2, XIAP	MCF-7 cells 4T1 cells	Qiu et al. (2019)
Crocin (0.5–6 mM)		Foxo3a, Bim, PTEN, activated caspase-3, BAX	Bcl-2	MCF-7 MDA-MB-231	Nasimian et al. (2020)
Tetrandrine (51 μM)		Activated caspase-8, activated caspase-9, activated caspase-3		MDA-MB-231	N et al. (2019)

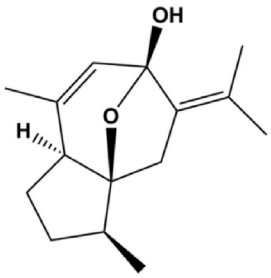
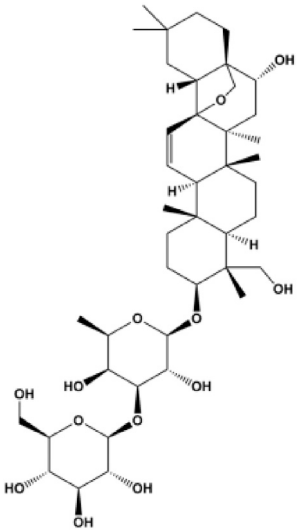
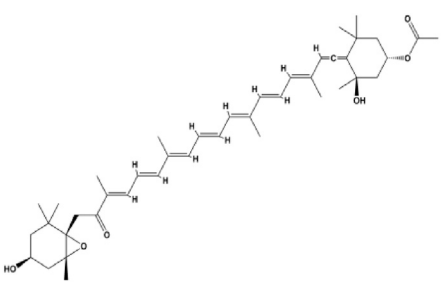
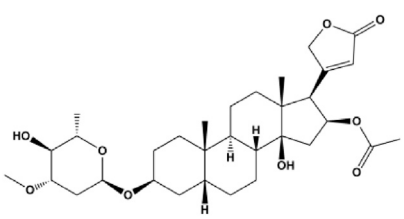
(Continued on following page)

TABLE 1 | (*Continued*) Proapoptotic effects of monomers from natural products on breast cancer cells.

Monomers	Chemical structure	Detail mechanisms		Cell model	Refs
(–)-Epicatechin (350 μM)		Bad, Bax		MCF-7 MDA-MB-231	Pereyra-Vergara et al. (2020)
Formononetin (8, 16, 32, 64, 128 μmol/L)		Bax, cleaved caspase-3	Bcl-2	MCF-7	Jia et al. (2020)
JAK-STAT3–mediated apoptosis					
Apigenin (0, 20, 40, 60 μM)		Cleaved caspase-8, cleaved caspase-3, cleaved PARP	p-JAK2, p-STAT3	MDA-MB-453 (HER2-overexpressing)	Seo et al. (2014)
Berberine (10, 20, 40 μg/mL)		Bax, cleaved PARP, cleaved caspase-3	p-JAK2, p-STAT3, Bcl-2	MCF-7	Zhang et al. (2015b)
7β-(3-Ethyl-*cis*-crotonoyloxy)-1α-(2-methylbutyryloxy)-3,14-dehydro-Z-notonipetranone (2.5, 5, 10 μM)		Cleaved caspase-3, cleaved caspase-8, cleaved PARP	p-STAT3 (Tyr705), p-JAK1, p-JAK2, p-Src, Bcl-2, COX-2, cyclin D1	MDA-MB-231	Jang et al. (2019)

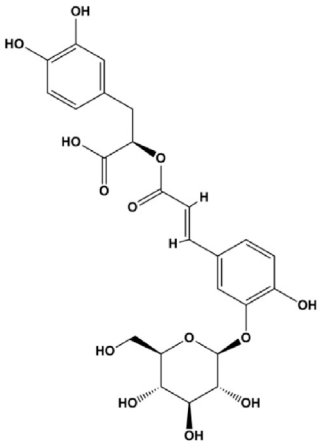
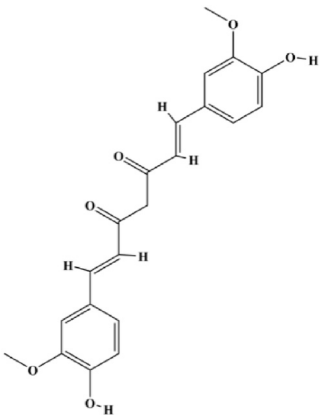
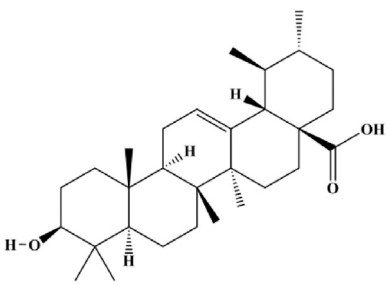
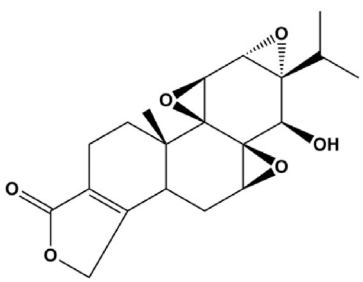
(Continued on following page)

TABLE 1 | (*Continued*) Proapoptotic effects of monomers from natural products on breast cancer cells.

Monomers	Chemical structure	Detail mechanisms	Cell model	Refs
Curcumol (0, 12.5, 25, 50, 100 μg/mL)		p-JAK2, p-STAT3	MCF-7	Ma et al. (2020)
Saikosaponin D (0, 5, 10, 20 μmol/L)		JAK2, STAT3, Ki-67	MCF-7	Feng et al. (2021)
Endoplasmic reticulum stress–mediated apoptosis				
Fucoxanthin (10, 20, 40 μmol/L)		Bax, activated caspase-4, activated caspase-7, activated caspase-9, CytoC	Bcl-2	MCF-7	Hou et al. (2014)
Oleandrin (with 14.5 nM in MCF-7, with 24.62 nM in MDA-MB-231)		Bax, Bim, IF2α, ATF4, CHOP, p-PERK, p-eIF2α	Bcl-2	MCF-7 MDA-MB-231	Li et al. (2020)

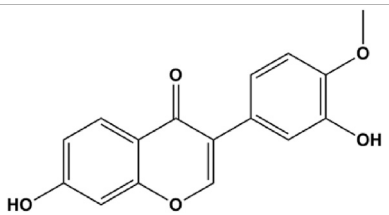
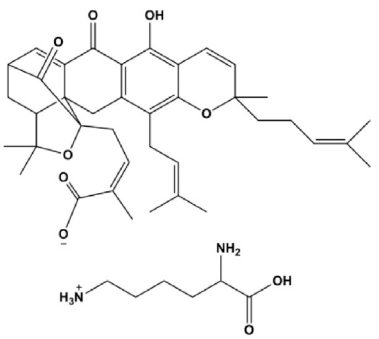
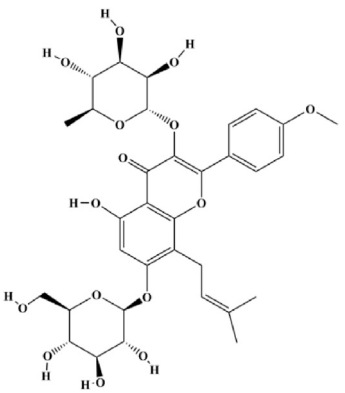
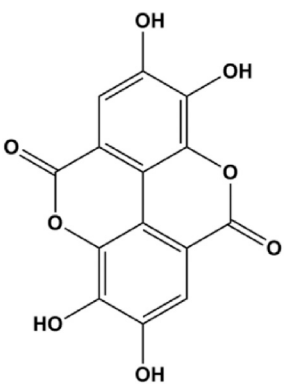
(Continued on following page)

TABLE 1 | (*Continued*) Proapoptotic effects of monomers from natural products on breast cancer cells.

Monomers	Chemical structure	Detail mechanisms		Cell model	Refs
Salviaflaside (0.1, 1, 10 μmol/L)		GRP78, ATF4, CHOP, p-PERK, p-eIF2α, cleaved caspase-3	Bcl-2/Bax	MDA-MB-231	Wu et al. (2018b)
Other pathways–mediated apoptosis					
Curcumin (30 μmol/mL)			pERK1/2, pEGFR	MDA-MB-231	Sun et al. (2012)
Ursolic acid (10, 20, 30 μmol/L)			FOXM1, cyclin D1, CDK4	MCF-7	Wang et al. (2012)
Triptolide (10, 25, 50 nM)			β-Catenin	MDA-MB-231 BT-474	Shao et al. (2014)

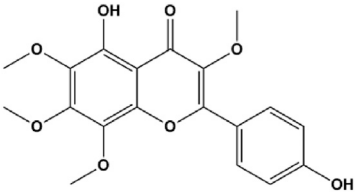
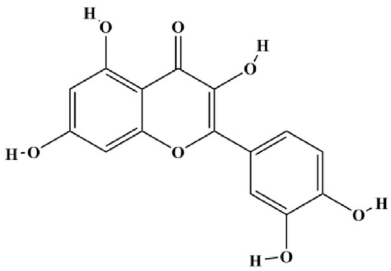
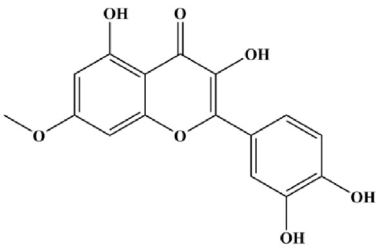
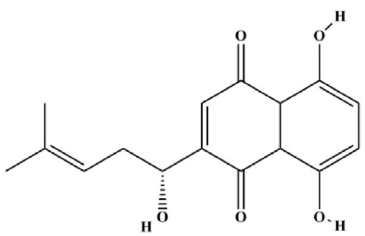
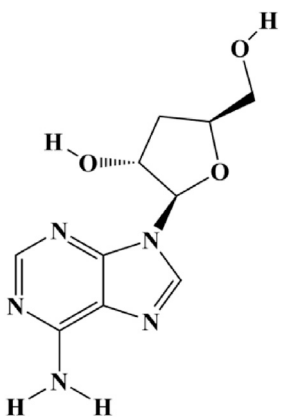
(Continued on following page)

TABLE 1 | (*Continued*) Proapoptotic effects of monomers from natural products on breast cancer cells.

Monomers	Chemical structure	Detail mechanisms		Cell model	Refs
Calycosin (10, 50, 100 μL)		p53, Cleaved caspase-3	SIRT1	MCF-7	Fang et al. (2015)
Gambogic acid lysinate (0.25, 0.50, 1.00, 2.00, 4.00, 8.00 μmol/L)		Cleaved caspase-3	SIRT1	MCF-7	Wei et al. (2015)
Icariin (10, 25, 50, 75 μM)		Caspase-3, PARP, p62	CDK2, CDK4, cyclin D1, Bcl-2, LC3-1, LC3-II, AGT5, Beclin-1	MCF-7/TAM	Cheng et al. (2019)
Ellagic acid (1–10 μM)			CDK6	MCF-7 MDA-MB-231	Yousuf et al. (2020)

(Continued on following page)

TABLE 1 | (*Continued*) Proapoptotic effects of monomers from natural products on breast cancer cells.

Monomers	Chemical structure	Detail mechanisms		Cell model	Refs
Flavonoid calycopterin (150 μM)		Bax, caspase-3, caspase-8	Bcl-2	MDA-MB-231	Moradi et al. (2020)
Quercetin (40, 80, 160 μmol/L)		GAS5, Bax, caspase-3	Notch1, Jagged1, Hes1, Bcl-2	MCF-7	Jiang et al. (2021)
Rhamnetin (15,FPHAR_fphar-2021-801662_gs_fx121 20, 25 μM)		Activated caspase-3, activated caspase-9, (miR-) 34a, p53	Notch1	MCF-7	Lan et al. (2019)
Shikonin (0.625, 1.25, 2.5 μM)			cIAP1, cIAP2, RIP1	MDA-MB-231	Wang et al. (2021)
Cordycepin (40, 80, 120 μM)		PUMA, CytoC, Fas, DR4/5, cleaved caspase-3	Bcl-2, XIAP, PDGFR-α	MDA-MB-231 MDA-MB-468 MCF-7	Liu et al. (2020)

MMP and activate the mitochondrial-mediated apoptotic pathway in MCF-7 cells, suggesting that stevioside is a potent inducer of apoptosis. Amentoflavone, isolated from an ethyl acetate extract of *Selaginella tamariscina* (P. Beauv.) Spring, has been reported to trigger apoptosis of MCF-7 cells by reducing MMP and promoting CytoC release and caspase-3 activation (Pei et al., 2012). In 2013, as shown in the study by Tian et al. (2013), calycosin decreased Bcl-2 and increased Bax expression to incur BC cell apoptosis through the mitochondrial pathway. Rajput et al. (2013) found that thymoquinone, the predominant bioactive ingredient of black seed oil (*Nigella sativa* L.), could induce apoptosis in MDA-MB-468 and T47D cells through upregulation of the levels of Bax, CytoC, cleaved caspase-3, and cleaved PARP, along with downregulation of the levels of Bcl-2, BclXL, and survivin. Embelin is a small-molecule compound extracted from the Myrsinaceae family. As shown in the study by Li et al. (2013), embelin can regulate Bax and Bcl-2, promote the release of CytoC, and activate caspase-3 and caspase-9, which indicates that the mechanism of embelin-induced MCF-7 apoptosis is related to the mitochondrial pathway. In 2013, Kim et al. reported that ginseng saponin rg3 induced MDA-MB-231 cell apoptosis through typical mitochondria-dependent caspase activation (Kim et al., 2013). In 2014, Ma et al. reported that ursolic acid reduced the proliferation and induced apoptosis of MDA-MB-231 cells by increasing the activities of caspase-3 and caspase-9 via the mitochondrial apoptosis pathway (Ma and Sun, 2014). Kim et al. proposed that dioscin induced apoptosis in MDA-MB-231, MDA-MB-453, and T47D cells by promoting the transfer of apoptosis-inducing factor (AIF) from the mitochondria to the nucleus and inhibiting antiapoptotic proteins Bcl-2, cIAP-1, and Mcl-1 (Kim et al., 2014). As shown in the study by Zhang et al. (2018a), 20(S)-protopanaxadiol (PDD) upregulated the expression of Bax/Bcl-2, cleaved PARP, and downregulated the expression of MMP of MCF-7 cells, and the caspase protein family was activated, indicating that MCF-7 cell apoptosis was induced by PDD *via* the mitochondrial pathway. Paratocarpin E, which belongs to prenylated chalcone, was extracted from *Euphorbia humifusa* Wild. In 2016, Gao et al. (2016) reported that paratocarpin E induced apoptosis in MCF-7 cells by altering the expression of Bax and Bcl-2 and inducing the release of CytoC from the mitochondria into the cytoplasm, suggesting that mitochondria-mediated pathways are activated during this process. In 2016, Lee et al. reported that amygdalin induced apoptosis of Hs578T TNBC cells, and the proapoptotic effect may be related to Bcl-2 downregulation, Bax upregulation, caspase-3 activation, and cleaved PARP increase (Lee and Moon, 2016). Cordycepin, a major compound isolated from *Cordyceps sinensis* (BerK.) Sacc., has been reported to increase the activation of proapoptotic proteins, such as caspase-8, caspase-9, caspase-3, and Bax, and inhibit Bcl-2 expression, suggesting that cordycepin could induce apoptosis in BC cells via the caspase-dependent pathway (Wang et al., 2016). Berberine is an isoquinoline alkaloid isolated from *Cotridis rhizoma*. In 2017, Zhao et al. (2017) demonstrated that berberine activated caspase-9/CytoC–mediated apoptosis to suppress TNBC cell proliferation *in vitro* and *in vivo*. *Clematis* hederagenin saponin (CHS), isolated from *Clematis chinensis* Osbeck, is a triterpenoid saponin family. Cheng et al. (2018) reported that CHS could significantly increase mitochondrial Apaf-1 and CytoC to activate caspase-3 and caspase-9 in BC cells and finally showed a proapoptotic effect. In 2019, Zhu et al. reported that kaempferol, a flavonoid, could induce apoptosis in MDA-MB-231 cells, which may be achieved by increasing the expression of cleaved caspase-9/3 and p-ATM (Zhu and Xue, 2019). Liao et al. (2019) demonstrated that diosgenin induced the loss of MMP, resulting in the release of CytoC and activation of the caspase signaling cascade in BC cells. In a 2020 study by Rosas Gonzalez et al.(2020), allicin reduced cell viability and led to apoptosis by activating caspase-3/8/9; upregulating NOXA, p21, and Bak; and downregulating BclXL expression. Ma et al. (2021) found that dehydrocostuslactone suppressed the growth and promoted apoptosis in SK-BR-3 BC cells, which may be associated with the inhibition of the antiapoptotic ability of BC cells by regulating Bax/Bcl-2 and caspase-3 expression.

Cofilin can regulate mitochondrial division by interacting with Drp1 at mitochondrial division sites, leading to mitochondrial damage and CytoC release and ultimately inducing apoptosis. 4-Methylthiobutyl isothiocyanate (erucin) is a compound isolated from cruciferous vegetables. In 2015, Li et al. (2015) showed that erucin induced mitochondrial division and apoptosis in human BC cells through mitochondrial translocation of cofilin, which was correlated with downregulated PARP and upregulated caspase-3 and caspase-9 cleavage. Li et al. (2017a) reported that polyphyllin I induced mitochondrial translocation of DRP1 by dephosphorylating the Ser637 site of DRP1, leading to mitochondrial division and CytoC release from mitochondria into the cytoplasm, ultimately leading to BC cell apoptosis. Arnidiol is a pentacyclic triterpenoid diol. In 2020, Hu et al. (2020) found that arnidiol induced apoptosis in human BC MDA-MB-231 cells *via* mitochondrial translocation of Drp1 and cofilin, which was correlated with reduced PARP expression and increased caspase-3 cleavage. Furthermore, in 2021, Shen et al. (2021) revealed that coadministration of cepharanthine and epirubicin markedly led to mitochondrial translocation of cofilin, thus inducing apoptosis in TNBC cells *via* the mitochondrial pathway.

P53 is a nuclear transcription factor that is negatively and positively regulated by MDM2 and ATM, respectively, and can regulate apoptosis-related gene expression, such as that of Bax and BclXL, to exhibit an anti-BC effect. P53 can also alter MMP and trigger CytoC release, ultimately inducing BC cell apoptosis via the mitochondrial pathway. The deficiency of p53 reduces the therapeutic effect and prognosis of BC. Therefore, accumulating evidence has shown that many natural products can increase or stabilize p53 to induce BC apoptosis. Liu et al. (2012) proposed that apigenin induced p53-dependent apoptosis in BC T47D cells. In 2014, Patel et al. revealed that L-carvone induced p53- and caspase-3–mediated apoptosis in MCF-7 and MDA-MB-231 cells (Patel and Thakkar, 2014). In 2014, Hassan et al. proposed that oleuropein-induced apoptosis via the p53 pathway in MCF-7 cells was related to the upregulation of p53 and Bax and downregulation of Bcl-2 (Hassan et al., 2014). In 2015, Zu et al. reported that emodin reduced Bcl-2 levels and increased cleaved caspase-3, PARP, p53, and Bax levels in BCAP-37 and ZR-75-30 BC cells, suggesting that it could induce apoptosis through the p53-mediated mitochondrial pathway (Zu et al., 2015). Gaillardin is a natural sesquiterpene lactone. In 2015,

Fallahian et al. found that the mechanism of apoptosis induced by gaillardin in MCF-7 and MDA-MB-468 cells involved upregulation the expression of Bax and p53, increased the production of ROS, and downregulated the expression of Bcl-2, inducing the loss of MMP (Fallahian et al., 2015). Sesamin is a major component of *Sesamum indicum* L. In 2015, Siao et al. demonstrated that sesamin could cause apoptosis in BC cells MCF-7 by improving the expression of the apoptosis markers Bax, caspase-3, and p53 (Siao et al., 2015). Zhang et al. found that osthole induced apoptosis in MCF-7 cells by the p53 pathway, which was related to high expression of Bax, p53, p21, and CytoC, as well as downregulation of Bcl-2 and MMP (Zhang and Zhu, 2016). Feng et al. (2016) showed that high concentrations of arecoline resulted in MCF-7 cell apoptosis, which may be achieved by increasing the protein expression of p53 and Bax and decreasing that of Bcl-2. Violacein is a natural purple pigment produced primarily by microorganisms. Alshatwi et al. (2016) showed that violacein induced apoptosis in MCF-7 cells through the upregulation the levels of Bax and p53 and downregulation the levels of MDM2. Li et al. (2017b) demonstrated that the mechanism of apoptosis induced by liriodenine in MCF-7 cells inhibited the expression of Bcl-2, cyclin D1, and vascular endothelial growth factor (VEGF) and upregulated the level of p53. As shown in the study by Liang et al. (2021), resveratrol can facilitate TNBC cell apoptosis *via* the p53-mediated pathway. In 2021, a study by Vazhappilly et al. indicated that catechol could inhibit proliferation and result in apoptosis in MCF-7 cells by activating p53, inhibiting of regulatory proteins such as DNMT1, P-BRCA1, Mcl-1, and PDCD6, and increasing the Bax/Bcl-2 ratio. Ultimately, caspase-mediated cell death is triggered (Vazhappilly et al., 2021). In their study, Sp et al. (2021) showed that 6-zingerol might induce apoptosis in MDA-MB-231 and MCF-7 BC cell lines by activating p53, regulating the Bax/Bcl-2 ratio, and increasing the release of CytoC.

Mitochondria are the main sites of ROS production. Accumulated ROS can directly act on the mitochondrial membrane, induce changes in MMP, release CytoC and other AIFs, and finally activate the caspase cascade, leading to apoptosis. 3β, 6β, 16β-trihydroxylup-20 (29)-ene (TTHL) is a pentacyclic triterpene isolated from the medicinal plant *Combretum leprosum* Mart. In 2014, Viau et al. demonstrated that TTHL induced MCF-7 cell apoptosis, and TTHL-induced apoptosis was accompanied by increased caspase-9 and intracellular ROS (Viau et al., 2014). Baicalein is a natural flavonoid extracted from *Scutellaria baicalensis* Georgi. A study by Liu et al. (2019) showed that baicalein damaged MMP, downregulated antiapoptotic protein Bcl-2 expression, upregulated proapoptotic protein Bax expression, and promoted the release of CytoC and activated caspase-9/3 in BC cells by increasing intracellular ROS levels. In a study conducted by Wang et al. (2020), diosmetin significantly upregulated the protein expression of p53, Bax, and caspase-3; downregulated the protein expression of Bcl-2; reduced MMP; and promoted ROS accumulation in MCF-7 cells, suggesting that diosmetin may promote apoptosis in MCF-7 cells through ROS- and p53-mediated mitochondrial apoptosis pathways.

FasL-Fas–Mediated Apoptosis

Upon FasL binding to the Fas receptor, it causes the formation of the complex of Fas, FADD, and pro–caspase-8, known as the death-inducing signaling complex. After caspase-8 is activated through self-cleavage of pro–caspase-8, it subsequently activates downstream effectors, including caspase-3 and caspase-7, resulting in cell apoptosis. Therefore, targeting to the FasL-Fas pathway is one of the strategies to induce cell apoptosis. Certain natural products have been shown to activate the FasL-Fas pathway to induce apoptosis in BC cells (**Figure 2**).

In 2012, Huang et al. (2012) reported that icariside II enhanced the expression of Fas and FADD, activated caspase-8 in MCF-7 BC cells, and played a role in promoting apoptosis. Gambogenic acid is the main active component isolated from the tree *Garcinia hanburyi* Hook. f. In 2013, Zhou et al. (2013) proposed that gambogic acid could induce BC cell apoptosis, and the mechanism was also related to increased expression of Fas, cleaved caspase-3/8/9, and Bax and decreased expression of antiapoptotic protein Bcl-2. In 2013, Wang et al. (2013a) proposed that genistein enhanced FasL, FADD, and cleaved caspase-8 protein expression in MDA-MB-231 cells, suggesting that genistein-induced apoptosis was mediated by the Fas/FasL pathway. In 2014, Li et al. (2014) demonstrated that α-mangostin significantly inhibited the expression of Fas and intracellular Fas activity to induce apoptosis in BC cells. In 2017, Liu et al. (2017a) reported that fraxetin suppressed cell proliferation and induced MCF-7 cell apoptosis by increasing the expression of Fas, FasL, and Bax and reducing Bcl-2 expression. Pulveraven A is a phenolic compound isolated from *Pulveroboletus ravenelii*. In 2021, Lee et al. proposed that apoptotic BC death was induced by the activation of promoter caspase-8 and executioner caspase-7 and upregulated the expression of FADD by pulveraven A. Furthermore, it was accompanied by an increase in the Bax/Bcl-2 ratio (Lee et al., 2021).

PI3K/AKT Pathway Mediated Apoptosis

The PI3K/AKT pathway is triggered by the binding of ligands, such as insulin, growth factors, and hormones. Upon PI3K activation, it phosphorylates AKT, and activated AKT plays an important role in regulating Bad, a proapoptotic member of the Bcl-2 family, to inhibit mitochondrial-mediated apoptosis. Alternatively, activated AKT phosphorylates other components, such as the mTOR complex and IkBα/NF-κB, which are ultimately involved in cell growth (Miricescu et al., 2020). Therefore, targeted inhibition of PI3K/AKT pathway activation can promote cell apoptosis. In recent decades, increasing evidence has indicated that nature produces can inactivate PI3K/AKT pathway to induce BC apoptosis (**Figure 3**).

In 2012, Sharma et al. (2012) reported that 18-β-glycyrrhetinic acid induced apoptosis by modulating the AKT/Foxo3a/Bim pathway in MCF-7 cells. In 2015, Hu et al. (2015) showed that isorhamnetin had a proapoptotic effect in MCF-7 and MDA-MB-468 BC cells, which was mediated by the AKT and MEK signaling pathways. In 2015, another report by Chen et al. (2015c) suggested that the phosphorylation level of AKT and the expression of its downstream target protein HOTAIR were decreased after treatment with calycosin, thus inducing

apoptosis in MCF-7 BC cells. In 2016, Peng et al. (2016) proposed that ginsenoside Rg3 promoted apoptosis in BC cells by interfering with the level of mammaglobin A in MDA-MB-231 cells, and this effect was achieved by affecting PI3K/AKT signaling pathway activity. α-Mangostin was extracted from mangosteen (*Garcinia mangostana* L.). In 2016, Kritsanawong et al. (2016) found that α-mangostin induced apoptosis in BC cells, which may be associated with PI3K/AKT signaling pathway regulation. Stachydrine hydrochloride is a well-known bioactive ingredient extracted from *Leonurus cardiac* L. Wang et al. (2017) reported that stachydrine hydrochloride inhibited cell division and growth and induced apoptosis in BC cells *via* deactivation of the AKT and ERK pathways. As a rare ginsenoside and the main ingredient extracted from fine black *Panax ginseng* C.A.Mey., ginsenoside Rg5, can induce apoptosis in a dose-dependent manner by inhibiting p-PI3K and p-AKT *in vivo* (Liu and Fan, 2018). In 2018, Liu et al. (2018b) reported that galangin inhibited MCF-7 cell proliferation and induced cell apoptosis *via* the mitochondrial and PI3K/AKT pathways. In 2018, Shen et al. (2018) showed that tetramethylpyrazine could significantly decrease the gene expression and the activity of AKT and increase the activity of caspase-3, thus inducing apoptosis in BC cells. Daucosterol linoleate, a steroid extracted from *Manihot esculenta* Crantz, has been reported to diminish the expression of the antiapoptotic proteins BclXL, Bcl-2, and XIAP; promote the levels of proapoptotic proteins Bax and Bad; and activate caspase-dependent apoptosis *in vivo*. Moreover, daucosterol linoleate invalidates the upstream of the PI3k/AKT/NF-κB pathway (Han et al., 2018). Crambescidin, separated from *Monanchora viridis*, a marine sponge, may be involved in the inactivation of phosphorylation of Akt, NF-κB, and MAPK pathways, resulting in apoptosis in TNBC cells according to the study by Shrestha et al. (2018). In 2019, Zhao et al. (2019) showed that kaempferol promoted the apoptosis of the SUM190 inflammatory BC cell line, and the proapoptotic effect might be associated with PI3K/AKT/GSK-3β pathway inhibition. Flavopereirine is a β-carboline alkaloid with antiplasmodial activity. In 2019, Yeh et al. (2019) reported that flavopereirine can induce apoptosis in MDA-MB-231cells by inhibiting the AKT/p38/ERK pathway. In 2021, Xu et al. (2021) reported that erianin can induce TNBC cell apoptosis, which may be ascribed to the inhibition of the PI3K/AKT pathway.

mTOR is one of the downstream members of the PI3K/AKT signaling pathway and is directly regulated by AKT. Activation of mTOR can phosphorylate p70S6K and 4EBP1 to promote cell survival. In 2017, Zhang et al. discovered that fangchinoline induced apoptosis in MDA-MB-231 cells. The mechanism was related to the downregulation of PI3K, AKT, mTOR, and p-PI3K, p-AKT, and p-mTOR proteins in a concentration-dependent manner (Zhang et al., 2017). In 2014, Takeshima et al. (2014) proposed that lycopene induced apoptosis in the MDA-MB-468 cell line by inhibiting the phosphorylation of AKT and its downstream molecule mTOR, enhancing PARP cleavage and upregulating Bax. In 2014, Shrivastava et al. proposed that piperlongumine, an alkaloid, reduced the expression of p-AKT, p70S6K1, 4EBP1, Bcl-2, and p53 and increased the expression of Bax and CytoC in human TNBC cells, suggesting that the proapoptotic function of piperlongumine was related to the inhibition of the PI3K/AKT/mTOR signaling axis (Shrivastava et al., 2014). Cepharanthine is a biscoclaurine alkaloid extracted from *Stephania cephalantha* Hayata. In 2017, Gao et al. (2017) reported that cepharanthine resulted in apoptosis in MCF-7 and MDA-MB-231 cells, which might be achieved by AKT/mTOR signaling pathway inhibition. In 2017, Sun et al. proposed that fisetin reduced the phosphorylation of PI3K, AKT, mTOR, and p70S6K and upregulated apoptosis factors such as Bax and caspase-3/8/9 in BC cells. These results indicated that fisetin inhibited cell growth and induced the apoptosis, which was attributed to the inhibition of the PI3K/AKT/mTOR signaling pathway (Sun et al., 2018). *Paris* saponins are saponin compounds isolated from *Paris polyphylla* Sm. A study by Xie et al. showed that the apoptotic effect of *Paris* saponins in BC cells was mediated through the Akt/mTOR signaling pathway. It was highly correlated with the downregulation of p-AKT, p-mTOR, p-P70S6K, and p-4EBP1 (Xie et al., 2017). According to another study by Yan et al., baicalein significantly reduced the expression of p-AKT, p-mTOR, NF-κB, and p-IκB in MCF-7 and MDA-MB-231 cells, demonstrating that baicalein can induce BC cell line apoptosis in animal models by inhibiting the PI3K/AKT signaling pathway (Yan et al., 2018). 20(S)-PPD belongs to one of the main active metabolites of *Panax ginseng* C.A.Mey. In 2018, Zhang et al. (2018a) reported that 20(S)-PPD could downregulate the protein expression of PI3K/AKT/mTOR in MCF-7 cells. In 2018, Sultan et al. (2018) reported that cannabidiol suppressed cell survival and prompted apoptosis in a dose-dependent manner, accompanied by downregulation of mTOR and upregulation and localization of PPARγ protein in the nuclei and cytoplasm. In 2018, another report by Hu et al. (2018) indicated that curcumin inhibited the phosphorylation of AKT and mTOR, decreased Bcl-2 and increased Bax, and cleaved caspase-3, subsequently inducing apoptosis in MCF-7 and MDA-MB-231 cells. In 2020, Wei et al. (2020) proposed that magnoflorine, a quaternary alkaloid separated from *Schisandra chinensis* (Turcz.) Baill or *Aristolochia clematitis* L., improved cell sensitivity to doxorubicin by inducing apoptosis through the Akt/mTOR and p38 signaling pathways.

Bcl-2 family proteins, which play a key role in determining cell death or survival, are downstream targets of AKT. For example, AKT directly phosphorylates Bad, which is then separated from Bcl-2. Then, Bcl-2 binds to the proapoptotic Bcl-2 family members such as Bax and Bak, thereby inhibiting apoptosis. In 2014, Kong et al. (2014) reported that cucurbitacin E can induce the MDA-MB-468 cell apoptosis by reducing the levels of cyclin D1, survivin, XIAP, Bcl-2, and Mcl-1 and inhibiting the activation of AKT. D-Rhamnose *β* hederin is an oleanane-type triterpenoid soap, which was found to induce apoptosis in BC cells by inhibiting the PI3K/AKT signaling pathway and regulating the protein expression of the Bcl-2 family (Cheng et al., 2014). Genistein, an estrogenic soy-derived compound, belongs to the isoflavone family. In 2015, Chen et al. (2015b) proposed that genistein induced apoptosis via the IGF-1R/p-Akt signaling pathway in MCF-7 cells, accompanied by a

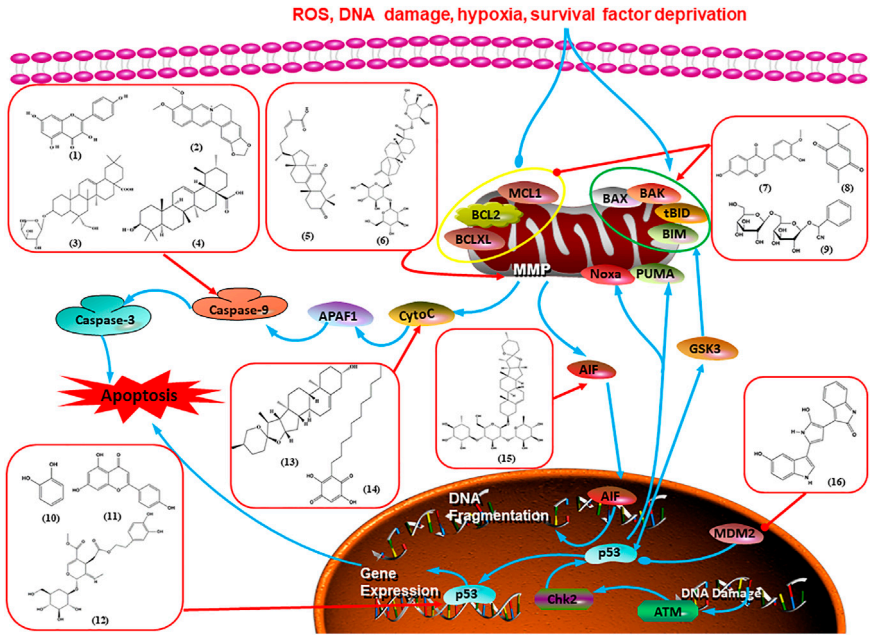


FIGURE 1 | Natural products induced apoptosis through mitochondrial pathway. (1) Kaempferol, (2) berberine, (3) *Clematis* hederagenin saponin, (4) ursolic acid, (5) ganoderic acid DM, (6) stevioside, (7) Calycosin, (8) thymoquinon, (9) amygdalin, (10) catechol, (11) apigenin, (12) oleuropein, (13) diosgenin, (14) embelin, (15) dioscin, (16) violacein.

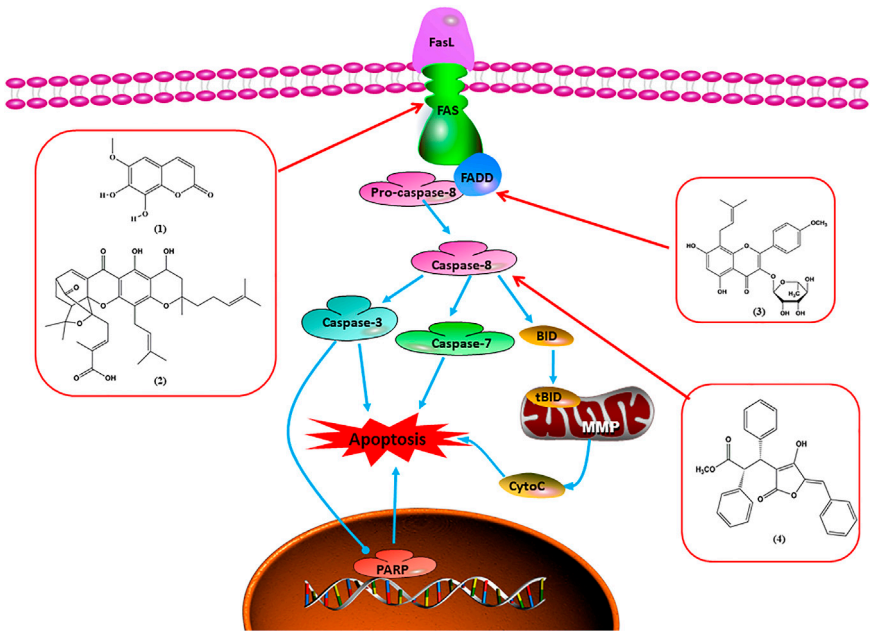


FIGURE 2 | Natural products induced apoptosis through FasL-Fas pathway. (1) Fraxetin, (2) gambogenic acid, (3) icariside II, (4) pulveraven A.

reduction in the ratio of Bcl-2/Bax. Ramentaceone, a naphthoquinone isolated from *Drosera rotundifolia* L., was reported to induce BC cell apoptosis by inhibiting the PI3K/AKT signaling pathway, which was highly correlated with upregulated Bax and Bak expression, downregulated Bcl-2 expression, and inhibition of PI3K and AKT phosphorylation (Kawiak and Lojkowska, 2016). A study by Razak et al. (2019) showed that eupatorine-induced apoptosis

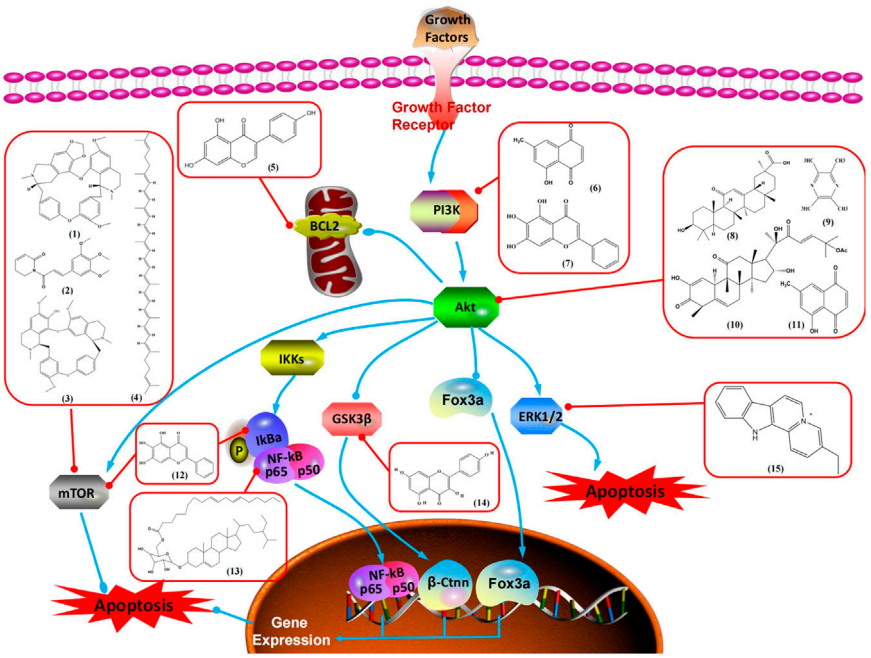


FIGURE 3 | Natural products induced apoptosis through PI3K/AKT pathway. (1) cepharanthine, (2) piperlongumine, (3) fangchinoline, (4) lycopene, (5) genistein, (6) ramentaceone, (7) baicalein, (8) 18β-glycyrrhetinic acid, (9) tetramethylpyrazine, (10) cucurbitacin e, (11) ramentaceone, (12) baicalein, (13) daucosterol linoleate, (14) kaempferol, (15) flavopereirine.

in MCF-7 and MDA-MB-231 cells was mediated by the upregulation of proapoptotic genes such as Bak1, HIF1A, Bax, and Bad, increasing CytoC release and SMAC/Diablo and blocking the p-AKT pathway. Hong et al. showed that ginsenoside Rk1 increased the levels of Bax, CytoC, and cleaved caspase-3/8/9 and reduced Bcl-2 by blocking the PI3K/AKT pathway (Hong and Fan, 2019). In 2019, Han et al. (2019) showed that parthenolide could lead to BC cell apoptosis by modulating the PI3K/AKT signaling pathway, which was highly correlated with downregulated Bcl-2 expression and upregulated cleaved caspase-3 expression. In 2020, Yu et al. proposed that avicularin induces MDA-MB-231

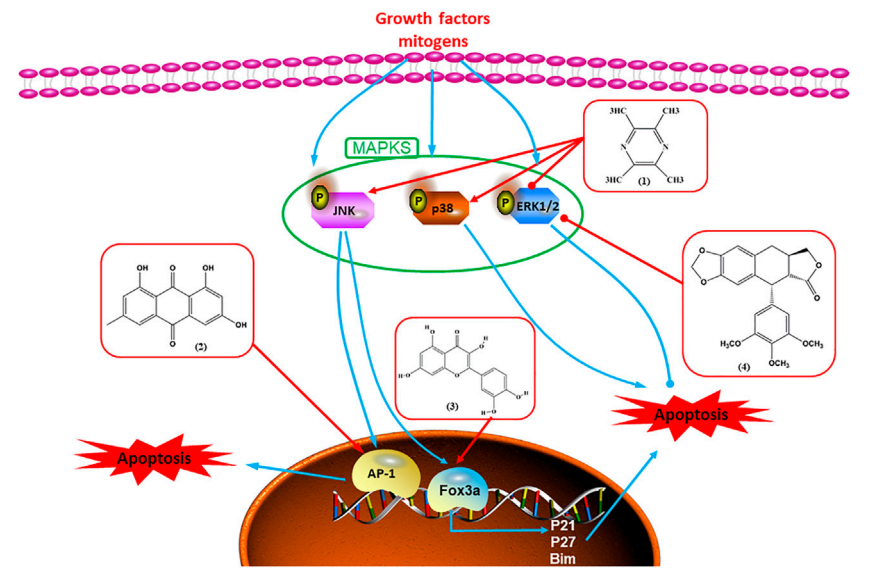


FIGURE 4 | Natural products induced apoptosis through MAPK pathway. (1) Tetramethylpyrazine, (2) emodin, (3) quercetin, (4) Deoxypodophyllotoxin.

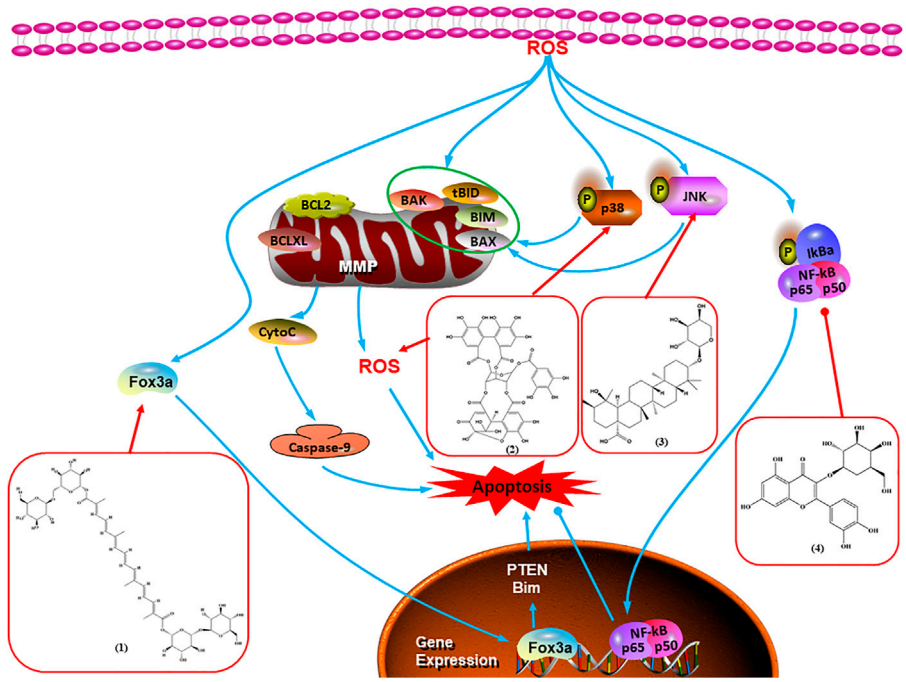


FIGURE 5 | Natural products induced apoptosis through ROS pathway. (1) Crocin, (2) geraniin, (3) ziyuglycoside II, (4) hyperoside.

cell apoptosis, which may be associated with the inhibition of the PI3K/AKT signaling pathway to decrease the gene expression of Bcl-2, BclXL, and CDK2 (Yu et al., 2020).

MAPK Pathway–Mediated Apoptosis

MAPK pathways are sequentially phosphorylated and activated by three protein kinases: MAPKKK activates MAPKK, which then activates MAPK. MAPKs are traditionally classified as ERK, JNK, and p38 kinase in mammalian cells. Through cascade reactions, MAPKs can transmit extracellular and intracellular signals to regulate cell growth, proliferation, differentiation, migration, and apoptosis.

Accumulating evidence suggests that MAPKs are important targets in natural product–induced BC cell apoptosis (**Figure 4**). In 2012, Chen and Sun found that formononetin elevated the Bax/Bcl-2 ratio in MCF-7 cells by activating the Ras-p38MAPK signaling pathway and finally induced cell apoptosis (Chen and Sun, 2012). Kim et al. reported that genipin, a constituent of *Gardenia jasminoides* J. Ellis, downregulated Bcl-2 and upregulated Bax and cleaved caspase-3 by activation of p38 and JNK signals, suggesting that genipin induced MDA-MB-231 cell apoptosis mediated by MAPK pathway activation (Kim et al., 2012). Deoxypodophyllotoxin (DTP) is a natural ingredient extracted from *Juniperus communis* L. In 2015, Benzina et al. proposed that DTP can induce BC cell apoptosis by inactivation of the ERK and NF-κB signaling pathways (Benzina et al., 2015). In 2015, Fan et al. (2015) proposed that emodin suppressed MCF-7 cell proliferation, and further studies showed that emodin promoted MCF-7 cell apoptosis by activating the JNK-AP1 signal transduction pathway. In 2015, Ranganathan et al. (2015) demonstrated that quercetin significantly inhibited cyclin D1, p21, Twist, and p-p38 expression in MCF-7 cells, demonstrating that quercetin increased BC cell apoptosis through the p38-Twist pathway mediated by cell cycle arrest. In 2017, Nguyen et al. also found that quercetin increased the signaling activities of p53, p21, and GADD45, and Foxo3a protein and mRNA expression and induced nuclear translocation of Foxo3a. The JNK inhibitor abolished quercetin-stimulated Foxo3a activity and apoptosis, suggesting that quercetin induced apoptosis by regulating Foxo3a signaling in TNBC cells (Nguyen et al., 2017). Isocryptotanshinone is a natural bioactive component isolated from *Salvia miltiorrhiza* Bunge. In 2015, Zhang et al. reported that isocryptotanshinone promoted apoptosis in human MCF-7 BC cells by activating MAPK signaling pathways, including p38, ERK, and JNK (Zhang et al., 2015a). In 2016, as shown in the study by Lai et al., tetramethylpyrazine (TMP) improved the expression of p-p38 and p-JNK proteins. However, it reduced p-ERK expression in MCF-7 cells. TMP can induce apoptosis in MCF-7 cells, and this may be related to MAPK signaling pathway activation (Lai et al., 2016). α-Mangostin was extracted from *Garcinia mangostana* L., and in 2016, Kritsanawong et al. (2016) found that α-mangostin could promote BC cell apoptosis by inhibiting PI3K/AKT and increasing p38 and JNK activation. In 2017, Lee et al. found that gallic acid decreased the expression of cyclin D1/CDK4 and cyclin E/CDK2, increased the expression of p21 and p27, and induced the activation of caspase-3/9 in MDA-MB-231 cells. In addition, p38 was found to be involved in gallic acid–induced apoptosis. The results indicated that gallic acid–induced apoptosis was related to the p38/p21/p27 axis (Lee et al., 2017). In 2019,

TABLE 2 | Extracts from natural products induced apoptosis in breast cancer.

Extracts	Compositions	Detail mechanisms		Cell model	Refs
		Upregulation	Downregulation		
Phaleria macrocarpa compound extract (DLBS1425) (5–50 μg/mL)	Phalerin	PTEN, p21, Bax, Bad, PUMA, activated caspase-9, cleaved PARP	p-Akt, BclxL	MDA-MB-231	Tandrasasmita et al. (2010)
Suillus collinitus methanolic extracts (25.2 ± 0.2 μg/mL)	Protocatechuic acid, p-hydroxybenzoic acid, cinnamic acid	p53, p21, cleaved PARP	Bcl-2, XIAP	MCF-7	Vaz et al. (2012)
Scrophularia oxysepala extracts (0–300 μg/mL)	Verbascosaponin, crokoelziside, isolated from these fractions	Caspase-3 mRNA, caspase-9 mRNA		MCF-7	Hosseini et al. (2015)
Ethyl acetate extracts of seeds of *Momordica cochinchinen* (ESMC2) (30, 60, 120 μg/mL)	Hexanoic acid, 2-heptenal, 2,4-nonadiena, 1,1′-carbonyldiimidazole, 1-oxaspiro [4,4]nonan-4-one, 5,5-dimethyl-cyclohex-3-en-1-ol, (E,E)-7,11,15, trimethyl-3-methylene-1,6,10,14-tetraene, l-(+), ascorbic acid 2,6-dihexadecanoate, 6-octadecenoic acid, octadecanoic acid, palmitin, octadecanoic acid 2,3-dihydroxypropyl ester	p53, Bax, Bak, Bad, cyclin B1, cyclin E, CDC2	NF-κB, Bcl-2, Mcl-1, p-ERK, p-p38, p-JNK, p-Akt	MDA-MB-231	Zheng et al. (2015)
Momordica cochinchinensis Aril extracts (50, 200, 400 μg/mL)	Lycopene, β-carotene	Bax, activated caspase-6, activated caspase-8, activated caspase-9		MCF-7	Petchsak and Sripanidkulchai, (2015)
Extracts from chickpea *Cicer arietinum* L. sprouts (20, 40, 60 μg/mL)	Ononin isoflavone, biochanin A-7-O-β-D-glucoside isoflavone, formononetin isoflavone, biochanin A isoflavone	Bax, caspase-7, caspase-9, p53, p21	Bcl-2 MCF-7	SKBr3	Chen et al. (2015a)
Dillenia suffruticosa dichloromethane root extracts (12.5, 25, 50 μg/mL)	Katonic acid, betulinic acid, koetjapic acid	JNK1	ERK1, Bcl-2	MDA-MB-231	Foo et al. (2016)
Green tea polyphenols (200, 300, 400 μg/mL)	Catechins	ROS, cleaved caspase-3, cleaved caspase-9		MCF-7	Liu et al. (2017b)
Fruit peel polyphenolic extracts flavine (F7) (150 μg/mL)	Myricetin, quercetin, kaempferol, rutin, isorhamnetine, catechin, epicatechin, malvidin-3-glucoside, caffeic acid, chrysin, galangin, apigenin, fisetin, luteolin, morin, anthocyanidins, stilbene resveratrol	Bax, cleaved PARP, activated caspase-7	Bcl-2	MCF-7	Kello et al. (2017)
Flavonoid compounds from *Tephroseris kirilowii* (IH: 10–40 μM, GN:20–80μM, Aca:50–150 μM)	IH: isorhamnetin, GN: genkwanin, and Aca: acacetin	p53, cleaved caspase-3, LC3-II, ATG5	p-Cdc2, cyclin B1, Bcl-2, BclxL, PARP1, p62, PI3Kγ-p110, p-PI3K, p-Akt, p-mTOR, p-p70S6K, p-ULK	MDA-MB-231	Zhang et al. (2018b)
Antrodia cinnamomea extracts (100, 200 μg/mL)	Antcin K, antcin C, antcin B, methyl, antcinate B, eburi-coic acid, dehydroeburicoic acid	miR-21-5p, miR-26-5p, miR-30-5p	Skp2	MCF-7	Lin et al. (2018)
Hexane fraction from *Inula helenium* (HFIH) (8 μg/mL)	Alantolactone, isoalantolactone, igalan, dugesialactone, alloantolactone	p-JNK, activated caspase-3, cleaved PARP	Cyclin D1, CytoC, Bcl-2, p-ERK	MDA-MB-231	Chun et al. (2018)
Ricinus communis L. fruit extract (0.05, 0.1, 0.5, 1 μg/mL)	Ricinine, p-coumaric acid, epigallocatechin, ricinoleic acid	Bax, CytoC, caspase-7, cleaved PARP	Bcl-2	MDA-MB-231 MCF-7	Majumder et al. (2019)
Fomes fomentarius ethanol Extract Exerts (100 μg/mL)	Betulin	Cleaved caspase-9, cleaved caspase-3, cleaved PARP	MMP9, p-Akt, cyclin A/E, Bcl-2	MDA-MB-231	Lee et al. (2019)
Extracts of *Rhus verniciflua* Stokes (200, 300, 400 μg/mL)	Gallic acid	p53, p21, cleaved caspase-3, caspase-9, PARP, Bax	Bcl-2	MCF-7	Kim et al. (2019)
Vitex rotundifolia Fractions (10 μg/mL)	Vitexicarpin	Caspase-8, caspase-9, caspases-3/7, Bax	Bcl-2	T-47D	Chaudhry et al. (2019)
Extracts from Ajwa dates pulp (15, 20 mg/mL)	Maltose, catechin, myricetin, quercetin, β-sitosterol, digalacturonic acid, chlorogenic acid, β-carotene	p53, Bax, cleaved caspase-3	Bcl-2, p-Akt, p-mTOR	MDA-MB-231	Khan et al. (2021)

Huang et al. (2019) reported that sophoraflavanone G suppressed the MAPK-related pathway to increase cleaved caspase-3/8/9 and Bax expression, decrease Bcl-2 and BclXL expression, and prompt the release of CytoC from mitochondria to the cytoplasm in MDA-MB-231 cells. Cardamonin is natural chalcone separated from large black *Elettaria cardamomum* (L.) Maton. As shown in the study by Kong et al. (2019), cardamonin increased the expression of Foxo3a and its target genes p21, p27, and Bim, and further studies suggested that cardamonin induced BC cell apoptosis by activating the JNK-Foxo3a pathway. In 2021, another report by Kim et al. (2021) indicated that silymarin induced BC cell apoptosis by regulating the MAPK signaling pathway, which increased the levels of Bax, cleaved PARP, cleaved caspase-9, and p-JNK and reduced the levels of Bcl-2, p-p38, and p-ERK.

NF-κB–Mediated Apoptosis

NF-κB can be activated physiologically and pathologically, such as by growth factors and oxidant-free radicals, particularly by pro-inflammatory cytokines interleukin 1 (IL-1) and tumor necrosis factor (TNF). Binding to the receptor TNFR1, TNF can recruit TNF-associated receptor death domain that binds to the TNF receptor–associated factor 2 and the kinase receptor–interacting protein 1, and then recruit IκB kinase (IKK), leading to the phosphorylation and subsequent degradation of IκBα, which activates NF-κB translocation into the nucleus, thereby regulating related gene expression to regulate cell apoptosis.

In 2013, Wang et al. (2013b) demonstrated that oridonin induced MDA-MB-231 BC cell apoptosis, which was associated with a reduction in the Bcl-2/Bax ratio, caspase-8, NF-κBp65, IKKα, IKKβ, and p-mTOR, and upregulated cleaved PARP, PPAR, and Fas expression levels. In 2018, Wu et al. (2018b) proposed that delphintin significantly downregulated the expression of p-NF-κBp65, p-IκBα, p-IKKα/β, and p-PKCα in MDA-MB-453 and BT-474 BC cells. The results showed that delphintin induced apoptosis by blocking the NF-κB signaling pathway. In 2018, Ren et al. demonstrated that chrysophanol upregulated caspase-3 and PARP cleavage and downregulated the apoptosis regulators Bcl-2, p-NF-κBp65, and p-IκB, which indicated that the proapoptotic function of chrysophanol was achieved by regulating the NF-κB/Bcl-2 signaling cascade (Ren et al., 2018). In 2021, Chen et al. found that capsaicin significantly reduced the expression of FBI-1, Ki-67, Bcl-2, and survivin; increased Bax protein expression; and activated caspase-3 in BC cells. Furthermore, NF-κB, the target gene of FBI-1, was also inactivated by capsaicin treatment. These results indicate that the proapoptotic effect of capsaicin is related to the FBI-1–mediated NF-κB pathway (Chen et al., 2021).

ROS-Mediated Apoptosis

Intracellular ROS can induce apoptosis through several signal pathways. First, ROS can cause oxidative damage to all mitochondrial components. Damaged mitochondrial DNA disrupts mitochondrial oxidative phosphorylation, thus increasing MMP and releasing CytoC to contribute to cell death. In addition, ROS can activate JNK and p38 and trigger mitochondria-mediated apoptosis. Moreover, Foxo3a is a nuclear transcription factor, and ROS can promote the translocation of Foxo3a, which regulates apoptosis-related gene expression. However, ROS can increase NF-κB activation and inhibit apoptosis. Hence, ROS-mediated apoptosis may increase with the use of natural components (**Figure 5**).

In 2014, a study showed that ziyuglycoside II treatment induced BC cell apoptosis by activating the ROS/JNK pathway (Zhu et al., 2014). In 2015, Xie et al. proposed that berberine also increased the production of ROS in MCF-7 and MDA-MB-231 cells, which promoted proapoptotic JNK signaling. Phosphorylated JNK triggers MMP depolarization and Bcl-2 downregulation, concomitant with the Bax upregulation, and release of CytoC and AIF from mitochondria, eventually leading to apoptosis (Xie et al., 2015). Geraniin, a typical ellagitannin extracted from *Phyllanthus urinaria* L., was found to contain a series of bioactive. In 2016, Zhai et al. (2016) reported that geraniin could generate intracellular ROS and activate p38, and inhibition of ROS can restrain the phosphorylation of p38 and reverse geraniin-induced apoptosis, which suggests that geraniin results in MCF-7 cell apoptosis via the ROS–p38 pathway. In 2019, Qiu et al. (2019) proposed that hyperoside induced apoptosis in MCF-7 and 4T1 cells through the ROS-mediated NF-κB signaling pathway, which was attributed to reduced levels of Bcl-2 and XIAP, and increased the expression of Bax and cleaved caspase-3. In 2020, Nasimian et al. found that crocin induced apoptosis in MCF-7 and MDA-MB-231 cells. The ROS-activated Foxo3a cascade played a crucial role in this process, and Foxo3a-mediated upregulation of PTEN further inhibited the AKT pathway (Nasimian et al., 2020).

Mitochondria are the primary site of ROS production and are also one of the most sensitive targets of ROS action. Intracellular ROS accumulation can activate the mitochondria-mediated apoptosis pathway. Fucoidan is an active ingredient in seaweeds. In 2013, according to the study by Banafa et al. (2013), fucoidan induced MCF-7 cell apoptosis by upregulating caspase-8 and Bax, downregulating Bcl-2, and increasing the release of CytoC and the production of ROS. Looi et al. also reported in 2013 that vernodalin can induce MCF-7 cell apoptosis by increasing the production of ROS in human BC cells, thereby inducing the reduction of MMP and the release of CytoC, thus triggering the caspase cascade and PARP cleavage (Looi et al., 2013). Tetrandrine is an alkaloid that is known for its anticancer activity. In 2020, N et al. (2019) demonstrated that tetrandrine separated from *Cyclea peltata* (Lam.) Hook. f. and Thomson induced cytotoxicity and apoptosis by increasing ROS and caspase-8/9/3 in MDA-MB-231 cells. Pereyra-Vergara et al. (2020) reported that apoptosis induced by (−)-epicatechin in human BC cells was mediated by ROS to increase the proapoptotic proteins Bad and Bax. In 2020, Jia et al. (2020) proposed that formononetin could induce mitochondrial damage and decrease MMP in BC cells by inhibiting antioxidant enzyme activity and increasing ROS levels, ultimately activating caspase-3-mediated apoptosis.

JAK-STAT3–Mediated Apoptosis

JAK/STAT signaling can transfer an extracellular signal into a transcriptional response that contributes to cancer progression

and metastatic development. IL-6, epidermal growth factor (EGF), interferon-α, and other extracellular signals can stimulate the activation of JAK2 and STAT3. Phosphorylated STAT3 then enters the nucleus; dimerized STAT3 binding to specific regulatory sequences could activate or inhibit transcription of target genes, such as BclXL, p21, and Myc, to regulate cell apoptosis.

For natural products, inhibiting the JAK/STAT3 pathway may be a potential strategy to induce BC cell apoptosis. In 2014, Xu et al. reported that apigenin can induce MDA-MB-453 cell apoptosis by upregulating cleaved caspase-8/3 and PARP, blocking the activation (phosphorylation) of JAK2 and STAT3, and decreasing the nuclear tillering of STAT3 (Seo et al., 2014). In 2015, Zhang et al. demonstrated that berberine upregulated Bax, cleaved PARP, and caspase-3 and downregulated p-JAK2, p-STAT3, and Bcl-2 levels. Berberine may induce MCF-7 cell apoptosis by regulating JAK2/STAT3 signaling in a concentration-dependent manner (Zhang et al., 2015b). 7β-(3-ethyl-*cis*-crotonoyloxy)-1α-(2-methylbutyryloxy)-3,14-dehydro-Z-notonipetranone, an ingredient isolated from *Tussilago farfara* L., was found to induce BC cell apoptosis by inhibiting JAK-STAT3 signaling and the expression of STAT3 target genes (Jang et al., 2019). In a study conducted by Ma et al. (2020), it was found that the mRNA expression of JAK2 and STAT3 was significantly decreased after curcumol treatment, suggesting that curcumol-induced apoptosis in BC cells might be realized through inhibition of the JAK2/STAT3 signaling pathway. In a study conducted in 2021, Feng et al. proposed that saikosaponin D can suppress cell growth and induce MCF-7 cell apoptosis, which may also be related to the JAK2/STAT3 pathway (Feng et al., 2021).

Endoplasmic Reticulum Stress–Mediated Apoptosis

Hypoxia, starvation, Ca^{2+} imbalance, and other factors can induce ERS. During the ERS phase, PERK dissociates from GRP78/BiP and is activated by phosphorylation. PERK activation also leads to increased translation of transcription factors, such as ATF4, which further promotes the synthesis of the proapoptotic factor CHOP. CHOP downregulates the antiapoptotic protein Bcl-2 and promotes apoptosis. Moreover, CHOP promotes GADD45 expression, which triggers apoptosis by completely blocking protein synthesis. In 2014, Hou et al. (2014) proposed that fucoxanthin upregulated intracellular free calcium content and the activation of calpain in MCF-7 cells through ERS pathway, and treatment with fucoxanthin also promoted the activation of caspase-4/7/9 and release of CytoC, thereby inducing BC cell apoptosis. In 2020, Li et al. (2020) proposed that oleandrin can induce apoptosis of MCF-7 cells by downregulating Bcl-2 and upregulating Bax, Bim, and ERS-related proteins such as EIF2α, ATF4, and CHOP, suggesting that ERS plays an important role in this process. In 2018, Wu et al. (2018b) proposed that salviaflaside can induce MDA-MB-231 cell apoptosis by activating the ERS response to upregulate GRP78/CHOP and interfere with the Bcl-2/Bax balance.

Other Pathway–Mediated Apoptosis

Multiple other signaling pathways can regulate BC cell apoptosis, such as the Wnt/β-catenin, Notch, and sirtuin-1 pathways. In 2012, curcumin, as the main ingredient of the spice turmeric isolated from the rhizomes of the plant *Curcuma longa* L., was reported to induce TNBC cell apoptosis by decreasing EGF receptor expression (Sun et al., 2012). In 2017, Zhao et al. (2017) also showed that curcumin suppressed cell growth and led to apoptosis in BT549 cells, and the mechanism was related to the inhibition of the Wnt/β-catenin signaling pathway. In 2014, Shao et al. (2014) reported that triptolide, a diterpene triepoxide compound, induced apoptosis *via* the Wnt/β-catenin signaling pathway. Ursolic acid is a natural pentacyclic triterpenoid compound. In 2012, Wang et al. (2012) demonstrated that ursolic acid inhibited FoxM1 expression and induced MCF-7 cell apoptosis, which was highly correlated with inactivation of cyclin D1/CDK4. In 2015, Fang et al. (2015) showed that calycosin promoted apoptosis of tumor cells MCF-7, possibly in part by reducing SIRT1 levels, thereby increasing p53 and cleaved caspase-3 expression to promote apoptosis. In 2015, Wei et al. (2015) reported that gambogic acid lysinate induced MCF-7 cell apoptosis in a dose-dependent manner by inhibiting SIRT1 protein expression levels and upregulating cleaved caspase-3 protein expression levels. In 2019, Cheng et al. (2019) indicated that icariin can significantly downregulate CDK2, CDK4, cyclin D1, and Bcl-2 and upregulate cleaved caspase-3 and PARP, thereby inducing apoptosis of the tamoxifen-resistant MCF-7/TAM BC cell line. In 2020, Yousuf et al. (2020) proposed that ellagic acid controlled cell proliferation and induced BC cell apoptosis by inhibiting CDK6. Moradi et al. (2020) also proposed in 2020 that flavonoid calycopterin can induce MDA-MB-231 cell apoptosis by increasing the caspase-3/8 expression. In addition, treatment with flavonoid calycopterin can also increase the ratio of Bax/Bcl-2.

Notch signaling can act as a therapeutic target to induce or resist cell apoptosis. When the Notch receptor is activated by DLL-1/2/3 and Jagged-1/2, the Notch intracellular domain (NIC) is released from the cell membrane. Then, the NIC translocates into the nucleus where it regulates the expression of target genes to induce a series of biochemical reactions. In 2021, Jiang et al. reported that quercetin could increase the expression of GAS5, Bax, and caspase-3 and decrease the expressions of Notch1, Jagged1, Hes1, and Bcl-2 in MCF-7 cells, suggesting that quercetin can induce BC cell apoptosis by the GAS5/Notch1 signaling pathway (Jiang et al., 2021). In 2019, a study by Lan et al. (2019) indicated that treatment with rhamnetin increased caspase-3/9 activity, upregulated p53 protein and miR-34a expression, and downregulated Notch-1 expression, suggesting that rhamnetin induced apoptosis of human BC cells through the miR-34a/Notch-1 signaling pathway. In 2021, Wang et al. (2021) reported that shikonin, a natural naphthoquinone isolated from *Arnebiae radix*, promoted the autoubiquitination and degradation of cIAP1 and cIAP2 to induce MDA-MB-231 cell apoptosis.

Abnormal expression of hedgehog ligands, overactivation of Smo proteins, and inappropriate disinhibition of Smo can lead to

abnormal activation of the hedgehog pathway. Once the hedgehog pathway is activated, Gli transcription factors are transported into the nucleus in a full-length form and function as transcriptional activators to promote the abnormal expression of downstream VEGF, C-MYC, and other target genes, resulting in excessive cell proliferation and ultimately the occurrence of tumors. In 2020, Liu et al. (2020) showed that cordycepin induced apoptosis by inhibiting the hedgehog pathway, and this effect was associated with elevated levels of PUMA, CytoC, Fas, DR4/5, and cleaved caspase-3 and decreased levels of Bcl-2, XIAP, and PDGFR-α.

EXTRACTS FROM NATURAL PRODUCT–INDUCED APOPTOSIS IN BC

In this study, we summarized the effects and mechanisms of extracts from natural products on the apoptosis of BC (**Table 2**). In 2010, Tandrasasmita et al. (2010) proposed that *Phaleria macrocarpa* (Scheff.) Boerl extract markedly decreased the PI3K/AKT signaling pathway and resulted in MDA-MB-231 cell apoptosis. In 2012, Vaz et al. (2012) reported that the methanol extract of *Suillus collinitus* (Fr.) Kuntze remarkably upregulated the levels of p53, p21 and cleaved PARP and downregulated the levels of Bcl-2 and XIAP in MCF-7 cell lines, suggesting that *S. collinitus*–induced apoptosis was realized by mediating p53. In a 2015 study conducted by Hosseini et al., the dichloromethane extract of *Scrophularia ningpoensis* Hemsl. *oxysepala* upregulated the mRNA expression of caspase-3 and caspase-9 in MCF-7 cells. Further, the expression study of caspase-9 mRNA confirmed that the fractions triggered apoptosis via the intrinsic mitochondrial pathway (Hosseini et al., 2015). In 2015, Zheng et al. (2015) proposed that ethyl acetate was isolated from the seeds of *Momordica cochinchinensis* (Lour.) Spreng. can induce cell apoptosis, which was correlated with high expression of p53, Bax, Bak, and Bad, along with downregulation of NF-κB. In a 2015 study conducted by Petchsak et al., *M. cochinchinensis* (Lour.) Spreng. aril extract induced BC cell apoptosis by increasing the expression of the proapoptotic gene Bax and enhancing caspase-6/8/9 activity (Petchsak and Sripanidkulchai, 2015). In 2015, Chen et al. (2015a) reported that extraction of isoflavones from chickpea *Cicer arietinum* L. sprouts induced apoptosis in SKBR3 and MCF-7 cells by increasing the expression of Bax, caspase-7/9, p53, and p21, and decreasing Bcl-2 expression. In 2016, Foo et al. reported that *Dillenia suffruticosa* (Griff.) Martelli root extract induced MDA-MB-231 cell apoptosis via activation of proapoptotic JNK1 and downregulation of antiapoptotic ERK1 and Bcl-2, increasing the Bax/Bcl-2 ratio and initiating the mitochondrial apoptosis pathway (Foo et al., 2016). In 2017, Liu et al. (2017b) reported that *Camellia sinensis* (L.) Kuntze polyphenols induced chromatin condensation, MMP reduction, ROS increase, and caspase-3/9 activation in BC cells, which indicated that *C. sinensis* (L.) Kuntze polyphenols induced mitochondrial pathway–mediated apoptosis. In 2017, Kello et al. (2017) found that peel polyphenol extracts induced apoptosis by increasing intracellular oxidative stress, activating p38 MAPK, and inhibiting ERK1/2 and AKT signaling pathways. In 2018, Zhang et al. (2018b) isolated three flavonoids from *Tephroseris kirilowii* (Turcz. ex DC.) Holub (isorhamnetin, genkwanin, and acacetin), which suppressed cell growth and induced apoptosis in MDA-MB-231 cells by downregulating the PI3K/AKT/mTOR/p70S6K/ULK signaling pathway. In 2018, Lin et al. (2018) proposed that the ethanol extract of *Antrodia cinnamomea* induced MCF-7 cell apoptosis by elevating the expression of miR-21-5p, miR-26-5p, and miR-30-5p and decreasing SKP2 mRNA expression. In 2018, Chun et al. (2018) found that the sesquiterpene lactones-enriched fraction of *Inula helenium* L. induced apoptosis *via* suppression of signal transducers and activators of the STAT3 signaling pathway in MDA-MB-231 cells. In 2019, Majumder et al. (2019) proposed that *Ricinus communis* L. fruit extract can contribute to apoptosis in MCF-7 and MDA-MB-231 cells by promoting the attenuation of antiapoptotic Bcl-2 and the accumulation of proapoptotic Bax and caspase-7 and PARP cleavage. In 2019, Lee et al. (2019) reported that *Fomes fomentarius* (L.Fr.) Kick. ethanol extracts induced apoptosis by inhibiting the PI3K/AKT pathway and activating the caspase pathway. In 2019, Kim et al. (2019) reported that the proapoptotic effect of *Toxicodendron vernicifluum* (Stokes) F.A. Barkley stokes extract in MCF-7 cells was attributed to p53, p21, and the intrinsic mitochondrial cascade. In a 2019 study, Chaudhry et al. (2019) reported that *Vitex agnus-castus* L. hexane and dichloromethane extracts induced T47D cell apoptosis by activating external and internal pathways, and this effect was concomitant with activation of caspase-8/9 and -3/7, upregulation of Bax and downregulation of Bcl-2. Khan et al. showed in a study in 2021 that *Phoenix dactylifera* L. ethanol extracts induced apoptosis in TNBC MDA-MB-231 cells. This effect was related to the upregulation of p53, Bax, and cleaved caspase-3 expression and downregulation of Bcl-2 and AKT/mTOR pathways (Khan et al., 2021).

CONCLUSION

Through a systematic summary, we found that numerous monomers/extracts have an anti-BC capacity, and the mechanism is closely associated with apoptosis. The mechanism of agent-induced apoptosis predominantly involves the mitochondrial pathway, PIK3K/AKT, NF-κB, MAPK, JAK-STAT3, and other pathways. Therefore, identifying potential anti-BC drugs from natural products is one of the most effective strategies. However, there are still some problems, and further studies should be performed in the future.

First, >50% of the studies mentioned in this review were performed *in vitro*. As we know, drugs undergo four processes *in vivo*, including absorption, distribution, metabolism, and excretion, all of which affect the therapeutic effect of drugs. Many drugs are effective *in vitro*. However, they have little or no effect *in vivo*. Therefore, animal experiments should be conducted to further confirm the proapoptotic effects of natural agents. Moreover, there is a lack of toxicity studies and

clinical data on the majority of the reported natural products. Therefore, the therapeutic effects, side effects, and toxicity of these drugs should be the focus on the future studies. More time is required before these natural products are used clinically. Furthermore, the evidence regarding the mechanism of certain natural products mentioned in our article to promote BC cell apoptosis is unclear and inadequate. Further, we can use diversified detection methods, such as CRISPR-Cas9, single-cell sequencing, and proteomic technology, to clarify the mechanism in detail, which will be conducive to the development and use of these natural products. Finally, most natural products still have flaws, such as low bioavailability, poor solubility, and poor selectivity, which interfere with their clinical application (Zhang et al., 2021a). Therefore, special processes can be considered to overcome these deficiencies. We can modify the structure of the compound. For example, polar groups can be joined to increase the solubility. Nanoparticle drug delivery systems for natural products can increase bioavailability and reduce toxicity to other organs.

In conclusion, we reviewed current studies on natural products that induced BC cell apoptosis and summarized the pro-apoptotic mechanisms. We hope that our review can provide direction in the search for candidate drugs derived from natural products to treat BC by inhibiting cell apoptosis.

AUTHOR CONTRIBUTIONS

LY collected documents and wrote the manuscript. YC drew the mechanism figures. LZ and SL collected the documents. PL polished the language and revised the manuscript. XL conceived ideas, designed the structure of the manuscript and revised the manuscript. All authors read and approved the submitted version.

FUNDING

This project is supported by Natural Science Foundation of Chongqing (No. csct2020jcyj-msxmX0223), Technology Project of Chongqing Health and Family Planning Commission (No. 2019MSXM010), and Basic Research and Frontier Exploration Project of Yuzhong District of Chongqing (No. 20190102).

REFERENCES

Alshatwi, A. A., Subash-Babu, P., and Antonisamy, P. (2016). Violacein Induces Apoptosis in Human Breast Cancer Cells through up Regulation of BAX, P53 and Down Regulation of MDM2. *Exp. Toxicol. Pathol.* 68 (1), 89–97. doi:10.1016/j.etp.2015.10.002

Ateba, S. B., Mvondo, M. A., Ngeu, S. T., Tchoumtchoua, J., Awounfack, C. F., Njamen, D., et al. (2018). Natural Terpenoids against Female Breast Cancer: A 5-year Recent Research. *Curr. Med. Chem.* 25 (27), 3162–3213. doi:10.2174/0929867325666180214110932

Banafa, A. M., Roshan, S., Liu, Y. Y., Chen, H. J., Chen, M. J., Yang, G. X., et al. (2013). Fucoidan Induces G1 Phase Arrest and Apoptosis through Caspases-dependent Pathway and ROS Induction in Human Breast Cancer MCF-7 Cells. *J. Huazhong Univ. Sci. Technolog Med. Sci.* 33 (5), 717–724. doi:10.1007/s11596-013-1186-8

Benzina, S., Harquail, J., Jean, S., Beauregard, A. P., Colquhoun, C. D., Carroll, M., et al. (2015). Deoxypodophyllotoxin Isolated from Juniperus Communis Induces Apoptosis in Breast Cancer Cells. *Anticancer Agents Med. Chem.* 15 (1), 79–88. doi:10.2174/1871520614666140608150448

Binkley, J. M., Harris, S. R., Levangie, P. K., Pearl, M., Guglielmino, J., Kraus, V., et al. (2012). Patient Perspectives on Breast Cancer Treatment Side Effects and the Prospective Surveillance Model for Physical Rehabilitation for Women with Breast Cancer. *Cancer* 118 (8 Suppl. l), 2207–2216. doi:10.1002/cncr.27469

Chaudhry, G. E., Jan, R., Naveed Zafar, M., Mohammad, H., and Muhammad, T. S. T. (2019). Vitex Rotundifolia Fractions Induced Apoptosis in Human Breast Cancer T-47D Cell Line via Activation of Extrinsic and Intrinsic Pathway. *Asian Pac. J. Cancer Prev.* 20 (12), 3555–3562. doi:10.31557/APJCP.2019.20.12.3555

Chen, H., Ma, H. R., Gao, Y. H., Zhang, X., Habasi, M., Hu, R., et al. (2015a). Isoflavones Extracted from Chickpea Cicer Arietinum L. Sprouts Induce Mitochondria-dependent Apoptosis in Human Breast Cancer Cells. *Phytother Res.* 29 (2), 210–219. doi:10.1002/ptr.5241

Chen, J., Duan, Y., Zhang, X., Ye, Y., Ge, B., and Chen, J. (2015b). Genistein Induces Apoptosis by the Inactivation of the IGF-1R/p-Akt Signaling Pathway in MCF-7 Human Breast Cancer Cells. *Food Funct.* 6 (3), 995–1000. doi:10.1039/c4fo01141d

Chen, J., Lin, C., Yong, W., Ye, Y., and Huang, Z. (2015c). Calycosin and Genistein Induce Apoptosis by Inactivation of HOTAIR/p-Akt Signaling Pathway in Human Breast Cancer MCF-7 Cells. *Cell Physiol Biochem* 35 (2), 722–728. doi:10.1159/000369732

Chen, J., and Sun, L. (2012). Formononetin-induced Apoptosis by Activation of Ras/p38 Mitogen-Activated Protein Kinase in Estrogen Receptor-Positive Human Breast Cancer Cells. *Horm. Metab. Res.* 44 (13), 943–948. doi:10.1055/s-0032-1321818

Chen, M., Xiao, C., Jiang, W., Yang, W., Qin, Q., Tan, Q., et al. (2021). Capsaicin Inhibits Proliferation and Induces Apoptosis in Breast Cancer by Down-Regulating FBI-1-Mediated NF-Kb Pathway. *Drug Des. Devel Ther.* 15, 125–140. doi:10.2147/DDDT.S269901

Cheng, L., Shi, L., Wu, J., Zhou, X., Li, X., Sun, X., et al. (2018). A Hederagenin Saponin Isolated from Clematis Ganpiniana Induces Apoptosis in Breast Cancer Cells via the Mitochondrial Pathway. *Oncol. Lett.* 15 (2), 1737–1743. doi:10.3892/ol.2017.7494

Cheng, L., Xia, T. S., Wang, Y. F., Zhou, W., Liang, X. Q., Xue, J. Q., et al. (2014). The apoptotic effect of D Rhamnose β-hederin, a novel oleanane-type triterpenoid saponin on breast cancer cells. *PLoS One* 9 (6), e90848. doi:10.1371/journal.pone.0090848

Cheng, X., Tan, S., Duan, F., Yuan, Q., Li, Q., and Deng, G. (2019). Icariin Induces Apoptosis by Suppressing Autophagy in Tamoxifen-Resistant Breast Cancer Cell Line MCF-7/TAM. *Breast Cancer* 26 (6), 766–775. doi:10.1007/s12282-019-00980-5

Chun, J., Song, K., and Kim, Y. S. (2018). Sesquiterpene Lactones-Enriched Fraction of Inula Helenium L. Induces Apoptosis through Inhibition of Signal Transducers and Activators of Transcription 3 Signaling Pathway in MDA-MB-231 Breast Cancer Cells. *Phytother Res.* 32 (12), 2501–2509. doi:10.1002/ptr.6189

Fallahian, F., Aghaei, M., Abdolmohammadi, M. H., and Hamzeloo-Moghadam, M. (2015). Molecular Mechanism of Apoptosis Induction by Gaillardin, a Sesquiterpene Lactone, in Breast Cancer Cell Lines : Gaillardin-Induced Apoptosis in Breast Cancer Cell Lines. *Cell Biol Toxicol* 31 (6), 295–305. doi:10.1007/s10565-016-9312-6

Fan, X. W., Zang, Y., Xi, L., and Li, S. D. (2015). The Emodin Inducted Human Breast Cancer MCF-7cell Apoptosis and Activated JNK Signal Transduction Pathways. *J. Chin. J. Surg. Oncol.* 7 (06), 346–350.

Fang, K., Liu, J. C., Qu, M. L., and Chang, N. D. (2015). Calycosin Promotes Apoptosis of Breast Cancer Cells MCF-7 through Inhibiting SIRT1. *J. Prog. Mod. Biomed.* 15 (23), 4431–4434.

Feng, J. X., Chen, J. H., and Lin, Q. H. (2021). Saikosaponin D Inhibits Proliferation and Promotes Apoptosis in Breast Cancer Cells through Down-Regulating JAK2/STAT3 Pathway. *J. J. Third Mil. Med. Univ.* 43 (09), 852–857.

Feng, S. D., Wu, D., Yang, S. S., He, J. Q., Zhang, K. F., and Ling, H. Y. (2016). Effect of Arecoline on Proliferation and Apoptosis of MCF-7 Human Breast Cancer Cells. *Zhongguo Ying Yong Sheng Li Xue Za Zhi* 32 (4), 370–372. doi:10.13459/j.cnki.cjap.2016.04.021

Foo, J. B., Saiful Yazan, L., Tor, Y. S., Wibowo, A., Ismail, N., Armania, N., et al. (2016). *Dillenia suffruticosa* Dichloromethane Root Extract Induced Apoptosis towards MDA-MB-231 Triple-Negative Breast Cancer Cells. *J. Ethnopharmacol* 187, 195–204. doi:10.1016/j.jep.2016.04.048

Gao, S., Li, X., Ding, X., Qi, W., and Yang, Q. (2017). Cepharanthine Induces Autophagy, Apoptosis and Cell Cycle Arrest in Breast Cancer Cells. *Cel Physiol Biochem* 41 (4), 1633–1648. doi:10.1159/000471234

Gao, S., Sun, D., Wang, G., Zhang, J., Jiang, Y., Li, G., et al. (2016). Growth Inhibitory Effect of Paratocarpin E, a Prenylated Chalcone Isolated from Euphorbia Humifusa Wild., by Induction of Autophagy and Apoptosis in Human Breast Cancer Cells. *Bioorg. Chem.* 69, 121–128. doi:10.1016/j.bioorg.2016.10.005

Georgalas, I., Paraskevopoulos, T., Koutsandrea, C., Kardara, E., Malamos, P., Ladas, D., et al. (2015). Ophthalmic Metastasis of Breast Cancer and Ocular Side Effects from Breast Cancer Treatment and Management: Mini Review. *Biomed. Res. Int.* 2015, 574086. doi:10.1155/2015/574086

Han, B., Jiang, P., Liu, W., Xu, H., Li, Y., Li, Z., et al. (2018). Role of Daucosterol Linoleate on Breast Cancer: Studies on Apoptosis and Metastasis. *J. Agric. Food Chem.* 66 (24), 6031–6041. doi:10.1021/acs.jafc.8b01387

Han, Y. Y., Yang, J. F., Sun, Y., and Li, L. H. (2019). Parthenolide on Proliferation and Apoptosis of Breast Cancer. *J. Northwest. J. Defense Med.* 40 (04), 205–211.

Hassan, Z. K., Elamin, M. H., Omer, S. A., Daghestani, M. H., Al-Olayan, E. S., Elobeid, M. A., et al. (2014). Oleuropein Induces Apoptosis via the P53 Pathway in Breast Cancer Cells. *Asian Pac. J. Cancer Prev.* 14 (11), 6739–6742. doi:10.7314/apjcp.2013.14.11.6739

Hematpoor, A., Paydar, M., Liew, S. Y., Sivasothy, Y., Mohebali, N., Looi, C. Y., et al. (2018). Phenylpropanoids Isolated from Piper Sarmentosum Roxb. Induce Apoptosis in Breast Cancer Cells through Reactive Oxygen Species and Mitochondrial-dependent Pathways. *Chem. Biol. Interact* 279, 210–218. doi:10.1016/j.cbi.2017.11.014

Hong, Y., and Fan, D. (2019). Ginsenoside Rk1 Induces Cell Cycle Arrest and Apoptosis in MDA-MB-231 Triple Negative Breast Cancer Cells. *Toxicology* 418, 22–31. doi:10.1016/j.tox.2019.02.010

Hosseini, B. A., Pasdaran, A., Kazemi, T., Shanehbandi, D., Karami, H., Orangi, M., et al. (2015). Dichloromethane Fractions of Scrophularia Oxysepala Extract Induce Apoptosis in MCF-7 Human Breast Cancer Cells. *Bosn J. Basic Med. Sci.* 15 (1), 26–32. doi:10.17305/bjbms.2015.1.226

Hou, L. L., Xu, Q. J., Hu, G. Q., and Xie, S. Q. (2014). Fucoxanthin Induces Human MCF-7 Breast Cancer Cells Apoptosis via Endoplasmic Reticulum Pathway. *J. Chin. Pharm. J.* 49 (02), 117–120.

Hu, J., Zhang, H., Li, J., Jiang, X., Zhang, Y., Wu, Q., et al. (2020). ROCK1 Activation-Mediated Mitochondrial Translocation of Drp1 and Cofilin Are Required for Arnidiol-Induced Mitochondrial Fission and Apoptosis. *J. Exp. Clin. Cancer Res.* 39 (1), 37. doi:10.1186/s13046-020-01545-7

Hu, S., Huang, L., Meng, L., Sun, H., Zhang, W., and Xu, Y. (2015). Isorhamnetin Inhibits Cell Proliferation and Induces Apoptosis in Breast Cancer via Akt and Mitogen-activated P-rotein K-inase K-inase S-ignaling P-athways. *Mol. Med. Rep.* 12 (5), 6745–6751. doi:10.3892/mmr.2015.4269

Hu, S., Xu, Y., Meng, L., Huang, L., and Sun, H. (2018). Curcumin Inhibits Proliferation and Promotes Apoptosis of Breast Cancer Cells. *Exp. Ther. Med.* 16 (2), 1266–1272. doi:10.3892/etm.2018.6345

Huang, C., Chen, X., Guo, B., Huang, W., Shen, T., Sun, X., et al. (2012). Induction of Apoptosis by Icariside II through Extrinsic and Intrinsic Signaling Pathways in Human Breast Cancer MCF7 Cells. *Biosci. Biotechnol. Biochem.* 76 (7), 1322–1328. doi:10.1271/bbb.120077

Huang, W. C., Gu, P. Y., Fang, L. W., Huang, Y. L., Lin, C. F., Liou, C. J., et al. (2019). Sophoraflavanone G from Sophora Flavescens Induces Apoptosis in Triple-Negative Breast Cancer Cells. *Phytomedicine* 61, 152852. doi:10.1016/j.phymed.2019.152852

Jang, H., Ko, H., Song, K., and Kim, Y. S. (2019). A Sesquiterpenoid from Farfarae Flos Induces Apoptosis of MDA-MB-231 Human Breast Cancer Cells through Inhibition of JAK-STAT3 Signaling. *Biomolecules* 9 (7). doi:10.3390/biom9070278

Jia, S. H., Liu, L. N., and Yan, T. H. (2020). Mechanism of Apoptosis and Oxidative Stress in MCF–7 Cells Induced by Formononetin. *J. West. China J. Pharm. Sci.* 35 (04), 385–391.

Jiang, D. C., Jin, L., Chen, H. X., and Zhang, L. (2021). Quercetin Promotes Apoptosis of Breast Cancer Cells by Targeting GAS5/Notch1 Signaling Pathway. *J. Chin. Pharmacol. Bull.* 37 (05), 637–644.

Kawiak, A., and Lojkowska, E. (2016). Ramentaceone, a Naphthoquinone Derived from Drosera sp., Induces Apoptosis by Suppressing PI3K/Akt Signaling in Breast Cancer Cells. *PLoS One* 11 (2), e0147718. doi:10.1371/journal.pone.0147718

Kello, M., Kulikova, L., Vaskova, J., Nagyova, A., and Mojzis, J. (2017). Fruit Peel Polyphenolic Extract-Induced Apoptosis in Human Breast Cancer Cells Is Associated with ROS Production and Modulation of p38MAPK/Erk1/2 and the Akt Signaling Pathway. *Nutr. Cancer* 69 (6), 920–931. doi:10.1080/01635581.2017.1339819

Khan, M. A., Siddiqui, S., Ahmad, I., Singh, R., Mishra, D. P., Srivastava, A. N., et al. (2021). Phytochemicals from Ajwa Dates Pulp Extract Induce Apoptosis in Human Triple-Negative Breast Cancer by Inhibiting AKT/mTOR Pathway and Modulating Bcl-2 Family Proteins. *Sci. Rep.* 11 (1), 10322. doi:10.1038/s41598-021-89420-z

Khojasteh Poor, F., Keivan, M., Ramazii, M., Ghaedrahmati, F., Anbiyaiee, A., Panahandeh, S., et al. (2021). Mini Review: The FDA-Approved Prescription Drugs that Target the MAPK Signaling Pathway in Women with Breast Cancer. *Breast Dis.* 40 (2), 51–62. doi:10.3233/bd-201063

Kim, B. M., Kim, D. H., Park, J. H., Na, H. K., and Surh, Y. J. (2013). Ginsenoside Rg3 Induces Apoptosis of Human Breast Cancer (MDA-MB-231) Cells.. *J. Cancer Prev.* 18 (2), 177–185. doi:10.15430/jcp.2013.18.2.177

Kim, E. A., Jang, J. H., Lee, Y. H., Sung, E. G., Song, I. H., Kim, J. Y., et al. (2014). Dioscin Induces Caspase-independent Apoptosis through Activation of Apoptosis-Inducing Factor in Breast Cancer Cells. *Apoptosis* 19 (7), 1165–1175. doi:10.1007/s10495-014-0994-z

Kim, E. S., Jeong, C. S., and Moon, A. (2012). Genipin, a Constituent of Gardenia Jasminoides Ellis, Induces Apoptosis and Inhibits Invasion in MDA-MB-231 Breast Cancer Cells. *Oncol. Rep.* 27 (2), 567–572. doi:10.3892/or.2011.1508

Kim, M. S., Lee, C. W., Kim, J. H., Lee, J. C., and An, W. G. (2019). Extract of Rhus Verniciflua Stokes Induces P53-Mediated Apoptosis in MCF-7 Breast Cancer Cells. *Evid. Based Complement. Alternat Med.* 2019, 9407340. doi:10.1155/2019/9407340

Kim, S. H., Choo, G. S., Yoo, E. S., Woo, J. S., Lee, J. H., Han, S. H., et al. (2021). Silymarin Inhibits Proliferation of Human Breast Cancer Cells via Regulation of the MAPK Signaling Pathway and Induction of Apoptosis. *Oncol. Lett.* 21 (6), 492. doi:10.3892/ol.2021.12753

Kong, W., Li, C., Qi, Q., Shen, J., and Chang, K. (2019). Cardamonin Induces G2/M Arrest and Apoptosis via Activation of the JNK-FOXO3a Pathway in Breast Cancer Cells. *Cell Biol Int* 44, 177–188. doi:10.1002/cbin.11217

Kong, Y., Chen, J., Zhou, Z., Xia, H., Qiu, M. H., and Chen, C. (2014). Cucurbitacin E Induces Cell Cycle G2/M Phase Arrest and Apoptosis in Triple Negative Breast Cancer. *PLoS One* 9 (7), e103760. doi:10.1371/journal.pone.0103760

Kritsanawong, S., Innajak, S., Imoto, M., and Watanapokasin, R. (2016). Antiproliferative and Apoptosis Induction of α-mangostin in T47D Breast Cancer Cells. *Int. J. Oncol.* 48 (5), 2155–2165. doi:10.3892/ijo.2016.3399

Kushwaha, P. P., Singh, A. K., Prajapati, K. S., Shuaib, M., Fayez, S., Bringmann, G., et al. (2020). Induction of Apoptosis in Breast Cancer Cells by Naphthylisoquinoline Alkaloids. *Toxicol. Appl. Pharmacol.* 409, 115297. doi:10.1016/j.taap.2020.115297

Lai, Y. B., Wang, Y. Q., and Yao, Q. H. (2016). Effect of Tetramethylpyrazine on Breast Cancer MCF-7 Cell Apoptosis and The Underlying Mechanism. *Zhejiang J. Integr. Traditional Chinese Western Med.* 26 (02), 105–107.

Lan, L., Wang, Y., Pan, Z., Wang, B., Yue, Z., Jiang, Z., et al. (2019). Rhamnetin Induces Apoptosis in Human Breast Cancer Cells via the miR-34a/Notch-1 Signaling Pathway. *Oncol. Lett.* 17 (1), 676–682. doi:10.3892/ol.2018.9575

Lee, D., Yu, J. S., Ryoo, R., Kim, J.-C., Jang, T. S., Kang, K. S., et al. (2021). Pulveraven A from the Fruiting Bodies of Pulveroboletus Ravenelii Induces Apoptosis in Breast Cancer Cell via Extrinsic Apoptotic Signaling Pathway. *J. Antibiot.* 74, 752–757. doi:10.1038/s41429-021-00435-0

Lee, H. L., Lin, C. S., Kao, S. H., and Chou, M. C. (2017). Gallic Acid Induces G1 Phase Arrest and Apoptosis of Triple-Negative Breast Cancer Cell MDA-MB-231 via P38 Mitogen-Activated Protein Kinase/p21/p27 axis. *Anticancer Drugs* 28 (10), 1150–1156. doi:10.1097/CAD.0000000000000565

Lee, H. M., and Moon, A. (2016). Amygdalin Regulates Apoptosis and Adhesion in Hs578T Triple-Negative Breast Cancer Cells. *Biomol. Ther. (Seoul)* 24 (1), 62–66. doi:10.4062/biomolther.2015.172

Lee, S. O., Lee, M. H., Lee, K. R., Lee, E. O., and Lee, H. J. (2019). Fomes Fomentarius Ethanol Extract Exerts Inhibition of Cell Growth and Motility Induction of Apoptosis via Targeting AKT in Human Breast Cancer MDA-MB-231 Cells. *Int. J. Mol. Sci.* 20 (5). doi:10.3390/ijms20051147

Li, G., Zhou, J., Budhraja, A., Hu, X., Chen, Y., Cheng, Q., et al. (2015). Mitochondrial Translocation and Interaction of Cofilin and Drp1 Are Required for Erucin-Induced Mitochondrial Fission and Apoptosis. *Oncotarget* 6 (3), 1834–1849. doi:10.18632/oncotarget.2795

Li, G. B., Fu, R. Q., Shen, H. M., Zhou, J., Hu, X. Y., Liu, Y. X., et al. (2017a). Polyphyllin I Induces Mitophagic and Apoptotic Cell Death in Human Breast Cancer Cells by Increasing Mitochondrial PINK1 Levels. *Oncotarget* 8 (6), 10359–10374. doi:10.18632/oncotarget.14413

Li, H., Prever, L., Hirsch, E., and Gulluni, F. (2021). Targeting PI3K/AKT/mTOR Signaling Pathway in Breast Cancer. *Cancers* 13 (14), 3517. doi:10.3390/cancers13143517

Li, P., Tian, W., and Ma, X. (2014). Alpha-mangostin Inhibits Intracellular Fatty Acid Synthase and Induces Apoptosis in Breast Cancer Cells. *Mol. Cancer* 13, 138. doi:10.1186/1476-4598-13-138

Li, X. X., Wang, D. Q., Sui, C. G., Meng, F. D., Sun, S. L., Zheng, J., et al. (2020). Oleandrin Induces Apoptosis via Activating Endoplasmic Reticulum Stress in Breast Cancer Cells. *Biomed. Pharmacother.* 124, 109852. doi:10.1016/j.biopha.2020.109852

Li, Y., Li, D., Yuan, S., Wang, Z., Tang, F., Nie, R., et al. (2013). Embelin-induced MCF-7 Breast Cancer Cell Apoptosis and Blockade of MCF-7 Cells in the G2/M Phase via the Mitochondrial Pathway. *Oncol. Lett.* 5 (3), 1005–1009. doi:10.3892/ol.2012.1084

Li, Z. H., Gao, J., Hu, P. H., and Xiong, J. P. (2017b). Anticancer Effects of Liriodenine on the Cell Growth and Apoptosis of Human Breast Cancer MCF-7 Cells through the Upregulation of P53 Expression. *Oncol. Lett.* 14 (2), 1979–1984. doi:10.3892/ol.2017.6418

Liang, Z. J., Wan, Y., Zhu, D. D., Wang, M. X., Jiang, H. M., Huang, D. L., et al. (2021). Resveratrol Mediates the Apoptosis of Triple Negative Breast Cancer Cells by Reducing POLD1 Expression. *Front. Oncol.* 11, 569295. doi:10.3389/fonc.2021.569295

Liao, W. L., Lin, J. Y., Shieh, J. C., Yeh, H. F., Hsieh, Y. H., Cheng, Y. C., et al. (2019). Induction of G2/M Phase Arrest by Diosgenin via Activation of Chk1 Kinase and Cdc25C Regulatory Pathways to Promote Apoptosis in Human Breast Cancer Cells. *Int. J. Mol. Sci.* 21 (1). doi:10.3390/ijms21010172

Lin, Y. S., Lin, Y. Y., Yang, Y. H., Lin, C. L., Kuan, F. C., Lu, C. N., et al. (2018). Antrodia Cinnamomea Extract Inhibits the Proliferation of Tamoxifen-Resistant Breast Cancer Cells through Apoptosis and skp2/microRNAs Pathway. *BMC Complement. Altern. Med.* 18 (1), 152. doi:10.1186/s12906-018-2204-y

Liu, B. W., Zhang, B., Zhang, Y., and Feng, W. H. (2012). Apigenin Induces P53-dependent Apoptosis and G/M Arrest in Breast Cancer T47D Cells. *J. Chin. J. Clin. Oncol.* 39 (06), 315–317.

Liu, C., Qi, M., Li, L., Yuan, Y., Wu, X., and Fu, J. (2020). Natural Cordycepin Induces Apoptosis and Suppresses Metastasis in Breast Cancer Cells by Inhibiting the Hedgehog Pathway. *Food Funct.* 11 (3), 2107–2116. doi:10.1039/c9fo02879j

Liu, C., Zhang, K., Shen, H., Yao, X., Sun, Q., and Chen, G. (2018a). Necroptosis: A Novel Manner of Cell Death, Associated with Stroke (Review). *Int. J. Mol. Med.* 41 (2), 624–630. doi:10.3892/ijmm.2017.3279

Liu, D., You, P., Luo, Y., Yang, M., and Liu, Y. (2018b). Galangin Induces Apoptosis in MCF-7 Human Breast Cancer Cells through Mitochondrial Pathway and Phosphatidylinositol 3-Kinase/Akt Inhibition. *Pharmacology* 102 (1-2), 58–66. doi:10.1159/000489564

Liu, G., Liu, Z., Yan, Y., and Wang, H. (2017a). Effect of Fraxetin on Proliferation and Apoptosis in Breast Cancer Cells. *Oncol. Lett.* 14 (6), 7374–7378. doi:10.3892/ol.2017.7143

Liu, S. M., Ou, S. Y., and Huang, H. H. (2017b). Green tea Polyphenols Induce Cell Death in Breast Cancer MCF-7 Cells through Induction of Cell Cycle Arrest and Mitochondrial-Mediated Apoptosis. *J. Zhejiang Univ. Sci. B* 18 (2), 89–98. doi:10.1631/jzus.B1600022

Liu, Y., and Fan, D. (2018). Ginsenoside Rg5 Induces Apoptosis and Autophagy via the Inhibition of the PI3K/Akt Pathway against Breast Cancer in a Mouse Model. *Food Funct.* 9 (11), 5513–5527. doi:10.1039/c8fo01122b

Liu, Z. H., Yang, C. X., Zhang, L., Yang, C. Y., and Xu, X. Q. (2019). Baicalein, as a Prooxidant, Triggers Mitochondrial Apoptosis in MCF-7 Human Breast Cancer Cells through Mobilization of Intracellular Copper and Reactive Oxygen Species Generation. *Onco Targets Ther.* 12, 10749–10761. doi:10.2147/OTT.S222819

Looi, C. Y., Arya, A., Cheah, F. K., Muharram, B., Leong, K. H., Mohamad, K., et al. (2013). Induction of Apoptosis in Human Breast Cancer Cells via Caspase Pathway by Vernodalin Isolated from Centratherum Anthelminticum (L.) Seeds. *PLoS One* 8 (2), e56643. doi:10.1371/journal.pone.0056643

Ma, C. L., Zhang, B. L., and Zhang, C. H. (2020). Effects of Curcuma on Proliferation and Apoptosis of Breast Cancer Cells and JAK2/STAT3 Signaling Pathway. *J. J. Chin. Oncol.* 26 (07), 616–620.

Ma, Q., Chen, J., Xiong, S., and Li, G. L. (2021). Effects of Dehydrocostuslactone on the Apoptosis of Human Breast Cancer SK- BR- 3 Cells and its Mechanism. *J. Traditional Chin. Drug Res. Clin. Pharmacol.* 32 (02), 200–207.

Ma, Y. P., and Sun, S. R. (2014). Effects of Ursolic Acid on Cell Apoptosis in MDA-MB-231 Cells and its Mechanisms. *J. J. Liaoning Univ. Traditional Chin. Med.* 16 (08), 59–62.

Majumder, M., Debnath, S., Gajbhiye, R. L., Saikia, R., Gogoi, B., Samanta, S. K., et al. (2019). Ricinus communis L. Fruit Extract Inhibits Migration/invasion, Induces Apoptosis in Breast Cancer Cells and Arrests Tumor Progression *In Vivo*. *Sci. Rep.* 9 (1), 14493. doi:10.1038/s41598-019-50769-x

Miricescu, D., Totan, A., Stanescu-Spinu, I. I., Badoiu, S. C., Stefani, C., and Greabu, M. (2020). PI3K/AKT/mTOR Signaling Pathway in Breast Cancer: From Molecular Landscape to Clinical Aspects. *Int. J. Mol. Sci.* 22 (1). doi:10.3390/ijms22010173

Mohammad, R. M., Muqbil, I., Lowe, L., Yedjou, C., Hsu, H. Y., Lin, L. T., et al. (2015). Broad Targeting of Resistance to Apoptosis in Cancer. *Semin. Cancer Biol.* 35 Suppl (Suppl. l), S78–s103. doi:10.1016/j.semcancer.2015.03.001

Moradi, M., Gholipour, H., Sepehri, H., Attari, F., Delphi, L., Arefian, E., et al. (2020). Flavonoid Calycopterin Triggers Apoptosis in Triple-Negative and ER-Positive Human Breast Cancer Cells through Activating Different Patterns of Gene Expression. *Naunyn Schmiedebergs Arch. Pharmacol.* 393 (11), 2145–2156. doi:10.1007/s00210-020-01917-y

N, B., Chandrashekar, K. R., Prabhu, A., and Rekha, P. D. (2019). Tetrandrine Isolated from Cyclea Peltata Induces Cytotoxicity and Apoptosis through ROS and Caspase Pathways in Breast and Pancreatic Cancer Cells. In Vitro *Cel Dev Biol Anim* 55 (5), 331–340. doi:10.1007/s11626-019-00332-9

Nasimian, A., Farzaneh, P., Tamanoi, F., and Bathaie, S. Z. (2020). Cytosolic and Mitochondrial ROS Production Resulted in Apoptosis Induction in Breast Cancer Cells Treated with Crocin: The Role of FOXO3a, PTEN and AKT Signaling. *Biochem. Pharmacol.* 177, 113999. doi:10.1016/j.bcp.2020.113999

Nguyen, L. T., Lee, Y. H., Sharma, A. R., Park, J. B., Jagga, S., Sharma, G., et al. (2017). Quercetin Induces Apoptosis and Cell Cycle Arrest in Triple-Negative Breast Cancer Cells through Modulation of Foxo3a Activity. *Korean J. Physiol. Pharmacol.* 21 (2), 205–213. doi:10.4196/kjpp.2017.21.2.205

Nøhr-Nielsen, A., Bagger, S. O., Brünner, N., Stenvang, J., and Lund, T. M. (2020). Pharmacodynamic Modelling Reveals Synergistic Interaction between Docetaxel and SCO-101 in a Docetaxel-Resistant Triple Negative Breast Cancer Cell Line. *Eur. J. Pharm. Sci.* 148, 105315. doi:10.1016/j.ejps.2020.105315

Pal, S., and Rakshit, T. (2021). Folate-Functionalized DNA Origami for Targeted Delivery of Doxorubicin to Triple-Negative Breast Cancer. *Front. Chem.* 9, 721105. doi:10.3389/fchem.2021.721105

Parton, M., Dowsett, M., and Smith, I. (2001). Studies of Apoptosis in Breast Cancer. *Bmj* 322 (7301), 1528–1532. doi:10.1136/bmj.322.7301.1528

Patel, P. B., and Thakkar, V. R. (2014). L-carvone Induces P53, Caspase 3 Mediated Apoptosis and Inhibits the Migration of Breast Cancer Cell Lines. *Nutr. Cancer* 66 (3), 453–462. doi:10.1080/01635581.2014.884230

Paul, S., Sengupta, S., Bandyopadhyay, T. K., and Bhattacharyya, A. (2012). Stevioside Induced ROS-Mediated Apoptosis through Mitochondrial Pathway in Human Breast Cancer Cell Line MCF-7. *Nutr. Cancer* 64 (7), 1087–1094. doi:10.1080/01635581.2012.712735

Pei, J. S., Liu, C. C., Hsu, Y. N., Lin, L. L., Wang, S. C., Chung, J. G., et al. (2012). Amentoflavone Induces Cell-Cycle Arrest and Apoptosis in MCF-7 Human Breast Cancer Cells via Mitochondria-dependent Pathway. *In Vivo* 26 (6), 963–970.

Peng, M., Zhai, H., Feng, Y. H., and Xin, L. W. (2016). Studies on Mechanisms of Rg3 Inducing Apoptosis through PI3K/Akt Mediating MGBA in Breast Cancer Cells. *J. J. Liaoning Med. Univ.* 37 (03), 114–115.

Pereyra-Vergara, F., Olivares-Corichi, I. M., Perez-Ruiz, A. G., Luna-Arias, J. P., and García-Sánchez, J. R. (2020). Apoptosis Induced by (−)-Epicatechin in Human Breast Cancer Cells Is Mediated by Reactive Oxygen Species. *Molecules* 25 (5). doi:10.3390/molecules25051020

Petchsak, P., and Sripanidkulchai, B. (2015). Momordica Cochinchinensis Aril Extract Induced Apoptosis in Human MCF-7 Breast Cancer Cells. *Asian Pac. J. Cancer Prev.* 16 (13), 5507–5513. doi:10.7314/apjcp.2015.16.13.5507

Qian, X. L., Pan, Y. H., Huang, Q. Y., Shi, Y. B., Huang, Q. Y., Hu, Z. Z., et al. (2019). Caveolin-1: a Multifaceted Driver of Breast Cancer Progression and its Application in Clinical Treatment. *Onco Targets Ther.* 12, 1539–1552. doi:10.2147/ott.S191317

Qiu, J., Zhang, T., Zhu, X., Yang, C., Wang, Y., Zhou, N., et al. (2019). Hyperoside Induces Breast Cancer Cells Apoptosis via ROS-Mediated NF-Kb Signaling Pathway. *Int. J. Mol. Sci.* 21 (1). doi:10.3390/ijms21010131

Rajabi, S., Maresca, M., Yumashev, A. V., Choopani, R., and Hajimehdipoor, H. (2021). The Most Competent Plant-Derived Natural Products for Targeting Apoptosis in Cancer Therapy. *Biomolecules* 11 (4). doi:10.3390/biom11040534

Rajput, S., Kumar, B. N., Dey, K. K., Pal, I., Parekh, A., and Mandal, M. (2013). Molecular Targeting of Akt by Thymoquinone Promotes G(1) Arrest through Translation Inhibition of Cyclin D1 and Induces Apoptosis in Breast Cancer Cells. *Life Sci.* 93 (21), 783–790. doi:10.1016/j.lfs.2013.09.009

Ranganathan, S., Halagowder, D., and Sivasithambaram, N. D. (2015). Quercetin Suppresses Twist to Induce Apoptosis in MCF-7 Breast Cancer Cells. *PLoS One* 10 (10), e0141370. doi:10.1371/journal.pone.0141370

Razak, N. A., Abu, N., Ho, W. Y., Zamberi, N. R., Tan, S. W., Alitheen, N. B., et al. (2019). Cytotoxicity of Eupatorin in MCF-7 and MDA-MB-231 Human Breast Cancer Cells via Cell Cycle Arrest, Anti-angiogenesis and Induction of Apoptosis. *Sci. Rep.* 9 (1), 1514. doi:10.1038/s41598-018-37796-w

Ren, L., Li, Z., Dai, C., Zhao, D., Wang, Y., Ma, C., et al. (2018). Chrysophanol Inhibits Proliferation and Induces Apoptosis through NF-κB/cyclin D1 and NF-κB/Bcl-2 Signaling cascade in Breast Cancer Cell Lines. *Mol. Med. Rep.* 17 (3), 4376–4382. doi:10.3892/mmr.2018.8443

Roos, W. P., and Kaina, B. (2013). DNA Damage-Induced Cell Death: from Specific DNA Lesions to the DNA Damage Response and Apoptosis. *Cancer Lett.* 332 (2), 237–248. doi:10.1016/j.canlet.2012.01.007

Rosas-González, V. C., Téllez-Bañuelos, M. C., Hernández-Flores, G., Bravo-Cuellar, A., Aguilar-Lemarroy, A., Jave-Suárez, L. F., et al. (2020). Differential Effects of Alliin and Allicin on Apoptosis and Senescence in Luminal A and Triple-Negative Breast Cancer: Caspase, ΔΨm, and Pro-apoptotic Gene Involvement. *Fundam. Clin. Pharmacol.* 34 (6), 671–686. doi:10.1111/fcp.12559

Seo, H. S., Ku, J. M., Choi, H. S., Woo, J. K., Jang, B. H., Shin, Y. C., et al. (2014). Induction of Caspase-dependent Apoptosis by Apigenin by Inhibiting STAT3 Signaling in HER2-Overexpressing MDA-MB-453 Breast Cancer Cells. *Anticancer Res.* 34 (6), 2869–2882.

Shao, H., Ma, J., Guo, T., and Hu, R. (2014). Triptolide Induces Apoptosis of Breast Cancer Cells via a Mechanism Associated with the Wnt/β-Catenin Signaling Pathway. *Exp. Ther. Med.* 8 (2), 505–508. doi:10.3892/etm.2014.1729

Sharma, G., Kar, S., Palit, S., and Das, P. K. (2012). 18β-glycyrrhetinic Acid Induces Apoptosis through Modulation of Akt/FOXO3a/Bim Pathway in Human Breast Cancer MCF-7 Cells. *J. Cel Physiol* 227 (5), 1923–1931. doi:10.1002/jcp.22920

Shen, J., Zeng, L., Pan, L., Yuan, S., Wu, M., and Kong, X. (2018). Tetramethylpyrazine Regulates Breast Cancer Cell Viability, Migration, Invasion and Apoptosis by Affecting the Activity of Akt and Caspase-3. *Oncol. Lett.* 15 (4), 4557–4563. doi:10.3892/ol.2018.7851

Shen, L.-w., Jiang, X.-x., Li, Z.-q., Li, J., Wang, M., Jia, G.-f., et al. (2021). Cepharanthine Sensitizes Human Triple Negative Breast Cancer Cells to Chemotherapeutic Agent Epirubicin via Inducing Cofilin Oxidation-Mediated Mitochondrial Fission and Apoptosis. *Acta Pharmacol. Sin.* doi:10.1038/s41401-021-00715-3

Shimanuki, Y., Shimomura, A., Yoshimura, K., Terakado, H., and Shimizu, C. (2021). Are Platinum Drugs Ineffective for Triple-Negative Breast Cancer with Residual Invasive Disease after Neoadjuvant Chemotherapy? *Jco* 39, 3521–3522. doi:10.1200/jco.21.01757

Shrestha, S., Sorolla, A., Fromont, J., Blancafort, P., and Flematti, G. R. (2018). Crambescidin 800, Isolated from the Marine Sponge Monanchora Viridis, Induces Cell Cycle Arrest and Apoptosis in Triple-Negative Breast Cancer Cells. *Mar. Drugs* 16 (2). doi:10.3390/md16020053

Shrivastava, S., Kulkarni, P., Thummuri, D., Jeengar, M. K., Naidu, V. G., Alvala, M., et al. (2014). Piperlongumine, an Alkaloid Causes Inhibition of PI3 K/Akt/mTOR Signaling axis to Induce Caspase-dependent Apoptosis in Human Triple-Negative Breast Cancer Cells. *Apoptosis* 19 (7), 1148–1164. doi:10.1007/s10495-014-0991-2

Siao, A. C., Hou, C. W., Kao, Y. H., and Jeng, K. C. (2015). Effect of Sesamin on Apoptosis and Cell Cycle Arrest in Human Breast Cancer Mcf-7 Cells. *Asian Pac. J. Cancer Prev.* 16 (9), 3779–3783. doi:10.7314/apjcp.2015.16.9.3779

Sindhu, R. K., Verma, R., Salgotra, T., Rahman, M. H., Shah, M., Akter, R., et al. (2021). Impacting the Remedial Potential of Nano Delivery-Based Flavonoids for Breast Cancer Treatment. *Molecules* 26 (17), 5163. doi:10.3390/molecules26175163

Sp, N., Kang, D. Y., Lee, J.-M., Bae, S. W., and Jang, K.-J. (2021). Potential Antitumor Effects of 6-Gingerol in P53-dependent Mitochondrial Apoptosis and Inhibition of Tumor Sphere Formation in Breast Cancer Cells. *Ijms* 22 (9), 4660. doi:10.3390/ijms22094660

Su, P., Ahmad, B., Zou, K., and Zou, L. (2020). β-Elemene Enhances the Chemotherapeutic Effect of 5-Fluorouracil in Triple-Negative Breast Cancer via PI3K/AKT, RAF-MEK-ErK, and NF-Kb Signaling Pathways. *Onco Targets Ther.* 13, 5207–5222. doi:10.2147/ott.S242820

Sultan, A. S., Marie, M. A., and Sheweita, S. A. (2018). Novel Mechanism of Cannabidiol-Induced Apoptosis in Breast Cancer Cell Lines. *Breast* 41, 34–41. doi:10.1016/j.breast.2018.06.009

Sun, X. D., Liu, X. E., and Huang, D. S. (2012). Curcumin Induces Apoptosis of Triple-Negative Breast Cancer Cells by Inhibition of EGFR Expression. *Mol. Med. Rep.* 6 (6), 1267–1270. doi:10.3892/mmr.2012.1103

Sun, X., Yu, M. W., Ma, X. M., and Zhang, G. L. (2018). *In Vitro* and *In Vivo* Study of the Regulation of Fisetin in PI3K/Akt/mTOR Pathway to Induce Apoptosis of Breast Cancer Cells," in The 15th National Conference of Integrated Traditional Chinese and Western Medicine oncology).2

Sung, H., Ferlay, J., Siegel, R. L., Laversanne, M., Soerjomataram, I., Jemal, A., et al. (2021). Global Cancer Statistics 2020: GLOBOCAN Estimates of Incidence and Mortality Worldwide for 36 Cancers in 185 Countries. *CA Cancer J. Clin.* 71 (3), 209–249. doi:10.3322/caac.21660

Suraweera, C. D., Hinds, M. G., and Kvansakul, M. (2020). Poxviral Strategies to Overcome Host Cell Apoptosis. *Pathogens* 10 (1). doi:10.3390/pathogens10010006

Takeshima, M., Ono, M., Higuchi, T., Chen, C., Hara, T., and Nakano, S. (2014). Anti-proliferative and Apoptosis-Inducing Activity of Lycopene against Three Subtypes of Human Breast Cancer Cell Lines. *Cancer Sci.* 105 (3), 252–257. doi:10.1111/cas.12349

Tandrasasmita, O. M., Lee, J. S., Baek, S. H., and Tjandrawinata, R. R. (2010). Induction of Cellular Apoptosis in Human Breast Cancer by DLBS1425, a Phaleria Macrocarpa Compound Extract, via Down-Regulation of PI3-Kinase/AKT Pathway. *Cancer Biol. Ther.* 10 (8), 814–823. doi:10.4161/cbt.10.8.13085

Tian, J., Duan, Y. X., Bei, C. Y., and Chen, J. (2013). Calycosin Induces Apoptosis by Upregulation of RASD1 in Human Breast Cancer Cells MCF-7. *Horm. Metab. Res.* 45 (8), 593–598. doi:10.1055/s-0033-1341510

Vaz, J. A., Ferreira, I. C., Tavares, C., Almeida, G. M., Martins, A., and Helena Vasconcelos, M. (2012). Suillus Collinitus Methanolic Extract Increases P53 Expression and Causes Cell Cycle Arrest and Apoptosis in a Breast Cancer Cell Line. *Food Chem.* 135 (2), 596–602. doi:10.1016/j.foodchem.2012.04.127

Vazhappilly, C. G., Hodeify, R., Siddiqui, S. S., Laham, A. J., Menon, V., El-Awady, R., et al. (2021). Natural Compound Catechol Induces DNA Damage, Apoptosis, and G1 Cell Cycle Arrest in Breast Cancer Cells. *Phytother Res.* 35 (4), 2185–2199. doi:10.1002/ptr.6970

Viau, C. M., Moura, D. J., Facundo, V. A., and Saffi, J. (2014). The Natural Triterpene 3β,6β,16β-Trihydroxy-Lup-20(29)-Ene Obtained from the Flowers of Combretum Leprosum Induces Apoptosis in MCF-7 Breast Cancer Cells. *BMC Complement. Altern. Med.* 14, 280. doi:10.1186/1472-6882-14-280

Wang, A., Liu, J., Yang, Y., Chen, Z., Gao, C., Wang, Z., et al. (2021). Shikonin Promotes Ubiquitination and Degradation of cIAP1/2-Mediated Apoptosis and Necrosis in Triple Negative Breast Cancer Cells. *Chin. Med.* 16 (1), 16. doi:10.1186/s13020-021-00426-1

Wang, C. J., Sheng, Y., Zhou, Q., and He, H. X. (2020). Anti-proliferation and Pro-apoptotic Activities of Diosmetin on MCF-7 Cells via Mitochondrial Apoptosis Pathway. *J. Traditional Chin. Drug Res. Clin. Pharmacol.* 31 (02), 149–155.

Wang, D., Zhang, Y., Lu, J., Wang, Y., Wang, J., Meng, Q., et al. (2016). Cordycepin, a Natural Antineoplastic Agent, Induces Apoptosis of Breast Cancer Cells via Caspase-dependent Pathways. *Nat. Prod. Commun.* 11 (1), 63–68. doi:10.1177/1934578x1601100119

Wang, H., Lu, C., Ma, W., and Mao, J. (2013a). Genistein-induced Apoptosis in Breast Cancer MDA-MB-231 Cells. *J. Chin. J. Breast Dis.* 7 (05), 322–328.

Wang, J. S., Ren, T. N., and Xi, T. (2012). Ursolic Acid Induces Apoptosis by Suppressing the Expression of FoxM1 in MCF-7 Human Breast Cancer Cells. *Med. Oncol.* 29 (1), 10–15. doi:10.1007/s12032-010-9777-8

Wang, M., Shu, Z. J., Wang, Y., and Peng, W. (2017). Stachydrine Hydrochloride Inhibits Proliferation and Induces Apoptosis of Breast Cancer Cells via Inhibition of Akt and ERK Pathways. *Am. J. Transl Res.* 9 (4), 1834–1844.

Wang, S., Zhong, Z., Wan, J., Tan, W., Wu, G., Chen, M., et al. (2013b). Oridonin Induces Apoptosis, Inhibits Migration and Invasion on Highly-Metastatic Human Breast Cancer Cells. *Am. J. Chin. Med.* 41 (1), 177–196. doi:10.1142/S0192415X13500134

Wei, J., Li, K. J., Wei, J. B., and Lv, C. P. (2015). Influence of Gambogic Acid Lysinate in Proliferation and Apoptosis in Breast Cancer MCF 7 Cells and its Mechanism. *J. J. Jilin Univ. (Medical Sci. Edition)* 41 (03), 476–480.

Wei, T., Xiaojun, X., and Peilong, C. (2020). Magnoflorine Improves Sensitivity to Doxorubicin (DOX) of Breast Cancer Cells via Inducing Apoptosis and Autophagy through AKT/mTOR and P38 Signaling Pathways. *Biomed. Pharmacother.* 121, 109139. doi:10.1016/j.biopha.2019.109139

Wu, G. L., Peng, J. Y., and Yu, X. P. (2018a). "Delphintin Induces Apoptosis and Molecular Mechanism of HER-2 Positive Breast Cancer Cells," in The 11th Special Nutrition Conference of Chinese Nutrition Society.1

Wu, G. S., Lu, J. J., Guo, J. J., Li, Y. B., Tan, W., Dang, Y. Y., et al. (2012). Ganoderic Acid DM, a Natural Triterpenoid, Induces DNA Damage, G1 Cell Cycle Arrest and Apoptosis in Human Breast Cancer Cells. *Fitoterapia* 83 (2), 408–414. doi:10.1016/j.fitote.2011.12.004

Wu, Y. Z., Zeng, Y., Zheng, K. S., and Wu, L. B. (2018b). Salviaflaside Induces the Breast Cancer Cell Apoptosis by Activating Endoplasmic Reticulum Stress. *J. Chin. J. Surg. Integrated Traditional West. Med.* 24 (06), 749–753.

Xie, J., Xu, Y., Huang, X., Chen, Y., Fu, J., Xi, M., et al. (2015). Berberine-induced Apoptosis in Human Breast Cancer Cells Is Mediated by Reactive Oxygen Species Generation and Mitochondrial-Related Apoptotic Pathway. *Tumour Biol.* 36 (2), 1279–1288. doi:10.1007/s13277-014-2754-7

Xie, Z. Z., Li, M. M., Deng, P. F., Wang, S., Wang, L., Lu, X. P., et al. (2017). Paris Saponin-Induced Autophagy Promotes Breast Cancer Cell Apoptosis via the Akt/mTOR Signaling Pathway. *Chem. Biol. Interact* 264, 1–9. doi:10.1016/j.cbi.2017.01.004

Xu, Y., Fang, R., Shao, J., and Cai, Z. (2021). Erianin Induces Triple-Negative Breast Cancer Cells Apoptosis by Activating PI3K/Akt Pathway. *Biosci. Rep.* 41 (6). doi:10.1042/BSR20210093

Yan, W., Ma, X., Zhao, X., and Zhang, S. (2018). Baicalein Induces Apoptosis and Autophagy of Breast Cancer Cells via Inhibiting PI3K/AKT Pathway *In Vivo* and Vitro. *Drug Des. Devel Ther.* 12, 3961–3972. doi:10.2147/DDDT.S181939

Yeh, H. T., Tsai, Y. S., Chen, M. S., Li, Y. Z., Lin, W. C., Lee, Y. R., et al. (2019). Flavopereirine Induces Cell Cycle Arrest and Apoptosis via the AKT/p38 MAPK/ERK1/2 Signaling Pathway in Human Breast Cancer Cells. *Eur. J. Pharmacol.* 863, 172658. doi:10.1016/j.ejphar.2019.172658

Yousuf, M., Shamsi, A., Khan, P., Shahbaaz, M., AlAjmi, M. F., Hussain, A., et al. (2020). Ellagic Acid Controls Cell Proliferation and Induces Apoptosis in Breast Cancer Cells via Inhibition of Cyclin-dependent Kinase 6. *Int. J. Mol. Sci.* 21 (10). doi:10.3390/ijms21103526

Yu, L., Strandberg, L., and Lenardo, M. J. (2008). The Selectivity of Autophagy and its Role in Cell Death and Survival. *Autophagy* 4 (5), 567–573. doi:10.4161/auto.5902

Yu, Q., Wang, W. S., and Zhu, B. B. (2020). Effect of Avicularin on the Apoptosis, Cell Cycle and PI3K/AKT Signaling Pathway in Human Breast Cancer MDA-MB-231 Cells. *J. Cent. South Pharm.* 18 (01), 48–52.

Zhai, J. W., Gao, C., Ma, W. D., Wang, W., Yao, L. P., Xia, X. X., et al. (2016). Geraniin Induces Apoptosis of Human Breast Cancer Cells MCF-7 via ROS-Mediated Stimulation of P38 MAPK. *Toxicol. Mech. Methods* 26 (5), 311–318. doi:10.3109/15376516.2016.1139025

Zhang, H., Xu, H. L., Wang, Y. C., Lu, Z. Y., Yu, X. F., and Sui, D. Y. (2018a). 20(S)-Protopanaxadiol-Induced Apoptosis in MCF-7 Breast Cancer Cell Line through the Inhibition of PI3K/AKT/mTOR Signaling Pathway. *Int. J. Mol. Sci.* 19 (4). doi:10.3390/ijms19041053

Zhang, H. W., Hu, J. J., Fu, R. Q., Liu, X., Zhang, Y. H., Li, J., et al. (2018b). Flavonoids Inhibit Cell Proliferation and Induce Apoptosis and Autophagy through Downregulation of PI3Kγ Mediated PI3K/AKT/mTOR/p70S6K/ULK Signaling Pathway in Human Breast Cancer Cells. *Sci. Rep.* 8 (1), 11255. doi:10.1038/s41598-018-29308-7

Zhang, H., and Zhu, L. (2016). Osthole Induce Human Breast Cancer Cells Lines MCF-7 Apoptosis by Activating P53 Signaling Pathway. *J. Chin. J. Mod. Appl. Pharm.* 33 (05), 547–551.

Zhang, P., Wang, Z. X., Zhang, Y. F., and Chen, Q. L. (2021a). Advances in the Research of Natural Products Anti-breast Tumor Nanometer Drug Delivery System. *J. Chin. Pharm. J.* 56(06), 429–435.

Zhang, R., Kang, R., and Tang, D. (2021b). The STING1 Network Regulates Autophagy and Cell Death. *Signal. Transduct Target. Ther.* 6 (1), 208. doi:10.1038/s41392-021-00613-4

Zhang, X., Luo, W., Zhao, W., Lu, J., and Chen, X. (2015a). Isocryptotanshinone Induced Apoptosis and Activated MAPK Signaling in Human Breast Cancer MCF-7 Cells. *J. Breast Cancer* 18 (2), 112–118. doi:10.4048/jbc.2015.18.2.112

Zhang, Y., Hao, C., wang, B. G., and Xing, Z. B. (2017). The Mechanism of Fangchinoline in Inducing the Apoptosis of MDA-MB-231 Human Breast Cancer Cells. *J. Oncol. Prog.* 15 (03), 250–254.

Zhang, Y. J., Qian, L., and Chen, C. J. (2015b). Effect of Berberine on Proliferation and Apoptosis of MCF-7 Cells. *J. Acta Universitatis Medicinalis Anhui* 50 (09), 1276–1280.

Zhao, M. Z., Zhang, L., Zhou, D., and Ding, Q. Q. (2019). Kaempferol Regulates PI3K/AKT/GSK-3β Signaling Pathway and Promotes Apoptosis of Human Inflammatory Breast Cancer Cell Line SUM190. *J. J. Guangxi Med. Univ.* 36 (06), 872–877.

Zhao, Y., Jing, Z., Lv, J., Zhang, Z., Lin, J., Cao, X., et al. (2017). Berberine Activates Caspase-9/cytochrome C-Mediated Apoptosis to Suppress Triple-Negative Breast Cancer Cells *In Vitro* and *In Vivo*. *Biomed. Pharmacother.* 95, 18–24. doi:10.1016/j.biopha.2017.08.045

Zheng, L., Zhang, Y., Liu, Y., Yang, X. O., and Zhan, Y. (2015). Momordica Cochinchinensis Spreng. Seed Extract Suppresses Breast Cancer Growth by Inducing Cell Cycle Arrest and Apoptosis. *Mol. Med. Rep.* 12 (4), 6300–6310. doi:10.3892/mmr.2015.4186

Zhou, J., Luo, Y. H., Wang, J. R., Lu, B. B., Wang, K. M., and Tian, Y. (2013). Gambogenic Acid Induction of Apoptosis in a Breast Cancer Cell Line. *Asian Pac. J. Cancer Prev.* 14 (12), 7601–7605. doi:10.7314/apjcp.2013.14.12.7601

Zhu, L., and Xue, L. (2019). Kaempferol Suppresses Proliferation and Induces Cell Cycle Arrest, Apoptosis, and DNA Damage in Breast Cancer Cells. *Oncol. Res.* 27 (6), 629–634. doi:10.3727/096504018X15228018559434

Zhu, X., Wang, K., Zhang, K., Zhu, L., and Zhou, F. (2014). Ziyuglycoside II Induces Cell Cycle Arrest and Apoptosis through Activation of ROS/JNK Pathway in Human Breast Cancer Cells. *Toxicol. Lett.* 227 (1), 65–73. doi:10.1016/j.toxlet.2014.03.015

Zu, C., Zhang, M., Xue, H., Cai, X., Zhao, L., He, A., et al. (2015). Emodin Induces Apoptosis of Human Breast Cancer Cells by Modulating the Expression of Apoptosis-Related Genes. *Oncol. Lett.* 10 (5), 2919–2924. doi:10.3892/ol.2015.3646

Conflict of Interest: The authors declare that the research was conducted in the absence of any commercial or financial relationships that could be construed as a potential conflict of interest.

Publisher's Note: All claims expressed in this article are solely those of the authors and do not necessarily represent those of their affiliated organizations, or those of the publisher, the editors and the reviewers. Any product that may be evaluated in this article, or claim that may be made by its manufacturer, is not guaranteed or endorsed by the publisher.

Copyright © 2022 Yuan, Cai, Zhang, Liu, Li and Li. This is an open-access article distributed under the terms of the Creative Commons Attribution License (CC BY). The use, distribution or reproduction in other forums is permitted, provided the original author(s) and the copyright owner(s) are credited and that the original publication in this journal is cited, in accordance with accepted academic practice. No use, distribution or reproduction is permitted which does not comply with these terms.

frontiers in Pharmacology

REVIEW
published: 31 January 2022
doi: 10.3389/fphar.2022.806148

Natural Products Modulate Cell Apoptosis: A Promising Way for the Treatment of Ulcerative Colitis

Chenhao Liu[1†‡], *Yiwei Zeng*[2†‡], *Yulong Wen*[1], *Xinggui Huang*[1] *and Yi Liu*[1*]

[1]School of Basic Medical Sciences, Chengdu University of Traditional Chinese Medicine, Chengdu, China, [2]School of Acupuncture-Moxibustion and Tuina, Chengdu University of Traditional Chinese Medicine, Chengdu, China

Ulcerative colitis (UC) is a chronic inflammatory bowel disease impacting patients' quality of life and imposing heavy societal and economic burdens. Apoptosis of intestinal epithelial cells (IECs) has been considered an early event during the onset of UC and plays a crucial role in disease development. Thus, effectively inhibiting apoptosis of IECs is of critical significance for the clinical management of UC, presenting a potential direction for the research and development of pharmacotherapeutic agents. In recent years, research on the ameliorative effects of natural products on UC through inhibiting IECs apoptosis has attracted increasing attention and made remarkable achievements in ameliorating UC. In this review, we summarized the currently available research about the anti-apoptotic effects of natural products on UC and its mechanisms involving the death-receptor mediated pathway, mitochondrial-dependent pathway, ERS-mediated pathway, MAPK-mediated pathway, NF-κB mediated pathway, P13k/Akt pathway, JAK/STAT3 pathway, and NLRP3/ASC/Caspase-1 pathway. Hopefully, this review may yield useful information about the anti-apoptotic effects of natural products on UC and their potential molecular mechanisms and provide helpful insights for further investigations.

Keywords: ulcerative colitis, inflammatory bowel disease, apoptosis, natural products, intestinal epithelia cells

OPEN ACCESS

Edited by:
Xin Luan,
Shanghai University of Traditional Chinese Medicine, China

Reviewed by:
Songqi Tang,
Hainan Medical University, China
Fengjie Zheng,
Beijing University of Chinese Medicine, China

****Correspondence:***
Yi Liu
tcmly@163.com

†ORCID:
Chenhao Liu
orcid.org/0000-0003-2563-2760
Yiwei Zeng
orcid.org/0000-0002-7042-2503

‡These authors have contributed equally to this work

Specialty section:
This article was submitted to Ethnopharmacology, a section of the journal Frontiers in Pharmacology

Received: *31 October 2021*
Accepted: *10 January 2022*
Published: *31 January 2022*

Citation:
Liu C, Zeng Y, Wen Y, Huang X and Liu Y (2022) Natural Products Modulate Cell Apoptosis: A Promising Way for the Treatment of Ulcerative Colitis. Front. Pharmacol. 13:806148. doi: 10.3389/fphar.2022.806148

1 INTRODUCTION

Ulcerative colitis (UC) is a chronic inflammatory bowel disease characterized by relapsing and remitting mucosal inflammation restricted to the colon and rectum. It is a global health challenge, and its typical clinical presentation consists of diarrhea, hematochezia, and abdominal pain with histological features of diffuse inflammation limited to mucosa and submucosa, crypt abscesses, crypt architectural distortion, mucin depletion, and goblet cell depletion (Conrad et al., 2014; Yu and Rodriguez, 2017). The prevalence of UC varies in different regions. A systematic review of population-based studies demonstrated that the prevalence ranges from 1.2–57.3 per 100,000 in Asia to14.5–505.0 per 100,000 and 139.8–286.3 per 100,000 in Europe and North America, respectively (Ng et al., 2017). UC can occur at any age and is most commonly diagnosed in the second to fourth decade of life (Du and Ha, 2020). Although the specific etiopathogenesis of UC remains obscure, it has been well-recognized that a complex interaction of intestinal microbiota, genetic susceptibility, and environmental factors may disturb the immune system and result in the immune-mediated chronic intestinal inflammatory response (Adams and Bornemann, 2013; Ananthakrishnan, 2015). The long-term inflammation leads to irreversible bowel damage and a higher risk of poor outcomes, such as colectomy and colorectal cancer (Rioux, 2008; Bopanna et al., 2017), impacting patients' quality of life, imposing heavy social and economic burdens, even

increasing mortality. Conventional treatments for UC, including aminosalicylates, corticosteroids, and immunosuppressants, only induce and maintain remission and often elicit adverse effects (Wan et al., 2014; Burri et al., 2020). Several bioagents have been developed to target such molecular mechanisms as tumor necrosis factor (TNF), integrin, and Janus kinase (JAK) (Pugliese et al., 2017; Wehkamp and Stange, 2018). However, these therapeutic agents have primarily focused on the inflammatory cascades to alleviate the disease process rather than histological healing, and most of these substances are expensive for the medium- and low-income populations. Therefore, researching effective and affordable medications with fewer side effects for UA is urgently needed.

Previous studies have demonstrated that the apoptosis of intestinal epithelial cells (IECs) in the colon contributes to chronic inflammatory bowel diseases. IECs play a significant role in host defense, mucosal homeostasis maintenance, and immune response (Eissa et al., 2019; Zhang J. et al., 2020). The intestinal mucosa structure is maintained by a sensitive balance between the apoptosis and proliferation of epithelial cells, which may be disturbed in the inflammatory intestine due to the increased proinflammatory cytokines, including tumor necrosis factor (TNF), interleukin (IL), and interferon family members (Schulzke et al., 2006; Qiu et al., 2011). Apoptosis of IECs has been considered an early event during the onset of UC and plays a crucial role in disease development (Iwamoto et al., 1996). Both extrinsic and intrinsic apoptotic pathways are involved in the UC pathology and regulated by multiple signaling pathways. IECs act as a barrier between lumina and the external environment. Excessive epithelial apoptosis disrupts the epithelial defense system and may cause the breakdown of epithelial barrier function, which may facilitate the mucosal invasion of intraluminal microorganisms and luminal antigen uptake (Hagiwara et al., 2002; Schulzke et al., 2009; Seidelin and Nielsen, 2009; Araki et al., 2010) and potentiate the prolonged inflammatory response. Therefore, effectively inhibiting apoptosis of IECs and retaining the integrated epithelial barrier are of critical significance for the clinical management of UC, presenting a potential direction for the research and development of pharmacotherapeutic agents (Verstege et al., 2006).

Recently, natural products, including extracts and isolated metabolites from medicinal botanical drugs and plants, have drawn increasing attention for their potential therapeutic effects on UC with high availability and fewer side effects (Wan et al., 2014; Santana et al., 2017). These natural agents have been demonstrated to possess anti-inflammatory, antioxidative, anti-apoptotic, antiplatelet, and immune-regulatory properties through mediating multiple signaling pathways related to the pathogenesis of UC (Ke et al., 2012; Triantafyllidi et al., 2015; Cao et al., 2019). Furthermore, several extracts and isolated metabolites from natural products have been reported to exert amelioratory effects on UC through inhibiting IECs apoptosis with multiple pathways, including death receptor-mediated pathway, mitochondria-dependent pathway, endoplasmic reticulum stress-mediated pathway, MAPK-mediated pathway, NF-κB mediated pathway, and P13K/Akt mediated pathway. Therefore, to yield helpful insights for further research and development of novel and efficacious pharmaceutic intervention in this field, a comprehensive review of the anti-apoptotic activities of natural products on UC and their potential molecular mechanisms is necessary. In this review, the following electronic databases were searched from the inception to July 2021 to identify the eligible studies: PubMed, Embase, Web of Science, China National Knowledge Infrastructure, China Biomedical Literature Database, Wanfang Database, VIP database, and Chinese Scientific Journals Database. The following terms were used in a combination for the search: Colitis, Ulcerative, ulcerative colitis, inflammatory bowel disease, colitis, apoptosis, apoptotic, cell death, natural product, natural medicine, traditional medicine, and traditional Chinese medicine. A meticulous review was performed, and the quality of all the included studies was assessed in accordance with the Best practice in research—Overcoming common challenges in phytopharmacological research (Heinrich et al., 2020). The detailed information of natural products and their potential effects with mechanisms on modulating apoptosis in UC is illustrated in **Tables 1**, **2**, and the chemical structures of isolated metabolites are summarized in **Table 3**.

2 EFFECTS AND MECHANISMS OF NATURAL PRODUCTS ON APOPTOSIS IN UC

2.1 Death Receptor-Mediated Pathway

The apoptosis pathway activated by death receptors is also known as the "extrinsic pathway". The ligand-bound death receptors refer to the proteins of tumor necrosis factor superfamily, such as tumor necrosis factor receptor, Fas, and tumor necrosis factor-related apoptosis initiating ligand-receptor (Vanamee and Faustman, 2018). These receptors can be activated by binding to their ligands, such as TNF-α, FasL, and TRAIL. The activated death receptors recruit Fas-associated death domain (FADD), the adaptor protein, which binds to the receptor and interacts with pro-caspase-8 to form a complex Death-inducing Signaling Complex (DISC), leading to the auto-cleavage and activation of caspase-8. Activated caspase-8 initiates the executioner caspase-3 to trigger the apoptotic cascades (Thorburn, 2004; Valmiki and Ramos, 2009). On the other hand, there is a cross-linking between the extrinsic pathway and intrinsic pathway (mitochondria-dependent apoptotic pathway), in which caspase-8 plays a critical role. Bid, a member of the bcl-2 family that regulates mitochondrial apoptosis, is cleaved by caspase-8 to activate the subsequent apoptotic events (Kantari and Walczak, 2011). Previous studies have already found that death receptor-mediated apoptosis is involved in the mucosal defect in UC (Yan et al., 2001; Yukawa et al., 2002; Fan et al., 2020).

In 2011, Liu et al. reported that *Sishen* Pill (2.5–10 g/kg), a prescription from traditional Chinese medicine (TCM), could inhibit epithelial apoptosis in rats through down-regulating Fas/FasL and up-regulating bcl-2 in colon tissues (Liu et al., 2011). In the same year, a study by Liu et al. found that Iridoid Glycosides (80–240 mg/kg), a fraction of *Folium syringae* [Myrtaceae: *Syringa vulgaris L.*] leaves, ameliorated epithelial apoptosis in experimental colitis of rats by

TABLE 1 | Anti-apoptotic activities of natural products on UC-induced intestinal epithelial apoptosis.

Potential mechanisms	Detailed mechanisms	Extracts/Isolated metabolites (dose/concentration)	Cells/Animal	Related targets	Refs
Death receptor apoptotic pathway	Down-regulating Fas and FasL; Down-regulating caspase-3, -9, and bax; Up-regulating bcl-2	Baicalin (30–120 mg/kg)	RAW264.7 cells stimulated by lipopolysaccharide; 2,4,6-trinitrobenzene sulfonic acid-induced rats	Fas, FasL, caspase-3, -9, bax, bcl-2	Yao et al. (2016)
	Down-regulating Fas; Increasing FasL, bcl-2	Sishen Wan (2.5, 5, 10 g/kg)	Sprague-Dawley rats stimulated by TNBS	Fas, FasL, bcl-2	Liu et al. (2011)
	Down-regulating Fas, FasL, bax, caspase-3; up-regulating bcl-2	Iridoid Glycosides (80, 160 and 240 mg/kg)	Sprague-Dawley rats stimulated by DSS	Fas, FasL, caspase-3, bcl-2	Liu and Wang, (2011)
	Decreasing Fas, FasL, caspase-3, bax; Increasing bcl-2	Wumei Pill (13.3–53.2 g/kg)	Sprague-Dawley rats stimulated by TNBS	Fas, FasL, caspase-3, bax, bcl-2	(Shuguang et al., 2016; Yi et al., 2016)
Mitochondria-dependent apoptotic pathway	Down-regulating bax; Up-regulating bcl-2	Aucklandia and Coptis Pills (1.6 g/kg)	Wistar rats stimulated by TNBS	Bax, bcl-2	Yan and Jingen., (2016)
	Down-regulating bax, caspase-3	Hesperetin (100 mg/kg)	Wistar rats stimulated by TNBS	Bax, caspase-3	Polat and Karaboga, (2019)
	Down-regulating cyt-c, caspase-9, -3, bcl-2/bax	Laggera Alata Flavone (100, 200, 400 mg/kg)	Sprague Dawley rats stimulated by TNBS	cyt-c, caspase-9, -3, bcl-2, bax	Xiaobin and Xiaodong., (2014)
	Down-regulating bax; Up-regulating bcl-2	Astragalus Polysaccharide (200 mg/kg)	Wistar rats stimulated by TNBS	Bax, bcl-2	Weijie et al. (2019)
	Down-regulating bax, caspase-3; Up-regulating bcl-2	Indigo (200, 400, 800 mg/kg)	C57BL/6 mice stimulated by DSS	Bax, caspase-3, bcl2	Wenqiang et al. (2019)
	Decreasing bax mRNA expression; Increasing bcl-2 mRNA expression	Aloe Vera Gel (200 mg/kg)	Sprague Dawley rats stimulated by 3% acetic acid	Bax, bcl-2	Hassanshahi et al. (2020)
	Decreasing bax, caspase-3	Coptidis Rhizoma and Magnoliae Officinalis Cortex (1, 2, 4 g/kg)	Sprague Dawley rats stimulated by TNBS	Bax, caspase-3	Xian-juan et al. (2020)
	Up-regulating bcl-2; Down regulating bax and caspase-3	Qingchang Wenzhong granule (0.42–2.20 g/kg)	Male Sprague Dawley rats stimulated by DSS	Bcl-2, bax, caspase-3	Shi et al. (2019)
	Down-regulating bax, caspase-3; Up-regulating bcl-2	Artesunate (30 mg/kg)	Female ICR mice stimulated by DSS	Bcl-2, bax, caspase-3	Yin et al. (2020)
	Decreasing bax, caspase-3; Increasing bcl-2, bcl-xL	Plumericin (0.5–2μg; 3 mg/kg)	IEC-6 cells induced by LPS and IFN; Male CD1 mice stimulated by DNBS	Bcl-2, bax, caspase-3	Rapa et al. (2021)
	Decreasing caspase-3, bax; Increasing bcl,2	Graviola (100 mg/kg)	Male Wistar rats induced by acetic acid	caspase-3, bax, bcl,2	Helal and Abd Elhameed, (2021)
Endoplasmic reticulum stress-mediated pathway	Down-regulating GRP78, caspase-3, -12	Berberine (100, 150, 200 mg/kg; 10 ml/kg)	Male BALB/c mice stimulated by DSS	GRP78, caspase-3, -12	(Yan et al., 2018; Yan et al., 2020)
	Decreasing GRP78, caspase-3, -12	Glycyrrhizin (0.5, 1, 2 mmol/L)	IECs induced by H2O2; Male BALB/c mice stimulated by DSS	GRP78, caspase-3, -12	Yan and Bin., (2020)
	Decreasing GRP78, PERK, CHOP, caspase-3, -12	Ginsenoside Rb1 (20,40 mg/kg)	C57BL/6 mice stimulated by DSS; IEC-6 rat intestinal epithelial cells induced by TNBS	GRP78, PERK, CHOP, caspase-3, -12	Dong et al. (2021)
	Inhibiting PERK-ATF4-CHOP pathway	Limonin (25, 50, 100 mg/kg)	Female C57BL/6 mice stimulated by DSS; RAW 264.7 cells induced by LPS	p-PERK, *p*-eIF2α, ATF4, CHOP	Song et al. (2021)
	Decreasing p-PERK, *p*-eIF2α, ATF4, CHOP, bax	Gancao Xiexin Decoction (10, 20,40 μL)	Caco-2 cells Male BALB/c mice stimulated by DSS	PERK, eIF2α, ATF4, CHOP, bax	Yan et al. (2021)
	Decreasing GRP78, CHOP, PERK, eIF2α, ATF4, XBP1s, capsase-12	Artesuante (30 mg/kg)	Female ICR mice stimulated by DSS	GRP78, CHOP, PERK, eIF2α, ATF4, XBP1s, capsase-12	Yin et al. (2021)
MAPK-mediated pathway	Suppressing p38, ERK1/2, and MAP2K1	SNE (50, 200 mg/kg)	Male ICR mice stimulated by DSS	p38, ERK1/2, MAP2K1	Taya et al. (2016)
	Modulating p38-, JNK-MAPK pathways	Curcumin (100 mg/kg)	Male Wistar albino rats stimulated by acetic acid	p38, JNK	Topcu-Tarladacalisir et al. (2013)

(Continued on following page)

TABLE 1 | (*Continued*) Anti-apoptotic activities of natural products on UC-induced intestinal epithelial apoptosis.

Potential mechanisms	Detailed mechanisms	Extracts/Isolated metabolites (dose/concentration)	Cells/Animal	Related targets	Refs
	Decreasing p38, p53, c-jun, c-fos, bax, caspase-3; Increasing bcl-2	Si ShenWan (5 g/kg)	C57/BL mice stimulated by TNBS	p38, c-jun, c-fos, bax, caspase-3, bcl-2	Zhao et al. (2013)
	Suppressing p38; down-regulating caspase-3; up-regulating PPARγ	Geraniol (250 mg/kg)	Male Wistar rats stimulated by TNBS	p38, caspase-3, PPARγ	Soubh et al. (2015)
	Inhibiting MAPK/NF-κB pathway; Up-regulating bcl-2; Down regulating bax and caspase-3, -9	Paeoniflorin (15, 30, 45 mg/kg; 2.5 g/kg)	Male Balb/c mice stimulated by TNBS; Male Wistar rats stimulated by DSS	ERK, p38, blc-2, bax, caspase-3, -9	(Gu et al., 2017; (Lanzhen et al., 2020)
	Inhibiting MAPK/NF-κB pathway; Increasing ERK1/2, *p*-ERK, p38, p-p38, JNK, *p*-JNK, *p*-IκB, p-p65 Decreasing cleaved caspase-3; Increasing bcl-2	Indirubin (10 mg/kg); Isatin (10 mg/kg)	Male BALB/c mice stimulated by DSS	ERK, p38, JNK, caspase-3, bcl-2	Gao et al. (2018)
	Increasing ERK1/2, p-ERK, p38, p-p38, JNK, p-JNK, p-IκB, p-p65	Chlorogenic Acid (30, 60, 120 mg/kg)	C57BL/6 mice stimulated by DSS	ERK, p38, JNK, p65	Gao et al. (2019)
	Inhibiting *p*-JNK, p-p38; Increasing bcl-2; Decreasing bax	Berberis lycium fruit extract (125–500 mg/kg)	Balb/C mice stimulated by DSS	JNK, p38, bcl-2, bax	Sharma et al. (2020)
	Inhibiting S100A9/MAPK/NF-κB pathway; Increasing bcl-2; Decreasing bax, caspase-3, p53	Anemoside B4 (5, 10 mg/kg)	SD rats stimulated by TNBS	S100A9, TLR4, JNK, p65, blc-2, bax, caspase-3, p53	(Yong et al., 2020; Zhang et al., 2021)
NF-κB mediated pathway	Inhibiting IκBα degradation, caspase-3 activation	Deoxyschisandrin (1–5 μg/ml)	HCT116 cells induced by H2O2	IκBα, caspase-3	Gu et al. (2010)
	Inhibiting IκBα degradation; Down-regulating caspase-3, -9	Corilagin (7.5, 15, 30 mg/kg)	Male C57BL/6 mice stimulated by DSS	IκBα, caspase-3, -9	Xiao et al. (2013)
	Inhibiting IκBα, and IKKβ Down-regulating Fas/FasL, bax, caspase-3; Up-regulating bcl-2	Iridoid Glycosides Fraction (80, 160 and 240mg/kg)	Sprague-Dawley rats stimulated by DSS	IκBα, IKKβ, Fas, FasL, Bax, caspase-3, bcl-2	(Liu and Wang, 2011; Zhang et al., 2020a)
	Down-regulating NF-kBp65, bax, caspase-3; Up-regulating bcl-2	Portulaca Extract (100 mg/kg)	Female mice stimulated by DSS	NF-kBp65, bax, bcl-2, caspase-3	Kong et al. (2018)
	Decreasing p-p65, caspase-3	QingBai decoction (0.0195 ml/g)	C57/bL mice stimulated by DSS	NF-kBp65, caspase-3	Lin et al. (2019)
	Inhibiting *p*-IκBα, p-p65; Decreasing caspase-3, -9; Increasing bcl-2	Gallic acid (20, 40, 60 mg/kg, mg/ml)	Balb/c mice stimulated by TNBS HIEC-6 cells induced by IL-1β	IκBα, NF-kBp65, caspase-3, -9, bcl-2	Zhu et al. (2019a)
	Suppressing NF-kB phosphorylation; Decreasing PARP	C. arietinum ethanol Extract (100, 200 mg/kg)	Male ICR mice stimulated by DSS	NF-kBp65, PARP	Kim et al. (2020)
	Down-regulating NF-kB, bax; Up-regulating bcl-2	Oleuropein (350 mg/kg)	Male laboratory albino rats stimulated by acetic acid	NF-kB, bax, bcl-2	Motawea et al. (2020)
	Suppressing NF-κBp65, pNF-κB, ERK1/2, COX-2 Down-regulating caspase-3	6,7-Dihydroxy-2,4-Dimethoxyphenanthrene (60,120, 240 mg/kg)	Male BALB/c mice stimulated by DSS	NF-κBp65, pNF-κB, ERK1/2, COX-2, caspase-3	Li et al. (2021)
	Down-regulating TLR4, NF-κB, caspase-3; Suppressing NLPR3, cleaved caspase-1, ASC mRNA	Canna x generalis L.H. Bailey rhizome extract (100, 200 mg/kg)	Mice stimulated by DSS	TLR4, NF-κB, NLPR3, ASC mRNA, caspase-3, -1	Mahmoud et al. (2021)
	Inhibiting NF-κBp65, IκBα Down-regulating bax, caspase-3, cyto-c; Up-regulating bcl-2	Coptisine (100 mg/kg)	Male BALB/c mice stimulated by DSS	NF-κBp65, IκBα, ax, caspase-3, cyto-c, bcl-2	Wang et al. (2021)
	Decreasing NF-κBp65, *p*-IKKβ/IKKβ, *p*-IKBα/IKBα; Decreasing cyt-c, caspase-3, -9, bcl-2/bax	Baicalin (30, 60, 90 mg/kg)	RAW264.7 cells induced by LPS; Sprague Dawley rats stimulated by TNBS	NF-κBp65, IKBα, IKKβ, cyt-c, caspase-3, -9, bcl-2, bax	Shen et al. (2019)

(Continued on following page)

TABLE 1 | (*Continued*) Anti-apoptotic activities of natural products on UC-induced intestinal epithelial apoptosis.

Potential mechanisms	Detailed mechanisms	Extracts/Isolated metabolites (dose/concentration)	Cells/Animal	Related targets	Refs
	Inhibiting TLR4, NF-κB; Decreasing bax, caspase-3; Increasing bcl-2	Deoxyschizandrin (20, 40, 80 mg/kg)	Sprague Dawley rats stimulated by DSS	TLR4, NF-κB, bcl-2, bax, caspase-3	Yu and Qian, (2021)
	Decreasing NF-κBp65, caspase-3	Hyperoside (25, 50, 100 mg/kg)	Wistar rats stimulated by TNBS	NF-κBp65, caspase-3	Yu et al. (2021)
P13K/Akt pathway	Regulating P13K/Akt pathway; Decreasing caspase-9, FasL	Baicalin (20, 50, 100 mg/kg)	Male Sprague Dawley rats stimulated by TNBS	P13K, Akt, caspase-9, FasL	Zhu et al. (2017)
	Regulating PI3K/Akt activation	Oxymatrine (25, 50, 100 mg/kg)	Male BALB/c mice stimulated by DSS	PI3K, Akt	Chen et al. (2017)
	Promoting P13K, Akt activity	Costus root granules (1,000 mg/kg)	Male Sprague Dawley rats stimulated by DSS	PI3K, Akt, caspase-3, bcl-2, bax, p53	Wang et al. (2018)
	Down-regulating caspase-3, bad; Up-regulating bcl-2, p53				
	Regulating Akt; Decreasing caspase-3, -9, PARP	Luteolin (50, 100 mg/kg)	Male C57BL/6 mice stimulated by DSS	Akt, caspase-3, -9, PARP	Vukelic et al. (2020)
Other	Decreasing caspase-3, -8	polysaccharide of Portulaca oleracea (200mg/0.33 ml)	Male Sprague Dawley rats stimulated by TNBS	Caspase-3, -8	Feng et al. (2010)
	Decreasing caspase-3	Honey (5 g/kg)	Male albino Wistar rats stimulated by DSS	Caspase-3	Nooh and Nour-Eldien, (2016)
	Inhibiting JAK2/STAT3 pathway	Aloe polysaccharide (15 mg/kg)	HT-29 cell induced by LPS; Male SD rats stimulated by TNBS	JAK2, *p*-JAK2, STAT3, p-STAT3	Lin et al. (2017)
	Up-regulating Sonic hedgehog signaling pathway; Decreasing caspase-3, bax; Increasing bcl-2	Polydatin (15, 30, 45 mg/kg)	Male C57BL/6 mice stimulated by DSS	Shh, caspase-3, bcl-2, bax	Lv et al. (2018)
	Down-regulating *p*-JAK2, pSTAT3, caspase-3, -9; Up-regulating bcl-2, bcl-xL	Tripterygium glycosides (27 mg/kg)	Male Sprague Dawley rats stimulated by TNBS	JAK2, STAT3, caspase-3, -9, bcl-2, bcl-xL	Nan et al. (2019)
	Down-regulating bax; Up-regulating bcl-2	Hydroxytyrosol (50 mg/kg)	Male laboratory albino rats stimulated by acetic acid	Bcl-2, bax	Elmaksoud et al. (2021)
	Inhibiting IL-10/JAK1/STAT3 pathway	Chushi Jianpi decoction (1 ml/kg)	BALB/c mice stimulated by DSS	IL-10, JAK, STAT3	Chen et al. (2021)
	Decreasing bax, caspase-3, TLR4, MyD88; Increasing bcl-2	Crocin (0.05, 0.1 g/kg)	Male Sprague Dawley rats stimulated by DSS	Bax, caspase-3, TLR4, MyD88, bcl-2	Yang et al. (2020)
	Decreasing bax, caspase-3, -9; Increasing VLDLR, bcl-2	Tanshinol (15, 30 mg/kg)	Male C57BL/6J mice stimulated by DSS	VLDLR, bax, bcl-2, caspase-3, -9	Zhu et al. (2021)
	Decreasing NRLP3, ASC, caspase-1	Walnut oil (2.5 ml/kg)	Kunming male mice stimulated by DSS	NRLP3, ASC, caspase-1	Miao et al. (2021)

TNBS, trinitrobenzene sulfonic acid; PPARγ, peroxisome proliferator activated receptor; CHOP, C/EBP, homologous protein; GRP78, glucose-regulated protein 78; PERK, protein kinase R-like ER, kinase; ATF4, activating transcription factor; JNK, c-jun N-terminal kinase; DSS, dextran sulfate sodium; DNBS, dinitrobenzenesulfonate; SNE, spirogyra neglecta extract; TLR4, toll-like receptor 4; IL-8, interleukin-8; PPAR-γ, peroxisome proliferator-activated receptor-γ; Cyto-c, cytochrome-c; LPS, lipopolysaccharide; TRAF6, tumor necrosis factor receptor-associated factor 6; NLRP3, NOD-like receptor protein; ASC, apoptosis-associated speck-like protein containing CARD; RJ, rumex japonicus houtt; JAK, janus kinase; STAT3, signal transducer and activator of transcription 3; IFN, interferon-γ; VLDLR, very low density lipoprotein receptor; Hh, Hedgehog.

modulating the expressions of Fas, FasL, caspase-3, bax, and bcl-2 (Liu and Wang, 2011). In 2016, a study by Yan et al. showed that a TCM prescription, *Wumei* Pill (13.3–53.2 g/kg), could inhibit the excessive apoptosis in colonic epithelial cells of rats via decreasing Fas, FasL, and caspase-3 (Shuguang. et al., 2016). Another study by Hui et al. also confirmed that *Wumei* Pill could decrease the bax expression and increase bcl-2 expression, exerting anti-apoptotic effects on colonic epithelial cells (Yi. et al., 2016). *In vitro* and *in vivo* studies on baicalin, a bioactive constituent from the root of *Scutellariae radix* [Lamiaceae: *Scutellaria baicalensis Georgi*], showed its anti-apoptotic activity, and the potential mechanisms were correlated to the down-regulation of Fas and FasL (Yao et al., 2016). The effects and mechanisms of natural products on death receptors-mediated apoptosis of UC are summarized in **Figure 1**.

2.2 Mitochondria-dependent Apoptotic Pathway

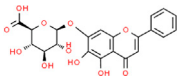
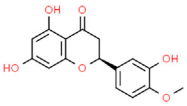
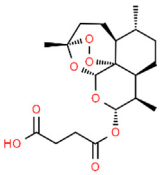
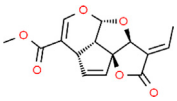
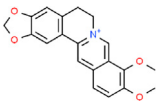
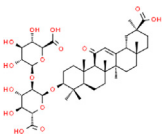
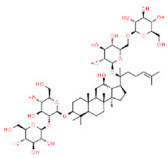
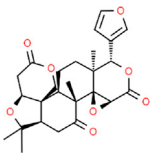
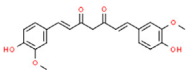
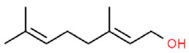
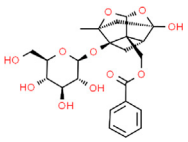
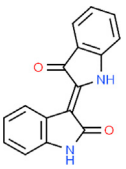
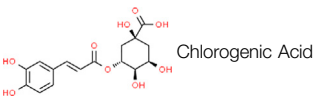
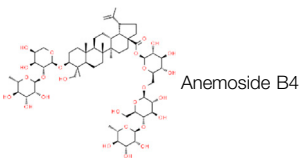
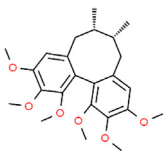
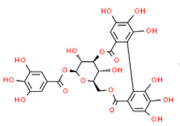
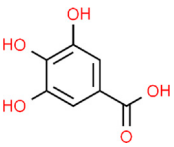
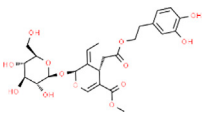
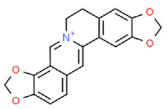
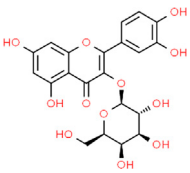
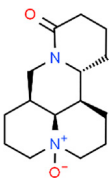
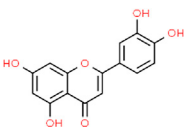
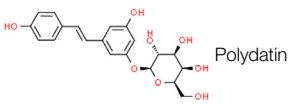
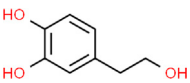
Diverse apoptotic stimuli may evoke the decrease of mitochondrial membrane potential (MMP) and the release of pro-apoptotic proteins to activate the mitochondria-dependent apoptotic pathway (intrinsic pathway) (Thorburn, 2004; Elmore, 2007). The MMP integrity is regulated by the bcl-2 family composed of the pro-apoptotic members (e.g. bax, bad, bak, bim, and bid) and anti-

TABLE 2 | Components of TCM prescriptions.

Prescription	Components [dosage(g)/ Concentrations (%)]	Scientific name	Refs
Sishen Wan	Wu Zhu Yu (6.67%) Bu Gu Zhi (26.67%) Wu Wei Zi (13.33%) Rou Dou Kou (13.33%) Sheng Jiang (26.67%) Da Zao (13.33%)	Rutaceae: *Tetradium ruticarpum (A.Juss.) T.G.Hartley* Fabaceae: *Cullen corylifolium (L.) Medik* Schisandraceae: *Schisandra chinensis (Turcz.) Baill* Myristicaceae: *Myristica fragrans Houtt* Zingiberaceae: *Zingiber officinale Roscoe* Rhamnaceae: *Ziziphus Jujuba Mill*	Liu et al. (2011), Zhao et al. (2013)
Wumei Pill	Wu Mei (16 g) Xi Xin (6 g) Gan Jiang (10 g) Gui Zhi (6 g) Fu Zi (6 g) Shu Jiao (4 g) Huang Lian (16 g) Ren Shen (6 g) Dang Gui (4 g) Huang Bo (6 g)	Rosaceae: *Prunus mume (Siebold) Siebold and Zucc* Aristolochiaceae: *Asarum heterotropoides F.Schmidt* Zingiberaceae: *Zingiber officinale Roscoe* Lauraceae: *Neolitsea cassia (L.) Kosterm* Ranunculaceae: *Aconitum carmichaeli Debeaux* Rutaceae: *Zanthoxylum bungeanum Maxim* Ranunculaceae: *Coptis chinensis Franch* Araliaceae: *Panax ginseng C.A.Mey* Apiaceae: *Angelica sinensis (Oliv.) Diels* Rutaceae: *Phellodendron amurense Rupr*	Yi et al. (2016)
Qingchang Wenzhong granule	Huang Lian (6 g) Pao Jiang (10 g) Ku Shen (15 g) Qing Dai (6 g) Di Yu (15 g) Mu Xiang (6 g) San Qi (6 g) Gan Cao (6 g)	Ranunculaceae: *Coptis chinensis Franch* Zingiberaceae: *Zingiber officinale Roscoe* Fabaceae: *Sophora flavescens Aiton* Brassicaceae: *Isatis tinctoria subsp. tinctoria* Rosaceae: *Sanguisorba officinalis L* Asteraceae: *Dolomiaea costus (Falc.) Kasana and A.K.Pandey* Araliaceae: *Panax notoginseng (Burkill) F.H.Chen* Fabaceae: *Glycyrrhiza glabra L*	Shi et al. (2019)
Gancao Xiexin decoction	Gan Cao (12 g) Gan Jiang (9 g) Ban Xia (9 g) Huang Qin (9 g) Huang Lian (3 g) Dang Shen (9 g) Da Zao (6 g)	Fabaceae: *Glycyrrhiza glabra L* Zingiberaceae: *Zingiber officinale Roscoe* Araceae: Pinellia ternata (Thunb.) Makino Lamiaceae: *Scutellaria baicalensis Georgi* Ranunculaceae: *Coptis chinensis Franch* Lamiaceae: *Salvia miltiorrhiza Bunge* Rhamnaceae: *Ziziphus Jujuba Mill*	Yan et al. (2021)
Qingbai decoction	Da Qing Ye (12 g) Ban Lan Gen (20 g) Huang Bo (9 g) Ku Shen (20 g) Yi Ren (30 g) Wu Zei Gu (25 g)	Brassicaceae: *Isatis tinctoria subsp. Tinctoria,* leaves Brassicaceae: *Isatis tinctoria subsp. Tinctoria,* roots Rutaceae: *Phellodendron amurense Rupr* Fabaceae: *Sophora flavescens Aiton* Poaceae: *Coix lacryma-jobi L* Cuttlebone	Lin et al. (2019)
Chushi Jianpi decoction	Bai Zhu (5 g) Cang Zhu (3 g) Fu Ling (3 g) Bai Shao (3 g) Dang Gui (2 g) Hou Po (2 g) Chen Pi (2 g) Zhu Ling (1.5 g) Ze Xie (1.5 g) Chai Hu (2 g) Sheng Ma (2 g) Fang Feng (2 g) Gan Cao (1 g)	Asteraceae: *Atractylodes macrocephala Koidz* Asteraceae: *Atractylodes lancea (Thunb.) DC.* Smilacaceae: *Smilax glabra Roxb* Paeoniaceae: *Paeonia lactiflora Pall* Apiaceae: *Angelica sinensis (Oliv.) Diels* Magnoliaceae: *Magnolia officinalis Rehder and E.H.Wilson* Rutaceae: *Citrus x aurantium L* Pteridaceae: *Adiantum capillus-veneris L* Alismataceae: *Alisma plantago-aquatica L* Apiaceae: *Bupleurum chinense DC.* Ranunculaceae: *Actaea cimicifuga L* Apiaceae: *Saposhnikovia divaricata (Turcz. ex Ledeb.) Schischk* Fabaceae: *Glycyrrhiza glabra L*	Chen et al. (2021)

apoptotic ones (e.g. bcl-2 and bcl-xL) (Jeong and Seol, 2008). Activating such apoptotic signaling pathways as p53-PUMA and death receptor pathways may enhance the pro-apoptotic proteins and reduce the anti-apoptotic proteins with a decrease in the MMP, disrupting the balance in the bcl-2 family. Increased mitochondrial membrane permeability induces the release of cytochrome-c (Cyt-c), which interacts with apoptosis protease-activating factor 1 (Apaf-1) to activate caspase-9 (Youle and Strasser, 2008; Qiu et al., 2011; Estaquier et al., 2012). Activated caspase-9 initiates pro-caspase-3 and -7, and in turn, the activated caspase-3 evokes pro-caspase-9, forming positive feedback. The activated executioner caspases cleave the downstream substrates, such as poly ADP-ribose polymerase (PARP), lamin, and fodrin, resulting in DNA fragmentation and apoptotic body formation (Fan et al., 2005). Increasing studies

TABLE 3 | Chemical structures of natural products.

 Baicalin	 Hesperetin	 Artesunate	 Plumericin
 Berberine	 Glycyrrhizin	 Ginsenoside Rb1	 Limonin
 Curcumin	 Geraniol	 Paeoniflorin	 Indirubin
 Chlorogenic Acid	 Anemoside B4	 Deoxyschisandrin	 Corilagin
 Gallic acid	 Oleuropein	 Coptisine	 Hyperoside
 Oxymatrine	 Luteolin	 Polydatin	 Hydroxytyrosol

demonstrated that many natural products could mediate mitochondria-dependent apoptosis in UC. The effects and mechanisms of natural products on the mitochondria-dependent apoptotic pathway of UC are summarized in **Figure 2**.

2.2.1 Extracts

In 2014, a study by Zhao et al. revealed that *Laggera Alata* [Asteraceae: *Laggera alata (D.Don) Sch. Bip. ex Oliv.*] Flavone (LAF) (100–400 mg/kg) could dramatically reduce apoptosis of colonic epithelial cells in trinitro-benzene-sulfonic acid (TNBS)-induced UC rats with the down-regulation of cyt-c, caspase-9, -3, and bcl-2/bax ratios (Xiaobin. and Xiaodong., 2014). In 2016, an investigation by Dong and Lu showed that Aucklandia [Asteraceae: *Dolomiaea costus (Falc.) Kasana and A.K.Pandey*] and Coptis [Ranunculaceae: *Coptis chinensis Franch.*] Pills (ACP) (1.6 g/kg) alleviated colonic epithelial apoptosis in TNBS-induced UC rats through decreasing bax expression and increasing bcl-2 expression (Yan. and Jingen., 2016). In 2018, Shi et al. found that a TCM clinical prescription, *Qingchang Wenzhong* granule (QCWZG), exerted anti-apoptotic effects (0.42–2.20 g/kg) in attenuating DSS-induced colitis rats via inhibiting bax and caspase-3 expressions and enhancing bcl-2 expression (Shi et al., 2019). In 2019, a study by Ma et al. indicated that Indigo [Brassicaceae: *Isatis tinctoria subsp. tinctoria*], one of the popular TCM botanical drugs, could reduce intestinal mucosa damage in experimental UC rats (200–800 mg/kg), and its mechanisms were associated with the down-regulation of caspase-3 and bax and the up-regulation of bcl-2 (Wenqiang et al., 2019). In 2020, an experiment by Hassanshahi et al. demonstrated that Aloe Vera Gel (AVG) could reduce cell apoptosis in the colon of acetic-acid-reduced colitis rats with a decreased bax and increased bcl-2 expressions (Hassanshahi et al., 2020). Yang et al. reported that the combination treatment with Coptidis Rhizoma [Ranunculaceae: *Coptis chinensis Franch.*] and Magnoliae Officinalis Cortex [Magnoliaceae: *Magnolia officinalis Rehder and E.H.Wilson*] (1, 2, and 4 g/kg) could protect colonic mucosa from apoptosis by decreasing bax and caspase-3 in TNBS-

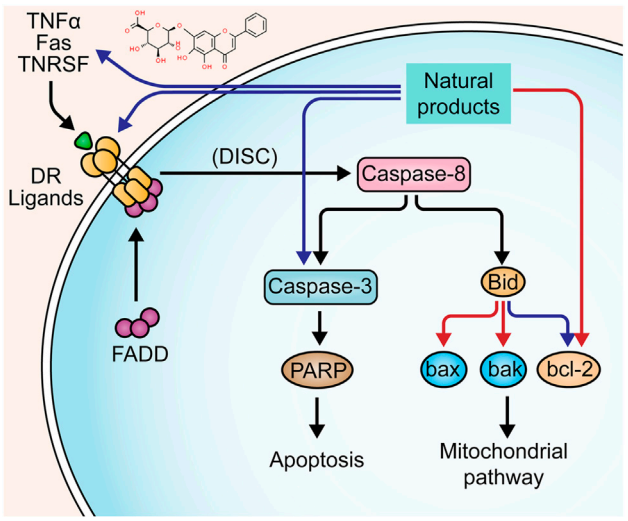


FIGURE 1 | Natural products modulate apoptosis of IECs through death receptors mediated pathway.

induced experimental rats (Xian-juan. et al., 2020). In 2021, Helal et al. elucidated the protective effects of graviola [Annonaceae: *Annona muricata L.*]. They observed that graviola treatment (100 mg/kg) attenuated apoptosis by modulating the expressions of bcl-2, bax, and caspase-3 (Helal and Abd Elhameed, 2021).

2.2.2 Isolated Metabolites

Hesperetin is a flavonoid compound found in many citrus fruits. In 2019, an investigation by Polat and Karaboga suggested that hesperetin treatment (100 mg/kg) could improve the histopathological changes in the colon mucosa of TNBS-induced UC rats through down-regulating bax and caspase-3 (Polat and Karaboga, 2019). In the same year, a study by Pan et al. showed that Astragalus Polysaccharide (AP) (200 mg/kg), one of the main constituents in *Astragalus mongholicus* [Fabaceae: *Astragalus mongholicus Bunge*], could alleviate colonic epithelial defect by decreasing bax expression and increasing bcl-2 expression (Weijie et al., 2019). Artesunate (ARS) is a semisynthetic derivative of Artemisinin. A study by Yin et al. demonstrated that ARS (30 mg/kg) suppressed apoptosis in colon tissues of DSS-induced colitis rats and notably protected epithelial integrity via inhibiting bax and caspase-3 and enhancing bcl-2 (Yin et al., 2020). In 2021, Plumericin, a major bioactive constituent of *Himatanthus sucuuba* [Apocynaceae: *Himatanthus articulatus (Vahl) Woodson*], was reported by Rapa to exert anti-apoptotic effects and protect the intestinal epithelium and its barrier function *in vitro* (0.5–2 μg) and *in vivo* (3 mg/kg), and its potential mechanisms were correlated to the decrease of bax and caspase-3 and the increase of bcl-2 and bcl-xL (Rapa et al., 2021).

2.3 Endoplasmic Reticulum Stress Mediated Pathway

Disrupted epithelial cell populations and functions can affect mucosal homeostasis of UC, leading to Endoplasmic reticulum stress (ERS). The protein-folding capacity of the endoplasmic reticulum is decreased, causing the unfolded protein response (UPR). This process can up-regulate the expression of chaperone proteins-encoding genes, such as glucose-2 regulated protein 78kD (GRP78) and Bip, triggering the downstream signaling of UPR,

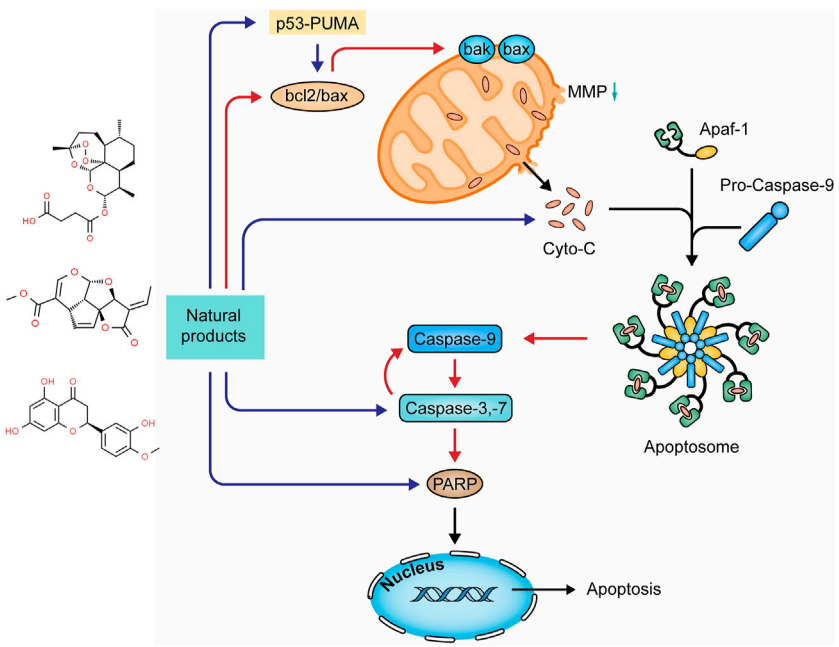


FIGURE 2 | Natural products modulate apoptosis of IECs through mitochondria-dependent pathway.

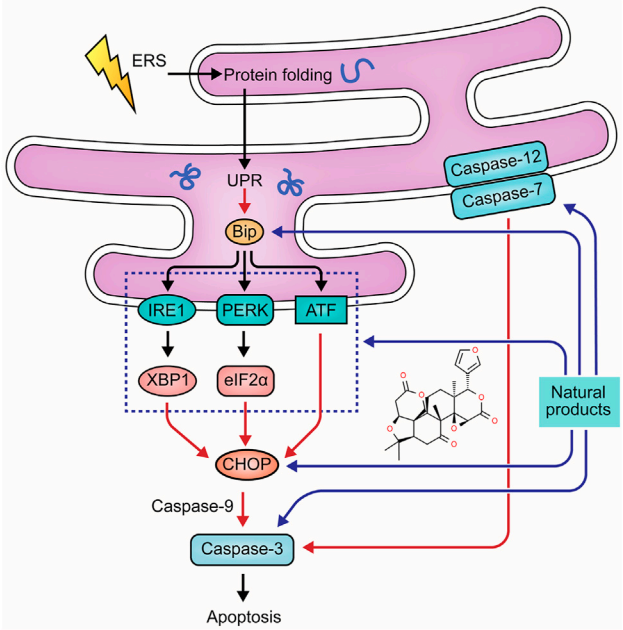


FIGURE 3 | Natural products modulate apoptosis of IECs through ERS-mediated pathway.

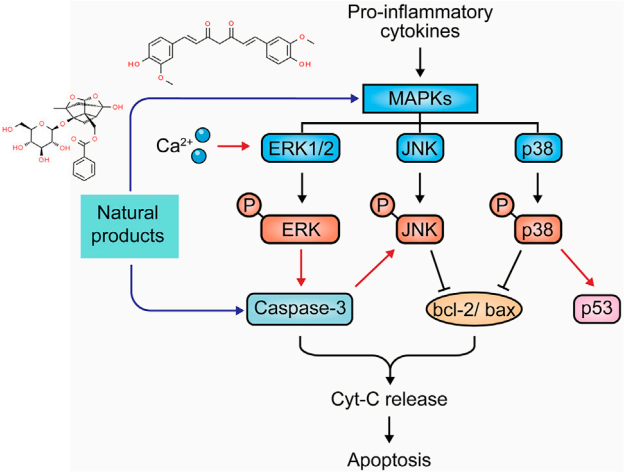


FIGURE 4 | Natural products modulate apoptosis of IECs through MAPK mediated pathway.

namely IRE1-XBP1, PERK-eIF2α, and ATF pathway. Activation of these pathways contributes to an increase in the C/EBP-homologous protein (CHOP), the bcl-2-interacting mediator of cell death (Bim), and the p53 up-regulated modulator of apoptosis (PUMA) to promote apoptosis (Hetz, 2012; Cao, 2016). ERS also induces apoptosis through the caspase-12 pathway. Pro-caspase-12 is pre-located on the cytoplasmic side of the ER, which can be cleaved in response to ERS. Caspase-12 can activate caspase-3, -9, and -7, directly inducing apoptosis (Tan et al., 2006; Liu et al., 2013). The role of ERS in UC pathogenesis has been recognized for decades, and numerous studies have yielded considerable evidence that natural products can protect intestinal epithelial cells from UC-induced apoptosis. The improvement effects and potential mechanisms of natural products on ERS-mediated apoptosis are summarized in **Figure 3**.

2.3.1 Extracts

In 2021, Shen et al. found that Gancao Xiexin Decoction (10–40 μL) could inhibit the activation of PERK- eIF2α-CHOP apoptotic signaling pathway to reduce the apoptosis of epithelial cells in UC, decreasing intestinal epithelial permeability and thus protecting intestinal mucosal barrier homeostasis (Yan et al., 2021).

2.3.2 Isolated Metabolites

Berberine (BBR) is one of the bioactive components in *Coptis Chinensis* [Ranunculaceae: *Coptis chinensis Franch.*]. In 2018, Shen et al. reported that BBR treatment (100–200 mg/kg) could decrease apoptosis in intestinal epithelial cells of UC rats, indicating that the anti-apoptotic effect of BBR was associated with the down-regulation of caspase-12 and -3 (Yan. et al., 2018). In 2020, Yan et al. further explored the anti-apoptotic mechanisms of BBR, and their results suggested that this component (10 ml/kg) also down-regulated GRP78 to alleviate UPR (Yan et al., 2020). *In vitro* and *in vivo* investigation of Shen et al. demonstrated glycyrrhizin (0.5–2.0 mmol/L) could regulate ERS-evoked intestinal epithelial apoptosis and protect cells from apoptosis by decreasing GRP78, caspase-12, and caspase-3 (Yan and Bin., 2020). In 2021, a study reported Ginsenoside Rb1 (20 and 40 mg/kg), the major ginsenoside in ginseng [Araliaceae: *Panax ginseng C.A.Mey.*] with multiple pharmacological activities, significantly alleviated ERS in DSS-induced UC rats and TNBS-stimulated rat intestinal epithelial cells through decreasing GRP78, PERK, CHOP, caspase-12, and caspase-3 (Dong et al., 2021). Song et al. found that limonin, a tetracyclic triterpenoid compound obtained from plants of *Rutaceae* and *Meliaceae*, could improve colon pathology both *in vitro* and *in vivo* by inhibiting the PERK-ATF4-CHOP pathway to relieve ERS and subsequent cell apoptosis (Song et al., 2021). ARS has been demonstrated to alleviate UC by multiple pathways. Besides regulating mitochondria-dependent apoptosis, it also suppressed the activation of PERK-eIF2α-ATF4-CHOP and IRE1α-XBP1 signaling pathways to prevent ERS-mediated apoptosis in colon tissues (Yin et al., 2021).

2.4 MAPK-Mediated Apoptotic Pathway

Mitogen-activated protein kinase (MAPK) family members conventionally include extracellular-regulated kinase (ERK1/2), c-Jun N-terminal kinase (JNK), p38 MAPK, and ERK5 (Sun et al., 2015). They play pivotal roles in transduction extracellular stimuli into cellular responses of cell growth, migration, proliferation, differentiation, and apoptosis. ERK can be stimulated by growth factors and cytokines in UC pathology, leading to phosphorylation. The ERK signaling can play anti-apoptotic and pro-apoptotic roles depending on the stimuli (Li et al., 2014). JNK and p38 MAPK regulate several bcl-2 family proteins. One of the best-known transcription factors, p53, is also modulated by JNK/p38MAPK cascades to promote apoptosis. In

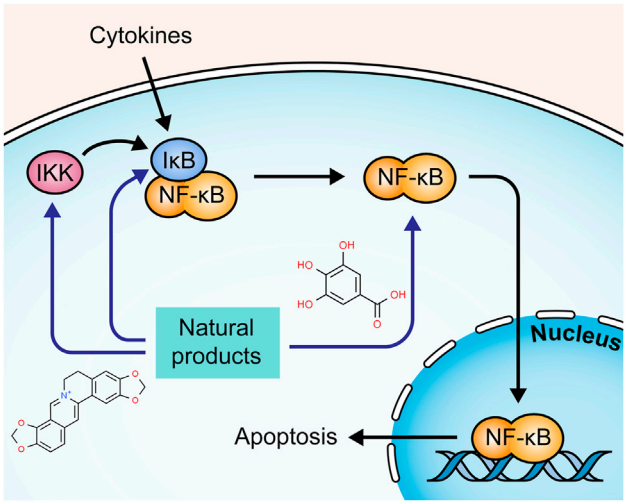


FIGURE 5 | Natural products modulate apoptosis of IECs through NFκB mediated pathway.

addition, JNK/p38MAPK has been reported to be associated with the activation of caspase cascades (Yue and Lopez, 2020). Currently, MAPKs are considered a potential target in the treatment of UC. The potential effectiveness and mechanism of natural products on MAPK-mediated apoptosis are summarized in **Figure 4**.

2.4.1 Extracts

Sishen Wan (SSW) is a notable TCM formula and has often been used in UC treatment. In 2013, Zhao et al. reported that SSW intervention (5 g/kg) in TNBS-induced colitis rats decreased colonic epithelial apoptosis by suppressing p38MAPK, p53, caspase-3, c-jun, c-fos, and bax expressions (Zhao et al., 2013). In 2016, a study by Taya et al. demonstrated that the extract (50 and 200 mg/kg) of Spirogyra neglecta, a freshwater green alga in the northern provinces of Thailand, diminished apoptosis of colonic epithelial cells in colitis mice via suppressing p38, ERK1/2, and MAP2K1 (Taya et al., 2016). Indirubin and Isatin are bioactive components in Qin Dai [Brassicaceae: *Isatis tinctoria subsp. tinctoria*]. In 2018, an investigation by Gao et al. demonstrated that the combination of Indirubin and Isatin inhibited cell apoptosis in DSS-induced UC mice through mediating the MAPK pathway, decreasing caspase-3, and increasing bcl-2 (Gao et al., 2018). *Qing Chang Hua Shi* granule (QCHS) also showed inhibitory effects on reducing UC-induced colonic apoptosis *in vitro* and *in vivo* by mediating MEK/ERK pathway and decreasing the expression of such apoptosis-related proteins as bax, bcl-2, caspase-3, -9, Fas, and Fas-L (Zhu et al., 2019a). In 2020, Sharma et al. reported that the extract of *Berberis lycium Royle* [Berberidaceae] fruit (125–500 mg/kg) could modulate intestinal epithelial cell apoptosis in mice through the inhibition of *p*-JNK and p-p38, increase of bcl-2, and decrease of bax, suggesting that it might be a viable candidate for UC treatment (Sharma et al., 2020).

2.4.2 Isolated Metabolites

Curcumin is a major constituent of medicinal turmeric [Zingiberaceae: *Curcuma longa L.*]. A study in 2013 revealed that curcumin (100 mg/kg) could reduce colon injury in UC rats through the modulation of p38-and JNK-MAPK pathways (Topcu-Tarladacalisir et al., 2013). In 2015, Soubh et al. reported that Geraniol, a natural monoterpene alcohol (250 mg/kg), hindered apoptosis in TNBS-induced UC rats by suppressing p38 and caspase-3 expressions. Ger also up-regulated PPARγ, a transcriptional factor whose down-regulation is highly associated with the activation of the p38MAPK pathway (Soubh et al., 2015). Paeoniflorin (PA) is one of the major bioactive components in Paeony [Paeoniaceae: *Paeonia lactiflora Pall.*] root. In 2017, Gu et al. revealed that PA treatment (15–45 mg/kg) for experimental colitis mice could ameliorate the apoptosis in colitis tissues through inhibiting MAPK/NF-κB pathway (Gu et al., 2017). Moreover, a study by Li et al., in 2020 showed that PA down-regulated bax, caspase-3, and caspase-9 and up-regulated bcl-2 to protect UC-induced apoptosis (Lanzhen. et al., 2020). Chlorogenic acid is found in coffee and various TCM botanical drugs, such as honeysuckle [Caprifoliaceae: *Lonicera japonica Thunb.*], hawthorn [Rosaceae: *Crataegus pinnatifida Bunge*], eucommia [Eucommiaceae: *Eucommia ulmoides Oliv.*], and chrysanthemum [Asteraceae: *Chrysanthemum x morifolium (Ramat.) Hemsl.*]. Gao et al. reported that Chlorogenic acid (30–120 mg/kg) could significantly alleviate colonic tissue apoptosis and inflammation via the mediation of the MAPK/ERK/JNK signaling pathway (Gao et al., 2019). Anemoside B4, a bioactive triterpenoid saponin isolated from Chinese pulsatilla [Ranunculaceae: *Pulsatilla chinensis (Bunge) Regel*], was demonstrated to exert anti-apoptotic effects on UC through inhibiting p53, caspase-3, and bax expressions and the S100A9/MAPK/NF-κB signaling pathway (Yong. et al., 2020; Zhang et al., 2021).

2.5 NF-κB Mediated Apoptotic Pathway

The transcription factor nuclear factor-kappaB (NF-κB) is also involved in the regulation of cell death. Under resting conditions, NF-κB is sequestered in the cytoplasm through interaction with IκB, an inhibitory protein. In the presence of NF-κB-activating stimuli, such as proinflammatory cytokines, IκB can be phosphorylated by IκB kinase (IKK) and degraded, leading to the translocation of NF-κB to the nucleus (Heyninck and Beyaert, 2001; Aranha et al., 2007). Activated NF-κB contributes to the transcription of multiple genes to regulate apoptosis induced by extrinsic and intrinsic apoptotic pathways (Baldwin, 2012; Liu et al., 2012). The potential mechanisms of natural products on NF-κB mediated apoptosis are summarized in **Figure 5**.

2.5.1 Extracts

A study by Liu and Wang showed that the Iridoid Glycosides fraction inhibited IkBα phosphorylation and IKK activity in intestinal epithelial cells, regulating the NF-κB signaling pathway (Liu and Wang, 2011). Another study by Zhang et al. presented similar results of IG in regulating the NF-κB signaling

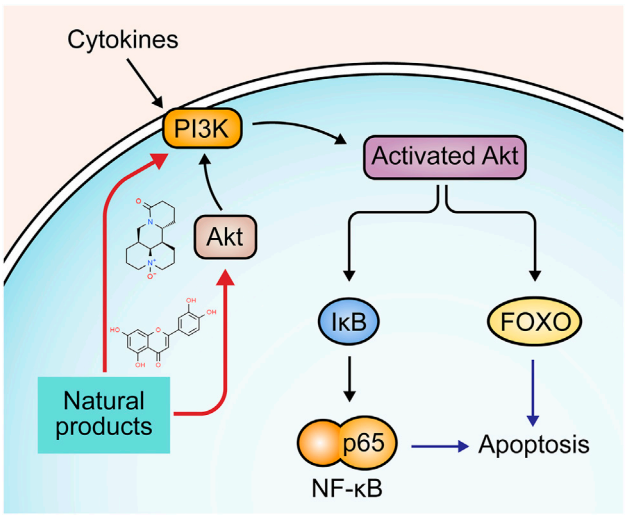


FIGURE 6 | Natural products modulate apoptosis of IECs through P13K/Akt pathway.

pathway (Zhang Y. et al., 2020). Corilagin is a major Gallotannin found in many medicinal plants. In 2013, a study by Xiao et al. demonstrated that Corilagin (7.5–30 mg/kg) suppressed the degradation of IκBα and down-regulated caspase-3 and -9, reducing apoptosis in colon tissues of UC mice (Xiao et al., 2013). Portulaca [Portulacaceae: *Portulaca oleracea L.*] is a wildly used botanical drug in TCM. In 2018, an investigation by Kong et al. revealed that Portulaca extract could alleviate colitis in mice and mediate colonic cell apoptosis through inhibiting the NF-κB pathway with decreased expressions of bax and caspase-3 and increased expression of bcl-2 (Kong et al., 2018). A study by Lin et al. displayed that QingBai decoction (QBD), a TCM prescription, effectively reduced apoptosis in the colon of DSS-induced UC mice via regulating the NF-κB pathway and decreasing caspase-3 (Lin et al., 2019). Gallic acid is widely present in many plants and fruits. In 2019, Zhu et al. found that it inhibited UC-induced apoptosis *in vitro* and *in vivo* by suppressing the expressions of *p*-IκBα and p-NF-κB, decreasing caspase-3 and -9, and increasing bcl-2 (Zhu et al., 2019b). Chickpea [Fabaceae: *Cicer arietinum L.*] is a staple food crop in tropical and subtropical areas. In 2020, Kim et al. reported that its ethanol extract (100 and 200 mg/kg) exerted a protective effect on DSS-induced apoptosis in colon tissue by the inhibition of nuclear factor-kappa B (NF-κB) and signal transducer and activator of transcription 3 (STAT3) (Kim et al., 2020). Canna [Cannaceae: *Canna x generalis L.H. Bailey*] is wildly used in folk medicine for the treatment of many diseases. In 2021, a study by Mahmoud et al. showed that its rhizome ethanol extract (100, 200 mg/kg) down-regulated NF-κB and caspase-3 expressions in colon tissues of colitis mice (Mahmoud et al., 2021).

2.5.2 Isolated Metabolites

In 2010, Gu et al. demonstrated that Deoxyschisandrin (5 μg/ml), one of the lignan components of *Schisandra Chinensis* [Schisandraceae: *Schisandra chinensis (Turcz.) Baill.*] fruits, could inhibit apoptosis of intestinal epithelial cells, and the potential mechanisms were associated with the inhibition of IκB degradation and the subsequent NF-κB activation (Gu et al., 2010). A study by Shen et al. discovered that Baicalin (30–90 mg/kg) presented a significant anti-apoptotic effect on TNBS-induced UC rats and LPS-induced RAW264.7 cells through regulating the IKK/IKB/NF-kB signaling and the expressions of such apoptosis-related proteins as cyt-c, caspase-3, -9, bcl-2, and bax (Shen et al., 2019). In 2020, Motawea et al. showed that Oleuropein (350 mg/mg), a major component of *Olea europaea L.*[Oleaceae], reduced apoptosis in colon tissues of experimental UC rats via down-regulating the expression of NF-kB and bax and up-regulating bcl-2 (Motawea et al., 2020). In 2021, a study by Li et al. revealed that 6,7-Dihydroxy-2,4-Dimethoxyphenanthrene (CYP4, 60–240 mg/kg) from Chinese Yam [Dioscoreaceae: *Dioscorea oppositifolia L.*] could protect intestinal mucosa from apoptosis in DSS-induced colitis mice by suppressing NF-κB and caspase-3 expressions (Li et al., 2021). In the same year, Wang et al. stated that Coptisine (100 mg/kg), a major bioactive component from Rhizoma Coptidis [Ranunculaceae: *Coptis chinensis Franch.*], markedly alleviated DSS-induced apoptosis in intestinal epithelial cells of rats by restraining IκBα phosphorylation and NF-κB translocation, down-regulating bax and caspase-3, and up-regulating bcl-2 (Wang et al., 2021). Yu et al. observed that hyperoside (25–100 mg/kg), a flavonol glycoside isolated from plants of Hypericum and Crataegus, could inhibit TNBS-induced intestinal epithelial apoptosis in rats via decreasing NF-κB and caspase-3 (Yu et al., 2021). Yu and Qian reported that Deoxyschizandrin treatment (20–80 mg/kg) could reduce apoptosis of colonic epithelial cells in UC model mice, which might be attributed to the inhibition of TLR4/NF-κB signaling pathway and the regulation of bcl-2, bax, and caspase-3 (Yu and Qian, 2021).

2.6 P13K/Akt Pathway

Phosphatidylinositol 3-kinase (PI3K)/Akt signaling is implicated in multiple cellular processes, such as survival, proliferation, differentiation, and apoptosis (Vivanco and Sawyers, 2002). P13K can be activated by various cytokines and be recruited to the membrane. Akt, the downstream target protein of P13K, migrates to the membrane and activates the sequential phosphorylation of P13K. Activated Akt releases from the membrane to cytosol to phosphorylate fork-head transcription factor (FOXO), triggering the downstream signaling pathways that regulate many apoptotic genes related to the intrinsic and extrinsic pathway (Franke et al., 2003; Fresno Vara et al., 2004; Zhang et al., 2011). P13K/Akt can also activate NF-κB through phosphorylating IκB (Chen et al., 2017). The involvement of the P13K/Akt signaling pathway in UC pathogenesis has been well-documented (Huang et al., 2011). Recently, compelling evidence has revealed that several natural products alleviate apoptosis in UC through regulating P13K/Akt signaling pathway. The potential mechanisms of natural products on P13K/Akt mediated apoptosis are summarized in **Figure 6**.

In 2017, Chen et al. reported that Oxymatrine (25–100 mg/kg), an alkaloid derived from the root of the

Sophora flavescens [Fabaceae: *Sophora flavescens Aiton*], could alleviate apoptosis through P13K/Akt pathway and exhibit potential therapeutic effects against DSS-induced colitis (Chen et al., 2017). In the same year, another study by Zhu et al. found that baicalin (20–100 mg/kg) reduced the expression of caspase-9 and FasL by regulating the P13K/Akt pathway (Zhu. et al., 2017). In 2018, an investigation by Wang et al. demonstrated that granules extracted from Costus root [Asteraceae: *Dolomiaea costus (Falc.) Kasana and A.K.Pandey*] (1000 mg/kg) could inhibit apoptosis of intestinal epithelial cells in UC rats via promoting the activities of P13K and Akt and subsequently down-regulating caspase-3 and bad while up-regulating bcl-2 and p53 (Wang et al., 2018). Luteolin is a common flavonoid in several plants, such as lemon, apple, and onion. In 2020, Vukelic et al. showed that luteolin (50–100 mg/kg) decreased caspase-3, -9, and PARP in UC mice, which may be related to Akt regulation (Vukelic et al., 2020).

2.7 Other Reported Pathways

Besides the major apoptotic pathways mentioned above, other mechanisms are also attributable to the anti-apoptotic activities of natural products on UC. For example, Aloe polysaccharide (AP) extracted from aloe vera [Asphodelaceae: *Aloe vera (L.) Burm. f.*] could effectively reduce the apoptosis in colonic tissues via inhibiting the JAK2/STAT-3 signaling pathway *in vivo* and *vitro* (Lin et al., 2017). Another study conducted in 2019 by Bu et al. revealed that Tripterygium glycosides (27 mg/kg) could attenuate intestinal mucosal apoptosis in UC rats through JAK2/STAT3 signaling pathway (Nan et al., 2019). Moreover, an investigation by Chen et al. demonstrated that *Chushi Jianpi* Decoction, a TCM prescription, could reduce intestinal epithelial apoptosis in colitis mice through inhibiting IL-10/JAK1/STAT3 pathway (Chen et al., 2021). Polydatin (15–45 mg/kg), a main component in Polygonum cuspidatum [Polygonaceae: *Reynoutria japonica Houtt.*], was reported to exert protective effects on DSS-induced apoptosis in mice by up-regulating the Sonic hedgehog signaling pathway, decreasing caspase-3 and bax, and increasing bcl-2 (Lv et al., 2018). In 2020, Yang et al. demonstrated that crocin (0.05–0.1 g/kg), a carotenoid compound derived from *Crocus sativus L.*(Iridaceae), could decrease bax and caspase3 and increase bcl-2 in the intestinal tissue of UC rats, and its potential mechanisms might be correlated with the down-regulation of the TLR4/MyD88 signaling pathway (Yang et al., 2020). In 2021, a study by Miao et al. revealed that Walnut oil (2.5 mg/kg) down-regulated the related gene proteins expression of the NLRP3/ASC/Caspase-1 pathway to inhibit apoptosis in DSS-induced colitis mice (Miao et al., 2021).

In addition, some natural agents have exerted therapeutic effects on UC-elicited apoptosis, but their mechanisms need to be further verified. In 2010, Pan et al. reported that polysaccharides of Portulaca oleracea (200mg/0.33 ml) could reduce intestinal epithelial apoptosis in TNBS-induced UC rats with decreased caspase-3 and -8 expression in the epithelium (Feng. et al., 2010). Interestingly, feeding DSS-induced colitis rats with honey (5 g/kg) could improve colonic histology by decreasing caspase-3 in colons (Nooh and Nour-Eldien, 2016). In 2021, Elmaksoud et al. demonstrated that Hydroxytyrosol (50 mg/kg), one of the main alcoholic compounds of the olive leaves extract, down-regulated the expression of bax and up-regulated that of bcl-2 in the colons of acetic acid-induced colitis rats (Elmaksoud et al., 2021). Tanshinol, a bioactive ingredient in DanShen [Lamiaceae: *Salvia miltiorrhiza Bunge*], was reported by Zhu et al. to alleviate apoptosis in UC model cells through promoting very low-density lipoprotein receptor expression (Zhu et al., 2021).

3 CONCLUSIONS AND PERSPECTIVES

Natural products refer to a wide range of bioactive extracts or isolated metabolites from natural materials. Their bioactivities are currently of great interest in many research fields (Ekiert and Szopa, 2020) and may yield promising pharmacological approaches for the prevention and treatment of UC due to their multiple regulatory effects with few adverse effects (Nascimento et al., 2020). In recent years, converging lines of evidence have demonstrated that apoptosis of IECs is highly associated with the occurrence and development of UC. This review reported that multiple natural products have anti-apoptotic activities *in vitro* and *in vivo* to protect intestinal epithelial cells against apoptosis in UC. Furthermore, their potential mechanisms are closely associated with the regulation of multiple apoptosis-related signaling pathways, including death-receptor mediated pathway, mitochondrial-dependent pathway, ERS-mediated pathway, MAPK-mediated pathway, NF-κB mediated pathway, P13k/Akt pathway, and other reported pathways such as JAK/STAT3 and NLRP3/ASC/Caspase-1. Thus, it is rational to presume that natural products may yield promising therapeutic agents to treat UC patients by modulating apoptosis of IECs.

Although many natural products have been demonstrated to be the potential candidates for UC treatment by targeting intestinal epithelial apoptosis, more sophisticated works in preclinical and clinical investigations need to be performed to research and develop effective pharmacotherapies. First, studies on the pharmacokinetics and pharmacodynamics of these natural agents are insufficient. Recently, with the increasing attention drawn on natural products, great attention has been paid to metabolism and pharmacokinetics research (Zeng et al., 2017), laying a foundation for subsequent research of toxicology and medication safety. Second, systematic evaluation for the toxicity and safety of natural products remains scarce. Though these natural plants and botanical drugs have been wildly used for thousands of years, well-designed studies for critical evaluation of safety are imperative for developing novel and effective pharmacotherapeutic agents. More concerns need to be paid on the potential toxicity and adverse effects of natural products (Wu et al., 2016; Byard et al., 2017; Liu et al., 2020). Third, current research of natural products targeting apoptosis in UC has primarily focused on their *in vivo* and *in vitro* effects and mechanisms. Well-designed clinical trials with high methodological quality are urgently needed for further verification of these natural products. Lastly, the exploration of

mechanisms of some natural products is still in the preliminary stage, and the specific targets and signaling pathways require further elucidation. In addition, some of the above-mentioned natural products, such as baicalin, Indirubin, and Paeoniflorin, are reported to modulate apoptosis through multiple pathways, and their underlying interactions or crosstalk with the core-target network of UC are worthy of further exploration.

In summary, we expect that this review will provide helpful information to understand the effects of natural products and their pharmacological mechanisms in regulating intestinal epithelial apoptosis of UC. These natural extracts and isolated metabolites are of potential value in clinical UC management. We also expect more researchers and clinicians to pay close attention to this field and conduct more relevant studies and trials.

AUTHOR CONTRIBUTIONS

All authors contributed substantially to the article. YL conceived and designed this paper. CHL, YWZ, YLW, and XGH summarized and analyzed the data. CHL and YWZ drafted, revised, and edited the paper.

FUNDING

This research was supported by the project of State Administration of Traditional Chinese Medicine of the People's Republic of China (No. GZY-KJS-2020-024) and the Major Research and Development Project of Sichuan Provincial Science and Technology Department (No. 22ZDYF2011).

REFERENCES

Adams, S. M., and Bornemann, P. H. (2013). Ulcerative Colitis. *Am. Fam. Physician* 87 (10), 699–705.

Ananthakrishnan, A. N. (2015). Epidemiology and Risk Factors for IBD. *Nat. Rev. Gastroenterol. Hepatol.* 12 (4), 205–217. doi:10.1038/nrgastro.2015.34

Araki, Y., Mukaisyo, K., Sugihara, H., Fujiyama, Y., and Hattori, T. (2010). Increased Apoptosis and Decreased Proliferation of Colonic Epithelium in Dextran Sulfate Sodium-Induced Colitis in Mice. *Oncol. Rep.* 24 (4), 869–874. doi:10.3892/or.2010.869

Aranha, M. M., Borralho, P. M., Ravasco, P., Moreira da Silva, I. B., Correia, L., Fernandes, A., et al. (2007). NF-kappaB and Apoptosis in Colorectal Tumourigenesis. *Eur. J. Clin. Invest.* 37 (5), 416–424. doi:10.1111/j.1365-2362.2007.01801.x

Baldwin, A. S. (2012). Regulation of Cell Death and Autophagy by IKK and NF-kappaB: Critical Mechanisms in Immune Function and Cancer. *Immunol. Rev.* 246 (1), 327–345. doi:10.1111/j.1600-065X.2012.01095.x

Bopanna, S., Ananthakrishnan, A. N., Kedia, S., Yajnik, V., and Ahuja, V. (2017). Risk of Colorectal Cancer in Asian Patients with Ulcerative Colitis: a Systematic Review and Meta-Analysis. *Lancet Gastroenterol. Hepatol.* 2 (4), 269–276. doi:10.1016/S2468-1253(17)30004-3

Burri, E., Maillard, M. H., Schoepfer, A. M., Seibold, F., Van Assche, G., Riviere, P., et al. (2020). Treatment Algorithm for Mild and Moderate-To-Severe Ulcerative Colitis: An Update. *Digestion* 101 (Suppl. 1), 2–15. doi:10.1159/000504092

Byard, R. W., Musgrave, I., Maker, G., and Bunce, M. (2017). What Risks Do Herbal Products Pose to the Australian Community? *Med. J. Aust.* 206 (2), 86–90. doi:10.5694/mja16.00614

Cao, S. S. (2016). Epithelial ER Stress in Crohn's Disease and Ulcerative Colitis. *Inflamm. Bowel Dis.* 22 (4), 984–993. doi:10.1097/MIB.0000000000000660

Cao, S. Y., Ye, S. J., Wang, W. W., Wang, B., Zhang, T., and Pu, Y. Q. (2019). Progress in Active Compounds Effective on Ulcerative Colitis from Chinese Medicines. *Chin. J. Nat. Med.* 17 (2), 81–102. doi:10.1016/S1875-5364(19)30012-3

Chen, Q., Duan, X., Fan, H., Xu, M., Tang, Q., Zhang, L., et al. (2017). Oxymatrine Protects against DSS-Induced Colitis via Inhibiting the PI3K/AKT Signaling Pathway. *Int. Immunopharmacol* 53, 149–157. doi:10.1016/j.intimp.2017.10.025

Chen, Z., Zheng, Y., Yang, J., and Lu, Y. (2021). Effect of Chushi Jianpi Decoction on IL-10/JAK1/STAT3 Pathway and Apoptosis of Intestinal Epithelial Cells in Mice with Ulcerative Colitis (China). *Guid J. Tradit Chin. Med. Pharm.* 27 (5), 13–17. doi:10.13862/j.cnki.cn43-1446/r.2021.05.001

Conrad, K., Roggenbuck, D., and Laass, M. W. (2014). Diagnosis and Classification of Ulcerative Colitis. *Autoimmun. Rev.* 13 (4-5), 463–466. doi:10.1016/j.autrev.2014.01.028

Dong, J. Y., Xia, K. J., Liang, W., Liu, L. L., Yang, F., Fang, X. S., et al. (2021). Ginsenoside Rb1 Alleviates Colitis in Mice via Activation of Endoplasmic Reticulum-Resident E3 Ubiquitin Ligase Hrd1 Signaling Pathway. *Acta Pharmacol. Sin* 42 (9), 1461–1471. doi:10.1038/s41401-020-00561-9

Du, L., and Ha, C. (2020). Epidemiology and Pathogenesis of Ulcerative Colitis. *Gastroenterol. Clin. North. Am.* 49 (4), 643–654. doi:10.1016/j.gtc.2020.07.005

Eissa, N., Hussein, H., Diarra, A., Elgazzar, O., Gounni, A. S., Bernstein, C. N., et al. (2019). Semaphorin 3E Regulates Apoptosis in the Intestinal Epithelium during the Development of Colitis. *Biochem. Pharmacol.* 166, 264–273. doi:10.1016/j.bcp.2019.05.029

Ekiert, H. M., and Szopa, A. (2020). Biological Activities of Natural Products. *Molecules* 25 (23). doi:10.3390/molecules25235769

Elmaksoud, H. A. A., Motawea, M. H., Desoky, A. A., Elharrif, M. G., and Ibrahimi, A. (2021). Hydroxytyrosol Alleviate Intestinal Inflammation, Oxidative Stress and Apoptosis Resulted in Ulcerative Colitis. *Biomed. Pharmacother.* 142, 112073. doi:10.1016/j.biopha.2021.112073

Elmore, S. (2007). Apoptosis: a Review of Programmed Cell Death. *Toxicol. Pathol.* 35 (4), 495–516. doi:10.1080/01926230701320337

Estaquier, J., Vallette, F., Vayssiere, J. L., and Mignotte, B. (2012). The Mitochondrial Pathways of Apoptosis. *Adv. Exp. Med. Biol.* 942, 157–183. doi:10.1007/978-94-007-2869-1_7

Fan, H., Li, X., Duan, X., and Shi, T. (2020). Cell Apoptosis in the Etiopathogenesis of Ulcerative Colitis. *Chin. J. Integrated Traditional West. Med. Digestion* 10 (3), 189–190.

Fan, T. J., Han, L. H., Cong, R. S., and Liang, J. (2005). Caspase Family Proteases and Apoptosis. *Acta Biochim. Biophys. Sin (Shanghai).* 37 (11), 719–727. doi:10.1111/j.1745-7270.2005.00108.x

Feng, P., Tao, Z., and Jianyong, C. (2010). The Polysaccharide of Portulaca Oleracea Interfered W Ith the Express Ion of Caspase-3 and Caspase-8 in a Rat Expermiental Model of TNBS-Induced Colitis. *CHINESE ARCHIVES TRADITIONAL CHINESE MEDICINE* 28 (8), 1639–1641. doi:10.13193/j.archtcm.2010.08.73.panf.074

Franke, T. F., Hornik, C. P., Segev, L., Shostak, G. A., and Sugimoto, C. (2003). PI3K/Akt and Apoptosis: Size Matters. *Oncogene* 22 (56), 8983–8998. doi:10.1038/sj.onc.1207115

Fresno Vara, J. A., Casado, E., de Castro, J., Cejas, P., Belda-Iniesta, C., and Gonzalez-Baron, M. (2004). PI3K/Akt Signalling Pathway and Cancer. *Cancer Treat. Rev.* 30 (2), 193–204. doi:10.1016/j.ctrv.2003.07.007

Gao, W., Wang, C., Yu, L., Sheng, T., Wu, Z., Wang, X., et al. (2019). Chlorogenic Acid Attenuates Dextran Sodium Sulfate-Induced Ulcerative Colitis in Mice through MAPK/ERK/JNK Pathway. *Biomed. Res. Int.* 2019, 6769789. doi:10.1155/2019/6769789

Gao, W., Zhang, L., Wang, X., Yu, L., Wang, C., and Gong, Y. (2018). The Combination of Indirubin and Isatin Attenuates Dextran Sodium Sulfate Induced Ulcerative Colitis in Mice. *Biochem. Cel Biol* 96 (5), 636–645. doi:10.1139/bcb-2018-0041

Gu, B. H., Minh, N. V., Lee, S. H., Lim, S. W., Lee, Y. M., Lee, K. S., et al. (2010). Deoxyschisandrin Inhibits H2O2-Induced Apoptotic Cell Death in Intestinal Epithelial Cells through Nuclear Factor-kappaB. *Int. J. Mol. Med.* 26 (3), 401–406.

Gu, P., Zhu, L., Liu, Y., Zhang, L., Liu, J., and Shen, H. (2017). Protective Effects of Paeoniflorin on TNBS-Induced Ulcerative Colitis through Inhibiting NF-kappaB Pathway and Apoptosis in Mice. *Int. Immunopharmacol* 50, 152–160. doi:10.1016/j.intimp.2017.06.022

Hagiwara, C., Tanaka, M., and Kudo, H. (2002). Increase in Colorectal Epithelial Apoptotic Cells in Patients with Ulcerative Colitis Ultimately Requiring Surgery. *J. Gastroenterol. Hepatol.* 17 (7), 758–764. doi:10.1046/j.1440-1746.2002.02791.x

Hassanshahi, N., Masoumi, S. J., Mehrabani, D., Hashemi, S. S., and Zare, M. (2020). The Healing Effect of Aloe Vera Gel on Acetic Acid-Induced Ulcerative Colitis in Rat. *Middle East. J. Dig. Dis.* 12 (3), 154–161. doi:10.34172/mejdd.2020.177

Heinrich, M., Appendino, G., Efferth, T., Furst, R., Izzo, A. A., Kayser, O., et al. (2020). Best Practice in Research - Overcoming Common Challenges in Phytopharmacological Research. *J. Ethnopharmacol* 246, 112230. doi:10.1016/j.jep.2019.112230

Helal, M. G., and Abd Elhameed, A. G. (2021). Graviola Mitigates Acetic Acid-Induced Ulcerative Colitis in Rats: Insight on Apoptosis and Wnt/Hh Signaling Crosstalk. *Environ. Sci. Pollut. Res. Int.* 28 (23), 29615–29628. doi:10.1007/s11356-021-12716-0

Hetz, C. (2012). The Unfolded Protein Response: Controlling Cell Fate Decisions under ER Stress and beyond. *Nat. Rev. Mol. Cel Biol* 13 (2), 89–102. doi:10.1038/nrm3270

Heyninck, K., and Beyaert, R. (2001). Crosstalk between NF-kappaB-Activating and Apoptosis-Inducing Proteins of the TNF-Receptor Complex. *Mol. Cel Biol Res Commun* 4 (5), 259–265. doi:10.1006/mcbr.2001.0295

Huang, X. L., Xu, J., Zhang, X. H., Qiu, B. Y., Peng, L., Zhang, M., et al. (2011). PI3K/Akt Signaling Pathway Is Involved in the Pathogenesis of Ulcerative Colitis. *Inflamm. Res.* 60 (8), 727–734. doi:10.1007/s00011-011-0325-6

Iwamoto, M., Koji, T., Makiyama, K., Kobayashi, N., and Nakane, P. K. (1996). Apoptosis of Crypt Epithelial Cells in Ulcerative Colitis. *J. Pathol.* 180 (2), 152–159. doi:10.1002/(SICI)1096-9896(199610)180:2<152:AID-PATH649>3.0.CO;2-Y

Jeong, S. Y., and Seol, D. W. (2008). The Role of Mitochondria in Apoptosis. *BMB Rep.* 41 (1), 11–22. doi:10.5483/bmbrep.2008.41.1.011

Kantari, C., and Walczak, H. (2011). Caspase-8 and Bid: Caught in the Act between Death Receptors and Mitochondria. *Biochim. Biophys. Acta* 1813 (4), 558–563. doi:10.1016/j.bbamcr.2011.01.026

Ke, F., Yadav, P. K., and Ju, L. Z. (2012). Herbal Medicine in the Treatment of Ulcerative Colitis. *Saudi J. Gastroenterol.* 18 (1), 3–10. doi:10.4103/1319-3767.91726

Kim, M., Chung, K. S., Hwang, S. J., Yoon, Y. S., Jang, Y. P., Lee, J. K., et al. (2020). Protective Effect of Cicer Arietinum L. (Chickpea) Ethanol Extract in the Dextran Sulfate Sodium-Induced Mouse Model of Ulcerative Colitis. *Nutrients* 12 (2). doi:10.3390/nu12020456

Kong, R., Luo, H., Wang, N., Li, J., Xu, S., Chen, K., et al. (2018). Portulaca Extract Attenuates Development of Dextran Sulfate Sodium Induced Colitis in Mice through Activation of PPARgamma. *PPAR Res.* 2018, 6079101. doi:10.1155/2018/6079101

Lanzhen, L., Shuangyan, L., Ye, W., and Xiaoli, S. (2020). Effects of Paeoniflorin on Expressions of Beclin1 and Bcl-2 in Colon Tissue of Rats with DSS-Induced Chronic Ulcerative Colitis (China). *Chin. J. Traditional Med. Sci. Technology* 27 (6), 885–889.

Li, Q., Chen, M., Liu, H., Yang, L., Yang, T., and He, G. (2014). The Dual Role of ERK Signaling in the Apoptosis of Neurons. *Front. Biosci. (Landmark Ed.* 19, 1411–1417. doi:10.2741/4291

Li, Q., Li, K., Hu, T., Liu, F., Liao, S., and Zou, Y. (2021). 6,7-Dihydroxy-2,4-Dimethoxyphenanthrene from Chinese Yam Peels Alleviates DSS-Induced Intestinal Mucosal Injury in Mice via Modulation of the NF-kappaB/COX-2 Signaling Pathway. *J. Agric. Food Chem.* 69 (16), 4720–4731. doi:10.1021/acs.jafc.1c00487

Lin, H., Honglang, L., Weifeng, L., Junmin, C., Jiantao, Y., and Junjing, G. (2017). The Mechanism of Alopolysaccharide Protecting Ulceralive Colitis. *Biomed. Pharmacother.* 88, 145–150. doi:10.1016/j.biopha.2016.11.138

Lin, J. C., Wu, J. Q., Wang, F., Tang, F. Y., Sun, J., Xu, B., et al. (2019). QingBai Decoction Regulates Intestinal Permeability of Dextran Sulphate Sodium-Induced Colitis through the Modulation of Notch and NF-kappaB Signalling. *Cell Prolif* 52 (2), e12547. doi:10.1111/cpr.12547

Liu, D., Huang, X., Cheng, S., Tong, W., Wan, P., Guan, Y., et al. (2011). Regulation of Sishen Wan on Bax/Bcl-2 mRNA, Fas/FasL in Colonic Tissue from Rats with Colitis (China). *Zhongguo Zhong Yao Za Zhi* 36 (24), 3484–3488.

Liu, D., Zhang, M., and Yin, H. (2013). Signaling Pathways Involved in Endoplasmic Reticulum Stress-Induced Neuronal Apoptosis. *Int. J. Neurosci.* 123 (3), 155–162. doi:10.3109/00207454.2012.746974

Liu, F., Bardhan, K., Yang, D., Thangaraju, M., Ganapathy, V., Waller, J. L., et al. (2012). NF-kappaB Directly Regulates Fas Transcription to Modulate Fas-Mediated Apoptosis and Tumor Suppression. *J. Biol. Chem.* 287 (30), 25530–25540. doi:10.1074/jbc.M112.356279

Liu, R., Li, X., Huang, N., Fan, M., and Sun, R. (2020). Toxicity of Traditional Chinese Medicine Herbal and mineral Products. *Adv. Pharmacol.* 87, 301–346. doi:10.1016/bs.apha.2019.08.001

Liu, X., and Wang, J. M. (2011). Iridoid Glycosides Fraction of Folium Syringae Leaves Modulates NF-kappaB Signal Pathway and Intestinal Epithelial Cells Apoptosis in Experimental Colitis. *PLoS One* 6 (9), e24740. doi:10.1371/journal.pone.0024740

Lv, T., Shen, L., Yang, L., Diao, W., Yang, Z., Zhang, Y., et al. (2018). Polydatin Ameliorates Dextran Sulfate Sodium-Induced Colitis by Decreasing Oxidative Stress and Apoptosis Partially via Sonic Hedgehog Signaling Pathway. *Int. Immunopharmacol* 64, 256–263. doi:10.1016/j.intimp.2018.09.009

Mahmoud, T. N., El-Maadawy, W. H., Kandil, Z. A., Khalil, H., El-Fiky, N. M., and El Alfy, T. (2021). Canna X Generalis L.H. Bailey Rhizome Extract Ameliorates Dextran Sulfate Sodium-Induced Colitis via Modulating Intestinal Mucosal Dysfunction, Oxidative Stress, Inflammation, and TLR4/NF-B and NLRP3 Inflammasome Pathways. *J. Ethnopharmacol* 269, 113670. doi:10.1016/j.jep.2020.113670

Miao, F., Shan, C., Ma, T., Geng, S., and Ning, D. (2021). Walnut Oil Alleviates DSS-Induced Colitis in Mice by Inhibiting NLRP3 Inflammasome Activation and Regulating Gut Microbiota. *Microb. Pathog.* 154, 104866. doi:10.1016/j.micpath.2021.104866

Motawea, M. H., Abd Elmaksoud, H. A., Elharrif, M. G., Desoky, A. A. E., and Ibrahimi, A. (2020). Evaluation of Anti-inflammatory and Antioxidant Profile of Oleuropein in Experimentally Induced Ulcerative Colitis. *Int. J. Mol. Cel Med* 9 (3), 224–233. doi:10.22088/IJMCM.BUMS.9.3.224

Nan, B., Ye, W., Rui, W., Li-ting, S., and Yan-qiu, F. (2019). Tripterygium Glycosides Attenuate Intestinal Mucosal Apoptosis and Inflammation in Rats with Ulcerative Colitis through JAK2/STAT3 Signaling Pathway (China). *Mod. Digestion & Intervention* 24 (5), 466–470.

Nascimento, R. P. D., Machado, A., Galvez, J., Cazarin, C. B. B., and Marostica Junior, M. R. (2020). Ulcerative Colitis: Gut Microbiota, Immunopathogenesis and Application of Natural Products in Animal Models. *Life Sci.* 258, 118129. doi:10.1016/j.lfs.2020.118129

Ng, S. C., Shi, H. Y., Hamidi, N., Underwood, F. E., Tang, W., Benchimol, E. I., et al. (2017). Worldwide Incidence and Prevalence of Inflammatory Bowel Disease in the 21st century: a Systematic Review of Population-Based Studies. *Lancet* 390 (10114), 2769–2778. doi:10.1016/S0140-6736(17)32448-0

Nooh, H. Z., and Nour-Eldien, N. M. (2016). The Dual Anti-inflammatory and Antioxidant Activities of Natural Honey Promote Cell Proliferation and Neural Regeneration in a Rat Model of Colitis. *Acta Histochem.* 118 (6), 588–595. doi:10.1016/j.acthis.2016.06.006

Polat, F. R., and Karaboga, I. (2019). Immunohistochemical Examination of Anti-inflammatory and Anti-apoptotic Effects of Hesperetin on Trinitrobenzene Sulfonic Acid Induced Colitis in Rats. *Biotech. Histochem.* 94 (3), 151–158. doi:10.1080/10520295.2018.1530454

Pugliese, D., Felice, C., Papa, A., Gasbarrini, A., Rapaccini, G. L., Guidi, L., et al. (2017). Anti TNF-Alpha Therapy for Ulcerative Colitis: Current Status and Prospects for the Future. *Expert Rev. Clin. Immunol.* 13 (3), 223–233. doi:10.1080/1744666X.2017.1243468

Qiu, W., Wu, B., Wang, X., Buchanan, M. E., Regueiro, M. D., Hartman, D. J., et al. (2011). PUMA-mediated Intestinal Epithelial Apoptosis Contributes to Ulcerative Colitis in Humans and Mice. *J. Clin. Invest.* 121 (5), 1722–1732. doi:10.1172/JCI42917

Rapa, S. F., Di Paola, R., Cordaro, M., Siracusa, R., D'Amico, R., Fusco, R., et al. (2021). Plumericin Protects against Experimental Inflammatory Bowel Disease by Restoring Intestinal Barrier Function and Reducing Apoptosis. *Biomedicines* 9 (1). doi:10.3390/biomedicines9010067

Rioux, K. (2008). What Is the Prognosis of Ulcerative Colitis? *Inflamm. Bowel Dis.* 14 (Suppl. 2), S52–S53. doi:10.1002/ibd.20574

Santana, M. T., Cercato, L. M., Oliveira, J. P., and Camargo, E. A. (2017). Medicinal Plants in the Treatment of Colitis: Evidence from Preclinical Studies. *Planta Med.* 83 (7), 588–614. doi:10.1055/s-0043-104933

Schulzke, J. D., Bojarski, C., Zeissig, S., Heller, F., Gitter, A. H., and Fromm, M. (2006). Disrupted Barrier Function through Epithelial Cell Apoptosis. *Ann. N. Y Acad. Sci.* 1072, 288–299. doi:10.1196/annals.1326.027

Schulzke, J. D., Ploeger, S., Amasheh, M., Fromm, A., Zeissig, S., Troeger, H., et al. (2009). Epithelial Tight Junctions in Intestinal Inflammation. *Ann. N. Y Acad. Sci.* 1165, 294–300. doi:10.1111/j.1749-6632.2009.04062.x

Seidelin, J. B., and Nielsen, O. H. (2009). Epithelial Apoptosis: Cause or Consequence of Ulcerative Colitis? *Scand. J. Gastroenterol.* 44 (12), 1429–1434. doi:10.3109/00365520903301212

Sharma, A., Tirpude, N. V., Kulurkar, P. M., Sharma, R., and Padwad, Y. (2020). Berberis Lycium Fruit Extract Attenuates Oxi-Inflammatory Stress and Promotes Mucosal Healing by Mitigating NF-kappaB/c-Jun/MAPKs Signalling and Augmenting Splenic Treg Proliferation in a Murine Model of Dextran Sulphate Sodium-Induced Ulcerative Colitis. *Eur. J. Nutr.* 59 (6), 2663–2681. doi:10.1007/s00394-019-02114-1

Shen, J., Cheng, J., Zhu, S., Zhao, J., Ye, Q., Xu, Y., et al. (2019). Regulating Effect of Baicalin on IKK/IKB/NF-kB Signaling Pathway and Apoptosis-Related Proteins in Rats with Ulcerative Colitis. *Int. Immunopharmacol* 73, 193–200. doi:10.1016/j.intimp.2019.04.052

Shi, L., Dai, Y., Jia, B., Han, Y., Guo, Y., Xie, T., et al. (2019). The Inhibitory Effects of Qingchang Wenzhong Granule on the Interactive Network of Inflammation, Oxidative Stress, and Apoptosis in Rats with Dextran Sulfate Sodium-Induced Colitis. *J. Cel Biochem* 120 (6), 9979–9991. doi:10.1002/jcb.28280

Shuguang, Y., Yi, H., and Jingtao, L. (2016). Effect of Wumei Pill on Apoptosis of Colonic Epithelial Cells in Rats with Ulcerative Colitis (China). *J. Basic Chin. Med.* 22 (6), 771–773.

Song, C., Chen, J., Li, X., Yang, R., Cao, X., Zhou, L., et al. (2021). Limonin Ameliorates Dextran Sulfate Sodium-Induced Chronic Colitis in Mice by Inhibiting PERK-ATF4-CHOP Pathway of ER Stress and NF-kappaB Signaling. *Int. Immunopharmacol* 90, 107161. doi:10.1016/j.intimp.2020.107161

Soubh, A. A., Abdallah, D. M., and El-Abhar, H. S. (2015). Geraniol Ameliorates TNBS-Induced Colitis: Involvement of Wnt/beta-Catenin, p38MAPK, NFkappaB, and PPARgamma Signaling Pathways. *Life Sci.* 136, 142–150. doi:10.1016/j.lfs.2015.07.004

Sun, Y., Liu, W. Z., Liu, T., Feng, X., Yang, N., and Zhou, H. F. (2015). Signaling Pathway of MAPK/ERK in Cell Proliferation, Differentiation, Migration, Senescence and Apoptosis. *J. Recept Signal. Transduct Res.* 35 (6), 600–604. doi:10.3109/10799893.2015.1030412

Tan, Y., Dourdin, N., Wu, C., De Veyra, T., Elce, J. S., and Greer, P. A. (2006). Ubiquitous Calpains Promote Caspase-12 and JNK Activation during Endoplasmic Reticulum Stress-Induced Apoptosis. *J. Biol. Chem.* 281 (23), 16016–16024. doi:10.1074/jbc.M601299200

Taya, S., Kakehashi, A., Wongpoomchai, R., Gi, M., Ishii, N., and Wanibuchi, H. (2016). Preventive Effects of Spirogyra Neglecta and a Polysaccharide Extract against Dextran Sodium Sulfate Induced Colitis in Mice. *Asian Pac. J. Cancer Prev.* 17 (4), 2235–2245. doi:10.7314/apjcp.2016.17.4.2235

Thorburn, A. (2004). Death Receptor-Induced Cell Killing. *Cell Signal* 16 (2), 139–144. doi:10.1016/j.cellsig.2003.08.007

Topcu-Tarladacalisir, Y., Akpolat, M., Uz, Y. H., Kizilay, G., Sapmaz-Metin, M., Cerkezkayabekir, A., et al. (2013). Effects of Curcumin on Apoptosis and Oxidoinflammatory Regulation in a Rat Model of Acetic Acid-Induced Colitis: the Roles of C-Jun N-Terminal Kinase and P38 Mitogen-Activated Protein Kinase. *J. Med. Food* 16 (4), 296–305. doi:10.1089/jmf.2012.2550

Triantafyllidi, A., Xanthos, T., Papalois, A., and Triantafillidis, J. K. (2015). Herbal and Plant Therapy in Patients with Inflammatory Bowel Disease. *Ann. Gastroenterol.* 28 (2), 210–220.

Valmiki, M. G., and Ramos, J. W. (2009). Death Effector Domain-Containing Proteins. *Cell Mol Life Sci* 66 (5), 814–830. doi:10.1007/s00018-008-8489-0

Vanamee, E. S., and Faustman, D. L. (2018). Structural Principles of Tumor Necrosis Factor Superfamily Signaling. *Sci. Signal.* 11 (511). doi:10.1126/scisignal.aao4910

Verstege, M. I., te Velde, A. A., and Hommes, D. W. (2006). Apoptosis as a Therapeutic Paradigm in Inflammatory Bowel Diseases. *Acta Gastroenterol. Belg.* 69 (4), 406–412.

Vivanco, I., and Sawyers, C. L. (2002). The Phosphatidylinositol 3-Kinase AKT Pathway in Human Cancer. *Nat. Rev. Cancer* 2 (7), 489–501. doi:10.1038/nrc839

Vukelic, I., Detel, D., Baticic, L., Potocnjak, I., and Domitrovic, R. (2020). Luteolin Ameliorates Experimental Colitis in Mice through ERK-Mediated Suppression of Inflammation, Apoptosis and Autophagy. *Food Chem. Toxicol.* 145, 111680. doi:10.1016/j.fct.2020.111680

Wan, P., Chen, H., Guo, Y., and Bai, A. P. (2014). Advances in Treatment of Ulcerative Colitis with Herbs: from Bench to Bedside. *World J. Gastroenterol.* 20 (39), 14099–14104. doi:10.3748/wjg.v20.i39.14099

Wang, X., Li, D., Zhang, Y., Wu, S., and Tang, F. (2018). Costus Root Granules Improve Ulcerative Colitis through Regulation of TGF-Beta Mediation of the PI3K/AKT Signaling Pathway. *Exp. Ther. Med.* 15 (5), 4477–4484. doi:10.3892/etm.2018.5946

Wang, Y., Liu, J., Huang, Z., Li, Y., Liang, Y., Luo, C., et al. (2021). Coptisine Ameliorates DSS-Induced Ulcerative Colitis via Improving Intestinal Barrier Dysfunction and Suppressing Inflammatory Response. *Eur. J. Pharmacol.* 896, 173912. doi:10.1016/j.ejphar.2021.173912

Wehkamp, J., and Stange, E. F. (2018). Recent Advances and Emerging Therapies in the Non-surgical Management of Ulcerative Colitis. *F1000Res* 7. doi:10.12688/f1000research.15159.1

Weijie, P., Lianfeng, Z., and Liang, L. (2019). A Study on Effect of Astragalus Polysaccharide on Rats with Ulcerative Colitis and its Mechanism (China). *JOURNAL NEW CHINESE MEDICINE* 51 (9), 13–16. doi:10.13457/j.cnki.jncm.2019.09.004

Wenqiang, M., Kun, Y., Xin, T., and Linxuan, S. (2019). The Therapeutic Effect and Mechanism of Indigo on Dextran Sulfate Sodium Induced Ulcerative Colitis in Mice (China). *Prog. Anatomical Sci.* 25 (2), 146–149. doi:10.16695/j.cnki.1006-2947.2019.02.010

Wu, H., Zhong, R. L., Xia, Z., Huang, H. C., Zhong, Q. X., Feng, L., et al. (2016). Research Progress on Potential Liver Toxic Components in Traditional Chinese Medicine. *Zhongguo Zhong Yao Za Zhi* 41 (17), 3209–3217. doi:10.4268/cjcmm20161715

Xian-juan, Y., Yin, F., Jian, W., and al, e. (2020). Protective Effect of Compatibility of Coptidis Rhizoma and Magnoliae Officinalis Cortex on Rat Model of Ulcerative Colitis and Influence of Apoptosis (China). *Chin. J. Exp. Traditional Med. Formulae* 26 (23), 83–91. doi:10.13422/j.cnki.syfjx.20202238

Xiao, H. T., Lin, C. Y., Ho, D. H., Peng, J., Chen, Y., Tsang, S. W., et al. (2013). Inhibitory Effect of the Gallotannin Corilagin on Dextran Sulfate Sodium-Induced Murine Ulcerative Colitis. *J. Nat. Prod.* 76 (11), 2120–2125. doi:10.1021/np4006772

Xiaobin, Z., and Xiaodong, X. (2014). Effects of Laggera Alata Flavone on Ulcerative Colitis and its Mechanism (China). *CHINESE ARCHIVES TRADITIONAL CHINESE MEDICINE* 32 (12), 3028–3030. doi:10.13193/j.issn.1673-7717.2014.12.069

Yan, D., and Jingen, L. (2016). The Effects of Aucklandia and Coptis Pills on Cellular Apoptosis and the Expression of Bcl-2 and Bax mRNA in Model Rats with Ulcerative Colitis (China). *West China Med. J.* 31 (6), 1046–1051. doi:10.7507/1002-0179.201600281

Yan, J., Ouyang, Q., Chen, D., et al. (2001). The Role of Fas/FasL-Mediated Colonic Epithelium Apoptosis in Ulcerative Colitis (China). *Chin. J. Dig.* 21 (7), 397–399.

Yan, S., and Bin, L. (2020). Study of Glycyrrhizin Regulating Caspase-12 Apoptosis Signaling Pathway of Endoplasmic Reticulum Stress to Alleviate the Colonic Inflammatory Response in Ulcerative Colitis. *CJTCMP* 35 (8), 3872–3877.

Yan, S., Si-yi, N., Hua-jun, Z., Si, L., and Bin, L. (2021). Mechanisms of Gancao Xiexin Decoction on Protecting Intestinal Mucosal Barrier by Regulating PERK-eIF2α-CHOP Signaling Pathway (China). *China J. Traditional Chin. Med. Pharm.* 36 (5), 2657–2663.

Yan, S., Yingchao, L., Zhangliu, W., Xianli, R., Si, L., Siyi, N., et al. (2020). Effect of Berberine from Coptis Chinensis on Apoptosis of Intestinal Epithelial Cells in a Mouse Model of Ulcerative Colitis: Role of Endoplasmic Reticulum Stress. *Evid. Based Complement. Alternat Med.* 2020, 3784671. doi:10.1155/2020/3784671

Yan, S., Zhangliu, W., Huajun, Z., and al, e. (2018). Effects of Berberine on Apoptosis of Intestinal Epithelial Cells in the Ulcerative Colitis Mice (China). *Zhejiang JITCWM* 28 (12), 992–996.

Yang, M., Liu, W., Tu, H., Li, L., and Fei, S. (2020). Protective Effect of Crocin in Ulcerative Colitis Rats and its Related Mechanism (China). *Chin. J. Tissue Eng. Res.* 24 (29), 4673–4679. doi:10.3969/j.issn.2095-4344.2817

Yao, J., Cao, X., Zhang, R., Li, Y. X., Xu, Z. L., Zhang, D. G., et al. (2016). Protective Effect of Baicalin against Experimental Colitis via Suppression of Oxidant Stress and Apoptosis. *Pharmacogn Mag.* 12 (47), 225–234. doi:10.4103/0973-1296.186342

Yi, H., Shuguang, Y., and Xiaolong, W. (2016). Study on Effect of Wumei Pill in Colonic Epithelial Cell Apoptosis and Expression of Bcl-2/Bax of Ulcerative Colitis in Rats (China). *CHINESE ARCHIVES TRADITIONAL CHINESE MEDICINE* 34 (1), 149–151.

Yin, S., Li, L., Tao, Y., Yu, J., Wei, S., Liu, M., et al. (2021). The Inhibitory Effect of Artesunate on Excessive Endoplasmic Reticulum Stress Alleviates Experimental Colitis in Mice. *Front. Pharmacol.* 12, 629798. doi:10.3389/fphar.2021.629798

Yin, S., Yang, H., Tao, Y., Wei, S., Li, L., Liu, M., et al. (2020). Artesunate Ameliorates DSS-Induced Ulcerative Colitis by Protecting Intestinal Barrier and Inhibiting Inflammatory Response. *Inflammation* 43 (2), 765–776. doi:10.1007/s10753-019-01164-1

Yong, Z., Wen-hua, S., Zheng-xia, Z., Luan, H., Yan-li, L., and Qiong-ming, X. (2020). Experimental Study on Pharmacological Mechanism ofAnemoside B4 in Ulcerative Colitis Induced by Acetic Acid in Rats (China). *Anti Infect. Pharm.* 17 (10), 1405–1410. doi:10.13493/j.issn.1672-7878.2020.10-002

Youle, R. J., and Strasser, A. (2008). The BCL-2 Protein Family: Opposing Activities that Mediate Cell Death. *Nat. Rev. Mol. Cel Biol* 9 (1), 47–59. doi:10.1038/nrm2308

Yu, S., and Qian, H. (2021). Deoxyschizandrin Treats Mice with Ulcerative Colitis Possibly via the TLR4/NF-kappaB Signaling Pathway. *Am. J. Transl Res.* 13 (4), 3856–3863.

Yu, X., Cai, Y., Zhou, S., Cheng, H., Zhou, W., and Li, X. (2021). Therapeutic Effect of Hyperoside in Rats with Ulcerative Colitis and its Mechanism (China). *IMMUNOLOGICAL JOURNAL* 37 (5), 417–424. doi:10.13431/j.cnki.immunol.j.20210058

Yu, Y. R., and Rodriguez, J. R. (2017). Clinical Presentation of Crohn's, Ulcerative Colitis, and Indeterminate Colitis: Symptoms, Extraintestinal Manifestations, and Disease Phenotypes. *Semin. Pediatr. Surg.* 26 (6), 349–355. doi:10.1053/j.sempedsurg.2017.10.003

Yue, J., and Lopez, J. M. (2020). Understanding MAPK Signaling Pathways in Apoptosis. *Int. J. Mol. Sci.* 21 (7). doi:10.3390/ijms21072346

Yukawa, M., Iizuka, M., Horie, Y., Yoneyama, K., Shirasaka, T., Itou, H., et al. (2002). Systemic and Local Evidence of Increased Fas-Mediated Apoptosis in Ulcerative Colitis. *Int. J. Colorectal Dis.* 17 (2), 70–76. doi:10.1007/s003840100340

Zeng, M., Yang, L., He, D., Li, Y., Shi, M., and Zhang, J. (2017). Metabolic Pathways and Pharmacokinetics of Natural Medicines with Low Permeability. *Drug Metab. Rev.* 49 (4), 464–476. doi:10.1080/03602532.2017.1377222

Zhang, J., Lei, H., Hu, X., and Dong, W. (2020a). Hesperetin Ameliorates DSS-Induced Colitis by Maintaining the Epithelial Barrier via Blocking RIPK3/MLKL Necroptosis Signaling. *Eur. J. Pharmacol.* 873, 172992. doi:10.1016/j.ejphar.2020.172992

Zhang, X., Tang, N., Hadden, T. J., and Rishi, A. K. (2011). Akt, FoxO and Regulation of Apoptosis. *Biochim. Biophys. Acta* 1813 (11), 1978–1986. doi:10.1016/j.bbamcr.2011.03.010

Zhang, Y., Han, D., Yu, S., An, C., Liu, X., Zhong, H., et al. (2020b). Protective Effect of Iridoid Glycosides of the Leaves of Syringa Oblata Lindl. On Dextran Sulfate Sodium-Induced Ulcerative Colitis by Inhibition of the TLR2/4/MyD88/NF-kappaB Signaling Pathway. *Biomed. Res. Int.* 2020, 7650123. doi:10.1155/2020/7650123

Zhang, Y., Zha, Z., Shen, W., Li, D., Kang, N., Chen, Z., et al. (2021). Anemoside B4 Ameliorates TNBS-Induced Colitis through S100A9/MAPK/NF-kappaB Signaling Pathway. *Chin. Med.* 16 (1), 11. doi:10.1186/s13020-020-00410-1

Zhao, H. M., Huang, X. Y., Zhou, F., Tong, W. T., Wan, P. T., Huang, M. F., et al. (20132013). Si Shen Wan Inhibits mRNA Expression of Apoptosis-Related Molecules in P38 MAPK Signal Pathway in Mice with Colitis. *Evid. Based Complement. Alternat Med.*, 432097. doi:10.1155/2013/432097

Zhu, H., Tong, S., Cui, Y., Wang, X., and Wang, M. (2021). Tanshinol Alleviates Ulcerative Colitis by Promoting the Expression of VLDLR. *Drug Dev. Res.*. doi:10.1002/ddr.21840

Zhu, L., Dai, L. M., Shen, H., Gu, P. Q., Zheng, K., Liu, Y. J., et al. (2019a). Qing Chang Hua Shi Granule Ameliorate Inflammation in Experimental Rats and Cell Model of Ulcerative Colitis through MEK/ERK Signaling Pathway. *Biomed. Pharmacother.* 116, 108967. doi:10.1016/j.biopha.2019.108967

Zhu, L., Gu, P., and Shen, H. (2019b). Gallic Acid Improved Inflammation via NF-kappaB Pathway in TNBS-Induced Ulcerative Colitis. *Int. Immunopharmacol* 67, 129–137. doi:10.1016/j.intimp.2018.11.049

Zhu, L., Shen, H., Zhang, L., and al, e. (2017). Effects of Baicalin on the Inflammation and Apoptosis in Ulcerative Colitis Rats Relating to PI3K/AKT Pathway (China). *China J. Traditional Chin. Med. Pharm.* 32 (9), 4001–4004.

Conflict of Interest: The authors declare that the research was conducted in the absence of any commercial or financial relationships that could be construed as a potential conflict of interest.

Publisher's Note: All claims expressed in this article are solely those of the authors and do not necessarily represent those of their affiliated organizations, or those of the publisher, the editors and the reviewers. Any product that may be evaluated in this article, or claim that may be made by its manufacturer, is not guaranteed or endorsed by the publisher.

Copyright © 2022 Liu, Zeng, Wen, Huang and Liu. This is an open-access article distributed under the terms of the Creative Commons Attribution License (CC BY). The use, distribution or reproduction in other forums is permitted, provided the original author(s) and the copyright owner(s) are credited and that the original publication in this journal is cited, in accordance with accepted academic practice. No use, distribution or reproduction is permitted which does not comply with these terms.

frontiers in Pharmacology

REVIEW
published: 09 February 2022
doi: 10.3389/fphar.2021.796300

Apoptosis Triggering, an Important Way for Natural Products From Herbal Medicines to Treat Pancreatic Cancers

Meiyan Li[†], *Dandan Tang*[†], *Ting Yang, Die Qian and Runchun Xu* *

School of Pharmacy, Chengdu University of Traditional Chinese Medicine, Chengdu, China

Pancreatic cancer, a poor prognosis and high morbidity and mortality cancer, is a malignant tumor occurring in pancreatic exocrine glands. Currently, surgery and gemcitabine (Gem) are commonly used to treat pancreatic cancers. However, the high recurrence rate and resistance makes the therapeutic effects still unsatisfied. Apoptosis is comprehensively recognized as one of the major ways of the programmed cell death, refers to the autonomous and orderly death process of cells in order to maintain the stability of the body's environment after receiving a certain signal or stimulation. Currently, it has also been proven to be a promising way for the treatment of pancreatic cancer. Nowadays, some active ingredients from herbal medicine have been reported to be effective for the treatment of pancreatic cancer via inducing cells apoptosis. Therefore, this article reviews the current references regarding anti pancreatic cancer effects of natural products derived from herbal medicines via triggering apoptosis, and summarizes the related potential signal pathways, including death receptors mediated apoptotic pathway, mitochondrial dependent apoptotic pathway, NF-κB mediated apoptotic pathways, MAPK mediated apoptotic pathway, ERS mediated apoptotic pathway, PI3K-Akt mediated apoptotic pathway, and other pathways such as JAK-STAT signal pathway, which can lay a certain foundation for the research and development of new natural products against pancreatic cancer.

Keywords: natural products, herbal medicine, pancreatic cancer, apoptosis, signal pathways

OPEN ACCESS

Edited by:
Hong Zhang,
Shanghai University of Traditional Chinese Medicine, China

Reviewed by:
Chunyu Li,
Chinese Academy of Medical Sciences and Peking Union Medical College, China
Xu Wu,
Southwest Medical University, China
Xiao Li Li,
Chongqing Medical University, China

***Correspondence:**
Runchun Xu
19972016@cdutcm.edu.cn

[†]These authors have contributed equally to this work

Specialty section:
This article was submitted to Pharmacology of Anti-Cancer Drugs, a section of the journal Frontiers in Pharmacology

Received: *16 October 2021*
Accepted: *08 December 2021*
Published: *09 February 2022*

Citation:
Li M, Tang D, Yang T, Qian D and Xu R (2022) Apoptosis Triggering, an Important Way for Natural Products From Herbal Medicines to Treat Pancreatic Cancers. Front. Pharmacol. 12:796300. doi: 10.3389/fphar.2021.796300

INTRODUCTION

Pancreatic cancer, also called "King of the cancer", is one of the most malignant tumors of the digestive tract, and mostly of them are ductal adenocarcinoma originating from the ductal epithelium (Xu, 2019). With the progress of China's population aging and changes in residents' lifestyle and diet, the incidence of pancreatic cancer would continue to increase, becoming a major public health problem threatening human life and health. Pancreatic cancer has the characteristics of high degree of malignancy, insidious onset, and poor prognosis. Currently, similar to other cancers, surgery remains the predominant way for radical cure of pancreatic cancer, however patients undergoing surgical treatment are prone to recurrence and metastasis, which is one of the main reasons for the extremely poor prognosis of pancreatic cancer. Therefore, the chance of being controlled by surgical resection is only 10–15%. Gemcitabine (Gem) is commonly used as one of the first line drugs for the treatment of advanced pancreatic cancers (Li et al., 2014) due to its main metabolites can be

incorporated into the DNA of tumor cells to activate apoptotic pathway of tumor cells. But after Gem acts on pancreatic cancer, NF-κB expression activity is abnormally increased in pancreatic cancer patients. NF-κB is an important regulator of the Bcl-2 promoter of the inhibitor of apoptosis protein. The abnormal increase in NF-κB activity leads to the activation of the Bcl-2 promoter, which ultimately leads to the acceleration of the proliferation and division of cancer cells via inhibition of apoptosis, which is an important reason for Gem resistance (Jin, 2013). Therefore, there is an urgent to develop new treatment methods and drugs for pancreatic cancer to provide better help for patients. Interestingly, current studies have shown that abundant natural effective ingredients could help induce apoptosis in various types of tumor cells, including lung cancers, pancreatic cancer cells and liver cancers, etc (Wu et al., 2015; Newman and Cragg, 2020). Compared to Gem, effective ingredients in herbal medicine are high curative effect, low toxic and resistance. Therefore, herbal medicine and ethnic medicines have become a hotspot to search for anti-cancer active ingredients. Apoptosis induction is an important mechanism of herbal medicine in the treatment of pancreatic cancer, which is a self-protection mechanism activated, expressed, and regulated by a series of specific genes. If the apoptosis signaling pathway is disordered, it will directly lead to the occurrence and progression of cancer.

Currently, much attentions have focused on the mechanism of herbal medicine inducing pancreatic cancer cell apoptosis, unfortunately the mechanisms were not clear. Therefore, the present paper aims to summarize the anticancer agents against pancreatic cancer cells derived from herbal medicines including extracts and monomers via inducing apoptosis, which would be beneficial for finding novel candidate drugs from herbal medicines for treating pancreatic cancers.

Apoptosis and Pancreatic Cancer

Currently, the cell death modes discovered mainly include apoptosis, necrosis, autophagy, and pyroptosis, which have great differences in morphological characteristics and biochemical signal transduction. Apoptosis is established as the major mechanism of development and programmed cell death (Peng et al., 2015). In 1972, Kerr first used the term "apoptosis" to describe the unique death pattern of cells. Apoptosis is characterized by morphological changes of the cell targeted for death that include nuclear fragmentation and condensation, mitochondrial outer membrane permeabilization, membrane blebbing, cell shrinkage and apoptotic body formation. The study of different model systems has revealed the important role of apoptosis in normal development and homeostasis. Apoptosis refers to the autonomous and orderly death process of cells in order to maintain the stability of the body's environment after receiving a certain signal or stimulation (Wang., 2018). That is to say, apoptosis is a self-protection mechanism activated, expressed, and regulated by a series of specific genes (Zhang et al., 2019). In addition, apoptosis also plays a defensive role in immune response or clearing damaged cells. Apoptosis can be used as a quality control for homeostasis (Liu et al., 2017). Pancreatic Cancer evolves through precursor lesions, known as pancreatic intraepithelial neoplasia (PanIN 1–3) to invasive ductal cancer. PanINs originate from the small pancreatic ducts, but the cell of origin of these PanINs or Pancreatic Cancer, whether ductal, acinar, or progenitor cell, remains elusive. But in the end different step-wise molecular alterations bring about the development of Pancreatic Cancer from PanINs. Other hits in the genome need to be sequentially accrued for the evolution of invasive cancer from the hyperplastic PanIN1. These include telomere shortening (PanIN1), loss of function of the tumor suppressor p16INK4a (PanIN2) and loss of function of tumor suppressors SMAD4 and TP53 (PanIN 3). These subcellular changes lead to down-regulation of apoptotic machinery (Modi, et al., 2016). Therefore, how to promote the apoptosis of pancreatic cancer cells provides a feasible direction for the development of anti-pancreatic cancer drugs.

Natural Products From Herbal Medicines Have Potential Effects Against Pancreatic Cancer Through Apoptosis.

Apoptosis ways mainly include mitochondrial dependent apoptotic pathway, and death receptors mediated apoptotic pathway, etc. In this part, we summarized the reported natural products including extracts and monomers against pancreatic cancers via triggering apoptosis, and introduced them based on the apoptotic pathways or signal transduction ways.

Death Receptors Mediated Apoptotic Pathway

The death receptor mediated apoptotic pathway, is mainly triggered by extracellular stimuli which are commonly recognized by the tumor necrosis factor receptor (TNFR) family of proteins, such as TNFR, Fas and TRAIL-R. Activated death receptors by their ligands, such as TNF-α, FasL, and TRAI, would further form the death inducing signaling complex, and subsequently bind to the Caspase-8, resulting in the activation of Caspase-8. Then, the activated Caspase-8 could further activate the Caspase-dependent apoptotic pathway via two routes. First, the activated Caspase-8 catalyzes Caspases (including Caspase-3 and -7) to induce apoptosis. Secondly, the activated Caspase-8 can activate the cleavage of Bid to trigger the mitochondrial dependent apoptotic pathway, promoting the release of Cytochrome C (Cyt-C) into cytoplasm from mitochondria, apoptosome formation, Caspase-cascade reaction, PARP cleavage, and ultimately leading to cell apoptosis (Scatizzi et al., 2007).

As early as 2006, Wang et al. found that the apoptosis induced by Triptolide is related to the activation of Caspase-3 and Caspase-8 and the cleavage of polymerase and Bid (Bcl-2 interacting domain death agonist) (Wang et al., 2006). DcR3 is a new member of TNFR superfamily, also known as TR6 or M68. It is a special apoptosis inhibitor that can be combined with tumor necrosis factor Fas L and negatively regulate their mediated cells (Sun et al., 2013). In 2012, Wang et al. found that Triptolide can induce apoptosis in pancreatic cancer cells by down-regulating DcR3 and up-regulating FADD, down-

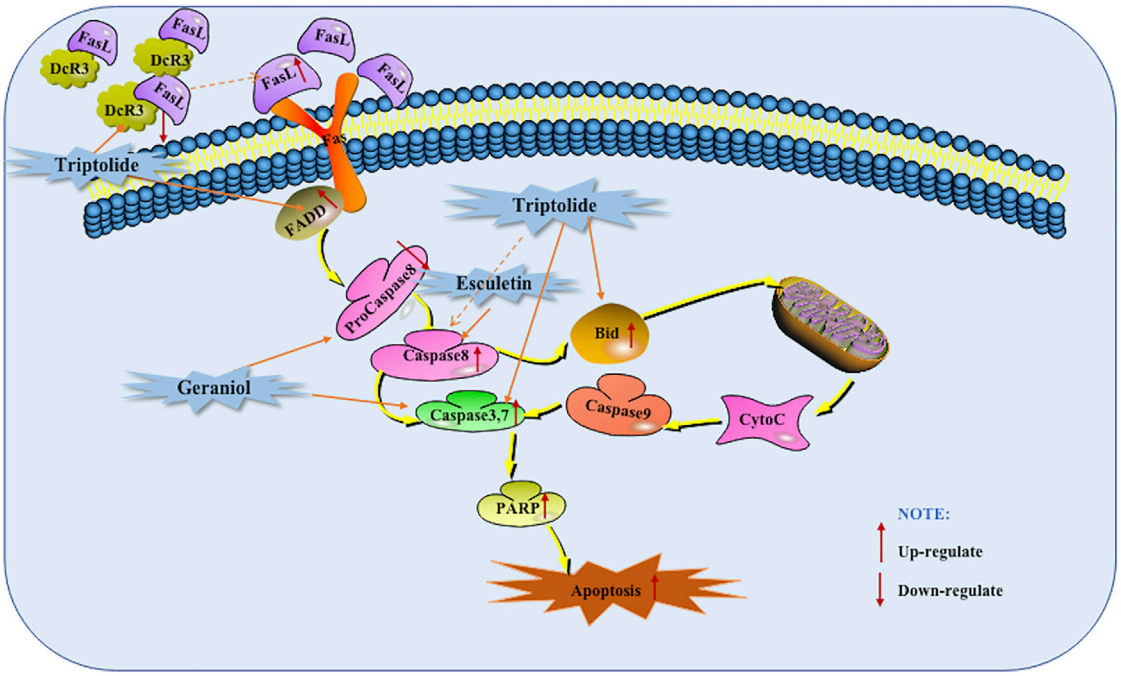


FIGURE 1 | Death receptors mediated apoptotic pathway of pancreatic cancer induced by herbal medicines.

regulating DcR3 promoted the cleavage of Bid and Caspase-3 and the activation of Caspase-8 was also found. And further *in vivo* studies found that Triptolide decreased DcR3 levels and increased cleaved caspase-3, and found that the tumor suppressor effect of Triptolide can be significantly enhanced by DcR3 siRNA (Wang et al., 2012). In 2013, Jin found that the use of Geraniol can reduce the tumor volume in BALB/c mice, and it becomes more obvious as the number of days increases. Further *in vitro* studies found that Geraniol induced BXPC-3 cells apoptosis is related to the down-regulation of pro-Caspase-8 and pro-Caspase-3 (Jin, 2013). In addition, Arora et al., in 2016 also found that the use of Esculetin increased the cleavage of Caspase-8, which also indicates that the extrinsic apoptotic pathway is activated (Arora et al., 2016). The potential mechanisms of herbal medicine for inducing apoptosis in this part are summarized in **Figure 1** and **Table 1**.

Mitochondrial Dependent Apoptotic Pathway

Mitochondria are the energy factories for cell activities, and the integrity of the structure and function of mitochondria is an important prerequisite to ensure the normal life activities of cells. Mitochondria mediated cell apoptosis is also known as the endogenous pathway of cell apoptosis, When the molecules separating the outer and inner mitochondrial membranes are released into the cytoplasm through the outer mitochondrial membrane permeabilization (MOMP), the Mitochondrial dependent apoptotic pathway begins. The process is controlled by anti-apoptotic proteins and pro-apoptotic proteins of Bcl-2 family.

In the Bcl-2 family, the anti-apoptotic proteins include Bcl-2, A1, Mcl-1, and the pro-apoptotic members were further divided into effector molecules, [e.g., Bak (Bcl-2 antagonist killer 1), Bax (Bcl-2 associated x protein)] and BH3-only proteins, [e.g., Bad (Bcl-2 antagonist of cell death), Bim (Bcl-2 interacting mediator of cell death), Bid (Bcl-2 interacting domain death agonist), Bik (Bcl-2 interacting killer) and Puma (p53-upregulated modulator of apoptosis)] (Chipuk and Green, 2008). If Bax and Bak are transferred from cytoplasm to mitochondrial membrane, forming transmembrane pores and decreasing the mitochondrial membrane potential (MCMP). At the same time, due to the disruption of the pro-apoptotic/anti-apoptotic protein balance, the permeability transition pore (PT) is induced to open, which further reduces the MCMP, thereby increasing the permeability of the mitochondrial membrane and promoting the release of Cyt-C. In turn, the mitochondrial respiratory chain will function abnormally and the cell will die due to lack of ATP. Cyt-C is not only involved in electron transport but also an important apoptosis initiation protein, because Cyt-C in the cytoplasm combines with APaf-1 protein and then combines with dATp/ATP to form a trimer and then oligomerizes to become apoptotic protein. The CARD domain is exposed after APaf-1 oligomerization and specifically adsorbs Caspase-9 zymogen into the apoptotic body. Caspase-9 is activated and therefore reaches a series of downstream Caspases into the apoptosis process and ultimately leads to apoptosis. (Jin., 2013; Lai et al., 2021). Nowadays, increasing scientific evidences have suggested that natural products are effective agents for the treatment of pancreatic cancer based on induction of mitochondrial dependent apoptosis.

TABLE 1 | Apoptosis-inducing activity of Chinese herbal medicine and its active ingredients in pancreatic cancer cells.

Potential pathways	Detail mechanisms	Extracts/ Monomers	Cells/animals	Related genes/Proteins	Refs
Death receptors mediated apoptotic pathway	Activate Caspase-3 and -8; Crack Bid	Triptolide	PANC-1 cells	Caspase-3, Caspase-8; Bid	Wang et al. (2006)
	Down-regulate DcR3	Triptolide	AsPC-1, MiaPaCa-2, BxPC-3, PANC-1, SW480 cells, Athymic mice	DcR3	Wang et al. (2012)
	Up-regulating Caspase-3 and -8	Geraniol	BXPC-3, HPC-Y5 cells; BALB/c Nude mice	Caspase-8, Caspase-3	Jin. (2013)
	Increase Caspase-8	Esculetin	PANC-1, MIA PaCa-2, AsPC-1 cell lines	Caspase-8	Arora et al. (2016)
Mitochondrial dependent apoptotic pathway	Increase Bax and Caspase-3; Increase Cyt-C and AIF	Capsaicin	AsPC-1, BxPC-3 cells	Bax, Caspase-3, Cyt-C, AIF	Zhang et al. (2008)
	Up-regulating Caspase-3 and Bax	Triptolide	SW1990 cell line	Caspase-3, Bax	Zhou et al. (2008)
	Increase miR-204, Decrease Mcl-1	Triptolide	Cancer patients; S2-VP10, AsPC-1, MIA PaCa-2	miR-204, Mcl-1	Chen et al. (2013)
	Up-regulating Bim; Activate Caspase-3	Resveratrol	PANC-1, MIA PaCa-2, Hs766T, AsPC-1 cells	Bim, Caspase-3	Roy et al. (2011)
	Down-regulate Mcl-1; Up-regulating Puma, Bim	Resveratrol	PANC-1, BxPC-3 cells	Mcl-1, Puma, Bim	Duan et al. (2016)
	Decrease Bcl-2/Bax	Casticin	PANC-1, BxPC3, HPAC, COS-7, FRT cells	Bcl-2, Bax	Ding., (2012)
	Up-regulating ROS; Decrease Bcl-2/Bax; Up-regulating Cyt-C; Activate Caspase-3	Isoalantolactone	PANC-1, BxPC3, HPAC, COS-7, FRT cells	Bcl-2, Bax, Cyt-C, Caspase-3	Ding., (2012)
	Down-regulate Bcl-2 and Bcl-xl; Up-regulating Bax; Activate Caspase-3	Proanthocyanidins	Female athymic nude mice; Miapaca-2, PANC-1, AsPC-1 cells	Bcl-2, Bcl-xl, Bax, Caspase-3	Prasad et al. (2012)
	Decrease Bcl-2/Bax; Activate Caspase-3	Oridonin	PANC-1 cells	Bcl-2, Bax, Caspase-3	Qi et al. (2012)
	Decrease MCMP (Δ ψ m); Down-regulate Bcl-2; Up-regulating caspase-3 and -9	Brucein D	Capan-2 cells	Bcl-2, Caspase-9; Caspase-3	Liu et al. (2012)
	Increase Cyt-C; Activate Caspase pathway	Geraniol	BXPC-3, HPC-Y5 cells; BALB/c Nude mice	Cyt-C	Jin., (2013)
	Up-regulating Bax, Bad, Puma; BIM, PARP, Caspase-7; Down-regulating Bcl-2, Bcl-XL	Terphenyllin	PANC-1, AsPC-1, CFPAC1, HPNE, SW 1990, Capan-2, HPAC cells	Bax, Bad, Puma, Bim, PARP, Caspase-7, Bcl-2, Bcl-x1, Bcl-2, Ser70, Caspase-7	Zhang.et al. (2020)
	Up-regulating Caspase-3 and -9, Bak; Down-regulating Bcl-XL; Increase; Decrease MCMP (Δ ψ m); Bcl-XL, Bak	Quercetin	PANC-1 cells	Caspase-9, Caspase-3	Lee et al. (2013)
	Up-regulating Bak, Caspase-3 &-9; Down-regulating Bcl-2, Bcl-XL; Increase Cyt-C	Bitter gourd juice	BxPC-3, MiaPaCa-2, AsPC-1, Capan-2 cells; BALB/c Nude mice	Bak, Bcl-2, Bcl-XL, Cyt-C, Caspase-3, Caspase-9	Kaur et al. (2013)
	Down-regulating Bcl-2, survivin; Up-regulating Bax, Caspase-3and -9	Ginsenoside Rh2	BxpC-3 cells	Bcl-2, Survivin, Bax, Caspase-3, Caspase-9	Tang et al. (2013)
	Activate Caspase-3; Up-regulating Bax; Down-regulating Bcl-2; Bcl-XL, c-Myc, Caspase-3	Longikaurin E	PANC1, AsPC-1, BxPC-3 cells	Bax, Bcl-2	Cheng et al. (2015)
	Up-regulating Bax; Down-regulating Bcl-2	YCHD	PANC-1 cells	Bax, Bcl-2	Zhou et al. (2015)
	Increase ROS; Up-regulating Bax, Caspase-3; Down-regulating Bcl-2	Nimbolide	hTERT HPNE, HPAC、PANC-1, MIAPaCa-2; BALB/c Nude mice	Bax, Caspase-3, PARP, Bcl-2	Subramani et al. (2016)
	Up-regulating Bax, Caspase-3 and -9; Down-regulating Bcl-2	Aconitine	Miacapa-2, PANC-1	Bax, Caspase-3, Caspase-9, PARP1, Bcl-2	Ji et al. (2016)
	Increase Cyt-C; Up-regulating Caspase-3 and -9	Esculetin	PANC-1, MIA PaCa-2, AsPC-1 cell lines	Cyt-C, Caspase-3, Caspase-9	Arora et al. (2016)
	Up-regulating p53 and Bax; Down-regulating Bcl-2	Ethylacetate fraction	PANC-1 cells	p53, Bax, Bcl-2	Ding et al. (2017)
	Up-regulating HTRA3, Bax	Paeoniflorin	Capan-1, MIAPaCa-2 cell lines	HTRA3, Bax	Li et al. (2017)
	Increase ROS; Decrease MCMP (Δ ψ m); Up-regulating Bax; Down-regulating Bcl-2	Glychionide-A	PANC-1, hTRET-HPNE cells	Bax, Bcl-2	Yu et al. (2019)

(Continued on following page)

TABLE 1 | (*Continued*) Apoptosis-inducing activity of Chinese herbal medicine and its active ingredients in pancreatic cancer cells.

Potential pathways	Detail mechanisms	Extracts/ Monomers	Cells/animals	Related genes/Proteins	Refs
	Up-regulating Caspase-3, Bax; Down-regulating Bcl-2	Piperine	PANC-1 cells	Caspase-3, Bax, Bcl-2	Zhong et al. (2020)
	Increase ROS, Cyt-C; Up-regulating Caspase-3 and -9	Tephrosin	A549, MCF-7, HepG2; SHG-44, CFPAC-1, MIAPaCa, PANC-1, SW1990 cell lines; BALB/c Nude mice	Cyt-C, Caspase-3, Caspase-9, PARP	Du et al. (2021)
	Up-regulating Bax and Caspase-3; Down-regulating Bcl-2	Icariin	BxPC-3 cells	Bax, Bcl-2, Caspase-3	Huang et al. (2021)
	Up-regulating Bax; Down-regulating Bcl-2, Wnt/β-catenin	Schisandrin B	PANC-1 cells	Bax, Bcl-2, Wnt4, Wnt5a, β-catenin	Wang et al. (2021a)
ERS mediated apoptotic pathway	Up-regulating GRP78, eIF2α, ATF4, GADD153	capsaicin	PANC-1, SW1990 cells; BALB/c Nude mice	eIF2 α, ATF4, GADD153	Lin et al. (2013)
	Up-regulating CHOP	Bitter gourd juice	BxPC-3, MiaPaCa-2, AsPC-1, Capan-2 cells; BALB/c Nude mice	CHOP	Kaur et al. (2013)
	Up-regulating phosphorylation-PERK, Grp78/BiP, GADD153/CHOP	Quercetin	PANC-1 cells	GADD153, CHOP	Lee et al. (2013)
PI3K-Akt mediated apoptotic pathway	Down-regulating Tyr458, Ser473; Up-regulating Caspase-3	Capsaicin	PANC-1 cells; BALB/c Nude mice	Tyr458, Ser473	Zhang et al. (2013)
	Down-regulating PI3K/AKT signaling	Longikaurin E	PANC1, AsPC-1, BxPC-3 cells	PI3K, Akt	Cheng et al. (2015)
	Down-regulating PI3K/AKT signaling	Brucein D	PANC-1, Capan-1, Capan-2, GES-1, SW-1990 cells; BALB/c Nude mice	PI3K, Akt	Lai et al. (2017)
	Down-regulating PI3K/AKT signaling	Timosaponin-AIII	PANC-1, BxPC-3 cells	PI3K, Akt	MarElia et al. (2018)
	Down-regulating Akt/mTOR signaling	Kaempferol	PANC-1, Mia PaCa-2 cells; BALB/C Nude mice	Akt, mTOR	Wang et al. (2021b)
NF-κB Mediated Apoptotic Pathways	Inhibit NF-κB, p65 activation; Decrease transcription of Bcl-2 and XIAP	Brucetin D	PANC-1 cells; BALB/c Nude mice	NF-κB	Lau et al. (2010)
	Down-regulating Bcl-2, Livin and Survivin; Up-regulating Bax	Geraniol	BXPC-3, HPC-Y5 cells; BALB/c Nude mice	Livin, Survivin, Bcl-2, Bax	Jin.,2013
	Inhibit Nrf2 phosphorylation, NF-κB	Esculetin	PANC-1, MIA PaCa-2, AsPC-1 cell lines	Nrf2, NF-κB	Arora et al. (2016)
	Down-regulating NF-κB, cIAP1, cIAP2, survivin, Bcl-2/Bax; Up-regulating Caspase-3	Lycopene	PANC-1 cells	NF-?B, cIAP1, cIAP2, Caspase-3, Bcl-2, Bax	Jeong et al. (2019)
	Inhibit NF-κB; Up-regulating Caspase-3	Sinomenine	Capan-1 cells	NF-κB, Caspase-3	Chen et al. (2020)
MAPK Mediated Apoptotic Pathway	Down-regulating $ERK_{1/2}$	Curcumin	H1299, PANC-1, p34, PC-14 cells	$ERK_{1/2}$	Lev-Ari et al. (2006)
	Increase ROS; Up-regulating p38	Brucetin D	PANC-1 cells; BALB/c Nude mice	p38	Lau et al. (2010)
	Activate p38	Bitter gourd juice	BxPC-3, MiaPaCa-2, AsPC-1, Capan-2 cells; BALB/c Nude mice	p38, $ERK_{1/2}$	Kaur et al. (2013)
	Activate JNK and p38; Inhibit ERK	Phycocyanin	PANC-1, Capan-1, BxPC3, H460, QSG-7701, AC-16, HepG2, BGC-823, DU145, MCF-7, HK-2 cells	JNK, p38, ERK	Liao et al. (2016)
Others	Increase miR-7; Decrease SET8	Curcumin	AsPC-1, BxPC-3 cells	miR-7	Ma et al. (2014)
	Up-regulating miR-340; Down-regulating XIAP	Curcumin	PANC-1, HEK293 cells	miR-340, XIAP	Yang et al. (2017)
	Up-regulating miR-101, Caspase-3; Down-regulating Mcl-1	Honokiol	PANC-1, SW1990 cells; BALB/c Nude mice	miR-101, Caspase-3, Mcl-1	Wang et al. (2020)
	Up-regulating miR-9	Icariin	BxPC-3 cells	miR-9	Huang et al. (2021)
	Inhibit Hsp70, 5-LOX	Triptolide	PANC-1, MiaPaCa-2, SW-1990 cells; Female nude mice	Hsp70, 5-LOX	Phillips et al., 2007 Zhou et al. (2007)

(Continued on following page)

TABLE 1 | (*Continued*) Apoptosis-inducing activity of Chinese herbal medicine and its active ingredients in pancreatic cancer cells.

Potential pathways	Detail mechanisms	Extracts/ Monomers	Cells/animals	Related genes/Proteins	Refs
	Down-regulation of EZH2, Trx; Activate ASK1	Capsaicin	AsPC-1, BxPC-3 cells; BALB/c Nude mice	Trx, ASK1	Pramanik and Srivastava, (2012)
		Diosgenin	Patu8988 and Panc-1, SW1990 cell line, Nude mice	EZH2	Guo et al. (2019)
	Inhibit IL-6/JAK2/STAT3 signaling	Gentiopicroside	PANC-1 cells	IL-6, JAK2, STAT3	Meng et al. (2020)
	Down-regulating PD-L1	Polyphyllin VII	PANC-1, Miapaca-2cells	PD-L1	He et al., 2021; Hu et al., 2020

YCHD, Yin Chen Hao Decoction; Cyt-C, cytochrome C; AIF, apoptosis inducing fact.

In 2008, Zhang et al. found that Capsaicin which is an interesting alkaloid isolated from the *Capsicum annuum* promoted the apoptosis of mice tumor cells, which was related to the up-regulated of Bax and Cleaved (C)-Caspase-3 and the increased of Cyt-C and AIF in the cytoplasm. The same results were also found for AsPC-1 and BxPC-3 cells when conducting *in vitro* studies (Zhang et al., 2008). Another research by Zhou et al., in 2008 found that Triptolide induced human pancreatic cancer cells to undergo apoptosis with typically apoptotic characteristics. Further research found that caspase-3 and Bax were significantly up-regulated in SW1990 cells treated with TL (Zhou et al., 2008). Mcl-1 is a member of the Bcl-2 superfamily. Recent genome-wide research suggests that Mcl-1 is subject to increased gene copy number across more than two dozen cancer types. Exploiting drug regimens targeting pathways that down-regulate Mcl-1 expression is therefore a current strategy in cancer therapy. In 2013, the results of Chen et al. showed that Triptolide can reduce the level of Mcl-1 by increasing the expression of miR-204, eventually induce apoptosis of pancreatic cancer cells (Chen et al., 2013). In 2011, Roy et al. found that Resveratrol which is a versatile natural monomer in grape skins and red wine can induce apoptosis in PANC-1, MIA PaCa-2, HS766T and AsPC-1 cells in a dose-dependent manner. Further researched found that Resveratrol induced apoptosis is related to the regulation of Bim and the activation of Caspase-3 (Roy et al., 2011). Subsequently, Duan et al. found in 2016 that Resveratrol significantly induces the PARP and Cleaved-Caspase-3 in PANC-1 and BxPC-3 cells. Resveratrol also can promote the down-regulation of Mcl-1, the up-regulation of Puma and the Bim (Duan et al., 2016). Under normal circumstances, the pro-apoptotic protein Bax, which exists in the cytoplasm, plays a negative regulatory effect against the anti-apoptotic protein Bcl-2, that is, Bcl-2/Bax determines cell apoptosis. In 2012, when Ding screened natural active compounds, it was found that Casticin could significantly increases the expression of Bax in PANC-1 cells while inhibiting the expression of Bcl-2. That is to say, Casticin caused cell apoptosis by reducing the ratio of Bcl-2/Bax. In this experiment, it was also found that Isoalantolactone can increase the level of ROS in PANC-1 cells in a dose-dependent manner, increase the expression of p38 and Bax, and accompanied by the release of Cyt-C and the activation of Caspase-3, it supports the view that Isoalantolactone induces pancreatic cancer PANC-1 cell apoptosis through an endogenous pathway (Ding., 2012). In the same year, Prasad R et al. found that Proanthocyanidins extracted from grape seeds significantly induced apoptosis of Miapaca-2 and PANC-1 cells. The potential mechanism of Grape seed Proanthocyanidins (GSPs) induction of apoptosis is related to the decrease of Bcl-2 and Bcl-xL levels, the increase of Bax and the activation of Caspase-3. Further *in vivo* studies found that the percentage of activated caspase-3 in the pancreatic tumor xenografts in athymic nude mice treated with GSPs was higher than that of mice that did not receive GSPs. It was also found that the level of Bax was increased, and the levels of Bcl-2 and Bcl-xL were reduced (Prasad et al., 2012). Qi et al. found that the apoptosis of PANC-1 cells induced by Oridonin is mediated by the decrease of Bcl-2/Bax ratio and activation of Caspase-3. This study also showed that Oridonin nanosuspension is more effective than free oridonin on G2/M cell cycle arrest and apoptosis in human pancreatic cancer PANC-1 cell line (Qi et al., 2012). In this year, Liu et al. found that Brucetin D can reduce the mitochondrial membrane potential in cells, weaken the expression of Bcl-2 protein, enhance the expression of Caspase-9 and Caspase-3 and increase Capan-2 cells apoptosis (Liu et al., 2012). Later in 2019, Huang found that the relative expression of Bcl-2, PARP, and Caspase-3 proteins after the combination of Brucein D and Taxol was significantly reduced. However, the relative expression of C-Caspase-3 protein was significantly increased. It shows that the combination can induce Capan-2 cells apoptosis by activating the Caspase-pathway (Huang et al., 2019). In 2013, Jin et al. found that Geraniol can reduce the expression of Cyt-C in the mitochondria of pancreatic cancer cells and increase the expression of Cyt-C in the cytoplasm. In turn, it activates the Caspase-pathway in the cytoplasm to promote the apoptosis of BXPC3 cells (Jin., 2013). In the same year, Lee et al. found that Quercetin increases the activity of Caspase-9 in PANC-1 cells, and induces the activation of Caspase-3. It also causes the change of PANC-1 mitochondrial membrane potential, decreases Bcl-xL and increases expression of Bak (Lee et al., 2013). Kaur et al. studied Bitter Gourd Juice (BMJ) and found that it significantly induced the pro-apoptotic protein Bak, and promoted the decrease of anti-apoptotic proteins Bcl-2 or Bcl-xL. The cytostatic levels of BMJ apoptotic molecules (survivin and XIAP) were significantly reduced, which also resulted in the

release of Cyt-C into the cytoplasm and activated both Caspase-3 and Caspase-9 (Kaur et al., 2013). Tang et al. also found that Ginsenoside Rh2 can down-regulate Bcl-2 and surviving, and up-regulate Bax, promote the cleavage of Caspase-3 and Caspase-9, and initiate the endogenous apoptotic pathway to induce BxpC-3 pancreatic cancer apoptosis (Tang et al., 2013). Longikaurin E is a substance from the *Rabdosia longitude* and has anti-proliferation and pro-apoptotic properties in a variety of cancers. In a 2015 study by Cheng et al., it was found that Longikaurin E promoted the apoptosis of PANC-1 human pancreatic cancer cells by reducing the Bcl-2/Bax ratio and activating Caspase-3 (Cheng et al., 2015). In 2016, Subramani et al. discovered Nimbolide, a phytochemical isolated from the leaves and flowers of Neem tree. The levels of ROS, Bax, C-Caspase-3 and lytic PARP were increased and the level of Bcl-2 was decreased, thus inducing cell apoptosis through the Mitochondrial Dependent Apoptotic Pathway. In pancreatic cancer xenograft models, it was found that Nimbolide induced apoptosis is related to the increase in the expression of Bax, C-Caspase-3 and lytic PARP; and the decrease in the expression of the anti-apoptotic protein Bcl-2. These findings also confirmed the *in vitro* observations. (Subramani et al., 2016). In the same year, Ji et al. found that Aconitine can induce cell apoptosis by up-regulating the expression of pro-apoptotic factors Bax, C-Caspase-3, C-Caspase-9 and lytic PARP1, and reducing anti-apoptotic Bcl-2. Importantly, NF-κB was also reduced after Aconitine treatment (Ji et al., 2016). In this year's study, Arora et al. found that Esculetin promotes the loss of mitochondrial membrane potential, leading to the release of Cyt-C into the cytoplasm. At the same time, the activation and cleavage of Caspase-3, Caspase-9 and Caspase-8 were also observed. All in all, Esculetin can induce apoptosis through both extrinsic apoptotic and endogenous pathways (Arora et al., 2016). In 2017, Ding et al. found that the Ethylacetate fraction (EAF) can inhibit proliferation and promote apoptosis of pancreatic cancer PANC-1 cells. The mechanism may be related to the up-regulation of p53, Bax expression and down-regulation of Bcl-2. HTRA3 belongs to the highly conserved HtrA family of stress-related serine proteases. HTRA3 sensitizes lung cancer cells to etoposide and cisplatin, where it may act as an effector of mitochondrial cell death, indicating its role as a tumor suppressor. In 2017, Li et al. found that Paeoniflorin increases the expression of HTRA3 in Capan-1 cells. The overexpression of HTRA3 also detectes an increase in the level of Bax protein. Therefore, HTRA3 exerts a new pro-apoptotic effect in pancreatic cancer cells by inducing Bax (Li et al., 2017). In 2019, Yu et al. discovered Glychionide-A, a new flavonosides have been isolated from the roots of Glychirriza glabra (Li et al., 2005). Glychionide-A increases ROS and reduces the mitochondrial membrane potential level of PANC-1 pancreatic cancer cells, indicating that Glychionide-A is ROS-mediated apoptosis and autophagy. Experiments also found that the expression of Bax increased and Caspase-9 reduced the expression of Bcl-2 in PANC-1 cells (Yu et al., 2019). In 2020, Zhong et al. found that Piperine can up-regulate the expression levels of Caspase-3 and Bax mRNA in PANC-1 cells, up-regulate the expression levels of C-Caspase-3 and Bax proteins, and down-regulate the expression levels of Bcl-2 mRNA and protein. It further shows that Piperine can induce PANC-1 cell apoptosis by regulating the Caspase-3/Bax/Bcl-2 apoptotic signaling pathway (Zhong et al., 2020). In the same year, Zhang discovered in his research that the natural drug Terphenyllin increased the expression of Bax, Bad, Puma and BIM, and inhibited the expression of Bcl-2 and Bcl-xL. The decrease of the Bcl-2/Bax ratio promotes the apoptosis of pancreatic cancer cells. At the same time, the expression of P-Bcl2-Ser70, Caspase-7 and PARP gradually decreased, and the expression of Cleaved PARP and Cleaved Caspase-7 gradually increased (Zhang, 2020). Recently, Du et al. discovered that Tephrosin, a natural carotenoid isoflavone, increases the production of reactive oxygen species (ROS) in the cell, depolarizes the mitochondrial membrane potential and releases Cyt-C to promote apoptosis. Tephrosin can also promote the apoptosis of PANC-1 and SW1990 pancreatic cancer cells by enhancing the cleavage of Caspase-3, Caspase-9 and PARP. To further study the anti-tumor effects of tephrosin in vivo, PANC-1 cells were injected subcutaneously into BALB/C nude mice. The study found that high-dose tephrosin (20 mg/kg) significantly reduced tumor growth *in vivo* compared with administration of vehicle. No pathological changes were observed in various organs after H&E staining. These results all proved the anti-tumor effect and low toxicity of tephrosin (Du et al., 2021). In the same year, Huang et al. found that Icariin increased the apoptosis rate of pancreatic cancer BxPC-3 cells, the expression of apoptosis marker proteins Bax and Cleaved Caspase-3, and down-regulated the expression of apoptosis marker protein Bcl-2 (Huang et al., 2021). In the same year, Wang et al. found that Schisandrin B can significantly induce the expression of the pro-apoptotic protein Bax and inhibit the expression of the anti-apoptotic protein Bcl-2. This study also found that the induction of pancreatic cancer PANC-1 cell apoptosis may be related to the inhibition of Wnt/β-catenin signaling pathway activation (Wang F. et al., 2021).

In addition to monomers, ancient allotment can also induce apoptosis in pancreatic cancer. Such as *Yin Chen Hao Decoction* (YCHD), which is a classic traditional Chinese medicine formula composed of three herbs: *Rheum officinale* Baill, *Artemisia capillaries* Thunb and *Gardenia iasminoides* Ellis. For a long time, YCHD can be used to treat cholestasis, hepatitis C, primary bil liver fibrosis. In addition, YCHD is an effective cancer suppressor. The anti-cancer activity of YCHD may induce cancer cell apoptosis. In 2015, Zhou et al. found that YCHD induced PANC-1 cell apoptosis, part of the mechanism was through up-regulation of Bax and down-regulation of Bcl-2 (Zhou et al., 2015). The potential mechanisms of herbal medicine for inducing apoptosis in this part are summarized in **Figure 2** and **Table 1**.

ERS Mediated Apoptotic Pathway

The endoplasmic reticulum (ER) is an organelle that receives various emergency stimuli and transmits relaxation signals. The endoplasmic reticulum can guide the synthesis, folding and secretion of proteins in eukaryotic cells. Endoplasmic reticulum stress (ERS) caused by endoplasmic reticulum dysfunction can enhance the folding ability of proteins, delay the translation of most proteins, and accelerate protein

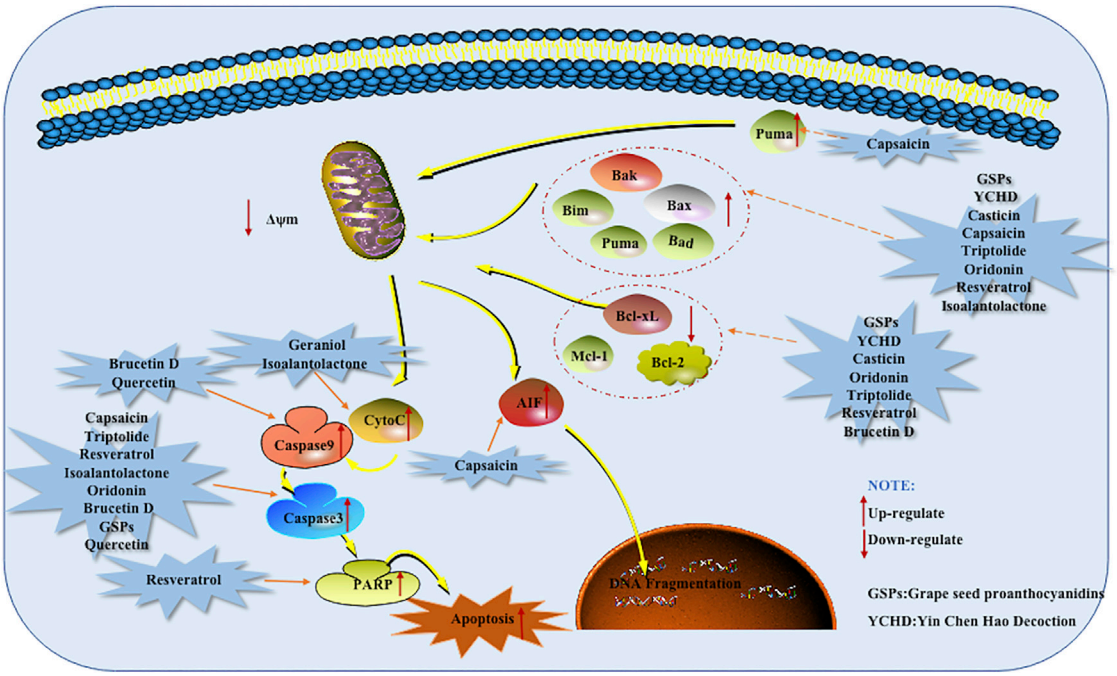


FIGURE 2 | Mitochondrial dependent apoptotic pathway of pancreatic cancer induced by herbal medicines.

degradation. It is the cell's self-protection mechanism. It can also activate the unfolded protein response (UPR), induce the expression of molecular chaperones such as GRP78, GRP94, Bip and so on, regulate the Irel/xBPT pathway, p-ERK/eIF2α pathway, up-regulate the expression of CCAAT/CHOP, and indirectly promote cell apoptosis. In addition, ESR can induce the opening of calcium channels, promote Ca^{2+} outflow, and break the BCL-2/Bax balance. These are all called ERS Mediated Apoptotic Pathway (Zhang et al., 2019). At present, there are many reports that Chinese herbal medicines and their monomers can induce pancreatic cancer cell apoptosis through the ERS Mediated Apoptotic Pathway.

In 2013, Lin et al. found that Capsaicin can significantly enhance the expression of GRP78 in PANC-1 and SW1990 cells. At the same time, GADD153, a marker of ERS mediated apoptotic pathway, was also added. Further research found that Capsaicin prolonged the survival rate of nude mice with orthotopic pancreatic cancer xenograft tumors.The results of western blot analysis showed that the protein expression of GRP78, phospho-PERK, phospho-eIF2α, ATF4 (eIF2 α downstream target), and GADD153 was much higher in the tumor tissues of Capsaicin-treated mice compared with that of control group. This study is the first to study the effect of Capsaicin on endoplasmic reticulum-mediated apoptosis in pancreatic cancer *in vitro* and *in vivo* (Lin et al., 2013). Kaur M et al. also found an increase in CHOP levels when studying the mechanism of BMJ induced apoptosis in 2013, so the induction of CHOP levels by BMJ may also help induce apoptosis (Kaur et al., 2013). In 2013, Lee et al. investigated the mechanism of Quercetin inducing apoptosis in pancreatic cancer, found that Quercetin went through the ERS mediated apoptotic pathway which induced the increase of GADD153/CHOP protein expression finally by increasing Grp78/Bip protein as well as activating PERK protein in PANC-1 cells. At the same time, it was also found that intracellular calcium accumulation in cell (Lee et al., 2013). The potential mechanisms of herbal medicine for inducing apoptosis in this part are summarized in **Figure 3** and **Table 1**.

PI3K-Akt Mediated Apoptotic Pathway

PI3K constitutes a family of lipid kinases whose role is that they can phosphorylate inositol ring 3′-OH group in inositol phospholipids to generate the second messenger phosphatidylinositol-3,4,5-triphosphate (PI -3,4,5 -P (3)). RPTK activation causes PI3K inside the plasma membrane to produce PI (3,4,5) P 3) and PI (3,4) P (2). Akt interacts with these phospholipids, causing its translocation to the inner membrane, which is phosphorylated and activated by PDK1 and PDK2. Activated Akt regulates the functions of a variety of substrates. These substrates are involved in regulating cell survival, cell cycle progression and cell growth. It has been shown that the components of the PI3K-Akt Mediated Apoptotic Pathway are often altered and inappropriately activated in human cancers (Fresno Vara et al., 2004). Bondar et al. studied 9 human pancreatic cancer cell lines *in vitro* and observed that onstitutive AKT phosphorylation (on S473) was consistent with pathway activation in seven of nine human pancreatic carcinoma cell lines *in vitro*. This study determined that the PI3K-Akt Mediated Apoptotic Pathway is constitutively activated in most human pancreatic cancer cell lines, and determined that this pathway is a promising target for therapeutic intervention

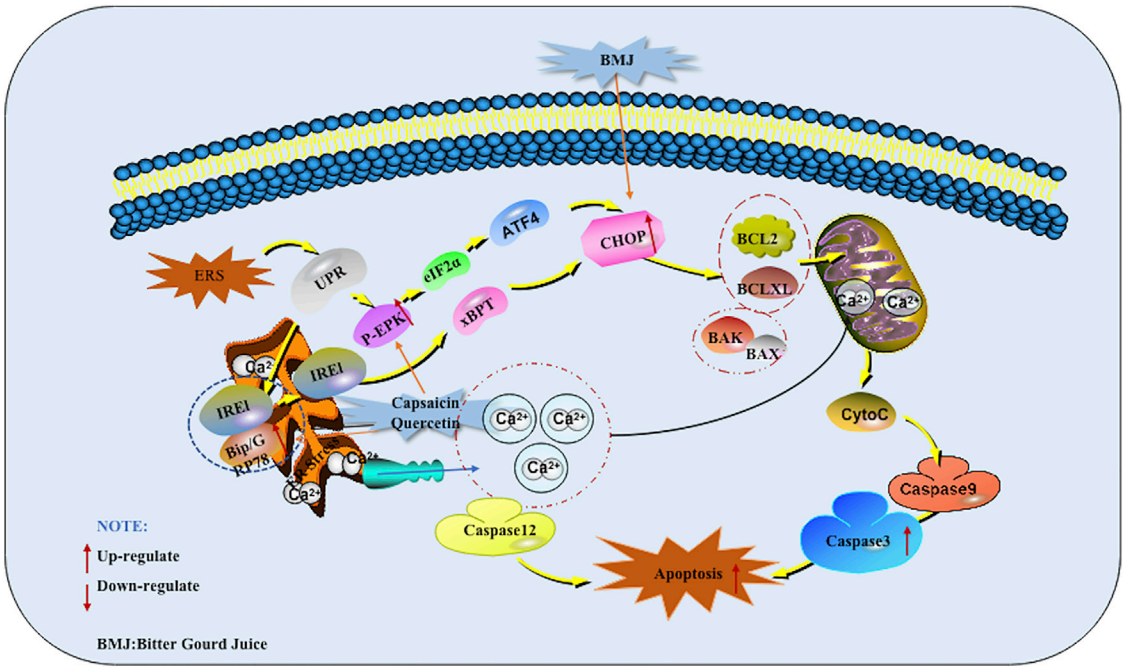


FIGURE 3 | Endoplasmic reticulum stress (ERS) mediated apoptotic pathway of pancreatic cancer induced by herbal medicines.

(Bondar et al., 2002). Therefore, the PI3K-Akt Mediated Apoptotic Pathway can be considered as a feasible and effective target for pancreatic cancer treatment. In 2013, Zhang et al. did a corresponding study on Capsaicin. In mice treated with Capsaicin, the expression of Tyr458 and Ser473 was down-regulated, and the expression of Caspase-3 was promoted. This indicates that the down-regulation of the PI3K-Akt mediated apoptotic pathway may be related to the apoptosis of PANC-1 cells induced by Capsaicin. The same result was found when conducting *in vitro* research experiments (Zhang et al., 2013). When Cheng et al. studied Longikaurin E in 2015, they found that p38 phosphorylation increased and decreased phosphorylation of PI3K/AKT pathway (Cheng et al., 2015). In 2017, Lai et al. studied the inhibitory effect of Brucein D on pancreatic cancer and found that Brucein D can induce PANC-1 and Capan-2 cells apoptosis through ROS-Associated PI3K-Akt mediated apoptotic pathway. Further research found Brucein D Suppresses the Tumor Progression in Orthotopic Xenograft Mouse Model. The protein expression of phosphorylated forms of Akt (Ser473) and Akt (Thr308) proteins was drastically suppressed by Brucein D treatment. These data suggested that modulation of PI3K/Akt activity might be an important molecular mechanism underlying the *in vivo* anti-PanCa effects exerted by Brucein D (Lai et al., 2017). MarElia et al. found in 2018 that the use of Anemarrhena and Anemarrhena saponins alone or together with Gem can inhibit the phosphorylation of PI3K-Akt Mediated Apoptotic Pathway proteins. Anemarrhena and Anemarrhena saponins enhance the effect of Gem in a dose-dependent manner. In addition, this study also found that Anemarrhena and Anemarrhena saponins can promote PANC-1 cell apoptosis through a Caspase-dependent apoptosis mechanism (MarElia et al., 2018). TGM2 is a multifunctional protein. It is the first mammalian transglutaminases (TGs) member to be discovered and is involved in the pathogenesis of many cancers. Recently. Wang F et al. found that Kaempferol increases ROS levels, which in turn suppresses the Akt/mTOR signaling pathway. At the same time, the down-regulation of TGM2 was also detected. *In vivo* research also found that Kaempferol promotes apoptosis via the TGM2-mediated ROS-dependent Akt/mTOR signaling pathway. TGM2 may be a potential target of kaempferol to inhibit pancreatic cancer and could serve as a promising prognostic biomarker for this disease (Wang J. W. et al., 2021). The potential mechanisms of herbal medicine for inducing apoptosis in this part are summarized in **Figure 4** and **Table 1**.

NF-κB Mediated Apoptotic Pathways

The transcription factor NF-κB is a major cell regulatory factor, as well as a chemical activator, growth factor, and cell adhesion molecule. NF-κB binds to its inhibitory protein IκB and is located in the cytoplasm. They are not active in normal cells. Once IκB is stimulated outside the cell, IκB is phosphorylated and degraded, so that NF-κB is activated and migrates to the nucleus, and then start or enhance the transcription of related genes. Cellular activities related to NF-κB include cell connection and repair, inflammatory cell displacement, early disease-causing signal amplification and spread, and tumor occurrence and development (Jin., 2013; Chen et al., 2020). At present, NF-κB Mediated Apoptotic Pathways has attracted more and more attention. Modern pharmacological studies have proved that Chinese herbal medicine can induce apoptosis of pancreatic cancer cells by regulating the NF-κB Mediated Apoptotic pathway.

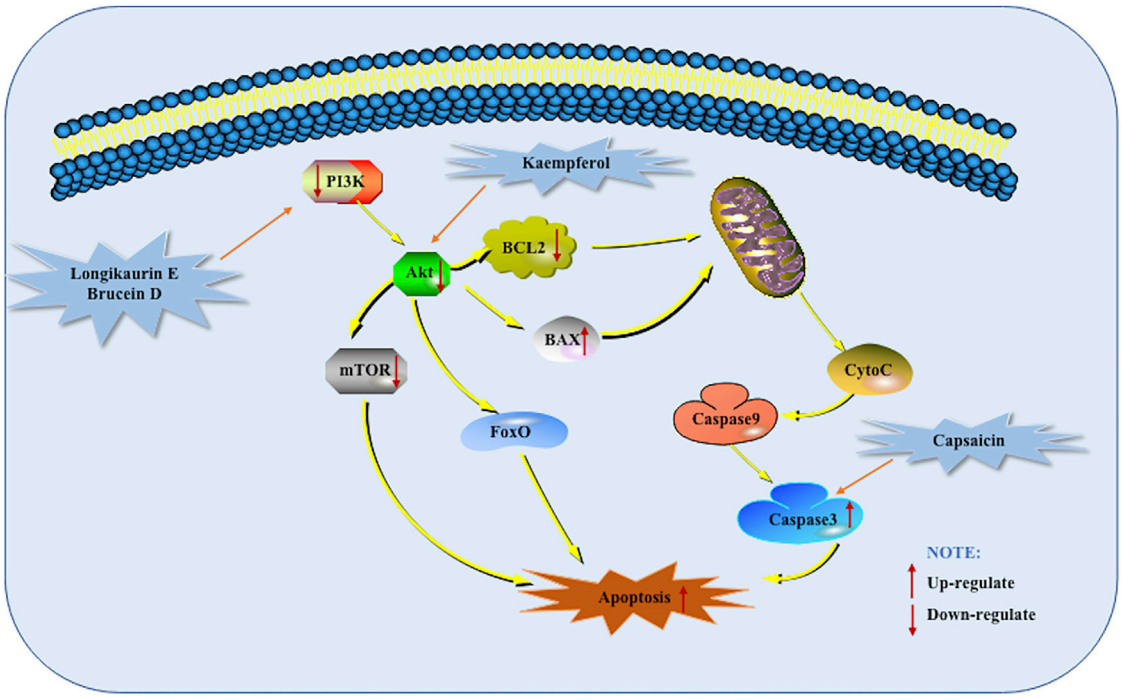


FIGURE 4 | PI3K-Akt mediated apoptotic pathway of pancreatic cancer induced by herbal medicines.

As early as 2010, Lau ST and others found that Brucetin D can inhibit the anti-apoptotic activity of NF-κB and promote apoptosis. Brucetin D treatment also weaken the p65 activation in PANC-1 cells, resulting in a decrease in the transcription of Bcl-2 and XIAP. Also found that Brucetin D inhibits the growth of CAPAN-2 human pancreatic tumor xenografts *in vivo* (Lau et al., 2010). Livin and Survivin, which are located in the nucleus of the apoptosis protein inhibitor family, are two downstream genes of NF-κB. They can inhibit cell apoptosis by inhibiting the expression of Caspase. Studies have shown that the two are not expressed or low expressed in normal pancreatic tissues, while they are highly expressed in pancreatic cancer tissues. In 2013, when Jin was researching Geraniol, she found that Geraniol inhibited the expression of Livin and Survivin, and might thereby enhance the sensitivity of pancreatic cancer to Gem. NF-κB is a regulatory factor for the promoter of the important apoptosis inhibitor protein Bcl-2. Due to the abnormal increase of NF-κB activity in pancreatic cancer, which leads to a large number of activation of the Bcl-2 promoter, eventually leading to the acceleration of cancer cell proliferation and the inhibition of apoptosis. This study also found that Geraniol inhibited the binding ability of NF-κB and the promoter. At the same time, Geraniol can also down-regulate the expression of the suppressor gene Bcl-2 and up-regulate the expression of the pro-apoptotic Bax gene, thereby promoting tumor cell apoptosis (Jin., 2013). In 2016, Arora et al. found that Esculetin binds to Keap1 and inhibits its interaction with Nrf2 in pancreatic cancer cells. Therefore, the nuclear accumulation of Nrf2 in PANC-1 cells is promoted. Nrf2 is phosphorylated and transported to the nucleus, where it binds to the promoter with the ARE sequence to eliminate ROS and weaken NF-κB to induce anti-proliferation and apoptosis (Arora et al., 2016). When studying Lycopene in 2019, Jeong et al. found that it inhibits NF-κB activation and the expression of NF-κB target genes such as cIAP1, cIAP2 and survivin by reducing ROS levels. The NF-κB target genes (cIAP1, cIAP2 and survivin) inhibit Caspase-3, which means that Lycopene promotes the activation of Caspase-3. Therefore, Lycopene induces Caspase-3 dependent apoptosis and increases the ratio of Bax to Bcl-2 in PANC-1 cells (Jeong et al., 2019). In 2020, Chen et al. found that Sinomenine can inhibit the activation of NF-κB mediated apoptotic pathways, down-regulate the expression of tumor cell anti-apoptotic factors and apoptosis inhibitor proteins, promote the lysis of Caspase-3, and promote pancreatic cancer Capan-1 apoptosis (Chen et al., 2020). The potential mechanisms of herbal medicine for inducing apoptosis in this part are summarized in **Figure 5** and **Table 1**.

MAPK Mediated Apoptotic Pathway

Mitogen-activated protein kinase (MAPK) is a silk protein/threonine kinase, an important molecule that transmits eukaryotic signals. MAPK is involved in the regulation of gene expression, cell proliferation and death, and plays a key role in the signal transmission process of multiple receptors. MAPKs mainly include extra cellular signal-regulated protein kinases (ERK), P38 mitogen activated protein kinase (p38MARK), and c-Jun N-terminal kinase (JNK). Among them, the p38MAPK plays an important role in the stress response such as inflammation and apoptosis. A variety of inflammatory factors, growth factors, and stress response will double phosphorylate the tyrosine and threonine of p38 protein, thereby activating p38. The activated

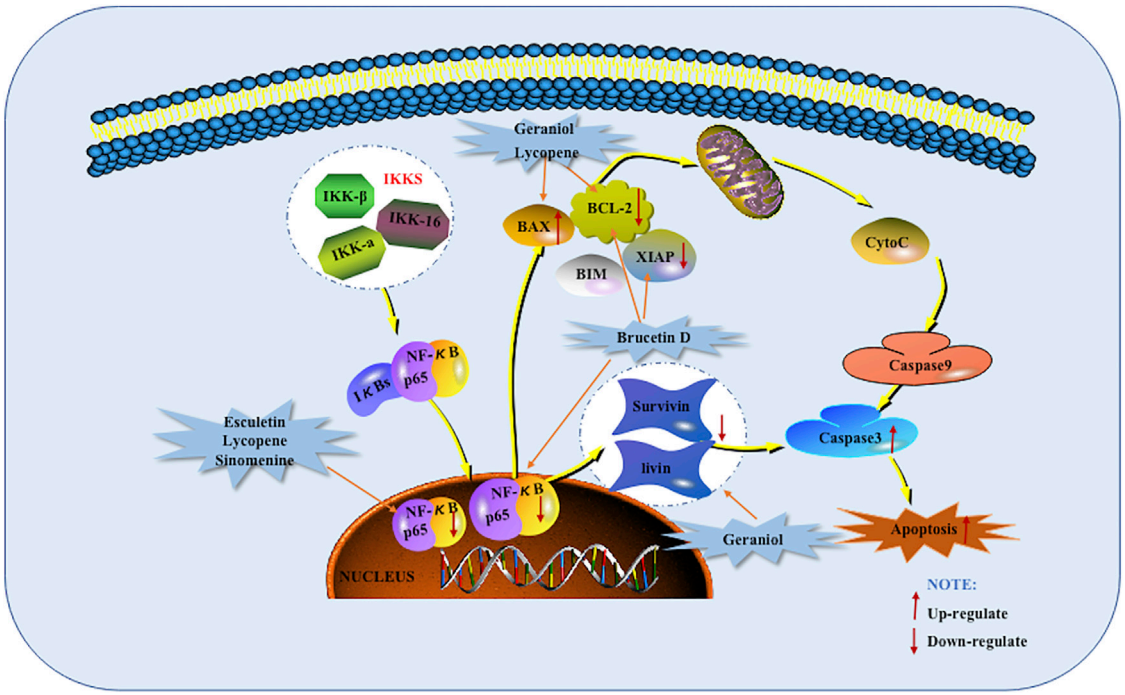


FIGURE 5 | NF-κB mediated apoptotic pathway of pancreatic cancer induced by herbal medicines.

p38 can enter the nucleus or transfer to other parts to activate transcription factors. Such as ATF2/6, ATH-1/2, ETS-1, MAX, HSF-1, nuclear transcription factor β, SAP-1, etc. These transcription factors in turn regulate the cytokines involved in cellular responses such as TNF-α, IL-1, IL-6, IL-8, and so on (Xu, 2019). When the cell is stimulated by the external environment, the c-Jun N-terminal kinase will be activated, and a part of the activated JNK will be translocated to the nucleus, and form p-JNK after phosphorylation modification. P-JNK can act on the pro-apoptotic proteins Bax and Bak in the Bcl family to induce the

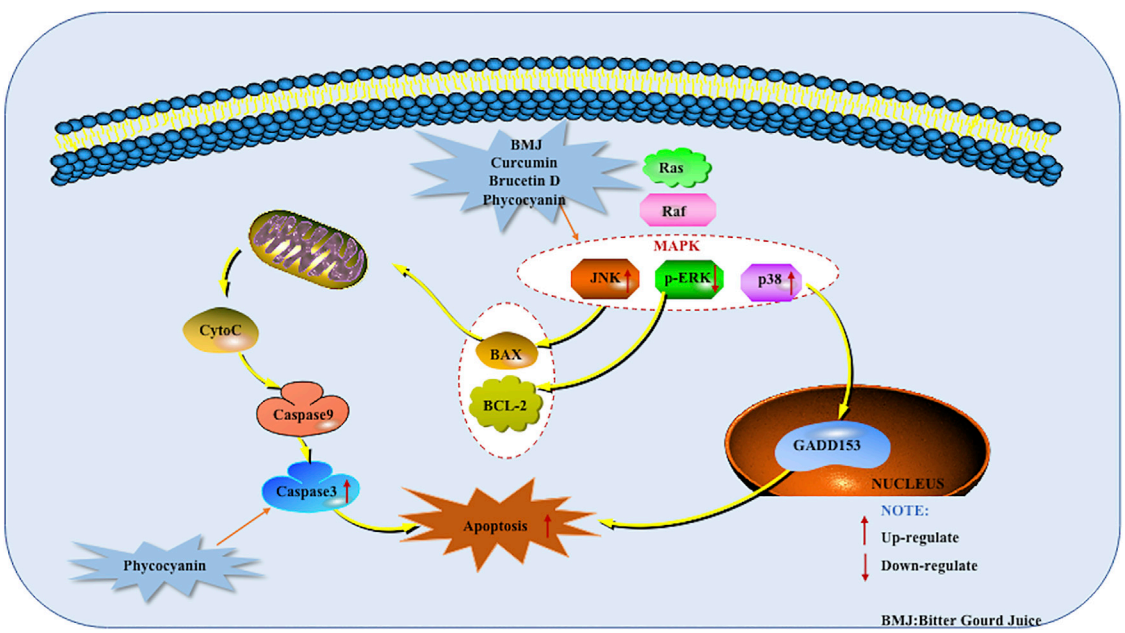


FIGURE 6 | Mitogen-activated protein kinase (MAPK) mediated apoptotic pathway of pancreatic cancer induced by herbal medicines.

TABLE 2 | Monomers for inducing apoptosis of pancreatic cancer.

Classification	Monomers	Apoptotic pathways	References
Terpenoids	Triptolide	Mitochondrial dependent apoptosis, Death Receptors mediated apoptosis, Inhibit Hsp70, 5-LOX	Chen et al. (2013), Wang et al. (2012), Phillips et al. (2007), Zhou et al. (2007)
	Geraniol	Death Receptors mediated apoptosis, Mitochondrial Dependent apoptosis, NF-κB mediated apoptosis	Jin. (2013)
	Oridonin	Mitochondrial dependent apoptosis	Qi et al. (2012)
	Brucein D	Mitochondrial dependent apoptosis, NF-κB mediated apoptosis, MAPK mediated apoptosis, PI3K-Akt mediated apoptosis	Huang et al. (2019), Lau et al. (2010), Lai et al. (2017)
	Lycopene	NF-κB mediated apoptosis	Jeong et al. (2019)
	Nimbolide	Mitochondrial dependent apoptosis	Subramani et al. (2016)
	Isoalantolactone	Mitochondrial dependent apoptosis	Ding. (2012)
	Longikaurin E	Mitochondrial dependent apoptosis	Cheng et al. (2015)
Alkaloids	Aconitine	Mitochondrial dependent apoptosis	Ji et al. (2016)
	Piperine	Mitochondrial dependent apoptosis	Zhong et al. (2020)
	Sinomenine	NF-κB mediated apoptosis	Chen et al. (2020)
Flavonoids	Casticin	Mitochondrial dependent apoptosis	Ding. (2012)
	Proanthocyanidins	Mitochondrial dependent apoptosis	Prasad et al. (2012)
	Quercetin	Mitochondrial dependent apoptosis, ERS mediated apoptosis	Lee et al. (2013)
	Icariin	Mitochondrial dependent apoptosis, Up-regulate miR-9	Huang et al. (2021)
	Kaempferol	PI3K-Akt-mTOR mediated apoptosis	Wang et al. (2021a)
	Tephrosin	Mitochondrial dependent apoptosis	Du et al. (2021)
Steroids	Ginsenoside Rh2	Mitochondrial dependent apoptosis	Tang et al. (2013)
	Diosgenin	Down-regulate EZH2	Guo et al. (2019)
	Timosaponin-AIII	PI3K-Akt mediated apoptosis	MarElia et al. (2018)
Lignans	Schisandrin B	Mitochondrial dependent apoptosis	Wang et al. (2021b)
	Honokiol	Up-regulate miR-101	Wang et al. (2020)
Coumarin	Esculetin	Mitochondrial dependent apoptosis, Death Receptors mediated apoptosis, NF-κB mediated apoptosis	Arora et al. (2016)
Phenols	Resveratrol	Mitochondrial dependent apoptosis	Roy et al. (2011), Duan et al. (2016)
	Terphenyllin	Mitochondrial dependent apoptosis	Zhang et al. (2020)
	Capsaicin	Mitochondrial dependent apoptosis, PI3K-Akt mediated apoptosis, ERS mediated apoptosis, Inhibit Trx, activate ASK1	Zhang et al. (2008), Zhang et al. (2013), Lin et al. (2013), Pramanik and Srivastava, (2012)
	Curcumin	MAPK mediated apoptosis, Increase miR-7, decrease SET8, miR-340/XIAP signal pathway	Lev-Ari et al. (2006), Ma et al. (2014), Yang et al. (2017)
Glucosides	Paeoniflorin	Mitochondrial dependent apoptosis	Li et al. (2017)
	Glychionide-A	Mitochondrial dependent apoptosis	Yu et al. (2019)
	Polyphyllin VII	Down-regulate PD-L1	He et al. (2021)
	Gentiopicroside	IL-6/JAK2/STAT3 signaling pathway	Meng et al. (2020)
Other	Phycocyanin	MAPK mediated apoptosis	Liao et al. (2016)

release of Cyt-C into the cytoplasm, thereby initiating the apoptosis program. It is reported that MAPK plays a vital role in inducing pancreatic cancer cells. In recent years, the influence of Chinese herbal medicine and its active monomers on MAPK Mediated Apoptotic Pathway in pancreatic cancer has been comprehensively reported *in vivo* and *in vitro*. When studying Curcumin in 2006, Lev-Ari S et al. found that it promotes the increase of apoptosis by inhibiting the activity of the ERK1/2 signaling pathway, and has a particularly strong effect on pancreatic cancer cell lines that express COX-2 (Lev-Ari et al., 2006). In 2010, Lau et al. found that Brucetin D mediates the activation of ROS to regulate the p38 signaling pathway to induce cell apoptosis. *In vivo* experiments found Brucetin D inhibits the growth of CAPAN-2 human pancreatic tumor xenografts (Lau et al., 2010). Later, in 2019, Huang et al. found that Brucein D combined with paclitaxel can also induce apoptosis of Capan-2 cells by activating JNK phosphorylation (Huang et al., 2019). When studying BMJ in 2013, Kaur et al. also found that the treatment of BMJ resulted in the prolongation and continuous activation of p38 and ERK1/2. Therefore, activation of p38 and ERK1/2 may also help induce apoptosis. Further use of IHC analysis found that BMJ's in vivo efficacy against MiaPaCa-2 xenograft growth is through inhibiting proliferation, inducing apoptosis and activating AMPK (Kaur et al., 2013). In 2016, Liao et al. found that the natural product Phycocyanin (from Spirulina) induced cell death in PANC-1 cells only partially dependent on the activation of Caspase-3. The activation of the JNK and p38 pathways while inhibiting ERK signaling indicates that the MAPK signaling pathway plays a key role in the apoptosis of cancer cells induced by Phycocyanin (Liao et al., 2016). The potential mechanisms of herbal medicine for inducing apoptosis in this part are summarized in **Figure 6** and **Table 1**.

Other Reported Pathways

MiRNAs/miRs are a class of small non-coding RNAs, and miRNAs play an important role in cytogenetics. In the process of tumor occurrence and development, it is related to the proliferation, apoptosis, differentiation, and metastasis of tumor cells. Therefore, miRNA has become a promising drug target. In 2014, Ma et al. found that curcumin inhibits cell growth,

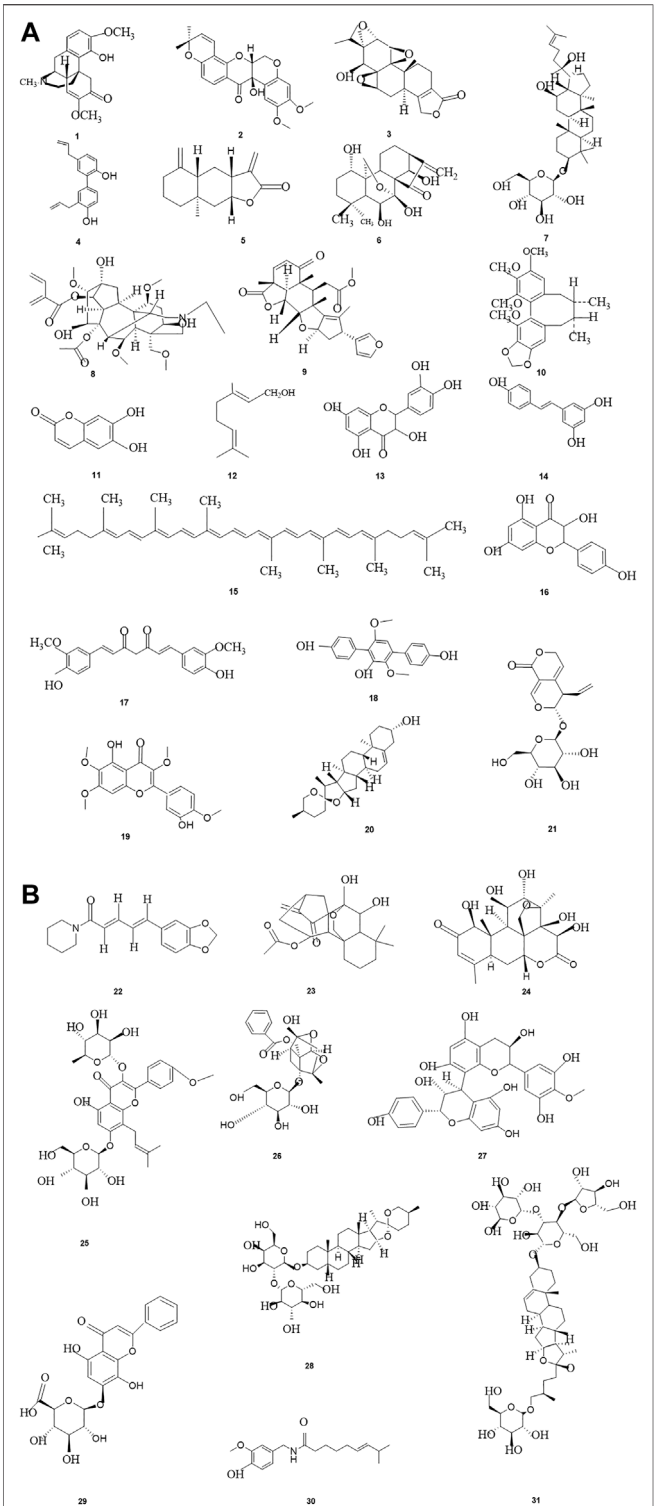


FIGURE 7 | (A–B) The related monomers of inducing apoptosis in Pancreatic cancer.Sinomenine (1), Tephrosin(2),Triptolide(3), Honokiol(4), Isoalantolactone(5), Oridonin(6), Ginsenosid-e Rh2(7), Aconitine(8), Nimbolide(9), Schisandrin B(10), Esculetin(11), Geraniol(12), Quercetin(13), Resveratrol(14), Lycopene(15), Kaempferol(16), Curcumin(17), Terphenyllin(18), Casticin(19), Diosgenin(20), Gentiopicroside(21), Piperine(22), Longikaurin E(23), Brucein D(24),Icariin(25), Paeoniflorin(26), Proanthocyanidins(27), Timosaponin-AIII(28), Glychionide-A(29), Capsaicin (30), Polyphyllin VII(31).

migration, and invasion, and induces apoptosis, which is related to the increased expression of miR-7 and the subsequent decrease in the expression of SET8 (one of the miR-7 targets) (Ma et al., 2014). Then in 2017, Yang et al. found that curcumin treatment significantly induced the expression of miR-340. In addition, an anti-apoptotic protein called XIAP was targeted by miR-340, leading to the pro-apoptotic effect of curcumin. Therefore, this study shows that the miR-340/XIAP signaling pathway is essential for curcumin-induced apoptosis of pancreatic cancer cells (Yang et al., 2017). In 2020, Wang et al. found that Honokiol induced the up-regulation of miR-101 in pancreatic cancer cells. Overexpression of miR-101 reduced cell viability and increased the activity of Caspase-3 and the rate of apoptosis. It also inhibited cell invasion, and it was also found that miR-101 down-regulated the expression of Mcl-1. As a downstream target of miR-101, Mcl-1 exerts an anti-apoptotic function. Further studies have found that Honokiol suppressed *in vivo* tumor growth of PANC-1 cells in a dose-dependent manner. It was also found that Honokiol dose-dependently up-regulated the expression of miR-101 and down-regulated the expression of Mcl-1, which is consistent with *in vitro* studies. (Wang et al., 2020). In 2021, Huang et al. found that Icariin can inhibit the proliferation of pancreatic cancer BxPC-3 cells and induce apoptosis of BxPC-3 cells by up-regulating miR-9 (Huang et al., 2021).

In addition, natural products also have other induction mechanisms. As early as 2007, Phillips et al. found that Triptolide induces the death of pancreatic cancer cells by inhibiting the expression of Hsp70. *in vivo* studies have also confirmed this (Phillips et al., 2007). In the same year, Zhou et al. found that the apoptosis of pancreatic tumor cell lines induced by Triptolide is related to the inhibition of 5-LOX (Zhou et al., 2007) ASK1 is a member of the mitogen-activated protein kinase family and is mainly activated by ROS. Previous studies have shown that ASK1 plays a key role in oxidative stress-mediated apoptosis by activating JNK and p38 signaling pathways. In 2012, Pramanik et al. found that Capsaicin can disrupt the Trx-ASK1 interaction through ROS, thereby inhibiting Trx to activate ASK1, leading to pancreatic tumor cell apoptosis. Further research found that Capsaicin suppresses AsPC-1 tumor growth *in vivo* in athymic nude mice. Capsaicin treatment also observed cleavage caspase-3 and PARP, inhibits Trx and activates ASK1 in pancreatic tumors (Pramanik and Srivastava, 2012). In 2019, Guo et al. found that diosgenin-induced apoptosis in pancreatic cancer cells may be related to down-regulation of EZH2 (oncoprotein). They also observed that administration of Diosgenin clearly inhibited subcutaneous tumor growth of nude mice compared with control group (Guo et al., 2019). Clinical studies have found that IL-6, JAK2, STAT3, etc. are abnormally expressed in tumor tissues of patients with pancreatic cancer. IL-6 is an important indicator for judging the prognosis of malignant tumors. After IL-6 binds to the corresponding IL-6 receptor on the target cell, it activates glycoprotein 130 (GP130) on the cell membrane surface, thereby activating JAK associated with GP130, thereby promoting the activation of receptor protein tyrosine kinases and binding to STAT3. Then the nuclear factor NF-κB is induced to dissociate from the IκB complex into free phosphorylation, and then enter the nucleus through the nuclear membrane. NF-κB

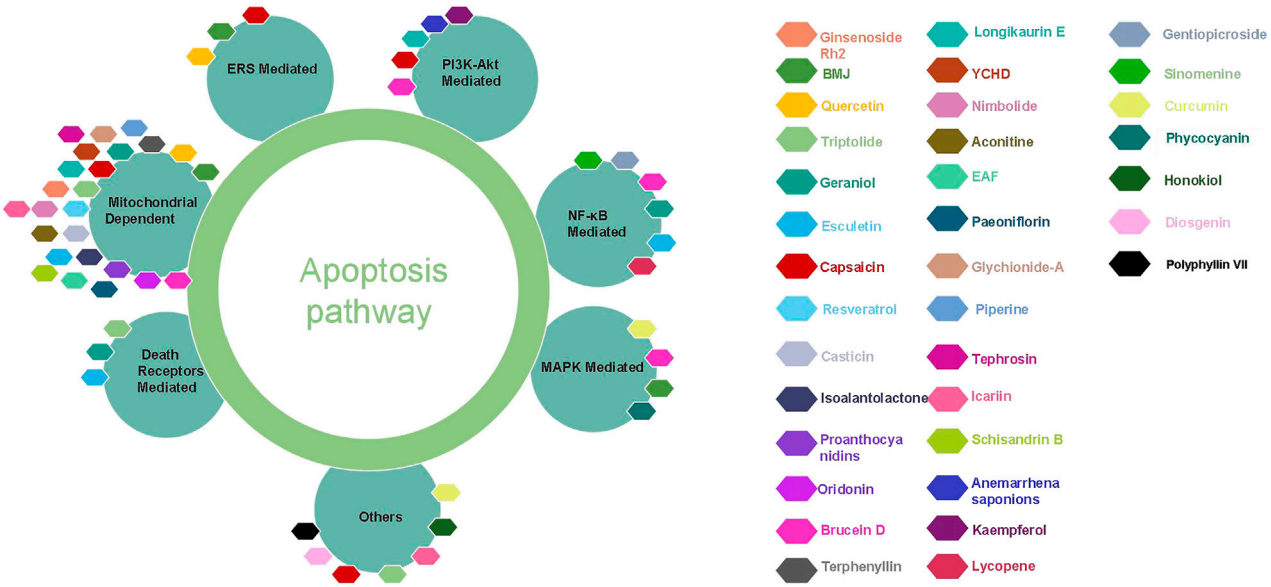


FIGURE 8 | The different apoptotic pathways of the natural monomers isolated from herbal medicines. YCHD, Yin Chen Hao Decoction; BMJ, Bitter Gourd Juice.

binds to its corresponding DNA response elements to regulate the expression of inflammation, apoptosis, or the proliferation of related factors. In 2020, Meng et al. found that Gentiopicroside can inhibit the proliferation and induce apoptosis of pancreatic cancer cells PANC-1. The mechanism may be related to the inhibition of the IL-6/JAK2/STAT 3 signaling pathway (Meng et al., 2020). In the same year, Hu et al. found that Polyphyllin VII induced Miapaca-2 cell apoptosis in a dose-dependent manner (Hu et al., 2020). Recently, He et al. found that Polyphyllin VII may induce PANC-1 cell apoptosis by down-regulating the expression of PD-L1 (He et al., 2021).

CONCLUSIONS

From ancient times to the present, herbal medicines play important roles in maintaining human health and curing diseases (Newman and Cragg, 2020; Zhang et al., 2021), and are generally regarded as valuable resources for screening and searching for new drug candidates with less toxicity. Pancreatic cancer, one of the most lethal malignancies and called the King of cancer, is the fourth leading cause of cancer-related death worldwide now, with an estimated 5-year survival rate less than 10%. Apoptosis, as the most typical way of programmed cell death and physiological cell suicide, is increasingly regarded as an ideal way to treat cancer. Increasing studies have found that herbal medicines and their monomers have pro-apoptotic effects on pancreatic cancer cells, we have summarized them in this review. The important mechanisms of herbal medicines in inducing apoptosis of pancreatic cancer cells include death receptors mediated apoptotic pathway, mitochondrial dependent apoptotic pathway, NF-κB mediated apoptotic pathways, MAPK mediated apoptotic pathway, ERS mediated apoptotic pathway, PI3K-Akt mediated apoptotic pathway, and other reported pathways such as JAK-STAT signal pathway. The classification of compounds that induce apoptosis in pancreatic cancer cells is shown in **Table 2**, the compound structure diagram is shown in **Figure 7A,B**, and the distribution diagram of compounds with different induction mechanisms is shown in **Figure 8**.

From the literature searched, mitochondrial dependent apoptosis is the most reported signaling pathway for herbal medicine to induce apoptosis in pancreatic cancer cells. For example, proanthocyanidins induced cells apoptosis through down-regulation of Bcl-2 and Bcl-xL, up-regulation of Bax and activate Caspase-3. Brucein D induced cells apoptosis via multi-pathways by mitochondrial dependent apoptotic pathway, down-regulate PI3K/AKT signaling, inhibit NF-κB, up-regulate p38 to activate MAPK mediated apoptotic pathway, so Brucetin D is one of the most promising active ingredients, but clinical research needs to be strengthened. Understanding that herbal medicine induces apoptosis of pancreatic cancer cells will not only help clarify the molecular mechanism of herbal medicine in treating diseases, but also help to find new drug candidates. Therefore, this review highlights the molecular mechanisms by which herbal medicines and their components induce apoptosis in pancreatic cancer cells, and provides some directions for the clinical future development of these herbal medicines against pancreatic cancer.

AUTHOR CONTRIBUTIONS

ML and DT collected documents and wrote the manuscript; TY and DQ systemically revised the manuscript before submission; RX designed the whole structure of the manuscript.

FUNDING

This research was supported by the National Natural Science Foundation of China (No.81873232).

REFERENCES

Arora, R., Sawney, S., Saini, V., Steffi, C., Tiwari, M., and Saluja, D. (2016). Esculetin Induces Antiproliferative and Apoptotic Response in Pancreatic Cancer Cells by Directly Binding to KEAP1. *Mol. Cancer* 15, 64. doi:10.1186/s12943-016-0550-2

Bondar, V. M., Sweeney-Gotsch, B., Andreeff, M., Mills, G. B., and McConkey, D. J. (2002). Inhibition of the Phosphatidylinositol 3'-Kinase-AKT Pathway Induces Apoptosis in Pancreatic Carcinoma Cells *In Vitro* and *In Vivo*. *Mol. Cancer Ther.* 1, 989–997.

Chen, W. Y., Qin, C. H., Tang, F., and Chen, Y. (2020). Sinomenine Inhibits Proliferation and Induces Apoptosis of Pancreatic Cancer Capan-1 Cells by Regulating NF-Kb Signaling Pathway. *Chin. J. Mod. Appl. Pharm.* 37, 2190–2195. doi:10.13748/j.cnki.issn1007-7693.2020.18.003

Chen, Z., Sangwan, V., Banerjee, S., Mackenzie, T., Dudeja, V., Li, X., et al. (2013). miR-204 Mediated Loss of Myeloid Cell Leukemia-1 Results in Pancreatic Cancer Cell Death. *Mol. Cancer* 12, 105. doi:10.1186/1476-4598-12-105

Cheng, H. B., Bo, Y., Shen, W. X., Ren, X. G., Tan, J. N., Jia, Z. R., et al. (2015). Longikaurin E Induces Apoptosis of Pancreatic Cancer Cells via Modulation of the P38 and PI3K/AKT Pathways by ROS. *Naunyn. Schmiedebergs Arch. Pharmacol.* 388, 623–634. doi:10.1007/s00210-015-1107-4

Chipuk, J. E., and Green, D. R. (2008). How Do BCL-2 Proteins Induce Mitochondrial Outer Membrane Permeabilization? *Trends Cel Biol* 18, 157–164. doi:10.1016/j.tcb.2008.01.007

Ding, C. (2012). *Identification and Characterization of Anti-Pancreatic Cancer Natural Compounds from Chinese Medicinal Herbs*. Changchun, China: Northeast Normal University.

Ding, X. G., Zhang, C. C., Qin, H. Y., Xiong, Y. K., Xu, J., and Zhang, T. (2017). Effect of EAF from Tetrastigma Hemsleyanum Root Tuber on Apoptosis of Human Pancreatic Cancer PANC-1 Cells and its Mechanism. *J. Toxicol.* 31, 182–186. doi:10.16421/j.cnki.1002-3127.2017.03.004

Du, J., Jiang, F., Xu, S. S., Huang, Z. F., Chen, L. L., and Li, L. (2021). Tephrosin Induces Apoptosis of Human Pancreatic Cancer Cells through the Generation of Reactive Oxygen Species. *J. Cancer* 12, 270–280. doi:10.7150/jca.50360

Duan, J., Yue, W., E, J., Malhotra, J., Lu, S. E., Gu, J., et al. (2016). *In Vitro* comparative Studies of Resveratrol and Triacetylresveratrol on Cell Proliferation, Apoptosis, and STAT3 and NFκB Signaling in Pancreatic Cancer Cells. *Sci. Rep.* 6, 31672. doi:10.1038/srep31672

Fresno Vara, J. A., Casado, E., de Castro, J., Cejas, P., Belda-Iniesta, C., and González-Barón, M. (2004). PI3K/Akt Signalling Pathway and Cancer. *Cancer Treat. Rev.* 30, 193–204. doi:10.1016/j.ctrv.2003.07.007

Guo, W., Chen, Y., Gao, J., Zhong, K., Wei, H., Li, K., et al. (2019). Diosgenin Exhibits Tumor Suppressive Function via Down-Regulation of EZH2 in Pancreatic Cancer Cells. *Cell Cycle* 18, 1745–1758. doi:10.1080/15384101.2019.1632624

He, H., Liu, Y., Qian, X. Y., Jin, M. F., Zheng, L., and Cheng, Z. (2021). Effect and Mechanism of Polyphyllin VII on Proliferation, Migration and Invasion of Pancreatic Cancer PANC-1 Cells. *Chin. Tradit. Herbal Drugs* 52, 1981–1986. doi:10.7501/j.issn.0253-2670.2021.07.015

Hu, S. S., Zhou, Y. Y., Wu, Z. H., Zhu, M., XX, Y., Du, B. Y., et al. (2020). The Effect of Polyphyllin Ⅶ on Pancreatic Carcinoma Cells. *J. HBUM.*, 544–550+528 .

Huang, Q. L., HuChen, Y. C. Y. J., Dai, L. M., and Dai, L. P. (2021). Effect of Icariin on Proliferation and Apoptosis of Pancreatic Cancer Cells BxPC-3 Is Related to Upregulation of miR-9. *Chin. J. Immunol.* 37, 289–294. doi:10.3969/j.issn.1000-484X.2021.03.006

Huang, Y. Y., Rao, M. J., Tan, B. Q., Wang, H. M., and Lin, N. M. (2019). Study on Inhibitory Effects and Mechanism of Bruceanine D Combined With Taxol on the Proliferation of Human Pancreatic Cancer Capan-2 Cells. *J. China. Pharm.* 30, 789–795. doi:10.6039/j06.14

Jeong, Y., Lim, J., and Kim, H. (2019). Inhibits Reactive Oxygen Species-Mediated NF-Kb Signaling and Induces Apoptosis in Pancreatic Cancer Cells. *Nutrients* 11, 762. doi:10.3390/nu11040762

Ji, B. L., Xia, L. P., Zhou, F. X., Mao, G. Z., and Xu, L. X. (2016). Aconitine Induces Cell Apoptosis in Human Pancreatic Cancer via NF-Kb Signaling Pathway. *Eur. Rev. Med. Pharmacol. Sci.* 20, 4955–4964.

Jin, X. X. (2013). *Empirical Study of Geraniol Anti-pancreatic Adenocarcinoma Effect and its Mechanism*. Central South University.

Kaur, M., Deep, G., Jain, A. K., Raina, K., Agarwal, C., Wempe, M. F., et al. (2013). Bitter Melon Juice Activates Cellular Energy Sensor AMP-Activated Protein Kinase Causing Apoptotic Death of Human Pancreatic Carcinoma Cells. *Carcinogenesis* 34, 1585–1592. doi:10.1093/carcin/bgt081

Lai, Q. J., Xiong, Z., Xu, X. H., Yang, M., Pang, B. Y., Li, J. T., et al. (2021). Research Progress of Emodin Induced Apoptosis of Hepatocellular Carcinoma Cells. *Chin. Arch. Tradit. Chin. Med.* 39, 129–132+273. doi:10.1200/jco.21.00027

Lai, Z. Q., Ip, S. P., Liao, H. J., Lu, Z., Xie, J. H., Su, Z. R., et al. (2017). Brucein D, A Naturally Occurring Tetracyclic Triterpene Quassinoid, Induces Apoptosis in Pancreatic Cancer Through ROS-Associated PI3K/Akt Signaling Pathway. *Front. Pharmacol.* 8, 936. doi:10.3389/fphar.2017.00936

Lau, S. T., Lin, Z. X., and Leung, P. S. (2010). Role of Reactive Oxygen Species in Brucein D-Mediated P38-Mitogen-Activated Protein Kinase and Nuclear Factor-kappa B Signaling Pathways in Human Pancreatic Adenocarcinoma Cells. *Br. J. Cancer* 102, 583–593. doi:10.1038/sj.bjc.6605487

Lee, J. H., Lee, H. B., Jung, G. O., Oh, J. T., Park, D. E., and Chae, K. M. (2013). Effect of Quercetin on Apoptosis of PANC-1 Cells. *J. Korean Surg. Soc.* 85, 249–260. doi:10.4174/jkss.2013.85.6.249

Lev-Ari, S., Starr, A., Vexler, A., Karaush, V., Loew, V., Greif, J., et al. (2006). Inhibition of Pancreatic and Lung Adenocarcinoma Cell Survival by Curcumin Is Associated with Increased Apoptosis, Down-Regulation of COX-2 and EGFR and Inhibition of Erk1/2 Activity. *Anticancer Res.* 26 (6B), 4423–4430.

Li, L., and Leung, P. S. (2014). Use of Herbal Medicines and Natural Products: an Alternative Approach to Overcoming the Apoptotic Resistance of Pancreatic Cancer. *Int. J. Biochem. Cel Biol.* 53, 224–236. doi:10.1016/j.biocel.2014.05.021

Li, Y., Gong, L., Qi, R., Sun, Q., Xia, X., He, H., et al. (2017). Paeoniflorin Suppresses Pancreatic Cancer Cell Growth by Upregulating HTRA3 Expression. *Drug Des. Devel. Ther.* 11, 2481–2491. doi:10.2147/DDDT.S134518

Li, Y. J., Gong, L. L., Qi, R. L., Sun, Q., Li, J. R., Wang, Y. Q., et al. (2005). Two New Compounds from Glycyrrhiza Glabra. *J. Asian Nat. Prod. Res.* 7, 677–680. doi:10.1016/j.biocel.2014.05.021

Liao, G., Gao, B., Gao, Y., Yang, X., Cheng, X., and Ou, Y. (2016). Phycocyanin Inhibits Tumorigenic Potential of Pancreatic Cancer Cells: Role of Apoptosis and Autophagy. *Sci. Rep.* 6, 34564. doi:10.1038/srep34564

Lin, S., Zhang, J., Chen, H., Chen, K., Lai, F., Luo, J., et al. (2013). Involvement of Endoplasmic Reticulum Stress in Capsaicin-Induced Apoptosis of Human Pancreatic Cancer Cells. *Compl. Alt.* 2013, 629750. doi:10.1155/2013/629750

Liu, G., Pei, F., Yang, F., Li, L., Amin, A., Liu, S., et al. (2017). Role of Autophagy and Apoptosis in Non-Small-Cell Lung Cancer. *Int. J. Mol. Sci.* 18, 367. doi:10.3390/ijms18020367

Liu, L., Lin, Z. X., Leung, P. S., Chen, L. H., Zhao, M., and Liang, J. (2012). Involvement of the Mitochondrial Pathway in Bruceine D-Induced Apoptosis in Capan-2 Human Pancreatic Adenocarcinoma Cells. *Int. J. Mol. Med.* 30, 93–99. doi:10.3892/ijmm.2012.980

Ma, J., Fang, B., Zeng, F., Pang, H., Zhang, J., Shi, Y., et al. (2014). Curcumin Inhibits Cell Growth and Invasion through Up-Regulation of miR-7 in Pancreatic Cancer Cells. *Toxicol. Lett.* 231, 82–91. doi:10.1016/j.toxlet.2014.09.014

MarElia, C. B., Sharp, A. E., Shemwell, T. A., Clare Zhang, Y., and Burkhardt, B. R. (2018). *Anemarrhena Asphodeloides* Bunge and its Constituent Timosaponin-AIII Induce Cell Cycle Arrest and Apoptosis in Pancreatic Cancer Cells. *FEBS Open Bio* 8, 1155–1166. doi:10.1002/2211-5463.12457

Meng, S., Zhou, Y. Z., Ma, Y. C., Xu, S. T., and J, S. J. (2020). Effects of Gentiopicroside on the Apoptosis of Human Pancreatic Cancer Cells PANC-1 and IL-6/JAK2/ STAT3 Signaling Pathway. *J. Chin. Pharm.* 31, 1836–1841. doi:10.6039/j.issn.1001-0408.2020.15.08

Modi, S., Kir, D., Banerjee, S., and Saluja, A. (2016). Control of Apoptosis in Treatment and Biology of Pancreatic Cancer. *J. Cel Biochem* 117, 279–288. doi:10.1002/jcb.25284

Newman, D. J., and Cragg, G. M. (2020). Natural Products as Sources of New Drugs over the Nearly Four Decades from 01/1981 to 09/2019. *J. Nat. Prod.* 83, 770–803. doi:10.1021/acs.jnatprod.9b01285

Peng, W., Wu, J. G., Jiang, Y. B., Liu, Y. J., Sun, T., Wu, N., et al. (2015). Antitumor Activity of 4-O-(2″-O-Acetyl-6″-O-P-Coumaroyl-β-D-Glucopyranosyl)-P-Coumaric Acid against Lung Cancers via Mitochondrial-Mediated Apoptosis. *Chem. Biol. Interact* 233, 8–13. doi:10.1016/j.cbi.2015.03.014

Phillips, P. A., Dudeja, V., McCarroll, J. A., Borja-Cacho, D., Dawra, R. K., Grizzle, W. E., et al. (2007). Triptolide Induces Pancreatic Cancer Cell Death via Inhibition of Heat Shock Protein 70. *Cancer Res.* 67, 9407–9416. doi:10.1158/0008-5472.CAN-07-1077

Pramanik, K. C., and Srivastava, S. K. (2012). Apoptosis Signal-Regulating Kinase 1-thioredoxin Complex Dissociation by Capsaicin Causes Pancreatic Tumor Growth Suppression by Inducing Apoptosis. *Antioxid. Redox Signal.* 17, 1417–1432. doi:10.1089/ars.2011.4369

Prasad, R., Vaid, M., and Katiyar, S. K. (2012). Grape Proanthocyanidin Inhibit Pancreatic Cancer Cell Growth *In Vitro* and *In Vivo* through Induction of Apoptosis and by Targeting the PI3K/Akt Pathway. *PLoS One* 7, e43064. doi:10.1371/journal.pone.0043064

Qi, X., Zhang, D., Xu, X., Feng, F., Ren, G., Chu, Q., et al. (2012). Oridonin Nanosuspension Was More Effective Than Free Oridonin on G2/M Cell Cycle Arrest and Apoptosis in the Human Pancreatic Cancer PANC-1 Cell Line. *Int. J. Nanomedicine.* 7, 1793–1804. doi:10.2147/IJN.S29483

Roy, S. K., Chen, Q., Fu, J., Shankar, S., and Srivastava, R. K. (2011). Resveratrol Inhibits Growth of Orthotopic Pancreatic Tumors through Activation of FOXO Transcription Factors. *PLoS One* 6, e25166. doi:10.1371/journal.pone.0025166

Scatizzi, J. C., Hutcheson, J., Bickel, E., Haines, G. K., 3rd, and Perlman, H. (2007). Pro-apoptotic Bid Is Required for the Resolution of the Effector Phase of Inflammatory Arthritis. *Arthritis Res. Ther.* 9, R49. doi:10.1186/ar2204

Subramani, R., Gonzalez, E., Arumugam, A., Nandy, S., Gonzalez, V., Medel, J., et al. (2016). Nimbolide Inhibits Pancreatic Cancer Growth and Metastasis through ROS-Mediated Apoptosis and Inhibition of Epithelial-To-Mesenchymal Transition. *Sci. Rep.* 6, 19819. doi:10.1038/srep19819

Sun, K. Y., Guo, S. H., Li, Z. W., and Li, Y. (2013). Research Progress of DcR3. Chin. *J. Trau. Disab. Med.* 21, 210–211.

Tang, X. P., Tang, G. D., Fang, C. Y., Liang, Z. H., and Zhang, L. Y. (2013). Effects of Ginsenoside Rh2 on Growth and Migration of Pancreatic Cancer Cells. *World J. Gastroenterol.* 19, 1582–1592. doi:10.3748/wjg.v19.i10.1582

Wang, F., Wang, L., Qu, C., Chen, L., Geng, Y., Cheng, C., et al. (2021a). Kaempferol Induces ROS-dependent Apoptosis in Pancreatic Cancer Cells via TGM2-Mediated Akt/mTOR Signaling. *BMC Cancer* 21, 396. doi:10.1186/s12885-021-08158-z

Wang, J. L. (2018). *Study on the Chemical Constituents and Pharmacological Activity Evaluation of Vernonia Anthelminticus*. Beijing, China: Beijing University of Chinese Medicine.

Wang, J. W., Hao, W. W., Li, S. T., and Zhou, N. (2021b). Schisandrin B Inhibits the Proliferation and Invasion, Promotes the Apoptosis of Human Pancreatic Cancer Cells via Wnt/β-Catenin Signaling Pathway. *Prog. Anat. Sci.* 27, 58–60+64. doi:10.3892/or.2016.4992

Wang, W., Li, X., Sun, W., Zhang, L., Zhang, M., Hong, B., et al. (2012). Triptolide Triggers the Apoptosis of Pancreatic Cancer Cells via the Downregulation of Decoy Receptor 3 Expression. *J. Cancer Res. Clin. Oncol.* 138, 1597–1605. doi:10.1007/s00432-012-1235-x

Wang, X., Matta, R., Shen, G., Nelin, L. D., Pei, D., and Liu, Y. (2006). Mechanism of Triptolide-Induced Apoptosis: Effect on Caspase Activation and Bid Cleavage and Essentiality of the Hydroxyl Group of Triptolide. *J. Mol. Med. (Berl)* 84, 405–415. doi:10.1007/s00109-005-0022-4

Wang, Y., Liu, Z., Liu, Q., Han, Y., Zang, Y., Zhang, H., et al. (2020). Honokiol Suppressed Pancreatic Cancer Progression via Mir-101/Mcl-1 Axis. *Cancer Manag. Res.* 12, 5243–5254. doi:10.2147/CMAR.S237323

Wu, L. S., Jia, M., Chen, L., Zhu, B., Dong, H. X., Si, J. P., et al. (2015). Cytotoxic and Antifungal Constituents Isolated from the Metabolites of Endophytic Fungus DO14 from *Dendrobium Officinale*. *Molecules* 21, 14. doi:10.3390/molecules21010014

Xu, Y. (2019). *Anti-Pancreatic Cancer Active Quassinoids From* Brucea Javanica *and Their Structure-Activit Relationship*. Nanjing, China: Nanjing University of Chinese Medicine.

Yang, D., Li, Y., and Zhao, D. (2017). Curcumin Induces Apoptotic Cell Death in Human Pancreatic Cancer Cells via the miR-340/XIAP Signaling Pathway. *Oncol. Lett.* 14, 1811–1816. doi:10.3892/ol.2017.6321

Yu, L., Chen, M., Zhang, R., and Xu, T. (2019). Antitumor Effects of Glychionide-A Flavonoid in Human Pancreatic Carcinoma Cells are Mediated by Activation of Apoptotic and Autophagic Pathways, Cell Cycle Arrest, and Disruption of Mitochondrial Membrane Potential. *Med. Sci. Monit.* 25, 962–969. doi:10.12659/MSM.913400

Zhang, J., Wang, W., Zhou, Y., Yang, J., Xu, J., Xu, Z., et al. (2020). Terphenyllin Suppresses Orthotopic Pancreatic Tumor Growth and Prevents Metastasis in Mice. *Front. Pharmacol.* 11, 457. doi:10.3389/fphar.2020.00457

Zhang, J. H., Lai, F. J., Chen, H., Luo, J., Zhang, R. Y., Bu, H. Q., et al. (2013). Involvement of the Phosphoinositide 3-kinase/Akt Pathway in Apoptosis Induced by Capsaicin in the Human Pancreatic Cancer Cell Line PANC-1. *Oncol. Lett.* 5, 43–48. doi:10.3892/ol.2012.991

Zhang, Q., Liu, J., Zhang, M., Wei, S., Li, R., Gao, Y., et al. (2019). Apoptosis Induction of Fibroblast-Like Synoviocytes is an Important Molecular-Mechanism for Herbal Medicine Along With its Active Components in Treating Rheumatoid Arthritis. *Biomolecules* 9, 795. doi:10.3390/biom9120795

Zhang, R., Humphreys, I., Sahu, R. P., Shi, Y., and Srivastava, S. K. (2008). *In Vitro* and *In Vivo* Induction of Apoptosis by Capsaicin in Pancreatic Cancer Cells Is Mediated through ROS Generation and Mitochondrial Death Pathway. *Apoptosis* 13, 1465–1478. doi:10.1007/s10495-008-0278-6

Zhang, Q., Liu, J., Duan, H. X. Y., Li, R. L., Peng, W., Wu, C. J., et al. (2021). Activation of Nrf2/HO-1 Signaling: An Important Molecular Mechanism of Herbal Medicine in the Treatment of Atherosclerosis via the Protection of Vascular Endothelial Cells From Oxidative Stress. *J. Adv. Res.* 34, 43–63. doi:10.1016/j.jare.2021.06.023

Zhong, D. C., Chen, C., Li, T., Ma, Ni., Zhao, L. F., Xu, W. L., et al. (2020). Study on the Caspase 3/Bax/Bcl-2 Signal Pathway Mechanism of Induction Apoptosis Effect of Piperine in Human Pancreatic Cancer PANC-1 Cell. *Chin. J. Mod. Appl. Pharm.* 37, 1687–1691.

Zhou, G. X., Ding, X. L., Huang, J. F., Zhang, H., Wu, S. B., Cheng, J. P., et al. (2008). Apoptosis of Human Pancreatic Cancer Cells Induced by Triptolide. *World J. Gastroenterol.* 14, 1504–1509. doi:10.3748/wjg.14.1504

Zhou, G. X., Ding, X. L., Huang, J. F., Zhang, H., and Wu, S. B. (2007). Suppression of 5-lipoxygenase Gene Is Involved in Triptolide-Induced Apoptosis in Pancreatic Tumor Cell Lines. *Biochim. Biophys. Acta* 1770, 1021–1027. doi:10.1016/j.bbagen.2007.03.002

Zhou, H. B., Chen, J. M., Shao, L. M., and Chen, Z. G. (2015). Apoptosis of Human Pancreatic Carcinoma Cell-1 Cells Induced by Yin Chen Hao Decoction. *World J. Gastroenterol.* 21, 8352–8357. doi:10.3748/wjg.v21.i27.8352

Conflict of Interest: The authors declare that the research was conducted in the absence of any commercial or financial relationships that could be construed as a potential conflict of interest.

Publisher's Note: All claims expressed in this article are solely those of the authors and do not necessarily represent those of their affiliated organizations, or those of the publisher, the editors and the reviewers. Any product that may be evaluated in this article, or claim that may be made by its manufacturer, is not guaranteed or endorsed by the publisher.

Copyright © 2022 Li, Tang, Yang, Qian and Xu. This is an open-access article distributed under the terms of the Creative Commons Attribution License (CC BY). The use, distribution or reproduction in other forums is permitted, provided the original author(s) and the copyright owner(s) are credited and that the original publication in this journal is cited, in accordance with accepted academic practice. No use, distribution or reproduction is permitted which does not comply with these terms.

frontiers in Pharmacology

ORIGINAL RESEARCH
published: 16 February 2022
doi: 10.3389/fphar.2022.794528

An Integrated Approach Based on Network Analysis Combined With Experimental Verification Reveals PI3K/Akt/Nrf2 Signaling Is an Important Way for the Anti-Myocardial Ischemia Activity of *Yi-Qi-Tong-Luo* Capsule

Huxinyue Duan[1†], Meiyan Li[1†], Jia Liu, Jiayi Sun[1], Chunjie Wu[1], Yu Chen[2], Xiaohui Guo[3*] and Xinglong Liu[1*]*

[1]Chengdu University of Traditional Chinese Medicine, Chengdu, China, [2]Guangyuan Hospital of Traditional Chinese Medicine, Guangyuan, China, [3]Hospital of Chengdu University of Traditional Chinese Medicine, Chengdu, China

OPEN ACCESS

Edited by:
Hong Zhang,
Shanghai University of Traditional Chinese Medicine, China

Reviewed by:
Bin Li,
Army Medical University, China
Ting Han,
Second Military Medical University, China

***Correspondence:**
Yu Chen
chenyu870411@163.com
Xiaohui Guo
guoxiaohui@cdutcm.edu.cn
Xinglong Liu
liuxinglong@cdutcm.edu.cn

[†]These authors have contributed equally to this work

Specialty section:
This article was submitted to Ethnopharmacology, a section of the journal Frontiers in Pharmacology

Received: *13 October 2021*
Accepted: *24 January 2022*
Published: *16 February 2022*

Citation:
Duan H, Li M, Liu J, Sun J, Wu C, Chen Y, Guo X and Liu X (2022) An Integrated Approach Based on Network Analysis Combined With Experimental Verification Reveals PI3K/Akt/Nrf2 Signaling Is an Important Way for the Anti-Myocardial Ischemia Activity of Yi-Qi-Tong-Luo Capsule. Front. Pharmacol. 13:794528. doi: 10.3389/fphar.2022.794528

Background: *Yiqi-Tongluo Capsule* (YTC) is a Chinese traditional patent medicine that has been used in the treatment of myocardial ischemia (MI). However, its molecular mechanisms against MI have not been clear.

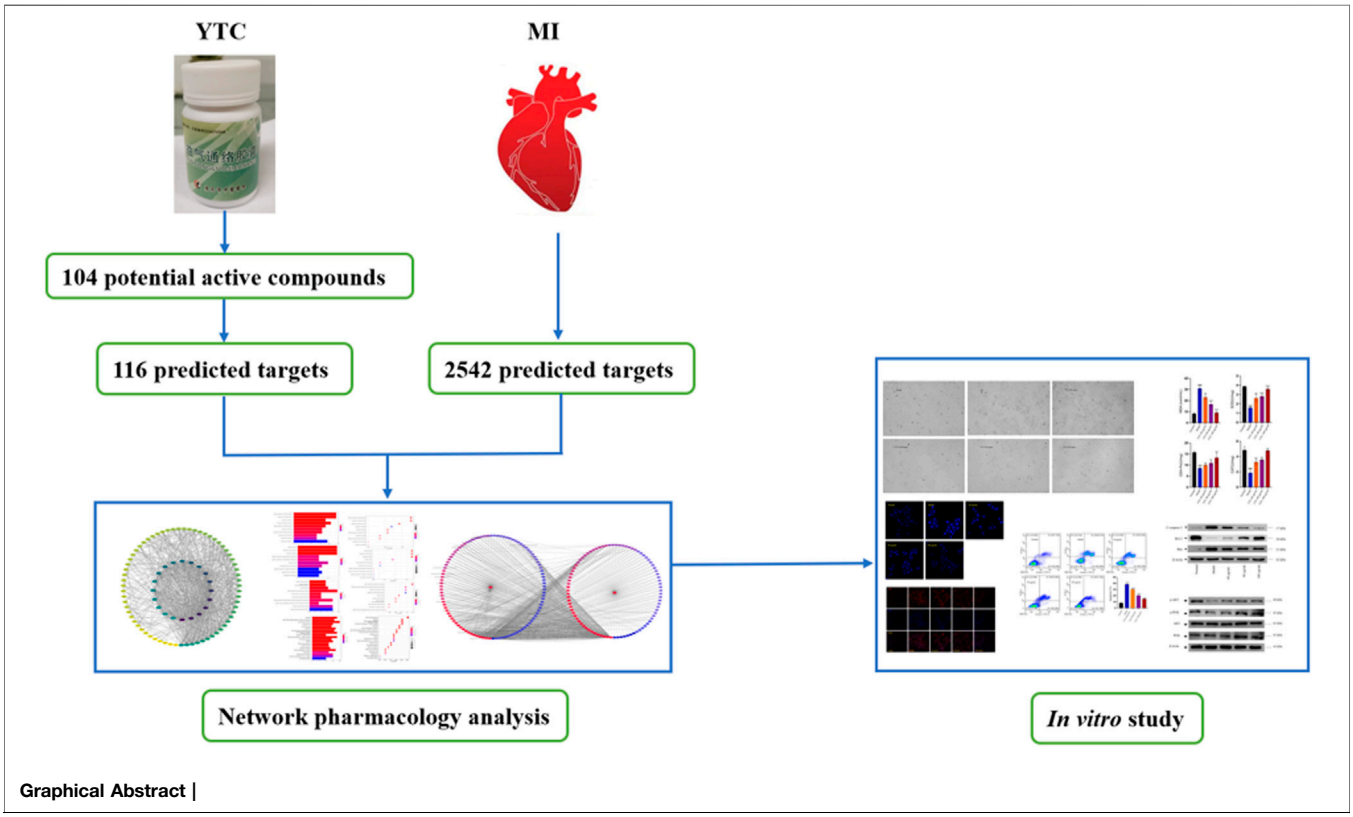
Methods: Network analysis and experimental verification were used to explore the potential molecular mechanisms of YTC for MI treatment. Firstly, the main components in the capsules and the potential targets of these components were predicted by online databases. The MI related genes were collected from Genecards and Online Mendelian Inheritance in Man (OMIM) databases. The drug targets and disease targets were intersected, and then the protein-protein interaction (PPI) and Drug-Molecular-Target-Disease Network (DMTD) were constructed, and GO enrichment analysis and KEGG pathway enrichment analysis were performed. Based on the H_2O_2-stimulated H9c2 cells, flow cytometry, western blot (WB) and immunofluorescence experiments were performed to verify the network analysis prediction.

Results: A total of 100 active components and 165 targets of YTC were predicted, in which there were 109 targets intersected with the targets of MI. GO and KEGG analysis showed that these potential targets were related to a variety of biological processes and molecular mechanisms, including oxidative stress and PI3K/AKT pathway. Astragaloside IV (AS IV) and paeoniflorin (PAE) might be the main active components in YTC. The results of cell counting kit-8 (CCK-8) showed that YTC alleviated the damage of H_2O_2 to H9c2 cells. The results of flow cytometry, DAPI staining and JC-1 probe showed that YTC alleviated H_2O_2 induced apoptosis in H9c2 cells. In addition, YTC reduced the level of intracellular superoxide anion, increased the activities of superoxide dismutase (SOD), catalase (CAT) and glutathione peroxidase (GSH-Px), and reduced the content of malondialdehyde (MDA) in H_2O_2-induced H9c2 cells. The results of

immunofluorescence and WB showed that the phosphorylation of PI3K and Akt were increased, the expression of Bcl-2 was up-regulated and the expression of cleaved caspase-3 and Bax were down-regulated. Besides, the nuclear translocation of Nrf2 were increased.

Conclusion: In conclusion, the results of this study showed that YTC might alleviate MI by suppressing apoptosis induced by oxidative stress via the PI3K/Akt/Nrf2 signal pathway.

Keywords: apoptosis, myocardial ischemia, network analysis, oxidative stress, Yi-Qi-Tong-Luo Capsule



Graphical Abstract |

INTRODUCTION

Myocardial ischemia (MI) is a physical condition in which the blood perfusion of heart is decreased, resulting in insufficient blood flow, insufficient oxygen supply and abnormal energy metabolism (Fan et al., 2019). As a common cardiovascular disease, MI can lead to irreversible myocardial damage, which has high incidence rate and mortality rate worldwide (Li et al., 2021). It has been reported that the pathogenesis of MI involves a variety of biological processes, including oxidative stress, apoptosis, inflammatory and immune responses (Zhao and Vinten, 2002; Kaul and Ito, 2004; Arslan et al., 2011; Yang et al., 2014). Currently, nitrates, calcium antagonists and β-blockers are the drugs commonly used in cardiovascular diseases; nonetheless, the mortality rate caused by MI is still high all over the world (Malakar et al., 2019). Therefore, it is necessary to identify more safe and effective drugs for MI. With a long history of clinic use, Traditional Chinese medicine (TCM) has great advantages to treat cardiovascular diseases (Duan et al., 2021; Zhang et al., 2021a), which can be seen as a resource library for alternative drugs of MI (Wu et al., 2020).

Yiqi-Tongluo Capsule (YTC) is a Chinese patent medicine of the Guangyuan Hospital of traditional Chinese medicine, and it has been used for decades in the treatment of MI with reliable therapeutical effects (Zhang, 2015). YTC is consisted of the roots of *Astragalus membranaceus* (Fisch.) Bge. var. mongholicus (Bge.) Hsiao (also called *Huangqi* in Chinese), the roots of *Angelica sinensis* (Oliv.) Diels (also called *Danggui* in Chinese), the body of *Pheretima aspergillum* (E. Perrier) (also called *Dilong* in Chinese), the root of *Paeonia lactiflora* Pall. (also

called *Chishao* in Chinese), the root of *Codonopsis pilosula* (Franch.) Nannf. (also called *Dangshen* in Chinese), the roots of *Ligusticum chuanxiong* Hort. (also called *Chuanxiong* in Chinese), the flower of *Carthamus tinctorius* L. (also called *Honghua* in Chinese), et al. It has been reported that extracts from *A. membranaceus* improved cardiac function in a rat model of MI by reducing myocardial cells apoptosis (Ma et al., 2013). Another study showed that astragalus polysaccharides alleviated inflammation and necrosis of myocardium in myocardial ischemia-reperfusion rats (He et al., 2018). In addition, *A. sinensis* polysaccharides were reported had cardioprotective activity in myocardial ischemia-reperfusion rats via its capacity of antioxidant, up-regulation of CT-1 and down-regulation of caspase-12 mRNA (Zhang et al., 2010). However, the active ingredients and molecular mechanisms of YTC are still unclear, which limits its further application and promotion.

Network analysis is an emerging technology, which integrates a variety of disciplines, including system biology, multi-directional pharmacology, network analysis and computational biology (Hopkins, 2008). In this approach, based on the interaction between drugs, components, targets and disease, incorporates biological networks and drug action networks are established to analyze and predict the potential active ingredients and mechanism of action of drugs (Xu et al., 2014). TCM is characterized by multi-components and multi-targets, which cause difficulty in illustrating the specific mechanism of TCM. Therefore, it is suitable to use network analysis to help us systematically study TCM and provide scientific basis for the research of TCM. In this study, the main components of YTC, the potential targets and underlying mechanisms were predicted by network analysis. And the predicted results of network analysis were verified by vitro experiments. The above study not only reveal the potential chemical and pharmacological basis of YTC, but also provides reference for the development and promotion of Chinese patent medicine. The main process of this study is presented in Graphical Abstract.

MATERIALS AND METHODS

Chemicals, Reagents, and Materials

All herbal medicines were provided by Guangyuan Hospital of Traditional Chinese Medicine (Guangyuan, China). Fetal bovine serum (FBS) and Dulbecco's modified Eagle medium (DMEM) were purchased from the Gibco Co. (Grand Island, NY, United States). BCA protein assay reagents, SDS-polyacrylamide gel electrophoresis (SDS-PAGE) preparation kit, penicillin-streptomycin mixture, trypsin, phosphate buffer saline (PBS) and cell counting kit-8 (CCK-8) were purchased from Boster Biological Technology Co., Ltd. (Wuhan, China). Annexin V-FITC/PI assay kit was purchased from Multisciences (Lianke) Biotechnology Corporate Limited (Hangzhou, China). H_2O_2 was purchased from Chengdu Chron Chemicals Co. Ltd. (Chengdu, China). Primary antibodies for PI3K, phosphorylation-PI3K (p-PI3K), AKT, phosphorylation-AKT (p-AKT), Nrf2, Bcl-2, Bax and cleaved-caspase-3 (C- caspase-3) were obtained from the ImmunoWay Biotechnology Co. (Suzhou, China). The assay kits for MDA, SOD, CAT, and GSH-PX were purchased from the Nanjing Jiancheng Bioengineering Institute (Nanjing, China). Ultrapure water purified by Millipore Ultra-pure Water Purifier (Millipore, Milford, MA, United States) was used. Other reagents were all of analytical grade.

Preparation of *Yiqi-Tongluo* Capsule Freeze-Dried Powder

All the dried herbal medicines including the roots of *Astragalus membranaceus* (Fisch.) Bge. var. mongholicus (Bge.) Hsiao (304 g), the roots of *Angelica sinensis* (Oliv.) Diels (190 g), the body of *Pheretima aspergillum* (E. Perrier) (114 g), the root of *Paeonia lactiflora* Pall. (152 g), the root of *Codonopsis pilosula* (Franch.) Nannf. (304 g), the roots of *Ligusticum chuanxiong* Hort. (190 g), the flower of *Carthamus tinctorius* L. (76 g), and the aboveground parts of *Mentha haplocalyx* Briq (76 g), were powdered and extracted with water by decoction for 3 times (1 hour each time). Then, the decoction was filtered and concentrated under 60°C to afford the thick paste with a vacuum rotary evaporator (EYELA, N-1300V, Tokyo, Japan). Subsequently, a lyophilizer (Labconco Co., Kansas, MI, United States) was used to freeze-dry the extracts to obtained the powder, which was sealed and stored at 4°C (yield 30%) for subsequent experiments.

Network Analysis

Screening of *Yiqi-Tongluo* Capsule Active Ingredients and Targets

The potential active components of YTC were screened from the Traditional Chinese Medicine Integrated Database (TCMSP, https://old.tcmsp-e.com/tcmsp.php). Subsequently, the ChemDraw professional 15.0 were used to draw the chemical structures. Then, the Mol. format files were uploaded to SwissTargetPrediction (http://www.swisstargetprediction.ch/) and TCMSP (https://old.tcmsp-e.com/tcmsp.php) online databases to obtain potential targets. In addition, some important components and targets of single drugs in YTC reported in literatures were supplemented (Sun et al., 2012; Qu et al., 2016; Bai et al., 2020; Wang et al., 2020).

To Establish Myocardial Ischemia Targets Library

The key word "myocardial ischemia" was input into the Online Mendelian Inheritance in Man database (OMIM) and the Genecards database (http://www.genecards.org) to screen target genes of MI. Then, the collected target genes were converted into standard gene names through the UniProt database (http://www.uniprot.org/).

Protein-Protein Interaction

Then, the potential targets of components in YTC and MI-related genes were overlapped as the objective targets. The PPI analysis was performed by the online STRING database (https://string-db.org/). The results of PPI analysis were updated into Cytoscape software (ver.3.7.1) to visualize these interactions and construct PPI network. Furthermore, CytohHubba plug-in tool was used to analyze the important proteins in PPI.

Drug-Molecular-Target-Disease Network Construction

Selected compounds and targets were uploaded into Cytoscape software (ver.3.7.1) to construct the Drug-Molecular-Target-Disease Network (DMTD) diagram. In this network diagram, nodes shoed the drug, disease, ingredients and genes, while edges represented the relationships between them. Finally, the importance of each node in the network was evaluated by calculating the degree, average shortest path length and closeness centrality in DMTD.

Bioinformatic Analysis

The clusterprofiler software package was downloaded in R language software to analyze the gene ontology (GO) term function and the Kyoto Encyclopedia of genes and genomes (KEGG) pathway enrichment, so as to obtain the function and pathway of the collected proteins. In this study, the criterion of statistically significant was $p < 0.05$, and only the top 10 were shown in the results.

In vitro Experiment

Cell Culture and Treatment

The H9c2 cells, a kind of cardiac myoblast isolated from rat, were purchased from Shanghai Yubo Biotech Co., Ltd. (Shanghai, China), and cultured in DMEM with FBS, 100 U/mL penicillin and 100 μg/ml streptomycin. Cells were cultured in a 37°C incubator with 95% air and 5% CO_2, and were subcultured every 2–3 days. Only cells in the exponential growth stage were used in this study.

Different concentrations of YTC (60, 80, and 100 μg/ml) were used to pretreat H9c2 cells for 24 h and then 200 μM H_2O_2 (Zhang et al., 2018) was incubated with cells for another 4 h. In the model group, YTC was replaced by the same amount of DMEM medium.

Cell Viability Assay

Cell viability was measured by a CCK-8 kit. H9c2 cells were seeded in a 96 well plate at 1×10^4 cells/well, and then treated with different concentrations of YTC (40, 60, 80, 100 and 120 μg/ml) for 24 h. After removing the medium containing YTC, 10 μl CCK8 solution and 90 μl fresh medium were added, and cells were incubated for 30 min in the incubator. At last, the optical density (OD) values were determined by a microplate reader at 450 nm. After that, H9c2 cells were pretreated with different concentrations of YTC (40, 60, 80, 100 and 120 μg/ml) for 24 h, and then treated with 200 μM H_2O_2 for 4 h.

Nuclear Staining with DAPI

H9c2 cells were incubated in a 6-well plate (1×10^5 cells/well) and pretreated with YTC (60, 80 and 100 μg/ml) for 24 h, and subsequently treated with 200 μM H_2O_2 for 4 h. After that, the cells were washed twice with PBS, and then fixed with 4% polyoxymethylene for 15 min. After fixation, the cells were incubated with DAPI solution in dark room for 10 min. Then, cells were washed with PBS and observed under a fluorescence microscope.

Apoptosis Assay by Flow Cytometer

The cells were incubated in a 6-well plate (1×10^5/well) and then treated as described above. Then, the cells were collected and washed with PBS, and the supernatant was removed by centrifugation. The diluted Annexin V binding buffer working solution was used to resuspend cells, and then 2.5 μl Annexin V-FITC and 2.5 μl PI staining solution was added. After mixed well and incubated at room temperature in the dark for 20 min, the apoptosis rate of cells was detected by a flow cytometry (Beckman Coulter Company, Brea, CA, United States).

Influence of Main Active Components on H9c2 Cells

According to the results of DMTD and many reported articles, two potential active components were selected as the main components of YTC, including astragaloside IV (AS IV) and paeoniflorin (PAE). Firstly, the effects of these two compounds on the viability of H_2O_2-induced H9c2 cells were detected by a CCK-8 kit. Then the anti-apoptosis effects of these components were detected by a flow cytometry. The experimental steps of CCK-8 and flow cytometry were described above.

Determination of Mitochondrial Membrane Potential

The cells were seeded in laser confocal dishes (1×10^4/well) and then treated with YTC and H_2O_2 as described above. Then, 10 μg/ml JC-1 probe was added and incubated for 30 min under dark conditions. Subsequently, after washing twice with PBS, cells were observed under a laser confocal microscope (Leica, SP8 SR, Wetzlar, Germany) to obtain the fluorescence images.

Detection of Intracellular ROS

The fluorescence probe dihydrogen ingot (DHE) was used to detect intracellular superoxide anion levels. Briefly, H9c2 cells were seeded in laser confocal dishes (1×10^4/well) and treated with YTC and H_2O_2 as described above. Subsequently, cells were incubated with 10 μM DHE for 20 min, and subsequently cultured with DAPI solution for 10 min. Then, the cells were washed with PBS and observed by a laser confocal microscope (Leica, SP8 SR, Wetzlar, Germany).

Determination of MDA, SOD, GSH-Px and CAT

Commercial assay kits were used to assay these antioxidant indexes according to the instructions. In brief, cells were seeded in 6-well plates (1×10^5 cells/well) and treated with H_2O_2 and YTC as described above after incubated for 24 h. Then the RIPA lysis buffer was added to lyse cells, and the supernatant was collected after centrifuging to obtain the total protein. Subsequently, the level of MDA and activities of SOD, GSH-Px and CAT were assayed by assay kits according to the steps described in instructions.

Detection of Nuclear Translocation of Nrf2

The H9c2 cells were seeded in laser confocal plates (1×10^4/well) and treated with YTC (60, 80 and 100 μg/ml) and H_2O_2 (200 μM) as described above. Then, the cells were incubated with 4% paraformaldehyde for 30 min and subsequently infiltrated with

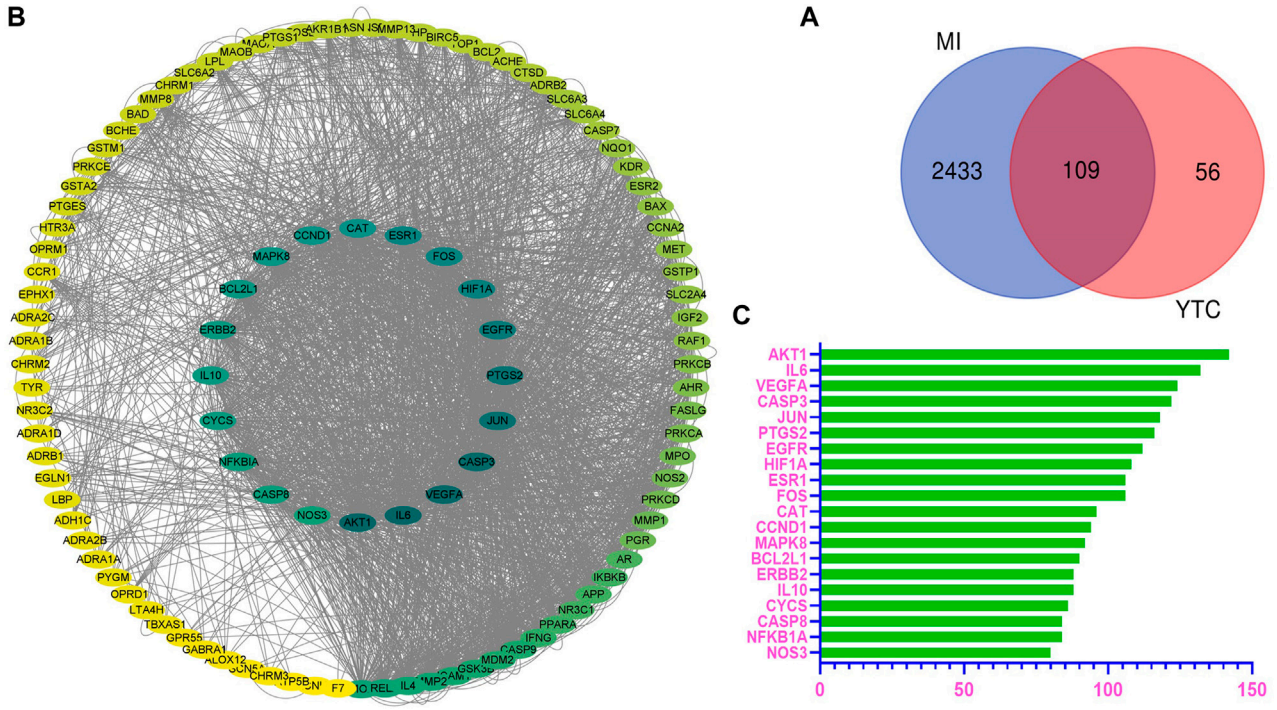


FIGURE 1 | Overlapped targets screen. **(A)** The protein-protein interaction (PPI) network of targets. The colors of the nodes are illustrated from green to yellow in descending order of degree values. **(B)** Overlap targets of YTC and MI. The blue circles represent MI targets and the red circles represent YTC targets. The overlapped area is the targets of YTC anti-MI. **(C)** The top 20 genes in the PPI network were selected based on the degree.

0.3% Triton for 30 min. After that, cells were incubated with 10% serum for 1 h. Then, the samples were incubated overnight with primary antibody Nrf2 at 4°C. Subsequently, the samples were washed with PBS for 3 times and incubated with fluorescent secondary antibody for 2 h. Finally, DAPI sealing agent was added and the samples were imaged under a laser confocal microscope (Leica, SP8 SR, Wetzlar, Germany).

Western Blotting Assay

After treating as described above, cells were collected and proteins were obtained by adding 100 μl RIPA lysis buffer at the end of the treatment. A BCA protein assay kit was used to assay the protein concentrations of the supernatants. Then, SDS-PAGE was prepared to separate the protein, and the separated protein was transferred onto polyvinylidene fluoride (PVDF) membrane. Then, the PVDF membrane was blocked with 5% fat-free milk at room temperature, and was subsequently incubated with primary antibodies of Bcl-2 (dilution of 1:1,000), Bax (dilution of 1:1,000), C-caspase-3 (dilution of 1:1,000), Akt (dilution of 1:1,000), p-Akt (dilution of 1:1,000), PI3K(dilution of 1:1,000) and p-PI3K(dilution of 1:1,000). After washed for three times, the membrane was incubated with HPR-conjugated antibody (1:5,000) for 1 hour. Finally, the membrane were imaged under an enhanced chemiluminescence (ECL) system, and β-actin was used as the internal reference. Gray analysis of each blot was performed by the ImageJ software (version 1.51, National Institutes of Health, MD, United States).

Immunofluorescence Assay

The H9c2 cells were seeded in laser confocal plates (1×10^4/well) and treated with YTC (60, 80 and 100 μg/ml) and H_2O_2 (200 μM) as described above. Then, the cells were incubated with 4% paraformaldehyde for 30 min and subsequently washed with PBS for 3 times. Then, the H9c2 cells were infiltrated with 0.3% Triton for 30 min. After that, cells were incubated with 10% serum for 1 h. Then, the samples were incubated overnight with primary antibody PI3K, p-PI3K, Akt, p-Akt, Bcl-2 and Bax at 4°C. Subsequently, the samples were washed with PBS for 3 times and incubated with fluorescent secondary antibody for 2 h. Finally, DAPI sealing agent was added and the samples were imaged under a laser confocal microscope (Leica, SP8 SR, Wetzlar, Germany).

Statistical Analysis

The results of this study were expressed as mean ± SD. Student's t-test and one-way analysis of variance (ANOVA) were used to analyze these data, and $p < 0.05$ was significant. Each experiment was repeated three times.

RESULTS

Chemical Composition of YTC Extract

161 components were collected, including 19 components in Huangqi, 3 components in Danggui, 3 components in Dilong, 22 components in Chishao, 18 components in Dangshen, 26

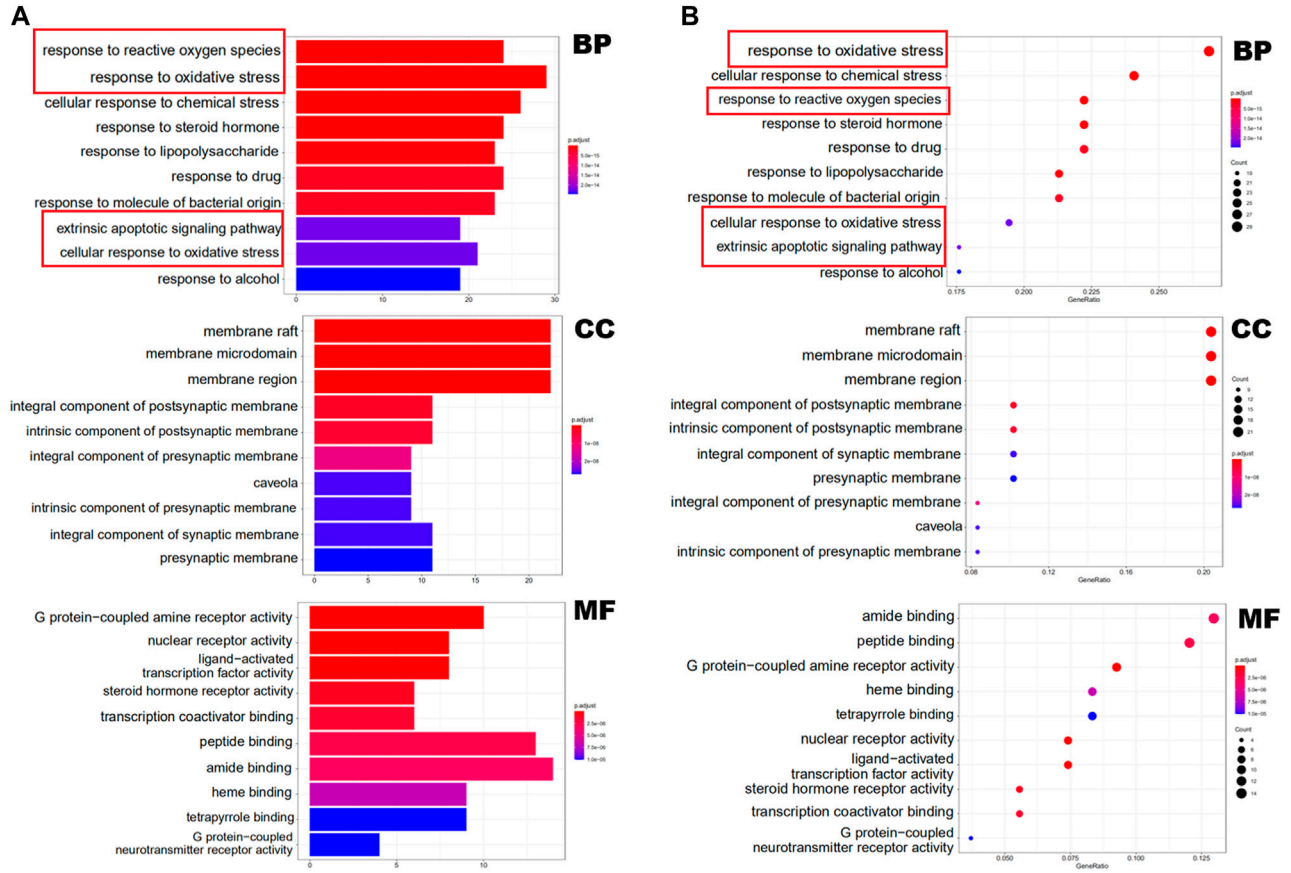


FIGURE 2 | GO functional enrichment analysis represented in bar chart **(A)** and bubble diagram**(B)**.

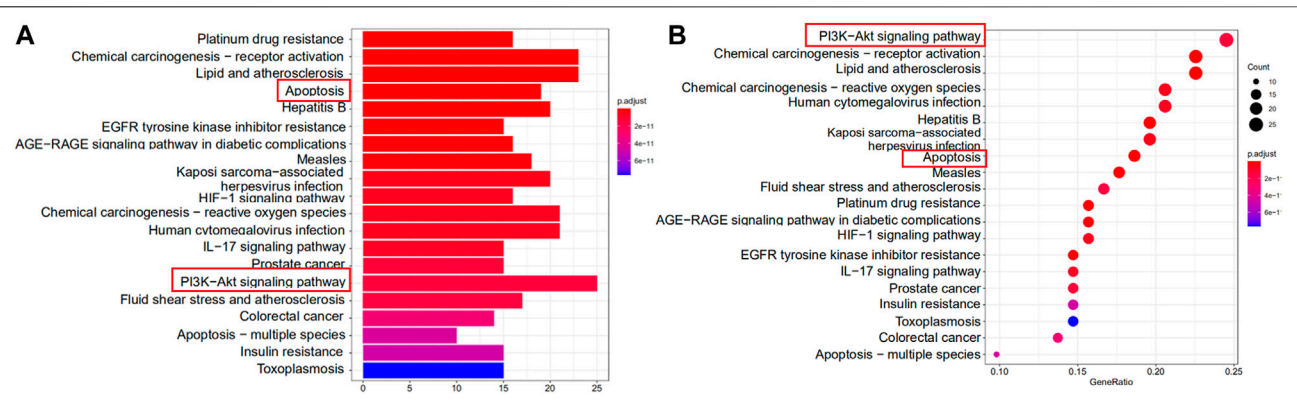


FIGURE 3 | KEGG functional enrichment analysis represented in bar chart **(A)** and bubble diagram **(B)**.

components in Chuanxiong, 15 components in Honghua, 4 components in Taoren, 33 components in Jiangxiang, 7 components in Xiebai, 1 components in Gualoupi and 10 components in Bohe. After the repetitive components were eliminated, 146 components were obtained (**Supplementary Table S1**).

Target Prediction of YTC Against MI

From online databases and previous reports, 165 targets of YTC were collected after deleting duplicated targets. And a total of 2542 MI-associated genes were collected from the OMIM and Genecards database. Subsequently, combining the potential target genes of YTC with MI-associated target genes, 109 overlapped genes were

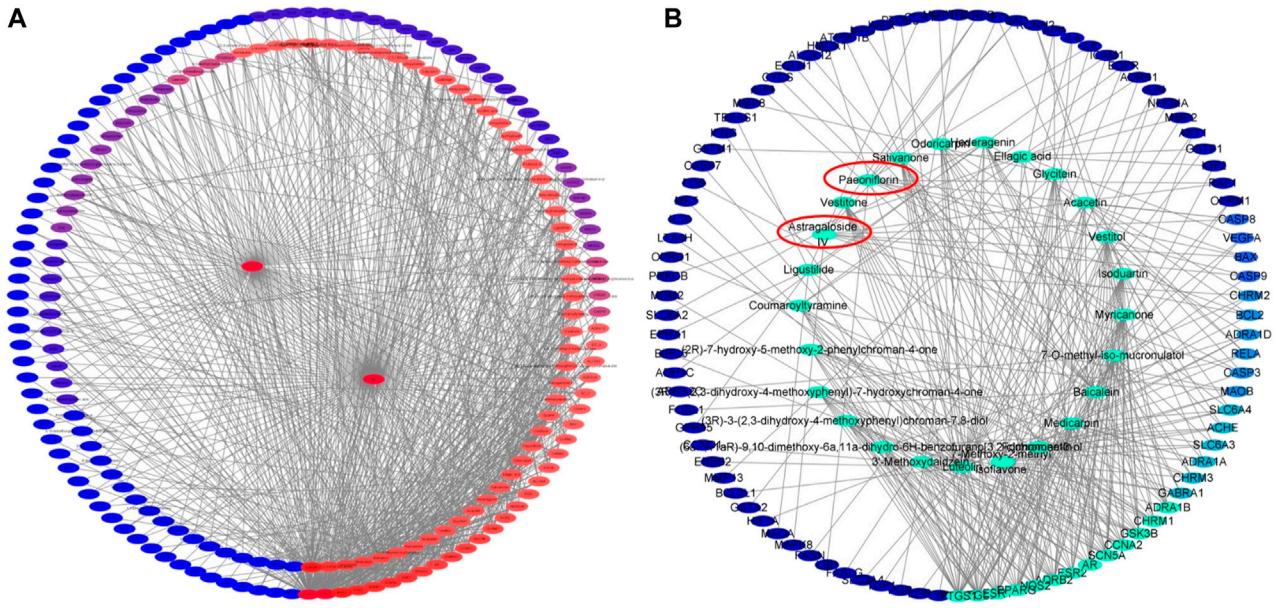


FIGURE 4 | Network analysis of potential active compounds and targets. **(A)**The drug, active compounds, disease and targets were input into Cytoscape to construct the DMTD diagram, and the colors of the nodes are illustrated from red to blue in descending order of degree values. **(B)** The top 25 components and their related targets in the DMTD network were selected based on the degree, and the colors of the nodes are illustrated from green to blue in descending order of degree values.

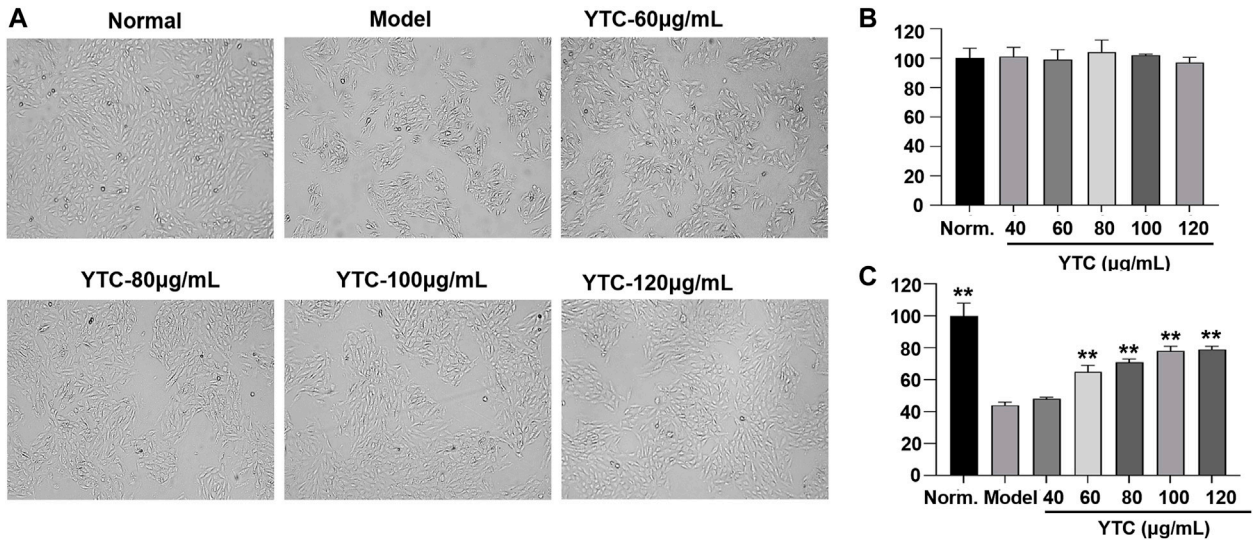


FIGURE 5 | Protective effects of YTC on the cell viability of H_2O_2-stimulated H9c2 cells. **(A)** The represented cell morphology of H9c2 cells with different treatment. **(B)** Effects of YTC on cell viability of normal H9c2 cell. **(C)** Effects of YTC on cell viability of H_2O_2-stimulated H9c2 cells under different concentration. The values were represented as the mean ± SD (n = 3). $^{**}p < 0.01$ vs the model group.

gained, as shown in the Venn diagram (**Figure 1A**). The 109 genes were considered the molecular targets of YTC against MI.

Results of PPI Network Analysis

Based on the potential protein targets of YTC against MI, the PPI network was constructed by STRING database and was entered into Cytoscape (ver.3.7.1) for visualization. As shown in **Figure 1B**, the edges represent the interaction between the two proteins, and the node represents the target proteins.

The most important 20 targets were selected according to node degree, as shown in **Figure 1C**, including AKT1, IL6, VEGFA, CASP3, JUN, PTGS2, EGFR, HIF1A, ESR1, FOS, CAT,

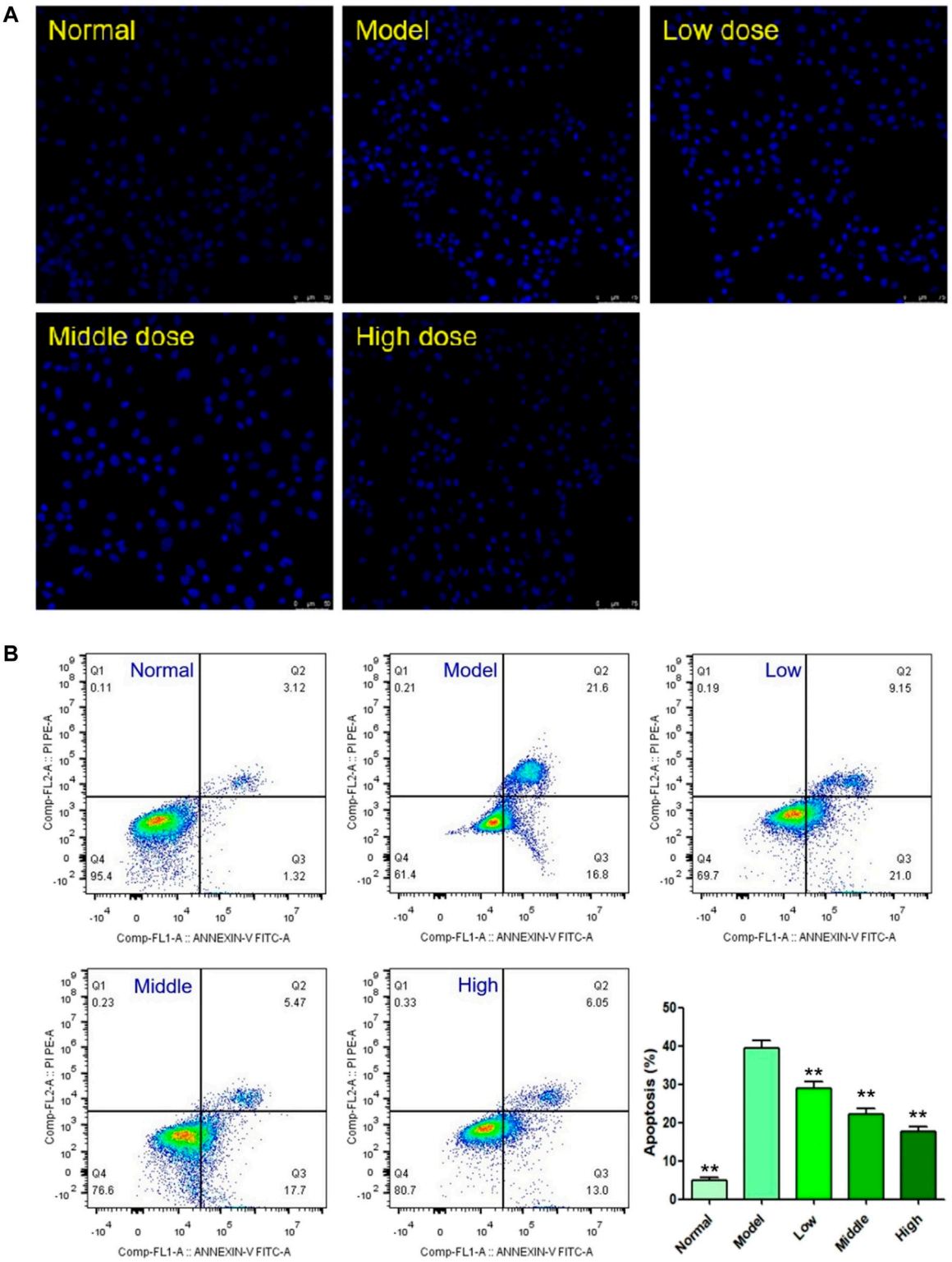


FIGURE 6 | Effects of YTC on apoptosis in H_2O_2-stimulated H9c2 cells. **(A)** Apoptotic assay by DAPI staining. **(B)** Apoptotic assay by flow cytometry. The values were represented as the mean ± SD (n = 3). $^{**}p < 0.01$ vs the model group.

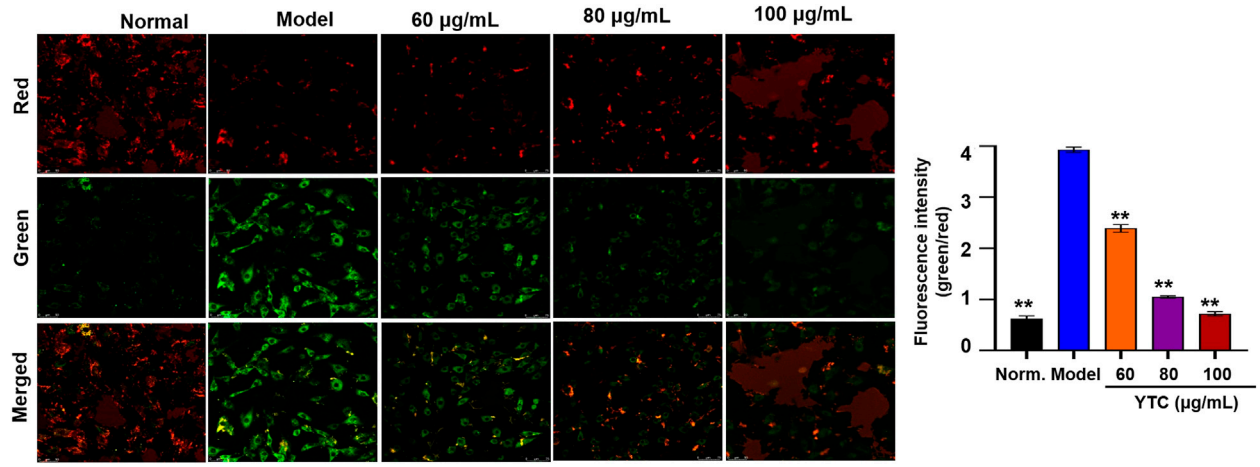


FIGURE 7 | Effects of YTC on the ΔΨm in H9c2 cells (×40). Cells were pretreated with YTC (60, 80 and 100 μg/ml) for 24 h, and then incubated in the presence of H_2O_2 (200 μM) for 4 h ΔΨm was measured using a JC-1 assay kit and observed using a laser confocal microscopy under a 100× microscope. Data were expressed as the mean ± SD (n = 3). $^{**}p < 0.01$ vs model group.

CCND1, MAPK8, BCL2L1, ERBB2, IL10, CYCS, CASP8, NFKBIA, NOS3, indicating these genes might be the main potential targets of YTC.

GO and KEGG Enrichment Analyses

In **Figure 2**, the terms of GO are located on the *y*-axis, and the number on the *x*-axis represents the degree of enrichment. The color of red indicates high reliability, whereas the color of blue indicates low reliability. The results of GO analysis indicates that the biological processes (BPs) of these targets are mainly in the response to reactive oxygen species, oxidative stress and chemical stress. Cellular components (CCs) are mainly related to membrane raft, membrane microdomain and membrane region. The main molecular functions (MFs) are the G protein-coupled amine receptor activity, nuclear receptor activity and ligand-activated transcription factor activity (**Supplementary Table S2**).

Enrichment analysis of KEGG pathway of the 109 potential therapeutic targets was performed to further identify the potential pathways, and the detail information was presented in **Supplementary Table S3**. The most important 20 signaling pathways are shown in **Figure 3**, including platinum drug resistance, chemical carcinogenesis-receptor activation, lipid and atherosclerosis, apoptosis, hepatitis B, measles, prostate cancer and PI3K-Akt signaling pathway. Among them, apoptosis signaling pathway and PI3K-Akt signaling pathway were mainly found to be involved in apoptosis or oxidative stress biological processes related to MI (Zhai et al., 2017; Yuan et al., 2020). In addition, the analysis results of GO also suggested that oxidative stress might be an important biological process of YTC to against MI. Combined with PPI analysis and previous literatures, it was shown that CASP3, MAPK8, FOS, HSP90AA1, NOS3, ERBB2 and CASP8 were associated with apoptosis or oxidative stress in MI (Sato et al., 2001; Scarabelli et al., 2002; Wei et al., 2011; Zhu et al., 2016; Bai et al., 2019; Ma and Jin, 2019). Therefore, we established a H_2O_2 stimulated H9c2 cell model *in vitro* to further explore and study the myocardial protection effects of YTC.

The Main Potential Active Component Against MI in YTC

As shown in **Figure 4A**, the DMTD diagram contained 193 nodes and 817 edges, including 1 disease, 1 drug, 100 components and 109 targets. The right circle consisted of targets, while the left circle consisted of components. The color changed from blue to red meant a greater number of connections and more important the connection is. The 100 components of YTC acted on different targets at the same time, which indicated that the effect of YTC on MI had the characteristics of multi-components and multi-targets. In addition, the top 25 components and related targets were selected, as shown in **Figure 4B.** According to the DMTD diagram and previous reports, AS IV and PAE, the characteristic components in YTC, were selected as the potential main active components and verified in subsequent experiments.

Experimental Validation In Vitro

Effect of YTC on Cell Viability

The H9c2 cells were treated with different concentrations of YTC (0, 40, 60, 80, 100 and 120 μg/ml) for 24 h. As shown in **Figure 5B**, YTC at the different concentrations had no obvious damages on the viability of H9c2 cells compared with the normal group ($p > 0.05$). Whereas, after incubating with 200 μM H_2O_2 for 4 h, the viability of H9c2 cells decreased to nearly 40% compared with the normal group ($p < 0.01$) (**Figures 5A,C**). The viability of cells pretreated with YTC (60, 80, 100 and 120 μg/ml) for 24 h before stimulating by H_2O_2 concentration-dependently increased compared with the model group ($p < 0.01$) (**Figures 5A,C**).

Effects of YTC on Cell Apoptosis

DAPI staining and flow cytometry were used to detect the effect of YTC on apoptosis in H9c2 cells. DAPI is a

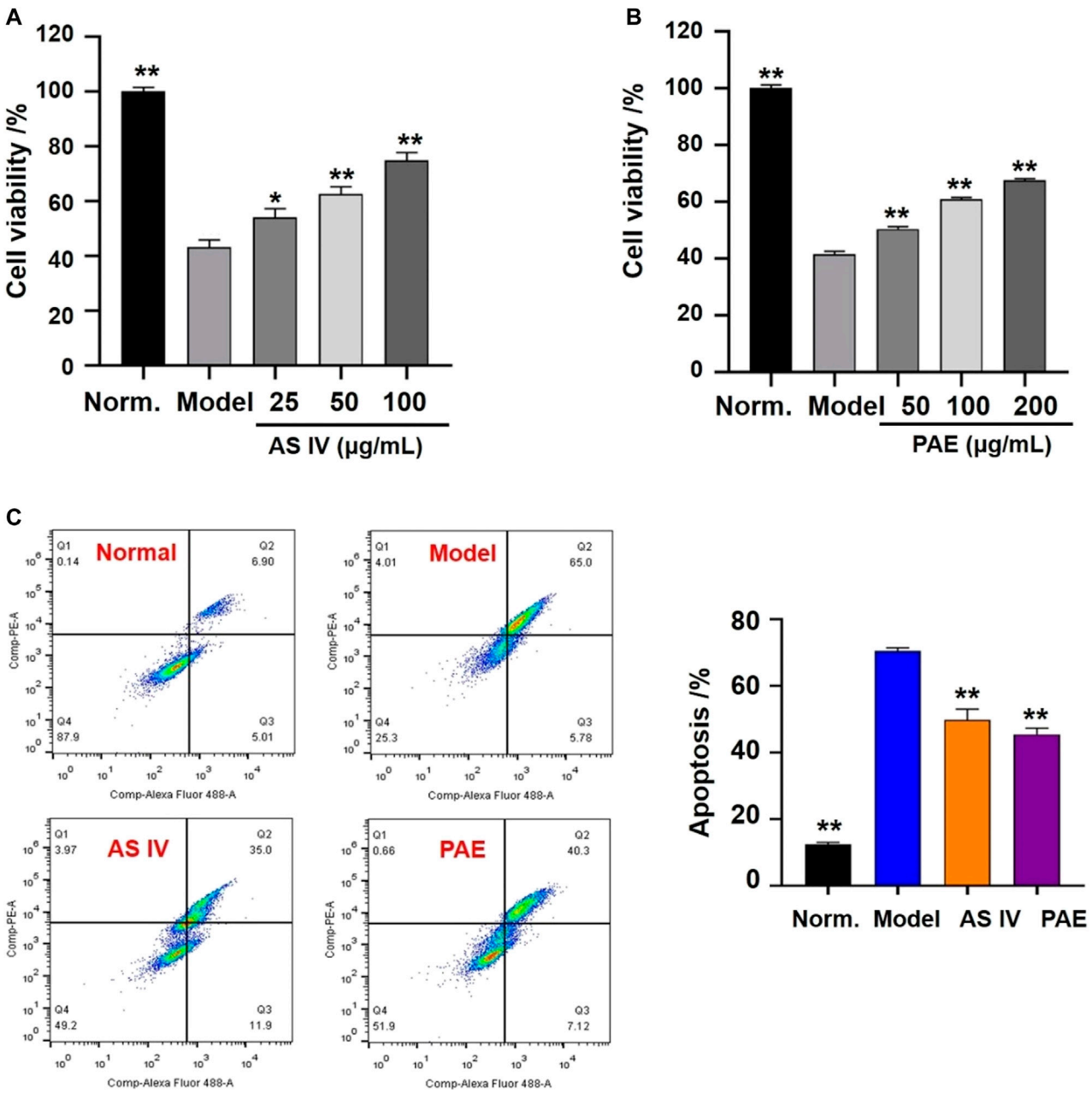


FIGURE 8 | Effects of the main active components (AS IV and PAE) on cell viability and apoptosis in H_2O_2-stimulated H9c2 cells. **(A)** Effects of AS IV on cell viability of H2O2-stimulated H9c2 cells under different concentration (25, 50 and 100 μM). **(B)** Effects of PAE on cell viability of H2O2-stimulated H9c2 cells under different concentration (50, 100 and 200 μM). **(C)** Apoptotic assay by flow cytometry. The values were represented as the mean ± SD ($n = 3$). $^{*}p < 0.05$, $^{**}p < 0.01$ vs model group.

fluorescent dye which can penetrate cell membrane and is widely used in apoptosis assay. As shown in **Figure 6A**, under a fluorescence microscope, normal H9c2 cells were alive with round and intact nucleus and faint blue fluorescence. On the contrary, the nuclear of H_2O_2-stimulated cells shrank and showed obviously bright blue fluorescence, indicating characteristic apoptotic features. However, YTC treatment could significantly attenuate above morphological changes induced by H_2O_2.

The results of DAPI staining assay were also confirmed by flow cytometry assay. As shown in **Figure 6B**, 200 μM H_2O_2 triggered a high magnitude of apoptosis (38.40%), which was significantly higher than the rate in the normal group (4.44%, $p < 0.01$). However, the cell viability of YTC (60, 80 and 100 μg/ml) treatment group was significantly improved, compared with the model group ($p < 0.01$). At the YTC concentrations of 60, 80 and 100 μg/ml, there were 30.15, 23.17 and 19.05% apoptotic cells, respectively.

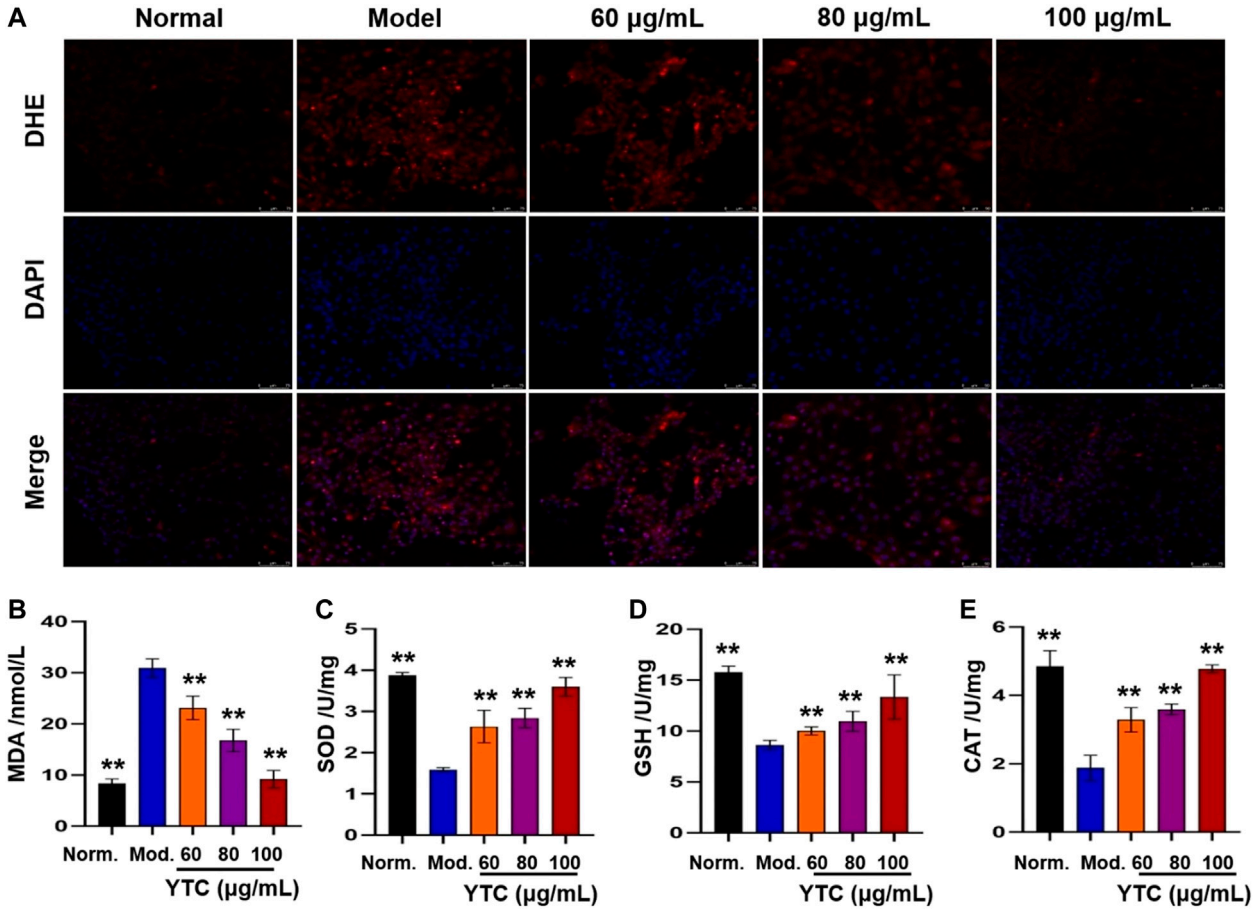


FIGURE 9 | Effects of YTC on ROS levels **(A)** and antioxidant enzyme activities **(B-E)** in H_2O_2-induced H9c2 cells. H9c2 cells were treated with YTC (60, 80 and 100 μg/ml) for 24 h, and then incubated in the presence of H_2O_2 (200 μM) for 4 h **(A)**The intracellular ROS levels were observed by laser confocal microscopy. **(B-E)**The levels of MDA and activities of SOD, GSH-Px, and CAT were determined by commercial assay kits. The values were represented as the mean ± SD ($n = 3$). $^{**}p < 0.01$ vs the model group.

Mitochondrial membrane potential (MMP, ΔΨm), to a large extent, is considered an important index to judge whether the physiological function of mitochondria is normal. Generally, the decrease of MMP is considered to be one of the indicators of mitochondrial dysfunction and an early feature of apoptosis cells. In this experiment, the changes of MMP were measured by using a fluorescent probe called JC-1. When the physiological conditions are normal, JC-1 usually aggregates in the matrix of mitochondrial, forming a polymer emitting red fluorescence. When MMP is reduced, there showed green fluorescence, suggesting the polymer disintegrated. As shown in **Figure 7**, in the H_2O_2-stimulated cells, the red fluorescence decreased and the green fluorescence increased. In contrast, YTC-pretreatment improved the above changes, and the red fluorescence increased compared with the model group. These results suggested that YTC alleviated the apoptosis of H9c2 cells induced by H_2O_2.

Effects of Main Active Components on Cell Viability and Apoptosis

The effects of the two components (AS IV and PAE) on cell viability were shown in **Figures 8A,B**. After the treatment with H_2O_2, the viability of H9c2 cells in the model group decreased significantly compared with the normal group ($p < 0.001$), while pretreatment with different concentrations of AS IV (25, 50 and 100 μM) and PAE (50, 100 and 200 μM) improved the viability of H2O2 stimulated- H9c2 cells ($p < 0.05$). In addition, as shown in **Figure 8C**, after stimulating by H_2O_2, the apoptosis rate of H9c2 cells in the model group was significantly higher than that of normal group ($p < 0.001$), while the apoptosis rate was decreased after pretreatment with the two main active components respectively ($p < 0.001$).

Effects of YTC on Intracellular ROS Generation

Excessive ROS will be produced after cells stimulating by H_2O_2, which is an important cause of cell apoptosis (Ogura and Shimosawa, 2014). Therefore, we used fluorescence probe DHE to detect the level of ROS. As shown in **Figure 9A**, compared with the normal group, the model group showed obvious red fluorescence, suggesting intracellular superoxide anion levels increased. Interestingly, the above phenomena could be alleviated by pretreatment with YTC (60, 80 and 100 μg/ml).

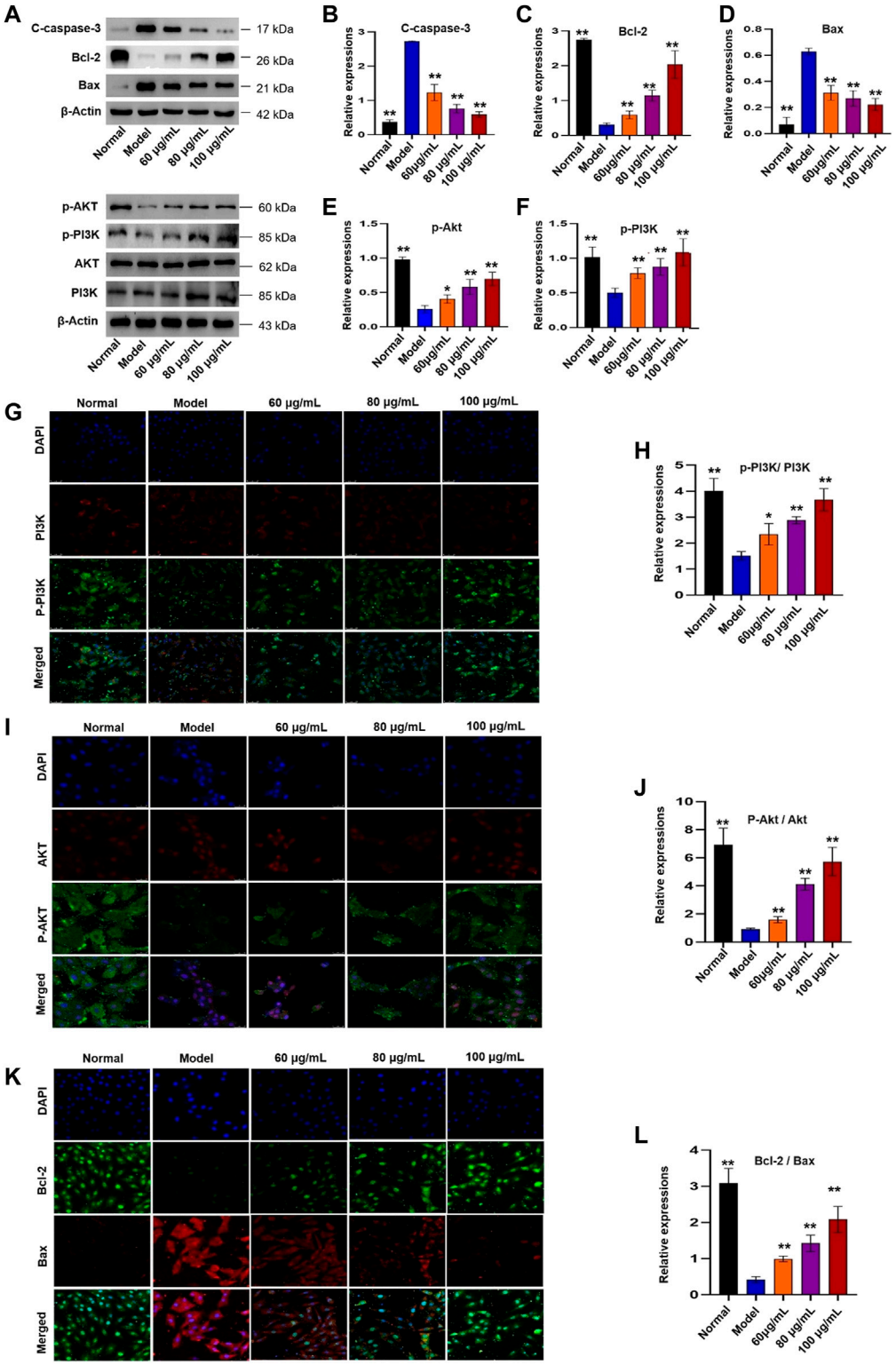


FIGURE 10 | Effects of YTC on PI3K/Akt signaling pathway in H_2O_2-induced H9c2 cells. **(A)** WB images of C-caspase-3, Bcl-2, Bax, p-Akt, p-PI3K, AKT and PI3K protein expression. **(B)** Analysis of C-caspase-3. **(C)** Analysis of Bcl-2. **(D)** Analysis of Bax. **(E)** Analysis of p-Akt. **(F)** Analysis of p-PI3K. **(G)** IF images of p-PI3K and PI3K. **(H)** Analysis of the p-PI3K/PI3K ratio. **(I)** IF images of p-Akt and Akt. **(J)** Analysis of the p-Akt/Akt ratio. **(K)** IF images of Bcl-2 and Bax. **(L)** Analysis of the Bcl-2/Bax ratio. Data were expressed as mean ± SD (n = 3), $^{**}p < 0.05$ and $^{**}p < 0{:}01$ vs model.

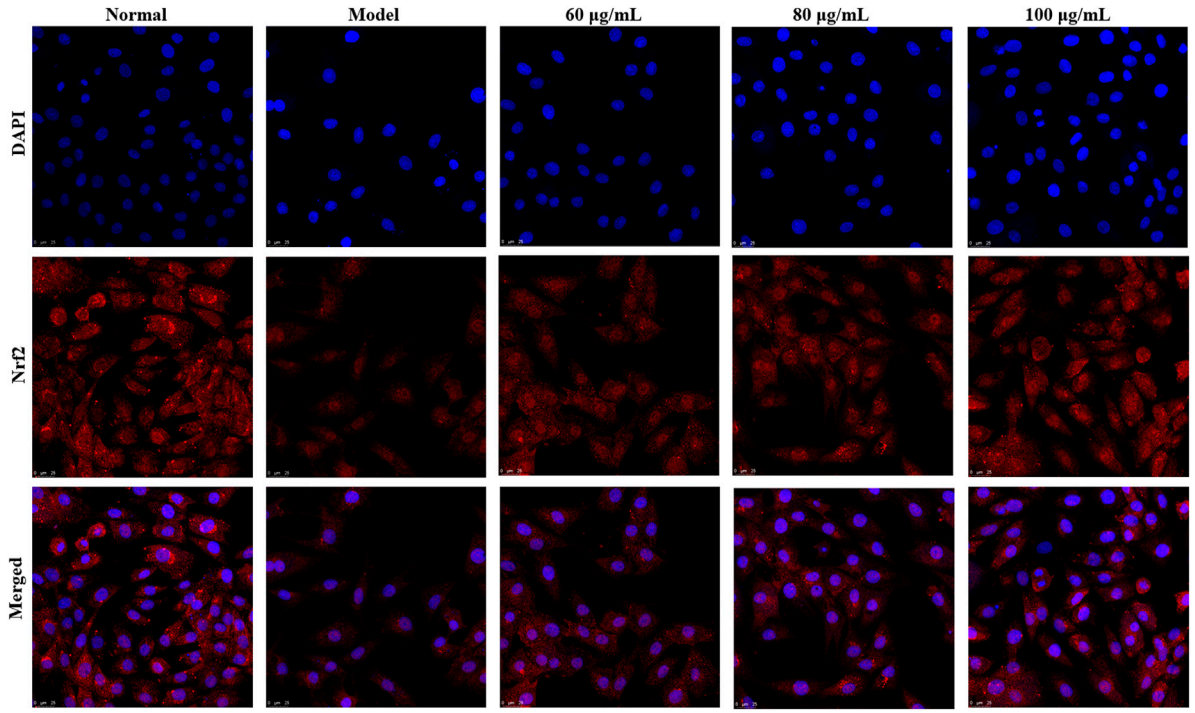


FIGURE 11 | Effects of YTC on nuclear transcription of Nrf2 in H_2O_2-induced H9c2 cells. H9c2 cells were treated with YTC (60, 80 and 100 μg/ml) for 24 h, subsequently subjected to H_2O_2 (200 μM) for 4 h. The nuclear transcription of Nrf2 was determined by laser confocal microscopy.

Effect of YTC on Antioxidant Enzyme

Oxidative stress injury is one of the important mechanisms of MI injury (Xie et al., 2021). In order to determine whether YTC affects biochemical enzymes related to oxidative stress, we measured the levels of intracellular lipid peroxidation products (MDA) and antioxidant enzymes (SOD, GSH-Px and CAT). As shown in **Figure 9B**, the content of MDA in H_2O_2-stimulated H9c2 cells was significantly increased compared with the normal group ($p < 0.01$). Whereas, YTC (60, 80 and 100 μg/ml) could alleviate this trend, compared to the model group ($p < 0.01$). In addition, the activities of SOD, GSH-Px and CAT in H_2O_2-treated cells were decreased compared with that in the normal group ($p < 0.01$), while the activities of the three enzymes were increased after YTC pretreatment ($p < 0.01$). The results indicated that YTC might have antioxidant capacity to protecting H9c2 cells from H_2O_2 damage.

Molecular Mechanism of the Protective Effects of YTC on H_2O_2-Treated H9c2 Cells

The KEGG analysis indicated that apoptosis and PI3K/Akt signaling pathway played an important role in YTC against MI. Therefore, western blot and immunofluorescence were utilized to evaluate the results. In **Figure 10**, the expressions of Bcl-2, Bcl-2/Bax, p-PI3K and p-Akt in the H_2O_2-stimulated model group were decreased, while the expressions of Bax and C-caspase-3 were increased, compared with the normal group ($p < 0.01$). However, 60, 80 and 100 μg/ml YTC could reverse these changes ($p < 0.01$). The expression of PI3K and Akt has no significant change in each group.

In addition, Nrf2 plays an important role in the regulation of redox homeostasis, so we further examined the effect of YTC on Nrf2 nucleation in H_2O_2-induced H9c2 cells. The results of immunofluorescence staining (**Figure 11**) showed that after pre-treatment with YTC, Nrf2 was mainly located in the nucleus compared with the model group, indicating that YTC might activate Nrf2 to transfer to the nucleus. The above results suggested that YTC might protect H_2O_2-induced H9c2 cells form oxidative stress and apoptosis by the PI3K/Akt/Nrf2 signalling pathway.

DISCUSSION

Currently, increasing reports have indicated that natural medicines, particularly the TCMs, are promising resources for finding useful agents for treating various diseases (Mozaffarian and Wu, 2018; Wang et al., 2019). One of the characteristics of TCM is that different components and targets play a role in different pathways, which makes it a challenge to study the molecular mechanisms of TCM. Network analysis has the characteristics of integrity and systematicness, which builds a bridge for different drugs to study interactions between them and is very suitable to research TCM. In this study, 162 potential compounds were collected from online databases. Then the 162 compounds were uploaded to TCMSP and SwissTarget online

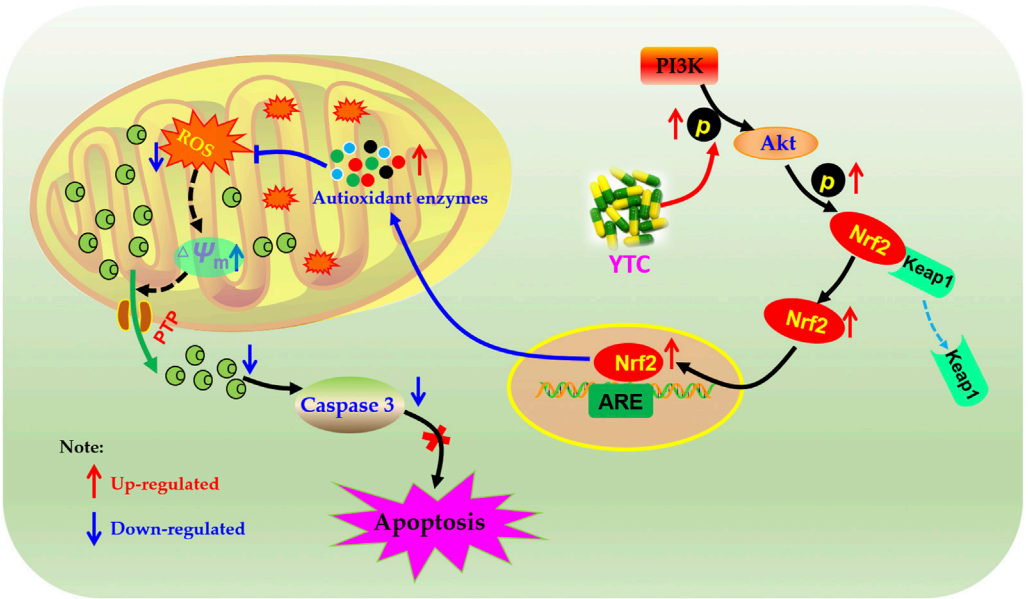


FIGURE 12 | Molecular mechanism of the protective effect of YTC. YTC possesses protective potentials on H_2O_2-stimulated H9c2 cells through suppression of oxidative stress-induced apoptosis via regulation of the PI3K/Akt/Nrf2 signal pathway.

databases, and 89 targets were predicted, while disease targets were collected from OMIM and Genecards database. According to the DMTD diagram and previous reports, AS IV and PAE were considered might be the key components of YTC against MI. It has been reported that AS IV could protect heart from MI and reperfusion injury through a variety of ways, including regulating autophagy, oxidative stress and energy metabolisms (Tu et al., 2013; Jiang et al., 2019; Huang et al., 2021). In addition, a study suggested that PAE had protective effect on myocardial ischemia-reperfusion by inhibiting apoptosis and reducing oxidative stress (Wu et al., 2020). *In vitro*, the results of CCK-8 assay and flow cytometry showed that the above two components significantly improved the decrease of cell viability and alleviated apoptosis in the H_2O_2-induced H9c2 cells.

The results of GO and KEGG analysis showed that the potential molecular mechanisms and signal pathways of YTC against MI were strongly related to apoptosis signal pathway. Similarly, the PPI analysis showed that the core target proteins of active ingredients in YTC were related to apoptosis, such as CASP3, CASP8, CASP9 and BCL2. Accumulated studies have also indicated that myocardial apoptosis was important in MI (Garg et al., 2003; Wang et al., 2013; Li et al., 2018). The results of GO analysis showed that oxidative stress may be related to mechanisms of YTC to against MI. Oxidative stress leads to excessive production of ROS, and then damages myocardial cells, which is an inevitable process in the pathogenesis of cardiovascular disease (Heistad et al., 2009; Zhang et al., 2018). Moreover, PI3K/Akt signaling pathway play the role of anti-oxidant stress by regulating Nrf2 (Li et al., 2016). Briefly, activated Akt leads to Nrf2 release from the Keap1-Nrf2 complex to the nucleus, and then Nrf2 reacts with the antioxidant response element sequences to protect the cell against oxidative stress (Li et al., 2018). Interestingly, KEGG results showed that PI3K/Akt pathway, an apoptosis-related signaling pathway, had a high anti-MI correlation in YTC, suggesting YTC may play an anti-MI role via alleviating oxidative stress and inhibiting apoptosis of cardiomyocyte via the PI3K/Akt pathway. In order to verify this hypothesis, *in vitro* studies were performed to verify the predicted results by network analysis.

In this study, we used H_2O_2 stimulated H9c2 cells to establish an oxidative stress injury model. The viability of H9c2 cells decreased significantly after incubation with H_2O_2; however, the decrease of cell viability induced by H_2O_2 reversed by pre-treatment with YTC. In addition, H_2O_2 stimulation significantly increased the accumulation of ROS in H9c2 cells, while pretreatment with YTC reduced the excessive accumulation of ROS. MDA is a biomarker of oxidative stress (Valko et al., 2007). SOD, CAT and GSH-Px are important ROS scavenging enzyme, which could maintain the redox balance in body (Chance et al., 1979). According to our results, in H_2O_2-timulated H9c2 cells, the content of MDA increased, while the activities of SOD, GSH-Px and CAT decreased. On the contrary, pretreatment with YTC reversed the above changes. In addition, after pretreatment with YTC, significant apoptosis of H9c2 cells induced by H_2O_2 alleviated. These results suggested that YTC may protect H9c2 cells from ROS-induced apoptosis.

Accumulating studies have suggested that the PI3K/Akt signalling pathway is important in regulating ROS expression and cellular oxidative stress pathways (Le Belle et al., 2011; Tsai et al., 2013; Lei et al., 2019). PI3K is an important signal transduction molecule in the growth factor superfamily, and Akt is a serine/threonine kinase, which is a key mediator of PI3K-mediated signal transduction (Lei et al., 2019). The result of PI3K phosphorylation is phosphorylation of Akt, which will

affect the expression of Bcl-2 and Bax proteins. Bcl-2 and Bax are a group of proteins closely related to apoptosis, and the anti-apoptotic protein Bcl-2 can inhibit the proapoptotic effect of Bax (Kønig et al., 2019). In the PI3K/Akt signalling, the expression of Bcl-2 increased and the expression of Bax decreased by activated p-Akt. In addition, Nrf2 was reported to be an essential protein for the production of antioxidant enzymes (Zhang et al., 2021b). Normally, Nrf2 is localized in the cytoplasm with keap 1. However, under conditions of oxidative stress, the structure of Keap1 is changed, resulting in the dissociation of Nrf2 from Keap1 into the nucleus. In the nucleus, Nrf2 combines with ARE to activate transcription to generate various antioxidant enzymes in the cytoplasm, including SOD, HO-1, CAT and GSH (Wen et al., 2018). In addition, PI3K/Akt is the main signaling pathway to activate Nrf2 (Zhang et al., 2021b). Our results showed that pretreatment with YTC promoted Nrf2 nuclear translocation and up-regulated the phosphorylation levels of PI3K and Akt, suggesting that the scavenging effect of YTC on ROS was closely related to the regulation of PI3K/Akt/Nrf2 signaling pathway in H_2O_2 stimulated-H9c2 cells (**Figure 12**).

CONCLUSION

In this study, network analysis and *in vitro* experiments were adopted to determine the active components and molecular mechanisms of YTC against MI. 162 compounds were obtained and the potential targets of these compounds were screened from online databases, and the intersection targets with the disease targets obtained from online databases were taken as the potential targets of YTC against MI. According to the analysis of PPI network and DMTD diagram, as well as GO and KEGG enrichment analysis, it is concluded that AS IV and PAE might be the most important component in YTC; YTC might play an anti-MI role by inhibiting apoptosis induced by oxidative stress via the PI3K/Akt/Nrf2 signal pathway. The results of *in vitro* experiments also verified the results of network analysis prediction. In conclusion, this study clarified the anti-MI mechanisms of YTC, and provided references for the research and promotion of Chinese traditional patent medicines.

DATA AVAILABILITY STATEMENT

The original contributions presented in the study are included in the article/**Supplementary Material**, further inquiries can be directed to the corresponding authors.

AUTHOR CONTRIBUTIONS

YC contributed to the design concepts of this whole study. HD, ML and JL carried out the study and collected important background information. HD and ML drafted the manuscript. JS carried out data acquisition and analysis. XG, XL and CW revised the article. All authors have read and approved the content of the manuscript.

FUNDING

This work was supported by Sichuan Science and Technology Program (no. 2020YFS0523).

SUPPLEMENTARY MATERIAL

The Supplementary Material for this article can be found online at: https://www.frontiersin.org/articles/10.3389/fphar.2022.794528/full#supplementary-material

REFERENCES

Arslan, F., de Kleijn, D. P., and Pasterkamp, G. (2011). Innate Immune Signaling in Cardiac Ischemia. *Nat. Rev. Cardiol.* 8, 292–300. doi:10.1038/nrcardio.2011.38

Bai, J., Wang, Q., Qi, J., Yu, H., Wang, C., Wang, X., et al. (2019). Promoting Effect of Baicalin on Nitric Oxide Production in CMECs via Activating the PI3K-AKT-eNOS Pathway Attenuates Myocardial Ischemia-Reperfusion Injury. *Phytomedicine* 63, 153035. doi:10.1016/j.phymed.2019.153035

Bai, X., Wang, W. X., Fu, R. J., Yue, S. J., Gao, H., Chen, Y. Y., et al. (2020). Therapeutic Potential of Hydroxysafflor Yellow A on Cardio-Cerebrovascular Diseases. *Front. Pharmacol.* 11, 01265. doi:10.3389/fphar.2020.01265

Chance, B., Sies, H., and Boveris, A. (1979). Hydroperoxide Metabolism in Mammalian Organs. *Physiol. Rev.* 59, 527–605. doi:10.1152/physrev.1979.59.3.527

Duan, H., Zhang, Q., Liu, J., Li, R., Wang, D., Peng, W., et al. (2021). Suppression of Apoptosis in Vascular Endothelial Cell, the Promising Way for Natural Medicines to Treat Atherosclerosis. *Pharmacol. Res.* 168, 105599. doi:10.1016/j.phrs.2021.105599

Fan, S., Sun, J. B., Li, R., Song, X., and Li, J. (2019). Lycopene Protects Myocardial Ischemia Injury through Anti-apoptosis and Anti-Oxidative Stress. *Eur. Rev. Med. Pharmacol. Sci.* 23, 3096–3104. doi:10.26355/eurrev_201904_17593

Garg, S., Hofstra, L., Reutelingsperger, C., and Narula, J. (2003). Apoptosis as a Therapeutic Target in Acutely Ischemic Myocardium. *Curr. Opin. Cardiol.* 18, 372–377. doi:10.1097/00001573-200309000-00009

He, S., Liu, X. Y., Qi, Q., Ma, Z. Z., Jiang, J. H., Jia, A., et al. (2018). Protective Effects of Astragalus Polysaccharides on Myocardial Ischemia-Reperfusion Injury in Rats. *Mod. Prev. Med.* 45, 3964–3967. CNKI:SUN:XDYF.0.2018-21-035.

Heistad, D. D., Wakisaka, Y., Miller, J., Chu, Y., and Pena-Silva, R. (2009). Novel Aspects of Oxidative Stress in Cardiovascular Diseases. *Circ. J.* 73, 201–207. doi:10.1253/circj.cj-08-1082

Hopkins, A. L. (2008). Network Pharmacology: the Next Paradigm in Drug Discovery. *Nat. Chem. Biol.* 4 (11), 682–690. doi:10.1038/nchembio.118

Huang, K. Y., Yu, Y. W., Liu, S., Zhou, Y. Y., Wang, J. S., Peng, Y. P., et al. (2021). A Single, Acute Astragaloside IV Therapy Protects Cardiomyocyte through Attenuating Superoxide Anion-Mediated Accumulation of Autophagosomes in Myocardial Ischemia-Reperfusion Injury. *Front. Pharmacol.* 12, 642925. doi:10.3389/fphar.2021.642925

Jiang, M., Ni, J., Cao, Y., Xing, X., Wu, Q., and Fan, G. (2019). Astragaloside IV Attenuates Myocardial Ischemia-Reperfusion Injury from Oxidative Stress by Regulating Succinate, Lysophospholipid Metabolism, and ROS Scavenging System. *Oxid Med. Cel. Longev.* 2019, 9137654. doi:10.1155/2019/9137654

Kaul, S., and Ito, H. (2004). Microvasculature in Acute Myocardial Ischemia: Part II: Evolving Concepts in Pathophysiology, Diagnosis, and Treatment. *Circulation* 109, 310–315. doi:10.1161/01.CIR.0000111583.89777.F9

Kønig, S. M., Rissler, V., Terkelsen, T., Lambrughi, M., and Papaleo, E. (2019). Alterations of the Interactome of Bcl-2 Proteins in Breast Cancer at the Transcriptional, Mutational and Structural Level. *Plos Comput. Biol.* 15, e1007485. doi:10.1371/journal.pcbi.1007485

Le Belle, J. E., Orozco, N. M., Paucar, A. A., Saxe, J. P., Mottahedeh, J., Pyle, A. D., et al. (2011). Proliferative Neural Stem Cells Have High Endogenous ROS Levels that Regulate Self-Renewal and Neurogenesis in a PI3K/Akt-Dependant Manner. *Cell Stem Cell* 8, 59–71. doi:10.1016/j.stem.2010.11.028

Lei, S., Su, W., Xia, Z. Y., Wang, Y., Zhou, L., Qiao, S., et al. (2019). Hyperglycemia-Induced Oxidative Stress Abrogates Remifentanil Preconditioning-Mediated Cardioprotection in Diabetic Rats by Impairing Caveolin-3-Modulated PI3K/Akt and JAK2/STAT3 Signaling. *Oxid Med. Cel. Longev.* 2019, 9836302. doi:10.1155/2019/9836302

Li, H., Song, F., Duan, L. R., Sheng, J. J., Xie, Y. H., Yang, Q., et al. (2016). Paeonol and Danshensu Combination Attenuates Apoptosis in Myocardial Infarcted Rats by Inhibiting Oxidative Stress: Roles of Nrf2/HO-1 and PI3K/Akt Pathway. *Sci. Rep.* 6, 23693. doi:10.1038/srep23693

Li, X., Huang, Q., Wang, M., Yan, X., Song, X., Ma, R., et al. (2018). Compound K Inhibits Autophagy-Mediated Apoptosis through Activation of the PI3K-Akt Signaling Pathway Thus Protecting against Ischemia/Reperfusion Injury. *Cel. Physiol. Biochem.* 47, 2589–2601. doi:10.1159/000491655

Li, L., Dai, W., Li, W., Zhang, Y., Wu, Y., Guan, C., et al. (2021). Integrated Network Pharmacology and Metabonomics to Reveal the Myocardial Protection Effect of Huang-Lian-Jie-Du-Tang on Myocardial Ischemia. *Front. Pharmacol.* 11, 589175. doi:10.3389/fphar.2020.589175

Ma, J., and Jin, G. (2019). Epidermal Growth Factor Protects against Myocardial Ischaemia Reperfusion Injury through Activating Nrf2 Signalling Pathway. *Free Radic. Res.* 53, 313–323. doi:10.1080/10715762.2019.1584399

Ma, X., Zhang, K., Li, H., Han, S., Ma, Z., and Tu, P. (2013). Extracts from Astragalus Membranaceus Limit Myocardial Cell Death and Improve Cardiac Function in a Rat Model of Myocardial Ischemia. *J. Ethnopharmacol.* 149, 720–728. Epub 2013 Aug 19. doi:10.1016/j.jep.2013.07.036

Malakar, A. K., Choudhury, D., Halder, B., Paul, P., Uddin, A., and Chakraborty, S. (2019). A Review on Coronary Artery Disease, its Risk Factors, and Therapeutics. *J. Cel Physiol* 234, 16812–16823. doi:10.1002/jcp.28350

Mozaffarian, D., and Wu, J. H. Y. (2018). Flavonoids, Dairy Foods, and Cardiovascular and Metabolic Health: a Review of Emerging Biologic Pathways. *Circ. Res.* 122 (2), 369–384. doi:10.1161/CIRCRESAHA.117.309008

Ogura, S., and Shimosawa, T. (2014). Oxidative Stress and Organ Damages. *Curr. Hypertens. Rep.* 16, 452. doi:10.1007/s11906-014-0452-x

Qu, D., Han, J., Ren, H., Yang, W., Zhang, X., Zheng, Q., et al. (2016). Cardioprotective Effects of Astragalin against Myocardial Ischemia/Reperfusion Injury in Isolated Rat Heart. *Oxid Med. Cel Longev* 2016, 8194690. doi:10.1155/2016/8194690

Sato, M., Bagchi, D., Tosaki, A., and Das, D. K. (2001). Grape Seed Proanthocyanidin Reduces Cardiomyocyte Apoptosis by Inhibiting Ischemia/reperfusion-Induced Activation of JNK-1 and C-JUN. *Free Radic. Biol. Med.* 31, 729–737. doi:10.1016/s0891-5849(01)00626-8

Scarabelli, T. M., Stephanou, A., Pasini, E., Comini, L., Raddino, R., Knight, R. A., et al. (2002). Different Signaling Pathways Induce Apoptosis in Endothelial Cells and Cardiac Myocytes during Ischemia/reperfusion Injury. *Circ. Res.* 90, 745–748. doi:10.1161/01.res.0000015224.07870.9a

Sun, B., Sun, G. B., Xiao, J., Chen, R. C., Wang, X., Wu, Y., et al. (2012). Isorhamnetin Inhibits H_2O_2-induced Activation of the Intrinsic Apoptotic Pathway in H9c2 Cardiomyocytes through Scavenging Reactive Oxygen Species and ERK Inactivation. *J. Cel Biochem* 113, 473–485. doi:10.1002/jcb.23371

Tsai, C. Y., Wang, C. C., Lai, T. Y., Tsu, H. N., Wang, C. H., Liang, H. Y., et al. (2013). Antioxidant Effects of Diallyl Trisulfide on High Glucose-Induced Apoptosis Are Mediated by the PI3K/Akt-dependent Activation of Nrf2 in Cardiomyocytes. *Int. J. Cardiol.* 168, 1286–1297. doi:10.1016/j.ijcard.2012.12.004

Tu, L., Pan, C. S., Wei, X. H., Yan, L., Liu, Y. Y., Fan, J. Y., et al. (2013). Astragaloside IV Protects Heart from Ischemia and Reperfusion Injury via Energy Regulation Mechanisms. *Microcirculation* 20 (8), 736–747. doi:10.1111/micc.12074

Valko, M., Leibfritz, D., Moncol, J., Cronin, M. T., Mazur, M., and Telser, J. (2007). Free Radicals and Antioxidants in normal Physiological Functions and Human Disease. *Int. J. Biochem. Cel Biol* 39, 44–84. doi:10.1016/j.biocel.2006.07.001

Wang, X., He, F., Liao, Y., Song, X., Zhang, M., Qu, L., et al. (2013). Baicalin Pretreatment Protects against Myocardial Ischemia/reperfusion Injury by Inhibiting Mitochondrial Damage-Mediated Apoptosis. *Int. J. Cardiol.* 168, 4343–4345. doi:10.1016/j.ijcard.2013.05.077

Wang, J., Wang, L., Lou, G. H., Zeng, H. R., Hu, J., Huang, Q. W., et al. (2019). Coptidis Rhizoma: a Comprehensive Review of its Traditional Uses, Botany, Phytochemistry, Pharmacology and Toxicology. *Pharm. Biol.* 57 (1), 193–225. doi:10.1080/13880209.2019.1577466

Wang, D. S., Yan, L. Y., Yang, D. Z., Lyu, Y., Fang, L. H., Wang, S. B., et al. (2020). Formononetin Ameliorates Myocardial Ischemia/reperfusion Injury in Rats by Suppressing the ROS-TXNIP-NLRP3 Pathway. *Biochem. Biophys. Res. Commun.* 525, 759–766. doi:10.1016/j.bbrc.2020.02.147

Wei, J., Wang, W., Chopra, I., Li, H. F., Dougherty, C. J., Adi, J., et al. (2011). c-Jun N-Terminal Kinase (JNK-1) Confers protection against Brief but Not Extended Ischemia during Acute Myocardial Infarction. *J. Biol. Chem.* 286, 13995–14006. doi:10.1074/jbc.M110.211334

Wen, Z., Hou, W., Wu, W., Zhao, Y., Dong, X., Bai, X., et al. (2018). 6′-O-Galloylpaeoniflorin Attenuates Cerebral Ischemia Reperfusion-Induced Neuroinflammation and Oxidative Stress via PI3K/Akt/Nrf2 Activation. *Oxid. Med. Cel. Longev.* 2018, 8678267. doi:10.1155/2018/8678267

Xie, F., Wu, Y. Y., Duan, G. J., Wang, B., and Gao, F. (2021). Anti-Myocardial Ischemia Reperfusion Injury Mechanism of Dried Ginger-Aconite Decoction Based on Network Pharmacology. *Front Pharmacol.* 12, 609702. doi:10.3389/fphar.2021.609702

Wu, L., Li, F., Zhao, C., Ming, Y., Zheng, C., Li, Y., et al. (2019). Effects and Mechanisms of Traditional Chinese Herbal Medicine in the Treatment of Ischemic Cardiomyopathy. *Pharmacol. Res.* 151, 104488. doi:10.1016/j.phrs.2019.104488

Wu, F., Ye, B., Wu, X., Lin, X., Li, Y., Wu, Y., et al. (2020). Paeoniflorin on Rat Myocardial Ischemia Reperfusion Injury of Protection and Mechanism Research. *Pharmacology* 105 (5-6), 281–288. doi:10.1159/000503583

Xu, H., Zhang, Y., Lei, Y., Gao, X., Zhai, H., Lin, N., et al. (2014). A Systems Biology-Based Approach to Uncovering the Molecular Mechanisms Underlying the Effects of Dragon's Blood Tablet in Colitis, Involving the Integration of Chemical Analysis, ADME Prediction, and Network Pharmacology. *PLoS One* 9, e101432. doi:10.1371/journal.pone.0101432

Yang, M., Chen, J., Zhao, J., and Meng, M. (2014). Etanercept Attenuates Myocardial Ischemia/reperfusion Injury by Decreasing Inflammation and Oxidative Stress. *PLoS One* 9, e108024. doi:10.1371/journal.pone.0108024

Yuan, X., Juan, Z., Zhang, R., Sun, X., Yan, R., Yue, F., et al. (2020). Clemastine Fumarate Protects against Myocardial Ischemia Reperfusion Injury by Activating the TLR4/PI3K/Akt Signaling Pathway. *Front. Pharmacol.* 11, 28. doi:10.3389/fphar.2020.00028

Zhai, M., Li, B., Duan, W., Jing, L., Zhang, B., Zhang, M., et al. (2017). Melatonin Ameliorates Myocardial Ischemia Reperfusion Injury through SIRT3-dependent Regulation of Oxidative Stress and Apoptosis. *J. Pineal Res.* 63, e12419. doi:10.1111/jpi.12419

Zhang, S., He, B., Ge, J., Li, H., Luo, X., Zhang, H., et al. (2010). Extraction, Chemical Analysis of Angelica Sinensis Polysaccharides and Antioxidant Activity of the Polysaccharides in Ischemia-Reperfusion Rats. *Int. J. Biol. Macromol.* 47, 546–550. doi:10.1016/j.ijbiomac.2010.07.012

Zhang, L., Liu, Y., Li, J. Y., Li, L. Z., Zhang, Y. L., Gong, H. Y., et al. (2018). Protective Effect of Rosamultin against H2O2-Induced Oxidative Stress and Apoptosis in H9c2 Cardiomyocytes. *Oxid. Med. Cel. Longev.* 2018, 8415610. doi:10.1155/2018/8415610

Zhang, Q., Li, R.-L., Tao, T., Sun, J.-Y., Liu, J., Zhang, T., et al. (2021a). Antiepileptic Effects of Cicadae Periostracum on Mice and its

Antiapoptotic Effects in H2O2-Stimulated PC12 Cells via Regulation of PI3K/Akt/Nrf2 Signaling Pathways. *Oxid. Med. Cel. Longev.* 2021, 1–19. doi:10.1155/2021/5598818

Zhang, Q., Liu, J., Duan, H., Li, R., Peng, W., and Wu, C. (2021b). Activation of Nrf2/HO-1 Signaling: An Important Molecular Mechanism of Herbal Medicine in the Treatment of Atherosclerosis via the protection of Vascular Endothelial Cells from Oxidative Stress. *J. Adv. Res.* 34, 43–63. doi:10.1016/j.jare.2021.06.023

Zhang, X. (2015). Effects of the Yiqi-Tongluo Capsule on the Thrombus, Serum Lipid, IL-8, CRP, TXA2, 6-Keto-PGF1αof Experimental Rats. *Chin. J. Integr. Med. Cardiovasc. Dis.* 13 (14), 1612–1614. doi:10.3969/j.issn.1672-1349.2015.14.009

Zhao, Z. Q., and Vinten-Johansen, J. (2002). Myocardial Apoptosis and Ischemic Preconditioning. *Cardiovasc. Res.* 55, 438–455. doi:10.1016/s0008-6363(02)00442-x

Zhu, W. S., Guo, W., Zhu, J. N., Tang, C. M., Fu, Y. H., Lin, Q. X., et al. (2016). Hsp90aa1: a Novel Target Gene of miR-1 in Cardiac Ischemia/reperfusion Injury. *Sci. Rep.* 6, 24498. doi:10.1038/srep24498

Conflict of Interest: The authors declare that the research was conducted in the absence of any commercial or financial relationships that could be construed as a potential conflict of interest.

Publisher's Note: All claims expressed in this article are solely those of the authors and do not necessarily represent those of their affiliated organizations, or those of the publisher, the editors, and the reviewers. Any product that may be evaluated in this article, or claim that may be made by its manufacturer, is not guaranteed or endorsed by the publisher.

Copyright © 2022 Duan, Li, Liu, Sun, Wu, Chen, Guo and Liu. This is an open-access article distributed under the terms of the Creative Commons Attribution License (CC BY). The use, distribution or reproduction in other forums is permitted, provided the original author(s) and the copyright owner(s) are credited and that the original publication in this journal is cited, in accordance with accepted academic practice. No use, distribution or reproduction is permitted which does not comply with these terms.

frontiers in Pharmacology

ORIGINAL RESEARCH
published: 24 February 2022
doi: 10.3389/fphar.2022.795613

Sesquiterpene Lactones Attenuate Paclitaxel Resistance Via Inhibiting MALAT1/STAT3/ FUT4 Axis and P-Glycoprotein Transporters in Lung Cancer Cells

Yaming Ding[1], Zhang Zhen[2], Muhammad Azhar Nisar[2], Farman Ali[3], Riaz Ud Din[2], Muhammad Khan[4], Tafail Akbar Mughal[5], Gulzar Alam[6], Linlin Liu[1] and Muhammad Zubair Saleem[2,7]**

[1]The Second Hospital of Jilin University, Changchun, China, [2]College of Basic Medical Sciences, Dalian Medical University, Dalian, China, [3]Academy of Integrative Medicine, Fujian University of Traditional Chinese Medicine, Fuzhou, China, [4]Institute of Zoology, University of the Punjab, Lahore, Pakistan, [5]Medical Toxicology Laboratory, Department of Zoology, Women University of Azad Jammu and Kashmir, Muzaffarabad, Pakistan, [6]Faculty of Rehabilitation and Allied Health Sciences, Riphah International University, Islamabad, Pakistan, [7]Fujian Provincial Key Laboratory of Natural Medicine Pharmacology, School of Pharmacy, Fujian Medical University, Fuzhou, China

OPEN ACCESS

Edited by:
Hong Zhang,
Shanghai University of Traditional Chinese Medicine, China

Reviewed by:
Hongmei Cui,
Lanzhou University, China
Hai Qian,
China Pharmaceutical University, China

***Correspondence:**
Linlin Liu
liull_123@126.com
Muhammad Zubair Saleem
dr_khattak@outlook.com
zubairsaleem@fjmu.edu.cn

Specialty section:
This article was submitted to Pharmacology of Anti-Cancer Drugs, a section of the journal Frontiers in Pharmacology

Received: 08 November 2021
Accepted: 03 February 2022
Published: 24 February 2022

Citation:
Ding Y, Zhen Z, Nisar MA, Ali F, Din RU, Khan M, Mughal TA, Alam G, Liu L and Saleem MZ (2022) Sesquiterpene Lactones Attenuate Paclitaxel Resistance Via Inhibiting MALAT1/ STAT3/ FUT4 Axis and P-Glycoprotein Transporters in Lung Cancer Cells. Front. Pharmacol. 13:795613. doi: 10.3389/fphar.2022.795613

Paclitaxel resistance is a challenging factor in chemotherapy resulting in poor prognosis and cancer recurrence. Signal transducer and activator of transcription factor 3 (STAT3), a key transcription factor, performs a critical role in cancer development, cell survival and chemoresistance, while its inactivation overwhelms drug resistance in numerous cancer types including lung cancer. Additionally, the fucosyltransferase 4 (FUT4) is a crucial enzyme in post-translational modification of cell-surface proteins involved in various pathological conditions such as tumor multidrug resistance (MDR). The P-glycoprotein (P-GP) is the well-known ABC transporter member that imparts drug resistance in different cancer types, most notably paclitaxel resistance in lung cancer cells. LncRNA-MALAT1 exerts a functional role in the cancer development as well as the drug resistance and is linked with STAT3 activation and activity of FUT4. Moreover, STAT3-mediated induction of P-GP is well-documented. Natural compounds of Sesquiterpene Lactone (SL) family are well-known for their anticancer properties with particular emphasis over STAT3 inhibitory capabilities. In this study, we explored the positive correlation of MALAT1 with STAT3 and FUT4 activity in paclitaxel resistant A549 (A549/T) lung cancer cells. Additionally, we investigated the anticancer activity of two well-known members of SLs, alantolactone (ALT) and Brevilin A (Brv-A), in A549/T lung cancer cells. ALT and Brv-A induced apoptosis in A549/T cells. Furthermore, these two natural SLs suppressed MALAT1 expression, STAT3 activation, and FUT4 and P-GP expression which are the hallmarks for paclitaxel resistance in A549 lung cancer cells. The inhibition of MALAT1 enhanced the competence of these SLs members significantly, which accounted for the growth inhibition as well as anti-migratory and anti-invasive effects of ALT and Brv-A. These findings suggest SLs to be the promising agents for overcoming paclitaxel resistance in A549 lung cancer cells.

Keywords: paclitaxel resistance, STAT3, FUT4, P-gp, MALAT1, alantolactone, brevilin A

INTRODUCTION

Among different types of cancer, the most lethal type is the lung cancer worldwide having highest mortality, morbidity, and metastatic rate. The most common malignant lung cancer is the non-small cell lung cancer (NSCLC) accounting approximately 90% of all type lung cancer cases whereas 70–80% of patients suffer with an intricate disease state and are unable to undergo the surgical removal of tumor (Wakelee et al., 2014; Siegel et al., 2017; Gong et al., 2018; Teng et al., 2019; Lin et al., 2020). Also, the side effects and drug tolerance in chemotherapy at the advanced stage are overwhelming factors. Due to the drug tolerance, patients within advanced stage of tumor have less response to the chemotherapy (Scheff and Schneider, 2013; Zhou et al., 2019). Paclitaxel is widely used in cancer treatment, primarily as a first-line chemotherapeutic drug against clinical manifestations of NSCLC (Pilkington et al., 2015; Yuan H. et al., 2016; Chen et al., 2017). Although, paclitaxel has improved the curative rates in both earlier and advanced stages of the disease and enhanced furtherance in the quality and life span of NSCLC patients (Zeng et al., 2015), however, paclitaxel resistance is a challenging obstacle to the successful treatment that creates a hiatus in the multimodal chemotherapeutic approach (Suda and Mitsudomi, 2015; Li et al., 2019).

Chemoresistance is a result of a variety of mechanisms that aid cancer cells in overcoming stress conditions. Previous studies have revealed that genetic and epigenetic modifications can lead to both acquired and intrinsic chemoresistance (Rebucci and Michiels, 2013). The long non-coding RNAs (lncRNAs) are the type of non-coding RNA transcripts containing more than 200 nucleotides that lack or have a limited protein-coding potential (Qu et al., 2016). It is known that lncRNAs perform important role in transcriptional and post-transcriptional regulation, chromatin remodeling, microRNA sponging, and chemoresistance in cancer biology (YiRen et al., 2017; Kim et al., 2020). MALAT1 (Metastasis-associated lung adenocarcinoma transcript 1), primarily discovered in NSCLC, is evolutionarily conserved lncRNA located at chromosome 11q13 that plays a variety of biological functions, i.e., glycolysis, vascular growth, retinal neurodegeneration, cancer progression, and chemotherapeutic resistance (Michalik et al., 2014; Latorre et al., 2016; Luo et al., 2016; Yao et al., 2016).

The increased levels of drug resistance-associated transporters encoded by ATP-binding cassette (ABC) genes in lung cancer are the most significant contributors to drug resistance (Zheng et al., 2021). Among seven sub-families, 13 out of 49 members of ABC genes are implicated in drug resistance. Among these, MDR1, also identified as P-GP (P-glycoprotein) plays a key role in the transportation or inhibition of 324 approved drugs and is known to ease the paclitaxel transport across the membrane (Nanayakkara et al., 2018). STAT3 is an imperative transcription factor involves in the regulation of MDR1 gene expression at transcriptional level. Recent studies have demonstrated that MALAT1 contributes to drug resistance by modulating STAT3 activation. STAT3 has also been implicated in cisplatin, doxorubicin, and gefitinib resistance (Phan et al., 2016; Fang et al., 2018; Li et al., 2018; Yue et al., 2020; Cao et al., 2021). Furthermore, STAT3 inactivation incapacitates paclitaxel resistance in several carcinomas as well as lung cancer in either independent or synergistic manner (Lee et al., 2015; Ji et al., 2017). Therefore, inactivating STAT3 *via* STAT3 inhibitors is a significant approach to devastate the resistance of paclitaxel in lung cancer.

Fucosyltransferase (FUT) family is involved in the post-translational modification of proteins by catalyzing the transfer of fucose residue to acceptor of oligosaccharide from the donor substrate GDP-fuc in various linkages, i.e., a1, 2-(FUT2 and FUT1), a1, 3/4-(FUT4, FUT3, FUT6, FUT5, FUT7, FUT10, FUT9, and FUT11) and a1, 6-linkage (FUT8) (de Vries et al., 2001; Ma et al., 2006; Cheng et al., 2013). The implications of these fucosylated oligosaccharides are noticed in different biological processes that include cell-cell interactions in differentiation, cancer development, and tumor multidrug resistance. In previous studies, FUT4 has been associated in cancer development and multidrug resistance *via* PI3K/AKT signaling pathway. Moreover, FUT4 regulation has also been elaborated in colorectal cancer where miR-26a/26b is sponged by MALAT1 to enhance the FUT4 fucosylation and promotes the metastasis *via* activation of PI3K/AKT pathway (Xu et al., 2020). Therefore, STAT3 activation and glycan alterations are the promising therapeutic targets to overcoming multidrug resistance in cancer.

Sesquiterpene lactones (SLs) are secondary metabolites comprise over 5,000 known compounds found in various plant families such as Cactaceae, Euphorbiaceae, Solanaceae, and Araceae (Wedge et al., 2000; Canales et al., 2005). These are commonly found in Asteraceae family which are one of the diverse plants in the world. SLs account up a significant portion of dry mass of these plants i.e., 3% in *Helenium amarum* (Ivie et al., 1975). SLs are colorless, lipophilic molecule with a 15-carbon backbone chain. To accomplish the goals, we used previously reported STAT3 inhibitors and members of SLs family, Alantolactone (ALT) and Brevilin A (Brv-A), based on their current effectiveness against multiple cancer cell lines. In previous study, the effect of ALT is investigated to reduce resistance of doxorubicin in A549 lung cancer cells *via* targeting MDR1 and STAT3 (Maryam et al., 2017). Beside, we have reported that Brv-A inhibits the activation of STAT3 even more significantly than the commercially available STAT3 inhibitors by direct binding (Khan et al., 2020; Saleem et al., 2020). This study represents the key role of these two compounds in reducing the expression of FUT4 in paclitaxel-resistant A549 (A549/T) cells for the first time. Several studies are previously conducted to discover the role of lncRNA MALAT1 in chemoresistance, however, how MALAT1 functions in the context of a therapeutic approach with special prominence to MALAT1/STAT3 and MALAT1/FUT4 axis in paclitaxel-resistant lung cancer is not well-known. Therefore, the feedback role of MALAT1 during STAT3 inhibition and FUT4 is needed to be justified analytically. The current work sought to provide novel insights into the functional response of MALAT1 and efficacy of common members of SLs (ALT and Brv-A) in paclitaxel-resistant lung cancer, vis-à-vis MALAT1/STAT3 and MALAT1/FUT4 axis.

MATERIALS AND METHODS

Reagents and Chemicals

Alantolactone (ALT) (>98% purity) was obtained from Tauto-Biotech (Shanghai, China) while Brevilin A (Brv-A) (purity >98%) and Paclitaxel (PTX) (purity >99%) was obtained from Selleck (China). DMEM (Dulbecco's modified Eagle's Medium), trypsin without or with EDTA, Streptomycin-Penicillin (10,000 U/ml), and fetal bovine serum (FBS) were all purchased from Gibco (Thermo Fisher Scientific, Inc.). Cell counting kit-8 (CCK-8) was purchased from KeyGen Biotech (Nanjing, China) and Protease-inhibitor cocktail from Sigma-Aldrich (St. Louis, MO). Dimethyl Sulfoxide (DMSO), Phenyl methyl sulfonyl fluoride (PMSF), Propidium Iodide (PI), crystal violet stain, Calcein acetoxymethyl ester (Calcein-AM), and annexin V-FITC kit for apoptosis detection were obtained from Beyotime Biotechnology (China). The primary antibodies for cleaved caspase-3, cleaved caspase-9 and cleaved PARP as well as p-STAT3, and STAT3 (Tyr 705) were obtained from Cell-Signaling Technology (Beverly, MA). FUT4 from Proteintech (Wuhan, China) while P-GP was obtained from abcam (Cambridge, MA). GAPDH was procured from Beyotime Biotechnology (China), while the HRP (Horseradish Peroxidase)-conjugated secondary type of antibodies (anti-mouse and anti-rabbit) were obtained from Sigma-Aldrich (St. Louis, MO).

Cell Culture

Human non-small cell lung cancer cell line (A549), and paclitaxel-resistant A549 (A549/T) cell line was purchased from iCell Biosciences Inc. (Shanghai, China). Both A549/T and A549 cell lines were cultured in 10% FBS containing DMEM, accompanied 100 μg/ml streptomycin and 100 U/ml concentration of penicillin. The cell lines were maintained in a logarithmic phase of growth for all experiments in humidified atmosphere with 5% CO_2 at 37°C.

Cell Treatment and Cell Viability Assay

DMSO (0.5% final concentration) was used to dissolve ALT, Brv-A, and PTX while the same DMSO concentration was kept as a control. CCK-8 kit was used to find out the percentage of cells viability. Briefly, cells (with density of 3×10^3) were added in 96-well culture plates for 24 h and treated with different concentrations of ALT and Brv-A (2.5, 5, 10, 15, 20, 40, 80 and 120 μM) for 24, 48, and 72 h, while various concentrations of PTX (0.0125, 0.25, 0.5, 1, 2, 4, 8, and 16 μM) were used to check the cell viability at 24, 48, and 72 h in A549 and A549/T lung cancer cells. The resistance index was calculated at 72 h time point. Afterwards, CCK-8 solution (10 μl) was added to each well and 96-well culture plate was kept at 37°C for 3 h. Optical density was measured at 450 nm wavelength through fluorescence-microplate reader (Synergy neo HTS multimode-microplate reader, BioTek). Following formula was used to calculate the cell viability in experiments performed in triplicate.

$$Cell\ viability\ (\%) = (A450\ sample - A450\ blank) / (A450\ control - A450\ blank) \times 100$$

where "sample" characterizes the optical density value of treated cells containing CCK-8 solution and culture media whereas "blank" displays the optical density of CCK-8 solution containing media without cells. IC_{50} values were calculated by SPSS 16.0 version.

Transfection

A549/T cells were taken for transfection with specific siRNA-MALAT1. The sequence of the sense strand used was MALAT1, 5′-CCCUCUAAAUAAGGAAUAATT-3′ obtained from GenePharma (Shanghai, China). For transfection, lipofectamine 2000 was used along with siRNA-MALAT1 followed by manufacturer's protocol. Cells were kept for 4–6 h, later, DMEM was removed and fresh DMEM was added. Transfected cells were used for multiple experiments after 48 h of transfection.

Extraction of RNA, Synthesis of cDNA, and Quantitative Polymerase Chain Reaction (qPCR)

Total RNAs were extracted and isolated through Trizol reagent (Invitrogen) as guided by the manufacturer's instructions. For reverse transcription, Prime Script TMRT-reagent kit (TransGen Biotech, China) was used while Trans Start Tip Top Green qPCR Super Mix (TransGen Biotech, China) was used for qPCR according to the instructions given by the manufacturer. The primers sequences were as follows. MALAT1: 5′-GCATTAATT GACAGCTGACCCA-3′ (F), 5′-GCTTGCTCCTCAGTCCTA GCTT-3′ (R); FUT4: 5′-ACAACTGTTCCCGATTCACG-3′(F), 5′-TGCCCTCCTCACCTTTCTC-3′(R); STAT3: 5′-CTTTGA GACCGAGGTGTATCACC-3′ (F), 5′-GGTCAGCATGTTGTACCACAGG-3′(R); GAPDH: 5′-AGC CCATCACCATCTTCCAG-3′ (F), 5′-ACCCATCACAAACAT GGGGG-3′. GAPDH was used to normalize the data and the relative measurements were determined using the $2^{-\Delta\Delta Ct}$ method. All the experiments were performed independently in triplicate.

Acquiring Chemical Structures

Chemical structures of ALT and Brv-A were acquired from SciFinder (http://scifinder.cas.org) by using Chem Bio Draw. Afterward, the data was downloaded in the "mol2" format.

Collection of Compound's Target and Correction of Protein's Names

To predict the targets of ALT and Brv-A, Pharm Mapper (http://lilabecust.cn/pharmmapper/), was used that contains a pharmacophore mapping method to identify potential drug targets (Liu et al., 2010). Due to the non-standard names of protein of the extracted targets, the official identifiers were corrected and obtained *via* UniProtKB (http://www.uniprot.org/).

GO, Pathway Enrichment and Network Construction

DAVID (version 6.8), accessed at https://david-d.ncifcrf.gov, was used for ontologies (GO) and KEGG pathway as mentioned

earlier (Sherman and Lempicki, 2009) while Cytoscape program (version 3.4.0) was used to create pathway networks (Missiuro et al., 2009).

Microscopic Observations of Cellular Morphological Changes

A549/T and A549 cancer cells were added in 96-well culture plates at 37°C overnight and designated treatment of ALT, Brv-A, and PTX was given for 24 h. To determine and photograph the morphological changes in the cells, Phase-contrast microscope (Leica, DMIL LED) was used.

Live/Dead Assay

To perform live/dead assay, A549/T cells were treated with 5, 10, and 15 μM of ALT and Brv-A for 24 h. After washing the cells with PBS, calcein-AM (2 μM) and PI (4 μM) were added to each sample for 15–20 min and kept at room temperature in the dark. The extra stain was removed by washing with PBS. Later, cells were mixed in PBS, and photographed using fluorescence microscope (Leica, DMI 4000B). To evaluate the live and dead cells, three different fields were selected and 100 cells in each field were calculated.

Colony Formation Assay

Colony formation assay was done to determine the cytotoxic and antiproliferative effect of ALT and Brv-A. Briefly, A549/T cells were cultured and treated with 5, 10, and 15 μM concentrations of ALT and Brv-A for 24 h. Afterwards, PBS was used to wash the cells, trypsinized, and were seeded in six-well culture plates with cells density of 500 per well. Cells were kept at 37°C for next 7 days to form colonies and given media was changed after each 48 h. After colony formation, cells were washed, and 4% paraformaldehyde (PFA) was used to fix colonies for 15–20 min. Colonies were further stained using crystal violet for 25–30 min. Extra stain was washed by PBS and colonies were photographed. The rate of proliferation was also evaluated by the addition of methanol to dissolve the stain taken by the colonies. Optical density at 595 nm wavelength was determined by fluorescent-spectrophotometer (Synergy neo HTS multi-mode microplate-reader; BioTek).

Apoptosis Assay

The impact of ALT and Brv-A in the induction of apoptosis was determined through flow cytometry where apoptosis detection kit was used. Annexin V-FITC/PI double staining was performed as directed by the manufacturer's instruction. In brief, A549/T cells were seeded in six-well culture plates and treated with 5, 10, and 15 μM ALT or Brv-A for 24 h. After washing with PBS, cells were mixed in the provided 1X binding-buffer. Each sample was incorporated with 5 μl annexin V-FITC and 10 μl PI and kept in the dark for 20 min, filtered and subjected to the flow cytometry (Beckmen Coulter, Life Sciences, United States) to investigate apoptotic rate. NovoExpress (version 1.3.0) was used for the analysis of data.

Cell Migration and Invasion Assay

Anti-migration and anti-invasive capabilities of ALT and Brv-A in A549/T lung cancer cells (transfected with or without siRNA MALAT1) were determined by transwell migration and invasion assays. In brief, cells were added in the transwell chamber without/with Matrigel with density of 3×10^3/chamber. The lower section contained DMEM (10% FBS) as chemoattractant while the DMEM (2% FBS) was poured in the upper chamber. To achieve the rate of migration and invasion among treated and untreated cells, the Transwell chamber was kept at 37°C. Next, the adhesive cells to the inner side of the upper chamber were detached with a soft cotton swab and the cells at the lower side of the chamber were fixed using 4% PFA for 15–20 min. Cells were stained for 30 min through 1% crystal violet, and later PBS was used to wash and remove the extra stain. The chambers were left air dried, photographed by using a fluorescence microscope (Leica, DMI 4000B), and quantified by counting in at least three random fields.

Protein and Ligand Preparation and Molecular Docking Analysis

To prepare FUT4 and P-GP proteins for molecular docking, dock prep was performed by using USCF Chimera (Pettersen et al., 2004; Yang et al., 2012). ALT and Brv-A were selected for docking purpose and compound's charges were minimized, and converted into PDBQT format before docking. The partial charges were added and non-polar hydrogen atoms were merged to the ligand atom by PYRX software (Dallakyan and Olson, 2015). Further, docking affinities were carried by selection of predicted ligand binding residues of FUT4 and P-GP proteins. Results were visualized by Discovery Studio software (Dassault Systemes BIOVIA, BIOVIA Discovery Studio Visualizer, v16).

Protein-Protein Interaction (PPI)

The Search Tool for the Retrieval of Interacting Genes (STRING) was used to evaluate and integrate the protein-protein interactions containing both physical (direct) and functional (indirect) interconnections.

Western Blot Analysis

Cells, after washing with chilled PBS, were lysed by using RIPA-lysis buffer (Beyotime Biotechnology) carrying 1% PMSF on ice for 30 min. Sodium fluoride (NaF) (2%) was also supplemented to RIPA buffer during extraction of phosphorylated proteins. Later, centrifuged the cells for 15 min at 12,000 rpm and the supernatant was transferred to ice-chilled Eppendorf tubes. The BCA protein assay kit (Beyotime Biotechnology) was used to determine the concentration of protein. Furthermore, by using 10–12% sodium dodecyl sulfate-polyacrylamide gel electrophoresis (SDS-PAGE) gels, an equal amount of 30–40 μg protein was separated, transferred to the PVDF (polyvinylidene difluoride) membranes, and kept in 5% skim milk for 2 h at room temperature. The membranes were further washed with TBST (Tris-buffered saline-tween) three times and incubated in specific primary antibodies overnight at 4°C on a shaker. Next, the membranes were washed by TBST three times

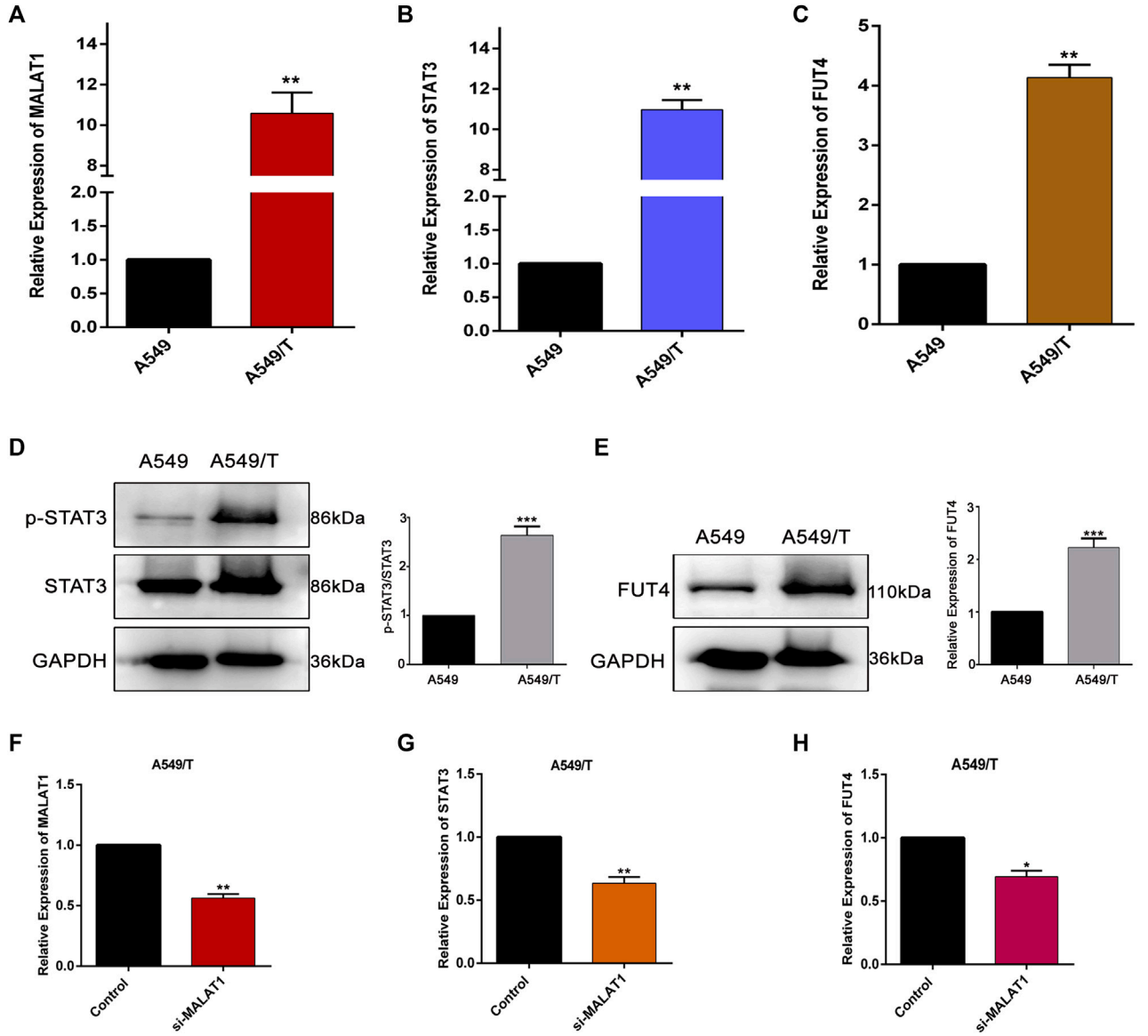


FIGURE 1 | Expression and correlation of MALAT1, STAT3, and FUT4 in A549/T lung cancer cells. **(A)** qPCR analysis for the determination mRNA level of MALAT1 in A549 lung cancer cells compared to that in A549/T cells. **(B)** a comparative qPCR-based analysis of mRNA level of STAT3 among A549/T and A549 lung cancer cells. **(C)** Relative mRNA levels of FUT4 among A549/T and A549 lung cancer cells. **(D)** Comparison of p-STAT3/STAT3 expression among A549/T and A549 cancer cells through western blotting. **(E)** Comparison of FUT4 expression among A549/T and A549 cancer cells through western blotting. **(F)** Functional confirmation of siRNA MALAT1 in inhibiting MALAT1 expression among A549/T cells. **(G)** Expression of STAT3 measured by qPCR in A549/T cells transfected with si-MALAT1 and compared to that in the control. **(H)** Expression of mRNA level of FUT4 measured by qPCR in A549/T cells transfected with si-MALAT1 and compared to that in the control. **(A–H)** Data are presented as Mean ± SD, whereas, the entire experiments were done in triplicate independently. ***$p < 0.001$, **$p < 0.01$, *$p < 0.05$ vs control group.

and kept in HRP-conjugated goat anti-mouse IgG or goat anti-rabbit IgG secondary antibodies at room temperature for 2 h. After washing by TBST, antibody binding was detected in DNR-bioimaging system MicroChemi 4.2 using ECL plus chemiluminescence kit. GAPDH was internal control for all triplicate experiments performed in the study. ImageJ software was used to analyze the variations in protein expression.

Statistical Analysis

Among three different performed experiments, all values are depicted as Mean ± SD and compared statistically with untreated, non-resistant, non-transfected samples as control. Student *t*-test was used to compare only two groups while one-way ANOVA followed by Tukey's Multiple Comparison Test was used for comparison between three or more groups. $p < 0.05$ was considered to be statistically significant.

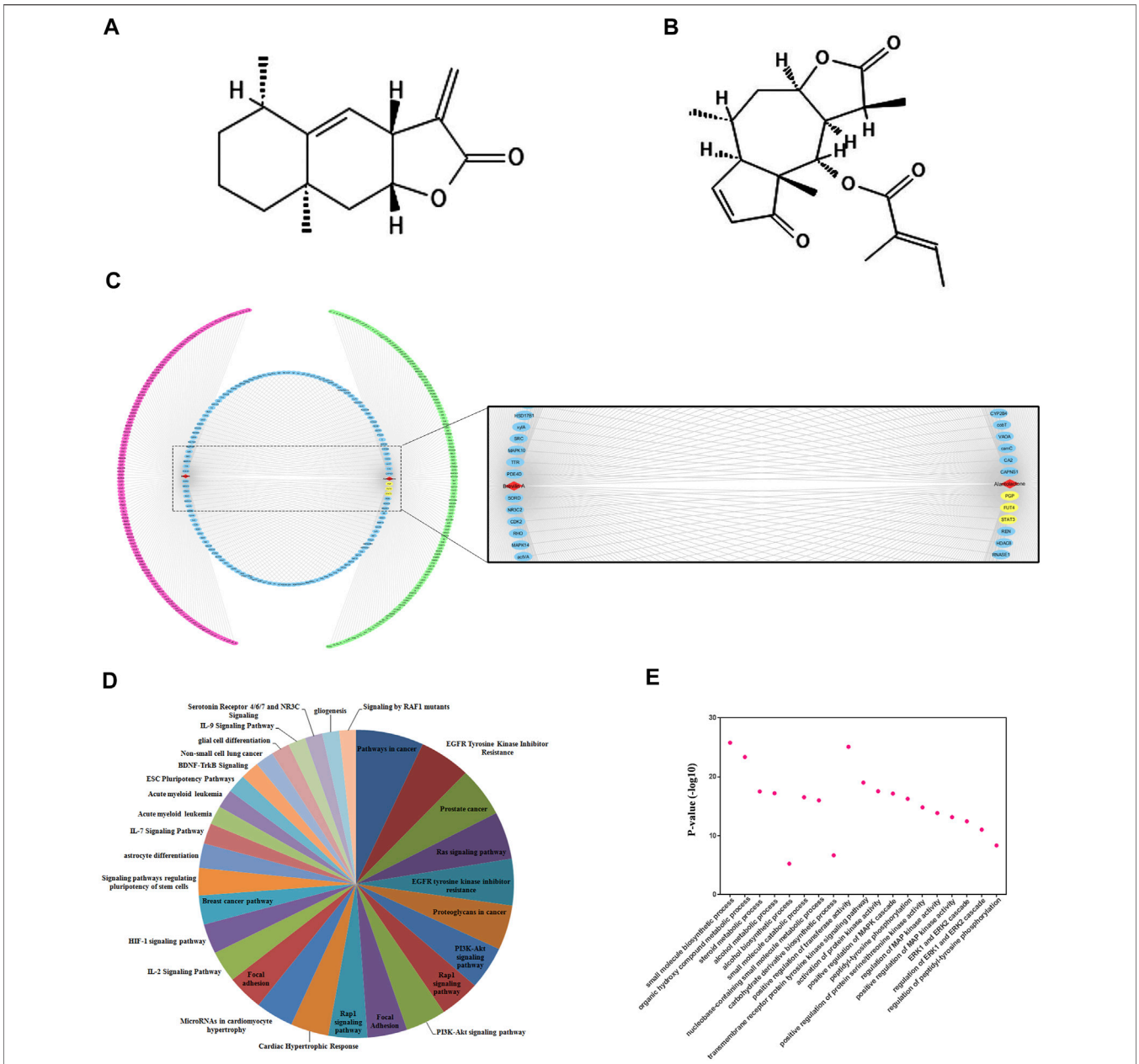


FIGURE 2 | Compound-target networking and evaluation of Gene Ontology (GO) and pathways. **(A)** Chemical structure of Alantolactone **(B)** Chemical structure of Brevilin A **(C)** Red and green circles represent the individual targets of ALT and Brv-A respectively. The blue circle represents some common targets of ALT and Brv-A. ALT and Brv-A are viewed in red triangles while the yellow marked targets are used for further study. **(D)** The *y*-axis depicts *p*-value enrichment score that are greatly enriched, while the names of these enriched biological processes are shown on *x*-axis. **(E)** KEGG Pathways categories.

RESULTS

MALAT1 Is Associated With STAT3 Activation and FUT4 Expression in Paclitaxel Resistant Lung Cancer Cells

To evaluate the significance of MALAT1, STAT3, and FUT4 in paclitaxel-resistance, initially, we compared the expression levels of lncMALAT1, STAT3, and FUT4 of A549/T cells with non-resistant A549 cells. We quantified the expressions at mRNA and protein level using qPCR and western blotting respectively. As indicated in **Figures 1A–C**, the mRNA expression of lncMALAT1, STAT3, and FUT4 was significantly high in A549/T cells as compared with the non-resistant A549 lung cancer cells. Similarly, the higher protein level of STAT3 and FUT4 was found in A549/T cells than A549 cells (**Figures 1D,E**). After establishing the expected role of MALAT1, STAT3, and FUT4 in resistant and non-resistant lung cancer cells, we further studied the association of MALAT1 with STAT3 and FUT4

expression in A549/T cells. Prior to find this association, we first measured the mRNA level for lncMALAT1 in siRNA MALAT1 transfected A549/T resistant cells to establish a control for our further readings. The expression of MALAT1 was downregulated successfully in siRNA MALAT1 transfected A549/T cells (**Figure 1F**). Later, we assessed the expression of STAT3 and FUT4 in A549/T cells transfected with siRNA-MALAT1. We detected a significant decrease in STAT3 activation and FUT4 expression in resistant cells transfected with siRNA-MALAT1 (**Figures 1G,H**). Collectively, our data indicate that STAT3 and FUT4 are overexpressed in A549/T cells and this overexpression is associated to the upregulation of lncRNA MALAT1.

Compound-Target Networking Analysis and Evaluation of Pathways and Gene Ontology (GO)

Prior to the mechanistic study, we validated the targets of SLs by compound-target networking analysis. Among SLs family, we chose ALT and Brv-A (**Figures 2A,B**) for the current study, as *1*) the anti-cancer effect and their pivotal role in the inhibition of STAT3 signaling has been extensively reported *2*) we confirmed that STAT3, FUT4, and P-GP were the common targets of ALT and Brv-A. There were 536 nodes (two compound nodes and 534 compound-targeted nodes) and 560 edges throughout this network (**Figure 2C**). The central nodes of this network, 128 nodes in blue, were found to be controlled by both ALT and Brv-A, whereas the external nodes, in green and red, are regulated individually by ALT and Brv-A, respectively. All such controlled nodes could be the core or central nodes in the treatment of lung cancer. As shown in this network, ALT and Brv-A would interact with these targets and exert a significant pharmacological effect.

The potential effect of ALT and Brv-A was further investigated using KEGG pathway evaluation. The analysis represented the enriched pathways in cancer affected by ALT and Brv-A include EGFR-tyrosine kinase inhibitor, PI3k-Akt signaling pathway, RAS signaling pathway, RAP1 signaling pathway, IL-17 signaling pathway, and breast cancer pathway along with EGFR tyrosine kinase inhibitor (**Figure 2D**). Lung cancer is associated with the aforementioned biological processes. As a result, these findings provided a theoretical support that the anti-cancer activity of ALT and BRV-A is closely connected to the above-mentioned cancer pathways.

We used GO enrichment to further investigate the molecular functions associated with ALT and BRV-A targets. These targets were found not only to be involved into the biosynthesis of small molecules, alcohol metabolism, regulation of ERK1 and ERK2 cascade, but also implicated in regulation of phosphatidyl-tyrosine phosphorylation and the positive regulation of MAPK cascade (**Figure 2E**).

ALT and Brv-A Restrict Growth and Proliferation in A549/T NSCLC Cells

First, we determined the resistance index of paclitaxel among A549 and A549/T cells at 72 h time point. As presented in **Figure 3A**, the IC_{50} of paclitaxel among A549 cells was approximately 0.195 μM while that in A549/T cells was 6.183 μM on average (almost 31 times higher in A549/T cells) at 72 h indicating that A549/T cells are resistant to paclitaxel. Following that, different concentrations of ALT and Brv-A were used to treat A549/T cells for 24, 48, and 72 h to assess cell viability. We detected a halted cell growth in presence of these two drugs followed by a substantial dose-dependent decrease in A549/T cells viability. The IC_{50} values for ALT were 20, 16, and 15 μM at 24, 48, and 72 h respectively. Moreover, the IC_{50} values for Brv-A at 24, 48, and 72 h were 18.31, 14.84, and 10.45 μM respectively representing the effectiveness of these natural compounds against paclitaxel resistance in lung cancer cells (**Figures 3B,C**). The most promising concentrations along the suggested concentration gradient of 2.5–120 μM were 5, 10, and 15 μM. The cytotoxic effect of ALT and Brv-A was further examined by observation of cell-morphological changes. Cells, treated with ALT and Brv-A for 24 h, developed a round shape and lost anchorage and cellular geometry (**Figures 3D,E**). We further confirmed the cell death *via* live/dead assay. PI and Calcein-AM were used to stain the dead (red) and live (green) cells respectively. Results showed that ALT and Brv-A treatment enhanced the proportion of PI intake among A549/T cells in concentration-dependent manner representing the dead cells (**Figures 3F,G**). Next, we performed colony forming assay to evaluate the anti-proliferative efficacy of ALT and Brv-A. After exposing the A549/T cells to ALT and Brv-A for 24 h, we noted that the capability of resistant cells to form colonies was reduced. We assessed the growth constraints in treated cells by liquifying the crystal violet stain (taken by the colonies) in methanol. Consistent with the reported alterations in cell viability and morphology, we observed lower uptake of crystal violet stain in ALT (**Figure 3H**) and Brv-A (**Figure 3I**) treated A549/T cells as compared to untreated cells. The collective data show that ALT and Brv-A has a considerable inhibitory effect over the growth and proliferation rate of A549/T cells.

ALT and Brv-A Induce Pro-apoptotic Effect in A549/T Cancer Cells

To ascertain the mode of cell death, we performed Annexin V-FITC and PI staining and subjected the cells to flow cytometric analysis. As presented in **Figures 4A,B**, ALT and Brv-A influenced the apoptotic event in dose-dependent way. The percentage of early and late apoptosis (average) was increased from 3.2 to 6.45, 12.9, and 29.08%, after treating the A549/T cells with 5, 10, and 15 μM concentration of ALT respectively (**Figure 4C**). Similarly, 5, 10, and 15 μM doses of Brv-A increased the rate of apoptosis from 2.65 to 3.68, 8.78, and 32.18% respectively (**Figure 4D**). Moreover, ALT and Brv-A increased the expression of cleaved PARP, cleaved caspase-9, and cleaved caspase-3 in dose-dependent manner which are the markers of apoptotic processes (**Figures 4E,F**).

ALT and Brv-A Inhibit STAT3 Activation and Attenuate FUT4 and P-GP Expression in A549/T Cells

Our previous studies established the direct binding of Brv-A to the STAT3 with a considerable effect compared to commercially

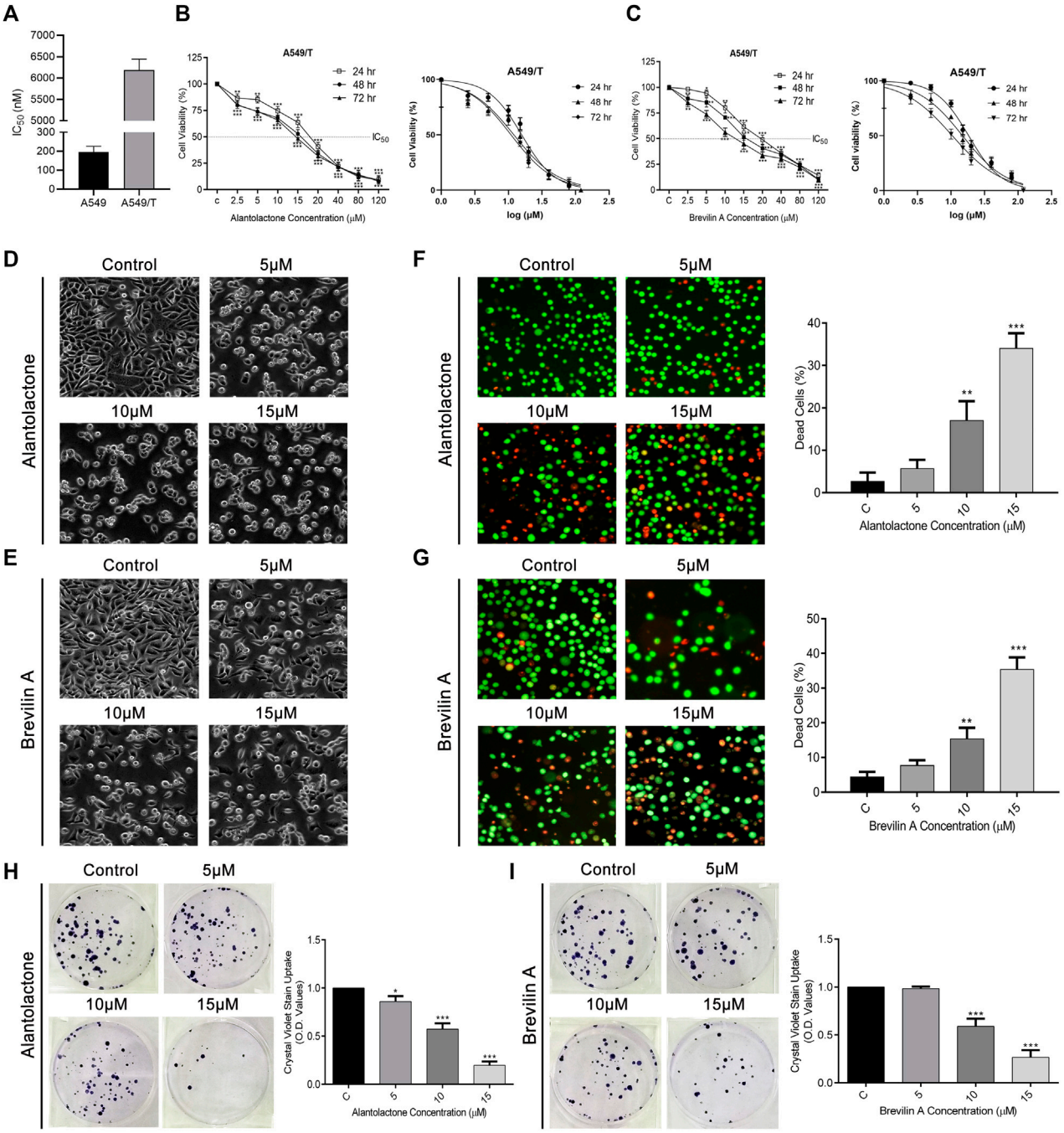


FIGURE 3 | ALT and Brv-A Restrict Growth and Proliferation in A549/T NSCLC Cells. **(A)** Paclitaxel resistance index in A549/T cells compared to the parental A549 cells after treating with various concentrations of paclitaxel for 72 h. **(B)** Cell viability percentage and S curve of A549/T cells treated with different concentrations of ALT (μM) for 24, 48, and 72 h. **(C)** Cell viability percentage and S curve of A549/T cells treated with different concentrations of Brv-A (μM) for 24, 48, and 72 h **(D,E)** Morphological changes observed in A549/T cells treated with 5, 10, and 15 μM concentrations of ALT and Brv-A for 24 h **(F,G)** Live/dead assay was performed to measure the alive and dead cells percentage by using calcein-AM and PI stain. Cells were treated with 5, 10, and 15 μM concentrations for 24 h and stained with calcein-AM and PI and photographed by using fluorescence microscope (Leica, DMI 4000B). **(H,I)** Clonogenic assay was performed to validate the cell viability of A549/T cells. **(D–G)** Scale bar is 100 mm. **(A–C,F–I)** Data are presented as Mean ± SD while the entire experiments were done in triplicate independently. ***$p < 0.001$, **$p < 0.01$, *$p < 0.05$ vs control group.

available STAT3 inhibitors (S31-201) (Khan et al., 2020). According to the findings of compound networking constructions and previous experimental research regarding anticancer activity of ALT and Brv-A (Maryam et al., 2017; Khan et al., 2020), we chose STAT3, FUT4, and P-GP (with a diverse role in chemoresistance) as the targets. In current study, molecular docking for FUT4 and P-GP was made to

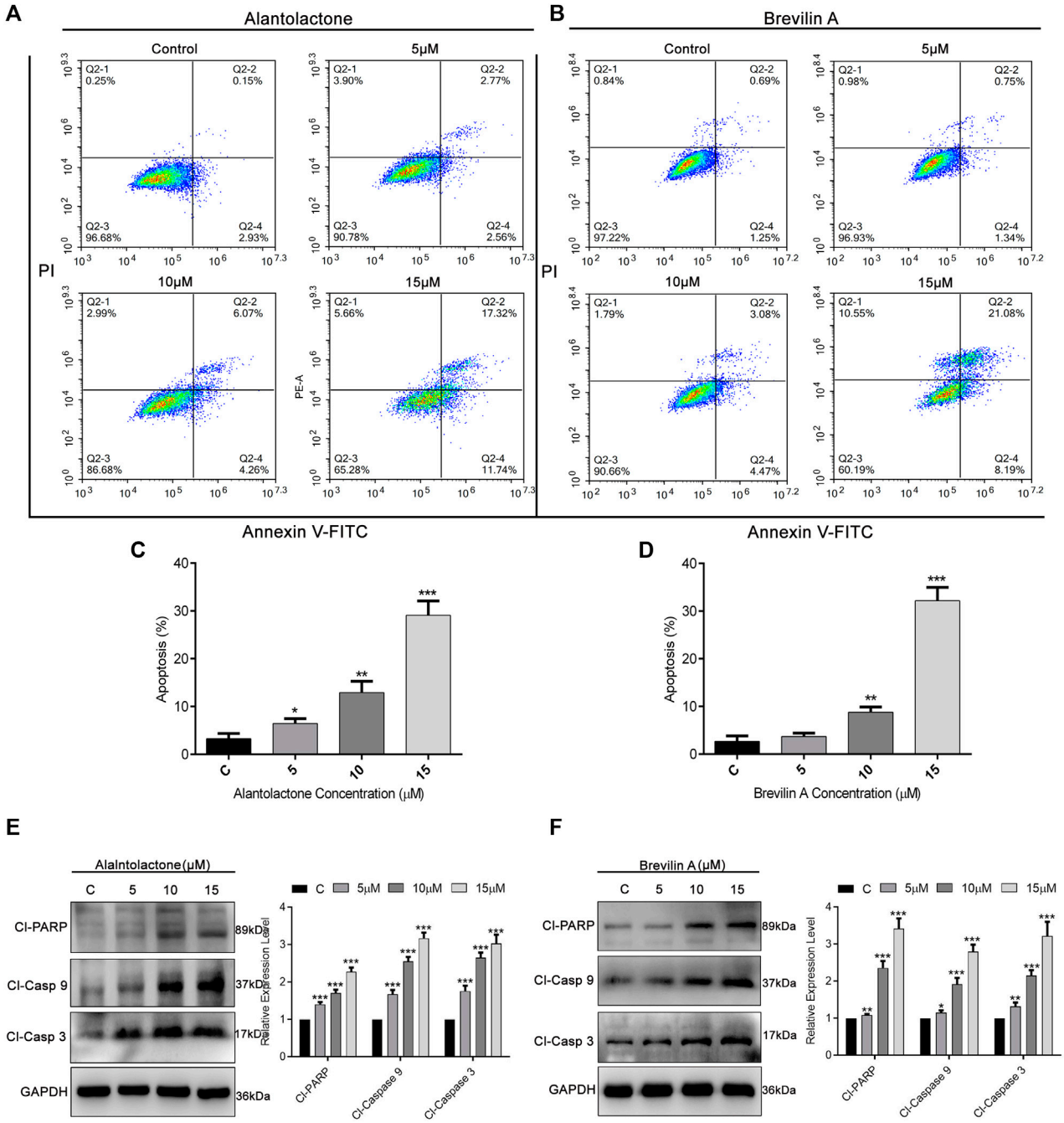


FIGURE 4 | Induction of apoptosis by ALT and Brv-A in A549/T cells. **(A,B)** Cells were treated with 5, 10, and 15 μM concentrations of ALT and Brv-A for 24 h. Cell were stained with annexin V-FITC and PI and analyzed by by flow cytometry. **(C,D)** Graphical presentation of apoptotic rate (percentage) among A549/T cells treated with ALT and Brv-A for 24 h **(E,F)** Expressions of cleaved PARP, cleaved caspase-9, and cleaved caspase-3 were determined by western blotting among treated and untreated A549/T cells. For loading control, GAPDH was used. **(C–F)** Data are presented as Mean ± SD while the entire experiments were done in triplicate independently. ***$p < 0.001$, **$p < 0.01$, *$p < 0.05$ vs control group.

assess the effectiveness of primary drug-protein associations and to examine the reliable binding interfaces, though the molecular docking of these two compounds for STAT3 has already been reported in previous studies (Chun et al., 2015; Khan et al., 2020). The molecular docking (protein-ligand complexes analysis) of FUT4 and P-GP with ALT and Brv-A were performed using PyRx software program. First, the validation method was conducted to ensure the capability of docking machine and the RMSD values were ≤2.0 Å. As presented in **Figure 5A**, the interaction of FUT4 structure with ALT forms a complex *via* carboxylic group of ALT interacted by hydrogen bonding with attractive charged residue Arg-201, pi-alkyl group bonded with residue Trp-31, and pi-sigma interacted to Trp-50

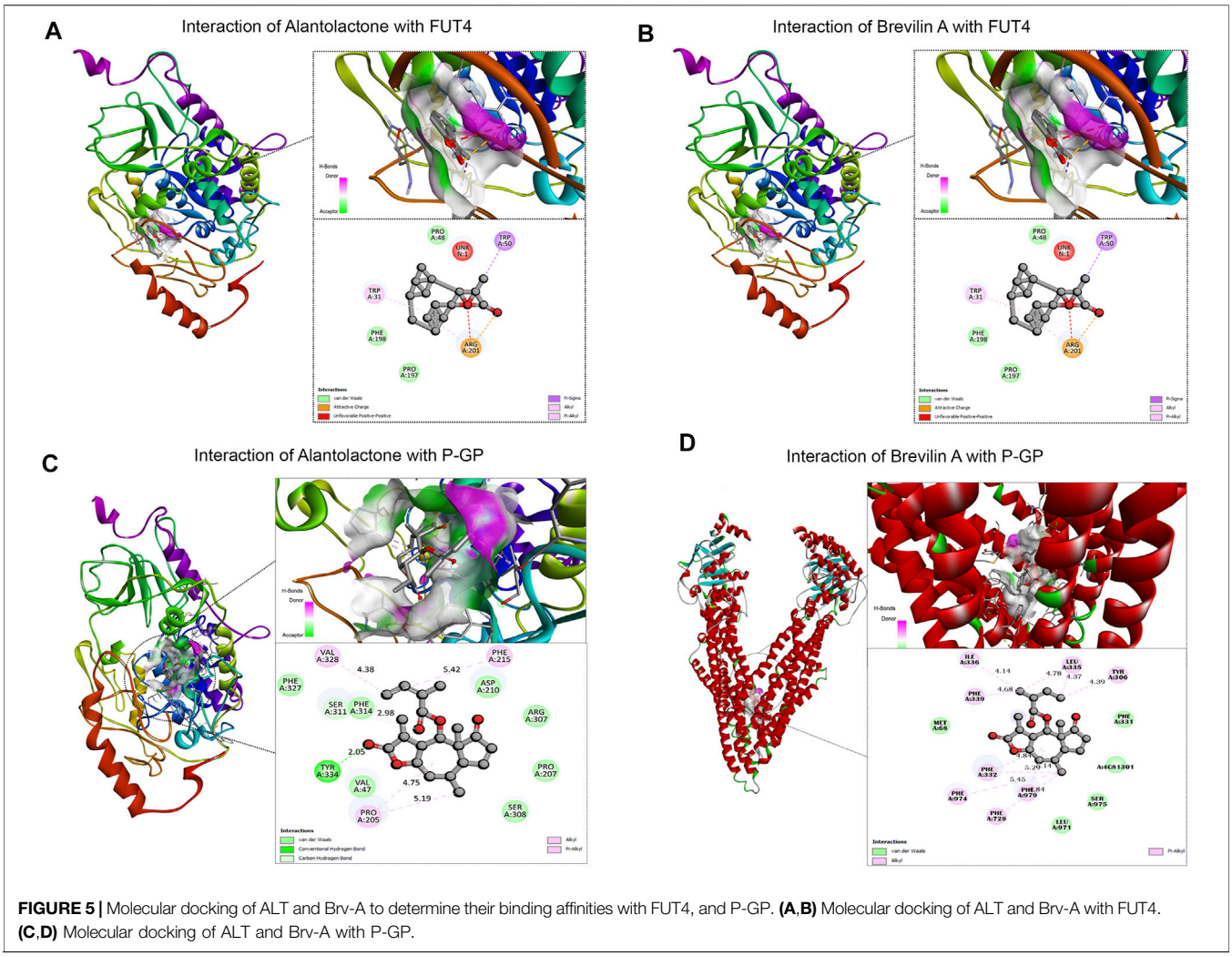


FIGURE 5 | Molecular docking of ALT and Brv-A to determine their binding affinities with FUT4, and P-GP. **(A,B)** Molecular docking of ALT and Brv-A with FUT4. **(C,D)** Molecular docking of ALT and Brv-A with P-GP.

amino acid. As shown in **Figure 5B**, Brv-A moieties form a complex with FUT4 *via* alkyl and pi-alkyl groups interacting with Phe-215, Val-328, Pro-205, and conventional hydrogen bond to Tyr334. These results showed that FUT4 had the binding affinity of −12.4 Kcal/mol and −8.1 Kcal/mol with ALT and Brv-A respectively. ALT also showed good interaction to P-GP binding site, where hydrogen bond forms interaction between pi-alkyl group and Phe-299 as well as Phe-766 residues (**Figure 5C**). Brv-A was found to be in interaction with P-GP residues Tyr-306, Phe-332, Leu 335 by alkyl group and pi-alkyl group interacts with amino acids Phe-979, Phe-974, Phe728, Phe-339, and Ile-336 (**Figure 5D**). On the basis of the binding energy scores of ALT (−10.5 Kcal/mol) and Brv-A (−8.7 Kcal/mol) with P-GP, it is estimated that P-GP has a better binding affinity with ALT.

On the basis of previously reported and obtained results from molecular docking, we were interested to analyze the effect of ALT and Brv-A over STAT3 activation, and FUT4 and P-GP expression *via* western blotting. As expected, ALT and Brv-A inhibited activation of STAT3 in A549/T cells in dose-dependent fashion (**Figures 6A,B**). Furthermore, ALT and Brv-A also inhibited FUT4 expression in dose-dependent manner (**Figures 6C,D**). P-GP, also known as MDR1, ABCB1 is a transmembrane transporter that works for the efflux of various anticancer drugs across the cell membrane *via* ATP hydrolysis and has been implicated in the promotion of drug resistance in various cancer cells. Additionally, STAT3 plays significant role in transcriptional regulation of P-GP expression (Wang R. et al., 2020). As mentioned in previous studies, targeting P-GP transporter is a viable strategy to overcome paclitaxel resistance in A549 cells (Lin et al., 2020). Therefore, we were interested in determining whether these two SLs members have the capability to downregulate P-GP expression among A549/T cells. To begin, we assessed and compared the expression of P-GP between A549 and A549/T cells. We distinguished a higher expression of P-GP in A549/T cells in contrast to A549 cells confirming the P-GP immersion in paclitaxel resistance (**Figure 6E**). Next, we determined the expression level of P-GP in A549/T cells treated with 5, 10, and 15 μM concentrations of ALT and Brv-A. Both of these drugs had a dose-dependent inhibitory effect on P-GP expression (**Figures 6F,G**). The purpose of inhibiting STAT3 activation, P-GP and FUT4 expressions in A549/T cells was to overcome the resistivity, as these proteins are considered to be the major contributors in developing preventive strategies by cancer cells against paclitaxel.

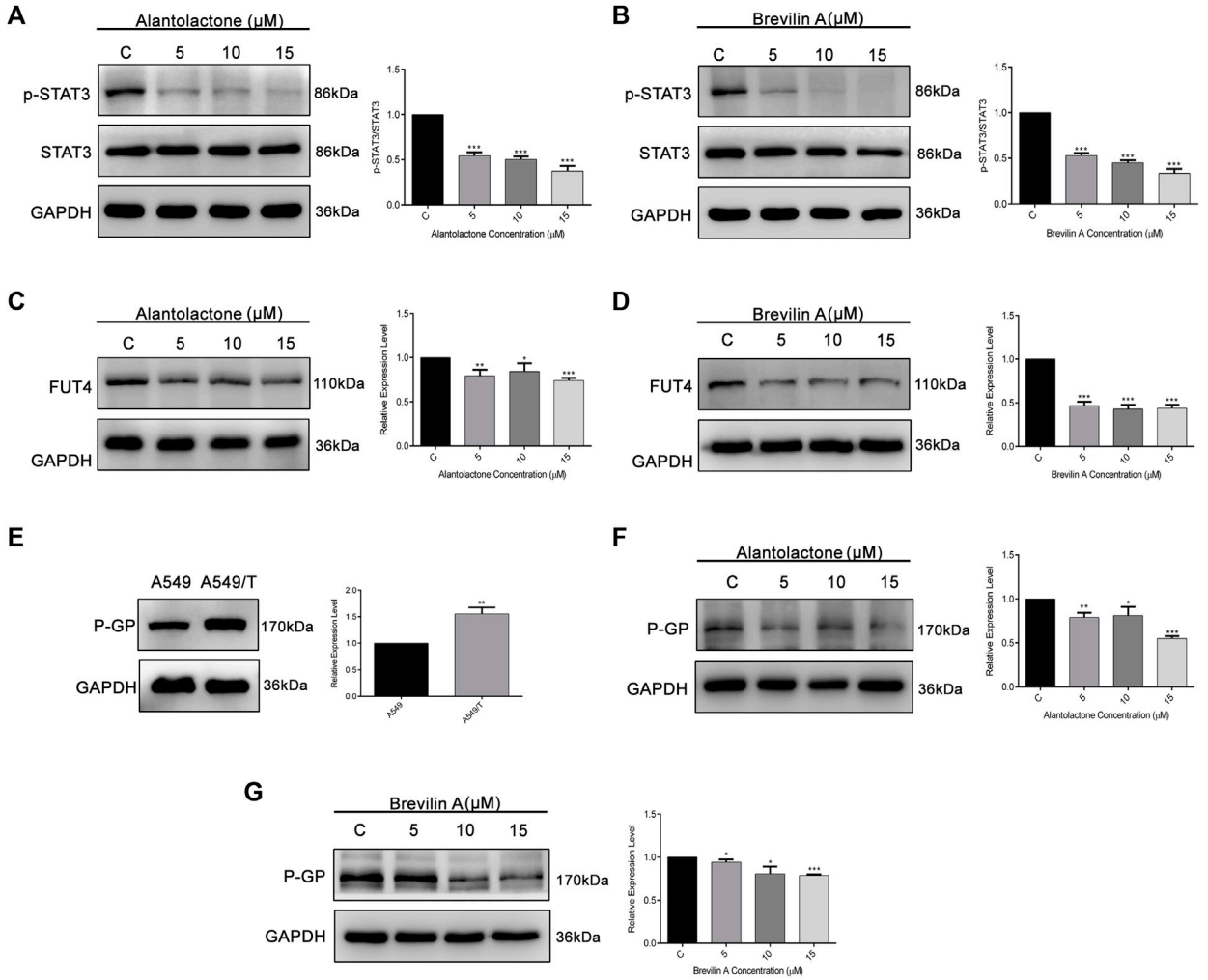


FIGURE 6 | ALT and Brv-A inhibit STAT3 activation, and FUT4 and P-GP expression in A549/T cells. **(A,B)** A549/T cells were exposed to the 5, 10, and 15 μM concentrations of ALT and Brv-A for 24 h and cell lysates were prepared. Expression of STAT3 and p-STAT3 was determined through western blotting. **(C,D)** Expression of FUT4 was determined through western blotting after treating the cells with 5, 10, and 15 μM concentrations of ALT and Brv-A. **(E)** A comparative expression level of P-GP was determined among A549 and A549/T cells *via* western blotting. **(F,G)** Expression of P-GP was determined through western blotting after treating the cells with 5, 10, and 15 μM concentrations of ALT and Brv-A. **(A–G)** For loading control, GAPDH was used. Data are presented as Mean ± SD while the entire experiments were done in triplicate independently. ***$p < 0.001$, **$p < 0.01$, *$p < 0.05$ vs control group.

Our study shows that ALT and Brv-A has a potential inhibitory effect over STAT3 activation, FUT4, and P-GP all of which are known to be linked to the drug resistance in cancer.

MALAT1 Inhibition Augments the Cytotoxic, Anti-migratory, and Anti-invasive Competence of ALT and Brv-A in A549/T Cells

After targeting three important modules responsible for paclitaxel drug resistance in cancer i.e., STAT3, FUT4, and P-GP, we were interested to determine the role of MALAT1 in this scenario. Prior to establish the effectiveness of ALT and Brv-A over the functional role of MALAT1, we predicted the protein-protein interactions (PPIs) by using STRING database. Our analysis revealed that MALAT1 interacts with 20 different types of proteins which included FUT4, STAT3, JAK1, JAK2, JAK3, EGFR, MAPK1, FOXP3, FOS, LEPR, PTPN2, HIF-1α, PIAS3, RELA, HSP90AA1, EP300, AR, CREBBP, IL10RA, and NANOG (**Figure 7A**). As given in **Figure 7B**, it is estimated that MALAT1 may interact with FUT4 *via* STAT3 that needs further experimental validation. Moreover, previous research has established that MALAT1 modulates STAT3, FUT4, and P-GP (Cheng et al., 2013; Fang et al., 2018; Yang et al., 2018; Wang R. et al., 2020; Xu et al., 2020). On the basis of MALAT1/STAT3, MALAT1/FUT4 and MALAT1/STAT3/P-GP interactions, we hypothesized that ALT and Brv-A may influence the expression of MALAT1. We assessed the MALAT1 levels in drug treated (ALT, Brv-A) groups and compared to the untreated and found a significant decrease in dose-dependent fashion (**Figure 8A**). Due to strong interactive properties of MALAT1 to STAT3, FUT4, and P-GP (selected markers to be

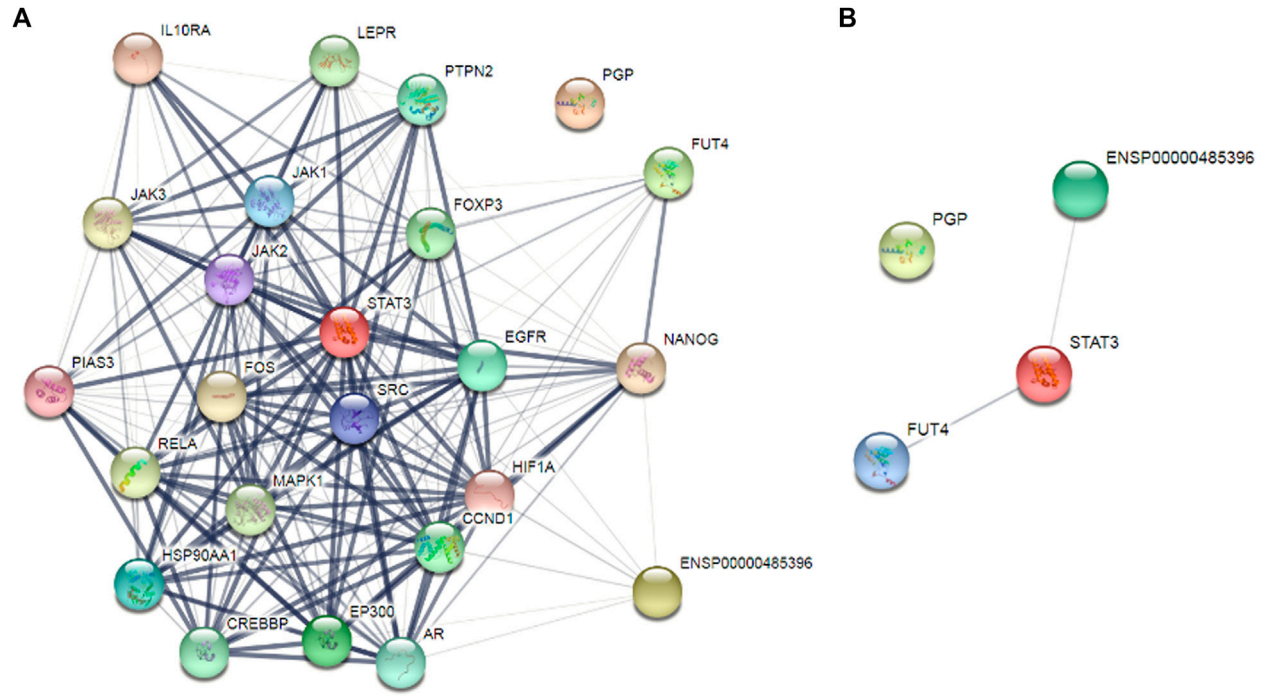


FIGURE 7 | Determination of the interrelating proteins through protein-protein interaction (PPI) network *via* the STRING online tool. **(A,B)** Lines in the network represent interaction of proteins among each other.

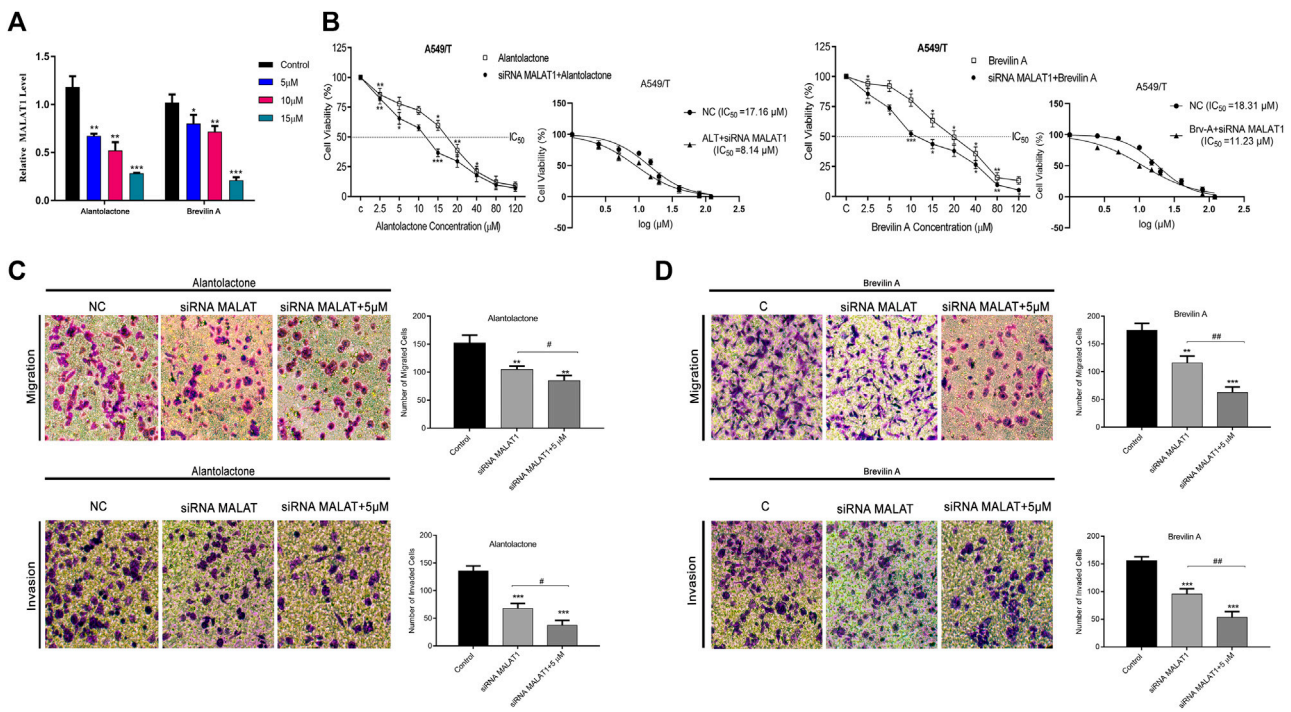


FIGURE 8 | ALT and Brv-A reduce MALAT1 expression to overcome paclitaxel-resistance in lung cancer cells. **(A)** The mRNA level of MALAT1 was measured in A549/T cells treated with 5, 10, and 15 μM concentrations of ALT and Brv-A for 24 h. **(B)** Cell viability (percentage) and S curve of non-transfected and siRNA MALAT1 transfected A549/T cells treated with ALT and Brv-A for 24 h **(C,D)** Rate of migration/invasion was measured in siRNA MALAT1 transfected A549/T cells individually and in combination with treatment of ALT and Brv-A (5 μM each). **(A–D)** Data are presented as Mean ± SD while the entire experiments were done in triplicate independently. ***$p < 0.001$, **$p < 0.01$, *$p < 0.05$ vs control group.

targeted in current study) we were interested to investigate the impact of knockdown MALAT1 over further improving the efficacy of ALT and Brv-A. This was accomplished by determining and comparing the viability of A549/T cells treated with different concentrations of ALT and Brv-A with and without siRNA MALAT1 transfection. As presented in **Figure 8B**, siRNA MALAT1 transfected cells were more sensitive to ALT and Brv-A at various dosages. Previously, some studies have confirmed the role of MALAT1 in the migration and invasive properties of various cancer cells (Chen et al., 2018; Tang et al., 2018; Yuan et al., 2019). Our data suggested that the inhibition of MALAT1 restricts A549/T cells from migration and invasion individually as well as in combination with treatment of ALT and Brv-A (**Figures 8C,D**). These results suggested that targeting the STAT3, FUT4, and P-GP and MALAT1 (by ALT and Brv-A as well as *via* gene knockdown) reduce the migration and invasion of paclitaxel-resistant A549 cells and enhance the competence of these two compounds significantly. These findings propose that along with targeting STAT3, FUT4, and P-GP transporters, inhibiting MALAT1 response would promote the rate of apoptosis in drug resistant cancer cells.

DISCUSSION

Metastasis and chemoresistance are the primary contributors for the terminal condition of lung cancer. Paclitaxel resistance is the major concern for researchers in field of therapeutic tactic towards NSCLC (Lin et al., 2020). Although, recent advancements in therapeutics have made it possible to overcome EGFR-TKIs resistant cancer types, however, the adverse effects, unmapped targets and cellular responses to the available drugs require further investigation (Yuan H. et al., 2016; Chen et al., 2017; Chen et al., 2019). More precisely, because paclitaxel resistance is multifactorial, it likely has various unknown motives that need further amplification with special emphasis on discovery of novel natural compounds with fewer side effects to counter the unexplored therapeutic targets and crucial aspects of resistance.

Several lncRNAs have been described to cause drug resistance in different cancer types which indicates that these lncRNAs serve as biological targets of drug resistance in cancer (Xue et al., 2018). LncRNA MALAT1 enhances tumor proliferation, migration, invasion, and growth of cancer cells. MALAT1 was known as a metastasis development marker for lung adenocarcinoma in the early stages (Ji et al., 2003). MALAT1 has been shown to contribute in a variety of functions in cancer cells such as, enhancement of EMT, acting as miRNA sponges, and stimulating autophagic events (Lin et al., 2007; Ji et al., 2013; Fan et al., 2014; Hirata et al., 2015; Qi et al., 2016). Recently, a numeral study has explored the fundamental role of MALAT1 in the development of drug resistance in different cancer cells. Some of these include resistance to the hepatocellular carcinoma cells by sponging miR-216b (Yuan P. et al., 2016), sunitinib-resistance by regulating miR-362-3p-mediated G3BP1 in renal cell carcinoma (Wang Z. et al., 2020), cisplatin resistance in gastric cancer (Dai et al., 2020), and docetaxel resistance of prostate cancer cells *via* miR-145-5p-mediated regulation of AKAP12 (Xue et al., 2018).

STAT3 is a transcriptional regulator of numerous factors that are involved in tumor progression. STAT3 activation has been shown to promote cancer proliferation, growth, and reduces the apoptotic rate (Timofeeva et al., 2013). Over-activation of STAT3 is linked with resistance to several drugs and therapeutic agents including, crizotinib, erlotinib, gefitinib, trastuzumab, and sorafenib (Sen et al., 2012; Li et al., 2013; Wu et al., 2013; Cuyàs et al., 2016; Aghazadeh and Yazdanparast, 2017; Sakurai et al., 2017). Additionally, alterations in the expression of fucosyltransferases, i.e., FUT4, FUT6, and FUT8 are also associated with MDR resistance (Cheng et al., 2013). Therefore, STAT3 along with FUT family proteins are attractive targets for overcoming drug resistance in cancer. In this study, we confirmed that MALAT1, STAT3, FUT4, and P-GP were higher in A549/T cells as compare to A549 cells. To validate whether MALAT1 is associated with STAT3 activation and FUT4 fucosylation, we knocked down MALAT1 *via* siRNA MALAT1 and determined the STAT3 activation and FUT4 expression. Interestingly, we found that MALAT1 knocked down in A549/T cells resulted in decreased FUT4 expression and STAT3 activation. Our findings were parallel to the findings of previous studies where MALAT1 promoted drug resistance in cancer cells *via* modulating STAT3 activation in lung cancer and enhanced FUT4 fucosylation by sponging miR-26a/26b involving PI3K/AKT pathway (Xu et al., 2020).

In the current study, we were interested in evaluating the anticancer activity of ALT and Brv-A against paclitaxel-resistant lung cancer cells. The aim was also extended to gain insight into whether simultaneous inhibition of STAT3 activation and FUT4 fucosylation *via* ALT and Brv-A have any impact on functional role of lncRNA MALAT1 in A549/T lung cancer cells. Prior to the mechanistic study, we also confirmed the targets of these two compounds by compound-target networking analysis where we found that STAT3, FUT4, and P-GP were common targets for both, ALT and Brv-A. The KEGG pathway analysis further justified the dominant involvement of these compounds in cancer pathways and EGFR tyrosine kinase inhibitor resistance. Therefore, these two natural compounds among SLs family were found more potent for this study. The results indicated that ALT and Brv-A significantly inhibited proliferation, growth, and cell viability of A549/T cells, accompanied by induction of apoptosis in a dose-dependent mode. Further study confirmed the apoptosis *via* measuring expression levels of apoptotic markers, i.e., PARP, caspase-9 and caspase-3 cleavage. Flow cytometric analysis was consistent with the finding where A549/T cells exhibited a significantly higher apoptotic rate than the untreated control group. Our results in terms of inducing apoptosis by ALT and Brv-A were consistent with previously conducted studies where ALT induced apoptosis in squamous lung cancer SK-MES-1 cells (Zhao et al., 2015) as well as in A549 lung adenocarcinoma cells (Maryam et al., 2017) while Brv-A induced apoptosis in breast cancer cells (MCF-7) through generation of ROS (Saleem et al., 2020) and lung cancer cells (Khan et al., 2020).

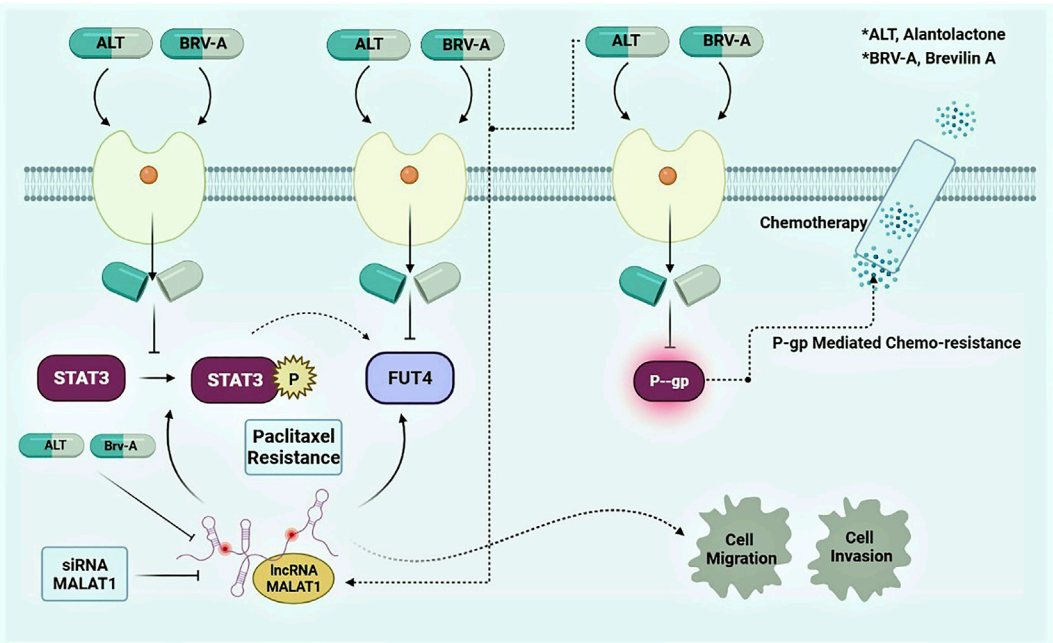


FIGURE 9 | Graphical presentation of mode of action of ALT and Brv-A and preemptive role of MALAT1 in A549/T lung cancer cells.

ALT and Brv-A are well-known natural SLs that inhibit STAT3 activation, while the inhibitory effect over FUT4 has been investigated for the first time in the current study. Moreover, the effect of ALT over P-GP has been investigated in the previous study (Maryam et al., 2017) however, Brv-A is used in the current study to explore its effectiveness against P-GP transporters that play a pivotal role in resistance. Our data confirmed that ALT and Brv-A, effectively inhibited STAT3 activation and decreased FUT4 and P-GP expression in A549/T cells in a dose-dependent manner. We also verified the primary drug-protein associations and reliable binding interfaces *via* molecular docking. The capability to restrict STAT3 activation and FUT4 and P-GP expressions simultaneously in A549/T cells enlist these two natural compounds as a comprehensive therapeutic strategy for incapacitating paclitaxel-resistance.

We also aimed to explore the effect of ALT and Brv-A over MALAT1 expression after exploring their effectiveness against STAT3 activation, FUT4, and P-GP expression. Interestingly, we found restricted MALAT1 expression in A549/T cells treated with ALT and Brv-A. To confirm whether restricting MALAT1 expression may affect the functional role of MALAT1 in paclitaxel resistance, we used siRNA-MALAT1 to knockdown MALAT1 and measured the viability of A549/T cells compared to the negative control. We observed a significant reduction in cell viability of MALAT1 knocked down cells treated with ALT and Brv-A. Inhibition of MALAT1 activity further promoted the effectiveness of these SLs. Our results were similar to the findings of Yang et al., where they showed that knockout of MALAT1 *via* shRNA MALAT1 improved the apoptotic rate of Polyphyllin I promoted in gefitinib-resistant NSCLC (Yang et al., 2018). Next, we were interested to know the role of MALAT1 in promoting invasion and migration of A549/T cells. Restriction of MALAT1 activity at the cellular level attenuated the migratory and invasive competence of A549/T cells. Furthermore, we also explored that ALT and Brv-A in combination with MALAT1 inhibition significantly reduced the migration/invasion among A549/T cells that further justified the role of MALAT1 in paclitaxel resistance and vindicated the rationale of the study.

In conclusion, the higher expression of lncRNA MALAT1 among resistant cancer types is alarming. The potential chemotherapeutic targets regarding chemoresistance e.g., STAT3, FUT4, and P-GP transporters are current center of attention for researcher to deal with drug resistance. It has been considered to be an inclusive strategy tactic for the management of drug resistance in cancer. This study concluded that MALAT1 is the main responsible factor that contributes to the paclitaxel resistance in A549 cells. Moreover, inhibiting STAT3 activation and FUT4 expression along with P-GP *via* SL, the widely used natural compounds for research and therapeutic purpose, demonstrated to overcome drug resistance (**Figure 9**; graphical presentation). In addition, restricting MALAT1 activity at cellular level could result in improvement in the promotion of apoptosis and prevent migration and invasion of paclitaxel-resistant lung cancer cells. Current study suggests these two SLs to be the promising agents for overcoming paclitaxel resistance in A549 lung cancer cells *via* MALAT1/STAT3/FUT4 axis. The profound insights at molecular level i.e., correlation of the physiological mechanism of MALAT1, STAT3, FUT4 and P-GP are lacking that needs further experimental investigations. However, the given findings suggest improved treatment strategies for patients with paclitaxel-resistant lung cancer with special emphasis over SLs.

DATA AVAILABILITY STATEMENT

The original contributions presented in the study are included in the article/Supplementary Material, further inquiries can be directed to the corresponding authors.

AUTHOR CONTRIBUTIONS

YD, ZZ, and MS conducted the experiments and prepared the original first draft of the manuscript. MN, MS, FA, and RD undertook the computational and statistical analysis. TM, MK, ZZ, and GA edited the manuscript and provided technical assistance. MS, LL, and MK assisted in conceptualization, data analysis, and provided support for project administration.

ACKNOWLEDGMENTS

The authors acknowledge all authorities of The Second Hospital of Jilin University for their support.

REFERENCES

Aghazadeh, S., and Yazdanparast, R. (2017). Activation of STAT3/HIF-1α/Hes-1 axis Promotes Trastuzumab Resistance in HER2-Overexpressing Breast Cancer Cells via Down-Regulation of PTEN. *Biochim. Biophys. Acta Gen. Subj* 1861 (8), 1970–1980. doi:10.1016/j.bbagen.2017.05.009

Canales, M., Hernández, T., Caballero, J., Romo de Vivar, A., Avila, G., Duran, A., et al. (2005). Informant Consensus Factor and Antibacterial Activity of the Medicinal Plants Used by the People of San Rafael Coxcatlán, Puebla, México. *J. Ethnopharmacol* 97 (3), 429–439. doi:10.1016/j.jep.2004.11.013

Cao, Y., Zhang, F., Wang, H., Bi, C., Cui, J., Liu, F., et al. (2021). LncRNA MALAT1 Mediates Doxorubicin Resistance of Hepatocellular Carcinoma by Regulating miR-3129-5p/Nova1 axis. *Mol. Cell Biochem* 476 (1), 279–292. doi:10.1007/s11010-020-03904-6

Chen, M., Xia, Z., Chen, C., Hu, W., and Yuan, Y. (2018). LncRNA MALAT1 Promotes Epithelial-To-Mesenchymal Transition of Esophageal Cancer through Ezh2-Notch1 Signaling Pathway. *Anti-Cancer Drugs* 29 (8), 767–773. doi:10.1097/cad.0000000000000645

Chen, S., Zhang, Z., and Zhang, J. (2019). Emodin Enhances Antitumor Effect of Paclitaxel on Human Non-small-cell Lung Cancer Cells In Vitro and In Vivo. *Drug Des. Devel Ther.* 13, 1145–1153. doi:10.2147/dddt.s196319

Chen, X., Sun, X., Guan, J., Gai, J., Xing, J., Fu, L., et al. (2017). Rsf-1 Influences the Sensitivity of Non-small Cell Lung Cancer to Paclitaxel by Regulating NF-Kb Pathway and its Downstream Proteins. *Cell Physiol Biochem* 44 (6), 2322–2336. doi:10.1159/000486116

Cheng, L., Luo, S., Jin, C., Ma, H., Zhou, H., and Jia, L. (2013). FUT Family Mediates the Multidrug Resistance of Human Hepatocellular Carcinoma via the PI3K/Akt Signaling Pathway. *Cell Death Dis* 4 (11), e923. doi:10.1038/cddis.2013.450

Chun, J., Li, R. J., Cheng, M. S., and Kim, Y. S. (2015). Alantolactone Selectively Suppresses STAT3 Activation and Exhibits Potent Anticancer Activity in MDA-MB-231 Cells. *Cancer Lett.* 357 (1), 393–403. doi:10.1016/j.canlet.2014.11.049

Cuyàs, E., Pérez-Sánchez, A., Micol, V., Menendez, J. A., and Bosch-Barrera, J. (2016). STAT3-targeted Treatment with Silibinin Overcomes the Acquired Resistance to Crizotinib in ALK-Rearranged Lung Cancer. *Cell Cycle* 15 (24), 3413–3418. doi:10.1080/15384101.2016.1245249

Dai, Q., Zhang, T., and Li, C. (2020). LncRNA MALAT1 Regulates the Cell Proliferation and Cisplatin Resistance in Gastric Cancer via PI3K/AKT Pathway. *Cancer Manag. Res.* 12, 1929–1939. doi:10.2147/cmar.s243796

Dallakyan, S., and Olson, A. J. (2015). Small-molecule Library Screening by Docking with PyRx. *Methods Mol. Biol.* 1263, 243–250. doi:10.1007/978-1-4939-2269-7_19

de Vries, T., Knegtel, R. M., Holmes, E. H., and Macher, B. A. (2001). Fucosyltransferases: Structure/function Studies. *Glycobiology* 11 (10), 119R–128Rr. doi:10.1093/glycob/11.10.119r

Fan, Y., Shen, B., Tan, M., Mu, X., Qin, Y., Zhang, F., et al. (2014). TGF-β-induced Upregulation of Malat1 Promotes Bladder Cancer Metastasis by Associating with Suz12. *Clin. Cancer Res.* 20 (6), 1531–1541. doi:10.1158/1078-0432.ccr-13-1455

Fang, Z., Chen, W., Yuan, Z., Liu, X., and Jiang, H. (2018). LncRNA-MALAT1 Contributes to the Cisplatin-Resistance of Lung Cancer by Upregulating MRP1 and MDR1 via STAT3 Activation. *Biomed. Pharmacother.* 101, 536–542. doi:10.1016/j.biopha.2018.02.130

Gong, J., Xu, L., Li, Z., Hu, X., Liu, J., Teng, Y., et al. (2018). A Clinical Prognostic Score to Predict Survival of Advanced or Metastatic Non-small Cell Lung Cancer (NSCLC) Patients Receiving First-Line Chemotherapy: a Retrospective Analysis. *Med. Sci. Monit.* 24, 8264–8271. doi:10.12659/MSM.911026

Hirata, H., Hinoda, Y., Shahryari, V., Deng, G., Nakajima, K., Tabatabai, Z. L., et al. (2015). Long Noncoding RNA MALAT1 Promotes Aggressive Renal Cell Carcinoma through Ezh2 and Interacts with miR-205. *Cancer Res.* 75 (7), 1322–1331. doi:10.1158/0008-5472.can-14-2931

Ivie, G. W., Witzel, D. A., and Rushing, D. D. (1975). Toxicity and Milk Bittering Properties of Tenulin, the Major Sesquiterpene Lactone Constituent of Helenium Amarum (Bitter Sneezeweed). *J. Agric. Food Chem.* 23 (5), 845–849. doi:10.1021/jf60201a012

Ji, L., Liu, X., Zhang, S., Tang, S., Yang, S., Li, S., et al. (2017). The Novel Triazolonaphthalimide Derivative LSS-11 Synergizes the Anti-proliferative Effect of Paclitaxel via STAT3-dependent MDR1 and MRP1 Downregulation in Chemoresistant Lung Cancer Cells. *Molecules* 22 (11), 1822. doi:10.3390/molecules22111822

Ji, P., Diederichs, S., Wang, W., Böing, S., Metzger, R., Schneider, P. M., et al. (2003). MALAT-1, a Novel Noncoding RNA, and Thymosin Beta4 Predict Metastasis and Survival in Early-Stage Non-small Cell Lung Cancer. *Oncogene* 22 (39), 8031–8041. doi:10.1038/sj.onc.1206928

Ji, Q., Liu, X., Fu, X., Zhang, L., Sui, H., Zhou, L., et al. (2013). Resveratrol Inhibits Invasion and Metastasis of Colorectal Cancer Cells via MALAT1 Mediated Wnt/β-Catenin Signal Pathway. *PLoS One* 8 (11), e78700. doi:10.1371/journal.pone.0078700

Khan, M., Maryam, A., Saleem, M. Z., Shakir, H. A., Qazi, J. I., Li, Y., et al. (2020). Brevilin A Induces ROS-dependent Apoptosis and Suppresses STAT3 Activation by Direct Binding in Human Lung Cancer Cells. *J. Cancer* 11 (13), 3725–3735. doi:10.7150/jca.40983

Kim, C. Y., Oh, J. H., Lee, J. Y., and Kim, M. H. (2020). The LncRNA HOTAIRM1 Promotes Tamoxifen Resistance by Mediating HOXA1 Expression in ER+ Breast Cancer Cells. *J. Cancer* 11 (12), 3416–3423. doi:10.7150/jca.38728

Latorre, E., Carelli, S., Raimondi, I., D'Agostino, V., Castiglioni, I., Zucal, C., et al. (2016). The Ribonucleic Complex HuR-MALAT1 Represses CD133 Expression and Suppresses Epithelial-Mesenchymal Transition in Breast Cancer. *Cancer Res.* 76 (9), 2626–2636. doi:10.1158/0008-5472.CAN-15-2018

Lee, J. H., Kim, C., Sethi, G., and Ahn, K. S. (2015). Brassinin Inhibits STAT3 Signaling Pathway through Modulation of PIAS-3 and SOCS-3 Expression and Sensitizes Human Lung Cancer Xenograft in Nude Mice to Paclitaxel. *Oncotarget* 6 (8), 6386–6405. doi:10.18632/oncotarget.3443

Li, B., Gu, W., and Zhu, X. (2019). NEAT1 Mediates Paclitaxel-Resistance of Non-small Cell of Lung Cancer through Activation of Akt/mTOR Signalling Pathway. *J. Drug Target.* 27 (10), 1061–1067. doi:10.1080/1061186X.2019.1585437

Li, R., Hu, Z., Sun, S. Y., Chen, Z. G., Owonikoko, T. K., Sica, G. L., et al. (2013). Niclosamide Overcomes Acquired Resistance to Erlotinib through Suppression of STAT3 in Non-small Cell Lung Cancer. *Mol. Cancer Ther.* 12 (10), 2200–2212. doi:10.1158/1535-7163.mct-13-0095

Li, S., Mei, Z., Hu, H. B., and Zhang, X. (2018). The lncRNA MALAT1 Contributes to Non-small Cell Lung Cancer Development via Modulating miR-124/STAT3 axis. *J. Cell Physiol* 233 (9), 6679–6688. doi:10.1002/jcp.26325

Lin, H., Hu, B., He, X., Mao, J., Wang, Y., Wang, J., et al. (2020). Overcoming Taxol-Resistance in A549 Cells: A Comprehensive Strategy of Targeting P-Gp Transporter, AKT/ERK Pathways, and Cytochrome P450 Enzyme CYP1B1 by 4-hydroxyemodin. *Biochem. Pharmacol.* 171, 113733. doi:10.1016/j.bcp.2019.113733

Lin, R., Maeda, S., Liu, C., Karin, M., and Edgington, T. S. (2007). A Large Noncoding RNA Is a Marker for Murine Hepatocellular Carcinomas and a Spectrum of Human Carcinomas. *Oncogene* 26 (6), 851–858. doi:10.1038/sj.onc.1209846

Liu, X., Ouyang, S., Yu, B., Liu, Y., Huang, K., Gong, J., et al. (2010). PharmMapper Server: a Web Server for Potential Drug Target Identification Using Pharmacophore Mapping Approach. *Nucleic Acids Res.* 38 (Suppl. l_2), W609–W614. doi:10.1093/nar/gkq300

Luo, F., Liu, X., Ling, M., Lu, L., Shi, L., Lu, X., et al. (2016). The lncRNA MALAT1, Acting through HIF-1α Stabilization, Enhances Arsenite-Induced Glycolysis in Human Hepatic L-02 Cells. *Biochim. Biophys. Acta* 1862 (9), 1685–1695. doi:10.1016/j.bbadis.2016.06.004

Ma, B., Simala-Grant, J. L., and Taylor, D. E. (2006). Fucosylation in Prokaryotes and Eukaryotes. *Glycobiology* 16 (12), 158R–184R. doi:10.1093/glycob/cwl040

Maryam, A., Mehmood, T., Zhang, H., Li, Y., Khan, M., and Ma, T. (2017). Alantolactone Induces Apoptosis, Promotes STAT3 Glutathionylation and Enhances Chemosensitivity of A549 Lung Adenocarcinoma Cells to Doxorubicin via Oxidative Stress. *Sci. Rep.* 7 (1), 1–18. doi:10.1038/s41598-017-06535-y

Michalik, K. M., You, X., Manavski, Y., Doddaballapur, A., Zörnig, M., Braun, T., et al. (2014). Long Noncoding RNA MALAT1 Regulates Endothelial Cell Function and Vessel Growth. *Circ. Res.* 114 (9), 1389–1397. doi:10.1161/CIRCRESAHA.114.303265

Missiuro, P. V., Liu, K., Zou, L., Ross, B. C., Zhao, G., Liu, J. S., et al. (2009). Information Flow Analysis of Interactome Networks. *Plos Comput. Biol.* 5 (4), e1000350. doi:10.1371/journal.pcbi.1000350

Nanayakkara, A. K., Follit, C. A., Chen, G., Williams, N. S., Vogel, P. D., and Wise, J. G. (2018). Targeted Inhibitors of P-Glycoprotein Increase Chemotherapeutic-Induced Mortality of Multidrug Resistant Tumor Cells. *Sci. Rep.* 8 (1), 967. doi:10.1038/s41598-018-19325-x

Pettersen, E. F., Goddard, T. D., Huang, C. C., Couch, G. S., Greenblatt, D. M., Meng, E. C., et al. (2004). UCSF Chimera-Aa Visualization System for Exploratory Research and Analysis. *J. Comput. Chem.* 25 (13), 1605–1612. doi:10.1002/jcc.20084

Phan, A. N. H., Hua, T. N. M., Kim, M.-K., Vo, V. T. A., Choi, J.-W., Kim, H.-W., et al. (2016). Gallic Acid Inhibition of Src-Stat3 Signaling Overcomes Acquired Resistance to EGF Receptor Tyrosine Kinase Inhibitors in Advanced Non-small Cell Lung Cancer. *Oncotarget* 7 (34), 54702–54713. doi:10.18632/oncotarget.10581

Pilkington, G., Boland, A., Brown, T., Oyee, J., Bagust, A., and Dickson, R. (2015). A Systematic Review of the Clinical Effectiveness of First-Line Chemotherapy for Adult Patients with Locally Advanced or Metastatic Non-small Cell Lung Cancer. *Thorax* 70 (4), 359–367. doi:10.1136/thoraxjnl-2014-205914

Qi, Y., Ooi, H. S., Wu, J., Chen, J., Zhang, X., Tan, S., et al. (2016). MALAT1 Long ncRNA Promotes Gastric Cancer Metastasis by Suppressing PCDH10. *Oncotarget* 7 (11), 12693–12703. doi:10.18632/oncotarget.7281

Qu, L., Ding, J., Chen, C., Wu, Z. J., Liu, B., Gao, Y., et al. (2016). Exosome-transmitted lncARSR Promotes Sunitinib Resistance in Renal Cancer by Acting as a Competing Endogenous RNA. *Cancer cell* 29 (5), 653–668. doi:10.1016/j.ccell.2016.03.004

Rebucci, M., and Michiels, C. (2013). Molecular Aspects of Cancer Cell Resistance to Chemotherapy. *Biochem. Pharmacol.* 85 (9), 1219–1226. doi:10.1016/j.bcp.2013.02.017

Sakurai, T., Yada, N., Hagiwara, S., Arizumi, T., Minaga, K., Kamata, K., et al. (2017). Gankyrin Induces STAT3 Activation in Tumor Microenvironment and Sorafenib Resistance in Hepatocellular Carcinoma. *Cancer Sci.* 108 (10), 1996–2003. doi:10.1111/cas.13341

Saleem, M. Z., Nisar, M. A., Alshwmi, M., Din, S. R. U., Gamallat, Y., Khan, M., et al. (2020). Brevilin A Inhibits STAT3 Signaling and Induces ROS-dependent Apoptosis, Mitochondrial Stress and Endoplasmic Reticulum Stress in MCF-7 Breast Cancer Cells. *Onco Targets Ther.* 13, 435–450. doi:10.2147/OTT.S228702

Scheff, R. J., and Schneider, B. J. (2013). Non–Small-Cell Lung Cancer: Treatment of Late Stage Disease: Chemotherapeutics and New Frontiers. *Semin. Interv. Radiol.* 30, 191–198. doi:10.1055/s-0033-1342961

Sen, M., Joyce, S., Panahandeh, M., Li, C., Thomas, S. M., Maxwell, J., et al. (2012). Targeting Stat3 Abrogates EGFR Inhibitor Resistance in Cancer. *Clin. Cancer Res.* 18 (18), 4986–4996. doi:10.1158/1078-0432.ccr-12-0792

Sherman, B. T., and Lempicki, R. A. (2009). Systematic and Integrative Analysis of Large Gene Lists Using DAVID Bioinformatics Resources. *Nat. Protoc.* 4 (1), 44–57. doi:10.1038/nprot.2008.211

Siegel, R. L., Miller, K. D., and Jemal, A. (2017). Cancer Statistics, 2017. *CA: A Cancer J. Clinicians* 67 (1), 7–30. doi:10.3322/caac.21387

Suda, K., and Mitsudomi, T. (2015). Role of EGFR Mutations in Lung Cancers: Prognosis and Tumor Chemosensitivity. *Arch. Toxicol.* 89 (8), 1227–1240. doi:10.1007/s00204-015-1524-7

Tang, Y., Xiao, G., Chen, Y., and Deng, Y. (2018). LncRNA MALAT1 Promotes Migration and Invasion of Non-small-cell Lung Cancer by Targeting miR-206 and Activating Akt/mTOR Signaling. *Anti-Cancer Drugs* 29 (8), 725–735. doi:10.1097/cad.0000000000000650

Teng, J. F., Qin, D. L., Mei, Q. B., Qiu, W. Q., Pan, R., Xiong, R., et al. (2019). Polyphyllin VI, a Saponin from Trillium Tschonoskii Maxim. Induces Apoptotic and Autophagic Cell Death via the ROS Triggered mTOR Signaling Pathway in Non-small Cell Lung Cancer. *Pharmacol. Res.* 147, 104396. doi:10.1016/j.phrs.2019.104396

Timofeeva, O. A., Tarasova, N. I., Zhang, X., Chasovskikh, S., Cheema, A. K., Wang, H., et al. (2013). STAT3 Suppresses Transcription of Proapoptotic Genes in Cancer Cells with the Involvement of its N-Terminal Domain. *Proc. Natl. Acad. Sci. U S A.* 110 (4), 1267–1272. doi:10.1073/pnas.1211805110

Wakelee, H., Kelly, K., and Edelman, M. J. (2014). 50 Years of Progress in the Systemic Therapy of Non-small Cell Lung Cancer. *Am. Soc. Clin. Oncol. Educ. Book* 34 (1), 177–189. doi:10.14694/EdBook_AM.2014.34.177

Wang, R., Lu, X., and Yu, R. (2020a). lncRNA MALAT1 Promotes EMT Process and Cisplatin Resistance of Oral Squamous Cell Carcinoma via PI3K/AKT/m-TOR Signal Pathway. *Onco Targets Ther.* 13, 4049–4061. doi:10.2147/ott.s251518

Wang, Z., Chang, X., Zhu, G., Gao, X., and Chang, L. (2020b). Depletion of lncRNA MALAT1 Inhibited Sunitinib Resistance through Regulating miR-362-3p-Mediated G3BP1 in Renal Cell Carcinoma. *Cell Cycle* 19 (16), 2054–2062. doi:10.1080/15384101.2020.1792667

Wedge, D. E., Galindo, J. C. G., and Macı´as, F. A. (2000). Fungicidal Activity of Natural and Synthetic Sesquiterpene Lactone Analogs. *Phytochemistry* 53 (7), 747–757. doi:10.1016/S0031-9422(00)00008-X

Wu, K., Chang, Q., Lu, Y., Qiu, P., Chen, B., Thakur, C., et al. (2013). Gefitinib Resistance Resulted from STAT3-Mediated Akt Activation in Lung Cancer Cells. *Oncotarget* 4 (12), 2430–2438. doi:10.18632/oncotarget.1431

Xu, J., Xiao, Y., Liu, B., Pan, S., Liu, Q., Shan, Y., et al. (2020). Exosomal MALAT1 Sponges miR-26a/26b to Promote the Invasion and Metastasis of Colorectal Cancer via FUT4 Enhanced Fucosylation and PI3K/Akt Pathway. *J. Exp. Clin. Cancer Res.* 39 (1), 54. doi:10.1186/s13046-020-01562-6

Xue, D., Lu, H., Xu, H. Y., Zhou, C. X., and He, X. Z. (2018). Long Noncoding RNA MALAT1 Enhances the Docetaxel Resistance of Prostate Cancer Cells via miR-145-5p-Mediated Regulation of AKAP12. *J. Cell Mol Med* 22 (6), 3223–3237. doi:10.1111/jcmm.13604

Yang, Q., Chen, W., Xu, Y., Lv, X., Zhang, M., and Jiang, H. (2018). Polyphyllin I Modulates MALAT1/STAT3 Signaling to Induce Apoptosis in Gefitinib-Resistant Non-small Cell Lung Cancer. *Toxicol. Appl. Pharmacol.* 356, 1–7. doi:10.1016/j.taap.2018.07.031

Yang, Z., Lasker, K., Schneidman-Duhovny, D., Webb, B., Huang, C. C., Pettersen, E. F., et al. (2012). UCSF Chimera, MODELLER, and IMP: an Integrated Modeling System. *J. Struct. Biol.* 179 (3), 269–278. doi:10.1016/j.jsb.2011.09.006

Yao, J., Wang, X. Q., Li, Y. J., Shan, K., Yang, H., Wang, Y. N., et al. (2016). Long Non-coding RNA MALAT1 Regulates Retinal Neurodegeneration through CREB Signaling. *EMBO Mol. Med.* 8 (4), 1113–1362. doi:10.15252/emmm.201606749

YiRen, H., YingCong, Y., Sunwu, Y., Keqin, L., Xiaochun, T., Senrui, C., et al. (2017). Long Noncoding RNA MALAT1 Regulates Autophagy Associated Chemoresistance via miR-23b-3p Sequestration in Gastric Cancer. *Mol. Cancer* 16 (1), 1–12. doi:10.1186/s12943-017-0743-3

Yuan, H., Sun, B., Gao, F., and Lan, M. (2016a). Synergistic Anticancer Effects of Andrographolide and Paclitaxel against A549 NSCLC Cells. *Pharm. Biol.* 54 (11), 2629–2635. doi:10.1080/13880209.2016.1176056

Yuan, J., Xu, X. J., Lin, Y., Chen, Q. Y., Sun, W. J., Tang, L., et al. (2019). LncRNA MALAT1 Expression Inhibition Suppresses Tongue Squamous Cell Carcinoma Proliferation, Migration and Invasion by Inactivating PI3K/Akt Pathway and Downregulating MMP-9 Expression. *Eur. Rev. Med. Pharmacol. Sci.* 23 (1), 198–206. doi:10.26355/eurrev_201901_16765

Yuan, P., Cao, W., Zang, Q., Li, G., Guo, X., and Fan, J. (2016b). The HIF-2α-MALAT1-miR-216b axis Regulates Multi-Drug Resistance of Hepatocellular Carcinoma Cells via Modulating Autophagy. *Biochem. Biophys. Res. Commun.* 478 (3), 1067–1073. doi:10.1016/j.bbrc.2016.08.065

Yue, X., Wu, W.-y., Dong, M., and Guo, M. (2020). LncRNA MALAT1 Promotes Breast Cancer Progression and Doxorubicin Resistance via Regulating miR-570–3p. *Biomed. J.* doi:10.1016/j.bj.2020.11.002

Zeng, H., Zheng, R., Guo, Y., Zhang, S., Zou, X., Wang, N., et al. (2015). Cancer Survival in China, 2003-2005: a Population-Based Study. *Int. J. Cancer* 136 (8), 1921–1930. doi:10.1002/ijc.29227

Zhao, P., Pan, Z., Luo, Y., Zhang, L., Li, X., Zhang, G., et al. (2015). Alantolactone Induces Apoptosis and Cell Cycle Arrest on Lung Squamous Cancer SK-MES-1 Cells. *J. Biochem. Mol. Toxicol.* 29 (5), 199–206. doi:10.1002/jbt.21685

Zheng, Y., Ma, L., and Sun, Q. (2021). Clinically-Relevant ABC Transporter for Anti-cancer Drug Resistance. *Front. Pharmacol.* 12 (705). doi:10.3389/fphar.2021.648407

Zhou, G.-H., Lu, Y.-Y., Xie, J.-L., Gao, Z.-K., Wu, X.-B., Yao, W.-S., et al. (2019). Overexpression of miR-758 Inhibited Proliferation, Migration, Invasion, and Promoted Apoptosis of Non-small Cell Lung Cancer Cells by Negatively Regulating HMGB. *Biosci. Rep.* 39 (1), BSR20180855. doi:10.1042/bsr20180855

Conflict of Interest: The authors declare that the research was conducted in the absence of any commercial or financial relationships that could be construed as a potential conflict of interest.

Publisher's Note: All claims expressed in this article are solely those of the authors and do not necessarily represent those of their affiliated organizations, or those of the publisher, the editors and the reviewers. Any product that may be evaluated in this article, or claim that may be made by its manufacturer, is not guaranteed or endorsed by the publisher.

Copyright © 2022 Ding, Zhen, Nisar, Ali, Din, Khan, Mughal, Alam, Liu and Saleem. This is an open-access article distributed under the terms of the Creative Commons Attribution License (CC BY). The use, distribution or reproduction in other forums is permitted, provided the original author(s) and the copyright owner(s) are credited and that the original publication in this journal is cited, in accordance with accepted academic practice. No use, distribution or reproduction is permitted which does not comply with these terms.

frontiers in Pharmacology

ORIGINAL RESEARCH
published: 25 February 2022
doi: 10.3389/fphar.2022.824652

Curcumin-Loaded mPEG-PLGA Nanoparticles Attenuates the Apoptosis and Corticosteroid Resistance Induced by Cigarette Smoke Extract

Xi Chen[1†], Di Wang[2†], Xuejun Guo[1], Xiaoming Li[1], Wenjing Ye[1], Yang Qi[3] and Wen Gu[1]**

[1]Department of Respirology Medicine, Xinhua Hospital, School of Medicine, Shanghai Jiaotong University, Shanghai, China, [2]Department of Intensive Care Medicine, The First Affiliated Hospital of USTC, Division of Life Sciences and Medicine, University of Science and Technology of China, Hefei, China, [3]Department of Pharmacy, No. 900 Hospital of the Chinese PLA Joint Support Forces, Fuzhou, China

OPEN ACCESS

Edited by:
Hong Zhang,
Shanghai University of Traditional Chinese Medicine, China

Reviewed by:
Jing Zhang,
Zhongshan Hospital, Fudan University, China
Wei Dong Chen,
Anhui University of Chinese Medicine, China
Guowei Wang,
Southwest University, China

***Correspondence:**
Yang Qi
qyangangle@sina.com
Wen Gu
guwen@xinhuamed.com.cn

[†]These authors have contributed equally to this work

Specialty section:
This article was submitted to Ethnopharmacology, a section of the journal Frontiers in Pharmacology

Received: 29 November 2021
Accepted: 07 February 2022
Published: 25 February 2022

Citation:
Chen X, Wang D, Guo X, Li X, Ye W, Qi Y and Gu W (2022) Curcumin-Loaded mPEG-PLGA Nanoparticles Attenuates the Apoptosis and Corticosteroid Resistance Induced by Cigarette Smoke Extract. Front. Pharmacol. 13:824652. doi: 10.3389/fphar.2022.824652

The present study was aim to prepare curcumin-loaded methoxypolyethylene-glycols-poly (lactic-co-glycolic acid) nanoparticles (Cur-mPEG-PLGA-NPs) and investigate curcumin's effect on reversing corticosteroid resistance induced by cigarette smoke extract (CSE) in rat tracheal epithelial (RTE) cells. The Cur-mPEG-PLGA-NPs were spherical, regular in shape with smooth surfaces, and well distributed and Cur-mPEG-PLGA-NP suspensions had good water solubility and presented prolonged release. Furthermore, we found that Cur-mPEG-PLGA-NPs were internalized more than curcumin into the cells and significantly alleviated apoptosis in RTE cells. In addition, 10% CSE reduced the maximal inhibition percentage and increased the half-inhibitory concentration of budesonide (BUD) on IL-8 secretion, and curcumin restored the efficacy of BUD inhibition. BUD in combination with Cur-mPEG-PLGA-NPs showed higher inhibitory rates for LPS- and CSE-induced IL-8 secretion than that in combination with curcumin. Moverover, the relative expression levels of HDAC2 was reduced after CSE exposure and curcumin could improve HDAC2 expression and reverse CSE-induced corticosteroid resistance. Curcumin in high concentration and Cur-mPEG-PLGA-NPs restored HDAC2 levels in RTE cells and thus Cur-mPEG-PCL-NPs have higher biological activity than curcumin.

Keywords: curcumin, chronic obstructive pulmonary disease, apotosis, IL-8, HDAC2

INTRODUCTION

Chronic obstructive pulmonary disease (COPD) is characterized by lung inflammation, airflow obstruction, and tissue destruction (Ito et al., 2005; Zhang et al., 2020). COPD is an aging disease with high prevalence and mortality. The aging of an ever-expanding world population, air pollution in the developing world, and high rates of smoking ensure that COPD will remain a global challenge in the 21st century (Lopez-Campos et al., 2016).The current drug management of COPD includes bronchodilators (muscarinic receptor antagonists and β2-agonists) associated with inhaled corticosteroids (ICSs), especially in patients with frequent exacerbations or severe COPD. However, in contrast to asthmatic patients, COPD patients are low and unresponsive to even

high doses of ICSs. ICSs have less effect on controlling the decline in lung function and suppressing chronic inflammation, leading to the development of corticosteroid resistance (Jiang and Zhu, 2016).

The molecular mechanisms of corticosteroid resistance in COPD are better understood now. A balance between histone acetyltransferase (HAT) and histone deacetylase (HDAC) is crucial for a normal inflammation reaction and effective inflammation suppression, and HDAC2-activity decrease is a contributing factor in corticosteroid resistance (Lai et al., 2018). In pro-inflammatory responses, activated NF-kappaB forms a protein complex with HAT, leading to histone acetylation and pro-inflammatory gene transcription. GR-alpha, one of 2 GR isoforms, can increase HDAC2 recruitment, resulting in deacetylation of histones in the promoter region of key pro-inflammatory cytokines, leading to inhibition of inflammation (Barnes, 2013b). Hence, modulating the activity of HDAC2 is a potential therapeutic approach to overcome corticosteroid resistance.

A variety of reagents such as phosphoinositide-3-kinase (PI3K) inhibitors and sulforaphane have been demonstrated to improve corticosteroid sensitivity by restoring the activity and expression of HDAC2 (Chen et al., 2012; Barnes, 2013a) . However, these agents are liable to cause systemic side effects and have a narrow therapeutic index. Therefore, developing drugs with only minor side effects and an ability to regulate HDAC2 activity has recently become the research focus for the reversal of corticosteroid resistance.

Curcumin (Cur), derived from the plant *Curcuma longa*, is used as a medicinal agent in many parts of the world, especially the Indian subcontinent. It has been reported that curcumin can restore HDAC2 protein levels by scavenging oxygen free radicals induced by cigarette smoke extract (CSE) and, hence, reverse corticosteroid resistance (Soflaei et al., 2018). Curcumin modulates the histone acetylation and deacetylation process in the promoter region of the pro-inflammatory cytokine gene, leading to reversal of corticosteroid resistance in type II alveolar epithelial cells (Ito et al., 2006). In addition, curcumin has the therapeutic potential to reverse corticosteroid resistance in COPD patients (Osoata et al., 2009). Curcumin has been extensively studied owing to its wide range of biological activities, which include anti-inflammatory, anti-infective, anti-arthritic, anti-cancer, and wound-healing potentials. Nevertheless, the clinical application of curcumin is limited, owing to its poor aqueous solubility, chemical instability, low oral bioavailability, inadequate absorption, rapid metabolism and elimination, and transmembrane permeation (To et al., 2010).

In recent years, nanotechnology-based delivery systems have been developed to overcome the pharmaceutical issues related to the delivery of therapeutic agents. Advantages such as avoiding enzymatic degradation of drugs, providing controlled release of therapeutic payloads, enhancing water solubility, improving cellular uptake, and optimizing target-specific delivery have made nanoparticles widely recognized (Umerska et al., 2018). At present, nanotechnology-based delivery carriers include liposomes, polymeric NPs, nanocomposite hydrogels, nanohybrid scaffolds, solid lipid nanoparticles, nanostructured lipid carriers, and nanofibers (Mohanty and Sahoo, 2010; Ungaro et al., 2012). Polymeric NPs have received extensive attention owing to some distinct properties, such as their ultra-small size, high encapsulation efficiency, adequate surface potential, biodegradability, and bio-compatibility (Zhang et al., 2014). Many studies have demonstrated that polymeric NPs can overcome the physical and chemical shortcomings of curcumin and improve its bioavailability. A polymeric NP delivery system improves the anti-oxidant, anti-inflammatory, and anti-tumor performance of curcumin (Yang et al., 2007). In addition, application of curcumin polymeric NPs as complementary agents is perfect for reducing the dose of the main therapeutic agent, resulting in enhanced therapeutic efficacy while reducing systemic toxicity (Umerska et al., 2018).

Therefore, we prepared Cur-mPEG-PLGA-NPs via emulsion solvent evaporation, to overcome the physical and chemical disadvantages of curcumin and improve its therapeutic activity. In addition, the effect of curcumin on reversing corticosteroid resistance induced by CSE was also investigated and biological activities between curcumin and Cur-mPEG-PLGA-NPs were investigated.

MATERIALS AND METHODS

Reagents and Materials

mPEG-PLGA (PLGA, DL-lactide-co-glycolide, 50/50 Poly, MW 20 kDa; mPEG, MW 2 kDa) was purchased from Daigang Biological Science and Technology Co.,, Ltd., (Shandong, China). Curcumin (purity ≥98%) and vitamin E-TPGS were purchased from Aladdin Industrial Corporation (Shanghai, China). Acetone and tetrahydrofuran (THF) were purchased from Sinopharm Chemical Reagent Co., Ltd., (Shanghai, China). Rat tracheal epithelial (RTE) cells were purchased from the Cell Culture Center of the Chinese Academy of Medical Sciences (Beijing, China). Budesonide (BUD) was purchased from AstraZeneca PLC (London, United Kingdom). β-actin (catalog #4970) antibody and HDAC Antibody Sampler Kit (catalog#9928) were bought from Cell Signaling Technology (Beverly, MA, United States).

Preparation of Nanoparticles

mPEG-PLGA nanoparticles containing curcumin (Cur-mPEG-PLGA-NPs) were synthesized via the emulsion solvent evaporation method. At room temperature, 30 mg mPEG-PLGA and 1 mg curcumin were dissolved in 3 ml acetone-ethanol solvent (volume ratio 1:1) to form an organic phase. The organic phase was slowly dropped into the PVA solution under magnetic stirring (300 rpm), which was continued for 5 min, to form a nanoparticle suspension. The acetone-ethanol solvent was removed via vacuum rotary evaporation for 40 min, and large particles were removed via centrifugation at 2000 rpm for 20 min. The nanoparticles were precipitated via centrifugation at 12,000 rpm for 30 min, and the supernatant was discarded to remove residual PVA and mPEG-PLGA. The residue was the colloidal suspension of Cur-mPEG-PLGA-NPs.

Characterization of Nanoparticles

The absorption wavelength of curcumin and standard curve of curcumin concentration were defined. mPEG-PLGA and curcumin were dissolved in THF, and then scanned using a Dinuolitai UV-Vis3000 spectrophotometer (Shanghai, China) in the wavelength of 200–600 nm with blank solvent as the reference. A standard curve correlating absorbance at 423 nm with the concentration of curcumin was created. The standard curve equation was used to calculate the concentration of curcumin or curcumin loaded into mPEG-PLGA nanoparticles in following studies.

Weight of drug feeded (Wt) was obtained by measuring total curcumin in a nanoparticle suspension. Another nanoparticle suspension was accelerated freezing centrifuged for 40 min at 20,000 rpm and weight of drug free (Wf) was obtained by measuring curcumin in the supernatant. Weight of feeding polymer and drug (Ws) was the total amount of drug and carrier added to the preparation. Encapsulation efficiency (EE) = (Wt − Wf)/Wt; drug loading (DL) = (Wt − Wf)/Ws.

The size distribution spectra, zeta potential, and morphology were determined using a HORIBA LB550 laser scattering particle size analyzer (Japan), Malvin zeta potentiometer (Malvern, United Kingdom), and transmission electron microscope (TEM), respectively.

In vitro Release of Curcumin From Nanoparticles

The *in vitro* drug release behavior of Cur-mPEG-PLGA-NPs was determined using the dynamic dialysis method. A nanoparticle suspension was loaded into a pre dialysis bag, both ends of which were clamped. Then, the bag was hung in a brown bottle containing 200 ml 0.5% SDS in water solution at (37.0 ± 0.5)° C with gentle shaking. At specific time points, 4 ml samples were collected, and 4 ml release medium was added. SDS in water solution (0.5%) was used as the blank control, and curcumin absorbance was measured at 423 nm. The concentration of curcumin was calculated according to the standard curve, and the cumulative drug release rate was determined.

Analysis of Cytotoxicity, Apoptosis and LDH Release Assay

The RTE cell line, obtained from GuangZhou Jennio Biotech Co., Ltd., was cultured in minimal essential medium with Earle's salts (MEM-EBSS, Life Technologies) supplemented with 20% fetal calf serum (HyClone; Thermo Scientific), 100 U/mL penicillin, and 100 mg/ml streptomycin in a 5% CO_2 humidified atmosphere at 37°C. RTE cells in the logarithmic growth phase were inoculated into a 96-well plate at a density of 5×10^3 cells/well and cultured for 24 h. Cells were then treated with curcumin of different concentrations (5 μM, 10 μM, 15 μM, 20 μM, 25 μM) or Cur-mPEG-PLGA-NPs (at doses equivalent to the concentration gradients of curcumin) and sequentially cultured for 48 h. The cell viability rate was determined by CCK8 assay according to the recommended protocol (Promega). After digestion with trypsin, the cells were collected, washed with PBS and resuspended by 1× Binding buffer. Annexin V-FITC and solution were added and react at room temperature for 15 min, then detected by flow cytometry (FACSCalibur, BD) within 1 h. LDH assay was performed by a commercial kit (Promega, Madison, WI, United States) according to the manufacturer's protocol.

Quantitative Cellular Uptake Study

The cellular uptake of curcumin and Cur-mPEG-PLGA-NPs was determined by following the method of Chandana et al. (Prasad et al., 2014). RTE cells were inoculated into 24-well plates at densities of 5×10^4 cells/well in 1 ml growth medium. The cells were incubated for 24 h at 37°C for adhesion. Then, the cells were treated with curcumin (100 nM) and Cur-mPEG-PLGA-NPs at a dose equivalent. After being incubated for different periods, the cells were washed twice with PBS to remove free drug molecules. Subsequently, the cells were lysed with methanol. The cell lysates were centrifuged at 10,000 rpm for 20 min at 4°C. Absorbance of curcumin in the supernatant of the two groups was measured and curcumin content was calculated.

Qualitative Cellular Uptake Study

The qualitative uptake of curcumin and Cur-mPEG-PLGA-NPs in RTE cells was detected by confocal microscopy. Cells were inoculated in a petri dish at a density of 1×10^4 cells/well and cultured for 24 h. Then, the cells were treated with curcumin (100 nM) and Cur-mPEG-PLGA-NPs at a dose equivalent and incubated at 37°C for different periods (2, 6, and 12 h). After incubation, the cells were fixed with 2% paraformaldehyde PBS solution for 10 min. Then, the cells were washed three times by physiological saline. Fluorescence from curcumin and curcumin loaded into mPEG-PLGA nanoparticles that entered into cells was observed using a fluorescence and light microscope with an argon laser (Olympus IX71; Olympus Corporation, Tokyo, Japan).

Preparation of Cigarette Smoke Extract Solutions

Smoke from 1 cigarette was dissolved in 10 ml medium under negative pressure in 2 min. Subsequently, the medium was filtered through a 0.22 μm membrane, and then used as a 100% smoke extract solution (100% CSE). The CSE preparation was standardized by measuring its absorbance at 320 nm, which showed very little variation between different preparations of CSE. CSE was freshly prepared for each experiment and diluted with culture medium.

Cell Stimulation, Intervention, and Inflammatory Mediators Assay

RTE cells in the logarithmic phase were inoculated into a 6-well plate at 2×10^4 cells/well. After cell adhesion was completed, medium containing 1% FBS was used for 12 h to starve cells. Then, the cells were treated with different concentration BUD, curcumin, or curcumin + BUD for 15 min and subsequently treated with 1 μg/ml LPS and stimulated by 10% CSE for 4 h

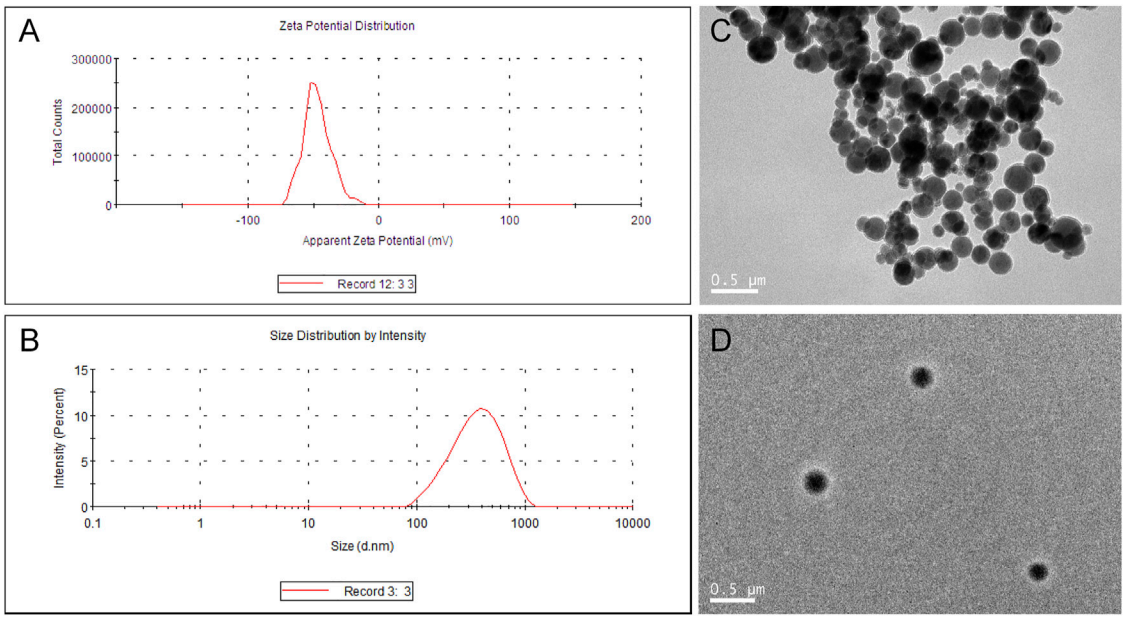


FIGURE 1 | (A) Mean particle size of Cur-mPEG-PLGA-NPs measured by a particle size analyzer. **(B)** Zeta potential of Cur-mPEG-PLGA-NPs measured by a Malvin zeta potentiometer. **(C,D)** Morphology of Cur-mPEG-PLGA-NPs measured by a transmission electron microscope.

before being treated by LPS. After the cells were incubated for 24 h, the supernatant was collected.

Another set of RTE cells was cultured by the above methods. The cells were treated by 100 nM curcumin + BUD or Cur-mPEG-PLGA-NPs (100 nM)+BUD for 15 min. Then, the cells were stimulated by 10% CES for 4 h, followed by stimulation by LPS. After the cells were incubated for 24 h, the supernatant was collected.

The cell supernatant was detected according to the operational guidelines provided by ELISA kit (eBioscience) according to the manufacturer's protocol. The inhibition rate and the half-inhibitory concentration (IC_{50}) of BUD on inhibiting IL-8 secretion were calculated.

Western Blot Analysis of HDACs

RTE cells were cultured according to the above methods. The cells were treated with BUD (100 nM), curcumin (100 nM), and Cur-mPEG-PLGA-NPs (100 nM) for 15 min and subsequently stimulated by 10% CSE. After incubation for 24 h, cells were collected and lysed by RIPA buffer. The total protein concentration of cell samples was measured by the Pierce BCA protein assay. The proteins were separated by electrophoresis on polyacrylamide gel, and then transferred to PVDF membranes. The PVDF membrane was incubated with primary antibody overnight at 4°C and secondary antibody for 120 min at room temperature. Semi-quantitative analysis was performed using ChemiDoc XRS gel imaging system (Bio-Rad, United States).

Statistical Analysis

Results were expressed as mean ± SEM from three independent experiments. The results were statistically evaluated using by one-way analysis of variance (ANOVA) followed by the Dunnett's test. A value of $p < 0.05$ indicates a significant difference.

RESULTS

Characteristics of Cur-NPs

Cur-mPEG-PLGA-NPs were synthesized with encapsulation efficiency of (83.05 + 1.07)% and drug loading rate of (10.87 + 0.58)%. The negative zeta potential and the average diameter of nanoparticles were −29.4 ± 5.47 mV (**Figure 1A**) and 376.3 ± 2.69 nm (**Figure 1B**), respectively. Moreover, the Cur-mPEG-PLGA-NPs were spherical, regular in shape with smooth surfaces, and well distributed (**Figures 1C,D**). Curcumin had maximum absorption at 400 nm, while mPEG-PLGA had little interference with the UV absorption of curcumin at this wavelength; therefore, the detection wavelength of curcumin was approximately 423 nm. Cur-mPEG-PLGA-NPs in distilled water exhibited a homogeneous suspension (**Figure 2B**); in contrast, curcumin was poorly soluble in distilled water (**Figure 2A**). As shown in **Figure 2C**, approximately (84.4 ± 3.58)% of the total curcumin was released in 7 days, showing a prolonged release behavior.

Cur and Cur-mPEG-PLGA-NPs Protected Against CSE-Induced Apoptosis

Accordingly, 20 μM and the concentration equivalent to 20 μM curcumin were chosen as the upper limit of the intervention concentrations of curcumin and Cur-mPEG-PLGA-NPs (**Figure 3A**). We next determined whether Cur and Cur-

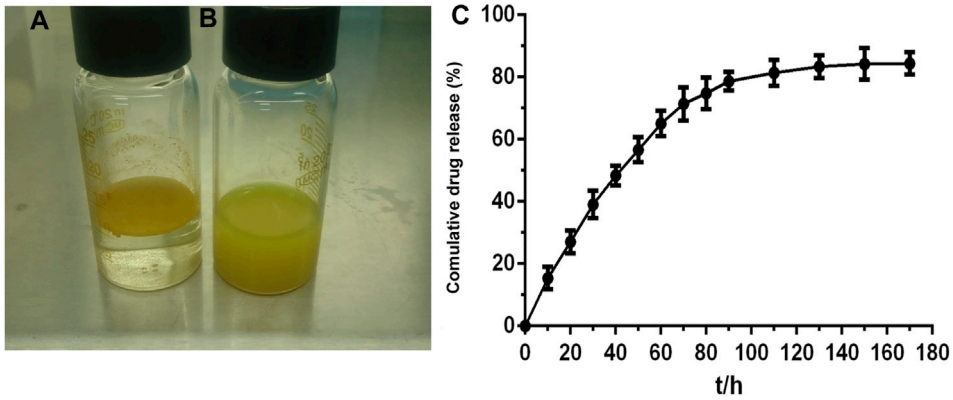


FIGURE 2 | (A) Cur (10 mg) dissolved in PBS (0.01 M, pH 7.4) was insoluble in aqueous solution. **(B)** Cur-mPEG-PLGA-NPs at a dose equivalent to 10 mg curcumin were dissolved in aqueous solution. **(C)** *In vitro* release profile of Cur in 0.5% SDS in water solution at (37.0 ± 0.5)°C from Cur- mPEG-PLGA-NPs.

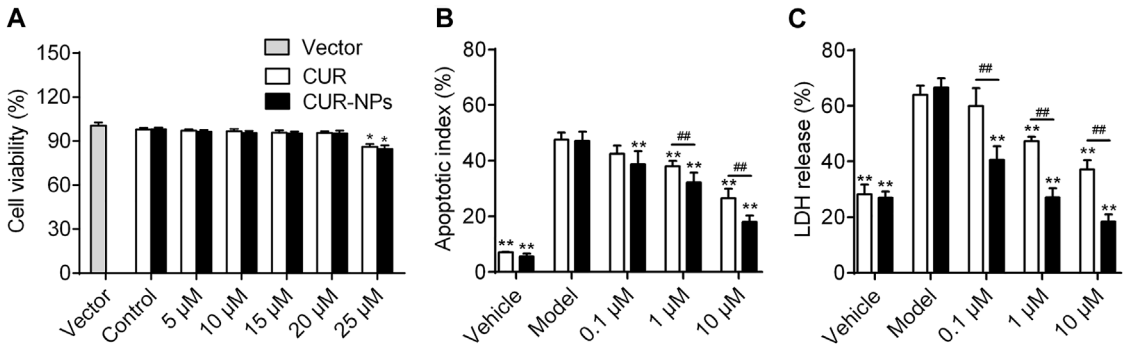


FIGURE 3 | Cur and Cur-mPEG-PLGA-NPs protected against CSE-induced cytotoxicity in RTE cells. **(A)** Viability of RTE cells with various concentrations of Cur and Cur-mPEG-PLGA-NPs for 48 h using a CCK8 bioassay. **(B)** Apoptosis assay of RTE cells exposed to CSE and different concentration administration of Cur or Cur-mPEG-PLGA-NPs were examined by flow cytometry. Cells were gated for an annexin V^+ (*x*-axis) versus PI^+ (*y*-axis) contour plot. **(C)** Cell cytotoxicity was determined by LDH activity. $^*p < 0.01$ and $^{**}p < 0.05$ related to the control group; $^{\#\#}p < 0.01$ compared to CUR group.

mPEG-PLGA-NPs could protect against CSE-induced apoptosis (**Figure 3B**). After the 10% CSE injure, RTE cells were suffered significantly apoptosis. Next, we found that Cur and Cur-mPEG-PLGA-NPs attenuated these apoptotic changes (**Figure 2B**).

Similar findings were also obtained with LDH release assays in RTE cells exposed to 10% CSE (**Figure 2C**). The data indicated that Cur and Cur-mPEG-PLGA-NPs protected against CSE-induced apoptosis.

Cellular Uptake of Curcumin Loaded in Nanoparticles

Our studies showed that curcumin loaded in mPEG-PLGA-NPs was internalized more than curcumin was in RTE cells (**Figure 4A**). The intracellular uptake of curcumin loaded in nanoparticles reached maximum at 4 h. In contrast, the intracellular uptake of curcumin reached maximum at 3 h. The highest cellular uptake of curcumin loaded in nanoparticles was nearly 3 times that of curcumin. Moreover, our results revealed an incubation time-dependent increase of intracellular fluorescence intensity of curcumin loaded in nanoparticles in RTE cells due to sustained release of encapsulated curcumin. In contrast, a decrease in fluorescence intensity was observed for curcumin, perhaps due to a loss of stability over time (**Figure 4B**).

Cur-mPEG-PLGA-NPs Inhibits LPS and CSE-Induced Inflammatory Mediators in RTE Cells

The levels of LPS and CSE-induced inflammatory mediators in RTE cells were detected by ELISA (**Figure 5**). We found that compared with the control group, the levels of TNF-α, MCP-1, MMP-9 and IL-8 in LPS + CSE group were significantly increased and Cur-mPEG-PLGA-NPs inhibits LPS and CSE-induced TNF-α, MCP-1 and IL-8 production in RTE Cells.

Effect of Curcumin on BUD Resistance Induced by CSE

In RTE cells, BUD concentration-dependently inhibited the secretion of IL-8 induced by LPS (**Figure 6A**; **Table 1**). In contrast, after being stimulated by LPS and 10% CSE, RTE

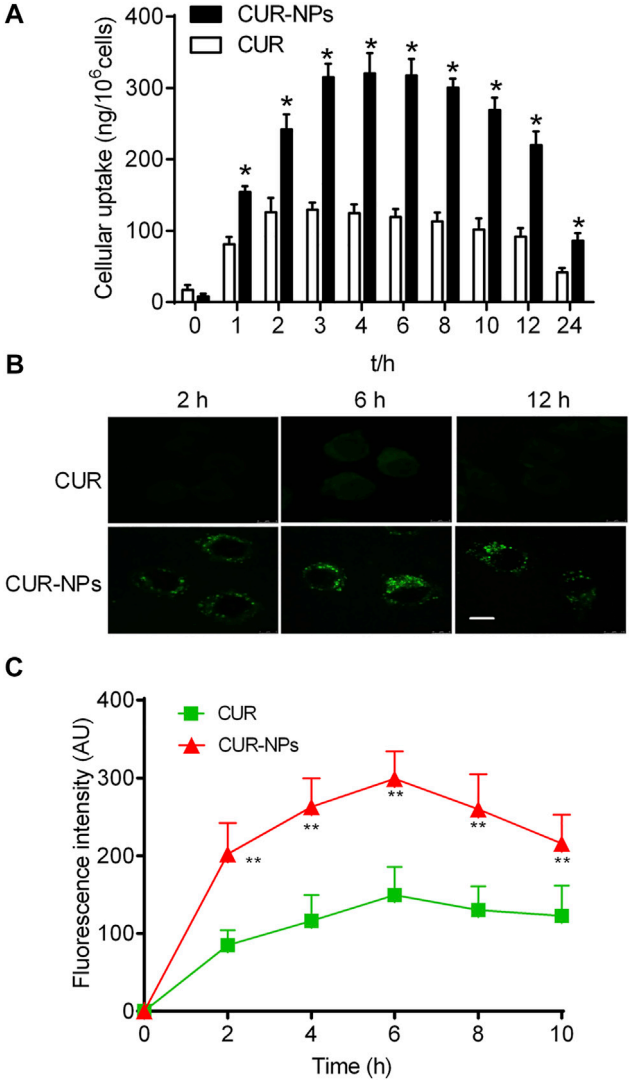


FIGURE 4 | Quantitative cellular uptake study of Cur and Cur-mPEG-PLGA-NPs for different periods on RTE cells **(A)**. **(B,C)** Confocal image showing time-dependent change in intracellular fluorescence intensity of Cur-mPEG-PLGA-NPs and Cur in RTE cells. Scale bar = 5 μm *$p < 0.05$ related to cells incubated with curcumin.

cells exhibited resistance to the anti-inflammatory effect of BUD (**Figure 6A**). The maximal inhibition percentage of BUD in RTE cells stimulated by LPS and 10% CSE was significantly lower than that in RTE cells stimulated by LPS alone. The half-inhibitory concentration of BUD showed a corresponding increase in RTE cells stimulated by LPS and 10% CSE (**Table 1**). The effect of curcumin on BUD resistance induced by 10% CSE was then investigated. Curcumin weakly reduced the LPS- and 10% CSE-induced IL-8 secretion (**Figure 6B**; **Table 1**). However, the combination of BUD and 100 nM curcumin achieved a higher maximum inhibition for LPS- and 10% CSE-induced IL-8 secretion than that for BUD alone (**Figure 6C**; **Table 1**). The half-inhibitory concentration of BUD in combination with curcumin was lower than that of BUD alone (**Table 1**).

Ability of Cur-mPEG-PLGA-NPs to Reverse Budesonide Resistance

The ability of curcumin and Cur-mPEG-PLGA-NPs to reverse budesonide resistance in RTE cells was compared. BUD in combination with Cur-mPEG-PLGA-NPs at doses equivalent to curcumin showed higher inhibitory rates for LPS- and 10% CSE-induced IL-8 secretion than that in combination with 100 nM curcumin (**Figure 6D**; **Table 2**). The obtained results demonstrated that curcumin loaded in nanoparticles was more effective in reversing budesonide resistance than curcumin.

Effect of Curcumin and Cur-mPEG-PLGA-NPs on Budesonide Resistant Markers Altered by Cigarette Smoke

In RTE cells, the effects of curcumin and Cur-mPEG-PLGA-NPs on HDACs were determined. Western blot analysis was employed to semi-quantitatively determine protein content levels of HDAC2. The results showed that 10% CSE exposure reduced HDAC2 protein levels, and curcumin and Cur-mPEG-PLGA-NPs restored HDAC2 levels in RTE cells (**Figure 7** and **Supplementary Material**). However, other HDAC members were not found to have a regulatory role in the CSE-mediated budesonide resistant in RTE cells. The results showed that curcumin was able to restore the expression level of HDAC2 and curcumin loaded in mPEG-PLGA-NPs was more effective than curcumin.

DISCUSSION

Inhaled corticosteroids (ICSs) have been widely used in the treatment of COPD and asthma. However, only 20–25% of severe COPD patients show effective responses to ICSs. In a large proportion of COPD patients, ICSs fail to control symptoms and prevent disease progression and are, therefore, challenged by corticosteroid resistance (Xie et al., 2011). It has been confirmed that reduced histone deacetylase (HDAC)-2 is a major contributor to corticosteroid resistance in COPD patients (Tsai et al., 2012). HDAC2 has the ability to promote histone deacetylation in target gene promoter regions and decrease pro-inflammatory gene transcriptional activity, such as TNF-alpha, IL-8, and IL-1 beta (Ghalandarlaki et al., 2014). In the anti-inflammatory process of corticosteroids, HDAC2 is recruited by activated GR to the promoter region of pro-inflammatory genes and switches off the transcription process (Zhang et al., 2013).

A body of evidence has indicated a decrease in HDAC2 activity in the alveolar macrophages of smokers and patients with COPD, and it is related to disease severity and exacerbation. For example, an *in vitro* study indicated that CSE exposure reduced HDAC2 expression and increased pro-inflammatory cytokine expression, such as IL-8 and TNF-alpha, in human macrophages (Adenuga et al., 2009). In peripheral blood mononuclear cells of patients with COPD and smokers, HDAC activities were decreased and negatively correlated to serum IL-8 levels (Meja et al., 2008).

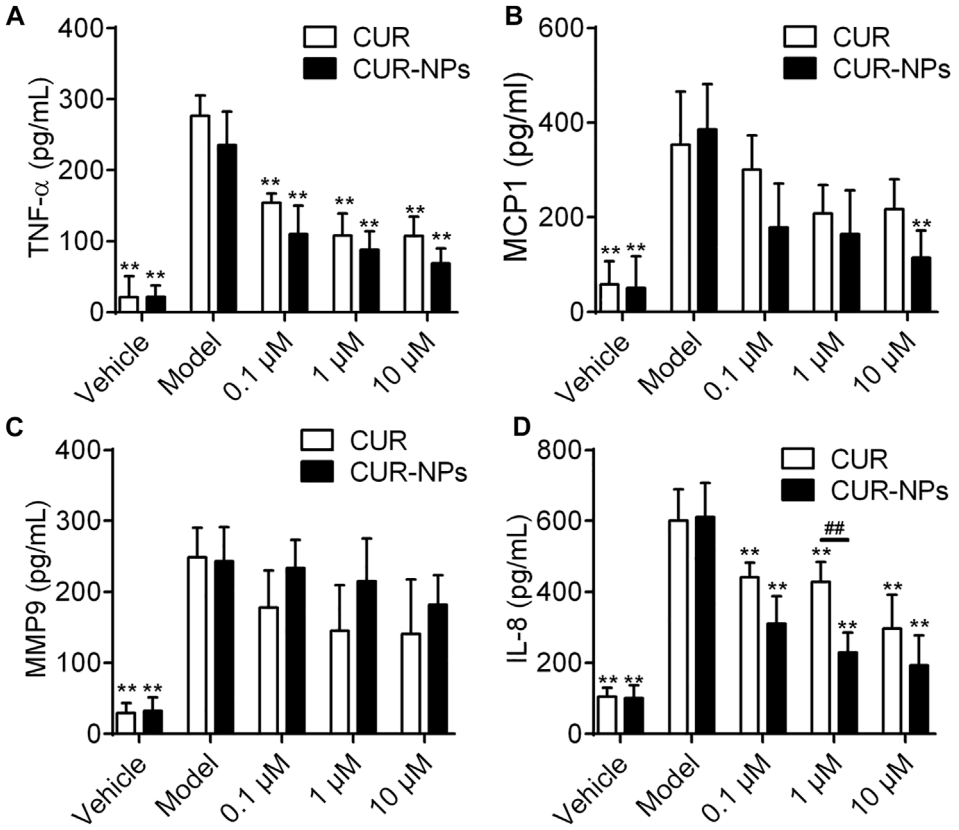


FIGURE 5 | Effect of Cur and Cur-mPEG-PLGA-NPs on the production of TNF-α **(A)**, MCP-1 **(B)**, MMP-9 **(C)** and IL-8 **(D)** in CSE-injured RTE cells. RTE cells were treated with 0.1, 1, 10 μM Cur or Cur-mPEG-PLGA-NPs for 2 h, then stimulated with 10% CSE, the supernatants were collected for the assay. $^{\#\#}p < 0.01$ versus curcumin group, $^{**}p < 0.01$ versus model group.

Another study confirmed that the messenger RNA (mRNA) and protein expressions of HDAC2 were also significantly lower in COPD patients and that the reduction in HDAC2 activity correlated with the severity of COPD disease (Lao et al., 2006).

The present study revealed that 10% CSE exposure reduced the level of HDAC2 protein in RTE cells. Consequently, the potency (maximum inhibitory percentage) and efficacy (median effective concentration) of BUD inhibiting IL-8 release were reduced in RTE cells incubated with10% CSE and LPS. Curcumin showed a relatively weak inhibitory effect on IL-8 induced by LPS and 10% CSE in RTE cells. However, by increasing HDAC2 levels, curcumin restored the diminished capacity of BUD to inhibit IL-8 release. These findings suggested that curcumin might reverse the 10% CSE-induced corticosteroid resistance by maintaining the level of HDAC2 protein.

A body of evidence indicates that curcumin has shown great therapeutic benefits in various diseases, including inflammatory disorders, cardiovascular disease, cancer, and Alzheimer's disease. However, rapid metabolism and systemic clearance from the body contribute to low bioavailability of curcumin, limiting its clinical application. After 12 h of the oral administration of 10 g/d and 12 g/d curcumin in a healthy human, only μg/mL quantities of curcumin conjugates (curcumin glucuronides and sulfates) were found in the serum, and among the eight subjects of study, only one had detectable free curcumin in the serum (Anand et al., 2010).

Nanotechnology is a new field of interdisciplinary investigation, and has been widely used in the diagnosis and treatment of diseases (Saka and Chella, 2020). MPEG and PLGA are two biodegradable materials approved by the United Satates Food and Drug Administration for human use. Block copolymers formed by mPEG and PLGA are often used for the preparation of nanoparticles as drug carrier materials. Some studies have indicated that curcumin-loaded mPEG-PLGA nanoparticles are able to overcome the chemical and physical drawbacks of curcumin and improve its biological activity. Besides, after intravenous administrations *in vivo*, curcumin achieved maximum plasma concentration in 5 min, leading to a short elimination half-time of approximately 1.07 h. In contrast, curcumin delivered by curcumin nanoparticles achieved maximum plasma concentration in 2 h, resulting in a significant increase in t1/2 (of about six-fold) compared with that of curcumin. The results concluded that the curcumin-loaded nanoparticles presented a relative threefold higher bioavailability than that of curcumin. In this study, the cellular uptake of Cur-mPEG-PLGA-NPs and curcumin in RTE cells was quantitatively evaluated by fluorescence spectroscopy. The data

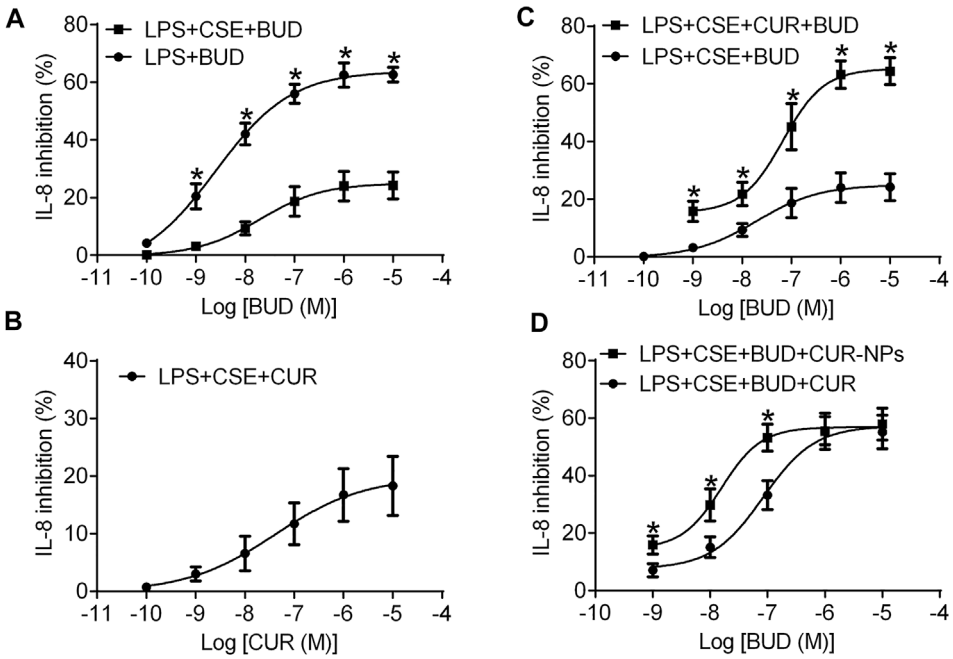


FIGURE 6 | Concentration dependent inhibitory effect of BUD or CUR on IL-8 release induced by LPS alone or in combination with CSE in RTE cells. **(A)** RTE cells were treated with BUD (10^{-10}–10^{-5} M) for 15 min and then stimulated with LPS (1 μg/ml) alone or in combination with 10% CSE. **(B)** RTE cells were treated with Cur and then stimulated with LPS (1 μg/ml) in combination with 10% CSE. **(C)** RTE cells were treated with BUD alone or in combination with Cur (100 nM) and then stimulated with LPS in combination with 10% CSE. Cell supernatants were collected after 24 h of cell stimulation and were used for IL-8 assays. *$p < 0.05$ related to cells incubated with BUD alone in the stimulation of CES and LPS. **(D)** Concentration dependent inhibitory effect of BUD in combination with CUR (100 nM) or Cur-mPEG-PLGA-NPs (equivalent to 100 nM CUR) on IL-8 release induced by LPS in combination with 10% CSE in RTE cells. *$p < 0.05$ related to cells incubated with BUD and CUR in the stimulation of CES and LPS.

TABLE 1 | Maximal efficacy and –log IC_{50} of BUD on IL-8 release.

B	RTE cells	
	Maximal inhibition (%)	**–log IC_{50}**
LPS + BUD	63.94 ± 1.48	8.60 ± 0.14
LPS + CSE + BUD	33.43 ± 1.24[a]	6.77 ± 0.08[a]
LPS + CSE + CUR + BUD	64.30 ± 1.74[b]	7.33 ± 0.10[b]

[a]*$p < 0.05$ related to cells incubated with BUD alone in the stimulation of LPS.*
[b]*$p < 0.05$ related to cells incubated with BUD alone in the stimulation of CES and LPS.*

TABLE 2 | Inhibitory effect of BUD in combination with CUR (100 nM) or Cur-mPEG-PLGA-NPs at a dose equivalent to 100 nM CUR on IL-8 release in RTE cells.

	Inhibition (%) of BUD (nM)		
	1	**10**	**100**
LPS + CSE + CUR	7.08 ± 2.25	15.08 ± 3.60	33.20 ± 5.06
LPS + CSE + CUR-NPS	15.92 ± 3.18[a]	29.82 ± 5.59[a]	53.26 ± 4.70[a]

[a]*$p < 0.05$ related to cells incubated with BUD and CUR (100 nM).*

demonstrated that the cellular uptake of curcumin-loaded mPEG-PLGA-NPs was statistically significantly higher than that of curcumin in RTE cells. This suggested that polymeric nanoparticles enhance the internalization and retention effects of curcumin. Then, the ability of Cur-mPEG-PLGA-NPs to restore corticosteroid-mediated inhibition on IL-8 was further studied. The data demonstrated that at low doses, BUD in combination with Cur-mPEG-PLGA-NPs represented higher inhibitory rates on IL-8 than that in combination with curcumin in RTE cells incubated with 10% CSE and LPS. These results were consistent with cellular uptake results and indicated that Cur-mPEG-PLGA-NPs offered higher bioavailability in reversing CSE-induced corticosteroid resistance. Further study intends to isolate and culture alveolar macrophages and airway epithelial cells from smoking COPD patients, smokers with normal lung function and normal controls, and use LPS stimulation to investigate the role of curcumin in reversing hormone resistance.

In summary, 10% CSE exposure reduced the potency and efficacy for BUD inhibiting IL-8 release in RTE cells, and induced corticosteroid resistance. Curcumin restored the diminished capacity of BUD to inhibit IL-8 release induced by LPS and 10% CSE. Curcumin loaded in mPEG-PLGA nanoparticles was uptaken more in RTE cells, and exhibited more effectiveness in reversing corticosteroid resistance than curcumin. All these findings indicate that Cur-mPEG-PLGA-NPs have great potential as a therapeutic agent. Both curcumin and Cur-mPEG-PLGA-NPs at high doses restored the decrease in HDAC2 levels caused by 10% CSE exposure. However, at relatively low doses, only Cur-mPEG-PLGA-NPs showed a

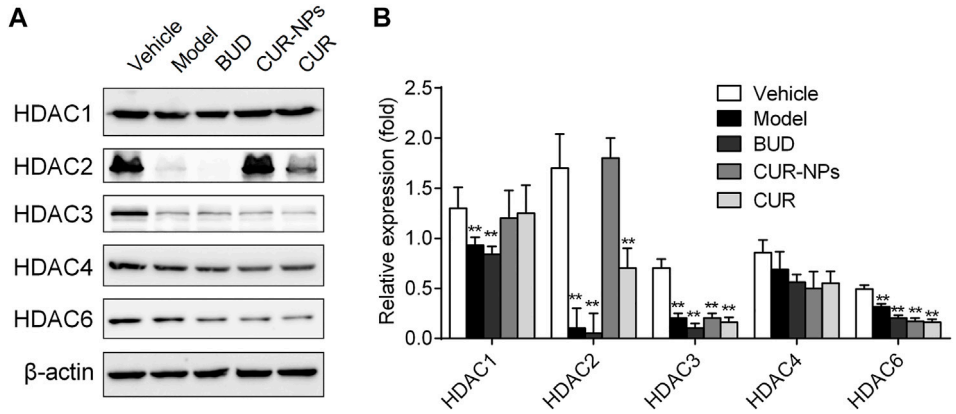


FIGURE 7 | Effects of CUR and Cur-mPEG-PLGA-NPs on HDACs level. **(A)** RTE cells were incubated with BUD (0.1 μM), Cur (1 μM), and Cur-mPEG-PLGA-NPs (equivalent to the concentrations of CUR) for 15 min and stimulated with 10% CSE. **(B)** HDACs levels were detected by western blotting. $^{**}p < 0.05$ related to CSE.

restoration effect on HDAC2 levels. This explains the greater efficacy of Cur-mPEG-PLGA-NPs in reversing corticosteroid resistance.

DATA AVAILABILITY STATEMENT

The raw data supporting the conclusion of this article will be made available by the authors, without undue reservation.

AUTHOR CONTRIBUTIONS

WG, XG, and XC designed research; DW, QY, and XL performed the experiments; WY analyzed data; and XC and DW wrote the manuscript.

FUNDING

This work was supported by the Youth Program of Natural Science Foundation of China (NO.81900017), the Natural Science Foundation of China (NO.81770023), the Natural Science Foundation of Fujian Province (2019J01529), the Startup Fund of Fujian Medical University (2018QH1233), and No. 900 Hospital of the Chinese PLA Joint Support Forces (2018Q03).

SUPPLEMENTARY MATERIAL

The Supplementary Material for this article can be found online at: https://www.frontiersin.org/articles/10.3389/fphar.2022.824652/full#supplementary-material

REFERENCES

Adenuga, D., Yao, H., March, T. H., Seagrave, J., and Rahman, I. (2009). Histone Deacetylase 2 Is Phosphorylated, Ubiquitinated, and Degraded by Cigarette Smoke. *Am. J. Respir. Cel Mol Biol* 40, 464–473. doi:10.1165/rcmb.2008-0255OC

Anand, P., Nair, H. B., Sung, B., Kunnumakkara, A. B., Yadav, V. R., Tekmal, R. R., et al. (2010). Design of Curcumin-Loaded PLGA Nanoparticles Formulation with Enhanced Cellular Uptake, and Increased Bioactivity *In Vitro* and superior Bioavailability *In Vivo*. *Biochem. Pharmacol.* 79, 330–338. doi:10.1016/j.bcp.2009.09.003

Barnes, P. J. (2013a). Corticosteroid Resistance in Patients with Asthma and Chronic Obstructive Pulmonary Disease. *J. Allergy Clin. Immunol.* 131, 636–645. doi:10.1016/j.jaci.2012.12.1564

Barnes, P. J. (2013b). New Anti-inflammatory Targets for Chronic Obstructive Pulmonary Disease. *Nat. Rev. Drug Discov.* 12, 543–559. doi:10.1038/nrd4025

Chen, Y., Huang, P., Ai, W., Li, X., Guo, W., Zhang, J., et al. (2012). Histone Deacetylase Activity Is Decreased in Peripheral Blood Monocytes in Patients with COPD. *J. Inflamm. (Lond)* 9, 10. doi:10.1186/1476-9255-9-10

Ghalandarlaki, N., Alizadeh, A. M., and Ashkani-Esfahani, S. (2014). Nanotechnology-applied Curcumin for Different Diseases Therapy. *Biomed. Res. Int.* 2014, 394264. doi:10.1155/2014/394264

Ito, K., Ito, M., Elliott, W. M., Cosio, B., Caramori, G., Kon, O. M., et al. (2005). Decreased Histone Deacetylase Activity in Chronic Obstructive Pulmonary Disease. *N. Engl. J. Med.* 352, 1967–1976. doi:10.1056/NEJMoa041892

Ito, K., Yamamura, S., Essilfie-Quaye, S., Cosio, B., Ito, M., Barnes, P. J., et al. (2006). Histone Deacetylase 2-mediated Deacetylation of the Glucocorticoid Receptor Enables NF-kappaB Suppression. *J. Exp. Med.* 203, 7–13. doi:10.1084/jem.20050466

Jiang, Z., and Zhu, L. (2016). Update on Molecular Mechanisms of Corticosteroid Resistance in Chronic Obstructive Pulmonary Disease. *Pulm. Pharmacol. Ther.* 37, 1–8. doi:10.1016/j.pupt.2016.01.002

Lai, T., Tian, B., Cao, C., Hu, Y., Zhou, J., Wang, Y., et al. (2018). HDAC2 Suppresses IL17A-Mediated Airway Remodeling in Human and Experimental Modeling of COPD. *Chest* 153, 863–875. doi:10.1016/j.chest.2017.10.031

Lao, C. D., Ruffin, M. T., Normolle, D., Heath, D. D., Murray, S. I., Bailey, J. M., et al. (2006). Dose Escalation of a Curcuminoid Formulation. *BMC Complement. Altern. Med.* 6, 10. doi:10.1186/1472-6882-6-10

López-Campos, J. L., Tan, W., and Soriano, J. B. (2016). Global burden of COPD. *Respirology* 21, 14–23. doi:10.1111/resp.12660

Meja, K. K., Rajendrasozhan, S., Adenuga, D., Biswas, S. K., Sundar, I. K., Spooner, G., et al. (2008). Curcumin Restores Corticosteroid Function in Monocytes Exposed to Oxidants by Maintaining HDAC2. *Am. J. Respir. Cel Mol Biol* 39, 312–323. doi:10.1165/rcmb.2008-0012OC

Mohanty, C., and Sahoo, S. K. (2010). The *In Vitro* Stability and *In Vivo* Pharmacokinetics of Curcumin Prepared as an Aqueous Nanoparticulate

Formulation. *Biomaterials* 31, 6597–6611. doi:10.1016/j.biomaterials.2010.04.062

Osoata, G. O., Yamamura, S., Ito, M., Vuppusetty, C., Adcock, I. M., Barnes, P. J., et al. (2009). Nitration of Distinct Tyrosine Residues Causes Inactivation of Histone Deacetylase 2. *Biochem. Biophys. Res. Commun.* 384, 366–371. doi:10.1016/j.bbrc.2009.04.128

Prasad, S., Tyagi, A. K., and Aggarwal, B. B. (2014). Recent Developments in Delivery, Bioavailability, Absorption and Metabolism of Curcumin: the golden Pigment from golden Spice. *Cancer Res. Treat.* 46, 2–18. doi:10.4143/crt.2014.46.1.2

Saka, R., and Chella, N. (2020). Nanotechnology for Delivery of Natural Therapeutic Substances: a Review. *Environ. Chem. Lett.* 19, 1097–1106. doi:10.1007/s10311-020-01103-9

Soflaei, S. S., Momtazi-Borojeni, A. A., Majeed, M., Derosa, G., Maffioli, P., and Sahebkar, A. (2018). Curcumin: A Natural Pan-HDAC Inhibitor in Cancer. *Curr. Pharm. Des.* 24, 123–129. doi:10.2174/1381612823666171114165051

To, Y., Ito, K., Kizawa, Y., Failla, M., Ito, M., Kusama, T., et al. (2010). Targeting Phosphoinositide-3-Kinase-delta with Theophylline Reverses Corticosteroid Insensitivity in Chronic Obstructive Pulmonary Disease. *Am. J. Respir. Crit. Care Med.* 182, 897–904. doi:10.1164/rccm.200906-0937OC

Tsai, Y. M., Chang-Liao, W. L., Chien, C. F., Lin, L. C., and Tsai, T. H. (2012). Effects of Polymer Molecular Weight on Relative Oral Bioavailability of Curcumin. *Int. J. Nanomedicine* 7, 2957–2966. doi:10.2147/IJN.S32630

Umerska, A., Gaucher, C., Oyarzun-Ampuero, F., Fries-Raeth, I., Colin, F., Villamizar-Sarmiento, M. G., et al. (2018). Polymeric Nanoparticles for Increasing Oral Bioavailability of Curcumin. *Antioxidants (Basel)* 7, 46. doi:10.3390/antiox7040046

Ungaro, F., D'angelo, I., Miro, A., La Rotonda, M. I., and Quaglia, F. (2012). Engineered PLGA Nano- and Micro-carriers for Pulmonary Delivery: Challenges and Promises. *J. Pharm. Pharmacol.* 64, 1217–1235. doi:10.1111/j.2042-7158.2012.01486.x

Xie, X., Tao, Q., Zou, Y., Zhang, F., Guo, M., Wang, Y., et al. (2011). PLGA Nanoparticles Improve the Oral Bioavailability of Curcumin in Rats: Characterizations and Mechanisms. *J. Agric. Food Chem.* 59, 9280–9289. doi:10.1021/jf202135j

Yang, A., Yang, L., Liu, W., Li, Z., Xu, H., and Yang, X. (2007). Tumor Necrosis Factor Alpha Blocking Peptide Loaded PEG-PLGA Nanoparticles: Preparation and *In Vitro* Evaluation. *Int. J. Pharm.* 331, 123–132. doi:10.1016/j.ijpharm.2006.09.015

Zhang, D. W., Fu, M., Gao, S. H., and Liu, J. L. (2013). Curcumin and Diabetes: a Systematic Review. *Evid. Based Complement. Alternat Med.* 2013, 636053. doi:10.1155/2013/636053

Zhang, K., Tang, X., Zhang, J., Lu, W., Lin, X., Zhang, Y., et al. (2014). PEG-PLGA Copolymers: Their Structure and Structure-Influenced Drug Delivery Applications. *J. Control. Release* 183, 77–86. doi:10.1016/j.jconrel.2014.03.026

Zhang, L., Valizadeh, H., Alipourfard, I., Bidares, R., Aghebati-Maleki, L., and Ahmadi, M. (2020). Epigenetic Modifications and Therapy in Chronic Obstructive Pulmonary Disease (COPD): An Update Review. *Copd* 17, 333–342. doi:10.1080/15412555.2020.1780576

Conflict of Interest: The authors declare that the research was conducted in the absence of any commercial or financial relationships that could be construed as a potential conflict of interest.

Publisher's Note: All claims expressed in this article are solely those of the authors and do not necessarily represent those of their affiliated organizations, or those of the publisher, the editors, and the reviewers. Any product that may be evaluated in this article, or claim that may be made by its manufacturer, is not guaranteed or endorsed by the publisher.

Copyright © 2022 Chen, Wang, Guo, Li, Ye, Qi and Gu. This is an open-access article distributed under the terms of the Creative Commons Attribution License (CC BY). The use, distribution or reproduction in other forums is permitted, provided the original author(s) and the copyright owner(s) are credited and that the original publication in this journal is cited, in accordance with accepted academic practice. No use, distribution or reproduction is permitted which does not comply with these terms.

frontiers in Pharmacology

REVIEW
published: 01 March 2022
doi: 10.3389/fphar.2022.806216

Inhibition of Myocardial Cell Apoptosis Is Important Mechanism for Ginsenoside in the Limitation of Myocardial Ischemia/Reperfusion Injury

Zhihan Chen[1†], *Jingping Wu*[2†], *Sijing Li*[1], *Caijiao Liu*[1] *and Yulan Ren*[3*]

[1]School of Acupuncture Moxibustion and Tuina, Chengdu University of Traditional Chinese Medicine, Chengdu, China,
[2]Department of Medical Cosmetology, Affiliated Hospital of Chengdu University of Traditional Chinese Medicine, Chengdu, China,
[3]School of Chinese Classics, Chengdu University of Traditional Chinese Medicine, Chengdu, China

Ischemic heart disease has a high mortality, and the recommended therapy is reperfusion. Nevertheless, the restoration of blood flow to ischemic tissue leads to further damage, namely, myocardial ischemia/reperfusion injury (MIRI). Apoptosis is an essential pathogenic factor in MIRI, and ginsenosides are effective in inhibiting apoptosis and alleviating MIRI. Here, we reviewed published studies on the anti-apoptotic effects of ginsenosides and their mechanisms of action in improving MIRI. Each ginsenoside can regulate multiple pathways to protect the myocardium. Overall, the involved apoptotic pathways include the death receptor signaling pathway, mitochondria signaling pathway, PI3K/Akt signaling pathway, NF-κB signaling pathway, and MAPK signaling pathway. Ginsenosides, with diverse chemical structures, regulate different apoptotic pathways to relieve MIRI. Summarizing the effects and mechanisms of ginsenosides contributes to further mechanism research studies and structure–function relationship research studies, which can help the development of new drugs. Therefore, we expect that this review will highlight the importance of ginsenosides in improving MIRI *via* anti-apoptosis and provide references and suggestions for further research in this field.

Keywords: ginsenosides, apoptosis, myocardial ischemia/reperfusion injury, *Panax ginseng*, review

OPEN ACCESS

Edited by:
Xin Luan,
Shanghai University of Traditional Chinese Medicine, China

Reviewed by:
Sheng-feng Lu,
Nanjing University of Chinese Medicine, China
Yanping Gong,
Chinese PLA General Hospital, China

***Correspondence:**
Yulan Ren
ryl@cdutcm.edu.cn

[†]*These authors have contributed equally to this work*

Specialty section:
This article was submitted to Ethnopharmacology, a section of the journal Frontiers in Pharmacology

Received: *31 October 2021*
Accepted: *09 February 2022*
Published: *01 March 2022*

Citation:
Chen Z, Wu J, Li S, Liu C and Ren Y (2022) Inhibition of Myocardial Cell Apoptosis Is Important Mechanism for Ginsenoside in the Limitation of Myocardial Ischemia/Reperfusion Injury. Front. Pharmacol. 13:806216. doi: 10.3389/fphar.2022.806216

INTRODUCTION

Ischemic heart disease (IHD) is characterized by insufficient blood flow to the cardiac tissue (Querio et al., 2021). In 2019, "The top 10 causes of death" presented that IHD was the world's biggest killer, responsible for 16% of total deaths worldwide (WHO, 2020). Myocardial blood flow blockage causes inflammatory reactions, energy metabolism disorders, micrangium damage, oxidative stress, calcium overload, and arrhythmia (Hao et al., 2021; Vilela and Fontes-Carvalho, 2021). Reperfusion therapy is the standard therapy for IHD; nevertheless, the restoration of blood flow to ischemic areas aggravates myocardial damage, namely, myocardial ischemia/reperfusion injury (MIRI) (Neri et al., 2017; Li et al., 2019). Evidence indicated that the death rate of acute myocardial infarction (AMI) patients treated with optimal reperfusion therapy was approximately 7% (Hausenloy and Yellon, 2016). MIRI involves multiple regulatory mechanisms, such as cell death, oxidative stress response, and mitochondrial dysfunction

(Neri et al., 2015; Dong et al., 2019; Bugger and Pfeil, 2020). Apoptosis, which is a programmed cell death, is the critical factor in the development of MIRI (Charununtakorn et al., 2016). Apoptosis causes myocardial infarction, damages cardiac systolic/diastolic dysfunction and electrophysiological performance (Li CY. et al., 2020; Cai et al., 2020), and even leads to irreversible damage (Liu et al., 2015). Previous studies indicated that inhibiting apoptotic pathways could effectively alleviate MIRI (Zhai et al., 2017; Cai et al., 2020; Liao et al., 2021). Regulating apoptosis is a promising therapeutic strategy.

Ginsenosides are triterpenoid saponins, which are deemed as the main bioactive components of *Panax ginseng* (Sabouri-Rad et al., 2017). *Panax* means "all healing" in Greek (Im and Nah, 2013), and *Panax ginseng* has effects in improving arrhythmia, decreasing the myocardial ischemic area, suppressing oxidative stress response, enhancing immune regulation, and inhibiting apoptosis (Sun et al., 2016; Wang H. et al., 2021). Ginsenosides have positive effects on MIRI via regulating oxidative stress, inflammation, calcium overload, and cell deaths (Fan et al., 2020; Wang et al., 2020). Previous evidence indicated that ginsenosides could improve myocardial cell (MC) apoptosis to promote cardiac functions and reduce infarct size in MIRI (Zhang et al., 2016; Li CY. et al., 2020). Ginsenosides are classified into three types: protopanaxadiol (PPD) type, oleanolic acid type, and protopanaxatriol (PPT) type (Sun et al., 2016). Ginsenosides inhibit MC apoptosis via different apoptotic pathways, owing to their distinct chemical structures (Kim et al., 2015).

In this review, PubMed, Embase, Web of Science, and China National Knowledge Infrastructure (CNKI) were searched from inception to 21 September 2021 by using the following terms: ginsenoside, myocardial reperfusion injury, etc. This research included and reviewed research studies addressing the anti-apoptosis effects of ginsenosides on MIRI to provide references and suggestions for further research in this field.

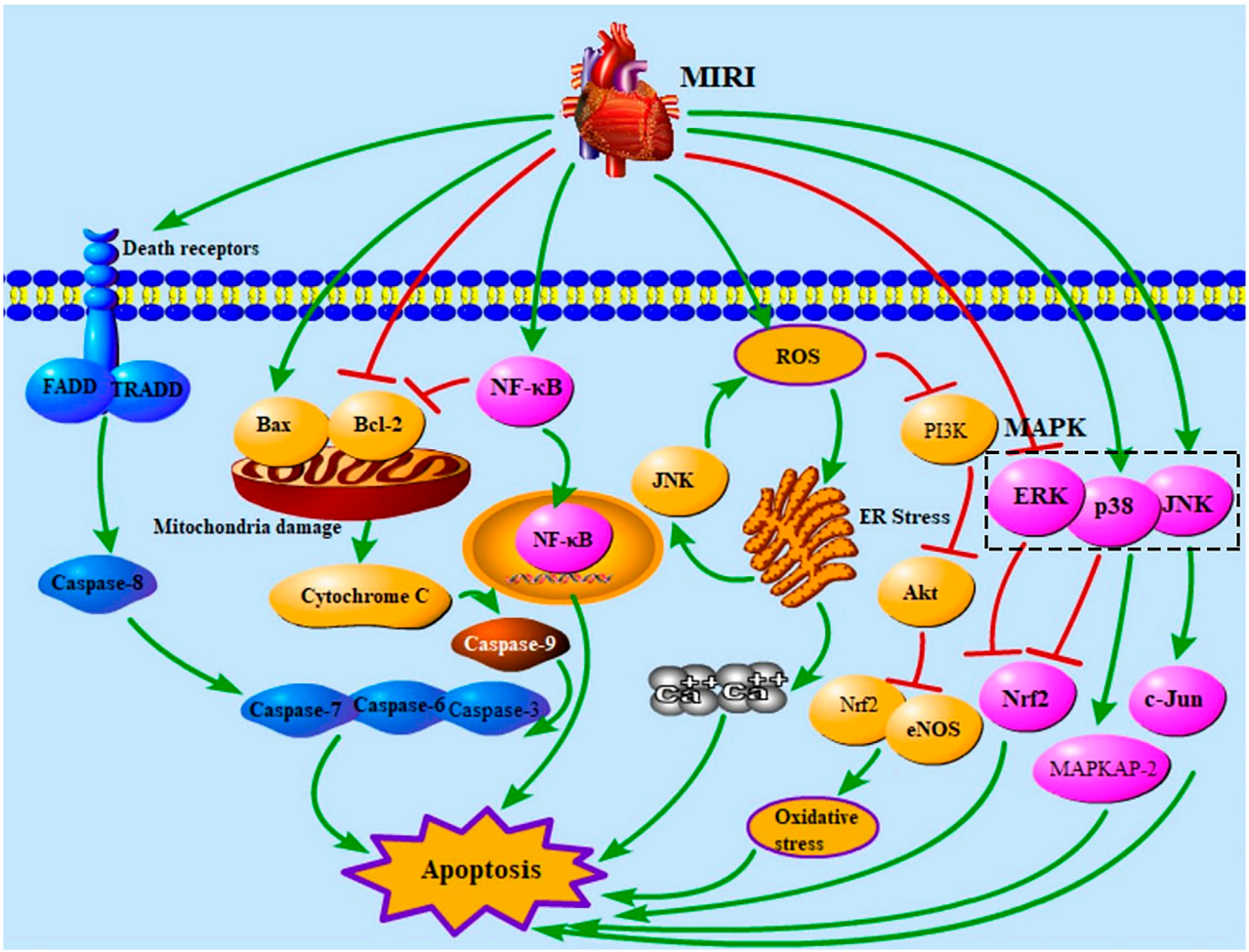


FIGURE 1 | Apoptotic pathways in MIRI. MIRI, myocardial ischemia/reperfusion injury; FADD, Fas-associated death domain protein; TRADD, TNFR1-associated death domain protein; NF-κB, nuclear factor of kappaB; ROS, reactive oxygen species; ER, endoplasmic reticulum; PI3K, phosphatidylinositol-3-kinase; MAPK, mitogen-activated protein kinase; ERK, extracellular signal–regulated kinase; Nrf2, nuclear factor E2–related factor 2; eNOS, endothelial nitric oxide synthase; c-Jun, c-Jun N-terminal kinase; MAPKAP-2, MAPK-activated protein kinase-2.

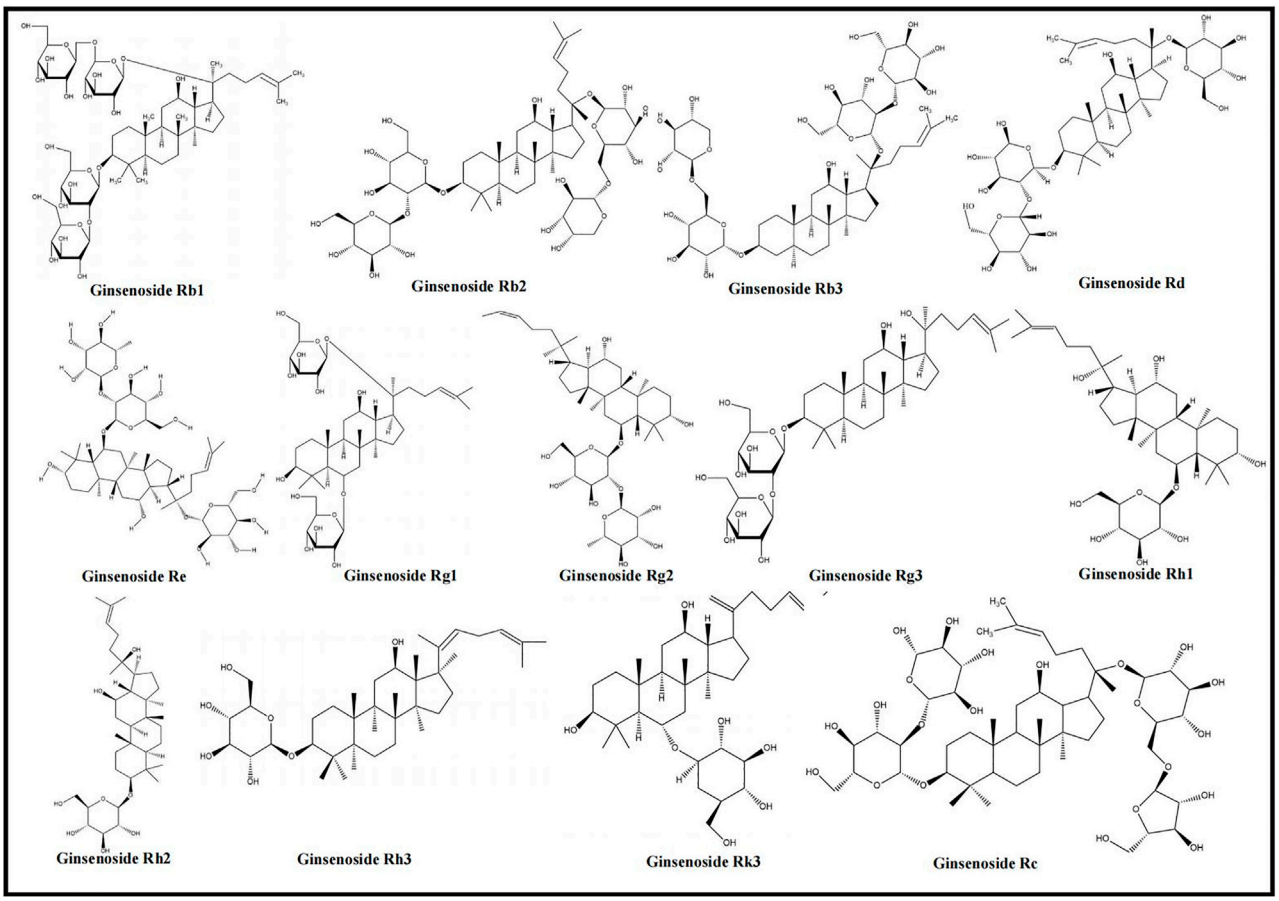


FIGURE 2 | Chemical structures of ginsenosides (ginsenosides Rb1, Rb2, Rb3, Rd, Re, Rg1, Rg2, Rg3, Rh1, Rh2, Rh3, Rk3, and Rc).

MYOCARDIAL CELL APOPTOSIS IN MYOCARDIAL ISCHEMIA/REPERFUSION INJURY

Myocardial ischemia (MI) is a complex pathological condition resulting from initial restriction of blood supply to the heart (Korshunova et al., 2021), which causes tissue hypoxia (Eltzschig and Eckle, 2011) and impediment of re-synthesis of energy sources (e.g., ATP) (Gunata and Parlakpinar, 2021). The lack of ATP reduces the activity of sodium–potassium pumps on the membrane, leading to calcium overload (Zhang et al., 2020). Calcium overload induces arrhythmias (Tribulova et al., 2016; Sugiyama et al., 2021), mitochondrial dysfunction (Tian and Zhang, 2021), and MC apoptosis (Gao et al., 2021). The recommended therapy of MI is reperfusion, namely, restoration of blood flow to ischemic areas (Jneid et al., 2017). Nevertheless, it also causes further myocardial damage (Virani et al., 2020; Ren et al., 2021). MIRI is characterized by metabolic disturbance, cardiac dysfunction, inflammatory reaction, and cell death (apoptosis, autophagy, necrocytosis, pyroptosis, ferroptosis) (Moens et al., 2005; Eltzschig and Eckle, 2011; Hwang et al., 2021; Lv et al., 2021; Peng et al., 2021).

Cell death occurs widely during pathological processes in multiple diseases and is one of the leading causes of death (Wang F. et al., 2021). Apoptosis is a type of programmed cell death, characterized by cell shrinkage, chromatin condensation, and nuclear shrinkage (Hotchkiss et al., 2009). Apoptosis pathways include the death receptor apoptosis pathway, mitochondria apoptosis pathway, endoplasmic reticulum (ER) pathway, PI3K/Akt signaling pathway, NF-κB signaling pathway, and mitogen-activated protein kinase (MAPK) signaling pathway (Hotchkiss et al., 2009; Lai et al., 2021; Zhu and Zhou, 2021). Death receptors are activated by their ligands, namely, FasL, TNF-α, and TRAIL (Zhang et al., 2019a). Death-inducing signaling complex formed by receptors and ligands can activate caspase-8, and activated caspase-8 further up-regulates caspase-3, caspase-6, and caspase-7, resulting in apoptosis (Jeremias et al., 2000; Hotchkiss et al., 2009; Zhang et al., 2019a). MIRI increases mitochondrial permeability and caspase-9 expression level to activate caspase-3, caspase-6, and caspase-7 (Gottlieb and Engler, 1999; Hotchkiss et al., 2009). The mitochondria pathway is regulated by Bax and Bcl-2, which dissociates cytochrome C (cyt-C) and further activates caspase proteins (Hamacher-Brady et al., 2006; Hotchkiss et al., 2009). NF-κB can be transported to the nucleus by binding to IκB, thus causing apoptosis (Hayden and Ghosh, 2004). And NF-κB has function of inhibiting anti-apoptotic protein Bcl-2 (Neamatallah et al., 2018). MIRI up-regulates the levels of reactive oxygen species (ROS) and ER stress and further leads to intracellular

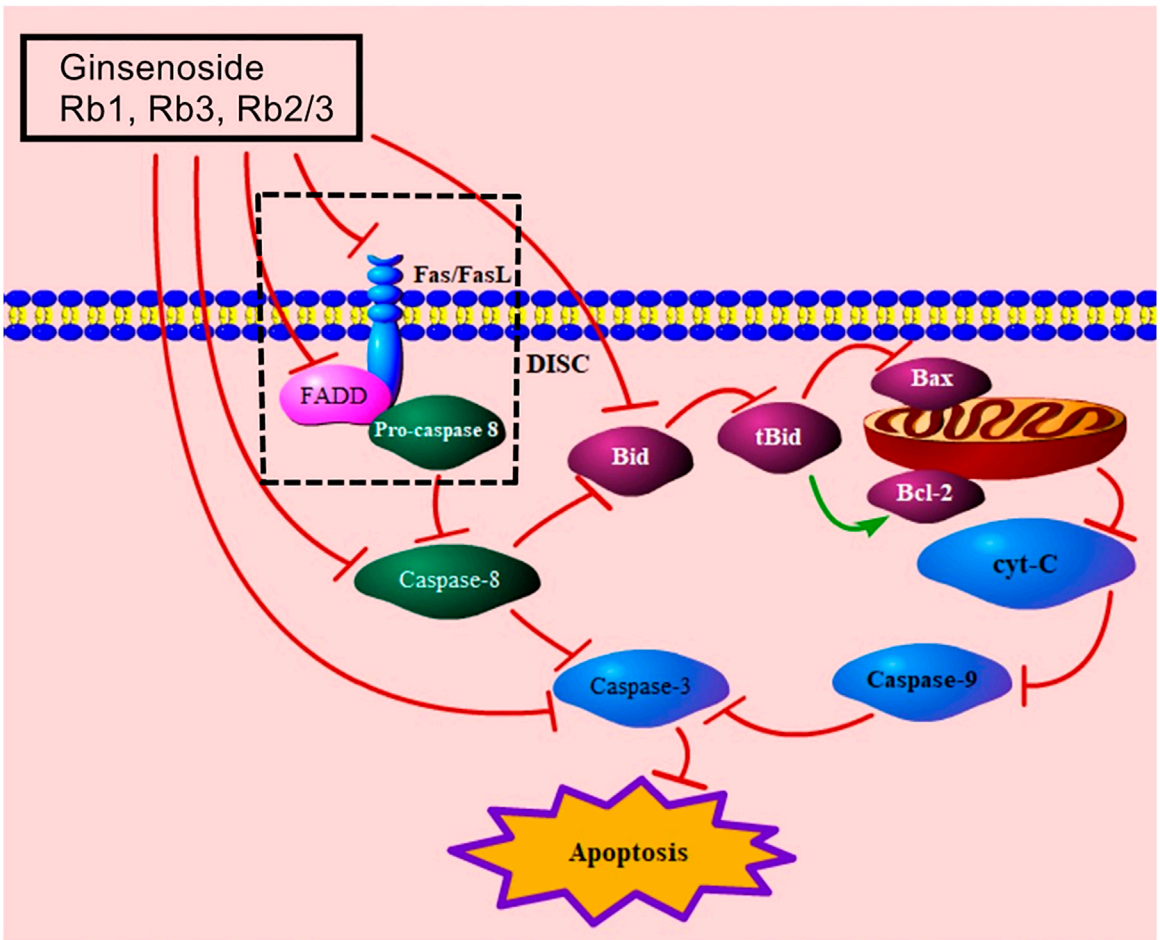


FIGURE 3 | Death receptor–mediated signaling pathway of ginsenoside in relieving MC apoptosis. FasL, Fas ligand; FADD, Fas-associated death domain protein; DISC, death-induced signal complex; tBid, truncated Bid; cyt-C, cytochrome C.

calcium overload and apoptosis (Chaudhari et al., 2014; Lai et al., 2020; Song et al., 2020; Shi et al., 2021). ROS activates ER stress and JNK to increase the content of ROS (Chaudhari et al., 2014; Son et al., 2014; Lu et al., 2017; Chu et al., 2019). Increased ROS activates the PI3K/Akt signaling pathway, and the PI3K/Akt signaling pathway can regulate Nrf2 and eNOS to affect apoptosis (Gao et al., 2002; Syamsunarno et al., 2021; Zheng et al., 2021). MAPK contains JNK, p38, and ERK (Chang and Karin, 2001). JNK, p38, and ERK affect cell apoptosis via regulating c-Jun, MAPKAP-2, and Nrf2 (Davis, 2000; Ai et al., 2015; Zhang et al., 2019a). **Figure 1** shows the apoptosis pathways in MIRI.

EFFECTS AND MECHANISMS OF GINSENOSIDES ON MYOCARDIAL CELL APOPTOSIS IN MYOCARDIAL ISCHEMIA/REPERFUSION INJURY

Panax ginseng, a medicinal plant, belongs to the Araliaceae family and has a long history of usage (Geng et al., 2010). The main active ingredients of *Panax ginseng* are ginsenosides (Wang H. et al., 2021), which inhibit oxidative stress, enhance immune regulation, promote physiological functions (Chen S. et al., 2019; Wang H. et al., 2021), and are adopted to improve IHD, depression, diabetes, etc. (Zhang JH. et al., 2021; Wang Q. et al., 2021; Jiang et al., 2021). Ginsenosides Rb1, Rb2, Rb3, Rd, Re, Rg1, Rg2, Rg3, Rh1, Rh2, Rh3, Rk3, and Rc were proved to alleviate MIRI. The chemical structures of ginsenosides determine their pharmacological effects, especially hydroxyl groups and sugar moieties (Kim et al., 2015). Based on the differences in the parent ring structure, ginsenosides are divided into PPD (Ra1/2/3, Rb1/2/3, Rc, Rd, Rg3, Rh2, F2, compound K), oleanolic acid (Rh3, Ro, Ri), and PPT (Re, Rf, Rg1/2, Rh1, F1) types (Sun et al., 2016). The parent ring structure of PPD type ginsenosides contains two hydroxyl groups at C-3 and C-12, and their sugar moieties attach to β-OH at C-3 and/or C-20 (Bai et al., 2014; Kim et al., 2015). The oleanolic acid type ginsenosides are comprised of a pentacyclic structure with the aglycone oleanolic acid (Choi, 2008; Kim et al., 2015). The parent ring structure of PPT type ginsenosides contains three hydroxyl groups at C-3, C-6, and C-12, and sugar moieties attach to β-OH

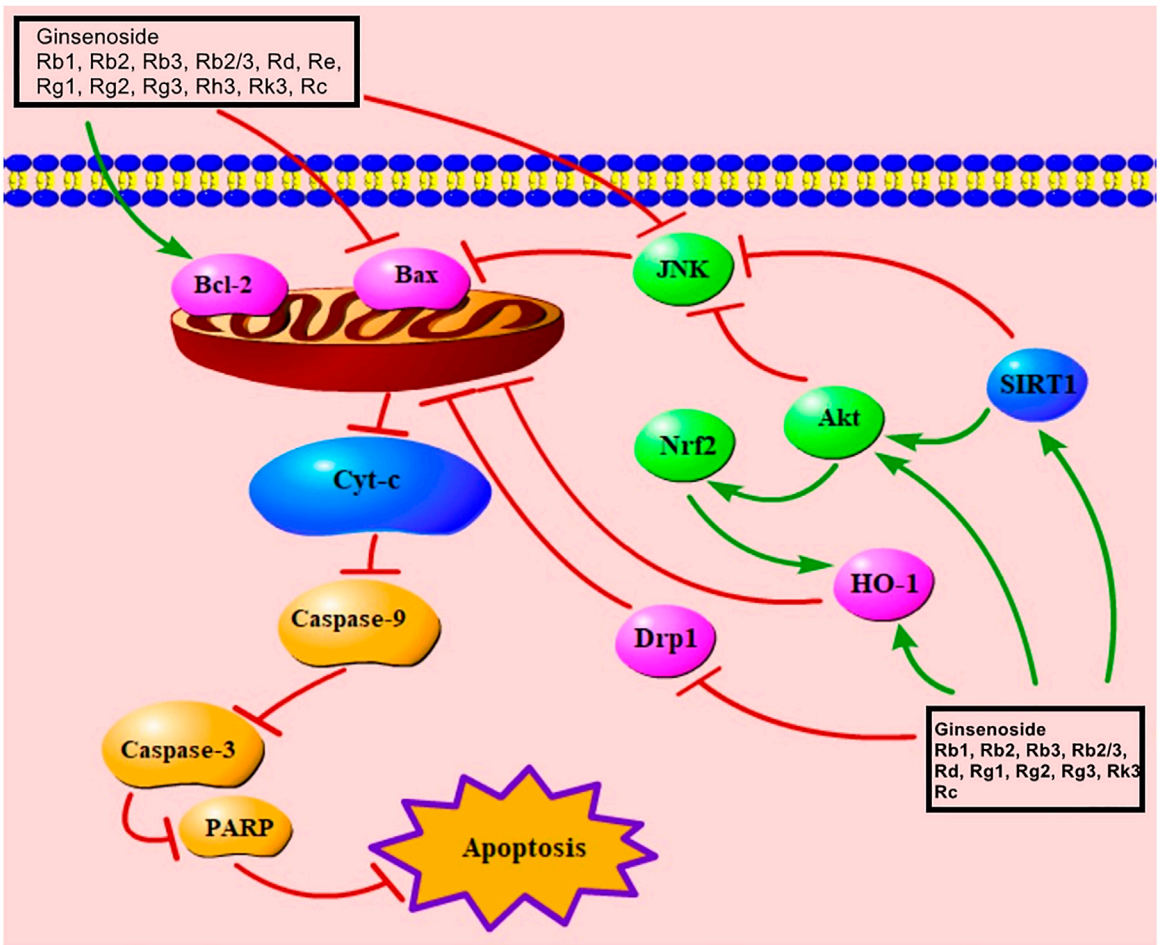


FIGURE 4 | Mitochondria-mediated signaling pathway of ginsenoside in relieving MC apoptosis. Cyt-C, cytochrome C; PARP, poly(ADP-ribose) polymerase; Nrf2, nuclear factor E2–related factor 2; SIRT1, sirtuin 1; Drp1, dynamin-related protein 1; HO-1, heme oxygenase-1.

at C-20 and/or α-OH at C-6 (Bai et al., 2014; Kim et al., 2015). It was demonstrated that the three types of ginsenosides were effective in inhibiting MC apoptosis and regulating different apoptotic pathways to relieve MIRI. According to the included studies, PPD type ginsenosides can trigger the death receptor–mediated signaling pathway; PPD and PPT type ginsenosides both regulate PI3K/Akt–mediated and NF-κB–mediated signaling pathways; furthermore, all three types of ginsenosides can affect mitochondria- and MAPK-mediated signaling pathways. The chemical structures of the ginsenosides included in this study are shown in **Figure 2**. The mechanisms of ginsenosides on MC apoptosis in MIRI are summarized in **Supplementary Table S1**.

Death Receptor–Mediated Signaling Pathway

The death receptor–mediated signaling pathway is the extrinsic pathway of apoptosis, induced by the binding of death receptors and their death ligands (Fas/FasL, TRAIL/TRAILR1, TRAIL/TRAILR2, TNF/TNFR1) (Galluzzi et al., 2012; Lee et al., 2012). Published studies addressing the death receptor–mediated MC apoptotic pathway of ginsenosides focus on the Fas/FasL signaling pathway. Fas/FasL binds to the FADD and transmits the apoptotic signal to procaspase-8, resulting in the formation of death-induced signal complex (DISC), which leads to caspase hydrolysis (Lee et al., 2012; Wang and Su, 2018). The combination of ginsenosides Rb3 and Rb2/Rb3 effectively regulates FasL and FADD to decrease the levels of caspase-8 and caspase-3 (Liu, 2014), while ginsenoside Rb1 improves MC apoptosis via the down-regulation of caspase-8 and caspase-3 (Ai et al., 2015). Moreover, caspase-8 can trigger the mitochondria-mediated signaling pathway by cleaving Bid (Chae et al., 2007). Bid decreases the level of Bcl-2 and increases the level of Bax to increase the release of cyt-C, and the levels of caspase-9 and caspase-3 (Chen et al., 2001; Pasdois et al., 2011; Kim et al., 2021). Ai et al. reported that ginsenoside Rb1 down-regulated caspase-8, bid, caspase-9, caspase-3, and cyt-C (Ai et al., 2015). The death receptor–mediated signaling pathway of ginsenosides in relieving MC apoptosis is shown in **Figure 3**.

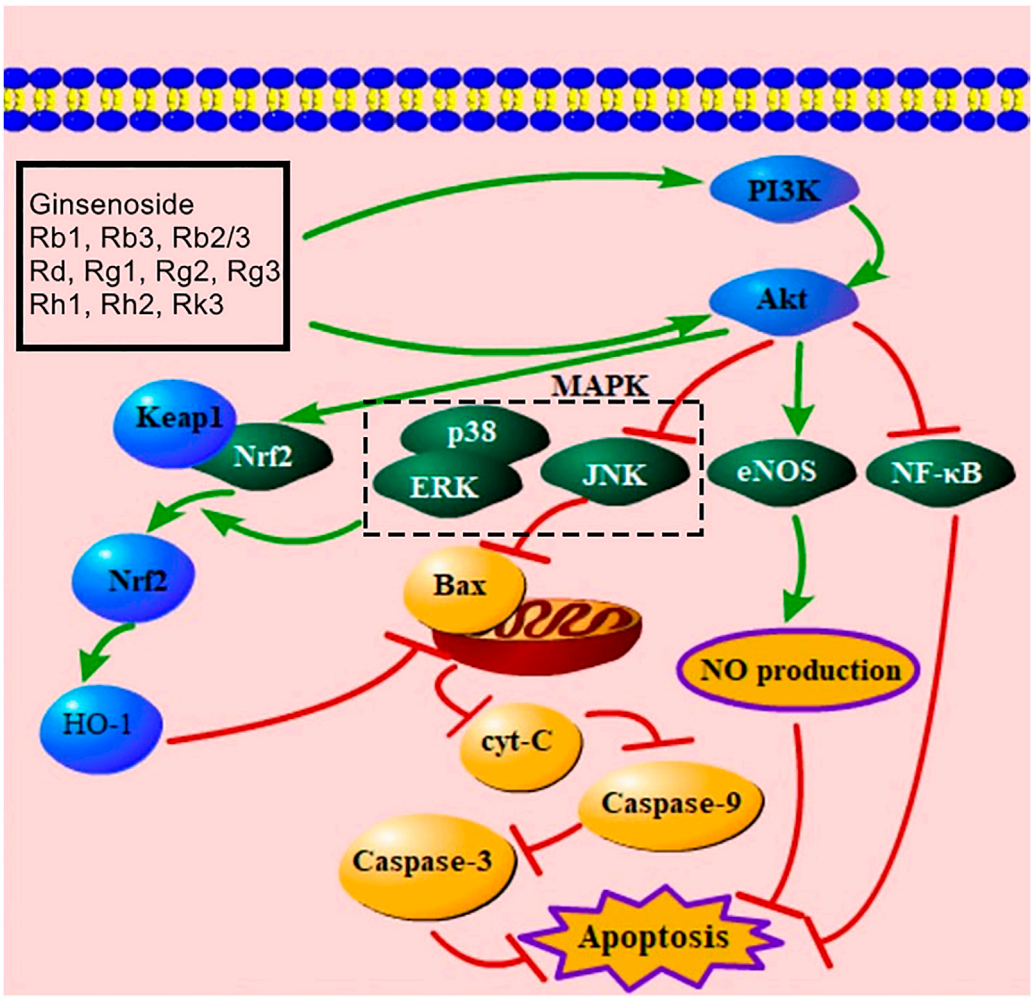


FIGURE 5 | PI3K/Akt-mediated signaling pathway of ginsenoside in relieving MC apoptosis. PI3K, phosphatidylinositol-3-kinase; MAPK, mitogen-activated protein kinase; Keap1, Kelch-like ECH-associated protein 1; Nrf2, nuclear factor E2–related factor 2; HO-1, heme oxygenase-1; ERK, extracellular signal–regulated kinase; Cyt-C, cytochrome C; eNOS, endothelial nitric oxide synthase; NF-κB, nuclear factor of kappaB; NO, nitric oxide.

Mitochondria-Mediated Signaling Pathway

Mitochondria play a significant role in adjusting metabolism, generating ROS, and guaranteeing cell activity (Zhang et al., 2019a; Zhang X. et al., 2021). Bcl-2 inhibits apoptosis, whereas Bax promotes it, causing damage to the membrane structure and potential of mitochondria (Wang Q. et al., 2016). When the balance between Bcl-2 and Bax is disrupted, the mitochondrial membrane potential is reduced and the permeability of mitochondrial membrane is increased (Wang G. et al., 2021). Damaged mitochondria release cyt-C, which then increases the levels of caspase-9 and caspase-3 (Zhang et al., 2019a; Pu et al., 2013); increased caspase-3 up-regulates ADP-ribose polymerase (PARP), leading to apoptosis (Aggeli et al., 2021; Toit et al., 2020). Previous studies indicated that ginsenoside Rb1, Rb2, Rb3, Rb2/Rb3 combination, Rd, Re, Rg1, Rg2, Rg3, Rh3, Rk3, Rc all relieved MC apoptosis via regulating Bax, Bcl-2, cyt-C, caspase-9, caspase-3, and PARP (**Supplementary Table S1**). Decreased SIRT1 can reduce Akt to trigger the mitochondria-mediated signaling pathway by regulating JNK, Nrf2, and Bax (Ai et al., 2015; Pai et al., 2021). Nrf2, an important signaling molecule involved in cardioprotection (Zhu et al., 2008), regulates HO-1, which also has a cardioprotective effect (Liu et al., 2007; Zhu et al., 2008). The mitochondria-mediated signaling pathway, induced by ginsenosides Rb1, Rk3, and Rg3, is associated with the regulation of Akt, Nrf2, and HO-1 (Sun, 2013; Ai et al., 2015; Li L. et al., 2020). Ginsenosides Rb2 and Rg2 also up-regulate SIRT1 to trigger the mitochondria-mediated apoptotic pathway (Fu et al., 2018; Xue et al., 2020). Ginsenoside Rb3 was found to be effective in regulating Nrf2 (Sun et al., 2019). Additionally, previous studies showed that Rb2/Rb3 combination, Rd and Rg1 reduced mitochondria damage via increment of Akt (Wang et al., 2013; Liu, 2014; Qin et al., 2018). Dephosphorylated Drp1 is recruited to the mitochondrial outer membrane to cause damage to mitochondria (Yang, 2013). Ginsenoside Rb1 can inhibit the mRNA level of Drp1 (Yang,

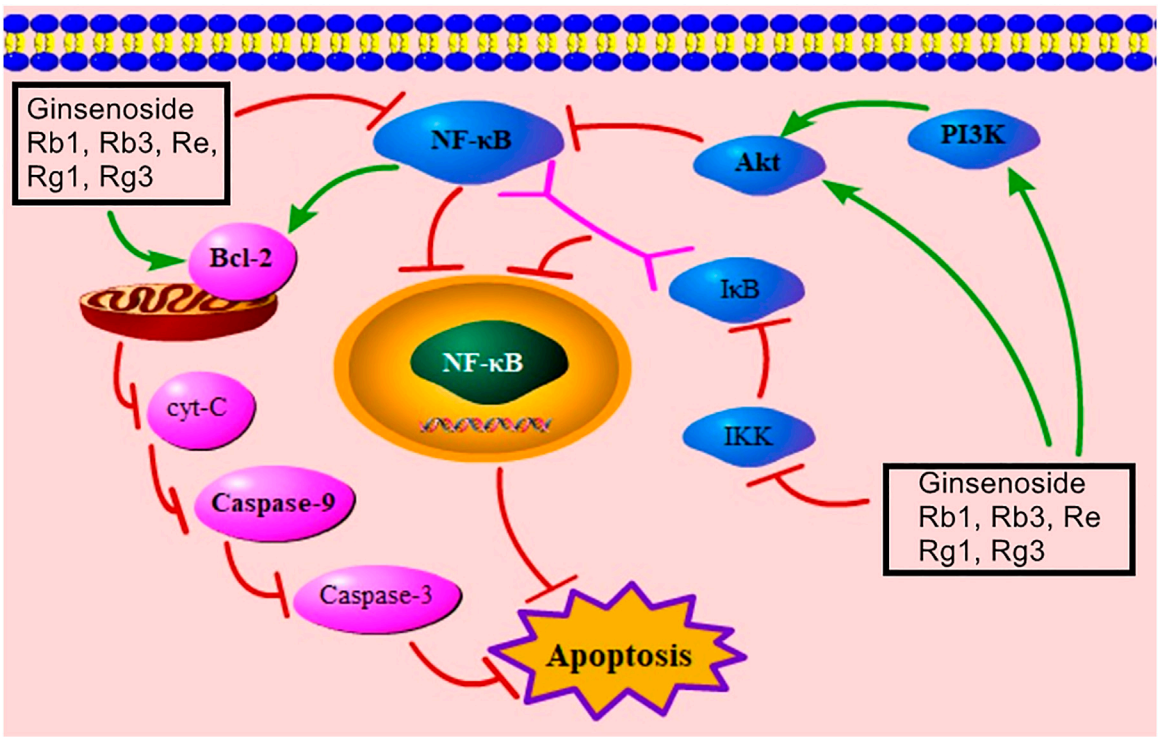


FIGURE 6 | NF-κB–mediated signaling pathway of ginsenoside in relieving MC apoptosis. NF-κB, nuclear factor of kappaB; cyt-C, cytochrome C; PI3K, phosphatidylinositol-3-kinase; IκB, inhibitor of NF-κB; IKK, IκB kinase.

2013). The mitochondria-mediated signaling pathway of ginsenosides in improving MIRI is presented in **Figure 4**.

PI3K/Akt-Mediated Signaling Pathway

The PI3K/Akt signaling pathway is an important pathway by which ginsenosides improve apoptosis. The activation of this pathway promotes angiogenesis, alleviates tissue hypoxia, suppresses cell damage, and improves MC apoptosis (Wang M. et al., 2021; Zhang J. et al., 2021; Cao et al., 2021). Evidence showed that ginsenoside Rb1, Rb3, Rb2/Rb3 combination, Rd, Rg1, Rg2, Rg3, Rh1, Rh2, Rk3 activated the PI3K/Akt-mediated signaling pathway (**Supplementary Table S1**). Activated PI3K can phosphorylate Akt to regulate Nrf2, JNK, eNOS, and NF-κB for decreasing the number of apoptotic cells (Liu SX. et al., 2012; Ai et al., 2015; Liu et al., 2017; Luan et al., 2019; Fu Y. et al., 2021). When MIRI occurs, Nrf2 is released from Keap1 to the nucleus and activates HO-1 to alleviate apoptosis (Mann et al., 2007). Moreover, Nrf2 nuclear export is regulated by the MAPK-mediated signaling pathway (Mann et al., 2007). Ginsenosides Rb1 and Rk3 both increase Nrf2 by down-regulating JNK, ERK, and p38 MAPK (Sun, 2013; Ai et al., 2015). As mentioned above, the PI3K/Akt signaling pathway can decrease JNK to trigger the mitochondria-mediated signaling pathway for inhibiting apoptosis. A previous study presented that ginsenosides Rg2, Rg3, Rh1, and Rh2 up-regulated Akt and down-regulated JNK to inhibit apoptosis (Feng et al., 2017). Phosphorylated eNOS increases NO production and improves MC apoptosis (He et al., 2016), and ginsenosides Rb1, Rg1, and Rg3 can induce the phosphorylation of eNOS (Wang, 2008; Wang et al., 2015; Qin et al., 2018). In addition, ginsenosides Rb3 and Rg1 both up-regulate Akt to decrease NF-κB (Li, 2014; Ma et al., 2014). The PI3K/AKT/NF-κB ginsenoside pathway is considered an important mediator of cell survival and immune responses (Peng et al., 2013). This PI3K/Akt-mediated signaling pathway is presented in **Figure 5**.

NF-κB–Mediated Signaling Pathway

NF-κB belongs to a family of related transcription factors and participates in the regulation of immune responses, proinflammatory cytokines' control, and cell death (Hussen et al., 2021; Hall et al., 2006). The Rel homology domain of NF-κB binds to IκB, and the complex of NF-κB/IκB inhibits the transport of NF-κB to the nucleus, thus inducing apoptosis (Hayden and Ghosh, 2004). Meanwhile, IκB is phosphorylated by IKK (Hayden and Ghosh, 2008). Recent studies have stated that ginsenosides Rb1, Rb3, Re, Rg1, and Rg3 can down-regulate IKKα, IκBα, and NF-κB, thus relieving MC apoptosis via inhibiting the NF-κB–mediated signaling pathway (**Supplementary Table S1**). Moreover, NF-κB can down-regulate Bcl-2 to trigger the mitochondria-mediated signaling pathway (Neamatallah et al., 2018; Duan et al., 2021). **Figure 6** presents the NF-κB–mediated signaling pathway of ginsenoside in relieving MC apoptosis.

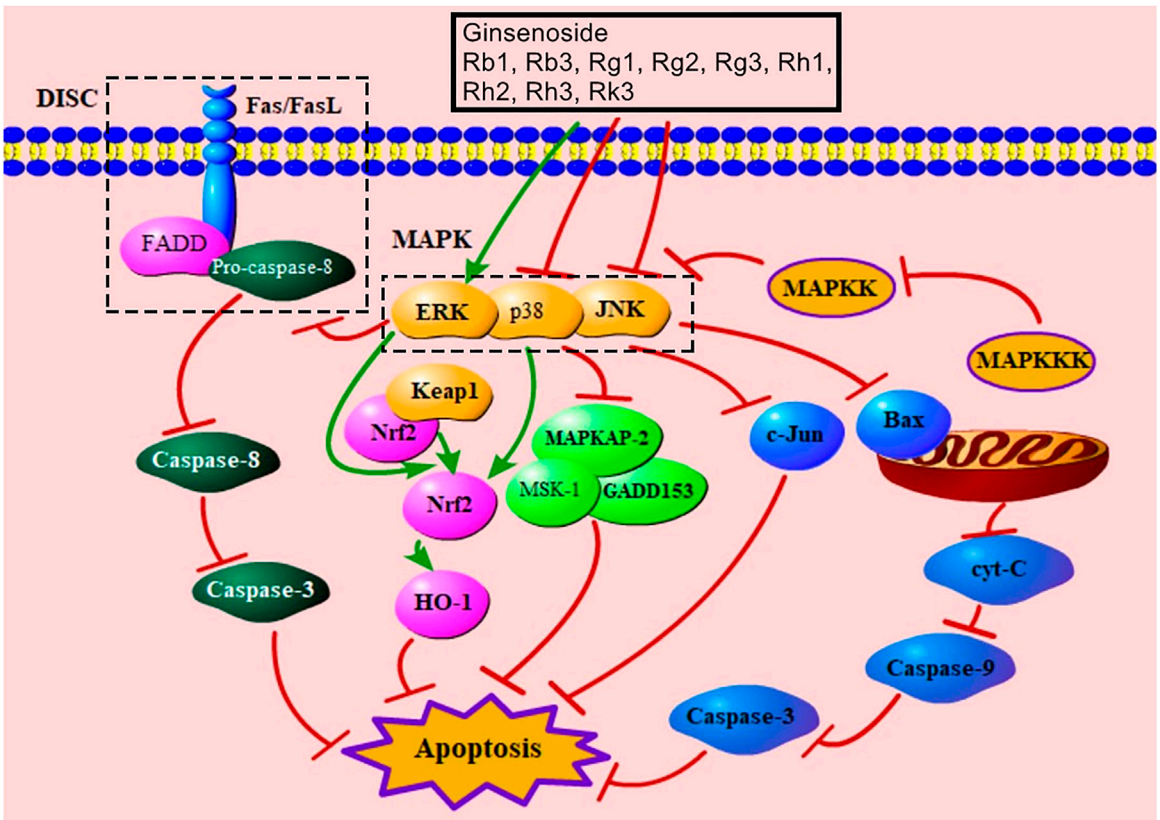


FIGURE 7 | MAPK-mediated signaling pathway of ginsenoside in relieving MC apoptosis. DISC, death-induced signal complex; FasL, Fas ligand; FADD, Fas-associated death domain protein; MAPK, mitogen-activated protein kinase; ERK, extracellular signal–regulated kinase; Keap1, Kelch-like ECH-associated protein 1; Nrf2, nuclear factor E2–related factor 2; HO-1, heme oxygenase-1; MAPKAP-2, MAPK-activated protein kinase-2; MSK-1, mitogen- and stress-activated protein kinase; MAPKK, MAPK kinase; MAPKKK, MAPK kinase kinase; c-Jun, c-Jun N-terminal kinase; cyt-C, cytochrome C.

MAPK-Mediated Signaling Pathway

MAPK is an important signal transducing enzyme that has effects on the regulation of gene expression, cell proliferation, and cell death (Chang and Karin, 2001). MAPK kinase (MAPKK) is activated by MAPK kinase kinase (MAPKKK) to reactivate MAPK (Junttila et al., 2008). MAPK includes JNK, p38, and ERK, which are activated by special MAPKK and have different functions (Chang and Karin, 2001). The activation of JNK and p38 mediates apoptosis (Junttila et al., 2008). JNK promotes apoptosis through regulating c-Jun, which is its most classical substrate (Davis, 2000). JNK also effectively regulates pro-apoptotic protein, Bax (Syeda et al., 2019). The p38 MAPK pathway is related to the regulation of inflammation, gene expression, and energetic metabolism (Bassi et al., 2008). p38 participates in the promotion of apoptosis via its substrates, such as MAPKAP-2, MSK-1, and GADD153 (Zhang et al., 2019a; Ashraf et al., 2014; Das et al., 2006). Inhibition of the p38 MAPK pathway up-regulates the levels of Nrf2 and HO-1 to increase antioxidative proteins and improve apoptosis (Chen et al., 2021). Evidence indicated that ginsenosides Rb1, Rb3, Rg2, Rg3, Rh1, Rh2, and Rk3 had a function of down-regulating JNK, and ginsenosides Rb1 and Rk3 decreased the level of p38 (**Supplementary Table S1**). ERK can proliferate cells and regulate cell growth, and activated ERK inhibits the formation of DISC to relieve death receptor–mediated signaling pathway–induced apoptosis (Meloche and Pouysségur, 2007; Holmström et al., 2000). Additionally, ERK can increase Nrf2 to alleviate mitochondria damage (Ai et al., 2015). Ginsenosides Rb1, Rg1, and Rk3 can up-regulate ERK (**Supplementary Table S1**). Notably, one study indicated that ginsenoside Rb1 down-regulated ERK to inhibit apoptosis (Ai et al., 2015). In this study, MIRI increases the level of ERK. And over-expressed ERK leads to reversible or permanent cell cycle arrest (Meloche and Pouysségur, 2007); thus, ginsenoside Rb1 may decrease over-expressed ERK induced by apoptosis to protect MCs. **Figure 7** showed MAPK-mediated signaling pathway of ginsenoside in relieving MC apoptosis.

Other Pathways

In addition to the above-mentioned apoptotic signaling pathway, other pathways have been reported in previous studies. Li et al. reported that ginsenoside Rb1 improved MIRI by preserving PDH activity and inhibiting SDH activity (Li et al., 2017). Ginsenoside Rb1 also inhibits apoptosis by regulating microRNAs (miRNAs), namely, mir-208, mir-1, mir-29a, mir-21, and mir-320 (Yan et al., 2015; Yan et al., 2016). In 2012, Zhang

et al. indicated that ginsenoside Rg1 increased ATP content and mTOR and decreased AMPKα, LC3B-1, and Beclin-1 to inhibit apoptosis and autophagy (Zhang et al., 2012). Moreover, ginsenoside Rg2 improves antioxidant enzyme activity (SOD, LDH, GXH-Px), and ginsenoside Rh3 increases SERCA (Zhou, 2009; Wang J. et al., 2016).

CONCLUSION AND PERSPECTIVE

MIRI is functional and organic damage to the heart, which results from restoration of blood flow in ischemic areas (Wang K. et al., 2021). Through a number of studies addressing MIRI, the mechanisms of MIRI have not been fully revealed. Previous studies indicated that MC apoptosis was one of the fundamental pathogenic factors of MIRI, and the inhibition of MC apoptosis was effective in alleviating MIRI (Zhou et al., 2018; Xu et al., 2019; Fu D. et al., 2021). Ginsenosides can improve MIRI by relieving mitochondria damage, resisting oxidation, reducing inflammatory response, and inhibiting the generation of DISC (Wang and Roh, 2020; Shaukat et al., 2021). Ginsenosides can relieve MIRI via multiple signaling pathways, such as the death receptor signaling pathway, mitochondria signaling pathway, PI3K/Akt signaling pathway, NF-κB signaling pathway, and MAPK signaling pathway. The occurrence and development of MIRI is complex and multi-factor interacted; thus, it is vital to investigate multi-target therapy in future studies. Ginsenosides, which are regarded as undoubtedly low-toxicity drugs (Xu JF. et al., 2021), have favorable safety profiles (Mancuso and Santangelo, 2017). Toxicity studies showed that most ginsenosides have no oral toxicity, such as Re, Rg2, and Rh2 (Wang et al., 2006; Lu et al., 2012; Gou et al., 2020). Undeniably, in vitro studies indicated that ginsenosides Rb1, Rg1, and Re had embryotoxic and teratogenic effects (Chan et al., 2004; Liu et al., 2005; Liu et al., 2006). However, results from in vitro animal studies may not reflect the true conditions in humans; thus, previous studies suggested that these ginsenosides need to be used with caution in clinics during the first trimester of gestation, before more data in humans are available (Liu et al., 2006; Mancuso and Santangelo, 2017). Overall, the development and application of ginsenosides in improving MIRI are significant, and the toxicity data from *in vivo* studies and clinical studies are needed.

Currently, multiple studies have explored the anti-apoptotic mechanism of ginsenosides; however, problems still exist, and further studies are needed. Firstly, the research studies about the structure–function relationship of ginsenosides in inhibiting MIRI are still needed to be conducted. The hydroxyl groups and sugar moieties have influences on the pharmacological effects of ginsenosides, which can interact with membrane lipids (Kim et al., 2015). Thus, the research of structure–function relationship of ginsenosides in anti-MIRI can contribute to developing safe and effective drugs via chemical modification. Secondly, the current results are mainly generated by *ex vivo* experiments or animal experiments. Rare clinical evidence has showed that ginsenoside Rb has protective effects on MIRI in patients undergoing mitral valve surgery (Zhan et al., 1994). Existing studies are in infancy, and more clinical research studies are needed to be designed and conducted to supply further clinical evidence. Thirdly, evidence showed that pyroptosis occurred during the development of MIRI (Xu XN. et al., 2021; Ji et al., 2021), and pro-apoptotic caspase-3 can cleave GSDME to induce pyroptosis (Wang Y. et al., 2017). However, no study has confirmed the anti-pyroptosis effect of ginsenosides in improving MIRI. Thus, the mechanisms of ginsenosides need to be further explored.

Overall, this review of anti-apoptotic mechanisms of ginsenoside in MIRI presents pharmacological mechanisms and lays the foundation for further research studies, hoping to contribute to the development of undiscovered mechanism and new drugs.

AUTHOR CONTRIBUTIONS

All authors listed have made a substantial, direct, and intellectual contribution to the work and approved it for publication.

FUNDING

This study was supported by the National Natural Science Foundation of China (Nos. 81873239 and 81573885) and Xinglin Scholar Research Premotion Project of Chengdu University of TCM (Nos. YXRC2018014).

SUPPLEMENTARY MATERIAL

The Supplementary Material for this article can be found online at: https://www.frontiersin.org/articles/10.3389/fphar.2022.806216/full#supplementary-material

REFERENCES

Aggeli, I. K., Kapogiannatou, A., Paraskevopoulou, F., and Gaitanaki, C. (2021). Differential Response of Cardiac Aquaporins to Hyperosmotic Stress; Salutary Role of AQP1 against the Induced Apoptosis. *Eur. Rev. Med. Pharmacol. Sci.* 25, 313–325. doi:10.26355/eurrev_202101_24397

Ai, Q., Sun, G., Luo, Y., Dong, X., Hu, R., Meng, X., et al. (2015). Ginsenoside Rb1 Prevents Hypoxia-Reoxygenation-Induced Apoptosis in H9c2 Cardiomyocytes via an Estrogen Receptor-dependent Crosstalk Among the Akt, JNK, and ERK 1/2 Pathways Using a Label-free Quantitative Proteomics Analysis. *RSC Adv.* 5, 26346–26363. doi:10.1039/c5ra02432c

Ashraf, M. I., Ebner, M., Wallner, C., Haller, M., Khalid, S., Schwelberger, H., et al. (2014). A p38MAPK/MK2 Signaling Pathway Leading to Redox Stress, Cell Death and Ischemia/reperfusion Injury. *Cell Commun Signal* 12, 6. doi:10.1186/1478-811X-12-6

Bai, M., Mao, Q., Xu, J. D., Zhu, L. Y., Zhu, H., Wang, Q., et al. (2014). Advance in Saponins of Aerial Parts of Panax Species. *Zhongguo Zhong Yao Za Zhi* 39, 412–422.

Bao, J., Zhang, X., Lu, X., and Rao, M. (2010). Effect of Panax Notoginsenoside Rb1 and Rg1 on Cell Apoptosis of Hypoxia-Reoxygenation Injury in Angiotensin II Induced Hypertrophied Neonatal Rat Myocytes. *Gansu Med. J.* 29, 121–124.

Bassi, R., Heads, R., Marber, M. S., and Clark, J. E. (2008). Targeting P38-MAPK in the Ischaemic Heart: Kill or Cure? *Curr. Opin. Pharmacol.* 8, 141–146. doi:10.1016/j.coph.2008.01.002

Bugger, H., and Pfeil, K. (2020). Mitochondrial ROS in Myocardial Ischemia Reperfusion and Remodeling. *Biochim. Biophys. Acta Mol. Basis Dis.* 1866, 165768. doi:10.1016/j.bbadis.2020.165768

Cai, Y., Ying, F., Liu, H., Ge, L., Song, E., Wang, L., et al. (2020). Deletion of Rap1 Protects against Myocardial Ischemia/reperfusion Injury through Suppressing Cell Apoptosis via Activation of STAT3 Signaling. *FASEB J.* 34, 4482–4496. doi:10.1096/fj.201901592RR

Cao, L., Gao, Y., Zhu, J., Zhang, J., Dong, M., and Mao, Y. (2020). Protective Action of the Ginsenoside Rh3 in a Rat Myocardial Ischemia-Reperfusion Injury Model by Inhibition of Apoptosis Induced via P38 Mitogen-Activated Protein Kinase/caspase-3 Signaling. *J. Int. Med. Res.* 48, 300060520969090. doi:10.1177/0300060520969090

Cao, X. (2004). *Experimental Studies on Protective Effects of Ginsenoside Re on Myocardium of Ischemia-Reperfusion Injury*. Jilin (China): Jilin University. [Doctor's Thesis].

Cao, Y., Li, Q., Yang, Y., Ke, Z., Chen, S., Li, M., et al. (2021). Cardioprotective Effect of Stem-Leaf Saponins from Panax Notoginseng on Mice with Sleep Deprivation by Inhibiting Abnormal Autophagy through PI3K/Akt/mTOR Pathway. *Front. Cardiovasc. Med.* 8, 694219. doi:10.3389/fcvm.2021.694219

Chae, S. U., Ha, K. C., Piao, C. S., Chae, S. W., and Chae, H. J. (2007). Estrogen Attenuates Cardiac Ischemia-Reperfusion Injury via Inhibition of Calpain-Mediated Bid Cleavage. *Arch. Pharm. Res.* 30, 1225–1235. doi:10.1007/BF02980263

Chan, L. Y., Chiu, P. Y., and Lau, T. K. (2004). Embryotoxicity Study of Ginsenoside Rc and Re in *In Vitro* Rat Whole Embryo Culture. *Reprod. Toxicol.* 19, 131–134. doi:10.1016/j.reprotox.2004.06.001

Chang, L., and Karin, M. (2001). Mammalian MAP Kinase Signalling Cascades. *Nature* 410, 37–40. doi:10.1038/35065000

Charununtakorn, S. T., Shinlapawittayatorn, K., Chattipakorn, S. C., and Chattipakorn, N. (2016). Potential Roles of Humanin on Apoptosis in the Heart. *Cardiovasc. Ther.* 34, 107–114. doi:10.1111/1755-5922.12168

Chaudhari, N., Talwar, P., Parimisetty, A., Lefebvre d'Hellencourt, C., and Ravanan, P. (2014). A Molecular Web: Endoplasmic Reticulum Stress, Inflammation, and Oxidative Stress. *Front Cel Neurosci* 8, 213. doi:10.3389/fncel.2014.00213

Chen, L., Guo, Y., Qu, S., Li, K., Yang, T., Yang, Y., et al. (2021). The Protective Effects of Shengmai Formula against Myocardial Injury Induced by Ultrafine Particulate Matter Exposure and Myocardial Ischemia Are Mediated by the PI3K/AKT/p38 MAPK/Nrf2 Pathway. *Front. Pharmacol.* 12, 619311. doi:10.3389/fphar.2021.619311

Chen, M., He, H., Zhan, S., Krajewski, S., Reed, J. C., and Gottlieb, R. A. (2001). Bid Is Cleaved by Calpain to an Active Fragment *In Vitro* and during Myocardial Ischemia/reperfusion. *J. Biol. Chem.* 276, 30724–30728. doi:10.1074/jbc.M103701200

Chen, S., Li, X., Wang, Y., Mu, P., Chen, C., Huang, P., et al. (2019a). Ginsenoside Rb1 Attenuates Intestinal Ischemia/reperfusion-induced I-nflammation and O-xidative S-tress via A-ctivation of the PI3K/Akt/Nrf2 S-ignaling P-athway. *Mol. Med. Rep.* 19, 3633–3641. doi:10.3892/mmr.2019.10018

Chen, X., Wang, Q., Shao, M., Ma, L., Guo, D., Wu, Y., et al. (2019b). Ginsenoside Rb3 Regulates Energy Metabolism and Apoptosis in Cardiomyocytes via Activating PPARα Pathway. *Biomed. Pharmacother.* 120, 109487. doi:10.1016/j.biopha.2019.109487

Choi, K. T. (2008). Botanical Characteristics, Pharmacological Effects and Medicinal Components of Korean Panax Ginseng C A Meyer. *Acta Pharmacol. Sin* 29, 1109–1118. doi:10.1111/j.1745-7254.2008.00869.x

Chu, Q., Zhang, Y., Zhong, S., Gao, F., Chen, Y., Wang, B., et al. (2019). N-n-Butyl Haloperidol Iodide Ameliorates Oxidative Stress in Mitochondria Induced by Hypoxia/Reoxygenation through the Mitochondrial C-Jun N-Terminal Kinase/Sab/Src/Reactive Oxygen Species Pathway in H9c2 Cells. *Oxid Med. Cel Longev* 2019, 7417561. doi:10.1155/2019/7417561

Cui, Y. C., Pan, C. S., Yan, L., Li, L., Hu, B. H., Chang, X., et al. (2017). Ginsenoside Rb1 Protects against Ischemia/reperfusion-Induced Myocardial Injury via Energy Metabolism Regulation Mediated by RhoA Signaling Pathway. *Sci. Rep.* 7, 44579. doi:10.1038/srep44579

Das, S., Tosaki, A., Bagchi, D., Maulik, N., and Das, D. K. (2006). Potentiation of a Survival Signal in the Ischemic Heart by Resveratrol through P38 Mitogen-Activated Protein Kinase/mitogen- and Stress-Activated Protein Kinase 1/cAMP Response Element-Binding Protein Signaling. *J. Pharmacol. Exp. Ther.* 317, 980–988. doi:10.1124/jpet.105.095133

Davis, R. J. (2000). Signal Transduction by the JNK Group of MAP Kinases. *Cell* 103, 239–252. doi:10.1016/s0092-8674(00)00116-1

Dong, Y., Chen, H., Gao, J., Liu, Y., Li, J., and Wang, J. (2019). Molecular Machinery and Interplay of Apoptosis and Autophagy in Coronary Heart Disease. *J. Mol. Cel Cardiol* 136, 27–41. doi:10.1016/j.yjmcc.2019.09.001

Du Toit, E. F., Tai, W. S., Cox, A., O'Connor, D., Griffith, T. A., Helman, T., et al. (2020). Synergistic Effects of Low-Level Stress and a Western Diet on Metabolic Homeostasis, Mood, and Myocardial Ischemic Tolerance. *Am. J. Physiol. Regul. Integr. Comp. Physiol.* 319, R347–R357. doi:10.1152/ajpregu.00322.2019

Duan, H., Zhang, Q., Liu, J., Li, R., Wang, D., Peng, W., et al. (2021). Suppression of Apoptosis in Vascular Endothelial Cell, the Promising Way for Natural Medicines to Treat Atherosclerosis. *Pharmacol. Res.* 168, 105599. doi:10.1016/j.phrs.2021.105599

Eltzschig, H. K., and Eckle, T. (2011). Ischemia and Reperfusion-Ffrom Mechanism to Translation. *Nat. Med.* 17, 1391–1401. doi:10.1038/nm.2507

Fan, H., Xiaoling, S., Yaliu, S., Mingming, L., Xiansheng, M., and Li, F. (2015). Tissue Distribution of Ginsenoside R g3 and its Metabolites in the Body of Rats. *Pharmacol. Clin. Chin. Materia Med.* 31, 16–19.

Fan, W., Huang, Y., Zheng, H., Li, S., Li, Z., Yuan, L., et al. (2020). Ginsenosides for the Treatment of Metabolic Syndrome and Cardiovascular Diseases: Pharmacology and Mechanisms. *Biomed. Pharmacother.* 132, 110915. doi:10.1016/j.biopha.2020.110915

Feng, R., Liu, J., Wang, Z., Zhang, J., Cates, C., Rousselle, T., et al. (2017). The Structure-Activity Relationship of Ginsenosides on Hypoxia-Reoxygenation Induced Apoptosis of Cardiomyocytes. *Biochem. Biophys. Res. Commun.* 494, 556–568. doi:10.1016/j.bbrc.2017.10.056

Fu, D., Gao, T., Liu, M., Li, C., Li, H., Li, H., et al. (2021b). LncRNA TUG1 Aggravates Cardiomyocyte Apoptosis and Myocardial Ischemia/reperfusion Injury. *Histol. Histopathol* 18381, 1–33. doi:10.14670/HH-18-381

Fu, W., Xu, H., Yu, X., Lyu, C., Tian, Y., Guo, M., et al. (2018). 20(S)-Ginsenoside Rg2 Attenuates Myocardial Ischemia/reperfusion Injury by Reducing Oxidative Stress and Inflammation: Role of SIRT1. *RSC Adv.* 8, 23947–23962. doi:10.1039/C8RA02316F

Fu, W., Yu, X., Lu, Z., Sun, F., Wang, Y., Zhang, Y., et al. (2016). Protective Effects of Ginsenoside Rb2 on Myocardial Ischemia *In Vivo* and *In Vitro*. *Int. J. Clin. Exp. Med.* 9, 9843–9855.

Fu, X., Zhang, Q., Luo, R., and Wang, P. (2020). Protective Effect of Ginsenoside Rh3 on Myocardial Ischemia-Reperfusion Injury in Rats by Regulation of P38 MAPK/caspase-3 Signaling Pathway. *Int. J. Clin. Exp. Med.* 13, 3212–3218.

Fu, Y., Zhou, J.-D., Sang, X.-Y., and Zhao, Q.-T. (2021a). Gualou-Xiebai-Banxia Decoction Protects against Type II Diabetes with Acute Myocardial Ischemia by Attenuating Oxidative Stress and Apoptosis via PI3K/Akt/eNOS Signaling. *Chin. J. Nat. Medicines* 19, 161–169. doi:10.1016/S1875-5364(21)60017-1

Galluzzi, L., Vitale, I., Abrams, J. M., Alnemri, E. S., Baehrecke, E. H., Blagosklonny, M. V., et al. (2012). Molecular Definitions of Cell Death Subroutines: Recommendations of the Nomenclature Committee on Cell Death 2012. *Cell Death Differ* 19, 107–120. doi:10.1038/cdd.2011.96

Gao, F., Gao, E., Yue, T. L., Ohlstein, E. H., Lopez, B. L., Christopher, T. A., et al. (2002). Nitric Oxide Mediates the Antiapoptotic Effect of Insulin in Myocardial Ischemia-Reperfusion: the Roles of PI3-Kinase, Akt, and Endothelial Nitric Oxide Synthase Phosphorylation. *Circulation* 105, 1497–1502. doi:10.1161/01.cir.0000012529.00367.0f

Gao, T., Yang, P., Fu, D., Liu, M., Deng, X., Shao, M., et al. (2021). The Protective Effect of Allicin on Myocardial Ischemia-Reperfusion by Inhibition of Ca2+ Overload-Induced Cardiomyocyte Apoptosis via the PI3K/GRK2/PLC-Γ/ip3r Signaling Pathway. *Aging (Albany NY)* 13, 19643–19656. doi:10.18632/aging.203375

Gao, Y., Yang, J., Wang, Y., and Wang, Q. (2011). Effect of Ginsenoside Re on Rat Myocardial Ischemia-Reperfusion Apoptosis and Caspase-3. *J. Liaoning Univ. TCM* 13, 123–124.

Geng, J., Dong, J., Ni, H., Lee, M. S., Wu, T., Jiang, K., et al. (2010). Ginseng for Cognition. *Cochrane Database Syst. Rev.* 2010, CD007769. doi:10.1002/14651858.CD007769.pub2

Gottlieb, R. A., and Engler, R. L. (1999). Apoptosis in Myocardial Ischemia-Reperfusion. *Ann. N. Y Acad. Sci.* 874, 412–426. doi:10.1111/j.1749-6632.1999.tb09255.x

Gou, D., Pei, X., Wang, J., Wang, Y., Hu, C., Song, C., et al. (2020). Antiarrhythmic Effects of Ginsenoside Rg2 on Calcium Chloride-Induced Arrhythmias without Oral Toxicity. *J. Ginseng Res.* 44, 717–724. doi:10.1016/j.jgr.2019.06.005

Guan, L., Li, W., and Liu, Z. (2002). Effect of Ginsenoside-Rb1 on Cardiomyocyte Apoptosis after Ischemia and Reperfusion in Rats. *J. Huazhong Univ. Sci. Technolog Med. Sci.* 22, 212–215. doi:10.1007/BF02828182

Gunata, M., and Parlakpinar, H. (2021). A Review of Myocardial Ischaemia/reperfusion Injury: Pathophysiology, Experimental Models, Biomarkers, Genetics and Pharmacological Treatment. *Cell Biochem Funct* 39, 190–217. doi:10.1002/cbf.3587

Hall, G., Hasday, J. D., and Rogers, T. B. (2006). Regulating the Regulator: NF-kappaB Signaling in Heart. *J. Mol. Cel Cardiol* 41, 580–591. doi:10.1016/j.yjmcc.2006.07.006

Hamacher-Brady, A., Brady, N. R., and Gottlieb, R. A. (2006). The Interplay between Pro-death and Pro-survival Signaling Pathways in Myocardial Ischemia/reperfusion Injury: Apoptosis Meets Autophagy. *Cardiovasc. Drugs Ther.* 20, 445–462. doi:10.1007/s10557-006-0583-7

Hausenloy, D. J., Barrabes, J. A., Bøtker, H. E., Davidson, S. M., Di Lisa, F., Downey, J., et al. (2016). Ischaemic Conditioning and Targeting Reperfusion Injury: a 30 year Voyage of Discovery. *Basic Res. Cardiol.* 111, 70. doi:10.1038/nrcardio.2016.510.1007/s00395-016-0588-8

Hayden, M. S., and Ghosh, S. (2008). Shared Principles in NF-kappaB Signaling. *Cell* 132, 344–362. doi:10.1016/j.cell.2008.01.020

Hayden, M. S., and Ghosh, S. (2004). Signaling to NF-kappaB. *Genes Dev.* 18, 2195–2224. doi:10.1101/gad.1228704

He, F., Xu, B. L., Chen, C., Jia, H. J., Wu, J. X., Wang, X. C., et al. (2016). Methylophiopogonanone A Suppresses Ischemia/reperfusion-Induced Myocardial Apoptosis in Mice via Activating PI3K/Akt/eNOS Signaling Pathway. *Acta Pharmacol. Sin* 37, 763–771. doi:10.1038/aps.2016.14

Holmström, T. H., Schmitz, I., Söderström, T. S., Poukkula, M., Johnson, V. L., Chow, S. C., et al. (2000). MAPK/ERK Signaling in Activated T Cells Inhibits CD95/Fas-Mediated Apoptosis Downstream of DISC Assembly. *EMBO J.* 19, 5418–5428. doi:10.1093/emboj/19.20.5418

Hotchkiss, R. S., Strasser, A., McDunn, J. E., and Swanson, P. E. (2009). Cell Death. *N. Engl. J. Med.* 361, 1570–1583. doi:10.1056/NEJMra0901217

Huang, Q., Su, H., Qi, B., Wang, Y., Yan, K., Wang, X., et al. (2021). A SIRT1 Activator, Ginsenoside Rc, Promotes Energy Metabolism in Cardiomyocytes and Neurons. *J. Am. Chem. Soc.* 143, 1416–1427. doi:10.1021/jacs.0c10836

Hussen, B. M., Azimi, T., Hidayat, H. J., Taheri, M., and Ghafouri-Fard, S. (2021). NF-KappaB Interacting LncRNA: Review of its Roles in Neoplastic and Non-neoplastic Conditions. *Biomed. Pharmacother.* 139, 111604. doi:10.1016/j.biopha.2021.111604

Hwang, J. W., Park, J. H., Park, B. W., Kim, H., Kim, J. J., Sim, W. S., et al. (2021). Histochrome Attenuates Myocardial Ischemia-Reperfusion Injury by Inhibiting Ferroptosis-Induced Cardiomyocyte Death. *Antioxidants (Basel)* 10, 1624. doi:10.3390/antiox10101624

Im, D. S., and Nah, S. Y. (2013). Yin and Yang of Ginseng Pharmacology: Ginsenosides vs Gintonin. *Acta Pharmacol. Sin* 34, 1367–1373. doi:10.1038/aps.2013.100

Jeremias, I., Kupatt, C., Martin-Villalba, A., Habazettl, H., Schenkel, J., Boekstegers, P., et al. (2000). Involvement of CD95/Apo1/Fas in Cell Death after Myocardial Ischemia. *Circulation* 102, 915–920. doi:10.1161/01.cir.102.8.915

Ji, N., Qi, Z., Wang, Y., Yang, X., Yan, Z., Li, M., et al. (2021). Pyroptosis: A New Regulating Mechanism in Cardiovascular Disease. *J. Inflamm. Res.* 14, 2647–2666. doi:10.2147/JIR.S308177

Jiang, N., Huang, H., Zhang, Y., Lv, J., Wang, Q., He, Q., et al. (2021). Ginsenoside Rb1 Produces Antidepressant-like Effects in a Chronic Social Defeat Stress Model of Depression through the BDNF-Trkb Signaling Pathway. *Front. Pharmacol.* 12, 680903. doi:10.3389/fphar.2021.680903

Jneid, H., Addison, D., Bhatt, D. L., Fonarow, G. C., Gokak, S., Grady, K. L., et al. (2017). 2017 AHA/ACC Clinical Performance and Quality Measures for Adults with ST-Elevation and Non-ST-elevation Myocardial Infarction: A Report of the American College of Cardiology/American Heart Association Task Force on Performance Measures. *J. Am. Coll. Cardiol.* 70, 2048–2090. doi:10.1161/HCQ.0000000000000003210.1016/j.jacc.2017.06.032

Junttila, M. R., Li, S. P., and Westermarck, J. (2008). Phosphatase-mediated Crosstalk between MAPK Signaling Pathways in the Regulation of Cell Survival. *FASEB J.* 22, 954–965. doi:10.1096/fj.06-7859rev

Kim, M. Y., Lee, H., Ji, S. Y., Kim, S. Y., Hwangbo, H., Park, S. H., et al. (2021). Induction of Apoptosis by Isoalantolactone in Human Hepatocellular Carcinoma Hep3B Cells through Activation of the ROS-dependent JNK Signaling Pathway. *Pharmaceutics* 13, 1627. doi:10.3390/pharmaceutics13101627

Kim, Y. J., Zhang, D., and Yang, D. C. (2015). Biosynthesis and Biotechnological Production of Ginsenosides. *Biotechnol. Adv.* 33, 717–735. doi:10.1016/j.biotechadv.2015.03.001

Korshunova, A. Y., Blagonravov, M. L., Neborak, E. V., Syatkin, S. P., Sklifasovskaya, A. P., Semyatov, S. M., et al. (2021). BCL2-regulated A-poptotic P-rocess in M-yocardial I-schemia-reperfusion I-njury (Review). *Int. J. Mol. Med.* 47, 23–36. doi:10.3892/ijmm.2020.4781

Lai, L., Liu, Y., Liu, Y., Zhang, N., Cao, S., Zhang, X., et al. (2020). Role of Endoplasmic Reticulum Oxidase 1α in H9C2 Cardiomyocytes Following Hypoxia/reoxygenation Injury. *Mol. Med. Rep.* 22, 1420–1428. doi:10.3892/mmr.2020.11217

Lai, T., Shen, Y., Chen, C., Huang, B., Deng, T., Zhao, Z., et al. (2021). Glycyrrhizic Acid Ameliorates Myocardial Ischemia-Reperfusion Injury in Rats through Inhibiting Endoplasmic Reticulum Stress. *Eur. J. Pharmacol.* 908, 174353. doi:10.1016/j.ejphar.2021.174353

Lee, E. W., Kim, J. H., Ahn, Y. H., Seo, J., Ko, A., Jeong, M., et al. (2012). Ubiquitination and Degradation of the FADD Adaptor Protein Regulate Death Receptor-Mediated Apoptosis and Necroptosis. *Nat. Commun.* 3, 978. doi:10.1038/ncomms1981

Li, C. Y., Yang, P., Jiang, Y. L., Lin, Z., Pu, Y. W., Xie, L. Q., et al. (2020a). Ginsenoside Rb1 Attenuates Cardiomyocyte Apoptosis Induced by Myocardial Ischemia Reperfusion Injury through mTOR Signal Pathway. *Biomed. Pharmacother.* 125, 109913. doi:10.1016/j.biopha.2020.109913

Li, G., Qian, W., and Zhao, C. (2016). Analyzing the Anti-ischemia-reperfusion Injury Effects of Ginsenoside Rb1 Mediated through the Inhibition of P38α MAPK. *Can. J. Physiol. Pharmacol.* 94, 97–103. doi:10.1139/cjpp-2014-0164

Li, J., Yang, Y. L., Li, L. Z., Zhang, L., Liu, Q., Liu, K., et al. (2017). Succinate Accumulation Impairs Cardiac Pyruvate Dehydrogenase Activity through GRP91-dependent and Independent Signaling Pathways: Therapeutic Effects of Ginsenoside Rb1. *Biochim. Biophys. Acta Mol. Basis Dis.* 1863, 2835–2847. doi:10.1016/j.bbadis.2017.07.017

Li, L., Pan, C. S., Yan, L., Cui, Y. C., Liu, Y. Y., Mu, H. N., et al. (2018). Ginsenoside Rg1 Ameliorates Rat Myocardial Ischemia-Reperfusion Injury by Modulating Energy Metabolism Pathways. *Front. Physiol.* 9, 78. doi:10.3389/fphys.2018.00078

Li, L., Wang, Y., Guo, R., Li, S., Ni, J., Gao, S., et al. (2020b). Ginsenoside Rg3-Loaded, Reactive Oxygen Species-Responsive Polymeric Nanoparticles for Alleviating Myocardial Ischemia-Reperfusion Injury. *J. Control. Release* 317, 259–272. doi:10.1016/j.jconrel.2019.11.032

Li, L. (2014). *The Effect and Mechanism of Ginsenoside Rg1 in Improving Myocardial Ischemia/Reperfusion Injury*. Beijing (China): Beijing University of Chinese Medicine.

Li, Y., Chen, B., Yang, X., Zhang, C., Jiao, Y., Li, P., et al. (2019). S100a8/a9 Signaling Causes Mitochondrial Dysfunction and Cardiomyocyte Death in Response to Ischemic/Reperfusion Injury. *Circulation* 140, 751–764. doi:10.1161/CIRCULATIONAHA.118.039262

Liao, S., Apaijai, N., Luo, Y., Wu, J., Chunchai, T., Singhanat, K., et al. (2021). Cell Death Inhibitors Protect against Brain Damage Caused by Cardiac Ischemia/reperfusion Injury. *Cell Death Discov* 7, 312. doi:10.1038/s41420-021-00698-4

Liu, C., Wu, S., and Ye, G. (2012b). Mechanism of Ginsenoside Rb1 against Myocardial Apoptosis during Ischemia-Reperfusion Injury in Diabetic Rats. *JETCM* 21, 1080–1081.

Liu, J., Sui, H., Zhao, J., and Wang, Y. (2017). Osmotin Protects H9c2 Cells from Simulated Ischemia-Reperfusion Injury through AdipoR1/PI3K/AKT Signaling Pathway. *Front. Physiol.* 8, 611. doi:10.3389/fphys.2017.00611

Liu, P., Xu, Y., Yin, H., Wang, J., Chen, K., and Li, Y. (2005). Developmental Toxicity Research of Ginsenoside Rb1 Using a Whole Mouse Embryo Culture

Model. *Birth Defects Res. B Dev. Reprod. Toxicol.* 74, 207–209. doi:10.1002/bdrb.20038

Liu, P., Yin, H., Xu, Y., Zhang, Z., Chen, K., and Li, Y. (2006). Effects of Ginsenoside Rg1 on Postimplantation Rat and Mouse Embryos Cultured *In Vitro*. *Toxicol. Vitro* 20, 234–238. doi:10.1016/j.tiv.2005.06.029

Liu, S. X., Zhang, Y., Wang, Y. F., Li, X. C., Xiang, M. X., Bian, C., et al. (2012a). Upregulation of Heme Oxygenase-1 Expression by Hydroxysafflor Yellow A Conferring protection from Anoxia/reoxygenation-Induced Apoptosis in H9c2 Cardiomyocytes. *Int. J. Cardiol.* 160, 95–101. doi:10.1016/j.ijcard.2011.03.033

Liu, X., Jiang, Y., Fu, W., Yu, X., and Sui, D. (2020). Combination of the Ginsenosides Rb3 and Rb2 Exerts Protective Effects against Myocardial Ischemia Reperfusion Injury in Rats. *Int. J. Mol. Med.* 45, 519–531. doi:10.3892/ijmm.2019.4414

Liu, X., Jiang, Y., Yu, X., Fu, W., Zhang, H., and Sui, D. (2014). Ginsenoside-Rb3 Protects the Myocardium from Ischemia-Reperfusion Injury via the Inhibition of Apoptosis in Rats. *Exp. Ther. Med.* 8, 1751–1756. doi:10.3892/etm.2014.2007

Liu, X., Simpson, J. A., Brunt, K. R., Ward, C. A., Hall, S. R., Kinobe, R. T., et al. (2007). Preemptive Heme Oxygenase-1 Gene Delivery Reveals Reduced Mortality and Preservation of Left Ventricular Function 1 Yr after Acute Myocardial Infarction. *Am. J. Physiol. Heart Circ. Physiol.* 293, H48–H59. doi:10.1152/ajpheart.00741.2006

Liu, X., Zhang, C., Qian, L., Zhang, C., Wu, K., Yang, C., et al. (2015). NF45 Inhibits Cardiomyocyte Apoptosis Following Myocardial Ischemia-Reperfusion Injury. *Pathol. Res. Pract.* 211, 955–962. doi:10.1016/j.prp.2015.09.018

Liu, X. (2014). *The Study on the Protective Effects and Mechanisms of Ginsenoside Rb3 and Rb2 Combination on Myocardial Ischemia Reperfusion Injury*. Changchun (China): Jilin University of China. [Doctor's thesis].

Liu, Z., Li, Z., and Liu, X. (2002). Effect of Ginsenoside Re on Cardiomyocyte Apoptosis and Expression of Bcl-2/Bax Gene after Ischemia and Reperfusion in Rats. *J. Huazhong Univ. Sci. Technolog Med. Sci.* 22, 305–309. doi:10.1007/BF02896771

Lu, D., Liu, J., Zhao, W., and Li, P. (2012). Chronic Toxicity of Ginsenoside Re on Sprague-Dawley Rats. *J. Ethnopharmacol* 144, 656–663. doi:10.1016/j.jep.2012.10.007

Lu, S., Zhang, Y., Zhong, S., Gao, F., Chen, Y., Li, W., et al. (2017). N-n-butyl Haloperidol Iodide Protects against Hypoxia/Reoxygenation Injury in Cardiac Microvascular Endothelial Cells by Regulating the ROS/MAPK/Egr-1 Pathway. *Front. Pharmacol.* 7, 520. doi:10.3389/fphar.2016.00520

Lu, X. (2009). *Studies on Influence of Ginsenoside-Re on Myocardium Ischemia-Reperfusion Injury and Apoptosis Pathway of Mitochondrial*. Jilin (China): Jinlin University. [Master's Thesis].

Luan, Y., Sun, C., Wang, J., Jiang, W., Xin, Q., Zhang, Z., et al. (2019). Baicalin Attenuates Myocardial Ischemia-Reperfusion Injury through Akt/NF-Kb Pathway. *J. Cel Biochem* 120, 3212–3219. doi:10.1002/jcb.27587

Lv, S., Li, X., Zhao, S., Liu, H., and Wang, H. (2021). The Role of the Signaling Pathways Involved in the Protective Effect of Exogenous Hydrogen Sulfide on Myocardial Ischemia-Reperfusion Injury. *Front Cel Dev Biol* 9, 723569. doi:10.3389/fcell.2021.723569

Ma, L., Liu, H., Xie, Z., Yang, S., Xu, W., Hou, J., et al. (2014). Ginsenoside Rb3 Protects Cardiomyocytes against Ischemia-Reperfusion Injury via the Inhibition of JNK-Mediated NF-Kb Pathway: a Mouse Cardiomyocyte Model. *PLoS One* 9, e103628. doi:10.1371/journal.pone.0103628

Mancuso, C., and Santangelo, R. (2017). Panax Ginseng and Panax Quinquefolius: From Pharmacology to Toxicology. *Food Chem. Toxicol.* 107, 362–372. doi:10.1016/j.fct.2017.07.019

Mann, G. E., Niehueser-Saran, J., Watson, A., Gao, L., Ishii, T., de Winter, P., et al. (2007). Nrf2/ARE Regulated Antioxidant Gene Expression in Endothelial and Smooth Muscle Cells in Oxidative Stress: Implications for Atherosclerosis and Preeclampsia. *Sheng Li Xue Bao* 59, 117–127.

Meloche, S., and Pouysségur, J. (2007). The ERK1/2 Mitogen-Activated Protein Kinase Pathway as a Master Regulator of the G1- to S-phase Transition. *Oncogene* 26, 3227–3239. doi:10.1038/sj.onc.1210414

Moens, A. L., Claeys, M. J., Timmermans, J. P., and Vrints, C. J. (2005). Myocardial Ischemia/reperfusion-Injury, a Clinical View on a Complex Pathophysiological Process. *Int. J. Cardiol.* 100, 179–190. doi:10.1016/j.ijcard.2004.04.013

Neamatallah, T., El-Shitany, N. A., Abbas, A. T., Ali, S. S., and Eid, B. G. (2018). Honey Protects against Cisplatin-Induced Hepatic and Renal Toxicity through Inhibition of NF-Kb-Mediated COX-2 Expression and the Oxidative Stress Dependent BAX/Bcl-2/caspase-3 Apoptotic Pathway. *Food Funct.* 9, 3743–3754. doi:10.1039/c8fo00653a

Neri, M., Fineschi, V., Di Paolo, M., Pomara, C., Riezzo, I., Turillazzi, E., et al. (2015). Cardiac Oxidative Stress and Inflammatory Cytokines Response after Myocardial Infarction. *Curr. Vasc. Pharmacol.* 13, 26–36. doi:10.2174/15701611131199900003

Neri, M., Riezzo, I., Pascale, N., Pomara, C., and Turillazzi, E. (2017). Ischemia/Reperfusion Injury Following Acute Myocardial Infarction: A Critical Issue for Clinicians and Forensic Pathologists. *Mediators Inflamm.* 2017, 7018393. doi:10.1155/2017/7018393

Pai, P. Y., Lin, Y. Y., Yu, S. H., Lin, C. Y., Liou, Y. F., Wu, X. B., et al. (2021). Angiotensin II Receptor Blocker Irbesartan Attenuates Sleep Apnea-Induced Cardiac Apoptosis and Enhances Cardiac Survival and Sirtuin 1 Upregulation. *Sleep Breath*, 1–12. doi:10.1007/s11325-021-02499-6

Pasdois, P., Parker, J. E., Griffiths, E. J., and Halestrap, A. P. (2011). The Role of Oxidized Cytochrome C in Regulating Mitochondrial Reactive Oxygen Species Production and its Perturbation in Ischaemia. *Biochem. J.* 436, 493–505. doi:10.1042/BJ20101957

Peng, L., Lei, Z., Rao, Z., Yang, R., Zheng, L., Fan, Y., et al. (2021). Cardioprotective Activity of Ethyl Acetate Extract of Cinnamomi Ramulus against Myocardial Ischemia/reperfusion Injury in Rats via Inhibiting NLRP3 Inflammasome Activation and Pyroptosis. *Phytomedicine* 93, 153798. doi:10.1016/j.phymed.2021.153798

Peng, Y., Huang, S., Wu, Y., Cheng, B., Nie, X., Liu, H., et al. (2013). Platelet Rich Plasma Clot Releasate Preconditioning Induced PI3K/AKT/NFκB Signaling Enhances Survival and Regenerative Function of Rat Bone Marrow Mesenchymal Stem Cells in Hostile Microenvironments. *Stem Cell Dev* 22, 3236–3251. doi:10.1089/scd.2013.0064

Pu, J., Yuan, A., Shan, P., Gao, E., Wang, X., Wang, Y., et al. (2013). Cardiomyocyte-expressed Farnesoid-X-Receptor Is a Novel Apoptosis Mediator and Contributes to Myocardial Ischaemia/reperfusion Injury. *Eur. Heart J.* 34, 1834–1845. doi:10.1093/eurheartj/ehs011

Qian, S., Kan, J., and Yang, Y. (2019). Protective Effects of the Combination of Ginsenoside Rgl and Resveratrol against Ischemia Reperfusion Injury of Cardiomyocytes. *J. Liaoning Univ. TCM* 21, 47–49.

Qin, L., Fan, S., Jia, R., and Liu, Y. (2018). Ginsenoside Rg1 Protects Cardiomyocytes from Hypoxia-Induced Injury through the PI3K/AKT/mTOR Pathway. *Pharmazie* 73, 349–355. doi:10.1691/ph.2018.8329

Querio, G., Antoniotti, S., Geddo, F., Tullio, F., Penna, C., Pagliaro, P., et al. (202110692). Ischemic Heart Disease and Cardioprotection: Focus on Estrogenic Hormonal Setting and Microvascular Health. *Vasc. Pharmacol.* 141, 106921. doi:10.1016/j.vph.2021.106921

Ren, Y., Lin, S., Liu, W., and Ding, H. (2021). Hepatic Remote Ischemic Preconditioning (RIPC) Protects Heart Damages Induced by Ischemia Reperfusion Injury in Mice. *Front. Physiol.* 12, 713564. doi:10.3389/fphys.2021.713564

Sabouri-Rad, S., Sabouri-Rad, S., Sahebkar, A., and Tayarani-Najaran, Z. (2017). Ginseng in Dermatology: A Review. *Curr. Pharm. Des.* 23, 1649–1666. doi:10.2174/1381612822666161021152322

Shaukat, A., Shaukat, I., Rajput, S. A., Shukat, R., Hanif, S., Jiang, K., et al. (2021). Ginsenoside Rb1 Protects from Staphylococcus Aureus-Induced Oxidative Damage and Apoptosis through Endoplasmic Reticulum-Stress and Death Receptor-Mediated Pathways. *Ecotoxicol Environ. Saf.* 219, 112353. doi:10.1016/j.ecoenv.2021.112353

Shen, W., Li, Y., and Yang, S. (2017). Effects of Ginsenoside Rg1 on Arrhythmias Induced by Ischemic/reperfusion Injury in Rats. *J. Clin. Cardiol.* 33, 465–469.

Shi, H., Zhao, T., Li, Y., Xiao, X., Wu, J., Zhang, H., et al. (2021). Velvet Antler Ameliorates Cardiac Function by Restoring Sarcoplasmic Reticulum Ca2+-ATPase Activity in Rats with Heart Failure after Myocardial Infarction. *Front. Pharmacol.Front Pharmaco* 12. doi:10.3389/fphar.2021.621194

Son, S. M., Byun, J., Roh, S. E., Kim, S. J., and Mook-Jung, I. (2014). Reduced IRE1α Mediates Apoptotic Cell Death by Disrupting Calcium Homeostasis via the InsP3 Receptor. *Cell Death Dis* 5, e1188. doi:10.1038/cddis.2014.129

Song, N., Ma, J., Meng, X. W., Liu, H., Wang, H., Song, S. Y., et al. (2020). Heat Shock Protein 70 Protects the Heart from Ischemia/Reperfusion Injury through Inhibition of P38 MAPK Signaling. *Oxid Med. Cel Longev* 2020, 3908641. doi:10.1155/2020/3908641

Sugiyama, A., Shimizu, Y., Okada, M., Otani, K., and Yamawaki, H. (2021). Preventive Effect of Canstatin against Ventricular Arrhythmia Induced by Ischemia/Reperfusion Injury: A Pilot Study. *Int. J. Mol. Sci.* 22, 1004. doi:10.3390/ijms22031004

Sun, J., Sun, G., Meng, X., Wang, H., Wang, M., Qin, M., et al. (20132013). Ginsenoside RK3 Prevents Hypoxia-Reoxygenation Induced Apoptosis in H9c2 Cardiomyocytes via AKT and MAPK Pathway. *Evid. Based Complement. Alternat Med.* 2013, 690190. doi:10.1155/2013/690190

Sun, J., Yu, X., Huangpu, H., and Yao, F. (2019). Ginsenoside Rb3 Protects Cardiomyocytes against Hypoxia/reoxygenation Injury via Activating the Antioxidation Signaling Pathway of PERK/Nrf2/HMOX1. *Biomed. Pharmacother.* 109, 254–261. doi:10.1016/j.biopha.2018.09.002

Sun, J. (2013). *Research on Active Ingredients of Chinese Medicine and Molecular Mechanisms Based on the Myocardial Protective Effec*. Beijing (China): Chinese Academy of Medical Sciences & Peking Union Medical College. [Doctor's Thesis].

Sun, Y., Liu, Y., and Chen, K. (2016). Roles and Mechanisms of Ginsenoside in Cardiovascular Diseases: Progress and Perspectives. *Sci. China Life Sci.* 59, 292–298. doi:10.1007/s11427-016-5007-8

Syamsunarno, M. R. A., Safitri, R., and Kamisah, Y. (2021). Protective Effects of Caesalpinia Sappan Linn. And its Bioactive Compounds on Cardiovascular Organs. *Front. Pharmacol.* 12, 725745. doi:10.3389/fphar.2021.725745

Syeda, M. Z., Fasae, M. B., Yue, E., Ishimwe, A. P., Jiang, Y., Du, Z., et al. (2019). Anthocyanidin Attenuates Myocardial Ischemia Induced Injury via Inhibition of ROS-JNK-Bcl-2 Pathway: New Mechanism of Anthocyanidin Action. *Phytother Res.* 33, 3129–3139. doi:10.1002/ptr.6485

Tian, F., and Zhang, Y. (2021). Overexpression of SERCA2a Alleviates Cardiac Microvascular Ischemic Injury by Suppressing Mfn2-Mediated ER/Mitochondrial Calcium Tethering. *Front. Cel Dev Biol* 9, 636553. doi:10.3389/fcell.2021.636553

Tian, J., Zheng, S., Guo, W., Ye, J., and Li, L. (2004). Ginsenoside Rg2 protection against Apoptosis in Ischemia and Reperfusion Rat Myocardium. *CHinese Pharmacol. Bull.* 20, 480.

Tribulova, N., Knezl, V., Szeiffova Bacova, B., Egan Benova, T., Viczenczova, C., Gonçalvesova, E., et al. (2016). Disordered Myocardial Ca(2+) Homeostasis Results in Substructural Alterations that May Promote Occurrence of Malignant Arrhythmias. *Physiol. Res.* 65 Suppl 1, S139–S148. doi:10.33549/physiolres.933388

Vilela, E. M., and Fontes-Carvalho, R. (2021). Inflammation and Ischemic Heart Disease: The Next Therapeutic Target? *Rev. Port Cardiol. (Engl Ed.* 40, 785–796. doi:10.1016/j.repc.2021.02.01110.1016/j.repce.2021.10.010

Virani, S. S., Alonso, A., Benjamin, E. J., Bittencourt, M. S., Callaway, C. W., Carson, A. P., et al. (2020). Heart Disease and Stroke Statistics-2020 Update: A Report from the American Heart Association. *Circulation* 141, e139–e596. doi:10.1161/CIR.0000000000000757

Wang, F., and Roh, Y. S. (2020). Mitochondrial Connection to Ginsenosides. *Arch. Pharm. Res.* 43, 1031–1045. doi:10.1007/s12272-020-01279-2

Wang, F., Yuan, Q., Chen, F., Pang, J., Pan, C., Xu, F., et al. (2021b). Fundamental Mechanisms of the Cell Death Caused by Nitrosative Stress. *Front. Cel Dev Biol* 9, 742483. doi:10.3389/fcell.2021.742483

Wang, G., Hao, M., Liu, Q., Jiang, Y., Huang, H., Yang, G., et al. (2021d). Protective Effect of Recombinant Lactobacillus Plantarum against H2O2-Induced Oxidative Stress in HUVEC Cells. *J. Zhejiang Univ. Sci. B* 22, 348–365. doi:10.1631/jzus.B2000441

Wang, H., Zheng, Y., Sun, Q., Zhang, Z., Zhao, M., Peng, C., et al. (2021a). Ginsenosides Emerging as Both Bifunctional Drugs and Nanocarriers for Enhanced Antitumor Therapies. *J. Nanobiotechnol* 19, 322. doi:10.1186/s12951-021-01062-5

Wang, J., Wang, H., Mou, X., Luan, M., Zhang, X., He, X., et al. (2020). The Advances on the Protective Effects of Ginsenosides on Myocardial Ischemia and Ischemia-Reperfusion Injury. *Mini Rev. Med. Chem.* 20, 1610–1618. doi:10.2174/1389557520666200619115444

Wang, J., Cui, Y., Wang, J., Li, H., Dai, J., and Ma, H. (2016b). Effect of Ginsenoside Rh3 Pretreatment on Expression of Myocardial Sarcoplasmic Reticulum Ca^{2+}-ATP in Rats Following I/R Injury. *Chin. J. Geriatr. Heart Brain Vessel Dis.* 18, 1077–1081.

Wang, J., Cui, Y., Wang, J., Li, H., Dai, J., Ma, H., et al. (2017b). Ginseng Saponin Rh3 Pretreatment to Protect Myocardial Ischemia-Reperfusion Injury in Rats. *Chin. Arch. Traditional Chin. Med.* 35, 2783–2786.

Wang, J., Cui, Y., Wang, J., Li, H., Dai, J., and Ma, H. (2019). Protective Effects of the Ginseng Saponin Rh1 Pretreatment to Myocardial Ischemia-Reperfusion Injury in Rats. *J. Liaoning Univ. TCM* 1, 42–45.

Wang, J., Cui, Y., Wang, J., Li, H., Dai, J., and Ma, H. (2017c). Protective Effects of the Ginseng Saponin Rh3 Pretreatment to Caspase-3 of Myocardial Ischemia-Reperfusion Injury in Rats. *J. Changchun Univ. Chin. Med.* 33, 13–15.

Wang, K., Li, Y., Qiang, T., Chen, J., and Wang, X. (2021f). Role of Epigenetic Regulation in Myocardial Ischemia/reperfusion Injury. *Pharmacol. Res.* 170, 105743. doi:10.1016/j.phrs.2021.105743

Wang, M., and Su, P. (2018). The Role of the Fas/FasL Signaling Pathway in Environmental Toxicant-Induced Testicular Cell Apoptosis: An Update. *Syst. Biol. Reprod. Med.* 64, 93–102. doi:10.1080/19396368.2017.1422046

Wang, M., Yang, D., Hu, Z., Shi, Y., Ma, Y., Cao, X., et al. (2021e). Extracorporeal Cardiac Shock Waves Therapy Improves the Function of Endothelial Progenitor Cells after Hypoxia Injury via Activating PI3K/Akt/eNOS Signal Pathway. *Front. Cardiovasc. Med.* 8, 747497. doi:10.3389/fcvm.2021.747497

Wang, Q., Fu, W., Yu, X., Xu, H., Sui, D., and Wang, Y. (2021c). Ginsenoside Rg2 Alleviates Myocardial Fibrosis by Regulating TGF-β1/Smad Signalling Pathway. *Pharm. Biol.* 59, 106–113. doi:10.1080/13880209.2020.1867197

Wang, Q., Zhang, L., Yuan, X., Ou, Y., Zhu, X., Cheng, Z., et al. (2016a). The Relationship between the Bcl-2/Bax Proteins and the Mitochondria-Mediated Apoptosis Pathway in the Differentiation of Adipose-Derived Stromal Cells into Neurons. *PLoS One* 11, e0163327. doi:10.1371/journal.pone.0163327

Wang, Y., Gao, W., Shi, X., Ding, J., Liu, W., He, H., et al. (2017a). Chemotherapy Drugs Induce Pyroptosis through Caspase-3 Cleavage of a Gasdermin. *Nature* 547, 99–103. doi:10.1038/nature22393

Wang, Y., Hu, Z., Sun, B., Xu, J., Jiang, J., and Luo, M. (2015). Ginsenoside Rg3 Attenuates Myocardial Ischemia/reperfusion Injury via Akt/endothelial Nitric Oxide Synthase Signaling and the B-cell lymphoma/B-cell L-ymphoma-associated X P-rotein P-athway. *Mol. Med. Rep.* 11, 4518–4524. doi:10.3892/mmr.2015.3336

Wang, Y., Li, X., Wang, X., Lau, W., Wang, Y., Xing, Y., et al. (2013). Ginsenoside Rd Attenuates Myocardial Ischemia/reperfusion Injury via Akt/GSK-3β Signaling and Inhibition of the Mitochondria-dependent Apoptotic Pathway. *PLoS One* 8, e70956. doi:10.1371/journal.pone.0070956

Wang, Y., and Zhang, Y. (2016). The Effect and Mechanism of Ginsenoside Rb1 in Improving Myocardial Ischemia/reperfusion Injury via P38MAPK Pathway. *World Latest Med. Inf.* 16, 89–90.

Wang, Z., Zheng, Q., Liu, K., Li, G., and Zheng, R. (2006). Ginsenoside Rh(2) Enhances Antitumour Activity and Decreases Genotoxic Effect of Cyclophosphamide. *Basic Clin. Pharmacol. Toxicol.* 98, 411–415. doi:10.1111/j.1742-7843.2006.pto_348.x

Wang, Z. (2008). *Protective Effects of Ginsenoside Rb1 on Myocardial Ischemia-Reperfusion Injury and its Mechanisms*. Guangzhou (China): Sun Yat-sen University. [Doctor's Thesis].

WHO (2020). The Top 10 Causes of Death. Available at: https://www.who.int/en/news-room/fact-sheets/detail/the-top-10-causes-of-death (Accessed October 30, 2021).

Wu, Y., Xia, Z. Y., Dou, J., Zhang, L., Xu, J. J., Zhao, B., et al. (2011). Protective Effect of Ginsenoside Rb1 against Myocardial Ischemia/reperfusion Injury in Streptozotocin-Induced Diabetic Rats. *Mol. Biol. Rep.* 38, 4327–4335. doi:10.1007/s11033-010-0558-4

Wu, Y. (2011). *An Experimental Study on the Effects of Ginsenoside Rb1 against Myocardial Ischemia/reperfusion Injury in Streptozotocin-Induced Diabetic Rats*. Wuhan (China): Wuhan University. [Doctor's Thesis].

Xin, G. (2020). *Study on the Mechanism of Shuangshen Ningxin Apsule Regulating FUNDC1 Mediated Mitochondrial Autophagy to Protect Myocardial Ischemia-Reperfusion Injury*. Beijing (China): China Academy of Chinese Medical Sciences. [Master's Thesis].

Xu, J. F., Wan, Y., Tang, F., Chen, L., Yang, Y., Xia, J., et al. (2021a). Emerging Significance of Ginsenosides as Potentially Reversal Agents of Chemoresistance in Cancer Therapy. *Front. Pharmacol.* 12, 720474. doi:10.3389/fphar.2021.720474

Xu, T., Zhang, K., Kan, F., Li, F., Yu, B., Du, W., et al. (2019). Adeno-associated Virus 9-mediated Small RNA Interference of TLR4 Alleviates Myocardial Ischemia and Reperfusion Injury by Inhibition of the NF-Kb and MAPK

Signaling Pathways in Rats. *Curr. Mol. Med.* 19, 127–135. doi:10.2174/1566524019666190311122521

Xu, X. N., Jiang, Y., Yan, L. Y., Yin, S. Y., Wang, Y. H., Wang, S. B., et al. (2021b). Aesculin Suppresses the NLRP3 Inflammasome-Mediated Pyroptosis via the Akt/GSK3β/NF-Kb Pathway to Mitigate Myocardial Ischemia/reperfusion Injury. *Phytomedicine* 92, 153687. doi:10.1016/j.phymed.2021.153687

Xue, Y., Fu, W., Liu, Y., Yu, P., Sun, M., Li, X., et al. (2020). Ginsenoside Rb2 Alleviates Myocardial Ischemia/reperfusion Injury in Rats through SIRT1 Activation. *J. Food Sci.* 85, 4039–4049. doi:10.1111/1750-3841.15505

Yan, X., Liu, J., Wu, H., Liu, Y., Zheng, S., Zhang, C., et al. (2016). Impact of miR-208 and its Target Gene Nemo-like Kinase on the Protective Effect of Ginsenoside Rb1 in Hypoxia/Ischemia Injuried Cardiomyocytes. *Cell Physiol Biochem* 39, 1187–1195. doi:10.1159/000447825

Yan, X., Xue, J., Wu, H., Wang, S., Liu, Y., Zheng, S., et al. (2015). Ginsenoside-Rb1 Protects Hypoxic- and Ischemic-Damaged Cardiomyocytes by Regulating Expression of miRNAs. *Evid. Based Complement. Alternat Med.* 2015, 171306. doi:10.1155/2015/171306

Yang, W., Lai, Q., Zhang, L., Zhang, Y., Zhang, Y., Yu, B., et al. (2021). Mechanisms Dissection of the Combination GRS Derived from ShengMai Preparations for the Treatment of Myocardial Ischemia/reperfusion Injury. *J. Ethnopharmacol* 264, 113381. doi:10.1016/j.jep.2020.113381

Yang, Y. (2013). *Influences of Ginsenoside Rbi on Mitochondrial Dynamics in NRVMs Hypoxia/reoxyenation Model*. Shantou (China): Shantou University. [Master's Thesis].

Yi-Dan, H., Ying-Xin, Z., Shi-Wei, Y., and Yu-Jie, Z. (2021). High-Energy Phosphates and Ischemic Heart Disease: From Bench to Bedside. *Front. Cardiovasc. Med.* 8, 675608. doi:10.3389/fcvm.2021.675608

Yuan, C., Wang, H., and Yuan, Z. (2019). Ginsenoside Rg1 Inhibits Myocardial Ischaemia and Reperfusion Injury via HIF-1 α-ERK Signalling Pathways in a Diabetic Rat Model. *Pharmazie* 74, 157–162. doi:10.1691/ph.2019.8858

Zhai, M., Li, B., Duan, W., Jing, L., Zhang, B., Zhang, M., et al. (2017). Melatonin Ameliorates Myocardial Ischemia Reperfusion Injury through SIRT3-dependent Regulation of Oxidative Stress and Apoptosis. *J. Pineal Res.* 63, e12419. doi:10.1111/jpi.12419

Zhang, C., He, M., Ni, L., He, K., Su, K., Deng, Y., et al. (2020). The Role of Arachidonic Acid Metabolism in Myocardial Ischemia-Reperfusion Injury. *Cell Biochem Biophys* 78, 255–265. doi:10.1007/s12013-020-00928-z

Zhang, F. L., Liu, X. Y., Linn, Y. C., and Zhang, K. Z. (2002). Insulin Resistance Model Induced by Dexamethasone in Rats. *Zhongguo Ying Yong Sheng Li Xue Za Zhi* 18, 98–100.

Zhang, H., Wang, X., Ma, Y., and Shi, Y. (2019b2019). The Effect of Ginsenoside RB1, Diazoxide, and 5-Hydroxydecanoate on Hypoxia-Reoxygenation Injury of H9C2 Cardiomyocytes. *Evid. Based Complement. Alternat Med.* 2019, 6046405. doi:10.1155/2019/6046405

Zhang, H. (2020). *Ginsenoside Rb1 Attenuates HR Injury of H9c2 Cells through Mitochondrial ATP-Sensitive Potassium Channels*. Jinzhou (China): Jinzhou Medical University. [Master's Thesis].

Zhang, J. H., Yang, H. Z., Su, H., Song, J., Bai, Y., Deng, L., et al. (2021a). Berberine and Ginsenoside Rb1 Ameliorate Depression-like Behavior in Diabetic Rats. *Am. J. Chin. Med.* 49, 1195–1213. doi:10.1142/S0192415X21500579

Zhang, J., Zhuge, Y., Rong, X., Ni, C., Niu, C., Wen, Z., et al. (2021c). Protective Roles of Xijiao Dihuang Tang on Coronary Artery Injury in Kawasaki Disease. *Cardiovasc. Drugs Ther.*, 1–14. doi:10.1007/s10557-021-07277-w

Zhang, L. (2017). *Effects and Mechanism of Alprostadil and Ginsenoside Rg3 on Myocardial Ischemia/reperfusion Injury in Rats*. Jilin (China): Jinlin University. [Doctor's Thesis].

Zhang, L. P., Jiang, Y. C., Yu, X. F., Xu, H. L., Li, M., Zhao, X. Z., et al. (20162016). Ginsenoside Rg3 Improves Cardiac Function after Myocardial Ischemia/Reperfusion via Attenuating Apoptosis and Inflammation. *Evid. Based Complement. Alternat Med.* 2016, 6967853. doi:10.1155/2016/6967853

Zhang, Q., Liu, J., Zhang, M., Wei, S., Li, R., Gao, Y., et al. (2019a). Apoptosis Induction of Fibroblast-like Synoviocytes Is an Important Molecular-Mechanism for Herbal Medicine along with its Active Components in Treating Rheumatoid Arthritis. *Biomolecules* 9, 795. doi:10.3390/biom9120795

Zhang, X., Agborbesong, E., and Li, X. (2021b). The Role of Mitochondria in Acute Kidney Injury and Chronic Kidney Disease and its Therapeutic Potential. *Int. J. Mol. Sci.* 22, 11253. doi:10.3390/ijms222011253

Zhang, Z. L., Fan, Y., and Liu, M. L. (2012). Ginsenoside Rg1 Inhibits Autophagy in H9c2 Cardiomyocytes Exposed to Hypoxia/reoxygenation. *Mol. Cel Biochem* 365, 243–250. doi:10.1007/s11010-012-1265-3

Zhao, H., Zhang, D., Pang, L., Zhang, H., and Yu, R. (2021). Effects of Astragaloside IV and Ginsenoside Rg1 on Myocardial Apoptosis after Myocardial Ischemia Reperfusion Injury Hyperlipidemia Rats. *Liaoning J. Traditional Chin. Med.* 48, 188–191.

Zheng, T., Yang, J., Zhang, J., Yang, C., Fan, Z., Li, Q., et al. (2021). Downregulated MicroRNA-327 Attenuates Oxidative Stress-Mediated Myocardial Ischemia Reperfusion Injury through Regulating the FGF10/Akt/Nrf2 Signaling Pathway. *Front. Pharmacol.* 12, 669146. doi:10.3389/fphar.2021.669146

Zhou, C. (2009). *The Protective Effect of Rg2 on Hypoxic Myocardial Cells*. Qingdao (China): Qingdao University. [Master's Thesis].

Zhou, Q. L., Teng, F., Zhang, Y. S., Sun, Q., Cao, Y. X., and Meng, G. W. (2018). FPR1 Gene Silencing Suppresses Cardiomyocyte Apoptosis and Ventricular Remodeling in Rats with Ischemia/reperfusion Injury through the Inhibition of MAPK Signaling Pathway. *Exp. Cel Res* 370, 506–518. doi:10.1139/cjpp-2021-028910.1016/j.yexcr.2018.07.016

Zhu, H., Jia, Z., Misra, B. R., Zhang, L., Cao, Z., Yamamoto, M., et al. (2008). Nuclear Factor E2-Related Factor 2-dependent Myocardiac Cytoprotection against Oxidative and Electrophilic Stress. *Cardiovasc. Toxicol.* 8, 71–85. doi:10.1007/s12012-008-9016-0

Zhu, H., and Zhou, H. (2021). Novel Insight into the Role of Endoplasmic Reticulum Stress in the Pathogenesis of Myocardial Ischemia-Reperfusion Injury. *Oxid Med. Cel Longev* 2021, 5529810. doi:10.1155/2021/5529810

Conflict of Interest: The authors declare that the research was conducted in the absence of any commercial or financial relationships that could be construed as a potential conflict of interest.

Publisher's Note: All claims expressed in this article are solely those of the authors and do not necessarily represent those of their affiliated organizations, or those of the publisher, the editors, and the reviewers. Any product that may be evaluated in this article, or claim that may be made by its manufacturer, is not guaranteed or endorsed by the publisher.

Copyright © 2022 Chen, Wu, Li, Liu and Ren. This is an open-access article distributed under the terms of the Creative Commons Attribution License (CC BY). The use, distribution or reproduction in other forums is permitted, provided the original author(s) and the copyright owner(s) are credited and that the original publication in this journal is cited, in accordance with accepted academic practice. No use, distribution or reproduction is permitted which does not comply with these terms.

frontiers in Pharmacology

REVIEW
published: 02 March 2022
doi: 10.3389/fphar.2022.806175

Induction of Apoptosis by Metabolites of Rhei Radix et Rhizoma (Da Huang): A Review of the Potential Mechanism in Hepatocellular Carcinoma

Huanyu Jiang[1], *Wuyinuo Tang*[1], *Yang Song*[2], *Wei Jin*[2]* *and Quanyu Du*[3]*

[1]Department of Geriatrics, Hospital of Chengdu University of Traditional Chinese Medicine, Chengdu, China, [2]Emergency Department, Hospital of Chengdu University of Traditional Chinese Medicine, Chengdu, China, [3]Department of Endocrinology, Hospital of Chengdu University of Traditional Chinese Medicine, Chengdu, China

Liver cancer is a global disease with a high mortality rate and limited treatment options. Alternations in apoptosis of tumor cells and immune cells have become an important method for detailing the underlying mechanisms of hepatocellular carcinoma (HCC). Bcl-2 family, Caspase family, Fas and other apoptosis-related proteins have also become antagonistic targets of HCC. Da Huang (Rhei Radix et Rhizoma, RR), a traditional Chinese herb, has recently demonstrated antitumor behaviors. Multiple active metabolites of RR, including emodin, rhein, physcion, aloe-emodin, gallic acid, and resveratrol, can successfully induce apoptosis and inhibit HCC. However, the underlying mechanisms of these metabolites inhibiting the occurrence and development of HCC by inducing apoptosis is complicated owing to the multi-target and multi-pathway characteristics of traditional Chinese herbs. Accordingly, this article reviews the pathways of apoptosis, the relationship between HCC and apoptosis, the role and mechanism of apoptosis induced by mitochondrial endoplasmic reticulum pathway and death receptor pathway in HCC and the mechanism of six RR metabolites inhibiting HCC by inducing apoptosis.

Keywords: hepatocellular harcinoma, apoptosis, emodin, rhein, physcion, aloe-emodin, gallic acid, resveratrol

OPEN ACCESS

Edited by:
Hong Zhang,
Shanghai University of Traditional Chinese Medicine, China

Reviewed by:
Huimei Wang,
Fudan University, China
Shilin Xia,
The First Affiliated Hospital of Dalian Medical University, China

***Correspondence:**
Wei Jin
jinwei1983@cdutcm.edu.cn
Quanyu Du
quanydu@cdutcm.edu.cn

Specialty section:
This article was submitted to Ethnopharmacology, a section of the journal Frontiers in Pharmacology

Received: *31 October 2021*
Accepted: *24 January 2022*
Published: *02 March 2022*

Citation:
Jiang H, Tang W, Song Y, Jin W and Du Q (2022) Induction of Apoptosis by Metabolites of Rhei Radix et Rhizoma (Da Huang): A Review of the Potential Mechanism in Hepatocellular Carcinoma. Front. Pharmacol. 13:806175. doi: 10.3389/fphar.2022.806175

INTRODUCTION

Liver cancer is one of the five most common malignancies worldwide and comprises the second leading cause of cancer-related deaths, with an increasing incidence rate (Marengo et al., 2016). Hepatocellular carcinoma (HCC) accounts for 80–85% of liver cancer cases, and its frequency of occurrence varies greatly from region to region. Most new cases occur in East Asia and southern Africa (Lafaro et al., 2015). Without early detection, HCC patients face extremely low survival rates and limited treatment options with high costs (Gravitz 2014; Orcutt and Anaya 2018). During the past decade, both pharmacologic and nonpharmacologic treatments for HCC, such as resection, suppression, transarterial chemoembolization, and ablation, have improved and become widely used. Small-molecule targeted agents, monoclonal antibodies, and other medicines have gradually been refined (Jindal et al., 2019; Chen et al., 2020). Recently, the role of insufficient apoptosis in the development and progression of some cells, including hepatocytes, has become the primary focus in detailing the underlying mechanism and potential treatment targets of HCC.

As a natural barrier inhibiting the development of cancer, apoptosis is a programmed cell death mechanism that is finely regulated at the genetic level, leading to the effective elimination of damaged

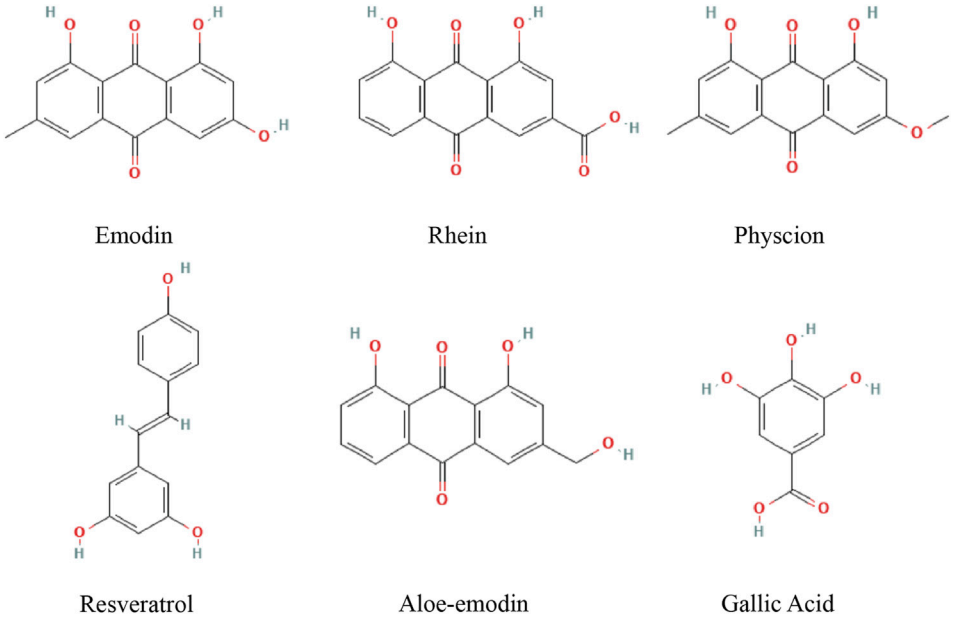


FIGURE 1 | Chemical structures of active metabolites of RR.

cells (such as DNA-damaged or infected cells) (Fuchs and Steller 2011). However, the evasion of and resistance to apoptosis are hallmarks of cancer cells, often leading to chemotherapy failure (Hanahan and Weinberg 2011; Cai et al., 2004). Therefore, a therapeutic strategy for apoptosis-resistant molecules may be effective.

RR comprises the dried roots and rhizomes of *Rheum palmatum* L., *Rheum tanguticum* Maxim. ex Balf., or *Rheum officinale* Baill. According to traditional Chinese medicine theory, RR eliminates heat toxicity, thereby eliminating stagnation and stasis. The most commonly used variety is *R. officinale* (Q. Huang et al., 2007). The main active metabolites of RR are anthraquinone derivatives. The 2020 edition of the Chinese Pharmacopoeia considers the contents of emodin, rhein, emodin, aloe-emodin, and chrysophanol in dried RR as quality control standards. Total anthraquinone content was calculated using these five metabolites. Some of these anthraquinone derivatives have attenuated HCC through apoptosis.

SEARCH STRATEGIES

For this review, research articles on the treatment of HCC with active ingredients of RR were collected from PubMed, the Cochrane Library Web of Science, and the EMBASE database. According to the quality control standard of RR in Chinese Pharmacopoeia and the quality evaluation index of RR in the articles, the relationship between 13 active ingredients and apoptosis in HCC was searched in the databases. Such as emodin, rhein, aloe-emodin, physcion, chrysophanol, sennoside B, sennoside A, gallic acid, catechins, resveratrol, epigallocatechin gallate, epicatechin and epicatechin gallate. Active metabolites that is not related to apoptosis were excluded. And the following types of article were excluded from our review: studies not lacking scientific value and those with obvious methodological errors. Overall, we have systematically explained the pharmacological mechanism of emodin, rhein, physcion, aloe-emodin, gallic acid, resveratrol regulating apoptosis in HCC cells, providing a reference for future research (**Figure1**).

APOPTOTIC PATHWAY

Apoptosis signals are mainly conducted through extrinsic and intrinsic apoptosis pathways (Pistritto et al., 2016). Intrinsic apoptosis mainly includes mitochondrial-dependent pathway and endoplasmic reticulum-dependent pathway. Intrinsic apoptosis is comprised of caspase-dependent apoptosis and caspase-independent apoptosis. Extrinsic apoptosis is mostly initiated by the binding of death receptors and ligands (Susin et al., 2000).

Intrinsic apoptosis pathways, which depend on mitochondria, are induced by a variety of highly heterogeneous intracellular stresses. These pathways are regulated by mitochondrial outer membrane permeabilization (MOMP), which can be changed by permeability transition pore complexes (PTPC) and the B-cell lymphoma-2 (Bcl-2) protein family members with pore-forming activity (Green and Kroemer 2004; Vande Walle et al., 2007). Intracellular stress signals, such as oxidative stress (OS), DNA damage, cytosolic Ca2+ overloads, and an accumulation of unfolded proteins in the endoplasmic reticulum, can activate the Bcl-2 protein family members of Bax and Bak, thereby damaging MOMP and releasing toxic proteins. These include

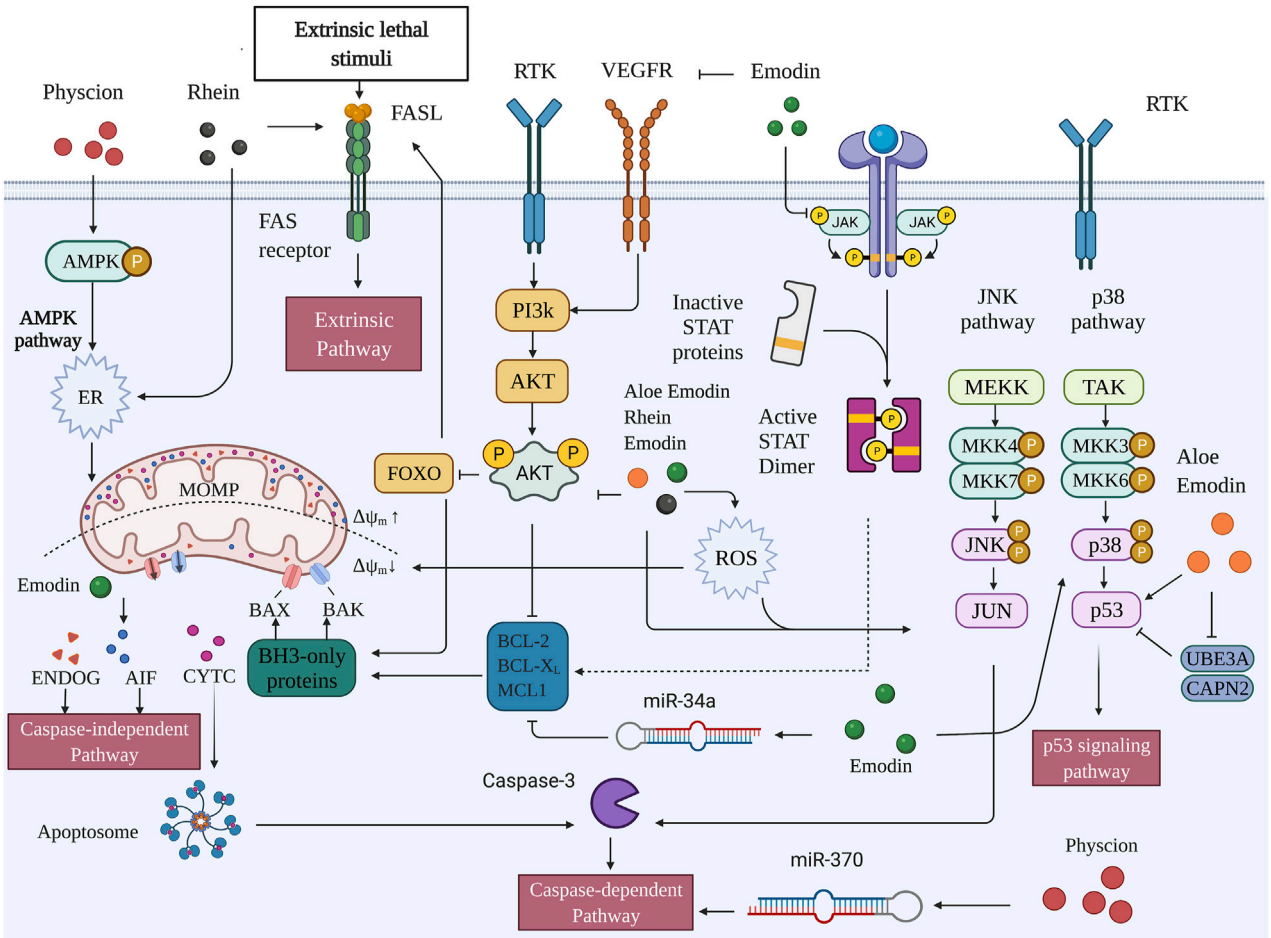


FIGURE 2 | Pro-apoptotic capacities of active metabolites of RR in HCC (Created with BioRender.com).

cytochrome C (CYTC), second mitochondria-derived activator of caspases (SMAC), high temperature requirement protein A2 (HTRA2), apoptosis-inducing factor (AIF), and endonuclease G (ENDOG), and are usually retained in the mitochondrial intermembrane space (IMS). These proteins are released to the cytosol, causing caspase-dependent and caspase-independent apoptosis (Danial and Korsmeyer 2004). Caspase is a cysteine protease family that contains 14 identified members, which are divided into two subgroups: interleukin 1β invertase (ICE) and abnormal cell death gene product 3 (CED-3). CED-3 subfamily, which is divided into initiator and executioner, is a major participant in the process of apoptosis. Caspase−2, −8, −9 and −10, as promoters of apoptosis, activate the executor of apoptosis through self-activation. Caspase−3, −6 and −7 are the executor of apoptosis and can directly degrade intracellular proteins to induce apoptosis after activation by promoter (Yan et al., 2021). Cytosolic CYTC promotes apoptosis by participating with apoptosis protease activating factor-1 (APAF-1) and dATP in forming apoptosomes, which recruit pro-caspase-9 and trigger the cleavage of pro-caspase-3. SMAC and HTRA2 depress caspase inactivation through inhibiting several members of the IAP family, thereby promoting the caspase-9→caspase-3 proteolytic cascade (Slee et al., 1999). AIF and ENDOG induce caspase-independent apoptosis by relocating to the nucleus, where they mediate large-scale DNA fragmentation (Büttner et al., 2007). In addition, HTRA2 can also act on the cytoskeleton because of its serine protease activity (Vande Walle et al., 2007). Endoplasmic reticulum stress (ERS) is the core of endoplasmic reticulum-dependent pathway. ERS refers to the accumulation of misfolded proteins, unfolded proteins, or correctly folded proteins in the endoplasmic reticulum, as well as changes in Ca2+ concentration and cholesterol synthesis, resulting in increased endoplasmic reticulum pressure and disturbance of cell balance (L. Zhang and Wang 2016). The unfolded protein reaction (UPR) triggered by the accumulation of unfolded proteins or misfolded proteins is the primary pathway of ERS. UPR is a self-protective measure for cells to promote endoplasmic reticulum folding ability. It depends on protein kinase R-like endoplasmic reticulum kinase (PERK), inositol requiring enzyme 1 (IRE1), and activating transcription factor-6 (ATF6). UPR can initiate cell apoptosis through signal molecules such as CHOP, caspase-12, JNK, Bax, etc. when cell damage is severe (Metcalf et al., 2020).

The extrinsic apoptosis pathway is a caspase-dependent subroutine of cell death induced by extracellular stress signals that are sensed and propagated by specific transmembrane receptors. When a death receptor is stimulated by its corresponding death ligand, its death domain (DD), a protein–protein interaction domain within the cell, interacts with other DD-containing proteins (Boldin et al., 1995; Schulze-Osthoff et al., 1998; Fulda and Debatin 2003; Guicciardi and Gores 2009). Subsequently, adaptor proteins recruited at the DD of Fas, i.e., a Fas-associated protein with a DD (FADD) or TNFR-associated DD (TRADD), capture other proteins. These may include receptor-interacting protein kinase 1 (RIP1), multiple isoforms of cellular FADD-like interleukin-1 converting enzyme inhibitory proteins (c-FLIP), cellular inhibitors of apoptosis proteins (cIAPs), and pro-caspase-8 and/or -10. These protein combinations form the death-inducing signal complex (DISC), which regulates the activation of caspase-8 (or -10) (Boatright and Salvesen 2003; Chang et al., 2003). Pro-caspase-8 (−10) catalyzes the proteolytic maturation of downstream effectors (e.g., caspase-3, -6, and -7), thereby triggering cell death (Budd et al., 2006; Kuribayashi et al., 2006). Some cells require an expansion step induced by caspase-8. In this case, capase-8 activates the cleavage of the BH3-interacting domain death agonist (BID), thereby generating truncated BID (tBID), which induces MOMP (Plati et al., 2008). Therefore, this works in conjunction with the intrinsic apoptosis pathway.

APOPTOSIS IN HCC

In normal hepatocytes, apoptosis is finely regulated by a series of genes to maintain homeostasis. Dysregulation of the balance between cell replication, growth, differentiation, and apoptosis is possibly related to the occurrence of preneoplastic lesions and hepatocarcinogenesis **Figure 2**.

Mitochondria-Mediated Apoptosis Pathway in HCC

Mitochondria mediated apoptosis is closely related to the Bcl-2 family which Bcl-2 family is divided into three main groups (Youle and Strasser, 2008). The first group is members of the anti-apoptotic family, including Bcl-2, Bcl-XL and Mc1-1, etc. Bcl-2 is usually located in the mitochondrial membrane and endoplasmic reticulum, and inhibits the activity of pro-apoptotic proteins and prevents MOMP by binding to the domain of pro-apoptotic protein BH3. The second group is pro-apoptotic family members, mainly including Bax, Bak and so on. Bax mostly exists in cytoplasm in the form of monomer, and after receiving apoptotic signal stimulation, Bax is transferred to the outer membrane of mitochondria, where Bax and Bak play a pro-apoptotic role together. A decrease in Bcl-2 leads to the fall of Bcl-2/Bax ratio, which is considered as a reliable signal of apoptosis. The third group is BH3-only pro-apoptotic family members, including Bad, Bid and BNIP3, which can induce apoptosis by blocking Bcl-2 or cooperating with Bax (Neophytou et al., 2021).

The expression of anti-apoptotic and pro-apoptotic members of Bcl-2 family is different at different stages of HCC. Most studies have shown that the expression of anti-apoptotic members such as Bcl-2 and Bcl-XL is elevated in tumor tissues of HCC patients (Hosseini-Khah et al., 2021; Y. YangZhu et al., 2011; Watanabe et al., 2004). Also, their elevation showed a significant anti-apoptotic effect on HCC cells such as HCC-9204 and SMMC-7721 *in vitro* (L. Yang et al., 2002; Yao et al., 2012) The decrease of Bax, Bad and other pro-apoptotic members in HCC tissues is associated with adverse clinical features such as vascular invasion, tumor differentiation and AFP (Hu et al., 2015; Garcia et al., 2002). Other studies have shown that Bcl-2 and Bcl-XL are expressed in a lower level in HCC than in normal liver tissues (X.Z. Guo et al., 2002). A research found that Bcl-2 expression was not even observed in HCC tumor tissues (Yoon et al., 1998). This is consistent with more active apoptosis in HCC cells than in normal liver tissues. Lower levels of Bcl-2 may inhibit the growth of tumors, and may also clear senescent tumor cells and promote the development of HCC. In conclusion, the Bcl-2 family tree changes in different tissues and stages of HCC. Interestingly, the expression of Bax decreased in different situations where Bcl-2 was increased or decreased. When Bcl-2 is lowered, Bax dropped more drastically, leading to the change of Bcl-2/Bax (X.Z. Guo et al., 2002). Changes in the ratio of anti-apoptotic members Bcl-2/MCL-1 also have an important impact on the efficacy of anti-tumor drugs in HCC (Tutusaus et al., 2018). Therefore, in mitochondria mediated apoptosis pathway, the balance of anti-apoptotic protein and pro-apoptotic protein is vital in the occurrence and development of HCC.

The anti-apoptotic mechanism of HCC is most closely related to MAPK and PI3K signaling pathways. MAPK pathway is an important signal transduction system of eukaryotic cells, which is comprised of four subfamilies. Extracellular signalregulated protein kinase (ERK), C-Jun N-terminal KINse/stress-activated protein kinase (JNK/SAPK), P38 kinase, and ERK5. Activation of ERK can promote the phosphorylation of Bcl-2, inhibit the apoptosis of HCC cells, and promote tumor development. The anti-apoptotic effect of ABT26-3, Gossypol and other Bcl-2 inhibitors is determined by the activation of ERK pathway (B. Wang et al., 2014; X. Zhao et al., 2011). The therapeutic effects of some natural products and anticancer drugs on HCC also involve the inhibition of ERK pathway, reduction of Bcl-2 (Tsai et al., 2020; W.T. Chen et al., 2019). Activation of JNK pathway promote the evasion from tumor surveillance. On the contrary, blocking JNK expression can inhibit the development of HCC cells, increase caspase recruitment, and induce apoptosis (Mucha et al., 2009). The p53 tumor suppressor gene (TP53) is a common downstream target of JNK and MAPK pathways. P53 can rely on the pro-apoptotic members of the Bcl-2 family such as Bax and Bak to send death stimuli to the mitochondria and induce apoptosis. P53 mutation is a common phenomenon in various cancers, and mutated P53 is also exist in HCC. The expression of Bax and Bak decreased significantly after p53 mutation, and the proliferation and metastasis of tumor cells induced by p53 mutation is an important mechanism of HCC (Meng et al., 2014). Bcl-2 and p53 antagonize each other. Bcl-2

can resist the pro-apoptotic effect of wild-type p53 in tumor cells, and the expression level of bcl-2 is increased in various tissues of p53 knockout mice. The induction of apoptosis through the activation of p53/Bcl-2 pathway in HCC cells is the main mechanism some antitumor drugs (Jiang et al., 2015). Coincidentally, the decreased p53 function is accompanied by overexpression of Bcl-xL and MCL-1, as well as a lack of response to Fas owing to the downregulation of FasL and the reduced expression of Bid in HCC associated with hepatitis B or C infections (May and May, 1999).

Phosphoinositide 3-kinase (PI3K) family is a proto-oncogene that regulates both inositol and phosphatidylinositol (PI). PI3K/Akt is an important pathway for regulating apoptosis in cancer cells. PI3k-activated Akt regulate apoptosis through the phosphorylation of downstream proteins mTOR, NF-KB, Bcl-2, Bad and Caspase-9 (G. Song et al., 2005). The activation of the PI3K/Akt/mTOR pathway negatively regulates Bad and positively regulates anti-apoptotic Bcl-2 family members, thereby promoting tumor growth and progression (Pollak, 2012). Additionally, the activation of nuclear factor-KB (NF-KB) upregulates the caspase-8 inhibitors c-FLIP, 191 c-IAP1, and c-IAP2, as well as the anti-apoptotic proteins Bcl-xL and Mcl-1 (Wajant et al., 2003). Activation of Akt in Hep3B increases cell resistance to antitumor drugs. Activation of Bcl-2 can increase the cancer stem cell-like behavior of Hep3B, promoting cell growth and tumor metastasis (You et al., 2017). CD133+ HCC cells contribute to chemoresistance through preferential activation of Akt/PKB and Bcl-2 cell survival response (S. Ma et al., 2008).

Endoplasmic Reticulum Mediated Apoptosis Pathway in HCC

When ERS is persistent, UPR is the main cause of apoptosis. UPR can initiate apoptosis through signal molecules such as CHOP, caspase-12, JNK, Bax, etc. CCAAT/enhancer binding protein homologous protein (CHOP) is infrequently expressed in normal cells and mostly activated in ERS state. CHOP triggers apoptosis through Inositol Requiring (IRE) 1-CHOP, PKR-like ER kinase (PERK)-CHOP, and activating factor (ATF) 6-CHOP, respectively. In HCC, CHOP can transcriptively up-regulate the death receptor TNF-related apoptosis ligand receptor 2 (TRAIL receptor 2), and then activate the extrinsic apoptosis pathway. In addition, CHOP induces apoptosis by the transcriptional induction of Bim (Yamaguchi and Wang 2004). ATP Citrate Lyase, a critical enzyme that inhibits cancer metabolic reprogramming, induces ERS in HCC cells and promotes apoptosis of HCC cells by activating the P-EIF2α/ATF4/CHOP axis (Zheng et al., 2021) Both PI3K inhibitors and melatonin can increase the expression of CHOP in HCC cells and inhibit the PI3K/Akt pathway to reverse ERS-induced adriamycin resistance (Fan et al., 2013). Silencing the expression of CHOP in HCC cells can significantly reduce ERS-induced apoptosis (Lei et al., 2017).

Caspase-12-mediated apoptosis is unique to the endoplasmic reticulum pathway. Caspase-12 exists in the outer membrane of the endoplasmic reticulum and is a key protein in the endoplasmic reticulum-mediated apoptosis pathway (Vande Walle et al., 2016). Caspase-12 is activated by tumor necrosis factor receptor associated factor 2 (TRAF2), calproteinase, and caspase-7, and induces apoptosis of HepG2 and BEL-7402 cells (Song et al., 2021).

Persistent ERS can also be activated by phosphorylation of JNK through IRE1-α. JNK directly regulates Bcl-2/Bax ratio and induces apoptosis by increasing death receptor level and mitochondrial permeability (Shigemi et al., 2017). *In vivo*, mice deficient in both JNK1 and JNK2 have an increased risk of developing HCC (Das et al., 2011). *In vitro*, activation of JNK promotes apoptosis of Hep3B cells (S.Y. Kim et al., 2020).

Death Receptors Mediated Apoptosis Pathway in HCC

Death receptors associated with HCC apoptosis include Fas, DR5, DR4, DR3 and TNFR1, which exist on the cell surface in the form of membrane molecules and bind with TNF-related apoptosis-inducing ligand (TRAIL) to induce apoptosis. The expression rate of Fas in serum of HCC patients is 100% while it is reduced in poorly differentiated cancer cells. The level of Fas/FasL in cancer cells can be used as a prognostic indicator for HCC patients and predict the recurrence of HCC (Ito et al., 2000; Sacco et al., 2000). The expression of Fas on immune cells also plays an important role in HCC. The interaction of Fas/FasL can lead to excessive turnover of $CD8^+$ T cells in HCC patients (C.L. Guo et al., 2014). Elevated Fas expression is related to increased apoptosis of circulating CD8 (+) T cell in HCC patients. This may be an important mechanism of immune escape of HCC cells. Death receptor 5 (DR5) is rarely expressed in normal liver cells, but highly expressed in HCC cell lines. The specific agonistic antibody against DR5 can selectively induce HCC cell apoptosis *in vitro* and is harmless to normal hepatocytes (Zhu et al., 2006). Therefore, DR5 is also a critical target in HCC cell apoptosis induced by a variety of natural drugs and anti-tumor drugs (Kawahara et al., 2013; J; Yang et al., 2011). Death receptor 4 (DR4) and death receptor 3 (DR3) also induce apoptosis in HCC cells. In Hep3B and other HCC cell lines, DR4 is targeted by Mir-106b, and Mir-106b inhibitors can induce increased DR4 expression and enhance TRAIL-mediated HCC apoptosis (Xu et al., 2017). The expression of DR3 increases in HepG2, Huh7, SMMC7721 and BEL-7402 HCC cells. Silencing DR3 in BEL-7402 inhibited the expression of NF-κB and p53, enhanced the expression of Fas, caspase-3 and caspase-8, and induced the apoptosis of HCC cells (Zhang Y. C. et al., 2015). Tumor necrosis factor receptor 1 (TNFR1) has a dual role in the development of HCC. The formation of TNFR1-complex I supports cell survival while TNFR1-complex II leads to apoptosis (Zou et al., 2020).

ACTIVE INGREDIENTS OF RHEI RADIX ET RHIZOMA USED FOR HCC TREATMENTS

Emodin

Emodin (1, 3, 8-trihydroxy-6-methylanthraquinone) is a natural product derived from several Chinese herbs, including *R. palmatum*, *Polygonum cuspidatum*, and *Polygonum*

multiflorum. It comprises an orange-red powder or crystal that exists in the form of its glycosides (X. Dong et al., 2016). Emodin is an insoluble compound with a melting point of 255°C and is soluble in alcohol and dimethyl sulfoxide (Semwal et al., 2021). Emodin directly regulates both intrinsic and extrinsic apoptosis as well as affects upstream pathways such as the MAPK, PI3K/AKT, VEGFR, and miRNA.

Lin et al. have demonstrated that emodin inhibits the proliferation of SMMC-7721 cells and induced apoptosis in a dose- and time-dependent manner and suppressed tumor growth in BALB/c-nu nude mice inoculated with SMMC-7721. Moreover, emodin may exert these effects by activating p38 and inhibiting p-AKT. In addition, emodin mildly suppresses the activation of c-Jun N-terminal kinase (JNK). Given that JNK is a sub-pathway of the MAPK pathway and plays an important role in apoptosis, the JNK pathway may minimally influence emodin's proapoptotic effect (Lin et al., 2016). Yang et al. incubated BEL-7402 cells with emodin at 25, 50, 100, 200, 400, and 600 μmol/L for 12, 24, and 48 h, and found the emodin successfully regulated intrinsic apoptosis by upregulating the expressions of BAX, CTYC, actin fiber-associated protein 1 (AFAP1), cleaved-caspase-9, cleaved-caspase-3, and Bcl-2. Moreover, the sterol regulatory element binding protein 1 (SREBP1) was also regulated, and a significant decrease in the expression of mRNA and proteins of SREBP1 was observed. Furthermore, apoptosis and similar changes in protein expressions were found in SREBP1 knockout B cells, but the apoptosis rate was lower than that in emodin-treated cells; this suggests that RR induces apoptosis through both SREBP1-dependent and SREBP1-independent pathways (N. Yang et al., 2019). A recent study by Cui et al. indicated that emodin induced intrinsic apoptosis and extrinsic apoptosis in HepG2 cells, in which treatment with 10–100 μM of emodin attenuated the phosphorylation of AKT and ERK and promoted phosphorylation of p38. Notably, inhibiting PI3K/Akt and ERK and activating p38 can strengthen emodin-induced apoptosis (Cui et al., 2016). Similar results were also observed in another study by Bai et al., who studied the mechanism of emodin from the perspective of the VEGF-AKT-ERK1/2 signaling pathway. In their study, emodin reduced p-VEGFR2, p-ERK, p-ERK1/2, and p-AKT levels in both HepG2 cells and BALB/C nude mice subcutaneously injected with HepG2. Additionally, emodin increased the expression level of miR-34a and reduced the protein levels of SMAD2, SMAD4, and p-SMAD2 (Bai et al., 2020). Subramaniam et al. treated HepG2 cells with 10, 25, and 50 μM of emodin and found that emodin induces apoptosis through inhibiting the STAT3 signaling cascade. Specifically, emodin suppressed STAT3 phosphorylation, its translocation to the nucleus, and its binding capacity to DNA in HepG2, which is mediated by modulating the activation of upstream kinases c-Src, JAK1, and JAK2 (Subramaniam et al., 2013). The Hippo pathway is closely related to OS with Yes-associated protein 1 (YAP1) as one of its key downstream targets and a transcriptional activator that mediates reactive oxygen species (ROS) signals. Large tumor suppressor homolog 1 (LATS1) is a signal protein related to the Hippo pathway. (Morinaka et al., 2011; Wada et al., 2011; Xiao et al., 2011). Lee et al. treated HepG2, SK-Hep-1, Huh-7, and HeLa cells with 3–30 μM of emodin and found that low-dose emodin exerted cytoprotective effects by attenuating arachidonic acid and iron-induced OS. Thus, lactate dehydrogenase (LDH) levels and apoptosis induced by OS decreased. In HepG2 cells, emodin induced the phosphorylation of YAP and LATS1, but HeLa cells did not show these changes. In addition, the AMPK marker p-liver kinase B1 (LKB1), which is the upstream target of acetyl CoA carboxylase and AMPK, was upregulated, whereas emodin demonstrated no cytoprotective effect in LKB1-deficient HeLa cells (Lee et al., 2020).

Emodin contains several free phenolic hydroxyl groups that are easily oxidized in air and have poor solubility, low oral bioavailability, and low stability (Liu et al., 2016a). Therefore, researchers are consistently attempting to improve its formulation, so that this compound can more accurately, efficiently, and stably promote apoptosis in HCC cells. Preparing hydrophobic drugs using nanoparticles as carriers increases the uptake by HCC cells and reduces drug resistance. Synergistic drug use can increase drug concentration in target organs, prolong drug action time, and reduce drug dose and toxic side effects in organs that are not the intended target, so that the drug has stronger anticancer effects. Nanoparticles can be internalized by tumor cells directly without the need for biofilm transport (Mei et al., 2013; Y. Guo et al., 2013). Liu et al., 2016a combined heparin and emodin with a nano-molecular carrier polylactic-co-glycolic acid-D-α-tocopheryl polyethylene glycol 1,000 succinate (PLGA-TPGS) to form heparin-loaded PLGA-TPGS nanoparticles and emodin-loaded PLGA-TPGS nanoparticles, respectively. Moreover, the researchers found that the two synergistically promote apoptosis *in vivo* and *in vitro*, and inhibit tumor growth *in vivo* (Liu et al., 2016a; Liu et al., 2016b). Dong et al. distributed emodin in a new type of biomaterial N-acetylaminogalactosyl-poly (lactide-co-glycolide)-succinyl-D-a-tocopherol polyethylene glycol 1,000 succinate (GalNAc-PLGA-sTPGS) to form a new type of nanoparticle, EGTPN, and found that EGTPN *in vitro* induced HepG2 apoptosis more effectively than emodin alone (H. Dong et al., 2018). In addition, combining emodin with other drugs is also a way to enhance its anticancer effects. Kim et al. revealed that 120 μM of emodin can enhance the antitumor effects of sorafenib at a low dose (2 μM) in Hep3B, HepG2, and Huh7 cells. Compared with emodin or sorafenib alone, the combination of the two drugs significantly increased the apoptosis rate of HepG2 cells, inhibited cell proliferation, and induced G1 phase arrest. Furthermore, the combination of the two drugs can regulate lipid metabolism in HepG2 and SK-HEP-1 cells and inhibit STAT3 phosphorylation in HepG2 and PLC/PRF5 cells. This group also performed *in vitro* experiments and found that emodin and sorafenib inhibited tumor growth in xenografted HepG2 and SK-HEP-1 mice (Y.S. Kim et al., 2018).

Rhein

Rhein (4,5-dihydroxyanthraquinone-2-carboxylic acid) is a lipophilic anthraquinone that exists in *R. palmatum*, *Cassia tora* L., *P. multiflorum*, and *Aloe barbadensis* Miller (Zhou

et al., 2015). Induction of ER stress by regulating the mitochondrial membrane potential (MMP) and mitochondrial permeability transition (MPT) are the primary mechanisms by which rhein promotes apoptosis in HCC cells.

In a previous study, swelling and leakage of Ca^{2+} were observed in isolated liver mitochondria when treated with 100 and 200 μM of rhein; however, these changes were inhibited by 1 μM cyclosporin A (CsA), an MPT inhibitor. In addition, rhein may also induce the loss of MMP, activate caspase-3, release CYTC, and reduce the production of ATP in HepG2 cells, whereas CsA may weaken these effects (Du et al., 2013). Moreover, treatment with 5–80 μM rhein may decrease the energy metabolism of SMMC-7221 and SMMC-7221/doxorubicin-resistant cells by inhibiting oxidative phosphorylation. However, CsA cannot reverse the inhibition of energy metabolism via rhein (Wu et al., 2019). Rhein can increase caspase-3 activity when combined with doxorubicin, which may be related to the increase in the concentration of doxorubicin in cells (Wu et al., 2020). Upregulation of the BIM gene (an ER stress-induced gene) is one of the key mechanisms of rhein-induced apoptosis in HCC cells. Wang et al. treated HepG2 cells with 75–150 μM of rhein, and apoptosis was enhanced, which was confirmed by the increase in the expression of the BIM gene, the cleavage of caspase-3,7,8, and the level of t-Bid (J. Wang et al., 2015). ROS can activate the JNK kinase, which subsequently phosphorylates its substrate c-Jun, and phosphorylated c-Jun further induces the activation of caspase-3 (Y. Wang et al., 2018). A recent study found that treatment with 50–200 μM of rhein significantly increased ROS in HepG2 cells and Huh7 cells in a dose-dependent manner. N-acetylcysteine, a ROS scavenger, significantly inhibited the pro-apoptotic effect of rhein. These results demonstrated that rhein-induced ROS activated the JNK/Jun/caspase-3 signaling pathway apoptosis *in vitro* (A. Wang et al., 2020).

Koramagazi et al. demonstrated that rhein can also promote apoptosis in normal hepatocytes. In HL-7702 cells, rhein induced caspase-dependent apoptosis by targeting ER stress-related pathways, including glucose-regulated protein 78 (GRP 78), PKR-like ER kinase (PERK), JNK, and the CCAAT/enhancer-binding protein homologous protein (CHOP) (Koramagazi et al., 2016). Li et al. investigated the activation of the intrinsic and extrinsic apoptosis pathways in L02 cells *via* rhein. Specifically, rhein increased ROS, tumor necrosis factor-α (TNF-α), tumor necrosis factor receptor (TNFR), and TRADD, cleaved caspase-3, and reduced MMP and pro-caspase-9 and -3. Notably, the decrease in the levels of the autophagy-related proteins LC3-II and Beclin-1 and increase in the expression of P62 indicated that rhein promoted apoptosis of L02 cells by inhibiting autophagy and decreasing their self-scavenging ability (Li et al., 2019).

Physcion

Physcion (1,8-dihydroxy-3-methoxy-6-methyl-anthraquinone), also known as parietin, is a natural anthraquinone derivative that has proven antitumor, antibacterial, anti-inflammatory, antioxidant, and lipid metabolism regulation effects (Xunli and Chen., 2019). Physcion mainly interferes with proteases of the intrinsic apoptosis pathway, ER stress, and miRNA.

Pan et al. revealed that physcion can induce ER stress by activating the AMPK signaling pathway, thus resulting in intrinsic apoptosis. In Huh-7 and Bel-7402 cells, physcion promoted the phosphorylation of AMPK and activated ER stress by increasing caspase-12 activation and protein levels of p-PERK, as well as activating transcription factor 6 (ATF6), heavy-chain binding protein (BIP), GRP78, GRP94, p-eukaryotic translation initiation factor 2A (p-EIF2A), and CHOP. The levels of caspase-12 and CHOP decreased following a treatment with compound C (an AMPK inhibitor) (X.P. Pan et al., 2018). Recombinant DNA methyltransferase 1 (DNMT1) is one of the major enzymes responsible for establishing and maintaining DNA methylation patterns in eukaryotic cells, and is involved in the regulation of miRNAs in tumor cells, including miR-370; by comparison, Sp1 is an upstream transcription factor that regulates the expression of DNMT1 (Datta et al., 2008; Zeng et al., 2012; Yie et al., 2015; Zhao et al., 2015). In another study, physcion increased the level of miR-370, and HCC cell lines transfected with miR-370 mimics showed higher miR-370 levels and apoptosis, whereas an miR-370 inhibitor abolished the physcion-induced apoptosis. Additionally, physcion upregulated pAMPK/tAMPK and downregulated the levels of DNMT1 and Sp1. Accordingly, physcion induced intrinsic apoptosis by upregulating miR-370 *via* the AMPK/Sp1/DNMT1 signaling pathway (X. Pan et al., 2016).

Aloe-Emodin

Aloe-emodin (1,8-dihydroxy-3-hydroxymethyl-anthraquinone), a common anthraquinone component derived from *Cassia occidentalis*, *R. palmatum*, *Aloe vera*, and *P. multiflorum*, exerts a wide range of pharmacological impacts, including antiviral, anti-inflammatory, antibacterial, anti-parasitic, neuroprotective, and liver-protective effects (X. Dong et al., 2020). The effect of aloe-emodin on apoptosis is closely related to p53 and OS.

In p53 positive HepG2 cells, 1–20 μM of aloe-emodin led to the accumulation of p53 as well as stimulated an increase in the expression of p21 (a cyclin-dependent kinase inhibitor), which was associated with cell cycle arrest in the G1 phase, cell surface molecule lefas/APO1, and Bax. In contrast, aloe emodin did not mediate the expression of Fas/APO1 or inhibited cell cycle progression in P53-deficient Hep3B cells. However, it did promote apoptosis by enhancing the expression of P21 and Bax. (Kuo et al., 2002). Calpain 2 (CAPN2) is a growth promoting protein, and ubiquitin protein ligase E3A (UBE3A) is an oncogenic associated protein, and is a member of the ligase family of E6AP. Both proteins participate in the degradation of p53 (Y. Huang and Wang 2001; L. Liu et al., 2008; Baron et al., 2006; Scheffner et al., 1993; Cooper et al., 2003). A study by Jeon et al. indicated that aloe-emodin can promote intrinsic apoptosis by improving DNA fragmentation and ROS accumulation, and by reducing CAPN2 and UBE3A levels (Jeon et al., 2012). Lu et al. focused on the potential mechanism underlying the pro-OS and pro-apoptotic effects of aloe-emodin. They found that treatment with 10–40 μM of aloe-emodin significantly increased the oxidation of peroxiredoxin (PRDX), a marker of OS and

antioxidant in liver tissue. It also increased intracellular ROS levels and decreased glutathione (GSH)/oxidized glutathione (GSSG) in HepG2 cells. Furthermore, a delayed and sustained phosphorylation of JNK and its downstream substrate c-Jun and a decreased phosphorylation of ERK occurred 3 h following aloe-emodin treatment. In addition, HepG2 cells treated with overexpressed antioxidant sod1 (pEGFP-c3/sod1) and aloe-emodin at the same dose decreased OS, JNK activation, and caspase-9. The same treatment was also performed on HCCM cells and Hep3B cells; the results showed that these effects of aloe-emodin were not cell line-specific (Lu et al., 2007).

Gallic Acid

Gallic acid (3,4,5-trihydroxybenzoic acid, GA) is a naturally occurring phenolic acid. It is widely found in a wide range of plants such as gallnuts, teas, grapes and RR (Ma et al., 2003). GA induce apoptosis in a variety of malignant tumors. GA can selectively induce apoptosis of HCC cell lines without affecting normal hepatocytes. Its mechanism of promoting apoptosis is most closely related to the mitochondrial pathway (Ma et al., 2003).

Sun treated SMMC-7721 cells and hepatocytes with 0, 6.25, 12.5 and 25.0 μg/mL GA and found GA increased the activity of caspase-3, caspase-9 and ROS, decreased MOMP, and induced apoptosis of SMMC-7721 cells. However, GA had no effect on apoptosis of hepatocytes HL-7702. These results indicate that GA has a selective anticancer agent that induces apoptosis in SMMC-7721 cells (Sun et al., 2016). Lima et al. demonstrated a dose-dependent decrease of vitality in GA-treated HepG2 cells and a significant increase of the percentage of cells in early apoptosis. Furthermore, the levels of IL-10 and IL-12 were significantly increased and the levels of IL-8 were decreased after GA treatment. These results suggest that GA has anti-proliferation, pro-apoptotic and anti-inflammatory effects on HepG2 cells (Lima et al., 2016). Shi et al. found GA promoted apoptosis of HepG2 cells and BEL-7402 cells in a dose-dependent manner by up-regulating Bax and down-regulating Bcl-2 and Bcl-XL. Long non-coding RNA (LncRNA) is considered to be a key regulator of tumorigenesis. Overexpression of metastatic lung adenocarcinoma transcript 1 (MALAT1) promotes the proliferation and metastasis of HCC through the MALAT1/Wnt signaling axis. MALAT1 was down-regulated in both GA-treated HCC cells, and overexpression of MALAT1 partially reversed GA-induced inhibitory proliferation and metastasis, and successfully eliminated the inhibition of Wnt/β-catenin signaling. These results suggest that the potential mechanism of GA promoting HCC apoptosis may be related to the inhibition of lncRNA Malat1-Wnt/β-catenin signaling axis (Shi et al., 2021). Methyl gallate (MG), a metabolite of GA, can also induce apoptosis of HCC cell lines, which is associated with activation of caspase-3 and regulation of Bcl2, Bax and Bad ligand levels (C.Y. Huang et al., 2021). Like many natural compounds, the clinical application of GA is limited by factors such as low bioavailability, poor oral absorption, and rapid metabolic elimination. Therefore, Ahmed encapsulated GA in PLGA-CS-PEG nanocomposite to form Gallic acid nanocomposite (GANC) and demonstrated that GANC could reduce AFP, ENG, HSP-90, Bcl-2, pro-caspase3 and LCN-2 levels of adult female Wistar rats afflicted with HCC. Pharmacokinetic analysis revealed that GANC displayed a characteristic sustained release profile with 4-fold increase in bioavailability in normal and HCC-induced rats (Ahmed et al., 2018).

Resveratrol

As a polyhumic compound, resveratrol (3,5,4′-trihydroxystilbene) exists naturally in more than 70 plant species (Gecibesler et al., 2021). It can inhibit the proliferation of a variety of human tumor cells, and the potential mechanism of its inhibition on HCC cells is related to the activation of mitochondria-dependent pathway.

Ou et al. found that resveratrol at a concentration of more than 10 μM could significantly inhibit the activity of HepG2 cells and induce apoptosis in a dose-dependent manner via activation of caspase-3 and caspase-9, up-regulation of the ratio of Bax/Bcl-2 and induction of p53 expression. In addition, cell cycle progresssion was arrested in the G1 and S phase. Moreover, the apoptosis-inducing effect of resveratrol can be potentiated by matrine, which is attributed to the cleavage of PARP-1, the activation of caspase-3 and caspase-9, production of ROS and disruption of MOMP (Ou et al., 2014). Karabekir treated HCC male Albino Wistar rats with 50, 75 and 100 mg/kg resveratrol, respectively, and found 50 and 100 mg/kg RSV can significantly decrease enzyme activity (ALT,AST, GGT and ALP). RSV at 75 mg/kg and 100 mg/kg could significantly enhance p53 expression. 100 mg/kg RSV significantly up-regulated Bax, down-regulated Bcl-2, and induced apoptosis of HCC cells (Karabekir and Özgörgülü 2020). Using the same model, Zhang proved that 50 mg/kg RSV can inhibit liver tumorigenesis by inducing cell apoptosis and down-regulating the expression of Myosin Light Chain kinase (MLCK) (X.L. Zhang et al., 2013). Olugbami et al. studied the effects of different doses of resveratrol on HepG2 and their outcomes revealed that resveratrol inhibited the proliferation of HepG2 in a dose-dependent and time-dependent manner. In addition, at lower concentrations (0.39–3.13 μg/ml), resveratrol has higher tendency to activate caspase-3 and caspase-7 (Olugbami et al., 2017).

DISCUSSION

With advancements of pharmacological technology such as high-throughput screening, an increasing number of natural products with certain chemical structures have exerted a variety of pharmacological effects on patients. As a result, these products have the potential to become new drugs that can be used to treat many diseases. Anthraquinones and their derivatives are widely found in nature and can be divided into three categories. Anthraquinone compounds are the main active metabolites of RR and have a variety of pharmacological activities, including antiviral, anti-inflammatory, antioxidant, and antibacterial effects. Among them, emodin, rhein, physcion, aloe-emodin, gallic acid, resveratrol demonstrate oral bioavailability (OB) values of 24.40, 83.38, 22.29, 47.07, 31.69, and 19.07 as well as

drug-likeness (DL) values of 0.24, 0.28, 0.27, 0.24, 0.04 and 0.11 respectively. Moreover, they have superior safety, and other advantages from the perspective of new drug development. The ADME parameters of rhein and aloe-emodin have certain advantages, whereas low bioavailability limits the clinical applications of emodin, resveratrol, and resveratrol; new formulations or structural modifications are needed to improve their pharmacokinetic parameters and promote their clinical applicability. According to current research, emodin, rhein, physcion, aloe-emodin, gallic acid, and resveratrol have considerable therapeutic effects on HCC, with apoptosis playing a critical role in their action mechanisms. Emodin has the most complex action mechanism, as it is related to both intrinsic and extrinsic apoptotic pathways and involves multiple upstream pathways that also interact with each other. Both rhein and physcion are related to the intrinsic apoptotic pathway and interfere with ER stress. The difference is that rhein can also downregulate MMP, whereas physcion can regulate miRNA expression. Aloe-emodin upregulates p53 and promotes OS, indirectly promoting cell apoptosis. Studies on other ways of treating HCC with these constituents, such as anti-angiogenic and anti-metastatic action, cell cycle arrest, and antioxidant and anti-inflammatory activities, are also being performed. These different action mechanisms share some common targets and synergistically provide antitumor benefits (He et al., 2009; Hsu et al., 2010; Zhang K et al., 2015; Xing et al., 2018; Cui et al., 2020).

RR is more commonly used as a laxative in TCM, and anthraquinones also have strong laxative effects (Srinivas et al., 2007). Therefore, it is necessary to watch for gastrointestinal side effects when using anthraquinones. Moreover, problems regarding how to more precisely target the liver, improve efficacy, and reduce side effects remain. There have been attempts to combine with other drugs or nanoparticles, but additional evidence is required (Akkol et al., 2021). Additionally, the current research still focuses on *in vitro* tests, with few animal and clinical tests. The anti-cancer effects of these ingredients *in vivo* still need to be verified. Although many experiments have proven that the active ingredients of RR can regulate various signals in the apoptosis of HCC cells, the specific link between its action mechanism, binding molecules, and binding sites are still unclear. Studies have used rhein and aloe-emodin as ligands and JUN proteins as protein receptors for molecular docking, and found that their affinity values were −6.3 and −6.1 kcal/mol, respectively, indicating strong binding activity between the two and JUN (Jiang L, et al., 2021). A molecular docking of BAX and aloe-emodin showed an affinity value of −15.72, implying a high binding affinity between them (Mulakayala C, et al., 2013). These studies are based on bioinformatic analyses and thus provide predictions for proteins or molecules that may interact with the metabolites of RR, but further experiments are needed to explore specific binding methods and sites.

As the main quality control indicators of RR, emodin, rhein, physcion, aloe-emodin, gallic acid, and resveratrol can inhibit the development of HCC through inducing apoptosis. RR may constitute a potential drug for treating HCC, and its clinical value is worth exploring in future studies.

AUTHOR CONTRIBUTIONS

HJ and WT contributed equally to this work. HJ conceived the study. WT was responsible for organizing the literature and drawing chemical formulas. QD, WJ, and YS reviewed and summarized the literature. HJ was in charge of consulting the literature. HJ and WT wrote the manuscript and drew the figures. QD supervised the study and gave final approval of the version to be published. The final version of the manuscript was read and approved by all authors.

ACKNOWLEDGMENTS

We thank Dr. F. Wang for constructive comments and his help in the field during the review process. We are grateful to Qian Dai for her help in producing several of the figures.

REFERENCES

Ahmed, H. H., Galal, A. F., Shalby, A. B., Abd-Rabou, A. A., and Mehaya, F. M. (2018). Improving Anti-cancer Potentiality and Bioavailability of Gallic Acid by Designing Polymeric Nanocomposite Formulation. *Asian Pac. J. Cancer Prev.* 19 (11), 3137–3146. doi:10.31557/apjcp.2018.19.11.3137

Akkol, E. K., TatlıII, Karatoprak, G. Ş., Ağar, O. T., Sobarzo-Sánchez, E., and Capasso, R. (2021). Is Emodin with Anticancer Effects Completely Innocent? Two Sides of the Coin. *Cancers (Basel)* 13 (11), 2733. doi:10.3390/cancers13112733

Bai, J., Wu, J., Tang, R., Sun, C., Ji, J., Yin, Z., et al. (2020). Emodin, a Natural Anthraquinone, Suppresses Liver Cancer *In Vitro* and *In Vivo* by Regulating VEGFR2 and miR-34a. *Invest. New Drugs* 38 (2), 229–245. doi:10.1007/s10637-019-00777-5

Baron, C. A., Tepper, C. G., Liu, S. Y., Davis, R. R., Wang, N. J., Schanen, N. C., et al. (2006). Genomic and Functional Profiling of Duplicated Chromosome 15 Cell Lines Reveal Regulatory Alterations in UBE3A-Associated Ubiquitin-Proteasome Pathway Processes. *Hum. Mol. Genet.* 15 (6), 853–869. doi:10.1093/hmg/ddl004

Boatright, K. M., and Salvesen, G. S. (2003). Mechanisms of Caspase Activation. *Curr. Opin. Cel Biol* 15 (6), 725–731. doi:10.1016/j.ceb.2003.10.009

Boldin, M. P., Mett, I. L., Varfolomeev, E. E., Chumakov, I., Shemer-Avni, Y., Camonis, J. H., et al. (1995). Self-association of the "death Domains" of the P55 Tumor Necrosis Factor (TNF) Receptor and Fas/APO1 Prompts Signaling for TNF and Fas/APO1 Effects. *J. Biol. Chem.* 270 (1), 387–391. doi:10.1074/jbc.270.1.387

Budd, R. C., Yeh, W. C., and Tschopp, J. (2006). cFLIP Regulation of Lymphocyte Activation and Development. *Nat. Rev. Immunol.* 6 (3), 196–204. doi:10.1038/nri1787

Büttner, S., Eisenberg, T., Carmona-Gutierrez, D., Ruli, D., Knauer, H., Ruckenstuhl, C., et al. (2007). Endonuclease G Regulates Budding Yeast Life and Death. *Mol. Cel* 25 (2), 233–246. doi:10.1016/j.molcel.2006.12.021

Cai, Y., Sun, M., Xing, J., and Corke, H. (2004). Antioxidant Phenolic Constituents in Roots of *Rheum officinale* and *Rubia cordifolia*: Structure-Radical Scavenging Activity Relationships. *J. Agric. Food. Chem.* 52 (26), 7884–7890. doi:10.1021/jf0489116

Chang, D. W., Xing, Z., Capacio, V. L., Peter, M. E., and Yang, X. (2003). Interdimer Processing Mechanism of Procaspase-8 Activation. *Embo j* 22 (16), 4132–4142. doi:10.1093/emboj/cdg414

Chen, W. T., Hsu, F. T., Liu, Y. C., Chen, C. H., Hsu, L. C., and Lin, S. S. (2019). Fluoxetine Induces Apoptosis through Extrinsic/Intrinsic Pathways and Inhibits ERK/NF-KB-Modulated Anti-Apoptotic and Invasive Potential in Hepatocellular Carcinoma Cells In Vitro. *Int. J. Mol. Sci.* 20 (3). doi:10.3390/ijms20030757

Chen, Z., Xie, H., Hu, M., Huang, T., Hu, Y., Sang, N., et al. (2020). Recent Progress in Treatment of Hepatocellular Carcinoma. *Am. J. Cancer Res.* 10 (9), 2993–3036.

Cooper, B., Schneider, S., Bohl, J., Jiang, Yh., Beaudet, A., and Vande Pol, S. (2003). Requirement of E6AP and the Features of Human Papillomavirus E6 Necessary to Support Degradation of P53. *Virology* 306 (1), 87–99. doi:10.1016/s0042-6822(02)00012-0

Cui, Y., Chen, L. J., Huang, T., Ying, J. Q., and Li, J. (2020). The Pharmacology, Toxicology and Therapeutic Potential of Anthraquinone Derivative Emodin. *Chin. J. Nat. Med.* 18 (6), 425–435. doi:10.1016/s1875-5364(20)30050-9

Cui, Y., Lu, P., Song, G., Liu, Q., Zhu, D., and Liu, X. (2016). Involvement of PI3K/Akt, ERK and P38 Signaling Pathways in Emodin-Mediated Extrinsic and Intrinsic Human Hepatoblastoma Cell Apoptosis. *Food Chem. Toxicol.* 92, 26–37. doi:10.1016/j.fct.2016.03.013

Danial, N. N., and Korsmeyer, S. J. (2004). Cell Death: Critical Control Points. *Cell* 116 (2), 205–219. doi:10.1016/s0092-8674(04)00046-7

Das, M., Garlick, D. S., Greiner, D. L., and Davis, R. J. (2011). The Role of JNK in the Development of Hepatocellular Carcinoma. *Genes Dev.* 25 (6), 634–645. doi:10.1101/gad.1989311

Datta, J., Kutay, H., Nasser, M. W., Nuovo, G. J., Wang, B., Majumder, S., et al. (2008). Methylation Mediated Silencing of MicroRNA-1 Gene and its Role in Hepatocellular Carcinogenesis. *Cancer Res.* 68 (13), 5049–5058. doi:10.1158/0008-5472.Can-07-6655

Dong, H., Wu, G., Xu, H., Zhang, C., Wang, J., Gao, M., et al. (2018). N-acetylaminogalactosyl-decorated Biodegradable PLGA-TPGS Copolymer Nanoparticles Containing Emodin for the Active Targeting Therapy of Liver Cancer. *Artif. Cell Nanomed Biotechnol* 46 (Suppl. 2), 260–272. doi:10.1080/21691401.2018.1455055

Dong, X., Fu, J., Yin, X., Cao, S., Li, X., Lin, L., et al. (2016). Emodin: A Review of its Pharmacology, Toxicity and Pharmacokinetics. *Phytother Res.* 30 (8), 1207–1218. doi:10.1002/ptr.5631

Dong, X., Zeng, Y., Liu, Y., You, L., Yin, X., Fu, J., et al. (2020). Aloe-emodin: A Review of its Pharmacology, Toxicity, and Pharmacokinetics. *Phytother Res.* 34 (2), 270–281. doi:10.1002/ptr.6532

Du, Q., Bian, X. L., Xu, X. L., Zhu, B., Yu, B., and Zhai, Q. (2013). Role of Mitochondrial Permeability Transition in Human Hepatocellular Carcinoma Hep-G2 Cell Death Induced by Rhein. *Fitoterapia* 91, 68–73. doi:10.1016/j.fitote.2013.08.008

Fan, L., Sun, G., Ma, T., Zhong, F., Lei, Y., Li, X., et al. (2013). Melatonin Reverses Tunicamycin-Induced Endoplasmic Reticulum Stress in Human Hepatocellular Carcinoma Cells and Improves Cytotoxic Response to Doxorubicin by Increasing CHOP and Decreasing Survivin. *J. Pineal Res.* 55 (2), 184–194. doi:10.1111/jpi.12061

Fuchs, Y., and Steller, H. (2011). Programmed Cell Death in Animal Development and Disease. *Cell* 147 (4), 742–758. doi:10.1016/j.cell.2011.10.033

Fulda, S., and Debatin, K. M. (2003). Death Receptor Signaling in Cancer Therapy. *Curr. Med. Chem. Anticancer Agents* 3 (4), 253–262. doi:10.2174/1568011033482404

Garcia, E. J., Lawson, D., Cotsonis, G., and Cohen, C. (2002). Hepatocellular Carcinoma and Markers of Apoptosis (bcl-2, bax, bcl-x): Prognostic Significance. *Appl. Immunohistochem. Mol. Morphol.* 10 (3), 210–217. doi:10.1097/00129039-200209000-00004

Gecibesler, I. H., Disli, F., Bayindir, S., Toprak, M., Tufekci, A. R., Sahin Yaglıoglu, A., et al. (2021). The Isolation of Secondary Metabolites from Rheum Ribes L. And the Synthesis of New Semi-synthetic Anthraquinones: Isolation, Synthesis and Biological Activity. *Food Chem.* 342, 128378. doi:10.1016/j.foodchem.2020.128378

Gravitz, L. (2014). Liver Cancer. *Nature* 516 (7529), S1. doi:10.1038/516s1a

Green, D. R., and Kroemer, G. (2004). The Pathophysiology of Mitochondrial Cell Death. *Science* 305 (5684), 626–629. doi:10.1126/science.1099320

Guicciardi, M. E., and Gores, G. J. (2009). Life and Death by Death Receptors. *Faseb j* 23 (6), 1625–1637. doi:10.1096/fj.08-111005

Guo, C. L., Yang, X. H., Cheng, W., Xu, Y., Li, J. B., Sun, Y. X., et al. (2014). Expression of Fas/FasL in CD8+ T and CD3+ Foxp3+ Treg Cells-Rrelationship with Apoptosis of Circulating CD8+ T Cells in Hepatocellular Carcinoma Patients. *Asian Pac. J. Cancer Prev.* 15 (6), 2613–2618. doi:10.7314/apjcp.2014.15.6.2613

Guo, X. Z., Shao, X. D., Liu, M. P., Xu, J. H., Ren, L. N., and Zhao, J. J. (2002). Effect of bax, bcl-2 and bcl-xL on Regulating Apoptosis in Tissues of Normal Liver and Hepatocellular Carcinoma. *World J. Gastroenterol.* 8 (6), 1059–1062. doi:10.3748/wjg.v8.i6.1059

Guo, Y., Luo, J., Tan, S., Otieno, B. O., and Zhang, Z. (2013). The Applications of Vitamin E TPGS in Drug Delivery. *Eur. J. Pharm. Sci.* 49 (2), 175–186. doi:10.1016/j.ejps.2013.02.006

Hanahan, D., and Weinberg, R. A. (2011). Hallmarks of Cancer: The Next Generation. *Cell* 144 (5), 646–674. doi:10.1016/j.cell.2011.02.013

He, Z. H., He, M. F., Ma, S. C., and But, P. P. (2009). Anti-angiogenic Effects of Rhubarb and its Anthraquinone Derivatives. *J. Ethnopharmacol* 121 (2), 313–317. doi:10.1016/j.jep.2008.11.008

Hosseini-Khah, Z., Babaei, M. R., Tehrani, M., Cucchiarini, M., Madry, H., and Ajami, A. (2021). SOX2 and Bcl-2 as a Novel Prognostic Value in Hepatocellular Carcinoma Progression. *Curr. Oncol.* 28 (4), 3015–3029. doi:10.3390/curroncol28040264

Hsu, C. M., Hsu, Y. A., Tsai, Y., Shieh, F. K., Huang, S. H., Wan, L., et al. (2010). Emodin Inhibits the Growth of Hepatoma Cells: Finding the Common Anti-cancer Pathway Using Huh7, Hep3B, and HepG2 Cells. *Biochem. Biophys. Res. Commun.* 392 (4), 473–478. doi:10.1016/j.bbrc.2009.10.153

Hu, W., Fu, J., Lu, S. X., Liu, L. L., Luo, R. Z., and Yun, J. P. (2015). Decrease of Bcl-xL/Bcl-2-Associated Death Promoter in Hepatocellular Carcinoma Indicates Poor Prognosis. *Am. J. Cancer Res.* 5 (5), 1805–1813.

Huang, C.-Y., Chang, Y.-J., Wei, P.-L., Hung, C.-S., and Wang, W. (2021). Methyl Gallate, Gallic Acid-Derived Compound, Inhibit Cell Proliferation through Increasing ROS Production and Apoptosis in Hepatocellular Carcinoma Cells. *PLoS One* 16 (3), e0248521. doi:10.1371/journal.pone.0248521

Huang, Y., and Wang, K. K. (2001). The Calpain Family and Human Disease. *Trends Mol. Med.* 7 (8), 355–362. doi:10.1016/s1471-4914(01)02049-4

Ito, Y., Monden, M., Takeda, T., Eguchi, H., Umeshita, K., Nagano, H., et al. (2000). The Status of Fas and Fas Ligand Expression Can Predict Recurrence of Hepatocellular Carcinoma. *Br. J. Cancer* 82 (6), 1211–1217. doi:10.1054/bjoc.1999.1065

Jeon, W., Jeon, Y. K., and Nam, M. J. (2012). Apoptosis by Aloe-Emodin Is Mediated through Down-Regulation of Calpain-2 and Ubiquitin-Protein Ligase E3A in Human Hepatoma Huh-7 Cells. *Cell Biol Int* 36 (2), 163–167. doi:10.1042/cbi20100723

Jiang, L., Zhang, Q., Ren, H., Ma, S., Lu, C., and Liu, B. (2015). Dihydromyricetin Enhances the Chemo-Sensitivity of Nedaplatin via Regulation of the p53/Bcl-2 Pathway in Hepatocellular Carcinoma Cells. *PLoS One* 10 (4), e0124994. doi:10.1371/journal.pone.0124994

Jindal, A., Thadi, A., and Shailubhai, K. (2019). Hepatocellular Carcinoma: Etiology and Current and Future Drugs. *J. Clin. Exp. Hepatol.* 9 (2), 221–232. doi:10.1016/j.jceh.2019.01.004

Karabekir, S. C., and Özgörgülü, A. (2020). Possible Protective Effects of Resveratrol in Hepatocellular Carcinoma. *Iran J. Basic Med. Sci.* 23 (1), 71–78. doi:10.22038/ijbms.2019.36821.8774

Kawahara, T., Toso, C., Yamaguchi, K., Cader, S., Douglas, D. N., Nourbakhsh, M., et al. (2013). Additive Effect of Sirolimus and Anti-death Receptor 5 Agonistic Antibody against Hepatocellular Carcinoma. *Liver Int.* 33 (9), 1441–1448. doi:10.1111/liv.12275

Kim, S. Y., Hwangbo, H., Lee, H., Park, C., Kim, G. Y., Moon, S. K., et al. (2020). Induction of Apoptosis by Coptisine in Hep3B Hepatocellular Carcinoma Cells through Activation of the ROS-Mediated JNK Signaling Pathway. *Int. J. Mol. Sci.* 21 (15). doi:10.3390/ijms21155502

Kim, Y. S., Lee, Y. M., Oh, T. I., Shin, D. H., Kim, G. H., Kan, S. Y., et al. (2018). Emodin Sensitizes Hepatocellular Carcinoma Cells to the Anti-cancer Effect of Sorafenib through Suppression of Cholesterol Metabolism. *Int. J. Mol. Sci.* 19 (10). doi:10.3390/ijms19103127

Koramagazi, A., Wang, D., Yousef, B., Guerram, M., and Yu, F. (2016). Rhein Triggers Apoptosis via Induction of Endoplasmic Reticulum Stress, Caspase-4 and Intracellular Calcium in Primary Human Hepatic HL-7702 Cells. *Biochem. Biophys. Res. Commun.* 473 (1), 230–236. doi:10.1016/j.bbrc.2016.03.084

Kuo, P. L., Lin, T. C., and Lin, C. C. (2002). The Antiproliferative Activity of Aloe-Emodin Is through P53-dependent and P21-dependent Apoptotic Pathway in Human Hepatoma Cell Lines. *Life Sci.* 71 (16), 1879–1892. doi:10.1016/s0024-3205(02)01900-8

Kuribayashi, K., Mayes, P. A., and El-Deiry, W. S. (2006). What Are Caspases 3 and 7 Doing Upstream of the Mitochondria? *Cancer Biol. Ther.* 5 (7), 763–765. doi:10.4161/cbt.5.7.3228

Lafaro, K. J., Demirjian, A. N., and Pawlik, T. M. (2015). Epidemiology of Hepatocellular Carcinoma. *Surg. Oncol. Clin. N. Am.* 24 (1), 1–17. doi:10.1016/j.soc.2014.09.001

Lee, E. H., Baek, S. Y., Park, J. Y., and Kim, Y. W. (2020). Emodin in Rheum Undulatum Inhibits Oxidative Stress in the Liver via AMPK with Hippo/Yap Signalling Pathway. *Pharm. Biol.* 58 (1), 333–341. doi:10.1080/13880209.2020.1750658

Lei, Y., Wang, S., Ren, B., Wang, J., Chen, J., Lu, J., et al. (2017). CHOP Favors Endoplasmic Reticulum Stress-Induced Apoptosis in Hepatocellular Carcinoma Cells via Inhibition of Autophagy. *PLoS One* 12 (8), e0183680. doi:10.1371/journal.pone.0183680

Li, Y., Shen, F., Bao, Y., Chen, D., and Lu, H. (2019). Apoptotic Effects of Rhein through the Mitochondrial Pathways, Two Death Receptor Pathways, and Reducing Autophagy in Human Liver L02 Cells. *Environ. Toxicol.* 34 (12), 1292–1302. doi:10.1002/tox.22830

Lima, K. G., Krause, G. C., Schuster, A. D., Catarina, A. V., Basso, B. S., De Mesquita, F. C., et al. (2016). Gallic Acid Reduces Cell Growth by Induction of Apoptosis and Reduction of IL-8 in HepG2 Cells. *Biomed. Pharmacother.* 84, 1282–1290. doi:10.1016/j.biopha.2016.10.048

Lin, W., Zhong, M., Yin, H., Chen, Y., Cao, Q., Wang, C., et al. (2016). Emodin Induces Hepatocellular Carcinoma Cell Apoptosis through MAPK and PI3K/AKT Signaling Pathways *In Vitro* and *In Vivo*. *Oncol. Rep.* 36 (2), 961–967. doi:10.3892/or.2016.4861

Liu, H., Gao, M., Xu, H., Guan, X., Lv, L., Deng, S., et al. (2016a). A Promising Emodin-Loaded Poly (Lactic-Co-Glycolic Acid)-D-α-Tocopheryl Polyethylene Glycol 1000 Succinate Nanoparticles for Liver Cancer Therapy. *Pharm. Res.* 33 (1), 217–236. doi:10.1007/s11095-015-1781-4

Liu, H., Xu, H., Zhang, C., Gao, M., Gao, X., Ma, C., et al. (2016b). Emodin-Loaded PLGA-TPGS Nanoparticles Combined with Heparin Sodium-Loaded PLGA-TPGS Nanoparticles to Enhance Chemotherapeutic Efficacy against Liver Cancer. *Pharm. Res.* 33 (11), 2828–2843. doi:10.1007/s11095-016-2010-5

Liu, L., Xing, D., Chen, W. R., Chen, T., Pei, Y., and Gao, X. (2008). Calpain-mediated Pathway Dominates Cisplatin-Induced Apoptosis in Human Lung Adenocarcinoma Cells as Determined by Real-Time Single Cell Analysis. *Int. J. Cancer* 122 (10), 2210–2222. doi:10.1002/ijc.23378

Lu, G. D., Shen, H. M., Chung, M. C., and Ong, C. N. (2007). Critical Role of Oxidative Stress and Sustained JNK Activation in Aloe-Emodin-Mediated Apoptotic Cell Death in Human Hepatoma Cells. *Carcinogenesis* 28 (9), 1937–1945. doi:10.1093/carcin/bgm143

Ma, J., Luo, X. D., Protiva, P., Yang, H., Ma, C., Basile, M. J., et al. (2003). Bioactive Novel Polyphenols from the Fruit of Manilkara Zapota (Sapodilla). *J. Nat. Prod.* 66 (7), 983–986. doi:10.1021/np020576x

Ma, S., Lee, T. K., Zheng, B. J., Chan, K. W., and Guan, X. Y. (2008). CD133+ HCC Cancer Stem Cells Confer Chemoresistance By Preferential Expression of the Akt/PKB Survival Pathway. *Oncogene* 27 (12), 1749–1758. doi:10.1038/sj.onc.1210811

Marengo, A., Rosso, C., and Bugianesi, E. (2016). Liver Cancer: Connections with Obesity, Fatty Liver, and Cirrhosis. *Annu. Rev. Med.* 67, 103–117. doi:10.1146/annurev-med-090514-013832

May, P., and May, E. (1999). Twenty Years of P53 Research: Structural and Functional Aspects of the P53 Protein. *Oncogene* 18 (53), 7621–7636. doi:10.1038/sj.onc.1203285

Mei, L., Zhang, Z., Zhao, L., Huang, L., Yang, X. L., Tang, J., et al. (2013). Pharmaceutical Nanotechnology for Oral Delivery of Anticancer Drugs. *Adv. Drug Deliv. Rev.* 65 (6), 880–890. doi:10.1016/j.addr.2012.11.005

Meng, X., Franklin, D. A., Dong, J., and Zhang, Y. (2014). MDM2-p53 Pathway in Hepatocellular Carcinoma. *Cancer Res.* 74 (24), 7161–7167. doi:10.1158/0008-5472.Can-14-1446

Metcalf, M. G., Higuchi-Sanabria, R., Garcia, G., Tsui, C. K., and Dillin, A. (2020). Beyond the Cell Factory: Homeostatic Regulation of and by the UPRER. *Sci. Adv.* 6 (29), eabb9614. doi:10.1126/sciadv.abb9614

Mucha, S. R., Rizzani, A., Gerbes, A. L., Camaj, P., Thasler, W. E., and Bruns, C. J. (2009). JNK Inhibition Sensitises Hepatocellular Carcinoma Cells but not Normal Hepatocytes to the TNF-Related Apoptosis-Inducing Ligand. *Gut.* 58 (5), 688–698. doi:10.1136/gut.2008.154625

Morinaka, A., Funato, Y., Uesugi, K., and Miki, H. (2011). Oligomeric Peroxiredoxin-I Is an Essential Intermediate for P53 to Activate MST1 Kinase and Apoptosis. *Oncogene* 30 (40), 4208–4218. doi:10.1038/onc.2011.139

Neophytou, C. M., Trougakos, I. P., Erin, N., and Papageorgis, P. (2021). Apoptosis Deregulation and the Development of Cancer Multi-Drug Resistance. *Cancers (Basel)* 13 (17). doi:10.3390/cancers13174363

Ng, I. O., Poon, R. T., Lee, J. M., Fan, S. T., Ng, M., and Tso, W. K. (2001). Microvessel Density, Vascular Endothelial Growth Factor and its Receptors Flt-1 and Flk-1/KDR in Hepatocellular Carcinoma. *Am. J. Clin. Pathol.* 116 (6), 838–845. doi:10.1309/fxnl-qtn1-94fh-ab3a

Olugbami, J. O., Damoiseaux, R., France, B., Onibiyo, E. M., Gbadegesin, M. A., Sharma, S., et al. (2017). A Comparative Assessment of Antiproliferative Properties of Resveratrol and Ethanol Leaf Extract of Anogeissus Leiocarpus (DC) Guill and Perr against HepG2 Hepatocarcinoma Cells. *BMC Complement. Altern. Med.* 17 (1), 381. doi:10.1186/s12906-017-1873-2

Ong, S. G., Lee, W. H., Kodo, K., and Wu, J. C. (2015). MicroRNA-Mediated Regulation of Differentiation and Trans-Differentiation in Stem Cells. *Adv. Drug Deliv. Rev.* 88, 3–15. doi:10.1016/j.addr.2015.04.004

Orcutt, S. T., and Anaya, D. A. (2018). Liver Resection and Surgical Strategies for Management of Primary Liver Cancer. *Cancer Control* 25 (1), 1073274817744621. doi:10.1177/1073274817744621

Ou, X., Chen, Y., Cheng, X., Zhang, X., and He, Q. (2014). Potentiation of Resveratrol-Induced Apoptosis by Matrine in Human Hepatoma HepG2 Cells. *Oncol. Rep.* 32 (6), 2803–2809. doi:10.3892/or.2014.3512

Pan, X., Wang, H., Tong, D., Wang, C., Sun, L., Zhao, C., et al. (2016). Physcion Induces Apoptosis in Hepatocellular Carcinoma by Modulating miR-370. *Am. J. Cancer Res.* 6 (12), 2919–2931.

Pan, X. P., Wang, C., Li, Y., and Huang, L. H. (2018). Physcion Induces Apoptosis through Triggering Endoplasmic Reticulum Stress in Hepatocellular Carcinoma. *Biomed. Pharmacother.* 99, 894–903. doi:10.1016/j.biopha.2018.01.148

Pistritto, G., Trisciuoglio, D., Ceci, C., Garufi, A., and D'Orazi, G. (2016). Apoptosis as Anticancer Mechanism: Function and Dysfunction of its Modulators and Targeted Therapeutic Strategies. *Aging (Albany NY)* 8 (4), 603–619. doi:10.18632/aging.100934

Plati, J., Bucur, O., and Khosravi-Far, R. (2008). Dysregulation of Apoptotic Signaling in Cancer: Molecular Mechanisms and Therapeutic Opportunities. *J. Cel Biochem* 104 (4), 1124–1149. doi:10.1002/jcb.21707

Pollak, M. (2012). The Insulin and Insulin-like Growth Factor Receptor Family in Neoplasia: an Update. *Nat. Rev. Cancer* 12 (3), 159–169. doi:10.1038/nrc3215

Sacco, R., Leuci, D., Tortorella, C., Fiore, G., Marinosci, F., Schiraldi, O., et al. (2000). Transforming Growth Factor Beta1 and Soluble Fas Serum Levels in Hepatocellular Carcinoma. *Cytokine* 12 (6), 811–814. doi:10.1006/cyto.1999.0650

Scheffner, M., Huibregtse, J. M., Vierstra, R. D., and Howley, P. M. (1993). The HPV-16 E6 and E6-AP Complex Functions as a Ubiquitin-Protein Ligase in the Ubiquitination of P53. *Cell* 75 (3), 495–505. doi:10.1016/0092-8674(93)90384-3

Schulze-Osthoff, K., Ferrari, D., Los, M., Wesselborg, S., and Peter, M. E. (1998). Apoptosis Signaling by Death Receptors. *Eur. J. Biochem.* 254 (3), 439–459. doi:10.1046/j.1432-1327.1998.2540439.x

Semwal, R. B., Semwal, D. K., Combrinck, S., and Viljoen, A. (2021). Emodin - A Natural Anthraquinone Derivative with Diverse Pharmacological Activities. *Phytochemistry* 190, 112854. doi:10.1016/j.phytochem.2021.112854

Shi, C. J., Zheng, Y. B., Pan, F. F., Zhang, F. W., Zhuang, P., and Fu, W. M. (2021). Gallic Acid Suppressed Tumorigenesis by an LncRNA MALAT1-Wnt/β-Catenin Axis in Hepatocellular Carcinoma. *Front. Pharmacol.* 12, 708967. doi:10.3389/fphar.2021.708967

Shigemi, Z., Manabe, K., Hara, N., Baba, Y., Hosokawa, K., Kagawa, H., et al. (2017). Methylseleninic Acid and Sodium Selenite Induce Severe ER Stress and Subsequent Apoptosis through UPR Activation in PEL Cells. *Chem. Biol. Interact* 266, 28–37. doi:10.1016/j.cbi.2017.01.027

Slee, E. A., Adrain, C., and Martin, S. J. (1999). Serial Killers: Ordering Caspase Activation Events in Apoptosis. *Cell Death Differ* 6 (11), 1067–1074. doi:10.1038/sj.cdd.4400601

Song, G., Ouyang, G., and Bao, S. (2005). The Activation of Akt/PKB Signaling Pathway and Cell Survival. *J. Cell Mol. Med.* 9 (1), 59–71. doi:10.1111/j.1582-4934.2005.tb00337.x

Song, P., Huang, H., Ma, Y., Wu, C., Yang, X., and Choi, H.-Y. (2021). Davidone C Induces the Death of Hepatocellular Carcinoma Cells by Promoting Apoptosis and Autophagy. *Molecules* 26 (17), 5219. doi:10.3390/molecules26175219

Srinivas, G., Babykutty, S., Sathiadevan, P. P., and Srinivas, P. (2007). Molecular Mechanism of Emodin Action: Transition from Laxative Ingredient to an Antitumor Agent. *Med. Res. Rev.* 27 (5), 591–608. doi:10.1002/med.20095

Subramaniam, A., Shanmugam, M. K., Ong, T. H., Li, F., Perumal, E., Chen, L., et al. (2013). Emodin Inhibits Growth and Induces Apoptosis in an Orthotopic Hepatocellular Carcinoma Model by Blocking Activation of STAT3. *Br. J. Pharmacol.* 170 (4), 807–821. doi:10.1111/bph.12302

Sun, G., Zhang, S., Xie, Y., Zhang, Z., and Zhao, W. (2016). Gallic Acid as a Selective Anticancer Agent that Induces Apoptosis in SMMC-7721 Human Hepatocellular Carcinoma Cells. *Oncol. Lett.* 11 (1), 150–158. doi:10.3892/ol.2015.3845

Susin, S. A., Daugas, E., Ravagnan, L., Samejima, K., Zamzami, N., Loeffler, M., et al. (2000). Two Distinct Pathways Leading to Nuclear Apoptosis. *J. Exp. Med.* 192 (4), 571–580. doi:10.1084/jem.192.4.571

Tsai, J. J., Chen, J. H., Chen, C. H., Chung, J. G., and Hsu, F. T. (2020). Apoptosis Induction and ERK/NF-KB Inactivation are Associated with Magnolol-Inhibited Tumor Progression in Hepatocellular Carcinoma In Vivo. *Environ. Toxicol.* 35 (2), 167–175. doi:10.1002/tox.22853

Tutusaus, A., Stefanovic, M., Boix, L., Cucarull, B., Zamora, A., and Blasco, L. (2018). Antiapoptotic BCL-2 Proteins Determine Sorafenib/Regorafenib Resistance and BH3-Mimetic Efficacy in Hepatocellular Carcinoma. *Oncotarget* 9 (24), 16701–16717. doi:10.18632/oncotarget.24673

Vande Walle, L., Jiménez Fernández, D., Demon, D., Van Laethem, N., Van Hauwermeiren, F., Van Gorp, H., et al. (2016). Does Caspase-12 Suppress Inflammasome Activation? *Nature* 534 (7605), E1–E4. doi:10.1038/nature17649

Vande Walle, L., Van Damme, P., Lamkanfi, M., Saelens, X., Vandekerckhove, J., Gevaert, K., et al. (2007). Proteome-wide Identification of HtrA2/Omi Substrates. *J. Proteome Res.* 6 (3), 1006–1015. doi:10.1021/pr060510d

Wada, K., Itoga, K., Okano, T., Yonemura, S., and Sasaki, H. (2011). Hippo Pathway Regulation by Cell Morphology and Stress Fibers. *Development* 138 (18), 3907–3914. doi:10.1242/dev.070987

Wajant, H., Pfizenmaier, K., and Scheurich, P. (2003). Tumor Necrosis Factor Signaling. *Cel Death Differ* 10 (1), 45–65. doi:10.1038/sj.cdd.4401189

Wang, A., Jiang, H., Liu, Y., Chen, J., Zhou, X., Zhao, C., et al. (2020). Rhein Induces Liver Cancer Cells Apoptosis via Activating ROS-dependent JNK/Jun/caspase-3 Signaling Pathway. *J. Cancer* 11 (2), 500–507. doi:10.7150/jca.30381

Wang, B., Chen, L., Ni, Z., Dai, X., Qin, L., and Wu, Y. (2014). Hsp90 Inhibitor 17-AAG Sensitizes Bcl-2 Inhibitor (-)-Gossypol by Suppressing ERK-Mediated Protective Autophagy and Mcl-1 Accumulation in Hepatocellular Carcinoma Cells. *Exp. Cell Res.* 328 (2), 379–387. doi:10.1016/j.yexcr.2014.08.039

Wang, J., Liu, S., Yin, Y., Li, M., Wang, B., Yang, L., et al. (2015). FOXO3-mediated Up-Regulation of Bim Contributes to Rhein-Induced Cancer Cell Apoptosis. *Apoptosis* 20 (3), 399–409. doi:10.1007/s10495-014-1071-3

Wang, Y., Guo, S. H., Shang, X. J., Yu, L. S., Zhu, J. W., Zhao, A., et al. (2018). Triptolide Induces Sertoli Cell Apoptosis in Mice via ROS/JNK-dependent Activation of the Mitochondrial Pathway and Inhibition of Nrf2-Mediated Antioxidant Response. *Acta Pharmacol. Sin* 39 (2), 311–327. doi:10.1038/aps.2017.95

Watanabe, J., Kushihata, F., Honda, K., Sugita, A., Tateishi, N., and Mominoki, K. (2004). Prognostic Significance of Bcl-xL in Human Hepatocellular Carcinoma. *Surgery* 135 (6), 604–612. doi:10.1016/j.surg.2003.11.015

Wu, L., Cao, K., Ni, Z., Wang, S., Li, W., Liu, X., et al. (2019). Rhein Reverses Doxorubicin Resistance in SMMC-7721 Liver Cancer Cells by Inhibiting Energy Metabolism and Inducing Mitochondrial Permeability Transition Pore Opening. *Biofactors* 45 (1), 85–96. doi:10.1002/biof.1462

Wu, L., Liu, X., Cao, K. X., Ni, Z. H., Li, W. D., and Chen, Z. P. (2020). Synergistic Antitumor Effects of Rhein and Doxorubicin in Hepatocellular Carcinoma Cells. *J. Cel Biochem* 121 (10), 4009–4021. doi:10.1002/jcb.27514

Xiao, L., Chen, D., Hu, P., Wu, J., Liu, W., Zhao, Y., et al. (2011). The C-Abl-MST1 Signaling Pathway Mediates Oxidative Stress-Induced Neuronal Cell Death. *J. Neurosci.* 31 (26), 9611–9619. doi:10.1523/jneurosci.0035-11.2011

Xing, Y. X., Li, M. H., Tao, L., Ruan, L. Y., Hong, W., Chen, C., et al. (2018). Anti-Cancer Effects of Emodin on HepG2 Cells as Revealed by 1H NMR Based Metabolic Profiling. *J. Proteome Res.* 17 (5), 1943–1952. doi:10.1021/acs.jproteome.8b00029

Xu, C., Shi, L., Chen, W., Fang, P., Li, J., Jin, L., et al. (2017). MiR-106b Inhibitors Sensitize TRAIL-Induced Apoptosis in Hepatocellular Carcinoma through Increase of Death Receptor 4. *Oncotarget* 8 (26), 41921–41931. doi:10.18632/oncotarget.16707

XunLiLiu, Y., Chu, Y., Yang, S., Peng, Y., Ren, S., et al. (2019). Physcion and Physcion 8-O-β-Glucopyranoside: A Review of Their Pharmacology, Toxicities and Pharmacokinetics. *Chem. Biol. Interact* 310, 108722. doi:10.1016/j.cbi.2019.06.035

Yamaguchi, H., and Wang, H. G. (2004). CHOP Is Involved in Endoplasmic Reticulum Stress-Induced Apoptosis by Enhancing DR5 Expression in Human Carcinoma Cells. *J. Biol. Chem.* 279 (44), 45495–45502. doi:10.1074/jbc.M406933200

Yan, J., Xie, Y., Si, J., Gan, L., Li, H., Sun, C., et al. (2021). Crosstalk of the Caspase Family and Mammalian Target of Rapamycin Signaling. *Ijms* 22 (2), 817. doi:10.3390/ijms22020817

Yang, J., Yang, Y., Tian, L., Sheng, X. F., Liu, F., and Cao, J. G. (2011). Casticin-induced Apoptosis Involves Death Receptor 5 Upregulation in Hepatocellular Carcinoma Cells. *World J. Gastroenterol.* 17 (38), 4298–4307. doi:10.3748/wjg.v17.i38.4298

Yang, L., Si, X., and Wang, W. (2002). Overexpression of bcl-2 Protects Hepatoma Cell Line HCC-9204 from Ethanol-Induced Apoptosis. *Chin. Med. J. (Engl)* 115 (1), 8–11.

Yang, N., Li, C., Li, H., Liu, M., Cai, X., Cao, F., et al. (2019). Emodin Induced SREBP1-dependent and SREBP1-independent Apoptosis in Hepatocellular Carcinoma Cells. *Front. Pharmacol.* 10, 709. doi:10.3389/fphar.2019.00709

Yang, Y., Zhu, J., Gou, H., Cao, D., Jiang, M., and Hou, M. (2011). Clinical Significance of Cox-2, Survivin and Bcl-2 Expression in Hepatocellular Carcinoma (HCC). *Med. Oncol.* 28 (3), 796–803. doi:10.1007/s12032-010-9519-y

Yao, Y., Li, L., Zhang, H., Jia, R., Liu, B., and Zhao, X. (2012). Enhanced Therapeutic Efficacy of Vitamin K2 by Silencing BCL-2 Expression in SMMC-7721 Hepatocellular Carcinoma Cells. *Oncol. Lett.* 4 (1), 163–167. doi:10.3892/ol.2012.682

Yie, Y., Zhao, S., Tang, Q., Zheng, F., Wu, J., Yang, L., et al. (2015). Ursolic Acid Inhibited Growth of Hepatocellular Carcinoma HepG2 Cells through AMPKα-Mediated Reduction of DNA Methyltransferase 1. *Mol. Cel Biochem* 402 (1-2), 63–74. doi:10.1007/s11010-014-2314-x

Yoon, D. S., Cheong, J. H., Park, Y. N., Kwon, S. W., Chi, H. S., and Kim, B. R. (1998). Cell Proliferation Index and the Expression of p53 and Bcl-2 in Tumorous and Non-Tumorous Lesions of Hepatocellular Carcinoma and Metastatic Liver Cancer. *Yonsei. Med. J.* 39 (5), 424–429. doi:10.3349/ymj.1998.39.5.424

You, M. L., Chen, Y. J., Chong, Q. Y., Wu, M. M., Pandey, V., and Chen, R. M. (2017). Trefoil Factor 3 Mediation of Oncogenicity and Chemoresistance in Hepatocellular Carcinoma is AKT-BCL-2 Dependent. *Oncotarget* 8 (24), 39323–39344. doi:10.18632/oncotarget.16950

Youle, R. J., and Strasser, A. (2008). The BCL-2 Protein Family: Opposing Activities that Mediate Cell Death. *Nat. Rev. Mol. Cell Biol.* 9 (1), 47–59. doi:10.1038/nrm2308

Zeng, B., Li, Z., Chen, R., Guo, N., Zhou, J., Zhou, Q., et al. (2012). Epigenetic Regulation of miR-124 by Hepatitis C Virus Core Protein Promotes Migration and Invasion of Intrahepatic Cholangiocarcinoma Cells by Targeting SMYD3. *FEBS Lett.* 586 (19), 3271–3278. doi:10.1016/j.febslet.2012.06.049

Zhang, K., Jiao, K., Zhu, Y., Wu, F., Li, J., and Yu, Z. (2015). Effect of Emodin on Proliferation and Cell Cycle of Human Oral Squamous Carcinoma Tca8113 Cells *In Vitro*. *Nan Fang Yi Ke Da Xue Xue Bao* 35 (5), 665–670.

Zhang, L., and Wang, H. H. (2016). The Essential Functions of Endoplasmic Reticulum Chaperones in Hepatic Lipid Metabolism. *Dig. Liver Dis.* 48 (7), 709–716. doi:10.1016/j.dld.2016.03.016

Zhang, X. L., Yu, H., Xiong, Y. Y., Ma, S. T., Zhao, L., and She, S. F. (2013). Resveratrol Down-Regulates Myosin Light Chain Kinase, Induces Apoptosis and Inhibits Diethylnitrosamine-Induced Liver Tumorigenesis in Rats. *Int. J. Mol. Sci.* 14 (1), 1940–1951. doi:10.3390/ijms14011940

Zhang, Y. C., Guo, L. Q., Chen, X., Wang, G. N., Ni, R., Wang, M. C., et al. (2015). The Role of Death Receptor 3 in the Biological Behavior of Hepatocellular Carcinoma Cells. *Mol. Med. Rep.* 11 (2), 797–804. doi:10.3892/mmr.2014.2858

Zhao, S., Wu, J., Zheng, F., Tang, Q., Yang, L., Li, L., et al. (2015). β-Elemene Inhibited Expression of DNA Methyltransferase 1 through Activation of ERK1/2 and AMPKα Signalling Pathways in Human Lung Cancer Cells: the Role of Sp1. *J. Cel Mol Med* 19 (3), 630–641. doi:10.1111/jcmm.12476

Zhao, X., Ogunwobi, O. O., and Liu, C. (2011). Survivin Inhibition is Critical for Bcl-2 Inhibitor-Induced Apoptosis in Hepatocellular Carcinoma Cells. *PLoS One* 6 (8), e21980. doi:10.1371/journal.pone.0021980

Zheng, Y., Zhou, Q., Zhao, C., Li, J., Yu, Z., and Zhu, Q. (2021). ATP Citrate Lyase Inhibitor Triggers Endoplasmic Reticulum Stress to Induce Hepatocellular Carcinoma Cell Apoptosis via P-eIF2α/ATF4/CHOP axis. *J. Cel Mol Med* 25 (3), 1468–1479. doi:10.1111/jcmm.16235

Zhou, Y. X., Xia, W., Yue, W., Peng, C., Rahman, K., and Zhang, H. (2015). Rhein: A Review of Pharmacological Activities. *Evid. Based Complement. Alternat Med.* 2015, 578107–578110. doi:10.1155/2015/578107

Zhu, R. X., Lin, J. S., Song, Y. H., Li, P. Y., and Tao, L. W. (2006). Relationship between Death Receptor 5 and Apoptosis in Hepatocellular Carcinoma. *Zhonghua Zhong Liu Za Zhi* 28 (4), 261–264.

Zou, X., Zhang, D., Song, Y., Liu, S., Long, Q., Yao, L., et al. (2020). HRG Switches TNFR1-Mediated Cell Survival to Apoptosis in Hepatocellular Carcinoma. *Theranostics* 10 (23), 10434–10447. doi:10.7150/thno.47286

Conflict of Interest: The authors declare that the research was conducted in the absence of any commercial or financial relationships that could be construed as a potential conflict of interest.

Publisher's Note: All claims expressed in this article are solely those of the authors and do not necessarily represent those of their affiliated organizations, or those of the publisher, the editors and the reviewers. Any product that may be evaluated in this article, or claim that may be made by its manufacturer, is not guaranteed or endorsed by the publisher.

Copyright © 2022 Jiang, Tang, Song, Jin and Du. This is an open-access article distributed under the terms of the Creative Commons Attribution License (CC BY). The use, distribution or reproduction in other forums is permitted, provided the original author(s) and the copyright owner(s) are credited and that the original publication in this journal is cited, in accordance with accepted academic practice. No use, distribution or reproduction is permitted which does not comply with these terms.

frontiers in Pharmacology

ORIGINAL RESEARCH
published: 04 March 2022
doi: 10.3389/fphar.2022.806869

Maackiain Modulates miR-374a/GADD45A Axis to Inhibit Triple-Negative Breast Cancer Initiation and Progression

Fu Peng[1], Li Wang[1], Liang Xiong[2], Hailin Tang[3], Junrong Du[1] and Cheng Peng[2]**

[1]Key Laboratory of Drug-Targeting and Drug Delivery System of the Education Ministry and Sichuan Province, Sichuan Engineering Laboratory for Plant-Sourced Drug and Sichuan Research Center for Drug Precision Industrial Technology, West China School of Pharmacy, Sichuan University, Chengdu, China, [2]State Key Laboratory of Southwestern Chinese Medicine Resources, Chengdu University of Traditional Chinese Medicine, Chengdu, China, [3]Department of Breast Oncology, Sun Yat-sen University Cancer Center, Guangzhou, China

Breast cancer ranks as the leading cause of death in lethal malignancies among women worldwide, with a sharp increase of incidence since 2008. Triple negative breast cancer (TNBC) gives rise to the largest proportion in breast cancer-related deaths because of its aggressive growth and rapid metastasis. Hence, searching for promising targets and innovative approaches is indispensable for the TNBC treatment. Maackiain (MA), a natural compound with multiple biological activities, could be isolated from different Chinese herbs, such as *Spatholobus suberectus* and *Sophora flavescens*. It was the first time to report the anti-cancer effect of MA in TNBC. MA could suppress TNBC cell proliferation, foci formation, migration, and invasion. MA also exerted a significant inhibitory effect on tumor growth of TNBC. Furthermore, MA could induce apoptosis with an increase of GADD45α and a decrease of miR-374a. In contrast, overexpressing miR-374a would result in at least partly affecting the proapoptotic effect of MA and suppressing GADD45α stimulated by MA. These results reveal the anti-TNBC effect of MA *in vitro* and *in vivo*, providing evidence for its potential as a drug candidate utilized in TNBC therapy.

Keywords: triple negative breast cancer, maackiain, miR-374a, GADD45α, EMT—epithelial to mesenchymal transformation

OPEN ACCESS

Edited by:
Hong Zhang,
Shanghai University of Traditional Chinese Medicine, China

Reviewed by:
Min Dai,
Chengdu Medical College, China
Jinqi Li,
Personalized Drug Therapy Key Laboratory of Sichuan Province, China

****Correspondence:***
Cheng Peng
pengchengchengdu@126.com
Junrong Du
dujr_1@163.com

Specialty section:
This article was submitted to Pharmacology of Anti-Cancer Drugs, a section of the journal Frontiers in Pharmacology

Received: *01 November 2021*
Accepted: *24 January 2022*
Published: *04 March 2022*

Citation:
Peng F, Wang L, Xiong L, Tang H, Du J and Peng C (2022) Maackiain Modulates miR-374a/GADD45A Axis to Inhibit Triple-Negative Breast Cancer Initiation and Progression. Front. Pharmacol. 13:806869. doi: 10.3389/fphar.2022.806869

INTRODUCTION

In 2020, breast cancer still ranked as the leading cause of death in cancer-related female patients worldwide, with the highest incidence (47.8 per 100,000 population) and the second highest mortality (13.6 per 100,000 population) based on the data from the Global Cancer Observatory database (An et al., 2021). According to molecular profiling, breast cancer is a complicated disease including various molecular subtypes, namely, luminal A, luminal B, human epidermal growth factor receptor 2 (HER2)-enriched, and triple-negative (Sinha et al., 2013). Approximately 15% of diagnosed breast cancers are triple negative breast cancer (TNBC), exerting higher recurrence, more aggressive growth, and more rapid metastasis (Tang et al., 2019). TNBC patients do not respond to hormone therapy or HER2 targeted agents because TNBC is the absence of hormone-receptor and HER2. Thus, it is urgent to search for novel targets and approaches to rise to the TNBC clinical challenge.

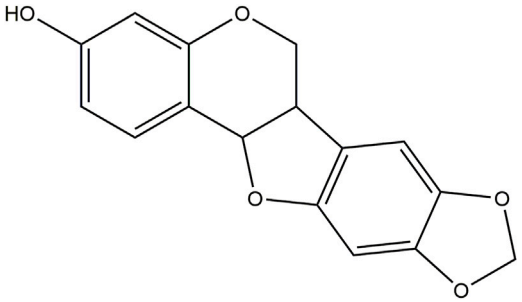


FIGURE 1 | The chemical structure of MA constructed using ChemBioDraw.

MicroRNAs (miRNAs) are classified as a class of small non-coding RNA molecules of 20-22 nucleotides negatively regulating their targets through cleavage or translational repression (Mendell et al., 2012). MiRNAs modulate diverse cellular processes relying on the impressive regulatory function even in cancer. The first study exploring the role of miRNAs in breast cancer was reported in 2005. The findings indicated overexpressed miR-21 and miR-155 in breast cancer patients as oncogenic gene (Iorio et al., 2005). Since then, a substantial number of studies started to focus on this novel conserved non-coding RNA in breast cancer management. Recently, it was pointed out that miR-374a could induce tumorigenicity and progression of breast cancer through the deregulation of β-lactamases, which was detected as part of the mitochondrial ribosomal complex (Zhang et al., 2018). Additionally, in TNBC, miR-374a promoted cancer development by directly targeting arrestin β 1, a member of the arrestin/β-arrestin family (Son et al., 2019). These reports suggested miR-374a as an oncogene in breast cancer. Therefore, it is worthwhile to expand the underlying mechanism of miR-374a regulation and discover approaches to suppress miR-374a in TNBC. *Spatholobus suberectus* Dunn (*S. suberectus*), a traditional Chinese medicine (TCM), could promote blood circulation and remove blood stasis according to TCM theory, implying its function to treat blood-stasis related diseases. *S. suberectus* was commonly used to treat rheumatism, anemia, and menoxenia in clinic (Qin et al., 2019). *S. suberectus* has been shown to have diverse pharmacological properties including anti-inflammatory, anti-bacterial, antioxidant, and antidiabetic effects (Fu et al., 2017; Do et al., 2018; Guo et al., 2018). Especially, *S. suberectus* treatment displayed cytotoxicity in myeloma cells and leukemia cells by promoting reactive oxygen species stress and inducing apoptosis (Lim et al., 2019). Recent studies declared that *S. suberectus* manifested an inhibitory effect on breast cancer *via* arresting the cell cycle and declining lactate dehydrogenase (Wang et al., 2013). *S. suberectus* could also inhibit TNBC *in vitro* and *in vivo* through ROS-induced pyroptosis (Zhang et al., 2021). Interestingly, pure compounds isolated from it also possessed potent anti-cancer effects in breast cancer according to our previous study (Peng et al., 2019). Maackiain (MA, **Figure 1**) could be extracted from *S. suberectus*, *Sophora flavescens,* and many other Chinese herbal medicines (Tsai et al., 2020). MA exerted multiple pharmacologic activities, such as anti-allergic, anti-cancer, and anti-inflammatory effects (Aratanechemuge et al., 2004; Mizuguchi et al., 2015). Accordingly, it is interesting to explore the inhibitory capacity of MA on TNBC as a promising drug candidate.

In this study, it is the first report to declare the anti-cancer propriety of MA in TNBC. MA exhibits a significant repressive impact on TNBC cell proliferation, epithelial-mesenchymal transition (EMT), migration, and invasion. MA also blocks foci formation and tumor growth of TNBC. In addition, MA could promote growth arrest and DNA damage-inducible 45α (GADD45α) protein as well as mRNA expression through the downregulation of miR-374a, resulting in a proapoptotic consequence. Conversely, overexpressed miR-374a could at least partly reverse the apoptosis-inducing capacity of MA and decrease GADD45A expression induced by MA. Taken together, our work indicates MA is a promising anti-TNBC agent owing to its ability to modulate miR-374a.

MATERIALS AND METHODS

Chemicals and Reagents

Reagents utilized in this study were obtained from typical companies. Specifically, the purity of MA reached 98% and was purchased from Chem Faces (Wuhan, China). The stocking solution of MA was dissolved in DMSO. When using MA to treat TNBC cells, the stocking solution was diluted until the percentage of DMSO was below 0.1%. Xylene, Eosin Y, Hematoxylin, and others were also purchased from typical companies such as Sigma (St. Louis, MO).

Cell Culture

TNBC cell line MDA-MB-231 and BT549 from American Type Culture Collection (ATCC, United States) were incubated in a 5% CO_2 37°C incubator. A total of 293 T cells was also obtained from ATCC. FBS was obtained from Gibco (Life Technologies, United States). All the mediums, penicillin, and trypsin were obtained from Hyclone (Cytiva, United States). MDA-MB-231, BT549, and 293 T were cultured in DMEM medium. When culturing cells, 10% FBS, 1% penicillin, and 1% streptomycin were added in cell medium.

CCK-8 Assay

TNBC cells were seeded in the 96 well plates at a concentration of 5×10^4 cells/ml treated with different doses (0, 2.5, 5, 10, 20, 40, 80, 100 μM) of MA for 24 and 48 h. After MA treatment, 10 μL CCK-8 reagents were added to the 96 well plates according to the manufacturer's instructions (MedChemExpress, United States). After incubation, the absorbance would be read by an ELISA plate reader at 450 nm. Triplicate experiments were performed independently.

Foci Formation Assay

Foci formation assay would be conducted as previously (Peng et al., 2020). Briefly, clones were stained with 0.5% crystal violet for 15 min. Foci numbers were counted after staining. Triplicate experiments were performed independently.

Flow Cytometry Analysis

Flow cytometry analysis would be conducted as previously (Peng et al., 2020). Briefly, FITC-conjugated Annexin V and PI staining were conducted through apoptosis analysis kit (BD Company, CA). After washing TNBC cells with cold PBS, the cells were resuspended in 1 × binding buffer at the concentration of 1×10^6 cells/ml. Then, we gently mixed cells with Annexin V and PI for 15 min at room temperature in the dark. Finally, stained cells were analyzed by flow cytometry within 1 h. Triplicate experiments were performed independently.

Chamber Invasion Assays

To determine the effect of MA on TNBC cell invasion, 6-well transwell chambers with Matrigel were utilized (Coring, United States). TNBC cells were planted at the upper compartment of the transwell plates at a concentration of 2.5×10^5 cells/well. After being treated with MA (0, 1 μM, 2.5 μM, 5 μM) for 24 h, invading cells were stained through 0.5% crystal violet. The remaining cells were detected through microscope (ZEISS, Germany).

Wound Scratch Assay

Wound scratch assays were performed as previously (Gong et al., 2018). Briefly, 3×10^5 cells/ml of TNBC cells were plated into Culture-Insert (ibidi GmbH, Martinsried, Germany). After 24 h cell attachment, Culture-Insert was gently removed. After MA treatment (0, 1, 2.5 and 5 μM) for another 24 h, scratches were recorded at the beginning and the end point of the experiment through microscope (ZEISS, Germany).

Western Blot

The protein in TNBC cells was extracted using cell lysis buffer (St. Louis, MO). There was 20-30 μg protein resolved on 10% SDS-PAGE gels and transferred onto PVDF membrane (Millipore, Merck, United States). We incubated sliced membranes and primary antibody against E-cadherin, N-cadherin, Vimentin, Bax, Bcl-2, GADD45α, GAPDH, and β-actin (Cell Signaling, Danvers, MA) overnight at 4°C. β-actin or GAPDH was selected as the loading control. After incubating sliced membranes and secondary antibody for 1 h, the detection was conducted *via* ECL Advance Reagent (Millipore, Merck, United States) and Image Lab Software (Bio-rad, Kidlington, UK).

Quantitative Real-Time PCR

We extracted total RNA *via* RNAiso Plus (Takara, Shiga, Japan) reagent after exposure to MA for 24 h. The RNA transcription into cDNA was performed *via* PrimeScript RT Reagent Kit with gDNA Eraser (Takara, Shiga, Japan). The real-time PCR for amplification was conducted through TB Green (Takara, Shiga, Japan). MiRNA was extracted through miRNeasy Mini Kit from Qiagen (Germany) after treatment. The miRNA transcription into cDNA was performed *via* TaqMan MicroRNA Reverse Transcription Kit (Ambion, Life Technologies, United States). The real-time PCR for amplification was conducted through ExiLENT SYBR Green master mix (QIAGEN, United States). GAPDH and U6 were selected as the loading control, and $2^{-\Delta\Delta CT}$ values were calculated. The following primers utilized for real time PCR were listed in **Supplementary Table S1**.

PCR Array

PCR assay was performed *via* microRNA PCR Panel (Qiagen, Germany) as previously described (Peng et al., 2020). Briefly, miRNA in TNBC cells was extracted using miRNeasy Mini Kit from Qiagen (Germany) in different groups. We used TaqMan MicroRNA Reverse Transcription Kit from Ambion (Life Technologies, United States) to conduct miRNA transcription. We conducted real-time PCR for amplification corresponding cDNA using ExiLENT SYBR Green master mix.

Cell Transfection

MirVana miRNA-374a mimic and mirVana miRNA mimic Negative Control were purchased from Ambion (Life Technologies, United States). We chose Lipofectamine RNAiMAX Transfection Reagent (Invitrogen, Life Technologies, United States) as transfection reagent. TNBC cells were plated on 6 well plates at a concentration of 2.5×10^5 cells/ml. The complexes of miRNA and transfection reagent were added to TNBC cells. Then, the plates were incubated at 37°C in the cell incubator for at least 24 h.

Luciferase Reporter Assay

The pMIR-REPOR miRNA Expression Reporter Vector System and Dual-Glo luciferase Assay System (Promega, Madison, WI) were utilized to verify the interaction between miR-374a and 3′UTR region of GADD45A. There are five groups, including the control group, miRNA mimic negative control + GADD45A 3′UTR wild type, miRNA-374a mimic + GADD45A 3′UTR wild type, miRNA mimic negative control + GADD45A 3′UTR mutated, and miRNA-374a mimic + GADD45A 3′UTR mutated, aiming at mimicking the modulation of miR-374a on GADD45A 3′UTR. The reagents were added based on the manufacturer's instruction. The luciferase activity was recorded by SpectraMax M5. The primers for amplification are shown in **Supplementary Table S2**.

Xenograft Tumor Growth Assays

Concisely, we conducted cell injection with 2×10^6 MDA-MB-231 cells into the dorsal flanks to establish a TNBC xenograft tumor model. After model establishment, 4-week-old nude mice were separated into the control group, low dose group (MA, 25 mg/kg/d), and high dose group (MA, 50 mg/kg/d) randomly (n = 10). We administered MA to mice through intraperitoneal injection for 28 days with a record of tumor volumes. After 28-days administration, mice were sacrificed and tumor weights were assessed. The animal experiments were conducted complying with the institutional guidelines of Sichuan University and Chengdu University of Traditional Chinese Medicine.

Immunohistochemistry

Immunohistochemistry (IHC) was utilized to detect GADD45α protein distribution and expression in tumor tissues. Tumor bulks

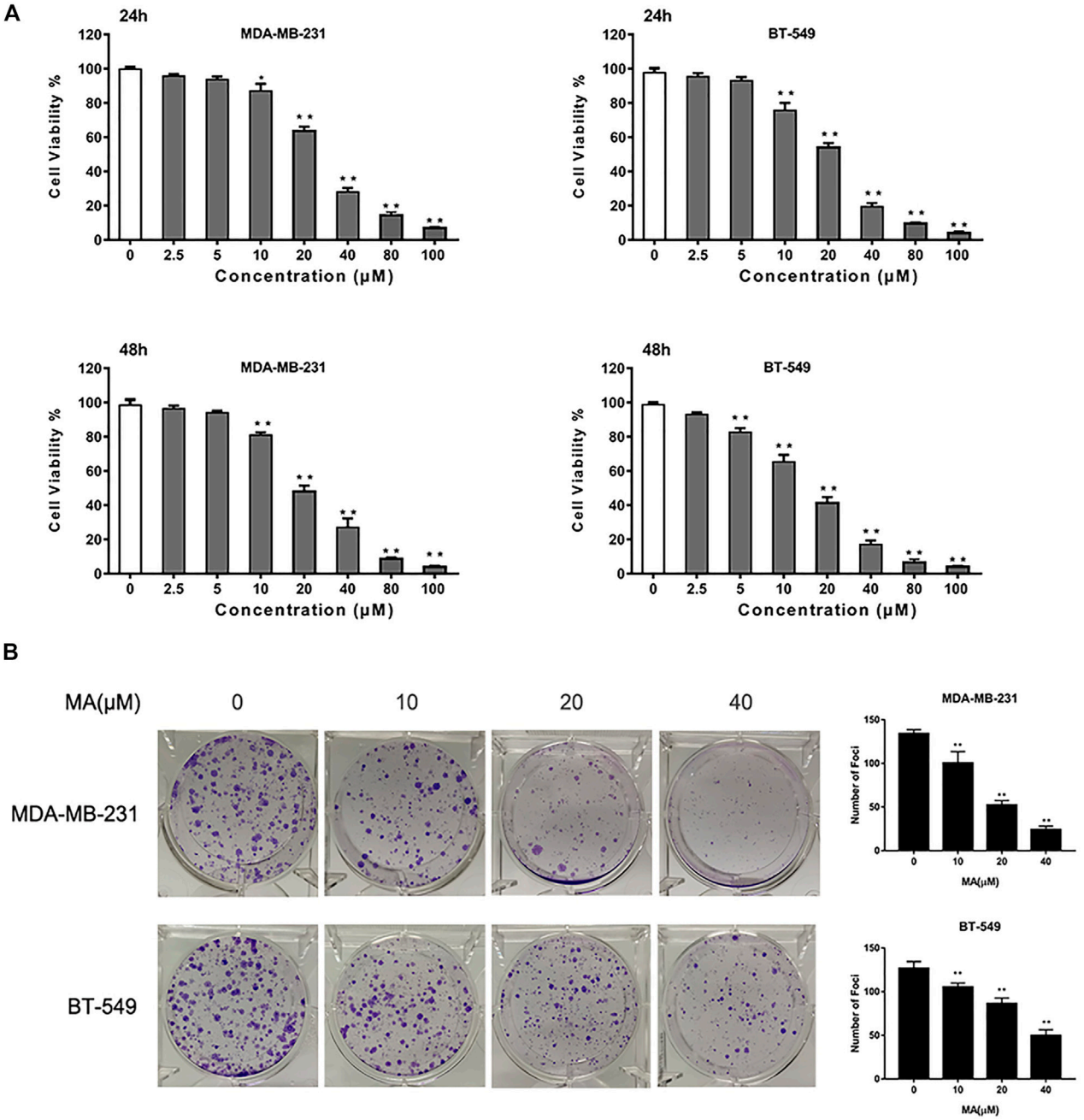


FIGURE 2 | MA attenuates TNBC cell growth. **(A)** Cell viability of TNBC cells after MA treatment. **(B)** Representative images and number of foci formation in TNBC cells after exposure to MA for 24 h. Compared with the control group (0 μM), $^{*}p < 0.05$, $^{**}p < 0.01$.

were collected after nude mice were sacrificed at the end point of the animal study. The tumor tissues were deparaffinized and rehydrated, before antigen retrieval with sodium citrate 10 mM, pH 6.0 at a high temperature. Before slides were incubated with the primary antibody against GADD45α (Cell Signaling, Danvers, MA), the section was blocked in 5% goat serum for 1 h at room temperature. After rinsing with TBST three times, we incubated the slides with HRP secondary conjugates for 30 min at room temperature. SignalStain DAB Substrate Kit was adopted to determine GADD45α protein in tumor tissues. We used hematoxylin to stain the nuclei. The results were recorded through a Zeiss microscope Axio Lab A1.

Data Analysis

We utilized GraphPad Prism 7.0 (Graph Pad Software, San Diego, CA) to conduct analyzing and visualizing data. The corresponding data were present as means ± standard deviations (SD). We used two-tailed student's test and one-way ANOVA to assess the statistical significance of data ($^{*}p < 0.05$, $^{**}p < 0.01$, $^{\#\#}p < 0.01$).

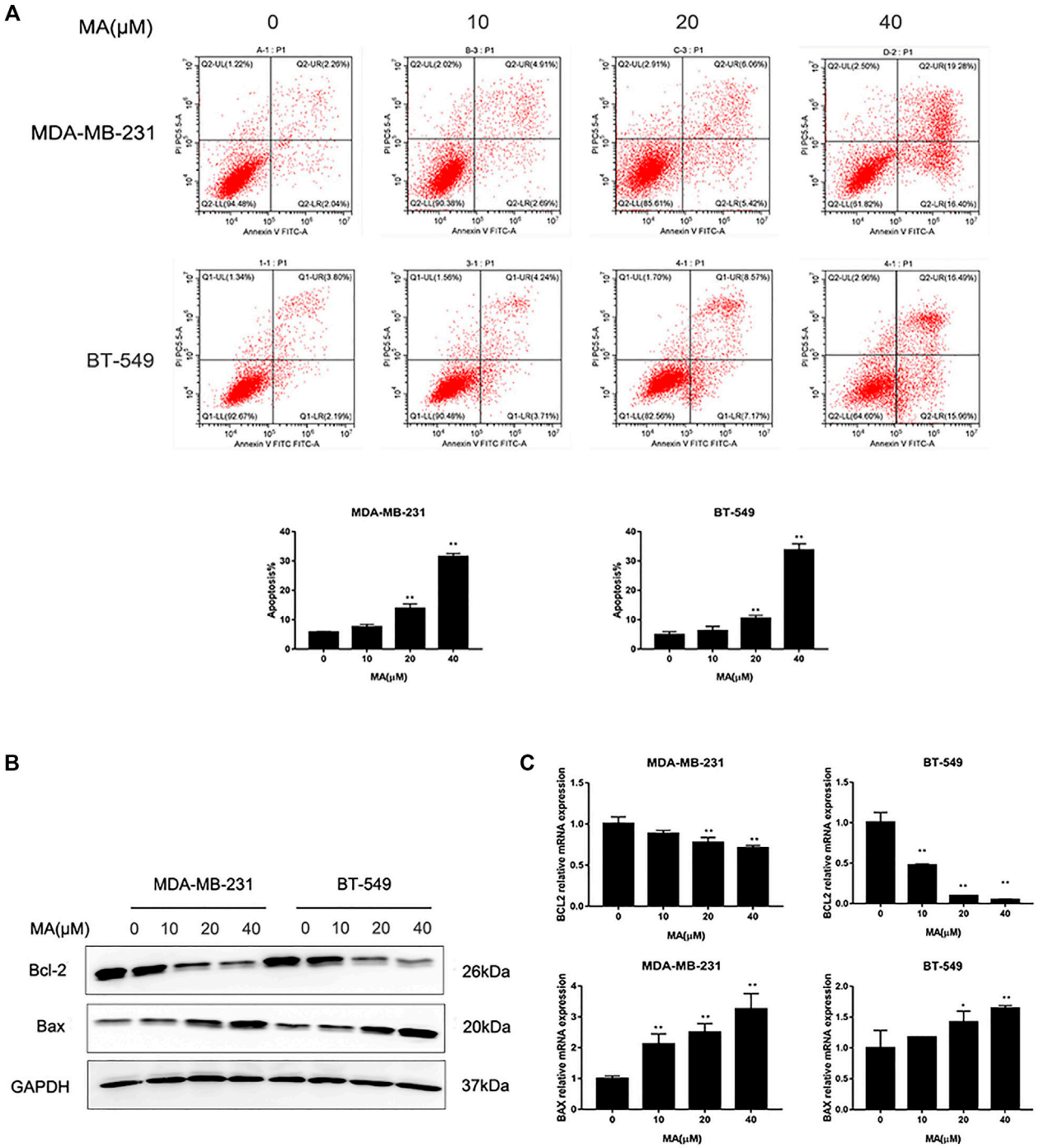


FIGURE 3 | MA promotes TNBC cell apoptosis. **(A)** Representative images of flow cytometry and percentages of apoptotic cells in TNBC cells determined after MA treatment for 24 h. **(B)** Western blot analysis of Bax and Bcl-2 protein expression after 24 h MA treatment. **(C)** Real-time PCR analysis of BAX and BCL-2 mRNA expression after 24 h MA treatment. Compared with the control group (0 μM), $^{**}p < 0.01$.

RESULTS

MA Exerts Cytotoxic Effects on TNBC Cells

To assess the inhibitory effect of MA on TNBC proliferation, we used a CCK-8 assay. After 24 h MA treatment, the cell viability was notably repressed above the concentration of 10 μM in BT549 and MDA-MB-231 cells. The IC_{50} values of MDA-MB-231 and BT549 cells were 25.24 and 20.99 μM, respectively (**Supplementary Figure S1**). MA could inhibit TNBC cell proliferation remarkedly at the concentration of 5 μM for 48 h

treatment ($p < 0.01$). In the meantime, MA demonstrated a dose-dependent suppression of cell viability in TNBC cells ($p < 0.01$) (**Figure 2A**). The cytotoxic effect of MA on TNBC cells was further determined *via* foci formation assay. As shown in **Figure 2B**, MA could reduce the number of foci in MDA-MB-231 and BT549 cells after 24 h inference. Taken conjointly, MA has a repressive effect on TNBC cell growth and foci formation.

MA Promotes Apoptosis in TNBC Cells

The results of Annexin V/PI staining apoptosis analysis showed that MA could induce an increase of a percentage of apoptotic cells after 24 h interference in TNBC cells ($p < 0.01$) (**Figure 2A**). The increasing percentage of apoptotic cells was consistent with the increasing of MA concentration. Additionally, MA could enhance Bax protein expression and reduce Bcl-2 protein expression (**Figure 3B**). Bax promotes mitochondrial apoptosis as a proapoptotic factor, while Bcl-2 restrains apoptosis progress as an anti-apoptotic factor. Meanwhile, MA could upregulate Bax mRNA expression and downregulate Bcl-2 mRNA expression (**Figure 3C**). These data signify that MA might inhibit TNBC cell proliferation by triggering mitochondrial-based apoptosis.

MA Inhibits EMT in TNBC Cells

Based on the data from the CCK-8 assay, MA could not affect cell proliferation of BT549 and MDA-MB-231 cells under the concentration of 5 μM for 24 h treatment. Thus, we adopted 0, 1, 2.5, and 5 μM MA to conduct the study further about the suppressive effect of MA on TNBC cell mobile capacity. Wound healing assay exerted that after MA treatment for 24 h, the percentages of BT549 and MDA-MB-231 cells to moving into the wound area were significantly repressed, compared with the control group (**Figure 4A**). Similarly, invading cell numbers were dramatically abated after MA treatment for 24 h according to the results of a chamber invasion assay (**Figure 4B**). The EMT process plays an essential role in cancer cell migration and invasion. Mesenchymal phenotype markers (N-cadherin, Vimentin) protein expression was remarkably decreased, while epithelial phenotype marker (E-cadherin) protein expression was noticeably increased after MA interference in TNBC cells (**Figure 4C**). Meanwhile, MA-treated cells manifested a significant increase of E-cadherin mRNA (**Figure 4D**). These findings thus imply that MA hinders EMT progression to successively hamper the migratory and invasive abilities of TNBC cells.

MA Suppresses TNBC Tumor Growth

To investigate the suppressive effect of MA *in vivo*, MDA-MB-231 cells were injected into mammary fat pads of 4-week-old nude mice. After 28 days MA intraperitoneal injection, the mice were sacrificed, and the tumors were collected. The volumes and weights of tumors were recorded and compared. The results displayed that MA could reduce the volume and weights of tumors compared to the control group, and the high-dose group had a significantly more inhibitory effect on tumor growth than the low-dose group (**Figures 5A–C**). Interestingly, even the high dose of MA did not affect the body weights significantly compared to the control group (**Figure 5E**). HE staining demonstrated that in the control group, there were a large number of agglomerated and closely arranged tumor cells with deeply stained nuclei. In MA-treated groups, especially the high-dose group, the number of tumor cells decreased dramatically and the arrangement was relatively loose (**Figure 5F**). Taken together, MA also has a critical inhibitory effect on TNBC tumor growth *in vivo*.

MA Downregulates Overexpressed miR-374a in TNBC Cells

Accumulating evidence indicates that miRNAs play an essential role in cell proliferation and tumor growth in breast cancer. A PCR array was performed to screen the varied miRNA with at least 1.5-fold change after MA treatment. According to the results, miR-374a was notably abated in both cell lines after exposure to 20 μM MA for 24 h (**Figure 6A**). According to the clinical data from the dbDEMC database (https://www.biosino.org/dbDEMC/index), miR-374a was highly expressed in various cancers compared to their corresponding normal tissues, suggesting miR-374a as an oncogene (**Figure 6B**) (Yang et al., 2017). Besides, miR-374a was confirmed to express at a high level in basal-like breast cancer tissues (**Supplementary Figure S2**). Also, data from the TCGA database using UALCAN analysis (http://ualcan.path.uab.edu/analysis.html) showed that miR-374a was dramatically overexpressed in TNBC tissues compared to other molecular types of breast cancer (**Figure 6C**) (Chandrashekar et al., 2017). Utilizing real-time PCR, we confirmed that MA had an inhibitory effect on miR-374a of TNBC cells in a dose-dependent manner (**Figure 6D**). Collectively, these data manifest that MA inhibits oncogenic miR-374a in TNBC cells.

MA Modulates miR-374a/GADD45α Axis

DIANA TOOLS (http://diana.imis.athena-innovation.gr/DianaTools/) predicted that GADD45A was one of the most potential targets of miR-374a (**Supplementary Figure S3**), and a present study suggested GADD45α as the downstream of miR-374a in a pheochromocytoma cell (Gong et al., 2018). Dual luciferase reporter assay confirmed that miR-374a could directly bind to the 3′UTR region of GADD45A (**Figure 6E**). Based on the data from the TCGA database using UALCAN analysis, GADD45A was lowly expressed in various types of cancer, including breast cancer. Moreover, GADD45A was dramatically expressed at a low level in TNBC, compared to normal tissues (**Figures 7A,B**). Pathway common (https://www.pathwaycommons.org/) exerted genes interacting with GADD45A (**Supplementary Table S3**), and KEGG annotation classification statistics of these genes indicated their role in cancer as well as MAPK pathway (**Figures 7C,D**). Further study displayed that MA could facilitate GADD45α mRNA and protein levels dose-dependently after 24 h treatment (**Figures 8A,B**). The *in vivo* results were inconsistent with *in vitro* findings. Determined by IHC staining, GADD45α was almost absent in tumor tissue and significantly increased in the MA high-dose group (**Figure 5F**). Results from real-time PCR exerted that

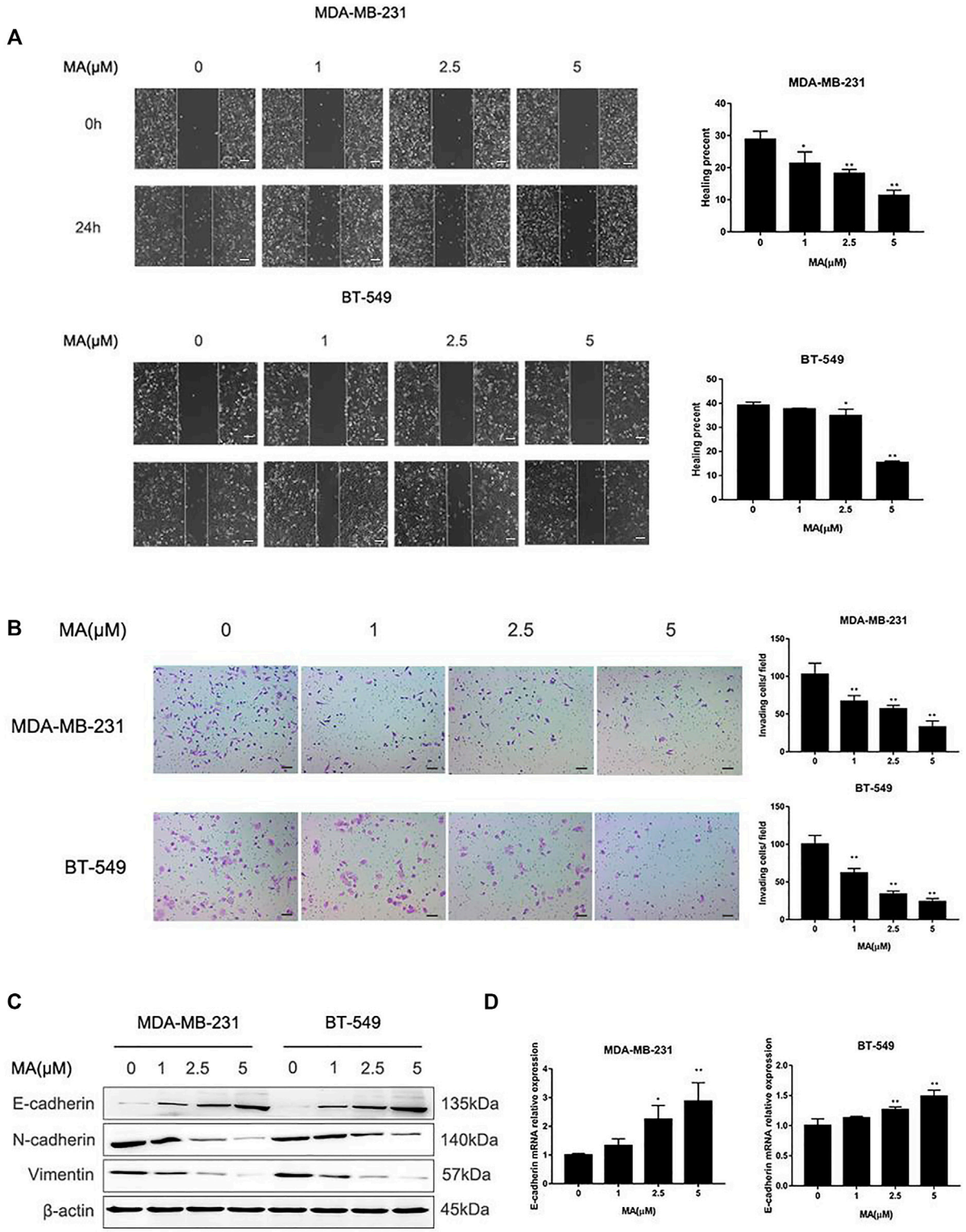


FIGURE 4 | MA alleviates migration and invasion of TNBC cells. **(A)** Representative images of wound healing assay and healing percentage of TNBC cells after 24 h MA treatment. **(B)** Representative images of chamber invasion assay and number of invading cells after 24 h MA treatment. **(C)** Western blot analysis of EMT-related protein levels after 24 h MA intervention. **(D)** Real-time PCR analysis of E-cadherin after exposure to MA for 24 h. Compared with the control group (0 μM), $^{*}p < 0.05$, $^{**}p < 0.01$.

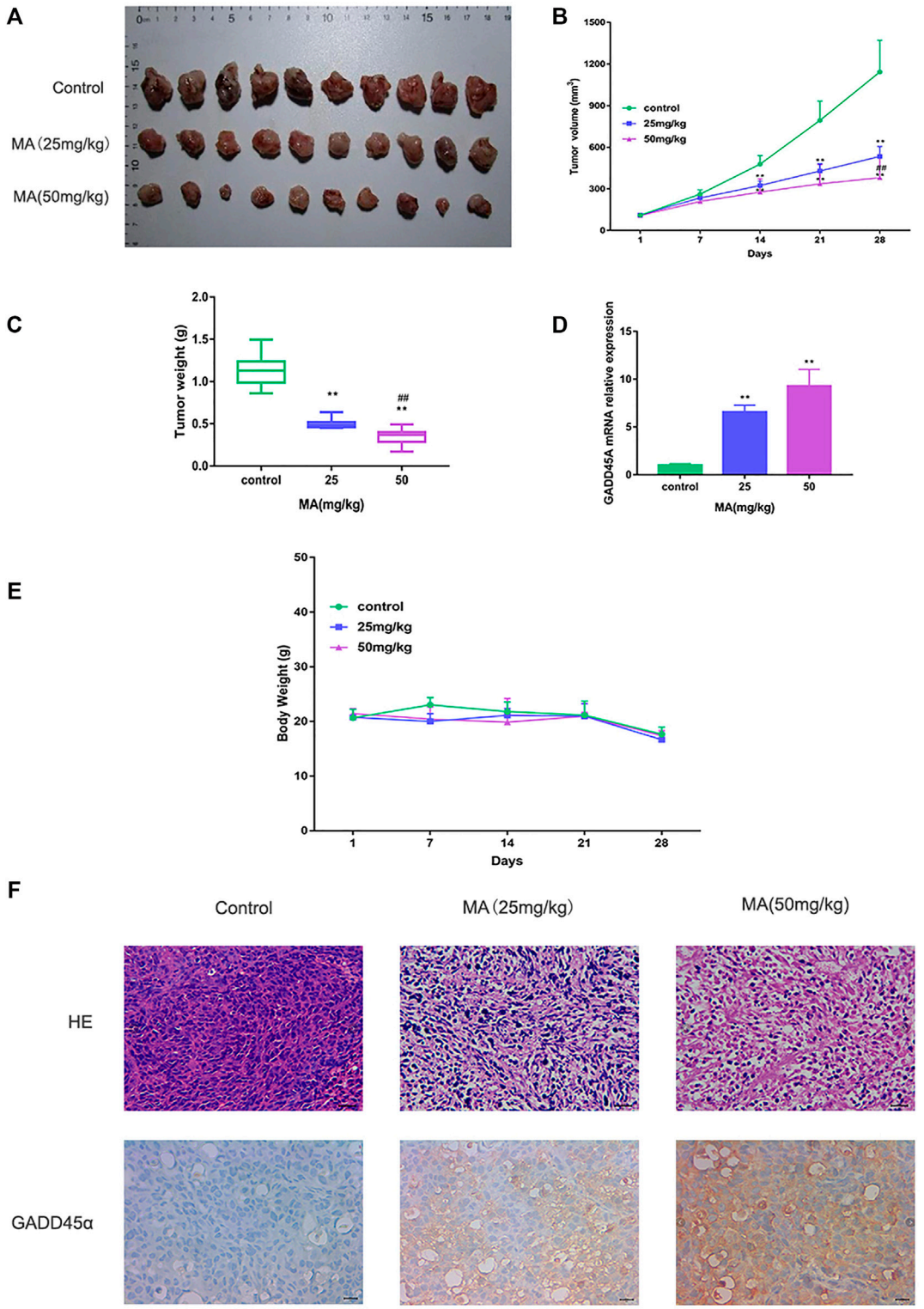


FIGURE 5 | MA restrains TNBC tumor growth. **(A)** Collected tumor tissues after MA administration. **(B)** Tumor volumes in different groups during the experiment. **(C)** Tumor weights in different groups after MA administration. **(D)** Real-time PCR analysis of GADD45α mRNA levels in xenograft models at the end point. **(E)** Body weights of mice in different groups during the experiment. **(F)** Representative images of HE staining and IHC analysis of GADD45α after MA administration. Compared to the control group, $^{**}p < 0.01$; compared to the low-dose group, $^{\#\#}p < 0.01$.

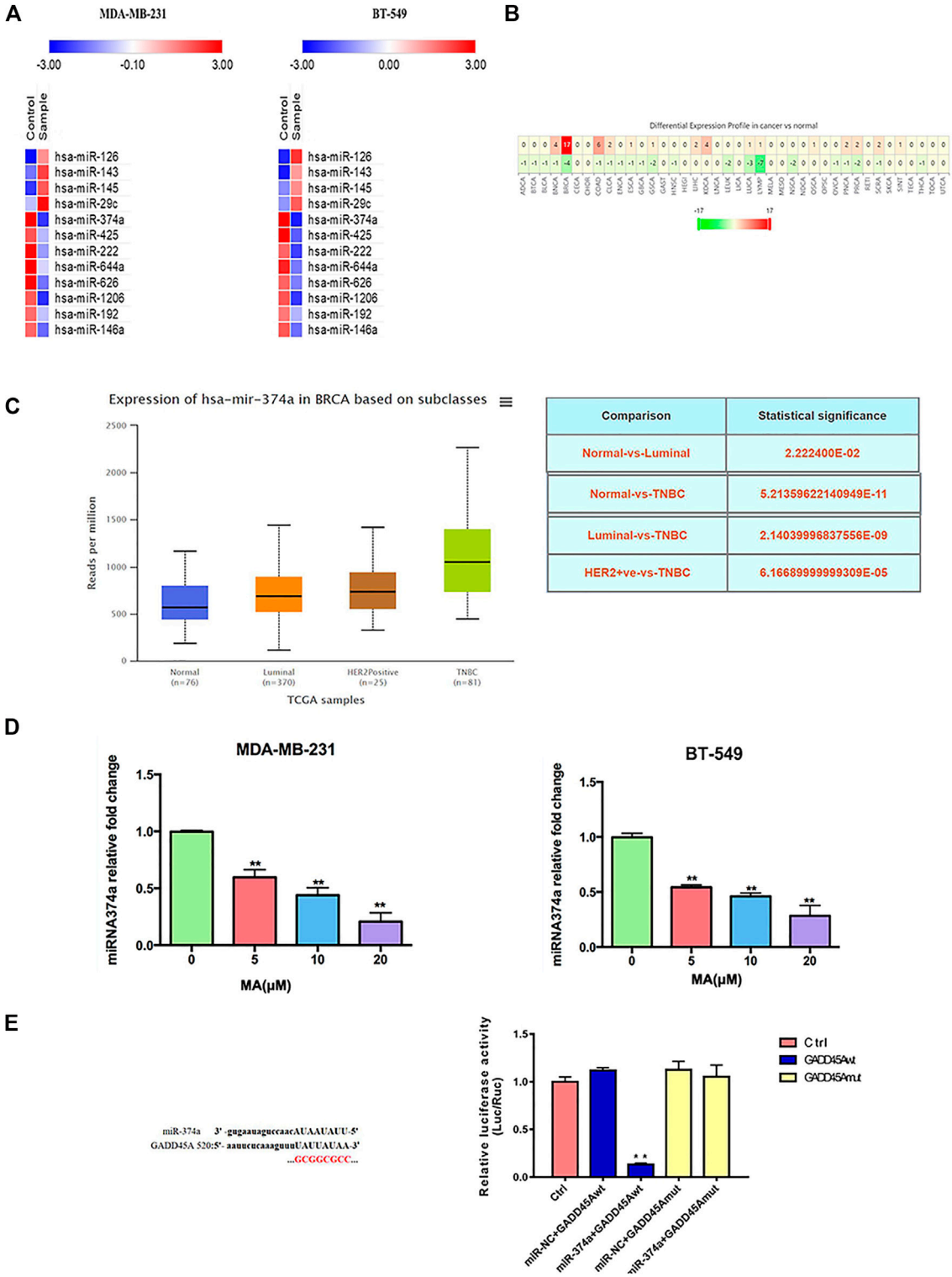


FIGURE 6 | Overexpressed miR-374a is inhibited by MA in TNBC cells. **(A)** PCR array analysis of miRNAs variation in TNBC cells after 24 h MA intervention. **(B)** MiR-374a expression in different types of cancer tissues and the corresponding normal tissues. **(C)** MiR-374a expression in different types of breast cancer tissues and normal tissues. **(D)** Real-time PCR analysis of miR-374a expression in TNBC cells after 24 h MA intervention. **(E)** Relative luciferase activity determined through dual luciferase reporter assay in 293 T cells. Compared to the control group, $^{**}p < 0.01$.

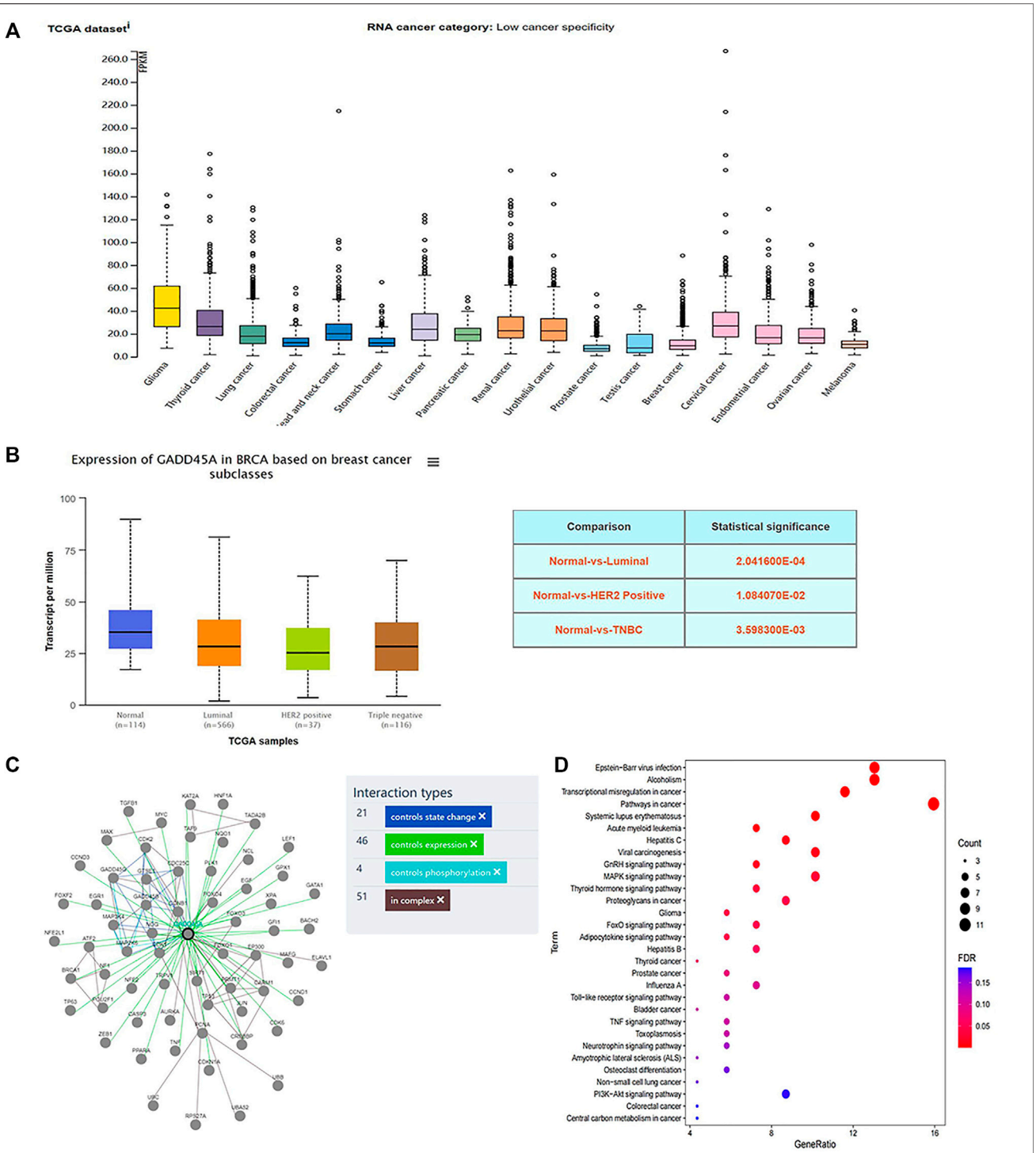


FIGURE 7 | GADD45A is expressed at a low level in TNBC. **(A)** GADD45A expression in different types of cancer tissues. **(B)** GADD45A expression in different types of breast cancer tissues and normal tissues. **(C)** GADD45A is interacted with multiple genes. **(D)** KEGG annotation classification statistics of GADD45A-related genes.

GADD45A was lowly expressed in tumor tissues, and MA treatment could enhance GADD45A expression dose-dependently *in vivo* (**Figure 5D**). To evaluate the effect of miR-374a downregulated by MA on GADD45A, we transfected BT-549 and MDA-MB-231 cells with miRNA mimic negative control and miR-374a mimic, and the successful transfection was confirmed by real-time PCR (**Figure 8C**). GADD45α mRNA and protein expression were

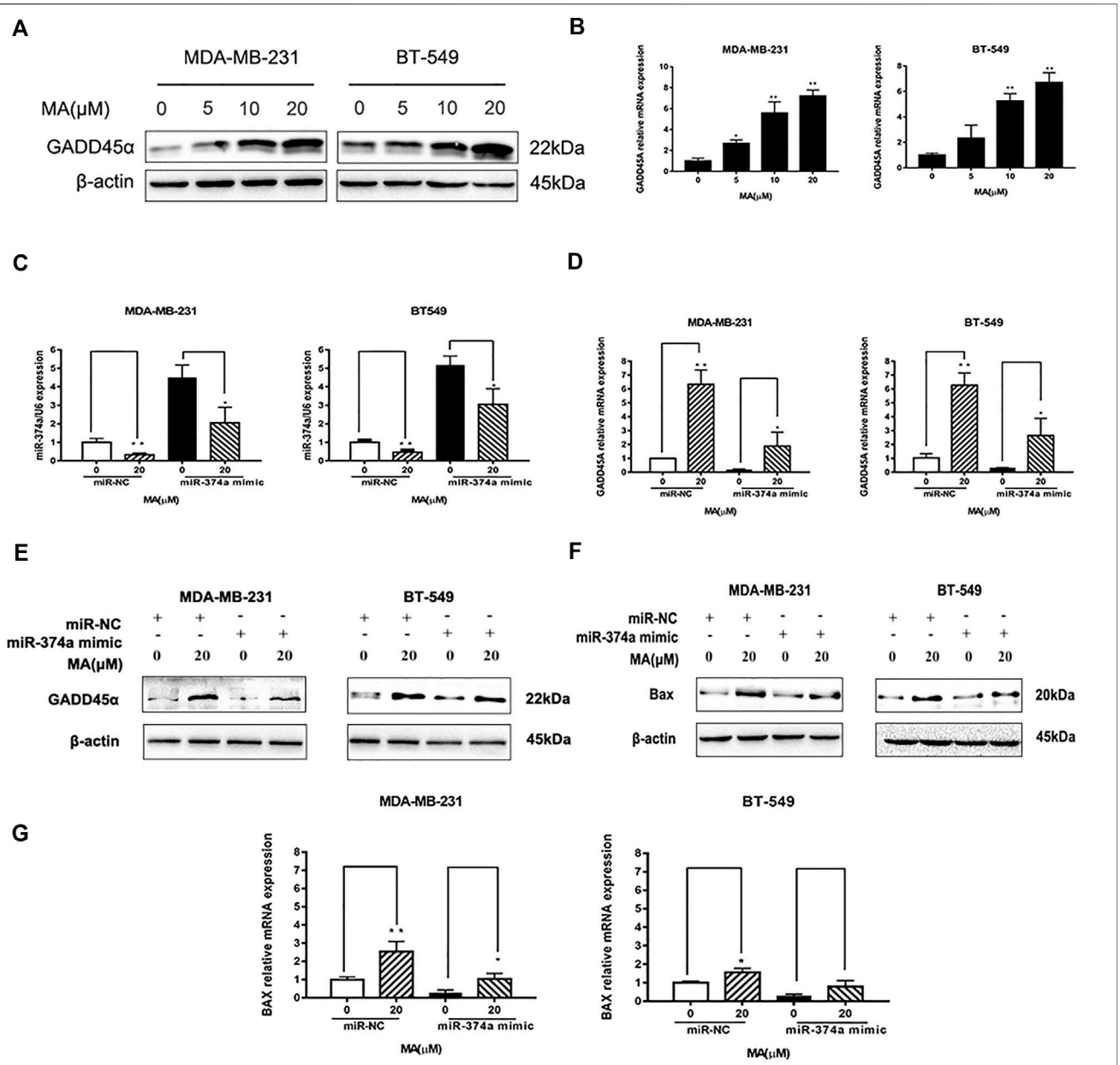


FIGURE 8 | MA regulates miR-374a/GADD45A axis. **(A)** Western blot analysis of GADD45α after 24 h MA treatment. **(B)** Real-time PCR analysis of GADD45α mRNA expression after 24 h MA treatment. **(C)** Real-time PCR analysis of miR-374a expression in different groups of TNBC cell **(D)** Real-time PCR analysis of GADD45A mRNA expression in different groups of TNBC cells. **(E)** Western blot analysis of GADD45α protein expression in different groups of TNBC cells. **(F)** Western blot analysis of Bax protein expression in different groups of TNBC cells. **(G)** Real-time PCR analysis of BAX in different groups of TNBC cells. Compared with the control group (0 μM), $^{*}p < 0.05$, $^{**}p < 0.01$.

detected after miR-374a mimic transfection and MA treatment. As shown in **Figures 8D,E**, MA could significantly promote GADD45α mRNA and protein levels at the concentration of 20 μM, and the effect was at least partly blocked after the miR-374a mimic pretreatment. Besides, Western blot results demonstrated that MA could promote Bax expression, and the upregulation of miR-374a would at least partly reverse the effect of MA (**Figure 8F**). As for BAX mRNA expression, the miR-374a mimic exerted a similar effect even after MA treatment (**Figure 8G**). Altogether, MA might activate GADD45α and related genes through downregulation of miR-374a in TNBC cells.

DISCUSSION

Breast cancer is the most common cancer occurring in women worldwide, with increasing incidence. TNBC belongs to the most

aggressive subtype of breast cancer, always accompanying worse clinical outcome (Feng Wang et al., 2021). Despite improvement in breast cancer therapeutic measures, the treatment for TNBC clinically without obvious side effects is still a huge challenge (Ghosh et al., 2021). Searching for complementary and alternative medicine is critical for the advancement of current TNBC therapies. Presently, TCM, with multiple biological capacities, gains credibility and reputation as a source of potential anti-cancer reagents (Yao et al., 2021). According to our previous work, several pure compounds isolated from *S. suberectus* could inhibit breast cancer (Peng et al., 2020; Peng et al., 2021b). We found that MA, extracted from *S. suberectus*, could also suppress the proliferative, migratory, and invasive abilities of TNBC cells (**Figures 2**, **3**, **4**). Apart from *in vitro* study, results from animal experiments further confirmed its anti-TNBC effect (**Figure 5**). Consequently, our study first clarified the anti-breast cancer property of MA. Meanwhile, it is interesting that we found that MA could downregulate miR-374a (**Figure 6**), an oncogenic regulator in TNBC cells promoting cell proliferation, migration, and invasion (Cai et al., 2013; Du et al., 2019; Son et al., 2019).

Triggering apoptosis relied on the balance between prosurvival and proapoptotic BCL-2 protein family members (Diepstraten et al., 2021). A recent study pointed out that DNA damage and oncogene deregulation could contribute to the activation of BCL-2-family-regulated pathway (Singh et al., 2019). Interestingly, miR-374a could act as an oncogenic factor in various types of cancer, and the down-regulation of miR-374a frequently led to stimulating apoptosis (Peng et al., 2021a). Our study exerted the proapoptotic effect of MA with a decrease of miR-374a, and miR-374a could directly bind to the 3′UTR region of GADD45A (**Figures 8, 5, 6**). GADD45A belongs to the growth arrest and DNA damage-inducible 45 family, mainly affecting cell cycle and interacting with cell growth modulators (Sytnikova et al., 2011). Furthermore, GADD45A had an inhibitory effect on cell cycle and cell proliferation through the regulation of P53 in bladder cancer (Han et al., 2019). More recent studies indicated GADD45A could even act as a tumor suppressive gene by facilitating apoptosis, maintaining cell-to-cell adhesion, inhibiting angiogenesis, modulating drug resistance, suppressing metastasis, promoting DNA repair, and stabilizing genomics (Yang et al., 2013; Bartoszewski et al., 2020; Runtian Wang et al., 2021). GADD45A was gradually considered as a promising target for tumor malignancy (Lin et al., 2022). More recent studies made an effort to prove that natural compounds could promote apoptosis through the activation of the cellular function of GADD45A (Jang et al., 2021). Meanwhile, MA could upregulate both GADD45α protein and mRNA expression, and overexpressing miR-374a would at least partly block the effect (**Figure 8**). These findings suggested the modulatory effect of MA in the mitochondria apoptotic signaling with the function to promote GADD45A through the inhibition of miR-374a in TNBC.

In addition to accelerating tumor growth, miR-374a is attributed to epithelial cells shifting into mesenchymal stem cells, namely, EMT process in cancer (Ma et al., 2019). In cancer cells, EMT initiates migration and invasion with the increase of more aggressive capacities (Bakir et al., 2020). EMT initiation is based on E-cadherin to N-cadherin switch, resulting in lessening cell-cell adhesion and gaining mobile ability (Biswas, 2020). Intriguingly, MA could upregulate E-cadherin and downregulate N-cadherin, accompanying a decrease of migratory and invasive TNBC cell numbers (**Figure 4**). In the meantime, MA could diminish miR-374a expression (**Figure 6**). These data first implied the role of MA as the mediator of the EMT process in TNBC cells.

CONCLUSION

TNBC cells tend to be more aggressive and EMT-activated than other molecular types of breast cancer. Our study demonstrated that MA had an inhibitory effect on TNBC proliferation, migration, invasion, and tumor growth as a promising drug candidate. Interestingly, MA could significantly repress miR-374a, which was usually considered as an oncogene regulating cancer initiation and development. Moreover, MA could promote GADD45α protein and mRNA expression through the downregulation of miR-374a. Further study confirmed that miR-374a directly targeted the 3′UTR region of GADD45A. Furthermore, the proapoptotic effect of MA was also negatively correlated to the expression of miR-374a. These findings first reported the anti-breast cancer effect of MA, pointed out GADD45A as the direct target of miR-374a in breast cancer, and partly offered evidence for *S. suberectus* as a resource of novel drug candidates in TNBC therapy.

DATA AVAILABILITY STATEMENT

Datasets generated for this article can be found in [TCGA] using the accession number TCGA-BRCA. The data are analyzed using UALCAN (http://ualcan.path.uab.edu/analysis.html).

ETHICS STATEMENT

The animal study was reviewed and approved by Ethics Committee of Chengdu University of Traditional Chinese Medicine.

AUTHOR CONTRIBUTIONS

The study was designed by FP and CP. The manuscript was written by FP and LW. FP performed experiments and analyzed data with LX and HT. LX and HT revised the manuscript. CP and JD supported the study.

FUNDING

The study was supported by National Natural Science Foundation of China (no. 82003879 and and U19A2010), the Key Project of Science and Technology Department of Sichuan Province (no. 2020YFS0053), and Youth Talent Promotion Project of China

Association for Science and Technology (CACM-2020-QNRC1-01) and the Open Research Fund of Chengdu University of Traditional Chinese Medicine Key Laboratory of Systematic Research of Distinctive Chinese Medicine Resources in Southwest China.

SUPPLEMENTARY MATERIAL

The Supplementary Material for this article can be found online at: https://www.frontiersin.org/articles/10.3389/fphar.2022.806869/full#supplementary-material

REFERENCES

An, J., Peng, C., Tang, H., Liu, X., and Peng, F. (2021). New Advances in the Research of Resistance to Neoadjuvant Chemotherapy in Breast Cancer. *Ijms* 22, 9644. doi:10.3390/ijms22179644

Aratanechemuge, Y., Hibasami, H., Katsuzaki, H., Imai, K., and Komiya, T. (2004). Induction of Apoptosis by Maackiain and Trifolirhizin (Maackiain Glycoside) Isolated from Sanzukon (Sophora Subprostrate Chen et T. Chen) in Human Promyelotic Leukemia HL-60 cells. *Oncol. Rep.* 12, 1183–1188. doi:10.3892/or.12.6.1183

Bakir, B., Chiarella, A. M., Pitarresi, J. R., and Rustgi, A. K. (2020). EMT, MET, Plasticity, and Tumor Metastasis. *Trends Cel. Biol.* 30, 764–776. doi:10.1016/j.tcb.2020.07.003

Bartoszewski, R., Gebert, M., Janaszak-Jasiecka, A., Cabaj, A., Króliczewski, J., Bartoszewska, S., et al. (2020). Genome-Wide mRNA Profiling Identifies RCAN1 and GADD45A as Regulators of the Transitional Switch from Survival to Apoptosis During ER Stress. *FEBS J.* 287, 2923–2947. doi:10.1111/febs.15195

Biswas, K. H. (2020). Molecular Mobility-Mediated Regulation of E-Cadherin Adhesion. *Trends Biochem. Sci.* 45, 163–173. doi:10.1016/j.tibs.2019.10.012

Cai, J., Guan, H., Fang, L., Yang, Y., Zhu, X., Yuan, J., et al. (2013). MicroRNA-374a Activates Wnt/β-Catenin Signaling to Promote Breast Cancer Metastasis. *J. Clin. Invest.* 123, 566–579. doi:10.1172/jci65871

Chandrashekar, D. S., Bashel, B., Balasubramanya, S. A. H., Creighton, C. J., Ponce-Rodriguez, I., Chakravarthi, B. V. S. K., et al. (2017). UALCAN: A Portal for Facilitating Tumor Subgroup Gene Expression and Survival Analyses. *Neoplasia* 19, 649–658. doi:10.1016/j.neo.2017.05.002

Diepstraten, S. T., Anderson, M. A., Czabotar, P. E., Lessene, G., Strasser, A., and Kelly, G. L. (2021). The Manipulation of Apoptosis for Cancer Therapy Using BH3-Mimetic Drugs. *Nat. Rev. Cancer* 22, 45–64. doi:10.1038/s41568-021-00407-4

Do, M., Hur, J., Choi, J., Kim, Y., Park, H.-Y., and Ha, S. (2018). Spatholobus Suberectus Ameliorates Diabetes-Induced Renal Damage by Suppressing Advanced Glycation End Products in Db/db Mice. *Ijms* 19, 2774. doi:10.3390/ijms19092774

Du, S., Hu, W., Zhao, Y., Zhou, H., Wen, W., Xu, M., et al. (2019). Long Non-coding RNA MAGI2-AS3 Inhibits Breast Cancer Cell Migration and Invasion *via* Sponging microRNA-374a. *Cancer Biomark.* 24, 269–277. doi:10.3233/cbm-182216

Wang, F., Kong, L., Pu, Y., Chao, F., Zang, C., Qin, W., et al. (2021). Long Noncoding RNA DICER1-AS1 Functions in Methylation Regulation on the Multi-Drugresistance of Osteosarcoma Cells *via* miR-34a-5p and GADD45A. *Front. Oncol.* 11, 685881. doi:10.3389/fonc.2021.685881

Fu, Y. F., Jiang, L. H., Zhao, W. D., Xi-Nan, M., Huang, S. Q., Yang, J., et al. (2017). Immunomodulatory and Antioxidant Effects of Total Flavonoids of Spatholobus Suberectus Dunn on PCV2 Infected Mice. *Sci. Rep.* 7, 8676. doi:10.1038/s41598-017-09340-9

Ghosh, S., Javia, A., Shetty, S., Bardoliwala, D., Maiti, K., Banerjee, S., et al. (2021). Triple Negative Breast Cancer and Non-small Cell Lung Cancer: Clinical Challenges and Nano-Formulation Approaches. *J. Control. Release* 337, 27–58. doi:10.1016/j.jconrel.2021.07.014

Gong, W., Qie, S., Huang, P., and Xi, J. (2018). Protective Effect of miR-374a on Chemical Hypoxia-Induced Damage of PC12 Cells *In Vitro* via the GADD45α/JNK Signaling Pathway. *Neurochem. Res.* 43, 581–590. doi:10.1007/s11064-017-2452-0

Guo, W.-L., Wang, W.-H., Hu, W.-T., Xie, Z.-Y., Wang, S.-F., Sun, Y., et al. (2018). Antibacterial Synergisms of Ji Xue Teng, Spatholobus Suberectus , Extract and Selected Antibiotics against Streptococcus Agalactiae from Nile Tilapia, *Oreochromis niloticus* (L.), *In Vitro* and *In Vivo*. *J. World Aquacult Soc.* 49, 1002–1013. doi:10.1111/jwas.12516

Han, N., Yuan, F., Xian, P., Liu, N., Liu, J., Zhang, H., et al. (2019). GADD45a Mediated Cell Cycle Inhibition Is Regulated by P53 in Bladder Cancer. *Onco Targets Ther.* 12, 7591–7599. doi:10.2147/ott.S222223

Iorio, M. V., Ferracin, M., Liu, C. G., Veronese, A., Spizzo, R., Sabbioni, S., et al. (2005). MicroRNA Gene Expression Deregulation in Human Breast Cancer. *Cancer Res.* 65, 7065–7070. doi:10.1158/0008-5472.Can-05-1783

Jang, H.-J., Yang, J. H., Hong, E., Jo, E., Lee, S., Lee, S., et al. (2021). Chelidonine Induces Apoptosis via GADD45a-P53 Regulation in Human Pancreatic Cancer Cells. *Integr. Cancer Ther.* 20, 153473542110061. doi:10.1177/15347354211006191

Lim, H., Park, M., Kim, C., Kang, B., Song, H.-S., Lee, H., et al. (2019). MiR-657/ATF2 Signaling Pathway Has a Critical Role in Spatholobus Suberectus Dunn Extract-Induced Apoptosis in U266 and U937 Cells. *Cancers* 11, 150. doi:10.3390/cancers11020150

Lin, H.-Y., Wu, H.-J., Chen, S.-Y., Hou, M.-F., Lin, C.-S., and Chu, P.-Y. (2022). Epigenetic Therapy Combination of UNC0638 and CI-994 Suppresses Breast Cancer via Epigenetic Remodeling of BIRC5 and GADD45A. *Biomed. Pharmacother.* 145, 112431. doi:10.1016/j.biopha.2021.112431

Ma, L., Shao, Z., and Zhao, Y. (2019). MicroRNA-374a Promotes Pancreatic Cancer Cell Proliferation and Epithelial to Mesenchymal Transition by Targeting SRCIN1. *Pathol. - Res. Pract.* 215, 152382. doi:10.1016/j.prp.2019.03.011

Mendell, J., and Olson, E. (2012). MicroRNAs in Stress Signaling and Human Disease. *Cell* 148, 1172–1187. doi:10.1016/j.cell.2012.02.005

Mizuguchi, H., Nariai, Y., Kato, S., Nakano, T., Kanayama, T., Kashiwada, Y., et al. (2015). Maackiain Is a Novel Antiallergic Compound that Suppresses Transcriptional Upregulation of the Histamine H 1 Receptor and Interleukin-4 Genes. *Pharmacol. Res. Perspect.* 3, e00166. doi:10.1002/prp2.166

Peng, F., Zhu, H., Meng, C.-W., Ren, Y.-R., Dai, O., and Xiong, L. (2019). New Isoflavanes from Spatholobus Suberectus and Their Cytotoxicity against Human Breast Cancer Cell Lines. *Molecules* 24, 3218. doi:10.3390/molecules24183218

Peng, F., Xiong, L., and Peng, C. (2020). (-)-Sativan Inhibits Tumor Development and Regulates miR-200c/PD-L1 in Triple Negative Breast Cancer Cells. *Front. Pharmacol.* 11, 251. doi:10.3389/fphar.2020.00251

Peng, F., Tang, H., Du, J., Chen, J., and Peng, C. (2021b). Isoliquiritigenin Suppresses EMT-Induced Metastasis in Triple-Negative Breast Cancer through miR-200c/C-JUN/β-Catenin. *Am. J. Chin. Med.* 49, 505–523. doi:10.1142/s0192415x21500233

Peng, F., Fan, H., Li, S., Peng, C., and Pan, X. (2021a). MicroRNAs in Epithelial-Mesenchymal Transition Process of Cancer: Potential Targets for Chemotherapy. *Ijms* 22, 7526. doi:10.3390/ijms22147526

Qin, S., Wu, L., Wei, K., Liang, Y., Song, Z., Zhou, X., et al. (2019). A Draft Genome for Spatholobus Suberectus. *Sci. Data* 6, 113. doi:10.1038/s41597-019-0110-x

Wang, R., Xu, K., Gao, F., Huang, J., and Guan, X. (2021). Clinical Considerations of CDK4/6 Inhibitors in Triple-Negative Breast Cancer. *Biochim. Biophys. Acta (Bba) - Rev. Cancer* 1876, 188590. doi:10.1016/j.bbcan.2021.188590

Singh, R., Letai, A., and Sarosiek, K. (2019). Regulation of Apoptosis in Health and Disease: the Balancing Act of BCL-2 Family Proteins. *Nat. Rev. Mol. Cel. Biol.* 20, 175–193. doi:10.1038/s41580-018-0089-8

Sinha, A., Agarwal, S., Parashar, D., Verma, A., Saini, S., Jagadish, N., et al. (2013). Down Regulation of SPAG9 Reduces Growth and Invasive Potential of Triple-Negative Breast Cancer Cells: Possible Implications in Targeted Therapy. *J. Exp. Clin. Cancer Res.* 32, 69. doi:10.1186/1756-9966-32-69

Son, D., Kim, Y., Lim, S., Kang, H. G., Kim, D. H., Park, J. W., et al. (2019). miR-374a-5p Promotes Tumor Progression by Targeting ARRB1 in Triple Negative Breast Cancer. *Cancer Lett.* 454, 224–233. doi:10.1016/j.canlet.2019.04.006

Sytnikova, Y. A., Kubarenko, A. V., Schäfer, A., Weber, A. N. R., and Niehrs, C. (2011). Gadd45a Is an RNA Binding Protein and Is Localized in Nuclear Speckles. *PLoS One* 6, e14500. doi:10.1371/journal.pone.0014500

Tang, Q., Ouyang, H., He, D., Yu, C., and Tang, G. (2019). MicroRNA-Based Potential Diagnostic, Prognostic and Therapeutic Applications in Triple-Negative Breast Cancer. *Artif. Cell Nanomed. Biotechnol.* 47, 2800–2809. doi:10.1080/21691401.2019.1638791

Tsai, R.-T., Tsai, C.-W., Liu, S.-P., Gao, J.-X., Kuo, Y.-H., Chao, P.-M., et al. (2020). Maackiain Ameliorates 6-Hydroxydopamine and SNCA Pathologies by Modulating the PINK1/Parkin Pathway in Models of Parkinson's Disease in *Caenorhabditis elegans* and the SH-SY5Y Cell Line. *Ijms* 21, 4455. doi:10.3390/ijms21124455

Wang, Z., Wang, D., Han, S., Wang, N., Mo, F., Loo, T. Y., et al. (2013). Bioactivity-Guided Identification and Cell Signaling Technology to Delineate the Lactate Dehydrogenase A Inhibition Effects of Spatholobus Suberectus on Breast Cancer. *PLoS One* 8, e56631. doi:10.1371/journal.pone.0056631

Yang, F., Zhang, W., Li, D., and Zhan, Q. (2013). Gadd45a Suppresses Tumor Angiogenesis via Inhibition of the mTOR/STAT3 Protein Pathway. *J. Biol. Chem.* 288, 6552–6560. doi:10.1074/jbc.M112.418335

Yang, Z., Wu, L., Wang, A., Tang, W., Zhao, Y., Zhao, H., et al. (2017). dbDEMC 2.0: Updated Database of Differentially Expressed miRNAs in Human Cancers. *Nucleic Acids Res.* 45, D812–D818. doi:10.1093/nar/gkw1079

Yao, C. L., Zhang, J. Q., Li, J. Y., Wei, W. L., Wu, S. F., and Guo, D. A. (2021). Traditional Chinese Medicine (TCM) as a Source of New Anticancer Drugs. *Nat. Prod. Rep.* 38, 1618–1633. doi:10.1039/d0np00057d

Zhang, J., He, Y., Yu, Y., Chen, X., Cui, G., Wang, W., et al. (2018). Upregulation of miR-374a Promotes Tumor Metastasis and Progression by Downregulating LACTB and Predicts Unfavorable Prognosis in Breast Cancer. *Cancer Med.* 7, 3351–3362. doi:10.1002/cam4.1576

Zhang, F., Liu, Q., Ganesan, K., Kewu, Z., Shen, J., Gang, F., et al. (2021). The Antitriple Negative Breast Cancer Efficacy of *Spatholobus Suberectus* Dunn on ROS-Induced Noncanonical Inflammasome Pyroptotic Pathway. *Oxid Med. Cel Longev* 2021, 5187569. doi:10.1155/2021/5187569

Conflict of Interest: The authors declare that the research was conducted in the absence of any commercial or financial relationships that could be construed as a potential conflict of interest.

Publisher's Note: All claims expressed in this article are solely those of the authors and do not necessarily represent those of their affiliated organizations, or those of the publisher, the editors and the reviewers. Any product that may be evaluated in this article, or claim that may be made by its manufacturer, is not guaranteed or endorsed by the publisher.

Copyright © 2022 Peng, Wang, Xiong, Tang, Du and Peng. This is an open-access article distributed under the terms of the Creative Commons Attribution License (CC BY). The use, distribution or reproduction in other forums is permitted, provided the original author(s) and the copyright owner(s) are credited and that the original publication in this journal is cited, in accordance with accepted academic practice. No use, distribution or reproduction is permitted which does not comply with these terms.

frontiers in Pharmacology

ORIGINAL RESEARCH
published: 14 March 2022
doi: 10.3389/fphar.2022.824579

Fengreqing Oral Liquid Exerts Anti-Inflammatory Effects by Promoting Apoptosis and Inhibiting PI3K/AKT and NF-κB Signaling Pathways

*Zhili Rao†, Xiangyu Li†, Xia Zhang, Jiuseng Zeng, Baojun Wang, Ruocong Yang and Nan Zeng**

State Key Laboratory of Southwestern Chinese Medicine Resources, School of Pharmacy, Chengdu University of TCM, Chengdu, China

OPEN ACCESS

Edited by:
Hong Zhang,
Shanghai University of Traditional Chinese Medicine, China

Reviewed by:
Ke Bian,
MIT, United States
Hang Ma,
University of Rhode Island, United States

***Correspondence:**
Nan Zeng
19932015@cdutcm.edu.cn

†These authors have contributed equally to this work

Specialty section:
This article was submitted to Ethnopharmacology, a section of the journal Frontiers in Pharmacology

Received: *29 November 2021*
Accepted: *27 January 2022*
Published: *14 March 2022*

Citation:
Rao Z, Li X, Zhang X, Zeng J, Wang B, Yang R and Zeng N (2022) Fengreqing Oral Liquid Exerts Anti-Inflammatory Effects by Promoting Apoptosis and Inhibiting PI3K/AKT and NF-κB Signaling Pathways. Front. Pharmacol. 13:824579. doi: 10.3389/fphar.2022.824579

Fengreqing oral liquid (FOL), a Chinese patent drug frequently used in clinical practice in China, is effective in treating inflammatory diseases of the upper respiratory tract such as colds and flu. However, its anti-inflammatory effects and mechanisms remain to be elucidated. In this study, the anti-inflammatory effects of FOL and its mechanisms on PI3K/AKT and NF-κB signaling pathways in LPS-induced RAW264.7 cells were explored, as well as the regulatory effect of FOL on apoptosis. In addition, the potential of FOL for the treatment of acute lung injury was explored in LPS-induced ALI mice. The results showed that treatment with FOL significantly reduced the levels of interleukin 1β (IL-1β), interleukin 6 (IL-6), nitric oxide (NO), and tumor necrosis factor α (TNF-α) in the supernatant of LPS-induced RAW264.7 cells, and also significantly reduced the phosphorylated protein levels of PI3K and AKT in the PI3K/AKT signaling pathway and also protein levels of NF-κB p50, phosphorylated NF-κB p65, and IκBα in the NF-κB signaling pathway. In addition, the results showed that FOL induced apoptosis in LPS-induced RAW264.7 cells at the level of 80%–90%, and significantly increased the protein expression levels of the pro-apoptotic Bax and cleaved-caspase-3. In LPS-induced ALI mice, FOL administration showed inhibition of IL-1β, IL-6, and TNF-α in Bronchoalveolar lavage fluid (BALF) and decreased protein expression levels of PI3K, AKT, NF-κB p50, and NF-κB p65, and elevated protein expression levels of Bax and cleaved-caspase-3 significantly. These results suggest that FOL may exert anti-inflammatory effects by inhibiting the PI3K/AKT signaling pathway to promote apoptosis and leading to attenuated activation of the NF-κB signaling pathway.

Keywords: Fengreqing oral liquid, anti-inflammation, apoptosis, acute lung injury, RAW 246.7 cells

INTRODUCTION

Fengreqing oral liquid (FOL), a Chinese patent medicine frequently used in clinical practice in China. In the theory of traditional Chinese medicine, it has the function of clearing away heat and toxic materials, expectorating, promoting the dispersing function of the lung, and expelling pathogenic factors from the exterior. Thus, it is mainly used for the treatment of fever, chills, headache, cough, runny nose, thirst, sore throat, and acute upper respiratory tract infections, which has a great curative

effect (Jie et al., 2021; Ruocong et al., 2021). FOL combines two ancient Chinese medical formulas, Qingdai Decoction in *Songfeng Shuoyi (On Pestilence Recorded by Song Feng)*, a TCM classic written by Liu Kui in the Qing Dynasty, and Jiegeng Decoction in *Shanghanlun (Treatise on Cold Damage)*, a TCM Canon written by Zhang Zhongjin and considered as the source of all prescription mannuals. These two formulas have been used in China for thousands of years and are highly effective for the treatment of inflammatory respiratory diseases. Recent studies have investigated the pharmacological effects of FOL and found that it had a significant inhibitory effect on xylene-induced ear swelling in mice (Kaixi et al., 2021b). A further study found that it significantly reduced tumor necrosis factor-α (TNF-α) and histamine content and obviously increased interleukin-4 (IL-4) content in swollen tissues of mice ears. In addition, the mechanism of analgesic effect of FOL may be related to the reduction of prostaglandin E2 and bradykinin levels and the increase of β-endorphin level in serum of mice (Kaixi et al., 2021b). Additional studies have shown that FOL has antiviral and antibacterial activity both *in vitro* and *in vivo*. It has also been reported that FOL enhances the immune function of immunocompromised mice by improving nonspecific immunity, humoral immunity, and cellular immunity (Kaixi et al., 2021a; Jie et al., 2021).

Acute lung injury (ALI) is a life-threatening disease with high morbidity and mortality rates that is characterized by severe inflammatory responses and tissue damage in the lungs (Mokra and Kosutova, 2015; Qu et al., 2019a). The main pathologies of ALI include diffuse alveolar injury, lung edema formation, neutrophil-derived inflammation, and surfactant dysfunction (Herold et al., 2013; Nieman et al., 2015). At present, it is well recognized that excessive-activated inflammatory response is the main cause of exacerbation of ALI or is causing multi-organ failure. Therefore, a novel strategy through suppressing the inflammatory cascade response in the lungs might be a promising therapy for the treatment of ALI (Rao et al., 2022).

It is well known that NF-κB regulates the expression of inflammation cytokine genes (Lambrou et al., 2020). The activation of NF-κB may lead to the release of proinflammatory cytokines (such as TNF-α, IL-6, and IL-1β), chemokines, and adhesion molecules, whereby enhancing the inflammatory response. Specifically, NF-κB signaling pathway activation is associated with the regulation of several signaling pathways, including apoptosis. Apoptosis, a programmed form of cell death, is a process actively selected through a series of pathways without causing an inflammatory response (Xu et al., 2019). Apoptosis plays an indispensable and irreplaceable role in both physiological and pathological conditions, while apoptotic dysfunction can lead to disease, and over-activated apoptosis may lead to disease exacerbation (Pietenpol and Stewart, 2002; García-Arriaza et al., 2017).

In our previous study, we predicted the potential targets of FOL *via* the network pharmacology approach and verified it by *in vitro* inflammation cells. The results showed that PI3K-AKT signaling transfer might be the key target in regulating the concentration of inflammation mediators of FOL in the Toll-like receptor signaling pathway. The vitro experiments confirmed that FOL may significantly reduce the levels of NO, IL-1β, IL-6, and TNF-α produced in LPS induced RAW264.7cells, which may be related to the regulation effect of FOL on PI3K-AKT pathway (Ruocong et al., 2021). In this study, we further investigated whether the anti-inflammatory effects of FOL were related to the regulation of NF-κB signaling pathway and apoptosis, and further evaluated its potential for the treatment of ALI.

MATERIALS AND METHODS

Preparation of FOL

FOL was provided by Xinlu Pharmaceutical Co. Ltd (Lot 200303; Sichuan, China) and composed of Gan Cao (*Glycyrrhiza uralensis* Fisch. ex DC. (Fabaceae)), Jie Geng (*Platycodon grandiflorus* (Jacq.) A. DC. (Campanulaceae)), Qing Dai (*Baphicacanthus cusia* (Nees) Bremek. (Acanthaceae)), Shan Yin Hua (Lonicera hypoglauca Miq. (Caprifoliaceae)), Gua Lou Pi (*Trichosanthes kirilowii* Maxim. (Cucurbitaceae)) and Xiong Dan Fen (Pulvis fellis ursi, Bile obtained from artificially cultured *Selenaretos thibetanus* Cuvier. by painless drainage). Briefly, 50 g of Qing Dai was macerated with 80% ethanol for 24 h and the percolate was collected. 850 g of Shan Yin Hua was extracted by redistillation to collect its aromatic water. The 500 g of Jie Gen, 400 g of Gua Lou Pi and 200 g of Gan Cao were steeped in water for half an hour and then decoction twice and the obtained filtrate was combined and concentrated by reducing pressure to a relative density of 1.10–1.15 g/ml at 90°C. Then ethanol was added to the above extract to reach 80% alcohol content and filtered, and the filtrate was combined with the percolate of Qing Dai and concentrated under reduced pressure to evaporate the ethanol. Then add the aromatic water of Shan Yin Hua and 5 g of Xiong Dan Fen, and adjust the pH to 6.0–6.5 with 10% sodium hydroxide solution. Finally, the extract was filtered and was added water to 1000 ml to fix the volume, sterilize and stored at 4°C until administration. In vitro study, 2 ml of FOL was taken and centrifuged at 3500 r/min for 10 min. The supernatant obtained was filtered through a 0.2 μm nylon microporous membrane and then stored at −20°C.

Determination of the Major Components of FOL by High-Performance Liquid Chromatography–Mass Spectrometry

The main chemical components of FOL were analyzed by high-performance liquid chromatography–mass spectrometry (HPLC-MS) (UltiMate 3000 LC, Orbitrap Elite; Thermo Scientific). In brief, FOL was centrifuged at 12,000 *g* and the supernatant was filtered at 0.22 μm and eluted with an Acclaim™ RSLC 120 C18 column (Thermo, Sichuan, China). The eluted components are fed into the mass spectrometer to collect the corresponding mass spectral information. The obtained mass spectral information was feature extracted and pre-processed using SIEVE software (Thermo, Sichuan, China), normalized, and edited into a two-dimensional data matrix including retention time, compound molecular weight, observed value (sample), and peak intensity using Excel 2010 software. The obtained compound mass spectral

information was compared with the mzcloud and mzvault databases, with information matching >85% as the screening condition.

Cell Culture

RAW264.7 cells were purchased from the Shanghai Cell Bank of the Chinese Academy of Sciences and cultured in complete Dulbecco's modified Eagle's medium (DMEM) containing 10% fetal bovine serum and 1% penicillin–streptomycin solution in an incubator at 37°C and 5% CO_2.

Animals

Male ICR mice (6 weeks old, 18–22 g) were obtained from Sichuan Dashuo Biotechnology Co. Ltd. (Sichuan, China) and given free access to water and a standard diet *ad libitum*. The mice were acclimated for 3 days before administration and housed in a controlled room with a constant temperature of 24 ± 2°C, relative humidity of 55 ± 10%, and a 12:12-h light:dark cycle. All animal studies were conducted in accordance with the guidelines of the Committee for Animal Care and Use of Laboratory Animals, College of Pharmacy, Chengdu University of Traditional Chinese Medicine (No. 20200320).

Determination of the Effect of FOL on Cell Viability by CCK-8 Assay

In our previous study, the effect of FOL on the viability of RAW264.7 cells was explored (Ruocong et al., 2021). We repeated this process in the current study and obtained the same results. Briefly, RAW264.7 cells (1×10^5 cells/ml) were uniformly seeded in a 96-well cell culture plate and incubated at 37°C and 5% CO_2 for 12 h. The cells were cultured with different concentrations of FOL (0.25%–0.50%) for 6 h before 100 μl of CCK-8 (Cell Counting Kit-8 Kit, Lot C1101130; YEASEN, Shanghai, China) solution (100 μl of DMEM containing 10 μl of CCK-8) was added to each well and incubated for 3 h. Then, the optical density value of each well was detected at 450 nm.

LPS Stimulation and Detection of NO, IL-6, IL-1β, and TNF-α in Culture Supernatant

RAW264.7 cells (1×10^6 cells/ml) were equally seeded in 6-well cell culture plates and cultured for 24 h. The cultured cells were divided into 5 groups, including control group, 0.30% of FOL group, LPS (1 μg/ml) group, LPS+0.30% of FOL group, and LPS+0.15% of FOL group. After aspirating the culture solutions, each group was pretreated with the corresponding concentrations of FOL for 6 h, while the control group and the LPS group contained an equal volume of DMEM. After 6 h of treatment, the culture solutions were removed. Except for the control group and 0.30% of FOL group in which DMEM was added, the cells in other groups were cultured with 1.5 ml of DMEM containing LPS (1 μg/ml) for 12 h. The cell culture supernatant was collected, and then the content of nitric oxide (NO) was determined by a Total Nitric Oxide Assay Kit (Beyotime Biotechnology, Lot 090420201102; Shanghai, China). The levels of IL-6, IL-1β, and TNF-α in the cell culture supernatant were measured by using enzyme-linked immunosorbent assay kits (ExCell Biotechnology, Lot 22A140, 22A128, 22A128; Shanghai, China), according to the manufacturer's instructions.

Effect of FOL on Apoptosis in LPS-Induced Inflammation Model of RAW264.7 Cells

RAW264.7 cells were seeded in a 6-well plate at a concentration of 10^6 cells/ml and divided into 5 groups: control group, 0.30% of FOL group, LPS group, 0.30% of FOL + LPS group, and 0.15% of FOL + LPS group. After each group was incubated with the corresponding concentration of drug for 6 h, LPS (1 μg/ml) was added to each group except the control group and 0.30% of FOL group for 12 h. Then, the cells were added to Annexin V-FITC and PI Staining Solution in an Annexin V-FITC/PI Apoptosis Detection Kit (Shanghai Yisheng Biotechnology Co. Lot 40302ES20, Shanghai, China), and the apoptotic cells were detected by flow cytometry according to the manufacturer's instructions.

To Investigate the Relationship Between the Anti-Inflammatory Effect of FOL and the Regulation of the PI3K/AKT Signaling Pathway by LY294002 and 740-YP

Our previous study predicted the potential targets of FOL via the approach of network pharmacology, and the results showed that PI3K-AKT signaling transfer might be the key part in regulating the concentration of inflammation cytokines. To investigate the relationship between the anti-inflammatory effect of FOL and the regulation of the PI3K/AKT signaling pathway, LY294002 (Selleck Biotech Technology Co. Lot S1105, USA), a PI3K inhibitor, and 740-YP (Shanghai TOPSCIENCE Biochemical Technology Co. Lot TQ0003, China), an activator of PI3K, were used in this study. Briefly, RAW264.7 cells (1×10^6 cells/ml) were equally seeded in 6-well cell culture plates and cultured for 24 h. The cultured cells were added with 1.5 ml of LY294002 (20 μM) or 740-YP (10 μM) solution for 2 h, and the other groups contained an equal volume of DMEM. Then, each group was pretreated with the corresponding concentrations of FOL for 6 h. After 6 h of treatment, the culture solutions were removed and cultured with 1.5 ml of DMEM containing LPS (1 μg/ml) for 12 h. The cytokines in the supernatant and proteins of cell lysate were measured.

LPS-Induced ALI and Administration

Mice were randomly divided into six groups: control group, sham-operation group, model group, LPS + FOL (12 ml/kg) group, LPS + FOL (6 ml/kg) group, and LPS + Dexamethasone (Sigma-Aldrich, Lot D4902, Shanghai, China) (LPS + DEX) (5 mg/kg) group. The mice in the LPS + FOL group (12 ml/kg, 6 ml/kg) were administered the corresponding concentrations of FOL by intragastric injection for 5 successive days, while the mice in the control group, sham-operation group, and model group were administered water instead. The mice in the LPS + DEX group were administered DEX dissolved in pure water. On day 6, after 12 h of fasting, all mice received

their final dose of the drug and then anesthetized by intraperitoneal injection of sodium pentobarbital (1%, 50 mg/kg) and immobilized. A sterile injection needle (1.0 ml) was used to puncture the trachea, which was then instilled with LPS (100 μl, 5 mg/kg) to induce ALI, while the mice in the sham-operation group were given an equal volume of sterile saline instead. After 8 h of LPS infusion, the mice were sacrificed, and the BALF and the lungs were collected for detection.

Detecting the Contents of IL-6, IL-1β, and TNF-α in BALF

After each mouse was sacrificed, a syringe with the tip cut off was inserted into the trachea and ligated. Then, 1 ml of saline was slowly injected into the syringe and lavaged three times to obtain the BALF. The BALF obtained was centrifuged at 3500 r/min for 10 min. The supernatant of BALF was separated out, and the contents of IL-6, IL-1β, and TNF-α in the BALF supernatant were measured by enzyme-linked immunosorbent assay kits (ExCell Biotechnology, Lot 22A05702, 22A02901 22A10608; Shanghai, China), according to the manufacturer's instructions.

The Content of Cells in BALF

After the supernatant of BALF was separated out, 1 ml of PBS was added to resuspension cells. Then, the number of cells in BALF were counted by a cell counting plate under an electron microscope.

Western Blotting

Proteins from cells and animal tissues were obtained by lysis of RIPA lysate buffer (Beyotime, Chengdu, China) containing 1 mM of phenylmethylsulfonyl fluoride (PMSF) (Med Chem Express, China). The protein concentrations were quantified by using the BCA kit (Beyotime, Chengdu, China), and all samples were adjusted to the same concentration. Then, the protein samples were mixed with 5 × loading buffer and heated to 95°C for 5 min. Afterwards, the proteins (10–30 μg) were separated by SDS-PAGE and electrophoretically transferred onto polyvinylidene fluoride membranes, and then blocked with 5% skimmed milk. The membranes were labeled with β-Actin (13E5) Rabbit mAb (Cell Signaling Technology, Lot #4970, USA), PI3 Kinase p85 Antibody (Cell Signaling Technology, Lot # 4292, USA), Akt (pan) (11E7) Rabbit mAb (Cell Signaling Technology, Lot #4685, USA), Phospho-PI3 Kinase p85 (Tyr458)/p55 (Tyr199) Antibody (Cell Signaling Technology, Lot#4228, USA), Phospho-Akt (Thr308) Antibody (Cell Signaling Technology, Lot#9275, USA), Apoptosis-Bcl-2 Antibody [Abmart Pharmaceutical Technology (Shanghai) Co. Lot P10415, Shanghai, China], Apoptosis regulator Bax [Abmart Pharmaceutical Technology (Shanghai) Co. Lot Q07812, Shanghai, China], Cleaved-Caspase 3 (Asp175), p17 Antibody [Abmart Pharmaceutical Technology (Shanghai) Co. Lot MB0711, Shanghai, China], Caspase-3 Antibody (Cell Signaling Technology, Lot #9662, USA), NF-κB1 p105/p50 (D4P4D) Rabbit mAb (Cell Signaling Technology, Lot#13586, USA), IκBα Antibody (Cell Signaling Technology, Lot #9242, USA), Phospho-IκBα (Ser32) (14D4) Rabbit mAb (Cell Signaling Technology, Lot #2859, USA), NF-κB p65 (D14E12) XP® Rabbit mAb (BSA and Azide Free) (Cell Signaling Technology, Lot #69994, USA), and Phospho-NF-κB p65 (Ser536) (93H1) Rabbit mAb (Cell Signaling Technology, Lot #3033, USA) antibody at 4°C overnight, and then incubated with anti-rabbit HRP-linked secondary antibody at room temperature for an hour. Antibody detections were performed using a ChemiDoc XRS+ (BioRad, Hercules, CA, United States) image analysis system.

Statistical Methods

The data are presented as mean ± S.D. SPSS 19.0 software (SPSS, Chicago, IL, United States) was used to determine the one-way analysis of variance with Fisher's protected least significant difference post hoc test to notarize the importance of multiple comparisons. The $p < 0.05$ was considered a statistically obvious difference, and the $p < 0.01$ was a significant difference.

RESULTS

Effects of FOL on RAW264.7 Cell Viability by CCK-8 Assay

The results showed that cells cultivated with 0.36%, 0.42%, and 0.50% of FOL for 6 h had a significant effect on RAW264.7 cell viability; the concentration of 0.30% and below had non-toxicity in RAW264.7 cells; therefore, the LPS-induced RAW264.7 cells were treated with 0.30% of FOL and 0.15% of FOL in the following experiments (**Figure 1**).

Effects of FOL on Secreted Expression of NO, IL-6, IL-1β, and TNF-α in RAW264.7 Inflammatory Cells

As shown in **Figure 1**, compared with the control groups, the levels of NO, IL-6, IL-1β, and TNF-α in the cell culture supernatant of LPS group were upregulated significantly. In addition, the contents of NO, IL-1β, IL-6, and TNF-α in the supernatant of the cells pretreated with FOL (0.30% and 0.15%) for 6 h have been downregulated significantly ($p < 0.01$). These results indicate that FOL has anti-inflammatory effects on LPS-stimulated RAW264.7 cells.

Effects of FOL on Inflammation *via* Inhibition of the PI3K/AKT Pathway

The results described above indicate that FOL can reduce the release of inflammatory cytokines. The PI3K/AKT signaling pathway may play a significant role in the release of pro-inflammatory cytokines. The results showed that 20 μM of LY294002 could only reduce the expression of IL-1β and have no effect on the secretion of IL-6, NO, and TNF-α in the LPS group. In addition, pretreatment with 20 μM LY294002 for 2 hours followed by treatment with 0.30% dose of FOL did not show significant differences in the secretion of IL-1β, IL-6, TNF-α, and NO compared to treatment with 0.30% dose of FOL

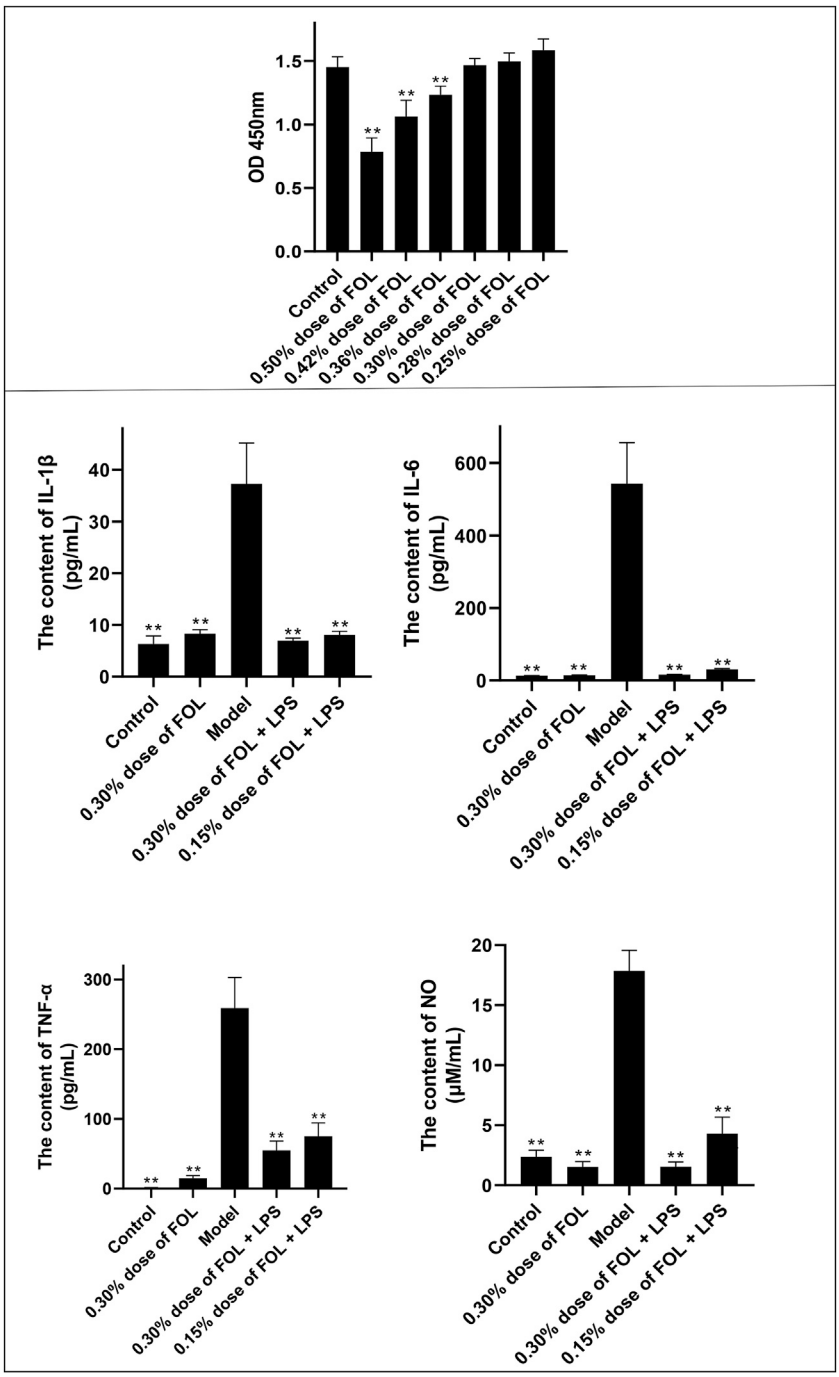


FIGURE 1 | Anti-inflammatory effect of FOL in LPS-induced RAW264.7 cells. The effect of FOL on the viability of RAW264.7 cells was determined by CCK-8 assay; results showed that 0.30% or below of FOL did not affect the cell viability of RAW264.7, and the effects of FOL on the expression levels of IL-1β, IL-6, TNF-α, and NO in LPS-induced cell supernatants were determined by ELISA. Data are presented as the mean ± SD compared with the LPS-only control group. $^{*}p < 0.05$; $^{**}p < 0.01$ ($n = 6$).

alone. What is more, the protein levels of p-PI3K/PI3K and *p*-AKT/AKT were detected and the results showed that the protein levels of p-PI3K/PI3K and *p*-AKT/AKT were obviously increased in the LPS group ($p < 0.01$). It was found that 0.30% and 0.15% dose of FOL could decrease the protein levels of p-PI3K/PI3K and *p*-AKT/AKT in LPS-induced RAW264.7

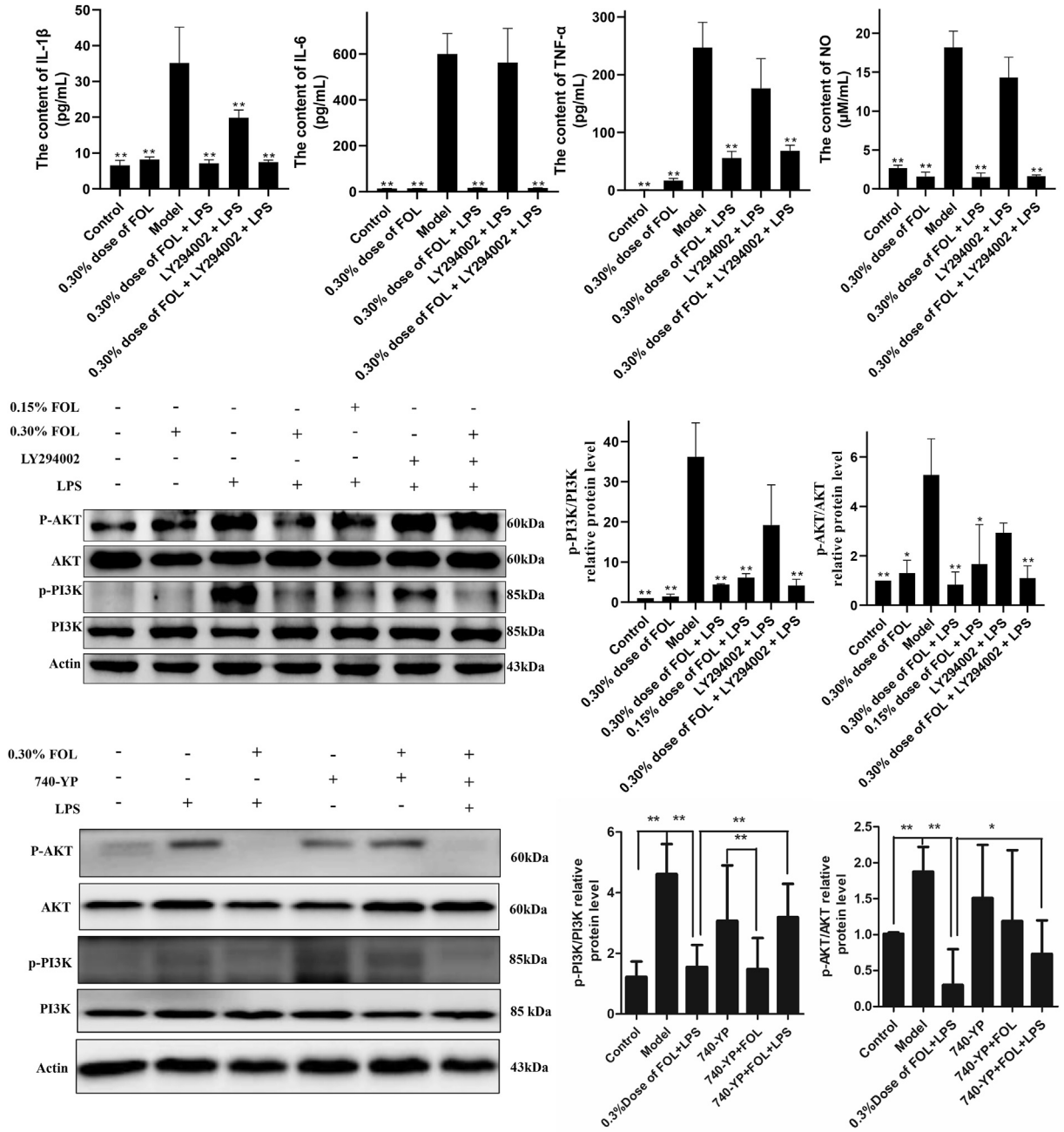


FIGURE 2 | Effect of FOL on the PI3K/AKT signaling pathway in LPS-induced RAW264.7 cells. Inhibit/activate the PI3K/AKT signaling pathway with LY294002/740-YP prior to FOL administration to determine whether FOL inhibits inflammatory cytokine expression by modulating the PI3K/AKT signaling pathway. The effect of FOL on phosphorylation of PI3K and AKT protein was also detected by Western blotting. Data are presented as the mean ± SD compared with the LPS-only control group. *$p < 0.05$; **$p < 0.01$ ($n = 6$).

inflammatory cells significantly ($p < 0.01$) (**Figure 2**). In addition, the PI3K agonist 740-YP significantly increased the expression levels of phosphorylated PI3K (p-PI3K) protein, while FOL inhibited PI3K activation induced by 740-YP. Meanwhile, in FOL-treated LPS-induced inflammatory cells, the inhibiting effect of FOL on phosphorylated PI3K and AKT was similarly attenuated by administration of 740-YP ($p < 0.05$).

FOL Suppresses Inflammatory Factor Expression by Inhibiting NF-κB Signaling Pathway Activation

The activation of the NF-κB signaling pathway is associated with the massive production of inflammatory cytokines, and the expression of key proteins of the NF-κB signaling pathway such as phosphorylated NF-κB p65, NF-κB p65, NF-κB p50,

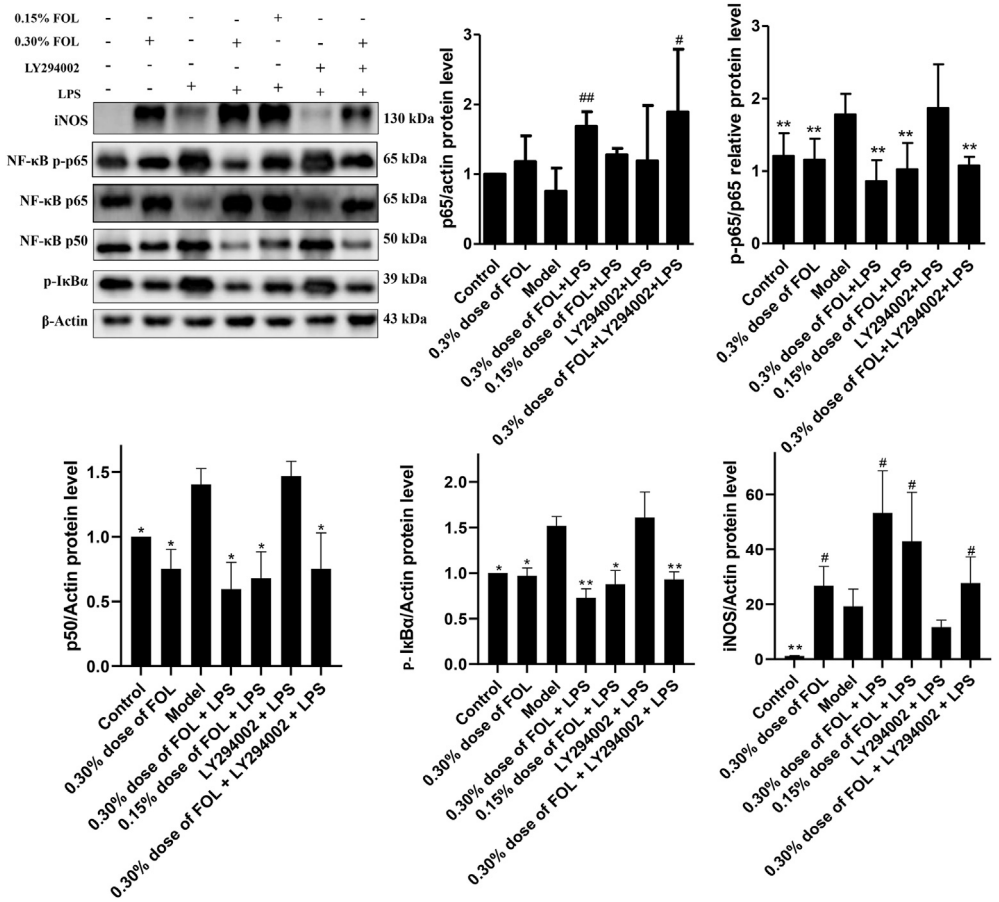


FIGURE 3 | Effect of FOL on the NF-κB signaling pathway in LPS-induced RAW264.7 cells. The effects of FOL on protein expression levels of iNOS, NF-κB p65, NF-κB p50, and phosphorylated IκBα and NF-κB p-p65 were detected by Western blotting in LPS-induced RAW264.7 cells. Data are presented as the mean ± SD compared with the LPS-only control group. $^{*}p < 0.05$; $^{**}p < 0.01$ ($n = 6$).

p-IκBα, and iNOS in LPS-induced RAW264.7cells was detected to investigate the regulatory effect of FOL on the NF-κB signaling pathway. The results showed that the NF-κB p50 and phosphorylated levels of NF-κB p65 and IκBα were significantly increased in LPS-induced RAW264.7 cells compared with the control group. In addition, the phosphorylated levels of NF-κB p65 were significantly decreased after 0.30% and 0.15% doses of FOL treatment, as well as the expression levels of NF-κB p50 and IκBα protein. Notably, the expression of iNOS was significantly increased in LPS-treated cells compared with controls, but the protein expression level of iNOS was further significantly increased after treatment with FOL. Meanwhile, LY294002 did not seem to show effective inhibition of NF-κB signaling pathway proteins such as NF-κB p65, NF-κB p65, NF-κB p50, and *p*-IκBα (**Figure 3**).

Effect of FOL on Apoptosis in LPS-Induced Raw264.7 Cells

To examine the regulatory effect of FOL on apoptosis, the apoptosis level of RAW264.7 cells was examined by flow cytometry. The results found that treatment with FOL could significantly increase the apoptosis level of RAW264.7 cells. Treatment with 0.30% dose of FOL for 3 h resulted in apoptosis levels of normal cells being 80.83%. The level of apoptosis in the 0.30% of FOL + LPS group and the 0.15% of FOL + LPS group was 94.77% and 75.74%, respectively. In addition, FOL significantly increased the expression of the pro-apoptotic protein Bax, and also significantly increased the activation level of the apoptosis executive protein caspase-3 (**Figure 4**). In addition, pretreatment with the PI3K agonist 740-YP significantly reduced FOL-induced activation of caspase-3 and Bax.

Main Chemical Components in FOL

In view of the good anti-inflammatory effect demonstrated by FOL in *in vitro* experiments, we further analyzed the main components in FOL by HPLC-MS. The ESI ± chromatograms are shown in **Figure 5**. By comparing and analyzing with the mzcloud and mzvalut database, we found that the chemical components with a high content in FOL include pyroglutamic acid, cryptochlorogenic acid, chlorogenic acid, caffeic acid, secoxyloganin, isochlorogenic acid B, isochlorogenic acid C, α-hederin, tanespimycin, glycyrrhizic acid, tauroursodeoxycholic

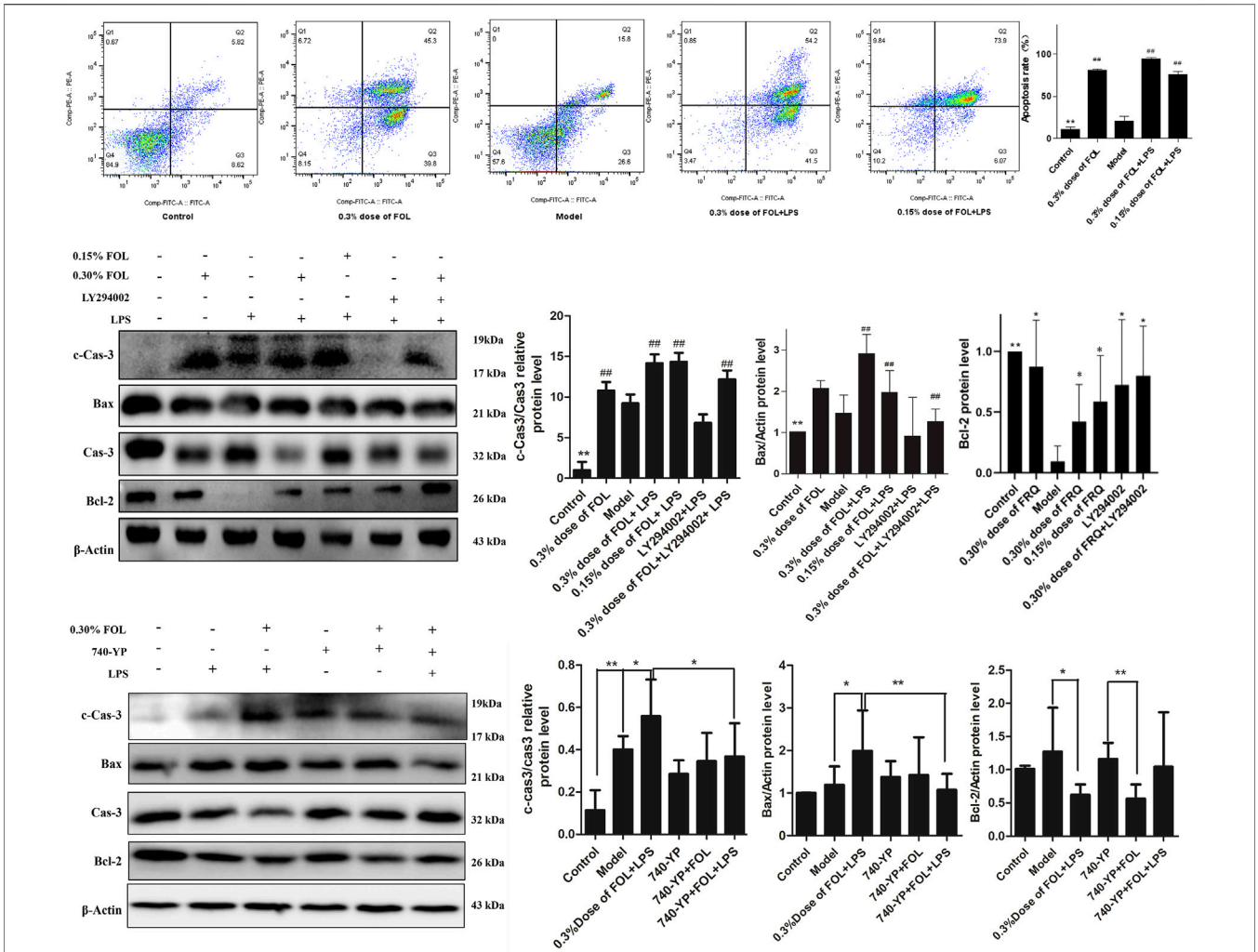


FIGURE 4 | Effect of FOL on apoptosis in LPS induced RAW264.7 cells. The effect of FOL on the apoptosis level of RAW264.7 cells was detected by flow cytometry. The effects of FOL on the expression levels of apoptosis-related proteins caspase-3, cleaved-caspase-3, and Bax and BCL-2 proteins were detected by Western blotting. Data are presented as the mean ± SD compared with the LPS-only control group. *$p < 0.05$; **$p < 0.01$; #$p < 0.05$; ##$p < 0.01$ ($n = 6$).

acid, hyodeoxycholic acid, and oleamide. The relative percentages of the top 30 compounds are shown in **Table 1**.

Effect of FOL on Inflammatory Cytokines in the BALF of LPS-Induced Acute Lung Injury Mice

As shown in **Figure 5**, the expression levels of IL-6, IL-1β, and TNF-α, and the total number of cells in BALF of LPS-induced ALI mice were measured. The results showed that the expression levels of IL-6, IL-1β, and TNF-α in the BALF of ALI mice were obviously higher than those of control and sham-operation mice. In addition, administration of FOL (6 ml/kg) could decrease the levels of IL-6 and TNF-α and the total number of cells in BALF of ALI mice significantly, and 12 ml/kg of FOL could significantly downregulate the level of IL-1β ($p < 0.05$). These results show that FOL can inhibit the release of IL-6, IL-1β, and TNF-α in ALI mice.

Effect of FOL on PI3K/AKT and NF-κB Signaling Pathways in LPS-Induced ALI Mice

As shown in **Figure 6**, the effects of FOL on the expression levels of proteins PI3K, AKT, and phosphorylated AKT in the lung tissue of LPS-induced ALI mice were examined. It was found that the protein expression levels of AKT, PI3K, and phosphorylated AKT were upregulated obviously in ALI mice ($p < 0.05$), and administration of FOL could reduce the protein expression levels of AKT significantly. In addition, the effect of FOL on the expression levels of key proteins of the NF-κB signaling pathway such as NF-κB p65, IκBα, iNOS, and the ratio of NF-κB p50 to NF-κB p105 in the lung tissue of LPS-induced ALI mice was also examined. The results showed that the expression levels of NF-κB p65, iNOS, and the ratio of NF-κB p50 to NF-κB p105 in LPS-induced ALI mice were increased significantly, and the expression level of IκBα was decreased; administration of FOL

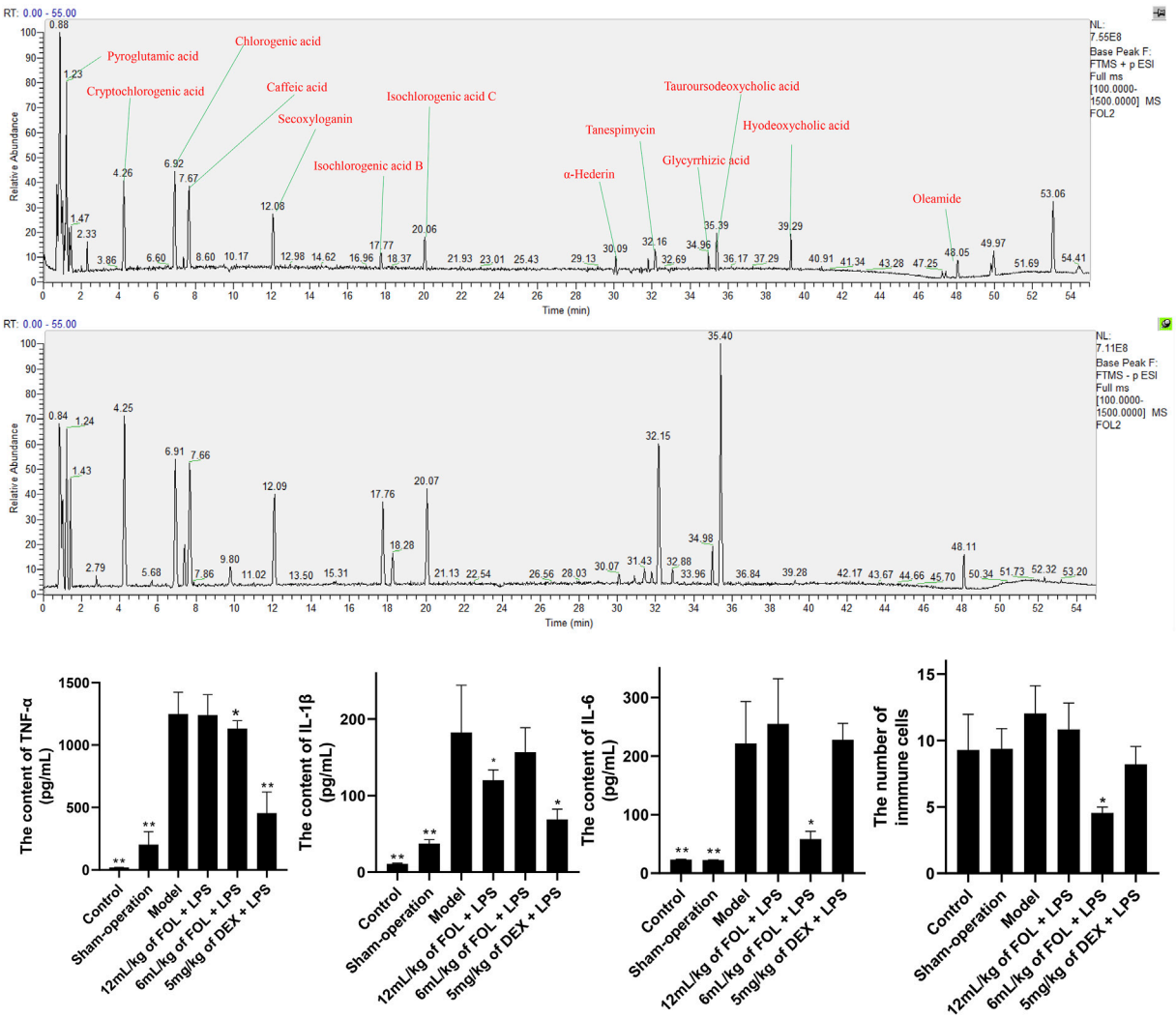


FIGURE 5 | The main compounds in FOL and the effects of FOL on the expression levels of IL-6, IL-1β, and TNF-α in BALF of ALI mice. ALI mice were induced by tracheal drip of LPS; BALF was collected; the contents of IL-6, IL-1β, and TNF-α in BALF were measured by ELISA; and the number of cells in BALF was counted by microscopy. Data are presented as the mean ± SD compared with the model-only control group. $^{*}p < 0.05$; $^{**}p < 0.01$ (n = 6–9).

showed an inhibiting effect on the ratio of NF-κB p50 to NF-κB p105 as well as the expression level of NF-κB p65. In addition, FOL also significantly elevated iNOS expression in the lung tissues of LPS-induced ALI mice.

Regulated Effects of FOL on Apoptosis in LPS-Induced ALI Mice

The protein expression levels of Bcl2, Bax, Caspase3, and cleaved-caspase 3 (c-caspase-3) were detected to investigate the regulated effects of FOL on apoptosis in LPS-induced ALI mice. As shown in **Figure 7**, compared with the control and sham-operated groups, the results showed that the expression of the pro-apoptotic protein Bax was significantly increased and the expression of the anti-apoptotic protein Bcl-2 was significantly decreased in LPS-induced ALI mice ($p < 0.05$). Furthermore, the ratio of c-Caspase3 to Caspase3 was also increased significantly. In comparison with LPS-induced ALI mice, Bax and c-Caspase3 were further increased in lung tissues of mice administration with a 12 ml/kg dose of FOL. This suggests that LPS-induced apoptosis was activated in mouse lung tissue, and treatment with FOL further exacerbated the level of apoptosis in lung tissue cells.

DISCUSSION

In the present study, we examined the anti-inflammatory effects of FOL in LPS-induced RAW264.7 cells and revealed the regulatory effects of FOL on apoptosis, PI3K/AKT, and NF-κB signaling pathways. In addition, the potential of FOL for the treatment of ALI was explored. FOL is widely used in China, and its clinical practice has been found to be effective in treating upper

TABLE 1 | The main chemical components in FOL.

NO.	Name	Formula	Molecular weight	RT [min]	Area (Max.)
1	Chlorogenic acid	$C_{16}H_{18}O_9$	354.09512	6.918	8965166431
2	Tauroursodeoxycholic acid	$C_{26}H_{45}NO_6S$	499.29715	35.396	7166230491
3	Cryptochlorogenic acid	$C_{16}H_{18}O_9$	354.0951	4.25	6634482676
4	Secoxyloganin	$C_{17}H_{24}O_{11}$	404.13205	12.083	6188063882
5	Cryptochlorogenic acid	$C_{16}H_{18}O_9$	354.09509	7.666	5768446177
6	Isochlorogenic acid C	$C_{25}H_{24}O_{12}$	516.12694	20.063	5591545088
7	Isochlorogenic acid B	$C_{25}H_{24}O_{12}$	516.12693	17.757	4381799389
8	L-Pyroglutamic acid	$C_5H_7NO_3$	129.04297	1.229	2517905360
9	Caffeic acid	$C_9H_8O_4$	180.04243	7.667	2473003990
10	3,5-Dicaffeoylquinic acid	$C_{25}H_{24}O_{12}$	516.12698	18.267	2443562323
11	Pyroglutamic acid	$C_5H_7NO_3$	129.04181	1.231	1905452321
12	Quinic acid	$C_7H_{12}O_6$	192.06295	0.902	1663621927
13	Gluconic acid	$C_6H_{12}O_7$	136.03666	0.863	1513125519
14	Succinic acid	$C_4H_6O_4$	118.02579	1.438	1365688355
15	2-(2-Acetyl-3,5-dihydroxyphenyl)acetic acid	$C_{10}H_{10}O_5$	210.05304	12.082	1350152380
16	Wilforlide A	$C_{30}H_{46}O_3$	454.3449	30.091	1345418190
17	Glycyrrhizic acid	$C_{42}H_{62}O_{16}$	840.41457	34.975	1118412349
18	Trigonelline	$C_7H_7NO_2$	137.04787	0.881	878398957.4
19	18-β-Glycyrrhetinic acid	$C_{30}H_{46}O_4$	470.33973	34.967	655461577.8
20	Caffeic acid	$C_9H_8O_4$	180.04247	20.064	622852246.7
21	Isoliquiritigenin	$C_{15}H_{12}O_4$	256.07402	14.849	607038615.6
22	Oleamide	$C_{18}H_{35}NO$	281.27213	48.058	505622534.2
23	Isoliquiritigenin	$C_{15}H_{12}O_4$	256.07402	15.19	493002608.5
24	Liguiritigenin-7-O-β-D-apiosyl-4′-O-β-D-glucoside	$C_{26}H_{30}O_{13}$	550.16923	15.206	408566018.8
25	Liquiritin	$C_{21}H_{22}O_9$	418.12676	14.85	402480550.4
26	D-Raffinose	$C_{18}H_{32}O_{16}$	526.15178	0.886	353507621.3
27	Formononetin	$C_{16}H_{12}O_4$	268.07383	33.188	326733854.5
28	Hyodeoxycholic acid	$C_{24}H_{40}O_4$	392.29285	39.297	320472298.1
29	Diammonium glycyrrhizinate	$C_{42}H_{62}O_{16}$	822.40396	35.763	290399140.7
30	Ethyl caffeate	$C_{11}H_{12}O_4$	208.07337	24.747	275746054.3

respiratory tract infections, effectively suppressing the level of inflammation in infected patients (Congxiao, 2020). Some studies have been conducted to evaluate the anti-inflammatory effect and mechanism of FOL. The results showed that FOL had an inhibitory effect on ear swelling in xylene ear swelling model mice, and reduced the levels of TNF-α and histamine and increased the levels of IL-4 in mouse ear tissues (Kaixi et al., 2021b). In addition, FOL reduced the number of torsions and serum levels of prostaglandin E2 and β-endorphin in acetic acid-induced torsion mice. FOL-treated mice showed prolonged foot-licking latency, a significant increase in serum β-EP content, and a significant decrease in PGE2 and bradykinin content (Kaixi et al., 2021b). These results show that FOL has a significant anti-inflammatory effect. In the present study, we found that FOL significantly reduced the levels of IL-6, IL-1β, TNF-α, and NO in the supernatant of LPS-induced RAW264.7 cells. It also reduced the concentration of IL-1β, IL-6, and TNF-α in BALF of LPS-induced ALI mice. These results further demonstrate the anti-inflammatory potential of FOL. However, the mechanism of the anti-inflammatory effect of FOL is still not elucidated.

In our previous study, the strategies and methods of network pharmacology were used to explore the characteristics and anti-inflammation effect of FOL and further verify it through an *in vitro* model (Ruocong et al., 2021). Through the enrichment and mapping analysis of network pharmacology, it is found that the PI3K-AKT pathway is the most critical intracellular signal transduction part of FOL intervention in wind-heat pattern. The PI3K/AKT signaling pathway is one of the important pathways associated with the regulation of cell survival in mammals that control cell growth, migration, proliferation, and metabolism (Pompura and Dominguez-Villar, 2018). The PI3K/AKT signaling pathway regulates a variety of cellular biological processes, including apoptosis, autophagy, inflammation, and oxidative stress (Du et al., 2017; Jiang et al., 2019; Shi et al., 2019). In this study, the LPS-induced ALI mice and LPS-induced RAW264.7 cells were implemented to validate the regulatory effects of FOL on the PI3K/AKT signaling pathway. The results showed that FOL exhibited inhibition of PI3K/AKT signaling pathway activation. In addition, FOL significantly inhibited PI3K phosphorylation activated by the PI3K agonist 740-YP. This information further confirmed the inhibitory effect of FOL on the PI3K/AKT signaling pathway. Notably, we used LY294002, a PI3K inhibitor shown to significantly inhibit PI3K and AKT activation, to further confirm the relationship between the anti-inflammatory effect of FOL and inhibition of the PI3K/AKT signaling pathway. However, the results showed that LY294002 could only reduce the content of IL-1β in the supernatant of LPS-induced RAW264.7 cells. In addition, treatment with LY294002 prior to FOL therapy versus FOL alone did not demonstrate a difference in the inhibition of inflammatory cytokine release. These results suggest that there are additional and more important regulatory pathways in the mechanisms of inhibiting the release of inflammatory cytokines in addition to the PI3K/AKT signaling pathway.

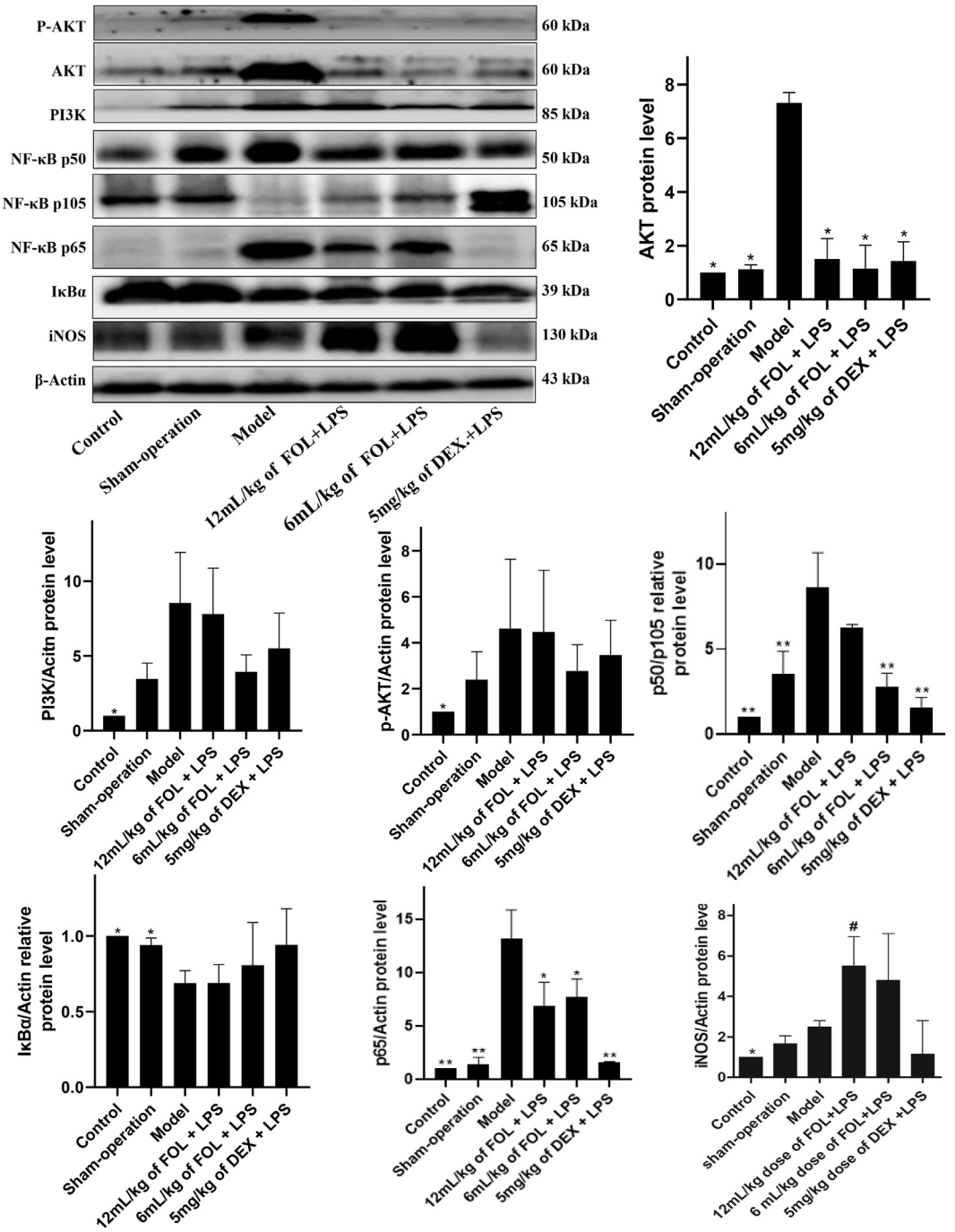


FIGURE 6 | Effect of FOL on PI3K/AKT and NF-κB signaling pathways in lung tissues of LPS-induced ALI mice. The main chemical components in FOL were determined by high-performance liquid chromatography–mass spectrometry (HPLC-MS). The protein expression levels of AKT, PI3K, NF-κB p50, NF-κB p105, NF-κB p65, IκBα, iNOS, and phosphorylated protein of AKT in lung tissues of LPS-induced ALI mice were detected by Western blotting. Data are presented as the mean ± SD compared with the model-only control group. $^{*}p < 0.05$; $^{**}p < 0.01$ ($n = 6–9$).

The NF-κB pathway is an important pathway for the regulation and release of inflammatory cytokines (Vallabhapurapu and Karin, 2009). The classical NF-κB pathway responds to stimuli from different immune receptors and leads to rapid NF-κB activation and inflammatory cytokine release (Sun, 2017). This process requires IκBα phosphorylation and loss of inhibition of NF-κB p50, which then mediates the nuclear translocation of NF-κB p50 and NF-κB p65 (Israël, 2010). Therefore, we also examined the effect of FOL on proteins related to the NF-κB signaling pathway in LPS-induced RAW264.7 cells.

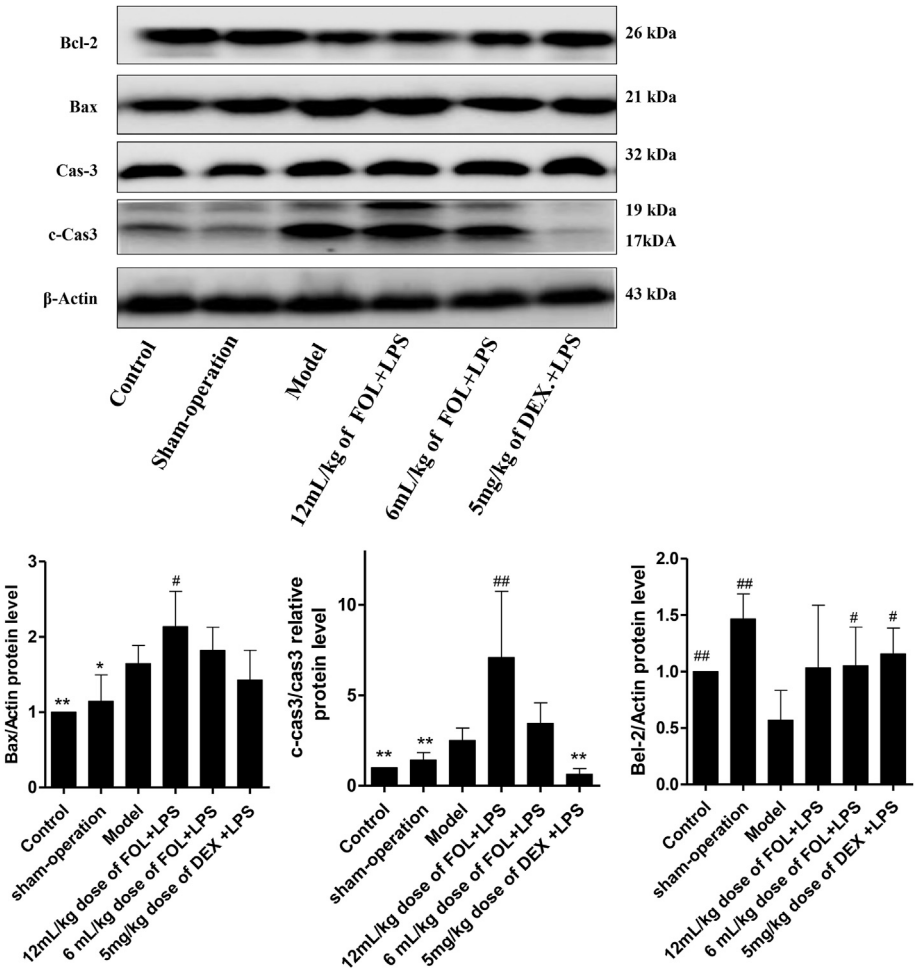


FIGURE 7 | Effect of FOL on apoptosis in lungs of LPS-induced ALI mice. The effects of FOL on the expression levels of apoptosis-related proteins of caspase-3, cleaved-caspase-3, and Bax and Bcl-2 were detected by Western blotting. Data are presented as the mean ± SD compared with the LPS-only control group. $*p < 0.05$; $**p < 0.01$; $\#p < 0.05$; $\#\#p < 0.01$ (n = 6–9).

The results showed that FOL significantly inhibited the phosphorylation level of IκBα, as well as the phosphorylation level of NF-κB p65 and the processing of NF-κB p50 in NF-κB p105 protein. In LPS-induced ALI, FOL administration also significantly reduced the protein expression levels of NF-κB p65 and NF-κB p50. These results suggest that the effect of FOL on reducing inflammatory cytokine release may be related to the inhibition of NF-κB activation.

In addition, PI3K/AKT inhibition may lead to increased levels of apoptosis (Yang et al., 2018; Sreenivasulu et al., 2020; Chen et al., 2021). We first examined the effect of FOL on LPS-induced apoptosis in RAW264.7 cells by flow cytometry and showed that even in the absence of LPS, FOL treatment resulted in a level of cell apoptosis at 80%, and in the presence of LPS induction, FOL treatment resulted in a level of apoptosis of 90.4%, while in the LPS group, the rate of apoptosis cells is about 41.2%. Further assays of apoptosis-related proteins such as Bax, caspase-3, and Bcl-2 revealed that treatment with FOL significantly increased the activation level of the apoptosis-executing protein caspase-3 and the expression level of the pro-apoptotic protein Bax. These results suggest that FOL has a certain induced apoptotic effect on macrophages. Apoptosis is known to be an active process and has anti-inflammatory properties (Henson and Bratton, 2013). These results suggest that the anti-inflammation effect of FOL may be associated with the promotion of macrophage apoptosis. This result was further validated in *in vivo* experiments, where FOL significantly increased caspase-3 activation in LPS-induced ALI, along with increased expression of the pro-apoptotic protein Bax. The promotion of apoptosis does play a role in inhibiting the release of inflammatory cytokines, but at the same time, excessive apoptosis may also aggravate ALI (Giordano et al., 2008; Chambers et al., 2018). Related studies have shown that apoptotic activation is already present in ALI, and over-activated apoptosis leads to alveolar capillary barrier dysfunction, which, in turn, leads to the development of pulmonary edema and pulmonary fibrosis (Gill et al., 2014; Gill et al., 2015). Therefore, we hypothesize that the anti-ALI effect of FOL at the 12 ml/kg dose is worse than that of 6 ml/kg *in*

vivo because of the stronger pro-apoptotic effect of higher doses of FOL. Even though it has a significant inhibitory effect on the inflammatory response, current evidence suggests that it may exacerbate ALI because of its pro-apoptotic effects.

Compositional analysis revealed high levels of pyroglutamic acid, cryptochlorogenic acid, chlorogenic acid, caffeic acid, secoxyloganin, isochlorogenic acid B, isochlorogenic acid C, α-hederin, tanespimycin, glycyrrhizic acid, tauroursodeoxycholic acid, hyodeoxycholic acid, and oleamide in FOL. Cryptochlorogenic acid, caffeic acid, chlorogenic acid, isochlorogenic acid B, and isochlorogenic acid C are the main active substances in Shan Yin Hua. The literature shows that cryptochlorogenic acid dose-dependently inhibits the production of NO, TNF-α, and IL-6 in LPS-induced RAW264.7 cells and inhibits the nuclear translocation of NF-κB by blocking the phosphorylation of IκB kinase (IKK) and degrading IκB (Zhao et al., 2020). Caffeic acid is a natural compound with a variety of biological activities that can be metabolized from chlorogenic acid, one of the metabolites of chlorogenic acid (Touaibia et al., 2011) and it has good anti-microbial activity against microbial pathogens (Khan et al., 2021). It has been shown that caffeic acid can induce apoptosis by inhibiting the activity of Bcl-2 (Chang et al., 2010). Isochlorogenic acid is also a natural compound with strong biological activity; isochlorogenic acid A could reduce the LPS-induced ALI by inhibiting the activation of the Nf-κB/NLRP3 signaling pathway, and it also has the effect of promoting apoptosis (Puangpraphant et al., 2011; Wang and Xiao, 2019; Liu et al., 2020). α-Hederin, a monodesmosidic triterpenoid saponin, exhibits promising antitumor potential against a variety of human cancer cell lines, and has a definite apoptosis-promoting effect (Sun et al., 2018; Wang et al., 2019; Wang et al., 2020). Tanespimycin, an inhibitor of HSP90, was found to inhibit AKT phosphorylation and demonstrate synergistic pro-apoptotic effects in combination with Tipifarnib (Krzykowska-Petitjean et al., 2012). Glycyrrhetinic acid and glycyrrhizin are the active ingredients in *Glycyrrhiza uralensis* Fisch. (Gan Cao) and have many pharmacological activities, such as anti-inflammatory, anti-viral, and anti-tumor activities, as well as participation in immune regulation (Chen et al., 2020). Studies have shown that glycyrrhetinic acid demonstrates inhibition of PI3K/AKT activation in LPS-induced ALI, which is consistent with our results (Wang et al., 2011; Qu et al., 2019b). Tauroursodeoxycholic acid, an endogenous bile acid, is the main compound of Fel Selenarcti (Xiong Dan Fen) and a strong modulator of apoptosis in several cell types (Castro et al., 2004). Hyodeoxycholic acid is also the main compound of Fel Selenarcti (Xiong Dan Fen) and can suppress intestinal epithelial cell proliferation through inhibiting the FXR-PI3K/AKT pathway (Song et al., 2020). In conclusion, FOL contains a variety of natural active ingredients, some of which have been reported to promote apoptosis and have regulatory effects on PI3K/AKT and NF-κB signaling pathways. This is consistent with the results we have obtained above.

Another interesting result showed that FOL administration resulted in a significant increase in iNOS protein expression, which apparently contradicts the result that FOL reduces NO content in cell supernatants. In the literature, iNOS expression was found to be induced by appropriate stimuli (e.g., cytokines and hypoxia), resulting in the production of NO (Wilmes et al., 2020). In addition, iNOS is a homodimer with a molecular weight of about 130–135 kDa. It adopts a dual structural domain structure where the homodimerization process required for enzyme activation occurs in both oxygen domains, leading to rapid conformational changes and depending on the activity of L-arginine (Kielbik et al., 2019). Therefore, the result of reduced NO content by FOL is not related to the inhibition of iNOS protein expression, and the FOL may inhibit the biological pathway of NO synthesis by inhibiting the activity of iNOS. This deserves further investigation, because iNOS over-activation is often associated with inflammation and malignant diseases.

In conclusion, FOL has significant anti-inflammatory potential, and its anti-inflammatory mechanism may be related to its inhibition effect on the PI3K/AKT signaling pathway, which, in turn, activates apoptosis and thus inhibits NF-κB signaling pathway activation. Although FOL has good anti-inflammatory effects, its application in the treatment of ALI requires more in-depth evaluation and consideration.

DATA AVAILABILITY STATEMENT

The original contributions presented in the study are included in the article/Supplementary Material, further inquiries can be directed to the corresponding author.

ETHICS STATEMENT

The animal study was reviewed and approved by the Committee for Animal Care and Use of Laboratory Animals, College of Pharmacy, Chengdu University of TCM (No: 20200320).

AUTHOR CONTRIBUTIONS

NZ and ZR were responsible for experimental design and manuscript writing, JZ and XL were responsible for data analysis, XZ and BW were responsible for target detection in animal experiments, and RY was responsible for manuscript quality. All data were generated in-house, and no paper mill was used. All authors agree to be accountable for all aspects of work ensuring integrity and accuracy.

FUNDING

This work was supported by the National Natural Science Foundation of China (No. 82074094), the Applied Basic Research Project of Science and Technology Department of Sichuan Province (20YYJC0640), the Open Research Fund of Chengdu University of Traditional Chinese Medicine Key Laboratory of Systematic Research of Distinctive Chinese Medicine Resources in Southwest China (No. 2020XSGG002), and the Xinglin Scholar Research Promotion Project of Chengdu University of Traditional Chinese Medicine (No. CDTD2018014).

REFERENCES

Castro, R. E., Solá, S., Ramalho, R. M., Steer, C. J., and Rodrigues, C. M. (2004). The Bile Acid Tauroursodeoxycholic Acid Modulates Phosphorylation and Translocation of Bad via Phosphatidylinositol 3-Kinase in Glutamate-Induced Apoptosis of Rat Cortical Neurons. *J. Pharmacol. Exp. Ther.* 311, 845–852. doi:10.1124/jpet.104.070532

Chambers, E., Rounds, S., and Lu, Q. (2018). Pulmonary Endothelial Cell Apoptosis in Emphysema and Acute Lung Injury. *Adv. Anat. Embryol. Cel. Biol.* 228, 63–86. doi:10.1007/978-3-319-68483-3_4

Chang, W. C., Hsieh, C. H., Hsiao, M. W., Lin, W. C., Hung, Y. C., and Ye, J. C. (2010). Caffeic Acid Induces Apoptosis in Human Cervical Cancer Cells through the Mitochondrial Pathway. *Taiwan J. Obstet. Gynecol.* 49, 419–424. doi:10.1016/S1028-4559(10)60092-7

Chen, K., Yang, R., Shen, F. Q., and Zhu, H. L. (2020). Advances in Pharmacological Activities and Mechanisms of Glycyrrhizic Acid. *Curr. Med. Chem.* 27, 6219–6243. doi:10.2174/0929867325666191011115407

Chen, Y. H., Yang, S. F., Yang, C. K., Tsai, H. D., Chen, T. H., Chou, M. C., et al. (2021). Metformin Induces Apoptosis and Inhibits Migration by Activating the AMPK/p53 axis and Suppressing PI3K/AKT Signaling in Human Cervical Cancer Cells. *Mol. Med. Rep.* 23, 88. doi:10.3892/mmr.2020.11725

Congxiao, Z. (2020). Multicenter Clinical Trial of Xiaoer Fengreqing Mixture in Treatment of Acute Upper Respiratory Tract Infection (Anemopyretic Cold) in Children. *Drug Eval. Res.* 43, 2450–2456. doi:10.7501/j.issn.1674-6376.2020.12.017

Du, C., Zhang, T., Xiao, X., Shi, Y., Duan, H., and Ren, Y. (2017). Protease-activated Receptor-2 Promotes Kidney Tubular Epithelial Inflammation by Inhibiting Autophagy via the PI3K/Akt/mTOR Signalling Pathway. *Biochem. J.* 474, 2733–2747. doi:10.1042/BCJ20170272

García-Arriaza, J., Perdiguero, B., Heeney, J. L., Seaman, M. S., Montefiori, D. C., Yates, N. L., et al. (2017). HIV/AIDS Vaccine Candidates Based on Replication-Competent Recombinant Poxvirus NYVAC-C-KC Expressing Trimeric Gp140 and Gag-Derived Virus-like Particles or Lacking the Viral Molecule B19 that Inhibits Type I Interferon Activate Relevant HIV-1-Specific B and T Cell Immune Functions in Nonhuman Primates. *J. Virol.* 91, e02182. doi:10.1128/JVI.02182-16

Gill, S. E., Taneja, R., Rohan, M., Wang, L., and Mehta, S. (2014). Pulmonary Microvascular Albumin Leak Is Associated with Endothelial Cell Death in Murine Sepsis-Induced Lung Injury *In Vivo*. *PLoS One* 9, e88501. doi:10.1371/journal.pone.0088501

Gill, S. E., Rohan, M., and Mehta, S. (2015). Role of Pulmonary Microvascular Endothelial Cell Apoptosis in Murine Sepsis-Induced Lung Injury *In Vivo*. *Respir. Res.* 16, 109. doi:10.1186/s12931-015-0266-7

Giordano, R. J., Lahdenranta, J., Zhen, L., Chukwueke, U., Petrache, I., Langley, R. R., et al. (2008). Targeted Induction of Lung Endothelial Cell Apoptosis Causes Emphysema-like Changes in the Mouse. *J. Biol. Chem.* 283, 29447–29460. doi:10.1074/jbc.M804595200

Henson, P. M., and Bratton, D. L. (2013). Antiinflammatory Effects of Apoptotic Cells. *J. Clin. Invest.* 123, 2773–2774. doi:10.1172/JCI69344

Herold, S., Gabrielli, N. M., and Vadász, I. (2013). Novel Concepts of Acute Lung Injury and Alveolar-Capillary Barrier Dysfunction. *Am. J. Physiol. Lung Cel. Mol. Physiol.* 305, L665–L681. doi:10.1152/ajplung.00232.2013

Israël, A. (2010). The IKK Complex, a central Regulator of NF-kappaB Activation. *Cold Spring Harb. Perspect. Biol.* 2, a000158. doi:10.1101/cshperspect.a000158

Jiang, T., Zhang, L., Ding, M., and Li, M. (2019). Protective Effect of Vasicine against Myocardial Infarction in Rats via Modulation of Oxidative Stress, Inflammation, and the PI3K/Akt Pathway. *Drug Des. Devel. Ther.* 13, 3773–3784. doi:10.2147/DDDT.S220396

Jie, L., Yuzuo, C., Kaixi, O., Baoning, W., Fu, P., and Chenghao, Y. (2021). Anti-bacterial and Anti-viral Effects of Fengreqing Oral Liquid (风热清口服液) *In Vitro* and *In Vivo*. *J. Tradit. Chin. Med.* 41, 530–538. doi:10.19852/j.cnki.jtcm.2021.03.005

Kaixi, O., Jie, L., Yuan, Z., Ziyi, Z., Yuming, Z., and Chenghao, Y. (2021a). Study on Immunomodulatory Property of Fengreqing Oral Liquid on Immunosuppressive Mice. *World Chin. Med.* 16, 2591–2595+2599. doi:10.3969/j.issn.1673-7202.2021.17.013

Kaixi, O., Jie, L., Yuming, Z., Yuan, Z., Ziyi, Z., and Chenghao, Y. (2021b). Anti-inflammatory and Analgesic Effects of Fengreqing Oral Liquid and its Mechanism. *Chin. J. Basic Med. Tradit. Chin. Med.* 27, 1104–1107+1110. doi:10.19945/j.cnki.issn.1006-3250.2021.07.016

Khan, F., Bamunuarachchi, N. I., Tabassum, N., and Kim, Y. M. (2021). Caffeic Acid and its Derivatives: Antimicrobial Drugs toward Microbial Pathogens. *J. Agric. Food Chem.* 69, 2979–3004. doi:10.1021/acs.jafc.0c07579

Kielbik, M., Szulc-Kielbik, I., and Klink, M. (2019). The Potential Role of iNOS in Ovarian Cancer Progression and Chemoresistance. *Int. J. Mol. Sci.* 20, 1751. doi:10.3390/ijms20071751

Krzykowska-Petitjean, K., Małecki, J., Bentke, A., Ostrowska, B., and Laidler, P. (2012). Tipifarnib and Tanespimycin Show Synergic Proapoptotic Activity in U937 Cells. *J. Cancer Res. Clin. Oncol.* 138, 537–544. doi:10.1007/s00432-011-1131-9

Lambrou, G. I., Hatziagapiou, K., and Vlahopoulos, S. (2020). Inflammation and Tissue Homeostasis: the NF-κB System in Physiology and Malignant Progression. *Mol. Biol. Rep.* 47, 4047–4063. doi:10.1007/s11033-020-05410-w

Liu, Y., Wang, Y., Liu, M., Yang, C., Cao, F., and Liang, J. (2020). Isochlorogenic Acid A Inhibits Proliferation and Migration and Promotes Apoptosis in MH7A Cells Induced by TNF-α. *Xi Bao Yu Fen Zi Mian Yi Xue Za Zhi* 36, 693–698. doi:10.13423/j.cnki.cjcmi.009047

Mokra, D., and Kosutova, P. (2015). Biomarkers in Acute Lung Injury. *Respir. Physiol. Neurobiol.* 209, 52–58. doi:10.1016/j.resp.2014.10.006

Nieman, G. F., Gatto, L. A., and Habashi, N. M. (2015). Impact of Mechanical Ventilation on the Pathophysiology of Progressive Acute Lung Injury. *J. Appl. Physiol. (1985)* 119, 1245–1261. doi:10.1152/japplphysiol.00659.2015

Pietenpol, J. A., and Stewart, Z. A. (2002). Cell Cycle Checkpoint Signaling: Cell Cycle Arrest versus Apoptosis. *Toxicology* 181-182, 475–481. doi:10.1016/s0300-483x(02)00460-2

Pompura, S. L., and Dominguez-Villar, M. (2018). The PI3K/AKT Signaling Pathway in Regulatory T-Cell Development, Stability, and Function. *J. Leukoc. Biol.* 103, 1065–1076. doi:10.1002/jlb.2mir0817-349r

Puangpraphant, S., Berhow, M. A., Vermillion, K., Potts, G., and Gonzalez De Mejia, E. (2011). Dicaffeoylquinic Acids in Yerba Mate (Ilex Paraguariensis St. Hilaire) Inhibit NF-κB Nucleus Translocation in Macrophages and Induce Apoptosis by Activating Caspases-8 and -3 in Human colon Cancer Cells. *Mol. Nutr. Food Res.* 55, 1509–1522. doi:10.1002/mnfr.201100128

Qu, L., Chen, C., Chen, Y., Li, Y., Tang, F., Huang, H., et al. (2019a). High-Mobility Group Box 1 (HMGB1) and Autophagy in Acute Lung Injury (ALI): A Review. *Med. Sci. Monit.* 25, 1828–1837. doi:10.12659/MSM.912867

Qu, L., Chen, C., He, W., Chen, Y., Li, Y., Wen, Y., et al. (2019b). Glycyrrhizic Acid Ameliorates LPS-Induced Acute Lung Injury by Regulating Autophagy through the PI3K/AKT/mTOR Pathway. *Am. J. Transl Res.* 11, 2042–2055.

Rao, Z., Zeng, J., Li, X., Peng, L., Wang, B., Luan, F., et al. (2022). JFNE-A Isolated from Jing-Fang n-Butanol Extract Attenuates Lipopolysaccharide-Induced Acute Lung Injury by Inhibiting Oxidative Stress and the NF-κB Signaling Pathway via Promotion of Autophagy. *Phytomed.* 96, 153891. doi:10.1016/j.phymed.2021.153891

Ruocong, Y., Zhili, R., Xiangyu, L., Dejian, W., Xi, P., and Nan, Z. (2021). Network Pharmacology and *In Vitro* Study of Fengreqing Oral Liquid (风热清口服液) in the Intervention of Wind-Heat Pattern. *J. Tradit. Chin. Med.* 41, 695–705. doi:10.19852/j.cnki.jtcm.2021.05.005

Shi, J., Yu, J., Zhang, Y., Wu, L., Dong, S., Wu, L., et al. (2019). PI3K/Akt Pathway-Mediated HO-1 Induction Regulates Mitochondrial Quality Control and Attenuates Endotoxin-Induced Acute Lung Injury. *Lab. Invest.* 99, 1795–1809. doi:10.1038/s41374-019-0286-x

Song, M., Yang, Q., Zhang, F., Chen, L., Su, H., Yang, X., et al. (2020). Hyodeoxycholic Acid (HDCA) Suppresses Intestinal Epithelial Cell Proliferation through FXR-PI3K/AKT Pathway, Accompanied by Alteration of Bile Acids Metabolism Profiles Induced by Gut Bacteria. *Faseb J.* 34, 7103–7117. doi:10.1096/fj.201903244R

Sreenivasulu, K., Nandeesha, H., Dorairajan, L. N., and Nachiappa Ganesh, R. (2020). Over Expression of PI3K-AkT Reduces Apoptosis and Increases Prostate Size in Benign Prostatic Hyperplasia. *Aging Male* 23, 440–446. doi:10.1080/13685538.2018.1519014

Sun, D., Shen, W., Zhang, F., Fan, H., Tan, J., Li, L., et al. (2018). α-Hederin Arrests Cell Cycle at G2/M Checkpoint and Promotes Mitochondrial Apoptosis by

Blocking Nuclear Factor-κB Signaling in Colon Cancer Cells. *Biomed. Res. Int.* 2018, 2548378. doi:10.1155/2018/2548378

Sun, S. C. (2017). The Non-canonical NF-κB Pathway in Immunity and Inflammation. *Nat. Rev. Immunol.* 17, 545–558. doi:10.1038/nri.2017.52

Touaibia, M., Jean-François, J., and Doiron, J. (2011). Caffeic Acid, a Versatile Pharmacophore: an Overview. *Mini Rev. Med. Chem.* 11, 695–713. doi:10.2174/138955711796268750

Vallabhapurapu, S., and Karin, M. (2009). Regulation and Function of NF-kappaB Transcription Factors in the Immune System. *Annu. Rev. Immunol.* 27, 693–733. doi:10.1146/annurev.immunol.021908.132641

Wang, Q., and Xiao, L. (2019). Isochlorogenic Acid A Attenuates Acute Lung Injury Induced by LPS via Nf-κB/NLRP3 Signaling Pathway. *Am. J. Transl. Res.* 11, 7018–7026.

Wang, C. Y., Kao, T. C., Lo, W. H., and Yen, G. C. (2011). Glycyrrhizic Acid and 18β-Glycyrrhetinic Acid Modulate Lipopolysaccharide-Induced Inflammatory Response by Suppression of NF-κB through PI3K P110δ and P110γ Inhibitions. *J. Agric. Food Chem.* 59, 7726–7733. doi:10.1021/jf2013265

Wang, J., Wu, D., Zhang, J., Liu, H., Wu, J., and Dong, W. (2019). α-Hederin Induces Apoptosis of Esophageal Squamous Cell Carcinoma via an Oxidative and Mitochondrial-dependent Pathway. *Dig. Dis. Sci.* 64, 3528–3538. doi:10.1007/s10620-019-05689-1

Wang, J., Deng, H., Zhang, J., Wu, D., Li, J., Ma, J., et al. (2020). α-Hederin Induces the Apoptosis of Gastric Cancer Cells Accompanied by Glutathione Decrement and Reactive Oxygen Species Generation via Activating Mitochondrial Dependent Pathway. *Phytother Res.* 34, 601–611. doi:10.1002/ptr.6548

Wilmes, V., Scheiper, S., Roehr, W., Niess, C., Kippenberger, S., Steinhorst, K., et al. (2020). Increased Inducible Nitric Oxide Synthase (iNOS) Expression in Human Myocardial Infarction. *Int. J. Leg. Med* 134, 575–581. doi:10.1007/s00414-019-02051-y

Xu, X., Lai, Y., and Hua, Z. C. (2019). Apoptosis and Apoptotic Body: Disease Message and Therapeutic Target Potentials. *Biosci. Rep.* 39, BSR20180992. doi:10.1042/BSR20180992

Yang, J., Pi, C., and Wang, G. (2018). Inhibition of PI3K/Akt/mTOR Pathway by Apigenin Induces Apoptosis and Autophagy in Hepatocellular Carcinoma Cells. *Biomed. Pharmacother.* 103, 699–707. doi:10.1016/j.biopha.2018.04.072

Zhao, X. L., Yu, L., Zhang, S. D., Ping, K., Ni, H. Y., Qin, X. Y., et al. (2020). Cryptochlorogenic Acid Attenuates LPS-Induced Inflammatory Response and Oxidative Stress via Upregulation of the Nrf2/HO-1 Signaling Pathway in RAW 264.7 Macrophages. *Int. Immunopharmacol.* 83, 106436. doi:10.1016/j.intimp.2020.106436

Conflict of Interest: The authors declare that the research was conducted in the absence of any commercial or financial relationships that could be construed as a potential conflict of interest.

Publisher's Note: All claims expressed in this article are solely those of the authors and do not necessarily represent those of their affiliated organizations, or those of the publisher, the editors, and the reviewers. Any product that may be evaluated in this article, or claim that may be made by its manufacturer, is not guaranteed or endorsed by the publisher.

Copyright © 2022 Rao, Li, Zhang, Zeng, Wang, Yang and Zeng. This is an open-access article distributed under the terms of the Creative Commons Attribution License (CC BY). The use, distribution or reproduction in other forums is permitted, provided the original author(s) and the copyright owner(s) are credited and that the original publication in this journal is cited, in accordance with accepted academic practice. No use, distribution or reproduction is permitted which does not comply with these terms.

frontiers | Frontiers in Pharmacology

ORIGINAL RESEARCH
published: 04 April 2022
doi: 10.3389/fphar.2022.827782

Extraction Optimization, Structural Characterization, and Anti-Hepatoma Activity of Acidic Polysaccharides From *Scutellaria barbata* D. Don

*Wenwen Su[1†], Leilei Wu[2†], Qichao Liang[2], Xiaoyue Lin[3], Xiaoyi Xu[4], Shikai Yu[5], Yitong Lin[1], Jiadong Zhou[6], Yang Fu[1], Xiaoyan Gao[1], Bo Zhang[7], Li Li[6], Dan Li[1], Yongkui Yin[8] and Gaochen Song[1]**

[1]Department of Biochemistry and Molecular Biology, Mudanjiang Medical University, Mudanjiang, China, [2]Collage of Pharmacology, Mudanjiang Medical University, Mudanjiang, China, [3]The First Clinical College of Medicine, Heilongjiang University of Chinese Medicine, Harbin, China, [4]The First Clinical College of Medicine, Mudanjiang Medical University, Mudanjiang, China, [5]Collage of Basic Medicine, Heilongjiang University of Chinese Medicine, Harbin, China, [6]Collage of Basic Medicine, Mudanjiang Medical University, Mudanjiang, China, [7]Department of Oncology, Mudanjiang Cancer Hospital, Mudanjiang, China, [8]College of Life Sciences, Mudanjiang Medical University, Mudanjiang, China

OPEN ACCESS

Edited by:
Hong Zhang,
Shanghai University of Traditional Chinese Medicine, China

Reviewed by:
Wang Lingchong,
Nanjing University of Chinese Medicine, China
Aling Shen,
Fujian University of Traditional Chinese Medicine, China

***Correspondence:**
Gaochen Song
songgaochen32@sina.com

[†]These authors have contributed equally to this work and share first authorship

Specialty section:
This article was submitted to Pharmacology of Anti-Cancer Drugs, a section of the journal Frontiers in Pharmacology

Received: 02 December 2021
Accepted: 07 March 2022
Published: 04 April 2022

Citation:
Su W, Wu L, Liang Q, Lin X, Xu X, Yu S, Lin Y, Zhou J, Fu Y, Gao X, Zhang B, Li L, Li D, Yin Y and Song G (2022) Extraction Optimization, Structural Characterization, and Anti-Hepatoma Activity of Acidic Polysaccharides From Scutellaria barbata D. Don. Front. Pharmacol. 13:827782. doi: 10.3389/fphar.2022.827782

The Chinese medicinal herb *Scutellaria barbata* D. Don has antitumour effects and is used to treat liver cancer in the clinic. *S. barbata* polysaccharide (SBP), one of the main active components extracted from *S. barbata* D. Don, exhibits antitumour activity. However, there is still a lack of research on the extraction optimization, structural characterization, and anti-hepatoma activity of acidic polysaccharides from *S. barbata* D. Don. In this study, the optimal extraction conditions for SBP were determined by response surface methodology (RSM): the material-liquid ratio was 1:25, the extraction time was 2 h, and the extraction temperature was 90°C. Under these conditions, the average extraction efficiency was 3.85 ± 0.13%. Two water-soluble polysaccharides were isolated from *S. barbata* D. Don, namely, SBP-1A and SBP-2A, these homogeneous acidic polysaccharide components with average molecular weights of 1.15×10^5 Da and 1.4×10^5 Da, respectively, were obtained at high purity. The results showed that the monosaccharide constituents of the two components were fucose, galactosamine hydrochloride, rhamnose, arabinose, glucosamine hydrochloride, galactose, glucose, xylose, and mannose; the molar ratio of these constituents in SBP-1A was 0.6:0.3:0.6:30.6:3.3:38.4:16.1:8:1.4, and that in SBP-2A was 0.6:0.5:0.8:36.3:4.4:42.7:9.2:3.6:0.7. In addition, SBP-1A and SBP-2A contained uronic acid and β-glucan, and the residue on the polysaccharide was mainly pyranose. The *in vitro* results showed that the anti-hepatoma activity of SBP-2A was better than that of SBP-1A and SBP. In addition, SBP-2A significantly enhanced HepG2 cell death, as cell viability was decreased, and SBP-2A induced HepG2 cell apoptosis and blocked the G1 phase. This phenomenon was coupled with the upregulated expression of P53 and Bax/Bcl-2 ratio, as well as the downregulated expression of the cell cycle-regulating protein cyclinD1, CDK4, and Bcl-2 in

Abbreviations: SBP, Crude Polysaccharide of *Scutellaria Barbata*; NEAAs, Non-Essential Amino Acids; FBS, Fetal Bovine Serum; MTT, 3-(4,5-Dimethylthiazol-2-yl)-2,5-diphenyltetrazolium bromide; FT-IR, Fourier Transform Infrared; CV, Coefficient of Variation; HPLC, High-Performance Liquid Chromatography.

this study. Further analysis showed that 50 mg/kg SBP-2A inhibited the tumour growth in H22 tumour-bearing mice, with an average inhibition rate of 40.33%. Taken together, SBP-2A, isolated and purified from *S. barbata* showed good antitumour activity *in vivo* and *in vitro*, and SBP-2A may be a candidate drug for further evaluation in cancer prevention. This study provides insight for further research on the molecular mechanism of the anti-hepatoma activity of *S. barbata* polysaccharide.

Keywords: *Scutellaria barbata* D. Don, polysaccharides, purification, structure, anti-hepatoma activity

BACKGROUND

Hepatocellular carcinoma (HCC) is the fourth leading cause of cancer-related death and ranks sixth among new cases of cancer worldwide (Yang et al., 2019). Because of the lack of symptoms at early stages and high heterogeneity of liver cancer, most patients are diagnosed in the late stages, resulting in a low cure rate. At the current rate, the number of new cases and deaths due to liver cancer worldwide are expected to increase from 841,080 to 781,631 in 2018–1,361,836 to 1,284,252 in 2040, which are increase of 62 and 64%, respectively (Singal et al., 2020). The methods for treating liver cancer include surgical resection, liver transplantation, arterial chemoembolization, and systemic pharmacological treatment with the kinase inhibitor sorafenib. However, nearly 70% of patients easily develop recurrent liver cancer or metachronous liver cancer (Tabrizian et al., 2015), with typical side effects such as hypertension, hypothyroidism, and leucopenia/neutropenia (Finn et al., 2020). Although the worldwide incidence and mortality rates of liver cancer are increasing compared with the burdens of many other cancers, the development of new drugs for liver cancer has been lacking historically. Therefore, developing low toxicity and high-efficiency antitumor drugs has become a research focus.

Polysaccharides are among the main bioactive substances of Chinese herbal medicine and have a wide range of pharmacological effects, including antitumor effects (Gan et al., 2020), antioxidant effects (Wei et al., 2015), anticoagulant effects (Zhao et al., 2012), effects in the treatment of ischemia-reperfusion injury (Yuan et al., 2021), liver protection effects (Qu et al., 2020), antiviral effects (Cao et al., 2020), effects in the control of blood lipids (Zhang et al., 2014), effects in the control of blood pressure (Xie et al., 2021) and immunoregulatory effects (Wang et al., 2021). *Scutellaria barbata* D. Don is a plant of the family Lamiaceae (Yeon et al., 2015), and is listed in the 2015 edition of the Chinese Pharmacopoeia. It has the characteristic effects of clearing away heat, detoxifying, diuresis and detumescence. *S. barbata* polysaccharide (SBP) exhibits anticomplement activity (Wu and Chen, 2009), inhibits lung cancer growth (Yang et al., 2014; Yang et al., 2015), and inhibits the proliferation and metastasis of colorectal cancer HT29 cells (Sun et al., 2017; Li H. et al., 2019) and high glucose-induced retinal vascular endothelial cells (Li and Xiao, 2021). However, most studies on SBP have examined crude polysaccharides, while the isolation and purification of SBP have not been performed, and its anti-hepatoma activity has not yet been studied. Furthermore, the lack of clear structural and mechanistic information limits the clinical application of the unique antitumour properties of SBP. *S.barbata* has been widely used in the treatment of digestive system tumours, especially liver cancer. In addition, our previous study showed that SBP inhibited tumour growth in H22 hepatoma-bearing mice (Li L. et al., 2019). However, there is still a lack of research on the effect of SBP on liver cancer and the underlying mechanism. Therefore, HCC cells were selected as the tumour target for this research.

Based on the above considerations, this study used water extraction and alcohol precipitation to extract crude polysaccharides from *S. barbata*, response surface methodology (RSM) to optimize the extraction process and column chromatography to purify SBP. We preliminarily identified the polysaccharides content, molecular weight, monosaccharide composition and basic structure of *S. barbata*. The anti-hepatoma activity and mechanism of SBP were further studied. We hope that this study will provide a basis for elucidating the antitumour effects of *Scutellaria barbata* polysaccharides.

MATERIALS AND METHODS

Materials

S. barbata was purchased from Hebei Jinyezi Pharmaceutical Co., Ltd. (Hebei, China); the finely sieved powder was dried to a constant weight. The fine powder was crushed through a 40 mesh sieve and stored in the dryer until use. DEAE-52 cellulose was purchased from Phygene Biotechnology Co., Ltd. (Fuzhou, China), and Sephadex G-100 was purchased from GE Healthcare Bio-Sciences AB (Uppsala, Sweden). Monosaccharide standards were provided by Shenzhen Bo Rui Sugar Biology Co., Ltd. (Shenzhen, China). All other reagents used in the tests were analytical grade and obtained from local chemical suppliers in China. The HepG2 cell line was purchased from the Chinese Academy of Sciences (Shanghai, China). Dry MEM powder, penicillin and streptomycin, trypsin, nonessential amino acids (NEAAs), and sodium pyruvate in a solution containing 100 μg/ml penicillin and 100 μg/ml streptomycin were purchased from GIBCO (Grand island biological company, NY, USA). The H22 cell line and Australian foetal bovine serum (FBS) were purchased from Wuxi Xinrun Biotechnology Co., Ltd. (Wuxi, China). 3-(4,5-Dimethylthiazol-2-yl)-2,5-diphenyltetrazolium bromide (MTT) cell proliferation and cytotoxicity test kits and DNA content test kits were purchased from Solebao (Beijing, China). A Hoechst 33258 apoptosis staining kit was purchased from Beyotime Institute of Biotechnology. (Nanjing, China).

Optimization of Water Extraction and Alcohol Precipitation With RSM

Single-Factor Experimental Design

Chunlin Ye used RSM to optimize the extraction parameters for *S. barbata*, and the polysaccharide extraction rate was only 2.43 ±

0.11% (Ye and Huang, 2012). To improve the crude polysaccharide extraction rate for *S. barbata*, we selected three factors: material-liquid ratio, extraction temperature and extraction time. Five levels were studied for each factor (Zhao et al., 2015; Qu et al., 2016), including material-liquid ratios of 1: 10, 1:15, 1:20, 1:25, and 1:30; extraction temperatures of 60, 70, 80, 90, and 100°C; and extraction time of 1, 2, 3, 4, and 5 h. The extraction rate was calculated from the measured SBP content.

RSM

According to the results of the single-factor experiments, the three factors and five levels were applied in a Box-Behnken experimental design to optimize the extraction conditions. The relevant experiments were performed by Design Expert 11 (State-Ease Inc., Minneapolis, MN, United States) RSM software and repeated three times for each group. RSM was used to perform regression analysis on the experimental data, and a nonlinear quadratic model was fitted according to the formula (Wang et al., 2012; Jia et al., 2014).

Extraction of SBP by Water Extraction and Alcohol Precipitation

S. barbata powder was soaked several times in 95% ethanol solution to decolorize the powder and remove alcohol-soluble components. The residue was dried for 24 h to prepare the *S. barbata* sample. With a material-liquid ratio of 1:25 (g/ml), the sample was extracted twice with hot water at 90°C for 2 h each time. The mixture was centrifuged at 3,500 rpm for 15 min, combined with the supernatant, and concentrated by rotary evaporation at 55°C to 1/4 of the original volume. While stirring, 4 volumes of absolute ethanol were slowly added to the concentrated solution, and the solution was cooled to 4°C. The precipitate was collected, diluted with water, and deproteinized with Sevage reagent (the chloroform: n-butanol volume ratio was 4:1) (volume ratio 1:5) (Chen and Xue, 2019; Yao et al., 2020). The solution was decolorized with macroporous resin D101 and filtered and concentrated under reduced pressure at 55°C to 1/4 of its original volume. SBP was prepared by vacuum drying at 50°C and stored in a desiccator until use.

SBP Purification

The crude polysaccharide was dissolved with distilled water to a concentration of 20 mg/ml and then injected into a DEAE-52 anionic cellulose chromatography column (2.5 cm × 100 cm). A gradient elution was performed with water and 0.1, 0.2, 0.3, 0.5, and 1 M NaCl solutions. The flow rate was adjusted to 1 ml/min, the eluent was collected at 10 ml/tube with an automatic collector, and the absorbance at 490 nm was measured with the phenol sulfuric acid method (Dubois et al., 1951). The elution fractions containing the same component were collected, concentrated to 1/8 of the original volume at 55°C; dialyzed with a dialysis bag with a molecular weight of 3,500 Da for 48 h, prefrozen at −40°C for 24 h, and then freeze-dried into powder (Zhang C. et al., 2019). Samples were placed on a SephadexG-100 dextran gel column and washed with ultrapure water, and the eluent was collected in a 5 ml tube. The polysaccharide content of each tube was measured by the phenol-sulfuric acid method, and elution curves were generated. The main peak components were concentrated, frozen and dried.

Polysaccharide and Protein Content

First, 0, 0.4, 0.6, 0.8, 1.0, 1.2, 1.4, 1.6, and 1.8 ml of the glucose standard with a concentration of 0.1 mg/ml were placed in nine test tubes with stoppers, and distilled water was added to bring the volume up to 2 ml. Then, 1 ml of 5% phenol was added, and 5 ml of concentrated sulfuric acid was quickly added, followed by through mixing. The tubes were placed at 40°C for 30 min. After cooling to room temperature, the absorbance value at 490 nm was measured with an ultraviolet spectrophotometer; the glucose standard concentration (μg/ml) was used as the abscissa and the absorbance value A was used as the ordinate to draw the glucose standard curve. Then, 1 mg of SBP was weighed out and fully dissolved in distilled water. According to the phenol-sulfuric acid method (Dubois et al., 1951), the absorbance value at 490 nm was measured and substituted into the standard curve to calculate the polysaccharide concentration. Then, according to the BCA kit instructions, the BCA working solution was prepared, and 10 μl of the BSA standard was diluted to 100 μl (0.5 mg/ml) with phosphate-buffered saline (PBS). The standard (0, 2, 4, 6, 8, 12, 16, and 20 μl) was added to 96-well plates, and PBS was added to bring the volumes in the wells to 20 μl. A 20 μl sample diluted with PBS and 200 μl/well BCA working solution were added to the plates, which were then incubated at 37°C for 30 min. The absorbance value at 562 nm was measured by an enzyme labelling instrument (Multiskan MK3, Thermo Fisher, United States), and the protein concentration was calculated according to the standard curve.

Monosaccharide Composition

Sixteen kinds of monosaccharide standards were added to test tubes at concentrations of 0.01, 0.1, 0.5, 1, 5, 10, and 20 mg/L. Ten milligrams of the sample was accurately weighed into an ampoule, and 10 ml of 3 M TFA was added to hydrolyse the substrate at 120°C for 3 h. The acid hydrolysis solution was aspirated, transferred into the tube, and dried with nitrogen. Next, 5 ml of water was added, and the mixture was vortexed, and diluted to 100 μl. Then, 900 μl of deionized water was added, and the mixture was centrifuged at 12,000 rpm for 5 min. The supernatant was removed, and a ICS5000 system (Thermo Fisher, Unites States) was used for ion chromatography (IC) analysis (Hui et al., 2019).

Molecular Weight Determination

High-performance liquid chromatography (HPLC) is widely used for the determination of molecular weight due to its high precision and efficiency (Li et al., 2020). Samples and standards were accurately weighed (the molecular weights were 5,000, 11,600, 2,800, 48600, 80900, 148,000, 273,000, 409,800, 667,800, and 3693000 Da), and 5 mg/ml solutions were prepared and centrifuged at 12,000 rpm for 10 min. The supernatant was filtered through 0.22 μm microporous filters, and the sample was transferred to a 1.8 ml injection vial. The chromatographic conditions for HPLC (LC-10A, Shimadzu, Japan) were as follows: chromatographic column: BRT105-

104-102 tandem gel column (8 × 300 mm); mobile phase: 0.05 M NaCl solution; flow rate: 0.6 ml/min, column temperature: 40°C; injection volume: 20 μl; detector: differential refractive index detector RID-1OA. Taking the logarithm of the molecular weight of the standard (log(Mw)) as the ordinate and the peak time (min) as the abscissa, regression fitting was performed on the curve to obtain the standard curve of the molecular weight distribution. The above chromatographic separation conditions were used to obtain a chromatogram of the sample, record the retention time of a single symmetrical peak, and calculate the molecular weight.

FT-IR Analysis

The samples were analysed in pressed KBr pellets by Fourier transform infrared (FT-IR) spectroscopy (Chylińska et al., 2016). Five milligrams of polysaccharide was placed in a mortar with dried KBr, mixed and ground fully, pressed into a thin sheet, and scanned with a Thermo Scientific Nicolet iS5 FT-IR spectrophotometer (Thermo Nicolet Co., Madison, WI, United States) at 500–4,000 cm^{-1}.

Anti-Hepatoma Activity of SBP-2A *In Vitro*

MTT Assay

The MTT assay was used to screen the SBP component with the highest antitumor activity. HepG2 cells were inoculated in a 96 well microplate, warmed in an incubator to 37°C under 5% CO_2 to adhere to the wall, and cultured with different concentrations (50–3,200 μg/ml) of SBP, SBP-1A, and SBP-2A for 48 h. Then, 20 μl/well of MTT solution (5 mg/ml) was added, and the cells were cultured for 4 h. Then, the liquid was discarded, and 150 μl/well DMSO was added. The plate was slowly oscillated for 10 min, and the absorbance (OD) value was measured at 490 nm with a SpectraMax M3 microplate reader (Molecular Devices, USA). A_0 represents the OD value of the black control group (10% FBS-MEM complete medium), A_1 represents the OD value of the experimental group, and A_2 represents the OD value of the negative control group.

The viability of HepG2 cells = $(A_1-A_0)/(A_2-A_0)\times100\%$

The IC_{50} values of the three polysaccharides at different concentrations were calculated by GraphPad Prism software. According to the IC_{50} value, the low, the medium, and the high doses of SBP-2A were used to study the anti-hepatoma effect.

Colony Formation Assay and Cell Morphology Observation

HepG2 cells were diluted and seeded at 4,000 cells/well in 35 mm dishes. After 10 h, the cells were treated with different concentrations of SBP-2A (0, 200 μg/ml, 400 μg/ml, 800 μg/ml) for 48 h and then cultured under standard conditions for 10 days. The MEM medium was replaced every 3 days. Finally, colonies were stained with 0.1% crystal violet, and colonies with more than 50 cells were counted. The colony formation assay was used to determine the colony formation ability of HepG2 cells treated with different concentrations of SBP-2A.

Colony formation rate (%) = number of cell colonies/number of inoculated cells.

HepG2 cells in the logarithmic growth stage were cocultured with SBP-2A for 48 h. The morphological changes in HepG2 cells were directly observed with a DMI 6000B Leica microsystem. Then, the culture medium was aspirated, 0.5 ml of fixing solution was added, and the cells were fixed for 20 min. Then, the cells were washed with PBS, cultured with Hoechst 33258 staining solution for 10 min, and rinsed with PBS. After blocking with an fluorescence quencher, the morphological changes in HepG2 cell apoptosis induced by SBP-2A were observed under a DMI 6000B Leica microsystem.

5-Ethynyl-2′–Deoxyuridine Assay

HepG2 cells were inoculated into 12-well plates containing sterile cell climbing tablets and then cultured in an incubator with SBP-2A for 48 h. According to the instructions provided with the BeyoClick™ EdU Cell Proliferation Kit with Alexa Fluor 594 (Beyotime, C0078S), an equal volume of EdU solution (20 μM) was added, and the cells were incubated for 2 h, followed by fixing with 4% paraformaldehyde. Then, 0.3% Triton X-100 was added at 200 μl/well for cell permeabilization (Solarbio, T8200), and the cells were placed in 1 × Apollo 567 reaction solution at room temperature for 30 min. Then, 2-(4-amidinophenyl)-6-indolecarbamidine dihydrochloride (DAPI, Beyotime, C1005) was used to counterstain the cells for 10 min. Finally, the images were captured by the DMI 6000B Leica microsystem in a live cell imager (Wetzlar, Germany), and the percentage of EdU-positive cells in each group and each well was randomly counted in five fields of view.

Cell Cycle Detection

The cell cycle distribution of the HepG2 cell line treated with SBP-2A was evaluated by flow cytometry. The cells were seeded at a density of 5×10^5 cells/well and inoculated in 35 mm cell culture dishes. After adding adherent, the cells were starved with MEM culture medium containing 1% FBS for 12 h. The cells were treated with SBP-2A solutions for 48 h. With a sample collection rate of 1×10^6 cells/piece, cell precipitates were obtained by centrifugation, and resuspended by adding 300 μl of precooled PBS, slowly adding 700 μl of precooled absolute ethanol with mixing, and then fixing the cells at −4°C overnight. The mixture was warmed in 37°C water for 30 min, 400 μl of PI staining solution was added to mixture, and the mixture was incubated at 4°C in the dark for 30 min. Finally, the cell cycle of the sample was detected by a Cytomics FC500 flow cytometry instrument with a CXP system (Beckman, United States), and the data were analysed by ModFit LT 5.0 software.

Real-Time Quantitative Polymerase Chain Reaction Assay

HepG2 cells were treated with different concentrations of SBP-2A for 48 h; the cells were lysed with TRIzol reagent (Solarbio, China) and total RNA was extracted. According to the manufacturer's protocol, the total RNA was reverse transcribed into cDNA by using an MMLV Reverse Transcriptase RNaseH-kit (Promega, United States) with 500 ng total RNA as a template. Real-time quantitative PCR was completed by an MX3000P real-time PCR Instrument

(Stratagene, United States) and SYBR Real-time PCR Universal Reagent (Aibosi, Shanghai). The mRNA expression levels of P53 and CyclinD1 were standardized to glyceraldehyde 3-phosphate dehydrogenase (GAPDH) level. The specific primer sequences were designed by Shanghai Aibosi Biotechnology Co., Ltd., and are shown in the table below.

Gene Name	Primer Name	Primer sequence (5'>3')
GAPDH	F primer	CATGAGAAGTATGACAACAGCCT
	R primer	AGTCCTTCCACGATACCAAAGT
	Product	113 bp
P53	F primer	CTATGAGCCGCCTGAGGTT
	R primer	AGCTGTTCCGTCCCAGTAGAT
	Product	152 bp
CCND1	F primer	AACAAACAGATCATCCGCAAACAC
	R primer	GTTGGGGCTCCTCAGGTTCAG
	Product	144 bp

Western Blot Assay

The HepG2 cells were cocultured with SBP-2A solution for 48 h. Then, the HepG2 cells and tumour tissue were lysed completely in a powerful RIPA (Solarbio, R0010, China) lysis buffer supplemented with protease and phosphatase inhibitors and centrifuged at 14000 × *g* for 5 min at 4°C. The total protein concentration was determined according to the instructions of a BCA protein quantitative kit (Beyotime Biotechnology, P0010, China). The total protein was separated by sodium dodecyl sulfate–polyacrylamide gel electrophoresis (SDS–PAGE) and transferred to 0.45 μm methanol-activated polyvinylidene fluoride (PVDF) membranes (Beyotime Biotechnology, Shanghai, China), followed by blocking with QuickBlock blocking buffer (P0252, Beyotime) at room temperature for 15 min. Next, diluted primary antibodies against *β*-actin (1: 1,000, 42 kDa, Beyotime, AF5003), P53 (1:1,000, 53 kDa, Wanleibio, WL01919), CyclinD1 (1:1,000; 35 kDa, Wanleibio, WL01435a), CDK4 (1:500, 34 kDa, Wanleibio, WL02274), Bax (1:10000, 23 kDa, Proteintech, 60267-1-lg) and Bcl-2 (1:500, 26 kDa, Beyotime, AF6285) were added and the membranes were incubated overnight at 4°C. The membranes were washed with TBST solution and then incubated with a diluted horseradish peroxidase-bound secondary antibody (1:5,000, Beyotime, A0208) for 1 h at 25°C. After washing with TBST solution, the bands were detected by Super-GL ECL hypersensitive luminescent solution and photographed with a hypersensitive multifunctional imager. Taking the grey value of the *β*-actin protein band as a reference, the protein bands of P53, CyclinD1, CDK4, Bax, and Bcl-2 were quantitatively analysed by ImageJ software.

Antitumour Activity of SBP-2A *In Vivo*

C57BL/6 mice were purchased from Liaoning Changsheng Biotechnology Co., Ltd. (Liaoning, China; Laboratory animal welfare and ethical review number: 20220314-1). The study was approved by the Ethics Committee of Mudanjiang Medical University (Mudanjiang, China). C57BL/6 male mice were raised in room without specific pathogen-free (SPF) conditions (Mudanjiang Medical University, Mudanjiang, China), and weighed 20 ± 2 g. H22 cells were cultured with RMPI 1640 complete medium, cells in the logarithmic growth phase were adjusted to 1.5×10^7 cells/mL, and washed with PBS 3 times. Then, the cells were suspended in 200 μl of PBS and injected subcutaneous into the right armpit of 30 C57BL/6 mice. The mice were randomly divided into 5 groups (n = 6 per group), included the model group, SBP-2A group (25, 50, and 100 mg/kg), and *Astragalus* polysaccharide (APS) group. On the second day after modelling, the model group was injected with saline and the treatment group was injected with SBP-2A via the peritoneal cavity, once a day for 12 consecutive days. On day 13, the mice were sacrificed, and the tumors were excised and weighed, the tumor volume was measured. The tumour inhibition rate of each group was calculated.

The tumor inhibition rate (%) = [1−(tumor weigh of the SBP-2A group/tumor weigh of the model group)] ×100%

Statistical Analyses

All data are expressed as the mean ± standard deviation (SD). All experiments were repeated three times. One-way ANOVA and multiple comparisons were used, and all statistical analyses were performed by using GraphPad Prism 7.0 software and plotted with Origin 2021. $p < 0.05$ was taken to indicate a statistically significant difference.

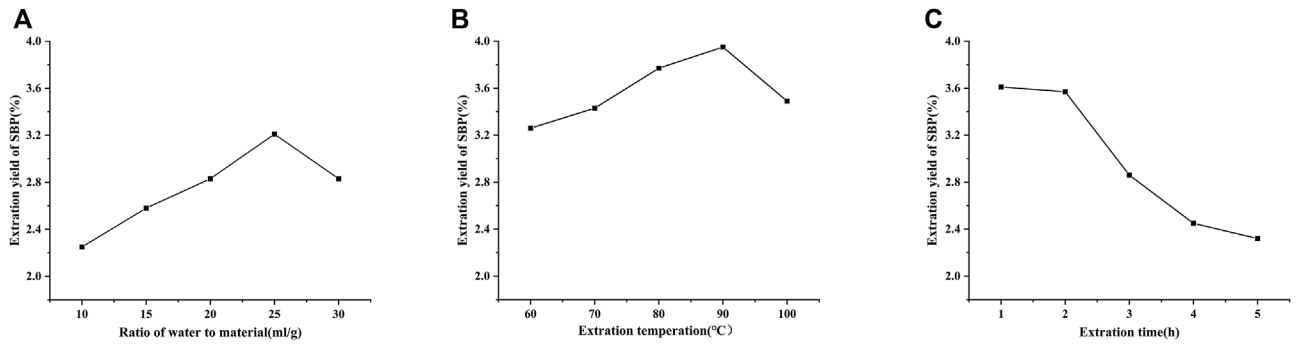


FIGURE 1 | Effects of different material-liquid ratios **(A)**, extraction time **(B)**, and extraction temperatures **(C)** on the SBP extraction rate.

TABLE 1 | Response surface experimental design and results.

Rang	A	B	C	Y
	Ratio of Water to Material (g/ml)	Extraction Time (h)	Extraction Temperature (°C)	Extraction Rate of SBP (%)
1	30	−1	0	2.64
2	25	1	1	8.84
3	25	1	−1	3.77
4	20	−1	0	2.42
5	25	0	0	3.97
6	30	0	−1	2.83
7	20	0	1	2.88
8	25	−1	1	3.81
9	30	1	0	2.74
10	25	0	0	3.9
11	25	−1	−1	3.27
12	25	0	0	3.95
13	20	1	0	2.79
14	25	0	0	3.91
15	20	0	−1	2.93
16	25	0	0	3.82
17	30	0	1	3.17

TABLE 2 | Regression Model and analysis of variance.

Source	Sum of squares	DF	Mean square	*F*-value	*p*-value
Model	4.94	9	0.55	143.86	<0.0001
A-Ratio of water to material	0.016	1	0.016	4.25	0.0783
B-Extraction time	0.12	1	0.13	32.77	0.0007
C-Extraction temperature	0.10	1	0.10	26.54	0.0013
AB	0.018	1	0.018	4.78	0.0651
AC	0.038	1	0.038	9.97	0.0160
BC	0.055	1	0.055	14.48	0.0067
A^2	4.14	1	4.14	1,084.65	<0.0001
B^2	0.31	1	0.31	81.22	<0.0001
C^2	0.005	1	0.005	1.26	0.2991
Residual	0.028	7	0.004		
Lack of Fit	0.013	3	0.004	1.32	0.3838
Pure Error	0.013	4	0.003		
Cor Total	4.97	16			

RESULTS

Single-Factor Design of SBP Extraction Conditions

Figure 1 shows the effects of different extraction parameters on the efficiency of the extraction of SBP. **Figure 1A** shows the effects of material-liquid ratios of 1:10, 1:15, 1:20, 1:25, and 1:30 on the extraction of SBP. The rates of polysaccharide extraction increased with increasing material-liquid ratio. When the material-liquid ratio was more than 1:25, the extraction rate increased rapidly, possibly because the increase in the material-liquid ratio allowed the polysaccharides to dissolve more fully (Wu et al., 2020; Bargougui et al., 2019). Therefore, 1:25 was chosen as the center of the response surface experiment. As shown in **Figure 1B**, the effects of 60, 70, 80, 90 and 100°C on the extraction of SBP were investigated. When the extraction temperature was 90°C, the polysaccharide extraction rate was highest. When the extraction temperature was increased from 60 to 90°C, the rate of polysaccharide extraction increased. As the temperature increased further, the extraction rate showed a decreasing trend. Therefore, the extraction temperature of 90°C was chosen as the central point of the response surface experiment. As shown in **Figure 1C**, when the extraction time was 1 h or 2 h, the rate of SBP extraction was higher, and extending the extraction time increased the polysaccharides extraction rate (Mkadmini Hammi et al., 2016); the rate of SBP extraction decreased as the time increased from 2 to 4 h, and it is possible that the structures of the polysaccharides were changed during the long-term extraction process (Ma et al., 2016). Therefore, 2 h was chosen as the centre of the response surface experiment.

Analysis of Response Surface Optimization Results

Regression Model and Analysis of Variance

A response surface optimization experiment with three factors and three levels was designed based on the results of the single-

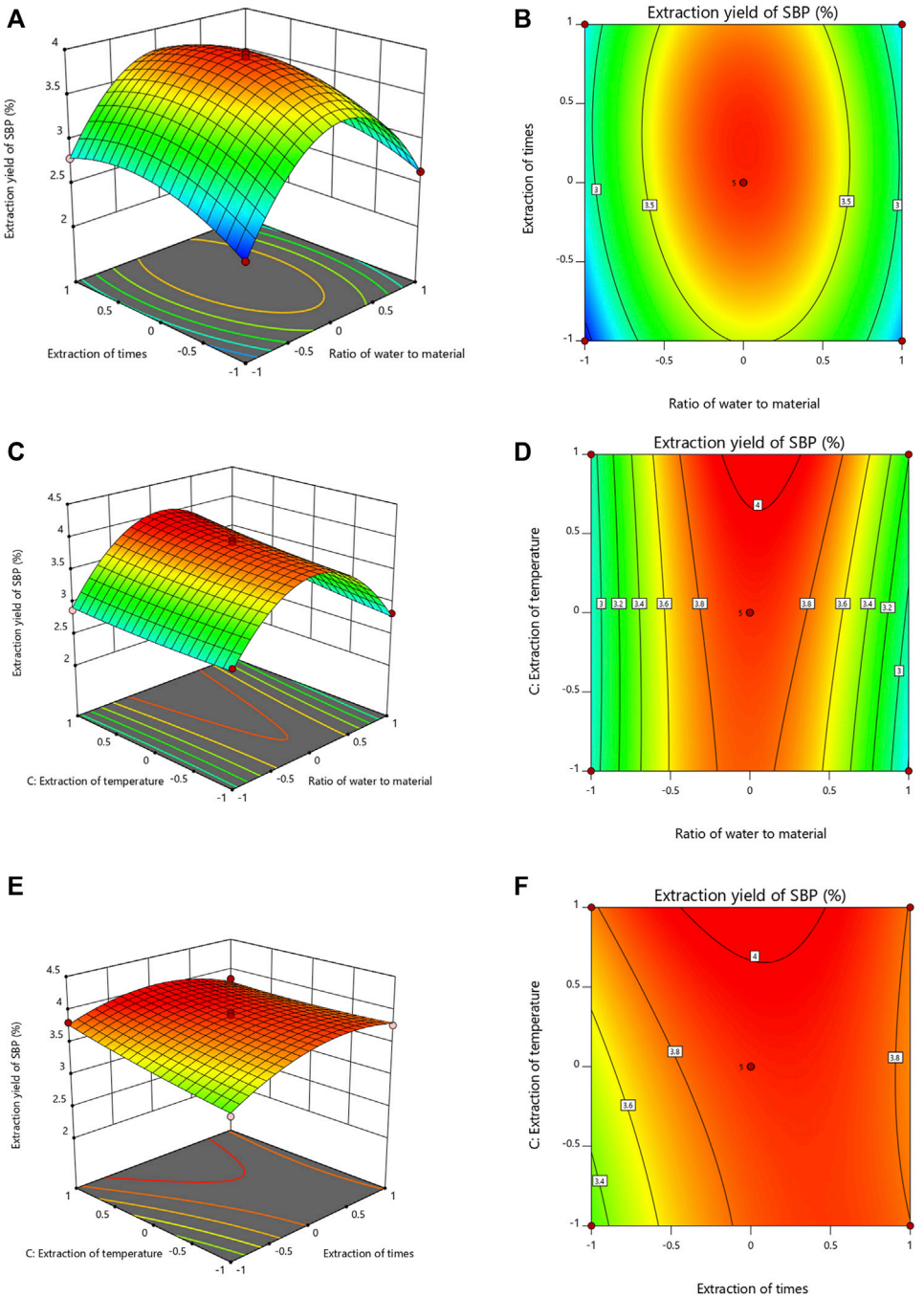


FIGURE 2 | Response surface and contour map of the three-factor interaction in the SBP extraction rate. **(A–F)** showing the effects of extraction time, ratio of water to material and extraction temperature on the extraction yields of SBP.

factor experiment. The polysaccharide extraction rate was the response value, and the material-liquid ratio (A), extraction temperature (B), and extraction time (C) were used as influencing factors. The Design Expert 11 software was used to process the data. As shown in **Table 1**, a binary multiple equation relating the extraction rate of SBP (y) and the three factors was obtained by data analysis:

$$Y = 3.91 + 0.045A + 0.125B + 0.113C - 0.068AB + 0.098AC - 0.118BC - 0.991A^2 - 0.271B^2 + 0.034C^2$$

Y is the SBP extraction efficiency; A is the ratio of material to liquid; B is the extraction time; and C is the extraction temperature.

Significance tests were conducted for all models and regression model coefficients, and the results are shown in **Table 2**. The F

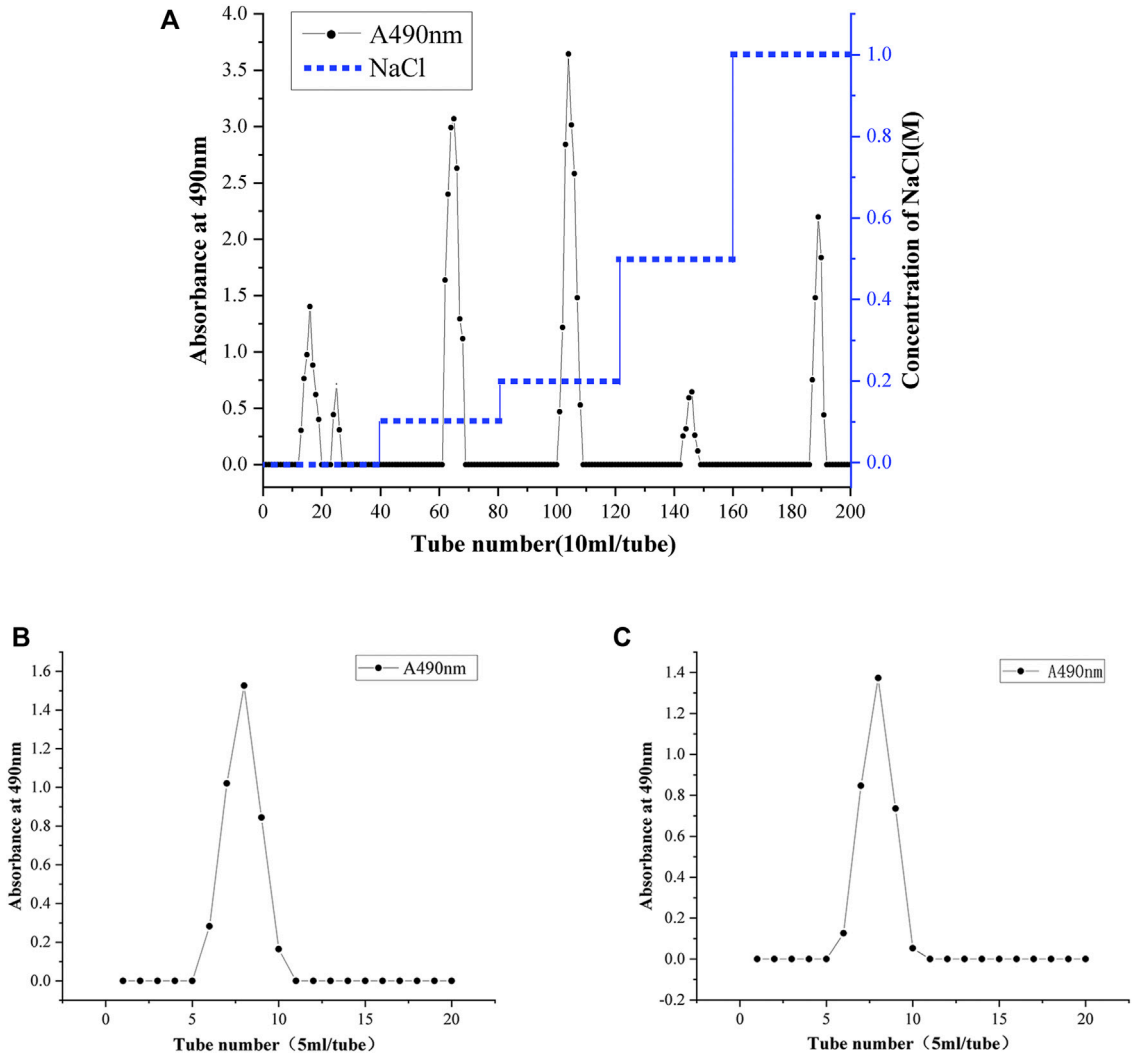


FIGURE 3 | Gradient elution profile of SBP on a DEAE-52 anion cellulose chromatography column with NaCl solutions (0, 0.1, 0.2, 0.5, and 1 M) **(A)**. Elution profiles of SBP-1A **(B)** and SBP-2A **(C)** on a Sephadex G-100 gel chromatography column with deionized water.

TABLE 3 | Preliminary characterization of SBP-1A and SBP-2A.

Sample	Total Sugar (%)	Uronic Acids (%)	Mw (Da)	Monosaccharide Composition (molar Ratio)						
				Rha	Fuc	Ara	Xyl	Man	Glc	Gal
SBP-1A	93.2	0.7	1.15 × 105	0.6	0.6	30.6	8.0	1.4	16.1	38.4
SBP-2A	95.5	1.2	1.4 × 105	0.8	0.6	36.3	3.6	0.7	9.2	42.7

value of the model was 143.86, and the p value was <0.0001, which indicates that the regression model had very high significant; the model mismatch term p value was 0.3838 ($p > 0.05$), so it was not significant at the level of $\alpha = 0.05$; this indicates that the model fitting was effective, and the experimental error was small. The correlation coefficient r was 0.9946, indicating that the simulated value of the model was consistent with the actual predicted value, and the prediction of the model was reasonable; the coefficient of variation (CV) was only 1.85%, so the model had good repeatability and high accuracy. From the F values of the three influencing factors (A, B, and C), it can be concluded that the effects of the influencing factors on the extraction rate of SBP decreased in the following order: extraction time > extraction temperature > material-liquid ratio.

Response Surface Analysis and Model Optimization

The response surface diagram and the contour map obtained by the multiple quadratic regression models were used to evaluate

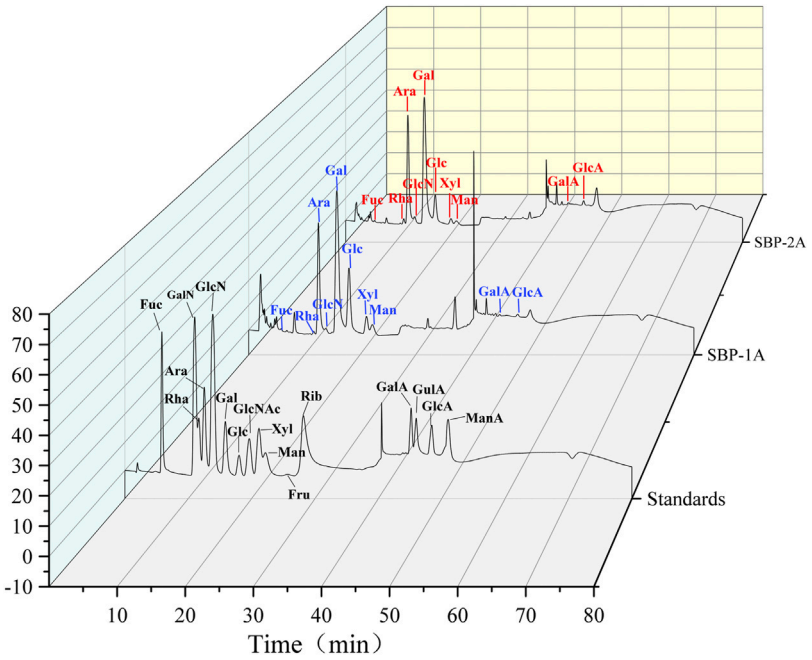


FIGURE 4 | IC chromatogram of mixed monosaccharide standards SBP-1A and SBP-2A.

the pairwise interactions of experimental factors and their impact on the extraction of SBP, which determined the optimal level range for each factor. The steeper the slope of the response surface is, the higher the response sensitivity. The shape of the contour line reflects the strength of the interaction. The contour lines for the material-liquid ratio and the extraction time tended to be oval, indicating that the interactions were significant; the interactions with other factors were not significant (**Figure 2**). The optimal extraction parameters for SBP were a material-liquid ratio of 1: 25.36, an extraction time of 120.3 min, and an extraction temperature of 100°C.

SBP Purification

Ion chromatography and gel column chromatography are usually used for the separation and purification of polysaccharides. The polysaccharide fractions with single peaks obtained by eluting with 0.1 and 0.2 M NaCl solutions were the largest (**Figure 3A**). Therefore, the eluates with these two elution peaks were collected and named SBP-1 and SBP-2. The two components SBP-1 and SBP-2 were purified by a SephadexG-100 gel column. As shown in **Figures 3B,C**, the two components showed a single and symmetrical elution peak respectively, demonstrating that both polysaccharides were relatively homogeneous; the samples with the single elution peak were collected and lyophilized to obtain white flocculent powders, which were named SBP-1A and SBP-2A.

Chemical Composition Analysis

Determination of Polysaccharide Content and Protein Content

Analysis showed that the polysaccharide content of SBP-1A was 93.2% and that of SBP-2A was 95.5%. A standard curve was obtained by using BSA protein standards, and the equation of the curve was $y = 1.1702x + 0.1401$, $R^2 = 0.9902$. The protein contents of the polysaccharide samples were determined: the protein content of SBP-1A was 2.87% and that of SBP-2A was 0.87% (**Table 3**).

Monosaccharide Composition

The monosaccharide compositions of SBP-1A and SBP-2A were analysed by IC. The peak sequences and retention time of the monosaccharide compositions were compared with those in chromatograms for the monosaccharide standard samples (**Figure 4**). For the mixed standard, the peak at 2.0 min represented sodium hydroxide, and the peak at 40 min represented sodium acetate. **Table 3** shows the molar ratios of the monosaccharide samples. SBP-1A consisted mainly of arabinose (30.6%) and galactose (38.4%), and the uronic acid content was 0.7%; SBP-2A consisted mainly of arabinose (36.3%) and galactose (42.7%), and the uronic acid content was 1.2%. The monosaccharide constituents of the two components were fucose, galactosamine hydrochloride, rhamnose, arabinose, glucosamine hydrochloride, galactose, glucose, xylose, and mannose, but the molar ratios were different: the molar ratio for SBP-1A was 0.6:0.3:0.6:30.6:3.3:38.4:16.1:8:1.4, and the molar ratio for SBP-2A was 0.6:0.5:0.8:36.3:4.4:42.7:9.2:3.6:0.7.

Molecular Weight Determination

The molecular weight distributions of SBP-1A and SBP-2A were determined by HPLC, and the following standard curve equation was obtained: lg Mw = −0.2078x + 12.968, $R^2 = 0.993$. **Figures 5A,B** shows a chromatogram with two polysaccharide components. Both SBP-1A and SBP-2A showed symmetrical single peaks, indicating that they were homogeneous acidic polysaccharides with high purity. The molecular weight of

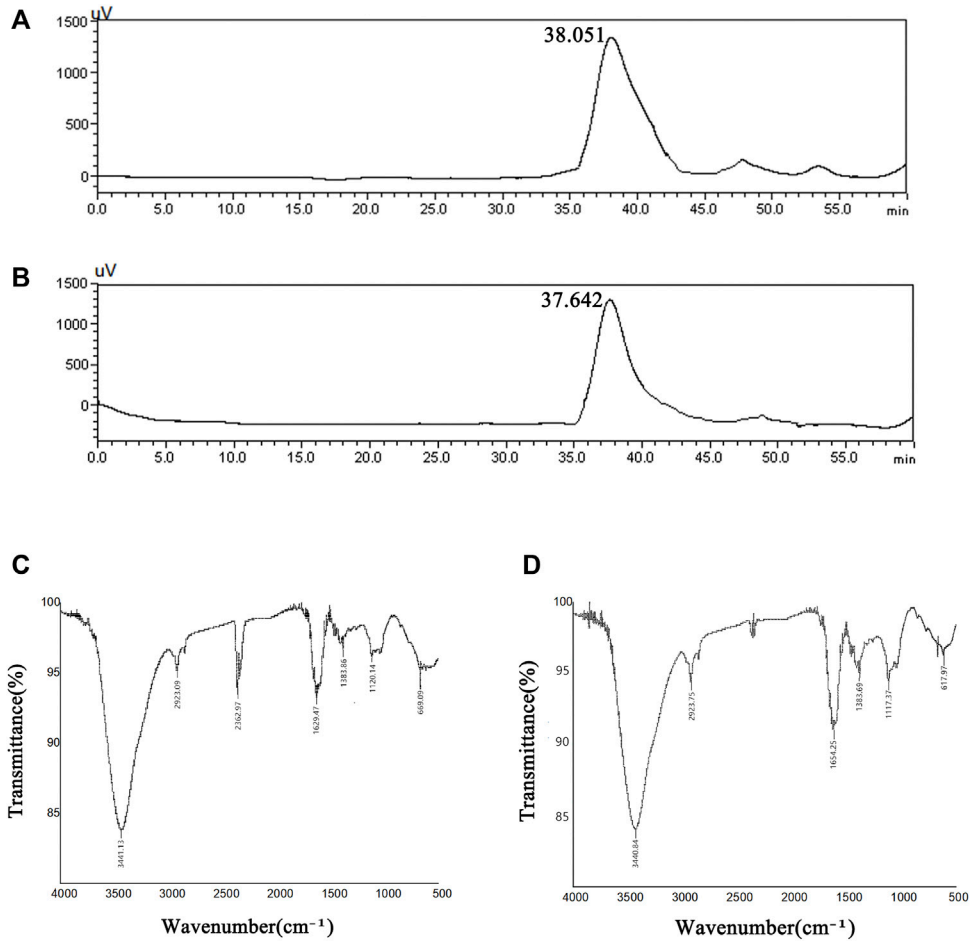


FIGURE 5 | HPLC profiles of SBP-1A **(A)** and SBP-2A **(B)**. FT-IR spectra of SBP-1A **(C)** and SBP-2A **(D)**.

SBP-1A was 1.15 × 105 Da (retention time: 38.051 min), and the molecular weight of SBP-2A was 1.4 × 105 Da (retention time: 37.642 min).

FT-IR Infrared Spectroscopy

As shown in **Figures 5C,D**, the FT-IR analysis showed that SBP-1A and SBP-2A had characteristic absorption peaks for polysaccharides near 3,400 cm^{-1}, and the strong absorption peak was the result of O-H stretching vibrations. The peak near 2,900 cm^{-1} was assigned to C-H stretching vibrations. There was a stretching vibration for C=O at 1,634 cm^{-1}, which may have been due to a carboxyl or acetyl group, indicating the presence of uronic acid. The absorption peak near 1,380 cm^{-1} was caused by the variable angle vibration of C-H, indicating that the polysaccharide had the β-characteristic absorption peak of dextran. A peak appeared near 1,120 cm^{-1}, indicating that the sugar residue of the polysaccharide was mainly pyranose.

Anti-Hepatoma Activity of SBP-2A *In Vitro*

MTT Assay

To identify the *in vitro* antitumour activities of isolated and purified SBP, the cell viability of HepG2 cells treated with different concentrations of *S. barbata* polysaccharides (SBP, SBP-1A, and SBP-2A) for 48 h was evaluated by the MTT method. **Figure 6B** shows that the inhibition of HepG2 cells growth, increased with increasing SBP concentration. The average inhibition rates for SBP, SBP-1A and SBP-2A increased from 17.29 to 66.35%, 2.13–70.19% and 18.02–76.53%, respectively. Compared with SBP, SBP-1A and SBP-2A significantly inhibited the growth of HepG2 cells in the dose range of 50–400 μg/ml, with IC_{50} values of 891.7 μg/ml and 548.3 μg/ml after 48 h. We found that when the concentration was 400 μg/ml, the average inhibition rate of SBP-2A for HepG2 cells was 49.52%, which was significantly higher than that of SBP-1A. Therefore, SBP-2A at concentrations of 200, 400, and 800 μg/ml was chosen for subsequent anti-hepatoma activity experiments. **Figures 6C,D** shows that the numbers of cell colonies formed by HepG2 cells treated with different concentrations of SBP-2A were significantly reduced compared with that of the control group. When the concentration was 800 μg/ml, the number of colonies formed decreased most significantly, indicating that SBP-2A significantly inhibited hepatoma cells colony formation; this was consistent with the results of the MTT assay.

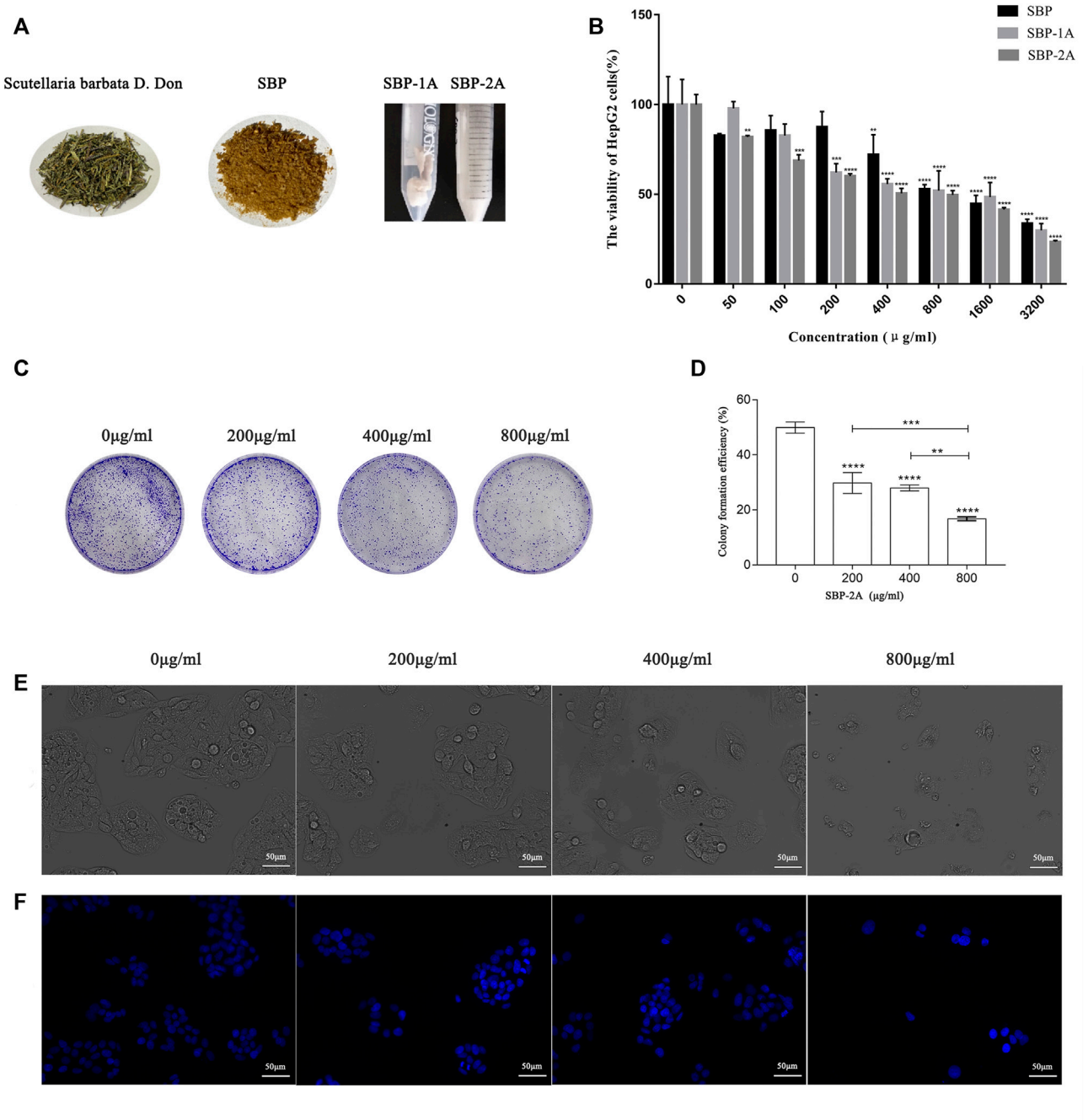


FIGURE 6 | (A) *Scutellaria barbata* D. Don, SBP, SBP-1A, and SBP-2A. The viability of HepG2 cells treated with SBP, SBP-1A and SBP-2A (0–3,200 μg/ml) for 48 h was measured by MTT assay **(B)**. Colony formation assays **(C,D)**, in contrast to the non-SBP-2A-treated group, $^{**}p < 0.01$, $^{***}p < 0.001$, $^{****}p < 0.0001$. The morphological characteristics **(E)** and Hoechst 33258 staining **(F)** of HepG2 cells treated with different concentrations of SBP-2A for 48 h.

Morphological Changes in Apoptosis Induced by SBP-2A

As illustrated in **Figure 6E**, HepG2 cells with normal morphologies showed irregular spindle shapes, high numbers, full shapes and clustered adherent growth. Compared with the control group, HepG2 cells gradually lost their original normal cell morphology with increasing SBP-2A concentrations, which showed that the number of cells decreased significantly, the cells became flat and contracted into a lump, and the cell membranes were broken, which resulted in unclear boundaries between the cells and cell fragments. These results showed that SBP-2A significantly inhibited the proliferation of HepG2 cells *in vitro*.

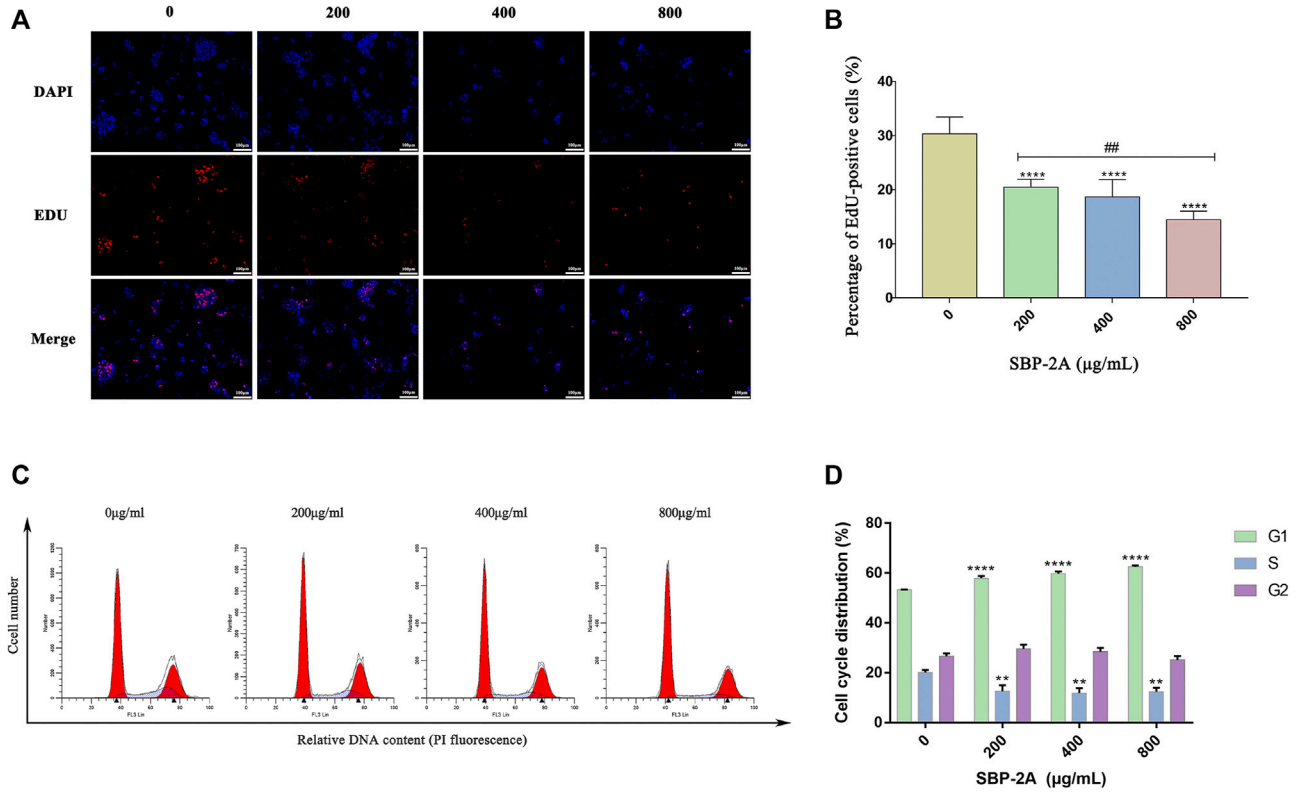


FIGURE 7 | Edu staining **(A)**, and Edu-positive (+) cells were counted by ImageJ software **(B)**. Compared to the non-SBP-2A-treated group, ****$p < 0.0001$. The number of apoptotic cells was determined by Annexin V-FITC/PI double staining **(C)**, and the DNA contents in the cell cycle was measured quantitatively by flow cytometry **(D)**.

TABLE 4 | Effect of SBP-2A on the cell cycle distribution of HepG2 cells for 48 h ($n = 3$).

Cell Cycle (%)	Concentration (μg/ml)			
	0	200	400	800
G1	53.34 ± 0.06	57.92 ± 0.94****	59.77 ± 0.77****	62.51 ± 0.54****
S	20 ± 1.1	12.55 ± 2.44**	11.82 ± 2.01**	12.34 ± 1.66**
G2\M	26.66 ± 1.14	29.53 ± 1.7	28.41 ± 1.55	25.15 ± 1.45

*Note: HepG2 cells were treated with SBP-2A (200 μg/ml, 400 μg/ml, 800 μg/ml) for 48 h (Mean ± SD, **p < 0.01, ****p < 0.0001 vs. non-SBP-2A-treated group).*

Figure 6F shows that HepG2 cells exhibited typical apoptotic characteristics compared with the control group, such as dense nuclear staining and an increased bright blue density after 48 h of treatment with SBP-2A. However, with increasing SBP-2A concentration, the number of bright blue spots first increased and then decreased, preliminarily indicating that SBP-2A induced apoptosis of HepG2 cells.

EdU Assay

An EdU assay was used to further evaluate the effect of SBP-2A on the proliferation of HepG2 cells. The nuclei of the proliferating cells were stained red by EdU and stained blue by DAPI (**Figure 7A**). Compared with the negative control group, the percentage of EdU-positive cells decreased significantly with increasing drug concentration ($p < 0.05$) (**Figure 7B**). This resultindicated that SBP-2A significantly inhibited the proliferation of HepG2 cells.

DNA Content Quantitation Assay

As displayed in **Figure 7C**, by analysing the percentage of DNA content in G0/G1, S and G2/M cells in the cell cycle, we found that compared with the untreated group, SBP-2A increased the percentage of cells in the G1 phase from 53.34 ± 0.06% to 62.51 ± 0.54% ($p < 0.0001$), and the percentage of cells in the S phase was decreased from 20 ± 1.1% to 12.34 ± 1.66% ($p < 0.01$), indicating a dose-dependent effect; the effect in cells in the G2/M phase was statistically insignificant (**Figure 7D** and **Table 4**). This observation was accompanied by an increase in the number of cells in the G0/G1 phase. HepG2 cells were blocked by SBP-2A in the G0/G1 phase of the cell cycle.

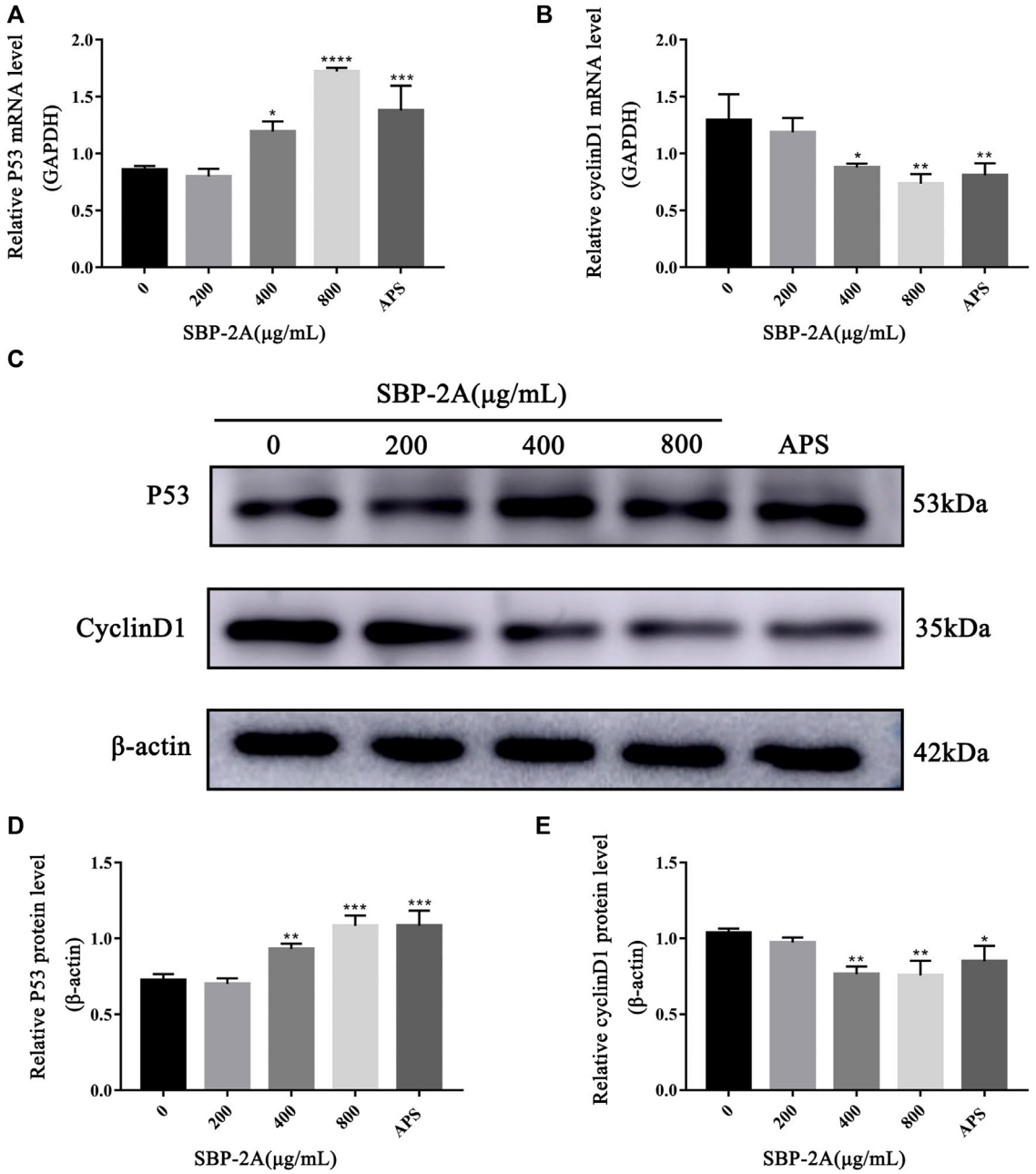


FIGURE 8 | The effect of SBP-2A on the mRNA expression of P53 and CyclinD1 was determined by qRT–PCR **(A,B)**. Compared to the non-SBP-2A-treated group, $^{*}p < 0.05$, $^{**}p < 0.01$, $^{***}p < 0.001$, $^{****}p < 0.0001$. The protein expression of p53 and cyclin D1 **(C–E)**. Compared to the non-SBP-2A-treated group, $^{*}p < 0.05$, $^{**}p < 0.01$, and $^{***}p < 0.001$.

qRT-PCR and Western Blot Analysis

Cell cycle progression is regulated by cell cycle-related molecules. We found that HepG2 cells were blocked by SBP-2A in the G1 phase of cell synthesis. In addition, P53 and CyclinD1 are the main genes that regulate the G1 phase of the cell cycle. Therefore, after treating HepG2 cells with different concentrations of SBP-2A for 48 h, we examined the relative expression levels of cyclin D1 and P53 mRNA by qRT-PCR (**Figures 8A,B**). Compared with the group without SBP-2A, there was no significant difference between the 200 μg/ml group and the negative group, but 400 μg/ml and 800 μg/ml SBP-2A significantly downregulated the mRNA expression of CyclinD1 and upregulated the mRNA expression of P53 in a concentration-dependent manner. Similarly, in the Western blot test, **Figures 8C–E** and **Figures 9B–D** showed that the protein level of P53 and Bax was significantly increased ($^{*}p$ <0.05), while the protein level of CyclinD1, CDK4, and Bcl-2 was significantly decreased ($^{*}p$ < 0.05) after SBP-2A treatment (**Figures 10A–C**). This

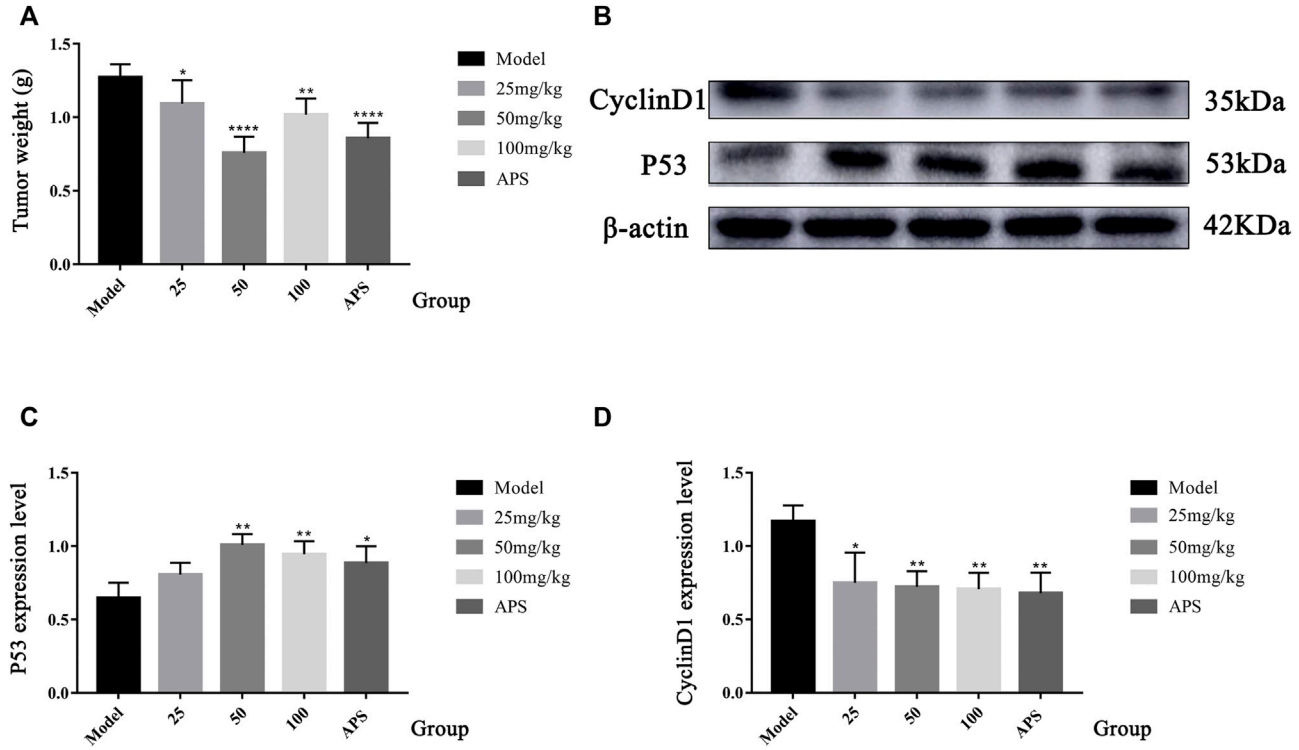


FIGURE 9 | Tumour weight of H22 tumour-bearing mice **(A)**. Compared to the model group, $^{*}p < 0.05$, $^{**}p < 0.01$, and $^{****}p < 0.0001$. The protein expression of P53 and CyclinD1 **(B–D)**. Contrast to the model group, $^{*}p < 0.05$, and $^{**}p < 0.01$.

phenomenon was consistent with the results obtained from the cell cycle assay. These data collectively indicated that SBP-2A blocked the DNA synthesis cycle in G1 phase by regulating the expression levels of P53 and CyclinD1 and induced apoptosis of HepG2 cells.

Antitumor Activity of SBP-2A *in vivo*

The antitumour efficacy of different SBP-2A doses was evaluated in H22 tumour-bearing mice (**Figure 10D**). **Figure 9A** showed that the tumour weights in the groups treated with different doses of SBP-2A were smaller than those in the tumour model group. (25 mg/kg SBP-2A compared with the model group, $^{*}p < 0.05$; 50 mg/kg SBP-2A compared with the model group, $^{****}p < 0.0001$; 100 mg/kg SBP-2A compared with the model group, $^{**}p < 0.01$). Furthermore, compared with the model group, the average inhibition rate of SBP-2A in doses of 50 mg/kg on tumor growth in mice was 40.33%, which significant inhibited the tumor growth of H22 tumor-bearing mice (**Table 5**).

DISCUSSIONS

The common design methods for the optimization of polysaccharide extraction include orthogonal tests and RSM. In the optimization of the SBP extraction process, previous studies used orthogonal testing. In this study, RSM was used for the first time to optimize the SBP extraction process. Compared with the orthogonal test, the RSM eliminated random errors in the experiment and allowed continuously analysis of the levels of the experiment during the optimization process to produce a continuous predictive model. In the single-factor experimental design, the polysaccharide extraction rate was lower at 100°C than at 90°C; this may have been due to the destruction of the polysaccharide structure when the temperature was too high (Zhang et al., 2015; Li et al., 2016; Cai et al., 2019). To facilitate practical operation, the process was improved as follows: the material–liquid ratio was 1:25, the extraction time was 2 h, and the extraction temperature was 90°C. Under these conditions, three groups of repeated validation experiments were carried out, and the SBP average extraction rate was 3.851 ± 0.13%, which was close to the predicted value of 4.06%. The result indicated that the model had good predictability and that the result of the RSM was reliable.

Five polysaccharide components were purified by ion column chromatography, and homogeneous acidic polysaccharide components with high purity, namely, SBP-1A and SBP-2A, were retained due to limitations of the experimental conditions. The molecular weight, monosaccharide composition and characteristics of SBP-1A and SBP-2A were preliminarily identified. The results showed that the molecular weight of SBP-1A (1.15×10^5 Da) was less than that of SBP-2A (1.4×10^5 Da), but both of them were medium-molecular-weight polysaccharides; these molecular weights were greater than that previously found for SBP. FT-IR analysis was used for rapid analysis of polysaccharides and to accurately identify specific

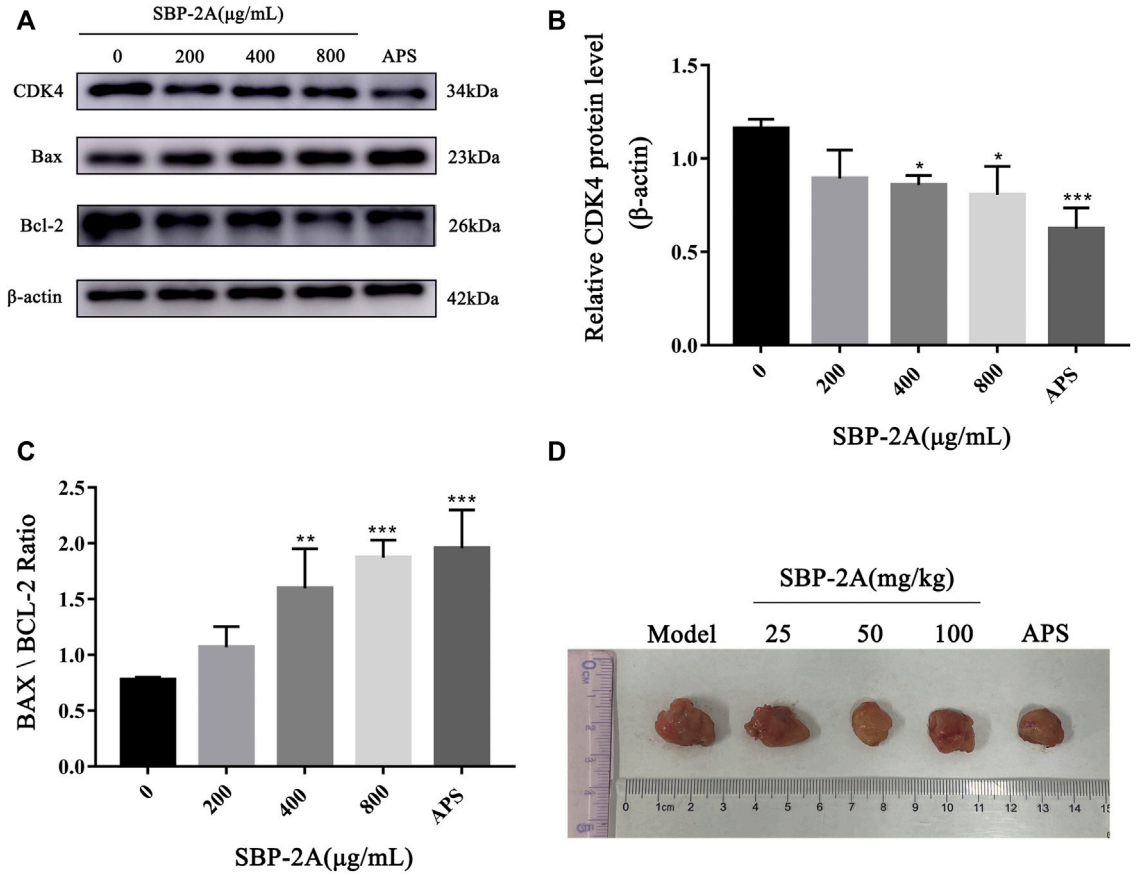


FIGURE 10 | The protein expression of CDK4, Bax and Bcl-2 **(A–C)**. Contrast to the without SBP-2A group, $*p < 0.05$, $**p < 0.01$, $***p < 0.001$. H22 mice tumor **(D)**.

TABLE 5 | Tumour inhibition rate (%) of SBP-2A in H22 mice ($n = 6$).

Group	Dose (mg/kg)	Tumour weight (g)	Inhibition Rate (%)
Model	—	1.27 ± 0.09	—
SBP-2A	25	1.09 ± 0.16*	14.09
SBP-2A	50	0.76 ± 0.11****	40.33
SBP-2A	100	1.02 ± 0.11**	19.93
APS	100	0.86 ± 0.11****	32.63

*Note: Mean ± SD, represent data, *p < 0.05, **p < 0.01, ****p < 0.0001 vs. the model group.*

absorption peaks (Vogt et al., 2019). SBP-1A and SBP-2A had a C=O stretching vibration at 1,634 cm^{-1} and contained uronic acid were proved, which is consistent with the monosaccharide composition of SBP determined by IC. In this study, comparing the anti-hepatoma activities of SBP, SBP-1A, and SBP-2A by MTT assay. The IC_{50} values for the 48 h inhibitory effect of SBP, SBP-1A, and SBP-2A on HepG2 cells were 1223, 891.7, and 548.3 μg/ml, respectively. It is worth noting that the IC_{50} value of SBP-2A was lower than that of SBP-1A, suggesting that SBP-2A may be more effective than SBP-1A in antitumour activity. Therefore, SBP-2A has high potential for application in cancer treatment research. The ability of the three polysaccharides from *Scutellaria barbata* to inhibit HepG2 cell proliferation was in order SBP-2A > SBP-1A > SBP. SBP-2A showed the strongest anti-hepatoma activity, which may be related to its high uronic acid content and the molecular weight of the polysaccharide molecules. The arabinose and galactose contents of SBP-2A are higher than those of SBP-1A. That is to say, the higher content of arabinose and galactose in the polysaccharide was, the stronger its antitumour effect. In addition, the C-H variable angle vibration occured near 1,380 cm^{-1}, causing the characteristic absorption peak of β-glucan to appear. The transmittance of SBP-2A was significantly lower than that of SBP-1A. These results indicate that the β-glucan functional group of SBP-2A was stronger than that of SBP-1A, possibly leading to the difference in anti-hepatoma activity between these polysaccharides.

Many studies have shown that the low-toxicity natural polysaccharides extracted from Chinese herbal medicines inhibit the proliferation of tumour cells and selectively induce apoptosis (Sohretoglu et al., 2019). Different biological macromolecules can be extracted from different raw materials, and the types and structural characteristics of polysaccharides affect their biological activities (Zhao et al., 2017; Chen et al., 2020; Liu et al., 2020). It has been shown that long-term *in vitro* culturing or drug treatment of cells can inhibit cell colony

formation (Lee et al., 2018; Chen et al., 2019). Therefore, we further verified the effect of SBP-2A on the inhibition of HepG2 cell proliferation with colony formation and Edu assays. *In vitro*, experiments preliminarily confirmed that SBP-2A inhibited the growth of HepG2 cells. We evaluated morphological changes of cells to determine the induced apoptosis response to drugs (Zhang et al., 2010; Drefs et al., 2017; Zhang W. et al., 2019). The morphological characteristics of HepG2 cells treated with SBP-2A for 48 h were directly observed by inverted microscopy. In this study, Hoechst 33258 staining confirmed that SBP-2A induced HepG2 cell apoptosis. To further evaluate the effect of SBP-2A on HepG2 cells, the DNA content was measured quantitatively after treatment with SBP-2A for 48 h by flow cytometry. In addition, the growth of normal and tumor cells was orderly in different stages of the cell cycle (Teloni et al., 2019), but cell cycle arrest and apoptosis can lead to programmed cell death (Zhang et al., 2017). We observed that SBP-2A induced apoptosis of HepG2 cells and arrested them in the G1 phase of the cell cycle. Cell cycle regulation is an important factor in tumorigenesis and development. There are many related molecules involved in the regulation of the G1 phase of the cell cycle, such as molecules belonging to the cyclin family and CDK family. CyclinD1 is the leading element in cell cycle regulation in the G1 phase; it promotes the transition from the G1 phase to S phase during the DNA synthesis cycle. The upregulation of CyclinD1 expression can induce tumour cell proliferation and lead to cancer characteristics (Choi et al., 2012). As a tumor suppressor, P53 is a key protein, which involved in DNA repair and apoptosis of damaged DNA cells. What's more, CyclinD1 has a certain synergistic effect with P53. When CyclinD1 is overexpressed, it can combine with intracellular inactivated P53, to promote the infinite proliferation and continuous deterioration of cells (Sauter et al., 2002). The expression of CyclinD1 were downregulated and that of P53 were upregulated when HepG2 cells were treated with SBP-2A is the fingings confirmed that the combination of wild-type P53 and antisense CyclinD1 in HepG2 cells could improve the ability of SBP to induce tumour cell apoptosis and block the DNA synthesis cycle in the G0/G1 phase, this is mainly achieved by downregulating the protein expression of CDK and upregulating the Bax/Bcl-2 ratio. *In vivo*, in contrast to APS, SBP-2A at a dose of 50 mg/kg significantly inhibited the tumour growth in H22 tumour-bearing mice. It is essential to further clarify the components of SBP and its molecular targets that play a role in the drug effects. This could provide a basis for determining the effects of *Scutellaria barbata* polysaccharides anti-hepatoma and support their potential use as a functional medicinal component.

CONCLUSION

In summary, the parameters for SBP extraction were optimized by RSM, and two homogeneous acidic polysaccharides with high purity were purified, SBP-1A and SBP-2A. The molecular weight, monosaccharide composition and characteristics of SBP-1A and SBP-2A were preliminarily identified. SBP, SBP-1A, and SBP-2A could inhibit the proliferation of HepG2 cells, but the ability of SBP-2A to inhibit the proliferation of HepG2 cells was better than that of SBP and SBP-1A. Moreover, SBP-2A could change the morphology of HepG2 cells and significantly induce apoptosis, which may be achieved by upregulating the expression of p53, Bax/Bcl-2 ratio and downregulating the expression of CyclinD1 and CDK4, to block HepG2 cells in the G0/G1 phase of the cell cycle. These results showed that SBP-2A isolated and purified from *Scutellaria barbata* showed antitumour activity *in vivo* and *in vitro*, which is worthy of further evaluation. This study, through in-depth exploration, provides information on the molecular mechanism of the anti-hepatoma effect of SBP.

CONSENT TO PUBLISH

All authors reviewed the results and approved the final version of the manuscript.

DATA AVAILABILITY STATEMENT

The raw data supporting the conclusions of this article will be made available by the authors, without undue reservation.

ETHICS STATEMENT

The animal study was reviewed and approved by the Ethics Committee of Mudanjiang Medical University (Mudanjiang, China). Written informed consent was obtained from the owners for the participation of their animals in this study.

AUTHOR CONTRIBUTIONS

GS and XX conceived and supervised the study; Experiments designed by GS and LW; LW, XL and WS completed the separation, purification and identification of Scutellaria barbata polysaccharide under the guidance of QL; The antitumor activity of Scutellaria barbata polysaccharide in vitro and in vivo was studied by WS, YL, SY, YF and LL; WS, JZ, DL and BZ analysis data and picture layout; WS wrote the manuscript; WS, QL, XG, LW, YY revised the manuscript.

FUNDING

This research was funded by the basic scientific research business fee project of Heilongjiang Provincial Department of Education (2018-KYYWFMY-0010), the Heilongjiang scientific research project of traditional Chinese Medicine (ZHY18-1168, ZQG-056), the innovative scientific research project for Postgraduates of Mudanjiang Medical University (YJSCX-MY16), the Postdoctoral Scientific Research Startup Fund of Heilongjiang Province (LBH-Q15141).

REFERENCES

Bargougui, K., Athmouni, K., and Chaieb, M. (2019). Optimization, Characterization and Hepatoprotective Effect of Polysaccharides Isolated from Stipa Parviflora Desf. Against CCl4 Induced Liver Injury in Rats Using Surface Response Methodology (RSM). *Int. J. Biol. Macromol* 132, 524–533. doi:10.1016/j.ijbiomac.2019.03.216

Cai, L., Chen, B., Yi, F., and Zou, S. (2019). Optimization of Extraction of Polysaccharide from Dandelion Root by Response Surface Methodology: Structural Characterization and Antioxidant Activity. *Int. J. Biol. Macromol* 140, 907–919. doi:10.1016/j.ijbiomac.2019.08.161

Cao, P., Wu, S., Wu, T., Deng, Y., Zhang, Q., Wang, K., et al. (2020). The Important Role of Polysaccharides from a Traditional Chinese Medicine-Lung Cleansing and Detoxifying Decoction against the COVID-19 Pandemic. *Carbohydr. Polym.* 240, 116346. doi:10.1016/j.carbpol.2020.116346

Chen, H., Huang, X., Fu, C., Wu, X., Peng, Y., Lin, X., et al. (2019). Recombinant Klotho Protects Human Periodontal Ligament Stem Cells by Regulating Mitochondrial Function and the Antioxidant System during H2O2-Induced Oxidative Stress. *Oxid Med. Cel Longev* 2019, 9261565. doi:10.1155/2019/9261565

Chen, J. Y., Sun, X. Y., and Ouyang, J. M. (2020). Modulation of Calcium Oxalate Crystal Growth and Protection from Oxidatively Damaged Renal Epithelial Cells of Corn Silk Polysaccharides with Different Molecular Weights. *Oxid Med. Cel Longev* 2020, 6982948. doi:10.1155/2020/6982948

Chen, Y. Y., and Xue, Y. T. (2019). Optimization of Microwave Assisted Extraction, Chemical Characterization and Antitumor Activities of Polysaccharides from Porphyra Haitanensis. *Carbohydr. Polym.* 206, 179–186. doi:10.1016/j.carbpol.2018.10.093

Choi, Y. J., Li, X., Hydbring, P., Sanda, T., Stefano, J., Christie, A. L., et al. (2012). The Requirement for Cyclin D Function in Tumor Maintenance. *Cancer Cell* 22 (4), 438–451. doi:10.1016/j.ccr.2012.09.015

Chylińska, M., Szymańska-Chargot, M., and Zdunek, A. (2016). FT-IR and FT-Raman Characterization of Non-cellulosic Polysaccharides Fractions Isolated from Plant Cell wall. *Carbohydr. Polym.* 154, 48–54. doi:10.1016/j.carbpol.2016.07.121

Drefs, M., Thomas, M. N., Guba, M., Angele, M. K., Werner, J., Conrad, M., et al. (2017). Modulation of Glutathione Hemostasis by Inhibition of 12/15-Lipoxygenase Prevents ROS-Mediated Cell Death after Hepatic Ischemia and Reperfusion. *Oxid Med. Cel Longev* 2017, 8325754. doi:10.1155/2017/8325754

Dubois, M., Gilles, K., Hamilton, J. K., Rebers, P. A., and Smith, F. (1951). A Colorimetric Method for the Determination of Sugars. *Nature* 168 (4265), 167. doi:10.1038/168167a0

Finn, R. S., Ikeda, M., Zhu, A. X., Sung, M. W., Baron, A. D., Kudo, M., et al. (2020). Phase Ib Study of Lenvatinib Plus Pembrolizumab in Patients with Unresectable Hepatocellular Carcinoma. *J. Clin. Oncol.* 38 (26), 2960–2970. doi:10.1200/jco.20.00808

Gan, Q. X., Wang, J., Hu, J., Lou, G. H., Xiong, H. J., Peng, C. Y., et al. (2020). Modulation of Apoptosis by Plant Polysaccharides for Exerting Anti-cancer Effects: A Review. *Front. Pharmacol.* 11, 792. doi:10.3389/fphar.2020.00792

Hui, Y., Jun-Li, H., and Chuang, W. (2019). Anti-oxidation and Anti-aging Activity of Polysaccharide from Malus Micromalus Makino Fruit Wine. *Int. J. Biol. Macromol* 121, 1203–1212. doi:10.1016/j.ijbiomac.2018.10.096

Jia, X., Ding, C., Yuan, S., Zhang, Z., Chen, Y., Du, L., et al. (2014). Extraction, Purification and Characterization of Polysaccharides from Hawk tea. *Carbohydr. Polym.* 99, 319–324. doi:10.1016/j.carbpol.2013.07.090

Lee, H., Jang, Y., Park, S., Jang, H., Park, E. J., Kim, H. J., et al. (2018). Development and Evaluation of a CEACAM6-Targeting Theranostic Nanomedicine for Photoacoustic-Based Diagnosis and Chemotherapy of Metastatic Cancer. *Theranostics* 8 (15), 4247–4261. doi:10.7150/thno.25131

Li, F., Gao, J., Xue, F., Yu, X., and Shao, T. (2016). Extraction Optimization, Purification and Physicochemical Properties of Polysaccharides from Gynura Medica. *Molecules* 21 (4), 397. doi:10.3390/molecules21040397

Li, H., Su, J., Jiang, J., Li, Y., Gan, Z., Ding, Y., et al. (2019a). Characterization of Polysaccharide from Scutellaria Barbata and its Antagonistic Effect on the Migration and Invasion of HT-29 Colorectal Cancer Cells Induced by TGF-B1. *Int. J. Biol. Macromol* 131, 886–895. doi:10.1016/j.ijbiomac.2019.03.053

Li, K., Cui, L. J., Cao, Y. X., Li, S. Y., Shi, L. X., Qin, X. M., et al. (2020). UHPLC Q-Exactive MS-Based Serum Metabolomics to Explore the Effect Mechanisms of Immunological Activity of Astragalus Polysaccharides with Different Molecular Weights. *Front. Pharmacol.* 11, 595692. doi:10.3389/fphar.2020.595692

Li, L., Xu, X., Wu, L., Zhu, H., He, Z., Zhang, B., et al. (2019b). Scutellaria Barbata Polysaccharides Inhibit Tumor Growth and Affect the Serum Proteomic Profiling of Hepatoma H22-bearing M-ice. *Mol. Med. Rep.* 19 (3), 2254–2262. doi:10.3892/mmr.2019.9862

Li, W., and Xiao, H. (2021). Scutellaria Barbata D. Don Polysaccharides Inhibit High Glucose-Induced Proliferation and Angiogenesis of Retinal Vascular Endothelial Cells. *Diabetes Metab. Syndr. Obes.* 14, 2431–2440. doi:10.2147/dmso.S296164

Liu, H., Sun, X. Y., Wang, F. X., and Ouyang, J. M. (2020). Regulation on Calcium Oxalate Crystallization and Protection on HK-2 Cells of Tea Polysaccharides with Different Molecular Weights. *Oxid Med. Cel Longev* 2020, 5057123. doi:10.1155/2020/5057123

Ma, T., Sun, X., Tian, C., Luo, J., Zheng, C., and Zhan, J. (2016). Polysaccharide Extraction from Sphallerocarpus Gracilis Roots by Response Surface Methodology. *Int. J. Biol. Macromol* 88, 162–170. doi:10.1016/j.ijbiomac.2016.03.058

Mkadmini Hammi, K., Hammami, M., Rihouey, C., Le Cerf, D., Ksouri, R., and Majdoub, H. (2016). Optimization Extraction of Polysaccharide from Tunisian Zizyphus lotus Fruit by Response Surface Methodology: Composition and Antioxidant Activity. *Food Chem.* 212, 476–484. doi:10.1016/j.foodchem.2016.06.004

Qu, J., Huang, P., Zhang, L., Qiu, Y., Qi, H., Leng, A., et al. (2020). Hepatoprotective Effect of Plant Polysaccharides from Natural Resources: A Review of the Mechanisms and Structure-Activity Relationship. *Int. J. Biol. Macromol* 161, 24–34. doi:10.1016/j.ijbiomac.2020.05.196

Qu, Y., Li, C., Zhang, C., Zeng, R., and Fu, C. (2016). Optimization of Infrared-Assisted Extraction of Bletilla Striata Polysaccharides Based on Response Surface Methodology and Their Antioxidant Activities. *Carbohydr. Polym.* 148, 345–353. doi:10.1016/j.carbpol.2016.04.081

Sauter, E. R., Takemoto, R., Litwin, S., and Herlyn, M. (2002). p53 Alone or in Combination with Antisense Cyclin D1 Induces Apoptosis and Reduces Tumor Size in Human Melanoma. *Cancer Gene Ther.* 9 (10), 807–812. doi:10.1038/sj.cgt.7700492

Singal, A. G., Lampertico, P., and Nahon, P. (2020). Epidemiology and Surveillance for Hepatocellular Carcinoma: New Trends. *J. Hepatol.* 72 (2), 250–261. doi:10.1016/j.jhep.2019.08.025

Sohretoglu, D., Zhang, C., Luo, J., and Huang, S. (2019). ReishiMax Inhibits mTORC1/2 by Activating AMPK and Inhibiting IGFR/PI3K/Rheb in Tumor Cells. *Signal. Transduct Target. Ther.* 4, 21. doi:10.1038/s41392-019-0056-7

Sun, P., Sun, D., and Wang, X. (2017). Effects of Scutellaria Barbata Polysaccharide on the Proliferation, Apoptosis and EMT of Human colon Cancer HT29 Cells. *Carbohydr. Polym.* 167, 90–96. doi:10.1016/j.carbpol.2017.03.022

Tabrizian, P., Jibara, G., Shrager, B., Schwartz, M., and Roayaie, S. (2015). Recurrence of Hepatocellular Cancer after Resection: Patterns, Treatments, and Prognosis. *Ann. Surg.* 261 (5), 947–955. doi:10.1097/sla.0000000000000710

Teloni, F., Michelena, J., Lezaja, A., Kilic, S., Ambrosi, C., Menon, S., et al. (2019). Efficient Pre-mRNA Cleavage Prevents Replication-Stress-Associated Genome Instability. *Mol. Cel* 73 (4), 670–e12. doi:10.1016/j.molcel.2018.11.036

Vogt, S., Löffler, K., Dinkelacker, A. G., Bader, B., Autenrieth, I. B., Peter, S., et al. (2019). Fourier-Transform Infrared (FTIR) Spectroscopy for Typing of Clinical *Enterobacter cloacae* Complex Isolates. *Front. Microbiol.* 10, 2582. doi:10.3389/fmicb.2019.02582

Wang, D., Liu, Y., and Zhao, W. (2021). The Adjuvant Effects on Vaccine and the Immunomodulatory Mechanisms of Polysaccharides from Traditional Chinese Medicine. *Front. Mol. Biosci.* 8, 655570. doi:10.3389/fmolb.2021.655570

Wang, R., Chen, P., Jia, F., Tang, J., and Ma, F. (2012). Optimization of Polysaccharides from Panax Japonicus C.A. Meyer by RSM and its Anti-oxidant Activity. *Int. J. Biol. Macromol* 50 (2), 331–336. doi:10.1016/j.ijbiomac.2011.12.023

Wei, D., Chen, T., Yan, M., Zhao, W., Li, F., Cheng, W., et al. (2015). Synthesis, Characterization, Antioxidant Activity and Neuroprotective Effects of Selenium Polysaccharide from Radix Hedysari. *Carbohydr. Polym.* 125, 161–168. doi:10.1016/j.carbpol.2015.02.029

Wu, H., Li, M., Yang, X., Wei, Q., Sun, L., Zhao, J., et al. (2020). Extraction Optimization, Physicochemical Properties and Antioxidant and Hypoglycemic Activities of Polysaccharides from Roxburgh Rose (Rosa Roxburghii Tratt.) Leaves. *Int. J. Biol. Macromol* 165 (Pt A), 517–529. doi:10.1016/j.ijbiomac.2020.09.198

Wu, Y., and Chen, D. F. (2009). Anti-complementary Effect of Polysaccharide B3-PS1 in Herba Scutellariae Barbatae (Scutellaria Barbata). *Immunopharmacol Immunotoxicol* 31 (4), 696–701. doi:10.3109/08923970903095314

Xie, M., Tao, W., Wu, F., Wu, K., Huang, X., Ling, G., et al. (2021). Anti-hypertensive and Cardioprotective Activities of Traditional Chinese Medicine-Derived Polysaccharides: A Review. *Int. J. Biol. Macromol* 185, 917–934. doi:10.1016/j.ijbiomac.2021.07.008

Yang, J., Yang, G., Hou, G., Liu, Q., Hu, W., Zhao, P. U., et al. (2015). Scutellaria Barbata D. Don Polysaccharides Inhibit the Growth of Calu-3 Xenograft Tumors via Suppression of the HER2 Pathway and Angiogenesis. *Oncol. Lett.* 9 (6), 2721–2725. doi:10.3892/ol.2015.3127

Yang, J. D., Hainaut, P., Gores, G. J., Amadou, A., Plymoth, A., and Roberts, L. R. (2019). A Global View of Hepatocellular Carcinoma: Trends, Risk, Prevention and Management. *Nat. Rev. Gastroenterol. Hepatol.* 16 (10), 589–604. doi:10.1038/s41575-019-0186-y

Yang, X., Yang, Y., Tang, S., Tang, H., Yang, G., Xu, Q., et al. (2014). Anti-tumor Effect of Polysaccharides from Scutellaria Barbata D. Don on the 95-D Xenograft Model via Inhibition of the C-Met Pathway. *J. Pharmacol. Sci.* 125 (3), 255–263. doi:10.1254/jphs.13276fp

Yao, Y. L., Shu, C., Feng, G., Wang, Q., Yan, Y. Y., Yi, Y., et al. (2020). Polysaccharides from Pyracantha Fortuneana and its Biological Activity. *Int. J. Biol. Macromol* 150, 1162–1174. doi:10.1016/j.ijbiomac.2019.10.125

Ye, C. L., and Huang, Q. (2012). Extraction of Polysaccharides from Herbal Scutellaria Barbata D. Don (Ban-Zhi-Lian) and Their Antioxidant Activity. *Carbohydr. Polym.* 89 (4), 1131–1137. doi:10.1016/j.carbpol.2012.03.084

Yeon, E. T., Lee, J. W., Lee, C., Jin, Q., Jang, H., Lee, D., et al. (2015). Neo-Clerodane Diterpenoids from Scutellaria Barbata and Their Inhibitory Effects on LPS-Induced Nitric Oxide Production. *J. Nat. Prod.* 78 (9), 2292–2296. doi:10.1021/acs.jnatprod.5b00126

Yuan, Q., Yuan, Y., Zheng, Y., Sheng, R., Liu, L., Xie, F., et al. (2021). Anti-cerebral Ischemia Reperfusion Injury of Polysaccharides: A Review of the Mechanisms. *Biomed. Pharmacother.* 137, 111303. doi:10.1016/j.biopha.2021.111303

Zhang, C., Zhao, F., Li, R., Wu, Y., Liu, S., and Liang, Q. (2019a). Purification, Characterization, Antioxidant and Moisture-Preserving Activities of Polysaccharides from Rosa Rugosa Petals. *Int. J. Biol. Macromol* 124, 938–945. doi:10.1016/j.ijbiomac.2018.11.275

Zhang, F., Shi, J. J., Thakur, K., Hu, F., Zhang, J. G., and Wei, Z. J. (2017). Anti-Cancerous Potential of Polysaccharide Fractions Extracted from Peony Seed Dreg on Various Human Cancer Cell Lines via Cell Cycle Arrest and Apoptosis. *Front. Pharmacol.* 8, 102. doi:10.3389/fphar.2017.00102

Zhang, T. T., Lu, C. L., Jiang, J. G., Wang, M., Wang, D. M., and Zhu, W. (2015). Bioactivities and Extraction Optimization of Crude Polysaccharides from the Fruits and Leaves of Rubus Chingii Hu. *Carbohydr. Polym.* 130, 307–315. doi:10.1016/j.carbpol.2015.05.012

Zhang, W., Lei, Z., Meng, J., Li, G., Zhang, Y., He, J., et al. (2019b). Water Extract of Sporoderm-Broken Spores of Ganoderma Lucidum Induces Osteosarcoma Apoptosis and Restricts Autophagic Flux. *Onco Targets Ther.* 12, 11651–11665. doi:10.2147/ott.S226850

Zhang, W. L., Zhu, L., and Jiang, J. G. (2014). Active Ingredients from Natural Botanicals in the Treatment of Obesity. *Obes. Rev.* 15 (12), 957–967. doi:10.1111/obr.12228

Zhang, Y., Soto, J., Park, K., Viswanath, G., Kuwada, S., Abel, E. D., et al. (2010). Nuclear Receptor SHP, a Death Receptor that Targets Mitochondria, Induces Apoptosis and Inhibits Tumor Growth. *Mol. Cel Biol* 30 (6), 1341–1356. doi:10.1128/mcb.01076-09

Zhao, L., Wang, Y., Shen, H. L., Shen, X. D., Nie, Y., Wang, Y., et al. (2012). Structural Characterization and Radioprotection of Bone Marrow Hematopoiesis of Two Novel Polysaccharides from the Root of Angelica Sinensis (Oliv.) Diels. *Fitoterapia* 83 (8), 1712–1720. doi:10.1016/j.fitote.2012.09.029

Zhao, X., Li, J., Liu, Y., Wu, D., Cai, P., and Pan, Y. (2017). Structural Characterization and Immunomodulatory Activity of a Water Soluble Polysaccharide Isolated from Botrychium Ternatum. *Carbohydr. Polym.* 171, 136–142. doi:10.1016/j.carbpol.2017.05.014

Zhao, Z. Y., Zhang, Q., Li, Y. F., Dong, L. L., and Liu, S. L. (2015). Optimization of Ultrasound Extraction of Alisma Orientalis Polysaccharides by Response Surface Methodology and Their Antioxidant Activities. *Carbohydr. Polym.* 119, 101–109. doi:10.1016/j.carbpol.2014.11.052

Conflict of Interest: The authors declare that the research was conducted in the absence of any commercial or financial relationships that could be construed as a potential conflict of interest.

Publisher's Note: All claims expressed in this article are solely those of the authors and do not necessarily represent those of their affiliated organizations, or those of the publisher, the editors, and the reviewers. Any product that may be evaluated in this article, or claim that may be made by its manufacturer, is not guaranteed or endorsed by the publisher.

Copyright © 2022 Su, Wu, Liang, Lin, Xu, Yu, Lin, Zhou, Fu, Gao, Zhang, Li, Li, Yin and Song. This is an open-access article distributed under the terms of the Creative Commons Attribution License (CC BY). The use, distribution or reproduction in other forums is permitted, provided the original author(s) and the copyright owner(s) are credited and that the original publication in this journal is cited, in accordance with accepted academic practice. No use, distribution or reproduction is permitted which does not comply with these terms.

Advantages of publishing in Frontiers

OPEN ACCESS
Articles are free to read for greatest visibility and readership

FAST PUBLICATION
Around 90 days from submission to decision

HIGH QUALITY PEER-REVIEW
Rigorous, collaborative, and constructive peer-review

TRANSPARENT PEER-REVIEW
Editors and reviewers acknowledged by name on published articles

Frontiers
Avenue du Tribunal-Fédéral 34
1005 Lausanne | Switzerland

Visit us: www.frontiersin.org
Contact us: frontiersin.org/about/contact

REPRODUCIBILITY OF RESEARCH
Support open data and methods to enhance research reproducibility

DIGITAL PUBLISHING
Articles designed for optimal readership across devices

FOLLOW US
@frontiersin

IMPACT METRICS
Advanced article metrics track visibility across digital media

EXTENSIVE PROMOTION
Marketing and promotion of impactful research

LOOP RESEARCH NETWORK
Our network increases your article's readership